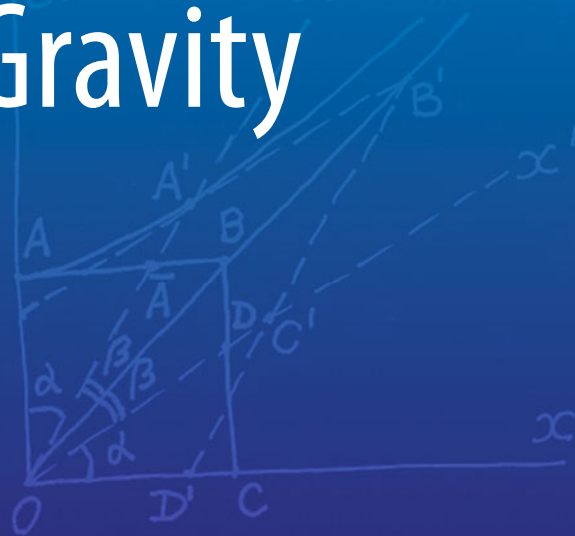


Dirk Puetzfeld
Claus Lämmerzahl
Bernard Schutz *Editors*

Equations of Motion in Relativistic Gravity



Proper length of the identical ball

$$l = \frac{PP'}{OC} = \frac{P'Q'}{PQ'}$$

Minkowski showed that:



Springer

Fundamental Theories of Physics

Volume 179

Series editors

Henk van Beijeren
Philippe Blanchard
Paul Busch
Bob Coecke
Dennis Dieks
Detlef Dürr
Roman Frigg
Christopher Fuchs
Giancarlo Ghirardi
Domenico J.W. Giulini
Gregg Jaeger
Claus Kiefer
Nicolaas P. Landsman
Christian Maes
Hermann Nicolai
Vesselin Petkov
Alwyn van der Merwe
Rainer Verch
R.F. Werner
Christian Wuthrich

More information about this series at <http://www.springer.com/series/6001>

Dirk Puetzfeld · Claus Lämmerzahl
Bernard Schutz
Editors

Equations of Motion in Relativistic Gravity

Editors

Dirk Puetzfeld
ZARM
University of Bremen
Bremen
Germany

Bernard Schutz
Max-Planck-Institut für Gravitationsphysik
Golm, Brandenburg
Germany

Claus Lämmerzahl
ZARM
University of Bremen
Bremen
Germany

Fundamental Theories of Physics
ISBN 978-3-319-18334-3 ISBN 978-3-319-18335-0 (eBook)
DOI 10.1007/978-3-319-18335-0

Library of Congress Control Number: 2015938091

Springer Cham Heidelberg New York Dordrecht London
© Springer International Publishing Switzerland 2015

This work is subject to copyright. All rights are reserved by the Publisher, whether the whole or part of the material is concerned, specifically the rights of translation, reprinting, reuse of illustrations, recitation, broadcasting, reproduction on microfilms or in any other physical way, and transmission or information storage and retrieval, electronic adaptation, computer software, or by similar or dissimilar methodology now known or hereafter developed.

The use of general descriptive names, registered names, trademarks, service marks, etc. in this publication does not imply, even in the absence of a specific statement, that such names are exempt from the relevant protective laws and regulations and therefore free for general use.

The publisher, the authors and the editors are safe to assume that the advice and information in this book are believed to be true and accurate at the date of publication. Neither the publisher nor the authors or the editors give a warranty, express or implied, with respect to the material contained herein or for any errors or omissions that may have been made.

Printed on acid-free paper

Springer International Publishing AG Switzerland is part of Springer Science+Business Media
(www.springer.com)

Preface

The derivation of the equations of motion for extended bodies represents a fundamental problem in relativistic gravitational physics. Since the early days of Einstein's theory of General Relativity, a wide spectrum of methods has been proposed to allow for the derivation in different physical settings. Without having such equations of motion at hand it is impossible to correctly describe, for example, the motion of binary systems, or to calculate the form of gravitational waves emitted by such systems. These equations are also crucial for astrometry and for high precision satellite missions.

In 2013 we organized¹ an international conference in Bad Honnef (Germany) on the "Equations of Motion in Relativistic Gravity". The conference brought together the leading experts in their respective fields, and was very well received by the speakers as well as by the audience. We would like to thank the WE-Heraeus Foundation for the generous support of this conference. Our thanks also go to the Physikzentrum Bad Honnef where the conference took place.

The very positive reception and the feedback after the conference made clear that there is a strong demand for an up-to-date textbook, covering the wide spectrum of methods employed in current research in the context of the relativistic problem of motion. This book intends to give a broad and up-to-date status report on this issue. It hopefully is of value for the experts working in this field and may also serve as a guideline for students with a background in General Relativity, who would like to enter the field.

The present volume is based on the lectures given at the conference, and gives an overview of the following topics:

- Derivation of the equations of motion in General Relativity (GR) and in alternative gravity theories for
 - Spinning and extended test bodies
 - Self-force effects

¹<http://puetzfeld.org/eom2013.html>.

- Self-gravitating/heavy bodies
- Microstructured bodies with internal degrees of freedom
- Approximation methods linked to the derivation of the equations of motion
 - Multipolar methods
 - Post-Newtonian and post-Minkowskian methods
- Current and future observations
 - Binary systems, in particular binary pulsars
 - Gravitational waves
 - Celestial mechanics and astrometry
 - Satellite experiments

The contributions in this book roughly follow the order of presentations at the conference, i.e. there are contributions on test bodies, self-force effects, the dynamics of self-gravitating bodies, as well as on current and future observations.

We as editors are deeply indebted to the contributors to this volume, who made great efforts to present their respective areas of research in an accessible way to a broader audience. We hope that the material presented here will prove to be useful as a reference for experienced researchers, as well as serve as an inspiration for younger researchers who want to enter this exciting field of gravitational physics.

Dirk Puetzfeld
Claus Lämmerzahl
Bernard Schutz

Contents

The New Mechanics of Myron Mathisson and Its Subsequent Development	1
W.G. Dixon	
Multipolar Test Body Equations of Motion in Generalized Gravity Theories	67
Yuri N. Obukhov and Dirk Puetzfeld	
Energy-Momentum Tensors and Motion in Special Relativity	121
Domenico Giulini	
Solutions of Mathisson-Papapetrou Equations for Highly Relativistic Spinning Particles	165
Roman Plyatsko, Mykola Fenyk and Oleksandr Stefanyshyn	
The MPD Equations in Analytic Perturbative Form	191
Dinesh Singh	
Center of Mass, Spin Supplementary Conditions, and the Momentum of Spinning Particles	215
L. Filipe O. Costa and José Natário	
General Relativistic Two-Body Problem: Theory and Experiment and the Role of Hidden Momentum	259
R.F. O’Connell	
Equations of Motion of Schwarzschild, Reissner–Nordström and Kerr Particles	265
Peter A. Hogan	

From Singularities of Fields to Equations of Particles Motion	285
Y. Itin	
Motion of Spinless Particles in Gravitational Fields.	303
Alexander J. Silenko	
On the Strong Field Point Particle Limit and Equation of Motion in General Relativity	317
Toshifumi Futamase	
Motion in Classical Field Theories and the Foundations of the Self-force Problem	327
Abraham I. Harte	
Motion of Small Objects in Curved Spacetimes: An Introduction to Gravitational Self-Force.	399
Adam Pound	
Self-force: Computational Strategies.	487
Barry Wardell	
On the Self-force in Electrodynamics and Implications for Gravity . . .	523
Volker Perlick	
Self-gravitating Elastic Bodies	543
Lars Andersson	
On Geodesic Dynamics in Deformed Black-Hole Fields	561
O. Semerák and P. Suková	
Higher Order Post-Newtonian Dynamics of Compact Binary Systems in Hamiltonian Form	587
Gerhard Schäfer	
Spin and Quadrupole Contributions to the Motion of Astrophysical Binaries	615
Jan Steinhoff	
Testing the Motion of Strongly Self-Gravitating Bodies with Radio Pulsars	651
Norbert Wex	
Equations of Motion in an Expanding Universe	689
Sergei M. Kopeikin and Alexander N. Petrov	

The Galactic Center Black Hole Laboratory	759
A. Eckart, S. Britzen, M. Valencia-S., C. Straubmeier, J.A. Zensus, V. Karas, D. Kunneriath, A. Alberdi, N. Sabha, R. Schödel and D. Puetzfeld	
Extreme Mass Ratio Inspirals: Perspectives for Their Detection.	783
Stanislav Babak, Jonathan R. Gair and Robert H. Cole	
Level Sets of the Lapse Function in Static GR	813
Carla Cederbaum	
Aberrational Effects for Shadows of Black Holes	823
Arne Grenzebach	
Time-Domain Inspiral Templates for Spinning Compact Binaries in Quasi-Circular Orbits.	833
Anuradha Gupta and Achamveedu Gopakumar	

Contributors

A. Alberdi Instituto de Astrofísica de Andalucía (CSIC), Glorieta de la Astronomía s/n, Granada, Spain

Lars Andersson Albert Einstein Institute, Potsdam, Germany

Stanislav Babak Albert Einstein Institute, Golm, Germany

S. Britzen Max-Planck-Institut für Radioastronomie, Bonn, Germany

Carla Cederbaum Mathematisches Institut, Universität Tübingen, Tübingen, Germany

Robert H. Cole Institute of Astronomy, University of Cambridge, Cambridge, UK

L. Filipe O. Costa CAMGSD, Instituto Superior Técnico, Universidade de Lisboa, Lisbon, Portugal; Departamento de Física e Astronomia, Centro de Física do Porto – CFP, Universidade do Porto, Porto, Portugal

W.G. Dixon Churchill College, University of Cambridge, Cambridge, England

A. Eckart I. Physikalisches Institut, Universität zu Köln, Cologne, Germany; Max-Planck-Institut für Radioastronomie, Bonn, Germany

Mykola Fenyk Pidstryhach Institute for APMM, Ukrainian National Academy of Sciences, Lviv, Ukraine

Toshifumi Futamase Astronomical Institute, Tohoku University, Sendai, Japan

Jonathan R. Gair Institute of Astronomy, University of Cambridge, Cambridge, UK

Domenico Giulini Riemann Center for Geometry and Physics, Institute for Theoretical Physics, Leibniz University Hannover, Hannover, Germany; Center for Applied Space Technology and Microgravity, University of Bremen, Bremen, Germany

Achamveedu Gopakumar Department of Astronomy and Astrophysics, Tata Institute of Fundamental Research, Mumbai, India

Arne Grenzebach ZARM, University of Bremen, Bremen, Germany

Anuradha Gupta Department of Astronomy and Astrophysics, Tata Institute of Fundamental Research, Mumbai, India

Abraham I. Harte Albert-Einstein-Institut, Max-Planck-Institut für Gravitationsphysik, Golm, Germany

Peter A. Hogan School of Physics, University College Dublin, Dublin 4, Ireland

Y. Itin Institute of Mathematics, Hebrew University of Jerusalem and Jerusalem College of Technology, Jerusalem, Israel

V. Karas Astronomical Institute, Academy of Sciences, Prague, Czech Republic

Sergei M. Kopeikin Department of Physics & Astronomy, University of Missouri, Columbia, MO, USA

D. Kunneriath Astronomical Institute, Academy of Sciences, Prague, Czech Republic

José Natário CAMGSD, Instituto Superior Técnico, Universidade de Lisboa, Lisbon, Portugal

R.F. O'Connell Department of Physics and Astronomy, Louisiana State University, Baton Rouge, LA, USA

Yuri N. Obukhov Theoretical Physics Laboratory, Nuclear Safety Institute, Russian Academy of Sciences, Moscow, Russia

Volker Perlick ZARM, University of Bremen, Bremen, Germany

Alexander N. Petrov Sternberg Astronomical Institute, Lomonosov Moscow State University, Moscow, Russia

Roman Plyatsko Pidstryhach Institute for APMM, Ukrainian National Academy of Sciences, Lviv, Ukraine

Adam Pound Mathematical Sciences, University of Southampton, Southampton, UK

Dirk Puetzfeld ZARM, University of Bremen, Bremen, Germany

N. Sabha I. Physikalisches Institut, Universität zu Köln, Cologne, Germany

Gerhard Schäfer Theoretisch-Physikalisches Institut, Friedrich-Schiller-Universität Jena, Jena, Germany

R. Schödel Instituto de Astrofísica de Andalucía (CSIC), Glorieta de la Astronomía s/n, Granada, Spain

O. Semerák Institute of Theoretical Physics, Faculty of Mathematics and Physics, Charles University in Prague, Prague, Czech Republic

Alexander J. Silenko Research Institute for Nuclear Problems, Belarusian State University, Minsk, Belarus; Bogoliubov Laboratory of Theoretical Physics, Joint Institute for Nuclear Research, Dubna, Russia

Dinesh Singh Department of Physics, University of Regina, Regina, SK, Canada

Oleksandr Stefanyshyn Pidstryhach Institute for APMM, Ukrainian National Academy of Sciences, Lviv, Ukraine

Jan Steinhoff Centro Multidisciplinar de Astrofísica (CENTRA), Instituto Superior Técnico (IST), Lisbon, Portugal

C. Straubmeier I. Physikalisches Institut, Universität zu Köln, Cologne, Germany

P. Suková Center for Theoretical Physics, Polish Academy of Sciences, Warsaw, Poland

M. Valencia-S. I. Physikalisches Institut, Universität zu Köln, Cologne, Germany

Barry Wardell Department of Astronomy, Cornell University, Ithaca, NY, USA

Norbert Wex Max-Planck-Institut für Radioastronomie, Bonn, Germany

J.A. Zensus I. Physikalisches Institut, Universität zu Köln, Cologne, Germany; Max-Planck-Institut für Radioastronomie, Bonn, Germany

The New Mechanics of Myron Mathisson and Its Subsequent Development

W.G. Dixon

Abstract In 1937, Myron Mathisson published a paper which initiated a program of work in general relativity that continues to the present day. The aim of this program was to obtain equations that determine the trajectory of an extended body in an external gravitational field. In Newtonian mechanics this is a straightforward task, but in general relativity even giving a precise meaning to the problem is fraught with difficulties. These difficulties are analysed, Mathisson's approach is described and it is shown how his approach has been carried to fulfillment by subsequent authors in the years since Mathisson's untimely death in 1940. This work, however, completes only a part of the overall program. The work is placed in context in this overall program and the issues remaining for that program are identified.

1 Introduction

In 1937, Myron Mathisson published a paper [1] in German in the Polish journal *Acta Physica Polonica* with the ambitious title, in translation, of *A New Mechanics of Material Systems*. Long neglected, this paper was finally made available in English translation in 2010 [2]. This was the first paper to consider how to describe an extended body in general relativity in a manner similar to that of Newtonian rigid body mechanics.

It was already known that a point particle with no internal structure follows a geodesic path. This had originally been a postulate of general relativity additional to the vacuum field equations, but Einstein and Grommer [3] had shown it to be a consequence of those equations and so not needed as a separate postulate. Their derivation treated the particle as a singularity in spacetime. The path followed by the particle was a geodesic in the background metric from which the field of the singularity itself had been subtracted. Einstein published a second paper [4] later that year, extending the work to include the presence of an electromagnetic field. The approach was dictated by Einstein's philosophical beliefs: the particles being considered are

W.G. Dixon (✉)

Churchill College, University of Cambridge, Cambridge CB3 0DS, England
e-mail: graham.dixon@ntlworld.com

the elementary particles of which all matter is composed, the vacuum field equations will break down in the immediate vicinity of such a particle, but as nothing is known about the manner of this breakdown, the best that can be done is provisionally to treat such particles as singularities in the gravitational and electromagnetic fields.

This philosophical view of Einstein causes problems when the question of interest is the motion of astronomical bodies, which is the only arena in which general relativity had been tested at that time, or indeed is likely to be tested in the foreseeable future. To treat such a body truly within Einstein's philosophy requires treating it as an assembly of elementary particles, each of which is represented as a spacetime singularity. In effect this requires the development of a general relativistic version of statistical mechanics, a formidable task.

The alternative is to say that, on an astronomical scale, the individual bodies to be considered are sufficiently small that they can themselves be treated as particles. This may seem plausible but it requires proof. A derivation of the geodesic postulate from this viewpoint was given first by Robertson [5], who expressed his philosophy thus:

In the general theory of relativity, as in many other branches of theoretical physics, the material and energetical content of space-time is considered, in the first instance, as an extended field, which is specified by means of field quantities (energy-momentum-stress tensor, charge-current density, electromagnetic field strength). From this point of view particles are constructs obtained by first considering the field quantities as non-vanishing only within certain world-tubes, and then passing by limiting processes to the idealisation in which these world tubes are shrunk into world-lines.

This was the philosophy adopted by Mathisson, who was writing at about the same time as Robertson but with much greater ambition. Mathisson wished not only to take the point particle limit but also to be able to treat the body as extended and to investigate the effects of its extended size on its motion. This approach raises its own questions, in particular what point to take as describing the position of an extended body and how to describe its structure. Mathisson addressed the second question first, by choosing initially an arbitrary world line within the body as describing its position and motion and then replacing the energy-momentum tensor with an equivalent infinite set of tensor fields defined along this world line which were considered to be multipole moments of the energy-momentum tensor. The covariant conservation equation satisfied by the energy-momentum tensor must then translate into a set of equations governing the form and evolution of the multipole moments. The first question, the choice of representative world line, is then answered by selecting one that simplifies these results in some way.

This is the ambitious plan of Mathisson's "New Mechanics". Despite its title, his paper of 1937 was only a first step towards this goal. He continued to work on this problem until his untimely death in 1940. This work was later taken up by others and the way his plan was eventually taken to completion is the subject of this paper.

2 Myron Mathisson, the Man

First a little of his history. See Sauer and Trautman [6], on which this account is based, for more details.

Myron Mathisson was a Polish Jew, born in Warsaw on 14 December 1897. He studied Civil Engineering at the Politechnika Warszawska from 1915. In 1919 he was drafted into the Polish Army, which was then fighting the Soviets. After that war he entered Warsaw University in 1920 to study physics. In 1925 he wrote a paper entitled *On the motion of a rotating body in a gravitational field*. This was never published, but the professor of theoretical physics at the University offered to accept it as a Ph.D. thesis. Mathisson was not satisfied with his own work and declined the offer.

In 1927, Einstein published the two papers described in the Introduction. As was seen there, Mathisson had a very different philosophy about the problem of motion in general relativity than did Einstein. This led him, on 18 December 1929 with no Ph.D. and no publications, to write the first of what eventually turned out to be around 20 letters to Einstein. The start of this letter is shown in Fig. 1. He wrote that Einstein neglects radiation and deviations from spherical symmetry, these approximations being due to the “mathematical insufficiency of your method”. The letter continues for 11 pages.

At the time that he received this letter, Einstein’s collaboration with Grommer had come to an end and he was looking for someone else. He responded to Mathisson’s audacious letter not by throwing it away but by inviting Mathisson to Berlin as a collaborator. Mathisson declined the invitation on the grounds that he did not yet feel ready for such a step.

Monsieur,

Votre Mémoire, publié dans les SITZUNGSBERICHTE DER PREUSS. AKADEMIE (séance du 8. décembre 1927), intitulé ALLGEMEINE RELATIVITÄTSTHEORIE UND BEWEGUNGSGESETZ, s'occupe d'un problème, dont j'ai établi, il y a deux ans et demi, une solution plus complète.

Fig. 1 The beginning of Mathisson’s first letter to Einstein, 18 December 1929 (Albert Einstein Archives at the Hebrew University of Jerusalem, 18-001)

In 1930, Einstein attempted unsuccessfully to obtain a stipend from the Rockefeller Foundation for Mathisson. Between 1932 and 1936, Mathisson lectured at Warsaw University but without a permanent position. In 1936 he left Warsaw for a position in Kazan in Soviet Russia. While there, he received a letter from Einstein inviting him to come for a year to the Princeton Institute for Advanced Study, where Einstein himself was at that time. Mathisson replied that he could come for the academic year 1937–1938 after a year in Russia. He added that he had found good conditions to work in Russia and that he would return to Kazan after his time in Princeton.

Einstein replied, expressing delight that Mathisson had found good conditions to work in Soviet Russia but also withdrawing his invitation to Princeton as it would not be right while there were so many scientists deprived of the possibility of work. Einstein then began a collaboration with Leopold Infeld and Banesh Hoffman and wrote to Mathisson in Kazan on 7 May 1937 that they have developed a new method (later known as the EIH method) of deriving the equations of motion for point masses. Infeld received the invitation to Princeton in place of Mathisson. The EIH paper [7] was submitted to *Annals of Mathematics* on 16 June 1937. Infeld arrived in Princeton in October 1937, the date when Mathisson had offered to arrive.

Mathisson returned to Warsaw from Kazan at the end of May 1937 as the situation for a foreigner there had become unbearable. On 5 September 1937 he submitted his most important paper [1] to *Acta Physica Polonica*. One can only wonder how different the development of equations of motion in general relativity might have been had Mathisson's visit to Princeton taken place and led to an Einstein-Mathisson collaboration instead of the Einstein-Infeld one.

In 1938 Mathisson went to Cracow where he collaborated with Adam Bielecki and Jan Weyssenhoff on unresolved issues of his 1937 paper, the results of which were published in [8]. While in Cracow he married Irena Jungermann. In the spring of 1939 the Mathissons went to Paris and later that year to Cambridge where he worked with Dirac. There he published a further paper [9] on his approach to equations of motion, this time considering a body under the influence of external forces within the framework of special relativity. Suffering from tuberculosis, he died in Cambridge on 13 September 1940. His work had so impressed Dirac that he edited Mathisson's unpublished notes into a posthumous paper [10].

In his historical account of work on the problem of motion, Havas [11] is very critical of the work on the problem of motion done by Einstein and, especially, Infeld and writes (p. 267) that “Mathisson's contributions were far more original than Infeld's and introduced far better mathematical methods”.

3 Mathisson's Paper of 1937 in Outline

The central concept introduced in Mathisson's paper of 1937 is what he termed the *gravitational skeleton* of a body. This describes a body occupying a world tube of finite spatial extent and is defined relative to a timelike world line L within this world tube. It provides an alternative description of an extended body to that provided by

the energy-momentum tensor $T^{\alpha\beta}$. It consists of an infinite set of multipole moments $m^{\alpha\beta}$, $m^{\gamma\alpha\beta}$, $m^{\gamma\delta\alpha\beta}$, ..., symmetric separately on their last two indices α, β and on all the remaining indices, such that

$$\int T^{\alpha\beta} \varphi_{\alpha\beta} Dx = \int_L \left(m^{\alpha\beta} \varphi_{\alpha\beta} + m^{\gamma\alpha\beta} \nabla_\gamma \varphi_{\alpha\beta} + \frac{1}{2!} m^{\gamma\delta\alpha\beta} \nabla_\gamma \nabla_\delta \varphi_{\alpha\beta} + \dots \right) ds \quad (1)$$

for symmetric tensor fields $\varphi_{\alpha\beta}$ of compact support. This is effectively treating the energy-momentum tensor as a distribution (generalised function) before the concept had been invented. The integral on the left extends over all spacetime, with $Dx \equiv \sqrt{-g} d^4x$ being the spacetime volume element. That on the right is over the world line L on which s is proper time, ∇_α denotes covariant differentiation and $\nabla_{\alpha\beta} \equiv \nabla_\alpha \nabla_\beta$. Note that this definition in fact differs slightly from that of Mathisson, in that he does not include the $1/n!$ factor in the 2^n -pole moment term. These factors are included here for agreement with later work of other authors.

In what follows, the signature of the spacetime metric is taken as -2 , so that the unit tangent vector v^α to L satisfies $v_\alpha v^\alpha = 1$. Round brackets around indices denote symmetrisation, square brackets denote antisymmetrisation. The sign of the curvature tensor is such that for a covariant vector field A_α the Ricci identity takes the form

$$\nabla_{[\beta\gamma]} A_\alpha = \frac{1}{2} R^\delta_{\cdot\alpha\beta\gamma} A_\delta. \quad (2)$$

The energy-momentum tensor satisfies the covariant conservation equation

$$\nabla_\beta T^{\alpha\beta} = 0. \quad (3)$$

There is an equivalent property of the gravitational skeleton, obtained by taking $\varphi_{\alpha\beta}$ in (1) to have the form

$$\varphi_{\alpha\beta} = \nabla_{(\alpha} \omega_{\beta)}. \quad (4)$$

The left hand side of (1) then vanishes as a consequence of (3), so the moments must satisfy

$$\int_L \left(m^{\alpha\beta} \varphi_{\alpha\beta} + m^{\gamma\alpha\beta} \nabla_\gamma \varphi_{\alpha\beta} + \frac{1}{2!} m^{\gamma\delta\alpha\beta} \nabla_\gamma \nabla_\delta \varphi_{\alpha\beta} + \dots \right) ds = 0 \quad (5)$$

for $\varphi_{\alpha\beta}$ of this form. Mathisson called this the *variational equation of dynamics*, the variation in question being the ability to vary ω_α at will. All the dynamics of the body is contained implicitly in this equation and his “new mechanics” consists of extracting its consequences as explicit restrictions on the form and evolution of the moments.

Mathisson continued by considering successively a body small enough that only the first one, two or three moments need be taken into account. For the case of a point mass, when only the monopole moment is retained, it follows from (5) that $m^{\alpha\beta}$ must have the form

$$m^{\alpha\beta} = M v^\alpha v^\beta \quad (6)$$

for some scalar function $M(s)$, where v^α is the unit tangent vector to L , and furthermore that

$$\frac{\delta}{ds}(M v^\alpha) \equiv v^\beta \nabla_\beta (M v^\alpha) = 0. \quad (7)$$

This in turn implies that M is independent of s and $\delta v^\alpha/ds = 0$, so L must be a geodesic.

When the dipole moment is also retained, he noted that (1) does not determine the moment tensors $m^{\alpha\beta}$ and $m^{\gamma\alpha\beta}$ uniquely. The transformation

$$m^{\alpha\beta} \rightarrow m^{\alpha\beta} + \frac{\delta n^{\alpha\beta}}{ds}, \quad (8)$$

$$m^{\gamma\alpha\beta} \rightarrow m^{\gamma\alpha\beta} + v^\gamma n^{\alpha\beta} \quad (9)$$

leaves the right hand side of (1) invariant for arbitrary symmetric $n^{\alpha\beta}$. The additional terms combine to give a total derivative that integrates to zero, since $\varphi_{\alpha\beta}$ has compact support. He used this freedom to impose the additional condition

$$v_\gamma m^{\gamma\alpha\beta} = 0 \quad (10)$$

and then deduced from (5) that $m^{\gamma\alpha\beta}$ must have the form

$$m^{\gamma\alpha\beta} = S^{\gamma(\alpha} v^{\beta)} + n^\gamma v^\alpha v^\beta \quad (11)$$

where $S^{\alpha\beta}$ is antisymmetric and both it and n^α are orthogonal to v^α on all indices. He later identifies $S^{\alpha\beta}$ as the angular momentum (spin) tensor of the body.

Next he chooses coordinates y^α such that $y^0 = s$, $y^i = 0$ on L for $i = 1, 2, 3$ and such that the hypersurfaces of constant y^0 meet L orthogonally. If (1) is written explicitly in these coordinates and $\varphi_{\alpha\beta}$ is expanded about $y^i = 0$ on each hypersurface of constant y^0 , the coefficients of $\partial\varphi_{00}/\partial y^i$ on both sides may be equated to give

$$n^i = \int y^i T^{00} \sqrt{-g} d^3 y \quad (12)$$

with the interpretation that n^α is the static dipole moment of the mass density $\mu \equiv T^{00}$. Its value will therefore depend on the choice of the world line L , enabling L to

be chosen as the world line of a centre of mass such that $n^i = 0$. Since $v_\alpha n^\alpha = 0$ it follows also that $n^0 = 0$ so that for all components

$$n^\alpha = 0, \quad (13)$$

with which (11) simplifies to

$$m^{\gamma\alpha\beta} = S^{\gamma(\alpha} v^{\beta)}. \quad (14)$$

With L determined by (13), Mathisson shows successively that (5) requires $S^{\alpha\beta}$ to satisfy

$$\frac{\delta S^{\alpha\beta}}{ds} + v^\alpha v_\gamma \frac{\delta S^{\beta\gamma}}{ds} - v^\beta v_\gamma \frac{\delta S^{\alpha\gamma}}{ds} = 0, \quad (15)$$

that $m^{\alpha\beta}$ must have the form

$$m^{\alpha\beta} = M v^\alpha v^\beta + v_\gamma v^{(\alpha} \frac{\delta S^{\beta)\gamma}}{ds} \quad (16)$$

for some scalar function M of s and that

$$\frac{\delta}{ds} \left(M v^\alpha + v_\beta \frac{\delta S^{\alpha\beta}}{ds} \right) = \frac{1}{2} v^\beta S^{\gamma\delta} R^\alpha_{\beta\gamma\delta}. \quad (17)$$

The equations of motion in this approximation are (15) and (17) which govern the evolution of variables M , v^α and $S^{\alpha\beta}$. Since v^α is a unit vector and $S^{\alpha\beta}$ is antisymmetric, these have respectively one, three and six linearly independent components. There appear at first to be ten equations for these ten variables but the left hand side of (15) vanishes identically when multiplied by v_β , reducing the number of equations from ten to seven.

For their solution to be determinate they must be supplemented by

$$v_\beta S^{\alpha\beta} = 0 \quad (18)$$

which forms part of the definition of $S^{\alpha\beta}$ through (11). This reduces the number of variables also to seven. When (18) holds, multiplying (15) by v_α shows that M is constant as in the monopole case, reducing the set to six equations for six variables.

A condition added to (15) and (17) to make them determinate has become known as a *supplementary condition*, although the term was not used by Mathisson. His condition results from his imposition of (13) in the derivation of the equations. Other authors have applied different conditions, as will be seen later.

Finally Mathisson considers the case where the quadrupole moment is also retained. He uses the non-uniqueness of the moments to impose, as an analogue of (10), the orthogonality condition

$$v_\gamma m^{\gamma\delta\alpha\beta} = 0 \quad (19)$$

and then decomposes the moment tensor into parts parallel to and orthogonal to v^α as

$$m^{\gamma\delta\alpha\beta} = b^{\gamma\delta\alpha\beta} + b^{\gamma\delta(\alpha} v^{\beta)} + b^{\gamma\delta} v^\alpha v^\beta. \quad (20)$$

The tensors b^{\dots} are orthogonal to v^α on all indices, are symmetric on their first two indices and $b^{\gamma\delta\alpha\beta}$ is also on its last two indices. He shows that (5) implies that

$$b^{(\gamma\delta\alpha)} = 0, \quad b^{(\gamma\delta\alpha)\beta} = 0 \quad (21)$$

but deduces incorrectly that the second of these implies, when taken together with the symmetry of $b^{\gamma\delta\alpha\delta}$ on γ, δ and α, β , that this tensor is identically zero. In fact these symmetry and orthogonality properties leave $b^{\gamma\delta\alpha\delta}$ with six linearly independent components, $b^{\gamma\delta\alpha}$ with eight and $b^{\gamma\delta}$ with six, a total of 20 for the quadrupole moment overall. The significance of this count will become clear in Sect. 11.

He continues by neglecting the $b^{\gamma\delta\alpha}$ contribution as he wants to retain only those quadrupole elements with classical counterparts. It follows that he would also have neglected the $b^{\gamma\delta\alpha\delta}$ contribution had he not incorrectly believed it to be zero. In the coordinate system and notation of (12) the remaining contribution $b^{\alpha\beta}$ is zero if either index is 0 and the purely spacelike components are given by

$$b^{ij} = \int y^i y^j T^{00} \sqrt{-g} d^3 y. \quad (22)$$

Due to the quadrupole presence, expression (11) for the dipole tensor $m^{\gamma\alpha\beta}$ gains additional terms that involve $b^{\alpha\beta}$, as does Eq. (15) governing the spin tensor $S^{\alpha\beta}$ which then becomes

$$\frac{\delta S^{\alpha\beta}}{ds} + v^\alpha v_\gamma \frac{\delta S^{\beta\gamma}}{ds} - v^\beta v_\gamma \frac{\delta S^{\alpha\gamma}}{ds} = \left(R^\alpha_{\cdot\gamma\delta\varepsilon} b^{\varepsilon\beta} - R^\beta_{\cdot\gamma\delta\varepsilon} b^{\varepsilon\alpha} \right) v^\gamma v^\delta. \quad (23)$$

Note that the result in Mathisson's paper has an additional factor 2 on the right-hand side. Both forms are correct, the difference being due to the presence in the quadrupole term of (1) of the $1/2!$ factor not present in Mathisson's paper, as discussed above in connection with (1).

The right hand side of (23) represents the torque exerted on the body by the gravitational field due to its quadrupole moment. He does not derive the modified form of Eq. (17) which would also be expected to gain additional terms.

4 Issues Arising from the Paper of 1937

There are several major issues left unresolved in this paper of 1937. It is useful to identify and study these as they provide a context in which to evaluate later work on the subject.

The first issue concerns the existence and uniqueness of the moment tensors. In that paper their existence was dealt with only briefly. Indeed, he arrived at (5) by a different route than that presented here, without ever writing (1) explicitly. The method presented here appears only in a footnote to his Eq.(2.31), where he says that it would be the shortest way to the result (5). He recognised their non-uniqueness but used it only to impose the orthogonality conditions (10) and (19) in the cases he studied.

This issue was the subject of his paper [8] of 1939 jointly with Bielecki and Weyssenhoff. There the definition (1) was given explicitly. The aim of the paper was to show that the moment tensors exist and that they become uniquely defined if in addition they are required to be orthogonal to v^α on all indices except the last two. This requirement includes (10) and (19) and is their natural generalisation to higher order moments.

The existence proof merits consideration because it too leaves an important issue unresolved, one that is crucial in the subsequent completion of his program. It begins by introducing a special coordinate system in which $y^0 = s$, $y^i = 0$ on L for $i = 1, 2, 3$ such that the hypersurfaces $\Sigma(s)$ given by $y^0 = s$ intersect L orthogonally. These are the same conditions used in the derivation of (12). It then defines quantities $M^{\alpha\beta}$, $M^{\gamma\alpha\beta}$, $M^{\gamma\delta\alpha\beta}$, ..., which are not tensors, whose components are zero if any index except the last two is 0 and whose other components are given by

$$M^{i\dots j\alpha\beta}(s) = \int_{\Sigma(s)} y^i \dots y^j T^{\alpha\beta} \sqrt{-g} d^3 y \quad (24)$$

where there are any number of indices $i \dots j$ and corresponding factors $y^i \dots y^j$, including none.

Expansion of $\varphi_{\alpha\beta}$ on $\Sigma(s)$ in a Taylor series about $y^i = 0$ then gives

$$\int T^{\alpha\beta} \varphi_{\alpha\beta} Dx = \int_L \left(M^{\alpha\beta} \varphi_{\alpha\beta} + M^{\gamma\alpha\beta} \partial_\gamma \varphi_{\alpha\beta} + \frac{1}{2!} M^{\gamma\delta\alpha\beta} \partial_\gamma \partial_\delta \varphi_{\alpha\beta} + \dots \right) ds. \quad (25)$$

An n -fold partial derivative can be expressed in terms of covariant derivatives of all orders from n downward, together with terms involving components of the affine connection $\Gamma_{\beta\gamma}^\alpha$. By a regrouping of terms, (25) can therefore be written in the form (1) where the m 's of any order are expressed in terms of the M 's of that and all higher orders and of the components of the affine connection and their partial derivatives. Transformations such as (8) with (9) can then be used to impose orthogonality to v^α on all indices of the m 's except the last two. Repeated use of the Ricci identity enables all except the totally symmetric part of repeated covariant derivatives to be eliminated, so that without loss of generality the m 's can be taken as symmetric on all indices except the last two. By construction they are already symmetric separately on the last two. These steps all involve further regrouping of terms but they leave the overall form of the result (1) unchanged.

This completes the existence proof. The paper gives explicit expressions for the m 's up to the quadrupole moment in terms of the M 's up to this same order, $\Gamma_{\beta\gamma}^\alpha$ and its partial derivatives. The uniqueness proof is straightforward and will not be described here.

The issues arising from the existence proof concern the various infinite series involved. The paper makes explicit at the outset that it assumes the convergence of the series that arise and the analyticity of functions so far as is required. The field $\varphi_{\alpha\beta}$ in (1) may be chosen freely, so there is no problem with the non-covariant Eq. (25) as it can be chosen to be analytic on the hypersurfaces $\Sigma(s)$. There is, however, a problem with its manipulation into the form (1).

To see this, note that the m 's at $z(s) \in L$ are determined by the M 's with this value of s and so in turn by the value of $T^{\alpha\beta}$ in the neighbourhood of $\Sigma(s)$ together with affine connection terms. *In the neighbourhood of* rather than *on* as derivatives with respect to s will arise from the transformations such as (8) with (9). But $\Sigma(s)$ is not uniquely defined. It is *any* spacelike hypersurface through $z(s)$ that meets L orthogonally. If the series for the m 's in terms of the M 's converged, the uniqueness of the m 's would imply that these series would sum to the same value for all such choices of $\Sigma(s)$.

If $T^{\alpha\beta}$ were also required to be analytic then this would be possible, as its value in the neighbourhood of one such hypersurface would determine its value throughout the domain in which it was analytic, and so in particular also on all other choices of $\Sigma(s)$. But $T^{\alpha\beta}$ is a physical field. It may not even be smooth, it is certainly not analytic. Its value in the neighbourhood of one such hypersurface does *not* determine its value on any other, except where they meet. So in general the series for the m 's in terms of the M 's cannot converge and the existence proof falls.

This may seem like unnecessary pedantry, criticism that would be appropriate for a piece of pure mathematics but out of place and of no significance in mathematics applied to the physical world. It is, however, of crucial importance. Mathisson's program is based on (1) being an implicit definition of the multipole moments. This definition leads to (5), a single equation that embodies all the consequences for the moments of the conservation equation (3) for the energy-momentum tensor. It needs to be possible both to extract explicit evolution equations for the moments from (5) *and* explicit expressions for the moments in terms of $T^{\alpha\beta}$ from (1), for without the latter the meaning of the moments governed by the former is unknown. The implicit analyticity of the energy-momentum tensor must be circumvented before Mathisson's program can be completed.

The second issue arising from the 1937 paper is the one that arose in his treatment of the quadrupole. In the monopole and dipole cases no further approximations were needed beyond the neglect of higher order moments. In the quadrupole case this was not so. Only certain components of the quadrupole moment were retained, those with a classical analogue. This was not because the other components lacked interest, or at least not only for this reason. Had all components been retained, it would have added an unmanageable level of complexity. Progression from the monopole to the dipole case added a second evolution equation, with both equations then involving time derivatives of the dipole moment, i.e., of the spin. In the same

way, progression from the dipole to the full quadrupole case would have added a third evolution equation and all three would have involved time derivatives of quadrupole components. Each successive approximation would add a further equation in this way, and a complete solution of the variational equation would have an infinite set of equations, each involving time derivatives of an infinite set of moments.

In Newtonian mechanics there would only be two evolution equations, those for momentum and angular momentum. Mathisson's new mechanics should aim at maintaining this simplicity. This would require eliminations between the full set of equations to leave only two, those governing momentum and angular momentum. The issue is whether or not this can be achieved, and if so how it can be done.

The final issue concerns the supplementary condition (18). Equation (17) is of second order in $S^{\alpha\beta}$. By use of (18) it can be put in a form that is of first order in $S^{\alpha\beta}$ but then it becomes second order in v^α . The set of equations (15), (17) and (18) then has solutions corresponding to arbitrary initial values of position, velocity, spin and acceleration. This is greater freedom than classical mechanics allows.

If the equations of motion are considered to represent a point particle then it is a matter of fact whether (18) is or is not satisfied. In a second paper [12] in 1937, Mathisson showed that this additional freedom in the solutions provides a classical analogue of the *zitterbewegung* of the quantum theory of the electron. But if the equations of motion are to represent an extended body then the supplementary condition selects the world line used to represent its position. It is no longer a matter of fact, but of choice, whether (18) holds. The freedom to specify an initial acceleration is now a defect. It does not correspond to a physical freedom but merely to the failure of (18) to determine a unique world line. It points to the need for a different supplementary condition that does not admit such solutions.

5 The Unphysical Solutions

The unphysical solutions allowed by the supplementary condition (18) are present also in special relativity. In this context they were studied by a number of authors in the period 1939–1950. It was noted above that they must be avoided when modelling an extended body. To achieve this, their origin needs to be properly understood. The following account is based on the work of Pryce [13] and Møller [14] and uses a Minkowskian coordinate system in the flat spacetime of special relativity.

Consider an extended body with symmetric energy-momentum tensor $T^{\alpha\beta}$ that satisfies the conservation equation (3). Given a spacelike hypersurface Σ that spans the body and a point z not necessarily on Σ , let

$$p^\alpha \equiv \int_{\Sigma} T^{\alpha\beta} d\Sigma_\beta \quad (26)$$

and

$$S^{\alpha\beta} \equiv 2 \int_{\Sigma} (x^{[\alpha} - z^{[\alpha}(s)) T^{\beta]\gamma} d\Sigma_{\gamma}. \quad (27)$$

The difference between their values for two different choices of Σ can be converted by Gauss's theorem to volume integrals. The integrands then vanish by the conservation equation for $T^{\alpha\beta}$ and because it is symmetric. These quantities are therefore independent of the choice of Σ . As the definition of p^{α} does not involve z , it follows that p^{α} is constant while $S^{\alpha\beta}$ becomes a function only of the point z . These properties have led to them becoming the generally accepted definitions of momentum and angular momentum (spin) for an isolated body in special relativity. Generalisations to more complex situations such as general relativity or the presence of external forces need to reduce to these in this special case.

Let z move along an arbitrary timelike world line L parameterised as $z(s)$ by proper time s and let $v^{\alpha} = dz^{\alpha}/ds$, which satisfies $v^{\alpha}v_{\alpha} = 1$. Differentiate (27) with respect to s , holding Σ fixed as the values of the integrals do not depend on it. This gives

$$\frac{dS^{\alpha\beta}}{ds} = 2p^{[\alpha}v^{\beta]} \quad (28)$$

from which

$$p^{\alpha} = Mv^{\alpha} + v_{\beta} \frac{dS^{\alpha\beta}}{ds} \quad (29)$$

where $M \equiv p^{\alpha}v_{\alpha}$. Since p^{α} is constant, (29) gives

$$\frac{d}{ds} \left(Mv^{\alpha} + v_{\beta} \frac{dS^{\alpha\beta}}{ds} \right) = 0 \quad (30)$$

while (28) and (29) together give

$$\frac{dS^{\alpha\beta}}{ds} + v^{\alpha}v_{\gamma} \frac{dS^{\beta\gamma}}{ds} - v^{\beta}v_{\gamma} \frac{dS^{\alpha\gamma}}{ds} = 0. \quad (31)$$

These are precisely the forms taken in flat spacetime by Mathisson's equations (15) and (17) in his dipole approximation, but now they are exact and the supplementary condition (18) has not yet been imposed. The variables also agree, to the accuracy of his approximation. To see this, note first that $m^{\alpha\beta\gamma} = M^{\alpha\beta\gamma}$ in the notation of (24) when quadrupole and higher contributions are neglected, and that the definition (27) of $S^{\alpha\beta}$ corresponds to $S^{\alpha\beta} = 2M^{[\alpha\beta]\gamma}v_{\gamma}$ to this accuracy. But (14) gives $2m^{[\alpha\beta]\gamma}v_{\gamma} = S^{\alpha\beta}$, so it follows that the two tensors $S^{\alpha\beta}$ are in agreement. The vector v^{α} is the unit tangent to L in both cases and in order for the right hand side of (29) to be constant with both definitions of M , these must also agree.

This agreement enables the origin of the unphysical solutions arising from the supplementary condition (18) to be studied in a context where the equations of

motion are exact. First suppose that z is any point on some L that satisfies (18). Choose Σ in (27) to be the hyperplane $v_\alpha(x^\alpha - z^\alpha) = 0$ through z . For this choice, $d\Sigma_\alpha$ is parallel to v_α so that $d\Sigma_\alpha = v_\alpha v^\gamma d\Sigma_\gamma$. Hence (18) with (27) gives

$$z^\alpha(s) = \int x^\alpha T^{\beta\gamma} v_\beta v_\gamma v^\delta d\Sigma_\delta \bigg/ \int T^{\beta\gamma} v_\beta v_\gamma v^\delta d\Sigma_\delta, \quad (32)$$

showing that z^α is a centre of mass for the mass (or energy) density $T^{\alpha\beta} v_\alpha v_\beta$ in the instantaneous rest frame. It follows that for a body with positive energy density throughout, i.e., $T^{\alpha\beta} v_\alpha v_\beta > 0$ for all choices of timelike v^α , L lies within the body (suitably interpreted if spacelike cross-sections of the body are not convex).

This is a restriction on the solutions for L but it does not make L unique. To study the non-uniqueness in more detail, let

$$K^{\alpha\beta} \equiv 2 \int x^{[\alpha} T^{\beta]\gamma} d\Sigma_\gamma \quad (33)$$

so that (27) gives

$$S^{\alpha\beta}(s) = K^{\alpha\beta} - 2z^{[\alpha}(s)p^{\beta]}. \quad (34)$$

This shows that there is a unique world line parameterised by a scalar λ , given by

$$z^\alpha = \lambda p^\alpha + \frac{p_\beta K^{\alpha\beta}}{p^\gamma p_\gamma}, \quad (35)$$

on which

$$p_\beta S^{\alpha\beta} = 0. \quad (36)$$

If the Minkowskian coordinate system is chosen so that this line is the time axis then it is also given by $z^\alpha = \lambda p^\alpha$, so (34) gives $S^{\alpha\beta}(s) = K^{\alpha\beta}$ and (36) becomes

$$p_\beta K^{\alpha\beta} = 0. \quad (37)$$

Let Latin indices take values 1, 2, 3 and let m be the magnitude of p^α , so $m^2 = p^\alpha p_\alpha$. Then with these coordinates $p^i = 0$, $p^0 = m$ and hence from (37) also $K^{i0} = 0$. From (34) the supplementary condition (18) can be put in the form

$$v_\beta \left(K^{\alpha\beta} - 2z^{[\alpha}(s)p^{\beta]} \right) = 0. \quad (38)$$

This has only three linearly independent components, which can be taken as those with $\alpha = 1, 2, 3$, since multiplication by v_α gives an identity. It is therefore equivalent to

$$v_j K^{ij} - m z^i v_0 = 0 \quad (39)$$

in the chosen Minkowskian coordinates. Since K^{ij} is antisymmetric it can be represented by a three-dimensional vector K_i such that $K^{ij} = \epsilon^{ikj} K_k$ where ϵ^{ijk} is the three-dimensional Levi-Civita symbol. If $t \equiv x^0$ is coordinate time then $v^i/v^0 = dz^i/dt$. These results enable (39) to be expressed in three-dimensional vector notation as

$$m\mathbf{z} - \frac{d\mathbf{z}}{dt} \times \mathbf{K} = 0. \quad (40)$$

Since \mathbf{K} is constant, the time derivative of (40) shows that $d\mathbf{z}/dt$ and \mathbf{K} are orthogonal. The vector product of (40) with \mathbf{K} therefore gives

$$\frac{d\mathbf{z}}{dt} = \frac{m}{K^2} \mathbf{K} \times \mathbf{z}. \quad (41)$$

This corresponds to motion about the origin in a circle with angular velocity m/K , where $K = |\mathbf{K}|$, in a plane perpendicular to \mathbf{K} . From (40) the radius of the circle is vK/m where $v = |d\mathbf{z}/dt|$. Units here have the velocity of light $c = 1$ so since L is timelike, $v < 1$. The possible circular motions therefore all lie in a disc of radius K/m in this plane and centred on the origin, but all such motions give an L that satisfies the supplementary condition, so confirming the non-uniqueness claimed above. For a body with positive energy density throughout, it was seen above that all choices of L that satisfy the supplementary condition lie within the body, suitably interpreted. It follows that this disc lies within the body, which gives a minimum size for such a body when its spin is nonzero.

A different perspective arises if the Eqs. (30) and (31) are taken in isolation, so that the quantities M and $S^{\alpha\beta}$ are considered to be properties of the body rather than constructs from the energy-momentum tensor. This is the situation when the equations of motion are used to model a point particle whose motion satisfies (18) as a matter of physical fact. The same results hold but they need to be cast in terms of M and $S^{\alpha\beta}$ rather than m and K . With the same choice of Minkowskian coordinate system used above, (34) gives $S^{ij} = K^{ij}$ but whereas $K^{i0} = 0$, S^{i0} is not zero. From (18),

$$S^{i0} = -S^{ij} v_j/v_0 = -K^{ij} v_j/v_0 = -\epsilon^{ikj} \frac{dz_j}{dt} K_k. \quad (42)$$

But $d\mathbf{z}/dt$ and \mathbf{K} are orthogonal three-dimensional vectors and $S_{i0} = -S^{i0}$ due to the form of the metric tensor, so

$$S^{i0} S_{i0} = -(vK)^2. \quad (43)$$

With the magnitude S of the spin tensor $S^{\alpha\beta}$ defined by $S^2 = S^{\alpha\beta} S_{\alpha\beta}/2$, (43) gives

$$S^2 = K^2(1 - v^2). \quad (44)$$

Also

$$M \equiv p^\alpha v_\alpha = mv_0 = m/\sqrt{1-v^2} \quad (45)$$

so

$$\frac{vK}{m} = \frac{vS}{M(1-v^2)} \quad (46)$$

which gives the radius of the circular orbit in terms of S and M as required. But whereas $v < 1$, which gave a limiting size to the radius, $v/(1-v^2)$ is unbounded as $v \rightarrow 1$. With this perspective there is no limit on the size of the circular orbits. As described above, the initial acceleration of the particle can be arbitrary and it is this choice that determines which orbit is followed.

This form of solution to the Eqs. (30) and (31) in flat spacetime was first given by Weyssenhoff and Raabe [15]. Mathisson [12] had earlier given a solution in the non-relativistic approximation that he had used to provide a classical analogue of the *zitterbewegung* of the electron. But as discussed in the preceding section, when the equations are used to model an extended body then these unphysical solutions must be avoided. The above analysis provides the clue to their avoidance, for it was seen that (36) *does* determine a unique world line. So in special relativity, if (36) is adopted as the supplementary condition in place of (18) then unphysical solutions are avoided. The issue in a curved spacetime is to find appropriate meanings for p^α and $S^{\alpha\beta}$. This will be addressed in Sect. 21.

6 The Period 1950–1970

At his death in 1940, Mathisson [9] had been studying his variational equation in special relativity for a body under the influence of external forces, maybe looking for clues as to how to progress further with it in general relativity. This work led to a paper by Shanmugadhasan [16] in 1946 that continued this development in special relativity. The multipole approach to equations of motion in general relativity went dormant, however, until the appearance of a paper by Papapetrou [17] in 1951 entitled “Spinning test-particles in general relativity. I”, a title that does not show anything like the same vision as did Mathisson’s.

Papapetrou defined a set of non-covariant moment integrals identical to those of Bielecki et al. [8] given as (24) above. He continued by developing equations of motion in terms of these quantities and other similarly defined ones, also non-covariant, constructing combinations of them along the way that he subsequently proved did transform as tensors. This was done first for a particle in which only the monopole moment is retained, and then when the dipole moment is also retained, which he calls a pole-dipole particle. In this way he finally arrives at the Eqs. (15) and (17) first obtained by Mathisson. Mathisson’s paper [1] of 1937 is given as a reference, but with the statement that it gives a discussion of the pole-dipole particle in special relativity. Since Papapetrou’s paper of 1951 in *Proceedings of the Royal*

Society is far more accessible than Mathisson's in a pre-war issue of *Acta Physica Polonica*, no-one seemed to check on this and for many years the equations of motion came to be associated with Papapetrou rather than Mathisson.

Papapetrou's work made one advance over Mathisson's results, in that (15) and (17) are derived without imposing a supplementary condition. This enables the merits of any such condition to be considered as a separate issue. Papapetrou was aware of the circular motions in special relativity that are possible with the supplementary condition $v_\beta S^{\alpha\beta} = 0$, describing them as internal motions for a pole-dipole particle. He asserted that these give a most successful classical analogue of the *zitterbewegung* of the electron, giving a paper of 1940 by Hönl and Papapetrou [18] but not Mathisson's second paper [12] of 1937 on this topic as a reference. He noted that for a macroscopic particle, however, these internal motions must be avoided. In a joint paper [19] with Corinaldesi submitted together with [17] they studied motion in a Schwarzschild field using a supplementary condition $k_\beta S^{\alpha\beta} = 0$ where k^α is the timelike Killing vector of the static spacetime. This has the merit of avoiding the internal motions but it is not applicable to non-static spacetimes.

In 1959, Tulczyjew [20] gave another derivation of (15) and (17). He noted that these equations were first derived by Mathisson and, later, "by a far less perfect method" by Papapetrou. His method simplified Mathisson's approach by the use of a singular energy-momentum tensor constructed from Dirac delta-functions. The main advance made by this paper, however, concerned the supplementary condition. Tulczyjew noted from the work of Weyssenhoff and Raabe [15] that in connection with the Eqs. (28)–(31) in special relativity, $v_\beta S^{\alpha\beta} = 0$ does not determine a unique world line in special relativity but that $p_\beta S^{\alpha\beta} = 0$ does so. He therefore adopted $p_\beta S^{\alpha\beta} = 0$ also in general relativity, setting

$$p^\alpha \equiv Mv^\alpha + v_\beta \frac{\delta S^{\alpha\beta}}{ds} \quad (47)$$

in his words "owing to the lack of another definition". This was the first use of a supplementary condition in general relativity that determined a unique world line without needing some variables external to the body concerned. This condition is not applicable to an extended body, however, as the variables it involves are defined only in the context of a singular energy-momentum tensor.

A paper by Tulczyjew and Tulczyjew [21] in 1962 gave yet another derivation of (15) and (17), this time by an improved version of Papapetrou's approach. The non-covariant moment integrals of Papapetrou were replaced by integrals made covariant by being defined in a special coordinate system based on the world line L chosen to represent the body. Consequently they do have well defined meaning for an extended body. It is noted that the equations need a supplementary condition of the form $p_\beta S^{\alpha\beta} = 0$ for a suitably defined momentum vector p^α but this vector is not one of the well defined moment integrals. It is defined only in the context of the pole-dipole approximation, so the condition is still not applicable to an extended body.

The present author had a go at this [22] in 1964. This was again a version of Papapetrou's approach, now with moment integrals made covariant by the use of

two-point tensors. The same equations were derived in the pole-dipole approximation and once again the main advance concerned the supplementary condition. This time the equations were derived in the form

$$\frac{\delta p^\alpha}{ds} = \frac{1}{2} v^\beta S^{\gamma\delta} R^\alpha{}_{\beta\gamma\delta} \quad (48)$$

and

$$\frac{\delta S^{\alpha\beta}}{ds} = 2p^{[\alpha} v^{\beta]} \quad (49)$$

where p^α and $S^{\alpha\beta}$ were among the quantities defined as covariant integrals of the energy-momentum tensor.

These equations have a well defined momentum vector but are nevertheless equivalent to (15) and (17) with $M \equiv p^\alpha v_\alpha$. To see this, multiply (49) by v_β and use $v^\beta v_\beta = 1$ to obtain an expression for p^α . Use of this to eliminate p^α from (48) and (49) gives (15) and (17) as required.

At last the condition

$$p_\beta S^{\alpha\beta} = 0 \quad (50)$$

becomes well defined for an extended body. It cannot yet be regarded as satisfactory, however, as the integral expressions are somewhat *ad hoc*. They could be modified in ways significant only in a quadrupole or higher approximation without changing the pole-dipole approximation but still affecting the world line that would be determined for an extended body.

Attempts to extend (15) and (17) to include the quadrupole moment were made by Taub [23] in 1965 and Madore [24] in 1969. Neither seemed aware that Mathisson had already considered the quadrupole case in 1937. As with Mathisson, both attempts needed further approximations beyond those implied by truncation of the multipole series. They needed this for the same reason as did Mathisson. As discussed in Sect. 4, retaining all quadrupole components leads to a third evolution equation and the need for a potentially unmanageable task of elimination between all three. Both Taub and Madore obtained quadrupole corrections to both the momentum and spin equations while Mathisson had only obtained that for spin. Both attempts were flawed, however, by algebraic errors that invalidated the results as published. Corrected versions of their results were given by the present author in [25] where they were seen to agree both with one another and with the results of that paper. The corrected versions also agree with Mathisson for the one equation that he obtained.

In the opinion of the present author, these advances over twenty years were only tiny steps. They had shed light on the problem of defining a unique centre of mass and made simplifications to the handling of the pole-dipole approximation but attempts to retain moments beyond the dipole had met a barrier that resisted all attacks. There seemed to be a locked door beyond which one could not pass.

I believe that Mathisson had realised that he had reached a door preventing his further progress. At his death, Mathisson had been studying his variational equation

in special relativity. This appeared to be a step backwards. Perhaps it was this that had led Papapetrou to believe that Mathisson's earlier work was also only in special relativity. It seems more likely to me that Mathisson had realised this would be a simpler arena in which to find the key to that door, but his untimely death prevented him from finding it.

In 1967 [26] I took up the search for the key in this special relativity arena and found it, or rather the two keys that are needed to progress beyond this door. Armed with these keys, the path to higher order multipole approximations in general relativity became accessible but there were still obstacles to be overcome. This further development occupied me until 1974 and was published in [25, 27, 28]. Those papers deal with the presence of both gravitational and electromagnetic fields. The following sections deal only with the purely gravitational case, for which they reveal the keys and the route past the obstacles and take Mathisson's program to completion.

7 Fourier Transforms Avoid Need for Analyticity

It was seen in Sect. 4 that Mathisson's moment-defining equation (1) does not lead to unique expressions for the moments as integrals of $T^{\alpha\beta}$ and that the reason for this is its assumption that $\varphi_{\alpha\beta}$ is analytic. The first key provides the means to avoid this assumption. It is the use of *Fourier transformation*.

Mathisson's defining equation (1) for the moments can be rewritten in full as

$$\int T^{\alpha\beta} \varphi_{\alpha\beta} Dx = \int_L \sum_{n \geq 0} \frac{1}{n!} m^{\delta \dots \gamma \alpha \beta}(s) \nabla_{\delta \dots \gamma} \varphi_{\alpha\beta}(z(s)) ds. \quad (51)$$

Here L is again parameterised as $z^\alpha(s)$, but now for generality s is not necessarily proper time. Here and throughout, n is the number of indices in the set marked with dots, in this case $\delta \dots \gamma$, including the possibilities $n = 0$ and $n = 1$.

Consider first the situation in flat spacetime, with a metric tensor whose components are constant but not necessarily diagonal. Define the Fourier transform $\tilde{\varphi}_{\alpha\beta}$ of $\varphi_{\alpha\beta}$ by

$$\tilde{\varphi}_{\alpha\beta}(k) = \int \varphi_{\alpha\beta}(x) \exp(ik \cdot x) Dx \quad (52)$$

where $k \cdot x \equiv k_\alpha x^\alpha$. This is well defined since x^α and k^α can be considered as position vectors when the metric tensor has constant components. If $\varphi_{\alpha\beta}$ in (51) is written in terms of $\tilde{\varphi}_{\alpha\beta}$ by the Fourier inversion formula, it gives

$$\begin{aligned} \int T^{\alpha\beta} \varphi_{\alpha\beta} Dx &= \frac{1}{(2\pi)^4} \int_L ds \sum_{n \geq 0} \int Dk \frac{(-i)^n}{n!} k_\delta \dots k_\gamma \\ &\quad \times m^{\delta \dots \gamma \alpha \beta}(s) \tilde{\varphi}_{\alpha\beta}(k) \exp(-i k \cdot z(s)). \end{aligned} \quad (53)$$

This is completely equivalent to (51) and holds no advantage over it. The key step is to exchange the order of the summation and the k -space integration, to give

$$\int T^{\alpha\beta} \varphi_{\alpha\beta} Dx = M^{\alpha\beta} [\Phi_{\alpha\beta}] \quad (54)$$

where

$$M^{\alpha\beta} [\Phi_{\alpha\beta}] = \frac{1}{(2\pi)^4} \int_L ds \int Dk \tilde{m}^{\alpha\beta}(s, k) \tilde{\Phi}_{\alpha\beta}(z(s), k) \quad (55)$$

with

$$\tilde{m}^{\alpha\beta}(s, k) = \sum_{n=0} \frac{(-i)^n}{n!} k_\delta \cdots k_\gamma m^{\delta \cdots \gamma \alpha\beta}(s) \quad (56)$$

and

$$\tilde{\Phi}_{\alpha\beta}(z, k) = \tilde{\varphi}_{\alpha\beta}(k) \exp(-i k \cdot z). \quad (57)$$

In general this exchange is not valid, but the Eq. (54) that results requires no assumption about the analyticity of $\varphi_{\alpha\beta}$. This is an improvement over (51) and so (54) will be taken, in flat spacetime, as the definition for the moments in its place.

What is now needed is a similar change of definition in a curved spacetime. The left hand side of (54) is well defined as an integral over the spacetime manifold M . The ultimate aim is to define the m 's at $z(s)$ to be tensors at this point. For (56) to be a covariant equation, this requires k_α to be a vector at $z(s)$. For fixed s this would make $\tilde{m}^{\alpha\beta}(s, k)$ be a tensor at $z(s)$ that is a function of a vector k_α at this point.

The right hand side of (54), as given by (55), then becomes well defined if $\tilde{\Phi}_{\alpha\beta}(z(s), k)$ is also such a field. The set of all vectors at a point z forms the *tangent space* $T_z(M)$ to M at z so these are functions that map the tangent space to tensors at z . The tangent space is a vector space that can be considered as a flat manifold with a natural metric tensor given by the metric tensor of M at z . From this viewpoint $\tilde{m}^{\alpha\beta}$ and $\tilde{\Phi}_{\alpha\beta}$ are tensor fields on $T_z(M)$. In (55), Dk is the volume element on this flat manifold. Fourier transforms on the tangent space are defined by (52), with $X \in T_z(M)$ replacing $x \in M$, just as for any flat manifold. So $\tilde{\Phi}_{\alpha\beta}(z(s), k)$ can be taken as the Fourier transform of a tensor field $\Phi_{\alpha\beta}(z(s), X)$ on the same tangent space. In the flat spacetime considered above, the $\tilde{\Phi}_{\alpha\beta}(z, k)$ defined by (57) is given in this way when

$$\Phi_{\alpha\beta}(z, X) = \varphi_{\alpha\beta}(x) \quad \text{with} \quad X \equiv x - z. \quad (58)$$

All that remains to make (54) be well defined in a curved spacetime is therefore to generalise (58) appropriately.

This next paragraph uses terminology from differential geometry to define the mapping needed to specify this generalisation. It puts the mapping in its proper context, but it is not necessary for understanding the remainder of this paper. Where details of the mapping are needed, the necessary properties will be developed before

use. Most of that development is in Sect. 14, but here for the record is the specification from differential geometry. When M is flat there is a natural identification of $T_z(M)$ with M , which is why (58) is meaningful in special relativity. In a curved spacetime the two are related by the exponential map $\text{Exp}_z : T_z(M) \rightarrow M$, for which see Bishop and Crittenden [29] or many other standard texts on differential geometry. If $X \in T_z(M)$ and $x = \text{Exp}_z X$ then the derivative map $((\text{Exp}_z)_*)_X$ of Exp_z at X maps $T_X(T_z(M))$ isomorphically onto $T_x(M)$. This mapping between tangent spaces has a unique extension to a mapping of the corresponding tensor algebras. This will be denoted by replacing the $*$ by A (for Algebra) in the notation. By letting X vary, this gives a map $(\text{Exp}_z)_A$ from tensor fields on $T_z(M)$ to tensor fields on M . Given such a tensor field for each z , application of the corresponding maps produces a family of tensor fields on M parameterised by z , i.e., a two-point function with scalar character at z and tensor character at the second point x . Let Exp_A denote this overall map and Exp^A denote its inverse.

What is needed at present is that there is a well defined linear mapping Exp_A that maps functions such as $\Phi_{\alpha\beta}(z, X)$, which is a tensor at $z \in M$ dependent on a vector X at z , into two-point functions such as $\varphi_{\alpha\beta}(z, x)$ which have tensor character at x and scalar character at z . Alternatively $\Phi_{\alpha\beta}(z, X)$ may be considered as mapping the tangent space $T_z(M)$ to tensors at z . The vector X and point x are related as follows. If $y(u)$ is a geodesic on M with affine parameter u such that $y = z$ and $dy^\alpha/du = X^\alpha$ when $u = 0$, then $x = y(1)$. The map from $T_z(M)$ to M that sends X to x is known as the *exponential map* Exp_z , so $x = \text{Exp}_z X$.

The inverse Exp^A of Exp_A acts in the opposite direction, so it acts on two-point functions such as $\varphi_{\alpha\beta}(z, x)$. It may therefore be applied to an ordinary tensor field on M by treating it as a two-point function that is independent of z . The interpretation of (54) in curved spacetime is completed by taking

$$\Phi_{\alpha\beta} = \text{Exp}^A \varphi_{\alpha\beta} \quad (59)$$

which has (58) as a special case.

8 The Route to Moments as Explicit Integrals

As with Mathisson's original definitions, (54) only determines a unique set of moments if additional symmetry and orthogonality conditions are imposed. These will be taken as

$$m^{\gamma \cdots \delta \alpha \beta}(s) = m^{(\gamma \cdots \delta)(\alpha \beta)}(s) \quad \text{for } n \geq 0, \quad (60)$$

$$n_\gamma(s) m^{\gamma \cdots \delta \alpha \beta}(s) = 0 \quad \text{for } n \geq 1 \quad (61)$$

where $n^\alpha(s)$ is a timelike unit vector at $z(s)$. Recall that n is the number of indices in the set marked with dots, so these apply to moments with at least two or three indices respectively. These conditions differ from those of Bielecki et al. [8] in that n^α need not be tangent to the world line L . This slight generalisation is for later convenience.

It will now be shown that with these conditions, (54) *does* determine explicit integral expressions for the moments, and in particular that the hypersurfaces of integration are uniquely determined. Choose a Minkowskian coordinate system on $T_{z(s)}(M)$ such that $n_\alpha \neq 0$ only for $\alpha = 4$. Then (56) and (61) show that $\tilde{m}^{\alpha\beta}(s, k)$ is independent of k_4 . The inversion formula for the Fourier transform $\tilde{f}(k)$ of a function $f(x)$ of a single variable shows that

$$\int \tilde{f}(k) dk = 2\pi f(0). \quad (62)$$

With this, the k_4 integration in the s -integrand on the right of equation (55) can be performed to show that its value for fixed s depends on $\Phi_{\alpha\beta}(z(s), X)$ only through its value on the hyperplane $X^4 = 0$, and hence on $\varphi_{\alpha\beta}$ only through its value on $\Sigma(s)$, the image of this hyperplane under Exp_z . This image is the hypersurface formed by all geodesics through $z(s)$ orthogonal to n_α .

Let $\tau(x)$ be the scalar function such that $\tau(x) = s$ if $x \in \Sigma(s)$ and let w^α be any vector field such that $w^\alpha \nabla_\alpha \tau = 1$. Then

$$\int T^{\alpha\beta} \varphi_{\alpha\beta} Dx = \int ds \int_{\Sigma(s)} T^{\alpha\beta} \varphi_{\alpha\beta} w^\gamma d\Sigma_\gamma \quad (63)$$

where $d\Sigma_\alpha$ is the vector-valued surface element on $\Sigma(s)$. The s -integrand here also depends on $\varphi_{\alpha\beta}$ only through its value on $\Sigma(s)$. Since $\varphi_{\alpha\beta}$ is no longer required to be analytic, (54) still holds if $\varphi_{\alpha\beta}$ is multiplied by an arbitrary smooth function that is constant on each $\Sigma(s)$. The above dependency results show that this multiplier can be brought outside the k -space integral in (55) and similarly outside the hypersurface integral in (63). Since this multiplier is arbitrary it follows that the s -integrands must be equal, so that

$$\int_{\Sigma(s)} T^{\alpha\beta} \varphi_{\alpha\beta} w^\gamma d\Sigma_\gamma = \frac{1}{(2\pi)^4} \int Dk \tilde{m}^{\alpha\beta}(s, k) \tilde{\Phi}_{\alpha\beta}(z(s), k). \quad (64)$$

It is now possible to express $\varphi_{\alpha\beta}$ in terms of $\tilde{\Phi}_{\alpha\beta}$ and so to identify $\tilde{m}^{\alpha\beta}(s, k)$ as an integral over $\Sigma(s)$. By expanding the resulting integrand as a series in k_α , explicit expressions can be obtained for the moments $m^{\delta \dots \gamma \alpha \beta}$ as integrals of $T^{\alpha\beta}$ over $\Sigma(s)$. The details will not be given here as there are further modifications needed to the moment definitions before an exact solution to the variational equation can be obtained. The method, however, will be used with the final definitions in Sects. 12, 23 and 24.

9 The Variational Equation Revisited

As was seen in Sect. 3, Mathisson's variational equation is obtained by taking $\varphi_{\alpha\beta}$ in the moment-defining equation to have the special form

$$\varphi_{\alpha\beta} = \nabla_{(\alpha}\omega_{\beta)} \quad (65)$$

for an arbitrary vector field ω_α of compact support. It follows from this that ω_α satisfies

$$\frac{\delta^2}{du^2}\omega_\alpha + \omega_{\beta\dot{\gamma}}\dot{x}^\gamma\dot{x}^\delta R^\beta_{\cdot\gamma\delta\alpha} = \dot{x}^\beta\dot{x}^\gamma\nabla_{\{\beta}\varphi_{\alpha\gamma\}} \quad (66)$$

along all affinely parameterised geodesics $x^\alpha(u)$, where $\dot{x}^\alpha = dx^\alpha/du$ and curly brackets around three indices are defined by

$$A_{\{\alpha\beta\gamma\}} = A_{\alpha\beta\gamma} - A_{\beta\gamma\alpha} + A_{\gamma\alpha\beta}. \quad (67)$$

A result of this form is to be expected since if $\varphi_{\alpha\beta} = 0$, ω_α is a Killing vector and (66) becomes the equation of geodesic deviation. This confirms the well-known fact that a Killing vector field satisfies the equation of geodesic deviation along any geodesic.

Suppose now that $\varphi_{\alpha\beta}$ is known everywhere, together with the values of ω_α and $\nabla_\alpha\omega_\beta$ at a point z . These values for ω_α determine initial conditions for the integration of (66) along any geodesic through z , so the entire field ω_α can be determined by integration along all such geodesics. But the value of $\nabla_{(\alpha}\omega_{\beta)}$ at z is given by (65), so the additional information needed about ω_α is actually only the values

$$A_\alpha \equiv \omega_\alpha(z) \quad \text{and} \quad B_{\alpha\beta} \equiv \nabla_{[\alpha}\omega_{\beta]}(z). \quad (68)$$

Let ξ_α be the unique vector field such that

$$\xi_\alpha = A_\alpha \quad \text{and} \quad \nabla_\alpha\xi_\beta = B_{\alpha\beta} \quad \text{at } z \quad (69)$$

and which satisfies the equation of geodesic deviation, *i.e.* (66) with the right hand side set to zero, along all geodesics through z . Note that $B_{\alpha\beta}$ is antisymmetric by its definition in (68). Put

$$\lambda_\alpha = \omega_\alpha - \xi_\alpha. \quad (70)$$

Then λ_α satisfies the full form of (66) along all such geodesics and has

$$\lambda_\alpha = 0 \quad \text{and} \quad \nabla_\alpha\lambda_\beta = \varphi_{\alpha\beta} \quad \text{at } z. \quad (71)$$

Note that λ_α and ξ_α are vectors at x that depend on both x and z . As such, they are functions to which Exp^A is applicable, so let

$$\Lambda_\alpha = \text{Exp}^A \lambda_\alpha, \quad \Xi_\alpha = \text{Exp}^A \xi_\alpha \quad \text{and} \quad G_{\alpha\beta} = \text{Exp}^A g_{\alpha\beta}. \quad (72)$$

The map $\text{Exp}_z : T_z(M) \rightarrow M$ under which $X \rightarrow x$ can be considered as giving a pointwise identification of the manifolds with one another. With this identification the components of $X^\alpha \in T_z(M)$ become coordinates of x , forming a normal coordinate system on M with pole z . In these coordinates Λ_α and $G_{\alpha\beta}$ become the components of λ_α and $g_{\alpha\beta}$. With this interpretation, $T_z(M)$ is not flat but is instead a Riemannian manifold with $G_{\alpha\beta}$ as its metric tensor. The coordinate expression

$$\nabla_\alpha \lambda_\beta = \frac{\partial}{\partial x^\alpha} \lambda_\beta - \Gamma_{\alpha\beta}^\gamma \lambda_\gamma \quad (73)$$

for components of the covariant derivative maps under this correspondence to

$$\text{Exp}^A \nabla_\alpha \lambda_\beta = \frac{\partial}{\partial X^\alpha} \Lambda_\beta - G_{\alpha\beta}^\gamma \Lambda_\gamma \quad (74)$$

where $G_{\alpha\beta}^\gamma$ is the Christoffel connection on $T_z(M)$ corresponding to the metric $G_{\alpha\beta}$.

In contrast to (73), the individual terms in (74) are tensors since the coordinate system given by the components of the position vector X^α is subject only to linear transformations. The notation

$$\nabla_{*\alpha} \equiv \frac{\partial}{\partial X^\alpha} \quad (75)$$

will be used to emphasise the covariant nature of this partial differentiation on $T_z(M)$ while at the same time distinguishing it from the covariant derivative ∇_α on M . With this notation the usual formula for the components of the Christoffel connection gives

$$G_{\alpha\beta}^\gamma = G^{\gamma\delta} G_{\alpha\beta\delta}^{-1} \quad \text{where} \quad G_{\alpha\beta\gamma} = \frac{1}{2} \nabla_{*\{\alpha} G_{\gamma\beta\}}. \quad (76)$$

Here $G^{\alpha\beta}$ is the matrix inverse of $G_{\alpha\beta}$, its contravariant form considered as a metric tensor, which needs to be distinguished from $G^{\alpha\beta}$ in which the indices have been raised with the flat metric $g_{\alpha\beta}$ on $T_z(M)$. It follows from (59), (65), (70) and (74) that

$$\Phi_{\alpha\beta} + G_{\alpha\beta}^\gamma \Lambda_\gamma = \nabla_{*(\alpha} \Lambda_{\beta)} + \Xi_{\alpha\beta} \quad (77)$$

where

$$\Xi_{\alpha\beta} \equiv \text{Exp}^A \nabla_{(\alpha} \xi_{\beta)}. \quad (78)$$

Since (74) assumes nothing about the form of λ_α , it may be applied also to ξ_α to give

$$\Xi_{\alpha\beta} = \nabla_{*(\alpha} \Xi_{\beta)} - G_{\alpha\beta}^\gamma \Xi_\gamma \quad (79)$$

where Ξ_α is given by (72).

The left hand side of (77) is well defined for all symmetric $\varphi_{\alpha\beta}$, whether or not it has the form (65), since the construction of λ_α by (66) with (71) does not depend on that special form. It is therefore possible to replace the moment-defining equation (54) by the modified form

$$\int T^{\alpha\beta} \varphi_{\alpha\beta} Dx = M^{\alpha\beta} [\Phi_{\alpha\beta} + G_{\alpha\beta}^\gamma \Lambda_\gamma] \quad (80)$$

where the functional $M^{\alpha\beta}$ is still defined by (55). This redefinition serves the same purpose as the rearrangement of terms in infinite series in Sect. 4, but without the associated problems of convergence.

This change only affects gravitational contributions to the moments since in flat spacetime $G_{\alpha\beta}^\gamma = 0$ but it has an important effect on the variational equation, which by (77) takes the form

$$M^{\alpha\beta} [\nabla_{*(\alpha} \Lambda_{\beta)} + \Xi_{\alpha\beta}] = 0. \quad (81)$$

Since $\nabla_{*\alpha}$ is just partial differentiation by (75), Fourier transformation gives

$$F[\nabla_{*\alpha} \Lambda_\beta] = -ik_\alpha \tilde{\Lambda}_\alpha \quad (82)$$

where $F[\dots]$ is used instead of a tilde for the Fourier transformation of a typographically complex expression. Hence from (55)

$$M^{\alpha\beta} [\nabla_{*(\alpha} \Lambda_{\beta)}] = \frac{1}{(2\pi)^4} \int ds \int Dk \tilde{t}^\alpha \tilde{\Lambda}_\alpha \quad (83)$$

where

$$\tilde{t}^\alpha(s, k) \equiv -ik_\beta \tilde{m}^{\alpha\beta}(s, k) = \sum_{n \geq 0} \frac{(-i)^n}{n!} k_\gamma \dots k_\beta t^{\gamma \dots \beta \alpha} \quad (84)$$

with

$$t^\alpha = 0 \quad \text{and} \quad t^{\delta \dots \gamma \beta \alpha} = (n+1) m^{(\delta \dots \gamma \beta) \alpha} \quad \text{for } n \geq 0. \quad (85)$$

Once again n is the number of indices in a set such as $\delta \dots \gamma$ marked with dots, with values 0 and 1 allowed. The contribution (83) to the variational equation therefore involves only certain linear combinations of the components of the m 's, those given by (85).

The other contribution $M^{\alpha\beta} [\Xi_{\alpha\beta}]$ involves the vector field ω_α only through the values A_α and $B_{\alpha\beta}$ of (68) along the world line L , as these are all the data required to construct ξ_α from which in turn $\Xi_{\alpha\beta}$ is constructed. Moreover for fixed $z \in L$ the dependence of $\Xi_{\alpha\beta}(z, X)$ on A_α and $B_{\alpha\beta}$ is linear. It follows that

$$M^{\alpha\beta} [\Xi_{\alpha\beta}] = \int \left(A^\alpha(s) F_\alpha(s) + \frac{1}{2} B^{\alpha\beta} L_{\alpha\beta}(s) \right) ds \quad (86)$$

for some F_α and antisymmetric $L_{\alpha\beta}$ that are defined on the world line L by this equation and which are independent of the field ω_α .

10 Tensor Decomposition Through Symmetry

The tensors t^{\dots} are formed from linear combinations of components of the m 's. This leads naturally to the question of what information remains in the m 's when that contained in the t 's is removed. It seems likely that this residual information will remain unconstrained by the variational equation and will therefore provide the desired description of the freely specifiable part of the higher moments.

The monopole and dipole moments are initially described by $m^{\alpha\beta}$ and $m^{\gamma\alpha\beta}$, tensors with two and three indices respectively, but their final description in the equations of motion is by a p^α and $S^{\alpha\beta}$ that have one fewer index. This seems to have led to a preconception among those who studied the quadrupole case that the free information in the quadrupole moment should be described by a three-index tensor.

The second key to the locked door was the realisation that this is not the case, that there is a mathematical tool to answer the question of what remains when the t 's are removed from the m 's. This tool is the theory of group representations, or more specifically of representations of the general linear group $GL(n)$ that describes the transformation of tensor components under a change of coordinate system. This in turn is provided by the theory of representations of the symmetric group, i.e., the group of all permutations of a given order. This is the group that describes the symmetry properties of tensors. It is a powerful tool but once this is realised, what is needed can also be arrived at without its use. as will now be shown.

Let

$$j^{\delta\dots\gamma\beta\alpha} = m^{\delta\dots\gamma\beta\alpha} + a t^{(\delta\dots\gamma\beta\alpha)} + 2b t^{\delta\dots\gamma(\beta\alpha)} \quad \text{for } n \geq 0 \quad (87)$$

where a and b are constants. These satisfy the same symmetry relations

$$j^{\delta\dots\gamma\beta\alpha} = j^{(\delta\dots\gamma)(\beta\alpha)} \quad (88)$$

as the m 's, while the t 's satisfy

$$t^{\delta\dots\gamma\beta\alpha} = t^{(\delta\dots\gamma\beta)\alpha}. \quad (89)$$

It is easily seen that for any $n \geq 0$, there exist a and b such that

$$\frac{1}{n+1} t^{\delta\dots\gamma\beta\alpha} + a t^{(\delta\dots\gamma\beta\alpha)} + b \left(t^{\delta\dots\gamma\beta\alpha} + t^{\alpha(\delta\dots\gamma\beta)} \right) = 0 \quad (90)$$

holds identically for all t^{\dots} satisfying (89). With these values, (85) and (87) show that the j^{\dots} also satisfy

$$j^{(\delta\dots\gamma\beta)\alpha} = 0 \quad \text{for } n \geq 0. \quad (91)$$

The cases $n = 0, 1$ give

$$j^{\beta\alpha} = 0, \quad j^{\gamma\beta\alpha} \equiv 3j^{(\gamma\beta\alpha)} - 2j^{(\beta\alpha)\gamma} = 0 \quad (92)$$

so that the m 's with two and three indices are equivalent to the corresponding t 's and need no counterpart.

These results show that a tensor m^{\dots} determines a corresponding j^{\dots} and t^{\dots} satisfying (88), (91) and (89) but it does not yet show that these two parts of m^{\dots} are independent. To see this, suppose now that a tensor j^{\dots} with four or more indices is given that satisfies (88) and (91), along with a t^{\dots} with the same number of indices satisfying (89). Construct m^{\dots} from them so that (87) holds. Then (85) will hold due to (90) and (91) while (87) holds by construction. These are the two equations that define j^{\dots} and t^{\dots} in terms of m^{\dots} so the j^{\dots} and t^{\dots} originally chosen will be recovered. This proves their independence, as required.

It follows that j^{\dots} meets all the conditions for the counterpart tensor to t^{\dots} , but its expression (87) is rather complicated once a and b have been evaluated as functions of n . An alternative and more useful counterpart is given by

$$J^{\zeta\dots\varepsilon\delta\gamma\beta\alpha} \equiv j^{\zeta\dots\varepsilon[\delta[\beta\gamma]\alpha]} = m^{\zeta\dots\varepsilon[\delta[\beta\gamma]\alpha]} \quad \text{for } n \geq 0. \quad (93)$$

The second equality follows from (87) and gives an expression for the J 's in terms of the m 's in which the number of indices does not enter explicitly. The nested square brackets denote antisymmetrisation independently over pairs of indices, the opening and closing brackets being paired in order from left to right. In (93) this means that the antisymmetrisation is applied to the index pairs $\delta\gamma$ and $\beta\alpha$.

It follows from this definition that the J 's have the symmetry properties

$$J^{\zeta\dots\varepsilon\delta\gamma\beta\alpha} = J^{(\zeta\dots\varepsilon)[\delta\gamma][\beta\alpha]} \quad \text{and} \quad J^{\zeta\dots\varepsilon\delta[\gamma\beta\alpha]} = 0 \quad \text{for } n \geq 0, \quad (94)$$

$$J^{\zeta\dots[\varepsilon\delta\gamma]\beta\alpha} = 0 \quad \text{for } n \geq 1, \quad (95)$$

which for $n = 0$ and $n = 1$ are the symmetries of the curvature tensor $R_{\delta\gamma/\beta\alpha}$ and its first derivative $\nabla_\varepsilon R_{\delta\gamma/\beta\alpha}$, in the latter case when the Bianchi identities are taken into account.

Some straightforward but tedious algebra shows that the j 's can be recovered from the J 's by

$$j^{\alpha\dots\beta\gamma\delta\varepsilon} = \frac{4n}{n+2} J^{(\alpha\dots\beta|\delta|\gamma)\varepsilon} \quad \text{for } n \geq 1 \quad (96)$$

where the vertical bars ‘|’ enclose indices that are to be excluded from the symmetrisation. If J^{\dots} satisfies (94) and (95) then the j^{\dots} constructed from it by (96) satisfies (88), (91) and (93). This completes the proof that the j ’s and J ’s are equivalent as counterparts to the t ’s in the decomposition of the m ’s.

11 The Orthogonality Conditions Revisited

As with Mathisson’s original moment-defining equation (51), its modified form (80) needs orthogonality conditions imposed for it to determine the moments uniquely. The conditions (61) used in Sect. 8 have the same symmetries as the moments themselves and so can be split into the two sets

$$n_{\delta} m^{\delta(\gamma \dots \beta) \alpha} = 0 \quad \text{for } n \geq 1 \quad (97)$$

and

$$n_{\zeta} m^{\zeta \dots \varepsilon [\delta [\beta \gamma] \alpha]} = 0 \quad \text{for } n \geq 1. \quad (98)$$

Note that n has a different meaning in each equation as it is the number of indices in the set marked by dots. Both conditions are $n \geq 1$ but the moments with three or four indices only occur in (97), so it is only for those with five or more indices that the orthogonality condition separates into two parts.

The second set can immediately be expressed in terms of the J ’s of (93) as

$$n_{\zeta} J^{\zeta \dots \varepsilon \delta \gamma \beta \alpha} \quad \text{for } n \geq 1. \quad (99)$$

The first set, however, is not a restriction purely on the t ’s. To complete the decomposition of the moments into two independent sets, it will therefore be modified for $n \geq 2$ by extending the index symmetrisation to include the δ . This then gives

$$n_{\delta} t^{\delta \gamma \dots \beta \alpha} = 0 \quad \text{for } n \geq 2. \quad (100)$$

This change does not affect the number of constraints placed on the components of the m ’s concerned as the new and old conditions have the same symmetries. It cannot be applied for $n = 1$, however, since $n_{\delta} m^{\delta \beta \alpha}$ is symmetric but $n_{\delta} t^{\delta \beta \alpha}$ is not, so in that case it would increase the number of constraints. For the time being $t^{\gamma \beta \alpha}$ will be left unconstrained, which leaves a little indeterminacy in the definition of the moments that will be resolved later.

The quadrupole and higher moments have both a J -part that satisfies (94), (95) and (99) and a t -part that satisfies (89) and (100). At first sight it seems difficult to count the number of linearly independent components in these parts due to the complexity of these conditions. In fact it is easy, though the count is best done on the equivalent j forms rather than directly on the J forms. In m dimensions the number of linearly independent components of a totally symmetric n -index tensor is given

by the binomial coefficient $\binom{n+m-1}{m-1}$. For the spacetime manifold $m = 4$. With this in mind, consider the tensors for a 2^n -pole moment for $n \geq 2$, for which both parts have $(n+2)$ indices. An $(n+2)$ -index tensor satisfying (88) or (89) will have $N_1(n)$ or $N_2(n)$ components respectively, where

$$N_1(n) = \binom{n+3}{3} \times \binom{5}{3}, \quad N_2(n) = \binom{n+4}{3} \times \binom{4}{3}. \quad (101)$$

The further condition (91) on the j -part gives $N_2(n)$ constraints, leaving it at this point with

$$N_3(n) \equiv N_1(n) - N_2(n) = (n+3)(n+2)(n-1) \quad (102)$$

components. This is therefore the number of linearly independent components of a J tensor satisfying (94) and (95). The orthogonality condition (99) has the same symmetries as the J 's but one fewer index, so it gives $N_3(n-1)$ constraints, leaving the $(n+2)$ -index J tensor with $N_3(n) - N_3(n-1) = (n+2)(3n-1)$ such components. The corresponding count for the $(n+2)$ -index t tensor is $N_2(n) - N_2(n-1) = 2(n+2)(n+3)$.

It will be seen in the next section that for $n \geq 2$ the t tensors actually vanish, leaving the J 's as the complete description of the quadrupole and higher moments. The quadrupole moment therefore has 20 such components, in agreement with Mathisson's full description of his quadrupole before he neglected components with a non-classical analogue. This again shows the advantage of Mathisson's approach over that of later authors; in their treatment of the quadrupole case neither Taub [23] nor Madore [24] had full descriptions of the quadrupole with 20 linearly independent components.

12 Solution of the Variational Equation

From (83) the contribution to $M^{\alpha\beta}[\nabla_{*(\alpha}\Lambda_{\beta)}]$ from the first term of the series (84) vanishes by (85) and the next two terms give

$$\int \left(t^{\beta\alpha} \nabla_{*\beta} \Lambda_{\alpha}(z(s), 0) + \frac{1}{2} t^{\gamma\beta\alpha} \nabla_{*\gamma} \nabla_{*\beta} \Lambda_{\alpha}(z(s), 0) \right) ds. \quad (103)$$

The Fourier transform has here been evaluated to give terms involving derivatives of $\Lambda_{\alpha}(z, X)$ at $X = 0$. Now it was seen in Sect. 9 that the components of X^{α} can be considered as a normal coordinate system on M with pole z . The $\nabla_{*\alpha}$ terms in (103) are partial derivatives of λ_{α} at z in this coordinate system. They can be replaced by covariant derivatives as each extra term vanishes, some because $\Gamma_{\alpha\beta}^{\gamma} = 0$ at the pole of a normal coordinate system, the others because $\lambda_{\alpha} = 0$ at this point by (71). If $t^{\beta\alpha}$ and $t^{\gamma\beta\alpha}$ are expressed in terms of the m 's by (85) then this contribution takes the form

$$\int \left(m^{\beta\alpha} \nabla_\beta \lambda_\alpha(z) + m^{\gamma\beta\alpha} \nabla_{(\gamma\beta)} \lambda_\alpha(z) \right) ds. \quad (104)$$

Now (71) gives

$$\nabla_\beta \lambda_\alpha = \varphi_{\beta\alpha} \quad \text{at } z \quad (105)$$

and since λ_α satisfies (66) along all geodesics through z it implies that

$$\nabla_{(\gamma\beta)} \lambda_\alpha = \nabla_{\{\gamma} \varphi_{\alpha\beta\}} \quad \text{at } z \quad (106)$$

where curly brackets around three indices are defined by (67). When this is put back into (104), two of the three terms in this curly bracket expansion cancel by the symmetry of $m^{\gamma\beta\alpha}$ on α and β . For $\varphi_{\alpha\beta}$ of the form (65), the result is

$$\int \left(m^{\beta\alpha} \nabla_\beta \omega_\alpha(z) + m^{\gamma\beta\alpha} \nabla_{\gamma\beta} \omega_\alpha(z) \right) ds. \quad (107)$$

Suppose now that ω_α is chosen so that it, $\nabla_\beta \omega_\alpha$ and $\nabla_{\gamma\beta} \omega_\alpha$ all vanish on the world line L . Then expression (107) vanishes, as do the parameters A_α and $B_{\alpha\beta}$ on L given by (68), and so also the contribution (86) to the variational equation (81). In addition the vector field ξ_α vanishes for all $z \in L$ by its definition through (69), so that $\lambda_\alpha = \omega_\alpha$. For such ω_α the variational equation therefore reduces to

$$\frac{1}{(2\pi)^4} \int ds \int Dk \tilde{\Omega}_\alpha \left(\sum_{n \geq 3} \frac{(-i)^n}{n!} k_\gamma \cdots k_\beta t^{\gamma \cdots \beta\alpha} \right) = 0 \quad (108)$$

with $\Omega_\alpha = \text{Exp}^A \omega_\alpha$.

The t 's in the summation are those on which the orthogonality condition (100) was imposed. By (85) they are also symmetric on all the indices contracted with k 's. The method of Sect. 8 may therefore be applied to show that the k -space integral in (108) depends on ω_α only through its value on $\Sigma(s)$, where as in that section, $\Sigma(s)$ is the hypersurface formed by all geodesics through $z(z)$ orthogonal to n_α . If ω_α is multiplied by any function that is constant on each $\Sigma(s)$, it still satisfies the vanishing conditions on L so (108) remains valid. Each k -space integral becomes multiplied by the value of the function on the corresponding $\Sigma(s)$ as it only depends on the value of ω_α on that hypersurface. Since (108) has to hold for all such multiplier functions, it follows that the k -space integral must itself be zero for all s .

Let $\tau(x)$ be the scalar function such that $\tau(x) = s$ if $x \in \Sigma(s)$, again as in Sect. 8. Let $\psi_\alpha(x)$ be any smooth vector-valued function of compact support. Choose any fixed coordinate system on M and set

$$\omega_\alpha(x) = a_{\beta\gamma\delta}(\tau(x))(x^\beta - z^\beta(\tau(x)))(x^\gamma - z^\gamma(\tau(x)))(x^\delta - z^\delta(\tau(x)))\psi_\alpha(x) \quad (109)$$

where $a_{\beta\gamma\delta}$ is a smooth function of s . This determines the vector field ω_α by giving its components in the chosen coordinate system. This ω_α and its first two derivatives vanish on L so the above results apply to it.

Consider the k -space integral in (108) with this ω_α for some fixed value s_0 of s . It depends on ω_α only through its value on $\Sigma(s_0)$, and for $x \in \Sigma(s_0)$, $\tau(x) = s_0$ by construction. The value of this k -space integral is therefore unchanged if $\tau(x)$ is replaced by s_0 throughout the definition (109) of ω_α . Now choose the coordinate system used in (109) to be the normal coordinates given by the components of $X \in T_z(M)$ for $z = z(s_0)$ as described above. Then $z^\alpha(s_0) = 0$ as this point is the pole of the normal coordinates so that (109), with the replacement just described, gives

$$\Omega_\alpha(z(s_0), X) = a_{\beta\gamma\delta}(s_0) X^\beta X^\gamma X^\delta \Psi_\alpha(z(s_0), X) \quad (110)$$

where $\Psi_\alpha = \text{Exp}^A \psi^\alpha$. The Fourier transform of (110) gives

$$\tilde{\Omega}_\alpha(z(s_0), k) = (-i)^3 a_{\beta\gamma\delta} \frac{\partial^3 \tilde{\Psi}_\alpha}{\partial k^\beta \partial k^\gamma \partial k^\delta}. \quad (111)$$

If this is put back into the k -space integral of (108), the vanishing of that integral gives

$$N^\alpha[\Psi_\alpha] \equiv \frac{1}{(2\pi)^4} \int \tilde{\Psi}_\alpha \tilde{N}_\alpha \text{D}k = 0 \quad (112)$$

where

$$\tilde{N}^\alpha = \sum_{n \geq 0} \frac{(-i)^n}{n!} k_\gamma \cdots k_\beta a_{\zeta\epsilon\delta} t^{\zeta\epsilon\delta\gamma \cdots \beta\alpha}. \quad (113)$$

Since ψ_α is an arbitrary smooth function of compact support on M , so also is Ψ_α on $T_z(M)$. Hence (112) completely defines N^α as a generalised function (distribution) on $T_z(M)$ with Fourier transform \tilde{N}^α . As N^α is identically zero, so also is \tilde{N}^α and hence also all coefficients in its power series expansion (113). Note that the Fourier transform of such a generalised function is analytic, see for example Gel'fand and Shilov [30] so the power series expansion is valid. Since $a_{\zeta\epsilon\delta}$ is also arbitrary, the vanishing of the power series coefficients gives

$$t^{\gamma \cdots \beta\alpha} = 0 \quad \text{for } n \geq 3. \quad (114)$$

For a general ω_α the only surviving part of $M^{\alpha\beta}[\nabla_{*(\alpha}\Lambda_{\beta)}]$ is (107). The other contribution to the variational equation (81) is $M^{\alpha\beta}[\Xi_{\alpha\beta}]$ given by (86), so with (68) that equation now takes the form

$$\int \left(F^\alpha \omega_\alpha + (m^{\beta\alpha} + \frac{1}{2} L^{\beta\alpha}) \nabla_\beta \omega_\alpha(z) + m^{\gamma\beta\alpha} \nabla_\gamma \omega_\alpha(z) \right) \text{d}s = 0 \quad (115)$$

for all smooth vector fields ω_α on M of compact support. Interestingly, this is Mathisson's original version in the case when only monopole and dipole moments are retained, but with the addition of external force and couple terms F^α and $L^{\beta\alpha}$.

It is solved by reducing it too to a form in which the s -integrand depends on ω_α only through its value on $\Sigma(s)$. To do this, at each point of L define the projection operators

$$P_\alpha^{\cdot\beta} \equiv \chi n_\alpha v^\beta \quad \text{and} \quad Q_\alpha^{\cdot\beta} \equiv A_\alpha^\beta - P_\alpha^{\cdot\beta} \quad (116)$$

where $\chi \equiv 1/(n_\alpha v^\alpha)$ and A_α^β is the unit tensor. If $x^\alpha(u)$ is an affinely parameterised geodesic through $z(s)$ orthogonal to n^α at z , as used in Sect. 9, ω_α on $\Sigma(s)$ determines $\dot{x}^\beta \nabla_\beta \omega_\alpha$ and $\dot{x}^\gamma \nabla_\gamma (\dot{x}^\beta \nabla_\beta \omega_\alpha)$ where $\dot{x}^\alpha = dx^\alpha/du$. But $\dot{x}^\gamma \nabla_\gamma \dot{x}^\beta = 0$ since $x(u)$ is geodesic, so it also determines $\dot{x}^\gamma \dot{x}^\beta \nabla_{\gamma\beta} \omega_\alpha$. Now at z the vector \dot{x}^α can be any vector orthogonal to n_α . It follows that ω_α on $\Sigma(s)$ determines the values of

$$\omega_\alpha, \quad Q_\beta^{\cdot\gamma} \nabla_\gamma \omega_\alpha \quad \text{and} \quad Q_\gamma^{\cdot\epsilon} Q_\beta^{\cdot\delta} \nabla_{(\epsilon\delta)} \omega_\alpha. \quad (117)$$

The derivatives in (115) can be decomposed by projection into the parts given in (117) together with similar parts in which one or more of the Q operators is replaced by a P . Wherever a P operator occurs, it can be eliminated by using the identity

$$P_\beta^{\cdot\gamma} \nabla_\gamma = \chi n_\beta \frac{\delta}{ds} \quad (118)$$

followed by an integration by parts. The integrated part will vanish as ω_α has compact support. If the P operator is not acting on the outermost derivative, the Ricci identity should first be used to commute the order of differentiation. In this way the integrand can be brought to a form in which ω_α occurs only through the projections (117).

If ω_α is multiplied by a function constant on each $\Sigma(s)$, the projections in (117) will each be multiplied by this same factor. It then follows by the argument used above that the s -integrand must itself be zero. But for a fixed value of s the values of ω_α , $\nabla_\beta \omega_\alpha$ and $\nabla_{(\gamma\beta)} \omega_\alpha$ at z can be specified independently, subject only to the last of these being symmetric in γ and β . For the s -integrand to vanish, the coefficients of each of these derivatives must be zero. These results complete the solution of the variational equation.

This process is best carried out in stages. The last projection in (117) can only arise from the last term of (115). The vanishing of the coefficient of $\nabla_{(\gamma\beta)} \omega_\alpha$ therefore gives

$$Q_\epsilon^{\cdot\gamma} Q_\delta^{\cdot\beta} m^{(\epsilon\delta)\alpha} = 0 \quad (119)$$

which with (116) shows that $m^{(\gamma\beta)\alpha}$ must have the form

$$m^{(\gamma\beta)\alpha} = \frac{1}{2} v^{(\gamma} S^{\beta)\alpha} \quad (120)$$

for some tensor $S^{\alpha\beta}$ that at this stage is not necessarily antisymmetric. But

$$m^{\gamma\beta\alpha} \equiv m^{(\gamma\beta)\alpha} + m^{(\gamma\alpha)\beta} - m^{(\beta\alpha)\gamma} \quad (121)$$

so that (120) gives

$$m^{\gamma\beta\alpha} = \frac{1}{2} \left(S^{[\gamma\beta]} v^\alpha + S^{[\gamma\alpha]} v^\beta + S^{(\beta\alpha)} v^\gamma \right) \quad (122)$$

from which

$$m^{\gamma\beta\alpha} \nabla_{\gamma\beta} \omega_\alpha = \frac{1}{2} S^{\beta\alpha} \frac{\delta}{ds} \nabla_\beta \omega_\alpha + \frac{1}{2} \omega_\alpha v^\beta S^{\gamma\delta} R^\alpha_{\cdot\beta\gamma\delta}. \quad (123)$$

If this is put back into (115), an integration by parts brings it to the form

$$\int \left(\left(\frac{1}{2} v^\beta S^{\gamma\delta} R^\alpha_{\cdot\beta\gamma\delta} + F^\alpha \right) \omega_\alpha + \left(m^{\beta\alpha} - \frac{1}{2} \frac{\delta S^{\beta\alpha}}{ds} + \frac{1}{2} L^{\beta\alpha} \right) \nabla_\beta \omega_\alpha(z) \right) ds = 0. \quad (124)$$

Now the second projection in (117) can only arise from the last term of (124), which leads to

$$Q_\gamma^{\cdot\beta} \left(m^{\gamma\alpha} - \frac{1}{2} \frac{\delta S^{\gamma\alpha}}{ds} + \frac{1}{2} L^{\gamma\alpha} \right) = 0. \quad (125)$$

In a similar manner to (120) it follows that

$$m^{\beta\alpha} - \frac{1}{2} \frac{\delta S^{\beta\alpha}}{ds} + \frac{1}{2} L^{\beta\alpha} = v^\beta p^\alpha \quad (126)$$

for some vector p^α , from which

$$\left(m^{\beta\alpha} - \frac{1}{2} \frac{\delta S^{\beta\alpha}}{ds} + \frac{1}{2} L^{\beta\alpha} \right) \nabla_\beta \omega_\alpha = p^\alpha \frac{\delta}{ds} \omega_\alpha. \quad (127)$$

Finally this can be put back into (124), when an integration by parts brings it to the form

$$\int \left(\frac{1}{2} v^\beta S^{\gamma\delta} R^\alpha_{\cdot\beta\gamma\delta} - \frac{\delta p^\alpha}{ds} + F^\alpha \right) \omega_\alpha ds = 0 \quad (128)$$

from which

$$\frac{1}{2} v^\beta S^{\gamma\delta} R^\alpha_{\cdot\beta\gamma\delta} - \frac{\delta p^\alpha}{ds} + F^\alpha = 0. \quad (129)$$

13 Equations of Motion

The results of the previous section provide a complete solution of the variational equation but they are not yet in the simplest form. There is still a little freedom in the moments that can be used to make one further simplification. In the same way that the first few terms of $M^{\alpha\beta}[\nabla_{*(\alpha}\Lambda_{\beta)}]$ were evaluated to give (104), so also the first two terms of $M^{\alpha\beta}[\Phi_{\alpha\beta}]$ as given by (55) can be evaluated to give

$$\int \left(m^{\beta\alpha} \varphi_{\beta\alpha} + m^{\gamma\beta\alpha} \nabla_{\gamma} \varphi_{\beta\alpha} \right) ds. \quad (130)$$

With $m^{\beta\alpha}$ and $m^{\gamma\beta\alpha}$ given in terms of p^{α} and $S^{\beta\alpha}$ by (122) and (126), the contribution to (130) from the symmetric part of $S^{\beta\alpha}$ is

$$\frac{1}{2} \int \left(\frac{\delta S^{(\beta\alpha)}}{ds} \varphi_{\beta\alpha} + S^{(\beta\alpha)} v^{\gamma} \nabla_{\gamma} \varphi_{\beta\alpha} \right) ds. \quad (131)$$

The two terms of the integrand combine to give a total derivative that integrates to zero since $\varphi_{\beta\alpha}$ has compact support. It follows that $S^{(\beta\alpha)}$ is not determined by the moment-defining equation (80).

This was foreseen in Sect. 11 where no new orthogonality condition was imposed to replace the case $n = 1$ of (97), namely $n_{\gamma} m^{\gamma\beta\alpha} = 0$. That condition set a symmetric two-index tensor to zero, so it is not surprising that omission of a replacement has left another symmetric two-index tensor undetermined. The definition of the moments is completed by imposing

$$S^{(\beta\alpha)} = 0. \quad (132)$$

Since $S^{\beta\alpha}$ and $L^{\beta\alpha}$ are now both antisymmetric, the symmetric part of (126) gives

$$m^{\alpha\beta} = p^{(\alpha} v^{\beta)} \quad (133)$$

while (122) simplifies to

$$m^{\alpha\beta\gamma} = S^{\alpha(\beta} v^{\gamma)}. \quad (134)$$

The result (129) can be written in the form

$$\frac{\delta p^{\alpha}}{ds} = \frac{1}{2} v^{\beta} S^{\gamma\delta} R^{\alpha}_{\cdot\beta\gamma\delta} + F^{\alpha} \quad (135)$$

while the antisymmetric part of (126) gives

$$\frac{\delta S^{\alpha\beta}}{ds} = 2p^{[\alpha} v^{\beta]} + L^{\alpha\beta}. \quad (136)$$

Equations (133) and (134) give the forms of the monopole and dipole moment tensors in terms of the momentum vector p^α and antisymmetric spin tensor $S^{\alpha\beta}$ while (135) and (136) are the equations of motion that the momentum and spin must satisfy.

These are the *only* equations that govern the evolution of the moments. The quadrupole and higher moments are completely specified by the tensors J^{\dots} since their t -parts vanish by (114). The J tensor for the 2^n -pole moment, $n \geq 2$, has $(n+2)$ indices. It satisfies the symmetry conditions (94) and (95) and orthogonality conditions (99) which leave it with $(n+2)(3n-1)$ linearly independent components, as seen in Sect. 11. These tensors determine the gravitational force F^α and torque $L^{\alpha\beta}$ as will be seen in Sect. 15 but their evolution with time is not constrained by the energy-momentum conservation equation (3). This is the same situation as in Newtonian mechanics. Such higher moments are of course still governed by physical laws, but these are solely the constitutive relations for the material of the body.

This resolves the second issue seen in Sect. 4 to arise from Mathisson's paper of 1937. The key to this resolution is the complete separation between the t and J tensors achieved by the modification of the orthogonality conditions made in Sect. 11. Had this not been done, there would have been higher order J tensors occurring in the variational equation. These would have led to the infinite set of evolution equations foreseen in Sect. 4, even if it had still been possible to solve that equation exactly, which may well not have been the case. The change of orthogonality conditions made a second modification to the moment definitions beyond that made in Sect. 9 even though it did not change the defining equation (80). This change achieved invisibly the elimination described in Sect. 4, but despite it being invisible the issue was real and the elimination essential.

Recall now that the world line L is still arbitrary and that, as mentioned at the start of Sect. 7, the parameter s in the development so far need not be proper time. For the rest of this section only, take it as such, so that $v^\alpha v_\alpha = 1$. If (136) is multiplied by v_β it then shows that

$$p^\alpha = M v^\alpha + v_\beta \frac{\delta S^{\alpha\beta}}{\delta s} - L^{\alpha\beta} v_\beta \quad (137)$$

where $M = p^\alpha v_\alpha$. Putting this back into (136) gives

$$\frac{\delta S^{\alpha\beta}}{\delta s} + v^\alpha v_\gamma \frac{\delta S^{\beta\gamma}}{\delta s} - v^\beta v_\gamma \frac{\delta S^{\alpha\gamma}}{\delta s} = L^{\alpha\beta} + 2v_\gamma v^{[\alpha} L^{\beta]\gamma}. \quad (138)$$

It can now be seen how these results are related to those of Mathisson and Papapetrou. Their results are obtained by eliminating p^α . When quadrupole and higher moments are neglected, F^α and $L^{\alpha\beta}$ are both zero. The form (138) then agrees with (15) and if (137) is put back into (135) it then gives (17). A comparison with Mathisson's quadrupole approximation will be made in Sect. 24 after the force and torque terms and the higher moments have been studied in more detail.

There is also a direct correspondence with the results of Pryce and Møller in flat spacetime that were studied in Sect. 5. In contrast to the results of Mathisson and

Papapetrou in general relativity, those results treat an extended body exactly, as do ours. They therefore provide an important check. If they cannot be reproduced by work that claims to be exact in curved spacetime, something is wrong. Fortunately there is agreement. Again, being flat spacetime, F^α and $L^{\alpha\beta}$ are both zero. The original form (136) of the equation for $S^{\alpha\beta}$ then agrees with (28) and correspondingly (137) and (138) agree with (29) and (31). These results add support to the identification of p^α and $S^{\alpha\beta}$ as the momentum and spin of the body.

14 The World Function

The exponential map played a central role in Sect. 7 in enabling the use of Fourier transforms in a curved spacetime. So far it has not been necessary to write explicit forms for the maps it induces between fields on the spacetime manifold M and those on its tangent spaces, but this cannot be put off indefinitely. There are two important tasks still remaining for which this is essential, namely evaluation of the force and torque F^α and $L^{\alpha\beta}$ and derivation of explicit expressions for the moments in terms of the energy-momentum tensor.

The tool needed for this is the *world function*, first used extensively in general relativity by Synge [31], although the notation used here follows that of DeWitt and Brehme [32]. As it is not in common use, however, this section will define the world function and derive the properties that will be needed.

The world function is the two-point scalar function defined by

$$\sigma(x(u_1), x(u_2)) = \frac{1}{2}(u_2 - u_1) \int_{u_1}^{u_2} g_{\alpha\beta}(x(u)) \frac{dx^\alpha}{du} \frac{dx^\beta}{du} du \quad (139)$$

for two points on a geodesic $x(u)$ with affine parameter u . This is well defined for any two points that can be joined by a unique geodesic. It will be assumed that this holds in the situations in which it will be used.

Let $\delta x(u)$ be a variation of the path of integration in (139) and $\delta\sigma$ be the corresponding change in the value of the integral. Then by an integration by parts, as in the standard derivation of the Euler-Lagrange equation of the calculus of variations,

$$\delta\sigma = (u_2 - u_1) \left\{ \left[g_{\alpha\beta} U^\beta \delta x^\alpha \right]_{u_1}^{u_2} - \int_{u_1}^{u_2} g_{\alpha\beta} \frac{\delta U^\beta}{du} \delta x^\alpha du \right\} \quad (140)$$

where $U^\alpha = dx^\alpha/du$. But $\delta U^\alpha/du = 0$ since $x(u)$ is an affinely parameterised geodesic, so the integral term vanishes.

For convenience of notation, from now on the two endpoints will be labelled as z , x corresponding to $u = u_1, u_2$ respectively. Indices $\alpha, \beta, \gamma, \dots$ will refer to the point x and $\kappa, \lambda, \mu, \dots$ to z . *This index convention will be used throughout the remainder of this paper and when results obtained so far are quoted, they will be amended to*

comply with it where necessary. Covariant derivatives of σ will be denoted simply by appropriate suffixes, e.g., $\sigma_{\alpha\beta\kappa} \equiv \nabla_\kappa \nabla_{\beta\alpha} \sigma$ where $\nabla_{\beta\alpha}$ acts at x and ∇_κ at z . With this notation (140) can be written as

$$\delta\sigma \equiv \sigma_\alpha \delta x^\alpha + \sigma_\kappa \delta z^\kappa = (u_2 - u_1) \left(g_{\alpha\beta} U^\beta \delta x^\alpha - g_{\kappa\lambda} U^\lambda \delta z^\kappa \right) \quad (141)$$

from which

$$\sigma^\alpha = (u_2 - u_1) U^\alpha, \quad \sigma^\kappa = (u_1 - u_2) U^\kappa. \quad (142)$$

The two equations are equivalent, the term in the bracket that has the positive sign being the u -value corresponding to the point at which the derivative of σ is evaluated.

The integrand in (139) is in fact constant along an affinely parameterised geodesic, so

$$\sigma = \frac{1}{2} (u_2 - u_1)^2 g_{\alpha\beta} U^\alpha U^\beta = \frac{1}{2} (u_2 - u_1)^2 g_{\kappa\lambda} U^\kappa U^\lambda \quad (143)$$

which with (142) gives

$$2\sigma = \sigma_\alpha \sigma^\alpha = \sigma_\kappa \sigma^\kappa. \quad (144)$$

Differentiating (144) then gives the important relations

$$\sigma^\alpha = \sigma_{\cdot\kappa}^\alpha \sigma^\kappa = \sigma_{\cdot\beta}^\alpha \sigma^\beta, \quad \sigma^\kappa = \sigma_{\cdot\alpha}^\kappa \sigma^\alpha = \sigma_{\cdot\lambda}^\kappa \sigma^\lambda \quad (145)$$

from which

$$\sigma_{\cdot\beta}^\kappa = \sigma_{\cdot\alpha\beta}^\kappa \sigma^\alpha + \sigma_{\cdot\alpha}^\kappa \sigma_{\cdot\beta}^\alpha. \quad (146)$$

This shows that

$$(u_2 - u_1) \frac{\delta}{\delta u} (\sigma_{\cdot\beta}^\kappa) + \sigma_{\cdot\alpha}^\kappa \sigma_{\cdot\beta}^\alpha - \sigma_{\cdot\beta}^\kappa = 0 \quad (147)$$

along geodesics through z , a result that will be useful later.

It is often useful to consider these two-point tensors in the limit $x \rightarrow z$, when they become ordinary tensors at z . This is known as their *coincidence limit* and denoted by $\langle \cdots \rangle$. If (142) is used in (145) and this limit taken, it can be seen that

$$\langle \sigma_{\cdot\beta}^\alpha \rangle = \delta_\beta^\alpha, \quad \langle \sigma_{\cdot\kappa}^\alpha \rangle = -\delta_\kappa^\alpha, \quad \langle \sigma_{\cdot\lambda}^\kappa \rangle = \delta_\lambda^\kappa \quad (148)$$

where the deltas are the Kronecker delta symbol.

Now the definition of the exponential map is that $x = \text{Exp}_z X$ for $X \in T_z(M)$ if

$$X^\kappa = (u_2 - u_1) U^\kappa. \quad (149)$$

By (142) this can be written as

$$X^\kappa = -\sigma^\kappa(z, x). \quad (150)$$

For fixed z the components X^κ are functions of x and can be considered as the coordinates of x in a new coordinate system. By its construction, this is a normal coordinate system with z as its pole.

The map Exp^A defined in Sect. 7 takes a two-point function $\varphi^{\dots}(z, x)$ on M that is a tensor at x and scalar at z and maps it to a function $\Phi^{\dots}(z, X)$ on $T_z(M)$ whose value is a tensor at z . In component form the components of Φ^{\dots} are nothing other than the components of φ^{\dots} in this normal coordinate system. The coordinate transformation is given by (150) from which

$$\frac{\partial X^\kappa}{\partial x^\alpha} = -\sigma^\kappa_{\cdot\alpha} \quad \text{and hence also} \quad \frac{\partial x^\alpha}{\partial X^\kappa} = -\sigma^{\alpha}_{\cdot\kappa}{}^{-1}. \quad (151)$$

The second form has the matrix inverse made explicit as otherwise $\sigma^\alpha_{\cdot\kappa}$ denotes the double derivative with the index α raised with $g^{\alpha\beta}(x)$, which has a different value. The tensor transformation rule therefore shows the map Exp^A to have the explicit form

$$\Phi^{\kappa\dots}_{\lambda\dots} = (-\sigma^\kappa_{\cdot\alpha}) \cdots (-\sigma^{\beta}_{\cdot\lambda})^{\dots -1} \varphi^{\alpha\dots}_{\beta\dots}. \quad (152)$$

The object Φ^{\dots} can also be considered as a two-point function on M with $x = \text{Exp}_z X$ as its second argument. With this interpretation it is a scalar at x and a tensor at z . The individual terms in (152) then all appear as tensors rather than as elements of a coordinate transformation. Different operators for differentiation apply in the two interpretations. When considered as a two-point function on M , the standard covariant derivatives ∇_α and ∇_κ apply. Considered as a function on $T_z(M)$, there should also be two covariant operations of differentiation. One is $\nabla_{*\kappa}$ defined by (75). What to take for the other will now be investigated.

Since Φ^{\dots} is a scalar function of the argument x , or X as appropriate, both ∇_α and $\nabla_{*\kappa}$ reduce to partial differentiation. The relationship between them is just the usual chain rule for a change of variables, which with (151) gives

$$\nabla_{*\kappa} \Phi^{\dots} = H^\alpha_{\cdot\kappa} \nabla_\alpha \Phi^{\dots} \quad \text{where} \quad H^\alpha_{\cdot\kappa} = -\sigma^{\alpha}_{\cdot\kappa}{}^{-1}. \quad (153)$$

When Φ^{\dots} is treated as a function on $T_z(M)$, the operator $\nabla_{*\kappa}$ describes variation of $X \in T_z(M)$. The point z can also be varied, but the tangent space on which Φ^{\dots} is defined then also varies. It therefore needs to be considered not as a function on a single tangent space but on the *tangent bundle* TM , which for an n -dimensional manifold M is a $2n$ -dimensional manifold formed from the union of all its tangent spaces. It is in this context that there is a counterpart to $\nabla_{*\kappa}$, a derivative operator $\nabla_{\kappa*}$ that describes variation of z and is such that $\nabla_{\kappa*} X^\lambda = 0$. To motivate its construction, consider X^λ as a function of z and x . Then (150) gives

$$\nabla_\kappa X^\lambda = -\sigma^\lambda_{\cdot\kappa}, \quad \nabla_\alpha X^\lambda = -\sigma^{\lambda}_{\cdot\alpha} \quad (154)$$

from which

$$\nabla_{\kappa} X^{\lambda} = \sigma^{\alpha}_{\cdot\mu} \sigma^{\mu}_{\cdot\kappa} \nabla_{\alpha} X^{\lambda}. \quad (155)$$

So if $\nabla_{\kappa*}$ is defined by

$$\nabla_{\kappa*} \Phi^{\dots} \equiv \nabla_{\kappa} \Phi^{\dots} + K^{\alpha}_{\cdot\kappa} \nabla_{\alpha} \Phi^{\dots} \quad \text{where} \quad K^{\alpha}_{\cdot\kappa} \equiv -\sigma^{\alpha}_{\cdot\lambda} \sigma^{\lambda}_{\cdot\kappa} \quad (156)$$

then $\nabla_{\kappa*} X^{\lambda} = 0$ as required. The minus signs in the definitions of $H^{\alpha}_{\cdot\kappa}$ and $K^{\alpha}_{\cdot\kappa}$ ensure that their coincidence limits are the unit tensor, as follows from (148). It is shown in [25] that $\nabla_{\kappa*}$ and $\nabla_{*\kappa}$ together form the covariant derivative on TM determined by the affine connection on TM induced by that on M .

There is a component form for $\nabla_{\kappa*}$ analogous to (75) for $\nabla_{*\kappa}$. To derive it, write the covariant derivatives in (156) in their component forms to give

$$\nabla_{\kappa*} \Phi^{\dots} = \left. \frac{\partial \Phi^{\dots}}{\partial z^{\kappa}} \right|_x + K^{\alpha}_{\cdot\kappa} \left. \frac{\partial \Phi^{\dots}}{\partial x^{\alpha}} \right|_z + \Gamma\text{-terms} \quad (157)$$

where the variables being held constant in the partial derivatives are marked explicitly and the connection terms arising from the tensor indices on Φ^{\dots} have been suppressed. In a component form for $\nabla_{\kappa*}$, partial derivatives need to be in terms of z^{κ} and X^{κ} rather than z^{κ} and x^{α} . To make this change, note that

$$\left. \frac{\partial \Phi^{\dots}}{\partial z^{\kappa}} \right|_x = \left. \frac{\partial \Phi^{\dots}}{\partial z^{\kappa}} \right|_X + \left. \frac{\partial \Phi^{\dots}}{\partial X^{\lambda}} \right|_z \left. \frac{\partial X^{\lambda}}{\partial z^{\kappa}} \right|_x \quad \text{and} \quad K^{\alpha}_{\cdot\kappa} \left. \frac{\partial \Phi^{\dots}}{\partial x^{\alpha}} \right|_z = \sigma^{\lambda}_{\cdot\kappa} \left. \frac{\partial \Phi^{\dots}}{\partial X^{\lambda}} \right|_z \quad (158)$$

where the second result makes use of (151) and (156). But

$$\sigma^{\lambda}_{\cdot\kappa} = -\nabla_{\kappa} X^{\lambda} = -\left. \frac{\partial X^{\lambda}}{\partial z^{\kappa}} \right|_x - \Gamma^{\lambda}_{\kappa\nu} X^{\nu}. \quad (159)$$

When these results are put back into (157), two partial derivative terms cancel to leave the final form

$$\nabla_{\kappa*} \Phi^{\lambda}_{\cdot\mu} = \frac{\partial \Phi^{\lambda}_{\cdot\mu}}{\partial z^{\kappa}} - \Gamma^{\rho}_{\kappa\nu} X^{\nu} \frac{\partial \Phi^{\lambda}_{\cdot\mu}}{\partial X^{\rho}} + \Gamma^{\lambda}_{\kappa\nu} \Phi^{\nu}_{\cdot\mu} - \Gamma^{\nu}_{\kappa\mu} \Phi^{\lambda}_{\cdot\nu}. \quad (160)$$

One contravariant and one covariant index has been retained here to show the Γ -terms suppressed above, which are simply the usual ones that arise from ∇_{κ} acting on the tensor indices at z .

The operator $\nabla_{\kappa*}$ has an important property related to integrals over the tangent spaces. Consider the absolute derivative along L of a tensor function $\Psi^{\dots}(z)$ formed by integrating $\Phi^{\dots}(z, X)$ over $T_z(M)$. To evaluate this, the various tangent spaces along L need to be mapped into one another so that the integrands can be compared. Let parallel transport be used to create this mapping. Then in component form

$$v^\kappa \frac{\partial}{\partial z^\kappa} \int \Phi^{\dots}(z, X) DX = \int \left(v^\kappa \frac{\partial \Phi^{\dots}}{\partial z^\kappa} + \frac{\partial \Phi^{\dots}}{\partial X^\lambda} \frac{\partial X^\lambda}{\partial s} \right) DX \quad (161)$$

where the dependence of X^κ on s is parallel transport, so that $\partial X^\lambda / \partial s + \Gamma_{\kappa\mu}^\lambda v^\kappa X^\mu = 0$. On substituting from this into (161), the result is seen to hold for all v^κ when

$$\frac{\partial}{\partial z^\kappa} \int \Phi^{\dots}(z, X) DX = \int \left(\frac{\partial \Phi^{\dots}}{\partial z^\kappa} - \Gamma_{\kappa\mu}^\lambda X^\mu \frac{\partial \Phi^{\dots}}{\partial X^\lambda} \right) DX. \quad (162)$$

The covariant derivative has connection terms arising from the tensor indices. If these are added in then comparison with (160) shows that

$$\nabla_\kappa \int \Phi^{\dots}(z, X) DX = \int \nabla_{\kappa*} \Phi^{\dots}(z, X) DX. \quad (163)$$

A similar method but with parallel transport also of the argument vector k^λ can be applied to the definition of the Fourier transform to show that $\nabla_{\kappa*}$ commutes with the operation of Fourier transformation.

Suppose now that $x(u, v)$ describes a family of geodesics with v constant and u an affine parameter on each geodesic. Let $V^\alpha \equiv \partial x^\alpha / \partial v$. Then V^α satisfies the equation of geodesic deviation along each geodesic. This is indeed the definition of that equation. Consider (142) for these geodesics with z denoting $z(v) \equiv x(u_1, v)$ but x now taken as the generic point $x(u, v)$ with u variable. It gives

$$\sigma^\kappa(z(v), x(u, v)) = (u_1 - u)U^\kappa(v). \quad (164)$$

Note that the tangent vector U^κ at $z(v)$ is independent of u . Both sides of (164) are vector fields along the line given by $u = u_1$, v variable. Its absolute derivative δ / dv along this line gives

$$\sigma^{\kappa}_{\cdot\lambda} V^\lambda + \sigma^{\kappa}_{\cdot\alpha} V^\alpha = (u_1 - u) \frac{\delta U^\kappa}{dv} \equiv (u_1 - u) \frac{\delta V^\kappa}{du}. \quad (165)$$

The vector field V^α is defined only on the surface formed by this family of geodesics, but if it is extended arbitrarily off this surface then $\delta V^\kappa / du = U^\lambda \nabla_\lambda V^\kappa$. The extension is required only to make the covariant derivative meaningful. With this and (164), (165) can be put in the form

$$\sigma^{\kappa}_{\cdot\lambda} V^\lambda + \sigma^{\kappa}_{\cdot\alpha} V^\alpha = \sigma^\lambda \nabla_\lambda V^\kappa \quad (166)$$

from which

$$V^\alpha = K^{\alpha}_{\cdot\kappa} V^\kappa - H^{\alpha}_{\cdot\kappa} \sigma^\lambda \nabla_\lambda V^\kappa \quad (167)$$

where

$$K^{\alpha}_{\cdot\kappa} = -\sigma^{\alpha}_{\cdot\lambda} \sigma^{\lambda}_{\cdot\kappa}, \quad H^{\alpha}_{\cdot\kappa} = -\sigma^{\alpha}_{\cdot\kappa} \quad (168)$$

as in (153) and (156). This gives a formal solution of the geodesic deviation equation with given initial conditions. As a Killing vector field satisfies this equation along all geodesics, it also determines the entire field from the value of it and its first derivative at one point.

15 The Gravitational Force and Torque

The solution (167) of the equation of geodesic deviation provides an explicit expression for ξ^α as defined by (69). It gives

$$\xi^\alpha = K^\alpha_{\cdot\kappa} A^\kappa - H^\alpha_{\cdot\kappa} \sigma_\lambda B^{\lambda\kappa}. \quad (169)$$

Now in the notation of (168) and as a special case of (152), the $G_{\kappa\lambda}$ defined by (72) is given by

$$G_{\kappa\lambda} = H^\alpha_{\cdot\kappa} H^\beta_{\cdot\lambda} g_{\alpha\beta}. \quad (170)$$

Note that indices κ, λ, \dots now need to be used on fields that are images under Exp^A as their values are tensors at z rather than at x . This is in accordance with the convention introduced in the previous section. Then Ξ_κ as defined in (72) can be put in the form

$$\Xi_\kappa = G_{\kappa\lambda} \Upsilon^\lambda \quad \text{where} \quad \Upsilon^\lambda = \sigma^\lambda_{\cdot\mu} A^\mu + X_\mu B^{\mu\lambda} \quad (171)$$

with (79) becoming

$$\Xi_{\kappa\lambda} = \nabla_{*(\kappa)}(G_{\lambda)\mu} \Upsilon^\mu - G_{\kappa\lambda\mu} \Upsilon^\mu. \quad (172)$$

This gives

$$\Xi_{\kappa\lambda} = A^\mu \left(G_{\nu(\kappa} \nabla_{*\lambda)} \sigma^\nu_{\cdot\mu} + \frac{1}{2} \sigma^\nu_{\cdot\mu} \nabla_{*\nu} G_{\kappa\lambda} \right) + B^{\mu\nu} (X_\nu G_{\kappa\lambda\mu} - \nabla_{*(\kappa)}(G_{\lambda)\mu} X_\nu) \quad (173)$$

when the explicit form (171) is used. But

$$\nabla_{*\lambda} \sigma^\nu_{\cdot\mu} = H^\alpha_{\cdot\lambda} \nabla_\alpha \sigma^\nu_{\cdot\mu} = H^\alpha_{\cdot\lambda} \nabla_\mu \sigma^\nu_{\cdot\alpha} = -\sigma^\nu_{\cdot\alpha} \nabla_\mu H^\alpha_{\cdot\lambda} \quad (174)$$

by (153) and because $\nabla_\mu(\sigma^\nu_{\cdot\alpha} H^\alpha_{\cdot\lambda}) = 0$, which holds as the product is minus the unit tensor. On using this product again with (170), this result gives

$$G_{\nu(\kappa} \nabla_{*\lambda)} \sigma^\nu_{\cdot\mu} = g_{\alpha\beta} (\nabla_\mu H^\alpha_{\cdot(\kappa)} H^\beta_{\cdot\lambda)}) = \frac{1}{2} \nabla_\mu G_{\kappa\lambda}. \quad (175)$$

Moreover, (153) and (168) give

$$\sigma^\nu_{\cdot\mu} \nabla_{*\nu} G_{\kappa\lambda} = -\sigma^\nu_{\cdot\mu} \sigma^{\alpha-1}_{\cdot\nu} \nabla_\alpha G_{\kappa\lambda} = K^\alpha_{\cdot\mu} \nabla_\alpha G_{\kappa\lambda}. \quad (176)$$

From (175) and (176) with (156), (173) can be put into its final form

$$\Xi_{\kappa\lambda} = \frac{1}{2} A^\mu \nabla_{\mu*} G_{\kappa\lambda} + B^{\mu\nu} (X_\nu G_{\kappa\lambda\mu} - \nabla_{*(\kappa} (G_{\lambda)\mu} X_\nu)) . \quad (177)$$

This expression for $\Xi_{\kappa\lambda}$ enables explicit expressions for the force and torque F_κ and $L_{\kappa\lambda}$ to be extracted from (86). With use of (55) and some straightforward manipulation of the Fourier transforms, it gives

$$F_\mu = \frac{1}{(2\pi)^4} \int \tilde{m}^{\kappa\lambda} F[\nabla_{\mu*} G_{\kappa\lambda}] Dk, \quad (178)$$

$$L_{\mu\nu} = \frac{2}{(2\pi)^4} \int \left(i \tilde{G}_{\kappa\lambda[\mu} \nabla_{*\nu]} \tilde{m}^{\kappa\lambda} - \tilde{m}^{\kappa\lambda} k_\kappa \nabla_{*[\mu} \tilde{G}_{\nu]\lambda} \right) Dk. \quad (179)$$

Now $\tilde{m}^{\kappa\lambda} k_\kappa = i \tilde{t}^\lambda$ by (84) and by (114) all the terms in the expansion of \tilde{t}^λ vanish except those involving $t^{\lambda\kappa}$ and $t^{\mu\lambda\kappa}$. The contributions from these two terms to the right hand side of (179) separately evaluate to zero. To see this, note that $t^{\lambda\kappa} = m^{\lambda\kappa}$ by (85) and so is symmetric, and that $G_{\lambda\kappa}(z, X) = g_{\lambda\kappa}(z)$ and $\nabla_{*\mu} G_{\lambda\kappa}(z, X) = 0$ at $X = 0$ since $G_{\kappa\lambda}$ gives the components of the metric tensor in a normal coordinate system with pole z .

It was shown in Sect. 14 that $\nabla_{\kappa*}$ commutes with the Fourier transform operator F , so in (178) it can be brought outside the F term. With these simplifications (178) and (179) now reduce to

$$F_\mu = \frac{1}{2(2\pi)^4} \int \tilde{m}^{\kappa\lambda} \nabla_{\mu*} \tilde{G}_{\kappa\lambda} Dk, \quad (180)$$

$$L_{\mu\nu} = \frac{2i}{(2\pi)^4} \int \left(\tilde{G}_{\kappa\lambda[\mu} \nabla_{*\nu]} \tilde{m}^{\kappa\lambda} \right) Dk. \quad (181)$$

These are the final exact expressions for the force and torque exerted on the body by the gravitational field. They do not depend on any assumptions of analyticity, as although $\tilde{m}^{\kappa\lambda}$ is defined by (56) as a power series, it is convergent for any body of finite spatial extent. Taken together with (135) and (136) they provide exact equations for the evolution of the momentum and spin along the chosen world line L . To provide complete and exact equations of motion, all that is required is to add a supplementary condition that specifies L uniquely as the world line of a suitably defined centre of mass. This will be addressed in Sect. 21.

16 Multipole Expansions

When the series (56) for $\tilde{m}^{\kappa\lambda}$ is substituted into (180) and (181), it shows that higher multipole moments of the body interact with successively higher derivatives of the gravitational field. It was noted in Sect. 4 that this was to be expected, but (135) and

(136) show that these interaction terms are the *only* occurrences of the quadrupole and higher moments in the equations of motion. It is only this latter fact that makes it valid to neglect higher moments when the size of the body is small in comparison with the length scale of variations in the gravitational field. This is the multipole approximation, valid as what is being neglected is not the higher moments themselves but is instead their diminishing contributions to the force and torque.

To make the multipole approximation the series (56) for $\tilde{m}^{\kappa\lambda}$ is truncated on substitution into (180) and (181). The k -space integration can then be performed term by term to give

$$F_\kappa = \frac{1}{2(2\pi)^4} \sum_{n \geq 0} \frac{(-i)^n}{n!} m^{\rho \cdots \sigma \lambda \mu} \int k_\rho \cdots k_\sigma \nabla_{\kappa*} \tilde{G}_{\lambda\mu} Dk, \quad (182)$$

$$L^{\kappa\lambda} = \frac{2}{(2\pi)^4} \sum_{n \geq 0} \frac{(-i)^n}{n!} g^{\rho[\kappa} m^{\lambda]\sigma \cdots \tau \mu \nu} \int k_\sigma \cdots k_\tau \tilde{G}_{\mu\nu\rho} Dk \quad (183)$$

where the series extend to the desired multipole order.

Note that k^λ in these integrands is the position vector in the tangent space, the rôle that was played by X^λ in (156). So as was seen following that equation, $\nabla_{\kappa*} k^\lambda = 0$ and since also $\nabla_{\kappa*} g_{\lambda\mu} = \nabla_{\kappa} g_{\lambda\mu} = 0$ then $\nabla_{\kappa*} k_\lambda = 0$. The $\nabla_{\kappa*}$ in (182) can therefore act on the whole integrand and so by (163) can be brought outside the integral as an ordinary covariant derivative. With (76) the k -space integrals in (182) and (183) can then be performed to give

$$F_\kappa = \frac{1}{2} \sum_{n \geq 0} \frac{1}{n!} m^{\rho \cdots \sigma \lambda \mu} \nabla_\kappa (\nabla_{*\rho} \cdots \nabla_{*\sigma} G_{\lambda\mu}), \quad (184)$$

$$L^{\kappa\lambda} = \sum_{n \geq 0} \frac{1}{n!} g^{\rho[\kappa} m^{\lambda]\sigma \cdots \tau \mu \nu} \nabla_{*\sigma} \cdots \nabla_{*\tau} \nabla_{*\{\mu} G_{\rho\nu\}}. \quad (185)$$

The G -terms are all evaluated at (z, X) with $X = 0$ and so, with the interpretation of the components of X^κ as normal coordinates on M with pole z , they are the tensors whose values at the pole of a normal coordinate system reduce to repeated partial derivatives of the metric tensor $g_{\lambda\mu}$.

Given any tensor field, there is a unique tensor at a point z whose components reduce to the n th partial derivative of that field at z in any normal coordinate system with pole z . This is known as the n th *extension* of that tensor field, a concept introduced by Veblen and Thomas [33], for which see also Thomas [34] and Schouten [35]. Following Veblen and Thomas, the additional n indices of the n th extension will be suffixed to the tensor and separated by a comma from the original indices. Note that such extensions are symmetric in their additional indices, unlike repeated covariant derivatives. So

$$\nabla_{*\rho} \cdots \nabla_{*\sigma} G_{\lambda\mu}(z, X) = g_{\lambda\mu, \sigma \cdots \rho}(z) \quad \text{when } X = 0 \quad (186)$$

which enables the multipole expressions for the force and torque to be put in the forms

$$F_{\kappa} = \frac{1}{2} \sum_{n \geq 2} \frac{1}{n!} m^{\rho \cdots \sigma \lambda \mu} \nabla_{\kappa} g_{\lambda\mu, \rho \cdots \sigma}, \quad (187)$$

$$L^{\kappa\lambda} = \sum_{n \geq 1} \frac{1}{n!} g^{\rho[\kappa} m^{\lambda]\sigma \cdots \tau \mu \nu} g_{(\rho\mu, \nu)\sigma \cdots \tau} \quad (188)$$

where, as before, the curly bracket notation for indices is defined by (67).

In principle the summations extend from $n = 0$ but since $g_{\kappa\lambda, \mu} = \nabla_{\mu} g_{\kappa\lambda} = 0$ then the first two terms of (187) and first one of (188) vanish. The lower limits to the summations have therefore been adjusted to take account of this.

The moments occurring in these expressions are the quadrupole and higher moments that are described primarily by the tensors J^{\cdots} . Since the tensors t^{\cdots} vanish for these moments, (87) and (96) show that the m 's are given in terms of the J 's by

$$m^{\mu \cdots \nu \rho \kappa \lambda} = \frac{4n}{n+2} J^{(\mu \cdots \nu | \kappa | \rho) \lambda} \quad \text{for } n \geq 1. \quad (189)$$

The general expressions for force and torque are simpler if left in terms of the m 's but this enables the expansion to any particular order to be expressed in terms of the J 's when required.

The Veblen extensions of the metric tensor occurring in these expressions can be expressed in terms of the curvature tensor and its covariant derivatives. This is not entirely straightforward, however, so the tools for doing so will be developed in the next section.

17 Evaluation of the Veblen Extensions

The relationship between Veblen extensions, covariant derivatives and the curvature tensor is most easily developed via another concept, *normal tensors*, also due to Veblen and Thomas [33]. The n th normal tensor $N^{\alpha}_{\beta\gamma\delta \cdots \varepsilon}$ is the tensor that reduces at the pole of a normal coordinate system to the n th partial derivative $\partial_{\delta \cdots \varepsilon} \Gamma^{\alpha}_{\beta\gamma}$ of the affine connection.

A normal coordinate system with pole z is one in which the coordinates of z are all zero and lines of the form $x^{\alpha}(u) = u X^{\alpha}$, X^{α} constant, are affinely parameterised geodesics through z . These lines therefore satisfy the geodesic equation

$$\frac{d^2 x^{\alpha}}{du^2} + \Gamma^{\alpha}_{\beta\gamma} \frac{dx^{\beta}}{du} \frac{dx^{\gamma}}{du} = 0. \quad (190)$$

Since also $d^n x^\alpha / du^n = 0$ for $n \geq 2$, differentiation of (190) n times shows that $X^\delta \cdots X^\varepsilon X^\beta X^\gamma \partial_{\delta \dots \varepsilon} \Gamma_{\beta\gamma}^\alpha = 0$. At z this must hold for all X^α , hence $\partial_{(\delta \dots \varepsilon} \Gamma_{\beta\gamma)}^\alpha = 0$ at z . Together with the definition of the normal tensors this shows that

$$N_{\cdot\beta\gamma\delta\dots\varepsilon}^\alpha = N_{\cdot(\beta\gamma)(\delta\dots\varepsilon)}^\alpha \quad \text{and} \quad N_{(\beta\gamma\delta\dots\varepsilon)}^\alpha = 0. \quad (191)$$

The curvature tensor is given in terms of the affine connection by

$$R_{\cdot\beta\gamma\delta}^\alpha = 2\partial_{[\delta} \Gamma_{\gamma]\beta}^\alpha + 2\Gamma_{\varepsilon[\delta}^\alpha \Gamma_{\gamma]\beta}^\varepsilon. \quad (192)$$

This, and successive covariant derivatives of it, evaluated at the pole of a normal coordinate system show that

$$\nabla_{\varepsilon\dots\zeta} R_{\cdot\beta\gamma\delta}^\alpha = 2N_{\cdot\beta[\gamma\delta]\varepsilon\dots\zeta}^\alpha + O(N^2) \quad (193)$$

where $O(N^2)$ denotes terms involving two or more normal tensors of lower order. Taken together with the first equation of (191), this enables any pair of indices of a normal tensor to be exchanged. If the symmetrisation in the second equation of (191) is expanded and the indices in each term rearranged in this way into a common order, it will give the n th normal tensor in terms of curvature terms and normal tensors of lower order. All normal tensors can then be evaluated successively in terms of the curvature tensor and its derivatives. With all lower indices, the first two are found to be

$$N_{\alpha\beta\gamma\delta} = \frac{2}{3} R_{\alpha(\beta\gamma)\delta} \quad \text{and} \quad N_{\alpha\beta\gamma\delta\varepsilon} = \frac{5}{6} \nabla_{(\delta} R_{\varepsilon)(\beta\gamma)\alpha} - \frac{1}{6} \nabla_{(\beta} R_{\gamma)(\delta\varepsilon)\alpha}. \quad (194)$$

The formula for the Christoffel connection gives

$$\partial_\gamma g_{\alpha\beta} = 2g_{\varepsilon(\alpha} \Gamma_{\beta)\gamma}^\varepsilon. \quad (195)$$

Evaluation of this and its partial derivatives at the pole of a normal coordinate system then gives the Veblen extensions of the metric tensor in terms of normal tensors, the first two being

$$g_{\alpha\beta,\gamma\delta} = 2N_{(\alpha\beta)(\gamma\delta)} = -\frac{2}{3} R_{\alpha(\gamma\delta)\beta}, \quad g_{\alpha\beta,\gamma\delta\varepsilon} = 2N_{(\alpha\beta)(\gamma\delta\varepsilon)} = -\nabla_{(\gamma} R_{\delta|\alpha\beta|\varepsilon)}. \quad (196)$$

Note that in the normal tensor expressions, the symmetrisation over the extension indices is not necessary and does not arise from (195). Even without this explicit symmetrisation the results must be symmetric in these indices as it has already been shown that the Veblen extensions have this property. Adding the explicit symmetrisation therefore does not affect the result and has the advantage of simplifying further evaluation with (194). Veblen extensions of other tensor fields can be similarly related to repeated covariant derivatives via normal tensors, but will not be needed here.

18 The Moment Definition Recast

It was seen in Sect. 4 that Mathisson's assumptions of analyticity made it impossible to deduce explicit expressions for the moments from his implicit definition of them through (51). Section 8 then showed that by modifying the defining equation into the form (54) the analyticity could be avoided and that this *would* enable explicit and unique expressions to be obtained for the moments as integrals of the energy-momentum tensor. But (54) was not the final definition. Motivated by a study of the variational equation, (54) was replaced by (80) which became the final form for the moment-defining equation.

Mathisson's orthogonality conditions were also modified as described in Sect. 11. All these changes mean that the methods of Sect. 8 can no longer be applied directly. The defining equation will now be recast into an equivalent form that *is* amenable to those methods.

Consider (80) now with a $\varphi_{\alpha\beta}$ that does not necessarily have the form (65). Let $\lambda_\alpha(s, x)$ be constructed from $\varphi_{\alpha\beta}$ as in Sect. 9, as the function that satisfies (66) along all geodesics through $z(s) \in L$ with initial conditions (71). Define

$$e_{\alpha\beta}(s, x) = \varphi_{\alpha\beta}(x) - \nabla_{(\alpha} \lambda_{\beta)}(s, x), \quad E_{\kappa\lambda} = \text{Exp}^\Lambda e_{\alpha\beta}. \quad (197)$$

Then with $\Phi_{\kappa\lambda}$ defined by (59) and Λ_κ by (72), (197) and (74) together give

$$\Phi_{\kappa\lambda} + G_{\kappa\lambda}^\mu \Lambda_\mu = E_{\kappa\lambda} + \nabla_{*(\kappa} \Lambda_{\lambda)}. \quad (198)$$

The defining equation (80) can therefore be put in the form

$$\int T^{\alpha\beta} \varphi_{\alpha\beta} \text{D}x = M^{\kappa\lambda} [E_{\kappa\lambda} + \nabla_{*(\kappa} \Lambda_{\lambda)}]. \quad (199)$$

The advantage of this version is that, as will be proved below, $E_{\kappa\lambda}$ necessarily has the form

$$E_{\kappa\lambda}(s, X) = X^\mu X^\nu E_{\kappa\mu\lambda\nu}(s, X) \quad (200)$$

for some $E_{\kappa\mu\lambda\nu}$ with the symmetry properties

$$E_{\kappa\mu\lambda\nu} = E_{[\kappa\mu][\lambda\nu]}, \quad E_{\kappa[\mu\lambda\nu]} = 0. \quad (201)$$

It follows from these that also $E_{\kappa\mu\lambda\nu} = E_{\lambda\nu\kappa\mu}$, so any $E_{\kappa\lambda}$ constructed from such an $E_{\kappa\mu\lambda\nu}$ by (200) is symmetric.

The Fourier transform of (200) gives

$$\tilde{E}_{\kappa\lambda}(s, k) = (-i)^2 g^{\mu\rho} g^{\nu\sigma} \nabla_{*\rho} \nabla_{*\sigma} \tilde{E}_{\kappa\mu\lambda\nu}(s, k) \quad (202)$$

so that from (55) and (93)

$$M^{\kappa\lambda}[E_{\kappa\lambda}] = \frac{1}{(2\pi)^4} \int_L ds \int Dk \tilde{J}^{\nu\mu\lambda\kappa}(s, k) \tilde{E}_{\nu\mu\lambda\kappa}(z(s), k) \quad (203)$$

where

$$\tilde{J}^{\nu\mu\lambda\kappa}(s, k) = \sum_{n \geq 0} \frac{(-i)^n}{n!} k_\sigma \cdots k_\rho J^{\sigma \cdots \rho \nu \mu \lambda \kappa}(s) \quad (204)$$

and as elsewhere, n is the number of indices in the set $\sigma \cdots \rho$. The fields $\tilde{J}^{\nu\mu\lambda\kappa}(s, k)$ and $\tilde{E}_{\nu\mu\lambda\kappa}(s, k)$ both have the same symmetry properties (201) as $E_{\nu\mu\lambda\kappa}(s, X)$, the former as a result of (94).

Due to the orthogonality condition (99) the method of Sect. 8 shows that the s -integrand of (203) depends on $E_{\nu\mu\lambda\kappa}$ only through its value on the hyperplane $n_\kappa X^\kappa = 0$ of $T_{z(s)}(M)$. If

$$e_{\delta\gamma\beta\alpha} = \text{Exp}_A E_{\nu\mu\lambda\kappa} \quad \text{so that } e_{\beta\alpha} = \sigma^\delta \sigma^\gamma e_{\beta\delta\alpha\gamma}, \quad (205)$$

this dependence translates as that on $e_{\delta\gamma\beta\alpha}(s, x)$ only through its value on the usual $\Sigma(s)$, as in (63).

The contribution $M^{\kappa\lambda}[\nabla_{*(\kappa}\Lambda_\lambda)]$ to the right hand side of (199) is given by (83). This has already been studied in Sect. 12, where it was found that only two terms survive in the series (84) for \tilde{t}^α due to (114). These terms still reduce to (104), and (105) and (106) still hold, giving

$$M^{\kappa\lambda}[\nabla_{*(\kappa}\Lambda_\lambda)] = \int \left(p^\kappa v^\lambda(s) \varphi_{\kappa\lambda}(z(s)) + S^{\kappa\lambda} v^\mu \nabla_\kappa \varphi_{\lambda\mu}(z(s)) \right) ds \quad (206)$$

in place of (107) since $\varphi_{\alpha\beta}$ no longer has the form (65) but $m^{\kappa\lambda}$ and $m^{\kappa\lambda\mu}$ have the forms (133) and (134).

The right hand side of (199) is therefore an s -integral whose integrand depends only on the values of $\varphi_{\beta\alpha}$ and $\nabla_\gamma \varphi_{\beta\alpha}$ at the point $z(s)$ and of $e_{\delta\gamma\beta\alpha}(s, x)$ on $\Sigma(s)$. This restricted dependence allows the methods of Sect. 8 to be used to evaluate all the moments as integrals of the energy-momentum tensor. This will be done explicitly for p^κ and $S^{\kappa\lambda}$ in the next section and for the higher moments in Sect. 24.

It remains to prove the existence of an $E_{\kappa\lambda\mu\nu}$ satisfying (200) and (201). The proof uses the results of Sect. 14 and is by construction, but for a given $E_{\kappa\lambda}$, $E_{\kappa\lambda\mu\nu}$ is not unique so no significance will be attached to the particular constructed value.

For a fixed s , let $x(u)$ be an affinely parameterised geodesic with $z(s) = x(0)$. Indices $\alpha, \beta, \gamma, \dots$ will refer to the generic point $x(u)$, so (142) gives $U^\alpha = u^{-1} \sigma^\alpha$ where $U^\alpha = dx^\alpha/du$ as in Sect. 14. Note first that

$$e_{\alpha\beta} = 0 \quad \text{at } x = z(s) \quad (207)$$

by (71) and that (66) applied to λ_κ can be put in the form

$$U^\beta U^\gamma \nabla_{\{\beta} e_{\alpha\gamma\}} = 0 \quad (208)$$

where curly brackets around three indices are defined by (67). Multiplication of (208) by U^α shows that $U^\alpha U^\beta e_{\alpha\beta}$ is constant along these geodesics and the initial condition (207) then shows its value is zero. By (142) this gives

$$\sigma^\alpha \sigma^\beta e_{\alpha\beta} = 0. \quad (209)$$

Differentiation of (209) and use of (208) shows that

$$\sigma^\alpha \sigma^\beta \nabla_\alpha e_{\beta\gamma} + \sigma^\alpha_{\cdot\gamma} \sigma^\beta e_{\alpha\beta} = 0. \quad (210)$$

If this is multiplied by $u^{-1} H^\gamma_{\cdot\kappa}$, use of

$$\frac{\delta}{du} (u H^\alpha_{\cdot\kappa}) = H^\gamma_{\cdot\kappa} \sigma^\alpha_{\cdot\gamma} \quad (211)$$

enables the result to be put in the form

$$\frac{\delta}{du} (H^\gamma_{\cdot\kappa} \sigma^\beta e_{\beta\gamma}) = 0. \quad (212)$$

The formula (211) follows from (147) on differentiation of $H^\alpha_{\cdot\kappa}$ as a matrix inverse. It follows that $H^\gamma_{\cdot\kappa} \sigma^\beta e_{\beta\gamma}$, which is a vector at z and scalar at x , is constant as x varies along any geodesic through z . As it vanishes at z , it therefore vanishes everywhere, so that

$$\sigma^\beta e_{\alpha\beta}(s, x) = 0 \quad \text{for all } x \quad (213)$$

from which

$$X^\mu E_{\mu\lambda}(s, X) = 0. \quad (214)$$

Differentiation of (214) gives

$$E_{\kappa\lambda}(s, X) = -X^\mu [\nabla_{*\kappa} E_{\mu\lambda}]_{(s, X)}. \quad (215)$$

But also

$$\frac{d}{du} E_{\kappa\lambda}(s, uX) = X^\mu [\nabla_{*\mu} E_{\kappa\lambda}]_{(s, uX)} \quad (216)$$

where u is a scalar parameter, which together with (215) gives

$$\frac{d}{du} (u E_{\kappa\lambda}(s, uX)) = 2u X^\mu [\nabla_{*[\mu} E_{\kappa]\lambda}]_{(s, uX)}. \quad (217)$$

Iterating this result for the second index of $E_{\kappa\lambda}$ shows that

$$\frac{d^2}{du^2} (u E_{\kappa\lambda}(s, uX)) = 4u X^\mu X^\nu [\nabla_{*[\mu} \nabla_{*[\nu} E_{\kappa]\lambda}]]_{(s, uX)}. \quad (218)$$

Since both $u E_{\kappa\lambda}(s, uX) = 0$ and $d(u E_{\kappa\lambda}(s, uX))/du = 0$ at $u = 0$, (218) can be integrated to give (200) with

$$E_{\kappa\mu\lambda\nu}(s, X) = 4 \int_0^1 u(1-u) [\nabla_{*[\mu} \nabla_{*[\nu} E_{\kappa]\lambda}]]_{(s, uX)} du \quad (219)$$

which satisfies the symmetry properties (201) identically. The existence proof is now complete.

19 Momentum and Spin as Integrals

By (63) the integration on the left hand side of (199) can be split into one over $\Sigma(s)$ followed by one over s . If (197) is used in the $\Sigma(s)$ integration, this gives

$$\int T^{\alpha\beta} \varphi_{\alpha\beta} Dx = \int_L ds \int_{\Sigma(s)} T^{\alpha\beta} (e_{\alpha\beta}(s, x) + \nabla_{(\alpha} \lambda_{\beta)}(s, x)) w^\gamma d\Sigma_\gamma \quad (220)$$

where, as in Sect. 8, w^γ is any vector field such that $w^\gamma \nabla_\gamma \tau = 1$ with $\tau(x)$ being the scalar function such that $\tau(x) = s$ if $x \in \Sigma(s)$. Now the forms obtained in the previous section for the two terms of the right hand side of (199) no longer involve λ_α . It should therefore be possible to eliminate it also from (220). To do so, put

$$\nu_\alpha(x) = \lambda_\alpha(\tau(x), x). \quad (221)$$

Then

$$\nabla_\beta \nu_\alpha = \nabla_\beta \lambda_\alpha + \nabla_\beta \tau \left[\frac{\partial \lambda_\alpha}{\partial s} \right]_{(s=\tau(x))}. \quad (222)$$

If this is used in (220) then the term with $\nabla_\beta \nu_\alpha$ can be converted back to an integration over all space and integrated by parts, when it vanishes by the covariant conservation equation (3). Also $\nabla_\beta \tau w^\gamma d\Sigma_\gamma = d\Sigma_\beta$ since $\nabla_\beta \tau$ and $d\Sigma_\beta$ are parallel and $w^\gamma \nabla_\gamma \tau = 1$. With this, (220) becomes

$$\int T^{\alpha\beta} \varphi_{\alpha\beta} Dx = \int_L ds \left(\int T^{\alpha\beta} e_{\alpha\beta} w^\gamma d\Sigma_\gamma - \int T^{\alpha\beta} \frac{\partial \lambda_\alpha}{\partial s} d\Sigma_\beta \right). \quad (223)$$

This does not yet eliminate λ_α but it will now be shown that $\partial \lambda_\alpha / \partial s$ can be evaluated on $\Sigma(s)$ from $e_{\alpha\beta}$ on that hypersurface, taken together with suitable initial

conditions. Since $\varphi_{\alpha\beta}(x)$ is independent of s , differentiation of (197) with respect to s shows that

$$\frac{\partial e_{\alpha\beta}}{\partial s} = -\nabla_{(\alpha} \frac{\partial \lambda_{\beta)}}{\partial s}. \quad (224)$$

This has the same form as (65), so by analogy with (66),

$$\frac{\delta^2}{du^2} \left(\frac{\partial \lambda_\alpha}{\partial s} \right) + \frac{\partial \lambda_\beta}{\partial s} \dot{x}^\gamma \dot{x}^\delta R^\beta_{\cdot\gamma\delta\alpha} = -\dot{x}^\beta \dot{x}^\gamma \nabla_{\{\beta} \frac{\partial e_{\alpha\gamma\}}{\partial s} \quad (225)$$

holds along all geodesics through $z(s)$. The initial conditions follow by differentiating (71) with respect to s . As $\lambda_\kappa(s, z(s))$ has two dependencies on s , this gives

$$\frac{\partial \lambda_\kappa}{\partial s} + v^\lambda \nabla_\lambda \lambda_\kappa = 0 \quad (226)$$

and

$$\nabla_\kappa \left(\frac{\partial \lambda_\lambda}{\partial s} \right) + v^\mu \nabla_{\mu\kappa} \lambda_\lambda = v^\mu \nabla_\mu \varphi_{\kappa\lambda} \quad (227)$$

at $x = z(s)$, which with (71) and (106) can be put in the form

$$\frac{\partial \lambda_\kappa}{\partial s} = a_\kappa, \quad \nabla_\kappa \left(\frac{\partial \lambda_\lambda}{\partial s} \right) = b_{\kappa\lambda} \quad (228)$$

where

$$a_\kappa(s) = -v^\lambda \varphi_{\kappa\lambda}(z(s)), \quad b_{\kappa\lambda}(s) = -2v^\mu \nabla_{[\kappa} \varphi_{\lambda]\mu}(z(s)). \quad (229)$$

This appears at first not to meet the need as $\partial e_{\alpha\beta}/\partial s$ cannot be evaluated from $e_{\alpha\beta}$ on $\Sigma(s)$ alone. However, $\sigma^\beta \partial e_{\alpha\beta}/\partial s$ is determined by $e_{\alpha\beta}$ on $\Sigma(s)$ as is seen by differentiating (213) and this enables the full right hand side of (225) to be evaluated. So $\partial \lambda_\alpha/\partial s$ can be determined on $\Sigma(s)$ from an equation that only requires knowing $e_{\delta\gamma\beta\alpha}(s, x)$ on this hypersurface, together with initial conditions that only require $\varphi_{\kappa\lambda}$ and $\nabla_\kappa \varphi_{\lambda\mu}$ at $z(s)$, all of which occur also in the two parts (203) and (206) of the right hand side of (199).

To match, for its left hand side, the separation of terms made by (203) and (206) for the right hand side of (199), it is necessary to split the calculated $\partial \lambda_\alpha/\partial s$ into two parts according to the data on which they depend. Let $\psi_\alpha(s, x)$ be the solution of (225) corresponding to initial conditions (228) with $a_\kappa = 0$ and $b_{\kappa\lambda} = 0$. This is determined by $e_{\alpha\beta}(s, x)$ alone. The difference between this and $\partial \lambda_\alpha/\partial s$ is a solution of (225) with the right hand side set to zero, i.e., a solution of the geodesic deviation equation determined by the initial conditions (228) with (229). That solution is given by (167). Putting both parts back into (223) gives

$$\int T^{\alpha\beta} \varphi_{\alpha\beta} Dx = \int_L ds \left(\int \left(T^{\alpha\beta} e_{\alpha\beta} w^\gamma - T^{\alpha\gamma} \psi_\alpha \right) d\Sigma_\gamma \right. \\ \left. + p^\kappa v^\lambda \varphi_{\kappa\lambda} + S^{\kappa\lambda} v^\mu \nabla_\kappa \varphi_{\lambda\mu} \right) \quad (230)$$

where

$$p^\kappa(s) = \int_{\Sigma(s)} K_\alpha^{\cdot\kappa} T^{\alpha\beta} d\Sigma_\beta, \quad S^{\kappa\lambda}(s) = 2 \int_{\Sigma(s)} H_\alpha^{[\kappa} \sigma^{\lambda]} T^{\alpha\beta} d\Sigma_\beta. \quad (231)$$

It follows that the defining equation (199) holds if, separately,

$$M^{\kappa\lambda}[E_{\kappa\lambda}] = \int ds \int_{\Sigma(s)} \left(T^{\alpha\beta} e_{\alpha\beta} w^\gamma - T^{\alpha\gamma} \psi_\alpha \right) d\Sigma_\gamma \quad (232)$$

and

$$M^{\kappa\lambda}[\nabla_{*(\kappa} \Lambda_{\lambda)}] = \int ds \left(p^\kappa v^\lambda \varphi_{\kappa\lambda} + S^{\kappa\lambda} v^\mu \nabla_\kappa \varphi_{\lambda\mu} \right), \quad (233)$$

while (203) and (205) show that (232) itself holds if

$$\int_{\Sigma(s)} \left(\sigma^{[\delta} T^{\alpha][\beta} \sigma^{\varepsilon]} e_{\alpha\delta\beta\varepsilon} w^\gamma - T^{\alpha\gamma} \psi_\alpha \right) d\Sigma_\gamma = \\ \frac{1}{(2\pi)^4} \int Dk \tilde{J}^{\nu\mu\lambda\kappa}(s, k) \tilde{E}_{\nu\mu\lambda\kappa}(s, k). \quad (234)$$

This latter equation is the true equivalent for the revised moment definitions of (64) for the original ones. Both sides depend on $e_{\alpha\beta\gamma\delta}(s, x)$ only through its value on $\Sigma(s)$. As seen in principle in Sect. 8, quadrupole and higher moments J^{\dots} therefore exist that satisfy (234) and expressions can be deduced for them as explicit integrals of $T^{\alpha\beta}$ over $\Sigma(s)$. Moreover, comparison of (233) with (206) shows that they have identical forms, so that (231) gives possible explicit integral expressions for the momentum p^κ and spin $S^{\kappa\lambda}$ constructed from the monopole and dipole moments by (133) and (134).

This shows that moments exist which satisfy the defining equation (199) and that explicit expressions can be obtained for all of them as integrals of the energy-momentum tensor. It does not, however, prove their uniqueness. Such a proof requires (232)–(234) to be *deduced* from (199) rather than being seen as just one possibility. The barrier to this deduction is that the expressions so far obtained for the two sides of (199) assume that $\varphi_{\alpha\beta}$ has been chosen arbitrarily and that $e_{\alpha\beta\gamma\delta}$ has been constructed from it. This is appropriate for the form (80) of the defining equation, but in (199) with (230) it is $e_{\alpha\beta\gamma\delta}(s, x)$ rather than $\varphi_{\alpha\beta}$ that serves as test function in the functionals concerned. A proof of uniqueness therefore requires it to be $e_{\alpha\beta\gamma\delta}(s, x)$ that is freely specifiable on each $\Sigma(s)$, or equivalently $e_{\alpha\beta\gamma\delta}(\tau(x), x)$ to be freely specifiable on M .

This will be taken up again in Sect. 23 and explicit integrals for the higher moments will be derived in Sect. 24, but there is one remaining aspect of uniqueness that can be dealt with now. The momentum and spin variables in (233) and (206) were identified with one another merely by similarity of form. The methods of Sect. 12 will now be used to prove that they are indeed the same. With the notation of (116) the projection procedure of Sect. 12 shows that

$$Q_{\nu}^{\cdot\kappa} \bar{S}^{\nu(\lambda} v^{\mu)} = 0 \quad (235)$$

where barred variables denote the difference between the two versions of the corresponding unbarred ones. This shows that $Q_{\nu}^{\cdot\kappa} \bar{S}^{\nu\lambda} = 0$. As $\bar{S}^{\nu\lambda}$ is antisymmetric it therefore vanishes with a projection by $Q_{\nu}^{\cdot\kappa}$ on either index, and for the same reason also with a projection by $P_{\nu}^{\cdot\kappa}$ on both indices. It follows that $\bar{S}^{\kappa\lambda} = 0$ so the two versions of $S^{\kappa\lambda}$ are equal. It then follows immediately that the two versions of p^{κ} are also equal.

The two-point tensors $K_{\alpha}^{\cdot\kappa}$ and $H_{\alpha}^{\cdot\kappa}$ both reduce to the unit tensor in a Minkowskian coordinate system in flat spacetime. The expressions (231) for momentum and spin therefore agree with the corresponding quantities defined by (26) and (27) in such a spacetime. This adds yet further support to their identification as the momentum and spin of the body.

Note that for a given world line L , the values of p^{κ} and $S^{\kappa\lambda}$ depend, through the construction of $\Sigma(s)$, on the choice of vector field n^{κ} along L . This is so even though this field enters the moment definitions only through orthogonality relations for the octopole and higher moments. This illustrates how sensitive the values of even the lower moments are to details of the full set of moment definitions.

20 Conserved Quantities

There is one crucial difference for the momentum and spin integrals between the situations in flat and curved spacetime. In a flat spacetime, where there are no gravitational forces, they were defined with respect to a spacelike hypersurface Σ and a point z not necessarily on Σ but were then shown to be independent of the choice of Σ . In physical terms they are conserved quantities. The definitions in curved spacetime can similarly be made with any such Σ replacing the specific $\Sigma(s)$ of (231), but then they *do* depend on the choice of Σ .

It will now be shown that whenever the spacetime admits a symmetry, there is a corresponding linear combination of components of the momentum and spin integrals that does have this independence from the choice of Σ . Flat spacetime is simply a special case in which there are as many symmetries, namely ten, as there are components of momentum and spin, so each component is conserved separately.

A spacetime symmetry corresponds to the existence of a Killing vector field ω_{α} . By (167) its value at any point x is given in terms of its value, and that of its first derivative, at any other point z by

$$\omega_\alpha = K_\alpha{}^\kappa \omega_\kappa + H_\alpha{}^\kappa \sigma^\lambda \nabla_\kappa \omega_\lambda. \quad (236)$$

Hence

$$\int_\Sigma T^{\alpha\beta} \omega_\alpha d\Sigma_\beta = p^\kappa \omega_\kappa + \frac{1}{2} S^{\kappa\lambda} \nabla_\kappa \omega_\lambda \quad (237)$$

for all points z and all spacelike hypersurfaces Σ that extend through the body. Here Σ is to be used instead of the prescribed $\Sigma(s)$ in the integrals (231) for p^κ and $S^{\kappa\lambda}$.

The difference between the value of the left hand side for two different choices of Σ can be converted to a volume integral that vanishes in virtue of the Killing equation and the covariant conservation equation for $T^{\alpha\beta}$. Its value is therefore independent of the hypersurface Σ of integration, so this is true also of the right hand side. This is therefore a linear combination of components of momentum and spin that is conserved in virtue of the spacetime symmetry, as required. For any choice of z on L , Σ can be taken to be the $\Sigma(s)$ used in (231). This linear combination is therefore constant along L when taken with the precise expressions (231) that occur in the equations of motion, which is perhaps a more natural interpretation of a conserved quantity.

An alternative view of this conservation property comes from the motion of z along L . The right hand side of (237) is constant as z moves, and differentiation of it with respect to s shows with (135) and (136) that

$$F^\kappa \omega_\kappa + \frac{1}{2} L^{\kappa\lambda} \nabla_\kappa \omega_\lambda = 0. \quad (238)$$

Each spacetime symmetry therefore leads to a component of the force and torque vanishing.

These results may seem so obvious as to be hardly worthy of mention. They are not really obvious, though, they are merely expected. Their truth with the definitions of momentum, spin, force and torque given here provides a sensitive test of those definitions. By way of illustration, it may have seemed more in keeping with Newtonian mechanics and special relativity to have defined the force by $\delta p^\kappa / ds = F^\kappa$, so treating the “spin-curvature interaction” term in (135) as a contribution to the force. Had this been done, a spacetime symmetry would no longer have led to the vanishing of a component of force and torque.

Now consider the expressions (231) in a flat spacetime. This has ten linearly independent Killing vector fields, so the force and torque vanish identically. Also, for a fixed point z , the values of p^κ and $S^{\kappa\lambda}$ are independent of the hypersurface of integration and therefore, for a given z , independent of the vector n^α that determines the hypersurface used in (231). By letting z vary they can therefore be considered as well defined fields on the spacetime manifold.

This is all true also for a spacetime of constant curvature, which provides another useful testbed for the definitions. In such a spacetime the curvature tensor has the form

$$R_{\alpha\beta\gamma\delta} = k(g_{\alpha\gamma}g_{\beta\delta} - g_{\alpha\delta}g_{\beta\gamma}) \quad (239)$$

where k is constant, so (135) and (136) reduce to

$$v^\lambda \nabla_\lambda p_\kappa = k v^\lambda S_{\kappa\lambda}, \quad v^\mu \nabla_\mu S_{\kappa\lambda} = 2 v^\mu p_{[\kappa} g_{\lambda]\mu}. \quad (240)$$

Since the choice of L is so far unspecified, this holds for all v^λ , giving

$$\nabla_\lambda p_\kappa = k S_{\kappa\lambda}, \quad \nabla_\mu S_{\kappa\lambda} = 2 p_{[\kappa} g_{\lambda]\mu}. \quad (241)$$

In a flat spacetime $k = 0$. In a Minkowskian coordinate system the first of these shows that p_κ is constant. The second is then trivially integrated to show that dependence of $S^{\kappa\lambda}$ on z has the form (34). When k is nonzero, (241) shows that $\nabla_{(\lambda} p_{\kappa)} = 0$ and hence that p^κ is a Killing vector field. Given this field, the first of (241) determines the field $S^{\kappa\lambda}$ which then satisfies the second equation as a result of (239). It follows that any Killing vector field p^κ determines an $S^{\kappa\lambda}$ which, taken together, satisfy (240) and therefore the equations of motion (135) and (136) along any choice of world line L . So as in the case of flat spacetime, p^κ and $S^{\kappa\lambda}$ can take any values at a single point z . The first of (241) gives $\nabla_\lambda p_\kappa$ at that point, (167) then gives p_κ everywhere from which $S^{\kappa\lambda}$ is determined everywhere by a second use of (241).

21 Centre of Mass

Although they have been referred to frequently as equations of motion, (135) and (136) are in fact only evolution equations. They describe how p^κ and $S^{\kappa\lambda}$ vary as the point z moves along an arbitrarily chosen timelike world line L . They become equations that describe the motion of the body only when a supplementary condition is given that determines L uniquely, preferably in a way that enables it to be considered as the world line of the centre of mass of the body. The problem of uniqueness was the final issue identified in Sect. 4 as arising from Mathisson's paper of 1937.

Section 5 identified a pointer towards the type of supplementary condition that would determine L uniquely. This was to use $p_\lambda S^{\kappa\lambda} = 0$ in place of Mathisson's choice $v_\lambda S^{\kappa\lambda} = 0$ that seems natural but which fails the uniqueness test. The big question this left unanswered was what definitions to use for momentum p^κ and spin $S^{\kappa\lambda}$ as they are not directly tensors within the moment set defined by (1) or its successors. Suitable quantities may be identified as constructs from the moments at any level of multipole approximation. These may provide uniqueness in that approximation but they do not provide a satisfactory definition of centre of mass, for two reasons. One is that there is an element of arbitrariness in the choice of constructs, the other is that the definition will change when higher multipole moments are retained.

It was seen in Sect. 13 that when the variational equation is solved exactly, $m^{\kappa\lambda}$ and $m^{\mu\kappa\lambda}$ have forms given by (133) and (134) that give precise definitions of p^κ and $S^{\kappa\lambda}$ within the moment scheme. Exact and uniquely determined integral expressions (231) were found for these in Sect. 19 where it was seen that in a flat spacetime they reduce to the generally accepted definitions (26) and (27) of momentum and spin in special

relativity. They are therefore the natural candidates to adopt in a supplementary condition $p_\lambda S^{\kappa\lambda} = 0$. But making this precise is not entirely straightforward. The tensors p^κ and $S^{\kappa\lambda}$ can be defined by (231) with respect to any base point z and timelike unit vector n^κ at z by taking, as before, $\Sigma(s)$ to be formed from all geodesics through z orthogonal to n^κ , but both tensors depend on both z and n^κ .

A two-stage process is therefore needed. First consider p^κ as a function of z and the vector n^κ , and for any z choose n^κ at z so that p^κ and n^κ are parallel, i.e.,

$$n^{[\kappa} p^{\lambda]}(z, n) = 0. \quad (242)$$

This is an implicit equation that can be solved by iteration. With any initial choice $n^\kappa = n_{(0)}^\kappa$, take $n_{(i+1)}^\kappa$ to be the unit vector parallel to $p^\kappa(z, n_{(i)})$. It is plausible that this process converges, at least for weak gravitational fields, as only one iteration is required in flat spacetime. Then with this choice of $n^\kappa(z)$, p^κ and $S^{\kappa\lambda}$ can be considered as functions of z alone. The line L can now be defined as the locus of points that satisfy

$$p_\lambda(z) S^{\kappa\lambda}(z) = 0. \quad (243)$$

Again it is plausible that this determines a unique L , at least for weak gravitational fields.

A set of sufficient conditions for this to be so has been given by Schattner [36, 37] where uniqueness is proved by use of a fixed point theorem for mappings. A definition with a two-stage process of this nature for an extended body was first given by the present author in [22] with different expressions for p^κ and $S^{\kappa\lambda}$, and with the present expressions by him in [27].

Support for this definition is provided by a test body in a spacetime of constant curvature. It was seen in the previous section that in this case p^κ and $S^{\kappa\lambda}$ are well defined functions of z that are independent of the choice of n^κ . This makes the solution of (242) be trivial. As in flat spacetime, only one iteration is required. By (241), (243) is equivalent to

$$p^\lambda \nabla_\lambda p^\kappa = 0. \quad (244)$$

It follows, with (241), that $p^\mu \nabla_\mu (p^\lambda \nabla_\lambda p^\kappa) = 0$ wherever (244) holds, so if (244) holds at a point then it holds also along the orbit of p^κ through that point. This orbit is therefore a solution for the desired world line L as (243) holds everywhere along it. By (244) that orbit is also a geodesic. It is *the* solution for L provided the solution is unique, a point which will be returned to in the next section where it will be seen that there is an exceptional case where uniqueness fails. This case corresponds to circumstances that cannot be physically realised, but its existence shows the need for conditions such as those of Schattner in order for uniqueness to be proved.

For a test body in a spacetime of constant curvature, the above definitions therefore lead to the world line of the centre of mass being a geodesic. Again this is to be expected since the force and torque have already been seen to vanish, but its truth is

a sensitive test of the definition of centre of mass. Note also that v^κ is parallel to p^κ so that also $v_\lambda S^{\kappa\lambda} = 0$ on L . The difference between the two conditions, however, is that the second one does not determine a unique world line but the first one does so, other than in physically unrealistic circumstances.

22 The Momentum-Velocity Relation

With L chosen as the world line of the centre of mass, the velocity $v^\kappa \equiv dz^\kappa/ds$ becomes determined by the motion of the body. It therefore becomes meaningful to ask how it is related to the momentum p^κ . The occurrence of v^κ in (135) and (136) is sufficiently involved that it is remarkable that an explicit solution can be found. Nevertheless there is such a solution, due to Ehlers and Rudolph [38].

Recall first that the entire development so far has left the choice of parameter s on L arbitrary, so v^κ is not necessarily a unit vector. Changing the parametrisation does not affect the form of the equations of motion (135) and (136), it only changes the force and torque F^κ and $L^{\kappa\lambda}$ by a scale factor. Several aspects of the development from these equations are simplified by choosing s not to be proper time along L but instead such that

$$n_\kappa v^\kappa = 1. \quad (245)$$

This corresponds to choosing ds , at each point of L , to be the elapsed time interval in the frame in which the 3-momentum is zero, even though the mass centre itself is moving in this frame. With this choice v^κ can be called the *kinematical velocity* and n^κ the *dynamical velocity* of the body, and it will be adopted in this section only.

With (242) in mind, define the mass $M(s)$ of the body by

$$M^2 = p^\kappa p_\kappa \quad \text{so that} \quad p^\kappa = M n^\kappa. \quad (246)$$

Note that $\delta(p_\lambda S^{\kappa\lambda})/ds = 0$ since (243) holds along L . Expand the derivative and use (135) and (136) to give

$$M^2(v^\kappa - h^\kappa) = S^{\kappa\lambda} W_\lambda \quad (247)$$

where

$$h^\kappa = n^\kappa + M^{-1} L^{\kappa\lambda} n_\lambda \quad (248)$$

and

$$W_\lambda = F_\lambda + \frac{1}{2} v^\rho S^{\mu\nu} R_{\lambda\rho\mu\nu}. \quad (249)$$

Now eliminate v^κ between (247) and (249) and multiply the result by $S^{\kappa\lambda}$ to give

$$S^{\kappa\lambda} W_\lambda = S^{\kappa\lambda} (F_\lambda + \frac{1}{2} h^\rho S^{\mu\nu} R_{\lambda\rho\mu\nu}) + \frac{1}{2} M^{-2} S^{\kappa[\lambda} S^{\rho]\sigma} S^{\mu\nu} W_\sigma R_{\lambda\rho\mu\nu}. \quad (250)$$

It follows from (243) that $S^{\kappa\lambda}$ has matrix rank at most 2, since it cannot have rank 3 in virtue of its antisymmetry. Hence $S^{[\kappa\lambda}S^{\rho]\sigma} = 0$, from which $2S^{\kappa[\lambda}S^{\rho]\sigma} = S^{\rho\lambda}S^{\kappa\sigma}$. If this is used in (250), it gives a linear equation for $S^{\kappa\lambda}W_\lambda$. When the solution is substituted into (247) it yields

$$(M^2 + \frac{1}{4}R_{\lambda\mu\nu\rho}S^{\lambda\mu}S^{\nu\rho})(v^\kappa - h^\kappa) = S^{\kappa\lambda}(F_\lambda + \frac{1}{2}R_{\lambda\mu\nu\rho}h^\mu S^{\nu\rho}) \quad (251)$$

which is the required result. The solution for v^κ satisfies the normalisation condition (245) since $n_\kappa h^\kappa = 1$, $n_\kappa S^{\kappa\lambda} = 0$.

It was seen in Sect. 20 that F^κ and $L^{\kappa\lambda}$ both vanish for a test body in a spacetime of constant curvature, where the curvature tensor has the form (239). The right hand side of (251) is then zero in virtue of (243). It follows that $v^\kappa = n^\kappa$ unless $M^2 + kS^2 = 0$, where S is the magnitude of the spin defined by $S^2 = (S^{\kappa\lambda}S_{\kappa\lambda})/2$. In this exceptional case (251) is satisfied identically so v^κ cannot be determined.

This confirms the result in the previous section that in such a spacetime the centre of mass follows a geodesic path with just one exception, the case $M^2 + kS^2 = 0$. This requires the spacetime to be of constant negative curvature, of radius R where $k = -R^{-2}$, and the body to be such that $S = MR$. Such a body has a size comparable with the radius of the universe, rotating at a speed comparable with that of light, so it is not physically realisable. As a mathematical case, however, it does genuinely give rise to non-uniqueness of the world line of the centre of mass as defined in the previous section. It was shown in [27] that in this case the points satisfying (242) and (243) form a timelike two-dimensional surface. The world line L can therefore be any timelike line in this surface, so v^κ really is indeterminate. This surface also contains a two-parameter family of timelike geodesics so the conclusion of the previous section that there are geodesic solutions was also correct, even in this exceptional case.

23 Uniqueness of the Moments

It was seen in Sect. 19 that to draw conclusions from the form (199) of the moment defining equation, $e_{\delta\gamma\beta\alpha}(s, x)$ needs to be freely specifiable on $\Sigma(s)$ for each s . This is needed in order to deduce (232)–(234) and then to extract unique integral expressions for the higher moments from the last of these. This issue was left open in Sect. 19. It will now be shown that for any choice of $e_{\delta\gamma\beta\alpha}(s, x)$ there exists a $\varphi_{\alpha\beta}(x)$ consistent with this choice, i.e., such that the $e_{\alpha\beta}(s, x)$ constructed from $\varphi_{\alpha\beta}(x)$ by (197) and that constructed from $e_{\delta\gamma\beta\alpha}(s, x)$ by (205) are equal on each $\Sigma(s)$. With this in hand, the uniqueness proof will then be completed.

The proof of existence is by construction. Let variables chosen *ab initio* and others used in the construction of $\varphi_{\alpha\beta}$ be marked with hats and those constructed from it be unhatted, as above. The requirement is to prove that the relevant hatted and unhatted variables are equal on the hypersurfaces $\Sigma(s)$. So assume now that a tensor field $\hat{e}_{\delta\gamma\beta\alpha}(s, x)$ is freely chosen on each $\Sigma(s)$, subject only to symmetry properties

$$\hat{e}_{\delta\gamma\beta\alpha} = \hat{e}_{[\delta\gamma][\beta\alpha]}, \quad \hat{e}_{\delta[\gamma\beta\alpha]} = 0. \quad (252)$$

Take the parameters \hat{a}_κ and $\hat{b}_{\kappa\lambda}$ to be zero. For each s , extend $\hat{e}_{\delta\gamma\beta\alpha}(s, x)$ smoothly away from $\Sigma(s)$ and set

$$\hat{e}_{\beta\alpha}(s, x) = \sigma^\delta \sigma^\gamma \hat{e}_{\beta\delta\alpha\gamma}(s, x). \quad (253)$$

Then $\hat{e}_{\beta\alpha}$ is symmetric,

$$\hat{e}_{\beta\alpha}(s, x) = 0, \quad \nabla_\gamma \hat{e}_{\beta\alpha}(s, x) = 0, \quad \frac{\partial \hat{e}_{\beta\alpha}}{\partial s}(s, x) = 0 \quad \text{at } x = z(s) \quad (254)$$

$$\text{and } \sigma^\beta \hat{e}_{\beta\alpha}(s, x) = 0 \quad \text{identically.} \quad (255)$$

Solve the hatted (225) with (228) along all geodesics through $z(s)$ to give $\partial \hat{\lambda}_\alpha / \partial s$ for x both on and off $\Sigma(s)$. With initial condition $\hat{\lambda}_\alpha(s, x) = 0$ for $x \in \Sigma(s)$, integrate the calculated $\partial \hat{\lambda}_\alpha / \partial s$ to give $\hat{\lambda}_\alpha(s, x)$ for all s and x . By (221), this construction gives $\hat{\nu}_\alpha(x) = 0$ for all x and since $\hat{a}_\kappa = 0$ and $\hat{b}_{\kappa\lambda} = 0$, (228) with (222) and its derivative give

$$\nabla_\beta \hat{\lambda}_\alpha(s, x) = 0, \quad \nabla_{\gamma\beta} \hat{\lambda}_\alpha(s, x) = 0 \quad \text{at } x = z(s). \quad (256)$$

Define

$$\hat{\varphi}_{\alpha\beta}(s, x) = \hat{e}_{\alpha\beta}(s, x) + \nabla_{(\alpha} \hat{\lambda}_{\beta)}(s, x) \quad (257)$$

which from (254) and (256) satisfies

$$\hat{\varphi}_{\alpha\beta}(s, x) = 0 \quad \text{and} \quad \nabla_\gamma \hat{\varphi}_{\alpha\beta}(s, x) = 0 \quad \text{at } x = z(s). \quad (258)$$

Then the required $\varphi_{\alpha\beta}$ is given by

$$\varphi_{\alpha\beta}(x) = \hat{\varphi}_{\alpha\beta}(\tau(x), x) \quad (259)$$

from which

$$\nabla_\alpha \varphi_{\beta\gamma}(x) = \nabla_\alpha \hat{\varphi}_{\beta\gamma}(\tau(x), x) + \nabla_\alpha \tau \frac{\partial \hat{\varphi}_{\beta\gamma}}{\partial s}(\tau(x), x). \quad (260)$$

It follows from (257) that

$$\frac{\partial \hat{\varphi}_{\alpha\beta}}{\partial s}(s, x) = \frac{\partial \hat{e}_{\alpha\beta}}{\partial s}(s, x) + \nabla_{(\alpha} \frac{\partial \hat{\lambda}_{\beta)}}{\partial s}(s, x). \quad (261)$$

Both terms on the right hand side vanish when $x = z(z)$, the first by (254) and the second by (228) since $\hat{b}_{\kappa\lambda} = 0$. So

$$\frac{\partial \hat{\varphi}_{\alpha\beta}}{\partial s}(s, x) = 0 \quad \text{at } x = z(s) \quad (262)$$

which with (258) to (260) gives

$$\varphi_{\alpha\beta}(x) = 0 \quad \text{and} \quad \nabla_\gamma \varphi_{\alpha\beta}(x) = 0 \quad \text{at } x = z(s). \quad (263)$$

It follows from (229) that $a_\kappa = 0$ and $b_{\kappa\lambda} = 0$ in agreement with the assumed values for their hatted counterparts.

There is now a complete parallel with (197), and with (66) as applied to λ_α , under the correspondence

$$e_{\alpha\beta} \rightarrow \frac{\partial \hat{\varphi}_{\alpha\beta}}{\partial s}, \quad \varphi_{\alpha\beta} \rightarrow \frac{\partial \hat{e}_{\alpha\beta}}{\partial s}, \quad \lambda_\alpha \rightarrow -\frac{\partial \hat{\lambda}_\alpha}{\partial s} \quad (264)$$

with the conditions (207) and (262) also corresponding. The $\varphi_{\alpha\beta}$ of (66) admittedly does not depend on s while its corresponding quantity does so, but s is not varied in (66) so this is immaterial. The steps leading to (213) remain valid under this correspondence, giving

$$\sigma^\beta \frac{\partial \hat{\varphi}_{\alpha\beta}}{\partial s} = 0 \quad \text{for all } x \quad (265)$$

which with (260) shows that

$$\sigma^\beta \sigma^\gamma \nabla_{\{\beta} \varphi_{\alpha\gamma\}}(x) = \sigma^\beta \sigma^\gamma \nabla_{\{\beta} \hat{\varphi}_{\alpha\gamma\}}(s, x) \quad \text{for } x \in \Sigma(s). \quad (266)$$

Differentiation of (255) shows that

$$\sigma^\beta \sigma^\gamma \nabla_{\{\beta} \hat{e}_{\alpha\gamma\}} = 0. \quad (267)$$

This is the hatted version of (208), which was there seen to be equivalent to (66) for λ_α , and (257) is the hatted version of (197). It follows that $\hat{\lambda}_\alpha$ satisfies (66) with $\hat{\varphi}_{\alpha\beta}$ replacing $\varphi_{\alpha\beta}$. But unhatted λ_α is constructed by solving (66) with unhatted $\varphi_{\alpha\beta}$ along all geodesics through $z(s)$. The hatted and unhatted right hand sides of (66) are equal on $\Sigma(s)$ by (266), so $\hat{\lambda}_\alpha$ and λ_α satisfy exactly the same equation along all geodesics in $\Sigma(s)$ through $z(s)$. The initial conditions are the same, too, since $\hat{\lambda}_\kappa(s, z(s))$ and $\nabla_\lambda \hat{\lambda}_\kappa(s, z(s))$ both vanish, the first by construction and the second by (256), and their unhatted counterparts vanish by (71) with (263). The solutions are therefore identical on $\Sigma(s)$ so that

$$\lambda_\alpha(s, x) = \hat{\lambda}_\alpha(s, x) \quad \text{for } x \in \Sigma(s) \quad (268)$$

or equivalently, by (221), $\nu_\alpha(x) = \hat{\nu}_\alpha(x)$ for all x . By construction $\hat{\nu}_\alpha(x) \equiv 0$ but this equality would have followed if any other value had been chosen such that it and its first derivative vanishes on L .

What remains is to show that $\nabla_\beta \lambda_\alpha(s, x)$ and $\nabla_\beta \hat{\lambda}_\alpha(s, x)$ are also equal on $\Sigma(s)$, for then it will follow from (197), (257) and (259) that $e_{\alpha\beta}(s, x)$ and $\hat{e}_{\alpha\beta}(s, x)$ are equal on $\Sigma(s)$, as required. Since $\nu_\alpha \equiv \hat{\nu}_\alpha$, (222) shows that $\nabla_\beta \lambda_\alpha(s, x) = \nabla_\beta \hat{\lambda}_\alpha(s, x)$ on $\Sigma(s)$ if $\partial \lambda_\alpha(s, x)/\partial s = \partial \hat{\lambda}_\alpha(s, x)/\partial s$ there. That these are equal at $x = z(s)$ already follows since $a_\kappa = \hat{a}_\kappa = 0$.

For simplicity let barred variables denote the difference between corresponding hatted and unhatted ones, e.g., $\bar{\varphi}_{\alpha\beta}(s, x) = \hat{\varphi}_{\alpha\beta}(s, x) - \varphi_{\alpha\beta}(x)$. The notation will be as in Sect. 18 from (207) onward. Since $\varphi_{\alpha\beta}(x)$ is independent of s , the unhatted version of (265) holds trivially, so

$$\sigma^\beta \frac{\partial \bar{\varphi}_{\alpha\beta}(s, x)}{\partial s} = 0 \quad \text{for all } x. \quad (269)$$

The barred version of (257) then gives

$$U^\beta \left(\frac{\partial \bar{e}_{\alpha\beta}}{\partial s} + \nabla_{(\alpha} \frac{\partial \bar{\lambda}_{\beta)}}{\partial s} \right) = 0 \quad (270)$$

along all geodesics through $z(s)$. But (213) and (255) give

$$\sigma^\beta \bar{e}_{\alpha\beta}(s, x) = 0 \quad \text{for all } x \quad (271)$$

from which $U^\alpha U^\beta \partial \bar{e}_{\alpha\beta} / \partial s = 0$, so multiplying (270) by U^α shows that $U^\alpha \partial \bar{\lambda}_\alpha / \partial s$ is constant along all geodesics through $z(s)$. This value is zero at $x = z(s)$ as noted above, so

$$\sigma^\alpha \frac{\partial \bar{\lambda}_\alpha}{\partial s} = 0 \quad \text{for all } x. \quad (272)$$

If (271) is differentiated with respect to s , the result with (272) enables (270) to be put in the form

$$\frac{d}{du} \left(u^{-1} \sigma^{\kappa\alpha} \frac{\partial \bar{\lambda}_\alpha}{\partial s} \right) = 2u^{-2} v_\lambda \sigma^{\kappa\alpha} \sigma^{\lambda\beta} \bar{e}_{\alpha\beta}. \quad (273)$$

The occurrence of $\bar{e}_{\alpha\beta}$ can be eliminated for geodesics in $\Sigma(s)$. The left hand side of (222) is zero when applied to the barred variables and $\bar{\varphi}_{\alpha\beta}(s, x) = 0$ for $x \in \Sigma(s)$ by construction, so

$$\bar{e}_{\alpha\beta} = \nabla_{(\alpha} \tau \frac{\partial \bar{\lambda}_{\beta)}}{\partial s} \quad \text{for } x \in \Sigma(s). \quad (274)$$

If (273) is multiplied by v_κ and restricted to geodesics in $\Sigma(s)$ then use of (274) turns it into a homogeneous equation in the variable $v_\kappa \sigma^{\kappa\alpha} \partial \bar{\lambda}_\alpha / \partial s$. This variable is zero at $x = z(s)$ as $\partial \bar{\lambda}_\alpha / \partial s = 0$ at this point, so it is zero throughout $\Sigma(s)$. This can be put back into the right hand side of (273) itself to turn it on $\Sigma(s)$ into a homogeneous equation for $\sigma^{\kappa\alpha} \partial \bar{\lambda}_\alpha / \partial s$, a function of x whose value is a vector at z . Once again

this vanishes at $x = z(s)$ and so this vector, and hence $\partial \bar{\lambda}_\alpha / \partial s$ itself, vanishes for all $x \in \Sigma(s)$.

As discussed above, this completes the proof that $e_{\alpha\beta}(s, x)$ and $\hat{e}_{\alpha\beta}(s, x)$ are equal on each $\Sigma(s)$. Because the constructed $\varphi_{\alpha\beta}$ satisfies (263), (199) reduces to (232) due to (206) and (230). This justifies (232) for all $e_{\alpha\beta}$, and so in particular for those constructed from a $\varphi_{\alpha\beta}$ that does not satisfy (263). Subtraction of (232) from the full defining equation (199) then shows that (233) is also valid.

Consider now a free choice of $e_{\delta\gamma\beta\alpha}(\tau(x), x)$ multiplied by a function that is constant on each $\Sigma(s)$. This multiplier can be brought outside the k -space integral of (203) and the hypersurface integral of (232) as both have been shown to depend on the value of $e_{\alpha\beta}(s, x)$ only through its value on $\Sigma(s)$. These are both expressions for $M^{\kappa\lambda}[E_{\kappa\lambda}]$, so as the multiplier is arbitrary, the s -integrands must be equal. This proves (234) and completes the proof of uniqueness for the results of Sect. 19.

24 Higher Moments as Integrals

The one issue standing in the way of extracting integral expressions for the moments J^{\dots} from (234) is the function ψ_α . This is defined as the solution of (225) corresponding to initial conditions (228) with $a_\kappa = 0$ and $b_{\kappa\lambda} = 0$. In practice it is easier to work with an alternative specification. The barred variables of (273) also satisfy (225) since the hatted and unhatted ones do so separately, and $\bar{a}_\kappa = 0$. Equation (273) is in fact a first integral of (225) in the case $a_\kappa = 0$, so ψ_α also satisfies it, giving

$$\frac{d}{du} \left(u^{-1} \sigma^{\kappa\alpha} \psi_\alpha \right) = 2u^{-2} v_\lambda \sigma^{\kappa\alpha} \sigma^{\lambda\beta} \sigma^\gamma \sigma^\delta e_{\alpha\gamma\beta\delta} \quad (275)$$

along all affinely parameterised geodesics $x(u)$ through $z(s)$ with $z(s) = x(0)$. Indices $\alpha, \beta, \gamma, \dots$ here refer to the generic point $x(u)$. Note that since $b_{\kappa\lambda} = 0$, $\psi_\alpha(x(u)) = O(u^2)$ as $u \rightarrow 0$, so the singularity at $u = 0$ is only apparent.

Now the Fourier inversion formula with (150) and (152) gives

$$\sigma^\delta \sigma^\varepsilon e_{\alpha\delta\beta\varepsilon}(s, x) = \frac{1}{(2\pi)^4} \sigma^\mu \sigma^\nu \sigma^\kappa_{\cdot\alpha} \sigma^\lambda_{\cdot\beta} \int Dk \sum \frac{1}{n!} (ik \cdot \sigma)^n \tilde{E}_{\kappa\mu\lambda\nu}(s, k) \quad (276)$$

where $k \cdot \sigma = k_\lambda \sigma^\lambda$. Since $\sigma^\kappa(x(u)) = u \sigma^\kappa(x(1))$ for the affinely parameterised geodesic $x(u)$, (276) can be put into (275) and the equation integrated to give

$$\psi_\alpha(s, x) = - \frac{2}{(2\pi)^4} H_{\alpha\kappa} v_\tau \sigma^\mu \sigma^\rho \int Dk \tilde{E}_{\lambda\mu\nu\rho} \sum_{n=0}^{\infty} \frac{1}{(n+1)!} (ik \cdot \sigma)^n {}_n\Theta^{\kappa\tau\lambda\nu} \quad (277)$$

where

$${}_n\Theta^{\kappa\lambda\mu\nu}(z, x(1)) = (n+1) \int_0^1 \sigma^{\kappa\alpha} \sigma^\mu_{\cdot(\alpha} \sigma^\nu_{\cdot\beta)} \sigma^{\lambda\beta} u^n du \quad (278)$$

with the arguments of the σ 's in (278) being $(z, x(u))$. The Θ 's are propagators dependent solely on the geometry and such that

$${}_n\Theta^{\kappa\lambda\mu\nu}(z, x) = g^{\kappa(\mu}g^{\nu)\lambda} \quad (279)$$

in a flat spacetime for all n .

If (276) and (277) are put into (234), the result may be compared with (204) to give

$$\begin{aligned} J^{\sigma\cdots\rho\nu\mu\lambda\kappa}(s) = & (-1)^n \int_{\Sigma(s)} \sigma^\sigma \cdots \sigma^\rho \sigma^{[\nu} \sigma^{\lambda} \left(\sigma^{\mu]}_{\alpha} \sigma^{\kappa]}_{\beta} T^{\alpha\beta} w^\gamma \right. \\ & \left. + \frac{2}{n+1} {}_n\Theta^{[\mu\kappa]\xi\tau} v_\tau H_{\alpha\xi} T^{\alpha\gamma} \right) d\Sigma_\gamma. \end{aligned} \quad (280)$$

Here, as everywhere, n is the number of indices in the set marked by dots, here $\sigma \cdots \rho$, and nested square brackets for antisymmetrisation are taken in order from left to right, so the pairs $\nu\mu$ and $\lambda\kappa$ are antisymmetrised. The factor $(-1)^n$ arises from the minus sign in (150); in a flat spacetime σ^κ is *minus* the position vector from $z(s)$ to the point x on $\Sigma(s)$.

This is the final expression for the quadrupole and higher moments as integrals of the energy-momentum tensor. They satisfy the symmetry conditions (94) and (95) identically and the orthogonality conditions (99) as $n_\kappa(s)\sigma^\kappa(z(s), x) = 0$ for $x \in \Sigma(s)$ by the definition of this hypersurface.

Mathisson took s as proper time along L and his orthogonality conditions used $n^\kappa = v^\kappa$. In his treatment of the quadrupole moment he neglected components that have no classical analogue. In doing so he is effectively considering an energy-momentum tensor of the form $T^{\alpha\beta} = \mu v^\alpha v^\beta$ where $\mu(x)$ is a mass density. Neglect of octopole and higher moments means that all tensors appearing in the expression for the quadrupole can be taken as evaluated at $z(s)$, so that effectively also $w^\gamma = v^\gamma$ and the distinction between indices at x and z can be ignored. If these assumptions are put into (280) for the case $n = 0$ it gives

$$J^{\nu\mu\lambda\kappa} = 3v^{[\nu}b^{\mu]\kappa}v^\lambda \quad (281)$$

where $b^{\kappa\lambda} = \int \mu \sigma^\kappa \sigma^\lambda v^\alpha d\Sigma_\alpha$ in agreement with Mathisson's expression (22).

This is the last piece in the jigsaw required to compare the quadrupole torque derived here with that of Mathisson. The required comparison is between his result (23) and the form (138) of the equation of motion for spin. The torque $L^{\kappa\lambda}$ in the quadrupole approximation is given by (188) with (189). The Veblen extension $g_{\nu\mu, \lambda\kappa}$ appearing in this is given by (196) and if $J^{\nu\mu\lambda\kappa}$ is taken as given by (281) then it is seen that Mathisson's result and ours are in agreement. It was noted in Sect. 6 that although Taub [23] and Madore [24] also developed quadrupole approximations, their work had algebraic errors. When those are corrected it is found that their expressions agree with one another and that both the force and torque of their results agrees with the quadrupole approximation obtained here.

25 Summary and Discussion

The multipole approach to equations of motion in general relativity originated with an ambitious paper by Myron Mathisson in 1937 entitled, in translation, “A New Mechanics of Material Systems”. This paper laid down a general program but carried through the details only in an approximation in which only monopole and dipole moments are retained, with a partial treatment also of the quadrupole moment.

He continued to work on this topic until his untimely death in 1940, after which this subject went dormant until Mathisson’s results were rediscovered, by a very different and much less satisfactory method, by Papapetrou in 1951. Over the next twenty years various authors, including myself, attempted to improve and extend the methods of Mathisson and Papapetrou but little advance was made. In particular the quadrupole case remained stubbornly intractable.

Further progress became possible only with the realisation that the supposed improvements of those twenty years were in fact not improvements at all, that they were leading to dead ends. Mathisson alone had been on the right track. There were important issues left unresolved by his work but the way forward was to identify these and find ways to handle them, not to go blindly off in other directions in the hope that they would prove fruitful. With this realisation, I was able to resolve those issues and take Mathisson’s program to completion. The results were published in three papers [25, 27, 28] over the period 1970–1974.

This paper began by summarising Mathisson’s work of 1937, identifying the issues it leaves and outlining the work of Papapetrou and the subsequent attempts to improve on his and Mathisson’s approaches. It then presented my developments of 1970–1974 by a route that follows Mathisson’s program as closely as possible. This differs somewhat from the way that it was presented in the original papers and in my opinion is a substantial improvement, being better motivated and easier to understand. This is yet one more illustration of the foresight that Mathisson had, right from the start of his work.

The results from the completion of Mathisson’s program show that an extended body can be described completely by an infinite set of moment tensors consisting of a momentum vector p^α , an antisymmetric spin tensor $S^{\alpha\beta}$ together with quadrupole and higher moment tensors. These are defined relative to a timelike world line L and a field n^α of timelike unit vectors chosen along L that enters the moment definitions through orthogonality relations satisfied by the octopole and higher moments.

This description is equivalent to the continuum description by a symmetric energy-momentum tensor $T^{\alpha\beta}$ in that either description completely determines the other. The moments initially have an implicit definition via an equation that expresses $T^{\alpha\beta}$ in terms of them. The development following Mathisson’s program then leads to explicit expressions for them as integrals of $T^{\alpha\beta}$ over spacelike cross-sections of the body. The hypersurfaces of integration are uniquely determined. For any point z on L the corresponding hypersurface is that formed by all geodesics through L orthogonal to n^α . This shows that the set of moment definitions must be taken in its entirety for any of them, even momentum and spin, to become well defined.

The energy-momentum tensor satisfies the covariant conservation equation

$$\nabla_\beta T^{\alpha\beta} = 0. \quad (282)$$

The corresponding property for the moments is the two equations of motion

$$\frac{\delta p^\alpha}{ds} = \frac{1}{2} v^\beta S^{\gamma\delta} R^\alpha_{\cdot\beta\gamma\delta} + F^\alpha \quad (283)$$

and

$$\frac{\delta S^{\alpha\beta}}{ds} = 2p^{[\alpha} v^{\beta]} + L^{\alpha\beta} \quad (284)$$

where F^α and $L^{\alpha\beta}$ are the force and torque exerted on the body by the gravitational field. These are determined by the quadrupole and higher moments. The sign convention for the curvature tensor is given by (2).

There are no other restrictions on the moments. They satisfy (283) and (284) as a consequence of (282) but conversely, given a set of moments that satisfy (283) and (284) then the energy-momentum tensor that they determine necessarily satisfies (282).

These results hold for an arbitrary choice of L and vector field n^α along it. For such a choice, (283) and (284) are really only evolution equations rather than equations of motion. They become true equations of motion only when supplemented by conditions that determine L as the world line of a uniquely defined centre of mass of the body. The conditions to achieve this are

$$n^{[\alpha} p^{\beta]} = 0 \quad (285)$$

and

$$p_\beta S^{\alpha\beta} = 0. \quad (286)$$

Note that (285) cannot be replaced by a simple statement to choose n^α as the unit vector parallel to p^α since p^α itself depends on n^α through the hypersurfaces of integration, as discussed above.

The 2^n -pole moment for $n \geq 2$ is described by a tensor J^{\dots} with $(n+2)$ indices that satisfies the symmetry and orthogonality conditions

$$J^{\zeta\dots\varepsilon\delta\gamma\beta\alpha} = J^{(\zeta\dots\varepsilon)[\delta\gamma][\beta\alpha]} \quad \text{and} \quad J^{\zeta\dots\varepsilon\delta[\gamma\beta\alpha]} = 0 \quad \text{for } n \geq 2, \quad (287)$$

$$J^{\zeta\dots[\varepsilon\delta\gamma]\beta\alpha} = 0 \quad \text{for } n \geq 3 \quad (288)$$

and

$$n_\zeta J^{\zeta\dots\varepsilon\delta\gamma\beta\alpha} \quad \text{for } n \geq 3. \quad (289)$$

This shows, in particular, that it has the symmetries of the curvature tensor on their last four indices. Note that n here continues to refer to the tensor being that for the 2^n -pole moment. Elsewhere in the paper it is the number of indices in the set elided by dots, here $\zeta \cdots \varepsilon$, namely $(n - 2)$ in the present context which is why the range of n appears to differ from that in (94), (95) and (99) from where these results are taken. As a result of these conditions the 2^n -pole moment tensor has $(n + 2)(3n - 1)$ linearly independent components. For the quadrupole this gives 20, which can be checked as it has the same symmetries as the curvature tensor for which this count is well known.

Explicit expressions as integrals of $T^{\alpha\beta}$ are developed for the momentum and spin in Sect. 19 and for the quadrupole and higher moments in Sect. 24. The gravitational force and torque are derived in an exact form in Sect. 15 and in any desired multipole approximation in Sect. 16. In the quadrupole approximation these give

$$F_\alpha = \frac{1}{6} J^{\beta\gamma\delta\varepsilon} \nabla_\alpha R_{\beta\gamma\delta\varepsilon} \quad \text{and} \quad L^{\alpha\beta} = \frac{2}{3} \left(J^{\alpha\gamma\delta\varepsilon} R_{\cdot\gamma\delta\varepsilon}^\beta - J^{\beta\gamma\delta\varepsilon} R_{\cdot\gamma\delta\varepsilon}^\alpha \right). \quad (290)$$

The completion of Mathisson's program is not the end of the story. The equations of motion in their exact form are satisfied exactly by an extended body but the gravitational field that occurs in it includes that produced by the body itself. Even for bodies of modest size, this self field dominates the external field in the neighbourhood of the body. This is certainly true for the Earth but is also for much smaller bodies. The multipole approximation depends on the size of the body being small in comparison with the length scale of the gravitational field, but the self field means that this is not normally true.

What is normally done is to ignore the self field by treating the body of interest as a test body, one whose size or mass is such that its contribution to the field can be neglected. There are two problems with treating a real body in this way. One is that it is assuming the field equations to be linear, in some suitable sense, so that the self field can be subtracted to leave an external field to be used in the equations of motion. The other is that it is assuming that the self field does not affect the motion, that the self force vanishes. This is ignoring such effects as radiation reaction.

What needs to be done is to give a precise meaning to the self field and the subtraction process, and so to the external field, in such a way that (282) still holds for the energy-momentum tensor of the body in the external field. The external field will not satisfy the Einstein field equations inside the body but this is not relevant to the results of the Mathisson program. They depend solely on the conservation equation (282). This problem will be addressed by others elsewhere in these proceedings.

Acknowledgments The author would like to thank the organisers of the 524th WE-Heraeus-Seminar "Equations of Motion in Relativistic Gravity", and Dirk Puetzfeld in particular, for inviting him to attend and speak at this seminar and the management of the Physikzentrum, Bad Honnef, for its hospitality.

References

1. M. Mathisson, Neue Mechanik materieller Systeme. *Acta Phys. Pol.* **6**, 163–200 (1937)
2. M. Mathisson, Republication of: new mechanics of material systems. *Gen. Relativ. Gravit.* **42**, 1011–1048 (2010)
3. A. Einstein, J. Grommer, Allgemeine Relativitätstheorie und Bewegungsgesetz. *Sitzungsber. Preuss. Akad. Wiss., Phys.-Math. Kl.* 2–13 (1927)
4. A. Einstein, Allgemeine Relativitätstheorie und Bewegungsgesetz. *Sitzungsber. Preuss. Akad. Wiss., Phys.-Math. Kl.* 235–245 (1927)
5. H.P. Robertson, Test corpuscles in general relativity. *Proc. Edinb. Math. Soc.* **5**(2), 63–81 (1937)
6. T. Sauer, A. Trautman, Myron Mathisson: what little we know of his life. *Acta Phys. Pol. B Suppl.* **1**, 7–26 (2008)
7. A. Einstein, L. Infeld, B. Hoffman, The gravitational equations and the problem of motion. *Ann. Math.* **39**, 65–100 (1938)
8. A. Bielecki, M. Mathisson, J.W. Weyssenhoff, Sur un théorème concernant une transformation d'intégrales quadruples en intégrales curvilignes dans l'espace de Riemann. *Bull. Int. Acad. Polonaise Sci. Lett., Cracovie Cl. Sci. Math. Natur., Sér. A* 22–28 (1939)
9. M. Mathisson, The variational equation of relativistic dynamics. *Proc. Camb. Philos. Soc.* **36**, 331–350 (1940)
10. M. Mathisson, Relativistic dynamics of a spinning magnetic particle. *Proc. Camb. Philos. Soc.* **38**, 40–60 (1942)
11. P. Havas, The early history of the “problem of motion” in general relativity, in *Proceedings of the 1986 Osgood Hill Conference*, ed. by D. Howard, J. Stachel (Birkhäuser, Boston, 1989), pp. 234–276
12. M. Mathisson, Das zitternde Elektron und seine Dynamik. *Acta Phys. Pol.* **6**, 218–227 (1937)
13. M.H.L. Pryce, The mass-centre in the restricted theory of relativity and its connection with the quantum theory of elementary particles. *Proc. R. Soc. (London)* **A195**, 62–81 (1948)
14. C. Möller, On the definition of the centre of gravity of an arbitrary closed system in the theory of relativity. *Comm. Dublin Inst. Adv. Studies* **A5**, 1 (1949)
15. J. Weyssenhoff, A. Raabe, Relativistic dynamics of spin-fluids and spin-particles. *Acta Phys. Pol.* **9**, 7–18 (1947)
16. S. Shanmugadhasan, On Mathisson's variational equation of relativistic dynamics. *Proc. Camb. Philos. Soc.* **42**, 54–61 (1946)
17. A. Papapetrou, Spinning test-particles in general relativity. I. *Proc. R. Soc. (London)* **A209**, 248–258 (1951)
18. H. Hönl, A. Papapetrou, Über die innere Bewegung des Elektrons III. *Z. Phys.* **116**, 153–183 (1940)
19. E. Corinaldesi, A. Papapetrou, Spinning test-particles in general relativity. II. *Proc. R. Soc. (London)* **A209**, 259–268 (1951)
20. W. Tulczyjew, Motion of multipole particles in general relativity theory. *Acta Phys. Pol.* **18**, 393–409 (1959)
21. B. Tulczyjew, W. Tulczyjew, On multipole formalism in general relativity, *Recent Developments in General Relativity* (Pergamon Press, London, 1962), pp. 465–472
22. W.G. Dixon, A covariant multipole formalism for extended test bodies in general relativity. *Nuovo Cimento* **34**, 317–339 (1964)
23. A.H. Taub, The motion of multipoles in general relativity, in *Proceedings Galileo IV Centenary Conference*, (Florence, 1965), pp. 77–89
24. J. Madore, The equations of motion of an extended body in general relativity. *Ann. Inst. Henri Poincaré* **11**, 221–237 (1969)
25. W.G. Dixon, Dynamics of extended bodies in general relativity III. Equations of motion. *Philos. Trans. R. Soc. (London)* **A277**, 59–119 (1974)
26. W.G. Dixon, Description of extended bodies by multipole moments in special relativity. *J. Math. Phys.* **8**, 1591–1605 (1967)

27. W.G. Dixon, Dynamics of extended bodies in general relativity I. Momentum and angular momentum. *Proc. R. Soc. (London)* **A.314**, 499–527 (1970)
28. W.G. Dixon, Dynamics of extended bodies in general relativity II. Moments of the charge-current vector. *Proc. R. Soc. (London)* **A.319**, 509–547 (1970)
29. R.L. Bishop, R.J. Crittenden, *Geometry of Manifolds* (Academic Press, New York, 1964)
30. I.M. Gel'fand, G.E. Shilov, *Generalized Functions Volume 1: Properties and Operations* (Academic Press, New York, 1964)
31. J.L. Synge, *Relativity: The General Theory* (North-Holland Publ. Co., Amsterdam, 1960)
32. B.S. DeWitt, R.W. Brehme, Radiation damping in a gravitational field. *Ann. Phys. (N. Y.)* **9**, 220–259 (1960)
33. O. Veblen, T.Y. Thomas, The geometry of paths. *Trans. Am. Math. Soc.* **25**, 551–608 (1923)
34. T.Y. Thomas, *The Differential Invariants of Generalized Spaces* (Cambridge University Press, Cambridge, 1934)
35. J.A. Schouten, *Ricci-Calculus*, chapter III, section 7, 2nd edn. (Springer, Berlin, 1954)
36. R. Schattner, The center of mass in general relativity. *Gen. Relativ. Gravit.* **10**, 377–393 (1979)
37. R. Schattner, The uniqueness of the center of mass in general relativity. *Gen. Relativ. Gravit.* **10**, 395–399 (1979)
38. J. Ehlers, E. Rudolph, Dynamics of extended bodies in general relativity: centre-of-mass description and quasirigidity. *Gen. Relativ. Gravit.* **8**, 197–217 (1977)

Multipolar Test Body Equations of Motion in Generalized Gravity Theories

Yuri N. Obukhov and Dirk Puetzfeld

Abstract We give an overview of the derivation of multipolar equations of motion of extended test bodies for a wide set of gravitational theories beyond the standard general relativistic framework. The classes of theories covered range from simple generalizations of General Relativity, e.g., encompassing additional scalar fields, to theories with additional geometrical structures which are needed for the description of microstructured matter. Our unified framework even allows to handle theories with nonminimal coupling to matter, and thereby for a systematic test of a very broad range of gravitational theories.

1 Introduction

In this work we present a general unified multipolar framework, which enables us to derive equations of motion of extended test bodies for a wide range of gravitational theories. The framework presented here can be applied to theories which significantly go beyond General Relativity (GR), and range from the most straightforward extensions of GR, like scalar-tensor theories, to theories with additional geometrical structures and nonminimal coupling.

The *multipolar method* which we employ here can be thought of as the direct generalization of the ideas pioneered by Mathisson [1], Papapetrou [2], and Dixon [3–6] to the case of generalized gravity theories. As sketched in Fig. 1, the main aim of such methods is to find a simplified *local* description of the motion of extended test bodies in terms of a suitable set of multipolar moments, which catches the essential properties of the body at the chosen order of approximation.

Y.N. Obukhov (✉)

Theoretical Physics Laboratory, Nuclear Safety Institute, Russian Academy of Sciences,
B.Tulskaya 52, Moscow 115191, Russia
e-mail: obukhov@ibrae.ac.ru

D. Puetzfeld

ZARM, University of Bremen, Am Fallturm, 28359 Bremen, Germany
e-mail: dirk.puetzfeld@zarm.uni-bremen.de
URL: <http://puetzfeld.org>

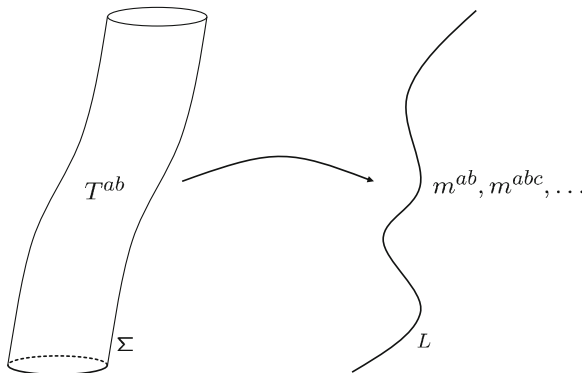


Fig. 1 General idea behind multipolar approximation schemes: The world-tube Σ of a body is replaced by a representative world-line L , whereas the original energy-momentum tensor T^{ab} is substituted by a set of multipole moments $m^{ab\dots}$ along this world-line. Such a multipolar description simplifies the equations of motion. This is achieved by consideration of only a finite set of moments. Different flavors of multipolar approximation schemes exist in the literature, in this work we define the moments à la Dixon in [3]

In this work, we use a covariant multipolar description, based on Synge's world-function formalism [7, 8]. The *multipolar moments* to be introduced, can be viewed as a direct generalization of the moments first introduced by Dixon in [3].

Central to the derivation of the equations of motion, by means of a multipolar method, is the knowledge of the corresponding conservation laws of the underlying gravity theory. In General Relativity, the starting point of all methods mentioned so-far is the conservation of the (symmetric) energy-momentum

$$\nabla_j T^{ij} = 0. \quad (1)$$

Many generalized gravity theories allow for a more detailed description of matter than standard GR, e.g., also taking into account internal matter degrees of freedom as source of the gravitational field. Consequently the conservation laws of such theories are more complex, and (1) has to be replaced by a suitable generalization.

Generalized gravity A metric and connection are the two fundamental geometrical objects on a spacetime manifold. They play an important role in the description of gravitational phenomena in the framework of what can be quite generally called an Einsteinian approach to gravity. The principles of equivalence and general coordinate covariance are the cornerstones of this approach. As Einstein himself formulated, the crucial achievement of his theory was the elimination of the notion of inertial systems as preferred ones among all possible coordinate systems.

In Einstein's theory, gravitation is associated with the metric tensor alone. Nevertheless, it is worthwhile to stress that Einstein clearly understood the different physical statuses of the metric and the connection (Appendix II in [9]):

[...] at first Riemannian metric was considered the fundamental concept on which the general theory of relativity and thus the avoidance of the inertial system were based. Later, however, Levi-Civita rightly pointed out that the element of the theory that makes it possible to avoid the inertial system is rather the infinitesimal displacement field Γ_{ik}^j . The metric or the symmetric tensor field g_{ik} which defines it is only indirectly connected with the avoidance of the inertial system insofar as it determines a displacement field.

There exists a variety of gravitational theories that generalize or extend the physical and mathematical structure of GR. Among these theories there are large classes of so-called $f(R)$ models, and of theories with nonminimal coupling to matter; they are developed in particular in the context of relativistic cosmology (but not only there), see [10–14]. The so-called Palatini approach represents another class of widely discussed theories in which the metric and the connection are treated as independent variables in the action principle [15–17]. Another early example of a generalized gravity theory with balance laws different from Einstein’s gravity can be found in [18, 19]. Last but not least, we should mention the vast family of the gauge gravity theories constructed using a Yang-Mills type of approach [20, 21].

Since our main aim is to present a unified multipolar framework for a very wide range of gravity theories, the theory underlying our analysis has to be sufficiently general. In this work we choose metric-affine gravity (MAG) as the foundation for the derivation of the equations of motion of extended deformable test bodies (Fig. 2).

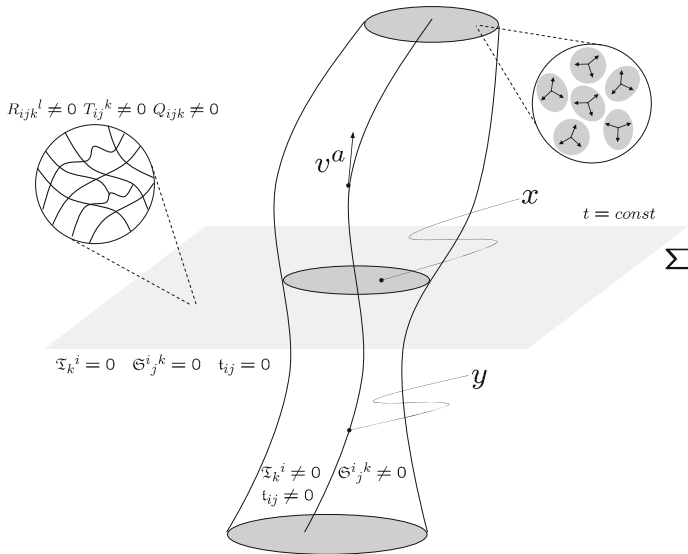


Fig. 2 In contrast to GR, MAG also allows to take into account the microstructural properties of matter (spin, dilation current, proper hypercharge). These additional currents couple to the post-Riemannian geometric degrees of freedom of the underlying spacetime. Our unified description of extended test bodies allows to cover a wide range of gravitational theories and matter models

In MAG, matter is characterized by three fundamental Noether currents—the canonical energy-momentum current, the canonical hypermomentum current, and the metrical energy-momentum current. These objects satisfy a set of conservation laws (or, more exactly, balance equations). In view of the multi-current characterization of matter in metric-affine gravity, we develop a general approach which is applicable to an arbitrary set of conservation laws for any number of currents. The latter can include gravitational, electromagnetic, and other physical currents if they are relevant to the model under consideration. In particular, our approach is flexible enough to be applied to the case in which there is a general nonminimal coupling between gravity to matter. Our presentation here is mainly based on the original works [22–24].

Structure of the paper The structure of the paper is as follows: In Sect. 2 we give an overview of the metric-affine theory of gravity. In particular we cover its geometrical and dynamical aspects. This is followed by a general Lagrange-Noether analysis in Sect. 3. The results of this general analysis are then used to derive the conservation laws of a metric-affine gravity with nonminimal coupling in Sect. 4. In Sect. 5 a unified multipolar framework is presented. This framework is then used Sect. 6 to derive the general equations of motion of extended test bodies in nonminimal metric-affine gravity. Several specializations to other gravity theories are discussed. Furthermore, in Sect. 7 the equations of motion in scalar-tensor theories are worked out. Section 8 contains a summary of our results.

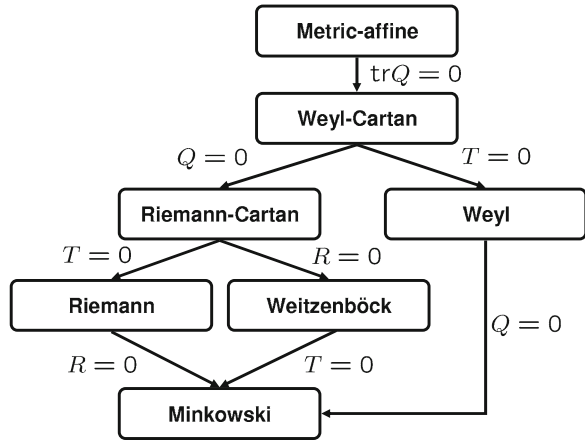
Our conventions are those of [25]. In particular, the basic geometrical quantities such as the curvature, torsion, and nonmetricity are defined as in [25], and we use the Latin alphabet to label the spacetime coordinate indices. Furthermore, the metric has the signature $(+, -, -, -)$. It should be noted that our definition of the metrical energy-momentum tensor differs by a sign from the definition used in [12, 14, 26]. A summary of our notation and conventions, as well as additional material for comparison to previous works can be found in the appendix.

2 Metric-Affine Gravity Primer

Metric-affine gravity [25] is a natural extension of Einstein’s general relativity theory. It is based on gauge-theoretic principles [20, 21], and it takes into account microstructural properties of matter (spin, dilation current, proper hypercharge) as possible physical sources of the gravitational field on an equal footing with macroscopic properties (energy and momentum) of matter. The formalism of MAG makes it possible to study all the above-mentioned alternative theories in a unified framework. The corresponding spacetime landscape [27] includes as special cases the geometries of Riemann, Riemann-Cartan, Weyl, Weitzenböck, etc. (cf. Fig. 3).

The standard understanding of metric-affine gravity is based on the gauge-theoretic approach for the general affine symmetry group. In this framework, we can naturally distinguish the *kinematics* of the gravity theory and its *dynamics*. The kinematics embraces all aspects that are related to the description of the fundamental

Fig. 3 Different spacetime types as special cases of a general metric-affine spacetime ($R_{kli}{}^j \neq 0$, $T_{kl}{}^i \neq 0$, $Q_{kij} \neq 0$). The abbreviations R (curvature), T (torsion), and Q (nonmetricity) over the arrows denote the vanishing of the corresponding geometrical object



variables, their mathematical properties and physical interpretation. The dynamics studies the choice of the Lagrangian and the field equations. We collect in this section all the relevant material. Although the Lagrange-Noether machinery is deeply interrelated with both kinematics and dynamics of the theory, we will discuss it in a separate section which will ultimately underlie the derivation of the multipole equations of motion.

2.1 Kinematics of Metric-Affine Gravity

We model spacetime as a four-dimensional smooth manifold. In this study we are not interested in the global (topological) aspects, and we will confine our attention only to local issues. The local coordinates x^i , $i = 0, 1, 2, 3$, are introduced in the neighborhood of an arbitrary point of the spacetime manifold. The geometrical (gravitational) and physical (material) variables are then fields of different nature (both tensors and nontensors) over the spacetime. They are characterized by their components and transformation properties under local diffeomorphisms $x^i \rightarrow x^i + \delta x^i$, where

$$\delta x^i = \xi^i(x). \quad (2)$$

The four arbitrary functions $\xi^i(x)$ parametrize an arbitrary local diffeomorphism.

2.1.1 Geometrical Variables

In the metric-affine theory of gravity, the gravitational physics is encoded in two fields: the metric tensor g_{ij} and an independent linear connection $\Gamma_{ki}{}^j$. The latter is not necessarily symmetric and compatible with the metric. From the geometrical point

of view, the metric introduces lengths and angles of vectors, and thereby determines the distances (intervals) between points on the spacetime manifold. The connection introduces the notion of parallel transport and defines the covariant differentiation ∇_k of tensor fields.

Under the spacetime diffeomorphisms (2), these geometrical variables transform as

$$\delta g_{ij} = -(\partial_i \xi^k) g_{kj} - (\partial_j \xi^k) g_{ik}, \quad (3)$$

$$\delta \Gamma_{ki}^j = -(\partial_k \xi^l) \Gamma_{li}^j - (\partial_i \xi^l) \Gamma_{kl}^j + (\partial_l \xi^j) \Gamma_{ki}^l - \partial_{ki}^2 \xi^j. \quad (4)$$

In general, the geometry of a metric-affine manifold is exhaustively characterized by three tensors: the curvature, the torsion and the nonmetricity. They are defined [27] as follows:

$$R_{kli}^j := \partial_k \Gamma_{li}^j - \partial_l \Gamma_{ki}^j + \Gamma_{kn}^j \Gamma_{li}^n - \Gamma_{ln}^j \Gamma_{ki}^n, \quad (5)$$

$$T_{kl}^i := \Gamma_{kl}^i - \Gamma_{lk}^i, \quad (6)$$

$$Q_{kij} := -\nabla_k g_{ij} = -\partial_k g_{ij} + \Gamma_{ki}^l g_{lj} + \Gamma_{kj}^l g_{il}. \quad (7)$$

The curvature and the torsion tensors determine the commutator of the covariant derivatives. For a tensor $A^{c_1 \dots c_k}_{d_1 \dots d_l}$ of arbitrary rank and index structure:

$$\begin{aligned} & (\nabla_a \nabla_b - \nabla_b \nabla_a) A^{c_1 \dots c_k}_{d_1 \dots d_l} = -T_{ab}^e \nabla_e A^{c_1 \dots c_k}_{d_1 \dots d_l} \\ & + \sum_{i=1}^k R_{abe}{}^{c_i} A^{c_1 \dots e \dots c_k}_{d_1 \dots d_l} - \sum_{j=1}^l R_{abd_j}{}^e A^{c_1 \dots c_k}_{d_1 \dots e \dots d_l}. \end{aligned} \quad (8)$$

The Ricci tensor is introduced by $R_{ij} := R_{kij}^k$, and the curvature scalar is $R := g^{ij} R_{ij}$.

A general metric-affine spacetime ($R_{kli}^j \neq 0$, $T_{kl}^i \neq 0$, $Q_{kij} \neq 0$) incorporates several other spacetimes as special cases, see Fig. 3 for an overview. The Riemannian connection $\tilde{\Gamma}_{kj}^i$ is uniquely determined by the conditions of vanishing torsion and nonmetricity which yield explicitly

$$\tilde{\Gamma}_{kj}^i = \frac{1}{2} g^{il} (\partial_j g_{kl} + \partial_k g_{lj} - \partial_l g_{kj}). \quad (9)$$

Here and in the following, a tilde over a symbol denotes a Riemannian object (such as the curvature tensor) or a Riemannian operator (such as the covariant derivative) constructed from the Christoffel symbols (9). The deviation of the geometry from the Riemannian one is then conveniently described by the *distortion* tensor

$$N_{kj}^i := \tilde{\Gamma}_{kj}^i - \Gamma_{kj}^i. \quad (10)$$

The system (6) and (7) allows to find the distortion tensor in terms of the torsion and nonmetricity. Explicitly:

$$N_{kj}^i = -\frac{1}{2}(T_{kj}^i + T^i_{kj} + T^i_{jk}) + \frac{1}{2}(Q^i_{kj} - Q_{kj}^i - Q_{jk}^i). \quad (11)$$

Conversely, one can use this to express the torsion and nonmetricity tensors in terms of the distortion,

$$T_{kj}^i = -2N_{[kj]}^i, \quad (12)$$

$$Q_{kij} = -2N_{k(ij)}. \quad (13)$$

Substituting (10) into (5), we find the relation between the non-Riemannian and the Riemannian curvature tensors

$$R_{adc}{}^b = \tilde{R}_{adc}{}^b - \tilde{\nabla}_a N_{dc}{}^b + \tilde{\nabla}_d N_{ac}{}^b + N_{an}{}^b N_{dc}{}^n - N_{dn}{}^b N_{ac}{}^n. \quad (14)$$

Applying the covariant derivative to (5)–(7) and antisymmetrizing, we derive the Bianchi identities [27]:

$$\nabla_{[n} R_{kl]i}{}^j = T_{[kl]}{}^m R_{n]mi}{}^j, \quad (15)$$

$$\nabla_{[n} T_{kl]}{}^i = R_{[kl n]}{}^i + T_{[kl]}{}^m T_{n]m}{}^i, \quad (16)$$

$$\nabla_{[n} Q_{k]ij} = R_{nk(ij)}. \quad (17)$$

2.1.2 Tensors, Densities, and Covariant Differential Operators

Along with tensors, an important role in physics is played by densities. A fundamental density $\sqrt{-g}$ is constructed from the determinant of the metric, $g = \det g_{ij}$. Under diffeomorphisms (2) it transforms as

$$\delta\sqrt{-g} = -(\partial_i \xi^i) \sqrt{-g}. \quad (18)$$

This is a direct consequence of (3). From any tensor $B_{i\dots}{}^{j\dots}$ one can construct a density $\mathfrak{B}_{i\dots}{}^{j\dots} = \sqrt{-g} B_{i\dots}{}^{j\dots}$. Although in this paper we will encounter only such objects, it is worthwhile to notice that not all densities are of this type—see the exhaustive presentation in the book of Synge and Schild [28].

There are two kinds of covariant differential operators on the spacetime manifold, depending on whether the connection is involved or not. The Lie derivative \mathcal{L}_ζ is defined along any vector field ζ^i and it maps tensors (densities) into tensors (densities) of the same rank. Let us recall the explicit form of the Lie derivative of the metric and the distortion:

$$\mathcal{L}_\zeta g_{ij} = \zeta^k \partial_k g_{ij} + (\partial_i \zeta^k) g_{kj} + (\partial_j \zeta^k) g_{ik}, \quad (19)$$

$$\mathcal{L}_\zeta N_{kj}^i = \zeta^n \partial_n N_{kj}^i + (\partial_k \zeta^n) N_{nj}^i + (\partial_j \zeta^n) N_{kn}^i - (\partial_n \zeta^i) N_{kj}^n. \quad (20)$$

In contrast, a covariant derivative ∇_k raises the rank of tensors (densities) and it is determined by the linear connection Γ_{kj}^i . Moreover, there are different covariant derivatives which arise for different connections that may coexist on the same manifold.

A mathematical fact is helpful in this respect: Every third rank tensor X_{kj}^i defines a map of one connection into a different new connection

$$\Gamma_{kj}^i \longrightarrow \Gamma_{kj}^i + X_{kj}^i. \quad (21)$$

There are important special cases of such a map. One example is obtained for $X_{kj}^i = N_{kj}^i$: then the connection Γ_{kj}^i is mapped into the Riemannian Christoffel symbols, $\tilde{\Gamma}_{kj}^i = \Gamma_{kj}^i + N_{kj}^i$, in accordance with (10).

Another interesting case arises for $X_{kj}^i = T_{jk}^i$. The result of the mapping

$$\bar{\Gamma}_{kj}^i = \Gamma_{kj}^i + T_{jk}^i = \Gamma_{kj}^i + \Gamma_{jk}^i - \Gamma_{kj}^i = \Gamma_{jk}^i. \quad (22)$$

is then called a *transposed connection*, or associated connection, see [29, 30].

The importance of the transposed connection is manifest in the following observation. Although the Lie derivative is a covariant operator—this is not apparent since it is based on partial derivatives—one can make everything explicitly covariant by noticing that it is possible to recast (19) and (20) into equivalent form

$$\mathcal{L}_\zeta g_{ij} = \zeta^k \nabla_k g_{ij} + (\bar{\nabla}_i \zeta^k) g_{kj} + (\bar{\nabla}_j \zeta^k) g_{ik}, \quad (23)$$

$$\mathcal{L}_\zeta N_{kj}^i = \zeta^n \nabla_n N_{kj}^i + (\bar{\nabla}_k \zeta^n) N_{nj}^i + (\bar{\nabla}_j \zeta^n) N_{kn}^i - (\bar{\nabla}_n \zeta^i) N_{kj}^n. \quad (24)$$

By the same token we can “covariantize” the Lie derivatives for all other tensors of any structure and of arbitrary rank.

A more nontrivial (and less known) fact is that we can define the Lie derivatives also for objects which are not tensors. In particular, the Lie derivative of the connection then reads [29]:

$$\mathcal{L}_\zeta \Gamma_{kj}^i = \nabla_k \bar{\nabla}_j \zeta^i - R_{klj}^i \zeta^l. \quad (25)$$

This quantity measures the noncommutativity of the Lie derivative with the covariant derivative

$$\begin{aligned} & (\mathcal{L}_\zeta \nabla_k - \nabla_k \mathcal{L}_\zeta) A^{c_1 \dots c_k}_{d_1 \dots d_l} \\ &= \sum_{i=1}^k (\mathcal{L}_\zeta \Gamma_{kb}^{ci}) A^{c_1 \dots b \dots c_k}_{d_1 \dots d_l} - \sum_{j=1}^l (\mathcal{L}_\zeta \Gamma_{kdj}^b) A^{c_1 \dots c_k}_{d_1 \dots b \dots d_l}. \end{aligned} \quad (26)$$

The connection Γ_{kj}^i , the transposed connection $\bar{\Gamma}_{kj}^i$, and the Riemannian connection $\tilde{\Gamma}_{kj}^i$ define the three respective covariant derivatives: ∇_k , $\bar{\nabla}_k$, and $\tilde{\nabla}_k$. The

covariant derivative defined by the Riemannian connection is conventionally denoted by a semicolon “;_a”.

We will assume that these differential operators act on tensors. In addition, we will need the covariant operators that act on densities. For an arbitrary tensor density $\mathfrak{B}^n_{i\dots}{}^{j\dots}$ we introduce the covariant derivative

$$\widehat{\nabla}_n \mathfrak{B}^n_{i\dots}{}^{j\dots} := \partial_n \mathfrak{B}^n_{i\dots}{}^{j\dots} + \Gamma_{nl}^j \mathfrak{B}^n_{i\dots}{}^{l\dots} - \Gamma_{ni}^l \mathfrak{B}^n_{l\dots}{}^{j\dots}, \quad (27)$$

which produces a tensor density of the same weight. We denote a similar differential operation constructed with the help of the Riemannian connection by

$$\check{\nabla}_n \mathfrak{B}^n_{i\dots}{}^{j\dots} := \partial_n \mathfrak{B}^n_{i\dots}{}^{j\dots} + \tilde{\Gamma}_{nl}^j \mathfrak{B}^n_{i\dots}{}^{l\dots} - \tilde{\Gamma}_{ni}^l \mathfrak{B}^n_{l\dots}{}^{j\dots}, \quad (28)$$

When $\mathfrak{B}^n_{i\dots}{}^{j\dots} = \sqrt{-g} B^n_{i\dots}{}^{j\dots}$, we find

$$\widehat{\nabla}_n \mathfrak{B}^n_{i\dots}{}^{j\dots} = \sqrt{-g} \nabla_n^* B^n_{i\dots}{}^{j\dots}, \quad (29)$$

$$\check{\nabla}_n \mathfrak{B}^n_{i\dots}{}^{j\dots} = \sqrt{-g} \tilde{\nabla}_n B^n_{i\dots}{}^{j\dots}, \quad (30)$$

where we introduced a modified covariant derivative

$$\nabla_i^* := \nabla_i + N_{ki}^k. \quad (31)$$

2.1.3 Matter Variables

We will not specialize the discussion of matter to any particular physical field. It will be more convenient to describe matter by a generalized field ψ^A . The range of the indices A, B, \dots is not important in our study. However, we do need to know the behavior of the matter field under spacetime diffeomorphisms (2):

$$\delta \psi^A = -(\partial_i \xi^j) (\sigma^A_B)_j{}^i \psi^B. \quad (32)$$

Here $(\sigma^A_B)_j{}^i$ are the generators of general coordinate transformations that satisfy the commutation relations

$$(\sigma^A_C)_j{}^i (\sigma^C_B)_l{}^k - (\sigma^A_C)_l{}^k (\sigma^C_B)_j{}^i = (\sigma^A_B)_l{}^i \delta_j^k - (\sigma^A_B)_j{}^k \delta_l^i. \quad (33)$$

We immediately recognize in (33) the Lie algebra of the general linear group $GL(4, R)$. This fact is closely related to the standard gauge-theoretic interpretation [25] of metric-affine gravity as the gauge theory of the general affine group $GA(4, R)$, which is a semidirect product of spacetime translation group times $GL(4, R)$.

The transformation properties (32) determine the form of the covariant and the Lie derivative of a matter field:

$$\nabla_k \psi^A := \partial_k \psi^A - \Gamma_{ki}^j (\sigma^A_B)_j^i \psi^B, \quad (34)$$

$$\mathcal{L}_\zeta \psi^A := \zeta^k \partial_k \psi^A + (\partial_i \zeta^j) (\sigma^A_B)_j^i \psi^B. \quad (35)$$

The commutators of these differential operators read

$$(\nabla_k \nabla_l - \nabla_l \nabla_k) \psi^A = -R_{klj}^i (\sigma^A_B)_i^j \psi^B - T_{kl}^i \nabla_i \psi^A, \quad (36)$$

$$(\mathcal{L}_\zeta \nabla_k - \nabla_k \mathcal{L}_\zeta) \psi^A = -(\mathcal{L}_\zeta \Gamma_{kj}^i) (\sigma^A_B)_i^j \psi^B. \quad (37)$$

2.1.4 Symmetries in MAG: Generalized Killing Vectors

As is well known, symmetries of a Riemannian spacetime are generated by Killing vector fields. Each such field defines a so-called *motion* of the spacetime manifold, that is a diffeomorphism which preserves the metric g_{ij} .

Suppose ζ^i is a Killing vector field. By definition, it satisfies

$$\tilde{\nabla}_i \zeta_j + \tilde{\nabla}_j \zeta_i = 0. \quad (38)$$

By differentiation, we derive from this the second covariant derivative

$$\tilde{\nabla}_i \tilde{\nabla}_j \zeta_k = \tilde{R}_{jki}^l \zeta_l. \quad (39)$$

Apply another covariant derivative and antisymmetrize:

$$\tilde{\nabla}_{[n} \tilde{\nabla}_{i]} \tilde{\nabla}_j \zeta_k = \tilde{\nabla}_{[n} (\tilde{R}_{|jk|i]}^l \zeta_l). \quad (40)$$

After some algebra, the last equation is recast into

$$\zeta^n \tilde{\nabla}_n \tilde{R}_{ijkl} + \tilde{R}_{njkl} \tilde{\nabla}_i \zeta^n + \tilde{R}_{inkl} \tilde{\nabla}_j \zeta^n + \tilde{R}_{ijnl} \tilde{\nabla}_k \zeta^n + \tilde{R}_{ijkn} \tilde{\nabla}_l \zeta^n = 0. \quad (41)$$

The Eqs. (38), (39) and (41) have a geometrical meaning:

$$\mathcal{L}_\zeta g_{ij} = 0, \quad (42)$$

$$\mathcal{L}_\zeta \tilde{\Gamma}_{ij}^k = 0, \quad (43)$$

$$\mathcal{L}_\zeta \tilde{R}_{ijkl} = 0. \quad (44)$$

That is, the Lie derivatives along the Killing vector field ζ vanish for all Riemannian geometrical objects. Moreover, one can show that the same is true for all higher covariant derivatives of the Riemannian curvature tensor [31]

$$\mathcal{L}_\zeta (\tilde{\nabla}_{n_1} \dots \tilde{\nabla}_{n_N} \tilde{R}_{ijkl}) = 0. \quad (45)$$

Let us generalize the notion of a symmetry to the metric-affine spacetime. We take an ordinary Killing vector field ζ and postulate the vanishing of the Lie derivative

$$\mathcal{L}_\zeta N_{kj}{}^i = 0 \quad (46)$$

of the distortion tensor. Combining this with (11) and (43), we find an equivalent formulation

$$\mathcal{L}_\zeta g_{ij} = 0, \quad (47)$$

$$\mathcal{L}_\zeta \Gamma_{ij}{}^k = 0. \quad (48)$$

We call a vector field that satisfies (47) and (48) a *generalized Killing vector* of the metric-affine spacetime. By definition, such a ζ generates a diffeomorphism of the spacetime manifold that is simultaneously an isometry (47) and an isoparallelism (48).

Since the Lie derivative along a Killing vector commutes with the covariant derivative, $\mathcal{L}_\zeta \tilde{\nabla}_i = \tilde{\nabla}_i \mathcal{L}_\zeta$, see (26), we conclude from (14) and (44) that the generalized Killing vector leaves the non-Riemannian curvature tensor invariant

$$\mathcal{L}_\zeta R_{klj}{}^i = 0. \quad (49)$$

It is also straightforward to verify that

$$\mathcal{L}_\zeta \left(\nabla_{n_1} \dots \nabla_{n_N} R_{klj}{}^i \right) = 0 \quad (50)$$

for any number of covariant derivatives of the curvature.

Later we will show that generalized Killing vectors have an important property: they induce conserved quantities on the metric-affine spacetime.

2.2 Dynamics of Metric-Affine Gravity

The explicit form of the dynamical equations of the gravitational field is irrelevant for the conservation laws that will form the basis for the derivation of the test body equations of motion. However, for completeness, we discuss here the field equations of a general metric-affine theory of gravity. The standard understanding of MAG is its interpretation as a gauge theory based on the general affine group $GA(4, R)$, which is a semidirect product of the general linear group $GL(4, R)$, and the group of local translations [25]. The corresponding gauge-theoretic formalism generalizes the approach of Sciama and Kibble [32, 33]; for more details about gauge gravity theories, see [20, 21]. In the standard formulation of MAG as a gauge theory [25], the gravitational gauge potentials are identified with the metric, coframe, and the linear connection. The corresponding gravitational field strengths are then the nonmetricity, the torsion, and the curvature, respectively.

Here we use an alternative formulation of MAG, in which gravity is described by a different set of fundamental field variables, i.e. the independent metric g_{ij} and connection Γ_{ki}^j , see [15–17, 34–40], for example. It is worthwhile to compare the field equations in the different formulations of MAG, and in particular, it is necessary to clarify the role and place of the *canonical* energy-momentum tensor as a source of the gravitational field. Since one does not have the coframe (tetrad) among the fundamental variables, the corresponding field equation is absent. Here we demonstrate that one can always rearrange the field equations of MAG in such a way that the canonical energy-momentum tensor is recovered as one of the sources of the gravitational field.

Assuming standard minimal coupling, the total Lagrangian density of interacting gravitational and matter fields reads

$$\mathcal{L} = \mathfrak{V}(g_{ij}, R_{ijk}^l, N_{ki}^j) + \mathcal{L}_{\text{mat}}(g_{ij}, \psi^A, \nabla_i \psi^A). \quad (51)$$

In general, the gravitational Lagrangian density \mathfrak{V} is constructed as a diffeomorphism invariant function of the curvature, torsion, and nonmetricity. However, in view of the relations (12) and (13), we can limit ourselves to Lagrangian functions that depend arbitrarily on the curvature and the distortion tensors. The matter Lagrangian depends on the matter fields ψ^A and their *covariant derivatives* (34).

The field equations of metric-affine gravity can be written in several equivalent ways. The standard form is the set of the so-called “first” and “second” field equations. Using the covariant derivative for densities (27), the field equations are given by

$$\widehat{\nabla}_n \mathfrak{H}^{in}{}_k + \frac{1}{2} T_{mn}^i \mathfrak{H}^{mn}{}_k - \mathfrak{E}_k^i = -\mathfrak{T}_k^i, \quad (52)$$

$$\widehat{\nabla}_l \mathfrak{H}^{kli}{}_j + \frac{1}{2} T_{mn}^k \mathfrak{H}^{mni}{}_j - \mathfrak{E}^{ki}{}_j = \mathfrak{S}^i{}_j{}^k. \quad (53)$$

Here the generalized gravitational field momenta densities are introduced by

$$\mathfrak{H}^{kli}{}_j := -2 \frac{\partial \mathfrak{V}}{\partial R_{kli}^j}, \quad \mathfrak{H}^{ki}{}_j := -\frac{\partial \mathfrak{V}}{\partial T_{ki}^j}, \quad \mathfrak{M}^{kij} := -\frac{\partial \mathfrak{V}}{\partial Q_{kij}}, \quad (54)$$

and the gravitational hypermomentum density

$$\mathfrak{E}^{ki}{}_j := -\mathfrak{H}^{ki}{}_j - \mathfrak{M}^{ki}{}_j = -\frac{\partial \mathfrak{V}}{\partial N_{ki}^j}. \quad (55)$$

Furthermore, the generalized energy-momentum density of the gravitational field is

$$\mathfrak{E}_k^i = \delta_k^i \mathfrak{V} + \frac{1}{2} Q_{kln} \mathfrak{M}^{iln} + T_{kl}^n \mathfrak{H}^{il}{}_n + R_{kln}^m \mathfrak{H}^{iln}{}_m. \quad (56)$$

The sources of the gravitational field are the canonical energy-momentum tensor and the canonical hypermomentum densities of matter, respectively:

$$\mathfrak{T}_k^i := \frac{\partial \mathfrak{L}_{\text{mat}}}{\partial \nabla_i \psi^A} \nabla_k \psi^A - \delta_k^i \mathfrak{L}_{\text{mat}}. \quad (57)$$

$$\mathfrak{S}^i_j{}^k := \frac{\partial \mathfrak{L}_{\text{mat}}}{\partial \Gamma_{ki}^j} = - \frac{\partial \mathfrak{L}_{\text{mat}}}{\partial \nabla_k \psi^A} (\sigma^A_B)_j^i \psi^B. \quad (58)$$

It is straightforward to verify that instead of the first field equation (52), one can use the so-called zeroth field equation which reads

$$2 \frac{\delta \mathfrak{V}}{\delta g_{ij}} = \mathfrak{t}^{ij}. \quad (59)$$

On the right-hand side, the matter source is now represented by the metrical energy-momentum density which is defined by

$$\mathfrak{t}_{ij} := 2 \frac{\partial \mathfrak{L}_{\text{mat}}}{\partial g^{ij}}. \quad (60)$$

The system (52) and (53) is completely equivalent to the system (53) and (59), and it is a matter of convenience which one to solve.

2.3 From Densities to Tensors

In actual metric-affine gravity models the Lagrangian densities are constructed in terms of the Lagrangian functions: $\mathfrak{L} = \sqrt{-g}L$, $\mathfrak{V} = \sqrt{-g}V$, $\mathfrak{L}_{\text{mat}} = \sqrt{-g}L_{\text{mat}}$. Accordingly, we find for the gravitational field momenta

$$\mathfrak{H}^{kli}{}_j = \sqrt{-g}H^{kli}{}_j, \quad \mathfrak{H}^{ki}{}_j = \sqrt{-g}H^{ki}{}_j, \quad \mathfrak{M}^{kij} = \sqrt{-g}M^{kij}, \quad (61)$$

and $\mathfrak{E}^i{}_j = \sqrt{-g}E^i{}_j$. The gravitational sources (57), (58) and (60) are rewritten in terms of the canonical energy-momentum tensor, the canonical hypermomentum tensor, and the metrical energy-momentum tensor, respectively:

$$\mathfrak{T}_k^i = \sqrt{-g}\Sigma_k^i, \quad \mathfrak{S}^i_j{}^k = \sqrt{-g}\Delta^i_j{}^k, \quad \mathfrak{t}_{ij} = \sqrt{-g}t_{ij}. \quad (62)$$

The usual spin arises as the antisymmetric part of the hypermomentum,

$$\tau_{ij}^k := \Delta_{[ij]}^k, \quad (63)$$

whereas the trace $\Delta^k = \Delta^i{}_i{}^k$ is the dilation current. The symmetric traceless part describes the proper hypermomentum [25].

As a result, the metric-affine field Eqs. (52) and (53) are recast into

$$\nabla_n^* H^{in}{}_k + \frac{1}{2} T_{mn}{}^i H^{mn}{}_k - E_k{}^i = -\Sigma_k{}^i, \quad (64)$$

$$\nabla_l^* H^{kli}{}_j + \frac{1}{2} T_{mn}{}^k H^{mni}{}_j - E^{ki}{}_j = \Delta^i{}_j{}^k. \quad (65)$$

2.3.1 Example: Matter Model with Microstructure

In order to give an explicit example of physical matter with microstructure, we recall the hyperfluid model [41]. This is a direct generalization of the general relativistic ideal fluid variational theory [42, 43] and of the spinning fluid model of Weyssenhoff and Raabe [44, 45]. Using the variational principle for the hyperfluid [41], one derives the canonical energy-momentum and hypermomentum tensors:

$$\Sigma_k{}^i = v^i P_k - p \left(\delta_k^i - v^i v_k \right), \quad (66)$$

$$\Delta_m{}^n{}^i = v^i J_m{}^n, \quad (67)$$

where v^i is the 4-velocity of the fluid and p is the pressure. Fluid elements are characterized by their microstructural properties: the momentum density P_k and the intrinsic hypermomentum density $J_m{}^n$.

3 General Lagrange-Noether Analysis

As a first step, we notice that the gravitational (geometrical) and material variables can be described together by means of a multiplet, which we denote by $\Phi^J = (g_{ij}, \Gamma_{ki}{}^j, \psi^A)$. We do not specify the range of the multi-index J at this stage. The matter fields may include, besides the true material variables, also auxiliary fields such as Lagrange multipliers. With the help of the latter we can impose various constraints on the geometry of the spacetime. Furthermore, we can use the Lagrange multipliers to describe models in which the Lagrangian depends on arbitrary-order covariant derivatives of the curvature, torsion, and nonmetricity. Then the general action reads

$$I = \int d^4x \mathcal{L}, \quad (68)$$

where the Lagrangian density $\mathcal{L} = \mathcal{L}(\Phi^J, \partial_i \Phi^J)$ depends arbitrarily on the set of fields Φ^J and their first derivatives.

Our aim is to derive Noether identities that correspond to general coordinate transformations. However, it is more convenient to start with arbitrary infinitesimal transformations of the spacetime coordinates and the matter fields. They are given as follows:

$$x^i \longrightarrow x'^i(x) = x^i + \delta x^i, \quad (69)$$

$$\Phi^J(x) \longrightarrow \Phi'^J(x') = \Phi^J(x) + \delta \Phi^J(x). \quad (70)$$

Within the present context it is not important whether this is a symmetry transformation under the action of any specific group. The total variation (70) is a result of the change of the form of the functions and of the change induced by the transformation of the spacetime coordinates (69). To distinguish the two pieces in the field transformation, it is convenient to introduce the *substantial variation*:

$$\delta_{(s)} \Phi^J := \Phi'^J(x) - \Phi^J(x) = \delta \Phi^J - \delta x^k \partial_k \Phi^J. \quad (71)$$

By definition, the substantial variation commutes with the partial derivative, $\delta_{(s)} \partial_i = \partial_i \delta_{(s)}$.

We need the total variation of the action:

$$\delta I = \int \left[d^4x \delta \mathcal{L} + \delta(d^4x) \mathcal{L} \right]. \quad (72)$$

A standard derivation shows that under the action of the transformation (69) and (70) the total variation reads

$$\delta I = \int d^4x \left[\frac{\delta \mathcal{L}}{\delta \Phi^J} \delta_{(s)} \Phi^J + \partial_i \left(\mathcal{L} \delta x^i + \frac{\partial \mathcal{L}}{\partial (\partial_i \Phi^J)} \delta_{(s)} \Phi^J \right) \right]. \quad (73)$$

Here the variational derivative is defined, as usual, by

$$\frac{\delta \mathcal{L}}{\delta \Phi^J} := \frac{\partial \mathcal{L}}{\partial \Phi^J} - \partial_i \left(\frac{\partial \mathcal{L}}{\partial (\partial_i \Phi^J)} \right). \quad (74)$$

3.1 General Coordinate Invariance

Now we specialize to general coordinate transformations. For infinitesimal changes of the spacetime coordinates and (matter and gravity) fields (69) and (70) we have $x^i \rightarrow x^i + \delta x^i$, $g_{ij} \rightarrow g_{ij} + \delta g_{ij}$, $\Gamma_{ki}^j \rightarrow \Gamma_{ki}^j + \delta \Gamma_{ki}^j$, and $\psi^A \rightarrow \psi^A + \delta \psi^A$, where variations are given by (2)–(4), and (32). Substituting these variations into (73), and making use of the substantial derivative definition (71), we find

$$\delta I = - \int d^4x \left[\xi^k \Omega_k + (\partial_i \xi^k) \Omega_k^i + (\partial_{ij}^2 \xi^k) \Omega_k^{ij} + (\partial_{ijn}^3 \xi^k) \Omega_k^{ijn} \right], \quad (75)$$

where explicitly

$$\begin{aligned}\Omega_k &= \frac{\delta \mathcal{L}}{\delta g_{ij}} \partial_k g_{ij} + \frac{\delta \mathcal{L}}{\delta \psi^A} \partial_k \psi^A + \frac{\partial \mathcal{L}}{\partial \Gamma_{ln}^m} \partial_k \Gamma_{ln}^m + \frac{\partial \mathcal{L}}{\partial \partial_i \Gamma_{ln}^m} \partial_k \partial_i \Gamma_{ln}^m \\ &\quad + \partial_i \left(\frac{\partial \mathcal{L}}{\partial \partial_i g_{mn}} \partial_k g_{mn} + \frac{\partial \mathcal{L}}{\partial \partial_i \psi^A} \partial_k \psi^A - \delta_k^i \mathcal{L} \right),\end{aligned}\quad (76)$$

$$\begin{aligned}\Omega_k^i &= 2 \frac{\delta \mathcal{L}}{\delta g_{ij}} g_{kj} + \frac{\delta \mathcal{L}}{\delta \psi^A} (\sigma^A_B)_k^i \psi^B + \frac{\partial \mathcal{L}}{\partial \partial_i \psi^A} \partial_k \psi^A - \delta_k^i \mathcal{L} \\ &\quad + \frac{\partial \mathcal{L}}{\partial \partial_i g_{mn}} \partial_k g_{mn} + \partial_j \left(2 \frac{\partial \mathcal{L}}{\partial \partial_j g_{in}} g_{nk} + \frac{\partial \mathcal{L}}{\partial \partial_j \psi^A} (\sigma^A_B)_k^i \psi^B \right) \\ &\quad + \frac{\partial \mathcal{L}}{\partial \Gamma_{li}^j} \Gamma_{lk}^j + \frac{\partial \mathcal{L}}{\partial \Gamma_{il}^j} \Gamma_{kl}^j - \frac{\partial \mathcal{L}}{\partial \Gamma_{lj}^k} \Gamma_{li}^j + \frac{\partial \mathcal{L}}{\partial \partial_i \Gamma_{ln}^m} \partial_k \Gamma_{ln}^m \\ &\quad + \frac{\partial \mathcal{L}}{\partial \partial_n \Gamma_{il}^m} \partial_n \Gamma_{kl}^m + \frac{\partial \mathcal{L}}{\partial \partial_n \Gamma_{li}^m} \partial_n \Gamma_{lk}^m - \frac{\partial \mathcal{L}}{\partial \partial_n \Gamma_{lm}^k} \partial_n \Gamma_{li}^m,\end{aligned}\quad (77)$$

$$\begin{aligned}\Omega_k^{ij} &= \frac{\partial \mathcal{L}}{\partial \partial_{(i} \psi^A} (\sigma^A_B)_{k}^{j)} \psi^B + \frac{\partial \mathcal{L}}{\partial \Gamma_{(ij)}^k} + \frac{\partial \mathcal{L}}{\partial \partial_{(i} \Gamma_{j)l}^m} \Gamma_{kl}^m \\ &\quad + 2 \frac{\partial \mathcal{L}}{\partial \partial_{(i} g_{j)n}} g_{kn} + \frac{\partial \mathcal{L}}{\partial \partial_{(i} \Gamma_{|l|j)}^m} \Gamma_{lk}^m - \frac{\partial \mathcal{L}}{\partial \partial_{(i} \Gamma_{|ln|}^k} \Gamma_{ln}^{j)},\end{aligned}\quad (78)$$

$$\Omega_k^{ijn} = \frac{\partial \mathcal{L}}{\partial \partial_{(n} \Gamma_{ij)}^k}.\quad (79)$$

If the action is invariant under general coordinate transformations, $\delta I = 0$, in view of the arbitrariness of the function ξ^i and its derivatives, we find the set of four Noether identities:

$$\Omega_k = 0, \quad \Omega_k^i = 0, \quad \Omega_k^{ij} = 0, \quad \Omega_k^{ijn} = 0.\quad (80)$$

General coordinate invariance is a natural consequence of the fact that the action (68) and the Lagrangian \mathcal{L} are constructed only from covariant objects. Namely, $\mathcal{L} = \mathcal{L}(\psi^A, \nabla_i \psi^A, g_{ij}, R_{kli}^j, N_{kj}^i)$ is a function of the metric, the curvature (5), the torsion (6), the matter fields, and their covariant derivatives (34). Denoting

$$\rho^{ijk}_l := \frac{\partial \mathcal{L}}{\partial R_{ijk}^l}, \quad \mu^{ij}_k := \frac{\partial \mathcal{L}}{\partial N_{ij}^k},\quad (81)$$

we find for the derivatives of the Lagrangian

$$\begin{aligned}\frac{\partial \mathcal{L}}{\partial \Gamma_{ij}^k} &= - \frac{\partial \mathcal{L}}{\partial \nabla_i \psi^A} (\sigma^A_B)_k^j \psi^B - \mu^{ij}_k \\ &\quad + 2 \rho^{inl}_k \Gamma_{nl}^j + 2 \rho^{nij}_l \Gamma_{nk}^l,\end{aligned}\quad (82)$$

$$\frac{\partial \mathcal{L}}{\partial \partial_i \Gamma_{jk}^l} = 2 \rho^{ijk}_l,\quad (83)$$

$$\frac{\partial \mathcal{L}}{\partial \partial_k g_{ij}} = \frac{1}{2} \left(\mu^{(ki)j} + \mu^{(kj)i} - \mu^{(ij)k} \right). \quad (84)$$

As a result, we straightforwardly verify that $\Omega_k^{ij} = 0$ and $\Omega_k^{ijn} = 0$ are indeed satisfied identically.

Using (82) and (83), we then recast the two remaining Noether identities (76) and (77) into

$$\begin{aligned} \Omega_k = & \frac{\delta \mathcal{L}}{\delta g_{ij}} \partial_k g_{ij} + \frac{\delta \mathcal{L}}{\delta \psi^A} \partial_k \psi^A + \partial_i \left(\frac{\partial \mathcal{L}}{\partial \nabla_i \psi^A} \nabla_k \psi^A - \delta_k^i \mathcal{L} \right) \\ & + \widehat{\nabla}_j \left(\frac{\partial \mathcal{L}}{\partial \nabla_j \psi^A} (\sigma^A_B)_m{}^n \psi^B \right) \Gamma_{kn}{}^m + \rho^{iln}{}_m \partial_k R_{iln}{}^m \\ & + \frac{\partial \mathcal{L}}{\partial \nabla_l \psi^A} (\sigma^A_B)_m{}^n \psi^B R_{lkn}{}^m + \mu^{ln}{}_m \partial_k N_{ln}{}^m \\ & + \frac{1}{2} \check{\nabla}_i \left(\mu^{(im)n} + \mu^{(in)m} - \mu^{(mn)i} \right) \partial_k g_{mn}, \end{aligned} \quad (85)$$

$$\begin{aligned} \Omega_k{}^i = & 2 \frac{\delta \mathcal{L}}{\delta g_{ij}} g_{kj} + \frac{\delta \mathcal{L}}{\delta \psi^A} (\sigma^A_B)_k{}^i \psi^B + \frac{\partial \mathcal{L}}{\partial \nabla_i \psi^A} \nabla_k \psi^A - \delta_k^i \mathcal{L} \\ & + \widehat{\nabla}_j \left(\frac{\partial \mathcal{L}}{\partial \nabla_j \psi^A} (\sigma^A_B)_k{}^i \psi^B \right) - \mu^{ln}{}_k N_{ln}{}^i + \mu^{il}{}_n N_{kl}{}^n + \mu^{li}{}_n N_{lk}{}^n \\ & + 2 \rho^{iln}{}_m R_{kl n}{}^m + \rho^{lni}{}_m R_{l n k}{}^m - \rho^{lnm}{}_k R_{l n m}{}^i \\ & + \check{\nabla}_n \left(\mu^{(ni)j} + \mu^{(nj)i} - \mu^{(ij)n} \right) g_{jk} = 0. \end{aligned} \quad (86)$$

Notice that the variational derivative (74) with respect to the matter fields can be identically rewritten as

$$\frac{\delta \mathcal{L}}{\delta \psi^A} \equiv \frac{\partial \mathcal{L}}{\partial \psi^A} - \widehat{\nabla}_j \left(\frac{\partial \mathcal{L}}{\partial \nabla_j \psi^A} \right), \quad (87)$$

and turns out to be a covariant tensor density. It is also worthwhile to note, that the variational derivative w.r.t. the metric is explicitly a covariant density. This follows from the fact that the Lagrangian depends on g_{ij} not only directly, but also through the objects Q_{kij} and $N_{ki}{}^j$. Taking this into account, we find

$$\begin{aligned} \frac{\delta \mathcal{L}}{\delta g_{ij}} &= \frac{d \mathcal{L}}{d g_{ij}} - \partial_n \left(\frac{\partial \mathcal{L}}{\partial \partial_n g_{ij}} \right) \\ &= \frac{\partial \mathcal{L}}{\partial g_{ij}} - \frac{1}{2} \check{\nabla}_n \left(\mu^{(ni)j} + \mu^{(nj)i} - \mu^{(ij)n} \right). \end{aligned} \quad (88)$$

The Noether identity (86) is a covariant relation. In contrast, (85) is apparently non-covariant. However, this can be easily repaired by replacing $\Omega_k = 0$ with an equivalent covariant Noether identity: $\Omega'_k := \Omega_k - \Gamma_{kn}{}^m \Omega_m{}^n = 0$. Explicitly, we find

$$\begin{aligned}
\Omega'_k &= \frac{\delta \mathcal{L}}{\delta \psi^A} \nabla_k \psi^A + \widehat{\nabla}_i \left(\frac{\partial \mathcal{L}}{\partial \nabla_i \psi^A} \nabla_k \psi^A - \delta_k^i \mathcal{L} \right) \\
&\quad - \left(\frac{\partial \mathcal{L}}{\partial \nabla_i \psi^A} \nabla_l \psi^A - \delta_l^i \mathcal{L} \right) T_{ki}{}^l + \frac{\partial \mathcal{L}}{\partial \nabla_l \psi^A} (\sigma^A{}_B)_{m}{}^n \psi^B R_{lkn}{}^m \\
&\quad + \left[-\frac{\delta \mathcal{L}}{\delta g_{ij}} - \frac{1}{2} \check{\nabla}_n \left(\mu^{(ni)j} + \mu^{(nj)i} - \mu^{(ij)n} \right) \right] Q_{kij} \\
&\quad + \mu^{ln}{}_m \nabla_k N_{ln}{}^m + \rho^{iln}{}_m \nabla_k R_{iln}{}^m \\
&= 0.
\end{aligned} \tag{89}$$

On-shell, i.e. assuming that the matter fields satisfy the field equations $\delta \mathcal{L} / \delta \psi^A = 0$, the Noether identities (86) and (89) reduce to the *conservation laws* for the energy-momentum and hypermomentum, respectively.

Equation (86) contains a relation between the canonical and the metrical energy-momentum tensor, and the conservation law of the hypermomentum. In the next section we turn to the discussion of models with general nonminimal coupling.

4 Conservation Laws in Models with Nonminimal Coupling

The results obtained in the previous section are applicable to *any* theory in which the Lagrangian depends arbitrarily on the matter fields and the gravitational field strengths. Now we specialize to the class of models described by an interaction Lagrangian of the form

$$L = F(g_{ij}, R_{kli}{}^j, N_{kl}{}^i) L_{\text{mat}}(\psi^A, \nabla_i \psi^A). \tag{90}$$

Here $L_{\text{mat}}(\psi^A, \nabla_i \psi^A)$ is the ordinary matter Lagrangian. We call $F = F(g_{ij}, R_{kli}{}^j, N_{kl}{}^i)$ the coupling function and assume that it can depend arbitrarily on its arguments, i.e. on all covariant gravitational field variables of MAG. When $F = 1$ we recover the minimal coupling case.

4.1 Identities for the Nonminimal Coupling Function

As a preliminary step, let us derive identities which are satisfied for the nonminimal coupling function $F = F(g_{ij}, R_{kli}{}^j, N_{kl}{}^i)$. For this, we apply the above Lagrange-Noether machinery to the auxiliary Lagrangian density $\mathcal{L}_0 = \sqrt{-g} F$. This quantity does not depend on the matter fields, and both (86) and (89) are considerably simplified. In particular, we have

$$\frac{\delta \mathcal{L}_0}{\delta g_{ij}} = \sqrt{-g} \left(\frac{1}{2} F g^{ij} + F^{ij} \right), \quad F^{ij} := \frac{\delta F}{\delta g_{ij}}. \quad (91)$$

Then we immediately see that (86) and (89) reduce to

$$\begin{aligned} \nabla_k F \equiv & \left[-F^{ij} - \frac{1}{2} \tilde{\nabla}_n \left(\mu^{(ni)j} + \mu^{(nj)i} - \mu^{(ij)n} \right) \right] Q_{kij} \\ & + \rho^{iln}_m \nabla_k R_{iln}{}^m + \mu^{ln}_m \nabla_k N_{ln}{}^m, \end{aligned} \quad (92)$$

$$\begin{aligned} 2F_k{}^i \equiv & -2\rho^{iln}_m R_{kln}{}^m - \rho^{lni}_m R_{lnk}{}^m + \rho^{lnm}_k R_{lnm}{}^i \\ & - \mu^{ln}_k N_{ln}{}^i + \mu^{il}_n N_{kl}{}^n + \mu^{li}_n N_{lk}{}^n \\ & + \tilde{\nabla}_n \left(\mu^{(ni)j} + \mu^{(nj)i} - \mu^{(ij)n} \right) g_{jk}. \end{aligned} \quad (93)$$

Here we denoted

$$\rho^{ijk}_l := \frac{\partial F}{\partial R_{ijk}{}^l}, \quad \mu^{ij}_k := \frac{\partial F}{\partial N_{ij}{}^k}. \quad (94)$$

Notice that for any tensor density we have relations (30) and (29).

The identity (92) is naturally interpreted as a generally covariant generalization of the chain rule for the total derivative of a function of several variables. This becomes obvious when we notice that (88) implies

$$\left[-F^{ij} - \frac{1}{2} \tilde{\nabla}_n \left(\mu^{(ni)j} + \mu^{(nj)i} - \mu^{(ij)n} \right) \right] Q_{kij} = \frac{\partial F}{\partial g_{ij}} \nabla_k g_{ij}. \quad (95)$$

It should be stressed that (92) and (93) are true identities, they are satisfied for any function $F(g_{ij}, R_{kli}{}^j, N_{kl}{}^i)$ irrespectively of the field equations that can be derived from the corresponding action.

4.2 Conservation Laws

Now we are in a position to derive the conservation laws for the general nonminimal coupling model (90). Recall the definitions of the canonical energy-momentum tensor (57), the canonical hypermomentum tensor (58) and the metrical energy-momentum tensor (60).

In view of the product structure of the Lagrangian (90), the derivatives are easily evaluated, and the conservation laws (86) and (89) reduce to

$$\begin{aligned}
& -F t_k^i - \tilde{\nabla}_n^* \left(F \Delta_k^{i n} \right) + F \Sigma_k^i + \left[2 F_k^i \right. \\
& + 2 \rho^{0 i l n} {}_m R_{k l n}^m + \rho^{0 l n i} {}_m R_{l n k}^m - \rho^{0 l n m} {}_k R_{l n m}^i \\
& + \mu^{0 l n} {}_k N_{l n}^i - \mu^{0 i l} {}_n N_{k l}^n - \mu^{0 l i} {}_n N_{l k}^n \\
& \left. - \tilde{\nabla}_n \left(\mu^{(n i) j} + \mu^{(n j) i} - \mu^{(i j) n} \right) g_{j k} \right] L_{\text{mat}} = 0, \tag{96}
\end{aligned}$$

$$\begin{aligned}
& \tilde{\nabla}_i^* \left(F \Sigma_k^i \right) + F \left[-\Sigma_l^i T_{k i}^l + \Delta_n^m {}^l R_{k l m}^n + \frac{1}{2} t^{ij} Q_{kij} \right] \\
& + \left\{ \rho^{0 i l n} {}_m \nabla_k R_{i l n}^m + \mu^{0 l n} {}_m \nabla_k N_{l n}^m + \left[-F^{ij} \right. \right. \\
& \left. \left. - \frac{1}{2} \tilde{\nabla}_n \left(\mu^{(n i) j} + \mu^{(n j) i} - \mu^{(i j) n} \right) \right] Q_{kij} \right\} L_{\text{mat}} = 0. \tag{97}
\end{aligned}$$

After we take into account the identities (92) and (93), the conservation laws (96) and (97) are brought to the final form:

$$F \Sigma_k^i = F t_k^i + \tilde{\nabla}_n^* \left(F \Delta_k^{i n} \right), \tag{98}$$

$$\tilde{\nabla}_i^* \left(F \Sigma_k^i \right) = F \left(\Sigma_l^i T_{k i}^l - \Delta_n^m {}^l R_{k l m}^n - \frac{1}{2} t^{ij} Q_{kij} \right) - L_{\text{mat}} \nabla_k F. \tag{99}$$

Lowering the index in (98) and antisymmetrizing, we derive the conservation law for the spin

$$F \Sigma_{[ij]} + \tilde{\nabla}_n^* \left(F \tau_{ij}^n \right) + Q_{nl[i} \Delta_{j]}^l = 0. \tag{100}$$

This is a generalization of the usual conservation law of the total angular momentum for the case of nonminimal coupling.

4.3 Rewriting the Conservation Laws

Using the definition (31) and decomposing the connection into the Riemannian and non-Riemannian parts (10), we can recast the conservation law (98) into an equivalent form

$$\tilde{\nabla}_j (F \Delta_k^{i j}) = F (\Sigma_k^i - t_k^i + N_{nm}^i \Delta_k^m {}^n - N_{nk}^m \Delta_m^i {}^n). \tag{101}$$

In a similar way we can rewrite the conservation law (99). At first, with the help of (12) and (13) we notice that

$$F \left(\Sigma_l^i T_{k i}^l - \frac{1}{2} t^{ij} Q_{kij} \right) = F (t_l^i - \Sigma_l^i) N_{k i}^l + F \Sigma_l^i N_{i k}^l. \tag{102}$$

Then substituting here (101) and making use of (10), (31), and the curvature decomposition (14), after some algebra we recast (99) into

$$\tilde{\nabla}_j \{F(\Sigma_k^j + \Delta^m_n{}^j N_{km}{}^n)\} = -F \Delta^m_n{}^i (\tilde{R}_{kim}{}^n - \tilde{\nabla}_k N_{im}{}^n) - L_{\text{mat}} \tilde{\nabla}_k F. \quad (103)$$

For the minimal coupling case, such a conservation law was derived in [46, 47]. The importance of this form of the energy-momentum conservation law lies in the clear separation of the Riemannian and non-Riemannian geometrical variables. As we see, the post-Riemannian geometry enters (103) only in the form of the distortion tensor $N_{kj}{}^i$ which is coupled only to the hypermomentum current $\Delta^m_n{}^i$. This means that, in the *minimal coupling* case, ordinary matter—i.e. without microstructure, $\Delta^m_n{}^i = 0$ —does *not* couple to the non-Riemannian geometry. In contrast, in the *nonminimal coupling* case, the derivative of the coupling function F on the right-hand side of (103) may lead to a coupling between non-Riemannian structures and ordinary matter.

4.4 Conserved Current Induced by a Spacetime Symmetry

Every generalized Killing vector field ζ^k generates a conserved current. This can be demonstrated from the analysis of the system (101) and (103) as follows. Let us contract equation (101) with $\tilde{\nabla}_i \zeta^k$ and Eq. (103) with ζ^k , then subtract the resulting expressions. Note that the contraction $t_k^i \tilde{\nabla}_i \zeta^k = 0$ vanishes because the first factor is a symmetric tensor and the second one is skew-symmetric. Then after some algebra we derive

$$\tilde{\nabla}_i \zeta^i = F \Delta^m_n{}^i \mathcal{L}_\zeta N_{im}{}^n - L_{\text{mat}} \mathcal{L}_\zeta F. \quad (104)$$

Here we associate a current with a Killing vector field via

$$\zeta^i := F \left[\zeta^k \Sigma_k^i - (\bar{\nabla}_m \zeta^m) \Delta^m_n{}^i \right]. \quad (105)$$

Note that the transposed connection appears here. The right-hand side of (104) depends linearly on the Lie derivatives along the Killing vector: $\mathcal{L}_\zeta F = \zeta^k \tilde{\nabla}_k F$ and

$$\mathcal{L}_\zeta N_{im}{}^n = \zeta^k \tilde{\nabla}_k N_{im}{}^n + (\tilde{\nabla}_i \zeta^k) N_{km}{}^n + (\tilde{\nabla}_m \zeta^k) N_{ik}{}^n - (\tilde{\nabla}_k \zeta^n) N_{im}{}^k. \quad (106)$$

When ζ^k is a *generalized Killing* vector, we have $\mathcal{L}_\zeta N_{im}{}^n = 0$ in view of (46). Furthermore, recalling that $F = F(g_{ij}, R_{klj}{}^i, N_{kj}{}^i)$, we find

$$\mathcal{L}_\zeta F = \frac{\partial F}{\partial g_{ij}} \mathcal{L}_\zeta g_{ij} + \frac{\partial F}{\partial R_{klj}{}^i} \mathcal{L}_\zeta R_{klj}{}^i + \frac{\partial F}{\partial N_{kj}{}^i} \mathcal{L}_\zeta N_{kj}{}^i = 0, \quad (107)$$

by making use of (46), (47), and (49).

As a result, the right-hand side of (104) vanishes for the generalized Killing vector field, and we conclude that the induced current (105) is conserved

$$\tilde{\nabla}_i \zeta^i = 0. \quad (108)$$

This generalizes the earlier results reported in [30, 48, 49]. In Sect. 6.1.2 we will show that there is a conserved quantity constructed from the multipole moments which is a direct counterpart of the induced current (105). It is worthwhile to give an equivalent form of the latter:

$$\zeta^i I = F \left[\zeta^k (\Sigma_k^i + \Delta_n^m N_{km}^n) - (\tilde{\nabla}_m \zeta^m) \Delta_n^m \right]. \quad (109)$$

4.5 Riemannian Limit

Our results contain the Riemannian theory as a special case. Suppose that the torsion and the nonmetricity are absent $T_{ij}^k = 0$, $Q_{kij} = 0$, hence $N_{ij}^k = 0$. Then for usual matter without microstructure (i.e. matter with $\Delta_n^m = 0$) the canonical and the metrical energy-momentum tensors coincide, $\Sigma_k^i = t_k^i$. As a result, the conservation law (99) reduces to

$$\tilde{\nabla}_i t_k^i = \frac{1}{F} \left(-L_{\text{mat}} \delta_k^i - t_k^i \right) \tilde{\nabla}_i F. \quad (110)$$

This conservation law for the general nonminimal coupling model was derived earlier in [26] without using the Noether theorem, directly from the field equations.¹ The old result established the conservation law for the case in which $F = F(\tilde{R}_{ijk}^l)$ depends arbitrarily on the components of the curvature tensor, correcting some erroneous derivations in the literature, see [26] for details.

Quite remarkably, (110) generalizes the earlier result to the case in which the nonminimal coupling function F is a general scalar function of the curvature tensor.

5 General Multipolar Framework

In this section we derive “master equations of motion” for a general extended test body, which is characterized by a set of currents

$$J^{Aj}. \quad (111)$$

¹Notice a different conventional sign, as compared to our previous work [26].

Normally, these are so-called Noether currents that correspond to an invariance of the action under a certain symmetry group. However, this is not necessary, and any set of currents is formally allowed. We call J^{Aj} dynamical currents. The generalized index (capital Latin letters A, B, \dots) labels different components of the currents.

As the starting point for the derivation of the equations of motion for generalized multipole moments, we consider the following conservation law:

$$\tilde{\nabla}_j J^{Aj} = -\Lambda_{jB}{}^A J^{Bj} - \Pi^A_{\dot{B}} K^{\dot{B}}. \quad (112)$$

On the right-hand side, we introduce objects that can be called material currents

$$K^{\dot{A}} \quad (113)$$

to distinguish them from the dynamical currents J^{Aj} . The number of components of the dynamical and material currents is different, hence we use a different index with dot \dot{A}, \dot{B}, \dots , the range of which does not coincide with that of A, B, \dots . At this stage we do not specify the ranges of both types of indices, this will be done for the particular examples which we analyze later. As usual, Einstein's summation rule over repeated indices is assumed for the generalized indices as well as for coordinate indices.

Both sets of currents J^{Aj} and $K^{\dot{A}}$ are constructed from the variables that describe the structure and the properties of matter inside the body. In contrast, the objects

$$\Lambda_{jB}{}^A, \quad \Pi^A_{\dot{B}}, \quad (114)$$

do not depend on the matter, but they are functions of the external classical fields which act on the body and thereby determine its motion. The list of such external fields include the electromagnetic, gravitational and scalar fields.

We will now derive the equations of motion of a test body by utilizing the covariant expansion method of Synge [7]. For this we need the following auxiliary formula for the absolute derivative of the integral of an arbitrary bitensor density $\mathfrak{B}^{x_1 y_1} = \mathfrak{B}^{x_1 y_1}(x, y)$ (the latter is a tensorial function of two spacetime points):

$$\frac{D}{ds} \int_{\Sigma(s)} \mathfrak{B}^{x_1 y_1} d\Sigma_{x_1} = \int_{\Sigma(s)} \tilde{\nabla}_{x_1} \mathfrak{B}^{x_1 y_1} w^{x_2} d\Sigma_{x_2} + \int_{\Sigma(s)} v^{y_2} \tilde{\nabla}_{y_2} \mathfrak{B}^{x_1 y_1} d\Sigma_{x_1}. \quad (115)$$

Here $v^{y_1} := dx^{y_1}/ds$, s is the proper time, $\frac{D}{ds} = v^i \tilde{\nabla}_i$, and the integral is performed over a spatial hypersurface. Note that in our notation the point to which the index of a bitensor belongs can be directly read from the index itself; e.g., y_n denotes indices at the point y . Furthermore, we will now associate the point y with the world-line of the test body under consideration. Here σ denotes Synge's [7] world-function and σ^y its first covariant derivative; g^y_x is the parallel propagator for vectors. For objects with more complicated tensorial properties the parallel propagator is straightforwardly

generalized to G^Y_X and $G^{\dot{Y}}_{\dot{X}}$. We will need these generalized propagators to deal with the dynamical and material currents J^{Aj} and $K^{\dot{A}}$. More details are collected in the appendix on our conventions.

After these preliminaries, we introduce integrated moments for the two types of currents via (for $n = 0, 1, \dots$)

$$j^{y_1 \dots y_n Y_0} = (-1)^n \int_{\Sigma(\tau)} \sigma^{y_1} \dots \sigma^{y_n} G^{Y_0}_{X_0} \mathfrak{J}^{X_0 x''} d\Sigma_{x''}, \quad (116)$$

$$i^{y_1 \dots y_n Y_0 y'} = (-1)^n \int_{\Sigma(\tau)} \sigma^{y_1} \dots \sigma^{y_n} G^{Y_0}_{X_0} g^{y'}_{x'} \mathfrak{J}^{X_0 x'} w^{x''} d\Sigma_{x''}, \quad (117)$$

$$m^{y_1 \dots y_n \dot{Y}_0} = (-1)^n \int_{\Sigma(\tau)} \sigma^{y_1} \dots \sigma^{y_n} G^{\dot{Y}_0}_{\dot{X}_0} \mathfrak{R}^{\dot{X}_0} w^{x''} d\Sigma_{x''}. \quad (118)$$

Here the densities are constructed from the currents: $\mathfrak{J}^{X_0 x_1} = \sqrt{-g} J^{X_0 x_1}$ and $\mathfrak{R}^{\dot{X}_0} = \sqrt{-g} K^{\dot{X}_0}$. Integrating (112) and making use of (115), we find the following “master equation of motion” for the generalized multipole moments:

$$\begin{aligned} \frac{D}{ds} j^{y_1 \dots y_n Y_0} = & -n v^{(y_1} j^{y_2 \dots y_n) Y_0} + n i^{(y_1 \dots y_{n-1} | Y_0 | y_n)} \\ & - \gamma^{Y_0}_{Y' Y'' y_{n+1}} \left(i^{y_1 \dots y_n Y' y''} + j^{y_1 \dots y_n Y' v^{y''}} \right) \\ & - \Lambda_{y' Y'' Y_0; y_1 \dots y_n Y'' y'} - \Lambda_{y' Y'' Y_0; y_{n+1}} i^{y_1 \dots y_{n+1} Y'' y'} \\ & - \Pi^{Y_0}_{\dot{Y}'} m^{y_1 \dots y_n \dot{Y}'} - \Pi^{Y_0}_{\dot{Y}'; y_{n+1}} m^{y_1 \dots y_{n+1} \dot{Y}'} \\ & + \sum_{k=2}^{\infty} \frac{1}{k!} \left[-(-1)^k n \alpha^{(y_1}_{y' y_{n+1} \dots y_{n+k}} i^{y_2 \dots y_n) y_{n+1} \dots y_{n+k} Y_0 y'} \right. \\ & + (-1)^k n v^{y'} \beta^{(y_1}_{y' y_{n+1} \dots y_{n+k}} j^{y_2 \dots y_n) y_{n+1} \dots y_{n+k} Y_0} \\ & + (-1)^k \gamma^{Y_0}_{Y' Y'' y_{n+1} \dots y_{n+k}} \left(i^{y_1 \dots y_{n+k} Y' y''} + j^{y_1 \dots y_{n+k} Y' v^{y''}} \right) \\ & - \Lambda_{y' Y'' Y_0; y_{n+1} \dots y_{n+k}} i^{y_1 \dots y_{n+k} Y'' y'} \\ & \left. - \Pi^{Y_0}_{\dot{Y}'; y_{n+1} \dots y_{n+k}} m^{y_1 \dots y_{n+k} \dot{Y}'} \right]. \quad (119) \end{aligned}$$

5.1 Electrodynamics in Minkowski Spacetime

To see how the general formalism works, let us consider the motion of electrically charged extended test bodies under the influence of the electromagnetic field in flat Minkowski spacetime. This problem was earlier analyzed by means of a different approach in [50].

In this case, it is convenient to recast the set of dynamical currents into the form of a column

$$J^{Aj} = \begin{pmatrix} J^j \\ \Sigma^{kj} \end{pmatrix}, \quad (120)$$

where J^j is the electric current and Σ^{kj} is the energy-momentum tensor. Physically, the structure of the dynamical current is crystal clear: the matter elements of an extended body are characterized by the two types of “charges”, the electrical charge (the upper component) and the mass (the lower component).

The generalized conservation law comprises two components of different tensor dimension:

$$\tilde{\nabla}_j \begin{pmatrix} J^j \\ \Sigma^{kj} \end{pmatrix} = \begin{pmatrix} 0 \\ -F^{kj} J_j \end{pmatrix}, \quad (121)$$

where the lower component of the right-hand side describes the usual Lorentz force.

Accordingly, we indeed recover for the dynamical current (120) the conservation law in the form (112), where $K^{\dot{B}} = 0$ and

$$\Lambda_{jB}^A = \left(\begin{array}{c|c} 0 & 0 \\ \hline F_j^k & 0 \end{array} \right). \quad (122)$$

The generalized moments (116)–(118) have the same column structure, reflecting the two physical charges of matter:

$$j^{y_1 \dots y_n} Y_0 = \begin{pmatrix} j^{y_1 \dots y_n} \\ p^{y_1 \dots y_n} Y_0 \end{pmatrix}, \quad (123)$$

$$i^{y_1 \dots y_n} Y_0 y' = \begin{pmatrix} i^{y_1 \dots y_n} y' \\ k^{y_1 \dots y_n} Y_0 y' \end{pmatrix}, \quad (124)$$

whereas $m^{y_1 \dots y_n} \dot{Y}_0 = 0$.

As a result, the master equation (119) reduces to the coupled system of the two sets of equations for the moments:

$$\frac{D}{ds} j^{y_1 \dots y_n} = -n v^{(y_1} j^{y_2 \dots y_n)} + n i^{(y_1 \dots y_n)}, \quad (125)$$

$$\begin{aligned} \frac{D}{ds} p^{y_1 \dots y_n} Y_0 &= -n v^{(y_1} p^{y_2 \dots y_n) Y_0} + n k^{(y_1 \dots y_{n-1}} | y_0 | y_n) \\ &\quad - F_{y'}^{y_0} i^{y_1 \dots y_n} y' - \sum_{k=1}^{\infty} \frac{1}{k!} F_{y'}^{y_0; y_{n+1} \dots y_{n+k}} i^{y_1 \dots y_{n+k}} y'. \end{aligned} \quad (126)$$

These equations should be compared to those of [50].

6 Equations of Motion in Metric-Affine Gravity

We are now in a position to derive the equations of motion for extended test bodies in metric-affine gravity. As a preliminary step, we rewrite the conservation laws (98) and (99) as [22]:

$$\tilde{\nabla}_j \Delta^i{}_k{}^j = -U_{jm}{}^{ni}{}_k \Delta^m{}_n{}^j + \Sigma_k{}^i - t_k{}^i, \quad (127)$$

$$\tilde{\nabla}_j \Sigma_k{}^j = -V_j{}^n{}_k \Sigma_n{}^j - R_{kjm}{}^n \Delta^m{}_n{}^j - \frac{1}{2} Q_{kj}{}^n t_n{}^j - A_k L_{\text{mat}}. \quad (128)$$

Here we denoted $A_k := \tilde{\nabla}_k \log F$, and

$$U_{jmn}{}^{ik} := A_j \delta_m^i \delta_n^k - N_{jm}{}^i \delta_n^k + N_j{}^k{}_n \delta_m^i, \quad (129)$$

$$V_{jn}{}^k := A_j \delta_n^k + N^k{}_{jn}. \quad (130)$$

Introducing the dynamical current

$$J^{Aj} = \begin{pmatrix} \Delta^{ikj} \\ \Sigma^{kj} \end{pmatrix}, \quad (131)$$

and the material current

$$K^{\dot{A}} = \begin{pmatrix} t^{ik} \\ L_{\text{mat}} \end{pmatrix}, \quad (132)$$

we then recast the system (127) and (128) into the generic conservation law (112), where we now have

$$\Lambda_{jB}{}^A = \left(\begin{array}{c|c} U_{ji'k'}{}^{ik} & -\delta_{j'}^i \delta_{k'}^k \\ \hline R^k{}_{ji'k'} & V_{jk'}{}^k \end{array} \right), \quad (133)$$

$$\Pi^A{}_{\dot{B}} = \left(\begin{array}{c|c} \delta_{i'}^i \delta_{k'}^k & 0 \\ \hline \frac{1}{2} Q^k{}_{i'k'} & A^k \end{array} \right). \quad (134)$$

Like in the previous example of an electrically charged body, the matter elements in metric-affine gravity are also characterized by two “charges”: the canonical hypermomentum (upper component) and the canonical energy-momentum (lower component). This is reflected in the column structure of the dynamical current (131). The material current (132) takes into account the metrical energy-momentum and the matter Lagrangian related to the nonminimal coupling. The multi-index $A = \{ik, k\}$, whereas $\dot{A} = \{ik, 1\}$. Accordingly, the generalized propagator reads

$$G^Y{}_X = \left(\begin{array}{c|c} g^{y_1}{}_{x_1} g^{y_2}{}_{x_2} & 0 \\ \hline 0 & g^{y_1}{}_{x_1} \end{array} \right), \quad (135)$$

and we easily construct the expansion coefficients of its derivatives from the corresponding expansions of the derivatives of vector propagator g^y_x :

$$\gamma^{Y_0}_{Y_1 Y_2 \dots Y_{k+2}} = \left(\frac{\gamma^{\{y_0 \tilde{y}\}}_{\{y' y''\} y_2 \dots y_{k+2}}}{0} \middle| \frac{0}{\gamma^{y_0}_{y' y_2 \dots y_{k+2}}} \right), \quad (136)$$

where we denoted

$$\gamma^{\{y_0 \tilde{y}\}}_{\{y' y''\} y_2 \dots y_{k+2}} = \gamma^{y_0}_{y' y_2 \dots y_{k+2}} \delta^{\tilde{y}}_{y''} + \gamma^{\tilde{y}}_{y'' y_2 \dots y_{k+2}} \delta^{y_0}_{y'} . \quad (137)$$

In particular, for the first expansion coefficient ($k = 1$), we find

$$\gamma^{\{y_0 \tilde{y}\}}_{\{y' y''\} y_2 y_3} = \frac{1}{2} \left(\tilde{R}^{y_0}_{y' y_2 y_3} \delta^{\tilde{y}}_{y''} + \tilde{R}^{\tilde{y}}_{y'' y_2 y_3} \delta^{y_0}_{y'} \right), \quad (138)$$

$$\gamma^{y_0}_{y' y_2 y_3} = \frac{1}{2} \tilde{R}^{y_0}_{y' y_2 y_3} . \quad (139)$$

For completeness, let us write down also another generalized propagator

$$G^{\dot{Y}}_{\dot{X}} = \left(\frac{g^{y_1}_{x_1} g^{y_2}_{x_2}}{0} \middle| \frac{0}{1} \right). \quad (140)$$

The last step is to write the generalized moments (116)–(118) in terms of their components:

$$j^{y_1 \dots y_n Y} = \left(\frac{h^{y_1 \dots y_n y' y''}}{p^{y_1 \dots y_n y'}} \right), \quad (141)$$

$$i^{y_1 \dots y_n Y y_0} = \left(\frac{q^{y_1 \dots y_n y' y'' y_0}}{k^{y_1 \dots y_n y' y_0}} \right), \quad (142)$$

$$m^{y_1 \dots y_n \dot{Y}} = \left(\frac{\mu^{y_1 \dots y_n y' y''}}{\xi^{y_1 \dots y_n}} \right). \quad (143)$$

For the two most important moments, “ h ” stands for the hypermomentum, whereas “ p ” stands for the momentum.² Finally, substituting all the above into the “master equation” (119), we obtain the system of multipolar equations of motion for extended test bodies in metric-affine gravity:

²Note that in order to facilitate the comparison with our previous work [51], we provide in appendix the explicit form of integrated conservation laws (127) and (128), as well as the generalized integrated moments (141)–(143) in the notation used in [51].

$$\begin{aligned}
\frac{D}{ds} h^{y_1 \dots y_n y_a y_b} = & -n v^{(y_1} h^{y_2 \dots y_n) y_a y_b} + n q^{(y_1 \dots y_{n-1} | y_a y_b | y_n)} \\
& + k^{y_1 \dots y_n y_b y_a} - \mu^{y_1 \dots y_n y_a y_b} \\
& - \frac{1}{2} \tilde{R}^{y_a}_{y' y'' y_{n+1}} \left(q^{y_1 \dots y_{n+1} y' y_b y''} + v^{y''} h^{y_1 \dots y_{n+1} y' y_b} \right) \\
& - \frac{1}{2} \tilde{R}^{y_b}_{y' y'' y_{n+1}} \left(q^{y_1 \dots y_{n+1} y_a y' y''} + v^{y''} h^{y_1 \dots y_{n+1} y_a y'} \right) \\
& - U_{y_0 y' y'' y_n y_a y_b} q^{y_1 \dots y_n y' y'' y_0} - U_{y_0 y' y'' y_n y_a y_b ; y_{n+1}} q^{y_1 \dots y_{n+1} y' y'' y_0} \\
& + \sum_{k=2}^{\infty} \frac{1}{k!} \left[(-1)^k v^{y'} n \beta^{(y_1}_{y' y_{n+1} \dots y_{n+k}} h^{y_2 \dots y_n) y_{n+1} \dots y_{n+k} y_a y_b} \right. \\
& + (-1)^k \gamma^{y_a}_{y' y'' y_{n+1} \dots y_{n+k}} \left(q^{y_1 \dots y_{n+k} y' y_b y''} + v^{y''} h^{y_1 \dots y_{n+k} y' y_b} \right) \\
& + (-1)^k \gamma^{y_b}_{y' y'' y_{n+1} \dots y_{n+k}} \left(q^{y_1 \dots y_{n+k} y_a y' y''} + v^{y''} h^{y_1 \dots y_{n+k} y_a y'} \right) \\
& - (-1)^k n \alpha^{(y_1}_{y' y_{n+1} \dots y_{n+k}} q^{y_2 \dots y_n) y_{n+1} \dots y_{n+k} y_a y_b y'} \\
& \left. - U_{y_0 y' y'' y_n y_a y_b ; y_{n+1} \dots y_{n+k}} q^{y_1 \dots y_{n+k} y' y'' y_0} \right], \tag{144}
\end{aligned}$$

$$\begin{aligned}
\frac{D}{ds} p^{y_1 \dots y_n y_a} = & -n v^{(y_1} p^{y_2 \dots y_n) y_a} + n k^{(y_1 \dots y_{n-1} | y_a | y_n)} \\
& - A^{y_a} \xi^{y_1 \dots y_n} - A^{y_a}_{; y_{n+1}} \xi^{y_1 \dots y_{n+1}} \\
& - V_{y'' y' y_a} k^{y_1 \dots y_n y' y''} - V_{y'' y' y_a ; y_{n+1}} k^{y_1 \dots y_{n+1} y' y''} \\
& - \frac{1}{2} \tilde{R}^{y_a}_{y' y'' y_{n+1}} \left(k^{y_1 \dots y_{n+1} y' y''} + v^{y''} p^{y_1 \dots y_{n+1} y'} \right) \\
& - R^{y_a}_{y_0 y' y''} q^{y_1 \dots y_n y' y'' y_0} - R^{y_a}_{y_0 y' y'' ; y_{n+1}} q^{y_1 \dots y_{n+1} y' y'' y_0} \\
& - \frac{1}{2} Q^{y_a}_{y'' y' \mu} \mu^{y_1 \dots y_n y' y''} - \frac{1}{2} Q^{y_a}_{y'' y' ; y_{n+1}} \mu^{y_1 \dots y_{n+1} y' y''} \\
& + \sum_{k=2}^{\infty} \frac{1}{k!} \left[(-1)^k n v^{y'} \beta^{(y_1}_{y' y_{n+1} \dots y_{n+k}} p^{y_2 \dots y_n) y_{n+1} \dots y_{n+k} y_a} \right. \\
& + (-1)^k \gamma^{y_a}_{y' y'' y_{n+1} \dots y_{n+k}} \left(k^{y_1 \dots y_{n+k} y' y''} + v^{y''} p^{y_1 \dots y_{n+k} y'} \right) \\
& - (-1)^k n \alpha^{(y_1}_{y' y_{n+1} \dots y_{n+k}} k^{y_2 \dots y_n) y_{n+1} \dots y_{n+k} y_a y'} \\
& - R^{y_a}_{y_0 y' y'' ; y_{n+1} \dots y_{n+k}} q^{y_1 \dots y_{n+k} y' y'' y_0} \\
& - V_{y'' y' y_a ; y_{n+1} \dots y_{n+k}} k^{y_1 \dots y_{n+k} y' y''} \\
& - \frac{1}{2} Q^{y_a}_{y'' y' ; y_{n+1} \dots y_{n+k}} \mu^{y_1 \dots y_{n+k} y' y''} \\
& \left. - A^{y_a}_{; y_{n+1} \dots y_{n+k}} \xi^{y_1 \dots y_{n+k}} \right]. \tag{145}
\end{aligned}$$

6.1 Special Cases

The general equations of motion (144) and (145) are valid to *any* multipolar order. In the following sections we focus on some special cases, in particular we work out the two lowest multipolar orders of approximation, and consider the explicit form of the equations of motion in special geometries.

6.1.1 General Pole-Dipole Equations of Motion

From (144) and (145), we can derive the general pole-dipole equations of motion. The relevant moments to be kept at this order of approximation are: p^a , p^{ab} , h^{ab} , q^{abc} , k^{ab} , k^{abc} , μ^{ab} , μ^{abc} , ξ^a , and ξ . Since all objects are now evaluated on the world-line, we switch back to the usual tensor notation.

For $n = 1$ and $n = 0$, Eq. (144) yields

$$0 = k^{acb} - \mu^{abc} + q^{bca} - v^a h^{bc}, \quad (146)$$

$$\frac{D}{ds} h^{ab} = k^{ba} - \mu^{ab} - U_{cde}{}^{ab} q^{dec}. \quad (147)$$

Furthermore for $n = 2, 1, 0$ Eq. (145) yields

$$0 = k^{(a|c|b)} - v^{(a} p^{b)c}, \quad (148)$$

$$\frac{D}{ds} p^{ab} = k^{ba} - v^a p^b - A^b \xi^a - V_{dc}{}^b k^{acd} - \frac{1}{2} Q^b{}_{dc} \mu^{acd}, \quad (149)$$

$$\begin{aligned} \frac{D}{ds} p^a &= -V_{cb}{}^a k^{bc} - R^a{}_{dbc} q^{bcd} - \frac{1}{2} Q^a{}_{cb} \mu^{bc} \\ &\quad - A^a \xi - \frac{1}{2} \tilde{R}^a{}_{cdb} (k^{bcd} + v^d p^{bc}) \\ &\quad - V_{dc}{}^a{}_{;b} k^{bcd} - \frac{1}{2} Q^a{}_{dc;b} \mu^{bcd} - A^a{}_{;b} \xi^b. \end{aligned} \quad (150)$$

Rewriting the equations of motion Let us decompose (146) and (147) into symmetric and skew-symmetric parts:

$$\mu^{abc} = k^{a(bc)} + q^{(bc)a} - v^a h^{(bc)}, \quad (151)$$

$$0 = -k^{a[bc]} + q^{[bc]a} - v^a h^{[bc]}, \quad (152)$$

$$\mu^{ab} = -\frac{D}{ds} h^{(ab)} + k^{(ab)} - U_{cde}{}^{(ab)} q^{dec}, \quad (153)$$

$$\frac{D}{ds} h^{[ab]} = -k^{[ab]} - U_{cde}{}^{[ab]} q^{dec}. \quad (154)$$

As a result, we can express the moments symmetric in the two last indices $\mu^{ab} = \mu^{(ab)}$ and $\mu^{cab} = \mu^{c(ab)}$ (in general, this is possible also for an arbitrary order $\mu^{c_1 \dots c_n ab} = \mu^{c_1 \dots c_n (ab)}$) in terms of the other moments.

Let us denote the skew-symmetric part $s^{ab} := h^{[ab]}$, as this simplifies greatly the subsequent manipulations and the comparison with [51].

The system of the two equations (148) and (152) can be resolved in terms of the 3rd rank k -moment. The result reads explicitly

$$\begin{aligned} k^{abc} = & v^a p^{cb} + v^c \left(p^{[ab]} - s^{ab} \right) + v^b \left(p^{[ac]} - s^{ac} \right) + v^a \left(p^{[bc]} - s^{bc} \right) \\ & + q^{[ab]c} + q^{[ac]b} + q^{[bc]a}. \end{aligned} \quad (155)$$

This yields some useful relations:

$$k^{a[bc]} = -v^a s^{bc} + q^{[bc]a}, \quad (156)$$

$$k^{[ab]c} = v^{[a} p^{c|b]} + v^c \left(p^{[ab]} - s^{ab} \right) + q^{[ab]c}. \quad (157)$$

The next step is to use the Eqs. (151), (153) together with (155) and to substitute the μ -moments and k -moments into (147), (149) and (150). This yields a system that depends only on the p , h , q , and ξ moments.

Let us start with the analysis of (150). The latter contains the combination $k^{[b|c|d]} + v^{[d} p^{b]c}$ where the skew symmetry is imposed by the contraction with the Riemann curvature tensor, which is antisymmetric in the two last indices. Making use of (155), we derive

$$k^{[a|c|b]} + v^{[b} p^{a]c} = \kappa^{abc} + \kappa^{acb} - \kappa^{bca}, \quad (158)$$

where we introduced the abbreviation

$$\kappa^{abc} := v^c \left(p^{[ab]} - s^{ab} \right) + q^{[ab]c}. \quad (159)$$

Note that by construction $\kappa^{abc} = \kappa^{[ab]c}$.

Then by making use of the Ricci identity we find

$$-\frac{1}{2} \tilde{R}^a{}_{cdb} \left(k^{bcd} + v^d p^{bc} \right) = \tilde{R}^a{}_{bcd} \left[q^{[cd]b} + v^b \left(p^{[cd]} - s^{cd} \right) \right]. \quad (160)$$

Substituting k^{bc} from (149) and μ^{bc} from (153), we find after some algebra

$$\begin{aligned} -V_{cb}{}^a k^{bc} - \frac{1}{2} Q^a{}_{cb} \mu^{bc} = & -A_b \frac{Dp^{ba}}{ds} - N^a{}_{cd} \frac{Dh^{cd}}{ds} - \left(p^a + N^a{}_{cd} h^{cd} \right) v^b A_b \\ -A^a A^b \xi_b - k^{bac} A_b A_c + & \left(N^a{}_{nb} N_{dc}{}^n - N^a{}_{cn} N_d{}^n{}_b \right) q^{cbd}. \end{aligned} \quad (161)$$

Further simplification is achieved by noticing that

$$v^b A_b = \frac{DA}{ds}, \quad k^{bac} A_b A_c = p^{ca} A_c \frac{DA}{ds}, \quad (162)$$

where we used (148) and recalled that $A_b = A_{;b}$.

Analogously, taking $k^{b[cd]}$ from (156) and μ^{bcd} from (151), we derive

$$-V_{dc}{}^a{}_{;b} k^{bcd} - \frac{1}{2} Q^a{}_{dc;b} \mu^{bcd} = -A_{b;c} k^{cab} + N^a{}_{cd;b} q^{cdb} - N^a{}_{cd;b} v^b h^{cd}. \quad (163)$$

We can again use $A_b = A_{;b}$ and (148) to simplify

$$-A_{b;c} k^{cab} = -p^{ba} \frac{DA_b}{ds}. \quad (164)$$

After these preliminary calculations, we substitute (160)–(164) into (150) to recast the latter into

$$\begin{aligned} \frac{D}{ds} \left(F p^a + F N^a{}_{cd} h^{cd} + p^{ba} \widehat{\nabla}_b F \right) &= F \tilde{R}^a{}_{bcd} v^b \left(p^{[cd]} - s^{cd} \right) \\ &- F q^{cbd} \left[R^a{}_{dcb} - \tilde{R}^a{}_{dcb} - N^a{}_{cb;d} - N^a{}_{nb} N_{dc}{}^n + N^a{}_{cn} N_d{}^n{}_b \right] \\ &- F A^a \left(\xi + \xi^b A_b \right) - F \xi^b A^a{}_{;b}. \end{aligned} \quad (165)$$

Finally, combining (147) and (149) to eliminate k^{ba} we derive the equation

$$\begin{aligned} \frac{D}{ds} \left(p^{ab} - h^{ab} \right) &= \mu^{ab} - v^a \left(p^b + N^b{}_{cd} h^{cd} \right) \\ &+ q^{cda} N^b{}_{cd} - q^{cbd} N_{dc}{}^a + q^{acd} N_d{}^b{}_c \\ &- \xi^a A^b + (q^{abc} - k^{abc}) A_c. \end{aligned} \quad (166)$$

Following [51], we introduce the total orbital and the total spin angular moments

$$L^{ab} := 2p^{[ab]}, \quad S^{ab} := -2h^{[ab]}, \quad (167)$$

and define the generalized total energy-momentum 4-vector and the generalized total angular momentum by

$$\mathcal{P}^a := F(p^a + N^a{}_{cd} h^{cd}) + p^{ba} \widehat{\nabla}_b F, \quad (168)$$

$$\mathcal{J}^{ab} := F(L^{ab} + S^{ab}). \quad (169)$$

Then, taking into account the identity (14), which with the help of the raising and lowering of indices can be recast into

$$\tilde{\nabla}^a N_{dcb} = -R^a{}_{dcb} + \tilde{R}^a{}_{dcb} + N^a{}_{cb;d} + N^a{}_{nb} N_{dc}{}^n - N_d{}^n{}_b N^a{}_{cn}, \quad (170)$$

we rewrite the pole-dipole equations of motion (165) and (166) in the final form

$$\begin{aligned} \frac{D\mathcal{P}^a}{ds} &= \frac{1}{2} \tilde{R}^a{}_{bcd} v^b \mathcal{J}^{cd} + F q^{cbd} \tilde{\nabla}^a N_{dcb} \\ &\quad - \xi \tilde{\nabla}^a F - \xi^b \tilde{\nabla}_b \tilde{\nabla}^a F, \end{aligned} \quad (171)$$

$$\begin{aligned} \frac{D\mathcal{J}^{ab}}{ds} &= -2v^{[a} \mathcal{P}^{b]} + 2F(q^{cd[a} N^{b]}{}_{cd} + q^{c[a|d|} N_{dc}{}^{b]} + q^{[a|cd|} N_d{}^{b]}{}_c) \\ &\quad - 2\xi^{[a} \tilde{\nabla}^{b]} F. \end{aligned} \quad (172)$$

The last equation arises as the skew-symmetric part of (166), whereas the symmetric part of the latter is a non-dynamical relation that determines the μ^{ab} moment

$$\begin{aligned} \mu^{ab} &= \frac{D\Upsilon^{ab}}{ds} + \frac{1}{F} v^{(a} (\mathcal{P}^{b)} + \mathcal{J}^{b)c} A_c) + \xi^{(a} A^{b)} \\ &\quad - q^{cd(a} N^{b)}{}_{cd} + q^{c(a|d|} N_{dc}{}^{b)} - q^{(a|cd|} N_d{}^{b)}{}_c \\ &\quad + (q^{[ac]b} + q^{[bc]a} - q^{(ab)c}) A_c. \end{aligned} \quad (173)$$

Here the symmetric moment of the total hypermomentum is introduced via

$$\Upsilon^{ab} := p^{(ab)} - h^{(ab)}. \quad (174)$$

6.1.2 Conserved Quantity

The equations of motion for the multipole moments are derived from the conservation laws of the energy-momentum and the hypermomentum currents Σ_k^i and $\Delta_n^m{}^i$. In Sect. 4.4 we demonstrated that every generalized Killing vector induces a conserved current constructed from Σ_k^i and $\Delta_n^m{}^i$. Quite remarkably, there is a direct counterpart of such an induced current built from the multipole moments.

Let ζ^k be a generalized Killing vector, and let us contract equation (171) with ζ_a and Eq. (172) with $\frac{1}{2} \tilde{\nabla}_a \zeta_b$, and then take the sum. This yields

$$\frac{D}{ds} \left(\mathcal{P}^a \zeta_a + \frac{1}{2} \mathcal{J}^{ab} \tilde{\nabla}_a \zeta_b \right) = F q^{cbd} \mathcal{L}_\zeta N_{dcb} - \xi \mathcal{L}_\zeta F - \xi^a \tilde{\nabla}_a \mathcal{L}_\zeta F. \quad (175)$$

On the right-hand side, the Lie derivatives of the distortion tensor and of the coupling function both vanish in view of (46) and (107).

Consequently, we conclude that for every generalized Killing vector field the quantity

$$\mathcal{P}^a \zeta_a + \frac{1}{2} \mathcal{J}^{ab} \tilde{\nabla}_a \zeta_b = \text{const.} \quad (176)$$

is conserved along the trajectory of an extended body.

We thus observe a complete consistency between (104), (105), (109) and (176), (175).

6.1.3 Coupling to the Post-Riemannian Geometry: Fine Structure

Let us look more carefully at how the post-Riemannian pieces of the gravitational field couple to extended test bodies. At first, we notice that the generalized energy-momentum vector (168) contains the term $N^a{}_{cd} h^{cd}$ that describes the direct interaction of the distortion (torsion plus nonmetricity) with the intrinsic dipole moment of the hypermomentum. Decomposing the latter into the skew-symmetric (spin) part and the symmetric (proper hypermomentum + dilation) part, we find

$$N^a{}_{cd} h^{cd} = -\frac{1}{2} N^a{}_{[cd]} S^{cd} - \frac{1}{2} Q^a{}_{cd} h^{(cd)}. \quad (177)$$

Here we made use of (13). This is well consistent with the gauge-theoretic structure of metric-affine gravity. The second term shows that the intrinsic proper hypermomentum and the dilation moment couple to the nonmetricity, whereas the first term displays the typical spin-torsion coupling.

Similar observations can be made for the coupling of higher moments which appear on the right-hand sides of (171) and (172)—and thus determine the force and torque acting on an extended body due to the post-Riemannian gravitational field. In order to see this, let us introduce the decomposition

$$-\frac{1}{2} q^{abc} = \overset{d}{q}{}^{abc} + \overset{s}{q}{}^{cab} \quad (178)$$

into the two pieces

$$\overset{d}{q}{}^{abc} := \frac{1}{2} \left(q^{[ac]b} + q^{[bc]a} - q^{(ab)c} \right), \quad (179)$$

$$\overset{s}{q}{}^{abc} := \frac{1}{2} \left(q^{[ab]c} + q^{[ac]b} - q^{[bc]a} \right). \quad (180)$$

The overscript “ d ” and “ s ” notation shows the relevance of these objects to the dilation plus proper hypermomentum and to the spin, respectively. By construction, we have the following algebraic properties

$$\overset{d}{q}{}^{[ab]c} \equiv 0, \quad \overset{s}{q}{}^{(ab)c} \equiv 0. \quad (181)$$

Making use of the decomposition (178) and of the explicit structure of the distortion (11), we then recast the equations of motion (171) and (172) into

$$\begin{aligned} \frac{D\mathcal{P}^a}{ds} &= \frac{1}{2} \tilde{R}^a{}_{bcd} v^b \mathcal{J}^{cd} \\ &\quad + F \tilde{q}^{cbd} \tilde{\nabla}^a T_{cbd} + F \tilde{q}^{cbd} \tilde{\nabla}^a Q_{dcb} \\ &\quad - \xi \tilde{\nabla}^a F - \xi^b \tilde{\nabla}_b \tilde{\nabla}^a F, \end{aligned} \quad (182)$$

$$\begin{aligned} \frac{D\mathcal{J}^{ab}}{ds} &= -2v^{[a} \mathcal{P}^{b]} \\ &\quad + 2F(\tilde{q}^{cd[a} T_{cd}{}^{b]} + 2\tilde{q}^{[a|cd|} T^{b]}{}_{cd}) \\ &\quad + 2F(\tilde{q}^{cd[a} Q^{b]}{}_{cd} + 2\tilde{q}^{[a|dc|} Q_{cd}{}^{b]}) \\ &\quad - 2\xi^{[a} \tilde{\nabla}^{b]} F. \end{aligned} \quad (183)$$

Now we clearly see the fine structure of the coupling of extended bodies to the post-Riemannian geometry. The first lines in the equations of motion describe the usual Mathisson-Papapetrou force and torque. They depend on the Riemannian geometry only. A body with the nontrivial moment (180) is affected by the torsion field, whereas the nontrivial moment (179) feels the nonmetricity. This explains the different physical meaning of the higher moments (179) and (180). In addition, the last lines in (182) and (183) describe contributions due to the nonminimal coupling.

6.1.4 General Monopolar Equations of Motion

At the monopolar order we have nontrivial moments p^a , k^{ab} , μ^{ab} and ξ . The nontrivial equations of motion then arise from (144) for $n = 0$ and from (145) for $n = 1$, $n = 0$:

$$0 = k^{ba} - \mu^{ab}, \quad (184)$$

$$0 = k^{ba} - v^a p^b, \quad (185)$$

$$\frac{Dp^a}{ds} = -V_{cb}{}^a k^{bc} - \frac{1}{2} Q^a{}_{cb} \mu^{bc} - A^a \xi. \quad (186)$$

The first two Eqs. (184) and (185) yield

$$k^{[ab]} = 0, \quad v^{[a} p^{b]} = 0, \quad (187)$$

and substituting (184), (185) and (187) into (186) we find

$$\frac{D(Fp^a)}{ds} = -\xi \tilde{\nabla}^a F. \quad (188)$$

From (187) we have $p^a = Mv^a$ with the mass $M := v^a p_a$, and this allows to recast (188) into the final form

$$M \frac{Dv^a}{ds} = -\xi(g^{ab} - v^a v^b) \frac{\tilde{\nabla}_b F}{F}. \quad (189)$$

Hence, in general the motion of nonminimally coupled monopole test bodies is non-geodesic. Furthermore, the general monopole equation of motion (189) reveals an interesting feature of theories with nonminimal coupling. There is an “indirect” coupling, i.e. through the coupling function $F(g_{ij}, R_{ijk}^l, T_{ij}^k, Q_{ij}^k)$, of post-Riemannian spacetime features to structureless test bodies.

6.1.5 Weyl-Cartan Spacetime

In Weyl-Cartan spacetime the nonmetricity reads $Q_{kij} = Q_k g_{ij}$, where Q_k is the Weyl covector. Hence the distortion is given by

$$N_{kj}^i = K_{kj}^i + \frac{1}{2} \left(Q^i g_{kj} - Q_k \delta_j^i - Q_j \delta_k^i \right). \quad (190)$$

The contortion tensor is constructed from the torsion,

$$K_{kj}^i = -\frac{1}{2} (T_{kj}^i + T^i_{kj} + T^i_{jk}). \quad (191)$$

As a result, the generalized momentum (168) in Weyl-Cartan spacetime takes the form:

$$\mathcal{P}^a = F p^a - \frac{F}{2} \left(K^a_{cd} S^{cd} - Q_b S^{ba} + Q^a D \right) + p^{ba} \tilde{\nabla}_b F. \quad (192)$$

Here we introduced the *intrinsic dilation* moment $D := g_{ab} h^{ab}$.

Substituting the distortion (190) into (171) and (172), we find the pole-dipole equations of motion in Weyl-Cartan spacetime:

$$\begin{aligned} \frac{D\mathcal{P}^a}{ds} &= \frac{1}{2} \tilde{R}^a_{bcd} v^b \mathcal{J}^{cd} + F \tilde{q}^{bcd} \tilde{\nabla}^a T_{cbd} \\ &\quad + Z^b \tilde{\nabla}^a Q_b - \xi \tilde{\nabla}^a F - \xi^b \tilde{\nabla}_b \tilde{\nabla}^a F, \end{aligned} \quad (193)$$

$$\begin{aligned} \frac{D\mathcal{J}^{ab}}{ds} &= -2v^{[a} \mathcal{P}^{b]} + 2F(\tilde{q}^{cd[a} T_{cd}^{b]} + 2\tilde{q}^{[a|cd|} T^{b]}_{cd}) \\ &\quad + 2F Z^{[a} Q^{b]} - 2\xi^{[a} \tilde{\nabla}^{b]} F. \end{aligned} \quad (194)$$

Here we introduced the trace of the modified moment (179)

$$Z^a := g_{bc} q^{d bca} = \frac{1}{2} g_{bc} (q^{bac} - q^{bca} - q^{abc}). \quad (195)$$

It is coupled to the Weyl nonmetricity.

6.1.6 Weyl Spacetime

Weyl spacetime [52] is obtained as a special case of the results above for vanishing torsion. Hence the contortion is trivial

$$K_{abc} = 0. \quad (196)$$

Taking this into account, the generalized momentum (192) and the equations of motion (193) and (194) are simplified even further.

It is interesting to note that besides a direct coupling of the dilation moment to the Weyl nonmetricity on the right-hand sides of (193) and (194), there is also a nontrivial coupling of the spin to the nonmetricity in (192).

6.1.7 Riemann-Cartan Spacetime

Another special case is obtained when the Weyl vector vanishes $Q_a = 0$. Equations (192)–(194) then reproduce *in a covariant way* the findings of Yasskin and Stoeger [53] when the coupling is minimal ($F = 1$). For nonminimal coupling we recover our earlier results in [51].

7 Equations of Motion in Scalar-Tensor Theories

The geometrical arena of scalar-tensor theories is the Riemannian spacetime, hence $N_{kj}^i = 0$ which means that both the torsion $T_{ij}^k = 0$ and the nonmetricity $Q_{kij} = 0$ vanish.

Scalar-tensor theories have a long history and they belong to the most straightforward generalizations of Einstein's general relativity theory. In the so-called Brans-Dicke theory [54–58] a scalar field is introduced as a variable “gravitational coupling constant” (which is thus more correctly called a “gravitational coupling function”). Similar formalisms were developed earlier by Jordan [59, 60], Thiry [61] and their collaborators using the 5-dimensional Kaluza-Klein approach. An overview of the history and developments of scalar-tensor theories can be found in [62–65].

Surprisingly little attention was paid to the equations of motion of extended test bodies in scalar-tensor theories. Some early discussions can be found in [56, 66, 67], and in [68] the dynamics of compact bodies was thoroughly studied in the framework of the post-Newtonian formalism.

7.1 Scalar-Tensor Theory: Jordan Frame

We consider the class of scalar-tensor theories along the lines of [68] where the action $I = \int d^4x \mathcal{L}$ is constructed on the manifold with the spacetime metric g_{ij}^J . The Lagrangian density $\mathcal{L} = \sqrt{-g}^J L$ has the following form

$$L = \frac{1}{2\kappa} \left(-F^2 \tilde{R}^J(g) + g^{ij} \gamma_{AB}^J \partial_i \varphi^A \partial_j \varphi^B - 2U \right) + L_m(\psi, \partial\psi, g_{ij}^J). \quad (197)$$

This action is an extension of standard Brans-Dicke theory [69] to the case when we have a multiplet of scalar fields φ^A (capital Latin indices $A, B, C = 1, \dots, N$ label the components of the multiplet). Here $\kappa = 8\pi G/c^4$ denotes Einstein's gravitational constant and in general we have several functions of scalar fields,

$$F = F(\varphi^A), \quad U = U(\varphi^A), \quad \gamma_{AB}^J = \gamma_{AB}^J(\varphi^A). \quad (198)$$

The Lagrangian $L_m(\psi, \partial\psi, g_{ij}^J)$ depends on the matter fields ψ and the gravitational field.

The metric g_{ij}^J determines angles and intervals in the *Jordan reference frame*. The Riemannian curvature scalar $\tilde{R}^J(g)$ is constructed from the Jordan metric. With the help of the conformal transformation

$$g_{ij}^J \longrightarrow g_{ij} = F^2 g_{ij}^J \quad (199)$$

we obtain a different metric on the spacetime manifold. This is called an Einstein reference frame.

7.2 Conservation Laws: Einstein Frame

In the *Einstein reference frame* the Lagrangian density in the scalar-tensor theory reads $\mathcal{L} = \sqrt{-g} L$ with

$$L = \frac{1}{2\kappa} \left(-\tilde{R} + g^{ij} \gamma_{AB} \partial_i \varphi^A \partial_j \varphi^B - 2U \right) + \frac{1}{F^4} L_{\text{mat}}(\psi, \partial\psi, F^{-2} g_{ij}). \quad (200)$$

Here the scalar curvature $\tilde{R}(g)$ is constructed from the Einstein metric g_{ij} , and

$$\gamma_{AB} = \frac{1}{F^2} (\gamma_{AB}^J + 6F_{,A} F_{,B}), \quad U = \frac{1}{F^4} U^J. \quad (201)$$

The metrical energy-momentum tensor for the matter Lagrangian L_{mat} is constructed as usual via (60). From the Noether theorem we find that it satisfies the generalized conservation law

$$\tilde{\nabla}^i t_{ij} = \frac{1}{F} (4t_{ij} - g_{ij}t) \partial^i F. \quad (202)$$

Here $t := g^{ij}t_{ij}$. The derivation is given in [23].

To begin with, we recast (202) into an equivalent form

$$\tilde{\nabla}_i t^{ij} = -A_i (\Xi^{ij} + t^{ij}) \quad (203)$$

by introducing

$$A_i := \partial_i \log F^{-4}, \quad \Xi^{ij} := -g^{ij}t/4. \quad (204)$$

7.3 General Equations of Motion: Arbitrary Multipole Order

We now derive the equations of motion for extended test bodies in scalar-tensor gravity by making use of the master equations obtained for the general case of MAG. In scalar-tensor theory, the hypermomentum is zero $\Delta^{ikj} = 0$. Following the general scheme, we introduce the dynamical current which is a special case of the MAG current:

$$J^{Aj} = \begin{pmatrix} 0 \\ \Sigma^{kj} \end{pmatrix}. \quad (205)$$

Taking into account the structure of the conservation laws (203) and (204), we define the material current

$$K^{\dot{A}} = \begin{pmatrix} t^{ik} \\ -t/4 \end{pmatrix}, \quad (206)$$

we then recast the system (203) into the generic conservation law, where we now have

$$\Lambda_{jB}{}^A = \left(\begin{array}{c|c} 0 & -\delta_j^i \delta_{k'}^k \\ \hline 0 & V_{jk'}{}^k \end{array} \right), \quad (207)$$

$$\Pi^A{}_{\dot{B}} = \left(\begin{array}{c|c} \delta_{i'}^i \delta_{k'}^k & 0 \\ \hline 0 & A^k \end{array} \right). \quad (208)$$

In accordance with (203) and (204) we now have

$$V_{jn}{}^k = A_j \delta_n^k, \quad A_i = \partial_i \log F^{-4}. \quad (209)$$

In view of (205) and (206) the generalized moments read

$$j^{y_1 \dots y_n Y} = \begin{pmatrix} 0 \\ p^{y_1 \dots y_n y'} \end{pmatrix}, \quad (210)$$

$$i^{y_1 \dots y_n Y y_0} = \begin{pmatrix} 0 \\ k^{y_1 \dots y_n y' y_0} \end{pmatrix}, \quad (211)$$

$$m^{y_1 \dots y_n \dot{Y}} = \begin{pmatrix} \mu^{y_1 \dots y_n y' y''} \\ \xi^{y_1 \dots y_n} \end{pmatrix}. \quad (212)$$

It is worthwhile to notice that although we formally use a different notation for the upper and lower components of the moment (212), they are not independent. Recalling (206), we have the obvious relation

$$\xi^{y_1 \dots y_n} = -\frac{1}{4} g_{y' y''} \mu^{y_1 \dots y_n y' y''}, \quad (213)$$

which we will take into account when rewriting the equations of motion.

Now we can make use of the general MAG equations of motion (119). The first equation is a degenerate version of (144) since we have $h^{y_1 \dots y_n y_a y_b} = 0$ and $q^{y_1 \dots y_{n-1} y_a y_b y_n} = 0$, and we are left with the algebraic relation

$$k^{y_1 \dots y_n y_b y_a} = \mu^{y_1 \dots y_n y_a y_b}. \quad (214)$$

for all n . Hence we find

$$\xi^{y_1 \dots y_n} = -\frac{1}{4} g_{y' y''} k^{y_1 \dots y_n y' y''}, \quad (215)$$

and the second equation (145) then gives rise to the equations of motion in scalar-tensor theory

$$\begin{aligned} \frac{D}{ds} p^{y_1 \dots y_n y_a} = & -n v^{(y_1} p^{y_2 \dots y_n) y_a} + n k^{(y_1 \dots y_{n-1} | y_a | y_n)} \\ & - A^{y_a} \xi^{y_1 \dots y_n} - A^{y_a}_{; y_{n+1}} \xi^{y_1 \dots y_{n+1}} \\ & - V_{y'' y' y_a} k^{y_1 \dots y_n y' y''} - V_{y'' y' y_a}_{; y_{n+1}} k^{y_1 \dots y_{n+1} y' y''} \\ & - \frac{1}{2} \tilde{R}^{y_a}_{y' y'' y_{n+1}} \left(k^{y_1 \dots y_{n+1} y' y''} + v^{y''} p^{y_1 \dots y_{n+1} y'} \right) \\ & + \sum_{k=2}^{\infty} \frac{1}{k!} \left[-(-1)^k n \alpha^{(y_1}_{y' y_{n+1} \dots y_{n+k}} k^{y_2 \dots y_n) y_{n+1} \dots y_{n+k} y_a} y' \right. \\ & + (-1)^k n v^{y'} \beta^{(y_1}_{y' y_{n+1} \dots y_{n+k}} p^{y_2 \dots y_n) y_{n+1} \dots y_{n+k} y_a} \\ & + (-1)^k \gamma^{y_a}_{y' y'' y_{n+1} \dots y_{n+k}} \left(k^{y_1 \dots y_{n+k} y' y''} + v^{y''} p^{y_1 \dots y_{n+k} y'} \right) \\ & \left. - V_{y'' y' y_a}_{; y_{n+1} \dots y_{n+k}} k^{y_1 \dots y_{n+k} y' y''} - A^{y_a}_{; y_{n+1} \dots y_{n+k}} \xi^{y_1 \dots y_{n+k}} \right]. \quad (216) \end{aligned}$$

The system (216) is valid up to any multipole order. In the following we specialize it to the dipole and the monopole case.

7.4 Pole-Dipole Equations of Motion in Scalar-Tensor Theory

For $n = 2, 1, 0$ Eq. (216) yields

$$0 = k^{(a|c|b)} - v^{(a} p^{b)c}, \quad (217)$$

$$\frac{D}{ds} p^{ab} = k^{ba} - v^a p^b - A^b \xi^a - V_{dc}{}^b k^{acd}, \quad (218)$$

$$\begin{aligned} \frac{D}{ds} p^a &= -V_{cb}{}^a k^{bc} - V_{dc}{}^a{}_{;b} k^{bcd} - A^a{}_{;b} \xi^b \\ &\quad - A^a \xi - \frac{1}{2} \tilde{R}^a{}_{cdb} (k^{bcd} + v^d p^{bc}). \end{aligned} \quad (219)$$

Taking into account that $k^{a[bc]} = 0$, we resolve (217) in a standard way to find explicitly

$$k^{abc} = v^a p^{cb} + v^c p^{[ab]} + v^b p^{[ac]} + v^a p^{[bc]}. \quad (220)$$

In view of (215), we have in addition

$$\xi^a = -\frac{1}{4} g_{bc} k^{abc}, \quad (221)$$

$$\xi = -\frac{1}{4} g_{ab} k^{ab}. \quad (222)$$

Then repeating the same algebra as we did in MAG, we recast the system (218) and (219) into

$$\frac{D\mathcal{P}^a}{ds} = \frac{1}{2} \tilde{R}^a{}_{bcd} v^b \mathcal{J}^{cd} - \xi \tilde{\nabla}^a F^{-4} - \xi^b \tilde{\nabla}_b \tilde{\nabla}^a F^{-4}, \quad (223)$$

$$\frac{D\mathcal{J}^{ab}}{ds} = -2v^{[a} \mathcal{P}^{b]} - 2\xi^{[a} \tilde{\nabla}^{b]} F^{-4}. \quad (224)$$

Here, following [51], we have the total orbital angular momentum $L^{ab} := 2p^{[ab]}$. Whereas the generalized total energy-momentum 4-vector and the generalized total angular momentum are introduced by

$$\mathcal{P}^a := F^{-4} p^a + p^{ba} \tilde{\nabla}_b F^{-4}, \quad (225)$$

$$\mathcal{J}^{ab} := F^{-4} L^{ab}. \quad (226)$$

7.5 Monopolar Equations of Motion in Scalar-Tensor Theory

At the monopolar order we find from Eq. (216) for $n = 1, n = 0$:

$$0 = k^{ba} - v^a p^b, \quad (227)$$

$$\frac{Dp^a}{ds} = -V_{cb}{}^a k^{bc} - A^a \xi. \quad (228)$$

Making use of $k^{[ab]} = 0$, the first equation yields $v^{[a} p^{b]} = 0$, hence we have

$$p^a = M v^a \quad (229)$$

with the mass $M := v^a p_a$. Substituting (209), (227) and (229) into (228) we find

$$\frac{D(F^{-4} M v^a)}{ds} = -\xi \tilde{\nabla}^a F^{-4}. \quad (230)$$

Contracting this with v_a , we derive

$$\frac{D(F^{-4} M)}{ds} = -\xi v^a \tilde{\nabla}_a F^{-4}, \quad (231)$$

we write (230) in the final form

$$M \frac{Dv^a}{ds} = -\xi (g^{ab} - v^a v^b) \frac{\tilde{\nabla}_b F^{-4}}{F^{-4}}. \quad (232)$$

Combining (222) with (227) we find

$$\xi = -\frac{v^a p_a}{4} = -\frac{M}{4}. \quad (233)$$

Substituting this into (232), we obtain

$$\frac{Dv^a}{ds} = -(g^{ab} - v^a v^b) \frac{\tilde{\nabla}_b F}{F}. \quad (234)$$

Quite remarkably, we thus find that the dynamics of an extended test body in the monopole approximation is independent of the body's mass. In case of a trivial coupling function F , Eq. (234) reproduces the well known general relativistic result.

Interestingly, the mass of a body is not constant. Substituting (233) into (231) we can solve the resulting differential equation to find explicitly the dependence of mass on the scalar function: $M = F^3 M_0$ with $M_0 = \text{const.}$

8 Conclusions

We have presented a general multipolar framework of covariant test body equations of motion for standard metric-affine gravity, as well as its extensions with nonminimal coupling between matter and gravity. Our results cover gauge theories of gravity (based on spacetime symmetry groups), and various so-called $f(R)$ models (and their generalizations), as well as scalar-tensor gravity.

Our results unify and extend a whole set of works [26, 51, 53, 70–78]. In particular they can be viewed as a completion of the program initiated in [73], in which a noncovariant Papapetrou [2] type of approach was used. The general equations of motion (144) and (145) cover *all* of the previously reported cases. As demonstrated explicitly, the master equation (119) allows for a quick adoption to any physical theory, as soon as the conservation laws and (multi-)current structure is fixed. Table 1 contains an overview of our main results in the context of metric-affine gravity. In particular, the explicit equations of motion at the pole-dipole and monopole order are given. We stress that these equations hold for the most general case, i.e. including a general nonminimal coupling between matter and gravity. The results for standard (minimal) MAG are easily recovered by choosing a trivial coupling function F .

Our analysis reveals how the new geometrical structures in generalized theories of gravity couple to matter, which in turn should be used for the design of experimental tests of gravity beyond the Einsteinian (purely Riemannian) geometrical picture. In the case of *minimal* coupling, we have once more confirmed—now in a very general context—that only matter with microstructure (such as the intrinsic hypermomentum, including spin, dilation and shear charges) allows for the detection of post-Riemannian structures. However, in gravitational theories with

Table 1 Overview: MAG equations of motion

<i>Lagrangian and conservation laws</i>	
$L = V(g_{ij}, R_{ijk}^l, N_{ki}^j) + F(g_{ij}, R_{kli}^j, N_{kl}^i) L_{\text{mat}}(\psi^A, \nabla_i \psi^A)$ $\tilde{\nabla}_j (F \Delta^i_k{}^j) = F(\Sigma_k^i - t_k^i + N_{nm}^i \Delta^m_k{}^n - N_{nk}^m \Delta^i_m{}^n)$ $\tilde{\nabla}_j \{F(\Sigma_k^j + \Delta^m_n{}^j N_{km}^n)\} = -F \Delta^m_n{}^i (\tilde{R}_{kim}^n - \tilde{\nabla}_k N_{im}^n) - L_{\text{mat}} \tilde{\nabla}_k F$	
<i>Equations of motion (any order)</i>	
See Eqs. (144) and (145)	
<i>Equations of motion (pole-dipole order)</i>	
$\frac{D\mathcal{P}^a}{ds} = \frac{1}{2} \tilde{R}^a_{bcd} v^b \mathcal{J}^{cd} + F q^{cbd} \tilde{\nabla}^a N_{dcb} - \xi \tilde{\nabla}^a F - \xi^b \tilde{\nabla}_b \tilde{\nabla}^a F$ $\frac{D\mathcal{J}^{ab}}{ds} = -2v^{[a} \mathcal{P}^{b]} + 2F(q^{cd[a} N^{b]}_{cd} + q^{c[a d } N_{dc}^{b]} + q^{[a cd } N_d^{b]}{}_{c}) - 2\xi^{[a} \tilde{\nabla}^{b]} F$ $L^{ab} = 2p^{[ab]} \quad S^{ab} = -2h^{[ab]}$ $\mathcal{P}^a = F(p^a + N^a_{cd} h^{cd}) + p^{ba} \tilde{\nabla}_b F \quad \mathcal{J}^{ab} = F(L^{ab} + S^{ab})$	
<i>Equations of motion (monopole order)</i>	
$M \frac{Dv^a}{ds} = -\xi(g^{ab} - v^a v^b) \frac{\tilde{\nabla}_b F}{F} \quad M = p^a v_a$	

Table 2 Overview: scalar-tensor equations of motion (Einstein frame)

<i>Lagrangian and conservation law</i>
$L = \frac{1}{2\kappa} (-\tilde{R} + g^{ij}\gamma_{AB}\partial_i\varphi^A\partial_j\varphi^B - 2U) + \frac{1}{F^4} L_{\text{mat}}(\psi, \partial\psi, F^{-2}g_{ij})$ $F = F(\varphi^A) \quad U = U(\varphi^A) \quad \gamma_{AB} = \gamma_{AB}(\varphi^A)$ $\tilde{\nabla}^i t_{ij} = \frac{1}{F} (4t_{ij} - g_{ij}t) \partial^i F$
<i>Equations of motion (any order)</i>
See Eq. (216)
<i>Equations of motion (pole-dipole order)</i>
$\frac{D\mathcal{P}^a}{ds} = \frac{1}{2}\tilde{R}^a{}_{bcd}v^b\mathcal{J}^{cd} - \xi\tilde{\nabla}^a F^{-4} - \xi^b\tilde{\nabla}_b\tilde{\nabla}^a F^{-4}$ $\frac{D\mathcal{J}^{ab}}{ds} = -2v^{[a}\mathcal{P}^{b]} - 2\xi^{[a}\tilde{\nabla}^{b]} F^{-4}$ $L^{ab} = 2p^{[ab]}$ $\mathcal{P}^a = F^{-4}p^a + p^{ba}\tilde{\nabla}_b F^{-4} \quad \mathcal{J}^{ab} = F^{-4}L^{ab}$
<i>Equations of motion (monopole order)</i>
$\frac{Dv^a}{ds} = -(g^{ab} - v^av^b)\frac{\tilde{\nabla}_b F}{F}$

nonminimal coupling, there seems to be a loophole which may prove to be interesting for possible experiments; i.e. there is an *indirect* coupling of new geometrical quantities to regular matter via the nonminimal coupling function F . This may be exploited to devise new strategies to detect possible post-Riemannian spacetime features in future experiments.

In addition to the results in MAG, we have explicitly worked out the test body equations of motion for a very general class of scalar-tensor gravitational theories. Table 2 contains an overview of our main results in the context of this theory class. Again the equations of motion at the pole-dipole and monopole order for a general coupling function F , which now depends on the scalar degrees of freedom, are explicitly given.

We hope that our covariant unified multipolar framework sheds more light on the systematic test of gravitational theories by means of extended and microstructured test bodies. We would like to conclude with a statement by Einstein [79] who stressed that

[...] the question whether this continuum has a Euclidean, Riemannian, or any other structure is a question of physics proper which must be answered by experience, and not a question of a convention to be chosen on grounds of mere expediency.

Acknowledgments We would like to thank A. Trautman (University of Warsaw), W.G. Dixon (University of Cambridge), J. Madore (University of Paris South), and W. Tulczyjew (INFN Napoli) for sharing their insights into gravitational multipole formalisms and discussing their pioneering works with us. Furthermore, we would like to thank F.W. Hehl (University of Cologne) for fruitful discussion on gauge gravity models, in particular on Metric-Affine Gravity (MAG). This work was supported by the Deutsche Forschungsgemeinschaft (DFG) through the grant LA-905/8-1/2 and SFB 1128/1 (D.P.).

Appendix

A Conventions and Symbols

In the following we summarize our conventions, and collect some frequently used formulas. A directory of symbols used throughout the text can be found in Tables 3, 4 and 5.

Table 3 Directory of symbols

Symbol	Explanation
<i>Geometrical quantities</i>	
x^a, s	Coordinates, proper time
g_{ab}	Metric
δ^a_b	Kronecker symbol
g	Determinant of the metric
σ	World-function
$\Gamma_{ab}{}^c$	Connection
$\widehat{\Gamma}_{ab}{}^c$	Riemannian connection
$\overline{\Gamma}_{ab}{}^c$	Transposed connection
$R_{abc}{}^d$	Curvature
Q_{abc}	Nonmetricity
Q_a	Weyl covector
$T_{ab}{}^c$	Torsion
$K_{ab}{}^c$	Contortion
$N_{ab}{}^c$	Distortion
R_{ab}, R	Ricci tensor/scalar
$(\sigma^A{}_B)_{j^i}$	Generators of general coordinate transformations
V, \mathfrak{V}	Gravitational Lagrangian (density)
$(H^{\cdots}, \mathfrak{H}^{\cdots}), (M^{\cdots}, \mathfrak{M}^{\cdots})$	Generalized gravitational field momenta (densities)
$E^{ab}{}_b, \mathfrak{E}^{ab}{}_b$	Gravitational hypermomentum (density)
$E_a{}^b, \mathfrak{E}_a{}^b$	Generalized gravitational energy-momentum (density)
I	General action
L, \mathfrak{L}	Total Lagrangian (density)
Φ^J	General set of fields
ζ^a	(Generalized) Killing vector
$J^{Aj}, \mathfrak{J}^{Aj}$	General dynamical currents (densities)
$^J g_{ij}$	Jordan frame metric
$^J L, \mathfrak{L}$	Total Lagrangian (density) in Jordan frame

Table 4 Directory of symbols

Symbol	Explanation
<i>Matter quantities</i>	
ψ^A	General matter field
$L_{\text{mat}}, \mathfrak{L}_{\text{mat}}$	Matter Lagrangian (density)
$\Sigma_a{}^b, \mathfrak{T}_a{}^b$	Canonical energy-momentum (density) of matter
$\Delta^a{}_b{}^c, \mathfrak{S}^a{}_b{}^c$	Canonical hypermomentum (density) of matter
$t_{ab}, \mathfrak{t}_{ab}$	Metrical energy-momentum (density)
$\tau_{ab}{}^c$	Spin current
Δ^a	Dilation current
v^a	Four velocity
p	Pressure (hyperfluid)
P_a	Momentum density (hyperfluid)
$J_a{}^b$	Intrinsic hypermomentum density (hyperfluid)
F, A	Coupling function
F^{ab}	Variation of the coupling function
ζ I^a	Induced conserved current
$K^{\hat{A}}, \mathfrak{K}^{\hat{A}}$	General material currents (densities)
$j^{\cdots}, i^{\cdots}, m^{\cdots}, p^{\cdots}, k^{\cdots},$	Integrated moments
$h^{\cdots}, q^{\cdots}, \mu^{\cdots}, \xi^{\cdots}$	
F^{ab}	Electromagnetic field
J^a	Electric current
L^{ab}, \mathcal{S}^{ab}	Total orbital/spin angular momentum
$\mathcal{P}^a, \mathcal{J}^{ab}$	Generalized total momentum/angular momentum
Υ^{ab}	Total hypermomentum
M	Generalized test body mass
D	Intrinsic dilation moment
φ^A	Multiplet of scalar fields
κ	Einstein's gravitational coupling constant

For an arbitrary k -tensor $T_{a_1 \dots a_k}$, the symmetrization and antisymmetrization are defined by

$$T_{(a_1 \dots a_k)} := \frac{1}{k!} \sum_{I=1}^{k!} T_{\pi_I \{a_1 \dots a_k\}}, \quad (235)$$

$$T_{[a_1 \dots a_k]} := \frac{1}{k!} \sum_{I=1}^{k!} (-1)^{|\pi_I|} T_{\pi_I \{a_1 \dots a_k\}}, \quad (236)$$

Table 5 Directory of symbols

Symbol	Explanation
<i>Auxiliary quantities</i>	
$\Omega_a, \Omega_a^b, \Omega_a^{bc}, \Omega_a^{bcd}, \Omega'_k$	Auxiliary variables (Noether identities)
ρ^{abc}_d, μ^{ab}_c	Partial derivatives of the total Lagrangian
\mathfrak{L}_0	Auxiliary Lagrangian density
$\overset{0}{\rho^{abc}}_d, \overset{0}{\mu^{ab}}_c$	Partial derivatives of the coupling function
$A, B, \dots; \dot{A}, \dot{B}, \dots$	General multi-indices
$\Lambda_{jB}^A, \Pi_{\dot{B}}^A$	General functions of external classical fields
$U_{abc}^d, V_{ab}^c, \kappa^{abc}$	Auxiliary variables (MAG equations of motion)
A_k	Derivative of the coupling function
$\alpha^{y_0}_{y_1 \dots y_n}, \beta^{y_0}_{y_1 \dots y_n}, \gamma^{y_0}_{y_1 \dots y_n}$	Expansion coefficients of the parallel propagator
$\overset{d}{q}^{abc}, \overset{s}{q}^{abc}$	Decomposition pieces of the q-moments
Z^a	Trace of the $\overset{d}{q}$ moment
$\gamma_{AB}, \overset{J}{\gamma}_{AB}$	General function of scalar fields (in Jordan frame)
$U, \overset{J}{U}$	General potential of scalar fields (in Jordan frame)
Ξ^{ab}	Auxiliary variable (Einstein frame)
$\Phi^{y_1 \dots y_n y_0}_{x_0}, \Psi^{y_2 \dots y_n + 1 y_0 y_1}_{x_0 x_1}$	Auxiliary variables multipole expansions
<i>Operators/accents</i>	
$\partial_a, \mathcal{L}_\zeta$	(Partial, Lie) derivative
∇_a	Covariant derivative
$\widehat{\nabla}_a, \text{“} \cdot \text{”}_a$	Riemannian covariant derivative
$\overline{\nabla}_a$	Transposed covariant derivative
$\widehat{\nabla}_a$	Covariant density derivative
$\check{\nabla}_a$	Riemannian covariant density derivative
$\overset{*}{\nabla}_a$	Modified covariant density derivative
$\frac{D}{ds} = \text{“} \cdot \text{”}$	Total derivative
$\delta, \delta_{(s)}$	Variation, substantial variation
\mathfrak{B}_{\dots}	(Bi-)Tensor density
$g^{y_0}_{x_0}, G^Y_X$	(Generalized) parallel propagator
$\text{“} J \text{”}$	Jordan frame quantity
\mathfrak{C}	Riemannian quantity
$\text{“} [\dots] \text{”}$	Coincidence limit

where the sum is taken over all possible permutations (symbolically denoted by $\pi_{I\{a_1 \dots a_k\}}$) of its k indices. As is well-known, the number of such permutations is equal to $k!$. The sign factor depends on whether a permutation is even ($|\pi| = 0$) or odd ($|\pi| = 1$). The number of independent components of the totally symmetric

tensor $T_{(a_1 \dots a_k)}$ of rank k in n dimensions is equal to the binomial coefficient $\binom{n-1+k}{k} = (n-1+k)!/[k!(n-1)!]$, whereas the number of independent components of the totally antisymmetric tensor $T_{[a_1 \dots a_k]}$ of rank k in n dimensions is equal to the binomial coefficient $\binom{n}{k} = n!/[k!(n-k)!]$. For example, for a second rank tensor T_{ab} the symmetrization yields a tensor $T_{(ab)} = \frac{1}{2}(T_{ab} + T_{ba})$ with 10 independent components, and the antisymmetrization yields another tensor $T_{[ab]} = \frac{1}{2}(T_{ab} - T_{ba})$ with 6 independent components.

In the derivation of the equations of motion we made use of the bitensor formalism, see, e.g., [7, 8, 80] for introductions and references. In particular, the world-function is defined as an integral $\sigma(x, y) := \frac{1}{2}\epsilon \left(\int_x^y d\tau \right)^2$ over the geodesic curve connecting the spacetime points x and y , where $\epsilon = \pm 1$ for timelike/spacelike curves. Note that our curvature conventions differ from those in [7, 80]. Indices attached to the world-function always denote covariant derivatives, at the given point, i.e. $\sigma_y := \tilde{\nabla}_y \sigma$, hence we do not make explicit use of the semicolon in case of the world-function. The parallel propagator by $g^y_x(x, y)$ allows for the parallel transportation of objects along the unique geodesic that links the points x and y . For example, given a vector V^x at x , the corresponding vector at y is obtained by means of the parallel transport along the geodesic curve as $V^y = g^y_x(x, y)V^x$. For more details see, e.g., [7, 8] or Sect. 5 in [80]. A compact summary of useful formulas in the context of the bitensor formalism can also be found in the appendices A and B of [26].

We start by stating, without proof, the following useful rule for a bitensor B with arbitrary indices at different points (here just denoted by dots):

$$[B_{\dots}]_{;y} = [B_{\dots;y}] + [B_{\dots;x}]. \quad (237)$$

Here a coincidence limit of a bitensor $B_{\dots}(x, y)$ is a tensor

$$[B_{\dots}] = \lim_{x \rightarrow y} B_{\dots}(x, y), \quad (238)$$

determined at y . Furthermore, we collect the following useful identities:

$$\sigma_{y_0 y_1 x_0 y_2 x_1} = \sigma_{y_0 y_1 y_2 x_0 x_1} = \sigma_{x_0 x_1 y_0 y_1 y_2}, \quad (239)$$

$$g^{x_1 x_2} \sigma_{x_1} \sigma_{x_2} = 2\sigma = g^{y_1 y_2} \sigma_{y_1} \sigma_{y_2}, \quad (240)$$

$$[\sigma] = 0, \quad [\sigma_x] = [\sigma_y] = 0, \quad (241)$$

$$[\sigma_{x_1 x_2}] = [\sigma_{y_1 y_2}] = g_{y_1 y_2}, \quad [\sigma_{x_1 y_2}] = [\sigma_{y_1 x_2}] = -g_{y_1 y_2}, \quad (242)$$

$$[\sigma_{x_1 x_2 x_3}] = [\sigma_{x_1 x_2 y_3}] = [\sigma_{x_1 y_2 y_3}] = [\sigma_{y_1 y_2 y_3}] = 0, \quad (243)$$

$$[g^{x_0}_{y_1}] = \delta^{y_0}_{y_1}, \quad [g^{x_0}_{y_1; x_2}] = [g^{x_0}_{y_1; y_2}] = 0, \quad (244)$$

$$[g^{x_0}_{y_1; x_2 x_3}] = \frac{1}{2} \tilde{R}^{y_0}_{y_1 y_2 y_3}. \quad (245)$$

B Covariant Expansions

Here we briefly summarize the covariant expansions of the second derivative of the world-function, and the derivative of the parallel propagator:

$$\sigma^{y_0}_{x_1} = g^{y'}_{x_1} \left(-\delta^{y_0}_{y'} + \sum_{k=2}^{\infty} \frac{1}{k!} \alpha^{y_0}_{y' y_2 \dots y_{k+1}} \sigma^{y_2} \dots \sigma^{y_{k+1}} \right), \quad (246)$$

$$\sigma^{y_0}_{y_1} = \delta^{y_0}_{y_1} - \sum_{k=2}^{\infty} \frac{1}{k!} \beta^{y_0}_{y_1 y_2 \dots y_{k+1}} \sigma^{y_2} \dots \sigma^{y_{k+1}}, \quad (247)$$

$$g^{y_0}_{x_1; x_2} = g^{y'}_{x_1} g^{y''}_{x_2} \left(\frac{1}{2} \tilde{R}^{y_0}_{y' y'' y_3} \sigma^{y_3} + \sum_{k=2}^{\infty} \frac{1}{k!} \gamma^{y_0}_{y' y'' y_3 \dots y_{k+2}} \sigma^{y_3} \dots \sigma^{y_{k+2}} \right), \quad (248)$$

$$g^{y_0}_{x_1; y_2} = g^{y'}_{x_1} \left(\frac{1}{2} \tilde{R}^{y_0}_{y' y_2 y_3} \sigma^{y_3} + \sum_{k=2}^{\infty} \frac{1}{k!} \gamma^{y_0}_{y' y_2 y_3 \dots y_{k+2}} \sigma^{y_3} \dots \sigma^{y_{k+2}} \right). \quad (249)$$

$$G^{Y_0}_{X_1; x_2} = G^{Y'}_{X_1} g^{y''}_{x_2} \sum_{k=1}^{\infty} \frac{1}{k!} \gamma^{Y_0}_{Y' y'' y_3 \dots y_{k+2}} \sigma^{y_3} \dots \sigma^{y_{k+2}}, \quad (250)$$

$$G^{Y_0}_{X_1; y_2} = G^{Y'}_{X_1} \sum_{k=1}^{\infty} \frac{1}{k!} \gamma^{Y_0}_{Y' y_2 y_3 \dots y_{k+2}} \sigma^{y_3} \dots \sigma^{y_{k+2}}. \quad (251)$$

The coefficients α, β, γ in these expansions are polynomials constructed from the Riemann curvature tensor and its covariant derivatives. The first coefficients read as follows:

$$\alpha^{y_0}_{y_1 y_2 y_3} = -\frac{1}{3} \tilde{R}^{y_0}_{(y_2 y_3) y_1}, \quad (252)$$

$$\beta^{y_0}_{y_1 y_2 y_3} = \frac{2}{3} \tilde{R}^{y_0}_{(y_2 y_3) y_1}, \quad (253)$$

$$\alpha^{y_0}_{y_1 y_2 y_3 y_4} = \frac{1}{2} \tilde{\nabla}_{(y_2} \tilde{R}^{y_0}_{y_3 y_4) y_1}, \quad (254)$$

$$\beta^{y_0}_{y_1 y_2 y_3 y_4} = -\frac{1}{2} \tilde{\nabla}_{(y_2} \tilde{R}^{y_0}_{y_3 y_4) y_1}, \quad (255)$$

$$\gamma^{y_0}_{y_1 y_2 y_3 y_4} = \frac{1}{3} \tilde{\nabla}_{(y_3} \tilde{R}^{y_0}_{|y_1| y_4) y_2}. \quad (256)$$

In addition, we also need the covariant expansion of a vector:

$$A_x = g^{y_0}_x \sum_{k=0}^{\infty} \frac{(-1)^k}{k!} A_{y_0; y_1 \dots y_k} \sigma^{y_1} \dots \sigma^{y_k}. \quad (257)$$

C Explicit Form

Here we make contact with our notation in [51] to facilitate a direct comparison to the results in there.

We introduce the auxiliary variables

$$\Phi^{y_1 \dots y_n y_0}_{x_0} := \sigma^{y_1} \dots \sigma^{y_n} g^{y_0}_{x_0}, \quad (258)$$

$$\Psi^{y_1 \dots y_n y_0 y'_0}_{x_0 x'} := \sigma^{y_1} \dots \sigma^{y_n} g^{y_0}_{x_0} g^{y'_0}_{x'}. \quad (259)$$

Their derivatives

$$\begin{aligned} \Psi^{y_1 \dots y_n y_0 y'_0}_{x_0 x'; z} &= \sum_{a=1}^n \sigma^{y_1} \dots \sigma^{y_a} g^{y_0}_{x_0} g^{y'_0}_{x'} \\ &\quad + \sigma^{y_1} \dots \sigma^{y_n} \left(g^{y_0}_{x_0; z} g^{y'_0}_{x'} + g^{y_0}_{x_0} g^{y'_0}_{x'; z} \right), \end{aligned} \quad (260)$$

$$\begin{aligned} \Phi^{y_1 \dots y_n y_0}_{x_0; z} &= \sum_{a=1}^n \sigma^{y_1} \dots \sigma^{y_a} g^{y_0}_{x_0} \\ &\quad + \sigma^{y_1} \dots \sigma^{y_n} g^{y_0}_{x_0; z}, \end{aligned} \quad (261)$$

can be straightforwardly evaluated by using the expansions from the previous appendix.

In terms of (258) and (259) the integrated conservation laws (127) and (128) take the form:

$$\begin{aligned} \frac{D}{ds} \int \Psi^{y_1 \dots y_n y_0 y'_0}_{x_0 x'} \mathfrak{S}^{x_0 x' x_2} d\Sigma_{x_2} &= \\ \int \Psi^{y_1 \dots y_n y_0 y'_0}_{x_0 x'} \left(-U_{x'''' x' x'' x_0} \mathfrak{S}^{x'' x''' x''''} + \mathfrak{T}^{x' x_0} - t^{x' x_0} \right) w^{x_2} d\Sigma_{x_2} \\ &+ \int \Psi^{y_1 \dots y_n y_0 y'_0}_{x_0 x'; x''} \mathfrak{S}^{x_0 x' x''} w^{x_2} d\Sigma_{x_2} \\ &+ \int v^{y_{n+1}} \Psi^{y_1 \dots y_n y_0 y'_0}_{x_0 x'; y_{n+1}} \mathfrak{S}^{x_0 x' x_2} d\Sigma_{x_2}, \end{aligned} \quad (262)$$

$$\begin{aligned} \frac{D}{ds} \int \Phi^{y_1 \dots y_n y_0}_{x_0} \mathfrak{T}^{x_0 x_2} d\Sigma_{x_2} &= \int \Phi^{y_1 \dots y_n y_0}_{x_0} \left(-V_{x'' x_0 x'} \mathfrak{T}^{x' x''} \right. \\ &\quad \left. - R^{x_0}_{x''' x' x''} \mathfrak{S}^{x' x'' x'''} - \frac{1}{2} Q^{x_0}_{x''' x'} t^{x' x''} - A^{x_0} \mathfrak{L}_{\text{mat}} \right) w^{x_2} d\Sigma_{x_2} \\ &+ \int \Phi^{y_1 \dots y_n y_0}_{x_0; x'} \mathfrak{T}^{x_0 x'} w^{x_2} d\Sigma_{x_2} + \int v^{y_{n+1}} \Phi^{y_1 \dots y_n y_0}_{x_0; y_{n+1}} \mathfrak{T}^{x_0 x_2} d\Sigma_{x_2}. \end{aligned} \quad (263)$$

This form allows for a direct comparison to (29) and (30) in [51]. Explicitly, in terms of (258) and (259) the integrated moments from (141)–(143) are given by:

$$p^{y_1 \dots y_n y_0} := (-1)^n \int_{\Sigma(\tau)} \Phi^{y_1 \dots y_n y_0}_{x_0} \mathfrak{T}^{x_0 x_1} d\Sigma_{x_1}, \quad (264)$$

$$k^{y_2 \dots y_{n+1} y_0 y_1} := (-1)^n \int_{\Sigma(\tau)} \Psi^{y_2 \dots y_{n+1} y_0 y_1}_{x_0 x_1} \mathfrak{T}^{x_0 x_1} w^{x_2} d\Sigma_{x_2}, \quad (265)$$

$$h^{y_2 \dots y_{n+1} y_0 y_1} := (-1)^n \int_{\Sigma(\tau)} \Psi^{y_2 \dots y_{n+1} y_0 y_1}_{x_0 x_1} \mathfrak{S}^{x_0 x_1 x_2} d\Sigma_{x_2}, \quad (266)$$

$$q^{y_3 \dots y_{n+2} y_0 y_1 y_2} := (-1)^n \int_{\Sigma(\tau)} \Psi^{y_3 \dots y_{n+2} y_0 y_1}_{x_0 x_1} g^{y_2}_{x_2} \mathfrak{S}^{x_0 x_1 x_2} w^{x_3} d\Sigma_{x_3}, \quad (267)$$

$$\mu^{y_2 \dots y_{n+1} y_0 y_1} := (-1)^n \int_{\Sigma(\tau)} \Psi^{y_2 \dots y_{n+1} y_0 y_1}_{x_0 x_1} t^{x_0 x_1} w^{x_2} d\Sigma_{x_2}, \quad (268)$$

$$\xi^{y_1 \dots y_n} := (-1)^n \int_{\Sigma(\tau)} \sigma^{y_1} \dots \sigma^{y_n} \mathfrak{L}_{\text{mat}} w^{x_2} d\Sigma_{x_2}. \quad (269)$$

References

1. M. Mathisson, Neue Mechanik materieller Systeme. Acta Phys. Pol. **6**, 163 (1937)
2. A. Papapetrou, Spinning test-particles in general relativity. I. Proc. Roy. Soc. Lond. A **209**, 248 (1951)
3. W.G. Dixon, A covariant multipole formalism for extended test bodies in general relativity. Nuovo Cimento **34**, 317 (1964)
4. W.G. Dixon, Dynamics of extended bodies in general relativity. III. Equations of motion. Philos. Trans. R. Soc. Lond. A **277**, 59 (1974)
5. W.G. Dixon, Extended bodies in general relativity: their description and motion, in *Proceedings of International School of Physics Enrico Fermi LXVII*, ed. by J. Ehlers (North Holland, Amsterdam, 1979), p. 156
6. W.G. Dixon, Mathisson's new mechanics: its aims and realisation. Acta Phys. Pol. B Proc. Suppl. **1**, 27 (2008)
7. J.L. Synge, *Relativity: The General Theory* (North-Holland, Amsterdam, 1960)
8. B.S. DeWitt, R.W. Brehme, Radiation damping in a gravitational field. Ann. Phys. (N.Y.) **9**, 220 (1960)
9. A. Einstein, *The Meaning of Relativity*, 5th revised edn. (Princeton University Press, Princeton, 1956)
10. T. Harko, Thermodynamic interpretation of the generalized gravity models with geometry—matter coupling. Phys. Rev. D **90**, 044067 (2014)
11. H.J. Schmidt, Fourth order gravity: equations, history, and applications to cosmology. Int. J. Geom. Methods Mod. Phys. **4**, 209 (2007)
12. O. Bertolami, C.G. Böhrer, T. Harko, F.S.N. Lobo, Extra force in $f(R)$ modified theories of gravity. Phys. Rev. D **75**, 104016 (2007)

13. N. Straumann, Problems with modified theories of gravity, as alternatives to dark energy (2008). [arXiv:0809.5148v1](https://arxiv.org/abs/0809.5148v1) [gr-qc]
14. S. Nojiri, S.D. Odintsov, Unified cosmic history in modified gravity: from $F(R)$ theory to Lorentz non-invariant models. *Phys. Rep.* **505**, 59 (2011)
15. F.W. Hehl, G.D. Kerlick, Metric-affine variational principles in general relativity. I. Riemannian spacetime. *Gen. Relativ. Gravit.* **9**, 691 (1978)
16. F.W. Hehl, G.D. Kerlick, Metric-affine variational principles in general relativity. II. Relaxation of the Riemannian constraint. *Gen. Relativ. Gravit.* **13**, 1037 (1981)
17. T.P. Sotiriou, V. Faraoni, $f(R)$ theories of gravity. *Rev. Mod. Phys.* **82**, 451 (2010)
18. P. Rastall, Generalization of the Einstein theory. *Phys. Rev. D* **6**, 3357 (1972)
19. L.L. Smalley, Modified Brans-Dicke gravitational theory with nonzero divergence of the energy-momentum tensor. *Phys. Rev. D* **9**, 1635 (1974)
20. M. Blagojević, *Gravitation and Gauge Symmetries* (IOP Publishing, London, 2002)
21. M. Blagojević, F.W. Hehl, *Gauge Theories of Gravitation. A Reader with Commentaries* (Imperial College Press, London, 2013)
22. Yu.N. Obukhov, D. Puetzfeld, Conservation laws in gravity: a unified framework. *Phys. Rev. D* **90**, 024004 (2014)
23. Yu.N. Obukhov, D. Puetzfeld, Equations of motion in scalar-tensor theories of gravity: a covariant multipolar approach. *Phys. Rev. D* **90**, 104041 (2014)
24. D. Puetzfeld, Yu.N. Obukhov, Equations of motion in metric-affine gravity: A covariant unified framework. *Phys. Rev. D* **90**, 084034 (2014)
25. F.W. Hehl, J.D. McCrea, E.W. Mielke, Y. Ne'eman, Metric-affine gauge theory of gravity: Field equations, Noether identities, world spinors, and breaking of dilation invariance. *Phys. Rep.* **258**, 1 (1995)
26. D. Puetzfeld, Yu.N. Obukhov, Covariant equations of motion for test bodies in gravitational theories with general nonminimal coupling. *Phys. Rev. D* **87**, 044045 (2013)
27. J.A. Schouten, *Ricci-Calculus. An Introduction to Tensor Analysis and its Geometric Applications*, 2nd edn. (Springer, Berlin, 1954)
28. J.L. Synge, A. Schild, *Tensor Calculus* (Dover, New York, 1978)
29. A. Lichnerowicz, *Geometry of Groups of Transformations* (Noordhoff International Publishing, Leyden, 1977)
30. A. Trautman, On the Einstein-Cartan equations. IV. *Bulletin de l'Académie Polonaise des Sciences, Sér. des Sciences Math., Astron. et Phys.* **21**, 345 (1973)
31. K. Yano, *The Theory of Lie Derivatives and its Applications* (North-Holland, Amsterdam, 1955)
32. D.W. Sciama, The analogy between charge and spin in general relativity, *Recent Developments in General Relativity, Festschrift for L. Infeld* (Pergamon Press, Oxford, 1962), p. 415
33. T.W.B. Kibble, Lorentz invariance and the gravitational field. *J. Math. Phys.* **2**, 212 (1961)
34. F.W. Hehl, G.D. Kerlick, P. von der Heyde, On hypermomentum in general relativity. I. The notion of hypermomentum. *Zeits. Naturforsch.* **31a**, 111 (1976)
35. F.W. Hehl, G.D. Kerlick, P. von der Heyde, On hypermomentum in general relativity. II. The geometry of spacetime. *Zeits. Naturforsch.* **31a**, 524 (1976)
36. F.W. Hehl, G.D. Kerlick, P. von der Heyde, On hypermomentum in general relativity. III. Coupling hypermomentum to geometry. *Zeits. Naturforsch.* **31a**, 823 (1976)
37. V.N. Ponomarev, Yu.N. Obukhov, The generalized Einstein-Maxwell theory of gravitation. *Gen. Relativ. Gravit.* **14**, 309 (1982)
38. D. Vassiliev, Quadratic metric-affine gravity. *Ann. Phys. (Leipzig)* **14**, 231 (2005)
39. T.P. Sotiriou, S. Liberati, Metric-affine $f(R)$ theories of gravity. *Ann. Phys. (N.Y.)* **322**, 935 (2007)
40. V. Vitagliano, T.P. Sotiriou, S. Liberati, The dynamics of metric-affine gravity. *Ann. Phys. (N.Y.)* **326**, 1259 (2011)
41. Yu.N. Obukhov, R. Tresguerres, Hyperfluid—a model of classical matter with hypermomentum. *Phys. Lett. A* **184**, 17 (1993)

42. A.H. Taub, General relativistic variational principle for perfect fluids. *Phys. Rev.* **94**, 1468 (1954)
43. B.F. Schutz, Perfect fluids in general relativity: velocity potentials and variational principles. *Phys. Rev. D* **2**, 2762 (1970)
44. J. Weyssenhoff, A. Raabe, Relativistic dynamics of spin-fluids and spin-particles. *Acta Phys. Pol.* **9**, 7 (1947)
45. Yu.N. Obukhov, V.A. Korotky, The Weyssenhoff fluid in Einstein-Cartan theory. *Class. Quantum Gravity* **4**, 1633 (1987)
46. Y. Ne'eman, F.W. Hehl, Test matter in a spacetime. *Class. Quantum Gravity* **14**, A251 (1997)
47. Yu.N. Obukhov, Poincaré gauge gravity: selected topics. *Int. J. Geom. Methods Mod. Phys.* **3**, 95 (2006)
48. Yu.N. Obukhov, G.F. Rubilar, Invariant conserved currents in gravity theories with local Lorentz and diffeomorphism symmetry. *Phys. Rev. D* **74**, 064002 (2006)
49. Yu.N. Obukhov, G.F. Rubilar, Invariant conserved currents in gravity theories: Diffeomorphisms and local gauge symmetries. *Phys. Rev. D* **76**, 124030 (2007)
50. W.G. Dixon, Description of extended bodies by multipole moments in special relativity. *J. Math. Phys.* **8**, 1591 (1967)
51. D. Puetzfeld, Yu.N. Obukhov, Equations of motion in gravity theories with nonminimal coupling: A loophole to detect torsion macroscopically? *Phys. Rev. D* **88**, 064025 (2013)
52. H. Weyl, *Raum-Zeit-Materie* (Springer, Berlin, 1923)
53. P.B. Yasskin, W.R. Stoeger, Propagation equations for test bodies with spin and rotation in theories of gravity with torsion. *Phys. Rev. D* **21**, 2081 (1980)
54. C. Brans, R.H. Dicke, Mach's principle and a relativistic theory of gravitation. *Phys. Rev.* **124**, 925 (1961)
55. C. Brans, Mach's principle and a relativistic theory of gravitation. II. *Phys. Rev.* **125**, 2194 (1962)
56. C. Brans, Mach's principle and locally measured gravitational constant in general relativity. *Phys. Rev.* **125**, 388 (1962)
57. R.H. Dicke, Mach's principle and invariance under transformation of units. *Phys. Rev.* **125**, 2163 (1962)
58. R.H. Dicke, *The Theoretical Significance of Experimental Relativity* (Gordon and Breach, New York, 1964)
59. P. Jordan, *Schwerkraft und Weltall*, 2nd edn. (Vieweg, Braunschweig, 1955)
60. P. Jordan, Zum gegenwärtigen Stand der Diracschen kosmologischen Hypothesen. *Z. Phys.* **157**, 112 (1959)
61. Y. Thiry, Etude mathématique des équations d'une théorie unitaire à quinze variables de champ. *J. Math. Pures et Appl. Sér. 9* **30**, 275 (1951)
62. Y. Fujii, K. Maeda, *The Scalar-tensor Theory of Gravity* (Cambridge University Press, Cambridge, 2003)
63. C. Brans, The roots of scalar-tensor theory: an approximate history (2005). [arXiv:gr-qc/0506063](https://arxiv.org/abs/gr-qc/0506063)
64. H. Goenner, Some remarks on the genesis of scalar-tensor theories. *Gen. Relativ. Gravit.* **44**, 2077 (2012)
65. T.P. Sotiriou, Gravity and scalar fields. *Lecture Notes in Physics*, ed. by E. Papantonopoulos **892**, 3 (2015)
66. P. Bergmann, Comments on the scalar-tensor theory. *Int. J. Theor. Phys.* **1**, 25 (1968)
67. R.V. Wagoner, Scalar-tensor theory and gravitational waves. *Phys. Rev.* **12**, 3209 (1970)
68. T. Damour, G. Esposito-Farèse, Tensor-multi-scalar theories of gravitation. *Class. Quantum Gravity* **9**, 2093 (1992)
69. C.M. Will, *Theory and Experiment in Gravitational Physics*, 2nd edn. (Cambridge University Press, Cambridge, 1993)
70. F.W. Hehl, How does one measure torsion of space-time? *Phys. Lett. A* **36**, 225 (1971)
71. I. Bailey, W. Israel, Lagrangian dynamics of spinning particles and polarized media in general relativity. *Commun. Math. Phys.* **42**, 65 (1975)

72. W.R. Stoeger, P.B. Yasskin, Can a macroscopic gyroscope feel torsion? *Gen. Relativ. Gravit.* **11**, 427 (1979)
73. D. Puetzfeld, Yu.N. Obukhov, Propagation equations for deformable test bodies with microstructure in extended theories of gravity. *Phys. Rev. D* **76**, 084025 (2007)
74. D. Puetzfeld, Yu.N. Obukhov, Motion of test bodies in theories with nonminimal coupling. *Phys. Rev. D* **78**, 121501 (2008)
75. D. Puetzfeld, Yu.N. Obukhov, Probing non-Riemannian spacetime geometry. *Phys. Lett. A* **372**, 6711 (2008)
76. F.W. Hehl, Yu.N. Obukhov, D. Puetzfeld, On Poincaré gauge theory of gravity, its equations of motion, and Gravity Probe B. *Phys. Lett. A* **377**, 1775 (2013)
77. D. Puetzfeld, Yu.N. Obukhov, Unraveling gravity beyond Einstein with extended test bodies. *Phys. Lett. A* **377**, 2447 (2013)
78. D. Puetzfeld, Yu.N. Obukhov, Prospects of detecting spacetime torsion. *Int. J. Mod. Phys. D* **23**, 1442004 (2014)
79. A. Einstein, *Geometrie und Erfahrung*. *Sitzungsber. Preuss. Akad. Wiss.* **1**, 123 (1921)
80. E. Poisson, A. Pound, I. Vega, The motion of point particles in curved spacetime. *Living Rev. Relativ.* **14**(7) (2011)

Energy-Momentum Tensors and Motion in Special Relativity

Domenico Giulini

Abstract The notion of “motion” and “conserved quantities”, if applied to extended objects, is already quite non-trivial in Special Relativity. This contribution is meant to remind us on all the relevant mathematical structures and constructions that underlie these concepts, which we will review in some detail. Next to the prerequisites from Special Relativity, like *Minkowski space* and its *automorphism group*, this will include the notion of a *body* in Minkowski space, the *momentum map*, a characterisation of the habitat of *globally conserved quantities* associated with Poincaré symmetry—so called *Poincaré charges*—the frame-dependent decomposition of global angular momentum into *Spin* and an orbital part, and, last not least, the likewise frame-dependent notion of *centre of mass* together with a geometric description of the *Møller Radius*, of which we also list some typical values. Two Appendices present some mathematical background material on Hodge duality and group actions on manifolds.

1 Introduction

This contribution deals with the “problem of motion” in Special Relativity. Thus we work entirely in Minkowski space M (to be defined below) and represent a material system by an energy-momentum tensor T the support of which is to be identified with the set of events (points) in Minkowski space where matter “exists”:

$$\text{supp}(T) := \overline{\{p \in M \mid T(p) \neq 0\}}. \quad (1)$$

D. Giulini (✉)

Institute for Theoretical Physics, Riemann Center for Geometry and Physics,
Leibniz University Hannover, Appelstrasse 2, 30167 Hannover, Germany
e-mail: giulini@itp.uni-hannover.de

D. Giulini

Center for Applied Space Technology and Microgravity, University of Bremen,
Am Fallturm, 28359 Bremen, Germany

A central assumption will be that the material system is *spatially well localised*, which here shall mean that $\text{supp}(\mathbf{T})$ has compact intersection with any Cauchy hypersurface in M . Note that Cauchy hypersurfaces end at spatial infinity I_0 and that $\text{supp}(\mathbf{T})$ need not have compact intersection with asymptotically hyperboloidal spacelike hypersurfaces which tend to lightlike rather than spacelike infinity. This is depicted in Fig. 1.

Definition 1 We say that an energy-momentum tensor \mathbf{T} describes a *body* iff the intersection of $\text{supp}(\mathbf{T})$ with any Cauchy hypersurface in Minkowski space is compact. \square

Hence we identify the event-set of a body with $\text{supp}(\mathbf{T})$, which, in the sense made precise above, is of finite spatial extent, though it clearly will extend to timelike infinity. This is visualised as the a tubular neighbourhood stretching all the way from past-timelike to future-timelike infinity, as indicated by the shaded vertical tube in Fig. 1. It is also clear from Fig. 1 that we generally cannot require compact support of \mathbf{T} on spacelike hypersurfaces which are not Cauchy, like L . In fact, if the body radiated in the finite past, given by the lighter-shaded part of the tubular region in the

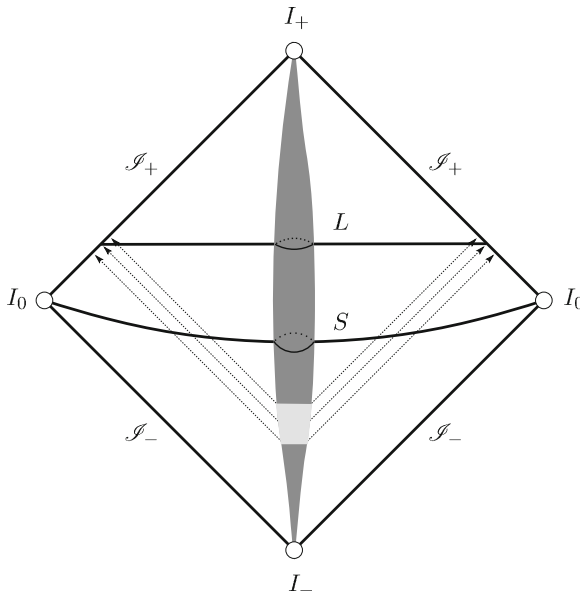


Fig. 1 History of a compact object in the conformal compactification of Minkowski space (Penrose Diagram). The five asymptotic regions of Minkowski space are future/past-timelike infinity I_{\pm} (each a single point), future/past-lightlike infinity \mathcal{I}_{\pm} (each a three-dimensional lightlike manifold of topology $\mathbb{R} \times S^2$), and spacelike infinity I_0 (a single point). The representation is not quite faithful because spacelike infinity, here represented by two points, is really just a single point. A faithful representation is obtained by wrapping the *diamond-shaped* 2-dimensional figure around a cylinder ($\mathbb{R} \times S^1$), so as to identify both points I_0 of the diagram to a single one. S and L are both spacelike hypersurfaces stretching out to “infinity”. But only S , which stretches out to spacelike infinity, is a Cauchy surface, i.e., covers all of spacetime in its domain of dependence

lower half of Fig. 1, the radiation will propagate to \mathcal{S}_+ and cover a neighbourhood in L of its 2-sphere of intersection with \mathcal{S}_+ , which is of non-compact closure. This can be avoided for spacelike hypersurfaces ending at I_0 if we require a neighbourhood of I_- to be free of radiation. This means that the body started to radiate a finite time in the past and that there is no incoming radiation from \mathcal{S}_- arbitrarily close to I_0 . In fact, describing a quasi-isolated body would presumably mean to exclude incoming radiation altogether. This explains our motivation for Definition 1.

A body should possess globally conserved quantities like linear and angular momentum. These are usually written down in a formulae like

$$P^a = \int_{\Sigma} T_b^a u^b d\mu, \quad (2a)$$

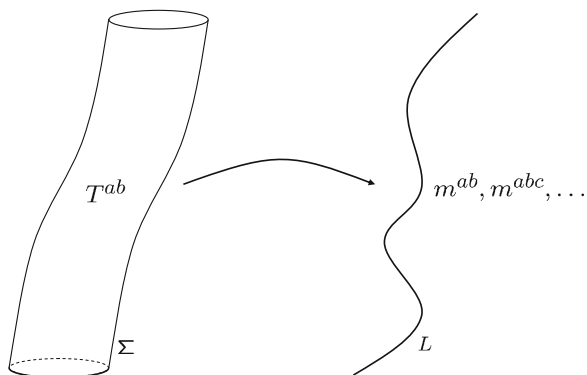
$$J^{ab}[z] = \int_{\Sigma} [(x^a - z^a)T_c^b - (x^b - z^b)T_c^a] u^c d\mu, \quad (2b)$$

where Σ is a Cauchy surface, u^a are the components of its future-pointing normal, and $d\mu$ is the measure on Σ induced from the ambient spacetime. See [1] for a conceptually exceptionally clear discussion.

The problem with these expressions is that, on face value, they do not make any sense. For one thing, the integrands are vector/tensor valued, and adding them at different points does not result in anything with an obvious meaning. If we wish to interpret P^a as the a th (covariant) component of the vector of total linear momentum, we should characterise the vector space of which P is an element. And, moreover, what does it mean to say that total linear (four-)momentum transforms like a four-vector (here covariant)? Likewise, we wish to interpret $J^{ab}[z]$ as the ab th (contravariant) component of the antisymmetric 2nd-rank tensor of angular momentum with respect to the centre z . Again it is unclear what tensor space this $J[z]$ is an element of and what is meant by stating its representation property under Poincaré transformations. Are these spaces defined at points in spacetime, perhaps at “infinity”, or in an abstract vector/tensor space globally associated to (but not *in*) spacetime? Also, the difference $(x^a - z^a)$ that appears in (2b) also makes no immediate sense. Is it supposed to be the a th component of some “difference function” on spacetime? Is it supposed to make sense in all coordinate systems, or just special ones; and if the latter holds, what selects these special ones?

Clearly, all these questions do have answers, but these answers delicately depend on the precise mathematical structures with which spacetime is endowed. In our (highly idealised) case of Minkowski space, it is the high degree of symmetry of spacetime that allows us to naturally interpret (2) so as to make unambiguous mathematical and physical sense. Removing or weakening these structures and pretending the expressions (2) to still make sense without further qualifications means to commit a mathematical and conceptual sin. This does not mean that (2) cannot be meaningfully generalised, but these generalisations will generally not be natural in a mathematical sense, that is, they will depend on additional structures and constructions to be imposed or selected “by hand”. The physical interpretation of what is then actually

Fig. 2 As emphasised by this conference logo, a central problem is to associate a timelike curve S to the energy-momentum tensor T . One would expect the line S to lie in the “convex hull” of the support of T , here represented by the extended tube Σ



represented by the integrals (2) will delicately depend on these by-hand additions. It is therefore the aim of this introductory exposition to clarify the mathematical and physical meaning of (2) in the simplest case, i.e. in Special Relativity. My strategy will be to fully display all the ingredients that go into the proper definition of (2). This, hopefully, will help to distinguish the generic difficulties of the gravitational case from those merely inherited from Special Relativity.

Related to the issue of giving proper meaning to (2) is the definition of “centre of mass” of an extended object. As you can see from its logo, this is a central concern of this conference (see Fig. 2). If “motion” is the change of position in time, we need to be clear about how to define “position” in the first place. The issue of how to define position observables in any special-relativistic theory, classical and quantum, is notorious. See, e.g., [2] for a good account. In my contribution I will give a derivation of the Møller radius which represents the ambiguity of defining position for systems with “spin”, i.e., “intrinsic angular momentum”, a notion also to be defined. So let us start at the beginning, asking for the reader’s patience!

2 Minkowski Space and Poincaré Group

In this section we wish to recall the definitions of Minkowski space and its automorphism group, despite the fact that this is generally considered a commonplace. But we think that there are some subtleties, in particular concerning the characterisation of its automorphism group, the *Poincaré group*, that deserve to be said more than once. We start with

Definition 2 *Minkowski space* is a quadruple $(M, V, \eta, +)$, consisting of:

1. A set, M , the elements of which are called spacetime points or events.
2. A real 4-dimensional vector space V .

3. A simply transitive action of V , considered as a group, on M , denoted by $+$, i.e.,

$$M \times V \rightarrow M, \quad (p, v) \mapsto p + v. \quad (3)$$

4. A non-degenerate symmetric bilinear form $\eta \in V^* \otimes V^*$ of signature $(+1, -1, -1, -1)$. \square

Remark 3 Every non-degenerate bilinear form $\eta : V \times V \rightarrow \mathbb{R}$ on a vector space V defines an isomorphism $\eta_\downarrow : V \rightarrow V^*$ to its dual space V^* via the requirement $\eta_\downarrow(v)(w) := \eta(v, w)$ for all $v, w \in V$; in short, $v \mapsto \eta_\downarrow(v) := \eta(v, \cdot)$. Its inverse map is $\eta_\uparrow : V^* \rightarrow V$, $\eta_\uparrow := (\eta_\downarrow)^{-1}$, which in turn defines a non-degenerate bilinear form on the dual space, $\eta^{-1} : V^* \times V^* \rightarrow \mathbb{R}$, via the requirement $\eta^{-1}(\alpha, \beta) := \alpha(\eta_\uparrow(\beta))$ for all $\alpha, \beta \in V^*$. On component-level this reads as follows: Let $\{e_a \mid 1 \leq a \leq n\}$ be a basis of V and $\{\theta^a \mid 1 \leq a \leq n\}$ its dual basis of V^* , so that $\theta^a(e_b) = \delta_b^a$. Then, writing $v = v^a e_a$, we get $\eta_\downarrow(v) = v_b \theta^b$ with $v_b := v^a \eta_{ab}$ and $\eta_{ab} := \eta(e_a, e_b)$. Similarly, writing $\alpha = \alpha_a \theta^a$, we get $\eta_\uparrow(\alpha) = \alpha^a e_a$ with $\alpha^a := \eta^{ab} \alpha_b$ and $\eta^{ab} := \eta^{-1}(\theta^a, \theta^b)$. This implies $\delta_b^a = \eta^{ac} \eta_{bc} = \eta^{ca} \eta_{cb} = \delta_b^a$ and, in particular, $\eta^{ab} = \eta^{ac} \eta^{bd} \eta_{cd}$ and $\eta_{ab} = \eta^{cd} \eta_{ca} \eta_{db}$. This explains why η_\uparrow and η_\downarrow are called the operations of “index-raising” and “index lowering”. Sometimes the images of η_\uparrow and η_\downarrow are indicated by the musical symbols \sharp (sharp) and \flat (flat) respectively, i.e., one writes $\eta_\uparrow(\alpha) = \alpha^\sharp$ and $\eta_\downarrow(v) = v^\flat$, which makes sense as long as the bilinear form η with respect to which these maps are defined is self understood. We shall also employ this notation. Note that so far we did not assume η to be symmetric, so that all formulae apply generally. However, from now on, and for the rest of this paper, the symbol η shall always denote the Minkowski metric, which specialises the general case by symmetry and signature. Once η is fixed, the isomorphisms between V and V^* as well as its extensions to tensor products is clear from the context and it is sufficient and useful to use shorthand notations, like $v \cdot w := \eta(v, w) = v^\flat(w)$, $v^2 := v \cdot v$, and $\|v\| := \sqrt{|v \cdot v|}$. Given $J = J^{ab} e_a \otimes e_b \in V \otimes V$ and $v \in V$, we shall also write $J \cdot v$ or $v \cdot J$ for the application of $J^{ab} e_a \otimes \eta_\downarrow(e_b) = J^a_b e_a \otimes \theta^b \in \text{End}(V)$ or $J^{ab} e_b \otimes \eta_\downarrow(e_a) = J_a^b e_b \otimes \theta^a \in \text{End}(V)$, respectively, to v . The inner products on V and V^* can be used to define inner products on any space built by taking tensor products of V and V^* just by slotwise contraction. However, in certain circumstances of high symmetry, e.g., for totally antisymmetric tensor products, it is more convenient to renormalise the slotwise inner product by combinatorial factors; like in formula (133) of the Appendix. Finally we recall that the transposed of a general linear map $A : V \rightarrow W$ between vector spaces V and W is the linear map $A^\top : W^* \rightarrow V^*$, defined by $A^\top(\alpha) := \alpha \circ A$ for all $\alpha \in W^*$. There is a natural isomorphism between a vector space V and its double dual V^{**} , so that we may identify these spaces without explicit mention. Symmetry of η is then equivalent to $\eta_\downarrow^\top = \eta_\downarrow$ and symmetry of η^{-1} to $\eta_\uparrow^\top = \eta_\uparrow$.

2.1 Affine Spaces

Note that 1–3 define the notion of an affine space. Minkowski space is thus just a real 4-dimensional affine space, the associated vector space of which carries a Lorentz metric. Any vector space V is a group under addition, with group identity being given by the zero vector and the inverse of $v \in V$ being $-v$. It is customary to use the same symbol, $+$, for the addition of vectors in V and the action of V on M . This allows to write the action property in the intuitive form (compare Appendix “Group Actions on Manifolds” for the general definition of a group action on a set)

$$p + (v + w) = (p + v) + w =: p + v + w. \quad (4)$$

But note the different meanings of $+$ in this equation. Moreover, we define the subtraction of a vector by the addition of the inverse:

$$p - v := p + (-v). \quad (5)$$

This allows one more simplifying notation: Since V acts simply transitive, there exists a *unique* $v \in V$ for any given pair $(p, q) \in M \times M$ so that $p = q + v$. We write

$$v = p - q. \quad (6)$$

Hence the minus sign should be understood as *difference map* $M \times M \rightarrow V, (p, q) \rightarrow p - q$, defined through $p = q + (p - q)$. Simple transitivity then implies

$$(p - o) + (o - q) = p - q, \quad (7)$$

which is equivalent to

$$p + (q - o) = q + (p - o). \quad (8)$$

2.2 Linear and Affine Frames

Definition 4 A *frame* F for an affine space $(M, V, +)$ consists of a tuple $F = (o, f)$, where $o \in M$ and $f \in \text{Lin}(\mathbb{R}^n, V)$ is a frame of the vector space V . Recall that a frame f of an n -dimensional real vector space V is an isomorphism from \mathbb{R}^n to V . This is equivalent to choosing n linear independent vectors $\{e_1, \dots, e_n\} \subset V$, the images under f of the canonical basis of \mathbb{R}^n . The map f is then defined by linear extension: $f(r^1, \dots, r^n) = \sum_{a=1}^n r^a e_a$. Its inverse map is given by $f^{-1}(v) = (\theta^1(v), \dots, \theta^n(v))$, where $\{\theta^1, \dots, \theta^n\} \subset V^*$ is the dual basis of $\{e_1, \dots, e_n\}$, i.e., $\theta^a(e_b) = \delta_b^a$. Similarly, an affine frame F defines a bijective map between \mathbb{R}^n and the underlying set M , denoted by the same letter F and defined by

$$\begin{aligned}
 F : \mathbb{R}^n \rightarrow \mathbf{M}, \quad (r_1, \dots, r_n) \mapsto F(r_1, \dots, r_n) &:= o + f(r^1, \dots, r^n) \\
 &= o + \sum_{a=1}^n r^a e_a.
 \end{aligned} \tag{9}$$

The inverse map is

$$\begin{aligned}
 F^{-1} : \mathbf{M} \rightarrow \mathbb{R}^n, \quad p \mapsto F^{-1}(p) &:= f^{-1}(p - o) \\
 &= (\theta^1(p - o), \dots, \theta^n(p - o)).
 \end{aligned} \tag{10}$$

Given two frames $F = (o, f)$ and $F' = (o', f')$, they are related by $F = F' \circ (F'^{-1} \circ F)$, where

$$F'^{-1} \circ F : \mathbb{R}^n \rightarrow \mathbb{R}^n, \quad (r, \dots, r^n) \mapsto (r'^1, \dots, r'^n) \tag{11a}$$

with

$$\begin{aligned}
 r'^a(r^1, \dots, r^n) &= [f'^{-1}(o - o') + f'^{-1} \circ f(r^1, \dots, r^n)]^a \\
 &= \theta'^a(o - o') + \sum_{b=1}^n \theta'^a(e_b) r^b.
 \end{aligned} \tag{11b}$$

We denote the set of all affine frames of \mathbf{M} by $\mathcal{F}_{\mathbf{M}}$. □

Remark 5 Affine spaces naturally inherit a topology from \mathbb{R}^n . It is defined to be the unique topology on \mathbf{M} for which all frame maps (9) are homeomorphisms, i.e., F and F^{-1} are continuous (hence F is an open map). Note that if a particular F' is a homeomorphism, then so is any other F , for $F = F' \circ (F'^{-1} \circ F)$ and $F'^{-1} \circ F : \mathbb{R}^n \rightarrow \mathbb{R}^n$, given by (11b), is clearly a homeomorphism. Hence the open sets in \mathbf{M} are precisely the images of open sets in \mathbb{R}^n under any F . Moreover, affine frames endow \mathbf{M} with the structure of a smooth (C^∞ , or even analytic) manifold since each frame defines a global chart with analytic transition functions (11b) between those charts. □

Definition 6 Affine frames define special, globally defined coordinates which are called *affine coordinates* or, in a physical context, *inertial coordinates*. Using these we may regard affine spaces as smooth (C^∞ , or even analytic) manifolds, as explained in Remark 5.

Recall that the algebra of all linear self-maps of a vector space \mathbf{V} onto itself is denoted by $\text{End}(\mathbf{V})$ (endomorphisms). The subset of all invertible elements in $\text{End}(\mathbf{V})$ is called $\text{GL}(\mathbf{V})$; it forms a group, the general-linear group (of self-isomorphisms, or Automorphisms regarding its structure as vector space) of \mathbf{V} . Accordingly, $\text{End}(\mathbb{R}^n)$ is just given by the algebra of all real $n \times n$ matrices and $\text{GL}(\mathbb{R}^n)$ by the group of all $n \times n$ matrices with non-vanishing determinant.

A frame of V defines an isomorphism of algebras $\text{End}(V) \rightarrow \text{End}(\mathbb{R}^n)$ through $A \mapsto A^f := f \circ A \circ f^{-1}$. Its restriction to $\text{GL}(V)$ defines an isomorphism of groups $\text{GL}(V) \rightarrow \text{GL}(\mathbb{R}^n)$. Let us denote by \mathcal{F}_V the set of all frames of V . There are two natural left actions of groups on \mathcal{F}_V : $\text{GL}(V)$ acts on the left according to $(A, f) \mapsto A \circ f$ and $\text{GL}(\mathbb{R}^n)$ also acts on the left according to $(B, f) \mapsto f \circ B^{-1}$. Note that $(B, f) \mapsto f \circ B$ would be a right action; see Appendix “Group Actions on Manifolds” for a general discussions of group actions. Both actions commute and are each simply transitive. A combined left action of $\text{GL}(V) \times \text{GL}(\mathbb{R}^n)$ on \mathcal{F}_V according to $((A, B), f) \mapsto A \circ f \circ B^{-1}$ results. The action of $\text{GL}(\mathbb{R}^n)$ is sometimes called *passive* since it merely moves the labels (coordinates) in label-space \mathbb{R}^n , whereas $\text{GL}(V)$ ’s action is called *active* since it really moves the points in the space V . Note that these adjectives refer to *different* groups, which are isomorphic but not naturally so since picking any isomorphism requires extra choices to be made. For example, picking a frame f , an f -dependent isomorphism $\text{GL}(\mathbb{R}^n) \rightarrow \text{GL}(V)$ is defined through the stabiliser subgroup in $\text{GL}(V) \times \text{GL}(\mathbb{R}^n)$ that fixes f under the common left action just described. This isomorphism then simply reads $\text{GL}(\mathbb{R}^n) \ni B \mapsto A := f \circ B \circ f^{-1} \in \text{GL}(V)$ (so that $A \circ f \circ B^{-1} = f$), which then also defines a frame-dependent left action of $\text{GL}(\mathbb{R}^n)$ on V . With respect to the fixed frame f the latter can then be used to define “active” transformations on V by means of what previously had been interpreted as mere label (coordinate) transformations. Failing to clearly state the groups, their domains of action, and the structures to be considered fixed is often the source of considerable confusion regarding the distinction of “active” and “passive” actions.

2.3 Affine Groups

Definition 7 Let $(M, V, +)$ be an n -dimensional real affine space. The *affine group*, denoted by $\text{Aff}(M)$, is the group of automorphisms of $(M, V, +)$. This means that $\text{Aff}(M)$ is the subgroup of bijections of M preserving the simply transitive action V on M . The word “preserving” means that for each $H \in \text{Aff}(M)$ there exists a unique $h \in \text{Aut}(V)$ so that $H(p + v) = H(p) + h(v)$ for all $p \in M$ and all $v \in V$. Here $\text{Aut}(V)$ is the automorphism group of V , which is $\text{GL}(V)$ if we consider its structure as vector space or as topological group, i.e., $\text{GL}(V)$ are the continuous automorphisms of the topological group V .

$$\text{Aff}(M) := \{H : M \rightarrow M \mid H(p + v) = H(p) + h(v), h \in \text{GL}(V), \forall v \in V\}. \quad (12)$$

Note that this definition makes sense, for if $p' + v' = p + v$, or $(p' - p) + v' = v$, we have $H(p' + v') = H(p') + h(v') = H(p + (p' - p)) + h(v') = H(p) + h((p' - p) + v') = H(p) + h(v) = H(p + v)$. \square

Remark 8 We said that $\text{Aut}(V)$ is $\text{GL}(V)$ if we consider V either as vector space or as topological group, comprising all the continuous automorphisms in the latter case. This qualification is indeed necessary, for if we considered V merely as algebraic group, as it might seem sufficient at this point, $\text{Aut}(V)$ would indeed be very much larger than $\text{GL}(V)$ in that it will also contain all the wildly discontinuous automorphisms that V inherits from the likewise wildly discontinuous automorphisms of the algebraic group $(\mathbb{R}, +)$. The latter are the discontinuous solutions $f : \mathbb{R} \mapsto \mathbb{R}$ to the so-called *Cauchy functional equation*, $f(x+y) = f(x) + f(y)$, which are also bijections. It is elementary to show that all its solutions necessarily satisfy $f(qr) = qf(r)$ for all $q \in \mathbb{Q}$ and all $r \in \mathbb{R}$. This implies that $f(q) = qf(1)$, i.e., that f is linear with slope $c := f(1)$ on all rational numbers, and hence linear with slope c on all real numbers if f were required to be continuous (requiring continuity at one point is sufficient). Without requiring continuity we can only conclude that for fixed $r \in \mathbb{R}$ and all $q \in \mathbb{Q}$ we must have $f(rq) = rq(f(r)/r)$, i.e., that f is again linear on the r -multiples of the rationals, but now with possibly r -dependent slope $c(r) := f(r)/r$. Indeed, plenty of such discontinuous solutions exist and can be constructed as follows [3]: Consider \mathbb{R} as vector space over \mathbb{Q} and let $B \subset \mathbb{R}$ be a (Hamel) basis, i.e., for each $r \in \mathbb{R}$ there exists a unique *finite* subset $\{e_1, \dots, e_n\} \subset B$ and unique $(q_1, \dots, q_n) \in \mathbb{Q}^n$, such that $r = \sum_{i=1}^n q_i e_i$. As was shown in [3], the existence of such a basis follows from the well-ordering theorem, though the cardinality of B is that of \mathbb{R} , i.e., the basis is uncountable. Now, any bijection $f : B \rightarrow B$ gives rise to an element of $\text{Aut}(\mathbb{R}, +)$ by uniquely extending f from $B \subset \mathbb{R}$ to \mathbb{R} in a \mathbb{Q} -linear fashion, i.e., by setting $f(\sum q_i e_i) := \sum q_i f(e_i)$ for all finite linear combinations of elements in B over \mathbb{Q} . Moreover, if the initial permutation $f : B \rightarrow B$ is not linear, i.e., if the function $B \ni e \mapsto f(e)/e$ is not constant, the automorphism $f : \mathbb{R} \rightarrow \mathbb{R}$ so defined is “wildly” discontinuous, in the sense that its graph $\{(x, f(x)) \mid x \in \mathbb{R}\} \subset \mathbb{R}^2$ is dense! In particular, given any $x \in \mathbb{R}$, the image of *any* interval containing x under f is dense in \mathbb{R} , no matter how small the interval was chosen to be. To see this, consider $e_1, e_2 \in B$ so that $f(e_1)/e_1 \neq f(e_2)/e_2$. Given any $(x, y) \in \mathbb{R}^2$ we can uniquely solve the two equations $x = r_1 e_1 + r_2 e_2$ and $y = r_1 f(e_1) + r_2 f(e_2)$, i.e., the single linear equation,

$$\begin{pmatrix} e_1 & e_2 \\ f(e_1) & f(e_2) \end{pmatrix} \begin{pmatrix} r_1 \\ r_2 \end{pmatrix} = \begin{pmatrix} x \\ y \end{pmatrix}, \quad (13)$$

for $(r_1, r_2) \in \mathbb{R}^2$ by rational operations, since the 2×2 matrix in (13) is invertible. In particular, (x, y) depends continuously on (r_1, r_2) so that with rational $(q_1, q_2) \in \mathbb{Q}^2$ in a neighbourhood of (r_1, r_2) we get arbitrarily close to (x, y) , as was to be proven. All this implies that the usual abelian group structure underlying vector addition cannot be uniquely specified without requiring continuity. Interestingly this problem was first encountered in analytical mechanics in connection with attempts to mathematically characterise the law for the composition of forces [4] and only later recognised as essential for general axiomatic formulations of vector addition; see, e.g., [5]. For us all this means that we cannot avoid invoking a continuity hypothesis

and that we must regard the abelian groups whose simply transitive action we require in the definition of affine spaces as topological groups acting continuously on affine space with its natural topology inherited from \mathbb{R}^n ; compare Remark 5. One might think that one gets away without continuity requirements if one defines $\text{Aff}(M)$ as that subgroup of the group of bijections (no continuity required here) of M which maps straight lines (physically: inertial trajectories) into straight lines (collinear sets of points into collinear sets would also suffice). A classic result in affine geometry then tells us that such transformations necessarily coincide with the standard continuous affine transformations; see, e.g., [6]. However, here a continuity requirement has tacitly slipped into the notion of “straight line” (inertial trajectory), which in affine space is defined to be the orbit of a *continuous* one-parameter subgroup of V . \square

Coming back to the group of affine automorphisms as defined above, we see that Hence an element $H \in \text{Aff}(M)$ is uniquely specified by an ordered pair of points $(p, q) \in M \times M$ and an element $h \in \text{GL}(V)$. The second point q is regarded as the image of the first point p under the map in question, whose definition is now given by $H(p + v) := q + h(v)$. Two such maps, H and H' , characterised by (p, q, h) and (p', q', h') , respectively, are easily seen to be the same iff $h = h'$ and $q' - q = h(p' - p)$. This defines an equivalence relation on the set $M \times M \times \text{GL}(V)$, the equivalence classes of which are

$$[p, q, h] = \bigcup_{v \in V} (p + v, q + h(v), h). \quad (14)$$

Hence we may identify $\text{Aff}(M)$ with this quotient space and write $H = [p, q, h]$ for any $H \in \text{Aff}(M)$. The composition of two maps $H = [p, q, h]$ and $H' = [p', q', h']$ can then be calculated

$$\begin{aligned} H' \circ H(p + v) &= H'(q + h(v)) = H'(p' + (q - p') + h(v)) \\ &= q' + h'(q - p') + h' \circ h(v). \end{aligned} \quad (15)$$

In other words

$$[p', q', h'] \circ [p, q, h] = [p, q' + h'(q - p'), h' \circ h]. \quad (16)$$

The first thing to note is that the equivalence class on the right-hand side is unchanged if we replace (p, q, h) with $(p + v, q + h(v), h)$ or (p', q', h') with $(p' + v', q' + h'(v'), h')$, which means that this prescription written down in terms of representatives defines indeed a multiplication of equivalence classes. Note that the neutral element is $[p, p, \text{id}_V]$ and the inverse of $[p, q, h]$ is

$$[p, q, h]^{-1} = [p, p - h^{-1}(q - p), h^{-1}]. \quad (17)$$

Furthermore, it is easy to check that (16) is associative and hence defines a group multiplication.

An obvious subgroup in $\text{Aff}(\mathbf{M})$ is given by the following subset

$$\text{Trans}(\mathbf{M}) := \{[p, q, h] \in \text{Aff}(\mathbf{M}) \mid h = \text{id}_V\}. \quad (18)$$

This subgroup is abelian,

$$\begin{aligned} [p', q', \text{id}_V] \circ [p, q, \text{id}_V] &= [p, q' + (q - p'), \text{id}_V] \\ &= [p' + (p - p'), q' + (q - p'), \text{id}_V] \\ &= [p', q' + (q - p') + (p' - p), \text{id}_V] \\ &= [p', q' + (q - p), \text{id}_V] \\ &= [p', q + (q' - p), \text{id}_V] \\ &= [p, q, \text{id}_V] \circ [p', q', \text{id}_V], \end{aligned} \quad (19)$$

(using (7) and (8) at the fourth and fifth equality) and normal,

$$\begin{aligned} [p, q, h] \circ [p', q', \text{id}_V] \circ [p, q, h]^{-1} &= [p, q, h] \circ [p', q', \text{id}_V] \circ [p, p - h^{-1}(q - p), h^{-1}] \\ &= [p, q, h] \circ [p, q' + (p - p') - h^{-1}(q - p), h^{-1}] \\ &= [p, q + h(q' - p') + (p - q), \text{id}_V] \\ &= [p, p + h(q' - p'), \text{id}_V]. \end{aligned} \quad (20)$$

It is called the *subgroup of translations*. It is the kernel of the projection homomorphism

$$\pi : \text{Aff}(\mathbf{M}) \rightarrow \text{GL}(V), \quad [p, q, h] \mapsto \pi([p, q, h]) := h. \quad (21)$$

If we denote the embedding (injective homomorphism) of $\text{Trans}(\mathbf{M})$ into $\text{Aff}(\mathbf{M})$ by i , we have the short sequence of groups and maps

$$\{1\} \rightarrow \text{Trans}(\mathbf{M}) \xrightarrow{i} \text{Aff}(\mathbf{M}) \xrightarrow{\pi} \text{GL}(V) \rightarrow \{1\}. \quad (22)$$

Here $\{1\}$ stands for the trivial group with unique group homomorphisms from and to any other group. The hooked arrow and the harpoon indicate injective and surjective homomorphisms respectively. This may be briefly summarised by saying that the short sequence is *exact*, where exactness means that at each group the image of the arriving map is the kernel of the departing one.

Moreover, our sequence (22) is not only exact but it also *splits*. By this is meant that there are also group embeddings (injective homomorphisms) $j : \text{GL}(V) \hookrightarrow \text{Aff}(\mathbf{M})$ so that $\pi \circ j = \text{id}_{\text{GL}(V)}$. To see this, choose a point $o \in \mathbf{M}$ and define (indicating the dependence of j on o by a subscript)

$$j_o : \text{GL}(V) \hookrightarrow \text{Aff}(\mathbf{M}), \quad h \mapsto j_o(h) := [o, o, h]. \quad (23)$$

Since $[o, o, h'] \circ [o, o, h] = [o, o + h'(o - o), h'h] = [o, o, h'h]$ one has indeed $i_o(h')i_o(h) = i_o(h'h)$ and $i_o(\text{id}_{\text{GL}(V)}) = \text{id}_{\text{Aff}(M)}$, that is, i_o is a group homomorphism. But note that we needed to select a point $o \in M$ to define the embedding. Two embeddings corresponding to different choices o and o' are related by conjugation with the translation from o to o' . Indeed, using that according to (17) we have $[o, o', \text{id}_V]^{-1} = [o, o - (o' - o), \text{id}_V] = [o', o, \text{id}_V]$, we have for all $h \in \text{GL}(V)$

$$\begin{aligned} [o, o', \text{id}_V] \circ i_o(h) \circ [o, o', \text{id}_V]^{-1} &= [o, o', \text{id}_V] \circ [o, o, h] \circ [o', o, \text{id}_V] \\ &= [o, o', \text{id}_V] \circ [o', o, h] \\ &= [o', o', h] \\ &= i_{o'}(h). \end{aligned} \quad (24)$$

The relation between the three groups $\text{Trans}(M)$, $\text{Aff}(M)$, and $\text{GL}(V)$ can then be compactly expressed by completing the short exact sequence (22) by a splitting homomorphism j_o :

$$\{1\} \rightarrow \text{Trans}(M) \xrightarrow{i} \text{Aff}(M) \begin{array}{c} \xrightarrow{\pi} \\ \xleftarrow{j_o} \end{array} \text{GL}(V) \rightarrow \{1\}. \quad (25)$$

This characterisation in terms of a split exact-sequence is the most natural in view of the homogeneity of M . The usual characterisation by means of a semi-direct product $V \rtimes \text{GL}(V)$ is unnatural insofar as the $\text{GL}(V)$ subgroup in $\text{Aff}(M)$ depends on the choice of a point $o \in M$, violating homogeneity. What one may say is that $\text{Aff}(M)$ is isomorphic to $V \rtimes \text{GL}(V)$, but the isomorphism depends on the selection of a point. Only *after* the point is selected can we locate a linear subgroup in $\text{Aff}(M)$ isomorphic to $\text{GL}(V)$, namely the image of $\text{GL}(V)$ under the embedding j_o (23). Once one agrees to select a point $o \in M$, we may write the general element of $\text{Aff}(M)$ in the form $[o, q, h]$. Group multiplication according to (16) then becomes

$$[o, q', h'] \circ [o, q, h] = [o, q' + h'(q - o), h' \circ h] = [o, o + (q' - o) + h'(q - o), h' \circ h]. \quad (26)$$

Having selected o we may identify M with V via $p \mapsto p - o$ (sometimes called the “vectorialisation” of M at o [6]) and the group $\text{Aff}(M)$ with the set $V \times \text{GL}(V)$. A general group element may then be written $[o, o + v, h] \mapsto (v, h)$ and (26) becomes

$$(v', h') \circ (v, h) = (v' + h'(v), h' \circ h), \quad (27)$$

which is just the product structure of a semi-direct product $V \rtimes \text{GL}(V)$ with respect to the homomorphism $\text{GL}(V) \rightarrow \text{Aut}(V)$ that is given by the defining representation of $\text{GL}(V)$.

Remark 9 The proper statement regarding the structure of the affine group $\text{Aff}(M)$ is that it is a *downward splitting extension* of $\text{GL}(V)$ by $\text{Trans}(M)$, as summarised by

(25). To be a downward extension¹ means that $\text{Trans}(M)$ is a normal (or “invariant”) subgroup of $\text{Aff}(M)$ so that the quotient $\text{Aff}(M)/\text{Trans}(M)$ is isomorphic to $\text{GL}(V)$. To be “splitting” means that $\text{GL}(V)$ may be identified with a subgroup in $\text{Aff}(M)$ whose intersection with $\text{Trans}(M)$ is merely the group identity. In our case there exist many such splitting embeddings of $\text{GL}(V)$ into $\text{Aff}(M)$, so that there is no unique way to regard $\text{GL}(V)$ as subgroup of $\text{Aff}(M)$. The ambiguity is faithfully labelled by the points in M (the point that is fixed under the action of the embedded copy of $\text{GL}(V)$ in $\text{Aff}(M)$ on M). Given such a splitting, $\text{Aff}(M)$ becomes isomorphic to the corresponding semi-direct product $V \rtimes \text{GL}(V)$. But this isomorphism depends on the choice of a point in M . If one says that $\text{Aff}(M)$ is isomorphic to $V \rtimes \text{GL}(V)$ one should add that this isomorphism is not “natural”, since by the very homogeneity of M there is clearly no preferred choice of a point in M .

2.4 Poincaré Group

Definition 10 Given Definition 2 of Minkowski space, we define the *Poincaré group*, $\text{Poin}(M)$, to be its group of automorphisms. This means that it must consist of affine transformations including all elements in $\text{Trans}(M)$, such that $\text{Aff}(M)/\text{Trans}(M) = \text{Lor}(V) \subset \text{GL}(V)$, where

$$\text{Lor}(V) := \left\{ h \in \text{GL}(V) \mid \eta(h(v), h(w)) = \eta(v, w), \forall v, w \in V \right\}. \quad (28)$$

Hence we have

$$\text{Poin}(M) := \left\{ H : M \rightarrow M \mid H(p + v) = H(p) + h(v), h \in \text{Lor}(V), \forall v \in V \right\}. \quad (29)$$

□

Totally analogous to (25), this leads to the splitting exact sequence

$$\{1\} \rightarrow \text{Trans}(M) \xrightarrow{i} \text{Poin}(M) \begin{array}{c} \xrightarrow{\pi} \\ \xleftarrow{j_o} \end{array} \text{Lor}(V) \rightarrow \{1\} \quad (30)$$

and to the $o \in M$ dependent(!) isomorphism

¹Here we recall that the usual terminology regarding extensions of groups is not quite uniform and hence ambiguous. Suppose three groups H , E and G are related by an exact sequence $1 \rightarrow H \rightarrow E \rightarrow G \rightarrow 1$, i.e. that H is a normal (or “invariant”) subgroup of E with quotient E/H isomorphic to G . Then this state of affairs is usually simply expressed by *either* saying that E is “an extension” of G by H , *or* of H by G . This ambiguity arises because views differ as to whether one likes to regard the *extending* or the *extended* group to be that one which becomes normal in the extension. To avoid such ambiguities the following refined terminology has been proposed in [7]: E is called an *upward extension* of H by G , or a *downward extension* of G by H .

$$\text{Poin}(M) \cong V \rtimes \text{Lor}(V). \quad (31)$$

If we complete o to a full affine frame $F = (o, f)$, where $f \in \text{Lin}(\mathbb{R}^n, V)$, and if in addition we require f to map the standard basis of \mathbb{R}^n to the orthonormal basis of V with respect to η , i.e., $\eta_{ab} := \eta(e_a, e_b) = \pm \delta_{ab}$ with one plus and $n - 1$ minus signs), we may identify M with \mathbb{R}^n , and then have

$$\text{Poin}(\mathbb{R}^n) = \mathbb{R}^n \rtimes \text{Lor}(\mathbb{R}^n). \quad (32)$$

where

$$\text{Lor}(\mathbb{R}^n) := \{L \in \text{GL}(\mathbb{R}^n) \mid \eta_{ab} L_c^a L_d^b = \eta_{cd}\}. \quad (33)$$

Now, $\text{Poin}(M)$ is a Lie group. The structure of a differentiable manifold with respect to which all group operations become smooth are again obtained by its isomorphism (non-naturalness is irrelevant here) with the matrix group just described. Note that the semi-direct product (32) can itself be embedded (i.e. mapped by an injective homomorphism) into the group $\text{GL}(\mathbb{R}^{n+1})$, via

$$\mathbb{R}^n \rtimes \text{Lor}(\mathbb{R}^n) \ni (v, L) \mapsto \begin{pmatrix} 1 & 0 \\ v & L \end{pmatrix} \in \text{GL}(\mathbb{R}^{n+1}) \quad (34)$$

which endows it with the differentiable structure inherited from $\text{GL}(\mathbb{R}^{n+1})$. All this is using the preferred affine (or inertial) coordinates of M ; compare Definition 6. Note also that the group multiplication in $\text{Aff}(M)$ has been explained simply by composition of maps ($\text{Aff}(M)$ was defined to consists of special bijections of M). This defines a left action of $\text{Aff}(M)$ on M and hence, by simple restriction, a left action of $\text{Poin}(M)$ on M . This, in turn, defines an anti-homomorphism between the Lie -algebra of $\text{Poin}(M)$ and the Lie algebra of vector fields on M (considered as differentiable manifold), where the Lie-algebra structure of the latter is defined by the commutator of vector fields. The reason why we have an anti- rather than a proper homomorphism of Lie algebras is explained in detail in Appendix “Group Actions on Manifolds”, in which we also review in some detail the notion of Lie-group actions on manifolds.

We recall that the Lie algebra, $\mathfrak{lor}(V)$, of $\text{Lor}(V)$ is the linear space of endomorphisms $A \in \text{End}(V)$ which are antisymmetric with respect to the Minkowski inner product η , i.e., satisfy $\eta(Av, w) = -\eta(v, Aw)$ for all $v, w \in V$. Using the η -induced isomorphism $\eta_\downarrow : V \rightarrow V^*$ and its inverse η_\uparrow (compare Remark 3), we can then write down the projection operators $P_S, P_A : \text{End}(V) \rightarrow \text{End}(V)$, which project onto the η -symmetric and η -antisymmetric endomorphisms:

$$P_S(M) := \frac{1}{2}(M + \eta_\uparrow \circ M^\top \circ \eta_\downarrow), \quad (35a)$$

$$P_A(M) := \frac{1}{2}(M - \eta_\uparrow \circ M^\top \circ \eta_\downarrow). \quad (35b)$$

Hence $\mathfrak{lor}(\mathbf{V})$ can be either characterised as the kernel of P_S or the image of P_A in $\text{End}(\mathbf{V})$. Using the first option we may write

$$\mathfrak{lor}(\mathbf{V}) = \text{Ker}(P_S) = \{A \in \text{End}(\mathbf{V}) \mid A = -\eta_{\uparrow} \circ A^{\top} \circ \eta_{\downarrow}\}. \quad (36)$$

Using the point-dependent isomorphism (31), the Lie algebra of $\text{Poin}(\mathbf{M})$, denoted by $\mathfrak{poin}(\mathbf{M})$, is the semi-direct product of the Lie algebras \mathbf{V} and $\mathfrak{lor}(\mathbf{V})$. Note that \mathbf{V} , considered as abelian group, has a Lie algebra which is isomorphic (as vector space) to \mathbf{V} with trivial Lie product (i.e. all Lie products are zero). Then we get the, likewise point-dependent, isomorphism

$$\begin{aligned} \mathfrak{poin}(\mathbf{M}) &\cong \mathbf{V} \rtimes \mathfrak{lor}(\mathbf{V}) \\ &= \left\{ (v, M) \in \mathbf{V} \times \mathfrak{lor}(\mathbf{V}) \mid [(v, M), (w, N)] = (Mw - Nv, [M, N]) \right\}. \end{aligned} \quad (37)$$

Here Mw is the action of $M \in \text{End}(\mathbf{V})$ on $w \in \mathbf{V}$ and $[M, N]$ is the commutator, which turns $\text{End}(\mathbf{V})$, considered as associative algebra, into a Lie algebra. An easy way to see that (37) does indeed give the right Lie product is to use the embedding (34), which induces an embedding

$$\mathbb{R}^n \rtimes \mathfrak{lor}(\mathbb{R}^n) \ni (v, M) \mapsto \begin{pmatrix} 0 & 0 \\ v & M \end{pmatrix} \in \text{End}(\mathbb{R}^{n+1}). \quad (38)$$

The Lie product of the images of (v, M) and (w, N) is then just their commutator, which is immediately seen to be the image of $(Mw - Nv, [M, N])$.

Now, as already mentioned above, the left action

$$\Phi : \text{Poin}(\mathbf{M}) \times \mathbf{M} \rightarrow \mathbf{M}, \quad (g, m) \mapsto \Phi(g, m) \equiv \Phi_g(m) \quad (39)$$

of $\text{Poin}(\mathbf{M})$ on \mathbf{M} induces a linear map from $\mathfrak{poin}(\mathbf{M})$ to the linear space of vector fields on \mathbf{M} , denoted by $\text{Vec}(\mathbf{M})$ (smooth sections in $T\mathbf{M}$). This map is just the differential of Φ with respect to the first (group valued) argument evaluated at the group identity. This is explained in all detail in Appendix “Group Actions on Manifolds”; compare (154). Since $\text{Vec}(\mathbf{M})$ is itself a Lie algebra, where the Lie product is defined to be the commutator of vector fields. With respect to these two Lie structures, the linear map $\mathfrak{poin}(\mathbf{M}) \ni X \mapsto V^X \in \text{Vec}(\mathbf{M})$ is a Lie anti-homomorphism. Again we refer to the Appendix “Group Actions on Manifolds” for details; compare (172b). Hence we have

$$[V^X, V^Y] = -V^{[X, Y]}, \quad (40)$$

where the “anti” is reflected by the minus-sign on the right-hand side.

Moreover, as the left action of $\text{Poin}(\mathbf{M})$ on \mathbf{M} lifts by push-forward (differential of Φ with respect to second (\mathbf{M} -valued) argument) to a left action on $T\mathbf{M}$ and hence $\text{Vec}(\mathbf{M})$, we can ask for the result of acting with $g \in \text{Poin}(\mathbf{M})$ on the special vector field V^X . The result is [see Eq. (173a) of Appendix “Group Actions on Manifolds”]

$$\Phi_{g*} V^X = V^{\text{Ad}_g(X)} \circ \Phi_g. \quad (41)$$

where Ad denotes the adjoint representation of $\text{Poin}(\mathbf{M})$ on $\mathfrak{poin}(\mathbf{M})$.

Let us at this point say a few words about the adjoint and co-adjoint representation; the latter will become important in what is to follow. An easy way to calculate the adjoint representation is again to identify $\text{Poin}(\mathbf{M})$ and $\mathfrak{poin}(\mathbf{M})$ according to (32) and (37), respectively, and perform the easy conjugation-calculation using the embeddings (34) and (38). The result is

$$\text{Ad}_{(a,L)}(v, M) = (Lv - LML^{-1}v, LML^{-1}). \quad (42)$$

The co-adjoint representation is the usual representation induced by Ad on the dual space, that is, the inverse transposed. As a vector space, $\mathfrak{poin}(\mathbf{M})$ is isomorphic to a linear subspace of $V \oplus \text{End}(V)$, namely the image of $\text{id}_V \oplus P_A$. Note that $V \oplus \text{End}(V)$ may be identified with $V \oplus (V \otimes V^*)$. The dual of the vector space $\mathfrak{poin}(\mathbf{M})$ is then isomorphic to a subspace of the dual to $V \oplus (V \otimes V^*)$, i.e., a subspace of $V^* \oplus (V^* \otimes V)$. This subspace is the image of $\text{id}_{V^*} \oplus P_A^\top$. It is called the dual of the Lie algebra $\mathfrak{poin}(\mathbf{M})$, denoted by $\mathfrak{poin}^*(\mathbf{M})$. It is merely considered as a vector space, not a Lie algebra. The natural pairing between $(p, J) \in \mathfrak{poin}^*(\mathbf{M})$ and $(v, M) \in \mathfrak{poin}(\mathbf{M})$ is

$$[(p, J)](v, M) = p(v) + \frac{1}{2} \text{Tr}(J^\top \circ M). \quad (43)$$

The factor $1/2$ in the second term is introduced because M obeys the condition $P_S(M) = 0$ and each independent component of M contributes twice to the trace. We have, by definition of the transposed map, $\text{Tr}(J^\top \circ P_A M) =: \text{Tr}((P_A^\top J)^\top \circ M)$ and likewise for P_S^\top , which immediately leads to the expressions

$$P_S^\top(J) := \frac{1}{2} (J + \eta_\downarrow \circ J^\top \circ \eta_\uparrow), \quad (44a)$$

$$P_A^\top(J) := \frac{1}{2} (J - \eta_\downarrow \circ J^\top \circ \eta_\uparrow). \quad (44b)$$

Hence we may characterise $\mathfrak{lot}^*(V)$ by:

$$\mathfrak{lot}^*(V) = \{J \in \text{End}(V^*) \mid J = -\eta_\downarrow \circ J^\top \circ \eta_\uparrow\}, \quad (45)$$

and furthermore (as vector spaces)

$$\mathfrak{poin}^*(\mathbf{M}) \cong V^* \times \mathfrak{lot}^*(V). \quad (46)$$

As already said, the co-adjoint representation, Ad^* of $\text{Poin}(\mathbf{M})$ on $\mathfrak{poin}^*(\mathbf{M})$ is defined to be the inverse-transposed:

$$\begin{aligned} \text{Ad}^* : \text{Poin}(\mathbf{M}) \times \mathfrak{poin}^*(\mathbf{M}) &\rightarrow \mathfrak{poin}^*(\mathbf{M}) \\ ((a, L), (p, J)) &\mapsto \text{Ad}_{(a,L)}^*(p, J) := (p, J) \circ \text{Ad}_{(a,L)}^{-1}. \end{aligned} \quad (47)$$

Note that the inverse is necessary to get a left action, i.e., $\text{Ad}_{(a,L)}^* \circ \text{Ad}_{(a',L')}^* = \text{Ad}_{(a,L)(a',L')}^*$. Using

$$\text{Ad}_{(a,L)}^{-1}(v, M) = (L^{-1}v + L^{-1}Ma, L^{-1}ML), \quad (48)$$

a straightforward calculation gives, writing $\tilde{L} := (L^\top)^{-1}$ and using the identity $p(w) = \text{Tr}(w \otimes p)$, valid for any $w \in V$ and $p \in V^*$,

$$[\text{Ad}_{(a,L)}^*(p, J)](v, M) = \tilde{L}p(v) + \frac{1}{2}\text{Tr}\left([2\tilde{L}p \otimes a + \tilde{L}J\tilde{L}^{-1}]^\top M\right). \quad (49)$$

This implies

$$\begin{aligned} \text{Ad}_{(a,L)}^*(p, J) &= (\tilde{L}p, \tilde{L}J\tilde{L}^{-1} + P_A^\top(2\tilde{L}p \otimes a) \\ &= (\tilde{L}p, \tilde{L}J\tilde{L}^{-1} + \tilde{L}p \otimes a - a^\flat \otimes (\tilde{L}p)^\sharp). \end{aligned} \quad (50)$$

For what follows it is important to compare the adjoint representation (42) of $\text{Poin}(M)$ on $\mathfrak{poin}(M)$ with the co-adjoint representation (50) of the same group on $\mathfrak{poin}^*(M)$. This is not quite straightforward since the representation spaces are different and hence it is not entirely obvious how to best appreciate their difference. However, it is true that, as vector spaces, $\mathfrak{poin}(M)$ and $\mathfrak{poin}^*(M)$ are isomorphic, though not naturally so. We need an extra structure to select a specific isomorphism, which in our case is already given to us by the inner product η , which was already seen to give an isomorphism $\eta_\flat : V \rightarrow V^*$; compare Remark 3. This structure can clearly also be used to define an isomorphism $\mathfrak{poin}(M) \rightarrow \mathfrak{poin}^*(M)$. However, it is more convenient to define isomorphisms between each of these vector spaces and $V \oplus \bigwedge^2 V$, where $\bigwedge^2 V := V \wedge V$ is the antisymmetric tensor product:

$$\mathfrak{poin}(M) \cong V \oplus P_A(V \otimes V^*) \cong V \oplus (V \wedge V) \cong V^* \oplus P_A^\top(V^* \otimes V) \cong \mathfrak{poin}^*(M). \quad (51)$$

Indeed, note that under this isomorphism $\mathfrak{lot}(V)$ gets mapped isomorphically onto the antisymmetric subspace $\bigwedge^2 V \subset V \otimes V$. The corresponding representations on $V \oplus \bigwedge^2 V$, which are equivalent to Ad and Ad^* under these isomorphisms, are respectively given by

$$\text{Ad}_{(a,L)}(v, M) = (Lv - (L \otimes LM) \cdot a, L \otimes LM), \quad (52a)$$

$$\text{Ad}_{(a,L)}^*(p, J) = (Lp, L \otimes LJ - a \wedge Lp), \quad (52b)$$

where the dot now abbreviates the inner product η in V , as explained in Remark 3. So for $a, b, c \in V$ we write

$$(a \wedge b) \cdot c = (a \otimes b - b \otimes a) \cdot c = a \eta(b, c) - b \eta(a, c) = a(b \cdot c) - b(a \cdot c). \quad (53)$$

These are now two inequivalent representations of the same group on the same vector space. It is the second, co-adjoint representation that will be physically relevant. It differs from the adjoint representation on how it implements the normal subgroup of translations. Let us, for clarity, just display the two representations if restricted to the subgroup $\text{Trans}(\mathbf{M})$:

$$\text{Ad}_{(a,\text{id})}(v, M) = (v - M \cdot a, M), \quad (54a)$$

$$\text{Ad}_{(a,\text{id})}^*(p, J) = (p, J - a \wedge p). \quad (54b)$$

The obvious difference is that under the adjoint representation translations act non-trivially only on the first summand in $V \oplus (V \wedge V)$ under the adjoint-, and non-trivially only on the second summand under the co-adjoint representation. As we will see below, the latter corresponds to the familiar origin-dependence of angular momentum and origin-independence of linear momentum.

Finally, using the identification $\text{LiePoin}(\mathbf{M}) \cong V \rtimes (V \wedge V)$, let us explicitly write down the Lie algebra (37) in terms of a basis. Let $\{e_a \mid 1 \leq a \leq n\}$ be a basis of V , such that $\eta(e_a, e_b) = e_a \cdot e_b = \eta_{ab}$ then $\{m_{ab} \mid 1 \leq a < b \leq n\}$ is a basis of $V \wedge V$, where $m_{ab} := e_a \wedge e_b = (e_a \otimes e_b - e_b \otimes e_a)$. Then the Lie products in (37) become

$$[e_a, e_b] = 0, \quad (55a)$$

$$[e_a, m_{bc}] = \eta_{ab} e_c - \eta_{ac} e_b, \quad (55b)$$

$$[m_{ab}, m_{cd}] = \eta_{ad} m_{bc} + \eta_{bc} m_{ad} - \eta_{ac} m_{bd} - \eta_{bd} m_{ac}. \quad (55c)$$

3 The Momentum Map and the Natural Habitat of Globally Conserved Poincaré-Charges

We now regard Minkowski space as a Semi-Riemannian manifold (M, g) with Lorentzian metric g , which in affine/inertial coordinates (compare Definition 6) is of the form (in four spacetime-dimensions)

$$g = \eta_{ab} dx^a \otimes dx^b, \quad \{\eta_{ab}\} = \text{diag}(1, -1, -1, -1). \quad (56)$$

As discussed above, and in more detail in the Appendix “Group Actions on Manifolds”, for each $X \in \text{poin}(\mathbf{M})$ we have a vector field $V^X \in \text{Vec}(\mathbf{M})$ that represents the “infinitesimal” left group-action of $\text{Poin}(\mathbf{M})$ on \mathbf{M} through an anti Lie-homomorphism $\text{poin}(\mathbf{M}) \rightarrow \text{Vec}(\mathbf{M})$, $X \mapsto V^X$, satisfying (40). Since $\text{Poin}(\mathbf{M})$ acts on \mathbf{M} by isometries, the Lie derivative of g with respect to each V^X is zero:

$$L_{V^X} g = 0. \quad (57)$$

In other words, each $V^X \in \text{Vec}(\text{M})$ is a Killing vector-field.

Now, suppose we have an energy-momentum tensor

$$\mathbf{T} = T_{ab} dx^a \otimes dx^b \quad (58)$$

which is divergence free with respect to the Levi-Civita covariant derivative determined by g . In components with respect to arbitrary coordinate systems this reads

$$\nabla_a T^{ab} = \partial_a T^{ab} + \Gamma_{ac}^a T^{cb} + \Gamma_{ac}^b T^{ac} = 0. \quad (59)$$

If the coordinates are affine/inertial, the Γ -coefficients are all zero.

Another way to look at \mathbf{T} is to regard it as a co-vector valued 3-form. This is achieved by Hodge-dualising the second tensor factor in (58):

$$\mathcal{T} = T_{ab} dx^a \otimes (\star dx^b), \quad (60)$$

where \star is the Hodge duality map the definition of which, together with our conventions, are summarised in Appendix “Exterior Products and Hodge-Duality”. Now comes the important point in the whole construction: using the vector fields V^X , we can, for each $X \in \text{poin}(\text{M})$ turn (60) into a 3-form that linearly depends on X via

$$\mathcal{T}_X := \star i_{V^X} \mathbf{T} = (V^X)^a T_{ab} (\star dx^b) = (V^X)^a g_{ab} T^{bc} \frac{1}{3!} \varepsilon_{cdef} dx^d \wedge dx^e \wedge dx^f. \quad (61)$$

here i_V denotes the map of inserting V into the first co-vector factor of the tensor it is applied to and ε_{abcd} are the components of the measure 4-form induced by g . The zero-divergence condition (59) implies, in view of (57), that each \mathcal{T}_X is closed:

$$d\mathcal{T}_X = 0. \quad (62)$$

This means that to each $X \in \text{poin}(\text{M})$ we can produce a number by integrating \mathcal{T}_X over a 3-dimensional hypersurface:

$$\mathfrak{M}[F, S](X) := \int_S \mathcal{T}_X[F] = \int_S \star \circ i_{V^X} \circ \mathbf{T}[F]. \quad (63)$$

Here we wrote the integrand as a composition of three maps. The first (\mathbf{T}) maps the field configuration F to a symmetric tensor, the second i_{V^X} contracts this tensor with the vector field V^X and turns it into a one form, and the last (\star) turns this one form into an $n - 1$ form (a three-form in four dimensions). The last map to be applied in order to get a number is to integrate this form over a hypersurface S . This number will depend on three arguments: The fields F on which \mathbf{T} depends, the surface S over which we integrate, and the Lie algebra element X which we use to build V^X to contract \mathbf{T} with. The value \mathfrak{M} takes on all these arguments is called the corresponding *momentum*.

Suppose now that the fields F on which \mathbf{T} depends carry a representation (not necessarily a linear one) of $\text{Poin}(\mathbf{M})$. That is, we assume there is a left action D of $\text{Poin}(\mathbf{M})$ on the space (not necessarily a vector space) of fields. We assume that the geometric object \mathbf{T} is built entirely out of such fields, and that there is no dependence on any other geometric structure not included in our F . Then we have the covariance property²

$$\mathbf{T}[D_h F] = \Phi_{h*} \mathbf{T}[F] \quad (64)$$

where Φ is as in (39) and Φ_{h*} denotes the push-forward of the diffeomorphism $\Phi_h : \mathbf{M} \rightarrow \mathbf{M}$. If F denote standard scalar, vector, and tensor fields, then (64) merely says that the energy-momentum distribution of the pushed-forward fields is just the push-forward of the energy-momentum distribution of the original fields.

Now we are interested in how the momentum changes if we act on the fields F by a Poincaré transformation, leaving the arguments S, X untouched for the moment. We get:

$$\begin{aligned} \mathfrak{M}[D_h(F), S](X) &= \int_S \star \circ i_{V^X} \circ T \circ D_h[F] \\ &\stackrel{1}{=} \int_S \star \circ i_{V^X} \circ \Phi_{h*} \circ T[F] \\ &\stackrel{2}{=} \int_S \star \circ \Phi_{h*} \circ i_{\Phi_h^{-1} V^X} \circ T[F] \\ &\stackrel{3}{=} \int_S \star \circ \Phi_{h*} \circ i_{V^{\text{Ad}_{h^{-1}}(X)}} \circ T[F] \\ &\stackrel{4}{=} \int_S \Phi_{h^{-1}}^* \left(\star \circ i_{V^{\text{Ad}_{h^{-1}}(X)}} \circ T[F] \right) \\ &\stackrel{5}{=} \int_{\Phi_{h^{-1}}(S)} \left(\star \circ i_{V^{\text{Ad}_{h^{-1}}(X)}} \circ T[F] \right) \\ &\stackrel{6}{=} \mathfrak{M}[F, \Phi_{h^{-1}}(S)](\text{Ad}_h^{-1}(X)) \\ &\stackrel{7}{=} \text{Ad}_h^*(\mathfrak{M})[F, \Phi_{h^{-1}}(S)](X) \end{aligned} \quad (65)$$

Here we broke up the derivation into seven steps, each one showing what happens as we commute the action of $\text{Poin}(\mathbf{M})$ from right to left through the various maps connected by the \circ symbols. At the first step we use (64), at the second step we just use the obvious commutation property of push-forwards with the vector-insertion map, at the third step we use property (41), at the fourth step we use the covariance (intertwining property) of the Hodge map and the definition of the push-forward of a form as the pull-back by the inverse map, in the fifth step we use the elementary

²This covariance property, which is crucial for the right representation-theoretic properties of the global charges, is hardly ever stated explicitly. A notable exception, more in words than in formulae, is Fock's book [8] Sect. 31, where it is referred to as "physical principle".

property of integrals, sometimes referred to as the “change-of-variables-formula”, in the sixth step we just use the definition (63), and in the seventh and last step we use the definition (47) of the co-adjoint representation.

Now, if S is a Cauchy surface and the support conditions discussed initially are satisfied, we are ensured that the integral converges and the momentum actually exists. Moreover, if \mathbf{T} is divergence free, as we assume here, the momentum does not depend on the particular Cauchy surface chosen, as follows from (62) and Gauss’ theorem. Hence we may delete S as an argument of \mathfrak{M} . Since Eq. (65) is valid for all $X \in \mathfrak{poin}(\mathbf{M})$, we may also delete the dependence on X , which is linear. We can then regard (65) as an equation between elements in the dual of the Lie algebra depending merely on F and expressing the fact that they transform under the co-adjoint representation.

Theorem 11 *A divergence-free energy-momentum tensor describing a body in the sense of Definition 1 and depending on fields which carry a (not necessarily linear) representation D of $\mathbf{Poin}(\mathbf{M})$ defines a map from the space of field configurations to $\mathfrak{poin}^*(\mathbf{M})$, called momentum map, given by*

$$\mathfrak{M}(X) := \int_S T_X[F], \quad (66)$$

where S is any Cauchy surface. The map is Ad^* -equivariant in the sense that

$$\mathfrak{M} \circ D_h = \text{Ad}_h^* \circ \mathfrak{M}, \quad (67)$$

for all $h \in \mathbf{Poin}(\mathbf{M})$. □

Let us finally see how, and in what sense, the general formula (66) implies the naive expressions (2). For this we express V^X in affine/inertial coordinates and choose for X basis elements of $\mathfrak{poin}(\mathbf{M})$ that are adapted to the decomposition of $\mathfrak{poin}(\mathbf{M})$ as semi-direct product $\mathbf{V} \rtimes \mathfrak{lor}(\mathbf{V})$. But here comes the point stressed above: there is no *natural* identification of $\mathbf{V} \rtimes \mathfrak{lor}(\mathbf{V})$ with $\mathfrak{poin}(\mathbf{M})$. Any such identification is equivalent to the choice of a point $o \in \mathbf{M}$. Only with respect to the choice of such a point does it make sense to speak of $\text{Lor}(\mathbf{V})$ as a subgroup of $\mathbf{Poin}(\mathbf{M})$ and of $\mathfrak{lor}(\mathbf{V})$ as a Lie subalgebra of $\mathfrak{poin}(\mathbf{M})$.

Let us now choose a system x^a of affine/inertial coordinates so that the vector fields $\partial/\partial x^a$ are orthonormal [i.e. the Minkowski metric g takes the standard form (56)]. The coordinate values of the preferred point o is denoted by $z^a := x^a(o)$. Then V^X for $X = (v, M) \in \mathbf{V} \oplus (\mathbf{V} \otimes \mathbf{V})$ is

$$V^{(v,M)}(z) = v^a \partial/\partial x^a + \frac{1}{2} M^{ac} \eta_{cb} [(x^a - z^a) \partial/\partial x^b - (x^b - z^b) \partial/\partial x^a]. \quad (68)$$

Note that $x^a : \mathbf{M} \rightarrow \mathbb{R}$ are coordinate functions on the manifold whereas $z^a = x^a(o)$ are fixed numbers (constant functions on \mathbf{M}). The corresponding *momentum* is then

$$\mathfrak{M}[X = (v, M)] = \eta_{ab} v^a P^b + \frac{1}{2} \eta_{ac} \eta_{bd} M^{ab} J^{cd}[z] \quad (69)$$

where, just as in (2),

$$P^a = \int_S T_b^a u^b d\mu, \quad (70a)$$

$$J^{ab}[z] = \int_S [(x^a - z^a)T_c^b - (x^b - z^b)T_c^a] u^c d\mu. \quad (70b)$$

Here u is the unit timelike normal to S and $d\mu = \star u^b$ (the Hodge-dual of the one-form $u^b := \eta_\downarrow(u)$) is the induced measure (3-form) on S . Note that only the J 's depend on z because only they refer to the non-natural (i.e. o -dependent) embedding of the Lorentz group into the Poincaré group. In contrast, the translation group $\text{Trans}(M)$ is normal and hence has a natural place in the Poincaré group. Correspondingly, the linear momenta P^a are natural and do not depend on any arbitrary choices. Note that it immediately follows from (70b) that

$$J[z + a] = J[z] - a \wedge P \quad (71)$$

which is just the co-adjoint representation of translations stated in (54b).

Remark 12 The discussion up to this point answers all the questions posed initially in connection with (70) in the case of Special Relativity. Globally conserved quantities (charges) in connection with Poincaré symmetry are valued in the vector space dual to the Lie algebra and transform according to the co-adjoint representation under Poincaré transformations of the fields to which these quantities belong. The splitting of the space in which the charges take their values into a “translational part” and a “homogeneous part” is not natural as far as the latter is concerned. Therefore the charges of the homogeneous (Lorentz-) part has an additional dependence on a spacetime point whose choice fixes the embedding of the Lorentz group into the Poincaré group. The very notion of, say, angular momentum depends on the choice of this point.

4 Supplementary Conditions and Mass Centres

The z dependence of J may be used to put further more or less physically motivated conditions on $J[z]$ to restrict the choices of z . Conditions of that sort are known as *supplementary conditions* whose aim is to narrow down the choices of z to a one-parameter family $z(\lambda)$ which is timelike and somehow interpreted as the worldline of the body. This line has many names depending on what supplementary conditions one uses. It can be “centre-of-mass”, “centre-of-inertia”, “centre-of-gravity”, “centre-of-spin”, “centre-of-motion”, “centroid”, etc. Early discussions of some of these concepts in Special Relativity were given in [8, 9]. For comprehensive discussions see [10] and in particular [2].

If $u \in V_1 := \{v \in V \mid \eta(u, u) = 1\}$ is a unit timelike vector characterising an inertial frame of reference, we may, e.g., consider the supplementary condition (recall that a dot indicates a contraction using the Minkowski metric)

$$J[z + a] \cdot u = 0 \Leftrightarrow J[z] \cdot u - (P \cdot u)a + (a \cdot u)P = 0. \quad (72)$$

This is equivalent to a linear inhomogeneous equation for a

$$\Pi(a) = \frac{J[z] \cdot u}{P \cdot u}, \quad (73a)$$

where

$$\Pi = \text{id} - \frac{P \otimes u^b}{P \cdot u} \quad (73b)$$

is the projector onto $u^\perp := \{v \in V \mid v \cdot u = 0\}$ parallel to P (caution: not parallel to u). Hence the solution space is one-dimensional timelike line in V parallel to P :

$$a(z, u; \lambda) = \frac{J[z] \cdot u}{P \cdot u} + \lambda P, \quad \lambda \in \mathbb{R}. \quad (74)$$

Its dependence on z immediately follows from (74) and (71):

$$a(z + b, u; \lambda) = a(z, u; \lambda + (u \cdot b)/(u \cdot P)) - b. \quad (75)$$

Equation (74) is a timelike line in V that represents the worldline of the *centre-of-mass* in M relative to the origin z . The wordline in M clearly does not depend on z (up to reparametrisation) and is simply given by

$$\gamma(u; \lambda) = z + a(z, u; \lambda). \quad (76)$$

Definition 13 The curve $\lambda \mapsto \gamma(u; \lambda)$ is called the *centre-of-mass* wordline relative to the inertial observer u . \square

The body's angular momentum with respect to this centre-of-mass is

$$S(u) := J[\gamma(u; \lambda)] := J[z + a(z, u; \lambda)]. \quad (77)$$

The right-hand side clearly does not depend on λ since shifting λ moves $a(z, u; \lambda)$ in the direction of P according to (74) and hence leaves J unchanged according to (71). It then also follows immediately from (75) that the right-hand side of (77) does not depend on z . Hence, as indicated, S only depends on u .

Definition 14 $S(u)$ is called the body's *spin* with respect to the inertial observer u . \square

Except for its dependence on u , this definition meets standard Newtonian intuition. Indeed, according to this intuition we would call

$$L(z, u) := a(z, u; \lambda) \wedge P \quad (78)$$

the orbital angular momentum relative to z and u (there is again no λ -dependence due to $P \wedge P = 0$). Equation (71) then just tells us that the total angular momentum is the sum of the spin and orbital parts:

$$J[z] = L[z + a(z, u; \lambda)] + a(z, u; \lambda) \wedge P = S(u) + L(z, u). \quad (79)$$

As in Newtonian mechanics, the z -dependence of angular momentum resides exclusively in the orbital part. But S and L each also depend on u , though in such a way that their sum is independent of u . This gives rise to the following

Remark 15 Unlike in Newtonian Mechanics, the splitting of the total angular momentum into a spin (z -independent) and an orbital (z -dependent) part depends on the inertial frame, here represented by u . \square

Finally, using the expression (74) for a , we get the following expression for the spin part,

$$S(u) := J[z] - a(z, u; \lambda) \wedge P = u \cdot \left(P \wedge \frac{J[z]}{P \cdot u} \right), \quad (80a)$$

which explicitly displays its u -dependence. Again note that the z -dependence of J (given by (72)) drops out due to the wedge product with P . The expression on the right-hand side of (80a) has a simple geometric interpretation, namely that of the (tensor-factor wise) projection of $J[Z]$ parallel to P onto u^\perp , we may also write

$$S(u) = \Pi \otimes \Pi (J[z]), \quad (80b)$$

where Π is as in (73a). Note that application of $\Pi \otimes \Pi$ cancels the z -dependence of J and, in exchange, introduces a u -dependence. From both expressions (80) the defining Eq. (72) for the centre-of-mass,

$$S(u) \cdot u = -u \cdot S(u) = 0 \quad (81)$$

follows trivially. In (75) we already stated the obvious dependence of the line $\lambda \mapsto a(z, u; \lambda)$ in V on z (which is just like in Newtonian physics). More interesting, and purely special-relativistic in nature, is its dependence on u . It is clear from (74) that any normal timelike vector $u \in V_1$ in Eq. (74) yields a worldline $\lambda \mapsto \gamma(u; \lambda)$ in M parallel to P . As u varies over the 3-dimensional hyperbola $V_1 \subset V$ we obtain a bundle of straight lines (geodesics) in M parallel to P :

$$B = \bigcup_{u \in V_1} \bigcup_{\lambda \in \mathbb{R}} \{\gamma(u; \lambda)\}. \quad (82)$$

In that bundle a particular line $\gamma = \gamma_*$ is distinguished, namely that for which $u \propto P$, i.e.

$$u = u_* := P / \|P\|. \quad (83)$$

Here we use the notation $\|P\| := \sqrt{|P \cdot P|}$. This is the only timelike direction the body determines by itself.³

Definition 16 The inertial frame for which $u \propto P$ is called the body's *rest frame* and

$$M_0 := (u_* \cdot P) / c \quad (84)$$

the body's *rest mass*. The line $\lambda \mapsto \gamma(u_*; \lambda)$, i.e. the centre-of-mass in the body's rest frame, is called its *centroid*, or wordline of the *centre-of-inertia* [2]. \square

Using (80) we can immediately write down the body's spin relative to its rest frame,

$$S_* := u_* \cdot (J[z] \wedge u_*), \quad (85)$$

which is clearly independent of z . With respect to the body's centroid, the bundle (82) of wordlines of mass-centres has a simple geometric description:

Theorem 17 *The intersection of the bundle \mathcal{B} with the hyperplane*

$$\Sigma(u_*, \sigma) := \{x \in M \mid (x - z) \cdot u_* = \sigma\} \quad (86)$$

is a 2-disc in perpendicular to the axis of rotation and with radius is

$$R_M = \frac{\|S_*\|}{\|P\|} = \frac{\|S_*\|}{M_0 c}. \quad (87)$$

Definition 18 The radius (87) is called the *Møller radius*, first defined in [11] and also discussed in, e.g., [1, 12]. It measures the degree to which different inertial observers disagree on the spatial location of the centre-of-mass perpendicular to the axis of rotation. Typical orders of magnitude for Møller radii will be given below. \square

Proof of Theorem 17 Note first that $\Sigma(u_*, \sigma)$ is the hyperplane with normal $u_* \propto P$ and timelike distance σ from the point z . As we may choose any convenient z , we take it to lie on the centroid. The hyperplane through z is then

$$\Sigma(u_*, \sigma = 0) = \{x \in M \mid (x - z) \cdot u_* = 0\}. \quad (88)$$

³Here we assume that P is timelike, which essentially means that we assume the energy-momentum tensor to satisfy the condition of energy dominance.

Relative to that choice of z (on the centroid) all other mass centres have worldlines

$$\gamma(u; \lambda) := z + \frac{S_* \cdot u}{P \cdot u} + \lambda P, \quad (89)$$

with λ parametrising the individual worldline and $u \in V_1$ the different mass-centres. Since $P \cdot S_* = 0$ the second and third term on the right-hand side are perpendicular, so that the wordline $\gamma(u; \lambda)$ intersects $\Sigma(u_*, \sigma = 0)$ at $\lambda = 0$. Hence

$$\mathcal{B} \cap \Sigma(u_*, \sigma = 0) = \left\{ z + \frac{S_* \cdot u}{P \cdot u} \mid u \in V_1 \right\} \quad (90)$$

The claim is that this is a 2-dimensional disc of radius (87) centred at z which lies in the plane perpendicular to the axis of rotation. To see this, we parametrise u by its boost-parameters relative to u_* , i.e., by its rapidity $\rho \in [0, \infty)$ and spatial direction $n \in u_*^\perp$, $n^2 = 1$, so that

$$u = \cosh(\rho) u_* + \sinh(\rho) n. \quad (91)$$

Then, assuming $\|S_*\| \neq 0$,

$$\frac{S_* \cdot u}{P \cdot u} = \frac{\|S_*\|}{\|P\|} \frac{S_* \cdot n}{\|S_*\|} \tanh(\rho). \quad (92)$$

Note that $n \mapsto \frac{S_* \cdot n}{\|S_*\|}$ maps u_*^\perp into itself. Since it is a non-zero antisymmetric endomorphism of the 3-dimensional vector space u_*^\perp it necessarily has a one-dimensional kernel, which is the rotation axis (the common fixed-point set of the rotations generated by the Lie-algebra element S_*) and maps the plane perpendicular to that axis into itself. In fact, since we divided by $\|S_*\|$, the map in the plane perpendicular to the rotation axis is a rotation by $\pi/2$. Hence, as n runs over the unit 2-sphere in u_*^\perp and $\tanh(\rho)$ over the interval $[0, 1)$, the image of the map $u \mapsto \frac{S_* \cdot u}{P \cdot u}$ becomes the unit 2-disc in u_*^\perp . \square

Remark 19 The condition $u_* \cdot S_* = 0$ makes S_* effectively a tensor in the antisymmetric tensor product of the 3-dimensional space u_*^\perp . Since u_*^\perp as well as its antisymmetric tensor product are 3-dimensional, there exists an isomorphism relating them. A preferred one is that of the 3-dimensional Hodge duality map, $\tilde{\star}$, which is obtained from the full (4-dimensional) Hodge duality map, denoted by \star , by first applying \star followed by left contraction with u_* , i.e., $\tilde{\star}T := u_* \cdot \star T = \star(T \wedge u_*)$; compare (146) of Appendix “Exterior Products and Hodge-Duality”. In this way we can uniquely associate a spin vector \vec{S}_* with the spin-tensor S_* as follows:

$$\vec{S}_* := -u_* \cdot \star S_* = -\star(S_* \wedge u_*), \quad (93a)$$

$$S_* = -u_* \cdot \star \vec{S}_* = -\star(\vec{S}_* \wedge u_*). \quad (93b)$$

Equation (93a) can be seen as definition of \vec{S}_* and (93b) as its inverse relation. The latter can be obtained from taking the \star of the first and using the fact that $\star \circ \star$ is the

identity on antisymmetric tensors of odd degree in even dimensions and Lorentzian signature, which follows from combining formulae (140) and (145) of Appendix “Exterior Products and Hodge-Duality”. This gives

$$\star \vec{S}_* = -S_* \wedge u_*. \quad (94)$$

Subsequent contraction with u_* , using $u_* \cdot S_* = 0$, yields (93b). In passing we also note that the component versions of (93) are

$$\vec{S}_*^n = -\frac{1}{2} \varepsilon_{abcd} \eta^{dn} S_*^{ab} u_*^c, \quad (95a)$$

$$S_*^{mn} = -\varepsilon_{abcd} \eta^{cm} \eta^{dn} \vec{S}_*^a u_*^b. \quad (95b)$$

We note from (93b) that

$$\vec{S}_* \cdot S_* = \star(\vec{S}_* \wedge \vec{S}_* \wedge u_*) = 0, \quad (96)$$

which means that \vec{S}_* lies in the intersection of u_*^\perp with the kernel of S_* . In other words, \vec{S}_* points along the axis of rotation. Finally we note that

$$\eta(\vec{S}_*, \vec{S}_*) = \eta_{ab} \vec{S}_*^a \vec{S}_*^b = -\frac{1}{2} \eta_{ac} \eta_{bd} S_*^{ab} S_*^{cd} = -\frac{1}{2} \eta \otimes \eta(S_*, S_*). \quad (97)$$

By the definition of the normalised inner product on antisymmetric tensors (i.e. dividing by $1/p!$ the p -fold tensor products of η on antisymmetric p -tensors) and setting

$$\|S_*\| := \sqrt{|\langle S_*, S_* \rangle_{\text{norm}}|} \quad (98)$$

we have (recall $\|\vec{S}_*\| := \sqrt{\eta(\vec{S}_*, \vec{S}_*)}$)

$$\|S_*\| = \|\vec{S}_*\|. \quad (99)$$

This justifies calling \vec{S}_* the *Spin vector*, which is associated to the (Lie-algebra valued) spin tensor S_* . \square

We end this section by justifying the terminology *centre-of-mass*. For this we recall that given an energy-momentum tensor \mathbf{T} and a unit timelike direction u , then $\mathbf{T}(u, u)$ is the spatial energy-density in the rest frame of the inertial observer represented by u . More precisely, let us foliate the affine space M by affine hyperplanes

$$\Sigma(u, \sigma) := \{x \in M \mid (x - z) \cdot u = \sigma\} \quad (100)$$

for some given $u \in V_1$ and $z \in M$. Each $\Sigma(u, \sigma)$ is a spacelike hyperplane of Einstein-simultaneity in the inertial frame characterised by u . It is clearly also a Cauchy surface in Minkowski space. The 3-form representing the spatial energy-density of \mathbf{T} on $\Sigma(u, \sigma)$ is then

$$\mathcal{E}(u, \sigma) = \mathbf{T}(u, u) \star u^b \big|_{\Sigma(u, \sigma)}, \quad (101)$$

where $\star u^b$ is the measure 3-form on $\Sigma(u, \sigma)$ (the Hodge-dual to the 1-form $u^b := \eta_{\downarrow}(u) := \eta(u, \cdot)$). The first moment of this energy distribution with respect to z is

$$m(z, u; \sigma) := \int_{\Sigma(u, \sigma)} (x - z) \mathcal{E}(u, \sigma) \bigg/ \int_{\Sigma(u, \sigma)} \mathcal{E}(u, \sigma), \quad (102)$$

where we explicitly indicated all dependencies on z, u , and σ and separated the latter by a semicolon to emphasise the special meaning of σ as “time-parameter” labelling the different leafs of the foliation orthogonal to u . The dependence on z is rather trivial: $m(z + b, u; \sigma) = m(z, u; \sigma) - b$ so that the set of points

$$\gamma(u; \sigma) = z + m(z, u; \sigma) \quad (103)$$

is independent of z . Moreover, from (102) it is obvious that $(\gamma(u, \sigma) - z) \cdot u = \sigma$ so that $\gamma(u, \sigma) \in \Sigma(u, \sigma)$. Note that the construction of the “first moment” refers to the affine structure of M . Given that \mathbf{T} satisfies the weak energy-condition we have $\mathbf{T}(u, u) \geq 0$, so that $\gamma(u, \sigma)$ lies in the convex hull of $\text{supp}(\mathbf{T}) \cap \Sigma(u, \sigma)$.

Now let us calculate the right-hand side of (102). The denominator is, in view of (70a),

$$\int_{\Sigma(u, \sigma)} \mathbf{T}(u, u) \star u^b = u \cdot P \quad (104)$$

independent of σ because P is independent of the Cauchy surface the integral is taken over. The a th component of the numerator can be transformed as follows (calling $\star u^b = d\mu$ and using component language)

$$\begin{aligned} \int_{\Sigma(u, \sigma)} (x - z)^a \mathcal{E}(u; \sigma) &= \int_{\Sigma(u, \sigma)} (x - z)^a T^{bc} u_b u_c d\mu \\ &= \int_{\Sigma(u, \sigma)} 2(x - z)^{[a} T^{b]c} u_b u_c d\mu \\ &\quad + \int_{\Sigma(u, \sigma)} (x - z)^b T^{ac} u_b u_c d\mu \\ &= J^{ab}[z] u_b + \sigma P^a \end{aligned} \quad (105)$$

where we used that $(x - z)^a u_a = \sigma$ for $x \in \Sigma(u, \sigma)$. In total we get

$$\gamma(u; \sigma) = z + \frac{J[z] \cdot u}{P \cdot u} + \frac{P}{P \cdot u} \sigma, \quad (106)$$

which, upon using the new parameter $\lambda := \sigma / (P \cdot u)$, just turns into (76) and (74). This justifies the term “centre-of-mass” in Definition 13, where “mass” is to be understood as proportional to energy. For a system of point particles this means

dynamical mass, not rest mass.⁴ We emphasise again that the essential use of the affine structure in this construction. In fact, the very notion of “first”, “second”, etc. “moments” of a distributions presuppose such a structure.

5 Typical Møller Radii

The ambiguity expressed in (87) only exists for bodies with spin. The formula suggest that for elementary particles it may well be of the order of magnitude of other radii, but that for laboratory-size or astrophysical bodies it is likely to be completely negligible. Let us therefore compute a few examples.

A spin-1/2 particle has $\|S\| = \hbar/2$ and thus

$$R_M = \frac{\hbar}{2M_0c} = \frac{1}{4\pi} \frac{h}{M_0c} = \frac{1}{4\pi} \lambda_C \quad (107)$$

where λ_C is the particle’s Compton wavelength. If the particle is electrically charged it has a classical charge-radius $R_{\text{classical}}$ determined by

$$\frac{e^2}{8\pi\epsilon_0 R_{\text{classical}}} = M_0 c^2. \quad (108)$$

Hence we have

$$R_M = R_{\text{classical}}/\alpha \approx 137 R_{\text{classical}} \quad (109)$$

Lets look at the Proton: Its experimentally determined “proton radius” (CODATA 2010) is

$$R_{\text{charge}}^{(\text{Proton})} = 0.87 \cdot 10^{-15} \text{ m}. \quad (110)$$

Its Compton wavelength is

$$\lambda_{\text{Proton}} = 1.32 \cdot 10^{-15} \text{ m}, \quad (111)$$

and its Møller radius is

$$R_M^{(\text{Proton})} = \frac{\lambda_{\text{Proton}}}{4\pi} = 1.05 \cdot 10^{-15} \text{ m} \approx \frac{1}{8} \cdot R_{\text{charge}}^{(\text{Proton})}. \quad (112)$$

⁴This definition of centre-of-mass, using the first moment of the dynamical-mass distribution, corresponds to cases (c) (for arbitrary u) and (d) (for $u = u_*$) in [10]. See this reference for a brief historical account of other definitions, e.g., based on the first moment of the rest-mass distribution, and a discussion of their partly peculiar properties, like moving mass centres in the zero momentum frame. There is also the issue of the Poisson structure for the coordinates of mass-centres, linear momentum, and spin, which for the mass centres based on dynamical mass where first discussed in [9]. Again we refer to [2] for a comprehensive discussion.

In comparison, a homogeneous rigid body of mass M and Radius R , rigidly spinning at angular frequency ω , has spin angular-momentum equal to

$$S = \frac{2}{5} MR^2 \omega \quad (113)$$

Hence the ratio of its Møller radius to its geometric radius is

$$\frac{R_M}{R} = \frac{S}{McR} = \frac{2}{5} \left(\frac{R\omega}{c} \right), \quad (114)$$

which shows that this ratio is of the order of magnitude of the circumferential velocity in units of the velocity of light. Applying this to Earth and Moon (somewhat idealised) gives

$$R_M^{(\text{Earth})} = 4 \text{ m}, \quad (115a)$$

$$R_M^{(\text{Moon})} = 1.1 \text{ cm}. \quad (115b)$$

Note that *Lunar Laser Ranging* also locates the moon's "position" within accuracy of centimeters. Hence the Møller radius is not as ridiculously small as one might have anticipated it to be for astronomical bodies. In fact, lets take the fast spinning Pulsar *PSR J1748-2446ad*, whose frequency is 716 Hz corresponding to a period of 1.4 milliseconds, for which we get $R\omega/c \approx 0.24$. Hence the ratio of its Møller radius to its geometric radius is

$$\left(\frac{R_M}{R} \right)_{\text{Pulsar}} \approx 0.1, \quad (116)$$

which is the typical ratio of relativistic effects for neutron stars.

Appendices

Exterior Products and Hodge-Duality

Let V be a real n -dimensional vector space, V^* its dual space and $T^p V^* = V^* \otimes \cdots \otimes V^*$ its p -fold tensor product.⁵ $T^p V^*$ carries a representation π_p of S_p , the symmetric group (permutation group) of p objects, given by

$$\pi_p : S_p \rightarrow \text{End}(T^p V^*), \quad \pi_p(\sigma)(\alpha_1 \otimes \cdots \otimes \alpha_p) := \alpha_{\sigma(1)} \otimes \cdots \otimes \alpha_{\sigma(p)} \quad (117)$$

⁵We follow standard tradition to define *forms*, i.e. the antisymmetric tensor product on the dual vector space V^* rather than on V . Clearly, all constructions that are to follow could likewise be made in terms of V rather than V^* .

and linear extension to sums of tensor products. On $T^p V^*$ we define the linear operator of antisymmetrisation by

$$\text{Alt}_p := \frac{1}{p!} \sum_{\sigma \in S_p} \text{sign}(\sigma) \pi_p, \quad (118)$$

where $\text{sign} : S_p \rightarrow \{1, -1\} \cong \mathbb{Z}_2$ is the sign-homomorphism. This linear operator is idempotent (i.e. a projection operator) and its image of $T^p V^*$ under Alt_p is the subspace of totally antisymmetric tensor-products. We write

$$\pi_p(T^p V^*) =: \bigwedge^p V^*. \quad (119)$$

Clearly

$$\dim \left(\bigwedge^p V^* \right) = \begin{cases} \binom{n}{p} & \text{for } p \leq n, \\ 0 & \text{for } p > n. \end{cases} \quad (120)$$

We set

$$\bigwedge V^* := \bigoplus_{p=0}^n \bigwedge^p V^*. \quad (121)$$

Let $\alpha \in \bigwedge^p V^*$ and $\beta \in \bigwedge^q V^*$, then we define their antisymmetric tensor product

$$\alpha \wedge \beta := \frac{(p+q)!}{p!q!} \text{Alt}_{p+q}(\alpha \otimes \beta) \in \bigwedge^{p+q} V^*. \quad (122)$$

One easily sees that

$$\alpha \wedge \beta = (-1)^{pq} \beta \wedge \alpha. \quad (123)$$

Bilinear extension of \wedge to all of $\bigwedge V^*$ endows it with the structure of a real 2^n -dimensional associative algebra, the so-called exterior algebra over V^* . If $\alpha_1, \dots, \alpha_p$ are in V^* , we have

$$\alpha_1 \wedge \dots \wedge \alpha_p = \sum_{\sigma \in S_p} \text{sign}(\sigma) \alpha_{\sigma(1)} \otimes \dots \otimes \alpha_{\sigma(p)}, \quad (124)$$

as one easily shows from (122) and (123) using induction.

If $\{\theta^1, \dots, \theta^n\}$ is a basis of V^* , a basis of $\bigwedge^p V^*$ is given by the following $\binom{n}{p}$ vectors

$$\{\theta^{a_1} \wedge \dots \wedge \theta^{a_p} \mid 1 \leq a_1 < a_2 < \dots < a_p \leq n\}. \quad (125)$$

An expansion of $\alpha \in \bigwedge^p V^*$ in this basis is written as follows

$$\alpha =: \frac{1}{p!} \alpha_{a_1 \dots a_p} \theta^{a_1} \wedge \dots \wedge \theta^{a_p}, \quad (126)$$

using standard summation convention and where the coefficients $\alpha_{a_1 \dots a_p}$ are totally antisymmetric in all indices. On the level of coefficients, (122) reads

$$(\alpha \wedge \beta)_{a_1 \dots a_{p+q}} = \frac{(p+q)!}{p!q!} \alpha_{[a_1 \dots a_p} \beta_{a_{p+1} \dots a_{p+q}]}, \quad (127)$$

where square brackets denote total antisymmetrisation in all indices enclosed:

$$\alpha_{[a_1 \dots a_p]} := \frac{1}{p!} \sum_{\sigma \in S_p} \text{sign}(\sigma) \alpha_{a_{\sigma(1)} \dots a_{\sigma(p)}}. \quad (128)$$

Suppose there is an inner product (non-degenerate symmetric bilinear form) η on V and the associated dual inner product η^{-1} on V^* (compare Remark 3). The latter extends to an inner product on each $T^p V^*$ by

$$\langle \alpha_1 \otimes \dots \otimes \alpha_p, \beta_1 \otimes \dots \otimes \beta_p \rangle := \prod_{a=1}^p \eta^{-1}(\alpha_a, \beta_a) \quad (129)$$

and bilinear extension:

$$\langle \alpha_{a_1 \dots a_p} \theta^{a_1} \otimes \dots \otimes \theta^{a_p}, \beta_{b_1 \dots b_p} \theta^{b_1} \otimes \dots \otimes \theta^{b_p} \rangle = \alpha_{a_1 \dots a_p} \beta^{a_1 \dots a_p}. \quad (130)$$

In particular, it extends to each subspace $\bigwedge^p V^* \subset T^p V^*$. We have

$$\langle \alpha_1 \wedge \dots \wedge \alpha_p, \beta_1 \wedge \dots \wedge \beta_p \rangle := p! \sum_{\sigma \in S_p} \text{sign}(\sigma) \prod_{a=1}^p \eta(\alpha_a, \beta_{\sigma(a)}) \quad (131)$$

and hence

$$\left\langle \frac{1}{p!} \alpha_{a_1 \dots a_p} \theta^{a_1} \wedge \dots \wedge \theta^{a_p}, \frac{1}{p!} \beta_{b_1 \dots b_p} \theta^{b_1} \wedge \dots \wedge \theta^{b_p} \right\rangle = \alpha_{a_1 \dots a_p} \beta^{a_1 \dots a_p}. \quad (132)$$

In the totally antisymmetric case it is more convenient to renormalise this product in a p -dependent fashion. One sets

$$\langle \cdot, \cdot \rangle_{\text{norm}} |_{\bigwedge^p V^*} := \frac{1}{p!} \langle \cdot, \cdot \rangle |_{\bigwedge^p V^*} \quad (133)$$

so that

$$\left\langle \frac{1}{p!} \alpha_{a_1 \dots a_p} \theta^{a_1} \wedge \dots \wedge \theta^{a_p}, \frac{1}{p!} \beta_{b_1 \dots b_p} \theta^{b_1} \wedge \dots \wedge \theta^{b_p} \right\rangle_{\text{norm}} = \frac{1}{p!} \alpha_{a_1 \dots a_p} \beta^{a_1 \dots a_p}. \quad (134)$$

Given a choice o of an orientation of V^* (e.g. induced by an orientation of V), there is a unique top-form $\varepsilon \in \bigwedge^n V^*$ (i.e. a *volume form* for V), associated with the triple (V^*, η^{-1}, o) , given by

$$\varepsilon := \theta^1 \wedge \cdots \wedge \theta^n, \quad (135)$$

where $\{\theta^1, \dots, \theta^n\}$ is any η^{-1} -orthonormal Basis of V^* in the orientation class o . The *Hodge-Duality* map at level $0 \leq p \leq n$ is a linear isomorphism

$$\star_p : \bigwedge^p V^* \rightarrow \bigwedge^{n-p} V^*, \quad (136a)$$

defined implicitly by

$$\alpha \wedge \star_p \beta = \varepsilon \langle \alpha, \beta \rangle_{\text{norm}}. \quad (136b)$$

This means that the image of $\beta \in \bigwedge^p V^*$ under \star_p in $\bigwedge^{n-p} V^*$ is defined by the requirement that (136b) holds true for all $\alpha \in \bigwedge^p V^*$. Linearity is immediate and uniqueness of \star_p follows from the fact that if $\lambda \in \bigwedge^{n-p} V^*$ and $\alpha \wedge \lambda = 0$ for all $\alpha \in \bigwedge^p V^*$, then $\lambda = 0$. To show existence it is sufficient to define \star_p on basis vectors. Since (136b) is also linear in α it is sufficient to verify (136b) if α runs through all basis vectors.

From now on we shall follow standard practice and drop the subscript p on \star , supposing that this will not cause confusion.

Let $\{e_1, \dots, e_n\}$ be a basis of V and $\{\theta^1, \dots, \theta^n\}$ its dual basis of V^* ; i.e. $\theta^a(e_b) = \delta_b^a$. Let further $\{\theta_1, \dots, \theta_n\}$ be the basis of V^* given by the image of $\{e_1, \dots, e_n\}$ under η_\downarrow (compare Remark 3), i.e. $\theta_a = \eta_{ab}\theta^b$. Then, on the basis $\{\theta_{a_1} \wedge \cdots \wedge \theta_{a_p} \mid 1 \leq a_1 < a_2 < \cdots < a_p \leq n\}$ of $\bigwedge^p V^*$ the map \star has the simple form

$$\star(\theta_{b_1} \wedge \cdots \wedge \theta_{b_p}) = \frac{1}{(n-p)!} \varepsilon_{b_1 \cdots b_p a_{p+1} \cdots a_n} \theta^{a_{p+1}} \wedge \cdots \wedge \theta^{a_n}. \quad (137)$$

This is proven by merely checking (136b) for $\alpha = \theta^{a_1} \wedge \cdots \wedge \theta^{a_p}$ and $\beta = \theta_{b_1} \wedge \cdots \wedge \theta_{b_p}$. Instead of (137) we can write

$$\begin{aligned} \star(\theta^{a_1} \wedge \cdots \wedge \theta^{a_p}) &= \frac{1}{(n-p)!} \eta^{a_1 b_1} \cdots \eta^{a_p b_p} \varepsilon_{b_1 \cdots b_p b_{p+1} \cdots b_n} \theta^{b_{p+1}} \wedge \cdots \wedge \theta^{b_n} \\ &= \frac{1}{(n-p)!} \varepsilon^{a_1 \cdots a_p}_{a_{p+1} \cdots a_n} \theta^{a_{p+1}} \wedge \cdots \wedge \theta^{a_n}, \end{aligned} \quad (138)$$

which makes explicit the dependence on ε and η .

If $\alpha = \frac{1}{p!} \alpha_{a_1 \cdots a_p} \theta^{a_1} \wedge \cdots \wedge \theta^{a_p}$, then $\star \alpha = \frac{1}{(n-p)!} (\star \alpha)_{b_1 \cdots b_{n-p}} \theta^{b_1} \wedge \cdots \wedge \theta^{b_{n-p}}$, where

$$(\star \alpha)_{b_1 \cdots b_{n-p}} = \frac{1}{p!} \alpha_{a_1 \cdots a_p} \varepsilon^{a_1 \cdots a_p}_{b_1 \cdots b_{n-p}}. \quad (139)$$

This gives the familiar expression of Hodge-Duality in component language. Note that on component level the first (rather than last) p indices are contracted.

Applying \star twice (i.e. actually $\star_{(n-p)} \circ \star_p$) leads to the following self-map of $\bigwedge^p V^*$:

$$\begin{aligned}
 & \star(\star(\theta^{a_1} \wedge \dots \wedge \theta^{a_p})) \\
 &= \frac{1}{p!(n-p)!} \varepsilon_{a_{p+1} \dots a_n}^{a_1 \dots a_p} \varepsilon_{b_1 \dots b_p}^{a_{p+1} \dots a_n} \theta^{b_1} \wedge \dots \wedge \theta^{b_p} \\
 &= \frac{(-1)^{p(n-p)}}{p!(n-p)!} \varepsilon_{a_1 \dots a_p a_{p+1} \dots a_n} \varepsilon_{b_1 \dots b_p a_{p+1} \dots a_n} \theta^{b_1} \wedge \dots \wedge \theta^{b_p} \\
 &= (-1)^{p(n-p)} \langle \varepsilon, \varepsilon \rangle_{\text{norm}} \theta^{a_1} \wedge \dots \wedge \theta^{a_p}.
 \end{aligned} \tag{140}$$

Note that

$$\langle \varepsilon, \varepsilon \rangle_{\text{norm}} = \frac{1}{n!} \eta^{a_1 b_1} \dots \eta^{a_n b_n} \varepsilon_{a_1 \dots a_n} \varepsilon_{b_1 \dots b_n} = (\varepsilon_{12 \dots n})^2 / \det\{\eta(e_a, e_b)\}. \tag{141}$$

This formula holds for any volume form ε in the definition (136b), independent of whether or not it is related to η .

Since the right-hand side of (136b) is symmetric under the exchange $\alpha \leftrightarrow \beta$, so must be the left-hand side. Using (140) we get

$$\begin{aligned}
 \langle \alpha, \beta \rangle_{\text{norm}} \varepsilon &= \alpha \wedge \star \beta = \beta \wedge \star \alpha = (-1)^{p(n-p)} \star \alpha \wedge \beta \\
 &= \langle \varepsilon, \varepsilon \rangle_{\text{norm}}^{-1} \star \alpha \wedge \star \star \beta = \langle \varepsilon, \varepsilon \rangle_{\text{norm}}^{-1} \langle \star \alpha, \star \beta \rangle_{\text{norm}} \varepsilon,
 \end{aligned} \tag{142}$$

hence

$$\langle \star \alpha, \star \beta \rangle_{\text{norm}} = \langle \varepsilon, \varepsilon \rangle_{\text{norm}} \langle \alpha, \beta \rangle_{\text{norm}}. \tag{143}$$

From this and (140) it follows for $\alpha \in \bigwedge^p V^*$ and $\beta \in \bigwedge^{n-p} V^*$, that

$$\langle \alpha, \star \beta \rangle_{\text{norm}} = \langle \varepsilon, \varepsilon \rangle_{\text{norm}}^{-1} \langle \star \alpha, \star \star \beta \rangle_{\text{norm}} = (-1)^{p(n-p)} \langle \star \alpha, \beta \rangle_{\text{norm}}. \tag{144}$$

This shows that the adjoint map of \star relative to $\langle \cdot, \cdot \rangle_{\text{norm}}$ is $(-1)^{p(n-p)} \star$.

Formulae (140), (142)–(144) are valid for general ε in the definition (136b). If we chose ε in the way we did, namely as the unique volume form that assigns unit volume to an oriented orthonormal frame, as does (135), then we have

$$\langle \varepsilon, \varepsilon \rangle_{\text{norm}} = (-1)^{n_-} \tag{145}$$

where n_- is the maximal dimension of subspaces in V restricted to which η is negative definite; i.e. η is of signature (n_+, n_-) . Equation (143) then shows that \star is an isometry for even n_- and an anti-isometry for odd n_- (as for Lorentzian η in any dimension).

Finally we note the following useful formula: If $v \in V$ let $i_v : T^p V^* \rightarrow T^{p-1} V^*$ the map which inserts v into the first tensor factor. It restricts to a map $i_v : \bigwedge^p V^* \rightarrow \bigwedge^{p-1} V^*$. Then, for any $\alpha \in \bigwedge^p V^*$, we have

$$i_v \star \alpha = \star(\alpha \wedge v^\flat). \quad (146)$$

where $v^\flat := \eta_\downarrow(v)$ (compare Remark 3). It suffices to prove this for basis elements $v = e_a$ of V and $\alpha = \theta^{a_1} \wedge \dots \wedge \theta^{a_p}$ of $\bigwedge^p V^*$, which is almost immediate using (138).

Group Actions on Manifolds

Let G be a group and M a set. An *action* of G of M is a map

$$\Phi : G \times M \rightarrow M \quad (147)$$

such that, for all $m \in M$ and $e \in G$ the neutral element,

$$\Phi(e, m) = m, \quad (148)$$

and where, in addition, one of the following two conditions hold:

$$\Phi(g, \Phi(h, m)) = \Phi(gh, m), \quad (149a)$$

$$\Phi(g, \Phi(h, m)) = \Phi(hg, m). \quad (149b)$$

If (147), (148) and (149a) hold we speak of a *left action*. A *right action* satisfies (147), (148) and (149b). For a left action we also write

$$\Phi(g, m) =: g \cdot m \quad (150a)$$

and for a right action

$$\Phi(g, m) =: m \cdot g. \quad (150b)$$

Equation (149) then simply become (group multiplication is denoted by juxtaposition without a dot)

$$g \cdot (h \cdot m) = (gh) \cdot m, \quad (151a)$$

$$(m \cdot h) \cdot g = m \cdot (hg). \quad (151b)$$

Holding either of the two arguments of Φ fixed we obtain the families of maps

$$\begin{aligned} \Phi_g : M &\rightarrow M \\ m &\mapsto \Phi(g, m) \end{aligned} \quad (152)$$

for each $g \in G$, or

$$\begin{aligned}\Phi_m : G &\rightarrow M \\ g &\mapsto \Phi(g, m)\end{aligned}\tag{153}$$

for each $m \in M$. Note that (148) and (149) imply that $\Phi_{g^{-1}} = (\Phi_g)^{-1}$. Hence each Φ_g is a bijection of M . The set of bijections of M will be denoted by $\text{Bij}(M)$. It is naturally a group with group multiplication being given by composition of maps and the neutral element being given by the identity map. Conditions (148) and (149a) are then equivalent to the statement that the map $G \rightarrow \text{Bij}(M)$, given by $g \mapsto \Phi_g$, is a group homomorphism. Likewise, (148) and (149b) is equivalent to the statement that this map is a group anti-homomorphism.

The following terminology is standard: The set $\text{Stab}(m) := \{g \in G \mid \Phi(g, m) = m\} \subset G$ is called the *stabiliser* of m . It is easily proven to be a normal subgroup of G satisfying $\text{Stab}(g \cdot m) = g(\text{Stab}(m))g^{-1}$ for left and $\text{Stab}(m \cdot g) = g^{-1}(\text{Stab}(m))g$ for right actions. The *orbit* of G through $m \in M$ is the set $\text{Orb}(m) := \{\Phi(g, m) \mid g \in G\} =: \Phi(G, m)$ (also written $G \cdot m$ for left and $m \cdot G$ for right action). It is easy to see that two orbits are either disjoint or identical. Hence the orbits partition M . A point $m \in M$ is called a *fixed point* of the action Φ iff $\text{Stab}(m) = G$. An action Φ is called *effective* iff $\Phi(g, m) = m$ for all $m \in M$ implies $g = e$; i.e., “only the group identity moves nothing”. Alternatively, we may say that effectiveness is equivalent to the map $G \mapsto \text{Bij}(M)$, $g \mapsto \Phi_g$, being injective; i.e., $\Phi_g = \text{id}_M$ implies $g = e$. The action Φ is called *free* iff $\Phi(g, m) = m$ for some $m \in M$ implies $g = e$; i.e., “no $g \neq e$ fixes a point”. This is equivalent to the injectivity of all maps $\Phi_m : G \rightarrow M$, $g \mapsto \Phi(g, m)$, which can be expressed by saying that all orbits of G in M are faithful images of G .

Here we are interested in *smooth* actions. For this we need to assume that G is a Lie group, that M a differentiable manifold, and that the map (147) is smooth. We denote by $\exp : T_e G \rightarrow G$ the exponential map. For each $X \in T_e G$ there is a vector field V^X on M , given by

$$\begin{aligned}V^X(m) &= \left. \frac{d}{dt} \right|_{t=0} \Phi(\exp(tX), m) \\ &= \Phi_{m*e}(X).\end{aligned}\tag{154}$$

Here Φ_{m*e} denotes the differential of the map Φ_m evaluated at $e \in G$. V^X is also called the *fundamental vector field* on M associated to the action Φ of G and to $X \in T_e G$. (We will later write $\text{Lie}(G)$ for $T_e G$, after we have discussed *which* Lie structure on $T_e G$ we choose.)

In passing we note that from (154) it already follows that the flow map of V^X is given by

$$\text{Fl}_t^{V^X}(m) = \Phi(\exp(tX), m).\tag{155}$$

This follows from $\exp(sX)\exp(tX) = \exp((s+t)X)$ and (149) (any of them), which imply

$$\text{Fl}_s^{V^X} \circ \text{Fl}_t^{V^X} = \text{Fl}_{s+t}^{V^X}. \quad (156)$$

on the domain of M where all three maps appearing in (156) are defined. Uniqueness of flow maps for vector fields then suffice to show that (155) is indeed the flow of V^X .

Before we continue with the general case, we have a closer look at the special cases where $M = G$ and Φ is either the left translation of G on G , $\Phi(g, h) = L_g(h) := gh$, or the right translation, $\Phi(g, h) = R_g(h) := hg$. The corresponding fundamental vector fields (154) are denoted by V_R^X and V_L^X respectively:

$$V_R^X(h) = \left. \frac{d}{dt} \right|_{t=0} (\exp(tX) h), \quad (157a)$$

$$V_L^X(h) = \left. \frac{d}{dt} \right|_{t=0} (h \exp(tX)). \quad (157b)$$

The seemingly paradoxical labeling of R for left and L for right translation finds its explanation in the fact that V_R^X is right and V_L^X is left invariant, i.e., $R_{g*} V_R^X = V_R^X$ and $L_{g*} V_L^X = V_L^X$. Recall that the latter two equations are shorthands for

$$R_{g*} V_R^X(h) = V_R^X(hg), \quad (158a)$$

$$L_{g*} V_L^X(h) = V_L^X(gh). \quad (158b)$$

The proofs of (158a) only uses (157a) and the chain rule:

$$\begin{aligned} R_{g*} V_R^X(h) &= R_{g*} \left. \frac{d}{dt} \right|_{t=0} (\exp(tX) h) \\ &= \left. \frac{d}{dt} \right|_{t=0} R_g (\exp(tX) h) \\ &= \left. \frac{d}{dt} \right|_{t=0} (\exp(tX) hg) \\ &= V_R^X(hg). \end{aligned} \quad (159a)$$

Similarly, the proof of (158b) starts from (157b):

$$\begin{aligned} L_{g*} V_L^X(h) &= L_{g*} \left. \frac{d}{dt} \right|_{t=0} (h \exp(tX)) \\ &= \left. \frac{d}{dt} \right|_{t=0} L_g (h \exp(tX)) \\ &= \left. \frac{d}{dt} \right|_{t=0} (gh \exp(tX)) \\ &= V_L^X(gh). \end{aligned} \quad (159b)$$

In particular, we have

$$V_R^X(g) = R_{g*e} V_L^X(e) = R_{g*e} X, \quad (160a)$$

$$V_L^X(g) = L_{g*e} V_R^X(e) = L_{g*e} X, \quad (160b)$$

showing that the vector spaces of right/left invariant vector fields on G are isomorphic to $T_e G$. Moreover, the vector spaces of right/left invariant vector fields on G are Lie algebras, the Lie product being their ordinary commutator (as vector fields). This is true because the operation of commuting vector fields commutes with push-forward maps of diffeomorphisms: $\phi_*[V, W] = [\phi_* V, \phi_* W]$. This implies that the commutator of right/left invariant vector fields is again right/left invariant. Hence the isomorphisms can be used to turn $T_e G$ into a Lie algebra, identifying it either with the Lie algebra of right- or left-invariant vector fields. The standard convention is to choose the latter. Hence, for any $X, Y \in \text{Lie}(G)$, one defines

$$[X, Y] := [V_L^X, V_L^Y](e). \quad (161)$$

$T_e G$ endowed with *that* structure is called $\text{Lie}(G)$. Clearly, this turns $V_L : \text{Lie}(G) \rightarrow \text{Vec}(G)$, $X \mapsto V_L^X$, into a Lie homomorphism:

$$V_L^{[X, Y]} = [V_L^X, V_L^Y]. \quad (162)$$

As a consequence, $V_R : \text{Lie}(G) \rightarrow \text{Vec}(G)$, $X \mapsto V_R^X$, now turns out to be an *anti* Lie isomorphism, i.e., to contain an extra minus sign:

$$V_R^{[X, Y]} := -[V_R^X, V_R^Y]. \quad (163)$$

This can be proven directly but will also follow from the more general considerations below.

On G consider the map

$$\begin{aligned} C : G \times G &\rightarrow G \\ (h, g) &\mapsto hgh^{-1}. \end{aligned} \quad (164)$$

For fixed h this map, $C_h : G \rightarrow G$, $g \mapsto C_h(g) = hgh^{-1}$, is an automorphism (i.e., self-isomorphism) of G . Automorphisms of G form a group (multiplication being composition of maps) which we denote by $\text{Aut}(G)$. It is immediate that the map $C \rightarrow \text{Aut}(G)$, $h \mapsto C_h$, is a homomorphism of groups; i.e.,

$$C_e = \text{id}_G, \quad (165a)$$

$$C_h \circ C_k = C_{hk}. \quad (165b)$$

Taking the differential at $e \in G$ of C_h we obtain a linear self-map of $T_e G$, which we call Ad_h :

$$\text{Ad}_h := C_{h*e} : T_e G \rightarrow T_e G. \quad (166a)$$

Differentiating both sides of both Eq. (165) at $e \in G$, using the chain rule together with $C_k(e) = e$ for the second, we infer that

$$\text{Ad}_e = \text{id}_{T_e G}, \quad (166b)$$

$$\text{Ad}_h \circ \text{Ad}_k = \text{Ad}_{hk}. \quad (166c)$$

This implies, firstly, that each linear map (166a) is invertible, i.e. an element of the *general linear group* $\text{GL}(T_e G)$ of the vector space $T_e G$, and, secondly, that the map

$$\begin{aligned} \text{Ad} : G &\rightarrow \text{GL}(T_e G) \\ h &\mapsto \text{Ad}_h \end{aligned} \quad (167)$$

is a group homomorphism. In other words, Ad is a linear representation of G on $T_e G$, called the *adjoint representation*.

In (158) we saw that V_R^X and V_L^X are invariant under the action of right and left translations respectively (hence their names). But what happens if we act on V_R^X with left and on V_L^X with right translations? The answer is obtained from straightforward computation. In the first case we get:

$$\begin{aligned} L_{g*h}(V_R^X(h)) &= L_{g*h} \frac{d}{dt} \Big|_{t=0} (\exp(tX) h) \\ &= \frac{d}{dt} \Big|_{t=0} (g \exp(tX) h) \\ &= \frac{d}{dt} \Big|_{t=0} (C_g(\exp(tX)) gh) \\ &= V_R^{\text{Ad}_g(X)}(gh), \end{aligned} \quad (168a)$$

where we used (166) in the last and the definition of V_R^X in the first and last step. Similarly, in the second case we have

$$\begin{aligned} R_{g*h}(V_L^X(h)) &= R_{g*h} \frac{d}{dt} \Big|_{t=0} (h \exp(tX) h) \\ &= \frac{d}{dt} \Big|_{t=0} (h \exp(tX) g) \\ &= \frac{d}{dt} \Big|_{t=0} (hg C_{g^{-1}}(\exp(tX))) \\ &= V_L^{\text{Ad}_{g^{-1}}(X)}(gh). \end{aligned} \quad (168b)$$

Taking the differential of Ad at $e \in G$ we obtain a linear map from $T_e G$ into $\text{End}(T_e G)$, the linear space of endomorphisms of $T_e G$ (linear self-maps of $T_e G$).

$$\begin{aligned} \text{ad} &:= \text{Ad}_{*e} : T_e G \rightarrow \text{End}(T_e G) \\ X &\mapsto \text{ad}_X. \end{aligned} \quad (169)$$

Now, we have

$$\text{ad}_X(Y) = [X, Y] \quad (170)$$

where the right-hand side is defined in (161). The proof of (170) starts from the fact that the commutator of two vector fields can be expressed in terms of the Lie derivative of the second with respect the first vector field in the commutator, and the definition of the Lie derivative. We recall from (155) that the flow of the left invariant vector fields is given by right translation: $\text{Fl}_t^{V_L^X}(g) = g \exp(tX)$. Then we have

$$\begin{aligned} [X, Y] &= [V_L^X, V_L^Y](e) \\ &= (L_{V_L^X} V_L^Y)(e) \\ &= \left. \frac{d}{dt} \right|_{t=0} \text{Fl}_{(-t)*}^{V_L^X} \left(V_L^Y(\text{Fl}_t^{V_L^X}(e)) \right) \\ &= \left. \frac{d}{dt} \right|_{t=0} \text{Fl}_{(-t)*}^{V_L^X} \left. \frac{d}{ds} \right|_{s=0} \text{Fl}_s^{V_L^Y} \left(\text{Fl}_t^{V_L^X}(e) \right) \\ &= \left. \frac{d}{dt} \right|_{t=0} \left. \frac{d}{ds} \right|_{s=0} \exp(tX) \exp(sY) \exp(-tX) \\ &= \left. \frac{d}{dt} \right|_{t=0} \text{Ad}_{\exp(tX)}(Y) \\ &= \text{ad}_X(Y). \end{aligned} \quad (171a)$$

A completely analogous consideration, now using $\text{Fl}_t^{V_R^X}(g) = \exp(tX)g$, allows to compute the commutator of the right-invariant vector fields evaluated at $e \in G$:

$$\begin{aligned} [V_R^X, V_R^Y](e) &= (L_{V_R^X} V_R^Y)(e) \\ &= \left. \frac{d}{dt} \right|_{t=0} \text{Fl}_{(-t)*}^{V_R^X} \left(V_R^Y(\text{Fl}_t^{V_R^X}(e)) \right) \\ &= \left. \frac{d}{dt} \right|_{t=0} \text{Fl}_{(-t)*}^{V_R^X} \left. \frac{d}{ds} \right|_{s=0} \text{Fl}_s^{V_R^Y} \left(\text{Fl}_t^{V_R^X}(e) \right) \\ &= \left. \frac{d}{dt} \right|_{t=0} \left. \frac{d}{ds} \right|_{s=0} \exp(-tX) \exp(sY) \exp(tX) \\ &= \left. \frac{d}{dt} \right|_{t=0} \text{Ad}_{\exp(-tX)}(Y) \\ &= -\text{ad}_X(Y) \\ &= -[X, Y]. \end{aligned} \quad (171b)$$

Equation (163) now follows if we act on both sides of $[V_R^X, V_R^Y](e) = -[X, Y]$ with R_{g*e} and use (158a).

We now return to the general case where M is any manifold and the vector field V^X is defined by an action Φ as in (154) and whose flow map is given by (155). Now, given that Φ is a *right action*, we obtain

$$\begin{aligned}
 [V^X, V^Y](m) &= (L_{V^X} V^Y)(m) \\
 &= \frac{d}{dt} \Big|_{t=0} \text{Fl}_{(-t)*}^{V^X} \left(V^Y(\text{Fl}_t^{V^X}(m)) \right) \\
 &= \frac{d}{dt} \Big|_{t=0} \text{Fl}_{(-t)*}^{V^X} \frac{d}{ds} \Big|_{s=0} \text{Fl}_s^{V^Y} \left(\text{Fl}_t^{V^X}(m) \right) \\
 &= \frac{d}{dt} \Big|_{t=0} \frac{d}{ds} \Big|_{s=0} \Phi(\exp(tX) \exp(sY) \exp(-tX), m) \\
 &= \frac{d}{dt} \Big|_{t=0} \Phi_{m*e}(\text{Ad}_{\exp(tX)}(Y)) \\
 &= V^{\text{ad}_X(Y)}(m) \\
 &= V^{[X,Y]}(m)
 \end{aligned} \tag{172a}$$

where we used (155) and (149b) at the fourth and (170) at the last equality. Similarly, if Φ is a *left action*, we have

$$\begin{aligned}
 [V^X, V^Y](m) &= (L_{V^X} V^Y)(m) \\
 &= \frac{d}{dt} \Big|_{t=0} \text{Fl}_{(-t)*}^{V^X} \left(V^Y(\text{Fl}_t^{V^X}(m)) \right) \\
 &= \frac{d}{dt} \Big|_{t=0} \text{Fl}_{(-t)*}^{V^X} \frac{d}{ds} \Big|_{s=0} \text{Fl}_s^{V^Y} \left(\text{Fl}_t^{V^X}(m) \right) \\
 &= \frac{d}{dt} \Big|_{t=0} \frac{d}{ds} \Big|_{s=0} \Phi(\exp(-tX) \exp(sY) \exp(tX), m) \\
 &= \frac{d}{dt} \Big|_{t=0} \Phi_{m*e}(\text{Ad}_{\exp(-tX)}(Y)) \\
 &= -V^{\text{ad}_X(Y)}(m) \\
 &= -V^{[X,Y]}(m)
 \end{aligned} \tag{172b}$$

where we used (155) and (149a) at the fourth and again (170) at the last equality.

Finally we derive the analog of (168) in the general case. This corresponds to computing the push-forward of V^X under Φ_g . If Φ is a left action we will obtain the analog of (168a), and the analog of (168b) if Φ is a right action. For easier readability we shall also make use of the notation (150). For a left action we then get

$$\begin{aligned}
\Phi_{g*m}(V^X(m)) &= \Phi_{g*m} \frac{d}{dt} \Big|_{t=0} \Phi(\exp(tX), m) \\
&= \frac{d}{dt} \Big|_{t=0} \Phi(g \exp(tX), m) \\
&= \frac{d}{dt} \Big|_{t=0} \Phi(C_g(\exp(tX)), g \cdot m) \\
&= \Phi_{(g \cdot m)*e} \frac{d}{dt} \Big|_{t=0} C_g(\exp(tX)) \\
&= \Phi_{(g \cdot m)*e}(\text{Ad}_g(X)) \\
&= V^{\text{Ad}_g(X)}(g \cdot m) \\
&= V^{\text{Ad}_g(X)}(\Phi(g, m)).
\end{aligned} \tag{173a}$$

Similarly, if Φ is a right action,

$$\begin{aligned}
\Phi_{g*m}(V^X(m)) &= \Phi_{g*m} \frac{d}{dt} \Big|_{t=0} \Phi(\exp(tX), m) \\
&= \frac{d}{dt} \Big|_{t=0} \Phi(\exp(tX) g, m) \\
&= \frac{d}{dt} \Big|_{t=0} \Phi(C_{g^{-1}}(\exp(tX)), m \cdot g) \\
&= \Phi_{(m \cdot g)*e} \frac{d}{dt} \Big|_{t=0} C_{g^{-1}}(\exp(tX)) \\
&= \Phi_{(m \cdot g)*e}(\text{Ad}_{g^{-1}}(X)) \\
&= V^{\text{Ad}_{g^{-1}}(X)}(m \cdot g) \\
&= V^{\text{Ad}_{g^{-1}}(X)}(\Phi(g, m)).
\end{aligned} \tag{173b}$$

References

1. W.G. Dixon, *Special Relativity. The Foundation of Macroscopic Physics* (Cambridge University Press, Cambridge, 1978)
2. G.N. Fleming, Covariant position operators, spin, and locality. *Phys. Rev. B* **137**, 188 (1965)
3. G. Hamel, Eine Basis aller Zahlen und die unstetigen Lösungen der Funktionalgleichung: $f(x+y) = f(x) + f(y)$. *Math. Ann.* **60**(3), 459–462 (1905)
4. J.G. Darboux, Sur la composition des forces en statique. *Bull. Sci. Math. Astron.* **9**, 281–288 (1875)
5. R. Schimmack, Ueber die axiomatische Begründung der Vektoraddition. *Nachr. Ges. d. Wiss. Gött., Math.-Phys. Kl.* **1903**, 257–278 (1903)
6. M. Berger, *Geometry*, vol. I, 1st edn (Springer, Berlin, 1987). Corrected second printing 1994
7. J.H. Conway et al., *ATLAS of Finite Groups* (Oxford University Press, Oxford, 1985)
8. V. Fock, *The Theory of Space Time and Gravitation*. First English edition (Pergamon Press, London, 1959)

9. M. Born, K. Fuchs, The mass centre in relativity. *Nature* **40**(3676), 587–587 (1940)
10. M.H.L. Pryce, The mass-centre in the restricted theory of relativity and its connexion with the quantum theory of elementary particles. *Proc. R. Soc. (London) A* **195**, 62 (1948)
11. C. Møller, On the definition of the centre of gravity of an arbitrary closed system in the theory of relativity. *Commun. Dublin Inst. Adv. Stud. Ser. A* **5**, 1 (1949)
12. R.U. Sexl, H.K. Urbantke, *Relativity, Groups, Particles*, 1st edn. (Springer, Wien, 2001). First English edition, succeeding the 1992 third revised German edition

Solutions of Mathisson-Papapetrou Equations for Highly Relativistic Spinning Particles

Roman Plyatsko, Mykola Fenyk and Oleksandr Stefanyshyn

Abstract Different types of essentially nongeodesic motions of highly relativistic spinning particles in Schwarzschild's and Kerr's background which follows from the Mathisson-Papapetrou (MP) equations are considered. It is shown that dependently on the correlation of signs of the spin and the particle's orbital velocity the spin-gravity coupling acts as a significant repulsive or attractive force. Numerical estimates for electrons, protons, and neutrinos in the gravitational field of black holes are presented. The correspondence between the general relativistic Dirac equation and MP equations is discussed. It is stressed that for the highly relativistic motions the adequate supplementary condition for the MP equations is the Mathisson-Pirani condition. In the following it is important to study the possible role of the highly relativistic spin-gravity coupling in astrophysics, cosmology, and high energy physics.

1 Introduction

After obtaining the general relativistic equations of motion for a test body with inner rotation/nonquantum spinning particle in [1, 2], investigations of their solutions for some backgrounds were started in [3–7]. Schwarzschild's metric was taken into account in [3, 5, 6], Lense-Thirring's and Melvin's metric were under consideration in [4, 7] correspondingly. The concrete physical effects of spin-gravity coupling on rotating body trajectories have been studied. For example, it was shown that the correction in perihelion motion of the planet Mercury because of its spin is negligible [3]. Similar results were obtained for other cases of spinning particle motions in the gravitational field which were considered at that time. Therefore, it is naturally that the corresponding statement was formulated in the known book [8] from 1973. However, the same year is dated paper [9] where another supposition one can read: "The simple act of endowing a black hole with angular momentum has led to an unexpected richness of possible physical phenomena. It seems appropriate to ask

R. Plyatsko (✉) · M. Fenyk · O. Stefanyshyn
Pidstryhach Institute for APMM, Ukrainian National Academy of Sciences,
3-b Naukova Str., Lviv 79060, Ukraine
e-mail: plyatsko@lms.lviv.ua

whether endowing the test body with intrinsic spin might not also lead to surprises.” This paper, together with [10], where the spin-spin and spin-orbit gravitational interactions were considered, gave the impulse for realizing our program of more detailed investigations of physical effects following from the MP equations. We began from searching possible new analytical solutions of the exact Mathisson-Papapetrou equations in Schwarzschild’s background without the supposition that they must be close to the corresponding solutions of the geodesic equations. That is, in our calculations we did not use the approach of small corrections because of the spin to the known geodesic solutions.

It is known that the exact MP equations have a simple analytical solution for the radial motion with any oriented spin in Schwarzschild’s background: this solution describe the particle’s world line which coincides with the corresponding geodesic world line. Other solutions of the MP equations in Schwarzschild’s background, which describe the circular orbits of a particle with spin orthogonal to the equatorial plane of its motion, is known as well. These solutions differ from the corresponding geodesic solutions because of the terms which describe the gravitational spin-orbit interaction. At the same time, it is not difficult to check that the MP equations do not admit solutions in Schwarzschild’s equatorial plane with the spin non-orthogonal to this plane. However, paper [10] inspired the question: do the MP equations admit any solution which describe circular orbits of a spinning particle beyond the equatorial plane of Schwarzschild’s background? Indeed, it was shown in [10] that according to the MP equations the spin-spin interaction cannot maintain a spinning test particle at rest on the axis of rotation of Kerr’s mass. Nevertheless, this fact does not exclude a priori an effect of particle hovering above Kerr’s or Schwarzschild’s mass due to the spin-orbit interaction, i.e., for some dynamical, nor statical, cases. Then it was shown that the MP equations admit the corresponding solutions both in the Schwarzschild [11, 12] and Kerr backgrounds [13] which describe just the circular non-equatorial orbits. It is important that for realizing these orbits a spinning particle must posses the highly relativistic velocity relative to a source of the gravitational field. Late those and other results of studying the highly relativistic spinning particle motions were summarized in book [14]. Further development of the corresponding direction of investigations for the last 15 years is presented in [15–23].

The important point in the description of spinning particle motions by the MP equations is the choice of an appropriate supplementary condition. From the first steps in our investigations we chose the Mathisson-Pirani supplementary condition [1, 24] as a basic one. In this choosing we took into account the results of papers [25, 26]: if we need to describe, in the proper sense, just the inner rotation of the body, it is necessary to use the Mathisson-Pirani condition. Nevertheless, in many cases, when the body/particle velocity is not very close to the velocity of light, this condition can be substitute by the Tulczyjew-Dixon condition with high accuracy (more on this subject we write below).

Here we present our results of the theoretical investigations of the highly relativistic spin-gravity coupling by analysis of the corresponding solutions of the MP equations in Schwarzschild’s and Kerr’s background. Naturally, from a practical point of view the situation with a macroscopic test particle moving relative to a

massive body with the velocity close to the velocity of light is not realistic. However, the highly relativistic velocities are usual in astrophysics for elementary particles. In this connection we stress the important fact: in many papers [27–35] it was shown that in a certain sense the MP equations follow from the quantum general relativistic Dirac equation [36–38] as a classical approximation.

2 Different Representations of Mathisson-Papapetrou Equations

Because the traditional form of the MP equations are presented above in other papers, in this section we write only their non-traditional forms which are convenient for further analysis of physical meaning of the corresponding solutions.

2.1 MP Equations Through Spin 3-Vector

For description of the particle spin by the MP equations, in many papers both the tensor of spin $S^{\lambda\mu}$ and the 4-vector of spin s_λ are used, where by definition

$$s_\lambda = \frac{1}{2} \varepsilon_{\lambda\mu\nu\sigma} \sqrt{-g} u^\mu S^{\nu\sigma}, \quad S^{\lambda\mu} = \varepsilon^{\lambda\mu\nu\sigma} u_\nu s_\sigma, \quad (1)$$

where $\varepsilon_{\lambda\mu\nu\sigma}$ and g are the Levi-Civita symbol and the determinant of the metric tensor correspondingly (here, and in the following, Greek indices run 1, 2, 3, 4 and Latin indices 1, 2, 3; the signature of the metric $-,-,-,+$ is chosen; units $c = G = 1$ are used). That is, instead of the six components $S^{\lambda\mu}$ one can deal with the four components s_λ . In the term of s_λ the Mathisson-Pirani condition is

$$s_\lambda u^\lambda = 0, \quad (2)$$

and the spin part of the MP equations takes the form

$$\frac{Ds^\lambda}{ds} = s_\mu \frac{Du^\mu}{ds} u^\lambda, \quad (3)$$

i.e., according to the MP equations at the Mathisson-Pirani the 4-vector of spin is Fermi transported [8].

For further reduction of the number of the spin components which are presented explicitly in the MP equations, it is possible to do another step: we can operate only with the three components of the spin tensor $S^{\lambda\mu}$ which contain only the spatial indices, i.e., S^{ik} , because the three other components of this tensor by the Mathisson-Pirani condition are expressed as

$$S^{i4} = \frac{u_k}{u_4} S^{ki}. \quad (4)$$

The useful form of the MP equation can be obtained if instead of the spin tensor components S^{ki} the 3-component value S_i is introduced by definition

$$S_i = \frac{1}{2u_4} \sqrt{-g} \varepsilon_{ikl} S^{kl}, \quad (5)$$

where ε_{ikl} is the spatial Levi-Civita symbol; the expression of S^{ki} through S_i is

$$S^{ik} = \frac{u_4}{\sqrt{-g}} \varepsilon^{ikl} S_l. \quad (6)$$

Then the transport part of the MP equations can be written as [14, 15]

$$\begin{aligned} m(\dot{u}^m + \Gamma_{\mu\nu}^m u^\mu u^\nu) - 2 \frac{d}{ds} \left[|g|^{-1/2} (\dot{u}^\mu + \Gamma_{\pi\rho}^\mu u^\pi u^\rho) (u_4 S_{[n} g_{p]\mu} + g_{4\mu} S_{[p} u_{n]}) \right] \\ - |g|^{-1/2} u^\nu (\dot{u}^\mu + \Gamma_{\pi\rho}^\mu u^\pi u^\rho) (u_4 \Gamma_{i\nu}^m g_{k\mu} + 2u_i \Gamma_{\nu[k}^m g_{4] \mu}) \varepsilon^{ikl} S_l \\ + \frac{1}{2} |g|^{-1/2} u^\pi (u_4 R_{\pi ik}^m + 2u_i R_{\pi k4}^m) \varepsilon^{ikl} S_l = 0, \end{aligned} \quad (7)$$

where for the free indices m, n and p it is necessary to put the circle combinations 1, 2, 3; 2, 3, 1; 3, 1, 2, and the fourth equation of the MP transport part can be transformed to the form

$$\begin{aligned} m(\dot{u}^4 + \Gamma_{\mu\nu}^4 u^\mu u^\nu) + \frac{d}{ds} \left[|g|^{-1/2} (\dot{u}^\mu + \Gamma_{\pi\rho}^\mu u^\pi u^\rho) g_{\mu k} u_i \varepsilon^{ikl} S_l \right] \\ - |g|^{-1/2} u^\nu (\dot{u}^\mu + \Gamma_{\pi\rho}^\mu u^\pi u^\rho) (u_4 \Gamma_{i\nu}^4 g_{k\mu} + 2u_i \Gamma_{\nu[k}^4 g_{4] \mu}) \varepsilon^{ikl} S_l \\ + \frac{1}{2} |g|^{-1/2} u^\pi (u_4 R_{\pi ik}^4 + 2u_i R_{\pi k4}^4) \varepsilon^{ikl} S_l = 0 \end{aligned} \quad (8)$$

(a dot denotes differentiation with respect to the proper time s , and square brackets denote antisymmetrization of indices).

The all three independent equations of the spin part of the MP equations can be written as [14, 21]

$$\begin{aligned} u_4 \dot{S}_i + 2(\dot{u}_{[4} u_{i]}) - u^\pi u_\rho \Gamma_{\pi[4}^\rho u_{i]} S_k u^k \\ + 2S_n \Gamma_{\pi[4}^n u_{i]} u^\pi = 0. \end{aligned} \quad (9)$$

In practical calculations for the concrete metric, both analytical and numerical, it is often more convenience to use the MP equation representation just through the

3-vector S_i . In particular, at a glance, from (9) we see that the spin part of the MP equations becomes much simpler if the condition $S_i u^i = 0$ is satisfied, i.e., when the spin is orthogonal to the particle's trajectory.

According to (1) and (5), there is a simple relationship between S_i and s_λ :

$$S_i = -s_i + \frac{u_i}{u_4} s_4. \quad (10)$$

2.2 MP Equations in Comoving Tetrad Representation

In many cases, it is important to describe a physical event in different frames of reference. Concerning the motion of a spinning test particle in the gravitational field, it is useful to consider the main properties of this motion from the point of view of an observer moving with the spinning particle, with respect to which the representative point of the particle is at rest.

As usual, the comoving frame of reference are determined by a set of orthogonal tetrads $\lambda_{(\nu)}^\mu$, where $\lambda_{(4)}^\mu = u^\mu$ and

$$\lambda_{(\nu)}^\mu \lambda_{(\rho)}^\pi g_{\mu\pi} = \eta_{(\nu)(\rho)}, \quad g_{\mu\nu} = \lambda_{(\mu)}^{(\pi)} \lambda_{(\nu)}^{(\rho)} \eta_{(\pi)(\rho)} \quad (11)$$

(here, and in the following, in contrast to the indices of the global coordinates, the local indices are placed in the parenthesis; $\eta_{(\nu)(\rho)}$ is the Minkowski tensor).

The local components of the spin 4-vector for a comoving observer satisfy the condition $s_{(4)} = 0$ [26]. Concerning the spatial components of this vector, without loss in generality, for convince we direct the first vector along the direction of spin, that is we write

$$s_{(1)} \neq 0, \quad s_{(2)} = 0, \quad s_{(3)} = 0, \quad s_{(4)} = 0. \quad (12)$$

The MP equations have the constant of motion $S_0^2 = s_{(\mu)} s^{(\mu)}$, where $|S_0|$ is the absolute value of the particle spin [26], and according to (12) $|s_{(1)}| = |S_0|$.

By relationships (11) and (12) for the local components of the spin 3-vector we have

$$S_{(1)} = -s_{(1)} \neq 0, \quad S_{(2)} = 0, \quad S_{(3)} = 0. \quad (13)$$

Then according to (10) the global components of this 3-vector are connected with its local components by the relationship

$$\lambda_4^{(4)} S_i = \left(\lambda_4^{(4)} \lambda_i^{(1)} - \lambda_i^{(4)} \lambda_4^{(1)} \right) S_{(1)}. \quad (14)$$

It follows from Eq. (9) that

$$\gamma_{(k)(1)(4)} = 0, \quad (15)$$

where $\gamma_{(k)(1)(4)}$ are the Ricci coefficients of rotation. Because these coefficients are antisymmetric in the first two indices, Eq. (15) contains the two relationships: $\gamma_{(2)(1)(4)} = 0$ and $\gamma_{(3)(1)(4)} = 0$. The similar third relationship, $\gamma_{(2)(3)(4)} = 0$, can be added if one need exclude the rotation of the second and the third local spatial vectors relative to the direction of the first vector, which in our consideration is connected with the spin orientation. Therefore, we are free to put

$$\gamma_{(i)(k)(4)} = 0. \quad (16)$$

Equation (16) is the known condition of the Fermi transport for the local orthonormal vectors.

By direct calculations, which are quite simple but rather lengthy, it follows from Eq. (7) that

$$m\gamma_{(1)(4)(4)} = S_{(1)}R_{(1)(4)(2)(3)}, \quad (17)$$

$$m\gamma_{(2)(4)(4)} = S_{(1)}(R_{(2)(4)(2)(3)} - \dot{\gamma}_{(3)(4)(4)} - \gamma_{(2)(4)(4)}\gamma_{(2)(3)(4)}), \quad (18)$$

$$m\gamma_{(3)(4)(4)} = S_{(1)}(R_{(3)(4)(2)(3)} + \dot{\gamma}_{(2)(4)(4)} - \gamma_{(3)(4)(4)}\gamma_{(2)(3)(4)}). \quad (19)$$

Here, as for the spin part of the MP equations, the first local spatial vector is determined by the spin orientation.

It is known that the value $\gamma_{(4)(4)}^{(i)}$ is the dynamical characteristic of the reference frame, namely, its acceleration.

In the linear spin approximation instead of Eqs. (17)–(19) we have the more simple equations

$$m\gamma_{(i)(4)(4)} = -S_{(1)}R_{(1)(4)(2)(3)}. \quad (20)$$

That is, according to (20) the force of the spin-gravity interaction, as estimated by the comoving observer in the linear spin approximation, is fully determined by the local components of the Riemann tensor. We shall analyze expression (20) in some concrete cases of spinning particle motions in the gravitational field.

3 Highly Relativistic Solutions of MP Equations in Schwarzschild's Background

We begin this section from consideration of a physical situation which is not connected directly with the MP equations and, in a certain sense, is similar to the known one in electrodynamics, when the electromagnetic field of a moving electric charge is under consideration. Now we are interested in the gravitational field of a moving mass. More exactly, let us analyze the expressions for Riemann's tensor components as evaluated by an observer which is moving with any velocity relative to Schwarzschild's mass.

3.1 Gravitational Field of a Moving Schwarzschild's Mass

As usual, to describe a moving observer we can use the corresponding set of orthogonal tetrads $\lambda_{(\nu)}^\mu$. Following many papers where the deeper analogies between gravitation and electromagnetism are under investigations we consider the gravitoelectric $E_{(k)}^{(i)}$ and gravitomagnetic $B_{(k)}^{(i)}$ components of the gravitational field. For example, in [39] these components are determined as

$$E_{(k)}^{(i)} = R^{(i)(4)}_{(k)(4)}, \quad (21)$$

$$B_{(k)}^{(i)} = -\frac{1}{2} R^{(i)(4)}_{(m)(n)} \varepsilon^{(m)(n)}_{(k)}. \quad (22)$$

Here our consideration is restricted by the gravitomagnetic components only for the observer which is moving relative to Schwarzschild's mass. The space local vectors can be oriented as: (1) The first vector is orthogonal to the plane that is determined by the instantaneous direction of the observer motion relative to the Schwarzschild mass and the radial direction; (2) The second vector is directed along the direction of the motion of the observer. Then using the standard Schwarzschild coordinates we obtain the nonzero components of the gravitomagnetic field

$$B_{(2)}^{(1)} = B_{(1)}^{(2)} = \frac{3Mu_{\parallel}u_{\perp}}{r^3\sqrt{u_4u^4-1}} \left(1 - \frac{2M}{r}\right)^{-1/2}, \quad (23)$$

$$B_{(3)}^{(1)} = B_{(1)}^{(3)} = \frac{3Mu_{\perp}^2u^4}{r^3\sqrt{u_4u^4-1}} \left(1 - \frac{2M}{r}\right)^{1/2}, \quad (24)$$

where $u_{\parallel} \equiv dr/ds$ and $u_{\perp} \equiv r d\varphi/ds$ are the radial and tangential components of the observer's 4-velocity, and M is Schwarzschild's mass.

Let us analyze expressions (23) and (24) at different velocities of the observer relative to Schwarzschild's mass. Note that the gravitomagnetic components are nonzero only at $u_{\perp} \neq 0$. That is, here the situation is similar to the known one in the electrodynamic for the components of the magnetic field of a moving electric charge. Then it is easy to see that the components (23) and (24) significantly depend on the velocity of an observer relative to the Schwarzschild mass. Indeed, at $|u_{\perp}| \ll 1$, $|u_{\parallel}| \ll 1$, the common term $3M/r^3$ in expressions (23) and (24) is multiplied on the corresponding small values. Whereas in the highly relativistic case, for $|u_{\perp}| \gg 1$, this term is multiplied by the large (as compare to 1) values and then we have

$$B_{(2)}^{(1)} = B_{(1)}^{(2)} \sim \frac{3M}{r^3} \gamma, \quad B_{(3)}^{(1)} = B_{(1)}^{(3)} \sim \frac{3M}{r^3} \gamma^2, \quad (25)$$

where γ is the relativistic Lorentz factor as calculated by the particle velocity relative to the Schwarzschild mass.

3.2 *Highly Relativistic Spin-Orbit Acceleration as Measured by a Comoving Observer*

What physical effects are caused by the gravitomagnetic components (23)–(25)? To answer this question, let us consider Eq. (20) which can be written as

$$a_{(i)} = -\frac{S_{(1)}}{m} R_{(i)(4)(2)(3)}, \quad (26)$$

where $a_{(i)}$ are the local components of the particle 3-acceleration relative to geodesic free fall as measured by the comoving observer; $S_{(1)}$ is the single nonzero component of the particle spin, i.e., here the first local space vector is oriented along the spin.

In the concrete case of particle motion in Schwarzschild's background, when the particle's spin is orthogonal to the plane determined by the direction of particle motion and the radial direction, by (22) and (26) we have

$$a_{(i)} = -\frac{S_{(1)}}{m} B_{(i)}^{(1)}, \quad (27)$$

where the nonzero values of $B_{(i)}^{(1)}$ come from (23) and (24). According to (25), the acceleration components (27) depend, in the case of highly relativistic nonradial motions, on γ such that $a_{(2)} \sim \gamma$, $a_{(3)} \sim \gamma^2$. The component $a_{(1)}$ remain equal to zero at any velocity. The absolute value of the 3-acceleration is proportional to γ^2 .

So, according to the MP equations, from the point of view of the observer comoving with a spinning particle in Schwarzschild's background, the spin-gravity interaction is much greater at the highly relativistic particle's velocity than at the low velocity. This interaction has the clear feature of the spin-orbit interaction. However, it is interesting to estimate the effects of this interaction for another observer, e.g., which is at rest relative to the Schwarzschild mass.

3.3 *Exact MP Equations in Schwarzschild's Background After Using Constants of Motion*

Due to the symmetry of Schwarzschild's and Kerr's metric here the MP equations have the constants of motion: the particle's energy E and the projection of its angular momentum J_z [5, 40–42]. It is known that in the case of the geodesic equations the analogous constants of motion were effectively used for analyzing possible orbits of a spinless particle in these metrics [43]. Namely, by the constants of energy and angular momentum the standard form of the geodesic equations, which are the differential equations of the second order by the coordinates, can be reduced to the differential equations of the first order. Naturally, it is interesting to apply the similar procedure to the exact MP equations. However, in contrast to the geodesic equations, the exact

MP equations at the Mathisson-Pirani condition contain the third derivatives of the coordinates.

The corresponding explicit form of the MP equations in Kerr's background is presented in [21]. Here we write these equations for Schwarzschild's background. As in [21], we use the set of the 11 dimensionless quantities y_i where by definition

$$\begin{aligned} y_1 &= \frac{r}{M}, \quad y_2 = \theta, \quad y_3 = \varphi, \quad y_4 = \frac{t}{M}, \\ y_5 &= u^1, \quad y_6 = Mu^2, \quad y_7 = Mu^3, \quad y_8 = u^4, \\ y_9 &= \frac{S_1}{mM}, \quad y_{10} = \frac{S_2}{mM^2}, \quad y_{11} = \frac{S_3}{mM^2}. \end{aligned} \quad (28)$$

In addition, we introduce the dimensionless quantities connected with the particle's proper time s and the constants of motion E, J_z :

$$x = \frac{s}{M}, \quad \hat{E} = \frac{E}{m}, \quad \hat{J} = \frac{J_z}{mM}. \quad (29)$$

Some quantities from (28) satisfy the four simple equations

$$\dot{y}_1 = y_5, \quad \dot{y}_2 = y_6, \quad \dot{y}_3 = y_7, \quad \dot{y}_4 = y_8, \quad (30)$$

here and in the following a dot denotes the usual derivative with respect to x . Other seven equations for the 11 functions y_i can be written as

$$\dot{y}_5 = A_1, \quad \dot{y}_6 = A_2, \quad \dot{y}_7 = A_3, \quad \dot{y}_8 = A_4, \quad (31)$$

$$\dot{y}_9 = A_5, \quad \dot{y}_{10} = A_6, \quad \dot{y}_{11} = A_7, \quad (32)$$

where

$$A_1 = A + \left(y_1 y_6^2 + y_1 y_7^2 \sin^2 y_2 - \frac{y_8^2}{y_1^2} \right) q + \frac{y_5^2}{y_1^2 q},$$

$$A_2 = B - \frac{2}{y_1} y_5 y_6 + y_7^2 \sin y_2 \cos y_2,$$

$$\begin{aligned} A_3 &= \left(-q^{-1} y_5 y_{10} + y_1^2 y_6 y_9 \right)^{-1} \times \left[q^{-1} (-y_7 y_{10} \sin^2 y_2 \right. \\ &\quad \left. + y_6 y_{11}) A + \left(-q^{-1} y_5 y_{11} + y_1^2 y_7 y_9 \sin^2 y_2 \right) B \right] \end{aligned}$$

$$\begin{aligned}
& -y_8 \sin y_2 + \frac{\hat{E}}{\varepsilon_0 q} \sin y_2 + \frac{1}{y_1^2 q} (y_7 y_{10} \sin^2 y_2 \\
& y_6 y_{11}) \Big] \sin^{-2} y_2 - \frac{2}{y_1} y_5 y_7 - 2 y_6 y_7 \cot y_2, \\
& A_4 = y_8 \left(-q^{-1} y_5 y_{10} + y_1^2 y_6 y_9 \right)^{-1} \\
& \times \left[-q^{-1} y_{10} A + y_1^2 y_9 B - y_1^2 \frac{y_7}{y_8 q} \sin y_2 \right. \\
& \left. + \frac{\hat{J}_z}{\varepsilon_0 \sin y_2} + \frac{y_{10}}{y_1} - y_9 \cot y_2 \right] - \frac{2}{y_1^2} y_5 y_8 q^{-1}, \\
& A = \varepsilon_0^{-2} q^{-1} \left(q^{-1} y_5 y_{10} - y_1^2 y_6 y_9 \right)^{-1} \\
& \times \left[[y_7 y_8 q (-y_5 y_{10} y_1^{-2} + q y_9 (y_6 y_{10} + y_7 y_{11})) \right. \\
& \left. + \frac{y_8 y_{11} q}{y_1^2 \sin^2 y_2} (q y_9 + y_5 (y_5 y_9 + y_6 y_{10})) \right] \\
& \times \left[y_1^2 \frac{\hat{E}}{q \varepsilon_0 y_8} \sin y_2 + \frac{1}{q y_8^2} (y_7 y_{10} \sin^2 y_2 - y_6 y_{11}) \right] \\
& + \frac{q y_8}{y_1^2} \left[y_5 y_{10}^2 + \frac{y_5 y_{11}^2}{\sin^2 y_2} - q y_1^2 y_9 (y_6 y_{10} + y_7 y_{11}) \right] \\
& \times \left(\frac{\hat{J}_z}{\varepsilon_0 \sin y_2} + \frac{q y_8 y_{10}}{y_1} - y_9 \cot y_2 \right) \Big] \\
& + \frac{q y_8}{\varepsilon_0^2 \sin y_2} [y_9 + q^{-1} y_5 (y_5 y_9 + y_6 y_{10} + y_7 y_{11})] \\
& \times \left[\frac{6 y_9}{y_1^3} q (-y_7 y_{10} \sin^2 y_2 + y_6 y_{11}) \right. \\
& \left. - y_{11} (q^{-1} y_5 y_{10} - y_1^2 y_6 y_9)^{-1} \right], \\
& B = y_1^{-2} \left[y_9 + q^{-1} y_5 (y_5 y_9 + y_6 y_{10} + y_7 y_{11}) \right]^{-1}
\end{aligned}$$

$$\begin{aligned}
& \times \left[q^{-1} (y_{10} + y_1^2 y_6 (y_5 y_9 + y_6 y_{10} + y_7 y_{11})) A \right. \\
& + \frac{\hat{E}}{q \varepsilon_0} y_1^2 y_7 \sin y_2 + q^{-1} y_7 (y_7 y_{10} \sin^2 y_2 - y_6 y_{11}) \\
& \left. - y_8 \left(\frac{\hat{J}_z}{\varepsilon_0 \sin y_2} + q y_8 y_{10} y_1^{-1} - q y_8 y_9 \cot y_2 \right) \right], \\
A_5 &= q y_8 \frac{y_6 y_{10} + y_7 y_{11}}{y_1} - q y_8 (y_5 y_9 + y_6 y_{10} + y_7 y_{11}) \\
& \times \left[\left(A_1 - \frac{y_5 A_4}{y_8} - \frac{y_5^2}{q y_1^2} \right) q^{-1} - y_1 y_6^2 - y_1 y_7^2 \sin^2 y_2 + \frac{y_8^2}{y_1^2} \right], \\
A_6 &= -q y_6 y_8 y_9 (y_1 - 3) + \frac{q y_5 y_8 y_{10}}{y_1} \\
& + q y_7 y_8 y_{11} \cot y_2 - q y_8 (y_5 y_9 + y_6 y_{10} + y_7 y_{11}) \\
& \times \left[y_1^2 A_2 - \frac{y_1^2 y_6}{y_8} A_4 + 2 y_5 y_6 (y_1 - q^{-1}) - y_1^2 y_7^2 \cos y_2 \sin y_2 \right], \\
A_7 &= \frac{q y_5 y_8 y_{11}}{y_1} - q y_7 y_8 y_9 (y_1 - 3) \sin^2 y_2 \\
& + q y_6 y_8 y_{11} \cot y_2 - q y_7 y_8 y_{10} \cos y_2 \sin y_2 \\
& - q y_8 (y_5 y_9 + y_6 y_{10} + y_7 y_{11}) \times \left[y_1^2 A_3 \sin^2 y_2 - \frac{y_1^2 y_7}{y_8} A_4 \sin^2 y_2 \right. \\
& \left. + 2 y_5 y_7 (y_1 - q^{-1}) \sin^2 y_2 + 2 y_1^2 y_6 y_7 \cos y_2 \sin y_2 \right]. \tag{33}
\end{aligned}$$

In all expressions (33) we note

$$q = 1 - \frac{2}{y_1}$$

and

$$\varepsilon_0 \equiv \frac{|S_0|}{mM}. \tag{34}$$

We stress that while dealing with the MP equations in Schwarzschild's or Kerr's background the condition for a spinning test particle

$$\frac{|S_0|}{mr} \equiv \varepsilon \ll 1 \quad (35)$$

must be taken into account [10].

3.4 Highly Relativistic Circular Equatorial Orbits of a Spinning Particle

Equations (31) and (32) can be used for description of all possible types of the spinning particle motions in Schwarzschild's background according to the MP equations under the Mathisson-Pirani condition. We begin from considering the important partial solutions which describe the circular orbits of a spinning particle in the equatorial plane $\theta = \pi/2$ of Schwarzschild's metric when the spin is orthogonal to this plane. Then all the MP equations are reduced to the single algebraic equation, where among the values y_i only y_1 , y_7 , and y_8 are present [22]:

$$\begin{aligned} & y_7^3(y_1 - 3)^2 y_8 y_1^2 \varepsilon_0 - y_7^2(y_1 - 3) y_1^3 \\ & + y_7(2y_1 - 3) \varepsilon_0 y_8 + y_1 = 0 \end{aligned} \quad (36)$$

(without any loss in generality, this equation is written for the orientation of the particle's spin when $S_2 \equiv S_\theta > 0$). Per relationship $u_\mu u^\mu = 1$ the value y_8 can be expressed through y_7 :

$$y_8 = \left(1 - \frac{2}{y_1}\right)^{-1/2} \sqrt{1 + y_1^2 y_7^2}. \quad (37)$$

In the limiting transition to the spinless particle ($\varepsilon_0 = 0$) we have from (36) the result known from the geodesic equations.

Equations (36) with (37) determine the region of existence of the circular orbits and the dependence of the particle's angular velocity, which in notation (28) correspond to y_7 , on the radial coordinate. Naturally, it is interesting to compare the situations with the spinless and spinning particle. The known result is that by the geodesic equations these orbits are allowed only for $r > 3M$ and the highly relativistic circular orbits exist only for $r = 3M(1 + \delta)$, where $0 < \delta \ll 1$. In this context we point out that Eq. (36) admits the highly relativistic circular orbit of a spinning particle with $r = 3M$, i.e., $y_1 = 3$. Indeed, it is easy to calculate the single real root y_7 of Eq. (36) in the simple analytical form

$$y_7 = -\frac{3^{-3/4}}{\sqrt{\varepsilon_0}} (1 + O(\varepsilon_0)) \quad (38)$$

(here we take into account that by (35) it is necessary $\varepsilon_0 \ll 1$). Then the absolute value of the particle orbital 4-velocity, which corresponds to (38), in the main spin approximation is equal to $3^{1/4}/\sqrt{\varepsilon_0}$. The same value has the relativistic Lorentz γ -factor of the spinning particle as calculated by an observer which is at rest relative to Schwarzschild's mass. Hence $\gamma^2 \gg 1$, i.e., for the motion on the circular orbit with $r = 3M$ the velocity of a spinning particle must be ultrarelativistic, the more ultrarelativistic the smaller is the ratio of spin to mass of the particle.

It is known that by the geodesic equations a spinless particle with nonzero mass of any velocity close to the velocity of light, starting in the tangential direction from the position $r = 3M$, will fall on the horizon surface within a finite proper time. On the other hand, a spinning particle can remain indefinitely on the circular orbit with $r = 3M$ due to the highly relativistic spin-gravity coupling if condition (38) is satisfied. It means that in this concrete situation the spin-gravity coupling acts as a strong repulsive force which compensates the usual (geodesic) attraction. By the way, from the point of view of an observer comoving with the spinning particle the value of this force is the same order as the formally calculated value of the Newtonian gravitational force for the masses M and m at distance $r = 3M$ [16].

Certainly, the picture described for the spinning particle on the circular orbit with $r = 3M$ holds in the ideal case only, when perturbations are neglected. Some cases with perturbations (noncircular motions) we shall consider below.

We stress the important feature of the partial circular solution of the MP equations with (38): this solution is common for the exact MP equations and their linear spin approximation and, as a result, both for the Mathisson-Pirani and Tulczyjew-Dixon condition [14, 17].

Let us consider other circular orbits of a spinning particle in Schwarzschild's background which are described by Eq. (38). The detailed analysis is presented in [22] and here we show some graphs which illustrate the domain of existence of the highly relativistic circular orbits and the dependence of the γ -factor, which is necessary for realizing these orbits, on the radial coordinate. Figure 1 describes the

Fig. 1 Lorentz factor versus r for the highly relativistic circular orbits with $d\varphi/ds < 0$ of the spinning particle beyond the small neighborhood of $r = 3M$ according to the exact MP equations

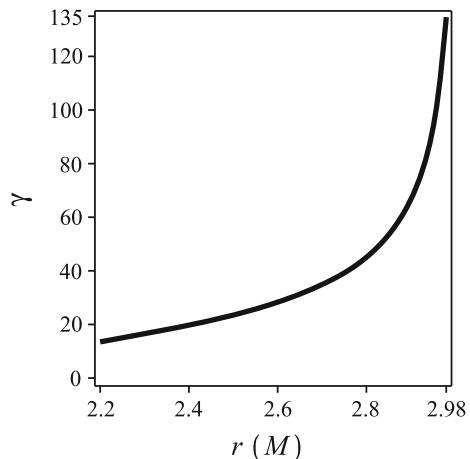
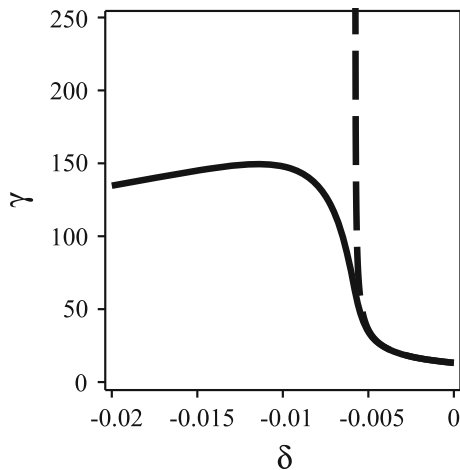


Fig. 2 Lorentz factor versus δ for the highly relativistic circular orbits with $d\varphi/ds < 0$ of the spinning particle in the small neighborhood of $r = 3M$ according to the exact MP equations (*solid line*) and their linear spin approximation (*dashed line*)



orbits with the negative values of the particle orbital velocity ($\gamma_7 < 0$) at $S_\theta > 0$, i.e., the signs of these values are the same as in the case of the highly relativistic circular orbit with $y_1 = 3$ and γ_7 from (38). (In these figures below we put $\varepsilon_0 = 10^{-2}$). The orbits corresponding to Fig. 1 exist in the space region $2M < r < 3M$ and, similarly to the circular orbit with $y_1 = 3$, these orbits are caused by the significant repulsive action of the highly relativistic spin-gravity coupling. However, in contrast to the orbit with $y_1 = 3$, which is fully determined by the linear spin terms, for the orbits in Fig. 1 the nonlinear terms are important. In this context Fig. 2 shows the difference in the description of the highly relativistic circular orbits of a spinning particle in the small neighborhood of $y_1 = 3$, that is when $y_1 = 3 + \delta$, $\delta < 0$, $|\delta| \ll 1$, by the exact MP equations and their linear spin approximation.

According to the solutions of Eq. (36) for different y_1 , the highly relativistic orbits of a spinning particle in Schwarzschild's background exist for $r > 3M$ as well. However, in contrast to the orbits from $2M < r < 3M$, they are caused by the significant attractive action of the spin-gravity coupling, and for realizing these orbits the sign of the particle orbital velocity must be positive ($d\varphi/ds > 0$) for $S_\theta > 0$. Figure 3 describes the small space domain, where $y_1 = 3 + \delta$, $0 < \delta \ll 1$, and Fig. 4 corresponds to the region for the large values of y_1 . There is an essential difference between the upper and lower part of the solid curve in Fig. 3. Namely, the last curve is close to the dashed line for $\delta > 0.00631$ and both these curves tend to the geodesic line if δ is growing, whereas the upper part of the solid curve in Fig. 3 significantly differs from the geodesic line. The dependence of the γ on r/M for this case on the interval from 3.02 is presented in Fig. 4, and for $r \gg 3M$ the value γ is proportional to \sqrt{r} . It means that for the motion on a circular orbit with $r \gg 3M$ the particle must possess much higher orbital velocity than in the case of the motion on a circular orbit near $r = 3M$.

For deeper understanding of physics of the highly relativistic circular orbits of a spinning particle in Schwarzschild's background, let us estimate the values of the

Fig. 3 Dependence of the Lorentz factor on $\delta > 0$ for the highly relativistic circular orbits with $d\varphi/ds > 0$ of the spinning particle in the small neighborhood of $r = 3M$ according to the exact MP equations and their linear spin approximation (*solid line*) and their linear spin approximation (*dashed line*). The *dotted line* corresponds to the geodesic circular orbits

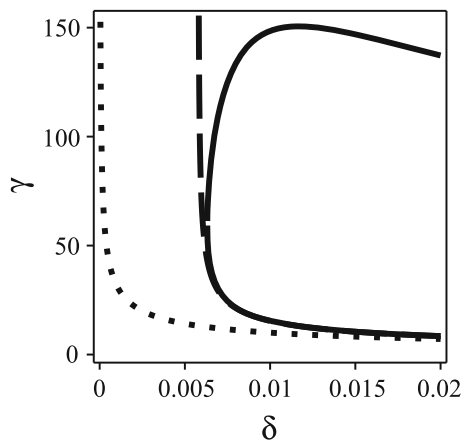
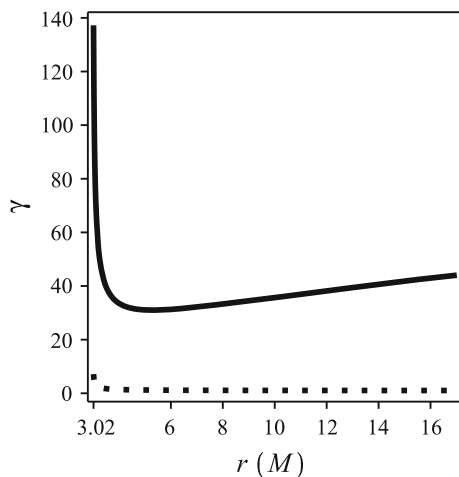


Fig. 4 Dependence of the Lorentz factor on r for the highly relativistic circular orbits with $d\varphi/ds > 0$ of the spinning particle beyond the small neighborhood of $r = 3M$ by the exact MP equations (*solid line*). The *dotted line* corresponds to the geodesic circular orbits



particle's energy E on these orbits. It is not difficult to calculate the values for E in the case of the circular orbits in the Schwarzschild background as [22]

$$E = m \left[\left(1 - \frac{2}{y_1} \right) y_8 - \varepsilon_0 y_1 (y_1 - 3) y_7^3 \right]. \quad (39)$$

It is easy to check that by (39) the energy of the spinning particle on the above considered highly relativistic circular orbits is positive and much less than the energy of the spinless particle on the corresponding geodesic circular orbits. For example, the energy of the spinless particle on the circular orbits with $r > 3M$ tends to ∞ if $r \rightarrow 3M$, whereas according to (36) the energy of the spinning particle is finite for its circular orbits with any r , including $r = 3M$. In the case of the highly relativistic circular orbits of the spinning particle beyond the small neighborhood of $3M$ it follows from (39) that

$$E = m \frac{\sqrt{\varepsilon_0}}{\sqrt{y_1}} \left(1 - \frac{2}{y_1}\right)^{1/4} \left|1 - \frac{3}{y_1}\right|^{-3/2} \left(1 - \frac{3}{y_1} + \frac{3}{y_1^2}\right). \quad (40)$$

Hence, by (40) we have $E^2 \ll m^2$ (note that the right-hand side of Eq. (40) is positive for all values y_1 beyond the horizon surface). That is, in this sense one can draw a conclusion concerning the strong binding energy for those orbits which is caused by the interaction of spin with the gravitational field.

3.5 Circular Nonequatorial Orbits

It is not difficult to verify that the MP equations in the standard coordinates of the Schwarzschild metric have the partial solution with

$$r = \text{const} \neq 0, \quad \theta = \text{const} \neq 0, \pi/2, \pi, \quad (41)$$

$$u^3 = \frac{d\varphi}{ds} = \text{const} \neq 0, \quad u^4 = \frac{dt}{ds} = \text{const} \neq 0, \quad (42)$$

$$S_r = \text{const} \neq 0, \quad S_\theta = \text{const} \neq 0, \quad S_\varphi = 0, \quad (43)$$

$$S_r \left(1 - \frac{3M}{r}\right) + S_\theta \frac{\cos \theta}{r \sin \theta} = 0. \quad (44)$$

Expressions (41)–(44) describe the nonequatorial circular orbits of a spinning particle with the constant orbital velocity when the spin lays in the meridional plane when the particle orbits the Schwarzschild mass. The necessary particle's velocity for motions on these orbits is determined by

$$u^3 = -\frac{K^{1/4} \left(1 - \frac{2M}{r}\right)^{-1/4}}{r \sqrt{6\varepsilon} |\sin \theta| \text{sign}(S_\theta \sin \theta)} [1 + O(\varepsilon)], \quad (45)$$

where we note

$$K = 1 + \left(1 - \frac{2M}{r}\right) \left(1 - \frac{3M}{r}\right)^{-2} \frac{\cos^2 \theta}{\sin^2 \theta} > 0, \quad (46)$$

and ε is the small value as determined by (35). The dependence of the angle θ on r is

$$\begin{aligned} \sin^2 \theta = & \left(1 - \frac{2M}{r}\right) \left[\frac{M}{r} \left(4 - \frac{9M}{r}\right) - 6 \left(1 - \frac{2M}{r}\right) \left(1 - \frac{3M}{r}\right) \right]^{-1} \\ & \times (1 + O(\varepsilon)). \end{aligned} \quad (47)$$

For the nonequatorial circular orbits it is necessary $0 < \sin^2 \theta < 1$. It follows from (47) that this condition is satisfied if and only if

$$\frac{15}{7}M(1 + O(\varepsilon)) < r < 3M(1 + O(\varepsilon)). \quad (48)$$

Therefore, relationships (45)–(48) give the necessary and sufficient conditions for the motion of a spinning test particle on the nonequatorial circular orbits in the Schwarzschild background. According to (48), the space region of existence of these orbits by the radial coordinate is determined (without small correction of the order ε) as

$$\frac{15}{7}M < r < 3M. \quad (49)$$

It follows from (47) that the minimum value of $\sin^2 \theta$ is achieved at

$$r = \frac{5\sqrt{5}}{3\sqrt{5} - 1} \approx 2.35M,$$

and

$$\sin^2 \theta|_{min} \approx 0.465, \quad \theta_{min} \approx 43^\circ.$$

whereas at $r = 2.35M$ and $r = 2.5M$ we have from (47) the common values $\sin^2 \theta = 0.5$ and $\theta = 45^\circ$.

We stress that for the realization of the considered nonequatorial circular orbits a spinning particle must possess the highly relativistic velocity, in the sense that $\gamma^2 \approx 1/\varepsilon \gg 1$.

Concerning the correlation between the direction of the particle orbital motion and its spin orientation we conclude from (45) that, for example, when $\sin \theta > 0$ ($0 < \theta < \pi/2$) the signs of S_θ and $u^3 = d\varphi/ds$ are opposite.

The considered circular orbits one can call *hovering*, because a spinning particle hovers above the Schwarzschild mass under the angle $\alpha_{hover} = \pi/2 - \theta$. According to (44) if r is in the small neighborhood of the value $3M$, the relationship $|S_r| \gg |S_\theta|$ takes place, i.e., in this case the particle's spin practically lays in the equatorial plane and by (47) α_{hover} is close to 0° . Whereas if r is in the small neighborhood of the value $15M/7$, the relationship $|S_\theta| \gg |S_r|$ is valid, i.e., here the spin is practically orthogonal to the equatorial plane and α_{hover} is close to 0° . Then it follows from (45) that if $r \rightarrow 15M/7$ the expression for the particle's orbital velocity passes the corresponding expression for the highly relativistic equatorial circular orbit with $r = 15M/7$.

We stress that Eqs. (44)–(47) were obtained from the exact MP equations under the Mathisson-Pirani supplementary condition. The MP equations in the linear spin approximation have the solutions which describe the nonequatorial highly relativistic circular orbits of a spinning particle in Schwarzschild's background as well. However,

these solutions exist only in the small neighborhood of the radial coordinate $r = 3M$ under the small hovering angle.

3.6 Highly Relativistic Noncircular Orbits

While investigating the highly relativistic noncircular orbits of a spinning particle in the Schwarzschild background it is necessary to integrate the set of the differential Equations (31)–(33). Note that this system contains the two parameters \hat{E} and \hat{J} proportional to the constants of the particle's motion: the energy and angular momentum. By choosing different values of these parameters for the fixed initial values of y_i one can describe the motions of different centers of mass. To describe the proper center of mass of a spinning particle in the Schwarzschild background, the method of separation of the corresponding solutions of the exact MP equations was proposed and realized in explicit relationships for the cases when the initial radial component of the particle velocity is much less than the tangential one [18]. The corresponding motions are considered and discussed in detailed in [18, 22]. Here we present three typical figures which illustrate some important features of the highly relativistic noncircular nonequatorial motions of a spinning particle in Schwarzschild's background (more illustrations are in [20]). Figures 5 and 6 show the situations when the highly relativistic spin-gravity coupling causes the significant attractive and repulsive action correspondingly (the circles with the radius 2 in these figures correspond to the horizon line).

Figure 7 illustrates the cases of the nonequatorial motions when the particle's spin is not orthogonal to the equatorial plane $\theta = \pi/2$. More exactly, this figure describes θ -oscillations for different values of the inclination angle of the spin to the equatorial plane due to $S_r \neq 0$ with $S_\varphi = 0$. All graphs in Fig. 7 are interrupted beyond the domain of validity of the linear spin approximation. Within the time

Fig. 5 Trajectories in the polar coordinates of the spinning (solid line) and spinless particle (dotted line) with the same initial values of their 4-velocity components: the tangential and radial velocities are equal to ≈ 35 and 10^{-2} correspondingly. The initial value of the radial coordinate is equal to $10M$, $\varepsilon_0 = 10^{-2}$

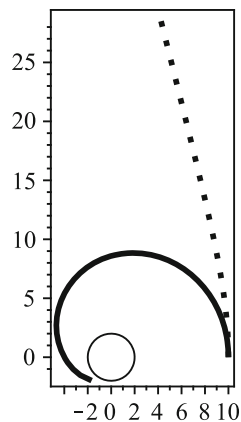
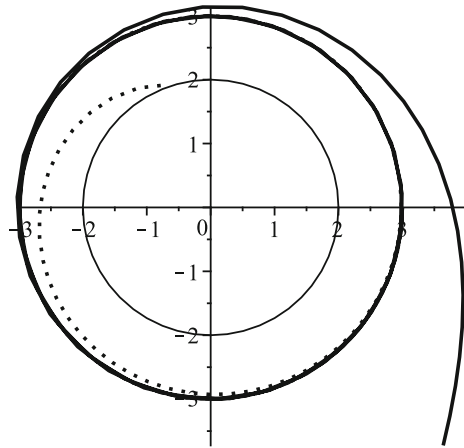


Fig. 6 Trajectories of the spinning (*solid line*) and spinless particle (*dotted line*) with the same initial value of the tangential velocity, which is equal to the spinning particle velocity on the circular orbit with $r = 3M$, and with much less radial velocity of order 10^{-7} . The initial value of the radial coordinate is equal to $3M$ and $\varepsilon_0 = 10^{-4}$



of this approximation validity, the period of the θ -oscillations coincides with the period of the particle's revolution by φ . Whereas on this interval the value of the spin component S_1 is *const*, just as the components S_2 , S_3 , and the coordinate r . This situation differs from the corresponding case of the circular motions of a spinning particle that are not highly relativistic. Indeed, then the nonzero radial spin component is not *const* but oscillates with the period of the particle's revolution by φ . Besides, in the last case the mean level of θ coincides with 90° , whereas in Fig. 7 the mean values of θ are above 90° . According to this figure the amplitude of the θ -oscillation increases with the inclination angle. However, $\theta - 90^\circ$ is small even for the inclination angle that is equal to 90° .

3.7 A Restriction on Using the Tulczyjew-Dixon Condition

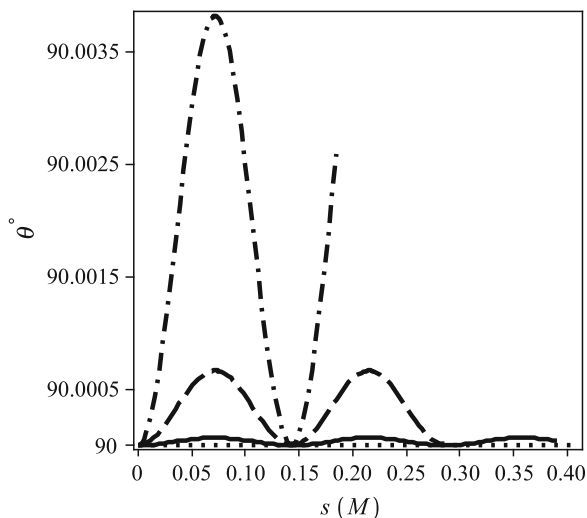
Now we consider some interesting situation which arise when the highly relativistic solutions of the MP equations under the Tulczyjew-Dixon condition are studied [21]. Let us write the main relationships following from the MP equations at Tulczyjew-Dixon condition. The mass of a spinning particle μ is defined as

$$\mu = \sqrt{P_\lambda P^\lambda} \quad (50)$$

and μ is the integral of motion. The quantity V^λ is the normalized momentum, where by definition

$$V^\lambda = \frac{P^\lambda}{\mu}. \quad (51)$$

Fig. 7 Graphs of the angle θ vs proper time for the inclination angle 0° (horizontal line $\theta = 90^\circ$), 1° (solid line), 10° (dash line), and 90° (dash and dot line) at $\varepsilon_0 = 10^{-4}$



As the normalized quantities u^λ and V^λ satisfy the relationships

$$u_\lambda u^\lambda = 1, \quad V_\lambda V^\lambda = 1. \quad (52)$$

There is the important relationship between u^λ and V^λ [40–42] :

$$u^\lambda = N \left[V^\lambda + \frac{1}{2\mu^2 \Delta} S^{\lambda\nu} V^\pi R_{\nu\pi\rho\sigma} S^{\rho\sigma} \right], \quad (53)$$

where

$$\Delta = 1 + \frac{1}{4\mu^2} R_{\lambda\pi\rho\sigma} S^{\lambda\pi} S^{\rho\sigma}. \quad (54)$$

Now our aim is to consider the explicit form of expression (53) for the concrete case of the Schwarzschild metric, for the particle motion in the plane $\theta = \pi/2$ when spin is orthogonal to this plane (we use the standard Schwarzschild coordinates). Then we have

$$u^2 = 0, \quad u^1 \neq 0, \quad u^3 \neq 0, \quad u^4 \neq 0, \quad (55)$$

$$S^{12} = 0, \quad S^{23} = 0, \quad S^{13} \neq 0. \quad (56)$$

In addition to (56) by Tulczyjew-Dixon condition we write

$$S^{14} = -\frac{P_3}{P_4} S^{13}, \quad S^{24} = 0, \quad S^{34} = \frac{P_1}{P_4} S^{13}. \quad (57)$$

Using corresponding expressions for the Riemann tensor in the Schwarzschild metric, from (53) we obtain

$$\begin{aligned} u^1 &= NV^1 \left(1 + \frac{3M}{r^3} V_3 V^3 \frac{S_0^2}{\mu^2 \Delta} \right), \quad u^2 = V^2 = 0, \\ u^3 &= NV^3 \left[1 + \frac{3M}{r^3} (V_3 V^3 - 1) \frac{S_0^2}{\mu^2 \Delta} \right], \\ u^4 &= NV^4 \left(1 + \frac{3M}{r^3} V_3 V^3 \frac{S_0^2}{\mu^2 \Delta} \right), \end{aligned} \quad (58)$$

According to (54) we write the expression for Δ as

$$\Delta = 1 + \frac{S_0^2 M}{\mu^2 r^3} (1 - 3V_3 V^3) \quad (59)$$

(the quantity M is the mass of a Schwarzschild source). Inserting (59) into (58) we get

$$\begin{aligned} u^1 &= \frac{NV^1}{\Delta} \left(1 + \frac{S_0^2 M}{m^2 r^3} \right), \\ u^3 &= \frac{NV^3}{\Delta} \left(1 - 2 \frac{S_0^2 M}{m^2 r^3} \right), \\ u^4 &= \frac{NV^4}{\Delta} \left(1 + \frac{S_0^2 M}{m^2 r^3} \right). \end{aligned} \quad (60)$$

Similarly to (35), we note

$$\varepsilon = \frac{|S_0|}{\mu r}, \quad (61)$$

where $\varepsilon \ll 1$.

The explicit expressions for N we obtain directly from the condition $u_\lambda u^\lambda = 1$ in the form

$$\begin{aligned} N &= \Delta \left[\left(1 + \varepsilon^2 \frac{M}{r} \right)^2 - 3V_3 V^3 \varepsilon^2 \frac{M}{r} \times \right. \\ &\quad \left. \times \left(2 - \varepsilon^2 \frac{M}{r} \right) \right]^{-1/2}. \end{aligned} \quad (62)$$

Inserting (62) into (60) we obtain the expression for the components V^λ through u^λ ($V^2 = u^2 = 0$):

$$\begin{aligned} V^1 &= u^1 R \left(1 - 2\varepsilon^2 \frac{M}{r} \right), \\ V^3 &= u^3 R \left(1 + \varepsilon^2 \frac{M}{r} \right), \\ V^4 &= u^4 R \left(1 - 2\varepsilon^2 \frac{M}{r} \right), \end{aligned} \quad (63)$$

where

$$R = \left[\left(1 - 2\varepsilon^2 \frac{M}{r} \right)^2 - 3(u^3)^2 \varepsilon^2 M r \left(2 - \varepsilon^2 \frac{M}{r} \right) \right]^{-1/2}. \quad (64)$$

The main feature of relationships (63) and (64) is that for the high tangential velocity of a spinning particle the values V^1 , V^3 , V^4 become imaginary. Indeed, if

$$|u^3| > \frac{1}{\varepsilon \sqrt{6Mr}}, \quad (65)$$

in (64) we have the square root of the negative value. (As writing (65) we neglect the small terms of order ε^2 ; all equations in this section before (65) are strict in ε .) Using the notation for the particle's tangential velocity $u_\perp \equiv ru^3$ by (65) we write

$$|u_\perp| > \frac{\sqrt{r}}{\varepsilon \sqrt{6M}}. \quad (66)$$

If r is not much greater than M , the velocity value of the right-hand side of Eq. (66) corresponds to the particle's highly relativistic Lorentz γ -factor of order $1/\varepsilon$.

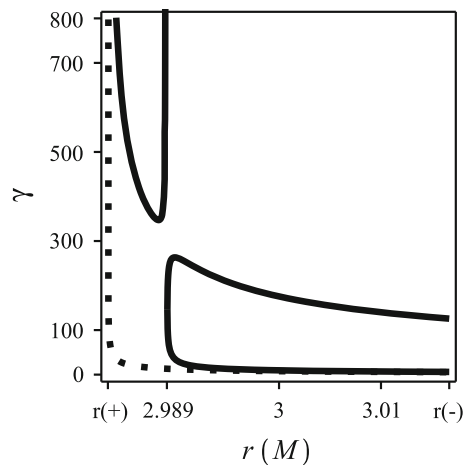
This fact that according to (51), (63)–(66) the expressions for the components of 4-momentum P^λ become imaginary (if μ in (50) is real) is an evidence that the Tulczyjew-Dixon condition cannot be used for the particle's velocity which is very close to the velocity of light. In this context it is clear the sense of a result of recent paper [44] concerning some solutions of the MP equations at the Tulczyjew-Dixon condition which allow acceleration of a spinning particle to the superluminal velocity in Schwarzschild's background. This result is connected with the situation when relationship (66) takes place, i.e., when the Tulczyjew-Dixon condition cannot be applied. Under the Mathisson-Pirani condition the corresponding result is not allowed by the MP equations.

4 Highly Relativistic Solutions of MP Equations in Kerr's Background

Some solutions of the MP equations under the Mathisson-Pirani condition in Kerr's background, which describe highly relativistic motions of a spinning particle, possess the feature common with the case of the corresponding motions in Schwarzschild's background, both for $a \ll M$ and $a \approx M$ (here a and M are the rotation parameter and the mass of the Kerr metric source; we put $a > 0$). For example, far from the horizon surface, when $r \gg r_g$, the highly relativistic equatorial circular orbits of a spinning particle in Kerr's background are allowed practically with the same dependence of the γ -factor on r as in Fig. 4 for the Schwarzschild background [23] (in [23] the Boyer-Lindquist coordinates are used). In this context we note that for growing values r the spin-orbit and spin-spin interactions decrease as $1/r^3$ and $1/r^4$ correspondingly; therefore, for $r \gg r_g$ the influence of the spin-orbit action on a particle is prevailing. Other situations arise when a particle is not far from r_g . For example, Fig. 8 illustrates a case of the circular orbits in the narrow space domain near $r_{ph}^{(+)}$ and $r_{ph}^{(-)}$ (these values are the radial coordinates of the co- and counter-rotation photon circular orbits correspondingly) at the small value of the parameter a . In contrast to Fig. 3 for $a = 0$, in Fig. 8 there is the upper graph which arises just due to $a \neq 0$, i.e., when spin-spin action is nonzero. Many other figures for different correlation of the signs a , $d\varphi/ds$, and S_θ are presented in [23].

Similarly to the case of Schwarzschild's background, the MP equations have the highly relativistic nonequatorial circular orbits in Kerr's background as well [13]. The space domain of these orbits existence increases with the increasing parameter a . If $a = M$, this domain is determined by $1.89M < r < 4M$. The maximum value of the hovering angle $\pi/2 - \theta$ is achieved at $a = M$ and is equal to $\approx 63^\circ$, in contrast to $\approx 47^\circ$ at $a = 0$.

Fig. 8 Dependence of the Lorentz factor on r for the highly relativistic equatorial circular orbits with $d\varphi/ds > 0$ of the spinning particle in Kerr's background at $a = 0.0145M$, $\varepsilon_0 = 10^{-2}$, and $S_\theta > 0$ (solid lines). The dotted line corresponds to the geodesic circular orbits. Here we use the notation $r^{(-)}$ for $r_{ph}^{(-)}$ and $r^{(+)}$ for $r_{ph}^{(+)}$



Some graphs which describe nonequatorial motions (in particular, the θ -oscillations) in Kerr's background when its spin is not orthogonal to the equatorial plane are presented in [20].

5 Numerical Estimates

Do some particles in cosmic rays possess the sufficiently high γ -factor for motions on the highly relativistic circular orbits, or on some their fragments, in the gravitational field of the Schwarzschild or Kerr black hole which are considered above? Yes, they do. By the numerical estimates for an electron in the gravitational field of a black hole with three of the Sun's mass the value $|\varepsilon_0|$ is equal 4×10^{-17} . Then the necessary value of the γ -factor for the realization of some highly relativistic circular orbits by the electron near this black hole is of order 10^8 . This γ -factor corresponds to the energy of the electron free motion of order 10^{14} eV. Analogously, for a proton in the field of such a black hole the corresponding energy is of order 10^{18} eV. For the massive black hole those values are greater: for example, if M is equal to 10^6 of the Sun's mass the corresponding value of the energy for an electron is of order 10^{17} eV and for a proton it is 10^{21} eV. Naturally, far from the black hole these values are greater because the necessary γ -factor is proportional to \sqrt{r} .

Note that for a neutrino near the black hole with three of the Sun's mass the necessary values of its γ -factor for motions on the highly relativistic circular orbits correspond to the neutrino's energy of the free motion of order 10^5 eV. If the black hole's mass is of order 10^6 of the Sun's mass, the corresponding value is of order 10^8 eV.

Can the highly relativistic spin-gravity effects be registered by the observation of the electromagnetic synchrotron radiation from some black holes? Perhaps, however, it is difficult to differ the situation when the circular orbits of a spinning charged particle and its synchrotron radiation are caused by the magnetic field or the spin-gravity coupling. The detailed analysis of the observational data is necessary.

6 On Correspondence Between the Dirac and MP Equations

Here we point out a question which arises after the comparison of the MP equations with the general relativistic Dirac equation. As we note in the Introduction, the first equations follow from the second equation in some classical approximation. However, this result has been obtained in the linear spin approximation only, when expression (3) for the Fermi transported spin practically coincides with the corresponding expression for the parallel transport. Note that the general relativistic Dirac equation was obtained for eight years before the MP equations and therefore the Fermi transport was not discussed in the context of possible description of a quantum spinning particle in the gravitational field. At the same time, if one wants to

satisfy the principle of correspondence between an equation for a quantum spinning particle and the MP equations, now it is necessary to take into account the known fact that according to the MP equations the spin of a test particle is transported by Fermi. However, in common sense, the notation “Fermi-transported spinor” cannot be introduced without violation of the Lorentz invariance. In this context it is interesting that for last years the possibility of the Lorentz invariance violation is discussed in the literature from different points of view. In any case (with violation of the Lorentz invariance or not), it is necessary to propose a more exact equations for fermions in gravitational field than the usual general relativistic Dirac equation (probably, this corrected equation must be nonlinear in the ψ -function [45]).

7 Conclusions

1. The MP equations are an important source (in the certain sense, even the unique source) of information on highly relativistic motions of spinning particles in the gravitational field.
2. Different solutions of the MP equations in Schwarzschild’s and Kerr’s background show clearly that the highly relativistic spin-gravity coupling can change significantly the trajectory of a spinning particle as compare to the corresponding geodesic trajectory of a spinless particle. In particular, the highly relativistic spin-orbit interaction reveals the strong repulsive action on a spinning particle.
3. In the highly relativistic regime of the spinning particle motions in the gravitational field the adequate supplementary condition for the MP equations is just the Mathisson-Pirani condition.
4. By the numerical estimates, some particles in cosmic rays posses a sufficiently high γ -factor for motions on the significantly nongeodesic orbits near Schwarzschild’s or Kerr’s black holes.
5. The MP equations can be useful for searching adequate corrections in the known general relativistic Dirac equation with the aim to investigate the highly relativistic spin-gravity coupling on the quantum level.

References

1. M. Mathisson, Acta Phys. Pol. **6**, 163 (1937)
2. A. Papapetrou, Proc. R. Soc. A **209**, 248 (1951)
3. E. Corinaldesi, A. Papapetrou, Proc. R. Soc. A **209**, 259 (1951)
4. A. Das, Prog. Theor. Phys. **17**, 373 (1957)
5. R. Micoulaut, Z. Phys. **206**, 313 (1967)
6. J.K. Lawrence, Acta Phys. Austr. **30**, 373 (1969)
7. A.R. Prasanna, N. Kumar, Progr. Theor. Phys. **49**, 1553 (1973)
8. C.W. Misner, K.S. Thorne, J.A. Wheeler, *Gravitation* (Freeman, San Francisco, 1973)
9. S. Rasband, Phys. Rev. Lett **30**, 111 (1973)

10. R. Wald, Phys. Rev. D **6**, 406 (1972)
11. R.M. Plyatsko, Preprint No. 158, Phys. Inst. Belor. Acad. Sci. (1978). (in Russian)
12. R.M. Plyatsko. Cand. thesis, Phys. Inst. Belor. Acad. Sci., (1979). Minsk (unpublished)
13. R.M. Plyatsko, A.L. Vynar, Sov. Phys. Dokl. **27**, 328 (1982)
14. R.M. Plyatsko, *Manifestations of gravitational ultrarelativistic spin-orbit interaction*, Naukova Dumka, Kyiv, (1988) (in Ukrainian)
15. R.M. Plyatsko, Phys. Rev. D **58**, 084031 (1998)
16. R. Plyatsko, O. Bilaniuk, Class. Quantum Gravity **18**, 5187 (2001)
17. R. Plyatsko, Class. Quantum Gravity **22**, 1545 (2005)
18. R. Plyatsko, O. Stefanyshyn, Acta Phys. Pol. B. **39**, 23 (2008)
19. R. Plyatsko, Acta Phys. Pol. B. Proc. Suppl. **1**, 173 (2008)
20. R. Plyatsko, O. Stefanyshyn, M. Fenyk, Phys. Rev. D **82**, 044015 (2010)
21. R.M. Plyatsko, O.B. Stefanyshyn, M.T. Fenyk, Class. Quantum Gravity **28**, 195025 (2011)
22. R. Plyatsko, M. Fenyk, Phys. Rev. D **85**, 104023 (2012)
23. R. Plyatsko, M. Fenyk, Phys. Rev. D **87**, 044019 (2013)
24. F.A.E. Pirani, Acta Phys. Pol. **15**, 389 (1956)
25. C. Møller, Commun. Dublin Inst. Adv. Stud., **A5**, 3 (1949)
26. B. Mashhoon, J. Math. Phys. **12**, 1075 (1971)
27. S. Wong, Int. J. Theor. Phys. **5**, 221 (1972)
28. L. Kannenberg. Ann. Phys., **103**, 64 (1977), (New York)
29. R. Catenacci, M. Martellini, Lett. Nuovo Cimento **20**, 282 (1977)
30. J. Audretsch, J. Phys. A **14**, 411 (1981)
31. A. Gorbatsievich, Acta Phys. Pol. B **17**, 111 (1986)
32. A. Barut, M. Pavsic, Class. Quantum Gravity **4**, 41 (1987)
33. F. Cianfrani, G. Montani, Europhys. Lett. **84**, 30008 (2008)
34. F. Cianfrani, G. Montani, Int. J. Mod. Phys. A **23**, 1274 (2008)
35. Yu.N. Obukhov, A. Silenko, O. Teryaev, Phys. Rev. D **80**, 064044 (2009)
36. V. Fock, D. Ivanenko, Z. Phys. **54**, 798 (1929)
37. V. Fock, Z. Phys. **57**, 261 (1929)
38. H. Weyl, Proc. Natl. Acad. Sci. USA **15**, 323 (1929)
39. K. Thorne, J. Hartle, Phys. Rev. D **31**, 1815 (1985)
40. K.P. Tod, F. de Felice, Nuovo Cimento **34**, 365 (1976)
41. R. Hojman, S. Hojman, Phys. Rev. D **15**, 2724 (1977)
42. S. Suzuki, K. Maeda, Phys. Rev. D **58**, 023005 (1998)
43. S. Chandrasekhar, *The Mathematical Theory of Black Holes* (Oxford University Press, Oxford, 1983)
44. S.A. Hojman, F.A. Asenjo, Class. Quantum Gravity **30**, 025008 (2013)
45. R. Plyatsko, arXiv: gr-qc/0601111; [arXiv: 1110.2386](https://arxiv.org/abs/1110.2386)

The MPD Equations in Analytic Perturbative Form

Dinesh Singh

Abstract A longstanding approach to the dynamics of extended objects in curved space-time is given by the Mathisson-Papapetrou-Dixon (MPD) equations of motion for the so-called “pole-dipole approximation.” This paper describes an analytic perturbation approach to the MPD equations via a power series expansion with respect to the particle’s spin magnitude, in which the particle’s kinematic and dynamical degrees of freedom are expressible in a completely general way to formally infinite order in the expansion parameter, and without any reference to pre-existent space-time symmetries in the background. An important consequence to emerge from the formalism is that the particle’s squared mass and spin magnitudes can shift based on a classical analogue of “radiative corrections” due to spin-curvature coupling, whose implications are investigated. It is explicitly shown how to solve for the linear momentum and spin angular momentum for the spinning particle, up to second order in the expansion. As well, this paper outlines two distinct approaches to address the study of many-body dynamics of spinning particles in curved space-time. The first example is the spin modification of the Raychaudhuri equation for worldline congruences, while the second example is the computation of neighbouring worldlines with respect to an arbitrarily chosen reference worldline.

1 Introduction

It is an undeniable fact that, for all practical purposes, macroscopic astrophysical objects in the Universe possess classical spin angular momentum during their formation and long-term evolution. In addition, it has been known for a long time that relativistic astrophysical objects, such as black holes and neutron stars with spin, also theoretically exist within the theory of General Relativity, with strong observational evidence to effectively confirm their presence within the Universe. Further to this, it becomes very relevant to consider, for example, the physical consequences involving the spin interaction of relativistic systems, such as the orbital dynamics of rapidly

D. Singh (✉)

Department of Physics, University of Regina, Regina, SK S4S 0A2, Canada
e-mail: dinesh.singh@uregina.ca

© Springer International Publishing Switzerland 2015

D. Puetzfeld et al. (eds.), *Equations of Motion in Relativistic Gravity*,

Fundamental Theories of Physics 179, DOI 10.1007/978-3-319-18335-0_5

spinning neutron stars around supermassive black holes expected to exist in the centres of most galaxies. Therefore, it is vital to properly understand the dynamics of extended bodies in curved space-time that incorporates classical spin.

The first attempt to introduce classical spin within the framework of General Relativity was presented by Mathisson [1], who demonstrated the existence of equations of motion involving an interaction due to the direct coupling of the Riemann curvature tensor with the moving particle's spin. Besides the so-called "pole-dipole approximation" for the case of a spinning point dipole as the leading order spin-dependent term alongside the mass monopole term, Mathisson's formalism includes a non-trivial set of higher-order multipole moment contributions that depend upon prior knowledge of the object's matter-energy tensor field. Several other contributions over the years also appear, most notably from Papapetrou [2] whose treatment of the problem was to describe the spinning object confined to within a space-time world tube that contains its centre-of-mass worldline, such that the associated matter field is given compact support. Other contributions, such as from Pirani [3], Tulczyjew [4], Madore [5], and several more have adopted competing perspectives on the treatment of higher-order multipole moments. Some years later, Dixon [6, 7] introduced what is arguably the most complete treatment of this problem by providing a fully self-consistent description of all multipole moment contributions to infinite order for the dynamics of extended bodies in curved space-time.

When considering the inspiral orbital motion of an equal-mass spinning binary neutron star system, for example, it is reasonable to demand an understanding of the higher-order multipole moment contributions when strong tidal disruptions are expected to occur to put stresses within the neutron stars' internal structure. However, for situations involving extreme mass-ratio systems, such as neutron stars or solar-mass black holes in orbit around supermassive black holes, it is justifiable to truncate the multipole moment expansion of the full equations of motion and focus exclusively on the pole-dipole approximation. Indeed, for most practical calculations involving an extreme mass ratio system, the essential physics of the dynamical motion is well-captured, provided that the spinning object's dimensions are sufficiently small compared to the background space-time's local radius of curvature in order for this justification to be well-motivated. Taking such an approach leads to what are commonly known as the Mathisson-Papapetrou-Dixon (MPD) equations of motion.

The application of the MPD equations for a variety of interesting astrophysical situations is evident within the literature. For obvious reasons, it is very natural to make use of the MPD equations to describe the dynamics of a spinning particle around spinning black holes, as described by the Kerr metric [8–12] to showcase the impact of spin-curvature interactions involving black hole spin on the spinning particle's long-term orbital motion. In so doing, the particle then becomes a sensitive probe of space-time curvature due to the MPD equations, from which it becomes possible to learn a great deal about the properties of the background source. From numerical simulations in particular, it is possible to explore the limits of stability for the MPD equations, such that deterministic chaos may result under extreme

circumstances [12–15]. Furthermore, it is possible within this framework to derive predictions of gravitational wave generation [16, 17] expected to occur from spin-induced deviations away from geodesic motion.

Besides the numerically driven treatments of the MPD equations, there also exist more formal analytic studies within the literature [18–20]. The direct precursor to the analytic perturbative approach presented in this article was first developed by Chicone, Mashhoon, and Punsly (CMP) [21], with a focus upon the study of spinning clumps of plasma in the formation of astrophysical jets columnated along a Kerr black hole’s axis of symmetry. For future reference, this approach to the MPD equations is hereafter known as the CMP approximation. This approach was then applied by Mashhoon and Singh [22] to identify analytic expressions for the leading-order perturbations for the circular orbit of a spinning particle around a Kerr black hole. Given the somewhat basic assumptions within the CMP approximation, the analysis is remarkably successful in reproducing the spinning particle’s kinematic properties when compared with the full MPD equations. This is self-evident for situations where, for spin magnitude s and mass m , with radial distance r away from the background source, the spinning particle’s Møller radius [22, 23] is confined to $s/m < 10^{-3} r$. This agreement, however, begins to break down when $s/(mr) \sim 10^{-2} - 10^{-1}$ for $r = 10 M$, where M is the Kerr black hole mass. It suggests strongly that higher-order spin-curvature coupling terms are necessary to more completely account for the orbital motions when compared with the numerical treatment of the MPD equations.

On the basis of this observation, a full generalization of the CMP approximation was introduced by Singh [24] to account for the need to have higher-order analytic contributions within the perturbation treatment. As will be shown within this paper, several attractive features emerge with the additional terms incorporated. First, the formalism in terms of a power series expansion with respect to the particle’s spin magnitude is extended to formally *infinite order*. Second, it is background independent and accommodates for *arbitrary motion* of the particle without any recourse to space-time symmetries within the metric. As such, it follows that this generalization is very robust and can be applied to a wide variety of astrophysical situations, examples of which are the modelling of globular clusters and other many-body dynamical systems in curved space-time. Explicit applications of this perturbation approach were presented by Singh to model the circular motion of a spinning test particle around a Kerr black hole [25] and that of a radially accreting or radiating Schwarzschild black hole, as described by the Vaidya metric [26]. Third, the formalism allows for the existence of a classical analogue for “radiative corrections” that shift the particle’s overall squared mass and spin magnitude with respect to some “bare mass” and “bare spin,” respectively. Such an observation under extreme conditions may well yield the ability to analytically determine the transition from stable to chaotic motion, which can be compared to existing studies [12–15] that involve numerical methods.

This paper presents the analytic perturbation treatment of the MPD equations based on the following outline. It begins in Sect. 2 with a general presentation of the MPD equations and its properties. Following that, Sect. 3 presents the perturbation approach based upon the CMP approximation. Afterwards, Sect. 4 gives a description of how to explicitly obtain the linear momentum and spin angular momentum

terms for a spinning test particle, up to second order in the perturbation expansion. Prior to the concluding remarks, Sect. 5 presents two lines of study for a many-body extension of the MPD equations that can incorporate the analytic perturbation approach. The first one concerns spin-induced modifications of the Raychaudhuri equation for a congruence of worldlines, while the second one involves the computation of neighbouring worldlines for spinning particles determined with respect to a reference spinning particle. In order to account for the anticipated spin-spin interactions to appear within this many-body extension, a novel approach is employed in the form of introducing a spin-induced torsion field satisfying the Riemann-Cartan U_4 geometry along the reference particle's worldline, details of which are explained in due course.

Throughout this paper, the metric convention is $+2$ signature with geometric units of $G = c = 1$ utilized. The Riemann tensor and its contractions are defined in accordance with Misner et al. [27].

2 The MPD Equations in General Form

2.1 Equations of Motion

Assuming the pole-dipole approximation for a spinning pointlike object, the MPD equations for its linear four-momentum $P^\mu(\tau)$ and spin tensor $S^{\alpha\beta}(\tau)$ are described by

$$\frac{DP^\mu}{d\tau} = -\frac{1}{2} R^\mu{}_{\nu\alpha\beta} u^\nu S^{\alpha\beta}, \quad (1)$$

$$\frac{DS^{\alpha\beta}}{d\tau} = P^\alpha u^\beta - P^\beta u^\alpha, \quad (2)$$

where (1) is the spin-curvature force equation due to the coupling of the Riemann curvature tensor $R_{\mu\nu\alpha\beta}$ with $S^{\alpha\beta}(\tau)$, plus the particle's four-velocity vector $u^\mu(\tau) = dx^\mu(\tau)/d\tau$ with affine parametrization τ , while (2) is the wedge product of the four-velocity with the four-momentum. An important consequence of the MPD equations is that the particle's four-momentum necessarily precesses around the centre-of-mass worldline. The affine parameter τ is formally left unspecified, but it is always possible to have it identified with proper time, such that $u^\mu u_\mu = -1$. When going beyond the pole-dipole approximation, (1) and (2) each have additional terms of the form \mathcal{F}^μ and $\mathcal{T}^{\alpha\beta}$ [18, 22], respectively. These contributions in turn require detailed knowledge of the spinning object's energy-momentum tensor $T^{\mu\nu}$ [6–8, 22], satisfying covariant conservation $\nabla_\nu T^{\mu\nu} = 0$. For the purposes of this paper, however, the expressions for (1) and (2) are sufficient.

2.2 Constraint Equations

By themselves, the MPD equations (1) and (2) are underdetermined. They require additional equations to specify the system, up to a parametrization constraint for τ . Specifically, it is necessary to determine some type of relationship involving the spin tensor that allows for the spinning particle's evolution to be understandable. Arguably, the most "reasonable" spin condition to be utilized, following Tulczyjew [4] and Dixon [6, 7] is to enforce orthogonality between the spin tensor and the linear four-momentum, such that

$$S^{\alpha\beta} P_\beta = 0. \quad (3)$$

It follows from use of both (3) and the MPD equations that the mass and spin magnitudes m and s , defined according to

$$m^2 = -P_\mu P^\mu, \quad (4)$$

$$s^2 = \frac{1}{2} S_{\mu\nu} S^{\mu\nu}, \quad (5)$$

are both *constants of the motion* [21].

In addition to this fact, use of (3) gives rise to determining the four-velocity u^μ with respect to P^μ and $S^{\alpha\beta}$ according to Tod et al. [10], such that

$$u^\mu = -\frac{P \cdot u}{m^2} \left[P^\mu + \frac{1}{2} \frac{S^{\mu\nu} R_{\nu\gamma\alpha\beta} P^\gamma S^{\alpha\beta}}{m^2 + \frac{1}{4} R_{\alpha\beta\rho\sigma} S^{\alpha\beta} S^{\rho\sigma}} \right]. \quad (6)$$

As noted above, the only remaining undetermined quantity is $P \cdot u$, which relates the particle's internal clock with respect to τ . While solving for $P \cdot u$ in terms of the normalization equation $u^\mu u_\mu = -1$ is obviously possible, it is also possible to impose a different constraint on τ , since the choice for $P \cdot u$ has no effect on the locus of the particle's worldline. For example, if it is desirable to measure time evolution in terms of a distant observer's clock, then letting $u^0 = dt/d\tau = 1$ and solving for $P \cdot u$ is a perfectly valid procedure to follow.

All these equations presented above will become useful for deriving the analytic perturbative approach to the MPD equations, based upon the CMP approximations to be presented next [24].

3 Analytic Perturbation Approach to the MPD Equations

3.1 CMP Approximation

The approximation of the MPD equations first introduced by Chicone et al. [21, 22] is based upon the assumption that $P^\mu - m u^\mu = E^\mu$ is small, where E^μ is the spin-

curvature force. Further to this, the Møller radius ρ [21–23] is chosen to be a small quantity, in terms of $\rho = s/m \ll r$, where r is the distance from the particle to the source of the gravitational background. When taken together, the CMP approximation emerges as a series expansion to first-order in s , in the form

$$\frac{DP^\mu}{d\tau} \approx -\frac{1}{2} R^\mu{}_{\nu\alpha\beta} u^\nu S^{\alpha\beta}, \quad (7)$$

$$\frac{DS^{\alpha\beta}}{d\tau} \approx 0. \quad (8)$$

According to (8), the spin tensor is parallel transported and the spin condition (3) becomes

$$S^{\alpha\beta} u_\beta \approx 0, \quad (9)$$

which agrees with the Pirani condition [3] for orthogonality between the spin tensor and the particle's four-velocity.

It is surprising to note that the CMP approximation is remarkably accurate for modelling the motion of a spinning test particle in curved space-time, with spin orientation as given in Fig. 1. This is illustrated very well when applied to circular motion around a Kerr black hole [22] and compared to the full MPD equations for $s/(mr) \sim 10^{-3}$ and $r = 10M$. However, when pushed to the more extreme situation of $s/(mr) \sim 10^{-2} - 10^{-1}$ for the same choice of r , a breakdown appears, as evidenced by Fig. 2 with the lack of any spin-induced modulation of the particle's τ -dependent radial position using the CMP approximation compared to the full MPD equations. This observation justifies the need for a generalization of the CMP approximation to be given below [24].

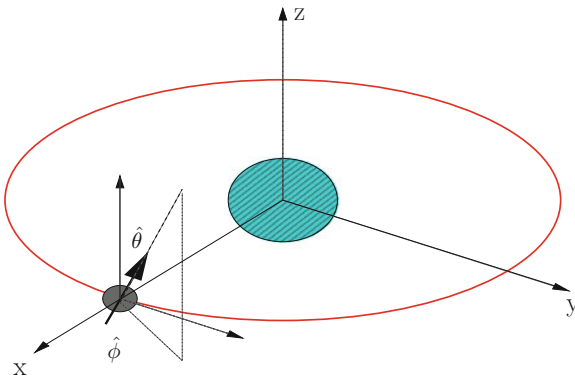


Fig. 1 Initial spin orientation $(\hat{\theta}, \hat{\phi})$ for a spinning particle in circular motion around a *black hole*. The observer is located along the *x*-axis

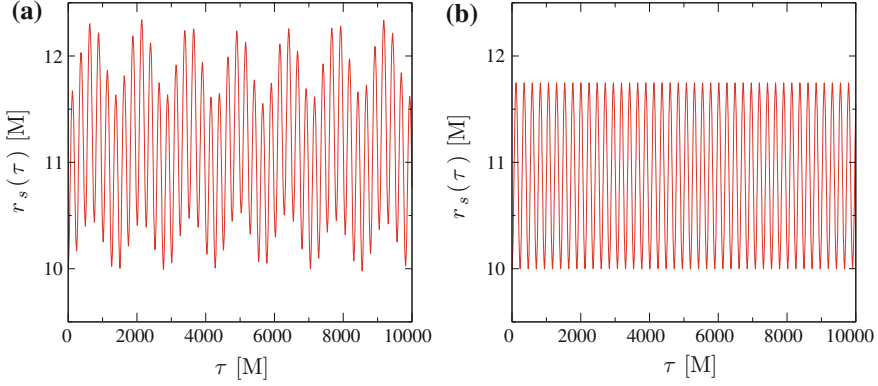


Fig. 2 The orbital radial co-ordinate $r_s(\tau)$ for $s/(mr) = 10^{-1}$, where $m = 10^{-2} M$, $r = 10 M$, $\hat{\theta} = \hat{\phi} = \pi/4$, and $a = 0.50$. **a** $s/(mr) = 10^{-1}$ (MPD). **b** $s/(mr) = 10^{-1}$ (Linear)

3.2 Generalization of the CMP Approximation

To develop the generalization of the CMP approximation [24, 25], the linear momentum and spin angular momentum are expressed in terms of a power series expansion in the form

$$P^\mu(\varepsilon) \equiv \sum_{j=0}^{\infty} \varepsilon^j P_{(j)}^\mu, \quad (10)$$

$$S^{\mu\nu}(\varepsilon) \equiv \varepsilon \sum_{j=0}^{\infty} \varepsilon^j S_{(j)}^{\mu\nu} = \sum_{j=1}^{\infty} \varepsilon^j S_{(j-1)}^{\mu\nu}. \quad (11)$$

For (10) and (11), ε is an expansion parameter that is identified with s , with $P_{(j)}^\mu$ and $S_{(j-1)}^{\mu\nu}$ as the respective j th-order contributions in ε of the linear momentum and spin angular momentum. For the zeroth-order expressions in ε , they correspond to the dynamics of a spineless particle in geodesic motion. In addition, it is also assumed that the four-velocity is described as

$$u^\mu(\varepsilon) \equiv \sum_{j=0}^{\infty} \varepsilon^j u_{(j)}^\mu. \quad (12)$$

When substituting (10), (11), and (12) into the MPD equations expressed as

$$\frac{DP^\mu(\varepsilon)}{d\tau} = -\frac{1}{2} R^\mu{}_{\nu\alpha\beta} u^\nu(\varepsilon) S^{\alpha\beta}(\varepsilon), \quad (13)$$

$$\frac{DS^{\alpha\beta}(\varepsilon)}{d\tau} = 2\varepsilon P^{[\alpha}(\varepsilon) u^{\beta]}(\varepsilon), \quad (14)$$

where for consistency an extra factor of ε is introduced in (14), the j th-order expressions of the MPD equations become

$$\frac{DP_{(j)}^\mu}{d\tau} = -\frac{1}{2} R^\mu{}_{\nu\alpha\beta} \sum_{k=0}^{j-1} u_{(j-1-k)}^\nu S_{(k)}^{\alpha\beta}, \quad (15)$$

$$\frac{DS_{(j-1)}^{\alpha\beta}}{d\tau} = 2 \sum_{k=0}^{j-1} P_{(j-1-k)}^{[\alpha} u_{(k)}^{\beta]}. \quad (16)$$

For $P_{(0)}^\mu = m_0 u_{(0)}^\mu$, where

$$m_0^2 \equiv -P_\mu^{(0)} P_{(0)}^\mu, \quad (17)$$

it follows that the zeroth-order term in ε is

$$\frac{DP_{(0)}^\mu}{d\tau} = 0, \quad (18)$$

while the respective first-order terms for the linear momentum and spin are then the CMP approximation, since

$$\frac{DP_{(1)}^\mu}{d\tau} = -\frac{1}{2} R^\mu{}_{\nu\alpha\beta} u_{(0)}^\nu S_{(0)}^{\alpha\beta}, \quad (19)$$

$$\frac{DS_{(0)}^{\alpha\beta}}{d\tau} = 0. \quad (20)$$

To complete the generalization, it is necessary to determine $u_{(j)}^\mu$ as a function of the linear and spin angular momentum expansion terms. To do this requires use of the supplementary equations (3)–(6), with important consequences to follow. From the spin condition (3), it is straightforward to show in terms of (10) and (11) that

$$P_\mu^{(0)} S_{(j)}^{\mu\nu} = - \sum_{k=1}^j P_\mu^{(k)} S_{(j-k)}^{\mu\nu}, \quad j \geq 1 \quad (21)$$

for the $(j+1)$ th-order contribution in ε , where the first-order perturbation in ε is

$$P_\mu^{(0)} S_{(0)}^{\mu\nu} = 0. \quad (22)$$

It is possible to identify a classical analogue for a *bare mass* m_0 defined by (17) and a *bare spin* s_0 , according to

$$s_0^2 \equiv \frac{1}{2} S_{\mu\nu}^{(0)} S_{(0)}^{\mu\nu}, \quad (23)$$

in analogy with the radiative corrections identified with the bare mass of quantum field theory, given that the m and s are dependent upon P^μ and $S^{\mu\nu}$, which are represented by (10) and (11), respectively. Therefore, it follows that the total mass and spin magnitudes can be identified as “radiative corrections” to m_0 and s_0 , such that

$$m^2(\varepsilon) = m_0^2 \left(1 + \sum_{j=1}^{\infty} \varepsilon^j \bar{m}_j^2 \right), \quad (24)$$

$$s^2(\varepsilon) = \varepsilon^2 s_0^2 \left(1 + \sum_{j=1}^{\infty} \varepsilon^j \bar{s}_j^2 \right), \quad (25)$$

where

$$\bar{m}_j^2 = -\frac{1}{m_0^2} \sum_{k=0}^j P_\mu^{(j-k)} P_{(k)}^\mu, \quad (26)$$

$$\bar{s}_j^2 = \frac{1}{s_0^2} \sum_{k=0}^j S_{\mu\nu}^{(j-k)} S_{(k)}^{\mu\nu}, \quad (27)$$

are dimensionless j th-order corrections to m_0^2 and s_0^2 , respectively. Since the m^2 and s^2 are already constant within the exact set of MPD equations, it follows that \bar{m}_j^2 and \bar{s}_j^2 must be individually constant for each order of ε .

With the four-velocity parametrized by ε in the form

$$u^\mu(\varepsilon) = -\frac{P \cdot u}{m^2(\varepsilon)} \left[P^\mu(\varepsilon) + \frac{1}{2} \frac{S^{\mu\nu}(\varepsilon) R_{\nu\gamma\alpha\beta} P^\gamma(\varepsilon) S^{\alpha\beta}(\varepsilon)}{m^2(\varepsilon) \Delta(\varepsilon)} \right], \quad (28)$$

$$\Delta(\varepsilon) \equiv 1 + \frac{1}{4 m^2(\varepsilon)} R_{\mu\nu\alpha\beta} S^{\mu\nu}(\varepsilon) S^{\alpha\beta}(\varepsilon), \quad (29)$$

it can be expanded out once the yet undetermined scalar product $P \cdot u$ is specified. A particularly useful choice is

$$P \cdot u \equiv -m(\varepsilon), \quad (30)$$

which leads to

$$\begin{aligned} u_\mu(\varepsilon) u^\mu(\varepsilon) &= -1 + \frac{1}{4 m^6(\varepsilon) \Delta^2(\varepsilon)} \tilde{R}_\mu(\varepsilon) \tilde{R}^\mu(\varepsilon) \\ &= -1 + O(\varepsilon^4), \end{aligned} \quad (31)$$

where

$$\tilde{R}^\mu(\varepsilon) \equiv S^{\mu\nu}(\varepsilon) R_{\nu\gamma\alpha\beta} P^\gamma(\varepsilon) S^{\alpha\beta}(\varepsilon). \quad (32)$$

Therefore, to at least third-order in ε , it is shown from (31) that τ is the *proper time* for parameterization of the particle's centre-of-mass worldline in accordance with (30). A resulting tedious but otherwise straightforward calculation shows from substituting (10), (11), and (24) into (28) that the spinning particle's four-velocity is

$$\begin{aligned} u^\mu(\varepsilon) = & \sum_{j=0}^{\infty} \varepsilon^j u_{(j)}^\mu = \frac{P_{(0)}^\mu}{m_0} + \varepsilon \left[\frac{1}{m_0} \left(P_{(1)}^\mu - \frac{1}{2} \bar{m}_1^2 P_{(0)}^\mu \right) \right] \\ & + \varepsilon^2 \left\{ \frac{1}{m_0} \left[P_{(2)}^\mu - \frac{1}{2} \bar{m}_1^2 P_{(1)}^\mu - \frac{1}{2} \left(\bar{m}_2^2 - \frac{3}{4} \bar{m}_1^4 \right) P_{(0)}^\mu \right] \right. \\ & + \left. \frac{1}{2m_0^3} S_{(0)}^{\mu\nu} R_{\nu\gamma\alpha\beta} P_{(0)}^\gamma S_{(0)}^{\alpha\beta} \right\} \\ & + \varepsilon^3 \left\{ \frac{1}{m_0} \left[P_{(3)}^\mu - \frac{1}{2} \bar{m}_1^2 P_{(2)}^\mu - \frac{1}{2} \left(\bar{m}_2^2 - \frac{3}{4} \bar{m}_1^4 \right) P_{(1)}^\mu \right. \right. \\ & - \left. \left. \frac{1}{2} \left(\bar{m}_3^2 - \frac{3}{2} \bar{m}_1^2 \bar{m}_2^2 + \frac{5}{8} \bar{m}_1^6 \right) P_{(0)}^\mu \right] \right. \\ & + \left. \frac{1}{2m_0^3} R_{\nu\gamma\alpha\beta} \left[\sum_{n=0}^1 S_{(1-n)}^{\mu\nu} \sum_{k=0}^n P_{(n-k)}^\gamma S_{(k)}^{\alpha\beta} - \frac{3}{2} \bar{m}_1^2 S_{(0)}^{\mu\nu} P_{(0)}^\gamma S_{(0)}^{\alpha\beta} \right] \right\} \\ & + O(\varepsilon^4), \end{aligned} \quad (33)$$

which satisfies (31) to third order in ε .

At this point, the worldline of the spinning particle can be explicitly determined by simple integration of (33), since it provides an iterative means to explicitly evaluate $u^\mu(\varepsilon)$ order by order in ε , based upon solving (15) and (16) in terms of quantities defined for lower orders of ε .

3.3 Perturbations of the Møller Radius and Stability Implications for Particle Motion

An important study with regard to the analytic perturbative approach to the MPD equations involves the study of transitions from stable to chaotic motion for spinning particles in curved space-time. From strictly numerical considerations [12–15], there is ample evidence to expect that there exists a critical point when, for sufficiently large s , the motion becomes chaotic. Indeed, when considering many-body particle dynamics for astrophysical systems, the importance of detecting chaotic dynamics is

very relevant. The pertinent question then concerns how to identify from presumably knowable and independent astrophysical parameters, such as the mass and spin of each constituent particle, the precise combination of factors that can trigger the transition from stable to chaotic motion.

It is understood from, for example, studying the case of a single MPD particle in circular orbit around a Kerr black hole [22] that the relevant parameter for determining the relative strength of the spin-curvature interaction to deviate from strictly geodesic motion is the Møller radius $\rho = s/m$. When $\rho \ll r$ for the particle orbit's radius of curvature, the capacity for entering an unstable region of phase space is minimized. For the choice of astrophysically realistic spins for MPD particles under numerical simulations [14, 15], it is shown that the particle motion never approaches instability.

Until now within this formalism, it is unclear how to extract useful analytic information about stability properties of MPD particle motion. Given the fact that the mass and spin parameters can shift in magnitude according to (24) and (25), this will have an impact upon the strength of the Møller radius, which in turn impacts upon the capacity for the spin-curvature interaction to induce unstable motion under potentially realistic physical situations. Therefore, determining the perturbations in ρ in analytic form may provide useful insight in determining the precise conditions to generate the transition from stable to chaotic motion for a single MPD particle.

It is straightforward to show from using (24) and (25) that

$$\begin{aligned} \rho(\varepsilon) &= \frac{s(\varepsilon)}{m(\varepsilon)} \\ &= \frac{s_0}{m_0} \left\{ \varepsilon + \varepsilon^2 \left[\frac{1}{2} (\bar{s}_1^2 - \bar{m}_1^2) \right] \right. \\ &\quad \left. + \varepsilon^3 \left[\frac{1}{2} (\bar{s}_2^2 - \bar{m}_2^2) - \frac{1}{4} \bar{s}_1^2 \bar{m}_1^2 - \frac{1}{8} (\bar{s}_1^4 - 3 \bar{m}_1^4) \right] + O(\varepsilon^4) \right\}, \quad (34) \end{aligned}$$

where the “radiative corrections” due to the second- and third-order contributions in ε cause a shift away from the zeroth-order Møller radius $\rho_0 = s_0/m_0$ defined by the “bare mass” m_0 and “bare spin” s_0 . What is important to note—perhaps not surprisingly—is that the corrections \bar{m}_j^2 and \bar{s}_j^2 counteract each other's effects, at least on a formal level. The precise nature of the shift from ρ_0 to ρ requires determining (34) in reference to a specific background and appropriately defined initial conditions. However, it is clearly evident that variations in the Møller radius are precisely identifiable, which can then be correlated with the computation of Lyapunov exponents and Poincaré maps, for example, while performing stability analysis studies using standard techniques available.

4 Evaluation of the Linear Momentum and Spin Angular Momentum Terms

4.1 Local Fermi Co-ordinate Frame

With the formalism behind the analytic perturbative approach to the MPD equations now established, it is possible to explicitly evaluate the linear momentum and spin angular momentum expansion terms [25] in (10) and (11). As noted earlier, this is accomplished in an iterative fashion by solving the first-order perturbation terms with respect to zeroth-order quantities, followed by solving the second-order and higher terms with respect to lower-order quantities. It becomes a very straightforward process to achieve this by framing the problem in terms of the tetrad formalism and Fermi normal co-ordinates [22], with the obvious benefit of expressing all contributions with respect to a freely falling worldline in a locally flat background. The metric deviations in Fermi normal co-ordinates to leading order are then proportional to the projected Riemann curvature tensor evaluated on the worldline.

To proceed, first start with an orthonormal tetrad frame $\lambda^\mu_{\hat{\alpha}}$ with the orthogonality condition

$$\eta_{\hat{\alpha}\hat{\beta}} = g_{\mu\nu} \lambda^\mu_{\hat{\alpha}} \lambda^\nu_{\hat{\beta}}, \quad (35)$$

such that the tetrad satisfies parallel transport in the general space-time background described by co-ordinates x^μ , with

$$\frac{D\lambda^\mu_{\hat{\alpha}}}{d\tau} = 0, \quad (36)$$

and where $\hat{\alpha}$ denote indices for the Fermi co-ordinates $X^{\hat{\alpha}}$ on a locally flat tangent space. The Riemann curvature tensor in the Fermi frame is then described by

$${}^F R_{\hat{\alpha}\hat{\beta}\hat{\gamma}\hat{\delta}} = R_{\mu\nu\rho\sigma} \lambda^\mu_{\hat{\alpha}} \lambda^\nu_{\hat{\beta}} \lambda^\rho_{\hat{\gamma}} \lambda^\sigma_{\hat{\delta}}. \quad (37)$$

4.2 Zeroth-Order Contributions to the Linear Momentum and Spin Angular Momentum

By ensuring that $\lambda^\mu_{\hat{0}} = u^\mu_{(0)}$ in the usual fashion and making use of (35) along with the leading-order spin condition $P^\mu_{(0)} S^{\mu\nu}_{(0)} = 0$, it becomes evident that

$$P^\mu_{(0)} = \lambda^\mu_{\hat{\alpha}} P^{\hat{\alpha}}_{(0)} = m_0 \lambda^\mu_{\hat{0}}, \quad (38)$$

$$S^{\mu\nu}_{(0)} = \lambda^\mu_{\hat{i}} \lambda^\nu_{\hat{j}} S^{\hat{i}\hat{j}}_{(0)}, \quad (39)$$

where $P_{(0)}^{\hat{\alpha}} = m_0 \delta^{\hat{\alpha}}_{\hat{0}}$ and $S_{(0)}^{\hat{i}\hat{j}}$ is a constant-valued spatial antisymmetric tensor, with components to be determined from initial conditions.

4.3 First-Order Perturbation Terms

For the linear momentum, the first-order perturbation in ε is very straightforward to evaluate. With (19) and (36), it is obvious that $DP_{(1)}^{\mu}/d\tau = \lambda^{\mu}_{\hat{\alpha}} \left(dP_{(1)}^{\hat{\alpha}}/d\tau \right)$, resulting in

$$\frac{dP_{(1)}^{\hat{\alpha}}}{d\tau} = -\frac{1}{2} {}^F R^{\hat{\alpha}}_{\hat{0}\hat{i}\hat{j}} S_{(0)}^{\hat{i}\hat{j}}. \quad (40)$$

This is immediately integrable, leading to

$$P_{(1)}^{\mu} = -\frac{1}{2} \lambda^{\mu}_{\hat{k}} \int \left({}^F R^{\hat{k}}_{\hat{0}\hat{i}\hat{j}} S_{(0)}^{\hat{i}\hat{j}} \right) d\tau. \quad (41)$$

Because of the tetrad formalism employed within this evaluation, it follows immediately upon contracting (41) with $P_{\mu}^{(0)}$ that

$$\bar{m}_1^2 = 0 \quad (42)$$

for a general space-time background. This immediately leads to simplified expressions for (33) and (34), expressed as

$$\begin{aligned} u^{\mu}(\varepsilon) &= \sum_{j=0}^{\infty} \varepsilon^j u_{(j)}^{\mu} = \frac{1}{m_0} \left[P_{(0)}^{\mu} + \varepsilon P_{(1)}^{\mu} \right] \\ &+ \varepsilon^2 \left\{ \frac{1}{m_0} \left[P_{(2)}^{\mu} - \frac{1}{2} \bar{m}_2^2 P_{(0)}^{\mu} \right] + \frac{1}{2m_0^3} S_{(0)}^{\mu\nu} R_{\nu\gamma\alpha\beta} P_{(0)}^{\gamma} S_{(0)}^{\alpha\beta} \right\} \\ &+ \varepsilon^3 \left\{ \frac{1}{m_0} \left[P_{(3)}^{\mu} - \frac{1}{2} \bar{m}_2^2 P_{(1)}^{\mu} - \frac{1}{2} \bar{m}_3^2 P_{(0)}^{\mu} \right] \right. \\ &\left. + \frac{1}{2m_0^3} R_{\nu\gamma\alpha\beta} \sum_{n=0}^1 S_{(1-n)}^{\mu\nu} \sum_{k=0}^n P_{(n-k)}^{\gamma} S_{(k)}^{\alpha\beta} \right\} + O(\varepsilon^4) \end{aligned} \quad (43)$$

and

$$\rho(\varepsilon) = \frac{s_0}{m_0} \left\{ \varepsilon + \varepsilon^2 \left[\frac{1}{2} \bar{s}_1^2 \right] + \varepsilon^3 \left[\frac{1}{2} \left(\bar{s}_2^2 - \bar{m}_2^2 \right) - \frac{1}{8} \bar{s}_1^4 \right] + O(\varepsilon^4) \right\}. \quad (44)$$

In contrast to the linear momentum to first-order, the corresponding expression for the spin tensor is considerably more complicated to evaluate. It is important first to note that, following (16) for $j = 2$,

$$\frac{DS_{(1)}^{\mu\nu}}{d\tau} = 0. \quad (45)$$

When $S_{(1)}^{\mu\nu}$ is described in terms of its tetrad projection, it is determined that

$$\begin{aligned} S_{(1)}^{\mu\nu} &= \lambda^\mu_{\hat{\alpha}} \lambda^\nu_{\hat{\beta}} S_{(1)}^{\hat{\alpha}\hat{\beta}} \\ &= 2 \lambda^{\mu}_{\hat{0}} \lambda^{\nu\hat{1}}_{\hat{j}} S_{(1)}^{\hat{0}\hat{j}} + \lambda^\mu_{\hat{i}} \lambda^\nu_{\hat{j}} S_{(1)}^{\hat{i}\hat{j}}. \end{aligned} \quad (46)$$

By using the spin condition relation (21) for $j = 1$ and the tetrad projection for (41), it is shown that

$$S_{(1)}^{\hat{0}\hat{j}} = -\frac{1}{m_0} P_i^{(1)} S_{(0)}^{\hat{i}\hat{j}}. \quad (47)$$

Regarding the components $S_{(1)}^{\hat{i}\hat{j}}$ in (46), they can be formally determined with respect to the “radiative correction” term \bar{s}_1^2 according to (27), such that

$$S_{(1)}^{\hat{i}\hat{j}} = \frac{1}{4} \bar{s}_1^2 S_{(0)}^{\hat{i}\hat{j}}. \quad (48)$$

At this point, a problem emerges with this approach, in that (46) still depends upon \bar{s}_1^2 , which remains an *undetermined parameter* to be computed. Given the discovery that $\bar{m}_1^2 = 0$ for the first-order mass shift correction, it would be tempting to simply make the same assumption about the corresponding spin shift correction. However, since \bar{s}_1^2 only needs to be *covariantly constant*, such an assumption is not well justified. This leads to the requirement of explicitly evaluating (45) independently of the tetrad in terms of the six-dimensional matrix differential equation¹

$$\frac{DS_{\mu\nu}^{(1)}}{d\tau} = \frac{dS_{\mu\nu}^{(1)}}{d\tau} + 2u_{(0)}^\alpha \Gamma_{\alpha[\mu}^\beta S_{\nu]\beta}^{(1)} = 0 \quad (49)$$

for a column vector of $\left(S_{\mu\nu}^{(1)}\right) \equiv \left(S_{01}^{(1)}, S_{02}^{(1)}, S_{03}^{(1)}, S_{12}^{(1)}, S_{23}^{(1)}, S_{31}^{(1)}\right)$. The solution to (49) is then used to evaluate the tetrad projected spin tensor $S_{(1)}^{\hat{\alpha}\hat{\beta}}$ and \bar{s}_1^2 .

¹A previous approach was reported in [25, 26] using a three-dimensional column vector of purely spatial components of $S_{\mu\nu}^{(1)}$ in combination with the spin condition to algebraically evaluate the remaining three components. In retrospect, this previous treatment is not viable in comparison to the approach presented in this paper. Therefore, this new perspective replaces the older one presented in [25, 26].

4.4 Second-Order Perturbation Terms

Once the challenge of evaluating the first-order perturbation term for the spin tensor is overcome, the second-order perturbation terms are easily determined. For example, from solving (15) for $j = 2$, the second-order linear momentum term is

$$P_{(2)}^\mu = -\frac{1}{2} \lambda^\mu_{\hat{\alpha}} \int \left(\frac{1}{m_0} {}^F R^{\hat{\alpha}}_{\hat{j}\hat{k}\hat{l}} P_{(1)}^{\hat{j}} S_{(0)}^{\hat{k}\hat{l}} + {}^F R^{\hat{\alpha}}_{\hat{0}\hat{\gamma}\hat{\beta}} S_{(1)}^{\hat{\gamma}\hat{\beta}} \right) d\tau, \quad (50)$$

which is the sum of terms with tetrad projections in both along the worldline and orthogonal to it. Therefore, it follows from (26) for $j = 2$ that $\bar{m}_2^2 \neq 0$ in general. Similarly, for the spin angular momentum, the corresponding second-order expression for (16) is

$$\frac{DS_{(2)}^{\mu\nu}}{d\tau} = \frac{1}{m_0^3} P_{(0)}^{[\mu} S_{(0)}^{\nu]\sigma} R_{\sigma\gamma\alpha\beta} P_{(0)}^\gamma S_{(0)}^{\alpha\beta}, \quad (51)$$

which when integrated leads to

$$S_{(2)}^{\mu\nu} = \frac{1}{m_0} \lambda^{[\mu}_{\hat{0}} \lambda^{\nu]}_{\hat{i}} \int S_{(0)}^{\hat{j}} {}^F R_{\hat{j}\hat{0}\hat{k}\hat{l}} S_{(0)}^{\hat{k}\hat{l}} d\tau. \quad (52)$$

As well, $\bar{s}_2^2 \neq 0$ in general. Further evaluation to higher orders in ε also suggests no obvious challenges to overcome, so the procedure can be extended indefinitely to any desired order.

5 Moving Towards an MPD Many-Body Description of Classical Spinning Particle Dynamics

5.1 Research Motivations

It would be very interesting to develop an extension of the analytic perturbative approach for the MPD equations that can be applied towards a many-body description of classical spinning particle dynamics. This is important to understand because virtually every composite astrophysical system, such as spiral galaxies, globular clusters, galactic superclusters, accretion disks around black holes, and so forth are all built in terms of components with spin angular momentum incorporated. These systems are often modelled using only many-body Newtonian gravitation, which may be a reasonable assumption under certain predetermined circumstances, but seems inadequate to address the full range of physical consequences that may be experienced due to relativistic effects that are necessarily excluded.

The essential intent for investigating a many-body description of classical spinning particles in curved space-time is to better understand the interaction dynamics between two or more spinning particles in relative motion with respect to one another. Given the interest shown in understanding the transition from stable to chaotic motion for a single particle, this consideration becomes even more relevant than before when dealing with a many-body system in curved space-time, in which the possibility of instabilities may emerge under astrophysically realistic conditions. As well, by compressing the many-body system into a very small volume of space, it seems possible to investigate the continuum limit for spinning matter subject to the MPD equations as applied to each unit cell endowed with spin.

This section presents the first stage of some long-term research [28] on understanding the extension of the MPD equations to incorporate many-body spinning particle systems. For now, it involves understanding the evolution of a single neighbouring worldline due to spin, determined with respect to some reference worldline in the following two contexts:

1. Raychaudhuri Equation:

$$\frac{d\theta}{d\tau} = -\frac{1}{3}\theta^2 - \sigma^{\alpha\beta}\sigma_{\alpha\beta} + \omega^{\alpha\beta}\omega_{\alpha\beta} - R_{\alpha\beta}u^\alpha u^\beta, \quad (53)$$

2. Generalized Jacobi Equation for tidal dynamics:

$$\frac{D^2\xi^\mu}{d\tau^2} + R^\mu{}_{\alpha\beta\gamma}u^\alpha\xi^\beta u^\gamma + \cdots = 0, \quad (54)$$

where θ is the expansion, $\sigma_{\alpha\beta}$ is the shear, and $\omega^{\alpha\beta}$ is the vorticity associated with a congruence of worldlines in (53), and where the unspecified extra terms in (54) refer to higher-order contributions involving the covariant time derivative of the separation vector ξ^μ between neighbouring worldlines.

In both contexts, there lies an important physical challenge to understand, which concerns the fact that the spinning particles moving along separate worldlines must *necessarily interact* with each other, which then significantly impacts upon their evolution in space-time. To put it another way, it is not reasonable to expect that one can just make multiple copies of MPD particles that are distributed throughout a given curved space-time background and have their worldlines determined *solely* by the background curvature. This issue can be best appreciated by appealing to the analogy of magnetostatics involving the attractive force felt by two parallel currents in a steady state, or conversely the repulsive force felt by two anti-parallel currents. Therefore, it is necessary to find an avenue that allows for the individual spinning particles to have non-trivial interactions.

5.2 Locally Induced Einstein-Cartan Interaction

In order to address the challenge of incorporating the interactions between two spinning particles that are separately subject to forces and torques as described by the MPD equations, it is useful to consider the situation in terms of the overall kinematics first without necessarily modifying the equations themselves.²

To this end, recall (28) and (29) with parametrization constraint (30) for the four-velocity $u^\mu(\varepsilon)$. Then the corresponding acceleration $a^\mu(\varepsilon)$ for the spinning particle, expanded out in ε , would formally read as

$$\begin{aligned} a^\mu(\varepsilon) &= \frac{Du^\mu(\varepsilon)}{d\tau} \\ &= \varepsilon \left[u_{(0)}^\alpha \nabla_\alpha u_{(1)}^\mu + u_{(1)}^\alpha \nabla_\alpha u_{(0)}^\mu \right] \\ &\quad + \varepsilon^2 \left[u_{(0)}^\alpha \nabla_\alpha u_{(2)}^\mu + u_{(1)}^\alpha \nabla_\alpha u_{(1)}^\mu + u_{(2)}^\alpha \nabla_\alpha u_{(0)}^\mu \right] + O(\varepsilon^3). \end{aligned} \quad (55)$$

Consider now a situation involving two spinning particles propagating in a curved space-time background. Because both particles are subject to forces and torques generated by the MPD equations, their worldlines are not geodesics. At the same time, because they are independent particles with distinct physical properties to them, their responses to the spin-curvature interaction are obviously expected to be distinct.

Now choose one of these two worldlines to act as a reference with respect to the other one. For the particle on that reference worldline, its propagation with respect to the background space-time can be determined in accordance with Fermi-Walker transport [29], such that

$$\frac{D_{(FW)} u^\mu}{d\tau} = u^\alpha \nabla_\alpha^{(FW)} u^\mu = 0, \quad (56)$$

where

$$\Gamma_{(FW)\alpha\beta}^\mu = \Gamma_{(0)\alpha\beta}^\mu + C_{(FW)\alpha\beta}^\mu, \quad (57)$$

$$C_{(FW)\alpha\beta}^\mu = a^\mu g_{\alpha\beta}^{(0)} - \delta^\mu_\beta a_\alpha, \quad (58)$$

and $\Gamma_{(0)\alpha\beta}^\mu$ is the metric connection for the space-time background.

At this point, it is important to make the following observation. From the perspective of an observer co-moving with the reference particle, it would appear from

²As presented, the MPD equations implicitly assume that all interactions are “local” in their description, at least within the context of General Relativity. If evidence emerges to show that gravitational interactions are necessarily “non-local” by some defining criterion, then it would follow that many-body spinning particle interactions as described here must incorporate non-locality. By implication, an appropriate modification of the MPD equations would then be well-motivated.

(56) that the particle is propagating along a *geodesic* in a *perturbed space-time background* due to particle acceleration generated by the MPD equations. Further to this perspective, it is self-evident from (58) that the Fermi-Walker connection (57) is *not symmetric* in its lower two indices, yielding an antisymmetric contribution. Therefore, it follows that $C_{(FW)\alpha\beta}^\mu$ is interpreted as the contortion tensor, with an induced torsion field generated by the reference particle that gets encoded within a new curvature tensor determined by (57).

The significance of this approach is that, in the instant of proper time as determined for the reference particle, the neighbouring particle is now subject to an MPD spin-curvature interaction *involving this new curvature tensor with induced torsion* due to the reference particle's acceleration. Furthermore, the geometry is now an instantaneous Riemann-Cartan U_4 [30], with the acceleration-dependent terms giving rise to what will now be called a *locally induced Einstein-Cartan (EC) interaction*.

Further details about the locally induced EC interaction and its subsequent application for the rest of this paper are deferred to a future publication [28]. However, it is worthwhile to show its presence in terms of the metric tensor of space-time in local Fermi normal co-ordinates (T, \mathbf{X}) .³ To linear order in the reference particle's acceleration, with $\mathbf{a}_j = a_j$ from the induced EC interaction labelled with boldface to distinguish these acceleration terms from others that arise elsewhere, it is shown that

$$g_{00}^{(FW)} = -1 - 2 a_k X^k - \left[R_{l0m0}^{(FW)}(T) + \frac{d}{dT} (\mathbf{a}_{(l,m)} \Delta T) \right] X^l X^m, \quad (59)$$

$$g_{(0j)}^{(FW)} = \frac{2}{3} R_{0(kl)j}^{(FW)}(T) X^k X^l, \quad (60)$$

$$g_{(ij)}^{(FW)} = \delta_{ij} + \frac{1}{3} R_{i(kl)j}^{(FW)}(T) X^k X^l, \quad (61)$$

$$g_{[0j]}^{(FW)} = \mathbf{a}_j \Delta T, \quad (62)$$

$$g_{[ij]}^{(FW)} = \mathbf{a}_i X^j - \mathbf{a}_j X^i, \quad (63)$$

with the metric tensor having now both symmetric and antisymmetric components, in which the latter set are dependent upon \mathbf{a}_j .

It is very important to point out that, while the induced EC interaction is a purely frame-dependent effect akin to a fictitious force, the new curvature tensor based upon (57) is perfectly well-defined because (58) is a tensor. For this reason, the explicit time-dependent contributions in (59) and especially (62) are labelled with ΔT , to symbolize that these contributions are ephemeral and can only persist within a limited time scale. In terms of the physical interpretations that can be ascribed to the EC interaction, it can be understood as something analogous to the Lense-Thirring effect that causes the precession of a nearby gyroscope due to the spin rotation of a massive body. This also fits well with an interpretation of Einstein-Cartan theory in terms of defects within space-time in like manner to that of classical defect theory concerning

³For ease of notation, the indices are left unhatted.

internal stresses within an elastic medium [31]. From such an interpretation, the induced torsion due to the reference particle causes a space-time defect that then has to be restored to its original state once the particle leaves that space-time region.

5.3 Spin Modifications of the Raychaudhuri Equation

When using the spin-perturbed space-time background to compute the Raychaudhuri equation, it takes the form

$$\begin{aligned} \frac{d\theta^{(FW)}}{d\tau} = & -\frac{1}{3}\theta^2 - \sigma^{\alpha\beta}\sigma_{\alpha\beta} + \omega^{\alpha\beta}\omega_{\alpha\beta} - R_{\alpha\beta}^{(FW)}u^\alpha u^\beta \\ & - 2a^\alpha u^\beta (\sigma_{\alpha\beta} - \omega_{\alpha\beta}) , \end{aligned} \quad (64)$$

where

$$\theta^{(FW)} = \theta = \nabla_\alpha u^\alpha , \quad (65)$$

$$\sigma_{\alpha\beta}^{(FW)} = \sigma_{\alpha\beta} + a_{(\alpha} u_{\beta)} = \left[\nabla_{(\beta} u_{\alpha)} - \frac{1}{3}\theta h_{\alpha\beta} \right] + a_{(\alpha} u_{\beta)} , \quad (66)$$

$$\omega_{\alpha\beta}^{(FW)} = \omega_{\alpha\beta} + a_{[\alpha} u_{\beta]} = \nabla_{[\beta} u_{\alpha]} + a_{[\alpha} u_{\beta]} . \quad (67)$$

are the modified forms of the expansion, shear, and vorticity with $h_{\alpha\beta} = g_{\alpha\beta}^{(0)} + u_\alpha u_\beta$, such that $u^\alpha h_{\alpha\beta} = 0$ and $h^\alpha_\alpha = 3$, while

$$R_{\alpha\beta}^{(FW)} u^\alpha u^\beta = R_{\alpha\beta}^{(0)} u^\alpha u^\beta - \frac{3}{2} a_\alpha a^\alpha \quad (68)$$

shows that the modified gravitational term includes the spin-dependent acceleration with opposite sign compared to the background Ricci term. This is interesting because it shows that the spin-curvature interaction causes a defocussing of the congruences. In particular, such a result may have relevance for cosmology as a way to account for a small repulsion that is currently attributed to dark energy, assuming that a sufficiently large MPD spin-curvature force can be generated due to the coupling of galactic spin with the cosmological space-time background. More details need to be examined to determine whether this possibility is physically realistic.

5.4 Generalized Jacobi Equation and Computation of Neighbouring Worldlines

The other approach towards finding a many-body description of spinning particles is to use the generalized Jacobi equation as a computational tool for determining a

neighbouring worldline with respect to a reference worldline. Since this approach [32, 33] specifically computes neighbouring geodesics with respect to a reference geodesic in a general space-time background, it can also be applied for the case of the perturbed space-time background as described by (57).

Suppose that σ is the parameter identifying a family of worldlines $x^\mu(\tau; \sigma)$ in a given space-time background, with the reference worldline as $x^\mu(\tau; 0) = x^\mu(\tau)$. Then the neighbouring worldline is related to the reference in terms of a Taylor expansion with respect to $\sigma = 0$, such that

$$\begin{aligned} x^\mu(\tau; \sigma) &= x^\mu(\tau) + \frac{\partial x^\mu(\tau)}{\partial \sigma} \sigma + \frac{1}{2} \frac{\partial^2 x^\mu(\tau)}{\partial \sigma^2} \sigma^2 + O(\sigma^3) \\ &= x^\mu(\tau) + \xi^\mu(\tau) \sigma \\ &\quad + \frac{1}{2} \left[k^\mu(\tau) - \Gamma_{(FW)\alpha\beta}^\mu \xi^\alpha(\tau) \xi^\beta(\tau) \right] \sigma^2 + O(\sigma^3), \end{aligned} \quad (69)$$

where

$$\xi^\mu(\tau) = \frac{\partial x^\mu(\tau)}{\partial \sigma} \quad (70)$$

is the separation vector between the neighbouring worldlines and

$$k^\mu(\tau) = \frac{D_{(FW)} \xi^\mu(\tau)}{d\sigma}. \quad (71)$$

The challenge is to solve for (70) and (71) for determining (69) to the desired order of the expansion in σ .

This study is currently a work in progress [28]. Nonetheless, it is still possible to outline the basic approach to solve for (70) and (71) necessary to obtain (69). This first point is to assume, just as in (10) and (11), that (70) and (71) can be written in the form

$$\xi^\mu(\varepsilon) \equiv \sum_{j=0}^{\infty} \varepsilon^j \xi_{(j)}^\mu, \quad (72)$$

$$k^\mu(\varepsilon) \equiv \sum_{j=0}^{\infty} \varepsilon^j k_{(j)}^\mu. \quad (73)$$

Focussing only on the first-order contribution in (69), the next step is to determine the generalized Jacobi equation (54) in order to determine the proper time-dependence of ξ^μ . This is best accomplished by solving the equation of motion for a test particle in a local Fermi frame [34, 35], in which the right-hand side is the acceleration of the neighbouring particle, denoted by the subscript “[1]” in what follows below. By again describing the background space-time in terms of the Fermi-Walker connection (57) and the locally induce EC interaction, it can be shown that

the generalized Jacobi equation is

$$\begin{aligned}
 & \frac{D_{(FW)}^2 \xi^\mu}{d\tau^2} + R_{(FW)\alpha\beta\gamma}^\mu u^\alpha \xi^\beta u^\gamma \\
 & + 2 \left[(\delta^\mu{}_\nu + u^\mu u_\nu) + \frac{D_{(FW)} \xi^\mu}{d\tau} u_\nu \right] R_{(FW)\alpha\beta\gamma}^\nu \frac{D_{(FW)} \xi^\alpha}{d\tau} \xi^\beta \\
 & \times \left(u^\gamma + \frac{1}{3} \frac{D_{(FW)} \xi^\gamma}{d\tau} \right) + \Omega_{accel.}^\mu + \Omega_{EC}^\mu = 0, \tag{74}
 \end{aligned}$$

where

$$\begin{aligned}
 \Omega_{accel.}^\mu = & (\delta^\mu{}_\nu + u^\mu u_\nu) \left\{ (a^\nu - a_{[1]}^\nu) + \frac{D_{(FW)} a_{[1]}^\nu}{d\sigma} \right. \\
 & + \frac{D_{(FW)} \xi^\nu}{d\tau} \left[\xi_\alpha \frac{D_{(FW)} a^\alpha}{d\tau} + \frac{D_{(FW)} \xi_\alpha}{d\tau} \left(a_{[1]}^\alpha - 2 a^\alpha + \frac{D_{(FW)} a^\alpha}{d\sigma} \right) \right. \\
 & + \left(a_\alpha^{[1]} + \frac{D_{(FW)} a_\alpha^{[1]}}{d\sigma} \right) \frac{D_{(FW)} \xi^\alpha}{d\tau} \frac{D_{(FW)} \xi_\beta}{d\tau} \frac{D_{(FW)} \xi^\beta}{d\tau} \\
 & \left. \left. - 2 \xi^\alpha \nabla_{(\alpha}^{(FW)} a_{\beta)} \frac{D_{(FW)} \xi^\beta}{d\tau} \right] \right\} \\
 & + \left(a_{[1]}^\nu + \frac{D_{(FW)} \xi^\nu}{d\sigma} \right) \frac{D_{(FW)} \xi_\alpha}{d\tau} \frac{D_{(FW)} \xi^\alpha}{d\tau} \left\{ \right. \\
 & - 2 g_{(0)}^{\mu\sigma} \left(R_{\alpha\beta\gamma\sigma}^{(FW)} - R_{\gamma\sigma\alpha\beta}^{(FW)} \right) \frac{D_{(FW)} \xi^\alpha}{d\tau} \xi^\beta u^\gamma \\
 & \left. - 8 \xi^\gamma \left[\delta^\mu{}_\alpha \nabla_{[\beta}^{(FW)} a_{\gamma]} - g_{(0)}^{\mu\sigma} g_{\gamma\alpha}^{(0)} \nabla_{[\beta}^{(FW)} a_{\sigma]} \right] \frac{D_{(FW)}}{d\tau} \left(\xi^{(\alpha} u^{\beta)} \right) \right\} \tag{75}
 \end{aligned}$$

and

$$\begin{aligned}
 \Omega_{EC}^\mu = & (\delta^\mu{}_\nu + u^\mu u_\nu) \left\{ \xi_\alpha \nabla_{(FW)}^{[\alpha} \mathbf{a}^{\nu]} - \left(1 + \Delta\tau \frac{D_{(FW)}}{d\tau} \right) \left(\mathbf{a}^\nu - \frac{D_{(FW)} \mathbf{a}^\nu}{d\sigma} \right) \right. \\
 & + \frac{D_{(FW)} \xi^\nu}{d\tau} \left[\left(2 \xi^\beta \nabla_{[\alpha}^{(FW)} \mathbf{a}_{\beta]} \right. \right. \\
 & \left. \left. - \mathbf{a}_\alpha - 2 \Delta\tau \frac{D_{(FW)}}{d\tau} \xi^\beta \nabla_{(\alpha}^{(FW)} \mathbf{a}_{\beta)} \right) \frac{D_{(FW)} \xi^\alpha}{d\tau} \right] \\
 & \left. + \left(\mathbf{a}^\nu \frac{D_{(FW)} \xi_\alpha}{d\tau} - \xi^\nu \frac{D_{(FW)} \mathbf{a}_\alpha}{d\tau} \right) \frac{D_{(FW)} \xi^\alpha}{d\tau} \right\}, \tag{76}
 \end{aligned}$$

with the neighbouring particle's acceleration already Lie transported for immediate evaluation. It is worth recalling that the neighbouring particle's acceleration is determined by use of the MPD equations, but with use of the modified Riemann curvature tensor $R_{\mu\nu\alpha\beta}^{(FW)}$ instead of $R_{\mu\nu\alpha\beta}^{(0)}$ for the background space-time.

The final step required is to substitute (72) and all other expansions of ε into (74), to then solve for each order of ε . The difficult part of the task is to evaluate the zeroth-order contribution for ξ^μ , which applies for geodesics, but once that contribution is determined, all the others can be obtained without difficulty through simple integration, at least in principle. It remains to be seen [28] whether there are any further technical challenges in determining (69), but it appears that the conceptual difficulties are overcome.

6 Conclusion

This paper illustrates the foundations and possible applications for the analytic perturbative approach to the MPD equations. It should be apparent that the approach is powerful, in that it is both background independent and applicable to any conceivable type of motion for the spinning particle. Furthermore, the outline of future work on many-body particle dynamics shows its potential to model many-body astrophysical systems that can be compared with observations. Nonetheless, it should also be noted that the formalism is always subject to refinements. For example, it would be useful to expand upon this perturbative approach to incorporate the quadrupole moment interaction of these otherwise pointlike particles, which would undoubtedly contribute to non-trivial motion under more extreme physical situations, such as orbital dynamics near the event horizon of a black hole. As well, the formalism does not take into account backreaction effects due to the gravitational self-force, which seems relevant for addressing more sophisticated considerations than outlined in this paper. These modifications do not seem very difficult to incorporate within the existing formalism. In its present form, however, there is already a lot of possibilities for useful applications to follow.

Acknowledgments The author wishes to thank the organizers of the *WE-Heraeus Seminar: Equations of Motion in Relativistic Gravity* for the invitation to present his research in Bad Honnef, Germany on February 18–22, 2013.

References

1. M. Mathisson, *Acta Phys. Pol.* **6**, 163 (1937)
2. A. Papapetrou, *Proc. R. Soc. Lond.* **209**, 248 (1951)
3. F. Pirani, *Acta Phys. Pol.* **15**, 389 (1956)
4. W. Tulczyjew, *Acta Phys. Pol.* **18**, 393 (1959)
5. J. Madore, *Ann. Inst. Henri Poincaré* **11**, 221 (1969)

6. W.G. Dixon, Phil. Trans. R. Soc. Lond. Ser. A, 277:59 (1974)
7. W.G. Dixon, *Isolated Gravitating Systems in General Relativity* (North-Holland Publishing Co., Amsterdam, 1979), pp. 156–219
8. B. Mashhoon, J. Math. Phys. **12**, 1075 (1971)
9. R. Wald, Phys. Rev. D **6**, 406 (1972)
10. F. de Felice, K.P. Tod, M. Calvani, Nuovo Cim. B **34**, 365 (1976)
11. O. Semerák, Mon. Not. R. Astron. Soc. **308**, 863 (1999)
12. S. Suzuki, K.I. Maeda, Phys. Rev. D **58**, 023005 (1998)
13. S. Suzuki, K.I. Maeda, Phys. Rev. D **61**, 024005 (1999)
14. M.D. Hartl, Phys. Rev. D **67**, 024005 (2003)
15. M.D. Hartl, Phys. Rev. D **67**, 104023 (2003)
16. M. Shibata, Y. Mino, T. Tanaka, Phys. Rev. D **53**, 622 (1996)
17. M. Sasaki, T. Tanaka, Y. Mino, M. Shibata, Phys. Rev. D **54**, 3762 (1996)
18. J. Ehlers, E. Rudolph, Gen. Relativity and Gravitation **8**, 197 (1977)
19. I. Bailey, W. Israel, Ann. Phys. **130**, 188 (1980)
20. T.W. Noonan, Astrophys. J. **291**, 422 (1985)
21. B. Mashhoon, C. Chicone, B. Punsly, Phys. Lett. A **343**, 1 (2005)
22. B. Mashhoon, D. Singh, Phys. Rev. D **74**, 124006 (2006)
23. C. Møller, Commun. Inst. Dublin Adv. Stud. Ser. A, **5** (1949)
24. D. Singh, Gen. Relativity and Gravitation **40**, 1179 (2008)
25. D. Singh, Phys. Rev. D **78**, 104028 (2008)
26. D. Singh, Gen. Relativity and Gravitation **78**, 104029 (2008)
27. K.S. Thorne, C.W. Misner, J.A. Wheeler, *Gravitation* (W. H. Freeman and Company, New York, 1973)
28. D. Singh, Work in progress
29. S.W. Hawking, G.F.R. Ellis, *The Large Scale Structure of Space-Time* (Cambridge University Press, Cambridge, 1973)
30. F.W. Hehl et al., Rev. Mod. Phys. **48**, 393 (1976)
31. M.L. Ruggiero, A. Tartaglia, Am. J. Phys. **71**, 1303 (2003)
32. J.W. van Holten, R. Kerner, R. Colistete Jr., Class. Quantum Gravity **18**, 4725 (2001)
33. G. Koekoek, J.W. van Holten, Phys. Rev. D **83**, 064041 (2011)
34. C. Chicone, B. Mashhoon, Class. Quantum Gravity **19**, 4231 (2002)
35. C. Chicone, B. Mashhoon, Class. Quantum Gravity **22**, 195 (2005)

Center of Mass, Spin Supplementary Conditions, and the Momentum of Spinning Particles

L. Filipe O. Costa and José Natário

Abstract We discuss the problem of defining the center of mass in general relativity and the so-called spin supplementary condition. The different spin conditions in the literature, their physical significance, and the momentum-velocity relation for each of them are analyzed in depth. The reason for the non-parallelism between the velocity and the momentum, and the concept of “hidden momentum”, are dissected. It is argued that the different solutions allowed by the different spin conditions are equally valid descriptions for the motion of a given test body, and their equivalence is shown to dipole order in curved spacetime. These different descriptions are compared in simple examples.

1 Introduction

An old problem in the description of the dynamics of test particles endowed with multipole structure is the fact that, even for a free *pole-dipole* particle (i.e. with a momentum vector P^α , and a spin 2-form $S_{\alpha\beta}$ as its only two relevant moments) in flat spacetime, the equations of motion resulting from the conservation laws $T^{\alpha\beta}_{;\beta} = 0$ do not yield a determinate system, since there exist 3 more unknowns than equations. The so-called “spin supplementary condition”, $S^{\alpha\beta}u_\beta = 0$, for some unit timelike vector u^α , first arose as a means of closing the system, by killing off 3 components of $S^{\alpha\beta}$. Its physical significance remained however obscure, especially in the earlier treatments that dealt with point particles [1–4] (see also in this respect [5]). Later treatments, most notably the works by Möller [6, 7], dealing with extended bodies, shed some light on the interpretation of the spin condition, as it being a choice of representative point in the body; more precisely, choosing it as the center of mass (“centroid”) as measured

L.F.O. Costa (✉) · J. Natário

CAMGSD, Instituto Superior Técnico, Universidade de Lisboa, Lisbon, Portugal

e-mail: lfpcosta@math.ist.utl.pt

J. Natário

e-mail: jnatar@math.ist.utl.pt

L.F.O. Costa

Centro de Física do Porto – CFP, Departamento de Física e Astronomia,
Universidade do Porto, Porto, Portugal

© Springer International Publishing Switzerland 2015

D. Puetzfeld et al. (eds.), *Equations of Motion in Relativistic Gravity*,

Fundamental Theories of Physics 179, DOI 10.1007/978-3-319-18335-0_6

in the rest frame of an observer of 4-velocity u^α —since in relativity, the center of mass of a spinning body is an observer-dependent point. Different choices have been proposed; the best known ones are the Frenkel-Mathisson-Pirani (FMP) condition [8, 16], which chooses the centroid as measured in a frame comoving with it; the Corinaldesi-Papapetrou (CP) condition [9], which chooses the centroid measured by the observers of zero 3-velocity ($u^i = 0$) in a given coordinate system; and the Tulczyjew-Dixon (TD) condition [10, 11], which chooses the centroid measured in the zero 3-momentum frame ($u^\alpha \propto P^\alpha$). A more recent condition, proposed in [12, 13], dubbed herein the “Ohashi-Kyrian-Semerák (OKS) condition” (which, as we shall see, seems to be favored in many applications), chooses the centroid measured with respect to some u^α parallel-transported along its worldline. The spin condition generally remained, however, a not well understood problem (this is true even today), not being clear, namely, its status as a choice (the discussion is sometimes put in terms of which are the “correct” and the “wrong” conditions for each type of particle, see introduction of [14] for a review), the differences arising from the different choices, and what it means to consider different solutions corresponding to *the same physical motion*. Also, some aspects of each condition have been poorly understood, especially the FMP condition and its famous helical motions [15]. The rules for transition between spin conditions, and the quantities that are fixed (for different solutions corresponding to the same physical body), were established in [13], where the numerical solutions were compared in the Kerr spacetime, and it was shown that, within the limit of validity of the pole-dipole approximation, the different solutions are contained within a minimal worldtube, formed by all the possible positions of the center of mass, which lies inside the convex hull of the body’s worldtube. These rules were further discussed in [16], and used to show that the helical motions are fully consistent solutions, always contained within the minimal worldtube (and to clarify the misunderstanding that led to the contrary claims in the literature).

The non-parallelism between the momentum and the velocity of a multipole particle subject to external fields, and its relation with the spin supplementary condition, is another old problem. A significant step towards its understanding was taken in [17], where a generalized concept of “hidden momentum” (first discovered in the context of classical electrodynamics [18–22]) was introduced in general relativity, and applied to the study of the TD and CP conditions (the latter designated therein by a different name, the “laboratory frame centroid”). These ideas were further worked out, with emphasis on the FMP condition, in recent works by the authors [16, 24].

In this paper, we discuss in detail the different spin conditions in general relativity, the centroids that they determine, their uniqueness/non-uniqueness, and the momentum-velocity relation arising from each of them. The different solutions given by the different spin conditions corresponding to the same physical motion are compared in simple examples, and their differences dissected. Building on the works in [13, 16] (where the equivalence was shown for free particles in flat spacetime), we prove the equivalence of the solutions to dipole order in curved spacetime; in particular, we clarify the dependence of the spin-curvature force on the spin condition, as being precisely what ensures the equivalence, and the connection of that with the geodesic deviation equation.

1.1 Notation and Conventions

1. Signature $-+++$; $\epsilon_{\alpha\beta\sigma\gamma} \equiv \sqrt{-g}[\alpha\beta\gamma\delta]$ is the Levi-Civita tensor, and we follow the orientation $[1230] = 1$ (i.e. in flat spacetime $\epsilon_{1230} = 1$); $\epsilon_{ijk} \equiv \epsilon_{ijk0}$. Riemann tensor: $R^\alpha_{\beta\mu\nu} = \Gamma^\alpha_{\beta\nu,\mu} - \Gamma^\alpha_{\beta\mu,\nu} + \dots$.
2. $(h^\mu)^\alpha_\beta \equiv \delta^\alpha_\beta + u^\alpha u_\beta$ denotes the projector orthogonal to a unit time-like vector u^α .
3. *The three basic vectors in the description of an extended body.* P^α is the momentum; $U^\alpha \equiv dz^\alpha/d\tau$ is the tangent vector to the reference worldline $z^\alpha(\tau)$; the vector field involved in the *spin condition* $S^{\alpha\beta}u_\beta = 0$ is generically denoted by u^α .
4. “Centroid”, “center of mass”, “CM”: have all the *same meaning* herein. $x^\alpha_{\text{CM}}(u) \equiv$ centroid as measured by an observer of 4-velocity u^α .

2 Center of Mass in Relativity and the Significance of the Spin Supplementary Condition

In the multipole scheme an extended body is represented by a set of moments of its current density 4-vector j^α (the “electromagnetic skeleton”) and a set of moments of the energy momentum tensor $T^{\alpha\beta}$, called “inertial” or “gravitational” moments (forming the so-called [8] “gravitational skeleton”), defined with respect to a reference worldline $z^\alpha(\tau)$ which is taken to be some representative point of the body, and whose motion aims to represent the “bulk” motion of the body. The natural choice for such point is the body’s center of mass (CM); however, in relativity, the CM of a spinning body is observer-dependent. This is illustrated in Fig. 1. In order to establish how the center of mass changes with the observer, we need reasonable definitions of momentum, angular momentum, mass and center of mass. In flat spacetime these are all well defined notions; but it is not so in curved spacetime, as they consist of integrals which amount to adding tensors defined at different (albeit close, if the body is assumed small) points; different generalizations of these notions have been proposed (see e.g. [11, 25, 26]). The discussion herein is aimed to be as general as possible; for that we use the following definitions that hold reasonable (at least to lowest orders) regardless of the particular multipole scheme followed.

Consider a system of Riemann normal coordinates $\{x^{\hat{\alpha}}\}$ (e.g. [25, 27]) centered at the point z^α of the reference worldline, associated to the orthonormal frame $\mathbf{e}_{\hat{\alpha}}$ at that point, and take it to be momentarily comoving with some observer \mathcal{O} of 4-velocity u^α (not necessarily tangent to the curve $z^\alpha(\tau)$); that is, at z^α , $\mathbf{e}_{\hat{0}} = u^\alpha$ and the triad $\mathbf{e}_{\hat{i}}$ spans the instantaneous local rest space of \mathcal{O} . We define the momentum P^α , angular momentum $S^{\alpha\beta}$, mass $m(u)$ and centroid $x^\alpha_{\text{CM}}(u)$ of the particle with respect to \mathcal{O} as the tensors at $z^\alpha(\tau)$ (respectively point) whose components (respectively coordinates) in this chart are



Fig. 1 A free spinning spherical body in flat spacetime. Observer \mathcal{O} , at rest relative to the axis of rotation, measures the centroid x_{CM}^α to coincide with the sphere's geometrical center (and with the rotation axis). $x_{\text{CM}}^\alpha \equiv x_{\text{CM}}^\alpha(P)$ is the centroid as measured in the $P^i = 0$ frame. Observers \mathcal{O}' and \mathcal{O}'' moving (relative to \mathcal{O}) with velocities \vec{v}' , \vec{v}'' opposite to the rotation of the body, see points on the *right side* of the body moving faster than those on the *left side*; hence for these observers the *right side* of the body is more massive, and the centroid they measure is shifted to the *right* by $\Delta \vec{x} = \vec{v} \times \vec{S}_*/M$. The larger the speed v the larger the shift; when v equals the speed of light, the shift takes its maximum value, with the centroid lying in the circle of radius $R_{\text{Moller}} = S_*/M$

$$P^{\hat{\alpha}} \equiv \int_{\Sigma(z,u)} T^{\hat{\alpha}\hat{\beta}} d\Sigma_{\hat{\beta}}, \quad (1)$$

$$S^{\hat{\alpha}\hat{\beta}} \equiv 2 \int_{\Sigma(z,u)} x^{[\hat{\alpha}} T^{\hat{\beta}]\hat{\gamma}} d\Sigma_{\hat{\gamma}}, \quad (2)$$

$$m(u) \equiv -P^\alpha u_\alpha = \int_{\Sigma(z,u)} T^{\hat{0}\hat{\gamma}} d\Sigma_{\hat{\gamma}}, \quad (3)$$

$$x_{\text{CM}}^{\hat{\alpha}}(u) \equiv \frac{\int_{\Sigma(z,u)} x^{\hat{\alpha}} T^{\hat{0}\hat{\gamma}} d\Sigma_{\hat{\gamma}}}{m(u)}. \quad (4)$$

Here $\Sigma(z, u) \equiv \Sigma(z(\tau), u)$ is the spacelike hypersurface generated by all geodesics orthogonal to the timelike vector u^α at the point z^α (in normal coordinates it coincides with the spatial hypersurface $x^{\hat{0}} = 0$), $d\Sigma$ is the 3-volume element on $\Sigma(z, u)$, and $d\Sigma_\gamma \equiv -n_\gamma d\Sigma$, where n^α is the (future-pointing) unit vector normal to $\Sigma(z, u)$ (at z^α , $n^\alpha = u^\alpha$). These definitions correspond to the ones given in [25], and have a well defined mathematical meaning, which can be written in the manifestly covariant form (66) and (67). They also correspond, to a good approximation, to the ones given in Dixon's schemes [11, 26]. This is discussed in detail in Appendix “Momentum and Angular Momentum in Curved Spacetime”. Note that although we used normal coordinates to perform the integrations above, the end results P^α and $S^{\alpha\beta}$ are tensors, which can now be expressed in any frame.¹

¹One could say the same about the point $x_{\text{CM}}^\alpha(u)$, although one must bear in mind when transforming its coordinates to the new frame that it will still be the CM as measured by the specific observer u^α , and *not* the CM as measured in the new frame.

The vector

$$(d_G^u)^\alpha \equiv -S^{\alpha\beta} u_\beta \quad (5)$$

yields the “mass dipole moment” as measured by the observer \mathcal{O} (of 4-velocity u^α), and

$$\Delta x^\alpha = -\frac{S^{\alpha\beta} u_\beta}{m(u)} \quad (6)$$

can be interpreted as the shift, or the “displacement”, of the centroid $x_{\text{CM}}^\alpha(u)$ relative to the reference worldline $z^\alpha(\tau)$. This is readily seen in the coordinate system $\{x^{\hat{\alpha}}\}$, where $u^{\hat{i}} = 0$ and $S^{\hat{i}\hat{\beta}} u_{\hat{\beta}} = -S^{\hat{i}\hat{0}}$, and so from Eq. (2) we have

$$S^{\hat{i}\hat{0}} = 2 \int_{\Sigma(z,u)} x^{\hat{l}} T^{\hat{0}\hat{l}\hat{\gamma}} d\Sigma_{\hat{\gamma}} = \int_{\Sigma(z,u)} x^{\hat{i}} T^{\hat{0}\hat{\gamma}} d\Sigma_{\hat{\gamma}} \equiv m(u) x_{\text{CM}}^{\hat{i}}(u); \quad (7)$$

note that $x^{\hat{0}} = 0$, since the integration is performed in the geodesic hypersurface $\Sigma(z, u)$ orthogonal to u^α at $z^\alpha(\tau)$. Hence $\Delta x^{\hat{i}} = S^{\hat{i}\hat{0}}/m(u)$ yields the coordinates $x_{\text{CM}}^{\hat{i}}(u)$ of the center of mass measured by \mathcal{O} , in the normal system $\{x^{\hat{\alpha}}\}$. Since the latter is constructed from geodesics radiating out of z^α , $\Delta \mathbf{x}$ is the vector at z^α tangent to the geodesic connecting z^α and $x_{\text{CM}}^\alpha(u)$, and whose length equals that of the geodesic; that is, $x_{\text{CM}}^\alpha(u)$ is the image by the geodesic exponential map of $\Delta \mathbf{x}$: $x_{\text{CM}}^\alpha(u) = \exp_z(\Delta \mathbf{x})$. In flat spacetime (where vectors are arrows connecting two points), $\Delta \mathbf{x}$ reduces to the displacement vector from z^α to $x_{\text{CM}}^\alpha(u)$; in curved spacetime it is still a reasonable notion of center of mass shift, and so (5) is a sensible definition of mass dipole moment. In particular, its vanishing for some observer means that one is choosing z^α as the center of mass $x_{\text{CM}}^\alpha(u)$ as measured by that observer. That is, the condition

$$S^{\alpha\beta} u_\beta = 0, \quad (8)$$

implying, in the system $\{x^{\hat{\alpha}}\}$, $S^{\hat{i}\hat{0}} = 0 \Rightarrow x_{\text{CM}}^{\hat{i}}(u) = 0$, states that the reference worldline is the center of mass as measured by the observer $\mathcal{O}(u)$ (or, equivalently, that the mass dipole vanishes for $\mathcal{O}(u)$). Equation (8), for some timelike vector field u^α defined (at least) along $z^\alpha(\tau)$, is known as the “spin supplementary condition”, which one needs to impose in order to have a determined system of equations of motion, as we shall see in the next section. As we have just seen, one can generically interpret it as a choice of center of mass.

In order to see how the center of mass changes with the observer, let us for simplicity consider the case with no electromagnetic field, $F^{\alpha\beta} = 0$; in this case, as explained in detail in Appendix “The Dependence of the Particle’s Momenta on Σ ”, under the assumption that the size of the body is small compared with the scale of the curvature, the moments (1) and (2) do not depend on the argument u^α of $\Sigma(z, u)$; that is, they depend on the point along the reference worldline $z^\alpha(\tau)$, but not on the particular geodesic hypersurface Σ through it. We may thus regard $P^\alpha(\tau)$ and $S^{\alpha\beta}(\tau)$

as well defined functions on $z^\alpha(\tau)$. We shall also introduce the following relations which will be useful throughout this paper. Let u^α and u'^α be the 4-velocities of two different observers. We can write (e.g. [28])

$$u'^\alpha = \gamma(u, u')(u^\alpha + v^\alpha(u', u)); \quad \gamma(u, u') \equiv -u^\alpha u'_\alpha = \frac{1}{\sqrt{1 - v^\alpha v_\alpha}}, \quad (9)$$

where $v^\alpha(u', u)$ is a vector orthogonal to u^α , whose space components v^i yield the ordinary 3-velocity of the observer u'^α in the frame $u^i = 0$ (i.e. the velocity of the observer u'^α relative to the observer u^α). Choose z^α to be the CM as measured by u^α : $z^\alpha = x_{\text{CM}}^\alpha(u)$; that is, choose $S^{\alpha\beta}u_\beta = 0$. In order to obtain the mass dipole measured by u'^α , one just has to contract $S^{\alpha\beta}$ with u'_β : $(d_G^{u'})^\alpha \equiv -S^{\alpha\beta}u'_\beta$; this is because, under the assumptions above, $S^{\alpha\beta}$ does not depend on the normal to the hypersurface $\Sigma(z)$, and thus, in the $u'^i = 0$ frame, we may write $-S^{\alpha\beta}u'_\beta$ in the form (7), only with u' in the place of u . The shift of the centroid $x_{\text{CM}}^\alpha(u')$ measured by u'^α relative to $x_{\text{CM}}^\alpha(u)$ is thus

$$\Delta x^\alpha = -\frac{S^{\alpha\beta}u'_\beta}{m(u')} = -\gamma(u, u') \frac{S^{\alpha\beta}v_\beta(u', u)}{m(u')}, \quad (10)$$

cf. Eq. (6). Especially interesting is the case $u^\alpha = P^\alpha/M$, where we denoted $M \equiv \sqrt{-P^\alpha P_\alpha}$; this amounts to choosing z^α as the CM as measured in the $P^i = 0$ frame, $z^\alpha = x_{\text{CM}}^\alpha(P)$. In this case

$$\Delta x^\alpha = -\frac{S_\star^{\alpha\beta}v_\beta}{M}, \quad (11)$$

where $v^\alpha \equiv v^\alpha(u', P)$ is the velocity of the observer u'^α relative to the $P^i = 0$ frame, and we denoted by $S_\star^{\alpha\beta}$ the angular momentum taken with respect to $z^\alpha = x_{\text{CM}}^\alpha(P)$ (note that the tensor $S^{\alpha\beta}$ depends on the choice of z^α , cf. Eq. (2); for the same body, $S^{\alpha\beta}$ is in general different for different z^α 's). Let us denote also the corresponding spin vector S_\star^α , so that $S_\star^{\alpha\beta} = \epsilon^{\alpha\beta}_{\gamma\delta} S_\star^\gamma P^\delta / M$. The space part (both in the $u'^i = 0$ and in the $P^i = 0$ frames, as Δx^α is orthogonal to both u'^α and P^α) reads

$$\Delta x^i = \frac{(\vec{S}_\star \times \vec{v})^i}{M}. \quad (12)$$

Thus the set of all shift vectors corresponding to all possible observers spans a disk of radius $R_{\text{Möller}} = S_\star/M$, centered at $x_{\text{CM}}^\alpha(P)$ and orthogonal to S_\star^α and P^α , in the tangent space at $x_{\text{CM}}^\alpha(P)$. This statement can roughly be rephrased as saying that the set of all possible positions of the center of mass as measured by the different observers is contained (and fills) such disk (in flat spacetime this is an exact statement, originally by Möller [7]). Let us dub such disk the “disk of centroids”, and its radius $R_{\text{Möller}}$ the *Möller radius*.

In order to illustrate how this works, consider for simplicity the setup in Fig. 1: a free spinning spherical body in flat spacetime. Observer \mathcal{O} , at rest relative to the axis of rotation, clearly must (by symmetry) measure the CM to coincide with the body's geometrical center (and with the rotation axis). The rest frame of such an observer corresponds in this case to the $P^i = 0$ frame (this statement will be made obvious in Sect. 3.2.3 by Eq. (23)). Consider now other observers, \mathcal{O}' and \mathcal{O}'' , moving (relative to \mathcal{O}) with velocities \vec{v}' and \vec{v}'' , opposite to the rotation of the body; for these observers the center of mass is shifted to the right, as they measure the right side of the body to be more massive. The larger the speed v the larger the shift; when v equals the speed of light, the shift takes its maximum value, with the centroid lying in the circle of radius R_{Moller} .

In spacetime, the set of all possible centroid worldlines forms a worldtube—the “minimal worldtube” [13], see Fig. 2—typically very narrow,² and always contained within the *convex hull* of the body's worldtube (see [25] for its precise definition). This can be shown in different ways. In flat spacetime, it is not difficult to show (see e.g. [29, p. 313]), that if the mass density-energy density $\rho(u) = T^{\alpha\beta}u_\beta u_\alpha$ is positive everywhere within the body and with respect to all observers u^α (i.e. if the weak energy condition holds everywhere within the body), then the center of mass with respect to any u^α must be within the body's convex hull. The flat spacetime arguments apply just as well in a local Lorentz frame $\{x^{\hat{\alpha}}\}$ (under the assumption above that the body is small enough so that we can take it to be nearly orthonormal throughout it). In the same framework one can show that R_{Moller} is the minimum size that a *classical* particle can have in order to have finite spin without containing mass-energy flowing faster than light, that is, without violating the dominant energy condition. The dominant energy condition implies $\rho \geq |\vec{J}|$, where $J^{\hat{i}} \equiv -T^{\hat{\alpha}\hat{i}}u_{\hat{\alpha}}$. Let a be the largest dimension of the body; in the local Lorentz frame centered at $x_{\text{CM}}^\alpha(P)$ and such that $P^{\hat{i}} = 0$, we may write,

$$S_\star = \left| \int \vec{x} \times \vec{J} d\Sigma \right| \leq \int x |\vec{J}| d\Sigma \leq \int \rho x d\Sigma \leq Ma \Leftrightarrow a \geq \frac{S_\star}{M}. \quad (13)$$

3 The Momentum-Velocity Relation

The force and the spin evolution equations for a multipole particle in an external electromagnetic and gravitational field are [11]

²For the fastest spinning celestial body known to date, the pulsar PSR J1748-2446ad (rotation frequency 716 Hz, estimated radius $a = 16$ km), whose equatorial velocity is $0.23c$, $R_{\text{Moller}} \simeq 0.1a$, see also the contribution by Giulini in this volume.

$$\begin{aligned} \frac{DP^\alpha}{d\tau} &= qF^\alpha_\beta U^\beta + \frac{1}{2}F^{\mu\nu;\alpha}\mu_{\mu\nu} + F^\alpha_{\gamma;\beta}U^\gamma d^\beta + F^\alpha_\beta \frac{Dd^\beta}{d\tau}, \\ &\quad - \frac{1}{2}R^\alpha_{\beta\mu\nu}S^{\mu\nu}U^\beta + F^\alpha(2^{N>1}) \end{aligned} \quad (14)$$

$$\frac{DS^{\alpha\beta}}{d\tau} = 2P^{[\alpha}U^{\beta]} + \tau^{\alpha\beta} \quad (15)$$

where q , d^α and $\mu_{\alpha\beta}$ are, respectively, the particle's charge, electric dipole vector, and magnetic dipole 2-form (for their precise definitions, see [24]). $F^\alpha(2^{N>1})$ denotes the force (gravitational and electromagnetic) due to the quadrupole and higher moments, and $\tau^{\alpha\beta}$ is sometimes called the “torque” tensor. $U^\alpha \equiv dz^\alpha/d\tau$ is the tangent to the reference worldline $z^\alpha(\tau)$. These equations form an undetermined system even in the case $DP^\alpha/d\tau = 0$ and $\tau^{\alpha\beta} = 0$ (for there would be 13 unknowns: P^α , 3 independent components of U^α , and 6 independent components of $S^{\alpha\beta}$, for only 10 equations), manifesting the need for a supplementary condition, which amounts to specify the worldline $z^\alpha(\tau)$, relative to which the moments are taken. The condition $S^{\alpha\beta}u_\beta = 0$, for some unit timelike vector field u^α defined along z^α , kills off 3 components of the angular momentum and makes that choice, requiring, as explained in the previous section, $z^\alpha(\tau)$ to be the centroid as measured by an observer of 4-velocity u^α . Contracting (15) with u_β one obtains an expression for the momentum of the particle,

$$P^\alpha = \frac{1}{\gamma(u, U)} \left(m(u)U^\alpha + S^{\alpha\beta} \frac{Du_\beta}{d\tau} + \tau^{\alpha\beta}u_\beta \right), \quad (16)$$

where $\gamma(U, u) \equiv -U^\alpha u_\alpha$, $m(u) \equiv -P^\alpha u_\alpha$, and in the second term we used $S^{\alpha\beta}u_\beta = 0$. Equation (16) tells us that, in general, P^α is not parallel to the CM 4-velocity U^α ; in this section we will discuss the reason for that.

The vector P^α can be split in its projections parallel and orthogonal to the CM 4-velocity U^α :

$$P^\alpha = P^\alpha_{\text{kin}} + P^\alpha_{\text{hid}}; \quad P^\alpha_{\text{kin}} \equiv mU^\alpha, \quad P^\alpha_{\text{hid}} \equiv (h^U)^\alpha_\beta P^\beta, \quad (17)$$

where $m \equiv -P^\alpha U_\alpha$ is the “proper mass”, i.e. the energy of the particle as measured in the CM frame, and

$$(h^U)^\alpha_\beta \equiv U^\alpha U_\beta + \delta^\alpha_\beta$$

is the projector orthogonal to U^α . We dub the parallel projection $P^\alpha_{\text{kin}} = mU^\alpha$ “kinetic momentum” associated with the motion of the center of mass; it is the most familiar part of P^α , formally similar to the momentum of a monopole particle. The component P^α_{hid} orthogonal to U^α is the so-called “hidden momentum” (e.g. [17]). The reason for the latter denomination is seen taking the perspective of an observer $\mathcal{O}(U)$ comoving with the particle: in the frame of $\mathcal{O}(U)$ (i.e. the $U^i = 0$ frame) the 3-momentum is in general not zero: $\vec{P} = \vec{P}_{\text{hid}} \neq 0$; however, by definition, the

particle's CM is at rest in that frame; hence this momentum must be somehow hidden in the particle. P_{hid}^α consists of two parts of distinct origin: $P_{\text{hid}}^\alpha = P_{\text{hidI}}^\alpha + P_{\text{hid}\tau}^\alpha$,

$$P_{\text{hidI}}^\alpha \equiv \frac{1}{\gamma(u, U)} (h^U)^\alpha_\sigma S^{\sigma\beta} \frac{Du_\beta}{d\tau}; \quad (18)$$

$$P_{\text{hid}\tau}^\alpha \equiv \frac{1}{\gamma(u, U)} (h^U)^\alpha_\sigma \tau^{\sigma\beta} u_\beta, \quad (19)$$

which we shall explain. P_{hidI}^α is a term that depends only on the spin supplementary condition, i.e. on the choice of the field u^α relative to which the centroid is computed. In this sense we say it is *gauge*. This type of hidden momentum was first discussed in [17] (dubbed “kinematical” therein). The vector u^α needs only to be defined *along* $z^\alpha(\tau)$; but if one takes it as belonging to some observer congruence in spacetime (one can always do such an extension), and decomposing

$$u_{\alpha;\beta} = -(a^u)_\alpha u_\beta - \epsilon_{\alpha\beta\gamma\delta} \omega^\gamma u^\delta + \theta_{\alpha\beta} \quad (20)$$

where $(a^u)^\alpha \equiv u^\alpha_{;\beta} u^\beta$ is the acceleration of the observers u^α , $\omega^\alpha = \frac{1}{2} \epsilon^{\alpha\lambda\sigma\tau} u_\tau u_{[\sigma;\lambda]}$ their vorticity, and $\theta_{\alpha\beta} \equiv (h^u)^\lambda_\alpha (h^u)^\nu_\beta u_{(\lambda;\nu)}$ the shear/expansion, we may write

$$P_{\text{hidI}}^\alpha = \frac{1}{\gamma(u, U)} (h^U)^\alpha_\sigma S^\sigma_\beta \left(\gamma(u, U) (a^u)^\beta - \epsilon^\beta_{\mu\gamma\delta} u^\delta U^\mu \omega^\gamma + \theta^{\beta\gamma} U_\gamma \right). \quad (21)$$

The kinematical quantities in Eq.(20) are connected to “inertial forces”, namely $G^\alpha = -(a^u)^\alpha$ and $H^\alpha = \omega^\alpha$ are, respectively, the “gravitoelectric field” and the “Fermi-Walker gravitomagnetic field” as measured by the congruence of observers u^α , see [23, 28]. For this reason we dub P_{hidI}^α “inertial” hidden momentum.

$P_{\text{hid}\tau}$ is associated to the “torque” tensor $\tau^{\alpha\beta}$ and (in general) consists of two parts: one which is again gauge and arises for certain choices of reference worldline z^α (i.e. of the field u^α) when a physical torque acts on the particle, plus another part which is not gauge, and cannot be made to vanish by any center of mass choice. Following [17] we dub the latter “dynamical hidden momentum”. To dipole order, this dynamical part consists of a form of mechanical momentum that arises in electromagnetic systems, first discovered in [18], and since discussed in number of papers, e.g. [19–21], including recent works [17, 22, 30]. To quadrupole and higher orders, there are both electromagnetic and gravitational contributions to $\tau^{\alpha\beta}$, and thus to $P_{\text{hid}\tau}$.

3.1 “Inertial Hidden Momentum”: Center of Mass Shift and the Decoupling of U^α from P^α

Equation (18) tells us that when u^α varies along $z^\alpha(\tau)$ (i.e. $Du^\alpha/d\tau \neq 0$), in general $P_{\text{hidI}}^\alpha \neq 0$, thus U^α is not parallel to P^α . This comes as a natural consequence of

what we discussed in Sect. 2 about the observer dependence of the center of mass. Recall the situation in Fig. 1, a *free* spinning particle in *flat* spacetime: the centroid measured by observers moving relative to \mathcal{O} are shifted relative to $x_{\text{CM}}(\mathcal{O})$. If the velocity of these observers changes along $z^\alpha(\tau)$, e.g. if at an instant τ' we have $u^\alpha(\tau') = u'^\alpha$, and at τ'' $u^\alpha(\tau'') = u''^\alpha$, the shift changes accordingly, giving rise to a non-trivial velocity of the centroid. That is, superfluous centroid motions can be generated just by changing u^α along $z^\alpha(\tau)$. The momentum, however, remains the same, $DP^\alpha/d\tau = 0$, cf. Eq. (14); thus the situation may be cast as the centroid acquiring a non-zero velocity in the $P^i = 0$ frame (which is in this case the rest frame of the observer \mathcal{O}). This amounts to saying that U^α gains a component orthogonal to P^α (denote it by U_\perp^α); conversely, there is a component of P^α orthogonal to U^α , which is the hidden momentum. Let us see this in detail. Denote by U_\parallel^α and U_\perp^α , respectively, the components of U^α parallel and orthogonal to P^α ,

$$U^\alpha = U_\parallel^\alpha + U_\perp^\alpha; \quad U_\parallel^\alpha \equiv \frac{m}{M^2} P^\alpha; \quad U_\perp^\alpha \equiv (h^P)^\alpha_\beta U^\beta, \quad (22)$$

where $m \equiv -U^\alpha P_\alpha$, and $(h^P)^\alpha_\beta \equiv P^\alpha P_\beta / M^2 + \delta^\alpha_\beta$ denotes the projector in the direction orthogonal to P^α . U_\perp^α is, up to a γ factor, the 3-velocity of the centroid in the $P^i = 0$ frame, cf. Eq. (9) above (substitute therein $u'^\alpha = U^\alpha$, $u^\alpha = P^\alpha / M$). In the special case $\tau^{\alpha\beta} = 0$, we have from Eq. (16)

$$U_\perp^\alpha = -\frac{1}{m(u)} (h^P)^\alpha_\sigma S^{\sigma\beta} \frac{Du_\beta}{d\tau}, \quad (23)$$

showing that indeed the variation of u^α along $z^\alpha(\tau)$ leads to a centroid moving in the zero 3-momentum frame, and to a non-parallelism between U^α and P^α (it is actually the sole reason for that in the special case $\tau^{\alpha\beta} = 0$). If we further specialize to the case of a free particle (depicted in Figs. 1 and 2), $DP^\alpha/d\tau = 0$, and noting that the centroid shift can be written as $\Delta x^\alpha = -(x_{\text{CM}}^\alpha(P) - x_{\text{CM}}^\alpha(u)) = S^{\alpha\beta} P_\beta / M^2$, cf. Eq. (10), the shift variation along z^α becomes

$$\frac{D\Delta x^\alpha}{d\tau} = \frac{P_\beta}{M^2} \frac{DS^{\alpha\beta}}{d\tau} = U^\alpha - \frac{m}{M^2} P^\alpha = U_\perp^\alpha. \quad (24)$$

In the second equality we used Eq. (15), in the third we used Eq. (22). That is, the variation of the shift equals the component of U^α orthogonal to P^α , mathematically formalizing the heuristic arguments in Figs. 1 and 2b. One should note however that, although this reasoning is useful to gain intuition, in the general case ($DP^\alpha/d\tau \neq 0$) Eq. (24) does not hold, and U_\perp^α is not just the variation of Δx^α ; this is because the centroid $x_{\text{CM}}^\alpha(P)$ is in general no longer at rest in the $P^i = 0$ frame. (When one employs the TD condition, $u^\alpha = P^\alpha / M$, if $DP^\alpha/d\tau \neq 0$ then the centroid 4-velocity is not in general parallel to P^α , cf. Eq. (23) or, explicitly, Eq. (28).) For the general case the argument can be given as follows: *the centroid position depends on the field u^α relative to which it is measured, and its velocity on the variation of*

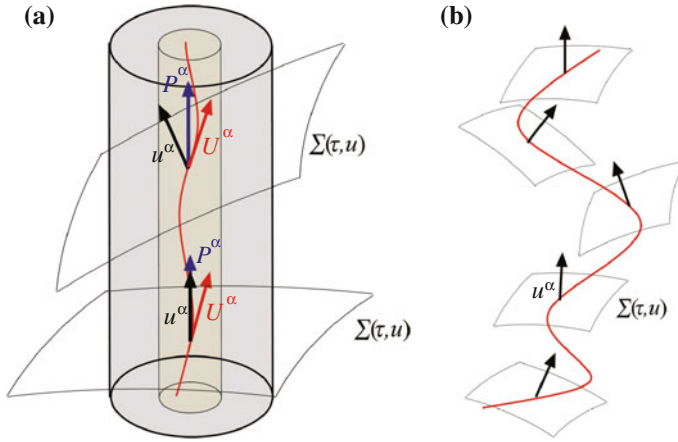


Fig. 2 **a** The body's worldtube (larger cylinder), the worldtube of centroids (narrow inner cylinder), and the *three* basic vectors involved in the description of the motion: the momentum P^α , the 4-velocity $U^\alpha = dz^\alpha/d\tau$, and the vector field u^α involved in the spin supplementary condition $S^{\alpha\beta}u_\beta = 0$. The vector u^α is orthogonal to the hypersurfaces $\Sigma(\tau, u)$ at z^α , and has the interpretation of the 4-velocity of the observer measuring the centroid. These three vectors are *not* parallel in general. **b** A curve with a varying u^α along it; that leads to a varying shift, see Fig. 1, leading to a non-zero velocity of the centroid in the $P^I = 0$ frame, cf. Eq. (23), and possibly to an acceleration without any force involved

u^α ; P^α , however, is unaffected by that, which means that in general $P^\alpha \nparallel U^\alpha$. This is precisely what Eq. (23) says.

When $U^\alpha_\perp \neq 0$, then (obviously) P^α has a component P^α_{hid} orthogonal to U^α . Noting from (22) that $P^\alpha = M^2(U^\alpha - U^\alpha_\perp)/m$, and from Eq. (17) that $U^\alpha = (P^\alpha - P^\alpha_{\text{hid}})/m$, we obtain the following relations between the hidden momentum and U^α_\perp :

$$U^\alpha_\perp = -\frac{1}{m}(h^P)^\alpha_\beta P^\beta_{\text{hid}}; \quad P^\alpha_{\text{hid}} = -\frac{M^2}{m}(h^U)^\alpha_\beta U^\beta_\perp \quad (25)$$

(these are fully general expressions, valid when $\tau^{\alpha\beta} \neq 0$).

Differentiating (23) with respect to τ , we see that when $D^2u^\alpha/d\tau^2 \neq 0$, in general the centroid acceleration $a^\alpha = DU^\alpha/d\tau$ will be non-zero, i.e. it will accelerate without the action of a force. That can lead to exotic motions; an example of that are the famous Mathisson helical motions, as shown in [16]; the same principle also leads to the bobbings in the “tetherballs” studied in [17] (in this case a force is involved, but it is not parallel to the acceleration), or the ones studied in Sect. 3.4. Of course, such effects can always be made to vanish by a choosing some u^α parallel transported along $z^\alpha(\tau)$; hence one can say that they are a complicated description for the same physics that, in principle, could be described in a simpler manner. In Fig. 2 we illustrate the situation for a free particle in flat spacetime: the worldline $z^\alpha(\tau)$ of a centroid measured by a field of observers u^α that varies along it has, in general,

superfluous motions. These are confined to the worldtube of centroids, which is a straight tube (always within the convex hull of the body's worldtube, see Sect. 2) parallel to the constant momentum P^α , and whose cross section orthogonal to P^α is the disk of centroids, orthogonal to S_\star^α , illustrated in Fig. 1. Choosing $Du^\alpha/d\tau = 0$ (e.g. inertial frames), the centroid worldlines obtained are straight lines parallel to P^α , yielding the simplest description possible for this problem.

3.2 Center of Mass and Momentum-Velocity Relation of the Different Spin conditions

In this section we shall consider, for simplicity, the case $\tau^{\alpha\beta} = 0$, so that the only hidden momentum present is the inertial hidden momentum P_{hidl}^α . Although all forms of hidden momentum have some sort of dependence on the spin condition, by the circumstance that $U^\alpha \equiv dz^\alpha/d\tau$ depends on the reference worldline $z^\alpha(\tau)$ chosen, P_{hidl}^α is the part that arises *solely* from it. Note that $\tau^{\alpha\beta} = 0$ corresponds for instance to the case of pole-dipole particles in purely gravitational systems.

3.2.1 The Corinaldesi-Papapetrou (CP) Condition

This spin condition was introduced in [9] for the Schwarzschild spacetime, where it was cast, in Schwarzschild coordinates, as $S^{i0} = 0$. One can write it covariantly as $S^\alpha_\beta u^\beta_{\text{lab}} = 0$, with u^α_{lab} corresponding to observers that have zero 3-velocity in such coordinates, $u^i_{\text{lab}} = 0$. These are the so-called “static observers”, whose 4-velocity is parallel to the time Killing vector: $u^\alpha_{\text{lab}} = u^\alpha_{\text{static}} \propto \partial/\partial t$. Hence, this condition chooses as reference worldline the centroid measured by the static observers. It can be generalized taking the static observers of other stationary spacetimes, or, as done in [13], to arbitrary metrics taking the congruence of observers with zero 3-velocity in the coordinate system chosen (let us dub it the “laboratory” frame). This effectively amounts to considering an arbitrary congruence of observers, which will be the problem discussed below: take a matter distribution described by the energy-momentum tensor $T^{\alpha\beta}(x)$, and a congruence of observers u^α_{lab} one may arbitrarily fix; then find the worldlines z^α obeying the condition $S^\alpha_\beta(z)u^\beta_{\text{lab}}(z) = 0$ —which demands z^α to be the center of mass as measured by the observer $u^\alpha_{\text{lab}}(z)$ located at that precise point. At first sight, it does not even seem obvious that such solutions exist. For when one considers an observer $u^\alpha_{\text{lab}}(x_1)$ at a given point x_1^α , the centroid with respect to $u^\alpha_{\text{lab}}(x_1)$ will be at some point x_2^α , in general not coinciding with x_1^α ; and then at the site x_2^α , the observer $u^\alpha_{\text{lab}}(x_2)$ that lies there is a different one, and measures its centroid to be in yet another different point x_3^α , and so on. This is illustrated in Fig. 3a.

We shall now show that the solution indeed always exists, but in general it is not unique. Consider the vector field (the mass dipole with respect to the

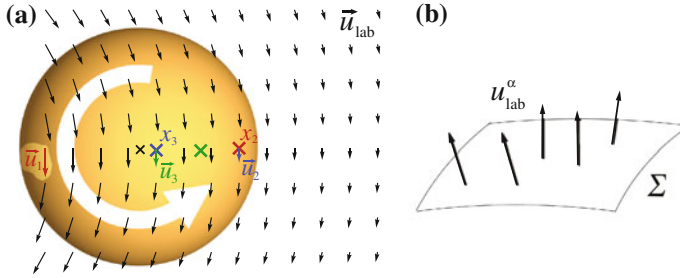


Fig. 3 **a** Centroid as measured by different observers of the congruence u_{lab}^α . Colors specify an observer and the corresponding centroid. Observer $u_{\text{lab}}^\alpha(x_1) \equiv u_1^\alpha$ measures the centroid to be at $x_2^\alpha \equiv x_{\text{CM}}^\alpha(u_1)$. The observer $u_{\text{lab}}^\alpha(x_2) \equiv u_2^\alpha$ at x_2^α is a different one, thus its centroid will in general be at a different point x_3^α . Observer $u_{\text{lab}}^\alpha(x_3) \equiv u_3^\alpha$ at x_3^α measures the centroid to be at yet another different point, and so on. **b** For the observers u_{lab}^α to agree on the centroid position, they must be orthogonal to the *same* totally geodesic hypersurface Σ . In this case the condition $S_{\beta}^{\alpha} u_{\text{lab}}^{\beta} = 0$ fixes an *unique* worldline

observer $u_{\text{lab}}^{\beta}(z)$

$$d_G^{\alpha}(z) = -S_{\beta}^{\alpha}(z, u_{\text{lab}}) u_{\text{lab}}^{\beta}(z),$$

which is a function of z^α , where $S_{\beta}^{\alpha}(z, u_{\text{lab}})$ is the angular momentum taken about z^α and in the geodesic hypersurface orthogonal to u_{lab}^α at z^α . Consider moreover the intersection of the convex hull of the body's worldtube W with some arbitrary spacelike hypersurface Σ , see Fig. 4; and let $\vec{d}_G(z)$ be the projection of $d_G^{\alpha}(z)$ on Σ . At the boundary of the region $W \cap \Sigma$ it is clear from the definition of $S^{\alpha\beta}(z, u)$ in Eq. (2) that $\vec{d}_G(z)$ points inwards (since, by virtue of the weak energy condition, $T_{\alpha\beta} u^\alpha u^\beta > 0$ for any time-like vector u^α). Given that $d_G^{\alpha}(z)$ is a *continuous* vector field (since u_{lab}^β is an observer *congruence*), the Brouwer fixed point theorem implies that the flow of \vec{d}_G must have a fixed point; i.e. $\vec{d}_G = 0$ at least one point within

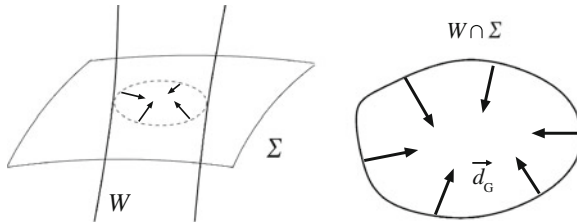


Fig. 4 The vector field $d_G^{\alpha}(z)$ (i.e. the mass dipole as measured by the observers u_{lab}^α at z^α), at the boundary of the region formed by the intersection of the convex hull W of the body's worldtube with some space-like hypersurface Σ , always points inwards. Since the field $d_G^{\alpha}(z)$ is spacelike and continuous, the Brouwer fixed point theorem ensures that $d_G^{\alpha}(z) = 0$ at *at least one* point $z^\alpha \in W \cap \Sigma$. In other words, there is at least one point which is the center of mass as measured by the observer u_{lab}^α *at that point*

$W \cap \Sigma$. Since $d_G^\alpha(z)$ is a space-like vector, this effectively means that $d_G^\alpha(z) = 0$ at that point.

The argument above is analogous to the one followed by Madore [25] to produce a similar proof for the vector field $S_\beta^\alpha(z, P)P^\beta(z)$.

Hence, at least one worldline z^α will exist such that $S_\beta^\alpha(z)u_{\text{lab}}^\beta(z) = 0$; but in general it is not unique. The analysis in Sect. 3.2.3 provides an example. Take, in flat spacetime, the congruence u_{lab}^α to be observers rotating rigidly with the angular velocity of Mathisson's helical motions, $\Omega = M/S_\star$ (i.e. take the laboratory frame to be the observers at rest in the coordinates associated to a frame rotating with angular velocity Ω), *opposite* to the sense of rotation of the body, and around the centroid measured in the $P^i = 0$ frame, $x_{\text{CM}}^\alpha(P)$. In this case, every point z^α within the worldtube of centroids is a center of mass with respect to the observers at rest in this frame, i.e. every such point is a solution of $S_\beta^\alpha(z)u_{\text{lab}}^\beta(z) = 0$.

In some cases the solution is unique; it is clearly so when the observers of the congruence agree on the centroid position (note however that this is a sufficient, but *not* necessary condition for uniqueness). The moments (thus the centroid, Eq. (4)) are defined integrating on geodesic hypersurfaces $\Sigma(z, u)$ orthogonal to $u^\alpha(z)$ at some z^α ; in order for different observers, e.g. u_1^α and u_2^α , to agree on the centroid position, their hypersurfaces $\Sigma(z_1, u_1)$ and $\Sigma(z_2, u_2)$ should be the same. Since $\Sigma(z_1, u_1)$ is geodesic at z_1^α (i.e., it is constructed from geodesics orthogonal to u_1^α radiating out of the point z_1^α), and $\Sigma(z_2, u_2)$ is geodesic at z_2^α and that must be true for every other point, then this means that the congruence $u_{\text{lab}}^\alpha(x)$ must be orthogonal to a *totally geodesic hypersurface* Σ . This implies $u_{\text{lab}}^\alpha(x)$ to be *vorticity-free*, $\omega^\alpha = 0$ (so that it is hypersurface orthogonal), and *rigid*, $\theta_{\alpha\beta} = 0$ (so that the second fundamental form of Σ vanishes). Since, from the general decomposition (20), we have, for any spatial vector X^α tangent to $\Sigma(z, u_{\text{lab}})$,

$$\nabla_X u_{\text{lab}}^\alpha = -\epsilon_{\alpha\beta\gamma\delta} X^\beta \omega^\gamma u_{\text{lab}}^\delta + \theta_{\alpha\beta} X^\beta, \quad (26)$$

then this implies that the congruence u_{lab}^α is parallel³ along $\Sigma(z, u_{\text{lab}})$, $\nabla_X u_{\text{lab}}^\alpha = 0$. This is the case of static observers in a static spacetime. When these conditions hold, and within the regime where the normal coordinates can be taken as nearly rectangular throughout the body⁴ (that amounts to taking $\lambda \ll 1$ in Eq. (69), which is reasonable in this context, see Appendix “Momentum and Angular Momentum in

³Such observers are said to be “kinematically comoving” (see [31, Sect. 6.1]).

⁴To see the reason for this assumption, consider two observers $u_1^\alpha = u_{\text{lab}}^\alpha(x_1)$ and $u_2^\alpha = u_{\text{lab}}^\alpha(x_2)$, orthogonal to the same geodesic hypersurface Σ . Let $\{x^{\hat{\alpha}}\}$ and $\{x^{\hat{\alpha}}\}$, respectively, denote their normal coordinate systems, related by $x^{\hat{\alpha}} = \Lambda^{\hat{\alpha}}_{\hat{\beta}}(x^{\hat{\beta}} - x_2^{\hat{\beta}})$ (where $\Lambda^{\hat{\alpha}}_{\hat{\beta}}$ is a function of $x^{\hat{\beta}}$). They will agree on the centroid position if $x_{\text{CM}}^{\hat{\alpha}}(u_2) = \Lambda^{\hat{\alpha}}_{\hat{\beta}}(x_{\text{CM}}^{\hat{\beta}}(u_1) - x_2^{\hat{\beta}})$. From Eq. (4) we see that it is the case when $\mathbf{d}x^{\hat{0}} = \mathbf{d}x^{\hat{0}}$, $x^{\hat{i}} = \Lambda^{\hat{i}}_{\hat{j}}(x^{\hat{j}} - x_2^{\hat{j}})$, with $\Lambda^{\hat{i}}_{\hat{j}}$ a constant matrix. Due to the curvature, however, this cannot be exactly so; choosing $\partial_{\hat{\alpha}}|_{x_2} \simeq \partial_{\hat{\alpha}}|_{x_2}$, we have $\Lambda^{\hat{\alpha}}_{\hat{\beta}} = \delta^{\hat{\alpha}}_{\hat{\beta}} + \mathcal{O}(\|\mathbf{R}\|\hat{x}\hat{x}_2) + \mathcal{O}(\|\mathbf{R}\|\hat{x}_2^2)$, e.g. Eq. 11.12 of [32]. It follows that, for all observers *within*

Curved Spacetime” and footnote 13), the observers u_{lab}^α will agree on the centroid position. If one starts with an observer $u_1^\alpha \equiv u_{\text{lab}}^\alpha(x_1)$ at a point x_1^α , and computes the centroid it measures from Eq. (4), the worldline $z^\alpha = x_{\text{CM}}^\alpha(u_1)$ obtained will therefore obey the CP condition $S_{\beta}^\alpha(z)u_{\text{lab}}^\beta(z) = 0$, since repeating the computation in the normal coordinates of the observer $u_{\text{lab}}^\alpha(z)$ at z^α yields the same result. An example is when u_{lab}^α are the observers associated to a global inertial frame in flat spacetime. In this case u_{lab}^α not only is the same vector everywhere, as one can set the Lorentz frames of each observer $u_{\text{lab}}^\alpha(x)$ in an hyperplane Σ to be the same up to spatial translations; so all observers of this frame will measure the centroid at the same point (i.e. there is a well defined, unique centroid associated to such frame). This is an *exact* statement in this case.

Momentum-velocity relation.—Since u_{lab}^α is a well defined vector field in the region of interest, we may write $Du_{\text{lab}}^\alpha/d\tau = u_{\text{lab}}^{\alpha;\beta}U_\beta$, and therefore, from Eq. (21), the momentum reads

$$P^\alpha = mU^\alpha + \frac{1}{\gamma}(h^U)^\alpha_\sigma S_{\beta}^\sigma \left(-\gamma G^\beta - \epsilon_{\mu\gamma\delta}^\beta u_{\text{lab}}^\delta U^\mu \omega^\gamma + \theta^{\beta\gamma} U_\gamma \right); \quad (27)$$

here $\gamma \equiv -u_{\text{lab}}^\alpha U_\alpha$, $G^\alpha = -\nabla_{\mathbf{u}_{\text{lab}}} u_{\text{lab}}^\alpha$ is minus the acceleration of the laboratory observers (i.e. the gravitoelectric field), ω^γ is their vorticity (or the Fermi-Walker gravitomagnetic field [23, 28]), and $\theta_{\alpha\beta}$ their shear/expansion tensor. Hence we have a well defined expression for P^α in terms of U^α , $S^{\alpha\beta}$ and the kinematics of the congruence u_{lab}^α , telling us that P^α differs from mU^α only if the laboratory observers measure inertial forces (i.e. if they are accelerated, rotating, or shearing/expanding).

3.2.2 The Tulczyjew-Dixon (TD) Condition

The condition $S^{\alpha\beta}P_\beta = 0$ amounts to choosing $u^\alpha = P^\alpha/M$, i.e. the centroid is the one as measured in the zero 3-momentum frame. As shown in [33, 34], for a given matter distribution, described by the energy-momentum tensor $T^{\alpha\beta}(x)$, there is only one worldline $z^\alpha(\tau)$ such that $S^{\alpha\beta}P_\beta = 0$ ($S^{\alpha\beta}$ and P^α being both evaluated at z^α , and using the hypersurface $\Sigma(z, P)$ orthogonal to P^α at z^α). In other words, this spin condition *specifies a unique worldline*. It is the central worldline of the worldtube of centroids, as seen from Eq. (12). From (16) and (17), we have the expressions for the momentum

$$P^\alpha = \frac{1}{m} \left(M^2 U^\alpha + S^{\alpha\beta} \frac{DP_\beta}{d\tau} \right) = mU^\alpha + \frac{1}{m} (h^U)^\alpha_\sigma S^{\sigma\beta} \frac{DP_\beta}{d\tau}. \quad (28)$$

(Footnote 4 continued)

the body's convex hull, $\|x_{\text{CM}}^{\tilde{\alpha}}(u_2) - x_{\text{CM}}^{\tilde{\alpha}}(u_1)\|/a \lesssim \lambda$, $\lambda = \|\mathbf{R}\|a^2$; hence $x_{\text{CM}}^{\tilde{\alpha}}(u_2) \simeq x_{\text{CM}}^{\tilde{\alpha}}(u_1)$ if $\lambda \ll 1$. This is, as expected, the condition that the metric $g_{\hat{\alpha}\hat{\beta}} = \eta_{\hat{\alpha}\hat{\beta}} + \mathcal{O}(\|\mathbf{R}\|\hat{x}^2)$ can be taken as nearly flat throughout the body.

Here $DP^\alpha/d\tau$ is the force, given by Eq. (14); in the absence of electromagnetic field, and to pole-dipole order, this expression can be manipulated into the well known expression (e.g. [14])

$$U^\alpha = \frac{m}{M^2} \left(P^\alpha + \frac{2S^{\alpha\nu} R_{\nu\tau\kappa\lambda} S^{\kappa\lambda} P^\tau}{4M^2 + R_{\alpha\beta\gamma\delta} S^{\alpha\beta} S^{\gamma\delta}} \right), \quad (29)$$

determining U^α *uniquely* in terms⁵ of P^α , $S^{\alpha\beta}$ and $R_{\alpha\beta\gamma\delta}$. A more general expression for the case when $F_{\alpha\beta} \neq 0$, and to arbitrary multipole order, is given in Eq. (35) of [17].

3.2.3 The Frenkel-Mathisson-Pirani (FMP) Condition. Helical Motions

The condition $S^{\alpha\beta}U_\beta = 0$, i.e. $u^\alpha = U^\alpha$, states that the centroid is measured in its own rest frame; in other words, it chooses the center of mass as measured by an observer comoving with it. This condition does not yield an unique worldline though: it is infinitely degenerate. For a given matter distribution, described by $T^{\alpha\beta}(x)$, there are infinitely many worldlines z^α through it such that $S^{\alpha\beta}U_\beta = 0$. Indeed, any point within the disk of centroids can be a solution (i.e. can be a center of mass as measured in its proper frame) provided that it moves with the appropriate velocity. In order to see that, we start by an heuristic argument, originally due to Möller [7]: consider, in Fig. 1, a point in circular motion *opposite* to the rotation of the body, with a radius $R = v'S_\star/M$ such that it passes through the centroid $x_{\text{CM}}^\alpha(u')$ measured by the observer \mathcal{O}' , and having *therein* the same velocity as \mathcal{O}' . Such point instantaneously coincides with $x_{\text{CM}}^\alpha(u')$, and at the same time is at rest with respect to \mathcal{O}' ; it is thus a center of mass computed in its own rest frame, and will be so at every instant as the motion is circular. The angular velocity of such points is constant, $\Omega = v'/R = M/S_\star$ (i.e. does not depend on R). That is, consider a disk of the same size of the disk of centroids, *rigidly* rotating about the centroid $x_{\text{CM}}^\alpha(P)$ measured by \mathcal{O} ; any point of such disk is a centroid computed in its rest frame, and is thus a solution of $S^{\alpha\beta}U_\beta = 0$. This is the origin of the helical motions (in a frame moving with respect to \mathcal{O} , the circular motions become helices).

These facts can be explicitly checked from the equations of motion. First we note that, with this spin condition, the momentum becomes, cf. Eq. (16),

$$P^\alpha = mU^\alpha + S^{\alpha\beta}a_\beta = mU^\alpha + \epsilon^{\alpha\beta}_{\gamma\delta} a_\beta S^\gamma U^\delta, \quad (30)$$

where S^α is the spin vector defined by

$$S^\alpha = \frac{1}{2} \epsilon^{\alpha}_{\beta\mu\nu} S^{\mu\nu} U^\beta; \quad S^{\alpha\beta} = \epsilon^{\alpha\beta\mu\nu} S_\mu U_\nu. \quad (31)$$

⁵The factor m/M^2 (involving U^α via m) can be determined by the normalization condition $U^\alpha U_\alpha = -1$.

Noting from (30) that $P^\alpha a_\alpha = P^\alpha S_\alpha = 0$, and using $S^{\alpha\beta} U_\beta = 0$, the component of the 4-velocity orthogonal to P^α is, from Eq. (23),

$$U_\perp^\alpha = -\frac{1}{M^2} \epsilon^{\alpha\beta\mu\nu} S_\mu P_\nu \frac{DU_\beta}{d\tau} \quad (32)$$

which in the $P^i = 0$ frame reads

$$\vec{U} + \frac{1}{M} \frac{D\vec{U}}{d\tau} \times \vec{S} = 0. \quad (33)$$

This is a differential equation for the space components \vec{U} ; as discussed above, $\vec{v} = \vec{U}/\gamma(P, U)$ has the interpretation of 3-velocity of the centroid in the $P^i = 0$ frame. Take now for simplicity the case of a free particle in flat spacetime; in this case, from Eq. (14) we have $DP^\alpha/d\tau = 0$; also, from Eq. (35), it follows that $DS^\alpha/d\tau = 0$ (since $S^\alpha a_\alpha = 0$, which can be seen substituting (30) in $DP^\alpha/d\tau = 0$); thus M and \vec{S} in (33) are constants, and the solution for the reference worldline z^α ($\vec{U} = d\vec{z}/d\tau$) is, in rectangular coordinates (taking \vec{S} along \vec{e}_z),

$$z^\alpha(\tau) = \left(\gamma\tau, -R \cos\left(\frac{v\gamma}{R}\tau\right), R \sin\left(\frac{v\gamma}{R}\tau\right), 0 \right) \quad (34)$$

where $R = v\gamma S/M$, and $\gamma \equiv \gamma(P, U) = -P^\alpha U_\alpha/M = \sqrt{1 - v^2}$; v can take any value between 0 and 1. These are circular motions of radius R and frequency $\Omega = M/\gamma S$, centered about the centroid $x_{\text{CM}}^\alpha(P)$ measured in the $P^i = 0$ frame. They may not seem at first the same motions we deduced from the heuristic argument above; in particular, the fact γ can be arbitrarily large has led some authors to believe that the radius of these motions, for a given body, can be arbitrary, and for this reason deemed them unphysical [35–37]. That is not the case; the reason for that is that S is different for all the helical representations corresponding to the same body. Let z^α and z'^α denote two different helical solutions. The scalar $S = \sqrt{S^\alpha S_\alpha} = \sqrt{S^{\alpha\beta} S_{\alpha\beta}/2}$, for a spin tensor obeying $S^{\alpha\beta} U_\beta = 0$, is the magnitude of the angular momentum taken about $z^\alpha = x_{\text{CM}}^\alpha(U)$. It should in be different, *for the same matter distribution* $T_{\alpha\beta}(x)$, from $S' = \sqrt{S'^{\alpha\beta} S'_{\alpha\beta}/2}$, since $S'^{\alpha\beta}$, obeying $S'^{\alpha\beta} U'_\beta = 0$, is the angular momentum about a different point, $z'^\alpha = x_{\text{CM}}^\alpha(U')$. It is shown in Sect. IV of [16] that, for all helical motions, $S = S_\star/\gamma$, where $S_\star = \sqrt{S_\star^{\alpha\beta} S_{\star\alpha\beta}/2}$ is the magnitude of the angular momentum taken about $x_{\text{CM}}^\alpha(P)$ (i.e. $S_\star^{\alpha\beta} P_\beta = 0$). So indeed these motions have a *finite* radius and constant frequency, as deduced above:

$$\Omega = \frac{M}{S_\star}; \quad R = \frac{v S_\star}{M}.$$

Hence we see that the famous helical motions are just another exotic effect generated by the variation, along $z^\alpha(\tau)$, of the field of observers $u^\alpha (= U^\alpha$, in this case) with respect to which the centroid is computed; what is special about them is that in this case the non-trivial motion induced on the centroid is such that the latter is always at rest with respect to the observer measuring it. Thus they are *not* unphysical, contrary to some claims in the literature; but they do not contain new physics either, they are just alternative, unnecessarily complicated descriptions for physical motions that can be described through simpler representations: for example, the non-helical solution that this spin condition also allows, which in the case of a free particle in flat spacetime is uniform straight line motion (corresponding to $v = 0$, $R = 0$, in Eq. (34)).

It is also worth noting that, from a dynamical perspective, the consistency of the helical motions (namely, the fact the centroid accelerates *without any force*) is explained through an interchange between kinetic momentum $P_{\text{kin}}^\alpha = mU^\alpha$ and hidden momentum $P_{\text{hidl}}^\alpha = S^{\alpha\beta}a_\beta$, which occurs in a way that their variations cancel out at every instant, such that $P^\alpha = mU^\alpha + P_{\text{hidl}}^\alpha$ remains constant; see Fig. 3 of [16]. This is exactly the same principle behind the bobbings due to P_{hidl}^α discussed in Sect. 3.4.

Features of the FMP Condition: Fermi-Walker Transport and Gravito-Electromagnetic Analogies

If one employs the Frenkel-Mathisson-Pirani condition, the spin vector of a gyroscope (if $\tau^{\alpha\beta} = 0$) is Fermi-Walker transported along the worldlines of *any of the centroids* obeying this condition. This can easily be seen substituting Eq. (31) in (15) to obtain

$$\frac{DS^\alpha}{d\tau} = S_\nu a^\nu U^\alpha. \quad (35)$$

This is the most natural description for the spin evolution, where the mathematical definition of a locally non-rotating frame meets the physical one: gyroscopes “oppose” changes in direction of their rotation axes; the axis of torque-free gyroscopes define *physically* the non-rotating frames. On the other hand, Fermi-Walker transport is the *mathematical* definition of a non-rotating frame $\mathbf{e}_{\hat{\alpha}}$ adapted to an arbitrarily accelerated observer: $\nabla_{\mathbf{U}}\mathbf{e}_{\hat{\beta}} = \Omega_{\hat{\beta}}^{\hat{\alpha}}\mathbf{e}_{\hat{\alpha}}$, $\Omega^{\alpha\beta} = 2U^{[\alpha}a^{\beta]}$; that is, it admits “rotation” (actually boost) in the time-space plane formed by U^α and a^α , unavoidable to keep the time axis of the tetrad parallel to the 4-velocity ($\mathbf{U} = \mathbf{e}_{\hat{0}}$), so that the triad $\mathbf{e}_{\hat{i}}$ spans the observer’s local rest space; but no additional spatial rotation (i.e. the axes $\mathbf{e}_{\hat{i}}$ orthogonal to a^α are parallel transported).

Another interesting feature of this spin condition is that it gives rise to three *exact* gravito-electromagnetic analogies [23, 24]: (i) the spin-curvature force (penultimate term of Eq. (14)) becomes $F_G^\alpha = -\mathbb{H}^{\beta\alpha}S_\beta$, where $\mathbb{H}_{\alpha\beta} \equiv \star R_{\alpha\mu\beta\nu}U^\mu U^\nu$, analogous to the force on a magnetic dipole (second term of Eq. (14)), $F_{\text{EM}}^\alpha = B^{\beta\alpha}\mu_\beta$, where

$B_{\alpha\beta} \equiv \star F_{\alpha\mu;\beta} U^\mu$; (ii) Eq. (35) becomes, in an orthonormal frame “adapted” to a congruence of observers, $d\hat{S}^i/d\tau = (\vec{S} \times \vec{H})^i/2$, where \vec{H} is the “gravitomagnetic field”, analogous to the precession of a magnetic dipole, $D\vec{S}/d\tau = \vec{\mu} \times \vec{B}$ (first term of Eq. (62)); (iii) the inertial hidden momentum, cf. Eq. (30), is $P_{\text{hidI}}^\alpha = \epsilon_{\beta\gamma\delta}^\alpha U^\delta S^\beta G^\gamma$, with $G^\alpha = -a^\alpha$ the “gravitoelectric” field as measured in the centroid frame, formally analogous to the electromagnetic hidden momentum, Eq. (65). These analogies (apart from their theoretical interest) provide useful insight to study some problems; they are discussed in detail in [24].

The downside of this condition is the fact that it is not always easy to set up the non-helical solution. It is done through suitable ansatz in Sect. 3.4 (at an approximate level), or at an exact level, in *very special* systems, in [24] (therein it is seen to be a good choice, as it takes advantage of the symmetries of the problems to yield the simplest equations). Prescriptions in the case of Schwarzschild and Kerr spacetimes are also proposed in [38, 39]; however no general rule is known.

3.2.4 The Ohashi-Kyrian-Semerák (OKS) Spin Condition

This condition, introduced in [12], and first discussed in depth in [13], amounts to choosing a vector field u^α parallel transported along $z^\alpha(\tau)$, $Du^\alpha/d\tau = 0$, which causes the inertial hidden momentum P_{hidI}^α and its associated gauge motions to vanish, cf. Eq. (18). In the general case where the torque tensor $\tau^{\alpha\beta}$ is non-zero, as we shall see in Sect. 3.5.1, some superfluous motions may still be present though, due to the pure gauge part of the hidden momentum $P_{\text{hid}\tau}^\alpha$ related to $\tau^{\alpha\beta}$ (in gravitational systems, $P_{\text{hid}\tau}^\alpha$ is usually less important, as it involves the particle’s quadrupole moment). When $\tau^{\alpha\beta} = 0$ (the problem at hand herein), it yields the simplest momentum velocity relation possible, $P^\alpha = mU^\alpha$, and a centroid that accelerates only when there is a force, $ma^\alpha = (h^U)^\alpha_\beta F^\beta$ (this becomes $ma^\alpha = F^\alpha$ for pole-dipole particles in gravitational fields, since $m = M \equiv \sqrt{-P^\alpha P_\alpha}$ is constant, as readily seen contracting Eqs. (14) or (40) with P^α). Equation (15) also takes a simple form, yielding a spin tensor $S^{\alpha\beta}$ parallel transported along $z^\alpha(\tau)$, $DS^{\alpha\beta}/d\tau = 0$.

This condition obviously does not specify a unique worldline through the body; it is infinitely degenerate, because there are infinite possible choices of u^α (the only restriction imposed is $Du^\alpha/d\tau = 0$); but another of its advantages [13] is that one does not need⁶ to explicitly determine u^α to solve the equations of motion (for pole-dipole particles), only its value at the initial point is needed. These properties together make this condition the most suitable (at least in that case) for numerical implementation.

⁶We thank O. Semerák and A. Harte for discussions on these issues.

3.2.5 Uniqueness of the Centroid Versus Determinacy of the Equations

There are some *apparent* contradictions in the literature regarding the uniqueness of the worldline specified by the different spin conditions, and what that means in terms of the determinacy of the equations of motion. On the one hand most authors (e.g. [7, 10, 13, 17, 26]) argue, in agreement with the discussion above, that the FMP condition does not uniquely specify a worldline through the body; on the other hand, it has recently been argued [40, 41] that it uniquely specifies the motion, given certain initial conditions. Also, in [10, 13], it is said that the CP condition yields an unique solution, whereas in the analysis above we have seen that, depending on the coordinate system chosen, it may or may not yield an unique center of mass. Our considerations above are based on starting with a test body whose matter distribution is described by an energy-momentum tensor $T^{\alpha\beta}(x)$, and asking the following question: given $T^{\alpha\beta}(x)$, does the condition $S^{\alpha\beta}u_\beta = 0$ yield an unique worldline? As we have seen, from the four conditions studied above, the answer is affirmative, as a general statement, only for the TD condition.

But if one takes the perspective of the initial value problem for the equations of motion (14) and (15), the impact of the uniqueness/non-uniqueness of the center of mass definition is not straightforward. First of all one should notice that, without further assumptions, the system (14) and (15), supplemented by (8), can be determined only to dipole order and if $F^{\alpha\beta} = 0$ (otherwise one needs evolution laws for $\mu^{\alpha\beta}$, d^α , and the higher order electromagnetic and gravitational moments). In this case, all the conditions yield a well defined solution if sufficient initial conditions are provided; and it is *the type of initial data* needed to determine the equations that depends on the nature of center of mass definition given by each of the conditions.

On general grounds one can say that if the equations of motion can be written as the *explicit* functions (dot denotes ordinary derivative along \mathbf{U})

$$\dot{z}^\alpha(\tau) \equiv U^\alpha = U^\alpha(\mathbf{z}, \mathbf{P}, S^{\mu\nu}); \quad \dot{P}^\alpha = f^\alpha(\mathbf{z}, \mathbf{P}, S^{\mu\nu}); \quad \dot{S}^{\alpha\beta} = g^{\alpha\beta}(\mathbf{z}, \mathbf{P}, S^{\mu\nu})$$

then, given the initial values $\{z^\alpha, P^\alpha, S^{\alpha\beta}\}|_{\text{in}}$, the system is determined. The first equation is the *explicit* velocity-momentum relation; but the other two also require such a relation, as can be seen by writing explicitly

$$\dot{P}^\alpha = \Gamma_{\nu\mu}^\alpha P^\mu U^\nu - \frac{1}{2} R_{\beta\gamma\delta}^\alpha U^\beta S^{\gamma\delta}; \quad \dot{S}^{\alpha\beta} = 2\Gamma_{\nu\mu}^{[\alpha} S^{\beta]\mu} U^\nu + 2P^{[\alpha} U^{\beta]}.$$

Thus, in order to have \dot{P}^α and $\dot{S}^{\alpha\beta}$ as explicit functions of $(\mathbf{z}, \mathbf{P}, S^{\mu\nu})$, we need to have an explicit relation $U^\alpha(\mathbf{z}, \mathbf{P}, S^{\mu\nu})$.

In the case of the OKS condition, since one has simply $U^\alpha = P^\alpha/m = P^\alpha/M$, cf. Sect. 3.2.4, the statements above obviously hold, and the solution is determined given $\{z^\alpha, P^\alpha, S^{\alpha\beta}\}|_{\text{in}}$, or, equivalently, $\{z^\alpha, S^{\alpha\beta}, U^\alpha, m\}|_{\text{in}}$.

The situation is similar for the TD condition (only with a more complicated velocity-momentum relation). Equation (29) is an explicit relation $U^\alpha(\mathbf{z}, \mathbf{P}, S^{\mu\nu})$; thus, given $\{z^\alpha, P^\alpha, S^{\alpha\beta}\}|_{\text{in}}$, the solution is determined. The initial data

$\{z^\alpha, S^{\alpha\beta}, U^\alpha, m\}|_{\text{in}}$ is equally sufficient because one can extract $P^\alpha|_{\text{in}}$ from Eq. (28) (substituting therein $DP^\alpha/d\tau$ by the explicit expression $-R^\alpha_{\beta\gamma\delta}U^\beta S^{\gamma\delta}/2$; an equation for M^2 is obtained by squaring (28)).

The case of the CP condition is also essentially similar. One obtains an explicit relation $U^\alpha(\mathbf{z}, \mathbf{P}, S^{\mu\nu})$ as follows.⁷ Substitute decomposition (20) into Eq. (16), with $u^\alpha = u^\alpha_{\text{lab}}$, to obtain

$$P^\alpha = \frac{-P_\alpha u^\alpha_{\text{lab}}}{\gamma} U^\alpha + \frac{1}{\gamma} S^\alpha_\beta \left(-\gamma G^\beta - \epsilon^\beta_{\mu\gamma\delta} u^\delta_{\text{lab}} U^\mu \omega^\gamma + \theta^{\beta\gamma} U_\gamma \right), \quad (36)$$

where $\gamma \equiv -U_\alpha u^\alpha_{\text{lab}}$. This is an equation for P^α in terms of U^α , $S^{\alpha\beta}$, and the quantities G^α , ω^α , and $\theta_{\alpha\beta}$ which are given in advance (see Sect. 3.2.1 and the equivalent Eq. (27)). We need now to solve for U^α . Expressing (36) in its components in a frame where $u^i_{\text{lab}} = 0$, we obtain

$$A^i_k v^k = P^i + S^i_j G^j, \quad A^i_k \equiv \left[P^0 \delta^i_k - S^i_j \left(\epsilon^j_{kl} \omega^l - \theta^j_k \right) \right],$$

where $v^i = U^i/U^0$ is the centroid velocity in the $u^i_{\text{lab}} = 0$ frame. This is a system of linear equations for the three components v^k , with solution $v^i = [A^{-1}]^i_k [P^k + S^k_j G^j]$. The component U^0 (and subsequently, U^i) is then obtained from the normalization condition $-1 = U^\alpha U_\alpha = -(U^0)^2(1 - v^2)$. We thus end up with an explicit relation $U^\alpha(\mathbf{z}, \mathbf{P}, S^{\mu\nu})$, meaning that, given the initial values $\{z^\alpha, S^{\alpha\beta}, P^\alpha\}|_{\text{in}}$, the solution is determined, as asserted in [13]. The set $\{z^\alpha, S^{\alpha\beta}, U^\alpha, m\}|_{\text{in}}$ is also sufficient, in agreement with the claim in [10], because one immediately obtains $P^\alpha|_{\text{in}}$ from (27). Finally, note that this is a distinct problem from the one addressed in Sect. 3.2.1 (where we started just with a matter distribution $T^{\alpha\beta}(x)$ and imposed $S^{\alpha\beta} u^\beta_{\text{lab}} = 0$, in which case, as we have seen, the solution always exists but in general is *not* unique). Herein one *assumes* the existence of some $T^{\alpha\beta}(x)$ that is compatible with the initial conditions prescribed (conversely, in the prescription of Sect. 3.2.1 there is no longer freedom to choose an arbitrary initial position z^α).

The case of the FMP condition has some important differences. The momentum-velocity relation is (30); the acceleration can be written as (cf. Eq. (24) of [13])

$$a^\alpha(\mathbf{z}, \mathbf{U}, S^{\mu\nu}) = \frac{1}{S^2} \left(\frac{1}{m} F^\mu S_\mu S^\alpha - P_\gamma S^{\alpha\gamma} \right) \quad (37)$$

with S^α defined by (31), $S^2 \equiv \sqrt{S^\alpha S_\alpha}$, and $F^\alpha \equiv DP^\alpha/d\tau$. Substituting in (30) one obtains an explicit relation $P^\alpha(\mathbf{z}, \mathbf{U}, S^{\mu\nu})$. However, one cannot a priori guarantee that such relation can be inverted into a relation $U^\alpha(\mathbf{z}, \mathbf{P}, S^{\mu\nu})$ (such problem, in the general case, has not yet been tackled in the literature, to the authors' knowledge). In the *special case of a free particle in flat spacetime*, we have, from (30),

⁷We thank O. Semerák for his input on this issue.

$$a^\alpha(\mathbf{P}, S^{\mu\nu}) = -\frac{S^{\alpha\beta}P_\beta}{S^2}; \quad U^\alpha(\mathbf{P}, S^{\mu\nu}) = \frac{1}{m} \left(P^\alpha + \frac{1}{S^2} S^{\alpha\mu} S_{\mu\beta} P^\beta \right). \quad (38)$$

This is an explicit relation $U^\alpha(\mathbf{P}, S^{\mu\nu})$ (m can be determined through the condition $U^\alpha U_\alpha = -1$); therefore, in agreement with the claims in [40, 41], the motion is indeed determined given the initial data $\{z^\alpha, S^{\alpha\beta}, P^\alpha\}|_{\text{in}}$ (i.e. this set of data specifies one particular solution of the *degenerate* condition $S^{\alpha\beta}U_\beta = 0$). On the other hand (unlike the situation for the other three spin conditions), the set of data $\{z^\alpha, S^{\alpha\beta}, U^\alpha, m\}|_{\text{in}}$ is *not* enough; one needs, additionally, the initial acceleration a^α , in agreement with the claims in e.g. [11, 17]. This is clear from Eqs. (30) and (38): the set of initial data $\{S^{\alpha\beta}, P^\alpha\}|_{\text{in}}$ is *equivalent* to $\{S^{\alpha\beta}, U^\alpha, m, a^\alpha\}|_{\text{in}}$. These features are readily understood in the framework of the discussion in Sect. 3.2.3: as we have seen, the motion of an helical solution $z^\alpha = x_{\text{CM}}^\alpha(U)$ is a superposition of a circular motion centered at the centroid measured in the $P^i = 0$ frame, $x_{\text{CM}}^\alpha(P)$, of radius $R = \|\Delta \mathbf{x}\|$ and angular velocity $\vec{\omega} = -M\vec{S}_\star/S_\star^2$, combined with a boost of 4-velocity P^α/M . $\Delta x^\alpha = z^\alpha - x_{\text{CM}}^\alpha(P)$ is the shift of z^α relative to the center of the helix. Given z_{in}^α , $S_{\text{in}}^{\alpha\beta}$, and P^α , one obtains $x_{\text{CM}}^\alpha(P)|_{\text{in}} = z_{\text{in}}^\alpha - \Delta x_{\text{in}}^\alpha$ from the expression $\Delta x^\alpha = S^{\alpha\beta}P_\beta/M^2$, cf. Eq. (10); $S_\star^{\alpha\beta}$ follows using $S^{\alpha\beta} = S_\star^{\alpha\beta} + 2P^{[\alpha}\Delta x^{\beta]}$, and therefore the motion is completely determined. On the other hand, if instead of $P^\alpha|_{\text{in}}$ one is given $\{U^\alpha, m\}|_{\text{in}}$, one cannot determine Δx^α ; that is the reason why one needs the acceleration, as it contains precisely the same information: $a^\alpha = -\Delta x^\alpha M^2/S^2$, cf. Eq. (38).

3.3 The Dependence of the Spin-Curvature Force on the Spin Condition; Equivalence of the Spin Conditions

We have seen that the significance of the spin condition $S^{\alpha\beta}u_\beta = 0$ is that of a choice of representative worldline z^α in the body, more precisely requiring such worldline to be, at each event, the center of mass as measured by an observer of 4-velocity u^α . We have thereby implied that the different spin conditions yield different, but *equivalent* descriptions of the motion of a given body, all contained within the worldtube of centroids, which in turn lies within the convex hull of the body's worldtube. That is easy to see for a free particle in flat spacetime, where indeed the different solutions stay close forever and within the straight worldtube depicted in Fig. 2. However, when external non-homogenous fields are present, changing z^α means not only changing the point where the fields (i.e. $F^{\alpha\beta}$ and $R_{\alpha\beta\gamma\delta}$) are evaluated, but also changing the moments ($S^{\alpha\beta}$, $\mu_{\alpha\beta}$, d^α , and the $2^{N>1}$ moments) themselves, on which the forces and torques also depend. These two changes would in principle compensate each other; the larger part of the compensation comes from the lower order terms, and a smaller part (negligible to some extent) from the higher order terms. Hence, in an approximation where only moments up to 2^N th order are kept, the different worldlines will eventually diverge. However, this does not mean that the spin condition is

not a gauge choice after all; in fact, it just marks the limit of validity of the given approximation [13]. The subtlety involved in this compensation is that, except for the case of flat spacetime, it does *not* mean that the force is the same for different choices of z^α .

In order to see this, let us consider first, in Newtonian mechanics, the problem of describing an extended body through different reference points; for more details on this problem, we refer to Sect. 3 of [42]. Consider a spherical body in a gravitational field $\vec{G}(\mathbf{x})$. If one takes z^i to be the body's center of mass $z^i = x_{\text{CM}}^i \equiv \int \rho x^i d^3x / m$ —a unique point, in Newtonian mechanics—then, with respect to z^i , the body is effectively a monopole, and the only force present is the usual (monopole) gravitational force $\vec{F} = \vec{F}_g = m\vec{G}(\mathbf{z})$. Now take a different reference point $\bar{z}^i = z^i + \Delta x^i$ (not a centroid) say, at the boundary of the sphere. The monopole force changes to $\vec{F}_g = m\vec{G}(\mathbf{z} + \Delta\mathbf{x})$; but, on the other hand, the particle has a mass dipole moment $\vec{d}_G = \int \rho \vec{x} d^3x = -m\Delta\vec{x}$ about \bar{z}^i (as well as quadrupole and higher order moments). The dipole force is $\vec{F}_{\text{dip}}^i = \nabla_j G^i d_G^j$; hence to dipole order, we have the *same net* Newtonian force:

$$\bar{F}^i = \bar{F}_g^i + \bar{F}_{\text{dip}}^i = mG^i(\mathbf{z} + \Delta\mathbf{x}) - m\nabla_j G^i(\mathbf{z} + \Delta\mathbf{x})\Delta x^j \simeq mG^i(\mathbf{z}) = F^i. \quad (39)$$

In General Relativity the situation is different because the lowest order gravitational force is the (dipole order) spin-curvature force

$$F^\alpha = -\frac{1}{2}R^\alpha_{\beta\mu\nu}S^{\mu\nu}U^\beta = \star R_{\beta\nu\mu}{}^\alpha U^\mu S^\beta u^\nu, \quad (40)$$

cf. Eq. (14), which depends explicitly on the spin condition $S^{\alpha\beta}u_\beta = 0$, i.e. on the choice of the centroid z^α . Such dependence is not compensated by a change in the monopole force (which does not exist), nor by the higher order terms (if that was the case, the pole-dipole approximation would not even make sense, for, as we shall see in Sect. 3.4.2, the differences in the force under different spin conditions are of the same order of magnitude as the force itself). Hence, the *net force* $F^\alpha = \nabla_U P^\alpha$ is different for different z^α 's, which is natural in a curved spacetime, since the differentiation is along different curves. On the other hand, although the monopole force \vec{F}_g (or \vec{G}) has no *physical* existence in the relativistic theory, there is a counterpart to the *tidal forces* arising from the variation of these fields from point to point, $\nabla_j G_i$, which comes from the curvature tensor (see below). And the crucial point here is that the change in the force F^α when one changes z^α is precisely the one needed to compensate for the tidal forces which “try” to make the worldlines diverge.

This can be formalized as follows. Take two different centroids with worldlines z^α and \bar{z}^α , defined by $S^{\alpha\beta}u_\beta = 0$ and $\bar{S}^{\alpha\beta}\bar{u}_\beta = 0$, respectively. $S^{\alpha\beta}$ is the angular momentum about z^α and $\bar{S}^{\alpha\beta}$ the angular momentum about \bar{z}^α . Extend (in a region small enough so that they do not intersect) these worldlines to a congruence of curves encompassing both z^α and \bar{z}^α ; take them to be infinitesimally close, so that one can employ the usual first order deviation equations (Eq. (42) below), and write

a connecting vector as $\Delta x^\alpha = \bar{z}^\alpha(\tau) - z^\alpha(\tau)$. Take moreover u^α to be parallel transported along z^α (i.e. it obeys Ohashi-Kyrian-Semerák spin condition), so that $P_{\text{hid}}^\alpha = 0 \Rightarrow P^\alpha = MU^\alpha$, and let the field \bar{u}^α be arbitrary. Noting that P^α can be taken as the same for z^α and \bar{z}^α (see Appendix “The Dependence of the Particle’s Momenta on Σ ”), it follows from Eq. (17) that $P^\alpha = \bar{m}\bar{U}^\alpha + \bar{P}_{\text{hid}}^\alpha$, where $\bar{m} \equiv -P^\alpha \bar{U}_\alpha$; contracting with P_α to obtain an expression for \bar{m}/M , and using Eq. (22), one obtains

$$\bar{U}^\alpha = \frac{P^\alpha}{M} + \left(\sqrt{1 + \frac{\bar{P}_{\text{hid}}^\alpha P_\alpha}{M^2}} - 1 \right) \frac{P^\alpha}{M} + \bar{U}_\perp^\alpha = \frac{P^\alpha}{M} + [\text{terms in } \bar{U}_\perp^\alpha]. \quad (41)$$

U_\perp^α and $P_{\text{hid}}^\alpha = P_{\text{hid}}^\alpha$ are gauge and reciprocal quantities; one can write one in terms of the other using Eq. (25). $\bar{U}^\alpha \neq P^\alpha/M$ only if $\bar{U}_\perp^\alpha \neq 0$ (or equivalently if $P_{\text{hid}}^\alpha \neq 0$). From the deviation equation for accelerated worldlines [43], we have

$$\begin{aligned} \frac{D^2 \Delta x^\alpha}{d\tau^2} &= -\mathbb{E}^{\alpha\beta} \Delta x_\beta + \nabla_{\Delta x} a^\alpha = -\mathbb{E}^{\alpha\beta} \Delta x_\beta + (\nabla_{\bar{U}} \bar{U}^\alpha - \nabla_U U^\alpha) \\ &= -\mathbb{E}^{\alpha\beta} \Delta x_\beta + \frac{1}{M} (\bar{F}^\alpha - F^\alpha) + [\text{terms in } \bar{U}_\perp^\alpha], \end{aligned} \quad (42)$$

where $\mathbb{E}_{\alpha\beta} \equiv R_{\alpha\mu\beta\nu} U^\mu U^\nu$ is the “gravitoelectric” tidal tensor, which is the relativistic counterpart of the Newtonian tidal tensor $\nabla_j G_i$. In the third equality we used Eq. (41) and the following: M is a conserved quantity for the OKS spin condition ($\nabla_U M = 0$ along z^α if $P^\alpha \parallel U^\alpha$, as readily seen contracting (40) with P^α), so that $F^\alpha = DP^\alpha/d\tau = Ma^\alpha$; and that along \bar{z}^α one has $\nabla_{\bar{U}} M = 0 + [\text{terms in } \bar{U}_\perp^\alpha]$.

Since Δx^α is infinitesimal, we can write (as in flat spacetime),

$$\bar{S}^{\alpha\beta} = S^{\alpha\beta} + 2P^{[\alpha} \Delta x^{\beta]} \quad (43)$$

and therefore the difference between the forces is

$$\begin{aligned} \bar{F}^\alpha - F^\alpha &= -\frac{1}{2M} R^\alpha_{\beta\gamma\delta} P^\beta (\bar{S}^{\gamma\delta} - S^{\gamma\delta}) + [\text{terms in } \bar{U}_\perp^\alpha] \\ &= M\mathbb{E}^{\alpha\beta} \Delta x_\beta + [\text{terms in } \bar{U}_\perp^\alpha] \end{aligned} \quad (44)$$

where the terms in \bar{U}_\perp^α are of order $\mathcal{O}(S^2)$. Substituting in (42), we obtain

$$\frac{D^2 \Delta x^\alpha}{d\tau^2} = 0 + [\text{terms in } \bar{U}_\perp^\alpha].$$

That is, the worldline deviation of the two solutions reduces to terms involving U_\perp^α (i.e. P_{hid}^α), that we have seen in Sect. 3.1 to be gauge (arising just from the choice of observers relative to which the centroids are computed). This is illustrated in Fig. 5. In particular, if one takes two different solutions of the OKS condition

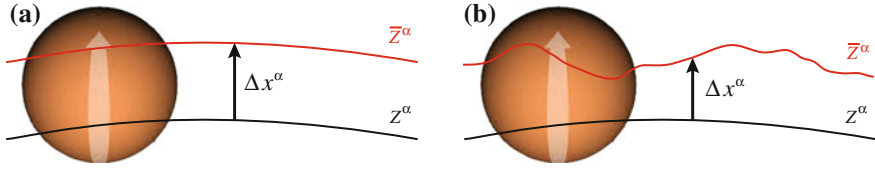


Fig. 5 **a** Two different centroids of the OKS condition move nearly parallel ($D\Delta x^\alpha/d\tau = 0$). In a curved spacetime, that implies that the force $DP^\alpha/d\tau$ along the two worldlines must be different (e.g. if $z^\alpha(\tau)$ is a geodesic, $\bar{z}^\alpha(\bar{\tau})$ cannot be). **b** Centroids $\bar{z}^\alpha(\bar{\tau})$ of other spin conditions accelerate relative to OKS centroids due to the gauge motions induced by the variation of u^α along \bar{z}^α (inertial hidden momentum)

(so that no superfluous motions come into play⁸) we have simply $D^2\Delta x^\alpha/d\tau^2 = 0$, i.e. there is no relative acceleration between the worldlines, which is *guaranteed* by the difference between the forces $F^\alpha = \nabla_{\mathbf{U}} P^\alpha$ and $\bar{F}^\alpha = \nabla_{\bar{\mathbf{U}}} P^\alpha$.

The situation becomes especially enlightening (and the correspondence with the Newtonian theory closer) in the limit of weak *static* fields and slow motion of Sect. 3.4. In this case the *coordinate* acceleration (for a stationary field) of the centroid \bar{z}^α is

$$m \frac{d^2 \bar{z}^i}{d\bar{\tau}^2} = m G^i(\mathbf{z}) + F^i - \frac{D P_{\text{hid}}^i}{d\tau}$$

where \vec{G} is the Newtonian field (more precisely, a fictitious, or “inertial” field, that mimics Newton’s \vec{G} in the coordinate acceleration. Is also known as the “gravitoelectric” field, e.g. [23]). The coordinate acceleration of the centroid \bar{z}^α is

$$m \frac{d^2 \bar{z}^i}{d\bar{\tau}^2} = m G^i(\bar{\mathbf{z}}) + \bar{F}^i - \frac{D \bar{P}_{\text{hid}}^i}{d\bar{\tau}} = m G^i(\bar{\mathbf{z}}) + F^i + m \mathbb{E}^{ij} \Delta x_j - \frac{D \bar{P}_{\text{hid}}^i}{d\bar{\tau}};$$

in the second equality we used (44) neglecting the U_\perp^α terms therein (as they are of order $\mathcal{O}(S^2)$). To first order in $\Delta \mathbf{x}$, $G^i(\bar{\mathbf{z}}) \simeq G^i(\mathbf{z}) + \nabla^j G^i \Delta x_j$; and since, for a stationary field, to linear order (see [23]), $\mathbb{E}_{ij} = -\nabla_j G_i$, then $m G^i(\bar{\mathbf{z}}) + \bar{F}^i = m G^i(\mathbf{z}) + F^i$, i.e. the sum of the spin curvature and the Newtonian forces is the same for both worldlines, the change in one compensating for the other, just like the case with the monopole and dipole forces in the Newtonian problem above, cf. Eq. (39). We have thus

$$m \frac{d^2 \bar{z}^i}{d\bar{\tau}^2} = m G^i(\mathbf{z}) + F^i - \frac{D \bar{P}_{\text{hid}}^i}{d\bar{\tau}} = m \frac{d^2 z^i}{d\tau^2} + \frac{D P_{\text{hid}}^i}{d\tau} - \frac{D \bar{P}_{\text{hid}}^i}{d\bar{\tau}}. \quad (45)$$

⁸Only when $\nabla_{\mathbf{U}} u^\alpha = \nabla_{\bar{\mathbf{U}}} \bar{u}^\alpha = 0$ should one expect two different centroids of the same body to move parallel, even in flat spacetime, as explained in Sect. 3.1 (see also Fig. 2b). Otherwise (i.e. when $P_{\text{hid}}^\alpha \neq 0$) they can have an arbitrary relative motion, cf. Fig. 5.

Hence, barring hidden momentum terms, the coordinate acceleration for $\bar{z}^\alpha(\bar{\tau})$ is the same as for $z^\alpha(\tau)$. This means, in particular, that the different solutions of the OKS condition are trajectories that run parallel (as both the coordinate acceleration and the velocity are the same for all of them).

3.4 Comparison of the Spin Conditions in Simple Examples

In this section we consider the two simple setups illustrated in Fig. 6—a spinning charged body (with $\vec{\mu} = 0$, and whose only non-vanishing electromagnetic moment is q , so that $P_{\text{hid}\tau}^\alpha = 0$) orbiting a Coulomb charge in flat spacetime, and a spinning body orbiting a Schwarzschild black hole, both particles having spin \vec{S} lying in the orbital plane—and compare the description of the motion given by the different spin conditions. Such comparison will be done ensuring that one is dealing with the worldlines of different centroids corresponding to the same physical body (i.e. the same matter distribution $T^{\alpha\beta}(x)$). We will be using the weak field slow motion approximation, for two reasons: first, because it is sufficient to illustrate the effects of interest; second, and more importantly, to make clear that the choice of spin condition (and the resulting hidden momentum) impacts the equations of motion at leading order, and thus these effects must be taken into account in any linearized theory or Post-Newtonian approximation.

3.4.1 Electromagnetic System

The Corinaldesi-Papapetrou (CP) condition, which sets the reference worldline z^α as being center of mass $x_{\text{CM}}^\alpha(u_{\text{lab}})$ measured in the “laboratory” frame (chosen as the congruence of static observers u_{lab}^α , at rest with respect to the source), coincides in this case with one of the solutions of the Ohashi-Kyrian-Semerák (OKS) condition, because such frame is inertial, and therefore $\nabla_{\mathbf{U}} u_{\text{lab}}^\alpha = 0 \Rightarrow P_{\text{hidl}}^\alpha = 0$, cf. Eq. (18). The momentum is thus parallel to the 4-velocity $P^\alpha = mU^\alpha$, and the equation of motion for the centroid reduces to ($Q \equiv$ charge of the source)

$$ma^\alpha = F^\alpha = qF^{\alpha\beta}U_\beta; \quad \vec{F} = q\vec{E}(U) = qQ\frac{\vec{r}}{r^3} + \mathcal{O}(v^2), \quad (46)$$

whose well known solution for a Coulomb field is an ellipse. In particular, a particle with an initial velocity in the xOy plane, and equaling that of a circular orbit, will follow a circular orbit in that plane (regardless of its spin); and a particle with initial radial velocity will move radially, cf. Fig. 6a. To compare with the description given by other centroids (corresponding to other OKS solutions, or to other spin conditions), we note that (i) these have worldlines $\bar{z}^\alpha(\bar{\tau})$ related to $z^\alpha(\tau)$ by (see Eq. (10))

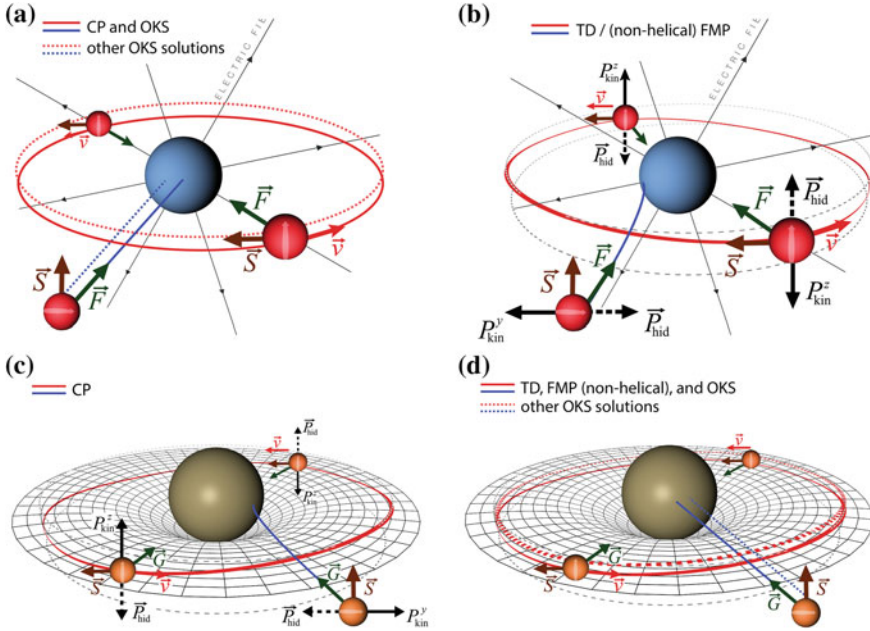


Fig. 6 Comparison of different spin conditions ($S^{\alpha\beta}u_\beta = 0$) in two analogous physical systems: **a–b** A spinning charged particle (but with $\vec{\mu} = 0$) orbiting a Coulomb charge in *flat spacetime*; **c–d** a spinning particle in the Schwarzschild spacetime. The CP condition, $u^\alpha = u^\alpha_{\text{lab}}$, chooses the centroid as measured by the observers at rest in the background (the “laboratory” frame); the FMP condition, $u^\alpha = U^\alpha$, and the TD condition, $u^\alpha = P^\alpha/M$, choose the centroid as measured in the frame comoving, or nearly comoving (respectively) with it. We consider only the *non-helical* FMP solution. In the electromagnetic system, the CP condition yields $Du^\alpha/d\tau = 0 \Rightarrow P^\alpha = mU^\alpha$ (since the laboratory frame is inertial), thus there is no hidden momentum nor exotic motions; trajectories are ellipses and, for particles with initial radial velocity, straight lines, cf. Fig. 6a. For the TD/FMP conditions, Fig. 6b, $Du^\alpha/d\tau \neq 0$ since a force \vec{F} acts on the particle, leading to a hidden momentum $\vec{P}_{\text{hid}} \simeq -\vec{S} \times \vec{F}/m$ that modifies the trajectories. A bobbing is added to the elliptical trajectories due to the oscillation of $\vec{P}_{\text{hid}} = P^z \vec{e}_z$ along the orbit; and instead of a radial motion, the centroid deflects. In the gravitational system the situation is *reversed*: $Du^\alpha/d\tau \approx 0 \Rightarrow P^\alpha_{\text{hid}} \approx 0$ for TD/FMP conditions, and it is for the CP condition (since the laboratory observers are accelerated) that there is a hidden momentum $\vec{P}_{\text{hid}} \simeq \vec{S} \times \vec{G} \neq 0$. The TD/FMP centroids with initial radial velocity move radially, whereas the corresponding CP centroid deflects. \vec{P}_{hid} also induces a bobbing in nearly elliptical orbits (adding to the existing bobbing caused by the spin-curvature force, which is *not* gauge, but has the same form up to a factor of three). In both systems P^α_{hid} and its induced motions are gauged away by the Ohashi-Kyrian-Semerák (OKS) condition; different OKS centroids move nearly parallel to each other.

$$\bar{z}^\alpha = z^\alpha + \Delta x^\alpha; \quad \Delta \vec{x} \simeq \frac{\vec{S} \times \vec{v}}{m}, \quad (47)$$

where \vec{v} is the particle's velocity with respect to the laboratory observers (i.e. $U^\alpha = \gamma(U, u_{\text{lab}}^\alpha)(u_{\text{lab}}^\alpha + v^\alpha)$, cf. Eq. (9)); (ii) the particle's momentum P^α is, to a good approximation, the same for all spin conditions, cf. Appendix “The Case with Electromagnetic Field”; and (iii) regardless of the reference worldline chosen, to the accuracy at hand, the net force on the body is the same, $\vec{F} = \vec{F}$ (unlike one might expect, since the fields are evaluated at different points). Point (iii) is explained by arguments analogous to the ones given in Sect. 3.3 for the Newtonian problem: when one changes z^α the particle's moments change as well; if the particle was a monopole with respect to z^α , then about \bar{z}^α it will have an electric dipole moment $\vec{d} = -q\Delta\vec{x}$, as well as higher order moments. Whereas \vec{F} is just the Coulomb force $\vec{F} = q\vec{E}(\mathbf{z})$, to dipole order $\vec{F} = q\vec{E}(\bar{\mathbf{z}}) + \vec{F}_{\text{dip}}^i$, where $\vec{F}_{\text{dip}}^i = \nabla_j E^i d^j + \mathcal{O}(v^2)$ is the force due to the electric dipole, cf. third term of Eq. (14). Hence

$$\bar{F}^i = qE^i(\bar{\mathbf{z}}) + \bar{F}_{\text{dip}}^i = qE^i(\mathbf{z} + \Delta\mathbf{x}) - q\nabla_j E^i(\mathbf{z} + \Delta\mathbf{x})\Delta x^j \simeq qE^i(\mathbf{z}) = F^i. \quad (48)$$

Therefore, any difference in the acceleration of the two centroids is due solely to the hidden momentum

$$m\bar{a} = \bar{F} - \frac{D\bar{P}_{\text{hid}}}{d\tau} = \vec{F} - \frac{D\vec{P}_{\text{hid}}}{d\tau} = m\vec{a} - \frac{D\vec{P}_{\text{hid}}}{d\tau} \quad (49)$$

This tells us that different solutions of the OKS condition, for which $\bar{P}_{\text{hid}}^\alpha = 0$ (corresponding to the centroids as measured by observers moving with constant velocity with respect to u_{lab}^α), yield different worldlines all (nearly) parallel to the CP solution, since they have the same acceleration, and the same 4-velocity $U^\alpha \parallel P^\alpha$. In particular, other OKS centroids \bar{z}^α corresponding the same physical motion whose description through z^α is radial motion, are non-radial straight lines parallel to z^α ; and the \bar{z}^α 's for which z^α is a circular motion are (non-concentric, in general non-complanar) circles, obtained from the latter by a constant spatial displacement $\Delta\vec{x}$; see Fig. 6a.

The situation is different if one chooses the Frenkel-Mathisson-Pirani (FMP), $u^\alpha = \bar{U}^\alpha$, or the Tulczyjew-Dixon (TD) condition, $u^\alpha = P^\alpha/M$, which pick as representative point the centroid as measured in the frame comoving, or nearly comoving, respectively, with it. Since a force acts on the particle (implying $DP^\alpha/d\tau \neq 0$ and $\bar{a}^\alpha \neq 0$), it follows that $Du^\alpha/d\tau \neq 0$ and $P_{\text{hid}}^\alpha \neq 0$, and therefore P^α is not parallel to \bar{U}^α , cf. Eqs. (28) and (30). From Eq. (28) (and noting from (29) that $M = m + \mathcal{O}(S^2)$), we have for the TD condition

$$P^\alpha = m\bar{U}^\alpha + \frac{S^{\alpha\beta}}{m}F_\beta + \mathcal{O}(S^2) = m\bar{U}^\alpha + \frac{1}{m}\epsilon_{\gamma\delta}^{\alpha\beta}F_\beta S^\gamma \bar{U}^\delta + \mathcal{O}(S^2). \quad (50)$$

This corresponds also to the momentum of the *non-helical* FMP solution. In order to see that, first take (50) as an ansatz, and observe it obeys, to the accuracy at hand, the FMP equations of motion. Namely, substituting (50) in the explicit equation for the acceleration⁹ (37), one gets

$$\bar{a}^\alpha = \frac{1}{S^2} \left(\frac{1}{m} F^\mu S_\mu S^\alpha - \frac{S_\gamma^\beta}{m} F_\beta S^{\alpha\gamma} \right) + \mathcal{O}(S) = \frac{F^\alpha}{m} + \mathcal{O}(S) \quad (51)$$

(in the second equality we noted that since $S_\gamma^\beta S^{\alpha\gamma} = S^\alpha S^\beta - (h^U)^{\alpha\beta} S^2$ and $F^\alpha U_\alpha = 0$, it follows that $-S_\gamma^\beta S^{\alpha\gamma} F_\beta / S^2 = F_\perp^\alpha \equiv$ projection of F^α orthogonal to S^α); then, substituting (51) in (30), leads consistently to (50). Equation (51) states that the acceleration comes, in first approximation (i.e. to zeroth order in S), from the force F^α , which is what one expects for a non-helical solution (and the rationale for taking (50) as an ansatz for (30)). Note from Eq. (34) that, for a free particle in flat spacetime, the acceleration of the helical motions is $a = \gamma^2 v M / S = \mathcal{O}(S^{-1}) \neq \mathcal{O}(S)$. The helices are effectively precluded from moment we impose $P^\alpha \simeq m \bar{U}^\alpha + S^{\alpha\beta} F_\beta / m$.

We can therefore write for the inertial hidden momentum of both the TD or (non-helical) FMP conditions

$$P_{\text{hidI}} \simeq \frac{1}{m} \epsilon^{\alpha\beta}_{\gamma\delta} F_\beta S^\gamma \bar{U}^\delta. \quad (52)$$

This hidden momentum leads to exotic motions of the centroid. From Eq. (49),

$$\begin{aligned} m \bar{\ddot{a}} &= m \ddot{a} - \frac{D \vec{P}_{\text{hid}}}{d\tau} = m \ddot{a} + \frac{1}{m} \vec{S} \times \vec{F}_I \bar{v}^I + \mathcal{O}(v^2) \\ &= m \ddot{a} + \frac{qQ}{m} \frac{1}{r^3} \left(\vec{v} \times \vec{S} - 3 \frac{(\vec{v} \cdot \vec{r}) \vec{r} \times \vec{S}}{r^2} \right). \end{aligned} \quad (53)$$

Here $\vec{r} = x \vec{e}_x + y \vec{e}_y$, since $\vec{F} (= \vec{\bar{F}})$ is the Coulomb force in the $x_O y$ plane.

Nearly circular motion.—Let us start by the motion above whose description through z^α (i.e. through the laboratory frame centroid, given by the CP/OKS conditions) was a circular motion in the $x_O y$ plane. Since we assume that \vec{S} lies on the $x_O y$ plane, it follows that $\vec{P}_{\text{hidI}} = P_{\text{hidI}} \vec{e}_z$,

$$P^x = m \bar{v}^x = m v^x; \quad P^y = m \bar{v}^y = m v^y; \quad P^z = m \bar{v}^z + P_{\text{hidI}}$$

(where we noted that since P^α is the same regardless of the spin condition, the components of the centroid velocity in the $x_O y$ plane are the same as for the CP condition: $\bar{v}^x = v^x$, $\bar{v}^y = v^y$). Therefore, $\vec{v} \cdot \vec{r} = 0$, $m \bar{a}^x = m a^x = F^x$, $m \bar{a}^y = m a^y = F^y$, and

⁹In [13], where Eq. (37) was originally derived, F^α was taken to be the spin-curvature force (40); it is however easy to check, following the derivation therein, that it holds for an arbitrary force, as long as Eq. (30) holds.

$$m\ddot{a}^z = \frac{qQ}{m} \frac{1}{r^3} (\vec{v} \times \vec{S})^z, \quad (54)$$

cf. Eq. (53). Thus, the projection of the motion in the $x_O y$ plane is circular, identical to z^α ; and since \vec{S} is constant to this accuracy,¹⁰ \ddot{a}^z oscillates between positive and negative values along the orbit, leading to a bobbing motion, depicted in Fig. 6b. This bobbing can easily be understood as follows. The particle's total momentum along z is constant (since there is no force along z , $DP^z/d\tau = 0$), and equal to zero, as one can see (since P^α is the same) from the results above of the CP/OKS conditions. On the other hand, from Eq. (52), there is a hidden momentum along z , $P_{\text{hid}}^z = -(\vec{S} \times \vec{F})^z/m$, oscillating along the orbit (from $P_{\text{min}}^z = -SF/m$ to $P_{\text{max}}^z = +SF/m$); this means that the centroid bobs up and down in order for the kinetic momentum $m\vec{v}^z$ to cancel out P_{hid}^z , keeping $P^z = 0$. Without loss of generality, we may take $\vec{S} = S\vec{e}_x$, $v^y = v \cos \omega\tau$, and thus $(\vec{v} \times \vec{S})^z = -vS \cos \omega\tau$; integrating $\ddot{z} = \ddot{a}^z$, Eq. (54), and noticing that $m\omega^2 r = Qq/r^2$ (as the motion is circular in the $x_O y$ plane), we obtain $z = (vS/m) \cos \omega\tau$, describing oscillations of half amplitude vS/m .

Nearly radial motion.—As we have seen above, for the CP or the OKS conditions, it follows from Eq. (46) that a particle with radial initial velocity will move radially, regardless of its spin. Take the case that the particle is dropped from rest at some point on the x axis; it will move in straight line along x towards the source, and we thus have that $P^y = P^z = 0$, $P^x = P$. Take \vec{S} to be along z . For the FMP or the TD conditions the situation is different; there is a hidden momentum, given by Eq. (52),

$$\vec{P}_{\text{hid}} = -\frac{1}{m} \vec{S} \times \vec{F} = \frac{1}{m} SF \vec{e}_y$$

(increasing as the particle approaches the source, since F increases), which causes the centroid to deflect in the negative y direction, in order to keep $P^y = P_{\text{hid}}^y + m\bar{U}^y = 0$. This is depicted in Fig. 6b.

3.4.2 Gravitational System

In the gravitational case, the situation is reversed in comparison to the electromagnetic system: now it is the “laboratory frame” (i.e. the observers at rest in the background) which is accelerated, therefore $\nabla_U u_{\text{lab}}^\alpha \neq 0$ and $P^\alpha \nparallel U^\alpha$ when the centroid is computed in such frame, cf. Eq. (27); and it is when the centroid is computed in the comoving (FMP condition) or nearly comoving frame (TD condition) that we have $P^\alpha \simeq mU^\alpha$, since the only force present is the spin curvature force (40), which yields a $\mathcal{O}(S^2)$ contribution to the hidden momentum, cf. Eq. (50). This is what we are now going to see in detail.

¹⁰Since $\tau^{\alpha\beta} = 0$, S^α is Fermi-Walker transported for the MP condition, Eq. (35), and approximately so for the TD condition (cf. Eq. (7.11) of [26]); since Eq. (54) is of first order in v , \vec{S} can be taken constant therein.

As we have seen in Sect. 3.3, the force (40) depends explicitly on the spin condition. For the FMP and the TD conditions, it can be written to lowest order as [24]

$$\bar{F}^i = -2\epsilon_{jkl}v^k G^{l,i} S^j + \epsilon_{lj}^i G^l_{,k} v^k S^j \simeq m\bar{a}^i, \quad (55)$$

where $\vec{G} = -m_S \vec{r}/r^3$ is the Newtonian (or gravitoelectric) field evaluated at \bar{z}^α , m_S is the mass of the Schwarzschild black hole, and in the second equality we used $\vec{P} = m\vec{U} + \mathcal{O}(S^2) \Rightarrow m\bar{a} \simeq \vec{F}$, as follows from (50). Explicitly:

$$m\bar{a} \simeq \vec{F} = -\frac{3m_S}{r^3} \left[\vec{v} \times \vec{S} + \frac{2\vec{r}[(\vec{v} \times \vec{r}) \cdot \vec{S}]}{r^2} + \frac{(\vec{v} \cdot \vec{r})\vec{S} \times \vec{r}}{r^2} \right]. \quad (56)$$

Notice the first term, formally analogous to the first term of (53), which caused the bobbing in the electromagnetic system; but note as well that despite the similarity, they have very different origins: the latter comes from the inertial hidden momentum, whereas the former comes from the spin-curvature force.

The coordinate acceleration is given by the sum of $m\bar{a}$ with the (radial) Newtonian “force” $m\vec{G}$,

$$m \frac{d^2 \bar{z}^i}{d\bar{\tau}^2} = mG^i(\bar{\mathbf{z}}) + \bar{F}^i.$$

For the CP condition the situation is different, because this is now the case where the field $u^\alpha = u^\alpha_{\text{lab}}$ (relative to which the centroid is computed) is not parallel transported along $z^\alpha(\tau)$, $\nabla_U u^\alpha_{\text{lab}} \neq 0$; therefore there is hidden momentum (cf. Eqs. (18) and (27)):

$$P_{\text{hid}}^\alpha = -(h^U)^\alpha_\sigma S^\sigma G^\beta = -(h^U)^\alpha_\sigma \epsilon^\sigma_{\beta\gamma\delta} G^\beta S^\gamma u^\delta_{\text{lab}} \Rightarrow \vec{P}_{\text{hid}} \simeq \vec{S} \times \vec{G}. \quad (57)$$

The spin-curvature force takes also a different form with this condition,

$$F^i = -\epsilon_{jkl}v^k G^{l,i} S^j + \epsilon_{lj}^i G^l_{,k} v^k S^j \quad (58)$$

(notice the relative factor of 2 comparing the first terms of (55) and (58)). The latter difference however is compensated by the difference between $\vec{G}(\mathbf{z})$ and $\vec{G}(\bar{\mathbf{z}})$, as explained in Sect. 3.3: $G^i(z) \simeq G^i(\bar{z}) - G^{i,j} \Delta x_j$, with $\Delta \vec{x} = \vec{S} \times \vec{v}/m$, cf. Eq. (47); that is, $G^i(z) \simeq G^i(\bar{z}) - \epsilon_{jkl} S^j v^k G^{l,i}/m$, and therefore $mG^i(\mathbf{z}) + F^i = mG^i(\bar{\mathbf{z}}) + \bar{F}^i$. The coordinate acceleration is thus given by

$$m \frac{d^2 z^i}{d\tau^2} = mG^i(\mathbf{z}) + F^i - \frac{DP_{\text{hid}}^i}{d\tau} = m \frac{d^2 \bar{z}^i}{d\bar{\tau}^2} - \frac{DP_{\text{hid}}^i}{d\tau}. \quad (59)$$

That is, the coordinate acceleration of the CP worldline $z^\alpha(\tau)$ differs from that of the worldline $\bar{z}^\alpha(\bar{\tau})$ of the TD/FMP conditions only by the hidden momentum term involved in the former. From (57) we have

$$\frac{DP_{\text{hid}}^i}{d\tau} \simeq P_{\text{hid},i}^\alpha v^i = \epsilon^i_{jl} S^j G^l_{,k} v^k = \frac{m_S}{r^3} \left(\vec{v} \times \vec{S} + 3 \frac{(\vec{v} \cdot \vec{r}) \vec{S} \times \vec{r}}{r^2} \right) \quad (60)$$

where we used the fact that, to this accuracy, $D\vec{S}/d\tau \approx 0$.

Nearly circular motion.—As in the electromagnetic case, we assume $\vec{S} \in xoy$, and so, for a nearly circular orbit, $(\vec{v} \times \vec{r}) \cdot \vec{S} \simeq 0$, $\vec{v} \cdot \vec{r} \simeq 0$; therefore, the second term of (56) and the last term of (56) and (60) vanish. We have thus for the FMP and TD conditions

$$m \frac{d^2 \bar{z}}{d\bar{\tau}^2} = m G^z(\bar{\mathbf{z}}) - \frac{3m_S}{r^3} (\vec{v} \times \vec{S})^z,$$

and for the CP condition

$$m \frac{d^2 z}{d\tau^2} = m \frac{d^2 \bar{z}}{d\bar{\tau}^2} - \frac{m_S}{r^3} (\vec{v} \times \vec{S})^z.$$

Both coordinate accelerations oscillate along the orbit, due to the terms $\vec{v} \times \vec{S}$ (since \vec{S} is approximately constant), leading to a bobbing motion depicted in Fig. 6c, d. Hence, by contrast with the electromagnetic system, in this case a bobbing is present regardless of the spin condition (or the presence of hidden momentum); it is just larger for the CP condition, because the contribution for the bobbing from the hidden momentum adds to the bobbing caused by the spin-curvature force (they have the same form, only different factors).

Nearly radial motion.—For a particle in radial motion in Schwarzschild space-time, the spin-curvature force under the FMP/TD conditions is *exactly* zero, $\bar{F}^\alpha = \nabla_{\bar{U}} P^\alpha = 0$, as shown in [24] (in the weak field and slow motion regime, one can check that from Eq. (56) above, by noting that the second term is zero, and the first and third terms cancel out when $\vec{r} \parallel \vec{v}$). The hidden momentum is also exactly zero for the TD and the non-helical FMP solutions, so $P^\alpha = m\bar{U}^\alpha$, and thus $D\bar{U}^\alpha/d\bar{\tau} = 0$. When dropped from rest, the particle moves along a geodesic towards the source. Take the motion to be along the x axis, so that $P^y = P^z = 0$, $P^x = P$, and take \vec{S} along z .

For the worldline $z^\alpha(\tau)$ given by the CP condition, there will be a non-vanishing spin-curvature force, cf. Eq. (44); which, as shown above and in Sect. 3.3, just compensates for the difference in the Newtonian field \vec{G} on the two worldlines, so that the coordinate acceleration differs only due to the hidden momentum terms, cf. Eqs. (45) and (59). Since the momentum P^α is the same regardless of the spin condition, the hidden momentum (57) that arises with this spin condition causes the centroid z^α to deflect in the y direction as it approaches the source, in order to keep

$$P^y = mU^y + (\vec{S} \times \vec{G})^y = 0,$$

just like the situation in the electromagnetic system for the FMP and the TD condition. This is depicted in Fig. 6c. Hence, the situation is *opposite* to the electromagnetic

analogue: for the FMP and TD conditions we have no hidden momentum, and \bar{z}^α has straight line radial motion; for the CP condition there is hidden momentum and a centroid that deflects from radial motion.

Finally, if one takes solutions $z'^\alpha(\tau')$ of the OKS condition, other than the one that (to this accuracy) coincides with the centroid z^α of the FMP and TD conditions, we have, from (45), $d^2 z'^i / d\tau'^2 = d^2 \bar{z}^i / d\bar{\tau}^2$, and thus $z'^\alpha(\tau')$ are curves that run approximately parallel to the trajectories of the TD/FMP (non-helical) conditions.

3.5 Hidden Momentum Arising from the “Torque” Tensor $\tau^{\alpha\beta}$

In this section we briefly discuss the hidden momentum (19) that is related to the torque tensor $\tau^{\alpha\beta}$. It is useful to split

$$\tau^{\alpha\beta} = \tau_{\text{DEM}}^{\alpha\beta} + \tau_{\text{QEM}}^{\alpha\beta} + \tau_{\text{QG}}^{\alpha\beta} + \dots \quad (61)$$

where [11]

$$\tau_{\text{DEM}}^{\alpha\beta} = 2\mu^{\theta[\beta} F^{\alpha]}_{\theta} + 2d^{[\alpha} F^{\beta]}_{\gamma} U^\gamma \quad (62)$$

is the electromagnetic dipole torque, $\tau_{\text{QEM}}^{\alpha\beta}$ and $\tau_{\text{QG}}^{\alpha\beta}$ are, respectively, the quadrupole electromagnetic and gravitational torques (the lowest order torque in the gravitational case), see [24] for the explicit expressions. All these torques (plus the higher order ones) will contribute to the momentum via Eqs. (17)–(19). A hidden momentum $P_{\text{hid}\tau}$ is originated whenever $\tau^{\alpha\beta}$ has a component along the vector field u^α , cf. Eq. (19), and it may be cast into two parts: a part which is pure gauge like the inertial hidden momentum P_{hidI}^α (comes from the choice of the reference worldline $z^\alpha(\tau)$; may be made to vanish by suitable choices), and another part, which arises in some physical systems, that is not gauge. Let us discuss these two subtypes of hidden momentum separately.

3.5.1 The Pure Gauge Hidden Momentum that Arises from $\tau_{\alpha\beta}$

This contribution is easier to understand if we think about a simple example. Consider a spinning particle in flat spacetime as depicted in Fig. 1, with no forces ($DP^\alpha/d\tau = 0$), but now under a torque. Consider moreover $\tau^{\alpha\beta}$ to be spatial and orthogonal¹¹ to P^α : $\tau^{\alpha\beta} P_\beta = 0$. In this case, just like for a torque-free particle, the centroid $x_{\text{CM}}^\alpha(P)$ (“ x_{CM} ” in Fig. 1), given by the condition $S^{\alpha\beta} P_\beta = 0$, is *at rest* in the $P^i = 0$ frame (note that $P^\alpha \parallel U^\alpha$ for the reference worldline $z^\alpha = x_{\text{CM}}^\alpha(P)$, as follows from Eq. (16) with $u^\alpha = P^\alpha/M$). Since $x_{\text{CM}}^\alpha(P)$ is unaffected by the torque,

¹¹E.g. the torque on an electric dipole in an uniform electromagnetic field, when z^α is the common centroid given by the TD or the (non-helical) FMP condition.

it remains at rest at the body's geometrical center, regardless of the fact that the spin of the particle is varying. Now consider another *inertial* observer (4-velocity \bar{u}^α) moving with respect to the $P^i = 0$ frame with *constant* velocity \bar{v} (so that $D\bar{u}^\alpha/d\tau = 0$, ensuring that no inertial hidden momentum comes into play); not only the centroid $x_{\text{CM}}^\alpha(\bar{u})$ it measures is shifted to the right relative to $x_{\text{CM}}^\alpha(P)$, as depicted in Fig. 1, *as the shift (10)–(12) also varies*, since S_\star^α varies due to the torque:

$$\frac{D\Delta x^\alpha}{d\tau} = -\frac{1}{m(\bar{u})} \frac{DS_\star^{\alpha\beta}}{d\tau} \bar{u}_\beta = -\frac{1}{m(\bar{u})} \tau^{\alpha\beta} \bar{u}_\beta \quad (63)$$

(i.e. the body's rotation velocity varies, causing Δx^α to vary). This means that the centroid $\bar{z}^\alpha = x_{\text{CM}}^\alpha(\bar{u})$ will be moving in the $P^i = 0$ frame; i.e. its 4-velocity $\bar{U}^\alpha = d\bar{z}^\alpha/d\bar{\tau}$ will have a component orthogonal to P^α , which reads (in this special case that $DP^\alpha/d\tau = 0$, so that Eq. (24) holds) $\bar{U}_\perp^\alpha = D\Delta x^\alpha/d\bar{\tau}$.

In the general case when there are forces acting on the particle, however, as already mentioned in Sect. 3.2, one should not think of \bar{U}_\perp^α as the velocity of the centroid \bar{z}^α relative to $z^\alpha = x_{\text{CM}}^\alpha(P)$, because the latter is *not* at rest in the $P^i = 0$ frame. The general argument should be given instead as: *the position of the centroid $\bar{z}^\alpha = x_{\text{CM}}^\alpha(\bar{u})$ as measured by a given observer \bar{u}^α depends on the body's angular momentum; when the latter varies due to the action of a torque, $x_{\text{CM}}^\alpha(\bar{u})$ moves accordingly; P^α , however, is unaffected, leading to $P^\alpha \nparallel U^\alpha$. The general (with $D\bar{u}^\alpha/d\tau = 0$) expression for \bar{U}_\perp^α formalizing this statement follows from Eqs. (16) and (22)¹²:*

$$\bar{U}_\perp^\alpha = -\frac{1}{m(\bar{u})} (h^P)_\sigma^\alpha \bar{\tau}^{\sigma\beta} \bar{u}_\beta. \quad (64)$$

Finally, if $U_\perp^\alpha \neq 0$, then $P_{\text{hid}}^\alpha \neq 0$ —i.e. when the centroid moves in the $P^i = 0$ frame, the momentum P^i is not zero in the centroid frame (the $\bar{U}^i = 0$ frame); thus there is hidden momentum, the two effects being reciprocal (and mere consequences of the fact that $P^\alpha \nparallel \bar{U}^\alpha$), cf. Eq. (25).

3.5.2 “Dynamical” Hidden Momentum

In general, the momentum of a multipole particle subject to electromagnetic and gravitational fields is not parallel to its 4-velocity regardless of the spin condition; that happens when $\tau^{\alpha\beta}$ is not a spatial tensor (i.e. when $\tau^{\alpha\beta}u_\beta \neq 0$ for all unit timelike vectors u^β), and is related to a type of hidden momentum which occurs in some physical systems and is *not* gauge. Following [17], we dub this part of $P_{\text{hid}\tau}^\alpha$ the “dynamical” hidden momentum. To dipole order, it arises in magnetic dipoles;

¹²To obtain (63) from (64) in the special case above, one uses $d\tau = \gamma(\bar{U}, P)d\bar{\tau}$ to write $\bar{U}_\perp^\alpha = \gamma(\bar{U}, P)D\Delta x^\alpha/d\tau$, computes $D\bar{S}^{\alpha\beta}/d\bar{\tau}$ from (43) using (15) to obtain $\bar{\tau}^{\alpha\beta} = \gamma(\bar{U}, P)\tau^{\alpha\beta}$, and finally uses the assumption above $\tau^{\alpha\beta}P_\beta = 0 \Rightarrow (h^P)_\sigma^\alpha \bar{\tau}^{\sigma\beta} = \bar{\tau}^{\alpha\beta}$.

let us then consider the case when $\tau^{\alpha\beta} = 2\mu^{\theta[\beta}F^{\alpha]}$ in Eqs. (61) and (62). Take the magnetic dipole moment to be proportional to the spin, $\mu^{\alpha\beta} = \sigma S^{\alpha\beta}$; we have from (19), for an arbitrary spin condition $S^{\alpha\beta}u_\beta = 0$,

$$P_{\text{hid}\tau}^\alpha = -\frac{1}{\gamma(u, U)}(h^U)^\alpha_\sigma \mu^{\sigma\beta}(E^u)_\beta \equiv P_{\text{hidEM}}^\alpha,$$

where $(E^u)^\alpha = F^\alpha_\beta u^\beta$. If $(E^u)^\alpha \nparallel \mu^\alpha$, P_{hidEM}^α can never be zero, because then $\mu^{\beta\sigma}(E^u)_\beta \neq 0$ and is a space-like vector, thus cannot be parallel to any U^α . For the FMP condition ($u^\alpha = U^\alpha$), P_{hidEM}^α takes the suggestive form

$$P_{\text{hidEM}}^\alpha = -\mu^{\alpha\beta}E_\beta = \epsilon^\alpha_{\beta\gamma\delta}\mu^\beta E^\gamma U^\delta, \quad (65)$$

where $E^\alpha = F^\alpha_\beta U^\beta$ is the electric field *as measured in the centroid frame*. In such frame, and in vector notation, $\vec{P}_{\text{hidEM}} = \vec{\mu} \times \vec{E}$, which is the most usual form in the literature for the hidden momentum that a magnetic dipole acquires under an external electromagnetic field (e.g. [19–22]). It equals *minus* the electromagnetic field momentum \vec{P}_\times generated by a magnetic dipole when placed in the external electromagnetic field, which, in the particle's frame, reads (see e.g. [19, 22, 24]) $\vec{P}_\times = \int \vec{E} \times \vec{B}_{\text{dipole}} = -\vec{\mu} \times \vec{E}$. It should however be noted that \vec{P}_{hidEM} is *not* field momentum; it is *purely mechanical in nature*, which can be understood through simple models, see e.g. [19, 22] (in particular Fig. 9 of [22]). Such momentum plays an important role in the conservation laws. Consider, for example, a magnetic dipole *at rest* in an external electric field; since no force is exerted on the particle, the setup is *stationary*; it follows from the conservation equations $(T_{\text{tot}})^{\alpha\beta}_{;\beta} = 0$ that the total spatial momentum $\vec{P}_{\text{tot}} \equiv \vec{P}_{\text{matter}} + \vec{P}_{\text{EM}}$ (i.e. the matter momentum plus the field momentum) must vanish. The momentum of the electromagnetic field, $\vec{P}_{\text{EM}} = \vec{P}_\times$, however, is not zero; it is the momentum $\vec{P}_{\text{matter}} = \vec{P}_{\text{hidEM}} = -\vec{P}_{\text{EM}}$, hidden in the dipole, that cancels out \vec{P}_{EM} , ensuring $\vec{P}_{\text{tot}} = 0$, as required by the conservation laws.

P_{hidEM}^α also leads to exotic motions, quite analogous to the ones coming from the inertial hidden momentum studied in Sect. 3.4, as one would expect from the formal analogy between (65) and the inertial hidden momentum under this spin condition, $P_{\text{hidI}}^\alpha = -\epsilon^\alpha_{\beta\gamma\delta}S^{\beta\gamma}a^\delta U^\delta$, cf. Eq. (30). Indeed, if in the application in Fig. 6a, b we considered particles with dipole moment $\mu^\alpha = \sigma S^\alpha \neq 0$, there would be a bobbing (in addition to the one caused by P_{hidI}^α) for a particle orbiting the source, and, in the case of a particle in *initially* radial motion, there would be a sideways dipole force on it, but due to P_{hidEM}^α the particle's sideways acceleration would actually be *opposite* to the force. This effect is discussed in detail in [24]. However, a crucial difference exists between these effects and the effects discussed in the previous sections: the hidden momentum in Eq. (65) is *not* gauge, nor the motions generated by it are (in general) made to vanish by any choice of center of mass.

4 Conclusion

In this paper we have discussed and compared in detail the different spin supplementary conditions in the literature, with special attention being given to the lesser-studied (but potentially useful) Corinaldesi-Papapetrou (CP) and Ohashi-Kyrian-Semerák (OKS) spin conditions. One of the main points is that the different solutions allowed by the different spin conditions are equivalent descriptions of the motion of a given body. We have shown this equivalence to pole-dipole order, explaining the change of the spin-curvature force under the different conditions—which is seen to be precisely what ensures the consistency of the different solutions, as it has the magnitude needed to prevent the worldlines from deviating due to tidal effects of a curved spacetime. This builds up on the work in [16] (dealing with free particles in flat spacetime) and backs the claims in [13] about the equivalence of all spin conditions in a curved spacetime.

We clarified the origin of the non-parallelism between U^α and P^α , which can be cast as the particle possessing a “hidden momentum”, a concept introduced in General Relativity in [17], and further developed herein. It consists of two main parts: an “inertial” part P_{hidI}^α that arises solely from the spin condition (i.e. from the choice of the observers relative to which the center of mass is measured), which we therefore cast as gauge, and another term $P_{\text{hid}\tau}^\alpha$ arising from the torque tensor $\tau_{\alpha\beta}$, which generically sub-divides into a part that again is gauge (arising from the motion of the centroid measured by *some* observers that is induced when $S^{\alpha\beta}$ varies due to $\tau_{\alpha\beta}$), and a “dynamical” part, which is not gauge. The latter, to dipole order, consists of a form of hidden momentum that arises in electromagnetic systems, and was previously known from treatments in classical electrodynamics.

The differences between the various spin conditions were discussed and illustrated with suitable examples; in particular the reciprocity (first noted in [17]) that exists when one compares spinning particles under an electromagnetic field in flat spacetime to spinning particles in a gravitational field: in the first case, when one picks the centroid as measured in the Laboratory frame (corresponding to the CP/OKS conditions), there is no inertial hidden momentum, $P_{\text{hidI}}^\alpha = 0$, and thus (if $P_{\text{hid}\tau}^\alpha = 0$) the momentum velocity relation is simply $P^\alpha = mU^\alpha$; and when one computes the center of mass in the comoving frame (FMP/TD conditions), P^α is no longer parallel to U^α , leading to exotic motions (like bobbings). In the gravitational case the situation is reversed: when one chooses the TD or the (non-helical) FMP conditions, P^α is approximately parallel to U^α ; and it is when one chooses the Laboratory centroid (CP condition) that hidden momentum arises.

All the spin conditions studied present interesting features. The CP condition yields a natural description, as it amounts to compute the centroid in the same frame where the motion is observed (the “Laboratory” frame, which is given in advance); it leads however to considerable superfluous motions in gravitational systems. The TD condition defines always an unique center of mass, which is the central worldline of the worldtube of centroids (can thus be thought of as describing the “bulk” motion of such worldtube). The FMP condition yields the most natural transport law for the

spin vector, and also gives rise to exact gravito-electromagnetic analogies (see [24]); however it is not always easy to single out the non-helical solution from the (infinite) helical solutions allowed by this condition (the latter should be avoided, as they are but unnecessarily complicated descriptions of the motion, as discussed in Sect. 3.2.3), and no general prescription for that is known. As for the OKS condition, it always gauges away the inertial hidden momentum and its induced motions, ensuring the simplest equations for the centroid motion; in the absence of torques, one has $F^\alpha = ma^\alpha$, i.e. these are Newtonian-like (or “dynamical”) centroids, which accelerate only if there is a force.

It is however crucial to notice that in spite of the equivalence of the descriptions, and the fact that the trajectories of the different spin conditions are contained within the (convex hull of the) body’s worldtube, their differences, and the superfluous motions induced by some of them are not negligible (even in weak field, slow motion approximations), and should not be overlooked. As it is also important to distinguish these motions from the physical effects. For, as we have exemplified in Sect. 3.4, the pure gauge contribution to the centroid acceleration with the CP condition is of the same order of magnitude as the one from the spin-curvature force itself; and it can actually be much larger, as is the case of the acceleration of the outer helical solutions of the FMP condition, which can be made arbitrarily large.

Acknowledgments We thank the participants of the 524 WE-Heraeus-Seminar for the enlightening discussions that helped shape this work. We thank also O. Semerák for useful correspondence, and Rui Quaresma (quaresma.rui@gmail.com) for his assistance in the illustrations. L.F.C. is funded by FCT through grant SFRH/BDP/85664/2012.

Momentum and Angular Momentum in Curved Spacetime

In rectangular coordinates in flat spacetime, the momenta P^α and $S^{\alpha\beta}$ of an extended body, as measured by some observer of 4-velocity u^α , are well defined by the integrals

$$P^\alpha = \int_{\Sigma(z,u)} T^{\alpha\beta} d\Sigma_\beta; \quad S^{\alpha\beta} = 2 \int_{\Sigma(z,u)} r^{[\alpha} T^{\beta]\gamma} d\Sigma_\gamma,$$

where $\Sigma(z, u)$ is the hyperplane orthogonal to u^α (the rest space of u^α), and $r^\alpha = x^\alpha - z^\alpha$ is the vector connecting the reference worldline z^α to the point of integration x^α . In curved spacetime the situation is different, as these integrals amount to summing tensors defined at different points; different generalizations of the flat spacetime notions have been proposed in the literature (e.g. [11, 25, 26]), none of them seeming a priori more natural than the others. Herein we discuss the mathematical meaning of the definitions used in this work, and how they relate to the schemes by Dixon [11, 26].

All schemes agree on generalizing $\Sigma(z, u)$ by the *geodesic* hypersurface orthogonal to u^α , and on replacing r^α by the vector $\mathbf{X} \in \mathcal{T}_z$ tangent to the geodesic connecting

z^α and x^α , and whose length equals that of the geodesic. That is, $\mathbf{X} = \Phi(x)$, where $\Phi \equiv \exp_z^{-1}$ is the *inverse* exponential map, mapping points in the spacetime manifold to vectors in the tangent space \mathcal{T}_z , $\Phi : \mathcal{M} \rightarrow \mathcal{T}_z$. Where the schemes differ is in the way the vector $\mathcal{A}^\alpha \equiv T^{\alpha\beta} d\Sigma_\beta$ is integrated. We adhere to the scheme proposed in [25]: using the natural map for tensors induced by \exp_z to pull back the energy-momentum tensor and the volume element to \mathcal{T}_z , and integrate therein, which is then a well defined tensor operation. Let $\Omega^{\hat{\alpha}}$ denote an orthonormal co-frame on \mathcal{T}_z ; the moments can then be written in the manifestly covariant form

$$\mathbf{P}(\Omega^{\hat{\alpha}}) = \int_{\Sigma(z,u)} \mathbf{T}(\Phi^* \Omega^{\hat{\alpha}}, d\Sigma) ; \quad (66)$$

$$\mathbf{S}(\Omega^{\hat{\alpha}}, \Omega^{\hat{\beta}}) = 2 \int_{\Sigma(z,u)} \mathbf{X}(\Omega^{[\hat{\alpha}}) \mathbf{T}(\Phi^* \Omega^{\hat{\beta}]}, d\Sigma). \quad (67)$$

Note that since $\mathbf{T}(\Phi^* \Omega^{\hat{\alpha}}, d\Sigma) = (\exp_z^* \mathbf{T})(\Omega^{\hat{\alpha}}, \exp_z^* d\Sigma)$, one is indeed pulling back the integrands from \mathcal{M} to \mathcal{T}_z . Note also that Eqs. (66) and (67) are *equivalent* to (1) and (2), i.e. they just amount to perform the integration in a system of Riemann normal coordinates $\{x^{\hat{\alpha}}\}$ centered at z^α (the coordinates naturally adapted to the exponential map). This is because such system is constructed from geodesics radiating out of z^α ; thus the components of \mathbf{X} , in global Lorentz coordinates in \mathcal{T}_z , are equal to the coordinates $x^{\hat{\alpha}}$ on \mathcal{M} ; also the basis 1-forms of such system are the pullbacks of $\Omega^{\hat{\alpha}}$ to \mathcal{M} , $dx^{\hat{\alpha}} = \Phi^* \Omega^{\hat{\alpha}}$; and, taking it comoving with u^α (i.e., at z , $\partial_0 = \mathbf{u}$), $\Sigma(z, u)$ coincides with the spatial hypersurface $x^{\hat{0}} = 0$.

Let us now compare these definitions with other schemes in the literature. In [11], P^α and $S^{\alpha\beta}$ are defined as

$$P_{\text{Dix}}^\kappa = \int_{\Sigma(z,u)} \bar{g}_\alpha{}^\kappa T^{\alpha\beta} d\Sigma_\beta; \quad S_{\text{Dix}}^{\kappa\lambda} = -2 \int_{\Sigma(z,u)} \sigma^{[\kappa} \bar{g}_\alpha{}^{\lambda]} T^{\alpha\beta} d\Sigma_\beta, \quad (68)$$

where $\sigma^\kappa(x, z) = -(\Phi(x))^\kappa = -X^\kappa$, cf. [44]. These definitions thus differ from (66) and (67) only in the way the vector $\mathcal{A}^\alpha \equiv T^{\alpha\beta} d\Sigma_\beta$ is integrated: $\bar{g}_\alpha{}^\kappa$ is a bitensor which parallel transports \mathcal{A}^α at x^α to z^κ along the geodesic connecting the two points, so that the integral is performed over vectors $\mathcal{A}^\kappa|_z = \bar{g}_\alpha{}^\kappa \mathcal{A}^\alpha|_x$ defined at z^κ (in [26, 44] different propagators, $K_\alpha{}^\kappa, H_\alpha{}^\kappa$ in the notation therein, are employed; the two schemes are not equivalent though, as noted in [26]). Writing $\bar{g}_{\hat{\beta}}{}^{\hat{\alpha}} \mathcal{A}^{\hat{\beta}}|_x = \mathcal{A}^{\hat{\alpha}}|_x + \Delta \mathcal{A}^{\hat{\alpha}}$, with $\Delta \mathcal{A}^{\hat{\alpha}} = - \int_x^z \Gamma_{\hat{\beta}\hat{\gamma}}^{\hat{\alpha}}(x') \mathcal{A}^{\hat{\beta}} dx'^{\hat{\gamma}}$, expanding the integrand in Taylor series around z^α , and noting that, in the normal coordinates $\{x^{\hat{\alpha}}\}$ (see e.g. [27]), we have $\Gamma_{\hat{\beta}\hat{\gamma}}^{\hat{\alpha}}(z) = 0$ and $\|\Gamma_{\hat{\beta}\hat{\gamma},\hat{\delta}}^{\hat{\alpha}}(z)\| \sim \|\mathbf{R}\|$, where $\|\mathbf{R}\| \equiv \sqrt{|R_{\alpha\beta\gamma\delta} R^{\alpha\beta\gamma\delta}|}$ denotes the magnitude of the curvature, we have $\Delta \mathcal{A}^\alpha = \mathcal{O}(\|\mathcal{A}\| \|\mathbf{R}\| x^2)$. Therefore $P_{\text{Dix}}^{\hat{\alpha}} = P^{\hat{\alpha}} + \mathcal{O}(\lambda \|\mathbf{P}\|)$, where

$$\lambda = \|\mathbf{R}\| a^2, \quad (69)$$

and a is the largest dimension of the body. Thus, when $\lambda \ll 1$, i.e. when the curvature is not too strong compared to the scale of the size of the body,¹³ $P_{\text{Dix}}^{\hat{\alpha}} \simeq P^{\hat{\alpha}}$. The two schemes are actually indistinguishable in a pole-dipole approximation, where only terms to linear order in x are kept in the integrals defining the moments; the resulting equations of motion are the same (compare Eqs. (43), (49) of [25] with Eqs. (6.31) and (6.32) of [11], or Eqs. (7.1) and (7.2) of [26]), both schemes leading to the well known Mathisson-Papapetrou equations (the latter derived using less sophisticated formalisms). These conclusions are natural, for the metric in Riemann normal coordinates is (e.g. [27]) of the form $g_{\hat{\alpha}\hat{\beta}} = \eta_{\hat{\alpha}\hat{\beta}} + \mathcal{O}(\|\mathbf{R}\|x^2)$; hence the assumption $\lambda \ll 1$ amounts to say that, *for the computation* of P^α and $S^{\alpha\beta}$, one may, to a good approximation, take the spacetime as nearly flat throughout the body.

The Dependence of the Particle's Momenta on Σ

The momenta (1) and (2) depend, in general, on the spacelike hypersurface $\Sigma(z, u) \equiv \Sigma(z(\tau), u)$ on which the integration is performed, see e.g. [11, 25, 26]. This is so even in flat spacetime; when forces and torques act on the body, it is clear that $P^\alpha(z, u)$, $S^{\alpha\beta}(z, u)$ depend on $z^\alpha(\tau)$, and also on the argument u^α of Σ . Curvature brings additional complications, as u^α is no longer a “free vector”, and Σ itself is in principle point dependent. Herein we shall show that, in the absence of electromagnetic field ($F^{\alpha\beta} = 0$), and under the assumption $\lambda \ll 1$ made above, for hypersurfaces $\Sigma(z, u)$ *through a point z^α within the body's convex hull*, the u^α dependence of the momentum and angular momentum is negligible.

Denote by $\xi = dx^{\hat{\alpha}}$ a particular basis 1-form of the Riemann normal coordinate system $\{x^{\hat{\alpha}}\}$; $P^\xi \equiv P^\alpha \xi_\alpha$ is thus the ξ component of P^α . From definition (1), and since ξ_α has constant components, we may write the ξ component of the momentum as the integral of a vector $A^\alpha \equiv T^{\alpha\beta} \xi_\beta$ on a 3-surface,

$$P^\xi(z, u) = \xi_{\hat{\alpha}} \int_{\Sigma(z, u)} T^{\hat{\alpha}\hat{\beta}} d\Sigma_{\hat{\beta}} = \int_{\Sigma(z, u)} T^{\hat{\alpha}\hat{\beta}} \xi_{\hat{\alpha}} d\Sigma_{\hat{\beta}} = \int_{\Sigma(z, u)} A^\beta d\Sigma_\beta.$$

Take $u^\alpha = P^\alpha/M$, and consider another vector u'^α at the same point z^α ; the ξ component of the difference between the momenta computed in the hypersurfaces $\Sigma(z, u')$ and $\Sigma(z, u)$, $\Delta P^\xi \equiv P^\xi(z, u') - P^\xi(z, u)$ is, from an application of the Gauss theorem (see Fig. 7),

$$\Delta P^\xi = \int_{\Sigma(z, u)} A^\beta d\Sigma_\beta - \int_{\Sigma(z, u')} A^\beta d\Sigma_\beta = \int_{V_{\text{Left}}} A^\beta_{;\beta} dV - \int_{V_{\text{Right}}} A^\beta_{;\beta} dV.$$

¹³For example, in the case of the Schwarzschild spacetime, $\|\mathbf{R}\| \sim m_S/r^3$, $\lambda = (m_S/r)(a^2/r^2)$; since $m_S/r < 1$ for any point outside the horizon, $\lambda \ll 1$ is guaranteed just by taking the size of the body much smaller than its the distance to the source, $r^2 \gg a^2$.

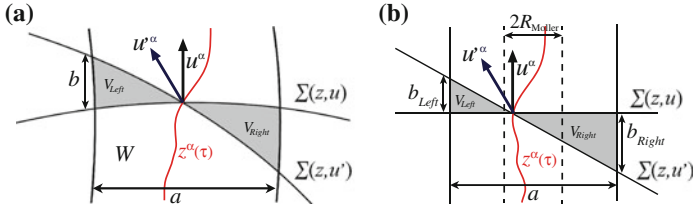


Fig. 7 *Shaded regions* V_{Left} and V_{Right} are the 4-volumes delimited by the hypersurfaces $\Sigma(z, u')$, $\Sigma(z, u)$, and the boundary of the body's worldtube, of convex hull W . u^α is chosen parallel to P^α . **a** Curved spacetime; **b** flat spacetime

Here V_{Left} and V_{Right} denote the shaded regions of Fig. 7 (where $A^\alpha \neq 0$), i.e. the “left” and “right” 4-volumes delimited by $\Sigma(z, u')$, $\Sigma(z, u)$ and the boundary of the body's worldtube. Now, using the conservation law $T^{\alpha\beta}_{;\beta} = 0$, one notes that

$$A^\beta_{;\beta} = T^{\alpha\beta}_{;\beta} \xi_\alpha + T^{\alpha\beta} \xi_{\alpha;\beta} = T^{\alpha\beta} \xi_{\alpha;\beta};$$

thus

$$\Delta P^\xi = \int_{V_{Left}} T^{\alpha\beta} \xi_{\alpha;\beta} dV - \int_{V_{Right}} T^{\alpha\beta} \xi_{\alpha;\beta} dV.$$

Since ξ is a basis 1-form, $\xi_{\hat{\alpha};\hat{\beta}} = 0$, and

$$\xi_{\hat{\alpha};\hat{\beta}} = -\Gamma^{\hat{\gamma}}_{\hat{\alpha}\hat{\beta}} \xi_{\hat{\gamma}} = \mathcal{O}(\|\mathbf{R}\|x);$$

therefore

$$|\Delta P^\xi| \lesssim \|\mathbf{R}\| \int_V T^{\hat{0}\hat{0}} |x| dV = \|\mathbf{R}\| V \langle T^{\hat{0}\hat{0}} |x| \rangle,$$

where $V \equiv V_{Left} + V_{Right}$, $\langle \cdot \rangle$ denotes the average on the shadowed region of Fig. 7a, and we noted that $T^{\hat{0}\hat{0}}$ is the largest component of $T^{\alpha\beta}$ and always positive. Since $b < av(u', u)$ (see Fig. 7), with $v^\alpha(u', u)$ defined by Eq. (9), and $v(u', u) < 1$, then $\langle |x| \rangle < a$; moreover (assuming $\partial_{\hat{0}} = \mathbf{u}$ at z), $V \langle T^{\hat{0}\hat{0}} \rangle < Mav(u', u)$; hence we get

$$|\Delta P^\xi| \lesssim M\lambda v(u', u) = \|\mathbf{P}\| \lambda v(u', u), \quad (70)$$

showing that ΔP^α is negligible¹⁴ compared to P^α under the restriction above on the strength of the gravitational field, $\lambda \ll 1$ (the same under which the different

¹⁴The inequality (69) means not only that the components of $\Delta \mathbf{P}$ in the system $\{x^{\hat{\alpha}}\}$ (where $\hat{P}^{\hat{i}} = 0$) are much smaller than M , but also much smaller than the typical spatial momentum in other frames. For instance, in normal coordinates $\{x^{\alpha'}\}$ comoving with u'^α , one has $|P^{i'}| \sim \gamma(u', u)v(u', u)M$ and $|\Delta P^{i'}| \lesssim |\Delta P^\xi| \gamma(u', u)$, thus $|\Delta P^{i'}| \ll |P^{i'}|$ when $\lambda \ll 1$.

multipole schemes become equivalent, and one can take local Lorentz coordinates as nearly rectangular throughout the extension of the body; see also footnote 13). In the application in Sect. 3.4—Schwarzschild spacetime, far field limit—we can write

$$|\Delta P^\xi| \lesssim \frac{M m_S}{r^3} a^2 v(u', u) \simeq \|P_{\text{hidl}}\| \frac{a}{R_{\text{Moller}}} \frac{a}{r} v(u', u)$$

where P_{hidl}^α is the inertial hidden momentum of the CP condition, Eq. (57) (P_{hidl}^α is zero or negligible for the other solutions). Thus ΔP^α is negligible compared to P_{hidl}^α under the condition $\frac{R_{\text{Moller}}}{a} \gg \frac{a}{r} v(u', u)$, which is reasonable in a problem where the particle's spin is worth taking into account (e.g. in the problem of nearly circular motion in Sect. 3.4 this amounts to taking $\omega_{\text{body}} \gg \omega_{\text{orbit}}$, where ω_{body} and ω_{orbit} are the body's rotation and orbital angular velocities).

Through an analogous procedure, one can show that the dependence of $S^{\alpha\beta}$ on u^α is negligible in this regime. Let $\mathcal{J}^{\hat{\alpha}\hat{\beta}\hat{\gamma}} \equiv 2x^{[\hat{\alpha}} T^{\hat{\beta}]\hat{\gamma}}$, so that $S^{\hat{\alpha}\hat{\beta}} = \int_{\Sigma(z,u)} \mathcal{J}^{\hat{\alpha}\hat{\beta}\hat{\gamma}} d\Sigma_{\hat{\gamma}}$; and consider the two basis spatial 1-forms ξ and η . Constructing the vector $\mathcal{J}^\gamma \equiv \mathcal{J}^{\alpha\beta\gamma} \xi_\alpha \eta_\beta$, we can write the $\xi \otimes \eta$ component of $S^{\alpha\beta}$ as $S^{\xi\eta}(z, u) = \int_{\Sigma(z,u)} \mathcal{J}^\beta d\Sigma_\beta$. By the Gauss theorem,

$$\begin{aligned} \Delta S^{\xi\eta} &= \int_{V_{\text{Left}}} \mathcal{J}^\beta_{;\beta} dV - \int_{V_{\text{Right}}} \mathcal{J}^\beta_{;\beta} dV \sim \|\mathbf{R}\| \int_V x^2 |\vec{J}| dV = \|\mathbf{R}\| V \langle |\vec{J}| x^2 \rangle \\ &< \|\mathbf{R}\| a^2 V \langle |\vec{J}| \rangle = \lambda V \langle |\vec{J}| \rangle \lesssim \lambda a^4 v(u', u) \langle |\vec{J}| \rangle, \end{aligned}$$

where $J^{\hat{i}} = T^{\hat{0}\hat{i}}$. In the second relation again we used $\Gamma^{\hat{\gamma}}_{\hat{\alpha}\hat{\beta}} = \mathcal{O}(\|\mathbf{R}\|x)$. Since $S = \mathcal{O}(a^4 \langle |\vec{J}| \rangle)$, cf. Eq. (13), we see that indeed when $\lambda \ll 1$, $\|\Delta S^{\xi\eta}\| \ll S$.

The Case with Electromagnetic Field

When $F^{\alpha\beta} \neq 0$, the conservation law is $T^{\alpha\beta}_{;\beta} = F^{\alpha\beta} j_\beta$ (denoting by $T^{\alpha\beta}$ the particle's energy momentum tensor). Consider for simplicity flat spacetime, and let ξ be a basis 1-form of a global Lorentz system; then $T^{\alpha\beta}_{;\beta} \xi_\alpha = (T^{\alpha\beta} \xi_\alpha)_{;\beta} \equiv A^\beta_{;\beta} = F^{\alpha\beta} j_\beta \xi_\alpha$. Note that $f^\alpha \equiv F^{\alpha\beta} j_\beta$ is the Lorentz force density. It follows (see Fig. 7b)

$$\Delta P^\xi = \int_{V_{\text{Left}}} A^\beta_{;\beta} dV - \int_{V_{\text{Right}}} A^\beta_{;\beta} dV = \xi_\alpha \left(V_{\text{Left}} \langle f^\alpha \rangle_{\text{Left}} - V_{\text{Right}} \langle f^\alpha \rangle_{\text{Right}} \right).$$

We have $V_{\text{Left}} = V_{\text{Left}}^{(3)} b_{\text{Left}}/2$, $V_{\text{Right}} = V_{\text{Right}}^{(3)} b_{\text{Right}}/2$ (where $V^{(3)}$ denote 3-volumes orthogonal to u^α). Herein we allow z^α to be any point within the worldtube of centroids; it follows that

$$b_{Left} \geq v(u, u') \left(\frac{a}{2} - R_{\text{Moller}} \right); \quad b_{Right} \leq v(u, u') \left(\frac{a}{2} + R_{\text{Moller}} \right)$$

$$V_{Left}^{(3)} \sim a^2 \left(\frac{a}{2} - R_{\text{Moller}} \right); \quad V_{Right}^{(3)} \sim a^2 \left(\frac{a}{2} + R_{\text{Moller}} \right).$$

Let $\langle f^\alpha \rangle_{Left} = \langle f^\alpha \rangle_{Right} + \Delta f^\alpha$, with $\|\Delta f^\alpha\| \lesssim \|\nabla_\beta f^\alpha\| a$; we obtain

$$|\Delta P^\xi| \lesssim \|F_L^\alpha\| R_{\text{Moller}} v(u', u) + \|\nabla_j F_L^\alpha\| v(u', u) a^2. \quad (71)$$

Hence ΔP^ξ has, as upper bound, the sum of two terms: the impulse of the Lorentz force F_L^α in the time interval $R_{\text{Moller}} v(u', u)$ (as measured in the $u^i = 0$ frame) between the two points where the hyperplane $\Sigma(z, u')$ crosses the worldtube of centroids, plus a term analogous to the gravitational one (70). For the field of a Coulomb charge, discussed in Sect. 3.4.1, they read

$$\|F_L^\alpha\| R_{\text{Moller}} v(u', u) = |E_p| v(u', u) \frac{R_{\text{Moller}}}{r} \sim \|P_{\text{hidl}}\| v(u', u)$$

$$\|\nabla_j F_L^\alpha\| v(u', u) a^2 = |E_p| v(u', u) \frac{a^2}{r^2} \sim \|P_{\text{hidl}}\| \frac{a}{R_{\text{Moller}}} \frac{a}{r} v(u', u)$$

where $E_p = qQ/r$ is the electric potential energy, and P_{hidl}^α is the inertial hidden momentum of the TD/FMP (non-helical) solutions, Eq. (52) (for the CP/OKS conditions, $P_{\text{hidl}}^\alpha = 0$). Assuming $|E_p| < M$, if $R_{\text{Moller}}/r \ll 1$ and $a^2/r^2 \ll 1$ (as is the case in the far-field regime), then $|\Delta P^\xi| \ll M = \|\mathbf{P}\|$, and ΔP^α is negligible compared to P^α by arguments analogous the ones given in footnote 14. It is also negligible compared to $\|P_{\text{hidl}}\|$ under the following conditions: (i) $v(u', u) \ll 1$ so that the first term of (71) can be neglected (this is guaranteed by the slow motion assumption in Sect. 3.4); (ii) that $\frac{R_{\text{Moller}}}{a} \gg \frac{a}{r} v(u', u)$, a condition analogous to the one we obtained gravitational case above, which is reasonable whenever the particle's spin is worth taking into account.

Note that the argument above can equally be used to show that P^α does not depend on the spin condition. Start with the TD centroid: $z^\alpha = x_{\text{CM}}^\alpha(u)$, with $u^\alpha = P^\alpha/M$; the centroids $x_{\text{CM}}^\alpha(u')$ of other spin conditions are reached by $x_{\text{CM}}^\alpha(u') = x_{\text{CM}}^\alpha(u) + \Delta x^\alpha$, with $\Delta x^\alpha \in \Sigma(u, z)$, cf. Eq. (10). Since the argument above applies to any spacelike hyperplane $\Sigma(u', z')$ through any arbitrary centroid z'^α on $\Sigma(u, z)$, it effectively means that, to the accuracy at hand, P^α does not depend on the particular centroid chosen.

References

1. J. Frenkel, Die Elektrodynamik des rotierenden Elektrons. Z. Phys. **37**, 243 (1926)
2. J. Frenkel, Spinning electrons. Nature **117**, 514 (1926)
3. H.J. Bhabha, H.C. Corben, General classical theory of spinning particles in a Maxwell field. Proc. R. Soc. Lond. A **178**, 273 (1940)

4. H.C. Corben, Spin in classical and quantum theory. *Phys. Rev.* **121**, 1833 (1961)
5. W.G. Dixon, Description of extended bodies by multipole moments in special relativity. *J. Math. Phys.* **8**, 1591 (1967)
6. C. Moller, On the definition of the centre of gravity in an arbitrary closed system in the theory of relativity. *Commun. Dublin Inst. Adv. Stud. A* **5**, 3 (1949)
7. C. Moller, Sur la dynamique des systemes ayant un moment angulaire interne. *Ann. Inst. Henri Poincaré* **11**, 251 (1949)
8. M. Mathisson, Neue Mechanik materieller Systeme. *Acta Phys. Pol.* **6**, 163 (1937)
9. E. Corinaldesi, A. Papapetrou, Spinning test-particles in general relativity II. *Proc. R. Soc. Lond. A* **209**, 259–268 (1951)
10. W. Tulczyjew, Motion of multipole particles in general relativity theory. *Acta Phys. Pol.* **18**, 393 (1959)
11. W.G. Dixon, A covariant multipole formalism for extended test bodies in general relativity. *II Nuovo Cimento* **34**, 317 (1964)
12. A. Ohashi, Multipole particle in relativity. *Phys. Rev. D* **68**, 044009 (2003)
13. K. Kyrian, O. Semerák, Spinning test particles in a Kerr field—II. *Mon. Not. R. Astron. Soc.* **382**, 1922 (2007)
14. O. Semerák, Spinning test particles in a Kerr field—I. *Mon. Not. R. Astron. Soc.* **308**, 863 (1999)
15. M. Mathisson, Das zitternde Elektron und seine Dynamik. *Acta Phys. Pol.* **6**, 218 (1937)
16. L.F. Costa, C. Herdeiro, J. Natário, M. Zilhão, Mathisson's helical motions for a spinning particle: are they unphysical? *Phys. Rev. D* **85**, 024001 (2012)
17. S. Gralla, A. Harte, R. Wald, Bobbing and Kicks in electromagnetism and gravity. *Phys. Rev. D* **81**, 104012 (2010)
18. W. Shockley, R.P. James, Try simplest cases discovery of hidden momentum forces on magnetic currents. *Phys. Rev. Lett.* **18**, 876 (1967)
19. L. Vaidman, Torque and force on a magnetic dipole. *Am. J. Phys.* **58**, 978 (1990)
20. V. Hnizdo, Hidden momentum and the electromagnetic mass of a charge and current carrying body. *Am. J. Phys.* **65**, 92 (1997)
21. S. Coleman, J.H. Van Vleck, Origin of hidden momentum forces on magnets. *Phys. Rev.* **171**, 1370 (1968)
22. D. Babson, S.P. Reynolds, R. Bjorquist, D.J. Griffiths, Hidden momentum, field momentum, and electromagnetic impulse. *Am. J. Phys.* **77**, 826 (2009)
23. L.F. Costa, J. Natário, Gravito-electromagnetic analogies. *Gen. Rel. Grav.* **46**, 1792 (2014)
24. L.F. Costa, J. Natário, M. Zilhão, Spacetime dynamics of spinning particles—exact gravito-electromagnetic analogies (2012) [arXiv:1207.0470](https://arxiv.org/abs/1207.0470)
25. J. Madore, The equations of motion of an extended body in general relativity. *Ann. Inst. Henri Poincaré* **11**, 221 (1969)
26. W.G. Dixon, Dynamics of extended bodies in general relativity. I. Momentum and angular momentum. *Proc. R. Soc. Lond. A* **314**, 499 (1970)
27. C.W. Misner, K.S. Thorne, J.A. Wheeler, *Gravitation* (W. H. Freeman and Company, San Francisco, 1973)
28. R.T. Jantzen, P. Carini, D. Bini, The many faces of gravitoelectromagnetism. *Ann. Phys.* **215**, 1 (1992)
29. J.L. Synge, *Relativity: The Special Theory* (North-Holland Publishing Company, Amsterdam, 1956)
30. S. Gralla, F. Herrmann, Hidden momentum and black hole kicks. *Class. Quantum Gravity* **30**, 205009 (2013)
31. V. Bolós, Intrinsic definitions of relative velocity in general relativity. *Commun. Math. Phys.* **273**, 217 (2007)
32. L. Brewin, Riemann normal coordinate expansions using Cadabra. *Class. Quantum Gravity* **26**, 175017 (2009)
33. W. Beiglbock, The center-of-mass in Einstein's theory of gravitation. *Commun. Math. Phys.* **5**, 106–130 (1967)

34. R. Schattner, The uniqueness of the center of mass in general relativity. *Gen. Relativ. Gravit.* **10**, 395–399 (1979)
35. J. Weyssenhoff, Relativistic dynamics of spin-fluids and spin-particles. *Nature* **157**, 766 (1946)
36. J. Weyssenhoff, A. Raabe, Relativistic dynamics of spin-fluids and spin particles. *Acta Phys. Pol.* **9**, 7 (1947)
37. W.G. Dixon, On a classical theory of charged particles with spin and the classical limit of the Dirac equation. *Il Nuovo Cimento* **38**, 1616 (1965)
38. R. Plyatsko, O. Stephanyshin, Mathisson equations: non-oscillatory solutions in a Schwarzschild field. *Acta Phys. Pol. B* **39**, 23 (2008)
39. R. Plyatsko, O. Stephanyshin, M. Fenyk, Mathisson-Papapetrou-Dixon equations in the Schwarzschild and Kerr backgrounds. *Class. Quantum Gravity* **28**, 195025 (2011)
40. N. Kudryashova, YuN Obukhov, On the dynamics of classical particles with spin. *Phys. Lett. A* **374**, 3801 (2010)
41. Yu.N. Obukhov, D. Puetzfeld, Dynamics of test bodies with spin in de Sitter spacetime. *Phys. Rev. D* **83**, 044024 (2011)
42. W.G. Dixon, The definition of multipole moments for extended test bodies. *Gen. Relativ. Gravit.* **4**, 199 (1973)
43. D. Bini, F. de Felice, A. Geralico, Strains in general relativity. *Class. Quantum Gravity* **23**, 7603 (2006)
44. W.G. Dixon, Dynamics of extended bodies in general relativity. III. Equations of motion. *Philos. Trans. R. Soc. Lond. A* **277**, 59 (1974)

General Relativistic Two-Body Problem: Theory and Experiment and the Role of Hidden Momentum

R.F. O'Connell

Abstract Emphasis will be placed on unusual aspects of our derivation, particularly the use of techniques from the more developed realm of QED (quantum electrodynamics). We obtain explicit results for the precession of the spin (rotation) and orbital effects and we discuss the relatively recent (2008) verification of our spin precession result. Unusual features of our orbital precession analysis is the appearance of hidden momentum effects whose origins may be traced to a special relativistic effect.

1 Introduction

The work of Schiff [1] in 1960 led to a resurgence of interest in analyzing and measuring the Lense-Thirring effect due to spin (rotation) effects. In particular, Barker and I [2], using a potential which we derived using techniques from QED, obtained the classical motion of a gyroscope in the gravitational field of a much larger mass with a quadrupole moment. Our method of derivation was much shorter and more straightforward than conventional methods especially as we made use of familiar Lagrangian concepts. Also, our results agreed with Schiff except that our equations of orbital motion appeared to be different than those of Schiff (although they both led to the same orbital precession results). Later, we traced this difference to the use of a different choice of coordinates [3], which was not due to the freedom enjoyed by the use of general relativity but due to a special relativistic effect, which we will discuss below in connection with hidden momentum.

When the first binary pulsar was discovered [4], we were motivated to extend our results to the two-body domain [5, 6]. However, due to the nature of their system, Hulse and Taylor were unable to observationally verify our results. However, with the discovery of the double pulsar, our results were verified to an accuracy of 13 % [7]. In Sect. 2, we discuss the derivation of our results and their experimental verification. Then, in Sect. 3, we discuss the origin of hidden momentum.

R.F. O'Connell (✉)

Department of Physics and Astronomy, Louisiana State University, Baton Rouge,
LA 70803-4001, USA
e-mail: oconnell@phys.lsu.edu

2 Two-Body Results: Theory and Experimental Verification

QED theory generally deals with the electromagnetic interaction of elementary particles whereas gravitation for the most part is confined to macroscopic systems. Thus, we decided to start with the gravitational interaction of two electrons, given by a one-graviton exchange interaction [8]. Next, making use of the universality of the gravitational interaction, we obtain the classical macroscopic result by letting

$$\begin{aligned}\frac{1}{2}\hbar\vec{\sigma}^{(1)} &\rightarrow \vec{S}^{(1)}, \\ \frac{1}{2}\hbar\vec{\sigma}^{(2)} &\rightarrow \vec{S}^{(2)},\end{aligned}\tag{1}$$

where $\vec{\sigma}^{(1)}$ and $\vec{\sigma}^{(2)}$ are the Pauli spin matrices associated with electrons 1 and 2 and where $\vec{S}^{(1)}$ and $\vec{S}^{(2)}$ are the classical spin angular momenta of the macroscopic masses m_1 and m_2 . Thus, we obtain the gravitational potential energy $V_1 + V_2$, correct to order c^{-2} (first post-Newtonian order). This leads to the spin-dependent Lagrangian and Hamiltonian. In order to obtain the spin-independent Hamiltonian H_0 in the center-of-mass system, we start with an expression give by Hiida and Okamura [9] which contains a quantity α which is an arbitrary dimensionless parameter which can take a number of different values, one of which ($\alpha = 0$) corresponds to the EIH Hamiltonian. However, we found it convenient to select a value in order to obtain a Hamiltonian without a G^2 term. Further work enabled us to include quadrupole moment terms for both masses so that we finally obtained, in an obvious notation, the total Hamiltonian

$$H_I(\alpha) = Mc^2 + H(\alpha) + V_{S1} + V_{S2} + V_{S1,S2} + V_{Q1} + V_{Q2},\tag{2}$$

from which the total Lagrangian readily followed. The Euler-Lagrange equations were then used to obtain the precessions of the spins and the precession of the orbit. Some general comments on our results are as follows:

(1) If we make the replacement $e^2 \rightarrow Gm^2$ in the result for the electromagnetic interaction for positronium [10, p. 286], we obtain terms of the same structure as our gravitational results. The numerical coefficients are generally different excepting the case for the spin-spin interaction term $V_{S1,S2}$ where they are the same.

(2) In the large mass approximation ($m_2 \gg m_1$), the results reduce to the Lense-Thirring results.

(3) Our procedure for calculating the precession of the orbit was greatly facilitated by making use of the fact that the Runge-Lenz vector \vec{A} is a constant in the non-relativistic case. In addition, \vec{A} and \vec{L} are always perpendicular, where \vec{L} is the orbital angular momentum and thus although both \vec{A} and \vec{L} precess in the more general case

they must do so in such a way as to ensure that $\vec{A} \cdot \vec{L} = 0$. In other words, the secular results for the precession of the orbit are of the form

$$\begin{aligned}\dot{\vec{L}}_{av} &= \vec{\Omega}^* \times \vec{L}, \\ \dot{\vec{A}}_{av} &= \vec{\Omega}^* \times \vec{A}.\end{aligned}\quad (3)$$

The fact that $\vec{\Omega}^*$ appears in both equations provided a beautiful check on the results.

(4) Defining the total angular momentum as

$$\vec{J} \equiv \vec{L} + \vec{S}^{(1)} + \vec{S}^{(2)}, \quad (4)$$

we found that

$$\dot{\vec{J}}_{av} = \vec{\Omega}^* \times \vec{L} + \vec{\Omega}_{av}^{(1)} \times \vec{S}^{(1)} + \vec{\Omega}_{av}^{(2)} \times \vec{S}^{(2)} \equiv 0, \quad (5)$$

where $\vec{\Omega}^*$ is the precession of \vec{L} and where $\vec{\Omega}_{av}^{(2)}$ is the precession of the spin of body 2, which can be obtained from the result for $\vec{\Omega}_{av}^{(1)}$ by interchanging the indices 1 and 2. In other words, the total angular momentum is conserved, which provides another excellent check on our results.

(5) The orbital precession $\vec{\Omega}^*$ was broken down into time derivatives of the longitude of the ascending node, the argument of the perihelion and the inclination of the orbit, following astronomical and space physics practise [5]. This is clearly displayed in Figs. 2 and 3 of [11]. In addition, we note that the first verification of the one-body Lense-Thirring results by Ciufolini and Pavlis [12] made use of nodal precession.

(6) One notable result which emerges is that, in the case of arbitrary masses m_1 and m_2 , the dominant spin-orbit contribution to the *spin* precession of body 1 is a factor $(m_2 + \mu/3)/(m_1 + m_2)$ times what it would be for a test body moving in the field of a fixed central mass $(m_1 + m_2)$. Here μ denotes the reduced mass $m_1 m_2 / (m_1 + m_2)$. This contrasts with the result of Robertson for the *periastron* precession where the corresponding factor is unity. This result, which was published in 1975 [5, 6] had to await until 2008 (a period of 33 years) for its verification by the work of Breton et al. [7] utilizing the double pulsar PSR J0737-3039A/B [13]. This pulsar consists of two neutron stars in a highly relativistic 2.45 h orbit, which displays an eclipse of pulsar A of the order of 30 s. when pulsar A passes behind pulsar B, enabling a measurement of the relativistic precession of the spin axis of pulsar B around the total orbital angular momentum \vec{L} .

The double pulsar system, is the only system observed so far in which both components are pulsing neutron stars and has the added advantage that the system is observed nearly perfectly edge-on. Its periastron precession of 16.9°/yr has been

measured with enormous accuracy (to 6 significant figures) which enabled the total mass $M = m_1 + m_2 = 2.2587 M_\odot$ to be measured also very accurately. However, in order to obtain the spin-orbit precession it is necessary to determine both m_1 and m_2 . These were determined from the projected semi-major values and the Shapiro time delay with the results $m(A) = m_2 = 1.3381 M_\odot$ and $m(B) = m_1 = 1.2489 M_\odot$ so that the measured precession rate of pulsar B is $4.77 \pm 0.66^\circ/\text{yr}$, in agreement, to an accuracy of 13 % [7], with the theoretical rate [5] of $5.0734 \pm 0.0007^\circ/\text{yr}$. Further details on our theoretical work and recent experiments appear in [11, 14].

(7) There is also a precession of \vec{L} in the double pulsar system due to spin precession effects, as is clear from Eq. (5). The dominant effect is due to pulsar A [15] since its spin frequency is 122 times larger than that of pulsar B. However, the effect is only about $4.06''/\text{yr}$ and thus may be difficult to observe.

3 Hidden Momentum

In the introduction, we stated that, even in the 1-body case, our results for the equations of orbital motion differed from these of Schiff but that they both led to the same orbital precession results. As we pointed out [3], the resolution of this problem may be traced to the work of Moller [16] and [17, p. 176]. He pointed out that in special relativity, a particle with structure and “spin” (its angular momentum vector in the rest system) is subject to a spin supplementary condition, which “—expresses in a covariant way that the proper center of mass is the center of mass in its own rest system (K^0)—” and that “—the difference between simultaneous positions of the centre of mass in K (obtained from K^0 by a Lorentz transformation with velocity (\vec{v}) and the proper centre of mass (in K^0)—” is

$$\Delta\vec{r} = \frac{\vec{S} \times \vec{v}}{mc^2}, \quad (6)$$

where (\vec{S}) is the spin and m is the rest mass. In essence, it is related to the fact that, in special relativity, there are two rest systems for the particle, zero velocity and zero momentum, reflecting the choice of spin supplementary conditions and the fact that only in special cases are the velocity and momentum proportional to each other [18] and [19, see Eq. (7) which for us the basis of a more rigorous quantum mechanical calculation]. We refer to an extensive review for more details [20].

It is clear that an increase in the coordinate by an amount of $\Delta\vec{r}$ will give rise to an increase in the momentum, which is generally referred to as hidden momentum $\Delta\vec{P}$. An expression for $\Delta\vec{P}$ was obtained in two extensive papers [21, 22] but a simple derivation is possible as we shall now demonstrate. Thus, taking the time derivative

of Eq. (6), and neglecting the very small second order terms in \vec{S} which arise in the relation between the velocity \vec{v} and momentum \vec{P} , we obtain

$$\Delta \vec{P} = \frac{\vec{S} \times \vec{a}}{c^2}, \quad (7)$$

where \vec{a} is the acceleration. This is a general expression for the hidden momentum.

In particular, in the realm of electrodynamics, since the expression for a magnetic dipole moment \vec{M} is derived from either the spin of a particle or from a steady current (bodies with structure in both cases), it is clear that

$$\Delta \vec{P} = k_1 \frac{\vec{M} \times \vec{a}}{c^2}, \quad (8)$$

where k_1 is a constant.

In the particular case where the particle with a magnetic moment \vec{M} is interacting with a pointlike electric charge e then, the electric field \vec{E} created gives rise to an acceleration that is given by $e\vec{E}/m$ so that

$$\Delta \vec{P} = k_2 \frac{\vec{M} \times \vec{E}}{c^2}, \quad (9)$$

where k_2 is a constant. This is essentially the expression used in all discussions in electromagnetism [23–29] for the hidden momentum. Thus, the hidden momentum of electrodynamics is a particular consequence of the motion of a spinning body (or, alternatively, a magnetic moment) for which, due to special relativistic effects, the simultaneous position of the center of mass in the moving system is different [by an amount given in Eq. (6)] than the proper center of mass.

Acknowledgments This work was partially supported by the National Science Foundation under grant no. ECCS-1125675.

References

1. L.I. Schiff, Proc. Natl. Acad. Sci. **46**, 871 (1960)
2. B.M. Barker, R.F. O’Connell, Phys. Rev. D **2**, 1428 (1970)
3. B.M. Barker, R.F. O’Connell, Gen. Relat. Gravit. **5**, 539 (1974)
4. R.A. Hulse, J.H. Taylor, Astrophys. J. Lett. **195**, L51 (1975)
5. B.M. Barker, R.F. O’Connell, Phys. Rev. D **12**, 329 (1975)
6. B.M. Barker, R.F. O’Connell, Astrophys. J. Lett. **199**, L25 (1975)
7. R.P. Breton, V.M. Kaspi, M. Kramer, M.A. McLaughlin, M. Lyutikov, S.M. Ransom, I.H. Stairs, R.D. Ferdman, F. Camilo, A. Possenti, Science **321**, 104 (2008)
8. B.M. Barker, S.N. Gupta, R.D. Haracz, Phys. Rev. **149**, 1027 (1966)
9. K. Hiida, H. Okamura, Prog. Theor. Phys. **47**, 1743 (1972)

10. V.B. Berestetskii, E.M. Lifshitz, L.P. Pitaevskii, *Relativistic Quantum Theory* (Pergamon Press, Oxford, 1971)
11. C. Feiler, M. Buser, E. Kajari, W.P. Schleich, E.M. Rasel, R.F. O'Connell, *Space Sci. Rev.* **148**, 123 (2009)
12. I. Ciufolini, E.C. Pavlis, *Nature* **431**, 958 (2004)
13. M. Burgay et al., *Nature* **426**, 531 (2003)
14. R.F. O'Connell, in *Atom Optics and Space Physics, Proceedings of Course CLXVIII of the International School of Physics, Enrico Fermi, Varenna, Italy, 2007*, ed. by E. Arimondo, W. Ertmer, W. Schleich (IOS, Amsterdam, 2009)
15. R.F. O'Connell, *Phys. Rev. Lett.* **93**, 081103 (2004)
16. C. Moller, *Commun. Dublin Inst. Adv. Stud.* **A5**, 1 (1949)
17. C. Moller, *The Theory of Relativity* (Oxford University Press, Oxford, 1972)
18. R.F. O'Connell, E.P. Wigner, *Phys. Lett.* **61A**, 353 (1977)
19. R.F. O'Connell, E.P. Wigner, *Phys. Lett.* **67A**, 319 (1978)
20. R.F. O'Connell, in *General Relativity and John Archibald Wheeler*, ed. by I. Ciufolini, R. Matzner (Springer, Netherlands, 2010)
21. S.E. Gralla, A.I. Harte, R.M. Wald, *Phys. Rev. D* **81**, 104012 (2010)
22. L.F. Costa et al., *Phys. Rev. D* **85**, 024001 (2012)
23. W. Shockley, R.P. James, *Phys. Rev. Lett.* **18**, 876 (1967)
24. M. Mansuripur, *Phys. Rev. Lett.* **108**, 193901 (2012)
25. D.A.T. Vanzella, *Phys. Rev. Lett.* **110**, 089401 (2013)
26. S.M. Barnett, *Phys. Rev. Lett.* **110**, 089402 (2013)
27. P.L. Saldanha, *Phys. Rev. Lett.* **110**, 089403 (2013)
28. M. Khorami, *Phys. Rev. Lett.* **110**, 089404 (2013)
29. M. Mansuripur, *Phys. Rev. Lett.* **110**, 089405 (2013)

Equations of Motion of Schwarzschild, Reissner–Nordström and Kerr Particles

Peter A. Hogan

Abstract A technique for extracting from the appropriate field equations the relativistic motion of Schwarzschild, Reissner–Nordström and Kerr particles moving in external fields is motivated and illustrated. The key assumptions are that (a) the particles are isolated and (b) near the particles the wave fronts of the radiation generated by their motion are smoothly deformed spheres. No divergent integrals arise in this approach. The particles are not test particles. The formalism is used, however, to derive the Mathisson–Papapetrou equations of motion of spinning test particles, neglecting spin–spin terms.

1 Introduction

We describe a method for modeling the relativistic motion of (uncharged or charged) particles moving in external gravitational and electromagnetic fields in general relativity. The particles modify the fields in which they move and thus are *not* test particles. The modified fields near the particles are predominantly the Schwarzschild, Reissner–Nordström or Kerr fields and thus the particles will be referred to as Schwarzschild, Reissner–Nordström or Kerr particles respectively. The origin of the approach described here is the seminal and challenging paper by Robinson and Robinson [1], with the disconcertingly modest title of “Equations of Motion in the Linear Approximation”, published in the festschrift in honor of Professor J.L. Synge. This paper inspired early work involving space-times which are more special than those required here and which can be found in a series of papers by Hogan and Imaeda [2–4] (see also [5]). A line element, which is a byproduct of a study of gravitational radiation from bounded sources [6], plays a key role in the development of our method. An early application can be found in [7]. The most up-to-date references to our technique and applications are in the paper [8] and the books [9] and [10]. Further development of this work has also involved graduate students Takashi Fukumoto and Shinpei Ogawa in Tohoku University, Aishling Nic an Tuile in University

P.A.Hogan (✉)

School of Physics, University College Dublin, Belfield, Dublin 4, Ireland
e-mail: peter.hogan@ucd.ie

College Dublin and Florian Bolgar in École Normale Supérieure, Paris and has taken the form of M.Sc. and Ph.D. theses and an Internship Report.

To introduce our approach we begin with the Eddington–Finkelstein form of the Schwarzschild line element:

$$ds^2 = -r^2 p_0^{-2} (dx^2 + dy^2) + 2 du dr + \left(1 - \frac{2m}{r}\right) du^2, \quad (1)$$

with

$$p_0 = 1 + \frac{1}{4}(x^2 + y^2). \quad (2)$$

Here x, y are stereographic coordinates taking values in the ranges $-\infty < x < +\infty$ and $-\infty < y < +\infty$, u is a null coordinate (in the sense that the hypersurfaces $u = \text{constant}$ are null) with $-\infty < u < +\infty$. The generators of these null hypersurfaces are null geodesics labelled by (x, y) and r (with $0 \leq r < +\infty$) is an affine parameter along them. When the mass parameter $m = 0$ the space-time is Minkowskian with line element

$$ds_0^2 = -r^2 p_0^{-2} (dx^2 + dy^2) + 2 du dr + du^2 = \eta_{ij} dX^i dX^j, \quad (3)$$

with $X^i = (X, Y, Z, T)$ rectangular Cartesian coordinates and time and $\eta_{ij} = \text{diag}(-1, -1, -1, +1)$. In this *background space-time* with line element (3) the hypersurfaces $u = \text{constant}$ are future null cones with vertices on the *time-like geodesic* $r = 0$. We can consider

$$\gamma_{ij} dx^i dx^j = -\frac{2m}{r} du^2, \quad (4)$$

in coordinates $x^i = (x, y, r, u)$, as a perturbation of this background which is singular on the time-like geodesic $r = 0$ and which, when added to the line element (3) produces the line element (1). Although we have no need to assume it now, we shall, in the sequel, assume that m is small of first order and write $m = O_1$ in order to simplify the complicated calculations that develop. We shall consider the background space-time a model of the *external field* in which the small mass is located. In the example here the background space-time is Minkowskian space-time and thus there is no external field present. Also in this example the time-like geodesic equations (satisfied by $r = 0$ in (3)) are the *equations of motion* of the small mass.

In the space-time with line element (3) let $X^i = w^i(u)$ be an arbitrary time-like world line with u proper time or arc length along it. Then $v^i(u) = dw^i/du$ is the unit tangent to this line and satisfies $v_j v^j = \eta_{ij} v^i v^j = +1$ along the world line. Equivalently v^i is the 4-velocity of the particle with world line $X^i = w^i(u)$. Thus $a^i = dv^i/du$ is the 4-acceleration and satisfies $a_j v^j = \eta_{ij} a^i v^j = 0$ along the world line. We shall lower and raise indices, referring to the coordinates X^i , using η_{ij} and η^{ij} respectively, with the latter defined by $\eta^{ij} \eta_{jk} = \delta_k^i$. We note that v^i and

a^i are the components of the 4-velocity and 4-acceleration of the particle expressed in the coordinates X^i . These features of the world line can be incorporated in the Minkowskian line element by replacing (3) by

$$ds_0^2 = -r^2 P_0^{-2} (dx^2 + dy^2) + 2 du dr + (1 - 2h_0 r) du^2, \quad (5)$$

with

$$P_0 = xv^1(u) + yv^2(u) + \left\{ 1 - \frac{1}{4}(x^2 + y^2) \right\} v^3(u) + \left\{ 1 + \frac{1}{4}(x^2 + y^2) \right\} v^4(u), \quad (6)$$

and

$$h_0 = \frac{\partial}{\partial u} (\log P_0) = a_j k^j, \quad (7)$$

with

$$k^j = P_0^{-1} \left[-x\delta_1^j - y\delta_2^j - \left\{ 1 - \frac{1}{4}(x^2 + y^2) \right\} \delta_3^j + \left\{ 1 + \frac{1}{4}(x^2 + y^2) \right\} \delta_4^j \right]. \quad (8)$$

In (5) $r = 0$ is the world line $X^i = w^i(u)$ with the 4-velocity components appearing in (5) via the function P_0 and the 4-acceleration appearing via h_0 . The future null cones with vertices on this world line are the null hypersurfaces $u = \text{constant}$. The generators of these null cones are the null geodesic integral curves of the vector field k^j , which satisfies $k_j k^j = 0$ and $k_j v^j = +1$. On each future null cone the generators are labeled by the stereographic coordinates x, y and $r \geq 0$ is an affine parameter along them. To see how Einstein's vacuum field equations can lead to the equations of motion as we have defined them in the paragraph above we consider a space-time with line element

$$ds^2 = -r^2 P_0^{-2} (dx^2 + dy^2) + 2 du dr + \left(1 - 2h_0 r - \frac{2m}{r} \right) du^2, \quad (9)$$

which is a generalization of the Schwarzschild space-time with line element (1). The Ricci tensor components in coordinates $x^i = (x, y, r, u)$ are now given exactly via

$$R_{ij} dx^i dx^j = \frac{6m h_0}{r^2} du^2. \quad (10)$$

With $m \neq 0$ we see that the vacuum field equations $R_{ij} = 0$ require $a_j k^j = h_0 = 0$ and this should hold for all possible k^j . Hence we must have, as equations of motion, the time-like geodesic equations

$$a^j = 0, \quad (11)$$

for the world line $r = 0$ in the Minkowskian background space-time. This simple example illustrates a connection between the equations of motion and the field

equations. In general we shall find, however, that the field equations by themselves will not be sufficient to determine the equations of motion. They will have to be supplemented by a smoothness condition on the wave fronts of the possible radiation produced by the motion of the particle. A singular point on a wave front translates in space-time into a singularity along a generator, extending to future null infinity, of the null hypersurface history of the wave front and thus violating the concept of an isolated source. A useful example with which to illustrate this is to consider the relativistic motion of a Reissner–Nordström particle moving in external electromagnetic and gravitational fields.

2 Reissner-Nordström Particle

We construct here a model of a Reissner–Nordström particle of small mass $m = O_1$ and small charge $e = O_1$ moving in external vacuum gravitational and electromagnetic fields. In this case the background space-time is a general solution of the vacuum Einstein–Maxwell field equations. We shall require a knowledge of this space-time, and the Maxwell field, in the neighborhood of an arbitrary time-like world line $r = 0$ (say). The charged mass will then be introduced as a perturbation of this space-time, which is singular on this world line in the background space-time (in similar fashion to (4) in the space-time with line element (3)), in such a way that the perturbed space-time is, for small values of r , predominantly the Reissner–Nordström space-time and Maxwell field. Since we have indicated in Sect. 1 that we shall make use of the field equations along with conditions on the wave fronts of possible radiation (electromagnetic and/or gravitational in the current example) produced by the motion of our particle, and since the histories of wave fronts are null hypersurfaces in space-time, we shall work in the background space-time and in the perturbed background space-time in a coordinate system based on a family of null hypersurfaces. Thus we begin by writing the line element of the background space-time as

$$ds^2 = -(\vartheta^1)^2 - (\vartheta^2)^2 + 2\vartheta^3\vartheta^4 = g_{ab}\vartheta^a\vartheta^b, \quad (12)$$

with the 1-forms ϑ^1 , ϑ^2 , ϑ^3 and ϑ^4 given by

$$\vartheta^1 = r p^{-1}(e^\alpha \cosh \beta dx + e^{-\alpha} \sinh \beta dy + a du), \quad (13)$$

$$\vartheta^2 = r p^{-1}(e^\alpha \sinh \beta dx + e^{-\alpha} \cosh \beta dy + b du), \quad (14)$$

$$\vartheta^3 = dr + \frac{c}{2} du, \quad (15)$$

$$\vartheta^4 = du. \quad (16)$$

The constants $g_{ab} = g_{ba}$ constitute the components of the metric tensor on the tetrad defined by the basis 1-forms. Tetrad indices will be denoted by the early letters of the alphabet a, b, c, \dots , and tetrad indices will be lowered with g_{ab} and raised with g^{ab}

where $g^{ab}g_{bc} = \delta_c^a$. This line element is completely general in that it involves six functions $p, \alpha, \beta, a, b, c$ each of the four coordinates x, y, r, u . It is thus equivalent to line elements constructed by Sachs [11] and by Newman and Unti [12]. It was constructed in [6] for the study of gravitational radiation from bounded sources and was specifically designed to have the Robinson–Trautman [13, 14] line elements appear as a convenient special case (got by simply putting $\alpha = \beta = 0$). This latter property also makes it convenient in the current context. We shall take $r = 0$ to be the equation of an arbitrary time-like world line in the space-time with line element (12). The space-time in the neighborhood of this world line has the well-known Fermi property (see, for example, [15, 16]) that there exist coordinates in terms of which the metric tensor components satisfy

$$g_{ij} = \eta_{ij} + O(r^2). \quad (17)$$

In view of the line element (5) we can implement this property in the context of the line element (12) by expanding the six functions appearing there in powers of r as follows:

$$p = P_0(1 + q_2 r^2 + q_3 r^3 + \cdots), \quad (18)$$

$$\alpha = \alpha_2 r^2 + \alpha_3 r^3 + \cdots, \quad (19)$$

$$\beta = \beta_2 r^2 + \beta_3 r^3 + \cdots, \quad (20)$$

$$a = a_1 r + a_2 r^2 + \cdots, \quad (21)$$

$$b = b_1 r + b_2 r^2 + \cdots, \quad (22)$$

$$c = c_0 + c_1 r + c_2 r^2 + \cdots, \quad (23)$$

where the coefficients of the powers of r are functions of x, y, u . Following (5) the function P_0 here is given by (6) and

$$c_0 = 1 = \Delta \log P_0 \quad \text{with} \quad \Delta = P_0^2 \left(\frac{\partial^2}{\partial x^2} + \frac{\partial^2}{\partial y^2} \right), \quad (24)$$

and

$$c_1 = -2h_0, \quad (25)$$

with h_0 given by (7). The operator Δ is the Laplacian on the unit 2-sphere. The relationship between the rectangular Cartesian coordinates and time X^i and the coordinates x, y, r, u near the arbitrary time-like world line $r = 0$ ($\Leftrightarrow X^i = w^i(u)$, introduced in Sect. 1) is given by (see, for example, [17])

$$X^i = w^i(u) + r k^i, \quad (26)$$

neglecting $O(r^2)$ -terms.

At this point in the discussion we should note some formulas associated with Minkowskian space-time with line element (5) or, equivalently, with metric tensor components η_{ij} in coordinates X^i . A useful basis of 1-forms suggested by (5) is

$$\omega^1 = r P_0^{-1} dx, \quad \omega^2 = r P_0^{-1} dy, \quad \omega^3 = dr + \left(\frac{1}{2} - h_0 r \right) du, \quad \omega^4 = du. \quad (27)$$

When expressed in terms of the coordinates X^i using the transformation (26) these read

$$\omega^1 = -P_0 \frac{\partial k_i}{\partial x} dX^i = -\omega_1, \quad (28)$$

$$\omega^2 = -P_0 \frac{\partial k_i}{\partial y} dX^i = -\omega_2, \quad (29)$$

$$\omega^3 = \left(v_i - \frac{1}{2} k_i \right) dX^i = \omega_4, \quad (30)$$

$$\omega^4 = k_i dX^i = \omega_3. \quad (31)$$

In coordinates X^i the vector fields with components $v^i, k^i, \partial k^i / \partial x, \partial k^i / \partial y$ form a basis and it is useful to express the metric tensor components η^{ij} on this basis as

$$\eta^{ij} = -P_0^2 \left(\frac{\partial k^i}{\partial x} \frac{\partial k^j}{\partial x} + \frac{\partial k^i}{\partial y} \frac{\partial k^j}{\partial y} \right) + k^i v^j + k^j v^i - k^i k^j. \quad (32)$$

Also the second partial derivatives of k^i play a key role in the calculations and when they are expressed on this basis we have

$$\frac{\partial^2 k^i}{\partial x^2} = P_0^{-2} (v^i - k^i) - \frac{\partial}{\partial x} (\log P_0) \frac{\partial k^i}{\partial x} + \frac{\partial}{\partial y} (\log P_0) \frac{\partial k^i}{\partial y}, \quad (33)$$

$$\frac{\partial^2 k^i}{\partial y^2} = P_0^{-2} (v^i - k^i) + \frac{\partial}{\partial x} (\log P_0) \frac{\partial k^i}{\partial x} - \frac{\partial}{\partial y} (\log P_0) \frac{\partial k^i}{\partial y}, \quad (34)$$

$$\frac{\partial^2 k^i}{\partial x \partial y} = -\frac{\partial}{\partial y} (\log P_0) \frac{\partial k^i}{\partial x} - \frac{\partial}{\partial x} (\log P_0) \frac{\partial k^i}{\partial y}. \quad (35)$$

As a simple indication of the usefulness of these formulas we notice that if we add (33) and (34) we obtain

$$\Delta k^i + 2 k^i = 2 v^i, \quad (36)$$

with the operator Δ defined in (24). Taking the scalar product, with respect to the Minkowskian metric tensor η_{ij} , of this equation with the 4-acceleration a^i yields

$$\Delta h_0 + 2 h_0 = 0, \quad (37)$$

with h_0 given by (7). This demonstrates that h_0 is an $l = 1$ spherical harmonic. A spherical harmonic Q of order l is a smooth solution, for $-\infty < x, y < +\infty$, of the equation $\Delta Q + l(l+1)Q = 0$ for $l = 0, 1, 2, \dots$

Returning now to the construction of the background Einstein–Maxwell field, the potential 1-form leading to the background electromagnetic field is given by

$$A = L dx + M dy + K du, \quad (38)$$

where L, M, K are functions of x, y, r, u . We have used the freedom to add an exact differential (i.e. a gauge transformation) to remove one component of this 1-form for convenience. The functions appearing in (38) will be expanded in powers of r in such a way that the resulting Maxwell 2-form $F = dA$, the exterior derivative of (38), is non-singular at $r = 0$, since this will be the *external* Maxwell field. The simplest expansions to achieve this are:

$$L = r^2 L_2 + r^3 L_3 + \dots, \quad (39)$$

$$M = r^2 M_2 + r^3 M_3 + \dots, \quad (40)$$

$$K = r K_1 + r^2 K_2 + \dots, \quad (41)$$

with the coefficients of the powers of r functions of x, y, u . The Maxwell 2-form is given by

$$F = dA = \frac{1}{2} F_{ab} \vartheta^a \wedge \vartheta^b, \quad (42)$$

where $F_{ab} = -F_{ba}$ are the components of the 2-form on the tetrad defined by the basis 1-forms (13)–(16). The leading terms, in powers of r , of the tetrad components F_{ab} which will interest us are, in light of the expansions (18)–(23) and (39)–(41),

$$F_{13} = -2P_0 L_2 + O(r), \quad F_{23} = -2P_0 M_2 + O(r), \quad F_{34} = K_1 + O(r). \quad (43)$$

Thus on $r = 0$ we can replace the basis (13)–(16) by the Minkowskian counterparts (28)–(31) and the coordinates x, y, r, u by the coordinates X^i following (26) to arrive at

$$L_2 = \frac{1}{2} F_{ij}(u) k^i \frac{\partial k^j}{\partial x}, \quad M_2 = \frac{1}{2} F_{ij}(u) k^i \frac{\partial k^j}{\partial y}, \quad K_1 = F_{ij}(u) k^i v^j, \quad (44)$$

where $F_{ij}(u) = -F_{ji}(u)$ are the components of the external Maxwell tensor on the world line $r = 0$ calculated in the coordinates X^i . With k^i given by (8) above we see that now the dependence of the functions L_2, M_2, K_1 on x, y is explicitly known. We can therefore use the useful formulas (33)–(35) to verify that Maxwell's vacuum field equations, $d^*F = 0$, where the star denotes the Hodge dual of the 2-form F , are satisfied by L_2, M_2, K_1 . The relevant equations obtained from the leading terms, in powers of r , in Maxwell's equations are

$$K_1 = P_0^2 \left(\frac{\partial L_2}{\partial x} + \frac{\partial M_2}{\partial y} \right), \quad \Delta K_1 + 2P_0^2 \left(\frac{\partial L_2}{\partial x} + \frac{\partial M_2}{\partial y} \right) = 0, \quad (45)$$

and

$$\frac{\partial K_1}{\partial x} + 2L_2 - \frac{\partial}{\partial y} \left\{ P_0^2 \left(\frac{\partial M_2}{\partial x} - \frac{\partial L_2}{\partial y} \right) \right\} = 0, \quad (46)$$

$$\frac{\partial K_1}{\partial y} + 2M_2 + \frac{\partial}{\partial x} \left\{ P_0^2 \left(\frac{\partial M_2}{\partial x} - \frac{\partial L_2}{\partial y} \right) \right\} = 0. \quad (47)$$

We see that the second equation in (45) is a consequence of (46) and (47) and the two equations in (45) imply that K_1 is an $l = 1$ spherical harmonic since

$$\Delta K_1 + 2K_1 = 0. \quad (48)$$

This latter equation can, of course, be verified directly using the last of (44) and the formulas (33)–(35).

The analogue, for the gravitational field, of the Maxwell 2-form with tetrad components F_{ab} given by (43) is the Weyl conformal curvature tensor with tetrad components C_{abcd} . The components which will be of interest to us in the neighborhood of the world line $r = 0$ are given by

$$C_{1313} + iC_{1323} = 6(\alpha_2 + i\beta_2) + O(r), \quad (49)$$

and

$$C_{3431} + iC_{3432} = \frac{3}{2}P_0^{-1} \left\{ a_1 + ib_1 + 4P_0^2 \frac{\partial q_2}{\partial \bar{\zeta}} \right\} + O(r), \quad (50)$$

where $\zeta = x + iy$ and a bar denotes complex conjugation. These must be examined in conjunction with the Einstein–Maxwell vacuum field equations for the background space-time:

$$R_{ab} = 2 \left\{ F_{ca} F^c{}_b - \frac{1}{4} g_{ab} F_{cd} F^{cd} \right\} = 2E_{ab}, \quad (51)$$

where R_{ab} are the tetrad components of the Ricci tensor of the background space-time, g_{ab} are the tetrad components of the metric tensor and, as indicated following (16), tetrad indices are raised using the components g^{ab} of the inverse of the matrix with components g_{ab} and $E_{ab} = E_{ba}$ are the tetrad components of the electromagnetic energy-momentum tensor. To satisfy the field equation $R_{33} = 2E_{33} + O(r)$ we find that

$$q_2 = \frac{2}{3} P_0^2 (L_2^2 + M_2^2). \quad (52)$$

This can be rewritten, using L_2 and M_2 given by (44) and the expression (32) for the components of the inverse of the Minkowskian metric tensor, simply as

$$q_2 = -\frac{1}{6} F^p{}_i(u) F_{pj}(u) k^i k^j. \quad (53)$$

Here $F_{pj}(u)$ are the components of the Maxwell tensor on the world line $r = 0$ in coordinates X^i while $F^p{}_i(u) = \eta^{pj} F_{ji}(u)$. Using this expression for q_2 in (50) and the basis (28)–(31), in similar fashion to the passage from (43) to (44) above, we conclude from (49) and (50) that

$$\alpha_2 = \frac{1}{6} P_0^2 C_{ijkl}(u) k^i \frac{\partial k^j}{\partial x} k^k \frac{\partial k^l}{\partial x}, \quad \beta_2 = \frac{1}{6} P_0^2 C_{ijkl}(u) k^i \frac{\partial k^j}{\partial x} k^k \frac{\partial k^l}{\partial y}, \quad (54)$$

and

$$a_1 = \frac{2}{3} P_0^2 \left(C_{ijkl}(u) k^i v^j k^k \frac{\partial k^l}{\partial x} + F^p{}_i(u) F_{pj}(u) k^i \frac{\partial k^j}{\partial x} \right), \quad (55)$$

$$b_1 = \frac{2}{3} P_0^2 \left(C_{ijkl}(u) k^i v^j k^k \frac{\partial k^l}{\partial y} + F^p{}_i(u) F_{pj}(u) k^i \frac{\partial k^j}{\partial y} \right), \quad (56)$$

where $C_{ijkl}(u)$ are the components of the Weyl tensor of the background space-time calculated on the world line $r = 0$ in the coordinates X^i . With P_0 given by (6) and k^j by (8), we see that the dependence of q_2 in (53), α_2 and β_2 in (54), and a_1 and b_1 in (55) and (56) on the coordinates x, y is explicitly known. The Einstein–Maxwell vacuum field equations $R_{12} = 2E_{12} + O(r)$ and $R_{11} - R_{22} = 2(E_{11} - E_{22}) + O(r)$ yield the pair of real field equations incorporated in the single complex equation:

$$2(\alpha_2 + i\beta_2) = -\frac{\partial}{\partial \bar{\zeta}} \left\{ a_1 + ib_1 + 4 P_0^2 \frac{\partial q_2}{\partial \bar{\zeta}} \right\}. \quad (57)$$

The pair of real field equations $R_{13} = 2E_{13} + O(r)$ and $R_{23} = 2E_{23} + O(r)$ can be written as the complex equation:

$$a_1 + ib_1 + 4 P_0^2 \frac{\partial q_2}{\partial \bar{\zeta}} = 2 P_0^4 \frac{\partial}{\partial \zeta} \{ P_0^{-2} (\alpha_2 + i\beta_2) \}. \quad (58)$$

The field equations (57) and (58) must be satisfied by $q_2, \alpha_2, \beta_2, a_1, b_1$ given by (53)–(56). This important check can be carried out using the useful formulas (33)–(35). We are now ready to introduce the Reissner–Nordström particle as a perturbation of this background space-time and Maxwell field.

The line element of the perturbed space-time is given by

$$ds^2 = -(\hat{\vartheta}^1)^2 - (\hat{\vartheta}^2)^2 + 2 \hat{\vartheta}^3 \hat{\vartheta}^4 = g_{ab} \hat{\vartheta}^a \hat{\vartheta}^b, \quad (59)$$

with the 1-forms $\hat{\vartheta}^1$, $\hat{\vartheta}^2$, $\hat{\vartheta}^3$ and $\hat{\vartheta}^4$ given by

$$\hat{\vartheta}^1 = r \hat{p}^{-1} (e^{\hat{\alpha}} \cosh \hat{\beta} dx + e^{-\hat{\alpha}} \sinh \hat{\beta} dy + \hat{a} du), \quad (60)$$

$$\hat{\vartheta}^2 = r \hat{p}^{-1} (e^{\hat{\alpha}} \sinh \hat{\beta} dx + e^{-\hat{\alpha}} \cosh \hat{\beta} dy + \hat{b} du), \quad (61)$$

$$\hat{\vartheta}^3 = dr + \frac{\hat{c}}{2} du, \quad (62)$$

$$\hat{\vartheta}^4 = du. \quad (63)$$

To achieve our aim of having a predominantly Reissner–Nordström field for small values of r we take the functions appearing here to have the following expansions in powers of r :

$$\hat{p} = \hat{P}_0 (1 + \hat{q}_2 r^2 + \hat{q}_3 r^3 + \dots), \quad (64)$$

$$\hat{\alpha} = \hat{\alpha}_2 r^2 + \hat{\alpha}_3 r^3 + \dots, \quad (65)$$

$$\hat{\beta} = \hat{\beta}_2 r^2 + \hat{\beta}_3 r^3 + \dots, \quad (66)$$

$$\hat{a} = \frac{\hat{a}_{-1}}{r} + \hat{a}_0 + \hat{a}_1 r + \hat{a}_2 r^2 + \dots, \quad (67)$$

$$\hat{b} = \frac{\hat{b}_{-1}}{r} + \hat{b}_0 + \hat{b}_1 r + \hat{b}_2 r^2 + \dots, \quad (68)$$

$$\hat{c} = \frac{e^2}{r^2} - \frac{2(m + 2\hat{f}_{-1})}{r} + \hat{c}_0 + \hat{c}_1 r + \hat{c}_2 r^2 + \dots \quad (69)$$

The coefficients of the various powers of r here are functions of x, y, u . The hatted functions differ from their background values by O_1 -terms. Thus in particular $\hat{a}_{-1} = O_1$, $\hat{a}_0 = O_1$, $\hat{b}_{-1} = O_1$, $\hat{b}_0 = O_1$, but $\hat{f}_{-1} = O_2$. The perturbed potential 1-form

$$A = \hat{L} dx + \hat{M} dy + \hat{K} du, \quad (70)$$

is predominantly the Liénard–Wiechert 1-form ($= e(r^{-1} - h_0) du$) up to a gauge term so that

$$\hat{L} = r^2 \hat{L}_2 + r^3 \hat{L}_3 + \dots, \quad (71)$$

$$\hat{M} = r^2 \hat{M}_2 + r^3 \hat{M}_3 + \dots, \quad (72)$$

$$\hat{K} = \frac{(e + \hat{K}_{-1})}{r} - e h_0 + r \hat{K}_1 + r^2 \hat{K}_2 + \dots, \quad (73)$$

where again the coefficients of the powers of r here are functions of x, y, u which differ from their background values by O_1 -terms and $\hat{K}_{-1} = O_2$. The expansions (64)–(69) and (71)–(73) appear to us to be the minimal assumptions necessary to have a small charged mass with gravitational and electromagnetic fields predominantly those of a Reissner–Nordström particle for small values of r . They certainly restrict

the model of such a particle moving in external gravitational and electromagnetic fields and their generalization or otherwise is a topic for further study.

When the metric tensor given by (59)–(63) and the potential 1-form (70), together with the expansions (64)–(69) and (71)–(73), are substituted into Maxwell's vacuum field equations and the Einstein–Maxwell vacuum field equations, and all terms are gathered on the left hand side of each equation with zero on the right hand side, we find a finite number of terms involving inverse powers of r and an infinite number of terms involving positive (or zero) powers of r . In an ideal world we would equate the coefficients of each of these powers to zero and from the resulting equations derive the coefficients in the expansions (64)–(69) and (71)–(73). However the reality is that we can at best make the coefficients small in terms of m and e . How small depends upon how accurately we require the equations of motion. Also the number of coefficients we require in the expansions (64)–(69) and (71)–(73) depends upon how accurately we require the equations of motion. For the purpose of the present illustration we shall calculate the equations of motion in first approximation and thus with an O_2 -error. The null hypersurfaces $u = \text{constant}$ in the space-time with line element (59) are the histories of possible wave fronts of radiation (electromagnetic and/or gravitational) produced by the motion of the Reissner–Nordström particle. For small values of r the degenerate metric on these hypersurfaces is given by the line element

$$ds_0^2 = -r^2 \hat{P}_0^{-2} (dx^2 + dy^2), \quad (74)$$

where \hat{P}_0 differs from its background value P_0 given in (6) by O_1 -terms and thus can be written

$$\hat{P}_0 = P_0 (1 + Q_1 + O_2), \quad (75)$$

with $Q_1(x, y, u) = O_1$. We will assume that the line elements (74) are smooth deformations of the line element of a 2-sphere. This means that Q_1 is a well behaved function for $-\infty < x, y < +\infty$ and thus free of singularities in x, y . Now the field equations yield

$$\hat{a}_{-1} = -4e P_0^2 L_2 + O_2 = O_2, \quad (76)$$

$$\hat{b}_{-1} = -4e P_0^2 M_2 + O_2 = O_1, \quad (77)$$

$$\hat{c}_0 = 1 + \Delta Q_1 + 2Q_1 + 8e F_{ij} k^i v^j + O_2, \quad (78)$$

and

$$-\frac{1}{2} \Delta (\Delta Q_1 + 2Q_1) = 6ma_i k^i - 6e F_{ij} k^i v^j + O_2. \quad (79)$$

Both terms on the right hand side of (79) are $l = 1$ spherical harmonics and thus (79) can be easily integrated (discarding the solution of the $l = 0$ spherical harmonic equation which is singular for infinite values of x and y) to read

$$\Delta Q_1 + 2Q_1 = 6ma_i k^i - 6e F_{ij} k^i v^j + A(u) + O_2, \quad (80)$$

where $A(u) = O_1$ is arbitrary (an $l = 0$ spherical harmonic). We note that spherical harmonics corresponding to $l = 0$ or $l = 1$ in the perturbation Q_1 in (75) are trivial, in the sense that the 2-sphere remains a 2-sphere under these perturbations, and can be neglected. Since the first two terms in (80) are both $l = 1$ spherical harmonics the solution Q_1 will necessarily have a singularity in x, y (a *directional singularity*) unless they combine to vanish or be at most small of second order. Thus we must have

$$ma_i k^i = 6e F_{ij} k^i v^j + O_2, \quad (81)$$

for all possible values of k^i and thus

$$ma_i = e F_{ij} v^j + O_2. \quad (82)$$

We have arrived at the Lorentz equations of motion in first approximation.

The example above serves to illustrate our approach. If it is continued to the next order of approximation the equations of motion which emerge are [8]

$$ma_i = e F_{ij} v^j + \frac{4}{3} e^2 h_i^k F^p{}_k F_{pj} v^j + \frac{2}{3} e^2 h_i^k \dot{a}^k + e^2 T_i + O_3, \quad (83)$$

where $h_j^i = \delta_j^i - v^i v_j$ is the projection tensor and the dot denotes differentiation with respect to proper time u . The second term on the right hand side here is an O_2 -correction to the external 4-force. The third term on the right hand side is the electromagnetic radiation reaction 4-force. The fourth term on the right hand side is a *tail term* given by an integral with respect to proper time u from $-\infty$ to the current proper time u of a vector whose components are proportional to the external Maxwell field $F_{ij}(u)$ and involve functions of u of integration and a pair of space-like vectors, which occur naturally, defined along the world line $r = 0$ in the background space-time. When $e = 0$ we obtain the equations of motion of a Schwarzschild particle in second approximation given by the approximate time-like geodesic equations

$$m a_i = O_3. \quad (84)$$

There is a formal similarity between the equations of motion (83) and equations of motion derived by DeWitt and Brehme [18]. However DeWitt and Brehme have removed an infinite term from their equations of motion and have considered a scenario (the world line of a charged test particle in a curved space-time, and hence utilize only Maxwell's equations on a curved space-time) which is different to that constructed here.

Finally, so that the reader is left in no doubt as to the procedure involved in the passage from (80) to (82), we can give a simplified example of the procedure. If $\lambda = \cos \theta$ for $0 \leq \theta \leq \pi$ (or equivalently for $-1 \leq \lambda \leq +1$) consider a function $f = f(\lambda)$ satisfying the inhomogeneous $l = 1$ Legendre equation (i.e. the inhomogeneous $l = 1$ spherical harmonic equation satisfied by a function of the single variable λ) with an $l = 1$ Legendre polynomial on the right hand side:

$$\Delta f + 2f \equiv \frac{d}{d\lambda} \left\{ (1 - \lambda^2) \frac{df}{d\lambda} \right\} + 2f = t_1 P_1(\lambda), \quad (85)$$

where t_1 is a constant. For this equation to have a solution which is non-singular at $\lambda = \pm 1$ (which are directional singularities) we must have $t_1 = 0$ (analogous to (81)). This easily follows from consideration of the general solution

$$f(\lambda) = -\frac{1}{6} t_1 \lambda \log(1 - \lambda^2) + t_2 P_1(\lambda) + t_3 Q_1(\lambda), \quad (86)$$

where t_2, t_3 are constants and $Q_1(\lambda)$ is the Legendre function corresponding to $l = 1$. Of course the required directional singularity-free solution also requires us to take $t_3 = 0$ here.

3 Kerr Particle

We outline here the application of our technique to the construction of a model of a spinning particle, or Kerr particle, moving in an external vacuum gravitational field, and the derivation of its equations of motion. This work, carried out by Shinpei Ogawa and the author, is reported in [10]. Although we consider only the equations of motion in first approximation here, the calculations are more intricate than those necessary for the study of the Reissner–Nordström particle. Consequently we must refer the interested reader to [10] for further details.

The fundamental aspects of our technique are the construction of a background space-time with an arbitrary time-like world line in the neighborhood of which the space-time is flat, following from the Fermi property, and then the introduction of the particle of interest as a perturbation of this space-time. In the flat neighborhood of the world line in the background space-time we wrote the line element in the form (5) which introduces the 4-velocity and 4-acceleration of the world line into the line element. To consider a particle with spin in this context we introduce the spin variables (what will become the three independent components of the angular momentum per unit mass of the particle) into the line element of Minkowskian space-time to accompany the 4-velocity and 4-acceleration already present. We do this in such a way that if $a^i = 0$ then the form of the line-element of Minkowskian space-time coincides with the Kerr line element, with three components of angular momentum per unit mass, in the special case in which the mass $m = 0$. The latter form of the Kerr line element can be found in ([19], p. 37). Let $s^i(u)$ be the components of the *spin vector* in coordinates X^i , defined along the arbitrary time-like world line $X^i = w^i(u)$ to be everywhere orthogonal to the 4-velocity $v^i(u)$ and Fermi transported, thus,

$$s^i v_i = 0 \quad \text{and} \quad \frac{ds^i}{du} = -(a_j s^j) s^i, \quad (87)$$

respectively. The equivalent *spin tensor* is defined by

$$s_{ij} = \epsilon_{ijkl} v^k s^l = -s_{ji}, \quad (88)$$

where ϵ_{ijkl} are the components of the Levi–Civita permutation tensor in coordinates X^i . We introduce s^i into the Minkowskian line element by replacing (26) by

$$X^i = w^i(u) + r k^i + P_0^2 \left(\frac{\partial k^i}{\partial x} F_y - \frac{\partial k^i}{\partial y} F_x \right), \quad (89)$$

where

$$F = s^i k_i, \quad (90)$$

and the subscripts on F denote partial differentiation with respect to x and y . We note that P_0 and k^i are given by (6) and (8). By (87) and the useful formulas (33)–(35) we easily find that F is an $l = 1$ spherical harmonic. Also we can rewrite (89) in the general form of (26) as

$$X^i = w^i(u) + r K^i \quad \text{with} \quad K^i = \left(\eta^{ij} + \frac{1}{r} s^{ij} \right) k_j, \quad (91)$$

showing that for large r in Minkowskian space-time K^i only differs from k^i by an infinitesimal Lorentz transformation generated by the spin tensor. The Minkowskian line element is given by $ds_0^2 = \eta_{ij} dX^i dX^j$ with X^i given now by (89). When $X^i = w^i(u)$ (no longer corresponding to $r = 0$) is a geodesic we can choose $v^i = \delta_4^i$ and the resulting line element is

$$ds_0^2 = -(r^2 + F^2) p_0^{-2} (dx^2 + dy^2) + 2d\Sigma \left\{ dr + \frac{1}{2} (du - F_y dx + F_x dy) \right\}, \quad (92)$$

with p_0 given by (2) and

$$d\Sigma = du - F_y dx + F_x dy. \quad (93)$$

We note that the latter is *not* an exact differential unless the spin vanishes. The Kerr solution with the three components of angular momentum (ms^1, ms^2, ms^3) (since now $s^4 = 0$) is

$$ds^2 = ds_0^2 - \frac{2mr}{r^2 + F^2} d\Sigma^2. \quad (94)$$

If the world line $X^i = w^i(u)$ is *not* a time-like geodesic then the Minkowskian line element is algebraically more complicated than (92). For simplicity we shall henceforth neglect spin–spin terms and assume that the 4-acceleration is proportional to the spin on the basis that we expect geodesic motion if the spin vanishes. Now the

Minkowskian part of the background line element, when the world-line $X^i = w^i(u)$ is not necessarily a time-like geodesic, is given by

$$ds_0^2 = -r^2 P_0^{-2} \left\{ dx^2 + dy^2 + \frac{2P_0^2 F_y}{r^2} dx du - \frac{2P_0^2 F_x}{r^2} dy du \right\} + 2 dr d\Sigma \\ + 2 F_y du dx - 2 F_x du dy + (1 - 2 h_0 r) du^2. \quad (95)$$

With this preparation we write the line element of the general background space-time as

$$ds^2 = -r^2 p^{-2} \left\{ (e^\alpha \cosh \beta dx + e^{-\alpha} \sinh \beta dy + a d\Sigma)^2 \right. \\ \left. + (e^\alpha \sinh \beta dx + e^{-\alpha} \cosh \beta dy + b d\Sigma)^2 \right\} + 2 dr d\Sigma + c d\Sigma^2, \quad (96)$$

with

$$p = P_0 (1 + q_2 r^2 + q_3 r^3 + \dots), \quad (97)$$

$$\alpha = \alpha_1 r + \alpha_2 r^2 + \dots, \quad (98)$$

$$\beta = \beta_1 r + \beta_2 r^2 + \dots, \quad (99)$$

$$a = \frac{P_0^2 F_y}{r^2} + \frac{a_{-1}}{r} + a_0 + a_1 r + \dots, \quad (100)$$

$$b = -\frac{P_0^2 F_x}{r^2} + \frac{b_{-1}}{r} + b_0 + b_1 r + \dots, \quad (101)$$

$$c = c_0 + c_1 r + \dots \quad (102)$$

We now require this background line element to be a solution of Einstein's vacuum field equations

$$R_{ab} = 0. \quad (103)$$

Equating to zero the powers of r in the Ricci tensor components R_{ab} we find the following expressions for the coefficients of the powers of r in the expansions (97)–(102):

$$q_1 = 0 = q_2, \quad \alpha_1 = 4F\beta_2, \quad \beta_1 = -4F\alpha_2, \quad (104)$$

$$\alpha_2 = \frac{1}{6} P_0^2 R_{ijkl}(u) \frac{\partial k^i}{\partial x} k^j \frac{\partial k^k}{\partial x} k^l + O(F), \quad (105)$$

$$\beta_2 = \frac{1}{6} P_0^2 R_{ijkl}(u) \frac{\partial k^i}{\partial x} k^j \frac{\partial k^k}{\partial y} k^l + O(F). \quad (106)$$

Also $a_{-1} = 0 = b_{-1}$ and

$$a_0 = -7P_0^2(\alpha_2 F_y - \beta_2 F_x), \quad b_0 = -7P_0^2(\alpha_2 F_x + \beta_2 F_y), \quad (107)$$

$$a_1 = \frac{2}{3}P_0^2 R_{ijkl}(u) k^i v^j k^k \frac{\partial k^l}{\partial x} + O(F), \quad (108)$$

$$b_1 = \frac{2}{3}P_0^2 R_{ijkl}(u) k^i v^j k^k \frac{\partial k^l}{\partial y} + O(F), \quad (109)$$

and $c_0 = 1$ while

$$c_1 = -2h_0 - FP_0^2 \left(\frac{\partial}{\partial y}(P_0^{-2}a_1) - \frac{\partial}{\partial x}(P_0^{-2}b_1) \right) + 5(a_1 F_y - b_1 F_x). \quad (110)$$

The $O(F)$ -terms not calculated here will get multiplied by F , as in (104), (107) and (110) and will therefore not contribute to the end result since we are systematically neglecting spin-spin terms. In these formulas $R_{ijkl}(u)$ are the components of the Riemann curvature tensor in coordinates X^i calculated on the world-line $X^i = w^i(u)$. As well as satisfying the algebraic symmetries of the Riemann tensor they satisfy Einstein's vacuum field equations $\eta^{ik} R_{ijkl}(u) = 0$ on the world-line $X^i = w^i(u)$.

We introduce the Kerr particle of small mass $m = O_1$ as a perturbation, which is predominantly the Kerr field for small values of r , of this background vacuum space-time. The simplest way to achieve this appears to be the expansions (remembering that we make no claim to uniqueness; see the comments following (73) above):

$$\begin{aligned} d\hat{s}^2 = & -r^2 \hat{p}^{-2} \left\{ (e^{\hat{\alpha}} \cosh \hat{\beta} dx + e^{-\hat{\alpha}} \sinh \hat{\beta} dy + \hat{a} d\Sigma)^2 \right. \\ & \left. + (e^{\hat{\alpha}} \sinh \hat{\beta} dx + e^{-\hat{\alpha}} \cosh \hat{\beta} dy + \hat{b} d\Sigma)^2 \right\} + 2 dr d\Sigma + \hat{c} d\Sigma^2, \end{aligned} \quad (111)$$

with

$$\hat{p} = \hat{P}_0 (1 + \hat{q}_2 r^2 + \hat{q}_3 r^3 + \dots), \quad (112)$$

$$\hat{\alpha} = \hat{\alpha}_1 r + \hat{\alpha}_2 r^2 + \dots, \quad (113)$$

$$\hat{\beta} = \hat{\beta}_1 r + \hat{\beta}_2 r^2 + \dots, \quad (114)$$

$$\hat{a} = \frac{P_0^2 F_y}{r^2} + \frac{\hat{a}_{-1}}{r} + \hat{a}_0 + \hat{a}_1 r + \dots, \quad (115)$$

$$\hat{b} = -\frac{P_0^2 F_x}{r^2} + \frac{\hat{b}_{-1}}{r} + \hat{b}_0 + \hat{b}_1 r + \dots, \quad (116)$$

$$\hat{c} = -\frac{2m}{r} + \hat{c}_0 + \hat{c}_1 r + \dots \quad (117)$$

As always the hatted functions of x, y, u differ from their background values by O_1 -terms. In addition \hat{P}_0 again has the form (75) involving the first order function $Q_1(x, y, u)$. Now we must impose the vacuum field equations to be satisfied by the metric given via the line element (111) with sufficient accuracy to enable us to derive the equations of motion for the world line $X^i = w^i(u)$ in the background space-time, in first approximation. The vacuum field equations provide us with a set of equations which parallel (79)–(81) in the Reissner–Nordström example. In addition to $\hat{q}_1 = O_2, \hat{q}_2 = O_2$ we find that

$$\hat{a}_0 = -7P_0^2(\alpha_2 F_y - \beta_2 F_x) - 2ma_1 + O(mF) + O_2, \quad (118)$$

$$\hat{b}_0 = -7P_0^2(\alpha_2 F_x + \beta_2 F_y) - 2mb_1 + O(mF) + O_2, \quad (119)$$

$$\hat{a}_{-1} = -4mF b_1 + O_2, \quad \hat{b}_{-1} = 4mF a_1 + O_2, \quad (120)$$

and

$$\begin{aligned} \hat{c}_0 = 1 + \Delta Q_1 + 2Q_1 - 10mF P_0^2 \left(\frac{\partial}{\partial y} (P_0^{-2} a_1) - \frac{\partial}{\partial x} (P_0^{-2} b_1) \right) \\ - 8m(a_1 F_y - b_1 F_x) + O_2. \end{aligned} \quad (121)$$

In the remaining field equation, which yields the analogue of (79) and thence the analogue of (80), the functions \hat{a}_0 and \hat{b}_0 are multiplied by m and so the uncalculated terms $O(mF)$ in (118) and (119) will not contribute to the equations of motion in first approximation (i.e. neglecting O_2 -terms). The equation we obtain, which is the analogue of (80), is

$$(\Delta + 2)(Q_1 + 2mJ_1 + mJ_2) = 6ma_i k^i - 6mR_{ijkl}(u)k^i v^j s^{kl} + A(u) + O_2, \quad (122)$$

where $A(u) = O_1$ is a function of integration as in (80) and J_1 and J_2 are spin-curvature terms given by

$$J_1 = P_0^2 F R_{ijkl}(u)k^i v^j \frac{\partial k^k}{\partial y} \frac{\partial k^l}{\partial x} + \frac{1}{5} R_{ijkl}(u)k^i v^j s^{kl}, \quad (123)$$

which is an $l = 3$ spherical harmonic and

$$J_2 = P_0^2 R_{ijkl}(u)s_m v^i k^j v^k \left(\frac{\partial k^l}{\partial x} \frac{\partial k^m}{\partial y} - \frac{\partial k^l}{\partial y} \frac{\partial k^m}{\partial x} \right), \quad (124)$$

which is an $l = 2$ spherical harmonic, results which are obtained using the useful formulas (33)–(35). The first two terms on the right hand side of (122) are $l = 1$ spherical harmonics and so, just as in the case of (80), the solution Q_1 will be free of directional singularities provided the sum of these terms is zero or at most small of second order, i.e.

$$m a_i k^i = m R_{ijkl}(u) k^i v^j s^{kl} + O_2, \quad (125)$$

for all possible k^i and thus we arrive at the equations of motion of the Kerr particle in first approximation:

$$m a_i = m R_{ijkl}(u) v^j s^{kl} + O_2. \quad (126)$$

The algebraic form of the right hand side of these equations is, perhaps, what one would expect. The numerical factor of unity distinguishes these equations of motion from those of Mathisson–Papapetrou for a spinning *test* particle. We have here a model of a Kerr particle and it is manifestly *not* a test particle. The rest mass m is already small and making it smaller does not make it a test particle since so long as $m \neq 0$ its presence perturbs the background space-time (96). However in the present context we can say something about spinning test particles and this is the topic we turn to now.

4 Spinning Test Particle

Since we are now concerned with test particles moving in vacuum gravitational fields we will concentrate on what we called background space-times above. We first consider the non-spinning test particle whose world line, according to the geodesic hypothesis, is a time-like geodesic. With the geodesic hypothesis accepted for a non-spinning test particle it is relatively easy to devise a strategy, using the formalism of this paper, which will lead us to the equations of motion of a spinning test particle. As in Sect. 3 we will neglect spin-spin terms, but this restriction can be relaxed (and indeed has been by Florian Bolgar in his Internship Report to the École Normale Supérieure (2012)). The background vacuum space-time with the spin vector $s^i = 0$ has line element given by (96)–(102) with $F = 0$ and the coefficients of the powers of r are given by (104)–(110) with $F = 0$. Thus in coordinates $x^i = (x, y, r, u)$, with $i = 1, 2, 3, 4$, the only coordinate component of the metric tensor involving the 4-acceleration a^i of the world line $X^i = w^i(u)$ is

$$g_{44} = 1 - 2r h_0 + O(r^2). \quad (127)$$

The coefficient of $-2r$ on the right hand side here is the $l = 1$ spherical harmonic h_0 , which vanishes if and only if $a^i = 0$. In this case the world line $X^i = w^i(u)$ is a time-like geodesic and is thus the history of a test particle moving in the vacuum gravitational field modeled by the space-time with line element (96) with $F = 0$. Now we consider a particle with spin $s^i \neq 0$ having world line $X^i = w^i(u)$ in the space-time with line element (96) with $F \neq 0$. Now (127) is replaced by

$$g_{44} = 1 - 2r \left(h_0 - \frac{1}{2} R_{ijkl}(u) k^i v^j s^{kl} + J_2 \right) + O(r^2), \quad (128)$$

with J_2 given by (124). The first two terms in the coefficient of $-2r$ here are $l = 1$ spherical harmonics while the third term J_2 is an $l = 2$ spherical harmonic. If the equations of motion of a spinning test particle are obtained in the same way as those of a non-spinning test particle then equating to zero the $l = 1$ terms in the coefficient of $-2r$ in (128) results in

$$a_i k^i = h_0 = \frac{1}{2} R_{ijkl}(u) k^i v^j s^{kl}, \quad (129)$$

for all possible values of k^i and thus the equations of motion of a spinning test particle, neglecting spin-spin terms, are

$$a_i = \frac{1}{2} R_{ijkl}(u) v^j s^{kl}, \quad (130)$$

in agreement with Mathisson [20] and Papapetrou [21].

5 Discussion

Perhaps the most striking aspect of the technique presented here for extracting equations of motion from field equations is the absence of infinities arising in the calculations, either in the form of infinite self energy of the Dirac type [18] or in the form of divergent integrals. We have already indicated following (84) above that in the case of the DeWitt and Brehme [18] work this may be due to the fact that they have considered a different problem to the one we have described in Sect. 2. Much work in recent years has been done under the general heading of “the self force problem” and, fortunately, this work is well represented in the current volume, offering the interested student a direct comparison with our work and the challenge of connecting the different points of view.

References

1. I. Robinson, J.R. Robinson, in *General Relativity*, ed. by L. O’Raifeartaigh (Clarendon Press, Oxford, 1972), p. 151
2. P.A. Hogan, M. Imaeda, Equations of motion in linearized gravity: I uniform acceleration. *J. Phys. A: Math. Gen.* **12**, 1051 (1979)
3. P.A. Hogan, M. Imaeda, Equations of motion in linearized gravity: II run-away sources. *J. Phys. A: Math. Gen.* **12**, 1061 (1979)
4. P.A. Hogan, M. Imaeda, On the motion of sources of some Robinson-Trautman fields. *J. Phys. A: Math. Gen.* **12**, 1071 (1979)
5. P.A. Hogan, G.M. O’Brien, On the motion of rotating bodies in linearized gravity. *Phys. Lett. A* **72**, 395 (1979)
6. P.A. Hogan, A. Trautman, in *Gravitation and Geometry*, ed. by W. Rindler, A. Trautman (Bibliopolis, Naples, 1987), p. 215
7. P.A. Hogan, I. Robinson, The motion of charged particles in general relativity. *Found. Phys.* **15**, 617 (1985)
8. T. Futamase, P.A. Hogan, Y. Itoh, Equations of motion in general relativity of a small charged black hole. *Phys. Rev. D* **78**, 104014-1 (2008)
9. H. Asada, T. Futamase, P.A. Hogan, *Equations of Motion in General Relativity* (Oxford University Press, Oxford, 2011)
10. C. Barrabès, P.A. Hogan, *Advanced General Relativity: Gravity Waves, Spinning Particles, and Black Holes* (Oxford University Press, Oxford, 2013)
11. R.K. Sachs, Gravitational waves in general relativity VIII. *Proc. R. Soc. (London) A* **270**, 103 (1962)
12. E.T. Newman, T.W.J. Unti, Behavior of asymptotically flat empty spaces. *J. Math. Phys. (N.Y.)* **3**, 891 (1962)
13. I. Robinson, A. Trautman, Spherical gravitational waves. *Phys. Rev. Lett.* **4**, 431 (1960)
14. I. Robinson, A. Trautman, Some spherical gravitational waves in general relativity. *Proc. R. Soc. (London) A* **265**, 463 (1962)
15. L. O’Raifeartaigh, Fermi coordinates. *Proc. R. Irish Acad. Sect. A* **59**, 15 (1958)
16. L. O’Raifeartaigh, Riemannian spaces of N dimensions which contain Fermi subspaces of N-1 dimensions. *Proc. R. Irish Acad. Sect. A* **62**, 63 (1962)
17. E.T. Newman, T.W.J. Unti, A class of null flat-space coordinate systems. *J. Math. Phys. (N.Y.)* **4**, 1467 (1963)
18. B.S. DeWitt, R.W. Brehme, Radiation damping in a gravitational field. *Ann. Phys. (N.Y.)* **9**, 220 (1960)
19. C. Barrabès, P.A. Hogan, *Singular Null Hypersurfaces in General Relativity* (World Scientific, Singapore, 2003)
20. M. Mathisson, New mechanics of material systems. *Acta Physica Polonica* **6**, 163 (1937)
21. A. Papapetrou, Spinning test-particles in general relativity I. *Proc. Roy. Soc. (London) A* **209**, 248 (1951)

From Singularities of Fields to Equations of Particles Motion

Y. Itin

Abstract Due to the well known Einstein's proposition, the non-linearity of the GR field equations allows to derive, from the singularities of the field, the geodesic principle i.e., the equations of motion of massive pointwise particles. In this paper, we illustrate how this construction can be realized explicitly in a simple case of a non-linear scalar field model. For a field singular at one point (a timelike curve in 4D description), we derive the inertial motion law. For a field with two singularities (two disjoint timelike curves), we obtain, in the lowest approximation, the second law of non-relativistic dynamics together with the proper expression of Newton's law of attraction. The ordinary used method in such type of derivation is the integration over a tube near the singular line. Instead, we are working with the singular terms themselves. We compare the terms of the field equation that have the same order of divergence. The dynamical equation is derived as the relation between the coefficients of two leading singular terms—the agent of inertia and the agent of interaction.

1 Introduction

It is usually declared that general relativity (GR) is unique and completely different from other classical field theories in its treatment of the particle motion. For a comparison, in linear classical field theories, such as Maxwell's electrodynamics, the equations of motion of the electric charges can and must be postulated independently from the field equations. It is in a contrast to GR where, due to Bianchi identities, the trajectories of sources cannot be assumed completely arbitrary and thus must be treated as a type of consequence of the field equations. The ordinary assertion is that this difference is related to the fact that Maxwell's equations are linear while Einstein's equations are non-linear. Namely the non-linearity forbids the unphysical solutions and thus turns out to be a positive feature of a good physical theory.

Y. Itin (✉)

Institute of Mathematics, Hebrew University of Jerusalem and Jerusalem
College of Technology, Jerusalem, Israel
e-mail: itin@math.huji.ac.il

It was stressed by Einstein, Infeld, Fock and others, that the treatment of the equations of motion is one of the key achievement of GR. The original Einstein's proposal can be formulated as follows:

The equations of motion of point-wise particles is completely determined by the source-free field equations and directly derived from them.

In other words, the assertion is that it is possible to prove the implication

$$R_{ij} = 0 \quad \implies \quad u_i D_j u^i = 0. \quad (1)$$

Here, the first equation is the source-free Einstein's equation. The second equation is the geodesic one. In the first approximation, being multiplied on the mass of the test particle, it is expressed in the form of the second law of dynamics, $ma = F$.

Observe that these two systems of equations are essentially different one from the other in their mathematical structure. In the left hand side of (1), we have the GR field equations that are combined into a system of 10 *partial differential equations* for 10 independent fields $g_{ij}(x^i)$. In a contrast, the equations of motion in the right hand side of (1) are dealing with a tangential vector of a curve in \mathbb{R}^4 , i.e., with a vector-function of one real variable $u^i(s)$. For N particles considered on a special-relativistic background, these equations constitute a system of $4N$ *ordinary differential equations*. In other words one of the problems that two equations in (1) are dealing with different sets of variables.

A relation between these two distinct systems is provided by *Einstein's model of a particle*. A point-wise particle is assumed to be represented by a solution of the field equation that is singular on some curve—a wordline of the particle. A system of two particles is represented by a solution that is singular on two separated curves. Certainly it is assumed that the different components of the physical field have the same domain and consequently the same singular curves.

Although, the implication (1) includes two pure geometric covariant equations, the proof of it was constructed with different approximation procedures [1–10]. The most known approximation procedure is based on the Einstein-Infeld-Hoffmann (EIH) equations. They were even extended to high order PPN approximations of the N -body problem [11–14], for calculation of the gravitational radiation reaction force [15] and for describing the motion of a gyroscope [16].

A new type of the proof that has proposed recently, see [17, 18], is based on a limiting procedure instead of an approximation scheme. These derivations are dealing with a full Einstein's equations including the energy-momentum tensor in the right side. In fact, only the existence of a generic energy-momentum tensor satisfying some natural conditions is required. Such consideration, however, is far from the original (source-free) Einstein's proposal. Another type of an exact (non-approximated) proofs [19, 20] are based on the notion of distributions and use the symmetry group arguments. Also here the full Einstein's equation is considered and the equations of motion are derived, in fact, from the energy-momentum tensor. For a complete review of the methods used in different proofs of the geodesic principle and on their logical meanings, we refer to [21]. This paper also includes a vast list of relevant literature.

In the current paper, we will show by elementary examples how, in principle, equations of particles motion can be identified into the field equations and how they actually can be extracted. To these purposes, we restrict ourselves to a scalar field equation (linear and non-linear). Moreover, we are looking for the lowest order approximation of the geodesic equation—Newton's law of dynamics together with Newton's expression of the force of attraction. In other words, instead of discussing the implication (1) we will study the implication

$$E\left(\phi(x^i), \partial\phi(x^i), \partial^2\phi(x^i)\right) = 0 \quad \Longrightarrow \quad m\ddot{\mathbf{x}} = \mathbf{F}. \quad (2)$$

Here and in the sequel, the Roman indices denote the components of four-dimensional vectors and tensors. The three-dimensional vectors are denoted by bold letters. We call the term $m\ddot{\mathbf{x}}$ *the agent of inertia*, the force term \mathbf{F} is referred to as *the agent of interaction*. So our problem is to identify these two agents in the field equation and to derive the equation between them.

The paper is organized as follows: In Sect. 2 we consider a linear scalar Lorentz invariant field model and derive the inertial motion of its 1-singular point solution. In Sect. 3, the non-inertial motion is discussed. We derive an exact solution with one singular point and an approximated solution with two singular points. We show that the balance between the singular contributions to the field equation yields, in the first order, the Newton law of attraction.

2 Inertial Motion as Derived from a Field Equation

First we must decide which class of the field equations is suitable for derivation of the equations of motion. In this section, we discuss a scalar field model which singular solution represents inertial motion of a single particle. We also make a first attempt to describe fields that are singular along curved trajectories.

2.1 Non-relativistic Scalar Field Model

As an introductory example, we consider the field equation

$$\Delta\phi := \frac{\partial^2\phi}{\partial x^2} + \frac{\partial^2\phi}{\partial y^2} + \frac{\partial^2\phi}{\partial z^2} = 0 \quad (3)$$

for a scalar function $\phi(t, \mathbf{r}) = \phi(t, x, y, z)$. This model can be viewed as the Newtonian gravity formulated as a field theory. The field equation (3) does not include time derivatives thus it cannot yield an agent of inertia. It has however some properties that will be instructive for our consideration.

The solution of (3) of the form

$$\phi(t, \mathbf{r}) = \frac{m}{r}, \quad r = ||\mathbf{r}|| = \sqrt{x^2 + y^2 + z^2} \quad (4)$$

is singular at the origin of the coordinates and have a free parameter m of the length dimension. When a system of units with Newton's constant equal to one is chosen, we are able to interpret this solution as a model of a point-wise particle localized at the origin with the mass m . Since Eq. (3) is independent of the time coordinate, it has a more general solution

$$\phi(t, \mathbf{r}) = \frac{m}{||\mathbf{r} - \psi(t)||} \quad (5)$$

with an arbitrary vector function $\psi(t)$. Such a solution is defined for every $\mathbf{r} \neq \psi(t)$ so it can be viewed as a model of a particle of the mass m moving along the curve $\mathbf{r} = \psi(t)$. Since this curve is arbitrary, the model (3) with the solution (5) does not have a lot of physical sense. It is well known that, in Newton's gravity, the arbitrariness of the function $\psi(t)$ in the solution (5) is restricted by an additional axiom, which is Newton's law of attraction. Only under these requirements, a proper trajectory $\mathbf{r} = \psi(t)$ is derived.

2.2 Dynamic Singular Ansatz—a First Attempt

We will discuss now another example of a field equation. In a close similarity to Maxwell's electrodynamics, we consider a relativistic scalar model

$$\square \phi := \frac{\partial^2 \phi}{\partial t^2} - \Delta \phi = 0. \quad (6)$$

This equation includes the second order time-derivative, we need it in order to construct the agent of inertia.

Similarly to the non-relativistic case, Eq. (6) also has a static solution

$$\phi(t, \mathbf{r}) = \frac{m}{||\mathbf{r}||}, \quad (7)$$

that is singular at the origin. We are looking now for a more generic time-dependent solution of Eq. (6). As in Eq. (5), we can try a generic ansatz

$$\phi(t, \mathbf{r}) = \frac{m}{||\mathbf{r} - \psi(t)||}. \quad (8)$$

This solution, if it exists for some non-trivial function $\psi(t)$, will be defined on a set $\mathbb{R}^3 \setminus \{\mathbf{r} - \psi(t) = 0\}$. Recall that we treat the exceptional set $\mathbf{r} = \psi(t)$ as the trajectory of a particle of the mass m . For instance, with $\psi(t) = \mathbf{r}_o + \mathbf{v}t$, Eq. (8) must represent a field of a free particle. We will see shortly that it is not a case.

We substitute (8) into (6). For an arbitrary function $\psi(t)$, we have

$$\Delta \left(\frac{m}{\|\mathbf{r} - \psi(t)\|} \right) = 0. \quad (9)$$

In order to calculate the time derivatives, we first observe an identity that holds for an arbitrary vector function $\mathbf{a} = \mathbf{a}(t, \mathbf{r})$

$$\frac{\partial}{\partial t} \|\mathbf{a}\| = \frac{\langle \dot{\mathbf{a}}, \mathbf{a} \rangle}{\|\mathbf{a}\|}. \quad (10)$$

Here and in the sequel, \langle, \rangle denotes the scalar product of two 3-dimensional vectors. Consequently, the time-derivatives read

$$\frac{\partial}{\partial t} \left(\frac{1}{\|\mathbf{r} - \psi(t)\|} \right) = \frac{\langle \dot{\psi}(t), \mathbf{r} - \psi(t) \rangle}{\|\mathbf{r} - \psi(t)\|^3}, \quad (11)$$

and

$$\frac{\partial^2}{\partial t^2} \left(\frac{1}{\|\mathbf{r} - \psi(t)\|} \right) = \frac{\langle \ddot{\psi}(t), \mathbf{r} - \psi(t) \rangle - \|\dot{\psi}(t)\|^2}{\|\mathbf{r} - \psi(t)\|^3} + 3 \frac{\langle \dot{\psi}(t), \mathbf{r} - \psi(t) \rangle^2}{\|\mathbf{r} - \psi(t)\|^5}. \quad (12)$$

We rewrite this expression as

$$\square \phi = \frac{\langle m \ddot{\psi}(t), \mathbf{r} - \psi(t) \rangle}{\|\mathbf{r} - \psi(t)\|^3} + m \frac{3 \langle \dot{\psi}(t), \mathbf{r} - \psi(t) \rangle^2 - \|\dot{\psi}(t)\|^2 \|\mathbf{r} - \psi(t)\|^2}{\|\mathbf{r} - \psi(t)\|^5}. \quad (13)$$

In the right hand side of Eq. (13), the first term is exactly what we need as an agent of inertia. The additional terms must be equal to zero. It is true, however, only for $\dot{\psi}(t) = 0$. Indeed, it is easy to check that even in the simplest case of the free motion trajectory, $\psi(t) = \mathbf{r}_o + \mathbf{v}t$, these terms give an expression which is non zero for $\mathbf{v} \neq 0$. It means that (8) is not a solution of Eq. (6) and we must look for a modification of our ansatz.

There is a principle reason why our simple ansatz (8) cannot make the job. The field equation (6) is relativistic invariant, but the ansatz (8) can be considered as be obtained by the non-relativistic transformation of the static ansatz.

2.3 Lorentz Transformation of a Static Singular Solution

Our problem can be formulated now as follows: We are looking for a solution of the equation (6) that represents inertial motion of a particle by the singularity of its solution. Let us consider a more complicated ansatz

$$\phi(t, \mathbf{r}) = \frac{m}{\|\mathbf{R}(t, \mathbf{r})\|} \quad (14)$$

with an unknown vector function $\mathbf{R}(t, \mathbf{r})$. Our requirements for $\mathbf{R}(t, \mathbf{r})$ are as follows:

- (1) The function $\mathbf{R}(t, \mathbf{r})$ must be regular in the whole space except for one singular curve.
- (2) $\mathbf{R}(t, \mathbf{r})$ must approach zero at the space infinity and at the time infinity.
- (3) In the static case $t = 0$, the vector $\mathbf{R}(t, \mathbf{r})$ must be equal to $(\mathbf{r} - \mathbf{r}_o)$.
- (4) The free-motion trajectory $\mathbf{r}(t) = \mathbf{r}_o + \mathbf{v}t$ must be a solution of the equation $\mathbf{R}(t, \mathbf{r}) = 0$.

The simplest way to derive a suitable expression for $\mathbf{R}(t, \mathbf{r})$ is to start with a static solution and apply to it the Lorentz transformation with a constant velocity \mathbf{v} . Most textbooks restrict to the one-dimensional Lorentz transformation. In particular, when a reference system $\{\tilde{t}, \tilde{x}, \tilde{y}, \tilde{z}\}$ moves with a velocity v parallel to the x -axis of the rest reference system $\{t, x, y, z\}$, the corresponding Lorentz transformation is given by

$$\tilde{x} = \beta(x + vt), \quad \tilde{y} = y, \quad \tilde{z} = z, \quad \tilde{t} = \beta(t + vx), \quad (15)$$

with the Lorentz parameter

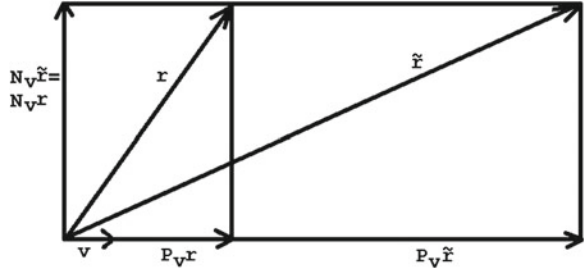
$$\beta = \frac{1}{\sqrt{1 - v^2}}. \quad (16)$$

Recall that we use here and in the sequel a system of units with $c = 1$. Since we want to describe a more generic trajectory of a particle, we need Lorentz transformation with an arbitrary directed velocity. Observe that two Lorentz's transformations with orthogonal velocities do not commute, so a general transformation can not be generated by a successive application of three orthogonal transformations (relative to three axes). The transformation with an arbitrary directed velocity can be derived as follows, see [22].

Consider a reference system which axes are parallel to the corresponding axes of a rest reference system. Let the origin of the first reference system moves with an arbitrary directed velocity \mathbf{v} . Consider a position vector \mathbf{r} directed to an arbitrary point. Its projection on the direction of \mathbf{v} reads

$$P_{\mathbf{v}}\mathbf{r} = \mathbf{v} \frac{\langle \mathbf{v}, \mathbf{r} \rangle}{\|\mathbf{v}\|^2}. \quad (17)$$

Fig. 1 The vectors \mathbf{r} and $\tilde{\mathbf{r}}$ are exhibited as the sum of their tangential and normal parts



We exhibit the vector \mathbf{r} as the sum of its tangential and normal parts (see Fig. 1).

$$\mathbf{r} = P_{\mathbf{v}}\mathbf{r} + N_{\mathbf{v}}\mathbf{r}, \quad N_{\mathbf{v}}\mathbf{r} = \mathbf{r} - \mathbf{v} \frac{\langle \mathbf{v}, \mathbf{r} \rangle}{\|\mathbf{v}\|^2}. \quad (18)$$

Due to Eq. (15), for a Lorentz transformation directed by \mathbf{v} , these two parts transform as

$$P_{\mathbf{v}}\tilde{\mathbf{r}} = \beta(P_{\mathbf{v}}\mathbf{r} + \mathbf{v}t), \quad \text{and} \quad N_{\mathbf{v}}\tilde{\mathbf{r}} = N_{\mathbf{v}}\mathbf{r}. \quad (19)$$

Consequently, the transform of the spatial vectors takes the form

$$\tilde{\mathbf{r}} = P_{\mathbf{v}}\tilde{\mathbf{r}} + N_{\mathbf{v}}\tilde{\mathbf{r}} = \beta(P_{\mathbf{v}}\mathbf{r} + \mathbf{v}t) + N_{\mathbf{v}}\mathbf{r}, \quad (20)$$

or, explicitly,

$$\tilde{\mathbf{r}} = \mathbf{r} + \mathbf{v}(\beta t - \alpha \langle \mathbf{r}, \mathbf{v} \rangle). \quad (21)$$

Here two Lorentz parameters are

$$\beta = \frac{1}{\sqrt{1 - \|\mathbf{v}\|^2}}, \quad \alpha = \frac{1 - \beta}{\|\mathbf{v}\|^2}. \quad (22)$$

The change of the time coordinate is also governed only by the tangential part of the vector \mathbf{r}

$$\tilde{t} = \beta(t + \|P_{\mathbf{v}}\mathbf{r}\| \|\mathbf{v}\|) = \beta(t + \langle P_{\mathbf{v}}\mathbf{r}, \mathbf{v} \rangle), \quad (23)$$

or, explicitly,

$$\tilde{t} = \beta(t + \langle \mathbf{r}, \mathbf{v} \rangle). \quad (24)$$

Therefore, an arbitrary directed Lorentz transformation takes the form

$$\begin{cases} \tilde{t} = \beta (t + \langle \mathbf{r}, \mathbf{v} \rangle), \\ \tilde{\mathbf{r}} = \mathbf{r} + \mathbf{v} (\beta t - \alpha \langle \mathbf{r}, \mathbf{v} \rangle). \end{cases} \quad (25)$$

In the special case of a velocity parallel to the axis x , the relations (25) reduce to the ordinary form of the Lorentz transformation (15).

2.4 A Dynamical Singular Solution

We consider now an ansatz

$$\phi(t, \mathbf{r}) = \frac{m}{||\mathbf{R}(t, \mathbf{r})||}, \quad (26)$$

where $\mathbf{R}(t, \mathbf{r})$ is the Lorentz transformation of the vector $(\mathbf{r} - \mathbf{r}_o)$ with a constant velocity $(-\mathbf{v})$, i.e.,

$$\mathbf{R}(t, \mathbf{r}) = (\mathbf{r} - \mathbf{r}_o) - \alpha \mathbf{v} \langle \mathbf{v}, (\mathbf{r} - \mathbf{r}_o) \rangle - \beta \mathbf{v} t. \quad (27)$$

Here α and β are Lorentz functions of the velocity \mathbf{v} given in Eq. (22).

First we check that (26) indeed a solution of the field equation (6). For the time derivatives of the vector $\mathbf{R}(t, \mathbf{r})$, we have

$$\dot{\mathbf{R}}(t, \mathbf{r}) = -\beta \mathbf{v}, \quad \ddot{\mathbf{R}}(t, \mathbf{r}) = 0. \quad (28)$$

Consequently, due to (10), the time derivatives of the field are

$$\frac{\partial \phi}{\partial t} = -m\beta \frac{\langle \mathbf{R}, \mathbf{v} \rangle}{||\mathbf{R}||^3}, \quad (29)$$

and

$$\frac{\partial^2 \phi}{\partial t^2} = -\frac{m\beta^2}{||\mathbf{R}||^3} \left(3 \langle \mathbf{R}, \mathbf{v} \rangle^2 - ||\mathbf{R}||^2 ||\mathbf{v}||^2 \right). \quad (30)$$

In order to calculate the spatial derivatives of the field (26), we introduce a set of unit vectors $\mathbf{e}_1, \mathbf{e}_2, \mathbf{e}_3$ directed along the axes x, y, z respectively. Using Eq. (10) the x -derivatives of the vector (27) is written as

$$\mathbf{R}_x = \mathbf{e}_1 - \alpha \mathbf{v} \langle \mathbf{v}, \mathbf{e}_1 \rangle \quad \mathbf{R}_{xx} = 0. \quad (31)$$

The second order derivative of the field takes now the form

$$\frac{\partial^2 \phi}{\partial x^2} = -\frac{m}{R^3} ||\mathbf{R}_x||^2 + 3 \frac{m}{R^5} \langle \mathbf{R}_x, \mathbf{R} \rangle^2. \quad (32)$$

Consequently, the three dimensional Laplacian of ϕ is expressed as

$$\begin{aligned} \Delta \phi = & -\frac{m}{R^3} \left(||\mathbf{R}_x||^2 + ||\mathbf{R}_y||^2 + ||\mathbf{R}_z||^2 \right) + \\ & 3 \frac{m}{R^5} \left(\langle \mathbf{R}_x, \mathbf{R} \rangle^2 + \langle \mathbf{R}_y, \mathbf{R} \rangle^2 + \langle \mathbf{R}_z, \mathbf{R} \rangle^2 \right). \end{aligned} \quad (33)$$

Since

$$\langle \mathbf{R}_x, \mathbf{R} \rangle = \langle \mathbf{R}, \mathbf{e}_1 \rangle - \alpha \langle \mathbf{v}, \mathbf{e}_1 \rangle \langle \mathbf{v}, \mathbf{R} \rangle, \quad (34)$$

we get

$$\begin{aligned} \langle \mathbf{R}_x, \mathbf{R} \rangle^2 + \langle \mathbf{R}_y, \mathbf{R} \rangle^2 + \langle \mathbf{R}_z, \mathbf{R} \rangle^2 = \\ R^2 - 2\alpha \langle \mathbf{v}, \mathbf{R} \rangle^2 + \alpha^2 ||\mathbf{v}||^2 \langle \mathbf{v}, \mathbf{R} \rangle^2, \end{aligned} \quad (35)$$

and

$$||\mathbf{R}_x||^2 + ||\mathbf{R}_y||^2 + ||\mathbf{R}_z||^2 = 3 - 2\alpha ||\mathbf{v}||^2 + \alpha^2 ||\mathbf{v}||^4. \quad (36)$$

Thus the three dimensional Laplacian of the field ϕ remains in the form

$$\Delta \phi = \frac{m}{R^5} (\alpha^2 ||\mathbf{v}||^2 - 2\alpha) (3 \langle \mathbf{v}, \mathbf{R} \rangle^2 - ||\mathbf{v}||^2 ||\mathbf{R}||^2). \quad (37)$$

With (30) and (37), we write the full d'Alembertian of the field as

$$\square \phi = \frac{m}{R^5} \left(\beta^2 + 2\alpha - \alpha^2 ||\mathbf{v}||^2 \right) \left(3 \langle \mathbf{v}, \mathbf{R} \rangle^2 - ||\mathbf{v}||^2 ||\mathbf{R}||^2 \right). \quad (38)$$

In the last step, we use the expressions (22) for the functions α, β to derive straightforwardly

$$\beta^2 + 2\alpha - \alpha^2 ||\mathbf{v}||^2 = 0. \quad (39)$$

Consequently, the 1-singular ansatz (26) with (27) is indeed a solution of the linear equation $\square \phi = 0$.

Let us check now what is the trajectory of the singular point related to this solution. It is encoded implicitly in the equation $\mathbf{R}(t, \mathbf{r}) = 0$, i.e.,

$$(\mathbf{r} - \mathbf{r}_o) - \alpha \mathbf{v} \langle \mathbf{v}, (\mathbf{r} - \mathbf{r}_o) \rangle - \beta \mathbf{v} t = 0. \quad (40)$$

Multiplying both sides of this equation by vector \mathbf{v} we obtain a scalar equation

$$\langle \mathbf{v}, (\mathbf{r} - \mathbf{r}_o) \rangle = \frac{\beta ||\mathbf{v}||^2 t}{1 - \alpha ||\mathbf{v}||^2} = ||\mathbf{v}||^2 t. \quad (41)$$

We substitute this expression into Eq. (40) and obtain

$$\mathbf{r} - \mathbf{r}_o = (\alpha ||\mathbf{v}||^2 + \beta) \mathbf{v} t = \mathbf{v} t. \quad (42)$$

It means that the singular set of the field ϕ coincides with the inertial trajectory. Thus starting with the singular solution of the linear equation $\square \phi = 0$ we derive the inertial motion trajectory.

3 Non-inertial Motion

Since it is imposible to get from the linear equation something more than the inertial motion, we turn to a non-linear scalar model. Its singular solutions must represent particles moving along curved trajectory. We identify the agent of inertia and the agent of interaction and derive, in the lowest approximation, Newton's law of attraction between two singularities.

3.1 Field Ansatz and Agent of Inertia

We are trying now to extend our results to a non-inertial motion. In general, it can be expressed by a curved trajectory of the form $\mathbf{r} = \mathbf{r}_o + \psi(t)$. In the inertial case, $\psi(t) = \mathbf{v}t$ with a constant velocity \mathbf{v} , we must return to the results from the previous section. Thus, in order to model a field of a single particle moving along a curved trajectory, we consider the ansatz

$$\phi(t, \mathbf{r}) = \frac{m}{||\mathbf{R}(t, \mathbf{r})||}. \quad (43)$$

Since the velocity of the point-wise singularity is not a constant now, we cannot use the Lorentz transformation directly. We are able to use it, however, in the infinitesimal sense. Similarly to (27), we assume

$$d\mathbf{R}(t, \mathbf{r}) = d\mathbf{r} - \alpha \dot{\psi} \langle \dot{\psi}, d\mathbf{r} \rangle - \beta \dot{\psi} dt. \quad (44)$$

Here α and β are Lorentz's functions of the velocity $||\dot{\psi}||^2$

$$\beta = \frac{1}{\sqrt{1 - ||\dot{\psi}||^2}} \approx 1 + \frac{1}{2}||\dot{\psi}||^2 + \frac{3}{8}||\dot{\psi}||^4 + \dots \quad (45)$$

and

$$\alpha = \frac{1}{||\dot{\psi}||^2} (1 - \beta) \approx -\frac{1}{2} \left(1 - \frac{3}{2}||\dot{\psi}||^2 - \frac{5}{8}||\dot{\psi}||^4 + \dots \right). \quad (46)$$

The function $\mathbf{R}(t, \mathbf{r})$ is presented now in the form of an integral expression of the unknown function ψ . In the case of the slow velocities of the particles, this technical difficult can be easily resolved. So we restrict our calculations to the condition $||\dot{\psi}|| \ll 1$ and remove all terms of the order $\mathcal{O}(||\dot{\psi}||^2)$ and higher. In Eq.(44), we can delete now the middle term and assume $\beta = 1$. The remaining equation is easily integrated and we come to our old non-relativistic ansatz

$$\phi(t, \mathbf{r}) = \frac{m}{||\mathbf{r} - \mathbf{r}_o - \psi(t)||}. \quad (47)$$

Recall that in order to use this ansatz, we must restrict to the lowest approximation. We are in a position now to generate an agent of inertia—the mass-times-acceleration term. Using the expression (13) and removing the terms of the order $\mathcal{O}(||\dot{\psi}||^2)$, we remain with

$$\square \phi(t, \mathbf{r}) = \frac{m}{||\mathbf{R}(t, \mathbf{r})||^3} < \ddot{\psi}, \mathbf{R}(t, \mathbf{r}) >. \quad (48)$$

This is a form of our *agent of inertia*.

3.2 Agent of Interaction

We are looking now how the interaction between two particles (two singularities of the field) can be generated by the field equation. It is clear that, for a linear equation, two distinct singular solutions are combined into a solution with two singular points without any interaction between them. Thus we need a non-linear operator acting on the field. Consider a Lorentz invariant term of the form

$$< \partial_\alpha \phi, \partial^\alpha \phi > = \left(\frac{\partial \phi}{\partial t} \right)^2 - ||\nabla \phi||^2. \quad (49)$$

For a field of the form, $\phi = {}^{(1)}\phi + {}^{(2)}\phi$, this expression gives

$${}^{(1)}\dot{\phi}^2 - ||\nabla^{(1)}\phi||^2 + {}^{(2)}\dot{\phi}^2 - ||\nabla^{(2)}\phi||^2 + 2 < \partial_\alpha {}^{(1)}\phi, \partial^\alpha {}^{(2)}\phi > . \quad (50)$$

Consider a case when ${}^{(1)}\phi$ and ${}^{(2)}\phi$ are two solutions of the field equation that contains the term (49). Now, the first four terms of (50) are canceled and we remain with

$$2 < \partial_\alpha {}^{(1)}\phi, \partial^\alpha {}^{(2)}\phi > . \quad (51)$$

This expression includes symmetric contributions of two singularities, so it can be interpreted as *the interaction term*.

We consider first what is going in the case of 1-point singularity. Let us calculate the expression (49) for the ansatz (47). Since the time derivative term of the field (47) is of the order $\mathcal{O}(|\dot{\psi}|^2)$, it can be neglected. As about the spatial derivative term, it takes the form

$$||\nabla\phi||^2 = -\frac{m^2}{||\mathbf{R}(t, \mathbf{r})||^4} . \quad (52)$$

This term remains non-zero even in the case of the inertial motion. Thus we must find out a way how to correlate two necessary terms: The inertia term (48) and the interaction term (49).

3.3 Non-linear Scalar Equation

We consider a non-linear Lorentz invariant scalar equation for a scalar field $\varphi = \varphi(x)$ given on a flat Minkowski space

$$\eta^{\alpha\beta} \left(\frac{\partial^2 \varphi}{\partial x^\alpha \partial x^\beta} - k \frac{\partial \varphi}{\partial x^\alpha} \frac{\partial \varphi}{\partial x^\beta} \right) = 0. \quad (53)$$

It is equivalent to

$$\square \varphi = k \left(\dot{\varphi}^2 - ||\nabla \varphi||^2 \right). \quad (54)$$

Here k is a dimensionless constant. We will discuss its value in the sequel. Let us derive now a static solutions of Eq.(53) with arbitrary values of the parameter k . First, we redefine the scalar field as

$$\varphi = -\frac{1}{k} \ln \phi, \quad \phi = e^{-k\varphi}. \quad (55)$$

It follows that

$$\square \varphi - k \left(\dot{\varphi}^2 - \|\nabla \varphi\|^2 \right) = -\frac{1}{k\phi} \square \phi. \quad (56)$$

Thus, under the transformation (55), the nonlinear equation (53) is transformed to the linear one $\square \phi = 0$. Consequently, every solution of the linear equation ϕ generates a solution φ of the nonlinear equation (53).

Starting with a function of the form

$$\phi = 1 - k \frac{m}{\|\mathbf{r} - \mathbf{r}_0\|}, \quad (57)$$

we come to a 1-singular solution of Eq.(53)

$$\varphi = -\frac{1}{k} \ln \left(1 - k \frac{m}{\|\mathbf{r} - \mathbf{r}_0\|} \right). \quad (58)$$

For an arbitrary value of the parameter k , this solution vanishes at infinity as $\varphi \rightarrow m/r$. Also, in the limiting case $k \rightarrow 0$, the solution (58) approaches the Newtonian potential. These two limits hold independently of the sign of k . We observe, however, that for $k > 0$ the solution (58) is defined only for $\|\mathbf{r} - \mathbf{r}_0\| > km$. In this case, we have some type of a scalar black hole. For $k < 0$, (58) is singular only at a point $\mathbf{r} = \mathbf{r}_0$ and smooth at all other points. We will see in the sequel that namely the negative values of the parameter k yield the attraction between the singularities, while the positive values of k yield their repulsion.

We consider now a non-static ansatz of the form (58)

$$\varphi = -\frac{1}{k} \ln \left(1 - \frac{km}{\mathbf{R}(t, \mathbf{r})} \right). \quad (59)$$

As we have already seen, it is enough to restrict, in the lowest approximation, to the denominator

$$\mathbf{R}(t, \mathbf{r}) = \mathbf{r} - \mathbf{r}_0 - \psi(t). \quad (60)$$

Substituting this expression into Eq.(53) and removing the terms of the order $\mathcal{O}(\|\dot{\psi}\|^2)$ we obtain

$$\eta^{\mu\nu} (\varphi_{,\mu\nu} - k\varphi_{,\mu}\varphi_{,\nu}) = \frac{m \langle \ddot{\psi}, \mathbf{R}(t, \mathbf{r}) \rangle}{\|\mathbf{R}(t, \mathbf{r})\|^3 \left(1 - \frac{km}{\|\mathbf{R}(t, \mathbf{r})\|} \right)}. \quad (61)$$

This is our new *agent of inertia*.

3.4 An Interaction Is Generated

Consider first a static solution of Eq. (53) with two singular points. In the lowest approximation, we may use the superposition of two individual static solutions,

$$\varphi = -\frac{1}{k} \ln \left(1 - k \frac{m_1}{\|\mathbf{r} - \mathbf{r}_1\|} \right) - \frac{1}{k} \ln \left(1 - k \frac{m_2}{\|\mathbf{r} - \mathbf{r}_2\|} \right). \quad (62)$$

Here \mathbf{r} is a generic point of observation, while $\mathbf{r}_1, \mathbf{r}_2$ are the positions of two singular points with the masses m_1 and m_2 respectively.

In order to generate a non-static (interaction) solution of Eq. (53) with two singular points moving on their own trajectories, we modify the definition of the denominators. Let $\psi_1(t)$ and $\psi_2(t)$ describe the trajectories of the singular points. Thus we come to an ansatz of the form

$$\varphi = -\frac{1}{k} \ln \left(1 - k \frac{m_1}{R_1} \right) - \frac{1}{k} \ln \left(1 - k \frac{m_2}{R_2} \right), \quad (63)$$

where

$$R_i = \|\mathbf{R}_i\| = \|(\mathbf{r} - \mathbf{r}_i) - \psi_i(t)\| \quad i = 1, 2. \quad (64)$$

We search for conditions on the functions $\psi_i(t)$ that turn (63) into an approximate solution of (53). Substituting (63) into Eq. (53) and removing the terms of the order $\mathcal{O}(\|\dot{\psi}_i\|^2)$, we get

$$\begin{aligned} \frac{m_1}{R_1^3} \cdot \frac{\langle \mathbf{R}_1, \ddot{\psi}_1 \rangle}{1 - k(m_1/R_1)} + \frac{m_2}{R_2^3} \cdot \frac{\langle \mathbf{R}_2, \ddot{\psi}_2 \rangle}{1 - k(m_2/R_2)} = \\ \frac{-km_1m_2 \langle \mathbf{R}_1, \mathbf{R}_2 \rangle}{R_1^3 R_2^3 (1 - k(m_1/R_1)) (1 - k(m_2/R_2))}. \end{aligned} \quad (65)$$

Both sides of Eq. (65) are functions of a point \mathbf{r} . They are singular at two points where $\mathbf{R}_1 = 0$ and $\mathbf{R}_2 = 0$, i.e., at the curves

$$\mathbf{r} = \mathbf{r}_1 - \psi_1(t), \quad \text{and} \quad \mathbf{r} = \mathbf{r}_2 - \psi_2(t), \quad (66)$$

and regular at all other points (Fig. 2).

Let us examine how the relation (65) can be satisfied in a neighborhood of a singular point. We consider near zones around two masses. They include points that are close enough to the singularities but yet far from the corresponding Schwarzschild spheres $R = km$. In these domains, we can essentially simplify Eq. (65)

$$\frac{m_1}{R_1^3} \langle \mathbf{R}_1, \ddot{\psi}_1 \rangle + \frac{m_2}{R_2^3} \langle \mathbf{R}_2, \ddot{\psi}_2 \rangle = \frac{-km_1m_2 \langle \mathbf{R}_1, \mathbf{R}_2 \rangle}{R_1^3 R_2^3}. \quad (67)$$

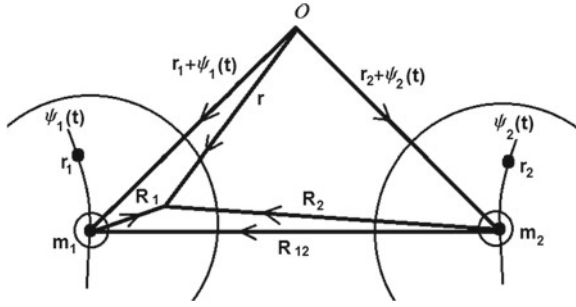


Fig. 2 On the picture, two masses m_1 and m_2 move along their trajectories $\psi_1(t)$ and $\psi_2(t)$ respectively. *Small circles* around the masses represent Schwarzschild spheres $R_1 = km_1$ and $R_2 = km_2$. *Big circles* show the near zones of the particles

We will examine the field at an arbitrary point \mathbf{r} close to the mass m_1 . Consequently we have $R_1 \rightarrow 0$. For the second singularity

$$R_1 \rightarrow 0 \quad \text{yields} \quad R_2 \rightarrow R_{12}, \quad (68)$$

where R_{12} is a vector directed from the point m_2 to the point m_1 .

On the left hand side of the equation (67), there is a singular term. It must be compensated by the corresponding singular term on the right hand side. These terms are of the same order $\mathcal{O}(R^{-2})$ near the first singularity. So they cancel each other in the case when the corresponding leading coefficients are equal. Consequently,

$$m_1 \langle \mathbf{R}_1, \ddot{\psi}_1 \rangle = \frac{-km_1 m_2 \langle \mathbf{R}_1, \mathbf{R}_2 \rangle}{R_2^3}. \quad (69)$$

Take into account that the point \mathbf{r} (in \mathbf{R}_1) is arbitrary. Hence (69) is valid only if

$$m_1 \ddot{\psi}_1 = \frac{-km_1 m_2 \mathbf{R}_2}{R_2^3}. \quad (70)$$

For small values of \mathbf{r} , we have in (70)

$$m_1 \ddot{\psi}_1 = \frac{-km_1 m_2 \mathbf{R}_{12}}{R_{12}^3}. \quad (71)$$

For $k > 0$, Eq.(71) results in repulsion between the particles. The negative values of the parameter k yield attraction. The absolute value of k is unimportant, since it amounts to the rescaling of the mass. This way the Newton-type law of attraction is derived from the scalar field equation.

4 Discussion

We present here an illustrative example of a non-linear scalar model that allows the derivation of the equation of motion. In fact, this model has some plausible features as Newton's behavior at infinity and Schwarzschild type form near the origin. So it can be used as a laboratory for the real gravity, compare [23, 24] .

Is it possible to extend our consideration to the electromagnetism? In fact, there is an essential difference in physics of electromagnetism and gravity. Observe first that we can hold two electric charges in arbitrary positions and study, with Maxwell's equations, the electric field between them. Quite similarly we can hold two masses and study, with Einstein's equations, the gravity field between them. In both cases, we are dealing with *open systems*.

For a *closed gravitational system* containing masses and gravity field, two massive particles cannot be in a rest or in a free motion. In Newton's gravity, such behavior is allowed by the field equation $\square\varphi = 0$ but it is forbidden by the second law of dynamics. In GR, such solution is forbidden already by the field equations themselves.

In an electromagnetic system containing only electric charges and electromagnetic field, Maxwell's system itself allows arbitrary motion of charges. In this sense, Maxwell's system itself is incomplete. In order to forbid these arbitrary motions, one must arranged the system with the second Newton's law, in particular with the notion of mass. Indeed the charges necessary have the non-zero masses. But the notion of mass is not related to the electromagnetism, it is a gravity phenomena. It means that electromagnetism cannot exist without gravity, even the gravity effects are very small in ordinary situations. In this sense electromagnetism itself must be considered as an *open system*. One can guess that in the Einstein-Maxwell system (or in some type of a unified theory), the equations of motion of massive charges must be derivable from the field equations as in the pure Einstein's system.

Acknowledgments I thank Claus Lämmerzahl and Dirk Pützfeld for an invitation to the 524. WE-Heraeus-Seminar on "Equations of Motion in Relativistic Gravity". I acknowledge support of the German-Israeli Research Foundation (GIF) by the grant GIF/No.1078-107.14/2009.

References

1. A. Einstein, J. Grommer, Sitzber. Deut. Akad. Wiss. Berlin, 2, (1927)
2. A. Einstein, L. Infeld, B. Hoffmann, Ann. Math. **39**, 65 (1938)
3. A. Einstein, L. Infeld, Ann. Math. **41**, 455 (1940)
4. L. Infeld, P.R. Wallace, Phys. Rev. **57**, 797 (1940)
5. A. Einstein, L. Infeld, Can. J. Math. **1**, 209 (1949)
6. L. Infeld, A. Schild, Rev. Mod. Phys. **21**, 408 (1949)
7. L. Infeld, Rev. Mod. Phys. **29**, 398 (1957)
8. B. Fock, JETP **9**, 375 (1939)
9. A. Papapetrou, Proc. Phys. Soc. (London) **209**, 248 (1951)
10. P. Havas, J.N. Goldberg, Phys. Rev. **128**, 398 (1962)

11. M. Carmeli, Phys. Lett. **9**, 132 (1964)
12. T. Damour, N. Deruelle, Ann. Inst. H. Poincaré **44**, 263 (1986)
13. T. Damour, in *Proceedings of Conference 300 Years of Gravity*, (Cambridge, England, 1987)
14. L. Blanchet, G. Faye, B. Ponsot, Phys. Rev. D **58**, 124002 (1998)
15. J.L. Anderson, Phys. Rev. D **36**, 2301 (1987)
16. L.I. Schiff, Proc. Natl. Acad. Sci. USA **46**, 871 (1960)
17. R. Geroch, P.S. Jang, J. Math. Phys. **16**, 65 (1975)
18. J. Ehlers, R. Geroch, Ann. Phys. **309**, 232 (2004)
19. J. Souriau, Ann. Inst. H. Poincaré **20**, 315 (1974)
20. S. Sternberg, Proc. Natl. Acad. Sci. USA **96**, 8845 (1999)
21. M. Tamir, Stud. Hist. Philos. Mod. Phys. **43**, 137 (2012)
22. S. Kaniel, Y. Itin, Ann. der. Phys. **15**, 877 (2006)
23. K. Watt, C.W. Misner, [gr-qc/9910032](#), (1999)
24. D. Giulini, [gr-qc/0611100](#), (2006)

Motion of Spinless Particles in Gravitational Fields

Alexander J. Silenko

Abstract The covariant Klein-Gordon equation describing a scalar particle in a Riemannian spacetime of general relativity is transformed to a Hamiltonian form by the generalized Feshbach-Villars method applicable for both massive and massless particles. The subsequent Foldy-Wouthuysen (FW) transformation allows to derive the relativistic FW Hamiltonian for a wide class of inertial and gravitational fields and find the new manifestation of conformal invariance for a massless scalar particle. Similarity of manifestations of conformal invariance for massless scalar and Dirac particles is proved. New exact FW Hamiltonians are derived for both massive and massless scalar particles in a general static spacetime and in a frame rotating in the Kerr field approximated by a spatially isotropic metric. The latter case covers an observer on the ground of the Earth or on a satellite and takes into account the Lense-Thirring (LT) effect. High-precision formulas are obtained for an arbitrary spacetime metric. General quantum-mechanical equations of motion are derived. Their classical limit coincides with corresponding classical equations. The quantum-mechanical description of the relativistic LT effect is presented. The exact evolution of the angular momentum operator in the Kerr field approximated by a spatially isotropic metric is found. The quantum-mechanical description of the full LT effect based on the Laplace-Runge-Lenz vector is given in the nonrelativistic and weak-field approximation. Relativistic quantum-mechanical equations for the velocity and acceleration operators are obtained. The equation for the acceleration defines the Coriolis-like and centrifugal-like accelerations and presents the quantum-mechanical description of the frame-dragging effect.

A.J. Silenko (✉)

Research Institute for Nuclear Problems, Belarusian State University,
220030 Minsk, Belarus
e-mail: alsilenko@mail.ru

A.J. Silenko

Bogoliubov Laboratory of Theoretical Physics, Joint Institute for Nuclear Research,
Dubna 141980, Russia

1 Introduction

The problem of quantum-mechanical description of a spinless particle in a Riemannian spacetime of general relativity (GR) has a long history. An appropriate form of the initial covariant Klein-Gordon (KG) equation [1–4] has been discovered fifty years ago by Penrose [5]. He has found an appropriate term describing a non-minimal coupling to the scalar curvature and conserving the conformal invariance of the equation for a massless scalar particle. Chernikov and Tagirov [6] have given clear explanations of this wonderful result. Their study involved the case of a nonzero mass and n -dimensional Riemannian spacetime. It is important that the inclusion of the Penrose-Chernikov-Tagirov term has been argued for both massive and massless particles [6].

Next step in investigation of the problem of conformal invariance of the KG equation has been made by Accioly and Blas [7, 8]. They have performed the exact FW transformation for a massive spin-0 particle in static spacetimes and have found new telling arguments in favour of the predicted coupling to the scalar curvature. A derivation of the relativistic FW Hamiltonian fulfilled in Refs. [7, 8] is important for a comparison of gravitational (and inertial) effects for scalar and Dirac particles. However, the transformation method used in Refs. [7, 8] is inapplicable to massless particles. In addition, it cannot be employed for nonstatic spacetimes. This does not allow to obtain an information about a specific manifestation of the conformal invariance in the FW representation.

A procedure of derivation of relativistic quantum-mechanical equations of motion from the FW Hamiltonians is fairly well known. Such a procedure was widely used for a Dirac particle in noninertial and gravitational fields (see Refs. [9–13] and references therein). It has been proved in Ref. [14] that satisfying the condition of the Wentzel-Kramers-Brillouin approximation allows to use this approximation in the relativistic case and to obtain a classical limit of the relativistic quantum-mechanical equations of motion.

In the present work, we consider a scalar particle in arbitrary Riemannian spacetimes. To obtain a Hamiltonian form of the initial covariant KG equation not only for massive particles but also for massless ones, we use the generalization of the Feshbach-Villars transformation [15] proposed in Ref. [16]. Then we fulfill the FW transformation and prove the conformal invariance of the relativistic FW Hamiltonian for a wide class of inertial and gravitational fields. We derive general quantum-mechanical equations of motion and obtain their classical limit. As an example, quantum-mechanical description of the LT effect is presented and its classical limit is found.

We denote world and spatial indexes by Greek and Latin letters $\alpha, \mu, \nu, \dots = 0, 1, 2, 3$, $i, j, k, \dots = 1, 2, 3$, respectively. Tetrad indexes are denoted by Latin letters from the beginning of the alphabet, $a, b, c, \dots = 0, 1, 2, 3$. Temporal and spatial tetrad indexes are distinguished by hats. The signature is $(+---)$, the Ricci scalar curvature is defined by $R = g^{\mu\nu} R_{\mu\nu} = g^{\mu\nu} R_{\mu\alpha\nu}^{\alpha}$, where $R_{\mu\beta\nu}^{\alpha} = \partial_{\beta}\Gamma_{\mu\nu}^{\alpha} - \dots$ is the Riemann curvature tensor. We use the system of units $\hbar = 1$, $c = 1$ except for some specific expressions.

2 Importance of the Penrose-Chernikov-Tagirov Term for Massive Scalar Particles

The covariant KG [1–4] equation with the additional term [5, 6] describes a scalar particle in a Riemannian spacetime and is given by

$$(\square + m^2 - \lambda R)\psi = 0, \quad \square \equiv \frac{1}{\sqrt{-g}}\partial_\mu \sqrt{-g} g^{\mu\nu} \partial_\nu. \quad (1)$$

Minimal (zero) coupling corresponds to $\lambda = 0$, while the Penrose-Chernikov-Tagirov coupling is defined by $\lambda = 1/6$. Sign of the Penrose-Chernikov-Tagirov term depends on the definition of R . For noninertial (accelerated and rotating) frames, the spacetime is flat and $R = 0$.

For massless particles, the conformal transformation

$$\tilde{g}_{\mu\nu} = O^{-2} g_{\mu\nu} \quad (2)$$

conserves the form of Eq. (1) but changes the operators and the wave function [5, 6]:

$$\left(\tilde{\square} - \frac{1}{6}\tilde{R}\right)\tilde{\psi} = 0, \quad \tilde{\psi} = O\psi. \quad (3)$$

In Ref. [6], higher dimensionality was also considered.

The corresponding classical equation

$$g^{\mu\nu} p_\mu p_\nu - m^2 = 0$$

is also conformal for a massless particle. It does not contain any nonminimal coupling to the scalar curvature. Therefore, the square of the classical momentum corresponds to the operator $-\hbar^2(\square - R/6)$ [6].

Chernikov and Tagirov [6] have shown the importance of the additional term for massive particles. They have proved that the requirement for motion to be quasiclassical for a large momentum is satisfied for massive and massless particles only when $\lambda = 1/6$. This choice of λ has been additionally substantiated in Refs. [17–19].

Important development of problem of the Penrose-Chernikov-Tagirov coupling in the GR for *massive* particles has been made by Accioly and Blas [7, 8]. They analyzed a dependence of the form of the FW Hamiltonian on the value of λ and considered the diagonal static metric in isotropic coordinates:

$$ds^2 = V(\mathbf{r})^2(dx^0)^2 - W(\mathbf{r})^2(d\mathbf{r})^2 \quad (4)$$

with arbitrary $V(\mathbf{r})$, $W(\mathbf{r})$. The choice of the metric allowed an *exact* FW transformation by the method used in Ref. [7, 8]. This method included the Feshbach-Villars transformation (unappropriate for massless particles) in order to bring initial Eq. (1)

to the Hamiltonian form. Next nonunitary and FW transformations resulted in the FW Hamiltonian [7, 8]:

$$\mathcal{H}_{FW} = \rho_3 \sqrt{m^2 V^2 + \mathcal{F} \mathbf{p}^2 \mathcal{F} - \frac{1}{4} \nabla \mathcal{F} \cdot \nabla \mathcal{F} + \mathcal{D}_\lambda(V, W)}, \quad (5)$$

where $\mathbf{p} = -i\nabla$ is the momentum operator, ρ_i ($i = 1, 2, 3$) are the Pauli matrices, $\mathcal{F} = V/W$, and the Darwin term is given by

$$\begin{aligned} \mathcal{D}_\lambda(V, W) = & \frac{V}{2W^2} \Delta V + \frac{V^2}{2W^3} \Delta W - 2\lambda \left[\frac{V}{W^2} \Delta V \right. \\ & \left. + \frac{V}{W^3} \nabla V \cdot \nabla W + 2 \frac{V^2}{W^3} \Delta W - \frac{V^2}{W^4} (\nabla W)^2 \right]. \end{aligned} \quad (6)$$

Only for $\lambda = 1/6$, this term has the simple form and is equal to $\frac{1}{6} \mathcal{F} \Delta \mathcal{F}$ [7, 8].

However, the important result obtained by Accioly and Blas demonstrates only a shadow of the conformal invariance, because it does not cover the case of $m = 0$. We perform general examination of the problem.

3 Generalized Feshbach-Villars Transformation

General form of the covariant KG equation is given by

$$\left(\partial_0^2 + \frac{1}{g^{00}\sqrt{-g}} \{ \partial_i, \sqrt{-g} g^{0i} \} \partial_0 + \frac{1}{g^{00}\sqrt{-g}} \partial_i \sqrt{-g} g^{ij} \partial_j + \frac{m^2 - \lambda R}{g^{00}} \right) \psi = 0. \quad (7)$$

The curly bracket $\{\dots, \dots\}$ denotes the anticommutator.

There is an ambiguity [20] in the definition of parameter of the Feshbach-Villars transformation. We use the generalized Feshbach-Villars (GFV) transformation proposed in Ref. [16] and based on this ambiguity. In the considered case, the GFV transformation consists in an introduction of the new wave function $\Psi = \begin{pmatrix} \phi \\ \chi \end{pmatrix}$ which components are given by wave function:

$$\begin{aligned} \psi &= \phi + \chi, \quad i(\partial_0 + \Upsilon) \psi = N(\phi - \chi), \\ \Upsilon &= \frac{1}{2g^{00}\sqrt{-g}} \{ \partial_i, \sqrt{-g} g^{0i} \}. \end{aligned} \quad (8)$$

Here N is an arbitrary nonzero real parameter. For the Feshbach-Villars transformation, it is definite and equal to the particle mass m . The two components form the wave function $\Psi = \begin{pmatrix} \phi \\ \chi \end{pmatrix}$ which normalization is defined by $\int (\phi^* \phi - \chi^* \chi) dV = 1$. The use of Eq. (8) results in

$$\phi^* \phi - \chi^* \chi = \frac{1}{N} \psi^* i(\partial_0 + \Upsilon) \psi.$$

Since the original Feshbach-Villars transformation corresponds to $N = m$, it becomes (unlike the GFV one) unapplicable for a massless particle.

The GFV transformation allows us to represent Eq. (7) in the Hamiltonian form describing both massive and massless particles [21]:

$$\begin{aligned} i \frac{\partial \Psi}{\partial t} &= \mathcal{H} \Psi, \quad \mathcal{H} = \rho_3 \frac{N^2 + T}{2N} + i \rho_2 \frac{-N^2 + T}{2N} - i \Upsilon, \\ T &= \frac{1}{g^{00} \sqrt{-g}} \partial_i \sqrt{-g} g^{ij} \partial_j + \frac{m^2 - \lambda R}{g^{00}} - \Upsilon^2. \end{aligned} \quad (9)$$

Similarly to Refs. [7, 8], then we perform the nonunitary transformation $\Psi' = f \Psi$ to obtain a pseudo-Hermitian (more exactly, ρ_3 -pseudo-Hermitian) Hamiltonian: $\mathcal{H}' = f \mathcal{H} f^{-1}$, $\mathcal{H}' = \rho_3 \mathcal{H}'^\dagger \rho_3$. In the case under consideration,

$$\begin{aligned} f &= \sqrt{g^{00} \sqrt{-g}}, \quad \Upsilon' = \frac{1}{2f} \left\{ \partial_i, \sqrt{-g} g^{0i} \right\} \frac{1}{f}, \\ T' &= \frac{1}{f} \partial_i \sqrt{-g} g^{ij} \partial_j \frac{1}{f} + \frac{m^2 - \lambda R}{g^{00}} - (\Upsilon^2)'. \end{aligned} \quad (10)$$

Transformed operators are denoted by primes and $(\Upsilon^2)' = (\Upsilon')^2$. Tedious but simple calculations result in [21]

$$\begin{aligned} \mathcal{H}' &= \rho_3 \frac{N^2 + T'}{2N} + i \rho_2 \frac{-N^2 + T'}{2N} - i \Upsilon', \\ T' &= \partial_i \frac{G^{ij}}{g^{00}} \partial_j + \frac{m^2 - \lambda R}{g^{00}} + \frac{1}{f} \nabla_i (\sqrt{-g} G^{ij}) \nabla_j \left(\frac{1}{f} \right) \\ &\quad + \sqrt{\frac{\sqrt{-g}}{g^{00}}} G^{ij} \nabla_i \nabla_j \left(\frac{1}{f} \right) + \frac{1}{4f^4} [\nabla_i (\Gamma^i)]^2 \\ &\quad - \frac{1}{2f^2} \nabla_i \left(\frac{g^{0i}}{g^{00}} \right) \nabla_j (\Gamma^j) - \frac{g^{0i}}{2g^{00} f^2} \nabla_i \nabla_j (\Gamma^j), \\ \Upsilon' &= \frac{1}{2} \left\{ \partial_i, \frac{g^{0i}}{g^{00}} \right\}, \quad G^{ij} = g^{ij} - \frac{g^{0i} g^{0j}}{g^{00}}, \quad \Gamma^i = \sqrt{-g} g^{0i}, \end{aligned} \quad (11)$$

where the nabla operators act only on the operators in brackets and the primes denote transformed operators. Equation (11) is exact and covers any inertial and gravitational fields.

4 Foldy-Wouthyusen Transformation

General methods of the FW transformation for relativistic particles have been developed in Refs. [16, 22, 23]. They belong to step-by-step methods performing the transformation as a result of subsequent iterations. We use the version [16] adapted to scalar particles.

The GFV Hamiltonian can be decomposed into operators commuting (\mathcal{M} and \mathcal{E}) and anticommuting (\mathcal{O}) with ρ_3 :

$$\begin{aligned}\mathcal{H}' &= \rho_3 \mathcal{M} + \mathcal{E} + \mathcal{O}, \quad \rho_3 \mathcal{M} = \mathcal{M} \rho_3, \\ \rho_3 \mathcal{E} &= \mathcal{E} \rho_3, \quad \rho_3 \mathcal{O} = -\mathcal{O} \rho_3, \\ \mathcal{M} &= \frac{N^2 + T'}{2N}, \quad \mathcal{E} = -i\Upsilon', \quad \mathcal{O} = i\rho_2 \frac{-N^2 + T'}{2N}.\end{aligned}\tag{12}$$

The relativistic FW transformation is carried out with the ρ_3 -pseudounitary operator ($U^\dagger = \rho_3 U^{-1} \rho_3$) [16]

$$U = \frac{\epsilon + \mathcal{M} + \rho_3 \mathcal{O}}{\sqrt{2\epsilon(\epsilon + \mathcal{M})}}, \quad \epsilon = \sqrt{\mathcal{M}^2 + \mathcal{O}^2}.\tag{13}$$

In the considered case,

$$U = \frac{\epsilon + N + \rho_1(\epsilon - N)}{2\sqrt{\epsilon N}}, \quad \epsilon = \sqrt{T'}.\tag{14}$$

It is important that the Hamiltonian obtained as a result of the transformation does not depend on N [16]:

$$\begin{aligned}\mathcal{H}_1 &= \rho_3 \epsilon + \mathcal{E}_1 + \mathcal{O}_1, \quad [\rho_3, \mathcal{E}_1] = [\rho_3, \mathcal{O}_1] = 0, \\ \mathcal{E}_1 &= -i\Upsilon' + \frac{1}{2\sqrt{\epsilon}} [\sqrt{\epsilon}, [\sqrt{\epsilon}, \mathcal{G}]] \frac{1}{\sqrt{\epsilon}}, \\ \mathcal{O}_1 &= \rho_1 \frac{1}{2\sqrt{\epsilon}} [\epsilon, \mathcal{G}] \frac{1}{\sqrt{\epsilon}}, \quad \mathcal{G} = -i\partial_0 - i\Upsilon'.\end{aligned}\tag{15}$$

This shows a self-consistency of the used transformation method.

Next transformation [16] eliminates the residual odd term and results in

$$\mathcal{H}_{FW} = \rho_3 \epsilon + \mathcal{E}_1 + \frac{\rho_3}{4} \left\{ \frac{1}{\epsilon}, \mathcal{O}_1^2 \right\}.\tag{16}$$

While relativistic step-by-step methods perfectly describe the contact (Darwin) interaction and strong field effects (see Refs. [9–13]), all of them are approximate [24, 25]. Allowance for the last term in Eq. (16) exceeds the achievable accuracy. Its omitting leads to the final form of the *approximate* relativistic FW Hamiltonian [21]:

$$\mathcal{H}_{FW} = \rho_3 \epsilon - i\Upsilon' - \frac{1}{2\sqrt{\epsilon}} [\sqrt{\epsilon}, [\sqrt{\epsilon}, (i\partial_0 + i\Upsilon')]] \frac{1}{\sqrt{\epsilon}}.\tag{17}$$

5 Exact Foldy-Wouthuysen Transformation and Conformal Invariance

The used method ensures the exact FW transformation for a wide class of spacetime metrics. The manifestation of conformal invariance can also be investigated in detail.

The sufficient condition of the exact FW transformation [16, 22, 23] applied to scalar particles is given by $[T', \mathcal{G}] = 0$ or, equivalently, $\partial_0 T' - [T', \Upsilon'] = 0$. When it is satisfied, the exact FW Hamiltonian reads

$$\mathcal{H}_{FW} = \rho_3 \sqrt{T'} - i\Upsilon'. \quad (18)$$

Equation (18) covers *all static spacetimes* ($\Upsilon' = 0$) and some important cases of stationary ones.

Since general expressions for the scalar Ricci curvature are very cumbersome, we restrict ourselves to an analysis of several special cases. For the metric defined by Eq. (4), the result of our calculations formally coincides with Eq. (5). However, the case of $m = 0$ can now be considered. Explicit expression for $\mathcal{D}_\lambda(V, W)$ [7, 8] shows the presence of conformal invariance for massless particles if and only if $\lambda = 1/6$. In this case, conformal transformation (2) does not change the FW Hamiltonian and the FW wave function Ψ_{FW} . These manifestations of conformal invariance radically differ from those for the covariant KG equation and the corresponding wave function.

The validity of the found properties can be checked for the scalar particle in nonstatic spacetimes. The metric of the rotating Kerr source has been reduced to the Arnowitt-Deser-Misner form [26] by Hergt and Schäfer [27]. This form reproduces the Kerr solution only approximately. The form of the metric can be additionally simplified due to an introduction of spatially isotropic coordinates and dropping terms violating the isotropy [13]:

$$ds^2 = V^2(dx^0)^2 - W^2\delta_{ij}(dx^i - K^i dx^0)(dx^j - K^j dx^0), \quad \mathbf{K} = \boldsymbol{\omega} \times \mathbf{r}. \quad (19)$$

The use of the approximate Kerr metric allows to fulfill the *exact* FW transformation when V , W , and $\boldsymbol{\omega}$ depend only on the isotropic radial coordinate r . In this approximation, the metric is defined by

$$V(r) = \frac{1 - \mu/(2r)}{1 + \mu/(2r)} + \mathcal{O}\left(\frac{\mu a^2}{r^3}\right), \quad W(r) = \left(1 + \frac{\mu}{2r}\right)^2 + \mathcal{O}\left(\frac{\mu a^2}{r^3}\right), \quad (20)$$

$$\boldsymbol{\omega}(r) = \frac{2\mu c}{r^3} \mathbf{a} \left[1 - \frac{3\mu}{r} + \frac{21\mu^2}{4r^2} + \mathcal{O}\left(\frac{a^2}{r^2}\right)\right].$$

Here $\mathbf{a} = \mathbf{J}/(Mc)$, $\mu = GM/c^2$; the total mass M and the total angular momentum \mathbf{J} (directed along the z axis) define the Kerr source uniquely. The leading term in the expression for $\boldsymbol{\omega}(r) = \omega(r)\mathbf{e}_z$ corresponds to the LT approximation.

We can pass on from the Kerr field approximated by Eqs. (19) and (20) to a frame rotating in this field with the angular velocity \mathbf{o} after the transformation $dx^i \rightarrow dX^i = dx^i + (\mathbf{o} \times \mathbf{r})dx^0$. The stationary metric of this frame can be obtained from Eqs. (19) and (20) with the replacement $\boldsymbol{\omega} \rightarrow \boldsymbol{\Omega} = \boldsymbol{\omega} - \mathbf{o}$. In particular, it covers an observer on the ground of a rotating source like the Earth or on a satellite. In this case, $\mathbf{o} = \mathbf{J}/I$, where I is the moment of inertia. It should be taken into account that frames rotating in the isotropic and Cartesian coordinates are not equivalent.

In the *isotropic* spherical coordinates, the metric takes the form

$$ds^2 = [V^2(r) - W^2(r)\Omega^2(r)r^2 \sin^2 \theta](dx^0)^2 - W^2(r)[2\Omega(r)r^2 \sin^2 \theta dx^0 d\varphi + dr^2 + r^2(d\theta^2 + \sin^2 \theta d\varphi^2)]. \quad (21)$$

The exact FW Hamiltonian is given by Eq. (18) where [21]

$$\begin{aligned} T' &= m^2 V^2 + \mathcal{F} \mathbf{p}^2 \mathcal{F} - \frac{1}{4} \nabla \mathcal{F} \cdot \nabla \mathcal{F} + \mathcal{D}_\lambda(V, W) \\ &+ \frac{\lambda}{2}(x^2 + y^2)(\Omega'_r)^2, \quad \mathcal{D}_\lambda(V, W) = \lambda \mathcal{F} \Delta \mathcal{F} \\ &+ (1 - 6\lambda) \frac{V}{2W^2} \left[\mathcal{F} \left(\frac{2W'_r}{r} + W''_{rr} \right) + \frac{2V'_r}{r} + V''_{rr} \right], \\ &- i \Upsilon' = \boldsymbol{\Omega} \cdot (\mathbf{r} \times \mathbf{p}), \end{aligned} \quad (22)$$

and derivatives with respect to r are denoted by indexes. In particular, for the LT metric

$$\boldsymbol{\Omega}(r) = \frac{2G\mathbf{J}}{c^2 r^3}, \quad V(r) = 1 - \frac{GM}{c^2 r}, \quad W(r) = 1 + \frac{GM}{c^2 r}. \quad (23)$$

While metric (19) and (20) reproduces the Kerr solution only approximately, the derivation of the exact FW Hamiltonian corresponding to this metric allows an independent unambiguous determination of the value of λ . If and only if $\lambda = 1/6$, conformal transformation (2) changes neither T' nor \mathcal{H}_{FW} , Ψ_{FW} . This property is the same as for the static metric.

6 General Equations of Motion

Equations for the FW Hamiltonian allow us to derive general quantum-mechanical equations of motion and then obtain their classical limit ($\hbar \rightarrow 0$). The quantum-mechanical equations of motion defining the force, velocity, and acceleration read ($p_0 \equiv \mathcal{H}_{FW}$)

$$\begin{aligned} F^i &\equiv \frac{dp^i}{dt} = \frac{\partial p^i}{\partial t} + \frac{i}{\hbar} [\mathcal{H}_{FW}, p^i] = \frac{1}{2} \frac{\partial}{\partial t} \{g^{i\mu}, p_\mu\} + \frac{i}{2\hbar} [\mathcal{H}_{FW}, \{g^{i\mu}, p_\mu\}], \\ \mathcal{V}^i &\equiv \frac{dx^i}{dt} = \frac{i}{\hbar} [\mathcal{H}_{FW}, x^i], \quad \mathcal{W}^i = \frac{\partial \mathcal{V}^i}{\partial t} + \frac{i}{\hbar} [\mathcal{H}_{FW}, \mathcal{V}^i]. \end{aligned} \quad (24)$$

Any commutation adds the factor \hbar as compared with the product of operators.

It has been proved in Ref. [14] that satisfying the condition of the Wentzel-Kramers-Brillouin approximation allows to use this approximation in the relativistic case and to obtain a classical limit of the relativistic quantum mechanics. Determination of the classical limit reduces to the replacement of operators in the FW Hamiltonian and quantum-mechanical equations of motion in the FW representation by the respective classical quantities. The classical limit of the general FW Hamiltonian is given by [21]

$$H = \left(\frac{m^2 - G^{ij} p_i p_j}{g^{00}} \right)^{1/2} - \frac{g^{0i} p_i}{g^{00}}. \quad (25)$$

It coincides with the classical Hamiltonian derived in Ref. [28]. The classical limit of Eq. (24) reads

$$\begin{aligned} \mathcal{V}^i &= \frac{G^{ij} p_j}{\sqrt{g^{00}(m^2 - G^{ij} p_i p_j)}} + \frac{g^{0i}}{g^{00}}, \\ F^i &= p_\mu \frac{\partial g^{i\mu}}{\partial t} + g^{0i} \frac{\partial H}{\partial t} + g^{ij} \partial_j H + p_\mu \mathcal{V}^j \partial_j g^{i\mu}. \end{aligned} \quad (26)$$

It coincides with the corresponding classical equations which follow from Hamiltonian (25) and the Hamilton equations. Thus, the quantum-mechanical and classical equations are in the best compliance.

For example, the exact metric of a general noninertial frame characterized by the acceleration \mathbf{a} and the rotation \mathbf{o} of an observer is defined by $V = 1 + \mathbf{a} \cdot \mathbf{r}$, $W = 1$, $\mathbf{\Omega} = -\mathbf{o}$ [29]. In this case, the classical limit of the Hamiltonian and equations of motion is given by [21]

$$\begin{aligned} H &= (1 + \mathbf{a} \cdot \mathbf{r}) \sqrt{m^2 + \mathbf{p}^2} - \mathbf{o} \cdot (\mathbf{r} \times \mathbf{p}), \\ \mathcal{V} &= (1 + \mathbf{a} \cdot \mathbf{r}) \frac{\mathbf{p}}{\sqrt{m^2 + \mathbf{p}^2}} - \mathbf{o} \times \mathbf{r}, \\ \mathcal{W} &= -\mathbf{a}(1 + \mathbf{a} \cdot \mathbf{r}) - 2\mathbf{o} \times \mathcal{V} - \mathbf{o} \times (\mathbf{o} \times \mathbf{r}) \\ &\quad + \frac{2\mathbf{a} \cdot \mathcal{V} + \mathbf{a} \cdot (\mathbf{o} \times \mathbf{r})}{1 + \mathbf{a} \cdot \mathbf{r}} (\mathcal{V} + \mathbf{o} \times \mathbf{r}), \end{aligned} \quad (27)$$

where $\mathbf{p} \equiv (-p_1, -p_2, -p_3)$. Leading terms in Eq. (27) reproduce well-known classical results [30, 31].

7 Quantum-Mechanical Description of the Lense-Thirring Effect

The results obtained allow to derive quantum-mechanical equations describing the LT effect. When a metric depends only on r , it is convenient to consider the evolution of the angular momentum operator $\mathbf{l} = \mathbf{r} \times \mathbf{p}$. Dynamics of this operator in a frame rotating in the Kerr field approximated by a spatially isotropic metric is defined by

$$\frac{d\mathbf{l}}{dt} = \frac{i}{\hbar} [\mathcal{H}_{FW}, \mathbf{l}] = \mathbf{\Omega} \times \mathbf{l}, \quad \mathbf{\Omega} = \boldsymbol{\omega} - \mathbf{o}. \quad (28)$$

Since the operators $\mathbf{\Omega}$ and \mathbf{l} commute, this equation is exact *for the chosen metric*.

The quantity $\boldsymbol{\omega}$ characterizes an evolution of the longitude of the ascending node, Υ : $\Upsilon = \Upsilon_0 + \boldsymbol{\omega}t$. Equations (20) and (28) provide for a relativistic post-Newtonian description of this evolution:

$$\boldsymbol{\omega} = \frac{2GJ}{c^2 r^3} \left[1 - \frac{3GM}{c^2 r} + \frac{21G^2 M^2}{4c^4 r^2} + \mathcal{O}\left(\frac{a^2}{r^2}\right) \right]. \quad (29)$$

This is a part of the LT effect. The longitude of the ascending node can be measured and its measurement is important for astrophysics.

A transition to the classical limit [14] and a calculation of the period average in the nonrelativistic and weak-field approximation results in

$$\left\langle \frac{1}{r^3} \right\rangle = \frac{1}{b^3(1-e^2)^{3/2}}, \quad \boldsymbol{\omega} = \frac{2GJ}{c^2 b^3(1-e^2)^{3/2}}, \quad (30)$$

where b is the semimajor axis and e is the eccentricity.

The quantum-mechanical description of the full LT effect is based on the Laplace-Runge-Lenz (LRL) vector. In this case, we confine ourselves by the nonrelativistic and weak-field approximation. The operator form of the LRL vector is given by

$$\mathbf{A} = \frac{1}{2} (\mathbf{p} \times \mathbf{l} - \mathbf{l} \times \mathbf{p}) - mk\hat{\mathbf{r}}, \quad \hat{\mathbf{r}} = \frac{\mathbf{r}}{r}, \quad k = GMm. \quad (31)$$

The nonrelativistic FW Hamiltonian for the Kerr field in the LT approximation reads

$$\mathcal{H}_{FW} = \rho_3 \left(mc^2 - \frac{k}{r} + \frac{\mathbf{p}^2}{2m} \right) + \mathbf{\Omega} \cdot \mathbf{l}, \quad (32)$$

where $\mathbf{\Omega}$ is defined by Eq. (23). The precession of pericenter of the orbit is defined by the commutator of the operators \mathcal{H}_{FW} and \mathbf{A} :

$$\frac{d\mathbf{A}}{dt} = \frac{i}{\hbar} [\mathcal{H}_{FW}, \mathbf{A}] = \frac{1}{2} (\mathbf{\Omega} \times \mathbf{A} - \mathbf{A} \times \mathbf{\Omega}) + \frac{3G}{2c^2} \left\{ \frac{\mathbf{J} \cdot \mathbf{l}}{r^5}, (\mathbf{r} \times \mathbf{l} - \mathbf{l} \times \mathbf{r}) \right\}. \quad (33)$$

The transition to the classical limit and the calculation of the period average brings the LT equation:

$$\frac{d\mathbf{A}}{dt} = \mathbf{\Omega}_{LT} \times \mathbf{A}, \quad \mathbf{\Omega}_{LT} = \frac{2G}{c^2 r^3} [\mathbf{J} - 3(\mathbf{J} \cdot \hat{\mathbf{l}})\hat{\mathbf{l}}], \quad (34)$$

where $\hat{\mathbf{l}} = \mathbf{l}/l$.

The existence of the frame dragging can also be shown. If we hold only main terms in the *relativistic* FW Hamiltonian presented by Eqs. (18) and (22), the velocity operator in the field defined by the LT metric (23) is given by

$$\mathcal{V} = \frac{\partial_3}{2} \left\{ \frac{c}{\sqrt{m^2 c^2 V^2 + \mathcal{F} p^2 \mathcal{F}}}, \mathcal{F} p \mathcal{F} \right\} + \boldsymbol{\Omega} \times \mathbf{r}. \quad (35)$$

In the weak-field approximation, the part of the acceleration operator defined only by the rotation of the source is equal to

$$\mathcal{W} = \boldsymbol{\Omega} \times \mathcal{V} - \mathcal{V} \times \boldsymbol{\Omega} - \boldsymbol{\Omega} \times (\boldsymbol{\Omega} \times \mathbf{r}). \quad (36)$$

This equation defines the Coriolis-like and centrifugal-like accelerations and therefore describes the quantum-mechanical frame-dragging effect.

It is important that the classical limit of quantum-mechanical equations coincides with the corresponding classical equations. This unambiguously shows a deep connection between the relativistic quantum mechanics of scalar particles in Riemannian spacetimes and the classical GR.

8 Conformal Invariance for Dirac and Classical Particles

It is possible to compare the conformal transformations in the GR for massless scalar, Dirac, and classical particles. Our analysis shows that the general Hermitian Dirac Hamiltonian for a massless particle in an arbitrary metric in the presence of an electromagnetic field [13] is not changed by the transformation (2). The FW transformation operator for particles in strong external fields obtained in Ref. [23] is also conformally invariant in the case of $m = 0$. As a result, the Dirac and FW wave functions, ψ and ψ_{FW} , and the FW Hamiltonian remain unchanged. These properties of Dirac particles are the same as for scalar ones. The Hamiltonian of massless classical particles is conformally invariant even if its spin-dependent part defined by Eqs. (3.18) and (4.12) in Ref. [13] is taken into account.

In the general case, the transformation of the initial covariant Dirac equation to the Hermitian Hamiltonian form is performed by the nonunitary operator $f_D = (\sqrt{-g}e_0^0)^{1/2}$ [13]. Since the transformation (2) leads to $\tilde{f}_D = O^{-3/2} f_D$, the conformally transformed wave function of the initial covariant Dirac equation, $\tilde{\Psi}$, reads

$$\tilde{\Psi} = \widetilde{f_D^{-1} \psi} = O^{3/2} f_D^{-1} \psi = O^{3/2} \Psi. \quad (37)$$

While its transformation is similar to that for the scalar particles, the powers of O in Eqs. (3) and (37) differ.

The second-order wave equation for the Dirac particles in general electromagnetic and gravitational fields derived in Ref. [13] includes the term describing a nonminimal coupling to the scalar curvature R . As the definitions of R in Ref. [13] and the present work differ in sign, this term corresponds to $\lambda = 1/4$.

9 Conclusions

The use of the GFV and relativistic FW transformations allows to describe the both massive and massless scalar particles in general noninertial frames and gravitational fields. The present work demonstrates the new manifestation of the conformal invariance for massless particles. The conformal transformation conserves the FW Hamiltonian and the FW wave function while it changes the wave function of the initial KG equation. The similar conclusion is valid for the Dirac particles. The nonminimal coupling to the scalar curvature is a common property of the scalar and Dirac particles.

The results obtained in Refs. [7, 8, 21] allow to state the general property of conformal symmetry for massive particles. Conformal transformation (2) changes only such terms in the FW Hamiltonian which are proportional to the particle mass m . This property is valid not only for real scalars (Higgs boson) but also for compound ones (zero-spin atoms and nuclei). Dirac particles possess the same property.

Contemporary methods of (pseudo)unitary and nonunitary transformations make it possible to derive new exact FW Hamiltonians for both massive and massless scalar particles i) in the general static spacetime and ii) in the frame rotating in the Kerr field approximated by a spatially isotropic metric. The latter result covers an observer on the ground of the Earth or on a satellite. It reproduces not only the well-known effects of the rotating frame but also the LT effect. For an arbitrary metric, high-precision formula (17) is obtained.

The classical limit of the derived general quantum-mechanical equations of motion coincides with corresponding classical equations. This important general conclusion is confirmed by the quantum-mechanical description of the relativistic LT effect. The exact evolution of the angular momentum operator in the Kerr field approximated by a spatially isotropic metric is found. The quantum-mechanical description of the full LT effect based on the Laplace-Runge-Lenz vector is given in the nonrelativistic and weak-field approximation. Relativistic quantum-mechanical equations for the velocity and acceleration operators are obtained. The equation for the acceleration defines the Coriolis-like and centrifugal-like accelerations and presents the quantum-mechanical description of the frame-dragging effect.

Acknowledgments The author is indebted to E.A. Tagirov for his interest in the present study and valuable discussions. The work was supported by the Belarusian Republican Foundation for Fundamental Research (Grant No. $\Phi 12D-002$).

References

1. O. Klein, Z. Phys. **37**, 895 (1926)
2. W. Gordon, Z. Phys. **40**, 117 (1926)
3. V. Fock, Z. Phys. **38**, 242 (1926)
4. E. Schrödinger, (unpublished)
5. V. Fock, *Relativity, Groups and Topology*, ed. by C. DeWitt, B. DeWitt (Gordon and Breach, London, 1964)
6. N. Chernikov, E. Tagirov, Ann. Inst. Henri Poincaré A **9**, 109 (1968)
7. A. Accioly, H. Blas, Phys. Rev. D **66**, 067501 (2002)
8. A. Accioly, H. Blas, Mod. Phys. Lett. A **18**, 867 (2003)
9. A.J. Silenko, O.V. Teryaev, Phys. Rev. D **71**, 064016 (2005)
10. A.J. Silenko, O.V. Teryaev, Phys. Rev. D **76**, 061101(R) (2007)
11. A.J. Silenko, Acta Phys. Polon. B Proc. Suppl. **1**, 87 (2008)
12. Yu.N. Obukhov, A.J. Silenko, O.V. Teryaev, Phys. Rev. D **80**, 064044 (2009)
13. Yu.N. Obukhov, A.J. Silenko, O.V. Teryaev, Phys. Rev. D **84**, 024025 (2011)
14. A.J. Silenko, Pis'ma Zh. Fiz. Elem. Chast. Atom. Yadra **10**, 144 (2013)
15. H. Feshbach, F. Villars, Rev. Mod. Phys. **30**, 24 (1958)
16. A. , J. Silenko. Teor. Mat. Fiz. **156**, 398 (2008)
17. S. Sonogo, V. Faraoni, Class. Quantum Gravity **10**, 1185 (1993)
18. V. Faraoni, Phys. Rev. D **53**, 6813 (1996)
19. A. Grib, E. Poberii, Helv. Phys. Acta **68**, 380 (1995)
20. A. Mostafazadeh, J. Phys. A **31**, 7829 (1998)
21. A.J. Silenko, J. Phys. Rev. D **88**, 045004 (2013)
22. A.J. Silenko, J. Math. Phys. **44**, 2952 (2003)
23. A.J. Silenko, Phys. Rev. A **77**, 012116 (2008)
24. E. Eriksen, M. Korlsrud, Nuovo Cimento Suppl. **18**, 1 (1960)
25. V.P. Neznamov, A.J. Silenko, J. Math. Phys. **50**, 122302 (2009)
26. R. Arnowitt, S. Deser, C.W. Misner, in *Gravitation: An Introduction to Current Research*, ed. by L. Witten (Wiley, New York, 1962)
27. S. Hergt, G. Schäfer, Phys. Rev. D **77**, 104001 (2008)
28. G. Cognola, L. Vanzo, S. Zerbinì, Gen. Relativ. Gravit **18**, 971 (1986)
29. F.W. Hehl, W.T. Ni, Phys. Rev. D **42**, 2045 (1990)
30. C.W. Misner, K.S. Thorne, J.A. Wheeler, *Gravitation* (Freeman, San Francisco, 1973)
31. H. Goldstein, C.P. Poole, J.L. Safko, *Classical Mechanics*, 3rd edn. (Addison-Wesley, San Francisco, 2001)

On the Strong Field Point Particle Limit and Equation of Motion in General Relativity

Toshifumi Futamase

Abstract Strong field point particle limit is developed in order to take into account strong internal gravity in the post-Newtonian approximation. The concept is also applicable to the motion of a fast moving particle. We give an introduction of the concept and show the application to the equation of motion.

1 Introduction

Recent interest on the equation of motion in general relativity is motivated by the development of gravitational telescope. It is expected that gravitational waves will be directly observed in very near future and will open up a new branch of astronomy, gravitational wave astronomy. However it is obvious that the detailed theoretical understanding for the source and the mechanism of wave generation are indispensable in order to interpret the observed data. This is particularly important for gravitational waves because the signals are extremely small. Without theoretical template no meaningful information can be obtained. This is the reason of renewed interest on the relativistic equation of motion. Although the equation of motion has a long history starting right after the development of general relativity, it has not been fully understood.

For systems whose velocity of typical motion are much less than the speed of light, one can use of the ratio between the speed of light and the typical velocity as a smallness parameter ϵ to develop the so-called slow motion approximation. If the system in concern is gravitationally bounded and the typical motion is governed by its gravitational potential, the slow-motion expansion is at the same time the expansion with respect to the gravitational potential and thus is called post-Newtonian approximation [1–4]. The post-Newtonian approximation is applied for various astrophysical systems including planetary motion in solar system and relativistic compact binaries with remarkable success [5–8]. The predicted orbital motion for the compact binaries is now used as a tool to determine physical parameters such as masses of component

T. Futamase (✉)

Astronomical Institute, Tohoku University, Sendai 980-8578, Japan
e-mail: tof@astr.tohoku.ac.jp

stars. However the usual treatment of the post-Newtonian approximation assumes that the field is everywhere weak including inside the component stars which is not applicable for relativistic binaries. Another difficulty of the post-Newtonian approximation is that the convergence of the expansion series becomes very slow in higher orders. At present 3.5 post-Newtonian approximation has been calculated [9–11], but there is a discussion that 4.5 post-Newtonian calculation will be necessary to make sufficiently accurate theoretical templates for predicting accurate waveform from coalescing binaries. Strong internal gravity in compact binaries becomes problematic in the calculation of higher-order post-Newtonian approximation because of high nonlinearity. The use of singular function such as Dirac delta function in higher order calculation is not satisfactory not only mathematically but also physically. Mathematically one cannot define singular function in nonlinear theory. Physically there is not singular source in general relativity. When one makes a singular source, one ends up a black hole which is regular horizon at least from outside. Although there are some elegant methods to deal with singular source in higher-order post-Newtonian calculation [12–14], it would be better to formulate the post-Newtonian approximation in such a way that it automatically take the strong internal gravity into account without singular sources. This is done by introducing the strong field point particle limit in the post-Newtonian approximation [15, 16].

For systems whose motion is highly relativistic, there are some development recent years and the equation of motion is known [17–20]. However it is still unsatisfactory in the sense that practical treatment is possible only for limited type of orbital motions [21–24] (however there have been some progresses in this direction recently [25–27]). Although higher order equation of motion in the relativistic case is not known yet, the use of singular source would cause serious theoretical difficulty. In this sense it is preferable to formulate the equation of motion without singular source. The strong field point particle limit may have a possibility to have such a formulation.

This article is the introduction to the concept of strong field point particle limit and its application to the equation of motion in general relativity. In Sect. 2, we give a formulation of the post-Newtonian approximation on the space of solutions of Einstein equation whose initial data satisfy the Newtonian scaling. Then we introduce the point particle limit introduce and derive the equation of motion in the surface integral form in Sect. 3. In Sect. 4, we apply the strong field point particle limit to derive the equation of motion for a fast moving particle. Although the derivation is still in the stage of formal, we expect to be useful for future practical application. Finally some discussions are given.

2 Newtonian Scaling and Strong Field Point Particle Limit

As discussed above, the strong field point particle limit is introduced in order to take the strong internal gravity of the relativistic binary system in the post-Newtonian approximation. This is done by realizing that the Newtonian scaling with respect

to the smallness parameter has a room to allow the strong internal gravity. Thus we first formulate the Newtonian approximation based on the Newtonian scaling. The post-Newtonian approximation is actually the asymptotic approximation to the sequence of solutions of Einstein equation which is defined by Newtonian initial data [28]. In the case of binary system, the Newtonian initial data is characterized by the following scaling relation.

$$v^i \sim \epsilon, \quad m \sim \epsilon^2 \quad (1)$$

where v^i is the orbital speed, and m is the mass of component stars. This relation guarantees the Newtonian orbit at least for some short time. Relativistic effects will deviate the scaling. The post-Newtonian approximation becomes accurate as the parameter goes to zero. This means that the limit $\epsilon \rightarrow 0$ should be understood, but the point is that the limit taken is along the trajectory on the sequence which connects physically equivalent events at each solution. Namely the time interval is also scaled as ϵ^{-1} , thus appropriate time coordinate on the sequence is not the coordinate time but the Newtonian time $\tau = \epsilon t$. In fact as ϵ goes zero, the Newtonian time stay constant and the limit is taken along the trajectory on which $\tau = \text{constant}$.

It should be noticed that it is sufficient for mass not the density to scale as ϵ^2 in order to guarantee the Newtonian behavior for the orbital motion. This is important because it allows us to have strong internal gravity for the component stars. Namely one can fix gravitational potential in the course of limit by assuming the size of the component stars shrink as ϵ^2 . This means the density scales as ϵ^{-4} . This scaling suggests the introduction of the body coordinates (α^i whose relation with the near zone coordinates (x^i) is as follows:

$$x^i(\tau) = z_A^i(\tau) + \epsilon^2 \alpha^i(\tau) \quad (2)$$

where we consider a system of compact binary and z_A^i is the center of mass coordinate of star A ($A = 1, 2$). We have used the Newtonian dynamical time τ because we neglect dynamical change of the internal structure. This is guaranteed by taking equilibrium internal configuration for the component stars as their initial data (the tidally induced change will appear at 4th post-Newtonian order). We further define the body zone B_A whose boundary is defined as

$$|\vec{x} - \vec{z}_A| = \epsilon R_A \quad (3)$$

where R_A is some fixed number. This boundary shrinks as ϵ in the limit $\epsilon \rightarrow 0$ in the near zone coordinate, but expands as ϵ^{-1} in the body zone coordinate. Thus the boundary is far zone from the point of view of component star and thus the gravitational field by the component star may be obtained by far zone expansion (multipole expansion).

This property is essential to calculate higher-order post-Newtonian approximation without any singular behavior and also deriving the formal equation of motion for a fast moving particle.

3 Bases of the Post-Newtonian Calculation

In this section we explain how the strong field point particle limit is implemented in the actual calculation of post-Newtonian approximation. This is done by writing equation of motion in the integral form.

We first define the 4-momentum P_A^μ of each component star as

$$P_A^\mu(\tau) = \int_{B_A} d^3x \Lambda^{\mu\tau} \quad (4)$$

where the integral is over the body zone B_A . $\Lambda^{\mu\nu}$ is defined as

$$\Lambda^{\mu\nu} = (-g) (T^{\mu\nu} + t_{LL}^{\mu\nu}) + \left(h^{\mu\nu} h^{\alpha\beta} - h^{\mu\alpha} h^{\nu\beta} \right)_{,\alpha\beta} \quad (5)$$

where $t_{LL}^{\mu\nu}$ is the Landau-Lifshitz pseudotensor [4], and $h^{\mu\nu} = \eta^{\mu\nu} - \sqrt{-g}g^{\mu\nu}$ is the Landau-Lifshitz variable. Then we have

$$\frac{dP_A^\mu}{d\tau} = - \oint_{\partial B_A} dS_k \Lambda^{k\mu} + v_A^k(\tau) \oint_{\partial B_A} dS_k \Lambda^{\tau\mu} \quad (6)$$

This is not the equation of motion in the usual sense. We need the relation between the energy P_A^τ and mass m_A as well as the relation between the momentum P_A^i and the velocity v_A^i . In the Newtonian order these are

$$P_A^\tau = m_A \quad (7)$$

$$P_A^i = M_A v_A^i \quad (8)$$

These relations suffer from higher-order post-Newtonian corrections. The energy-mass relation is obtained from the time component of the above equation. The momentum-velocity relation is given by

$$P_A^i = P_A^\tau v_A^i + Q_A^i + \frac{dD_A^i}{d\tau} \quad (9)$$

where $y_A^i = y^i - z_A^i(\tau)$ and

$$Q_A^i = \oint_{\partial B_A} dS_k \left(\Lambda^{\tau k} - v_A^k \Lambda^{\tau\tau} \right) \quad (10)$$

$$D_A^i = \oint_{\partial B_A} d^3y \Lambda^{\tau\tau} y_A^i \quad (11)$$

D_A^i is the dipole moment of the star A which we can choose arbitrary value. The above relation is obtained from the identity

$$\Theta^{\tau i} = \left(\Lambda^{\tau\tau} y_A^i \right)_{,\tau} + \left(\Lambda^{\tau j} y_A^i \right)_{,j} + v_A^i \Lambda^{\tau\tau} \quad (12)$$

This is the consequence of the conservation law $\Lambda^{\mu\nu}_{;\nu} = 0$.

Then we have the following equation of motion in the integral form.

$$P_A^\tau \frac{dv_A^i}{d\tau} = - \oint_{\partial B_A} dS_k \Lambda^{ki} + v_A^i \oint_{\partial B_A} dS_k \Lambda^{\tau i} \quad (13)$$

$$+ v_A^i \left(\oint_{\partial B_A} dS_k \Lambda^{k\tau} - v_A^i \oint_{\partial B_A} dS_k \Lambda^{\tau\tau} \right) - \frac{dQ_A^i}{d\tau} - \frac{d^2 D_A^i}{d\tau^2} \quad (14)$$

As mentioned above the energy mass relation is obtained from the time component of the Eq. (5).

The first step of the calculation is to write down the formal solution of the Einstein equation.

$$h^{\mu\nu}(\tau, \vec{x}) = 4 \int d^3 y \frac{\Lambda^{\mu\nu}(\tau - \epsilon|\vec{x} - \vec{y}|, \vec{y})}{|\vec{x} - \vec{y}|} \quad (15)$$

This integral is divided into two parts, one from the body zone and the other from the other region except the body zone.

$$h_B(\tau, \vec{x}) = 4 \sum_{A=1,2} \int_{B_A} d^3 \alpha \frac{\Lambda^{\mu\nu}(\tau - \epsilon|\vec{r}_A - \epsilon^2 \vec{\alpha}_A|, \vec{z}_A + \epsilon^2 \vec{\alpha}_A)}{|\vec{r}_A - \epsilon^2 \vec{\alpha}_A|} \quad (16)$$

$$h^{\mu\nu}(\tau, \vec{x}) = 4 \int_{N/B} d^3 y \frac{\Lambda^{\mu\nu}(\tau - \epsilon|\vec{x} - \vec{y}|, \vec{y})}{|\vec{x} - \vec{y}|} \quad (17)$$

where $\vec{r}_A = \vec{y} - \vec{z}_A$ and N/B means the near zone region except the body zones. One can show by explicit calculation that the artificial boundary does not contribute to the final result [29].

In the surface integral approach we only need the gravitational field on the body zone boundary ∂B_A . Since the body zone boundary is the far zone in the body zone coordinate the field h_B is calculated by multipole expansion. On the other hand the field $h_{B/N}$ is calculated by using the following formula.

$$\int_{N/B} d^3 y \frac{f(\vec{y})}{|\vec{x} - \vec{y}|} = -4\pi g(\vec{x}) + \oint_{\partial(B/N)} dS_k \left[\frac{1}{|\vec{x} - \vec{y}|} \frac{\partial g(\vec{y})}{\partial y^k} - g(\vec{y}) \frac{\partial}{\partial y^k} \left(\frac{1}{|\vec{x} - \vec{y}|} \right) \right] \quad (18)$$

where g is the super potential of f , namely

$$\Delta g(\vec{x}) = f(\vec{x}) \quad (19)$$

For example, if $f = 1/(r_1 r_2)$, then

$$g = \ln(r_1 + r_2 + r_{12}) \quad (20)$$

Up to 2.5 post-Newtonian order all the necessary super-potentials have been known by the work of Jaranowski and Schäfer [30, 31]. In higher-order calculation we have integrals in which super-potential cannot be found. Even in these cases, we can evaluate the field at the body zone boundary [11].

The surface integral expression for the equation of motion allows us to calculate the higher-order equation of motion step by step starting from only non-vanishing Newtonian field.

$$h^{\tau\tau} = 4\epsilon^4 \sum_A \frac{m_A}{r_A} \quad (21)$$

with

$$m_A = \lim_{\epsilon \rightarrow 0} P_A^\tau \quad (22)$$

$$P_A^i = m_A v_A^i \quad (23)$$

Detailed calculation are presented in the references [16, 29, 32].

4 Application to the Fast Motion Equation of Motion

We shall apply the point particle limit to the equation of motion for a fast moving small body in an arbitrary background field. Our starting point is the integral form of equation of motion derived in the previous section.

$$\frac{dP_A^\mu}{d\tau} \simeq \lim_{\epsilon \rightarrow 0} \oint_{\partial B_A} dS n_\nu \Theta^{\mu\nu} = - \lim_{\epsilon \rightarrow 0} \epsilon^2 \int d\Omega n_\nu (1 + \epsilon a \cdot n) t_{LL}^{\mu\nu} |_{\partial B} \quad (24)$$

Here we used $\Theta = (-g)(T + t_{LL})$ instead of Λ in the integrand because the essential contribution comes from this part, and n^μ is the unit normal vector to the surface and $a^\mu = Du^\mu/d\tau$ the 4-acceleration.

Let suppose we have a background field g_b and write the deviation from the background as h in this section (do not confuse h in the previous section). The deviation field contains the singular field at the position of the particle if it is really a point. For the irrotational extended source the field which fall off as r^{-1} corresponds to the singular field. We shall write down the monopole field as δg , then the whole field at the body boundary may be written as follows.

$$g = g_b + h = g_s + \delta g \quad (25)$$

where g_s is the sum of the background and the regular part of the self field. There is no ambiguity of separating the regular and singular field because the separation is done on the body zone boundary. Then the Landau-Lifshitz pseudotensor at the body zone boundary may be symbolically written as follows

$$\begin{aligned}\Theta|_{\partial B} &\simeq t_{LL}|_{\partial B} \simeq \Gamma(g_s + \delta g)\Gamma(g_s + \delta g) \\ &\simeq \Gamma(g_s)\partial(g_s) + \Gamma(g_s)\partial(\delta g) + \Gamma(\delta g)\partial(\delta g)\end{aligned}$$

where Γ represents Christoffel symbol. Each term has different ϵ dependences because $g_s \sim O(\epsilon^0)$, $\delta g \sim \epsilon^{-1}$, and thus the second term $\Gamma(g_s)\partial(\delta g)$ cancels another ϵ^2 dependence coming from surface element and gives nonzero contribution. The third term vanishes by the angular integral.

Let us make the above argument more explicit. The singular part of the self field may be written as follows.

$$\delta g^{\mu\nu}(x) = 2 \int d^4y \sqrt{-g} u^{\mu\nu}_{\alpha\beta}(x, y) \delta(\sigma(x, y)) T^{\alpha\beta} \quad (26)$$

where σ is the world function and the field point is supposed to be on the body zone boundary, and $u^{\mu\nu}_{\alpha\beta}$ is the coefficient of singular part in the retarded tensor Greens function [20, 33]. In the above expression we do not consider the spinning particle. Note that our field point x is on the body zone boundary which is in the far zone of the star. This allows us to make use of the multipole expansion. For this purpose we choose our coordinate as

$$y^\alpha = z^\alpha(\tau) + \delta y^\alpha, \quad z^0(\tau) = \tau, \quad \delta y^0 = 0 \quad (27)$$

where $z(\tau)$ is the world line of the center of the star. The center is assumed always to be inside the body in the point particle limit, and thus there is no ambiguity regarding the choice of the center. Thus we have

$$\delta g^{\mu\nu}(x) = \frac{2m}{\dot{\sigma}(x, z(\tau_z))} u^{\mu\nu}_{\alpha\beta}(x, z(\tau_z)) \dot{z}^\alpha(\tau_z) \dot{z}^\beta(\tau_z) \quad (28)$$

where τ_z is the retarded time at the center given by $\sigma(x, z(\tau_z)) = 0$, and

$$m \dot{z}^\alpha(\tau_z) \dot{z}^\beta(\tau_z) \equiv \lim_{\epsilon \rightarrow 0} \int \delta^3 y \sqrt{-g} T^{\alpha\beta} \quad (29)$$

Since we are going to take the point particle limit, the world function is simply approximated as $1/2\eta_{\mu\nu}(x - z)^\mu(x - z)^\nu$ and $u^{\mu\nu}_{\alpha\beta} \simeq \delta_\alpha^{(\mu} \delta_\beta^{\nu)}$, we have

$$\delta g^{\alpha\beta} \simeq \frac{4m u^\alpha u^\beta}{u_\mu r^\mu} \quad (30)$$

where $u^\mu = \dot{z}$, $r^\mu = x^\mu - z^\mu$ and the z and u are evaluated at the retarded time. Thus its derivative may be evaluated at the body zone boundary as follows

$$\partial_\alpha (\delta g^{\mu\nu}) \simeq \frac{4m\delta_\alpha^\mu u^\nu}{\epsilon^2} + O(\epsilon^{-1}) \quad (31)$$

Using the above expressions in the LL tensor, we have the following result in the point particle limit:

$$\frac{dP^\mu}{d\tau} = -m\Gamma_{\alpha\beta}^\mu(g_s)u^\alpha u^\beta - \frac{1}{2}m\Gamma_{\alpha\beta}^\alpha(g_s)u^\beta u^\mu \quad (32)$$

Here we need the relation between 4-momentum and the mass. Higher-order post-Newtonian result indicates that the ADM mass is related to the 4-momentum as

$$P^\mu = \sqrt{-g_s} m u^\mu \quad (33)$$

Finally we have the equation of motion for a fast moving particle.

$$\frac{du^\mu}{d\tau} + \Gamma_{\alpha\beta}^\mu(g_s)u^\alpha u^\beta = 0 \quad (34)$$

This is the geodesic equation but not in the background geometry, but on the smooth part of the geometry which is the sum of the background and the smooth part of the self field.

5 Conclusions

We have reviewed the strong field point particle limit which allows one to take the strong internal gravity into account in the equation of motion without any artificial and unphysical singularities. Although the concept is developed within the framework of post-Newtonian approximation, it can be applicable to the equation of motion for a fast moving small body in an arbitrary background spacetime as long as the size of the body is much smaller than the typical scale of background geometry. It has been shown that the strong field point particle limit can be applicable to the equation of motion up to 3.5 post-Newtonian order without any mathematical difficulty. It is interesting to see if it is applicable to ,ore higher order calculation. In particularly there will be tidal effect at the 4th order and a simple point particle limit should be modified. Since our limit allows us to calculate higher-order moments of the component star as a simple expansion with respect to ϵ , the tidal effect should be calculated without difficulty. In fact it is straightforward to formally calculate all the effect of Newtonian mass multipole moments in the equation of motion in the surface integral approach.

$$m_1 \frac{d^2 \vec{z}_1}{d\tau^2} = \sum_p \sum_q \frac{(-1)^{p+1} (2p + 2q + 1)!!}{p!q!} \frac{I_1^{<M_p> I^{<N_q>}}}{r_{12}^{p+q+2}} N^{<iM_p N_q>} \quad (35)$$

where $\vec{r}_{12} = \vec{z}_1 - \vec{z}_2$, $N_i = r_{12}^i / r_{12}$, $M_p = m_1 m_2 \dots m_p$ is a corrective index, $< \dots >$ denotes the symmetric-tracefree operation on the indices between the brackets, and $I_A^{M_p}$ are the Newtonian mass multipole moments of order $2p$.

Unfortunately the present derivation of equation of motion for a fast moving small body is still on a formal level, the strong field point particle limit dose not have any ambiguity for the separation of the singular part in the self field, there might be some way of deriving more tractable expression for the equation of motion.

Acknowledgments This review is based on my talk at 524th WE Heraeus seminar on the “Equations of Motion in Relativistic Gravity” I would like to thank Dirk Puetzfeld for giving me a chance to contribute in the seminar. I would also thank Yousuke Itoh for fruitful collaborations and useful discussions. I apologize not to cite and mention many relevant works on the subject of equation of motion, and strongly recommend reader to read the review articles such as Living Reviews. This work is supported by a Grant-in-Aid for Scientific Research from JSPS (Nos. 18072001, 20540245).

References

1. A. Einstein, L. Infeld, B. Hoffmann, *Annals. Math.* **39**, 65 (1938)
2. S. Chandrasekhar, F.P. Esposito, *Astrophys. J.* **160**, 153 (1970)
3. V. Fock, *The Theory of Space Time and Gravitation* (Pergamon, Oxford, 1959)
4. L.D. Landau, E.M. Lifshitz, *The Classical Theory of Fields* (Pergamon, Oxford, 1962)
5. L. Blanchet, T. Damour, *Phys. Rev. D* **37**, 1410 (1988)
6. L.P. Grishchuk, S.M. Kopejkin, *Sov. Astron. Lett.* **9**, 230 (1983)
7. A.G. Wiseman, C.M. Will, *Phys. Rev. D* **44**, 2945 (1991)
8. M. Walker, C.M. Will, *Phys. Rev. Lett.* **45**, 1751 (1980)
9. C. Königsdörffer, G. Faye, G. Schäfer, *Phys. Rev. D* **68**, 044004 (2003)
10. S. Nissanke, L. Blanchet, *Class. Quantum Gravity* **22**, 1007 (2005)
11. Y. Itoh, *Phys. Rev. D* **80**, 124003 (2009)
12. T. Damour, P. Jaranowski, G. Schäfer, *Phys. Rev. D* **63**, 044021 (2001)
13. L. Blanchet, *Living Rev. Relativ.* **5**(3) (2002)
14. L. Blanchet, T. Damour, G. Esposito-Farese, *Phys. Rev. D* **69**, 124007 (2004)
15. T. Futamase, *Phys. Rev. D* **36**, 321 (1987)
16. T. Futamase and Y. Itoh, *Living Rev. Relativity*, **10**(2) (2007)
17. T. Mino, M. Sasaki, T. Tanaka, *Phys. Rev. D* **55**, 3457 (1997)
18. T. Quinn, B. Wald, *Phys. Rev. D* **56**, 3381 (1997)
19. S. Fukumoto, T. Futamase, Y. Itoh, *Prog. Theor. Phys.* **116**, 423 (2006)
20. E. Poisson, *Living Rev. Relativity*, **7**(6) (2004)
21. A. Pound, *Phys. Rev. D* **81**, 024023 (2010)
22. L. Barack, A. Ori, *Phys. Rev. D* **61**, 061502(R) (2000)
23. L. Barack, A. Ori, *Phys. Rev. D* **67**, 024029 (2003)
24. L. Barack, N. Sago, *Phys. Rev. D* **75**, 064021 (2007)
25. A. Pound, C. Merlin, L. Barack, *Phys. Rev. D* **89**, 024009 (2014)
26. N. Warburton, S. Akcay, L. Barack, J.R. Gair, N. Sago, *Phys. Rev. D* **85**, 061501(R) (2012)
27. T. Damour, *Phys. Rev. D* **81**, 024017 (2010)
28. T. Futamase, B.F. Schutz, *Phys. Rev. D* **28**, 2363 (1983)

- 29. Y. Itoh, T. Futamase, H. Asada, Phys. Rev. D **63**, 064038 (2001)
- 30. P. Jaranowski, G. Schäfer, Phys. Rev. D **55**, 4712 (1997)
- 31. P. Jaranowski, G. Schäfer, Phys. Rev. D **60**, 124003 (1999)
- 32. Y. Itoh, Phys. Rev. D **69**, 064018 (2004)
- 33. B.S. DeWitt, R.W. Brehme, Ann. Phys. **9**, 220 (1960)

Motion in Classical Field Theories and the Foundations of the Self-force Problem

Abraham I. Harte

Abstract This article serves as a pedagogical introduction to the problem of motion in classical field theories. The primary focus is on self-interaction: How does an object's own field affect its motion? General laws governing the self-force and self-torque are derived using simple, non-perturbative arguments. The relevant concepts are developed gradually by considering motion in a series of increasingly complicated theories. Newtonian gravity is discussed first, then Klein-Gordon theory, electromagnetism, and finally general relativity. Linear and angular momenta as well as centers of mass are defined in each of these cases. Multipole expansions for the force and torque are derived to all orders for arbitrarily self-interacting extended objects. These expansions are found to be structurally identical to the laws of motion satisfied by extended test bodies, except that all relevant fields are replaced by effective versions which exclude the self-fields in a particular sense. Regularization methods traditionally associated with self-interacting point particles arise as straightforward perturbative limits of these (more fundamental) results. Additionally, generic mechanisms are discussed which dynamically shift—i.e., renormalize—the apparent multipole moments associated with self-interacting extended bodies. Although this is primarily a synthesis of earlier work, several new results and interpretations are included as well.

1 Introduction

How are charges accelerated by electromagnetic fields? How do masses fall in curved spacetimes? Such questions can be answered in many different ways. Consider, for example, the Newtonian n -body problem. This is typically solved using a certain system of ordinary differential equations which govern the locations of n points in \mathbb{R}^3 . Besides its location, each point is characterized only by its mass. This is a considerable abstraction from the stars or planets whose motion the n -body problem is intended

A.I. Harte (✉)

Albert-Einstein-Institut, Max-Planck-Institut für Gravitationsphysik,
Am Mühlenberg 1, 14476 Golm, Germany
e-mail: harte@aei.mpg.de

to describe. Physically, each mass point is really an extended body described by the laws of continuum mechanics. The internal density distributions, velocity fields, and temperatures of these bodies might be governed by complicated sets of nonlinear partial differential equations. From one point of view, it is the solutions to these equations which represent “the motion” of each mass.

This is not, however, the approach which is typically adopted in celestial mechanics. In that context, one instead focuses only on each body’s center of mass (and perhaps its spin angular momentum). These are observables which describe motion “in the large.” It is a central result of Newtonian gravity that much of the dynamics of these observables can be understood without detailed knowledge of each body’s internal structure. This is why the extended stars and associated partial differential equations of the “physical n -body problem” can often be modeled as discrete points satisfying a simple set of ordinary differential equations—an enormous simplification.

This work is intended as an introduction to techniques which have recently been developed [1–5] to similarly simplify problems of motion in a wide variety of contexts. Is it possible, for example, to describe extended masses in general relativity using appropriately-defined centers of mass? Do these mass centers obey simple laws of motion? Of course, the same questions may also be asked for charged matter coupled to electromagnetic fields. In simple cases, appropriate laws of motion are well-known in both electromagnetism and general relativity: Sufficiently small test charges accelerate via the Lorentz force law and sufficiently small test masses fall on geodesics. Test body motion is also understood in cases where a body’s higher multipole moments cannot be neglected [6].

Although it has historically been difficult to relax the test body assumption in relativistic theories, several important cases have nevertheless been understood [7–14]. The majority of this work has been intrinsically perturbative. It makes detailed assumptions about the systems to be studied and uses these assumptions at all stages in the analysis. Concepts like the mass and momentum of individual objects typically arise as purely perturbative structures with no clear connection to the full theory. This review takes a different approach. Although approximations may be needed to understand specific applications, we adopt the point of view that approximating exact concepts is preferable to considering structures which emerge only as artifacts of a particular approximation scheme. We therefore focus on non-perturbative descriptions of motion. Somewhat surprisingly, considerable progress can be made from this perspective. Indeed, applying perturbation theory “too early” serves mainly to increase the computational burden and to obscure the underlying physics.

The first step in our program is to define exact linear and angular momenta for arbitrary extended objects.¹ It is these momenta which are used to characterize an object’s motion. Their evolution equations are derived without placing any significant

¹Classical point particles are sometimes discussed as though they were the fundamental building blocks of all classical matter. This viewpoint is severely problematic on both mathematical and physical grounds, and is rejected here. That said, appropriately-regularized point particles do arise as *mathematical structures* obtained from certain well-defined limits involving families of extended bodies. All mention of point particles here is to be understood in this (effective) sense.

constraints on an object's shape, composition, or degree of rigidity. Despite this generality, the methods used here are very easy to apply once the main concepts have been understood. Almost all difficulties lie in finding appropriate definitions and interpreting relations between those definitions; complicated calculations are not required.² Nevertheless, many of the concepts used here are likely to be unfamiliar. Considerable effort has therefore been devoted to explaining these concepts slowly and carefully by applying them in a series of increasingly complicated contexts.

The prototype for all of our discussion is Newtonian celestial mechanics. The laws of motion for this theory are reviewed in Sect. 2. This serves two purposes. First, Sect. 2.1 uses standard techniques to remind the reader which ideas are important and why they are true. What, for example, is a self-field? Why do the self-force and self-torque vanish in Newtonian gravity? The methods used to discuss these questions make essential use of the vector space structure of Euclidean space, and cannot be generalized to curved spacetimes.

Section 2.2 therefore uses Newtonian gravity as a familiar setting with which to introduce techniques that do make sense in curved spacetimes. The problem is reformulated such that no reference is made to any particular coordinate system or to the detailed properties of Euclidean space. All that is needed is a Riemannian space which admits a maximal set of Killing vector fields. It is then possible to introduce a "generalized momentum" which serves to describe a body's large-scale behavior. The ordinary linear and angular momenta arise as two aspects of this more fundamental structure. Using the generalized momentum has many advantages and plays an essential role throughout this review. Employing it, Newtonian self-forces and self-torques are seen to vanish using a one-line computation which requires only the symmetry of an appropriate Green function. That symmetry is physically related to Newton's third law.

From this perspective, certain generalizations of Newtonian gravity may be considered with almost no additional effort. The standard Euclidean background space can, for example, be replaced by one which is spherical or hyperbolic. The usual laws of motion still hold in these cases, except for the addition of Mathisson-Papapetrou spin-curvature couplings. Such terms arise kinematically even in these non-relativistic problems, and are shown to have a simple geometrical interpretation.

Fully relativistic motion is first discussed in Sect. 3, although only in flat or otherwise maximally-symmetric backgrounds. We consider for simplicity the motion of matter coupled to a linear scalar field. A non-perturbative self-field is defined in this context using a slight generalization of its Newtonian analog. Unlike in the non-relativistic case, forces and torques exerted by relativistic self-fields do not necessarily vanish. They instead act to renormalize³ an object's linear and angular momenta. This effect is finite and non-perturbative. Physically, it represents the inertia associated with an object's self-field. Mathematically, it is related to the hyperbolicity of the

²As is typical throughout physics, simple underlying principles do not imply simple applications to explicit problems. Applications typically do require significant computations.

³It is common in the literature to use the words renormalization and regularization interchangeably, both implying the removal of unwanted infinities. This is not the usage here. Renormalization is intended in this review essentially as a synonym for "dynamical shift." These shifts need not be

underlying field equations. Similar effects apply generically for all matter coupled to long-range hyperbolic fields.

Section 4 considers motion in fully generic curved spacetimes. The Killing vectors used to define momenta in simpler cases must then be replaced by an appropriate set of “generalized Killing fields.” This is accomplished in Sect. 4.1. The scalar problem of motion is analyzed first in this more general context, where a new type of renormalization is found to occur. This affects the quadrupole and higher multipole moments of a body’s stress-energy tensor, and may be viewed as a consequence of the “passive gravitational mass distribution” of an object’s self-field. Matter coupled to electromagnetic fields in generic background spacetimes may be understood similarly, and is discussed in Sect. 4.3. Finally, Sect. 4.4 considers motion in general relativity.

Notation

The sign conventions used here are those of Wald [15]. Metrics have positive signature. The Riemann tensor satisfies $2\nabla_{[a}\nabla_{b]}\omega_c = R_{abc}{}^d\omega_d$ for any 1-form ω_a , and the Ricci tensor is defined by $R_{ab} = R_{acb}{}^c$. Abstract indices are denoted using letters a, b, \dots from beginning of the Latin alphabet, while i, j, \dots represent coordinate components. Boldface symbols are used to denote Euclidean vectors and tensors. Units are chosen such that $c = G = 1$.

2 Newtonian Gravity

Consider a Newtonian test body immersed in a gravitational potential $\phi(\mathbf{x}, t)$. If such a body is sufficiently small, it is well-known that its center of mass location γ_t at time t evolves via

$$\ddot{\gamma}_t = -\nabla\phi(\gamma_t, t). \quad (1)$$

This is not the correct equation of motion for (non-spherical) objects with significant self-gravity. Relaxing the test body assumption while still imposing an appropriate smallness condition results in

$$\ddot{\gamma}_t = -\nabla\hat{\phi}(\gamma_t, t), \quad (2)$$

where $\hat{\phi}$ denotes that part of the potential which is determined only by masses external to the body of interest. Comparison of these two equations shows that the field $\nabla\hat{\phi}$

(Footnote 3 continued)

infinite. Regularizations, by contrast, always refer to rules for handling singular behavior. Almost all discussion here focuses on finite renormalizations. Regularizations arise only in certain limiting cases.

which accelerates a large mass can differ⁴ from the field $\nabla\phi$ which would be inferred by measuring the accelerations of nearby test particles. Although it is not often emphasized, this is a standard result in Newtonian gravity. The well-known laws of motion which describe “Newtonian point masses” are, for example, equivalent to (2), not (1).

A central goal of this review is to explain how similar results hold in more complicated relativistic theories. In all cases, the laws of motion are structurally identical to those associated with test bodies. The fields which appear in those laws of motion are not, however, the physical ones. Effective fields appear instead, their details depending on appropriate notions of self-interaction. Once the precise nature of the effective field has been determined in a particular theory, “point particle limits” and related approximations follow very easily.

Many of the difficulties encountered in the relativistic theory motion already appear in the Newtonian problem (where they can be so simple as to easily pass by unnoticed). It is therefore instructive to open this review by carefully discussing the Newtonian theory of motion. Section 2.1 accomplishes this using essentially standard arguments. Concepts such as the self-field and self-force are emphasized, as well as their connections to physical principles like Newton’s third law. Similar discussions may be found in, e.g., [14, 16, 17]. Unfortunately, the familiar techniques used in Sect. 2.1 cannot be readily applied to more complicated theories. Section 2.2 therefore uses Newtonian gravity as a familiar setting with which to introduce a different, more geometrical, approach. The resulting formulation, some of which originally appeared in [2, 5], does generalize. It is used throughout the remainder of this review.

2.1 Newtonian Celestial Mechanics

Consider an extended body residing inside a finite (and possibly time-dependent) region of space $\mathfrak{B}_t \subset \mathbb{R}^3$ which contains no other matter. The mass density ρ and momentum density⁵ $\rho\mathbf{v}$ of this body are both assumed to be smooth. Local mass and momentum conservation then imply that [17–19]

$$\frac{\partial\rho}{\partial t} + \nabla \cdot (\rho\mathbf{v}) = 0 \quad (3)$$

⁴Although the gradients of ϕ and $\hat{\phi}$ coincide at the center of a spherically-symmetric mass, they can be quite different in general. Consider, for example, a barbell constructed by joining two unequal spheres with a massless strut.

⁵In simple cases, \mathbf{v} represents a velocity field in the standard sense. More generally, it might be only an effective construction. This occurs, for example, if a body is composed of multiple interpenetrating fluids.

and

$$\frac{\partial}{\partial t}(\rho \mathbf{v}) + \nabla \cdot (\rho \mathbf{v} \otimes \mathbf{v} - \boldsymbol{\tau}) = \mathbf{f}. \quad (4)$$

The Cauchy stress tensor $\boldsymbol{\tau}$ describes how matter interacts via contact forces, while the force density \mathbf{f} describes longer-range interactions (also known as body forces). If the only long-range forces are gravitational, there exists a potential ϕ such that⁶

$$\mathbf{f} = -\rho \nabla \phi. \quad (5)$$

Inside \mathfrak{B}_t , the potential must satisfy Poisson's equation

$$\nabla^2 \phi = 4\pi \rho. \quad (6)$$

The influence of masses external to \mathfrak{B}_t may be encoded using, e.g., ϕ or its normal derivative on the boundary $\partial \mathfrak{B}_t$.

Equations (3)–(6) are very general. They are not, however, complete. Imposing appropriate boundary conditions, Poisson's equation determines ϕ in terms of ρ , mass conservation evolves ρ using \mathbf{v} , and momentum conservation evolves \mathbf{v} using $\boldsymbol{\tau}$. The stress tensor cannot, however, be determined without additional assumptions. Its evolution is not universal. Stresses depend on an object's detailed composition, reflecting the trivial fact that different types of materials move differently. This is but a minor obstacle in celestial mechanics, and no particular form for $\boldsymbol{\tau}$ is assumed here.

Observables which describe a body's "large-scale" motion may be obtained by integrating the conservation laws (3) and (4). This results in the total mass m , linear momentum $\mathbf{p}(t)$, and angular momentum $\mathbf{S}(\mathbf{z}_t, t)$:

$$m := \int_{\mathfrak{B}_t} \rho d^3 \mathbf{x}, \quad \mathbf{p} := \int_{\mathfrak{B}_t} \rho \mathbf{v} d^3 \mathbf{x}, \quad \mathbf{S} := \int_{\mathfrak{B}_t} \rho (\mathbf{x} - \mathbf{z}_t) \times \mathbf{v} d^3 \mathbf{x}. \quad (7)$$

The general philosophy of celestial mechanics is to focus on \mathbf{p} and \mathbf{S} while ignoring ρ and \mathbf{v} as much as possible. The vast majority of information concerning an object's internal structure is set aside; only its momenta matter. Evolution equations for these momenta are easily obtained from (3) and (4), which show that the mass remains constant and that

$$\dot{\mathbf{p}} = - \int_{\mathfrak{B}_t} \rho \nabla \phi d^3 \mathbf{x}, \quad \dot{\mathbf{S}} = - \int_{\mathfrak{B}_t} \rho (\mathbf{x} - \mathbf{z}_t) \times \nabla \phi d^3 \mathbf{x} - \dot{\mathbf{z}}_t \times \mathbf{p}. \quad (8)$$

⁶This follows from noting that any sufficiently small piece of matter with finite density responds to gravitational forces as though it were a test body.

The gravitational force and torque acting on an extended body therefore depend on its mass distribution, its internal gravitational potential, and a “choice of origin” parametrized by \mathbf{z}_t .

One reason for considering \mathbf{p} is its close relation to the center of mass position γ_t . This can be defined by

$$\gamma_t := \frac{1}{m} \int_{\mathfrak{B}_t} \mathbf{x} \rho(\mathbf{x}, t) d^3 \mathbf{x}, \quad (9)$$

or equivalently by demanding that a body’s mass dipole moment vanish when evaluated about γ_t :

$$\int_{\mathfrak{B}_t} (\mathbf{x} - \gamma_t) \rho(\mathbf{x}, t) d^3 \mathbf{x} = 0. \quad (10)$$

Regardless, it follows from (3) and (9) that the center of mass velocity must satisfy

$$m \dot{\gamma}_t = \mathbf{p}. \quad (11)$$

Note that this is a derived result, not a definition; m , γ_t and \mathbf{p} are defined in terms of ρ and \mathbf{v} via (7) and (9). In more complicated theories, the center of mass velocity need not be parallel to the momentum.

Once γ_t has been defined, its time evolution is easily found by combining (8) and (11) to yield

$$m \ddot{\gamma}_t = - \int_{\mathfrak{B}_t} \rho \nabla \phi d^3 \mathbf{x}. \quad (12)$$

Evaluating $\mathbf{S}(\mathbf{z}_t, t)$ with $\mathbf{z}_t = \gamma_t$ isolates the spin component of the angular momentum from the orbital component which can appear more generally, resulting in

$$\dot{\mathbf{S}} = - \int_{\mathfrak{B}_t} \rho (\mathbf{x} - \gamma_t) \times \nabla \phi d^3 \mathbf{x}. \quad (13)$$

In astrophysical applications, ρ and $\nabla \phi$ are typically only very coarsely constrained by observations. Integral expressions like (12) and (13) are therefore unsuitable for applications. They must first be simplified.

Such simplifications are immediate if $\nabla \phi$ varies negligibly throughout \mathfrak{B}_t , as can occur if the mass in question is a test body whose dimensions are small compared with the distances to all other masses in the universe. In these cases, it follows from (12) and (13) that the center of mass acceleration satisfies (1) and that $\dot{\mathbf{S}} = 0$. Simplifying the laws of motion in more general contexts requires understanding the influence of an object’s own gravitational field.

A precise definition for the self-field may be obtained via a two-point function (or propagator) $G(\mathbf{x}, \mathbf{x}')$ describing “the gravitational potential at \mathbf{x} per unit mass at \mathbf{x}' .” Any potential constructed from such a propagator can reasonably be called a self-field only if it is a Green function for the Poisson equation:

$$\nabla^2 G(\mathbf{x}, \mathbf{x}') = 4\pi\delta^3(\mathbf{x} - \mathbf{x}'). \quad (14)$$

There are, of course, many possible Green functions. A particular one may be singled out by demanding that self-fields described by G be compatible with Newton’s third law. Consider two distinct points $\mathbf{x}, \mathbf{x}' \in \mathfrak{B}_t$. It is then natural to interpret “the force on mass at \mathbf{x} due to mass at \mathbf{x}' ” to mean

$$-\rho(\mathbf{x}, t)\nabla \left[G(\mathbf{x}, \mathbf{x}')\rho(\mathbf{x}', t)d^3\mathbf{x}' \right] d^3\mathbf{x}. \quad (15)$$

The weak form of Newton’s third law states that the force at \mathbf{x} due to \mathbf{x}' must be equal and opposite to the force at \mathbf{x}' due to \mathbf{x} , which implies that

$$\nabla G(\mathbf{x}, \mathbf{x}') = -\nabla' G(\mathbf{x}', \mathbf{x}). \quad (16)$$

The strong form of Newton’s third law instead requires that the force at \mathbf{x} due to \mathbf{x}' point along the line which connects these two points. Imposing this,

$$\nabla G(\mathbf{x}, \mathbf{x}') \propto \mathbf{x} - \mathbf{x}'. \quad (17)$$

Any $G(\mathbf{x}, \mathbf{x}')$ which is compatible with the strong form of Newton’s third law can therefore depend only on the distance $|\mathbf{x} - \mathbf{x}'|$ between its arguments. Up to an irrelevant additive constant, it follows from (14) that

$$G(\mathbf{x}, \mathbf{x}') = G(\mathbf{x}', \mathbf{x}) = -\frac{1}{|\mathbf{x} - \mathbf{x}'|}. \quad (18)$$

The total self-field is then

$$\phi_S(\mathbf{x}, t) := \int_{\mathfrak{B}_t} \rho(\mathbf{x}', t)G(\mathbf{x}, \mathbf{x}')d^3\mathbf{x}' = - \int_{\mathfrak{B}_t} \frac{\rho(\mathbf{x}', t)}{|\mathbf{x} - \mathbf{x}'|}d^3\mathbf{x}'. \quad (19)$$

The physical field ϕ may be viewed as the sum of the self-field ϕ_S and an appropriate remainder $\hat{\phi}$:

$$\hat{\phi} := \phi - \phi_S. \quad (20)$$

It follows from (6), (14), and (19) that the effective potential $\hat{\phi}$ satisfies the vacuum field equation $\nabla^2 \hat{\phi} = 0$ throughout \mathfrak{B}_t .

Now consider the total force exerted by ϕ_S , the “self-force.” Noting (8), it is natural to let this refer to

$$\mathbf{F}_S := - \int_{\mathfrak{B}_t} \rho \nabla \phi_S d^3 \mathbf{x}. \quad (21)$$

Substituting (19) into this expression results in an integral over the product space $\mathfrak{B}_t \times \mathfrak{B}_t$:

$$\mathbf{F}_S = - \int_{\mathfrak{B}_t \times \mathfrak{B}_t} \rho(\mathbf{x}, t) \rho(\mathbf{x}', t) \nabla G(\mathbf{x}, \mathbf{x}') d^3 \mathbf{x} d^3 \mathbf{x}'. \quad (22)$$

Recalling (16) or (18), the integrand is antisymmetric under interchange of \mathbf{x} and \mathbf{x}' . The Newtonian self-force therefore vanishes. This is an exact result. It holds for all compact mass distributions. Whatever the shape a particular body happens to be in \mathfrak{B}_t , the self-force vanishes because that shape is trivially symmetric when copied into $\mathfrak{B}_t \times \mathfrak{B}_t$. A similar argument may be used to show that the self-torque, the net torque exerted by ϕ_S , vanishes as well.

The main point of this discussion is that the net gravitational force exerted on any isolated extended mass satisfies

$$\dot{\mathbf{p}} = - \int_{\mathfrak{B}_t} \rho \nabla (\hat{\phi} + \phi_S) d^3 \mathbf{x} = - \int_{\mathfrak{B}_t} \rho \nabla \hat{\phi} d^3 \mathbf{x}. \quad (23)$$

Not necessarily choosing \mathbf{z}_t to be the center of mass, the equivalent evolution equation for $\mathbf{S}(\mathbf{z}_t, t)$ is

$$\dot{\mathbf{S}} = - \int_{\mathfrak{B}_t} \rho(\mathbf{x} - \mathbf{z}_t) \times \nabla \hat{\phi} d^3 \mathbf{x} - \dot{\mathbf{z}}_t \times \mathbf{p}. \quad (24)$$

The vanishing self-force and self-torque allows ϕ to be replaced by $\hat{\phi}$ in the evolution equations for both the linear and angular momenta. Although forces and torques may be computed using either the physical field ϕ or the fictitious effective field $\hat{\phi}$, the latter computation is often simpler. In most cases of practical interest, $\nabla \hat{\phi}$ varies far more slowly in \mathfrak{B}_t than does $\nabla \phi$. The integral involving $\nabla \hat{\phi}$ can therefore be amenable to approximation when the (otherwise equivalent) integral involving $\nabla \phi$ is not.

Recalling that $\hat{\phi}$ is harmonic inside the body region, it must be analytic there. This means that its Taylor series about an arbitrary point $\mathbf{z}_t \in \mathfrak{B}_t$ converges at least in some neighborhood of \mathbf{z}_t . If that series converges throughout the body, it may be substituted into (23) and integrated term by term. The integral expression for the force is then equivalent to

$$\dot{p}_i(t) = -m \partial_i \hat{\phi}(\mathbf{z}_t, t) - \sum_{n=1}^{\infty} \frac{1}{n!} m^{j_1 \dots j_n}(\mathbf{z}_t, t) \partial_i \partial_{j_1} \dots \partial_{j_n} \hat{\phi}(\mathbf{z}_t, t), \quad (25)$$

where $m^{j_1 \dots j_n}(\mathbf{z}_t, t)$ denotes the body's 2^n -pole mass moment about \mathbf{z}_t :

$$m^{j_1 \dots j_n}(\mathbf{z}_t, t) := \int_{\mathfrak{B}_t} (\mathbf{x} - \mathbf{z}_t)^{j_1} \dots (\mathbf{x} - \mathbf{z}_t)^{j_n} \rho(\mathbf{x}, t) d^3 \mathbf{x}. \quad (26)$$

The series (25) is referred to as a multipole expansion for the force. A similar series also exists for the angular momentum. If \mathbf{z}_t is chosen to coincide with the center of mass γ_t , the dipole moment $m^i(\gamma_t, t)$ vanishes by (10). The $n = 1$ term in (25) therefore vanishes as well, so

$$\ddot{\gamma}_t^i = -\partial^i \hat{\phi}(\gamma_t, t) - \frac{1}{m} \sum_{n=2}^{\infty} \frac{1}{n!} m^{j_1 \dots j_n}(\gamma_t, t) \partial^i \partial_{j_1} \dots \partial_{j_n} \hat{\phi}(\gamma_t, t). \quad (27)$$

The utility of this expression is that there are many cases of interest where the multipole series can be truncated at low order without significant loss of accuracy. The simplest such truncation recovers (2). More generally, there are correction to this equation which involve a body's quadrupole and higher multipole moments.

Lastly, note that the moments (26) are somewhat different from the ones which are found in textbooks. The harmonicity of $\hat{\phi}$ implies that arbitrary traces may be added to the $m^{j_1 \dots j_n}$ without affecting the force. The $m^{j_1 \dots j_n}$ appearing in (25) may therefore be replaced by different moments $\tilde{m}^{j_1 \dots j_n}$ which are trace-free in all pairs of indices. It is these trace-free moments which are typically used in practical calculations. Besides the elimination of irrelevant components, the trace-free moments are also useful in that they may be determined purely using external measurements of an object's gravitational field.

2.2 Reformulating Newtonian Celestial Mechanics

The discussion which has just been presented relies heavily on the geometric peculiarities of Euclidean space. This is not essential. The only characteristic of (three-dimensional) Euclidean space which is truly important is that it is maximally symmetric: There exist a total of six linearly independent Killing vector fields. The Newtonian laws of motion are now rederived using methods which make this manifest.

As a consequence, certain aspects of the Newtonian problem are significantly clarified. The geometrical nature of the linear and angular momenta is made precise, for example. These are shown to be two aspects of a more fundamental vector which lives not in the physical space, but in a space which is dual to the space of Killing vector fields. The approach introduced in this section also emphasizes the importance of symmetries. It is fundamental to understanding motion in more complicated theories.

Another advantage of the reformulation discussed in this section is that certain generalizations of Newtonian gravity may be understood essentially “for free.” Noting that spherical and hyperbolic spaces are both maximally-symmetric, there are no new complications if the usual Euclidean background of Newtonian gravity is replaced by a space of constant curvature. It is also trivial to change the number of spatial dimensions, or to add, e.g., a mass term to the field equation. For concreteness, we restrict to three spatial dimensions and keep the gravitational field equation as-is. We do, however, allow the background space to be curved. This has interesting consequences which reappear in the more complicated relativistic theories considered in later sections.

2.2.1 Geometric Preliminaries

The locations of Newtonian events may be viewed as points in a four-dimensional manifold \mathcal{M} . While a relativistic spacetime is defined using only a manifold and a non-degenerate metric, Newtonian spacetimes require more structure [18–20]. One such structure is a preferred notion of time. This takes the form of an equivalence class⁷ of functions which associate each event in spacetime with “the time” at which it occurs. Associated with this is a preferred foliation of \mathcal{M} into a one-parameter family of hypersurfaces $\{\mathcal{S}_t\}$. These are the spaces of constant time.

Newtonian spacetimes are difficult to work with directly. They simplify considerably in the presence of a frame, a structure that identifies events at different times as being at “the same” spatial point. It is assumed here that a frame has been fixed in such a way that all \mathcal{S}_t are mapped into a single space consisting of a three-dimensional manifold \mathcal{S} together with a (fixed) Riemannian metric g_{ab} . This process also fixes a particular time function. It permits all physical quantities in spacetime to be viewed as time-dependent quantities on \mathcal{S} . We allow the spatial metric to be curved, but assume that its curvature is everywhere constant. Letting ∇_a and $R_{abc}{}^d$ denote the covariant derivative and Riemann tensor associated with g_{ab} , $\nabla_a R_{bcd}{}^f = 0$. This implies that (\mathcal{S}, g_{ab}) is maximally symmetric.

Consider the motion of a material object instantaneously confined to a submanifold $\mathfrak{B}_t \subset \mathcal{S}$ which contains no other matter and has finite volume. Denote this body’s mass density at time t by $\rho(\cdot, t)$ and its velocity field at time t by $v^a(\cdot, t)$. Local conservation of mass and momentum continue to hold in this context, so (3) and (4) carry over essentially without change:

$$\frac{\partial}{\partial t} \rho + \nabla_a (\rho v^a) = 0, \quad (28)$$

$$\frac{\partial}{\partial t} (\rho v^a) + \nabla_b (\rho v^a v^b - \tau^{ab}) = -\rho \nabla^a \phi. \quad (29)$$

⁷For any single time function $T : \mathcal{M} \rightarrow \mathbb{R}$ and any $c, d \in \mathbb{R}$ such that $c > 0$, the map $cT + d$ is also an acceptable time function.

The gravitational potential ϕ which appears here satisfies the obvious generalization of Poisson's equation:

$$\nabla^a \nabla_a \phi = g^{ab} \nabla_a \nabla_b \phi = 4\pi\rho. \quad (30)$$

2.2.2 Generalized Momentum

Our first significant departure from the elementary discussion of Newtonian motion found in Sect. 2.1 arises in the definitions for a body's linear and angular momenta. The usual integrals (7) make sense only when evaluated in a Cartesian coordinate system. Alternatively, they require a canonical identification of tangent spaces associated with different points in the spatial manifold. While this is easily accomplished in Euclidean space, it is not obvious what to do more generally. Our first task is therefore to define momenta which do not make reference to a specific coordinate system. Accomplishing this provides a notion of momentum which is easily generalized to curved Newtonian backgrounds, and even to completely generic relativistic spacetimes. It is a basic building block for all results discussed in this review.

One problem with elementary definitions of mechanical momentum is that they attempt to represent this concept via a spatial vector or covector. This is physically unnatural (except for point particles or momentum densities). Momenta are associated with extended regions, not individual points. There is no natural tangent or cotangent space in which to place the momentum contained in an extended region $\mathfrak{R} \subset \mathfrak{B}_t$. The simplest mathematical structure with which to represent a quasi-local quantity must itself be quasi-local. Spatial tensors are not, of course, examples of such structures.

Besides being quasi-local, momenta must also be extensive. For any two disjoint regions $\mathfrak{R}_1, \mathfrak{R}_2 \subset \mathfrak{B}_t$ which are "physically independent," there must be a sense in which

$$(\text{momentum in } \mathfrak{R}_1) + (\text{momentum in } \mathfrak{R}_2) = (\text{momentum in } \mathfrak{R}_1 \cup \mathfrak{R}_2) \quad (31)$$

for some binary operation "+" which is both associative and commutative. If \mathfrak{R}_1 and \mathfrak{R}_2 are identically prepared, it is also natural to suppose that

$$(\text{momentum in } \mathfrak{R}_1) + (\text{momentum in } \mathfrak{R}_2) = 2(\text{momentum in } \mathfrak{R}_1). \quad (32)$$

This motivates a notion of scalar multiplication.

Together, these considerations and others suggest that momenta should be elements of a vector space. The most natural vector space is not, however, the space of tensors at any particular spatial point. A better choice may be motivated by recalling that conserved linear momenta arise naturally in theories which are derived from translation-invariant Lagrangians. Similarly, conserved angular momenta arise from Lagrangians which are invariant with respect to rotations. This suggests that both types of momenta can be associated explicitly with a collection of continuous

symmetries. Consider, in particular, those symmetries—the continuous isometries—which preserve the spatial metric. While these are not necessarily symmetries for all physically-interesting quantities, they are extremely useful.

The continuous isometries of a Riemannian space (\mathcal{S}, g_{ab}) are generated by its Killing vector fields. By definition,

$$\mathcal{L}_\xi g_{ab} = 0 \quad (33)$$

for every Killing vector ξ^a , where \mathcal{L}_ξ denotes the Lie derivative with respect to ξ^a . We use K to denote the collection of all Killing vector fields together with obvious notions of addition and scalar multiplication. This is a vector space. Moreover, the dimension of this vector space is finite. If the dimension of the physical space is $\dim \mathcal{S} = \dim \mathfrak{B}_t = N$, it may be shown that (see, e.g., Appendix C of [15])

$$\dim K \leq \frac{1}{2}N(N+1). \quad (34)$$

This section restricts attention to maximally-symmetric spaces where $\dim K = \frac{1}{2}N(N+1)$. When $N = 3$, Euclidean, spherical, and hyperbolic spaces are all maximally-symmetric. They admit six linearly-independent Killing fields. Given a preferred point, three Killing fields may be interpreted as translations and three as rotations. This makes sense only near the given point, and is best avoided at this stage. Doing so implies that the linear and angular momenta should be treated as elements of a single object “conjugate to” the space of all Killing vector fields.

Consider a representation of a body’s momentum as a vector in the space K^* which is dual to K . An element of K^* is, by definition, a linear map from K to \mathbb{R} . The specific linear map which has the desired properties is

$$P_t[\mathfrak{R}](\xi) := \int_{\mathfrak{R}} \rho(x, t) v_a(x, t) \xi^a(x) dV, \quad (35)$$

where $\xi^a \in K$ and the volume element is the natural one associated with g_{ab} . We call this the *generalized momentum contained in $\mathfrak{R} \subseteq \mathfrak{B}_t$ at time t* . It is often convenient to omit the dependence on \mathfrak{R} , in which case it is to be understood that $P_t = P_t[\mathfrak{B}_t]$.

The dimension of K^* is equal to the dimension of K , so this momentum has six components in three spatial dimensions. These components correspond to the usual three components of linear momentum and three components of angular momentum. Such a split can be made explicit by introducing additional structure, namely a preferred point $z_t \in \mathfrak{B}_t$. For any such point, $P_t[\mathfrak{R}]$ can be re-expressed in terms of spatial tensors p_a , S^a at z_t . This is explained in Sect. 2.2.6. For now, it suffices to consider $P_t[\mathfrak{R}]$ on its own. While the introduction of a preferred point allows this map to be replaced by spatial tensors, avoiding such representations whenever possible provides considerable calculational and conceptual simplifications.

In relativistic contexts where there exists a maximally-symmetric background geometry, the generalized momentum remains essentially unchanged. The infinitesimal momentum $\rho v_a dV$ is merely replaced by $T_a{}^b dS_b$, where $T_a{}^b$ is an appropriate stress-energy tensor and dS_b is the natural volume element on a three-dimensional hypersurface. If a spacetime is not maximally-symmetric, one also replaces K by another vector space which has the correct dimensionality. The “generalized Killing fields” used for this purpose are discussed in Sect. 4.1.

2.2.3 Generalized Force

How does Newtonian gravity affect the time evolution of the generalized momentum? Using local momentum conservation (29) and assuming that the boundary $\partial\mathfrak{R}$ is independent of time (or that there is no matter there),

$$\frac{d}{dt} P_t[\mathfrak{R}](\xi) = \int_{\mathfrak{R}} \left[-\rho \mathcal{L}_\xi \phi + \frac{1}{2} (\rho v^a v^b - \tau^{ab}) \mathcal{L}_\xi g_{ab} \right] dV = - \int_{\mathfrak{R}} \rho \mathcal{L}_\xi \phi dV. \quad (36)$$

The second equality here follows from Killing’s equation (33). If $\mathcal{L}_\psi \phi = 0$ for some specific Killing field ψ^a , it is clear that the associated momentum $P_t[\mathfrak{R}](\psi)$ is conserved. This means that if ϕ is constant along a translational Killing field, there can be no force in that direction. Similarly, a field which is invariant about rotations around a given axis exerts no torque about that axis. Both of these statements are physically obvious. They are also of limited value. Once the field equation (30) is taken into account, $\mathcal{L}_\psi \phi = 0$ implies that $\mathcal{L}_\psi \rho \propto \mathcal{L}_\psi \nabla^a \nabla_a \phi = \nabla^a \nabla_a \mathcal{L}_\psi \phi = 0$ as well. This is clearly impossible for any compact body if ψ^a is a pure translation. Rotational symmetries fare better, although they are still a rather special case.

Transforming (36) into a surface integral results in a more interesting conservation law. Using the field equation and integrating by parts shows that

$$\frac{d}{dt} P_t[\mathfrak{R}](\xi) = - \oint_{\partial\mathfrak{R}} T^a{}_b \xi^b dS_a, \quad (37)$$

where

$$T_{ab} := \frac{1}{4\pi} (\nabla_a \phi \nabla_b \phi - \frac{1}{2} g_{ab} \nabla^c \phi \nabla_c \phi) \quad (38)$$

is the stress tensor associated with ϕ . At least in flat space, one might imagine extending $\partial\mathfrak{R}$ (and perhaps $\partial\mathfrak{B}_t$) far outside of all matter of interest. If ϕ falls off sufficiently fast in this region, the surface integral can be seen to vanish. The generalized momentum is therefore conserved in such cases. Of course, the momentum associated with a single object in a larger system is not conserved. Understanding its dynamics requires a different argument.

2.2.4 The Self-field

The generalized force (36) involves the physical field ϕ . As discussed in Sect. 2.1, this is too complicated to work with directly. We therefore isolate its most complicated part—the self-field—and compute what it does directly. Once this is accomplished, the remaining undetermined portion of the force is relatively simple to understand.

The self-field in this context is defined in Sect. 2.1 in terms of a certain two-point function G . This must still be a Green function. If $G(x, x') = G(x', x)$, the two constraints (16), (17) which implied a notion of Newton’s third law in Euclidean space generalize to the statement that

$$\mathcal{L}_\xi G(x, x') = [\xi^a(x) \nabla_a + \xi^{a'}(x') \nabla_{a'}] G(x, x') = 0 \quad (39)$$

for all $\xi^a \in K$. In the Euclidean case, translational invariance alone implies the weak form of Newton’s third law. Further imposing rotational invariance recovers the strong form of Newton’s third law. In general, though, symmetries of G imply only “portions of” Newton’s third law.

It is always possible to find Green functions which satisfy (39) in maximally-symmetric backgrounds. Indeed, these Green functions depend only on the geodesic distance between their arguments. Introducing Synge’s function (also known as the world function) [10, 21, 22]

$$\sigma(x, x') := \frac{1}{2} (\text{squared geodesic distance between } x \text{ and } x'), \quad (40)$$

the Euclidean Green function (18) can be written as $G = -1/\sqrt{2\sigma}$. Green functions associated with spherical and hyperbolic spaces are merely more complicated functions of σ [23]. In any of these cases, $\mathcal{L}_\xi G \propto \mathcal{L}_\xi \sigma = 0$.

Using the symmetric Green function which satisfies (39) to define the self-field, let

$$\phi_S(x, t) := \int_{\mathfrak{B}_t} \rho(x', t) G(x, x') dV'. \quad (41)$$

Substituting this into (36) shows that

$$\begin{aligned} \frac{d}{dt} P_t &= - \int_{\mathfrak{B}_t} \rho(x, t) \mathcal{L}_\xi \hat{\phi}(x, t) dV \\ &\quad - \frac{1}{2} \int_{\mathfrak{B}_t} dV \int_{\mathfrak{B}_t} dV' \rho(x, t) \rho(x', t) \mathcal{L}_\xi G(x, x') \\ &= - \int_{\mathfrak{B}_t} \rho(x, t) \mathcal{L}_\xi \hat{\phi}(x, t) dV, \end{aligned} \quad (42)$$

where $\hat{\phi} = \phi - \phi_S$ and \mathfrak{R} has been replaced by the entire body region \mathfrak{B}_t . It is clear from this that the self-force and self-torque both vanish as an immediate consequence of (39). All forces and torques may therefore be computed using $\hat{\phi}$ instead of ϕ . Furthermore, the effective field satisfies the vacuum equation

$$\nabla^a \nabla_a \hat{\phi} = 0. \quad (43)$$

It can clearly be computed by subtracting the self-field from the physical field. Alternatively, Stokes' theorem may be used together with (43) to write $\hat{\phi}$ as a kind of average of ϕ over a closed surface which surrounds the body of interest.

It has already been mentioned that $P_t(\psi)$ is conserved if $\mathcal{L}_\psi \phi = 0$. Equation (42) shows that this is also true if $\mathcal{L}_\psi \hat{\phi} = 0$, a much weaker condition. For a closed system, one typically has $\phi = \phi_S$ and hence $\hat{\phi} = 0$. All components of the generalized momentum are therefore conserved in such cases.

Equation (42) has been established by showing that the generalized force exerted by ϕ_S always vanishes. This force involves an integral over $\mathfrak{B}_t \times \mathfrak{B}_t$, and may therefore be interpreted as a two-point interaction. It can sometimes be interesting to also consider interactions between three or more points. Let

$$\tilde{\phi}_S(x, t) := \sum_{n=1}^{n_{\max}} c_n \int_{\mathfrak{B}_t} dV_1 \cdots \int_{\mathfrak{B}_t} dV_n \rho(y_1, t) \cdots \rho(y_n, t) G_n(x, y_1, \dots, y_n), \quad (44)$$

where the c_n are arbitrary constants and the $(n+1)$ -point propagators G_n are symmetric in their arguments and satisfy $\mathcal{L}_\xi G_n$ for all $\xi^a \in K$. It is straightforward to show that the generalized force exerted by any such field vanishes. Given the two-point G used to define ϕ_S , an appropriate three-point interaction may be chosen using, e.g.,

$$G_3(x, y, z) = G(x, y)G(y, z)G(z, x). \quad (45)$$

Other choices are also possible, of course. Higher-order propagators typically lead to fields $\tilde{\phi}_S$ which are not really Newtonian self-fields in the sense that $\nabla^a \nabla_a \tilde{\phi}_S \neq 4\pi\rho$. Series like (44) can nevertheless be useful for understanding different theories where matter couples to nonlinear fields. In those cases, the sum in $\tilde{\phi}_S$ might be compared to a kind of Dyson series for an object's self-field. Regardless of the field equation, however, the existence of a Killing field ψ^a which satisfies $\mathcal{L}_\psi(\phi - \tilde{\phi}_S) = 0$ for *some* $\tilde{\phi}_S$ always implies that $P_t(\psi)$ is conserved. Although this conservation law might be manifest only for a particular choice of $\tilde{\phi}_S$, the value of $P_t(\psi)$ does not depend on that choice.

2.2.5 Multipole Expansions

Returning to the main development, note that (36) and (42) differ only by the replacement $\phi \rightarrow \hat{\phi}$. Although both of these integrals are numerically equivalent, the latter is often simpler to evaluate. This is because $\mathcal{L}_\xi \hat{\phi}$ can be readily approximated throughout \mathfrak{B}_t in many more physically-interesting situations than can $\mathcal{L}_\xi \phi$. Such approximations are based on a Taylor expansion of $\hat{\phi}$. While this has an obvious meaning in Euclidean space, a technical diversion is needed to explain what is meant by Taylor expansions more generally.

Given an origin $z_t \in \mathfrak{B}_t$ about which a particular Taylor expansion is to be performed, the most natural Cartesian-like coordinate systems are the Riemann normal coordinates with origin z_t . These are unique up to rotations, and may be used to perform Taylor expansions in the usual way.

To be more precise, recall that the exponential map $\exp_x X^a = x'$ takes as input a point x and a vector X^a at that point. The point x' which is returned is found by considering an affinely-parametrized geodesic y_u satisfying $y_0 = x$ and $\dot{y}_0^a = X^a$. The point x' is then equal to y_1 . An equivalent statement may be expressed using Synge's function (40). Letting $\sigma_a(x', x)$ denote $\nabla_a \sigma(x', x)$,

$$\exp_x[-\sigma^a(x', x)] = x'. \quad (46)$$

First derivatives of Synge's function therefore generalize the concept of a "separation vector." The $x' - x$ of a conventional Taylor series in Cartesian coordinates naturally turns into $-\sigma^a(x', x)$ in more general contexts. If a scalar field $\lambda(x)$ is to be expanded in a Taylor series about some x , it is convenient to first rewrite this as a function on the tangent bundle by defining

$$\Lambda(x, X^a) := \lambda(\exp_x X^a). \quad (47)$$

Now let the n th tensor extension of λ at x be

$$\lambda_{,a_1 \dots a_n}(x) := \left[\frac{\partial^n \Lambda(x, X^b)}{\partial X^{a_1} \dots \partial X^{a_n}} \right]_{X^b=0}. \quad (48)$$

This is the unique tensor field which reduces to n partial derivatives of λ in a Riemann normal coordinate system with origin x . In flat space, $\lambda_{,a_1 \dots a_n} = \nabla_{a_1} \dots \nabla_{a_n} \lambda$. More generally, the curvature can appear. Further discussion of tensor extensions may be found in [4, 6].

Combining all of these concepts, a natural Taylor series for $\hat{\phi}$ which applies regardless of the background geometry is

$$\hat{\phi}(x', t) = \sum_{n=0}^{\infty} \frac{(-1)^n}{n!} \sigma^{a_1}(x', z_t) \dots \sigma^{a_n}(x', z_t) \hat{\phi}_{,a_1 \dots a_n}(z_t, t). \quad (49)$$

All distances are assumed to be sufficiently small that σ remains single-valued and its derivative is well-defined. Furthermore, a Taylor series like this is—even if it does not converge everywhere of interest—assumed to be at least a useful asymptotic approximation throughout \mathfrak{B}_s . Substituting (49) into (42) and integrating term-by-term results in a multipole expansion for the generalized force. Noting that

$$\mathcal{L}_\xi \sigma^a = \mathcal{L}_\xi (g^{ab} \nabla_b \sigma) = g^{ab} \nabla_b \mathcal{L}_\xi \sigma = 0 \quad (50)$$

for any Killing field ξ^a , the multipole expansion for the generalized force is

$$\frac{d}{dt} P_t(\xi) = - \sum_{n=0}^{\infty} \frac{1}{n!} m^{a_1 \dots a_n}(z_t, t) \mathcal{L}_{\xi} \hat{\phi}_{, a_1 \dots a_n}(z_t, t). \quad (51)$$

The mass moments which appear here depend on ρ via

$$m^{a_1 \dots a_n}(z_t, t) := (-1)^n \int_{\mathfrak{B}_t} \sigma^{a_1}(x', z_t) \dots \sigma^{a_n}(x', z_t) \rho(x', t) dV'. \quad (52)$$

It follows from (28) that the zeroth moment, the mass, is independent of time. Conservation laws do not, however, fix the evolution of the higher moments. These depend on the type of matter under consideration.

If $\mathcal{L}_{\psi} \hat{\phi} = 0$ for some Killing field ψ^a , it follows that $\mathcal{L}_{\psi} \hat{\phi}_{, a_1 \dots a_n} = 0$ for any n . The conservation of $P_t(\psi)$ in such a case is therefore preserved by any approximation which truncates the multipole series at finite n . This is an important property which helps such approximations have accurate long-time behavior.

2.2.6 Linear and Angular Momenta

Thus far, $P_t = P_t[\mathfrak{B}_t]$ has been loosely described as equivalent to a body's linear and angular momenta at time t . Similarly, time derivatives of the generalized momentum have been interpreted as “forces and torques.” These identifications are now made precise.

Recall that the generalized momentum is a vector in K^* , the vector space dual to K . While it is productive to view P_t simply as a linear map from K to \mathbb{R} , it can also be useful to find its components with respect to a particular basis. It is in this context that the linear and angular momenta arise in their more familiar form.

A basis for K may be found by recalling that knowledge of a Killing field and its first derivative at any one point fixes it everywhere [15]. Choosing an arbitrary point x , the space of Killing vectors is in one-to-one correspondence with the space of all 1- and 2-forms at x . There exist two-point tensor fields $\Xi^{a'a}(x', x)$, $\Xi^{a'ab}(x', x)$ such that

$$\xi^{a'}(x') = \Xi^{a'a}(x', x) A_a + \Xi^{a'ab}(x', x) B_{ab} \quad (53)$$

is an element of K for any A_a and any $B_{ab} = B_{[ab]}$. The “Killing data” satisfies

$$A_a = \xi_a(x), \quad B_{ab} = B_{[ab]} = \nabla_a \xi_b(x). \quad (54)$$

In a physical space of dimension N , there exist N linearly independent 1-forms and $N(N-1)/2$ linearly independent 2-forms. Together, these generate the requisite $N(N+1)/2$ linearly independent Killing vectors. In Euclidean space and in a Cartesian coordinate system,

$$\Xi^{i'i}(x', x) = \delta^{ii'}, \quad \Xi^{i'ij}(x', x) = (x' - x)^{[i} \delta^{j]i'}. \quad (55)$$

More generally, $\Xi^{a'a}$ and $\Xi^{a'ab}$ are related to the geodesic deviation equation and form a basis for K . They can be computed using the first two derivatives of Synge’s function [24]. Defining $\sigma_{ab} := \nabla_b \sigma_a = \nabla_b \nabla_a \sigma$, $\sigma_{aa'} := \nabla_{a'} \sigma_a$, and $H^{a'}_a := [-\sigma^a_{a'}]^{-1}$,

$$\Xi^{a'a} = H^{a'}_b \sigma^{ba}, \quad \Xi^{a'ab} = H^{a'}_{[a} \sigma^{b]}. \quad (56)$$

Substituting (53) into (35) shows that $P_t(\xi)$ can be written as a linear combination of $\xi_a(x)$ and $\nabla_a \xi_b(x)$. The coefficients in this combination are identified with the linear momentum $p^a(x, t)$ and the angular momentum bivector $S^{ab} = S^{[ab]}(x, t)$:

$$P_t(\xi) = p^a(x, t) \xi_a(x) + \frac{1}{2} S^{ab}(x, t) \nabla_a \xi_b(x). \quad (57)$$

This is an implicit definition. Varying amongst all possible ξ_a and $\nabla_a \xi_b$ recovers the explicit formulae

$$p^a(x, t) = \int_{\mathfrak{B}_t} \rho(x', t) v_{a'}(x', t) H^{a'}_b(x', x) \sigma^{ba}(x', x) dV', \quad (58)$$

$$S^{ab}(x, t) = 2 \int_{\mathfrak{B}_t} \rho(x', t) v_{a'}(x', t) H^{a'}_{[a}(x', x) \sigma^{b]}(x', x) dV'. \quad (59)$$

In three spatial dimensions, the angular momentum bivector is dual to an angular momentum 1-form S_a via

$$S_a = \frac{1}{2} \epsilon_{abc} S^{bc}. \quad (60)$$

Introducing Cartesian coordinates in a flat background, it is easily verified that the p^i and S_i derived from P_t in this way reproduce the elementary definitions (7). Explicit coordinate expressions are more difficult to obtain in curved backgrounds, but these are rarely necessary.

Thus far, the spatial curvature has played no explicit role in any of our discussion. It does appear, however, in the evolution equations for p^a and S^{ab} . First note the general identity [15]

$$\nabla_a \nabla_b \xi_c = -R_{bca}{}^d \xi_d, \quad (61)$$

which holds for any Killing field ξ^a . Time derivatives of the Killing data (A_a, B_{ab}) along a path z_t therefore satisfy

$$\frac{D}{dt} A_a = \dot{z}_t^b B_{ba}, \quad \frac{D}{dt} B_{ab} = -R_{abc}{}^d \dot{z}_t^c A_d. \quad (62)$$

These are known as the Killing transport equations [15, 25]. They are ordinary differential equations which can be used to relate Killing data at one point to Killing data at another point.

Consider linear and angular momenta defined about some z_t , so, e.g., $p^a = p^a(z_t, t)$. Substituting (54) and (62) into (57) then shows that

$$\left(\frac{Dp^a}{dt} - \frac{1}{2} R_{bcd}{}^a S^{bc} \dot{z}_t^d \right) \xi_a + \frac{1}{2} \left(\frac{DS^{ab}}{dt} - 2p^{[a} \dot{z}_t^{b]} \right) \nabla_a \xi_b = \frac{d}{dt} P_t(\xi) \quad (63)$$

for all $\xi^a \in K$. Varying over all Killing vector fields recovers the individual evolution equations

$$\dot{p}^a = \frac{1}{2} R_{bcd}{}^a S^{bc} \dot{z}_t^d + F^a, \quad \dot{S}^{ab} = 2p^{[a} \dot{z}_t^{b]} + N^{ab}. \quad (64)$$

The force F^a and torque $N^{ab} = N^{[ab]}$ appearing here are determined by matching appropriate coefficients in dP_t/dt . Integral expressions follow from (42), (53), and (56):

$$F_a = - \int_{\mathfrak{B}_t} \rho H^{a'b} \sigma_{ab} \nabla_{a'} \hat{\phi} dV', \quad (65)$$

$$N_{ab} = -2 \int_{\mathfrak{B}_t} \rho H^{a'[a} \sigma^{b]} \nabla_{a'} \hat{\phi} dV'. \quad (66)$$

These expressions are exact. Their multipole expansions follow from (51):

$$F_a = - \sum_{n=0}^{\infty} \frac{1}{n!} m^{b_1 \dots b_n} \nabla_a \hat{\phi}_{, b_1 \dots b_n}, \quad (67)$$

$$N^{ab} = \sum_{n=0}^{\infty} \frac{2}{n!} g^{c[a} m^{b]d_1 \dots d_n} \hat{\phi}_{, cd_1 \dots d_n}. \quad (68)$$

Note that the velocity \dot{z}_t^a of the (arbitrarily-chosen) origin does not appear in F_a or N^{ab} . Those portions of (64) which do involve the velocity are spatial analogs of the Mathisson-Papapetrou terms typically used to describe the motion of spinning particles in general relativity. It is apparent here that similar terms arise even in non-relativistic theories. Their origin is essentially kinematic, being related to the decomposition of K into pure translations and pure rotations. It follows from (57) that $p_a(z_t, t)$ is associated with Killing vectors which appear translational at z_t in the sense that $\nabla_a \xi_b(z_t) = 0$. Similarly, $S_{ab}(z_t, t)$ is associated with Killing fields which are purely rotational in the sense that $\xi_a(z_t) = 0$. The Mathisson-Papapetrou terms arise in the laws of motion because, e.g., a Killing vector which is purely translational at z_t is not necessarily purely translational at a neighboring point z_{t+dt} . A given Killing field may have different proportions of “translation” and “rotation” at different points, and this inevitably mixes the evolution equations for p^a and S^{ab} . A simple version of this effect occurs even in flat space, where a pure rotation about one origin is not necessarily a pure rotation about another origin. This explains the $p^{[a} \dot{z}_t^{b]}$ term in (64) and the $-\dot{z}_t \times p$ term in (24).

Essentially the same explanation for the Mathisson-Papapetrou terms applies in general relativity. In that case, the spacetime may not admit any Killing vectors at all. Regardless, there still exists a ten-dimensional space of “generalized Killing fields” as described in Sect. 4.1. Given a particular event, these are naturally decomposed into a four-dimensional space of translations and a six-dimensional space of rotations and boosts. Whether or not a particular generalized Killing field is, e.g., purely translational varies from point to point just as it does for ordinary Killing fields. The evolution equations for relativistic momenta therefore acquire velocity-dependent terms which are closely analogous to those which appear in the generalized Newtonian theory discussed here.

Confining attention only to the generalized momentum whenever possible avoids the complications associated with the Mathisson-Papapetrou terms. It also simplifies the discussion of conservation laws. Recall that the presence of a particular spatial Killing field ψ^a which satisfies $\mathcal{L}_\psi \hat{\phi} = 0$ implies that $P_t(\psi)$ must be conserved. It follows from (57) that a particular linear combination of p_a and S_{ab} must be conserved as well:

$$p^a(z_t, t)\psi_a(z_t) + \frac{1}{2}S^{ab}(z_t, t)\nabla_a\psi_b(z_t) = (\text{constant}). \quad (69)$$

This constant is independent of z_t . Its existence implies that a particular combination of forces and torques must vanish. Specifically, comparison with (63) shows that

$$F^a\psi_a + \frac{1}{2}N^{ab}\nabla_a\psi_b = 0. \quad (70)$$

Although these results could be deduced directly from (64)–(66), they are considerably more clear from the perspective of the generalized momentum and its evolution equation (42).

2.2.7 Center of Mass

The laws of motion for p^a and S^{ab} have left z_t undetermined. One convenient choice is to set $z_t = \gamma_t$, where γ_t denotes the body's center of mass at time t .

This is straightforward when the background space is flat. It is then standard to define the center of mass to be the origin about which the mass dipole moment vanishes: $m^a(\gamma_t, t) = 0$. Enforcing this while differentiating (52) recovers the standard relation $p^a = m\dot{\gamma}_t^a$ between an object's velocity and its linear momentum. Using (64) and (67),

$$\ddot{\gamma}_t^a = -\nabla^a \hat{\phi}(\gamma_t, t) - \frac{1}{m} \sum_{n=2}^{\infty} \frac{1}{n!} m^{b_1 \cdots b_n}(\gamma_t, t) \nabla^a \nabla_{b_1} \cdots \nabla_{b_n} \hat{\phi}(\gamma_t, t). \quad (71)$$

This is equivalent to (27).

Similar results do not appear to hold when the background space is curved. It is still possible to demand that the dipole moment vanish [which, among other benefits, eliminates the $n = 1$ term in (67) and the $n = 0$ term in (68)]. The velocity of such a trajectory may be shown to satisfy

$$\dot{\gamma}_t^b \int_{\mathfrak{B}_t} \rho(x', t) \sigma^a_b(x', \gamma_t) dV' = - \int_{\mathfrak{B}_t} \rho(x', t) v^{a'}(x', t) \sigma^a_{a'}(x', \gamma_t) dV'. \quad (72)$$

The integral on the left-hand side of this equation can (typically) be inverted to yield an explicit expression for $\dot{\gamma}_t^a$. Unfortunately, the result does not depend on p^a in any simple way. Simplifications are possible when a body's dimensions are much smaller than the curvature scale. In these cases σ^a_b and $\sigma^a_{a'}$ can be expanded in Taylor series about γ_t , yielding the ordinary momentum-velocity relation at lowest order. More generally, this is problematic. Higher-order corrections require more information about the body than is required for the evolution equations of the momenta alone. Moments of a body's momentum distribution—its “current moments”—are required together with its mass moments.

It is only in this very last step where a celestial mechanics of “curved Newtonian gravity” appears to be problematic. Similar complications do not arise in relativistic systems. Among other differences, the presence of boost-type Killing fields (or their generalizations) provide additional constraints which imply well-behaved momentum-velocity relations.

2.2.8 Equations of Motion

Results such as (64) are properly described as laws of motion, not equations of motion [26, 27]. They are incomplete. Even if z_t is chosen as a body's center of mass, we still have not described how to compute $\hat{\phi}$ or the higher multipole moments.

The traditional approach is to introduce smallness assumptions. Consider, for simplicity, the n -body problem in flat space. If a particular body in such a system has characteristic size ℓ and mass m , its 2^n -pole moments must be smaller⁸ than approximately $m\ell^n$. Letting r denote a minimum distance between bodies and assuming that all masses are comparable, the n th term in (71) is at most of order $\frac{1}{n!}(m/r)^2(\ell/r)^n$. Considerable simplifications therefore result if $\ell \ll r$. At lowest order, only the monopole term is retained in the law of motion. Furthermore, each $\hat{\phi}$ may be computed in this approximation by assuming that all other masses are pure monopoles. This recovers the typical Newtonian n -body equations of motion. More details may be found in, e.g., [16, 17].

3 An Introduction to Relativistic Motion

Despite being considerably more abstract than the traditional presentation of Newtonian gravity, the formalism which has just been described is very powerful. It does not rely on any particular coordinate systems, and the majority of the discussion doesn't even require that the metric be flat. Indeed, most of the results well-known in ordinary Newtonian gravity continue to hold in generalizations of this theory which employ spherical or hyperboloidal geometries. It is also trivial to change the number of spatial dimensions, or even to amend the field equation in certain ways. It is physically more interesting, however, to consider motion in relativistic theories such as electromagnetism or general relativity.

This section describes how the formalism of Sect. 2.2 generalizes for objects coupled to relativistic fields. For simplicity, we consider the motion of an extended mass coupled to a scalar field ϕ which satisfies the Klein-Gordon equation

$$(\nabla^a \nabla_a - \mu^2)\phi = 4\pi\rho. \quad (73)$$

μ represents a (constant) field mass and ρ the body's charge density. Following the Newtonian problem as closely as possible, the four-dimensional background spacetime (\mathcal{M}, g_{ab}) is assumed to be maximally-symmetric. Understanding motion in more general curved spacetimes requires eliminating our reliance on a maximal set of Killing vector fields. This is indeed possible, but is somewhat technical. Its discussion is therefore delayed to Sect. 4. Motion in electromagnetic fields is discussed there as well.

Scalar charges in maximally-symmetric spacetimes provide a simple example with which to introduce the relativistic theory of motion. They differ from their Newtonian counterparts in only one important respect: Self-forces no longer vanish. Still,

⁸Large astrophysically-relevant objects like planets tend to be very nearly spherical due to the limited shear stresses which can be supported. The trace-free components of the moments, which are all that couple to the motion, are then much smaller than $m\ell^n$. These tend to be induced mainly by rotation and external tidal fields, and are typically modeled using Love numbers.

self-forces are “almost ignorable.” They effectively renormalize a body’s momentum, but do nothing else.⁹ This is a finite renormalization, meaning only that self-forces conspire to, e.g., make the mass computed by integrating over a body’s stress-energy tensor differ from the mass inferred by watching how that body accelerates in response to external fields.

Physically, renormalization arises because as a charge accelerates, its field must be accelerated as well. Although portions of that field may break away as radiation or otherwise change, there is a sense in which charges and their fields remain inseparably coupled. The energy contained in a body’s self-field implies that it must resist acceleration and contribute to that body’s inertia.

Now, self-forces vanish in Newtonian theory because of Newton’s third law. The self-field is sourced by a body’s instantaneous mass distribution and exerts forces on that same mass distribution. Interactions are no longer instantaneous, however, in theories which involve hyperbolic field equations. Fields are sourced by charge in a four-dimensional region of spacetime, but act only on configurations in three-dimensional hypersurfaces. It is impossible to maintain an exact concept of “action-reaction pairs” in this context. The imbalance which results turns out to exert forces and torques which precisely mimic changes to a body’s linear and angular momenta. This type of effect is generic for any coupling to long-range fields which satisfies hyperbolic field equations (or otherwise depends on a system’s history).

3.1 Relativistic Continuum Mechanics

The simplest relativistic modification of Newtonian gravity¹⁰ involves objects with scalar charge density ρ interacting via a field ϕ which satisfies the wave equation (73). Suppose that the body of interest resides inside a worldtube $\mathfrak{W} \subset \mathcal{M}$ containing no other matter. Also assume that \mathfrak{W} is spatially bounded in the sense that its spacelike slices have finite volume.

Our description for the motion of a compact object is based on its stress-energy tensor T_{body}^{ab} . This encodes many of a body’s mechanical properties, and is analogous to the (ρ, v^a, τ^{ab}) triplet used to analyze Newtonian objects in Sect. 2. Like those variables, the stress-energy satisfies differential equations which are independent of the specific type of material under consideration. Although these laws do not determine T_{body}^{ab} completely, they do provide significant constraints.

If ϕ vanishes everywhere and there are no other long-range fields, $\nabla_b T_{\text{body}}^{ab} = 0$. More generally, scalar fields contribute to a system’s total stress-energy. It is only

⁹The notion of self-force used here is consistent with the usual Newtonian definition, but is unconventional in relativistic contexts. Its precise meaning is made clear below.

¹⁰This is to be considered as a model problem. If interpreted as a theory of gravity, the type of scalar field theory described here is not compatible with observations. Of course, it is not necessary to interpret ϕ as a gravitational potential (so ρ needn’t be a “mass density” in any sense).

this total $T_{\text{tot}}^{ab} = T_{\text{tot}}^{(ab)}$ which is necessarily¹¹ conserved:

$$\nabla_b T_{\text{tot}}^{ab} = 0. \quad (74)$$

Consider splitting this total into “body” and “field” components:

$$T_{\text{tot}}^{ab} = T_{\text{field}}^{ab} + T_{\text{body}}^{ab}. \quad (75)$$

Away from any matter, it is clear that $T_{\text{body}}^{ab} = 0$ and

$$T_{\text{field}}^{ab} = \frac{1}{4\pi} \left[\nabla^a \phi \nabla^b \phi - \frac{1}{2} g^{ab} (\nabla_c \phi \nabla^c \phi + \mu^2 \phi^2) \right]. \quad (76)$$

Elsewhere, local interactions between the matter and the field make it physically difficult to motivate any particular split.

One possible way forward is to work only with T_{tot}^{ab} . Unfortunately, the momentum obtained from this stress-energy tensor might be very different if computed first in a slice of \mathfrak{M} , and then in a slightly larger hypersurface. There is no natural boundary where integrations can be stopped. Although momentum integrals might settle down when performed over very large volumes, it is unclear how useful this is. The relevant distance scale could be so large that the only “total momenta” which are useful encompass the entire (modeled) universe, precluding any ability to learn about the dynamics of individual masses. Results based on T_{tot}^{ab} alone can be useful in certain approximations involving the motion of very small bodies [28], but this is insufficiently general for our purposes.

The approach adopted here is mathematically the simplest. Let T_{field}^{ab} be given by (76) throughout \mathfrak{M} . The remaining stress-energy tensor is then defined to be the body’s: $T_{\text{body}}^{ab} = T_{\text{body}}^{(ab)} := T_{\text{tot}}^{ab} - T_{\text{field}}^{ab}$. Equations (73)–(76) imply that this satisfies

$$\nabla_b T_{\text{body}}^{ab} = -\rho \nabla^a \phi, \quad (77)$$

which generalizes the Newtonian conservation laws (28) and (29).

3.2 Generalized Momentum

Recall the generalized momentum (35) defined for Newtonian mass distributions. This requires very little modification for use in relativistic systems. The one complication which does arise is that there is no longer any preferred notion of time. A time parameter must be supplied as an additional ingredient, which is accomplished

¹¹In a Lagrangian formalism, the total stress-energy tensor considered here is derived from a functional derivative of the action with respect to the metric. It is conserved whenever the action is diffeomorphism-invariant [15].

by foliating \mathcal{W} with a 1-parameter family of hypersurfaces $\{\mathfrak{B}_s\}$. Each \mathfrak{B}_s may be viewed as the body region at time s , and is assumed to have finite volume. The precise nature of the body regions may be considered arbitrary for now. They can be spacelike or even null.¹²

Supposing that a particular foliation has been fixed, the generalized momentum contained in any three-dimensional region $\mathfrak{R} \subseteq \mathfrak{B}_s$ is most obviously defined as

$$P_s[\mathfrak{R}](\xi) = \int_{\mathfrak{R}} T_{\text{body}}^{ab} \xi_a dS_b, \quad (78)$$

where ξ^a is any Killing vector field. $P_s[\mathfrak{R}](\cdot)$ defines a linear map on the space of K of Killing vector fields. It is therefore a vector in the dual space K^* . For the maximally-symmetric four-dimensional spacetimes considered here, $\dim K = \dim K^* = 10$. Given a particular event, four of these dimensions correspond to translations and six to rotations and boosts. As in the Newtonian case, such decompositions allow the generalized momentum to be expressed in a basis which recovers linear and angular momenta associated with a preferred event. The details of this correspondence are described more precisely in Sect. 3.7.

3.3 Generalized Force

Forces and torques are determined by s -derivatives of the generalized momentum. Considering only the momenta in \mathfrak{B}_s , it is convenient to simplify the notation by defining $P_s = P_s[\mathfrak{B}_s]$. Using (77) together with Killing's equation then shows that

$$\frac{d}{ds} P_s(\xi) = - \int_{\mathfrak{B}_s} \rho \mathcal{L}_\xi \phi dS \quad (79)$$

for all $\xi^a \in K$, where $dS := t^a dS_a$ and t^a denotes a time evolution vector field for the foliation $\{\mathfrak{B}_s\}$. The relativistic generalized force (79) is essentially identical to its Newtonian analog (36). As in that context, the force can be immediately put into a practical form only if the object of interest does not significantly contribute to ϕ . More generally, the self-field introduces considerable complications. Progress is made by finding a precise definition for the self-field, computing its effects analytically, and then subtracting it out. The “effective field” which remains after this process is typically much simpler to analyze than the physical one.

¹²Consider, e.g., the past-directed light cones associated with a timelike worldline.

3.4 The Self-field

At least in part, the Newtonian self-field (19) can be generalized essentially as-is. Let the relativistic self-field ϕ_S be obtained by convolving an object's charge density with a particular two-point¹³ scalar G . This must be a Green function, so

$$(\nabla^a \nabla_a - \mu^2)G(x, x') = 4\pi\delta(x, x'). \quad (80)$$

Still more constraints are necessary to fix G uniquely. One of these follows from requiring that the self-field¹⁴ depend only quasi-locally on a body's "instantaneous" configuration. It should not, for example, involve distantly-imposed boundary conditions, the behavior of other objects, or a body's history in the distant past. Such conditions can be ensured by demanding that $G(x, x') = 0$ whenever x and x' are timelike-separated. Lastly, suppose that $G(x, x') = G(x', x)$. Such objects exist (at least in finite regions), are unique, and are referred to as S-type or "singular" Detweiler-Whiting Green functions [10, 29]. In the maximally-symmetric backgrounds considered here, G satisfies $\mathcal{L}_\xi G = 0$ for all $\xi^a \in K$. It implies a relativistic form of Newton's third law. For massless fields in Minkowski spacetime, $G = \frac{1}{2}(G_+ + G_-)$ where G_\pm are the advanced and retarded Green functions. More generally,

$$G = \frac{1}{2}(G_+ + G_- - V) \quad (81)$$

for a certain symmetric biscalar $V(x, x')$ which satisfies the homogeneous field equation. G can also be expressed in terms of Synge's function σ . Using Δ to denote the van Vleck determinant [10] (which depends on second derivatives of σ), δ the Dirac distribution, and Θ the Heaviside distribution,

$$G = \frac{1}{2}[\Delta^{1/2}\delta(\sigma) - V\Theta(\sigma)]. \quad (82)$$

This shows that $G(x, \cdot)$ can have support on and outside the light cones of x .

The self-field "due to" charge contained in a given spacetime volume $\mathfrak{R} \subseteq \mathfrak{W}$ can now be expressed in terms of the S-type Detweiler-Whiting Green function:

$$\phi_S[\mathfrak{R}](x) = \int_{\mathfrak{R}} G(x, x')\rho(x')dV'. \quad (83)$$

If the argument \mathfrak{R} is omitted, the integral is understood to be carried out over an object's entire worldtube \mathfrak{W} .

¹³It is also possible to introduce $(n+1)$ -point self-fields similar to (44). This is not considered any further here.

¹⁴The term self-field is used in several different ways in the literature. The definition adopted here is uncommon, and is sometimes described as the "Coulomb-like" component of the self-field.

We now compute the self-force. It is simpler not to consider this directly, but rather its integral over a finite interval of time. Letting $s_f > s_i$, it is clear from (79) that

$$P_{s_f}(\xi) - P_{s_i}(\xi) = \int_{s_i}^{s_f} \frac{d}{ds} P_s(\xi) ds = - \int_{\mathcal{I}} \rho \mathcal{L}_\xi \phi dV \quad (84)$$

for any $\xi^a \in K$. The 4-volume $\mathcal{I} = \mathcal{I}(s_i, s_f) \subset \mathcal{W}$ which appears here represents that part of an object's worldtube which lies in between the initial and final hypersurfaces $\mathfrak{B}_{s_i}, \mathfrak{B}_{s_f}$. See Fig. 1. Substitution of the self-field definition (83) into (84) shows that the total change in momentum due to ϕ_S alone is

$$\int_{\mathcal{I}} dV \int_{\mathcal{W}} dV' f(x, x'), \quad (85)$$

where

$$f(x, x') = -\rho(x)\rho(x')\xi^a(x)\nabla_a G(x, x') \quad (86)$$

may be interpreted as the density of generalized force exerted at x by x' . Independently of any specific form for f , double integrals with the form (85) can be rewritten as

$$\frac{1}{2} \int_{\mathcal{I}} dV \left(\int_{\mathcal{W}} dV' [f(x, x') + f(x', x)] + \int_{\mathcal{W} \setminus \mathcal{I}} dV' [f(x, x') - f(x', x)] \right) \quad (87)$$

whenever the relevant integrals commute. This identity is very general, and is central to understanding motion in every relativistic theory we discuss. It is therefore worthwhile to examine it in detail.

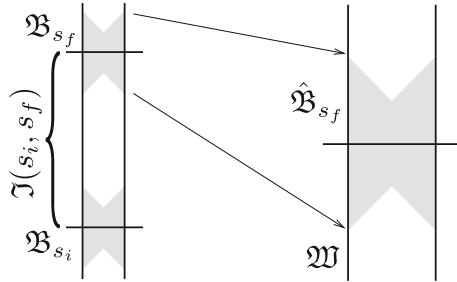


Fig. 1 Schematic illustrations of a body's worldtube \mathcal{W} together with hypersurfaces \mathfrak{B}_{s_i} and \mathfrak{B}_{s_f} (drawn spacelike). The region $\mathcal{I}(s_i, s_f) \subset \mathcal{W}$ bounded by these hypersurfaces and appearing in (84) is indicated. The shaded 4-volumes $\hat{\mathfrak{B}}_{s_i}$ and $\hat{\mathfrak{B}}_{s_f}$ [see (97)] denote the domains of dependence associated with the self-momenta E_{s_i} and E_{s_f} defined by (90). Although $P_{s_f}(\xi) - P_{s_i}(\xi)$ depends on $\rho \mathcal{L}_\xi \hat{\phi}$ throughout $\mathcal{I}(s_i, s_f)$, it depends on more complicated aspects of a body's internal structure only in the shaded regions. These contributions are always confined to within approximately one light-crossing time of the bounding hypersurfaces, and are therefore “quasi-local”

The first term in (87) can be interpreted as an average of “action-reaction pairs” in the sense of Newton’s third law. It is very similar to the types of identities used to simplify the motion of objects coupled to elliptic fields in Sect. 2. Recalling that discussion, the reciprocity relation $G(x, x') = G(x', x)$ implies that

$$\int_{\mathcal{I}} dV \int_{\mathfrak{M}} dV' [f(x, x') + f(x', x)] = - \int_{\mathcal{I}} dV \int_{\mathfrak{M}} dV' \rho(x) \rho(x') \mathcal{L}_\xi G(x, x'). \quad (88)$$

As in the Newtonian theory, Lie derivatives of G are associated here with sums over action-reaction pairs. As in that case, these sums vanish. All of the self-force is therefore determined by the second group of terms in (87). These do not vanish in general. They are intrinsically connected to the finite speed of propagation associated with the wave equation, and are responsible for renormalizing a body’s momentum.

3.5 Renormalization

The generalized force exerted by ϕ_S is entirely determined by the final part of (87). To understand this, first let \mathfrak{B}_s^+ (resp. \mathfrak{B}_s^-) denote the four-dimensional future (past) of \mathfrak{B}_s inside the body’s worldtube:

$$\mathfrak{B}_s^\pm(s) := \bigcup_{\pm(\tau-s)>0} \mathfrak{B}_\tau. \quad (89)$$

Also define

$$E_s(\xi) := \frac{1}{2} \left(\int_{\mathfrak{B}_s^+} \rho \mathcal{L}_\xi \phi_S [\mathfrak{B}_s^-] dV - \int_{\mathfrak{B}_s^-} \rho \mathcal{L}_\xi \phi_S [\mathfrak{B}_s^+] dV \right). \quad (90)$$

Like P_s , this represents an s -dependent vector in K^* . Using it, the second term in the expansion (87) for the self-force is simply

$$\frac{1}{2} \int_{\mathcal{I}} dV \int_{\mathfrak{M} \setminus \mathcal{I}} dV' [f(x, x') - f(x', x)] = -[E_{s_f}(\xi) - E_{s_i}(\xi)]. \quad (91)$$

Taking the limit $s_f \rightarrow s_i$ while combining (84), (87), (88), and (91) finally shows that the generalized force can be written as

$$\frac{d}{ds} P_s(\xi) = - \int_{\mathfrak{B}_s} \rho \mathcal{L}_\xi \hat{\phi} dS - \frac{d}{ds} E_s(\xi). \quad (92)$$

Replacing the physical field ϕ with $\hat{\phi} = \phi - \phi_S$ can therefore be accomplished only at the cost of the counterterm $-dE_s/ds$. That this is a total derivative suggests the introduction of an “effective generalized momentum” \hat{P}_s satisfying

$$\hat{P}_s := P_s + E_s. \quad (93)$$

For any finite scalar charge in a maximally-symmetric spacetime,

$$\frac{d}{ds} \hat{P}_s(\xi) = - \int_{\mathfrak{B}_s} \rho \mathcal{L}_\xi \hat{\phi} dS. \quad (94)$$

There is a sense in which E_s renormalizes the (bare) momentum P_s . The sum of P_s and E_s behaves instantaneously as though it were the momentum of a test charge placed in the effective field $\hat{\phi}$. Furthermore,

$$(\nabla^a \nabla_a - \mu^2) \hat{\phi} = 0. \quad (95)$$

Physically, it is not sufficient to motivate the renormalization $P_s \rightarrow \hat{P}_s$ merely by fact that the self-force is a total derivative. Essentially *any* function of one variable can be written as the total derivative of its integral. Indeed, one might introduce a constant s_0 and define

$$\tilde{P}_s(\xi) := P_s(\xi) + E_s(\xi) + \int_{s_0}^s d\tau \int_{\mathfrak{B}_\tau} dS \rho \mathcal{L}_\xi \hat{\phi}. \quad (96)$$

This does not vary at all with s . While it may be useful for some purposes, \tilde{P}_s is not a physically acceptable momentum. This is because it depends in an essential way on the configuration of the system for all times between s_0 and s . While \tilde{P}_s would be approximately local for $s \approx s_0$, it otherwise depends on a system's history in a complicated way.

The renormalized momentum \hat{P}_s defined by (93) does not share this deficiency. Like P_s , it depends only on the body's configuration in regions “near” \mathfrak{B}_s . The relevant region is, however, somewhat larger for \hat{P}_s than it is for P_s . Definitions (83) and (90) imply that $E_s(\xi)$ depends on a neighborhood $\hat{\mathfrak{B}}_s \supset \mathfrak{B}_s$ defined to be the set of all points in \mathfrak{W} which are null- or spacelike-separated to at least one point in \mathfrak{B}_s . In terms of Synge's function,

$$\hat{\mathfrak{B}}_s = \{x \in \mathfrak{W} \mid \sigma(x, y) \geq 0 \text{ for some } y \in \mathfrak{B}_s\}. \quad (97)$$

$\hat{\mathfrak{B}}_s$ is a (finite) four-dimensional region of spacetime. It extends into the past and future of \mathfrak{B}_s by roughly the body's light-crossing time. See Fig. 1.

One might have guessed that a self-momentum at time s could be defined by integrating the stress-energy tensor associated with¹⁵ ϕ_S over a large hypersurface which contains \mathfrak{B}_s . Unfortunately, such integrals depend on gradients of ϕ_S far outside of \mathfrak{B}_s . These, in turn, depend on the body's state in the distant past and future. Such a definition is physically unacceptable in general. Nevertheless, it does

¹⁵Recalling (76), T_{field}^{ab} is quadratic in ϕ . The stress-energy tensor “associated with ϕ_S ” is taken to mean that portion of T_{field}^{ab} which is quadratic in ϕ_S . Terms linear in ϕ_S are not included.

make sense in the stationary limit, and may be shown to coincide with E_s in that case [2]. In more dynamical cases, the E_s defined here appears to be the only well-motivated possibility.

3.6 Multipole Expansions

Forces and torques exerted on relativistic scalar charges may be expanded exactly as in the Newtonian theory. Assuming that $\hat{\phi}$ can be accurately approximated using a Taylor series about some origin $z_s \in \mathfrak{B}_s$, the techniques of Sect. 2.2.5 may be used to show that (94) admits the multipole expansion

$$\frac{d}{ds} \hat{P}_s(\xi) = - \sum_{n=0}^{\infty} \frac{1}{n!} q^{a_1 \cdots a_n}(z_s, s) \mathcal{L}_{\xi} \hat{\phi}_{,a_1 \cdots a_n}(z_s). \quad (98)$$

The 2^n -pole moment of ρ which appears here is defined by

$$q^{a_1 \cdots a_n}(s) := (-1)^n \int_{\mathfrak{B}_s} \sigma^{a_1}(x, z_s) \cdots \sigma^{a_n}(x, z_s) \rho(x) dS, \quad (99)$$

and $\hat{\phi}_{,a_1 \cdots a_n}$ denotes the n th tensor extension of $\hat{\phi}$. Equation (98) may be compared with the Newtonian generalized force (51). Unlike its Newtonian counterpart, however, the relativistic scalar monopole moment q may depend on time; the total charge is not necessarily conserved. Also note that the relativistic multipole expansion is intended only to be asymptotic. It may require truncation at large n (see, e.g., [30]).

3.7 Linear and Angular Momenta

Like P_s , the effective generalized momentum \hat{P}_s is an element of K^* . Expanding this in an appropriate basis recovers objects which may be interpreted as a body's linear and angular momenta. The appropriate arguments are almost identical to those described in Sect. 2.2.6.

Choosing a point $z_s \in \mathfrak{B}_s$, every Killing field may be written as a linear combination of 1- and 2-forms at z_s [cf. (53)]. $P_s(\xi)$ and $\hat{P}_s(\xi)$ are clearly linear in ξ^a , so they too may be expanded in linear combinations of 1- and 2-forms at z_s . Recalling (57), the coefficients in this combination may be identified as a body's linear and angular momentum:

$$\hat{P}_s(\xi) = \hat{p}^a(z_s, s) \xi_a(z_s) + \frac{1}{2} \hat{S}^{ab}(z_s, s) \nabla_a \xi_b(z_s). \quad (100)$$

Hats have been placed on \hat{p}^a and \hat{S}^{ab} to emphasize that these are renormalized momenta. Bare quantities defined in terms of P_s may be introduced as well and shown to coincide with the momenta introduced by Dixon [6, 17, 24] for objects without electromagnetic charge-currents. The bare momenta obey more complicated laws of motion, and are not considered any further.

Differentiating (100) while using (61) leads to an implicit evolution equation for \hat{p}^a and \hat{S}^{ab} :

$$\left(\frac{D\hat{p}^a}{ds} - \frac{1}{2}R_{bcd}{}^a\hat{S}^{bc}z_s^d\right)\xi_a + \frac{1}{2}\left(\frac{D\hat{S}^{ab}}{ds} - 2\hat{p}^{[a}z_s^{b]}\right)\nabla_a\xi_b = \frac{d}{ds}\hat{P}_s(\xi). \quad (101)$$

Varying over all ξ_a and all $\nabla_a\xi_b = \nabla_{[a}\xi_{b]}$ recovers the explicit equations

$$\frac{D\hat{p}^a}{ds} = \frac{1}{2}R_{bcd}{}^a\hat{S}^{bc}z_s^d + \hat{F}^a, \quad \frac{D\hat{S}^{ab}}{ds} = 2\hat{p}^{[a}z_s^{b]} + \hat{N}^{ab}. \quad (102)$$

The force \hat{F}^a and torque $\hat{N}^{ab} = \hat{N}^{[ab]}$ appearing here may be found in integral form by comparing (94) and (101). Using the multipole expansion (98) instead,

$$\hat{F}_a = -\sum_{n=0}^{\infty} \frac{1}{n!} q^{b_1 \dots b_n} \nabla_a \hat{\phi}_{,b_1 \dots b_n}, \quad (103)$$

$$\hat{N}^{ab} = \sum_{n=0}^{\infty} \frac{2}{n!} g^{c[a} q^{b]d_1 \dots d_n} \hat{\phi}_{,cd_1 \dots d_n}. \quad (104)$$

The laws of motion (102)–(104) describe bulk features of essentially arbitrary self-interacting scalar charge distributions in maximally-symmetric backgrounds. As in the Newtonian case, all explicit dependence on z_s^a is contained in the Mathisson-Papapetrou terms. These terms are kinematic, and may again be traced to the changing character of Killing fields evaluated at different points.

All conservation laws discussed in the Newtonian context generalize immediately. If $\mathcal{L}_{\psi}\hat{\phi} = 0$ for some particular Killing field ψ^a ,

$$\hat{P}_s(\psi) = \hat{p}^a\psi_a + \frac{1}{2}\hat{S}^{ab}\nabla_a\psi_b = (\text{constant}). \quad (105)$$

Similarly,

$$\hat{F}^a\psi_a + \frac{1}{2}\hat{N}^{ab}\nabla_a\psi_b = 0. \quad (106)$$

These results are exact. They hold independently of any choices made for z_s . They also apply to approximate momenta evolved via any consistent truncation of the multipole series.

Although the relativistic multipole expansions are structurally almost identical to their Newtonian counterparts, it is important to emphasize that the effective field is far more difficult to compute in relativistic contexts. In Newtonian gravity, $\hat{\phi}$ is simply the external potential and is easily computed given the instantaneous external mass distribution of the universe. The relativistic effective potential can, however, depend in complicated ways on boundary conditions, initial data, and past history. Using retarded boundary conditions, the relativistic $\hat{\phi}$ typically depends on ρ , and is therefore not interpretable as a purely external field.

Another property of the relativistic theory is that the angular momentum has six independent components rather than three. Consider a unit timelike vector u^a at z_s . This acts like a local frame which may be used to decompose \hat{S}^{ab} into two components. Given u^a , there exist \hat{S}^a and \hat{m}^a which satisfy

$$\hat{S}_{ab} = \epsilon_{abcd}u^c\hat{S}^d - 2u_{[a}\hat{m}_{b]} \quad (107)$$

and $u_a\hat{S}^a = u_a\hat{m}^a = 0$. Writing out \hat{S}^{ab} explicitly in flat spacetime in the limit of negligible self-interaction suggests that \hat{S}^a represents a body's "ordinary" angular momentum about z_s . Similarly, \hat{m}^a may be interpreted as the dipole moment of a body's energy distribution. Relativistically, these are two aspects of the same physical structure. The split $\hat{S}^{ab} \rightarrow (\hat{S}^a, \hat{m}^a)$ is closely analogous to the decomposition $F_{ab} \rightarrow (E_a, B_a)$ of an electromagnetic field into its electric and magnetic components.

3.8 Center of Mass

Thus far, the foliation $\{\mathfrak{B}_s\}$ of \mathfrak{W} used to define the generalized momentum has been left unspecified. The collection of events $\{z_s\}$ used to perform the multipole expansion (98) has been arbitrary as well. This constitutes a considerable amount of freedom.

One simplifying strategy is to first associate a hypersurface with each possible point in \mathfrak{W} . This could be accomplished by, e.g., defining \mathfrak{B}_s to be the past- (or future-) null cone with vertex z_s . A timelike worldline parametrized by $\{z_s\}$ then results in a null foliation of \mathfrak{W} . Alternatively, a spacelike foliation may be chosen as described in [17, 24, 31].

Regardless, defining each \mathfrak{B}_s in terms of z_s reduces all freedom in the law of motion to the choice of a single worldline (and its parametrization). Recall that in Newtonian gravity, a body's center of mass is the location about which its mass dipole moment vanishes. Relativistically, the dipole moment of a body's stress-energy tensor is proportional to $\hat{S}^{ab}(z_s, s)$. In general, there is no choice of z_s which can be used to make this vanish entirely. It is, however, possible to use translations to set $\hat{m}^a = 0$ as defined in (107). This requires the introduction of a frame with which to choose an appropriate dipole moment. Consider the zero-momentum frame u^a where

$$\hat{p}^a = \hat{m} u^a. \quad (108)$$

u^a is defined to be a unit vector, so the rest mass \hat{m} must satisfy

$$\hat{m} := \sqrt{-\hat{p}^a \hat{p}_a}. \quad (109)$$

A center of mass γ_s may now be defined by demanding that

$$\hat{S}^{ab}(\gamma_s, s) \hat{p}_a(\gamma_s, s) = 0. \quad (110)$$

This can be interpreted as requiring that the dipole moment of a body's energy distribution vanish as seen by a zero-momentum observer at γ_s . It is a highly implicit definition. Good existence and uniqueness results are known for the closely-related Dixon momenta [32, 33], but not more generally. We nevertheless assume that a unique worldline (and associated foliation) can be found in this way. Other choices are also possible, however.

A general relation between the center of mass 4-velocity and the linear momentum may be found by differentiating (110). The result of this differentiation is solved explicitly for $\dot{\gamma}_s^a$ in [17, 31], resulting in¹⁶

$$\hat{m} \dot{\gamma}_s^a = \hat{p}^a - \hat{N}^a{}_b u^b - \frac{\hat{S}^{ab} \left[\hat{m} \hat{F}_b - \frac{1}{2} (\hat{p}^c - \hat{N}^c{}_h u^h) \hat{S}^{df} R_{bcdf} \right]}{\hat{m}^2 + \frac{1}{4} \hat{S}^{pq} \hat{S}^{rs} R_{pqrs}}. \quad (111)$$

This assumes that the parameter s has been chosen such that $\dot{\gamma}_s^a \hat{p}_a = -\hat{m}$, and also that all instances of z_s have been replaced with γ_s . In principle, it is possible for the denominator $\hat{m}^2 + \frac{1}{4} \hat{S}^{pq} \hat{S}^{rs} R_{pqrs}$ here to vanish, indicating a breakdown of the center of mass condition. This can occur only if the curvature scale is comparable to a body's own size, in which case it is unlikely that any simple description of an extended body in terms of its center of mass is likely to be useful. In more typical cases, it is straightforward to obtain multipole approximations of (111) by substituting appropriately-truncated versions of (103) and (104).

Also note that $\dot{\gamma}_s^a$ is not necessarily collinear with \hat{p}^a . The difference $\hat{p}^a - \hat{m} \dot{\gamma}_s^a$ may be interpreted as a “hidden mechanical momentum.” Simple examples of hidden momentum are commonly discussed in electromagnetic problems (see, e.g., [8, 34, 35]), but occur much more generally. Some consequences of the hidden momentum are discussed in [36, 37].

The center of mass condition provides more than just a relation between the momentum and the velocity. It also implies that $\hat{S}^{ab}(\gamma_s, s)$ can be written entirely in terms of the spin vector $\hat{S}^a(\gamma_s, s)$. Inverting (107) while using (110),

¹⁶References [17, 31] derive the momentum-velocity relation using Dixon's momenta without a scalar field, but in a spacetime which is not maximally-symmetric. Here, Dixon's momenta are modified by E_s , there is a scalar field, and the spacetime is maximally-symmetric. Despite these differences, the relevant tensor manipulations are identical.

$$\hat{S}_a(\gamma_s, s) = -\frac{1}{2}\epsilon_{abcd}u^b\hat{S}^{cd}. \quad (112)$$

Differentiating this and applying (102), the spin vector evaluated about the center of mass is seen to satisfy

$$\frac{D\hat{S}_a}{ds} = -\frac{1}{2}\epsilon_{abcd}u^b\hat{N}^{cd} + u_a\left(\hat{S}_b\frac{Du^b}{ds}\right). \quad (113)$$

The first term here represents a torque in the ordinary sense. The second term is responsible for the Thomas precession, and may be made more explicit by substituting (102) and (108).

An evolution equation may also be derived for the mass \hat{m} , which is not necessarily constant. Variations in \hat{m} are not an exotic effect; masses change even for monopole test bodies coupled to relativistic scalar fields. In general, use of (102) and (109) shows that the mass evaluated using $z_s = \gamma_s$ satisfies [24]

$$\frac{d\hat{m}}{ds} = -\dot{\gamma}_s^a\hat{F}_a + \hat{N}_{ab}u^a\frac{Du^b}{ds}. \quad (114)$$

The final term here may be made more explicit by using (102) and (108) to eliminate Du^b/ds .

3.9 Monopole Approximation

The equations derived here are quite complicated in general. Some intuition for them may be gained by truncating the multipole series at monopole order. Inspection of (103) and (104) then shows that

$$\hat{F}_a = -q\nabla_a\hat{\phi}, \quad \hat{N}_{ab} = 0. \quad (115)$$

Further restricting to cases where $q = (\text{constant})$, it follows from (114) that

$$\hat{m} - q\hat{\phi} = (\text{constant}). \quad (116)$$

$\hat{m} - q\hat{\phi}$ may therefore be viewed as a conserved energy for the system. Note that it is the effective field $\hat{\phi}$ which occurs here, not the physical field ϕ .

Contracting (113) with \hat{S}^a also shows that $\hat{S}^2 := \hat{S}^a\hat{S}_a = (\text{constant})$, meaning that the spin vector can only precess in the monopole approximation. The rate at which this occurs may be simplified by first recalling that in any maximally-symmetric spacetime, there exists a constant κ such that

$$R_{abcd} = \kappa g_{a[c}g_{d]b}. \quad (117)$$

Of course, $\kappa = 0$ in the flat background of special relativity. Regardless, the spin evolution is independent of κ :

$$\frac{D\hat{S}_a}{ds} = -(q/\hat{m})u_a\hat{S}^b\nabla_b\hat{\phi}. \quad (118)$$

It experiences a purely Thomas-like precession. The momentum-velocity relation (111) does, by contrast, retain explicit evidence of the curvature, reducing to

$$\hat{m}\dot{\gamma}_s^a = \hat{p}^a + \left(\frac{q/\hat{m}}{1 + \frac{1}{2}\kappa(\hat{S}/\hat{m})^2} \right) \epsilon^{abcd}u_b\hat{S}_c\nabla_d\hat{\phi}. \quad (119)$$

The linear momentum is also affected by κ :

$$\frac{D\hat{p}_a}{ds} = -q\nabla_a\hat{\phi} + q\left(\frac{\frac{1}{2}\kappa(\hat{S}/\hat{m})^2}{1 + \frac{1}{2}\kappa(\hat{S}/\hat{m})^2} \right) \left(\delta_a^b + u_a u^b - \hat{S}_a\hat{S}^b/\hat{S}^2 \right) \nabla_b\hat{\phi}. \quad (120)$$

The overall force is therefore a particular linear transformation of $-q\nabla_a\hat{\phi}$. Up to an overall factor, the second term here extracts that component of $q\nabla_a\hat{\phi}$ which is orthogonal to both \hat{p}^a and \hat{S}^a .

Together, (116) and (118)–(120) determine the evolution of a scalar charge in the monopole approximation. Despite the approximations which have already been made, these equations remain rather formidable. They may be simplified further by demanding that $\hat{S} = 0$ at some initial time. The monopole approximation implies that an initially non-spinning particle remains non-spinning, so it is consistent to set $\hat{S} = 0$ for all time. It also follows that $\hat{p}^a = \hat{m}\dot{\gamma}_s^a$ and

$$\ddot{\gamma}_s^a = -(q/\hat{m})(g^{ab} + \dot{\gamma}_s^a\dot{\gamma}_s^b)\nabla_b\hat{\phi}. \quad (121)$$

In the test body limit where $\hat{\phi} \approx \phi$, this is the typical equation adopted for the motion of a point particle with scalar charge q . A point particle limit of this equation which still allows for self-interaction is equivalent to what is known as the Detweiler-Whiting regularization [10, 29]. This regularization—which originally arose via heuristic arguments associated with the singularity structure of point particle fields—is a special case of the much more general results derived here (and which first appeared in [2]). Its origin is unrelated to any point particle limits or to the singularities associated with them.

It is shown in Sect. 4.2 that standard self-force results follow easily from (121). That section also generalizes all laws of motion derived here to apply to scalar charges moving in arbitrarily-curved spacetimes.

4 Motion in Curved Spacetimes

The discussion up to this point has made extensive use of Killing vector fields. This is familiar and simple, but not necessary. The first step towards understanding motion in generic spacetimes is to find a suitable replacement for the space of Killing vector fields. Once this is accomplished, the problem of motion for extended charges coupled to scalar fields is considered once again. This example is used to illustrate a new type of renormalization which occurs in spacetimes without symmetries. The techniques used to solve the scalar problem are then adapted to discuss motion in electromagnetic fields. Lastly, we consider motion in general relativity, where the objects of interest dynamically modify the geometry itself.

4.1 Generalized Killing Fields

Recalling (35) or its relativistic analog (78), the generalized momenta used in maximally-symmetric spacetimes are defined as linear operators over the space K of Killing vector fields. There is, however, no obstacle to replacing K by some other vector space K_G . This is the approach we take to defining momenta in generic spacetimes. Although several notions of generalized or approximate Killing fields exist in the literature [38–40], only one of these [1] appears to be suitable for our purposes. We describe it now.

The space of generalized Killing fields used here can be motivated axiomatically. First note that avoiding significant modifications to the formalism developed thus far requires that all elements of K_G be vector fields on spacetime (or space in non-relativistic problems). It is also reasonable to require that:

1. All genuine Killing vectors which might exist are also generalized Killing vectors:
 $K \subseteq K_G$.
2. $K = K_G$ in maximally-symmetric spacetimes.
3. The dimensionality of K_G can depend only on the number of spacetime dimensions.

The first of these conditions is clearly necessary for any K_G which may be said to generalize K . The second condition ensures that there are not “too many” generalized Killing fields in simple cases. The final condition is more subtle. It guarantees that the generalized momentum contains the “same amount” of information regardless of the metric. More specifically, a generalized momentum defined using K_G must be decomposable in terms of linear and angular momenta with the correct number of components. Recalling (34),

$$\dim K_G = \frac{1}{2}N(N+1) \geq \dim K \quad (122)$$

in any N -dimensional space.

The given conditions restrict K_G , but do not define it. An additional constraint is needed which describes how those elements of K_G which are not also elements of K preserve an appropriate geometric structure. It is not, of course, possible to demand that they preserve the metric. Symmetries of the connection or curvature are unsuitable as well. The only reasonable possibilities are nonlocal.

4.1.1 Symmetries About a Point

First consider the Riemannian case.¹⁷ Recalling (50), any Killing vector field used to drag two points x and x' preserves the separation vector $-\sigma^a(x, x')$ between those points. A slightly weaker condition can be used to define generalized Killing vectors even when no genuine Killing vectors exist. Suppose that a particular point x has been fixed and demand that $A_G(x)$ be defined as the set of all vector fields ξ^a satisfying

$$\mathcal{L}_\xi \sigma^a(x', x) = 0. \quad (123)$$

The result clearly forms a vector space. Unfortunately $A_G(x)$ is too large. In flat space, it becomes independent of x and coincides with the space of affine collineations: vector fields satisfying $\nabla_a \mathcal{L}_\xi g_{bc} = 0$. Geometrically, affine collineations represent symmetries which preserve the connection. In generic spaces, $A_G(x)$ may be described as a space of generalized affine collineations with respect to x .

The space of Killing vector fields is known to be a vector subspace of the affine collineations. Similarly, generalized Killing fields $K_G(x)$ may be obtained as an appropriate subspace of $A_G(x)$. It is sufficient to demand only that the appropriate vector fields be exactly Killing at x :

$$\mathcal{L}_\xi g_{ab}(x) = 0. \quad (124)$$

The set of all vector fields satisfying this and (123) are denoted by $K_G(x)$. They are the generalized Killing fields with respect to x . Any genuine Killing fields which may exist are also elements of $K_G(x)$.

Many geometric structures are preserved by generalized Killing fields. Equation (124) can be shown to generalize to

$$\mathcal{L}_\xi g_{ab}(x) = \nabla_a \mathcal{L}_\xi g_{bc}(x) = 0, \quad (125)$$

¹⁷The same geometric conditions can also be imposed in Lorentzian geometries. Physically, however, the vector fields discussed here are most useful in non-relativistic contexts. A more complicated structure described in Sect. 4.1.2 is better-suited to Lorentzian physics.

which holds only at the special point x . More generally, “projected Killing equations” are valid wherever the generalized Killing fields are defined [1]:

$$\sigma^{a'}(x, x') \mathcal{L}_\xi g_{a'b'}(x') = \sigma^{a'}(x, x') \sigma^{b'}(x, x') \nabla_{a'} \mathcal{L}_\xi g_{b'c'}(x') = 0. \quad (126)$$

The elements of $K_G(x)$ also preserve all distances from x in the sense that $\mathcal{L}_\xi \sigma(x, x') = 0$. In general, $\xi^{a'}(x')$ is a solution to the geodesic deviation (or Jacobi) equation along the geodesic connecting x and x' .

The generalized Killing fields may be shown to admit an expansion in terms of 1- and 2-forms at x . Expanding (123) in terms of covariant derivatives shows that for every $\xi^a \in K_G(x)$,

$$\xi^{a'} = \Xi^{a'a} \xi_a + \Xi^{a'ab} \nabla_a \xi_b. \quad (127)$$

The bitensors $\Xi^{a'a}$ and $\Xi^{a'ab}$ which appear here—known as Jacobi propagators—are explicitly given by (56). The expansion (53) of Killing vector fields is therefore identical to the expansion (127) of generalized Killing vector fields. Varying ξ_a and $\nabla_a \xi_b$ arbitrarily, it is clear that $\dim K_G(x) = N + \frac{1}{2}N(N-1) = \frac{1}{2}N(N+1)$ in N spatial dimensions.

The generalized Killing fields defined by (123) and (124) provide a notion of symmetry with respect to a point. They may be used to analyze non-relativistic motion in geometries which do not admit any exact symmetries. This is not pursued here. We instead focus on relativistic motion, in which case it is more appropriate to consider a different kind of generalized Killing field which provides a notion of symmetry near a worldline instead of a point.

4.1.2 Symmetries About a Worldline

In relativistic contexts, it is useful to define a K_G which takes as arguments a timelike worldline and a foliation instead than a single point. Given a worldtube $\mathfrak{W} = \{\mathfrak{B}_s \mid s \in \mathbb{R}\}$ in a Lorentzian spacetime (\mathcal{M}, g_{ab}) of dimension N , consider a foliation $\{\mathfrak{B}_s\}$. Also consider a timelike worldline \mathcal{Z} parametrized by $z_s := \mathcal{Z} \cap \mathfrak{B}_s$. The definition of $K_G(\mathcal{Z}, \{\mathfrak{B}_s\})$ in this context is as follows: First, (125) is enforced for all z_s . This provides a sense in which the elements of $K_G(\mathcal{Z}, \{\mathfrak{B}_s\})$ generalize Poincaré symmetries “near” \mathcal{Z} . It implies that the generalized Killing fields and their first derivatives satisfy the Killing transport equations on \mathcal{Z} . Moreover,

$$\nabla_a \nabla_b \xi_c|_{\mathcal{Z}} = -R_{bca}{}^d \xi_d, \quad (128)$$

which generalizes (61). This describes, e.g., how generalized Killing fields which might appear purely rotational or boost-like at one point acquire translational components at nearby points. When applied to problems of motion, it leads to the Mathisson-Papapetrou spin-curvature force.

Demanding that (125) hold on \mathcal{Z} describes the generalized Killing fields only on that worldline. They may be extended outwards into \mathfrak{W} by demanding that

$$\mathcal{L}_\xi \sigma^{a'}(x', z_s) = 0 \quad (129)$$

for each $x' \in \mathfrak{B}_s$. This is merely a restriction of (123). It implies that (127) holds whenever there exists some s such that $x = z_s$ and $x' \in \mathfrak{B}_s$. Elements of $K_G(\mathcal{Z}, \{\mathfrak{B}_s\})$ may therefore be specified using an arbitrary pair of 1- and 2-forms at any point on \mathcal{Z} . As required, the generalized Killing fields form a vector space with dimension $\frac{1}{2}N(N+1)$. Additionally, $\mathcal{L}_\xi \sigma(x', z_s) = 0$ and

$$\sigma^{a'}(x', z_s) \sigma^{b'}(x', z_s) \mathcal{L}_\xi g_{a'b'}(x', z_s) = 0 \quad (130)$$

whenever $x' \in \mathfrak{B}_s$ [1]. The elements of $K_G(\mathcal{Z}, \{\mathfrak{B}_s\})$ are the generalized Killing fields used in the remainder of this work.

4.2 Scalar Charges in Curved Spacetimes

We now return to the motion of scalar charges as discussed in Sect. 3, but no longer require that the background spacetime admit any symmetries. Consider a body coupled to a Klein-Gordon field ϕ in a four-dimensional spacetime (\mathcal{M}, g_{ab}) . This body is assumed to be contained inside a worldtube $\mathfrak{W} \subset \mathcal{M}$ with finite spatial extent and no other matter. Its stress-energy tensor T_{body}^{ab} is assumed to satisfy (77).

A generalized momentum is easily defined by reusing (78), but with the space K employed there replaced by an appropriate space $K_G(\mathcal{Z}, \{\mathfrak{B}_s\})$ of generalized Killing fields as described in Sect. 4.1. This requires the introduction of a timelike worldline \mathcal{Z} and a foliation $\{\mathfrak{B}_s\}$ of \mathfrak{W} . Supposing that these structures have been chosen—perhaps using center of mass conditions—let

$$P_s(\xi) := \int_{\mathfrak{B}_s} T_{\text{body}}^{ab} \xi_a dS_b \quad (131)$$

for all $\xi^a \in K_G(\mathcal{Z}, \{\mathfrak{B}_s\})$. For each s , this is a vector in the ten-dimensional space $K_G^*(\mathcal{Z}, \{\mathfrak{B}_s\})$. The associated linear and angular momenta p_a and S_{ab} coincide with those introduced by Dixon [6, 17, 24] for matter which does not couple to an electromagnetic field.¹⁸

Using stress-energy conservation to differentiate the generalized momentum with respect to the time parameter s ,

¹⁸Dixon's papers never considered matter coupled to scalar fields. The momenta associated with (131) are those which arise naturally for objects falling freely in curved spacetimes.

$$\frac{d}{ds} P_s(\xi) = \int_{\mathfrak{B}_s} \left(\frac{1}{2} T_{\text{body}}^{ab} \mathcal{L}_\xi g_{ab} - \rho \mathcal{L}_\xi \phi \right) dS. \quad (132)$$

The first term on the right-hand side of this expression is not present in its maximally-symmetric counterpart (79); extra forces arise when the ξ^a are not Killing. These may be interpreted as gravitational effects. While sufficiently small test bodies fall along geodesics in curved spacetimes, the same is not true for more extended masses. Gravity then exerts nonzero 4-forces and 4-torques which are described by the $\mathcal{L}_\xi g_{ab}$ term in (132). If expanded in a multipole series, (125) implies that such effects first appear at quadrupole order. This is described more fully in Sect. 4.2.2.

The effect of the scalar field on the second term on the right-hand side of (132) may be understood by repeating the arguments of Sects. 3.4 and 3.5. This results in Eq. (94) being replaced by

$$\begin{aligned} \frac{d}{ds} \hat{P}_s(\xi) = \int_{\mathfrak{B}_s} & \left[\frac{1}{2} T_{\text{body}}^{ab}(x) \mathcal{L}_\xi g_{ab}(x) - \rho(x) \mathcal{L}_\xi \hat{\phi}(x) \right. \\ & \left. - \frac{1}{2} \int_{\mathfrak{M}} dV' \rho(x) \rho(x') \mathcal{L}_\xi G(x, x') \right] dS. \end{aligned} \quad (133)$$

The effective field which appears here is defined by $\hat{\phi} := \phi - \phi_S$, where ϕ_S satisfies (83) and G is the Detweiler-Whiting S-type Green function described in Sect. 3.4. The generalized momentum P_s has also been replaced by the renormalized momentum $\hat{P}_s := P_s + E_s$, where the self-momentum E_s is given by (90).

An absence of spacetime symmetries explicitly affects self-interaction only via the second line of (133). Unlike in maximally-symmetric backgrounds, the Detweiler-Whiting Green function does not satisfy $\mathcal{L}_\xi G = 0$ in general. Indeed, no Green function can be constructed with this property, a result which could be viewed as implying that it is impossible to define an analog of Newton's third law in generic spacetimes. It follows that the self-force cannot be entirely absorbed into a redefinition of the momentum. Understanding it requires another type of renormalization which affects the quadrupole and higher multipole moments of T_{body}^{ab} .

4.2.1 Breakdown of Newton's Third Law

The self-force which remains after renormalizing P_s depends on $\mathcal{L}_\xi G$. It may be understood physically by recalling that there is a sense in which G is constructed purely from the spacetime metric. It therefore follows that for any vector field ξ^a , whether it is a generalized Killing field or not, $\mathcal{L}_\xi G$ must depend linearly on $\mathcal{L}_\xi g_{ab}$. In this sense, the first and third terms on the right-hand side of (133) are both linear in $\mathcal{L}_\xi g_{ab}$. They are physically very similar, both representing different aspects of the gravitational force [4].

As remarked in Sect. 3, a body's inertia depends on both its own stress-energy tensor and the properties of its self-field. The inertia due to T_{body}^{ab} is described by

P_s and the inertia due to ϕ_S by E_s . A body's passive gravitational mass experiences a similar split. The gravitational force exerted on a body due to its stress-energy tensor is

$$\frac{1}{2} \int_{\mathfrak{B}_s} T_{\text{body}}^{ab} \mathcal{L}_\xi g_{ab} dS, \quad (134)$$

while the gravitational force exerted on a body's self-field is instead described by

$$-\frac{1}{2} \int_{\mathfrak{B}_s} dS \int_{\mathfrak{W}} dV' \rho \rho \mathcal{L}_\xi G. \quad (135)$$

Although it is difficult to do so explicitly, this latter expression can be transformed into a linear operator on $\mathcal{L}_\xi g_{ab}$. It effectively adds to a body's gravitational mass distribution as inferred by observing responses to different spacetime curvatures. *In a multipole expansion, the force (135) may be viewed as renormalizing the quadrupole and higher multipole moments of a body's stress-energy tensor.*

The failure of Newton's third law provides a second mechanism by which self-fields induce renormalizations. It is distinct—both in its origin and in the quantities it affects—from the mechanism described in Sect. 3.5. The renormalization of a body's momentum was shown to be closely connected to the hyperbolicity of the underlying field equation. The geometry-induced¹⁹ failure of Newton's third law can instead arise even for matter coupled to elliptic field equations. It affects only the quadrupole and higher moments of a body's stress-energy tensor. Combined, the two types of renormalization affect all multipole moments of T_{body}^{ab} . In this sense, one is led to the concept of an effective stress-energy tensor. This is defined quasi-locally, and can be identified with T_{tot}^{ab} only in special cases.

A fully explicit discussion of this effect is not known. To motivate it more directly, it is instructive to find a wave equation satisfied by $\mathcal{L}_\xi G$. Noting that

$$\mathcal{L}_\xi \delta(x, x') = -\frac{1}{2} \delta(x, x') g^{ab}(x) \mathcal{L}_\xi g_{ab}(x), \quad (136)$$

a Lie derivative of (80) yields

$$\begin{aligned} (\nabla^a \nabla_a - \mu^2) \mathcal{L}_\xi G &= \nabla_a \left[(g^{ac} g^{bd} - \frac{1}{2} g^{ab} g^{cd}) \nabla_b G \mathcal{L}_\xi g_{cd} \right] \\ &\quad + \frac{\mu^2}{2} (g^{ab} \mathcal{L}_\xi g_{ab}) G. \end{aligned} \quad (137)$$

¹⁹This type of renormalization fundamentally arises from the connection between $\mathcal{L}_\xi G$ and $\mathcal{L}_\xi g_{ab}$ which occurs for Green functions associated with the Klein-Gordon equation. In different theories, Lie derivatives of G can depend on fields other than the metric. Self-forces renormalize whichever moments are coupled to these fields.

Viewing $\mathcal{L}_\xi G$ on the left-hand side of this equation as “independent” of the G appearing on the right-hand side suggests that $\mathcal{L}_\xi G$ is a solution to a wave equation sourced by $\mathcal{L}_\xi g_{ab}$ and its first derivative. A source which is independent of G may be found by applying the Klein-Gordon operator to both sides:

$$(\nabla^{a'} \nabla_{a'} - \mu^2)(\nabla^a \nabla_a - \mu^2) \mathcal{L}_\xi G = 4\pi \nabla_a \left[(g^{ac} g^{bd} - \frac{1}{2} g^{ab} g^{cd}) (\mathcal{L}_\xi g_{cd}) \nabla_b \delta \right] - 2\pi \mu^2 (g^{ab} \mathcal{L}_\xi g_{ab}) \delta. \quad (138)$$

This describes $\mathcal{L}_\xi G$ as the solution to a fourth-order distributional differential equation sourced by $\mathcal{L}_\xi g_{ab}$ and $\nabla_a \mathcal{L}_\xi g_{bc}$.

Results like these may be used together with the field equation to integrate (135) by parts. Let

$$T_{\text{field},S}^{ab} := \frac{1}{4\pi} \left[\nabla^a \phi_S \nabla^b \phi_S - \frac{1}{2} g^{ab} (\nabla_c \phi_S \nabla^c \phi_S + \mu^2 \phi_S^2) \right] \quad (139)$$

be the stress-energy tensor associated with ϕ_S and define

$$\begin{aligned} \mathcal{I}^a := & \frac{1}{8\pi} (g^{ac} g^{bd} - \frac{1}{2} g^{ab} g^{cd}) \phi_S \nabla_b \phi_S \mathcal{L}_\xi g_{cd} \\ & + \frac{1}{8\pi} \int_{\mathfrak{W}} \rho' (\nabla^a \phi_S \mathcal{L}_\xi G - \phi_S \nabla^a \mathcal{L}_\xi G) dV'. \end{aligned} \quad (140)$$

The law of motion (133) then reduces to

$$\begin{aligned} \frac{d}{ds} \hat{P}_s = & \int_{\mathfrak{B}_s} \left[\frac{1}{2} (T_{\text{body}}^{ab} + T_{\text{field},S}^{ab}) \mathcal{L}_\xi g_{ab} - \rho \mathcal{L}_\xi \hat{\phi} \right] dS \\ & - \frac{d}{ds} \int_{\mathfrak{B}_s} \mathcal{I}^a dS_a - \oint_{\partial \mathfrak{B}_s} \mathcal{I}^a t^b dS_{ab}. \end{aligned} \quad (141)$$

The gravitational force in this expression clearly acts on the combined stress-energy tensor $T_{\text{body}}^{ab} + T_{\text{field},S}^{ab}$. Unfortunately, the stress-energy tensor associated with the self-field does not have compact spatial support. The finite integration volume \mathfrak{B}_s must therefore be compensated by the two boundary terms involving \mathcal{I}^a . If these can be ignored, it is evident that gravitational forces are determined only by $T_{\text{body}}^{ab} + T_{\text{field},S}^{ab}$. This cannot, however, be expected to hold generically. In general, there does not appear to be any reason to neglect \mathcal{I}^a .

Approximations may instead be introduced which allow the renormalized multipole moments to be computed essentially using local Taylor series [4]. Another approach, described here for the first time, is to use Hadamard series. Recalling the Hadamard form (82) for G ,

$$\mathcal{L}_\xi G = \frac{1}{2} \left[\Delta^{1/2} \delta'(\sigma) \mathcal{L}_\xi \sigma + (\mathcal{L}_\xi \Delta^{1/2} - H \mathcal{L}_\xi \sigma) \delta(\sigma) - \mathcal{L}_\xi V \Theta(\sigma) \right]. \quad (142)$$

Our task is now to convert this into an expression where all Lie derivatives act on the metric.

This is easily accomplished for the Lie derivatives of σ and Δ . Differentiating the well-known identity $\sigma^a \sigma_{a'} = 2\sigma$ shows that

$$\sigma^{a'} \nabla_{a'} \mathcal{L}_\xi \sigma - \mathcal{L}_\xi \sigma = \frac{1}{2} \sigma^{a'} \sigma^{b'} \mathcal{L}_\xi g_{a'b'}. \quad (143)$$

The differential operator $\sigma^{a'}(x, x') \nabla_{a'}$ appearing here is a covariant derivative along the geodesic connecting x and x' , so (143) may be viewed as an ordinary differential equation for $\mathcal{L}_\xi \sigma$. Letting y_τ denote a geodesic which is affinely parametrized by τ while satisfying $y_0 = x$ and $y_1 = x'$, it follows that

$$\mathcal{L}_\xi \sigma(x, x') = \frac{1}{2} \int_0^1 \dot{y}_\tau^a \dot{y}_\tau^b \mathcal{L}_\xi g_{ab}(y_\tau) d\tau. \quad (144)$$

Moreover, an argument found in [4] shows that Lie derivatives of the van Vleck determinant Δ depend on $\mathcal{L}_\xi \sigma$:

$$\mathcal{L}_\xi \ln \Delta^{1/2} = -\frac{1}{4} \left[g^{ab} \mathcal{L}_\xi g_{ab} + g^{a'b'} \mathcal{L}_\xi g_{a'b'} + 2H^{aa'} \nabla_a \nabla_{a'} \mathcal{L}_\xi \sigma \right]. \quad (145)$$

Both $\mathcal{L}_\xi \sigma$ and $\mathcal{L}_\xi \Delta^{1/2}$ may therefore be written as line integrals—solutions to transport equations—which are linear in $\mathcal{L}_\xi g_{ab}$. Substituting these expressions into (142) goes much of the way towards expressing $\mathcal{L}_\xi G$ in terms of $\mathcal{L}_\xi g_{ab}$.

All that remains is to consider $\mathcal{L}_\xi V$. This is more difficult. Even V itself is complicated to compute. It is a solution to the homogeneous field equation which is symmetric in its arguments and satisfies

$$V(x, x') = G_+(x, x') + G_-(x, x') \quad (146)$$

whenever x' is timelike-separated from x . Alternatively, V can be computed using a transport equation along null geodesics [10]. For each x' , this transport equation may be used as boundary data with which to obtain $V(\cdot, x')$. Extending this data outside of the null cones is essentially an “exterior characteristic problem:” One seeks a solution to a hyperbolic differential equation in the exterior of a null cone given values of the solution on that cone. Unlike interior characteristic problems, the general mathematical status of such problems is unclear.

One way to proceed is to construct a Hadamard series. This is an ansatz which supposes that V can be expanded via [41]

$$V(x, x') = \sum_{n=0}^{\infty} V_n(x, x') \sigma^n(x, x'). \quad (147)$$

The V_n here are determined by demanding that each explicit power of σ vanish separately when this series is inserted into $(\nabla^a \nabla_a - \mu^2)V = 0$. The result is an infinite tower of ordinary differential equations. The $n = 0$ case is governed by

$$\Delta^{1/2} \sigma^a \nabla_a (\Delta^{-1/2} V_0) + V_0 = \frac{1}{2} \nabla^a \nabla_a \Delta^{1/2}. \quad (148)$$

For each x' , this determines $V(\cdot, x')$ on the light cones of x' . Higher-order terms are needed in the exteriors of these light cones. For all $n \geq 1$,

$$\Delta^{1/2} \sigma^a \nabla_a (\Delta^{-1/2} V_n) + (n+1)V_n = -\frac{1}{2n} \nabla^a \nabla_a V_{n-1}. \quad (149)$$

It should be emphasized that the Hadamard series is not a Taylor expansion. The V_n are two-point scalar fields, not constants. Furthermore, the Hadamard series is known to converge only if the metric is analytic (and even then, it might converge only in a finite region) [41]. Although analyticity is quite a strong assumption, there may be other interesting cases where a finite Hadamard series can be used to approximate V up to a well-controlled remainder.

Assuming that (147) is valid, it is easily used to compute Lie derivatives of V . This results in

$$\mathcal{L}_\xi V = \sum_{n=0}^{\infty} [\mathcal{L}_\xi V_n + (n+1)V_{n+1} \mathcal{L}_\xi \sigma] \sigma^n. \quad (150)$$

Lie derivatives of σ may already be transformed into Lie derivatives of g_{ab} via (144). Lie derivatives of the V_n may instead be found by differentiating (148) and (149). The $n = 0$ case satisfies

$$\begin{aligned} \Delta^{1/2} \sigma^a \nabla_a (\Delta^{-1/2} \mathcal{L}_\xi V_0) + \mathcal{L}_\xi V_0 &= \frac{1}{2} (\mathcal{L}_\xi \nabla^a \nabla_a \Delta^{1/2} - V_0 \mathcal{L}_\xi \sigma^a{}_a) \\ &\quad + (g^{ab} \sigma^c \mathcal{L}_\xi g_{bc} - \nabla^a \mathcal{L}_\xi \sigma) \nabla_a V_0, \end{aligned} \quad (151)$$

for example. The left-hand side of this equation may be interpreted as an ordinary differential operator along the geodesic which connects the two arguments of V_0 . All Lie derivatives in the source on the right-hand of this equation may, with the help of (144) and (145), be rewritten in terms of $\mathcal{L}_\xi g_{ab}$. It follows that $\mathcal{L}_\xi V_0$ can be expressed as a line integral involving $\mathcal{L}_\xi g_{ab}$. Similar results also hold for $\mathcal{L}_\xi V_n$ with $n > 0$. The detailed forms of these integrals are complicated and are not displayed here. The important point, however, is that all parts of $\mathcal{L}_\xi G$ may be expressed as line integrals involving $\mathcal{L}_\xi g_{ab}$. Changing variables appropriately and using the spatially-compact support of ρ then shows that the self-force (135) does indeed renormalize the gravitational force (134).

4.2.2 Multipole Expansions

It is useful to expand the scalar force in a multipole series when $\hat{\phi}$ varies slowly. Similarly, the gravitational force may be expanded in its own multipole series when there is an appropriate sense in which g_{ab} does not vary too rapidly²⁰ inside each \mathfrak{B}_s . Such expansions can be obtained using the techniques of Sects. 2.2.5 and 3.6. Recalling (94), (98), and (133), first note that

$$\begin{aligned} \frac{d}{ds} \hat{P}_s(\xi) = & - \sum_{n=0}^{\infty} \frac{1}{n!} q^{a_1 \dots a_n} \mathcal{L}_{\xi} \hat{\phi}_{,a_1 \dots a_n} + \frac{1}{2} \int_{\mathfrak{B}_s} T_{\text{body}}^{ab} \mathcal{L}_{\xi} g_{ab} dS \\ & - \frac{1}{2} \int_{\mathfrak{B}_s} dS \int_{\mathfrak{M}} dV' \rho \rho' \mathcal{L}_{\xi} G. \end{aligned} \quad (152)$$

The two integrals which remain here are intrinsically gravitational.

Given (125), it is evident that multipole expansion for the generalized force must begin at quadrupole order. More specifically, it may be shown that [4, 6, 17]

$$\frac{1}{2} \int_{\mathfrak{B}_s} T_{\text{body}}^{ab} \mathcal{L}_{\xi} g_{ab} dS = \frac{1}{2} \sum_{n=2}^{\infty} \frac{1}{n!} I^{c_1 \dots c_n ab} \mathcal{L}_{\xi} g_{ab, c_1 \dots c_n}, \quad (153)$$

where $g_{ab, c_1 \dots c_n}$ represents the n th tensor extension of g_{ab} and $I^{c_1 \dots c_n ab}$ is the 2^n -pole moment of T_{body}^{ab} . Tensor extensions in this context are somewhat more complicated than in the scalar case discussed in Sect. 2.2.5. While they are still defined as those tensors which reduce to n partial derivatives when evaluated at the origin of a Riemann normal coordinate system, equations like (48) must be generalized for objects with nonzero tensorial rank (see, e.g., [4]). For this reason, explicit integrals relating $I^{c_1 \dots c_n ab}$ to T_{body}^{ab} are significantly more complicated than their scalar analogs. These are not needed here, and may be found in [4, 6]. They are Dixon's multipole moments. Additionally, note that the first few tensor extensions of the metric are $g_{ab, c} = 0$ and

$$g_{ab, c_1 c_2} = \frac{2}{3} R_{a(c_1 c_2) b}, \quad g_{ab, c_1 c_2 c_3} = \nabla_{(c_1} R_{|a| c_2 c_3) b}, \quad (154)$$

$$g_{ab, c_1 c_2 c_3 c_4} = \frac{6}{5} \nabla_{(c_1 c_2} R_{|a| c_3 c_4) b} + \frac{16}{15} R_{a(c_1 c_2}{}^d R_{|b| c_3 c_4) d}. \quad (155)$$

Expanding both integrals in (152) while identifying coefficients in front of $\mathcal{L}_{\xi} g_{ab, c_1 \dots c_n}$ results in a series structurally identical to (153), but with all bare multipole moments $I^{c_1 \dots c_n ab}$ replaced by their renormalized counterparts $\hat{I}^{c_1 \dots c_n ab}$. The

²⁰More precisely, the coordinate components g_{ij} must not vary too rapidly when expressed in a Riemann normal coordinate system with origin z_s . Physically, this is a significant restriction. It would be far better to perform multipole expansions only using effective metrics where gravitational self-fields have been appropriately removed. It is not known how to do this for the full Einstein-Klein-Gordon system.

final multipole expansion for the generalized force acting on a self-interacting scalar charge distribution is therefore

$$\frac{d}{ds} \hat{p}_s(\xi) = \frac{1}{2} \sum_{n=2}^{\infty} \frac{1}{n!} \hat{I}^{c_1 \dots c_n ab} \mathcal{L}_{\xi} g_{ab, c_1 \dots c_n} - \sum_{n=0}^{\infty} \frac{1}{n!} q^{a_1 \dots a_n} \mathcal{L}_{\xi} \hat{\phi}_{, a_1 \dots a_n}. \quad (156)$$

Gravitational terms first arise at quadrupole order, while scalar terms appear even at monopole order.

4.2.3 Forces and Torques

As in Sects. 2.2.6 and 3.7, the generalized momentum can be decomposed into linear and angular components \hat{p}^a , \hat{S}^{ab} . These obey the law of motion (102), where the force and torque are now supplemented by gravitational terms at quadrupole and higher orders:

$$\hat{F}_a = \frac{1}{2} \sum_{n=2}^{\infty} \frac{1}{n!} \hat{I}^{d_1 \dots d_n bc} \nabla_a g_{bc, d_1 \dots d_n} - \sum_{n=0}^{\infty} \frac{1}{n!} q^{b_1 \dots b_n} \nabla_a \hat{\phi}_{, b_1 \dots b_n}, \quad (157)$$

$$\begin{aligned} \hat{N}^{ab} = & \sum_{n=2}^{\infty} \frac{2}{n!} g^{f[b} (\hat{I}^{c_1 \dots c_n | a] d} g_{df, c_1 \dots c_n} + \frac{n}{2} \hat{I}^{a] c_1 \dots c_{n-1} dh} g_{dh, c_1 \dots c_{n-1} f}) \\ & + \sum_{n=0}^{\infty} \frac{2}{n!} g^{c[a} q^{b] d_1 \dots d_n} \hat{\phi}_{, cd_1 \dots d_n}. \end{aligned} \quad (158)$$

A center of mass may be defined exactly as described in Sect. 3.8. Applying (110), the momentum-velocity relation remains (111).

4.2.4 Monopole Approximation

Suppose that \mathcal{Z} is identified with the center of mass worldline $\{\gamma_s\}$. It is then interesting to consider the laws of motion truncated at monopole order. As explained in Sect. 3.9, the spin magnitude is conserved in such cases. It is therefore consistent to consider cases where \hat{S}_a is negligible. Assuming this, an object's mass \hat{m} and center of mass γ_s satisfy

$$\hat{m} - q \hat{\phi} = (\text{constant}), \quad \hat{m} \ddot{\gamma}_s^a = -q (g^{ab} + \dot{\gamma}_s^a \dot{\gamma}_s^b) \nabla_b \hat{\phi} \quad (159)$$

whenever $q = (\text{constant})$. These are formally equivalent to the standard equations of motion adopted for scalar test charges, but with the physical field replaced everywhere by the effective field. Laws of motion applicable to self-interacting charges involve $\hat{\phi}$, not ϕ .

Classical results on the scalar self-force are easily derived from (159). In the absence of any external charges (which does not necessarily imply trivial motion in curved spacetimes), it is natural to suppose that initial data for ϕ has been prescribed in the distant past. If all details of that data have decayed sufficiently, the only remaining field is the retarded solution associated with the body's own charge distribution. Generalizing this somewhat to also allow for a prescribed “external field” ϕ_{ext} ,

$$\phi(x) = \phi_{\text{ext}}(x) + \int_{\mathfrak{M}} \rho(x') G_{-}(x, x') dV'. \quad (160)$$

While the retarded Green function G_{-} can be difficult to compute in nontrivial spacetimes, we assume that this problem has been solved. Using (81) and (83) then results in the effective potential²¹

$$\hat{\phi} = \phi_{\text{ext}} + \frac{1}{2} \int_{\mathfrak{M}} \rho'(G_{-} - G_{+} + V) dV'. \quad (161)$$

Although the “self-field” ϕ_{S} has been removed from ϕ , remnants of the body's charge distribution do remain. These are responsible for self-forces as they are commonly defined in the literature, and give rise to physical phenomena such as radiation reaction.

The “traditional” self-force problem involves point particle limits. Such limits consist of appropriate one-parameter families of charge distributions $\lambda\rho$ and stress-energy tensors $\lambda T_{\text{body}}^{ab}$ whose supports collapse to a single timelike worldline as $\lambda \rightarrow 0$ (see, e.g., [28]). Suppose that these families are chosen such that a body's physical size and mass asymptotically scale like λ^1 as $\lambda \rightarrow 0$, suggesting that $\lambda q^{a_1 \dots a_n}$ scales like λ^{n+1} for all $n \geq 0$ and that $\lambda \hat{I}^{c_1 \dots c_n ab}$ scales like λ^{n+1} for all $n \geq 2$. These conditions guarantee that the multipole series can be truncated at low order [as has already been assumed in (159)].

It is also important to demand that the time dependence of $\lambda\rho$ remain smooth as $\lambda \rightarrow 0$. This guarantees that a body's internal dynamics remain slow compared to its light-crossing timescale, which is required to ensure that a charge does not self-accelerate in the absence of any external influence. Self-acceleration could occur if, e.g., internal oscillations conspired to generate strongly-collimated beams of radiation. Such cases are physically possible, but are typically excluded from self-force discussions.

The $\lambda \rightarrow 0$ limit of the approximation which has just been sketched results in a timelike worldline satisfying the usual equations for a monopole test charge accelerated by ϕ_{ext} . Effects typically described as self-forces occur at the following order. In principle, interactions between dipole moments and ϕ_{ext} also occur at this order. These are dropped here for simplicity, leaving only (159). Without entering

²¹The two-point scalar V is to be understood here as equivalent to G_{\pm} when its arguments are timelike-separated. This defines it even in the presence of caustics and other potential complications.

into technical details, the appropriate approximation for the effective field in this limit may be shown to be given by (161) with a point particle charge density. Dropping all labels involving λ ,

$$\hat{\phi}(x) = \phi_{\text{ext}}(x) + \frac{1}{2}q \int [G_-(x, \gamma_{s'}) - G_+(x, \gamma_{s'}) + V(x, \gamma_{s'})] ds' \quad (162)$$

plus terms of order λ^2 . Unlike the $\lambda \rightarrow 0$ limit of ϕ , the limit of $\hat{\phi}$ is well-defined even at the particle's location. The same is also true of its gradient. All necessary regularizations have automatically been taken into account by first deriving the correct laws of motion for nonsingular extended bodies.

The computations needed to evaluate $\nabla_a \hat{\phi}$ at γ_s are rather tedious, so we merely cite²² the result [10]. Defining the projection operator $h^{ab} := g^{ab} + \dot{\gamma}_s^a \dot{\gamma}_s^b$ and assuming that $q = (\text{constant})$,

$$\begin{aligned} \nabla^a \hat{\phi} = & \nabla^a \phi_{\text{ext}} + \frac{1}{3}(q^2/\hat{m})h^{ab}\dot{\gamma}_s^c [\nabla_b \nabla_c \phi_{\text{ext}} - 2(q/\hat{m})\nabla_b \phi_{\text{ext}} \nabla_c \phi_{\text{ext}}] \\ & + \frac{1}{12}q(R\dot{\gamma}_s^a - 2h^{ab}R_{bc}\dot{\gamma}_s^c) + q \lim_{\epsilon \rightarrow 0^+} \int_{-\infty}^{s-\epsilon} \nabla^a G_-(\gamma_s, \gamma_{s'}) ds'. \end{aligned} \quad (163)$$

Substituting this into (159), the final equations of motion are

$$\begin{aligned} \ddot{\gamma}_s^a = & -(q/\hat{m})h^{ab} \left(\nabla_b \phi_{\text{ext}} + \frac{1}{3}(q^2/\hat{m})\dot{\gamma}_s^c [\nabla_b \nabla_c \phi_{\text{ext}} - 2(q/\hat{m})\nabla_b \phi_{\text{ext}} \nabla_c \phi_{\text{ext}}] \right. \\ & \left. - \frac{1}{6}qR_{bc}\dot{\gamma}_s^c + q \lim_{\epsilon \rightarrow 0^+} \int_{-\infty}^{s-\epsilon} \nabla_b G_-(\gamma_s, \gamma_{s'}) ds' \right) \end{aligned} \quad (164)$$

and

$$\hat{m} - q\phi_{\text{ext}} + q^2 \left(\frac{1}{12}R - \lim_{\epsilon \rightarrow 0^+} \int_{-\infty}^{s-\epsilon} G_-(\gamma_s, \gamma_{s'}) ds' \right) = (\text{constant}) \quad (165)$$

through first order in λ . Essentially²³ the same results were first obtained by Quinn using an axiomatic argument [42]. Their derivation from first principles was later discussed in [2]. The integrals over the tail of G_- indicate that a charge's motion can depend on its past history. This is related to the failure of Huygens' principle,

²²The point particle field derived in [10] includes a derivative of the particle's acceleration. A careful treatment of the perturbation theory shows that such terms refer only to accelerations at lower order [28]. The self-consistent discussion which is implicit here therefore requires that accelerations be simplified using the zeroth order equation of motion. This is taken into account in (163).

²³Some sign conventions in [2, 42] are different from those adopted here.

in which case the field a body sources in the past can scatter back towards it at later times. This effect disappears for matter coupled to massless fields in flat spacetime, but is almost always present otherwise.

4.3 Electromagnetic Charges

The problem of electromagnetic self-force has inspired considerable discussion over the past century. Here, we show how it can be understood using a straightforward application of the formalism just described for scalar charges. The body of interest is assumed to be smooth and to be confined to a finite worldtube $\mathfrak{W} \subset \mathcal{M}$ in a fixed four-dimensional spacetime (\mathcal{M}, g_{ab}) . It couples to an electromagnetic field $F_{ab} = F_{[ab]}$ satisfying Maxwell's equations

$$\nabla_{[a} F_{bc]} = 0, \quad \nabla^b F_{ab} = 4\pi J_a, \quad (166)$$

from which it follows as an integrability condition that the body's 4-current J^a must be divergence-free. Its total charge

$$q := \int_{\mathfrak{B}_s} J^a dS_a \quad (167)$$

is therefore a constant independent of \mathfrak{B}_s (as long as this hypersurface completely contains the body of interest). Furthermore, the stress-energy tensor associated with F_{ab} can be defined throughout \mathfrak{W} via

$$T_{\text{field}}^{ab} = \frac{1}{4\pi} (F_a{}^c F_{bc} - \frac{1}{4} g_{ab} F^{cd} F_{cd}). \quad (168)$$

Identifying all remaining stress-energy as T_{body}^{ab} , stress-energy conservation implies that

$$\nabla_b T_{\text{body}}^{ab} = F^{ab} J_b. \quad (169)$$

The right-hand side of this equation is the Lorentz force density.

4.3.1 An Electromagnetic Momentum

A generalized momentum may again be defined using (131). This requires a choice of worldline \mathcal{Z} and a foliation $\{\mathfrak{B}_s\}$, leading to a vector which resides in $K_G^*(\mathcal{Z}, \{\mathfrak{B}_s\})$. Applying (169) shows that forces and torques follow from

$$\frac{d}{ds} P_s(\xi) = \int_{\mathfrak{B}_s} \left(\frac{1}{2} T_{\text{body}}^{ab} \mathcal{L}_\xi g_{ab} + F_{ab} \xi^a J^b \right) dS. \quad (170)$$

This is the simplest approach. It is not, however, the only reasonable possibility. P_s has the unfortunate property that symmetries do not necessarily imply conservation laws. Even if there exists a vector field ψ^a satisfying $\mathcal{L}_\psi F_{ab} = \mathcal{L}_\psi g_{ab} = 0$, the associated momentum $P_s(\psi)$ is not necessarily conserved.

Dixon [6, 24, 43] has proposed a different set of linear and angular momenta in this context which do form simple conservation laws in the presence of symmetries (among other desirable properties more generally). Translating his definitions into a generalized momentum P_s^D results in

$$P_s^D(\xi) := P_s(\xi) + \int_{\mathfrak{B}_s} dS_a J^a(x) \int_0^1 du u^{-1} \sigma^{b'}(y'_u, z_s) \xi^{c'}(y'_u) F_{b'c'}(y'_u). \quad (171)$$

The curve $\{y'_u \mid u \in [0, 1]\}$ describes an affinely-parametrized geodesic satisfying $y_0 = z_s$ and $y_1 = x$. The correction to P_s which is used here represents a type of interaction between the electromagnetic field and its source. It can be motivated using symmetry considerations [24], the theory of multipole moments [6], or Lagrangian methods [43]. Some intuition for this interaction may be gained by introducing a vector potential A_a so that $F_{ab} = 2\nabla_{[a} A_{b]}$. Then,

$$P_s^D + q(A_a \xi^a)|_{z_s} = P_s + \int_{\mathfrak{B}_s} dS_a J^a \left(A_b \xi^b - \int_0^1 du u^{-1} \sigma^{b'} \mathcal{L}_\xi A_{b'} \right). \quad (172)$$

Although this has been written in terms of a gauge-dependent vector potential, it is manifest from (171) that P_s and P_s^D are both gauge-invariant.

Combining (172) with (170) shows that the generalized force associated with Dixon's momentum is

$$\begin{aligned} \frac{d}{ds} (P_s^D + q A_a \xi^a) &= \int_{\mathfrak{B}_s} dS \left(\frac{1}{2} T_{\text{body}}^{ab} \mathcal{L}_\xi g_{ab} + J^a \mathcal{L}_\xi A_a \right) \\ &\quad - \frac{d}{ds} \int_{\mathfrak{B}_s} dS_a J^a \int_0^1 du u^{-1} \sigma^{a'} \mathcal{L}_\xi A_{a'}. \end{aligned} \quad (173)$$

This is awkward to write more explicitly without introducing additional technical tools. Even so, it is simple to temporarily consider special cases where there exists a Killing vector field ψ^a satisfying $\mathcal{L}_\psi F_{ab} = \mathcal{L}_\psi g_{ab} = 0$. It is then possible to find a vector potential $A_a^{(\psi)}$ such that $\mathcal{L}_\psi A_a^{(\psi)} = 0$. The component of momentum conjugate to ψ^a is therefore conserved in the sense that

$$P_s^D(\psi) + q A_a^{(\psi)} \xi^a = (\text{constant}), \quad (174)$$

where $A_a^{(\psi)} \xi^a$ is understood to be evaluated at z_s . Although this is reminiscent of the canonical momentum associated with a pointlike test charge, it is valid for essentially arbitrary extended charge distributions.

4.3.2 The Self-field and Self-force

Electromagnetic self-forces may be defined and removed from either P_s or P_s^D . In both cases, it is convenient to work in the Lorenz gauge:

$$\nabla^a A_a = 0. \quad (175)$$

Maxwell's equations then reduce to the single hyperbolic equation

$$\nabla^b \nabla_b A_a - R_a{}^b A_b = -4\pi J_a. \quad (176)$$

Introducing the parallel propagator $g^a{}_{a'}(x, x')$ [10], consider a Green function $G_{aa'}$ satisfying

1. $\square G_{aa'} - R_a{}^b G_{ba'} = -4\pi g_{aa'} \delta(x, x')$,
2. $G_{aa'}(x, x') = G_{a'a}(x', x)$,
3. $G_{aa'}(x, x') = 0$ when x, x' are timelike-separated.

These are the closest possible analogs of the constraints used to define G in Sect. 3.4. They characterize the S-type Detweiler-Whiting Green function for the reduced Maxwell equation (176). In terms of the advanced and retarded Green functions $G_{aa'}^\pm$, there exists a homogeneous solution $V_{aa'}$ such that

$$G_{aa'} = \frac{1}{2}(G_{aa'}^+ + G_{aa'}^- - V_{aa'}) = \frac{1}{2}[g_{aa'} \Delta^{1/2} \delta(\sigma) - V_{aa'} \Theta(\sigma)]. \quad (177)$$

Although it can be difficult to find $G_{aa'}$ explicitly in a particular spacetime, we assume that it is known.

A self-field A_a^S may be defined by convolving J^a with $G_{aa'}$. Considering a space-time volume $\mathfrak{R} \subseteq \mathfrak{W}$, let

$$A_a^S[\mathfrak{R}] := \int_{\mathfrak{R}} G_{aa'} J^{a'} dV'. \quad (178)$$

In the scalar case, the analog of this expression represents the “self-field” sourced in the region \mathfrak{R} . The interpretation here is somewhat more obscure, as the restriction of J^a to arbitrary regions is not necessarily conserved and is therefore unphysical. This definition is nevertheless useful. Without specification of any particular region, it is to be understood that $\mathfrak{R} = \mathfrak{W}$ so $A_a^S = A_a^S[\mathfrak{W}]$. This (full) self-field is sourced by a conserved current, implying that $F_{ab}^S := 2\nabla_{[a} A_{b]}^S$ satisfies the complete Maxwell equations

$$\nabla_{[a} F_{bc]}^S = 0, \quad \nabla^b F_{ab}^S = 4\pi J_a. \quad (179)$$

The same cannot necessarily be said for fields $2\nabla_{[a} A_{b]}^S[\mathfrak{R}]$ where $\mathfrak{R} \neq \mathfrak{M}$.

Now consider changes in P_s due to A_a^S . Applying the arguments of Sects. 3.4 and 3.5 to (170) shows that the self-force has the form (85) with

$$f(x, x') = 2\xi^a J^b J^{b'} \nabla_{[a} G_{b]b'}. \quad (180)$$

The average $f(x, x') + f(x', x)$ of action-reaction pairs reduces in this case to

$$J^a J^{a'} \mathcal{L}_\xi G_{aa'} - \nabla_a (J^a J^{a'} \xi^b G_{ba'}) - \nabla_{a'} (J^a J^{a'} \xi^b G_{ab'}). \quad (181)$$

The divergences which appear here are new features of the electromagnetic problem. Only their integrals matter, however, so they are easily dealt with. Defining the homogeneous effective field

$$\hat{F}_{ab} := F_{ab} - F_{ab}^S, \quad (182)$$

the final result is that

$$\frac{d}{ds} \hat{P}_s = \int_{\mathfrak{B}_s} dS \left(\frac{1}{2} T_{\text{body}}^{ab} \mathcal{L}_\xi g_{ab} + \xi^a J^b \hat{F}_{ab} + \frac{1}{2} \int_{\mathfrak{M}} dV' J^a J^{a'} \mathcal{L}_\xi G_{aa'} \right), \quad (183)$$

where $\hat{P}_s := P_s + E_s$ and

$$\begin{aligned} E_s := \frac{1}{2} \left(\int_{\mathfrak{B}_s^+} dV J^a \mathcal{L}_\xi A_a^S[\mathfrak{B}_s^-] - \int_{\mathfrak{B}_s^-} dV J^a \mathcal{L}_\xi A_a^S[\mathfrak{B}_s^+] \right) \\ + \int_{\mathfrak{B}_s} (\xi^a A_a^S) J^b dS_b. \end{aligned} \quad (184)$$

The renormalized momentum \hat{P}_s therefore evolves via \hat{F}_{ab} rather than F_{ab} . As explained in Sect. 4.2.1, the forces involving $\mathcal{L}_\xi g_{ab}$ and $\mathcal{L}_\xi G_{aa'}$ in (183) combine in a natural way to form an effective gravitational force. Furthermore, E_s is known to reduce in simple cases to the expected expression involving the stress-energy tensor associated with F_{ab}^S [3]. More generally, it should be thought of as a quasi-local functional of J^a .

A very similar result may be derived using the Dixon momentum P_s^D . This is most easily accomplished if a new self-momentum is introduced which satisfies

$$E_s^D := E_s - \int_{\mathfrak{B}_s} dS_a J^a \int_0^1 du u^{-1} \sigma^{b'} \xi^{c'} F_{b'c'}^S. \quad (185)$$

Defining $\hat{P}_s^D := P_s^D + E_s^D$, it follows that

$$\begin{aligned} \frac{d}{ds} \hat{P}_s^D = \int_{\mathfrak{B}_s} dS \left(\frac{1}{2} T_{\text{body}}^{ab} \mathcal{L}_\xi g_{ab} + \xi^a J^b \hat{F}_{ab} + \frac{1}{2} \int_{\mathfrak{M}} dV' J^a J^{a'} \mathcal{L}_\xi G_{aa'} \right) \\ + \frac{d}{ds} \int_{\mathfrak{B}_s} dS_a J^a \int_0^1 du u^{-1} \sigma^{b'} \xi^{c'} \hat{F}_{b'c'}, \quad (186) \end{aligned}$$

or equivalently

$$\begin{aligned} \frac{d}{ds} (\hat{P}_s^D + q \hat{A}_a \xi^a) = \int_{\mathfrak{B}_s} dS \left(\frac{1}{2} T_{\text{body}}^{ab} \mathcal{L}_\xi g_{ab} + J^a \mathcal{L}_\xi \hat{A}_a + \frac{1}{2} \int_{\mathfrak{M}} dV' J^a J^{a'} \mathcal{L}_\xi G_{aa'} \right) \\ - \frac{d}{ds} \int_{\mathfrak{B}_s} dS_a J^a \int_0^1 du u^{-1} \sigma^{a'} \mathcal{L}_\xi \hat{A}_{a'} \quad (187) \end{aligned}$$

for any vector potential \hat{A}_a satisfying $\hat{F}_{ab} = 2\nabla_{[a} \hat{A}_{b]}$.

If a Killing vector field ψ^a exists which satisfies $\mathcal{L}_\psi \hat{F}_{ab} = \mathcal{L}_\psi g_{ab} = 0$, it is possible to choose a vector potential for \hat{F}_{ab} with the property that $\mathcal{L}_\psi \hat{A}_a^{(\psi)} = 0$. It then follows immediately that $\hat{P}_s^D + q \hat{A}_a^{(\psi)} \xi^a$ is conserved. No similarly-simple conservation law is associated with \hat{P}_s .

4.3.3 Multipole Expansions

Integral expressions for the generalized force are not particularly useful on their own. It is instead more interesting to consider their multipole expansions. Unlike in the scalar theories discussed earlier, more than one “reasonable” force may be considered in the electromagnetic case. As a matter of computation, it is simplest to expand the force associated with \hat{P}_s . Dixon’s momentum is otherwise more attractive, however. Multipole series for the associated forces and torques have already been derived in a test body approximation [6]. The mechanics of the calculation are exactly the same here, and result in

$$\begin{aligned} \frac{d}{ds} \hat{P}_s^D = \frac{1}{2} \sum_{n=2}^{\infty} \frac{1}{n!} \hat{I}^{c_1 \dots c_n ab} \mathcal{L}_\xi g_{ab, c_1 \dots c_n} + q \hat{F}_{ab} \xi^a \dot{z}_s^b \\ + \sum_{n=1}^{\infty} \frac{n}{(n+1)!} q^{b_1 \dots b_n a} \mathcal{L}_\xi \hat{F}_{ab_1, b_2 \dots b_n}. \quad (188) \end{aligned}$$

The coefficients $q^{b_1 \dots b_n a}$ represent 2^n -pole moments of J^a as defined (using the notation $m^{b_1 \dots b_n a}$) by Dixon [6, 44]. They are not to be confused with the scalar charge moments satisfying (99). The $\hat{I}^{c_1 \dots c_n ab}$ appearing in (188) represent 2^n -pole moments of T_{body}^{ab} as renormalized by Lie derivatives of $G_{aa'}$. Again, these are different from the renormalized stress-energy moments which appear in the scalar law of motion

(156). In the limit of negligible self-interaction, however, both definitions reduce to Dixon's stress-energy moments [6]. For reference, the first tensor extensions of \hat{F}_{ab} are explicitly

$$\hat{F}_{ab,c} = \nabla_c \hat{F}_{ab}, \quad \hat{F}_{ab,cd} = \nabla_{(c} \nabla_{d)} \hat{F}_{ab} - \frac{2}{3} \hat{F}_{f[a} R_{b](cd)}{}^f. \quad (189)$$

If there exists a Killing vector ψ^a which satisfies $\mathcal{L}_\psi \hat{F}_{ab} = \mathcal{L}_\psi \hat{A}_a^{(\psi)} = 0$, it has already been stated that $\hat{P}_s^D(\psi) + q \hat{A}_a^{(\psi)} \psi^a$ is conserved exactly. It is evident from (188) that this quantity is also conserved in any consistent truncation of the multipole series. If a particular ψ^a is Killing but does not necessarily preserve \hat{F}_{ab} , all gravitational terms vanish from (188) and

$$\frac{d}{ds} \hat{P}_s^D(\psi) = q \hat{F}_{ab} \psi^a \dot{z}_s^b + \sum_{n=1}^{\infty} \frac{n}{(n+1)!} q^{b_1 \dots b_n a} \mathcal{L}_\psi \hat{F}_{ab_1, b_2 \dots b_n}. \quad (190)$$

This holds for all $\psi^a \in K \subseteq K_G$. It is all that arises for charges moving in flat or de Sitter spacetimes.

4.3.4 Linear and Angular Momentum

Linear and angular momenta may be extracted from \hat{P}_s^D using the methods described in Sects. 2.2.6 and 3.7. Let \hat{p}^a and \hat{S}^{ab} be defined by

$$\hat{P}_s^D = \hat{p}^a \xi_a + \frac{1}{2} \hat{S}^{ab} \nabla_a \xi_b. \quad (191)$$

Differentiating this and varying over all generalized Killing fields shows that

$$\frac{D\hat{p}^a}{ds} = q \hat{F}^a{}_{b} \dot{z}_s^b + \frac{1}{2} R_{bcd}{}^a \hat{S}^{bc} \dot{z}_s^d + \hat{F}^a, \quad \frac{D\hat{S}^{ab}}{ds} = 2 \hat{p}^{[a} \dot{z}_s^{b]} + \hat{N}^{ab}, \quad (192)$$

where

$$\hat{F}_a = \frac{1}{2} \sum_{n=2}^{\infty} \frac{1}{n!} \hat{I}^{d_1 \dots d_n bc} \nabla_a g_{bc, d_1 \dots d_n} + \sum_{n=1}^{\infty} \frac{n}{(n+1)!} q^{c_1 \dots c_n b} \nabla_a \hat{F}_{bc_1, c_2 \dots c_n}, \quad (193)$$

$$\begin{aligned} \hat{N}^{ab} = & \sum_{n=2}^{\infty} \frac{2}{n!} g^{f[b} (\hat{I}^{c_1 \dots c_n | a] d} g_{df, c_1 \dots c_n} + \frac{n}{2} \hat{I}^{a] c_1 \dots c_{n-1} dh} g_{dh, c_1 \dots c_{n-1} f}) \\ & + \sum_{n=0}^{\infty} \frac{2}{n!} g^{f[b} q^{a] c_1 \dots c_n d} \hat{F}_{df, c_1 \dots c_n}. \end{aligned} \quad (194)$$

Electromagnetic forces and torques defined in this way first arise at dipole order. The (monopole) Lorentz force depends—unlike any other electromagnetic terms—on \dot{z}_s^a . It has therefore been separated out explicitly in (192). There is no similarly velocity-dependent electromagnetic torque.

Defining the force to exclude the Lorentz force has the advantage that if ψ^a is Killing and preserves \hat{F}_{ab} , the associated conservation law implies that

$$\hat{F}_a \psi^a + \frac{1}{2} \hat{N}_{ab} \nabla^a \psi^b = 0. \quad (195)$$

This does not involve q , and is directly analogous to the scalar result (106).

4.3.5 Center of Mass

The electromagnetic laws of motion (192)–(194) depend on both the foliation $\{\mathfrak{B}_s\}$ and the worldline \mathcal{Z} . Center of mass conditions may be used to fix these structures as described in Sect. 3.8. An evolution equation for the center of mass position γ_s can then be obtained by differentiating $\hat{p}_a \hat{S}^{ab} = 0$. The result differs slightly from (111) due to the additional velocity-dependence associated with the Lorentz force. Adapting the methods of [31], the electromagnetic momentum-velocity relation may be shown to be

$$\hat{m} \dot{\gamma}_s^a = \hat{p}^a - \hat{N}^a{}_b u^b - \frac{\hat{S}^{ab} [\hat{m} \hat{F}_b + (\hat{p}^c - \hat{N}^c{}_h u^h) (q \hat{F}_{bc} - \frac{1}{2} R_{bcdf} \hat{S}^{df})]}{\hat{m}^2 - \frac{1}{2} \hat{S}^{pq} (q \hat{F}_{pq} - \frac{1}{2} R_{pqrs} \hat{S}^{rs})} \quad (196)$$

when s has been chosen such that $\dot{\gamma}_s^a \hat{p}_a = -\hat{m}$ and u^a is the unit timelike vector satisfying $\hat{p}^a = \hat{m} u^a$.

Although a precise set of assumptions which imply this are not known, it is assumed here that the center of mass condition (111) admits a unique timelike solution in a sufficiently broad class of physical systems. Inspection of (196) shows that a breakdown of the center of mass condition must occur whenever

$$\hat{m}^2 - \frac{1}{2} \hat{S}^{bc} \left(q \hat{F}_{bc} - \frac{1}{2} R_{bcdf} \hat{S}^{df} \right) = 0. \quad (197)$$

This is sufficient but not necessary. While the $q = 0$ case was dismissed in Sect. 3.8 as unlikely to be physically relevant, the charged case is potentially more interesting. Consider an electron²⁴ in a magnetic field of order B . Setting $q = e$, $\hat{m} = m_e$, $R_{abc}{}^d = 0$, and $\hat{S} = \hbar/2$, the denominator in (196) can diverge when $B \sim 2m_e^2/e\hbar \sim 10^{14}$ Gauss. This may be viewed as the field strength at which an electron's dipole energy $\hbar B/2$ becomes comparable to its rest mass. Quantum mechanically, it is also

²⁴It is unclear that there is any sense in which an electron's behavior can be modeled using equations derived for classical extended charges. Nevertheless, the example appears to be suggestive.

the field strength at which the separation between (Landau) energy levels becomes comparable to the rest mass energy. Indeed, this is the scale at which quantum electrodynamics is expected to become dominant. Although systems with 10^{14} Gauss magnetic fields are far from direct laboratory experience, such fields are believed to exist around some neutron stars [45]. Even in somewhat smaller magnetic fields, hidden momentum effects predicted by the classical theory can become very large. Whether or not this has qualitative consequences for neutron star astrophysics is an open question.

If the center of mass can be defined and the classical laws of physics remain valid, (196) may be combined with (192)–(194) to yield very general laws of motion. As in the scalar case, \hat{S}^{ab} can also be reduced to a single spin vector \hat{S}^a satisfying (113). Similarly, the mass varies according to (114). Unlike in the scalar case, matter coupled to electromagnetic fields can change mass only at dipole and higher orders. Such effects are related to changes in a body's internal energy due to work performed by (or against) the ambient fields [24].

4.3.6 Monopole Approximation

In simple cases, the laws of motion governing an extended charge distribution may be truncated at monopole order. Within this approximation, $\hat{F}_a = \hat{N}_{ab} = 0$ and (192) reduces to

$$\frac{D\hat{p}^a}{ds} = q\hat{F}^a{}_b\dot{\gamma}_s^b + \frac{1}{2}R_{bcd}{}^a\hat{S}^{bc}\dot{\gamma}_s^d, \quad \frac{D\hat{S}_{ab}}{ds} = 2\hat{p}^{[a}\dot{\gamma}_s^{b]}. \quad (198)$$

Contracting the second of these equations with \hat{S}_{ab} while using (110) again shows that $\hat{S}^2 := \hat{S}^a\hat{S}_a = (\text{constant})$. An object which is initially not spinning therefore remains non-spinning in this approximation. Consider these cases for simplicity. The momentum-velocity relation then reduces to $\hat{p}^a = \hat{m}\dot{\gamma}_s^a$, the mass remains constant, and the body accelerates via the Lorentz force law

$$\hat{m}\ddot{\gamma}_s^a = q\hat{F}^a{}_b\dot{\gamma}_s^b \quad (199)$$

in the effective electromagnetic field \hat{F}_{ab} . The effective field always satisfies the vacuum Maxwell equations. It is generically distinct from the physical field F_{ab} which governs the acceleration of nearby test charges.

In many cases of interest, it is useful to model F_{ab} as the sum of some external field F_{ab}^{ext} and the retarded field associated with a body's charge distribution:

$$F_{ab} = F_{ab}^{\text{ext}} + 2 \int_{\mathfrak{M}} \nabla_{[a} G_{b]b'}^- J^{b'} dV'. \quad (200)$$

In these cases, it follows from (177) and (182) that the effective field must satisfy

$$\hat{F}_{ab} = F_{ab}^{\text{ext}} + \int_{\mathcal{W}} \nabla_{[a} (G_{b]b'}^- - G_{b]b'}^+ + V_{b]b'}) J^{b'} dV'. \quad (201)$$

Performing a point particle limit as discussed in Sect. 4.2.4 and [3, 28], the lowest-order self-interaction effects follow from (201) with a pointlike current. Through first order in the expansion parameter λ ,

$$\hat{F}_{ab} = F_{ab}^{\text{ext}} + q \int \nabla_{[a} (G_{b]b'}^- - G_{b]b'}^+ + V_{b]b'}) \dot{\gamma}_s^{b'} ds'. \quad (202)$$

Evaluating this on γ_s and recalling the projection operator $h^{ab} = g^{ab} + \dot{\gamma}_s^a \dot{\gamma}_s^b$, it may be shown that [10]

$$\begin{aligned} \hat{F}_{ab} = F_{ab}^{\text{ext}} + \frac{4}{3} q \dot{\gamma}_s^l g_{l[a} h_{b]}^c \dot{\gamma}_s^d [(q/\hat{m}) \dot{\gamma}_s^f \nabla_f F_{cd}^{\text{ext}} + (q/\hat{m})^2 g^{fh} F_{cf}^{\text{ext}} F_{hd}^{\text{ext}} \\ + \frac{1}{2} R_{cd}] + 2q \lim_{\epsilon \rightarrow 0^+} \int_{-\infty}^{s-\epsilon} \nabla_{[a} G_{b]b'}^-(\gamma_s, \gamma_{s'}) \dot{\gamma}_s^b \dot{\gamma}_{s'}^{b'} ds'. \end{aligned} \quad (203)$$

Substitution into (199) finally yields the equation of motion for a self-interacting “pointlike” electric charge:

$$\begin{aligned} \hat{m} \ddot{\gamma}_s^a = q g^{ab} F_{bc}^{\text{ext}} \dot{\gamma}_s^c + \frac{2}{3} (q^3/\hat{m}) h^{ab} \dot{\gamma}_s^c [\dot{\gamma}_s^d \nabla_d F_{bc}^{\text{ext}} + (q/\hat{m}) g^{df} F_{bd}^{\text{ext}} F_{fc}^{\text{ext}}] \\ + \frac{1}{3} q^2 h^{ab} R_{bc} \dot{\gamma}_s^c + 2q^2 \lim_{\epsilon \rightarrow 0^+} \int_{-\infty}^{s-\epsilon} \nabla_{[a} G_{b]b'}^-(\gamma_s, \gamma_{s'}) \dot{\gamma}_s^b \dot{\gamma}_{s'}^{b'} ds'. \end{aligned} \quad (204)$$

In curved spacetime, this is a reduced-order version—see Footnote 22—of a result first obtained by DeWitt and Brehme [21] (with corrections due to Hobbs [46]). The second line of (204) vanishes in flat spacetime, leaving only

$$\hat{m} \ddot{\gamma}_s^a = q g^{ab} F_{bc}^{\text{ext}} \dot{\gamma}_s^c + \frac{2}{3} (q^3/\hat{m}) h^{ab} \dot{\gamma}_s^c [\dot{\gamma}_s^d \nabla_d F_{bc}^{\text{ext}} + (q/\hat{m}) g^{df} F_{bd}^{\text{ext}} F_{fc}^{\text{ext}}]. \quad (205)$$

This is essentially the Abraham-Lorentz-Dirac equation [8], but in a reduced-order form typically attributed to Landau and Lifshitz [47].

While instructive, the neglect of spin and electromagnetic dipole effects in (204) can be overly restrictive. This restriction is easily dropped by making use of the general multipole expansions derived above. The resulting changes are qualitatively significant [3] (see also [28]): A hidden momentum appears, external fields may change an object’s rest mass, and the spin magnitude may change due to torques exerted by F_{ab}^{ext} .

For monopole point particles in flat spacetime, the use of \hat{F}_{ab} instead of F_{ab} in the laws of motion was first suggested by Dirac [48]. The appropriate generalization for monopole particles in curved spacetimes was obtained much more recently by Detweiler and Whiting [29]. Both of these proposals were essentially physically-motivated axioms intended to define the dynamics of point charges. The discussion here, which follows [3], shows that these regularization schemes are actually limits of laws of motion which hold rigorously for nonsingular extended charge distributions. Once the general laws of motion (192)–(194) and (196) have been derived, more explicit results such as (204) follow very easily. So do their spin-dependent generalizations.

4.4 General Relativity

All results discussed up to this point assume that the spacetime metric is known beforehand and has been fixed. This assumption may be relaxed. Doing so allows the consideration of self-gravitating masses in general relativity. We take a minimal approach to this problem by adapting the techniques of the previous sections as closely as possible. Although there are some deficiencies to this approach, considerable progress can still be made.

Let the spacetime be described by (\mathcal{M}, g_{ab}) and the body of interest be contained inside a spatially-compact worldtube $\mathfrak{W} \subset \mathcal{M}$. Only the purely gravitational problem is considered here, meaning that objects can interact with each other solely via their influence on the metric; electromagnetic and similar long-range interactions are excluded. It follows that $T_{\text{body}}^{ab} = T_{\text{tot}}^{ab}$ inside \mathfrak{W} . Letting g_{ab} be a solution to Einstein's equation

$$R_{ab} - \frac{1}{2}g_{ab}R = 8\pi g_{ac}g_{bd}T_{\text{body}}^{cd}, \quad (206)$$

it follows that

$$\nabla_b T_{\text{body}}^{ab} = 0. \quad (207)$$

These two equations replace, e.g., (73) and (77) used to understand the motion of scalar charges. Unlike in the scalar or electromagnetic cases, the gravitational law of motion (207) is a consequence of the field equation, not an independent assumption.

Both T_{body}^{ab} and the metric inside \mathfrak{W} are assumed to be smooth. This precludes the consideration of black holes. Although unfortunate, it appears difficult to remove this restriction in a non-perturbative theory which describes the motions of individual objects (and not only characteristics of the entire spacetime). While quantities such as momenta might be associated with a black hole horizon [49, 50], adopting such definitions typically excludes the discussion of objects without horizons. Alternatively, one may consider an effective background and compute momenta associated

with, e.g., the Landau-Lifshitz pseudotensor [51, 52]. This is troublesome as well. Nevertheless, the motion of black holes can be sensibly discussed within certain approximation schemes [10, 53, 54]. These consider only the metric outside of the body of interest, and apply versions of matched asymptotic expansions in appropriate “buffer regions.” We instead consider internal metrics as well as external ones, but do not require the existence of a buffer region.

As in other theories, the laws of motion derived here involve an effective field which is distinct from the physical one. In general relativity, the relevant field is the metric. We therefore use two metrics, which makes index raising and lowering ambiguous. All factors of the appropriate metric are therefore displayed explicitly in this section.

4.4.1 Generalized Momentum

As in scalar and electromagnetic systems, the first step to understanding the motion of a self-gravitating mass is to write down a generalized momentum. It is this momentum which is used to describe an object’s large-scale behavior. Introducing a foliation $\{\mathfrak{B}_s\}$ of \mathfrak{W} and a worldline \mathcal{Z} , the linear and angular momenta proposed by Dixon [6, 17, 24] are conjugate to generalized Killing fields constructed using the physical metric g_{ab} . Adding an extra argument to K_G to reflect this, the appropriate generalized momentum is

$$P_s^D(\xi) := \int_{\mathfrak{B}_s} T_{\text{body}}^{ab} g_{bc} \xi^c dS_a, \quad \xi^a \in K_G(\mathcal{Z}, \{\mathfrak{B}_s\}; g). \quad (208)$$

For each s , this is an element of the ten-dimensional vector space $K_G^*(\mathcal{Z}, \{\mathfrak{B}_s\}; g)$. The associated linear and angular momenta have a number of useful properties [6, 31, 55, 56]. Using (207), their time evolution satisfies

$$\frac{d}{ds} P_s^D(\xi) = \frac{1}{2} \int_{\mathfrak{B}_s} T_{\text{body}}^{ab} \mathcal{L}_\xi g_{ab} dS. \quad (209)$$

If $\mathcal{L}_\xi g_{ab}$ varies slowly throughout \mathfrak{B}_s , forces and torques can be expanded in multipole series as described in [4, 6] and in Sect. 4.2.2.

While such assumptions can be useful for test bodies, they are too strong for self-gravitating masses. Moving beyond the test body regime first requires the introduction of an effective metric \hat{g}_{ab} such that—after appropriate renormalizations—the $\mathcal{L}_\xi g_{ab}$ appearing in (209) can be replaced by $\mathcal{L}_\xi \hat{g}_{ab}$. If $\mathcal{L}_\xi \hat{g}_{ab}$ varies slowly, the resulting integral for the generalized force can be expanded in a multipole series in the usual way. One additional subtlety which occurs in the gravitational problem is that even if a particular \hat{g}_{ab} can itself be adequately approximated using a low-order Taylor expansion, the same can not necessarily be said for $\mathcal{L}_\xi \hat{g}_{ab}$ when $\xi^a \in K_G(\mathcal{Z}, \{\mathfrak{B}_s\}; g)$. The generalized Killing fields associated with Dixon’s momenta involve the physical metric and all of its attendant difficulties. These difficulties are partially inherited by the generalized Killing fields used to define P_s^D .

One way out of this problem²⁵ is to choose a bare momentum $P_s(\xi)$ defined by an integral which is structurally identical to (209), but where all ξ^a are elements of $K_G(\mathcal{Z}, \{\mathfrak{B}_s\}; \hat{g})$ rather than $K_G(\mathcal{Z}, \{\mathfrak{B}_s\}; g)$. Let

$$P_s(\xi) := \int_{\mathfrak{B}_s} T_{\text{body}}^{ab} g_{bc} \xi^c dS_a, \quad \xi^a \in K_G(\mathcal{Z}, \{\mathfrak{B}_s\}; \hat{g}). \quad (210)$$

We take this to be the bare momentum of a self-gravitating mass. The effective metric which appears here is to be regarded at this stage as an additional parameter. The generalized force dP_s/ds follows from a trivial modification of (209). Furthermore, Dixon's momenta are recovered in a test mass limit where $\hat{g}_{ab} \approx g_b$. If there exists a $\psi^a \in K_G(\mathcal{Z}, \{\mathfrak{B}_s\}; \hat{g})$ such that $\mathcal{L}_\psi g_{ab} = 0$, it is evident that $P_s(\psi)$ must be conserved.

4.4.2 Self-fields and Laws of Motion

There are many possible ways to extract an effective metric \hat{g}_{ab} from the physical metric g_{ab} . The simplest generalization of the previous discussions involves a two-point tensor field $G_{aba'b'}(x, x')$ which satisfies

$$G_{aba'b'} = G_{(ab)a'b'} = G_{ab(a'b')} \quad (211)$$

and

$$G_{aba'b'}(x, x') = G_{a'b'ab}(x', x). \quad (212)$$

For any such propagator, consider an effective metric \hat{g}_{ab} defined via

$$g_{ab} = \hat{g}_{ab} + g_{ab}^S, \quad (213)$$

where

$$g_{ab}^S[\mathfrak{R}] := \int_{\mathfrak{R}} G_{aba'b'} T_{\text{body}}^{a'b'} dV' \quad (214)$$

and $g_{ab}^S = g_{ab}^S[\mathfrak{M}]$. Note that the volume element in this “self-field” is the one associated with g_{ab} , not \hat{g}_{ab} . Substituting (213) into the appropriately-modified form of (209) shows that the s -integral of the self-field's contribution to dP_s/ds has the form (85) with force density

²⁵It would be more elegant to instead demand that $K_G(\mathcal{Z}, \{\mathfrak{B}_s\}; \hat{g})$ and $K_G(\mathcal{Z}, \{\mathfrak{B}_s\}; g)$ be identical or otherwise closely related. Such an assumption would restrict possible relations between g_{ab} and \hat{g}_{ab} , and is an avenue which has not been explored.

$$f = \frac{1}{2} T_{\text{body}}^{ab} T_{\text{body}}^{a'b'} (\xi^c \nabla_c G_{aba'b'} + 2 \nabla_a \xi^c G_{bca'b'}). \quad (215)$$

Applying (87) and related results then transforms the law of motion into

$$\frac{d}{ds} \hat{P}_s = \frac{1}{2} \int_{\mathfrak{B}_s} T_{\text{body}}^{ab} \mathcal{L}_\xi \hat{g}_{ab} dS + \frac{1}{4} \int_{\mathfrak{B}_s} dS \int_{\mathfrak{M}} dV' T_{\text{body}}^{ab} T_{\text{body}}^{a'b'} \mathcal{L}_\xi G_{aba'b'}, \quad (216)$$

where $\hat{P}_s = P_s + E_s$ and

$$E_s = \frac{1}{4} \left(\int_{\mathfrak{B}_s^+} T_{\text{body}}^{ab} \mathcal{L}_\xi g_{ab}^S [\mathfrak{B}_s^-] dV - \int_{\mathfrak{B}_s^-} T_{\text{body}}^{ab} \mathcal{L}_\xi g_{ab}^S [\mathfrak{B}_s^+] dV \right). \quad (217)$$

E_s is a functional of T_{body}^{ab} which effectively acts like the momentum of the self-field. If $\mathcal{L}_\xi G_{aba'b'}$ is a linear functional of $\mathcal{L}_\xi \hat{g}_{ab}$, the term involving $\mathcal{L}_\xi G_{aba'b'}$ in (216) renormalizes a body's quadrupole and higher multipole moments. In these cases, a multipole expansion of (216) yields

$$\frac{d}{ds} \hat{P}_s(\xi) = \frac{1}{2} \sum_{n=2}^{\infty} \frac{1}{n!} \hat{I}^{c_1 \dots c_n ab} \mathcal{L}_\xi \hat{g}_{ab, c_1 \dots c_n}. \quad (218)$$

The tensor extensions appearing here are extensions of \hat{g}_{ab} in a spacetime with metric \hat{g}_{ab} . This means, for example, that $\hat{g}_{ab,c} = 0$ and $\hat{g}_{ab,cd} = \frac{2}{3} \hat{R}_{a(cd)}^f \hat{g}_{bf}$ [cf. (154)].

Equation (218) represents not a particular law of motion, but a class of them. This is because many different propagators may be found which satisfy (211) and (212), and whose Lie derivatives with respect to ξ^a are quasi-local in $\mathcal{L}_\xi \hat{g}_{ab}$. Choosing different propagators with these properties leads to different effective metrics, different self-momenta, and different effective multipole moments. Any of these combinations satisfies (216), and also (218) when the appropriate \hat{g}_{ab} is sufficiently well-behaved. It is of course preferable to choose a propagator such that the associated multipole series may “typically” be truncated at low order without significant loss of accuracy. This condition is vague. In the electromagnetic and scalar theories, a (rather imperfect) proxy was the requirement that the effective fields be solutions to the vacuum field equation. The analogous condition in general relativity would be $\hat{R}_{ab} = 0$, where \hat{R}_{ab} denotes the Ricci tensor associated with \hat{g}_{ab} . This does not appear to be possible within the currently-considered class of effective metrics.

We take a pragmatic approach and suppose that $G_{aba'b'}$ is the Detweiler-Whiting S-type Green function associated with

$$\begin{aligned} & \hat{g}^{cd} \hat{\nabla}_c \hat{\nabla}_d G_{aba'b'} - [2 \hat{g}^{cf} \hat{R}_{f(ab)}^d + \frac{1}{2} (\hat{g}^{cd} \hat{R}_{ab} + \hat{g}_{ab} \hat{g}^{cf} \hat{g}^{dh} \hat{R}_{fh})] G_{cda'b'} \\ & = -16\pi (\hat{g}_{ac} \hat{g}_{bd} - \frac{1}{2} \hat{g}_{ab} \hat{g}_{cd}) \hat{g}^c_{(a} \hat{g}^d_{b')} \hat{\delta}(x, x'). \end{aligned} \quad (219)$$

This is essentially the prescription suggested in [5]. In terms of retarded and advanced solutions $G_{aba'b'}^\pm$ to (219), the S-type Green function satisfies

$$G_{aba'b'} = \frac{1}{2}(G_{aba'b'}^+ + G_{aba'b'}^- - V_{aba'b'}) \quad (220)$$

for some bitensor $V_{aba'b'}$ which is an appropriate solution to the homogeneous version of (219). Somewhat more explicitly,

$$G_{aba'b'} = 2(\hat{g}_{ac}\hat{g}_{bd} - \frac{1}{2}\hat{g}_{ab}\hat{g}_{cd})\hat{g}^c_{(a'}\hat{g}^d_{b')}\hat{\Delta}^{1/2}\delta(\hat{\sigma}) - \frac{1}{2}V_{aba'b'}\Theta(\hat{\sigma}). \quad (221)$$

Coupling this Green function with (213) and (214) defines \hat{g}_{ab} in terms of g_{ab} . Unlike in scalar or electromagnetic theories, the definition of the effective field is highly implicit in general relativity. It reduces to a simple subtraction only in linear perturbation theory. More generally, the Green function itself depends on the field which one intends to find, and must be found by iteration or related methods.

Despite the nonlinearity of the map $g_{ab} \rightarrow \hat{g}_{ab}$, the effective metric does not necessarily satisfy the vacuum Einstein equation. The specific differential equation (219) is nevertheless inspired by Lorenz-gauge perturbation theory, and has the following desirable properties:

1. If g_{ab} is sufficiently close to a background metric \bar{g}_{ab} satisfying the vacuum Einstein equation $\bar{R}_{ab} = 0$, \hat{g}_{ab} satisfies the vacuum Einstein equation linearized about \bar{g}_{ab} .
2. The differential operator is self-adjoint.
3. The trace of (219) can be solved independently of the full equation.

The first condition guarantees that the effective metric is reasonable at least in first order perturbation theory. Self-adjointness is useful because it allows the reciprocity condition (212) to be enforced. Finally, it is important for technical reasons to know the trace $\hat{g}^{ab}G_{aba'b'}$ of $G_{aba'b'}$. The form of (219) may be used to show that this satisfies

$$\hat{g}^{ab}G_{aba'b'} = \mathcal{G}\hat{g}_{a'b'}, \quad (222)$$

where \mathcal{G} is an S-type Detweiler-Whiting Green function for the nonminimally-coupled scalar equation

$$(\hat{g}^{ab}\hat{\nabla}_a\hat{\nabla}_b + \frac{1}{2}\hat{R})\mathcal{G} = 16\pi\hat{\delta}(x, x'). \quad (223)$$

4.4.3 Linear and Angular Momentum

Using the Green function associated with (219) to construct \hat{g}_{ab} and \hat{P}_s , linear and angular momenta may be extracted in the usual way. For any $\xi^a \in K_G(\mathcal{Z}, \{\mathfrak{B}_s\}; \hat{g})$ and any $z_s \in \mathcal{Z}$, let

$$\hat{P}_s(\xi) = \hat{p}_a(z_s, s)\xi^a(z_s) + \frac{1}{2}\hat{S}^a{}_b\hat{\nabla}_a\xi^b(z_s). \quad (224)$$

The angular momentum defined in this way is antisymmetric in the sense the $\hat{S}^{(a}{}_{c}\hat{g}^{b)c} = 0$. Differentiating (224) using a covariant derivative associated with \hat{g}_{ab} shows that

$$\frac{\hat{D}\hat{p}_a}{ds} = -\frac{1}{2}\hat{R}_{abc}{}^d\hat{z}_s^b\hat{S}^c{}_d + \hat{F}_a, \quad \frac{\hat{D}\hat{S}^a{}_b}{ds} = (\hat{g}^{ac}\hat{g}_{bd} - \delta_d^a\delta_b^c)\hat{p}_c\hat{z}_s^d + \hat{N}^a{}_b, \quad (225)$$

where

$$\hat{F}_a = \frac{1}{2}\sum_{n=2}^{\infty}\frac{1}{n!}\hat{I}^{d_1\cdots d_n bc}\hat{\nabla}_a\hat{g}_{bc, d_1\cdots d_n}, \quad (226)$$

and

$$\hat{N}^a{}_c\hat{g}^{bc} = \sum_{n=2}^{\infty}\frac{2}{n!}\hat{g}^{f[b}\left(\hat{I}^{c_1\cdots c_n]a]d}\hat{g}_{df, c_1\cdots c_n} + \frac{n}{2}\hat{I}^{a]c_1\cdots c_{n-1}dh}\hat{g}_{dh, c_1\cdots c_{n-1}f}\right). \quad (227)$$

$\hat{I}^{c_1\cdots c_n ab}$ represents the renormalized 2^n -pole moment of the body's stress-energy tensor. Despite the notation, these are not the same as the moments appearing in the scalar and electromagnetic multipole expansions (156) and (188), which are renormalized differently. In the test body limit where $\hat{g}_{ab} \approx g_{ab}$, (225)–(227) reduce to the multipole expansions derived by Dixon [6]. More generally, they show—that if the multipole expansion is valid—that with appropriate renormalizations, a self-gravitating body moves instantaneously as though it were a test body in the effective metric \hat{g}_{ab} . Note in particular that the derivatives of the momenta which appear in the evolution equations are derivatives associated with \hat{g}_{ab} , not g_{ab} . This is a consequence of choosing the generalized Killing fields to be constructed using \hat{g}_{ab} instead of g_{ab} .

4.4.4 Center of Mass

A center of mass frame may be defined by choosing an appropriate foliation together with the worldline $\{\gamma_s\}$ which guarantees that $\hat{p}_a\hat{S}^a{}_b = 0$ when $z_s = \gamma_s$. A body's linear momentum is then related to its center of mass velocity via an appropriately “hatted” version of (111).

4.4.5 A Simple Case

If $d\hat{P}_s/ds$ is sufficiently small, a body's quadrupole and higher multipole moments might be neglected. In these cases, it follows from (225) that the motion is described by the Mathisson-Papapetrou equations in the effective metric:

$$\frac{\hat{D}\hat{p}_a}{ds} = -\frac{1}{2}\hat{R}_{abc}{}^d \dot{z}_s^b \hat{S}^c{}_d, \quad \frac{\hat{D}\hat{S}^a{}_b}{ds} = (\hat{g}^{ac}\hat{g}_{bd} - \delta_d^a \delta_b^c) \hat{p}_c \dot{z}_s^d. \quad (228)$$

Choosing $z_s = \gamma_s$, the squared spin magnitude $\hat{S}^a{}_b \hat{S}^b{}_a$ is necessarily conserved. It is therefore consistent to once again consider systems with vanishing spin. Assuming that $\hat{S}^a{}_b = 0$,

$$\frac{\hat{D}}{ds} \dot{\gamma}_s^a = 0. \quad (229)$$

Non-spinning masses whose quadrupole and higher interactions may be neglected therefore fall on geodesics associated with \hat{g}_{ab} . This generalizes the well-known result that small test bodies in general relativity fall on geodesics associated with the background spacetime.

Moving beyond the test body limit, the difficult step is to compute \hat{g}_{ab} . What is typically referred to as the first order gravitational self-force may nevertheless be derived by considering an appropriate family of successively-smaller extended masses. To lowest nontrivial order, the effective metric looks like the metric of a point particle moving on an appropriate vacuum background \bar{g}_{ab} which is close to \hat{g}_{ab} . Using overbars to denote quantities associated with \bar{g}_{ab} and assuming retarded boundary conditions,

$$\hat{g}_{ab} = \bar{g}_{ab} + \frac{1}{2}\hat{m} \int (\bar{G}_{aba'b'}^- - \bar{G}_{aba'b'}^+ + \bar{V}_{aba'b'}) \dot{\gamma}_s^{a'} \dot{\gamma}_s^{b'} ds'. \quad (230)$$

This is well-behaved even on the body's worldline. So is the connection associated with it, which may be computed using, e.g., methods described in [10]. Substituting the result into (229) recovers the MiSaTaQuWa equation commonly used to describe the first order gravitational self-force [5]. Comparisons have not yet been made with second order calculations of the gravitational self-force which have recently been completed using other methods [57, 58].

4.4.6 Future Directions

The formulation of the gravitational problem of motion remains somewhat unsatisfactory. Most importantly, the effective metric which has been adopted here (and in [5]) is somewhat ad hoc. It is inspired by Lorenz-gauge perturbation theory, but this has no particular significance other than being one way to guarantee hyperbolic field

equations. More seriously, the \hat{g}_{ab} defined here does not satisfy the vacuum Einstein equation except in certain limiting cases. This seems unnatural. It would be preferable if the general relativistic laws of motion were completely identical in structure to the laws satisfied by test bodies moving in vacuum backgrounds. A condition like $\hat{R}_{ab} = 0$ would also suggest, at least intuitively, that the associated \hat{g}_{ab} might vary slowly in a wide variety of physical systems. The importance of slow variation to the application of multipole expansions makes it extremely interesting to search for an effective metric which admits a multipole expansion like (218) while also being an exact solution to the vacuum Einstein equation. Although such a metric²⁶ has not yet been found, there are several promising routes by which progress might be made.

The simplest conceivable modifications of the formalism described here retains the bare momentum (210) while altering the effective metric \hat{g}_{ab} . It is trivial to accomplish this by, for example, modifying the differential equation satisfied by $G_{aba'b'}$ or by introducing n -point propagators similar to those in (44). It can also be useful to alter the functional relation (213) between g_{ab} , \hat{g}_{ab} , and any integrals which may be present. Despite being very simple analytically, relating two metrics to one another via the addition of a second-rank tensor is geometrically rather awkward.

Better-motivated functional relationships between the physical and effective metrics may be more convenient. Geometrically, perhaps the simplest conceivable map between two metrics is a conformal transformation. If $g_{ab} = \Omega^2 \hat{g}_{ab}$ for an appropriate Ω , it is straightforward²⁷ to obtain an effective metric which exactly satisfies the trace $\hat{R} = 0$ of the vacuum Einstein equation. This is not enough, however. More degrees of freedom are necessary. It may be possible to go further by combining an appropriate conformal factor with a “generalized Kerr-Schild transformation” so that

$$g_{ab} = \Omega^2(\hat{g}_{ab} + \ell_{(a}k_{b)}) \quad (231)$$

for some 1-forms ℓ_a and k_a which are null with respect to \hat{g}_{ab} (and therefore null with respect to g_{ab} as well). Despite the simplicity of this expansion, there is strong evidence that it is very general: Given any analytic g_{ab} , (Ω, ℓ_a, k_a) triplets can always be chosen, at least locally, which guarantee that \hat{g}_{ab} is flat [59]. Although it is not known how such choices interact with the laws of motion, the possibility of a flat (or conformally flat) effective metric is intriguing. Among other benefits, it might eliminate the need for generalized Killing vectors.²⁸

²⁶It could also be interesting to consider reformulations where an effective connection is sought instead of an effective metric.

²⁷Analyzing the effect of a conformal factor on the laws of motion is similar to considering objects coupled to a particular type of nonlinear scalar field. Despite the nonlinearity, such systems can be understood exactly using only minimal adaptations of the formalism used to analyze the (linear) Klein-Gordon problem.

²⁸Quasi-local momenta have recently been proposed in general relativity which use isometric embeddings to lift flat Killing fields into arbitrary spacetimes [60, 61]. See also [62] for a proposal which allows conformal Killing vectors to be introduced in geometries without symmetries.

Combinations of these observations can perhaps be combined to provide one (implicit) map $g_{ab} \rightarrow \hat{g}_{ab}$ with the desired properties. It is likely simpler, however, to instead use them to construct a continuous flow of metrics ${}_{\lambda}\tilde{g}_{ab}$ which smoothly deforms $g_{ab} = {}_0\tilde{g}_{ab}$ into an appropriate $\hat{g}_{ab} = {}_{\infty}\tilde{g}_{ab}$. The λ parameter is not necessarily physical, but might be interpreted roughly as the reciprocal of the influence of a body's internal scales. Flows like these have the advantage that individual "steps" $\lambda \rightarrow \lambda + d\lambda$ can be viewed as (easily-controlled) linear perturbations. Indeed, it is straightforward to impose differential relations on the λ -dependence of ${}_{\lambda}\tilde{g}_{ab}$ which ensure that a flow removes any initial stress-energy as $\lambda \rightarrow \infty$. This requires using a 1-parameter family of Green functions ${}_{\lambda}G_{aba'b'}$ associated with Einstein's equation linearized about each ${}_{\lambda}\tilde{g}_{ab}$. Separately, it is also straightforward to construct flows which lead to well-behaved laws of motion. What is more difficult is to find a flow which accomplishes both of these tasks simultaneously. If this were found, varying λ would likely vary an object's effective metric, its effective momentum, and its effective multipole moments. While only the $\lambda \rightarrow \infty$ limit might be physical, such variations are highly reminiscent of the running couplings which arise in renormalization group flows.

Regardless, a great deal of freedom clearly exists and may be exploited to better understand the problem of motion in general relativity. The resulting insights may also shed new light on nonlinear problems more generally.

5 Discussion

The techniques described in this review provide a unified and largely non-perturbative formalism with which to better understand how objects move. Although these techniques have thus far been applied only to a handful of specific theories—Newtonian gravity, Klein-Gordon theory, electromagnetism, and general relativity—they are easily generalized.

One of the central concepts employed here is what we have called the "generalized momentum." This is used as a convenient observable with which to describe an object's motion in the large, and represents a body's momentum not as a tensor either in the interior of the spacetime or at infinity, but instead as a linear map over a more abstract vector space. This automatically takes into account the nonlocality inherent in the momentum concept and also makes explicit how particular components of the momentum can be "conjugate to," e.g., symmetry-generating vector fields.

Another important property of the generalized momentum is that it unifies a body's linear and angular momenta into a single object. Given a generalized momentum, linear and angular components can easily be extracted. This process depends, however, on extra information, namely a choice of "observer" in the sense of a preferred origin. This origin is arbitrary. It affects the angular momentum even in elementary discussions of Newtonian mechanics, but more generally influences an object's linear momentum as well. This has an interesting physical consequence: *Mathisson-Papapetrou terms arise in the evolution equations governing a body's linear and*

angular momenta due to the motion of the origin used to extract these components of the generalized momentum. Mathisson-Papapetrou effects are therefore kinematic in nature, arising from the changing “character” of each generalized (or genuine) Killing field at different points.

Once a generalized momentum has been defined as a particular linear map on a particular vector space, stress-energy conservation may be used to derive its rate of change. The resulting generalized force is another linear map on the same vector space. Letting ξ^a be a particular element of that space, generalized forces typically have the form

$$F = \int_{\mathfrak{B}_s} \rho \mathcal{L}_\xi \phi dS, \quad (232)$$

where ϕ represents some (not necessarily scalar) long-range field and ρ its source. \mathfrak{B}_s is an appropriate 3-volume and dS an associated volume element. Integrals like these can be difficult to evaluate directly, so it is important to seek approximations in practical problems. The simplest such approximations involve some combination of test body and smallness conditions which guarantee that $\mathcal{L}_\xi \phi$ “varies slowly” throughout \mathfrak{B}_s . A multipole expansion can then be performed to express F in terms of ϕ and its derivatives as well as the multipole moments of ρ computed on a (largely arbitrary) worldline $\{z_s\}$: $F = q(z_s, s) \mathcal{L}_\xi \phi(z_s) + q^a(z_s, s) \mathcal{L}_\xi \nabla_a \phi(z_s) + \dots$

It is far more difficult to obtain useful multipole expansions when an object’s self-field can no longer be ignored. The potentially-complicated nature of ρ is then inherited by ϕ via the field equation, and there is typically no sense in which $\mathcal{L}_\xi \phi$ can be approximated using Taylor-like expansions inside \mathfrak{B}_s . Coping with this is perhaps the main theoretical problem associated with self-interaction in the classical theory of motion.

Self-interaction is dealt with here by considering methods which alter the integrand in (232) without affecting the integral as a whole (or affecting it only via terms which can be interpreted as renormalizations). Particularly useful for this purpose are nonlocal deformations $\phi \rightarrow \hat{\phi}$ generated by appropriate classes of propagators. Although the cases discussed here have used 2-point Green functions associated with appropriate field equations, other types of propagators can be more useful in other contexts. Regardless, the large variety of possible deformations may be tailored to optimally simplify whichever problem is at hand.

In particular, it is often possible to find a deformation $\phi \rightarrow \hat{\phi}$ such that $\mathcal{L}_\xi \hat{\phi}$ varies slowly even when $\mathcal{L}_\xi \phi$ does not. Appropriately-modified multipole expansions can then be applied much more generally than might have been expected. This leads to the main physical principle which dictates motion in each of the theories we have considered: *Laws governing the motion of self-interacting masses are structurally identical to laws governing the motion of test bodies.* The fields appearing in these laws are nontrivial, however. Objects generally act as though they were accelerated not by the physical fields (i.e., ϕ), but by certain “effective fields” instead.

The use of effective fields to understand problems of motion is not new per se. Standard formulations of Newtonian celestial mechanics heavily rely, for example, on external gravitational potentials which are distinct from the physical potentials. What has been stressed here is that generalizing the external field concept (where the “external” label is replaced by the more appropriate “effective”) is similarly essential for a simple understanding of motion even in highly non-Newtonian regimes. All classical results on the self-force can easily be recovered, for example, once the appropriately-formulated laws of motion have been derived. Even point particle limits of these laws are well-defined precisely as stated; they require no independent postulates or regularizations.

The standard deformation $\phi \rightarrow \hat{\phi}$ of the physical Newtonian gravitational potential into its effective counterpart leaves forces and torques completely unaffected: The Newtonian self-force and self-torque both vanish. Other theories are not so simple. Writing generalized forces in terms of effective fields generally requires the introduction of compensating counterterms. It is only when these counterterms have a particularly simple form that the associated effective field is likely to be useful. Indeed, we have considered systems where these terms act only to make a body’s momenta or other multipole moments appear to be shifted from those moments which might have been deduced using knowledge of a body’s internal structure. The details of this structure are rarely known in practice, in which case it is natural to “remove” residual forces and torques by appropriately redefining an object’s momenta or other multipole moments. These are renormalizations. They affect generic extended objects, and are always finite in this context. Considerable effort has been devoted here to identifying renormalizations and interpreting them physically.

The resulting techniques have shown that a large variety of renormalizations are possible even in simple theories. The effective 4-momentum of an electric charge may differ from its bare momentum not only in length (i.e., mass), but also in direction. Spins and center of mass positions can be renormalized as well. Adding the additional complication of a curved spacetime, even the quadrupole and higher multipole moments associated with a body’s stress-energy tensor may be dynamically shifted via the forces exerted by its self-field.

Two general mechanisms have been shown responsible for these effects. Both of these are associated with generalizations of—or failures to generalize—Newton’s third law. One mechanism relates from a direct violation of this law, while the other arises from an inability to fully take advantage of “action-reaction cancellations.” The second of these is simpler and affects a body’s linear and angular momenta. It is associated with self-fields which are nonlocal in time, in which case forces are sourced in four dimensions but act on matter only in three-dimensional slices. If the propagators associated with these statements satisfy certain minimal constraints, the inability to construct action-reaction pairs in this context conspires to dynamically shift an object’s momenta. Such effects are essentially universal in relativistic theories, but can also be relevant for some non-relativistic systems.

The second renormalization mechanism discussed here stems from more direct violations of Newton’s third law. Mathematically, it is related to the behavior of

the relevant propagators under Lie dragging. If, say, a self-field is defined in terms of a propagator G , and $\mathcal{L}_\xi G$ depends only on $\mathcal{L}_\xi \phi$ for some field ϕ , the multipole moments coupling to ϕ are renormalized by the self-force. In the cases considered here, ϕ was the metric and the relevant moments were those associated with a body's stress-energy tensor. The same mechanism applied to a nonlinear scalar theory would instead renormalize a body's charge moments.

Despite the generality of these results, much remains to be learned. Besides the various technical details which remain open—some of which have been mentioned in the text—it would also be interesting to understand how the techniques developed here can be applied in new ways. It may be possible, for example, to adapt these techniques to systems where long-range fields couple to an object's surface instead of its volume. Such problems arise when considering the motion of solid objects through fluids, among other cases. More generally, it might be possible to investigate problems which are not related to motion at all. Quantities similar to (232) occur in many fields of physics and mathematics, as do various types of regularizations and renormalizations. It appears likely that the methods developed here can be applied to better understand at least some of these systems. Such speculations have only just begun to be explored.

References

1. A.I. Harte, Approximate spacetime symmetries and conservation laws. *Class. Quantum Gravity* **25**, 205008 (2008)
2. A.I. Harte, Self-forces from generalized Killing fields. *Class. Quantum Gravity* **25**, 235020 (2008)
3. A.I. Harte, Electromagnetic self-forces and generalized killing fields. *Class. Quantum Gravity* **26**, 155015 (2009)
4. A.I. Harte, Effective stress-energy tensors, self-force and broken symmetry. *Class. Quantum Gravity* **27**, 135002 (2010)
5. A.I. Harte, Mechanics of extended masses in general relativity. *Class. Quantum Gravity* **29**, 055012 (2012)
6. W.G. Dixon, Dynamics of extended bodies in general relativity. III. Equations of motion. *R. Soc. Lond. Philos. Trans. Ser. A* **277**, 59 (1974)
7. T. Erber, The classical theories of radiation reaction. *Fortschritte der Physik* **9**, 343 (1961)
8. J.D. Jackson, *Classical Electrodynamics* (Wiley, New York, 1999)
9. H. Spohn, *Dynamics of Charged Particles and Their Radiation Field* (Cambridge University Press, Cambridge, 2004)
10. E. Poisson, A. Pound, I. Vega, The motion of point particles in curved spacetime. *Living Rev. Relativ.* **14**, (2011)
11. L. Barack, Gravitational self-force in extreme mass-ratio inspirals. *Class. Quantum Gravity* **26**, 213001 (2009)
12. L. Blanchet, Gravitational radiation from post-Newtonian sources and inspiralling compact binaries. *Living Rev. Relativ.* **17**, (2014)
13. T. Futamase, Y. Itoh, The post-Newtonian approximation for relativistic compact binaries. *Living Rev. Relativ.* **10** (2007)
14. S. Kopeikin, M. Efroimsky, G. Kaplan, *Relativistic Celestial Mechanics of the Solar System* (Wiley, Berlin, 2011)

15. R.M. Wald, *General Relativity* (University of Chicago Press, Chicago, 1984)
16. T. Damour, The problem of motion in Newtonian and Einsteinian gravity, in *Three Hundred Years of Gravitation*, ed. by S.W. Hawking, W. Israel (Cambridge University Press, Cambridge, 1989), p. 128
17. W.G. Dixon, Extended bodies in general relativity: their description and motion, in *Isolated Gravitating Systems in General Relativity*, ed. by J. Ehlers (1979), p. 156
18. J.E. Marsden, T.J.R. Hughes, *Mathematical Foundations of Elasticity* (Dover, New York, 1994)
19. C. Truesdell, W. Noll, *The Non-linear Field Theories of Mechanics* (Springer, Berlin, 1992)
20. W.G. Dixon, *Special Relativity: The Foundation of Macroscopic Physics* (Cambridge University Press, New York, 1978)
21. B.S. DeWitt, R.W. Brehme, Radiation damping in a gravitational field. *Ann. Phys. (NY)* **9**, 220 (1960)
22. J.L. Synge, *Relativity: The General Theory* (North-Holland, Amsterdam, 1960)
23. F. Diacu, *Relative Equilibria of the Curved N-Body Problem* (Atlantis Press, Amsterdam, 2012)
24. W.G. Dixon, Dynamics of extended bodies in general relativity. I. Momentum and angular momentum. *R. Soc. Lond. Proc. Ser. A* **314**, 499 (1970)
25. R. Geroch, Limits of spacetimes. *Commun. Math. Phys.* **13**, 180 (1969)
26. P. Havas, J.N. Goldberg, Lorentz-invariant equations of motion of point masses in the general theory of relativity. *Phys. Rev.* **128**, 398 (1962)
27. J. Ehlers, Isolated systems in general relativity. *Ann. Phys. (NY)* **336**, 279 (1980)
28. S.E. Gralla, A.I. Harte, R.M. Wald, Rigorous derivation of electromagnetic self-force. *Phys. Rev. D* **80**, 024031 (2009)
29. S. Detweiler, B.F. Whiting, Self-force via a Green's function decomposition. *Phys. Rev. D* **67**, 024025 (2003)
30. W.G. Dixon, Description of extended bodies by multipole moments in special relativity. *J. Math. Phys.* **8**, 1591 (1967)
31. J. Ehlers, E. Rudolph, Dynamics of extended bodies in general relativity center-of-mass description and quasirigidity. *Gen. Relativ. Gravit.* **8**, 197 (1977)
32. R. Schattner, The center of mass in general relativity. *Gen. Relativ. Gravit.* **10**, 377 (1979)
33. R. Schattner, The uniqueness of the center of mass in general relativity. *Gen. Relativ. Gravit.* **10**, 395 (1979)
34. W. Shockley, R.P. James, "Try simplest cases" discovery of "hidden momentum" forces on "magnetic currents". *Phys. Rev. Lett.* **18**, 876 (1967)
35. S. Coleman, J.H. van Vleck, Origin of "hidden momentum forces" on magnets. *Phys. Rev.* **171**, 1370 (1968)
36. S.E. Gralla, A.I. Harte, R.M. Wald, Bobbing and kicks in electromagnetism and gravity. *Phys. Rev. D* **81**, 104012 (2010)
37. L.F.O. Costa, J. Natário, M. Zilhão, Spacetime dynamics of spinning particles—exact gravito-electromagnetic analogies. (2012) [arXiv:1207.0470](https://arxiv.org/abs/1207.0470)
38. R.A. Matzner, Almost symmetric spaces and gravitational radiation. *J. Math. Phys.* **9**, 1657 (1968)
39. G.B. Cook, B.F. Whiting, Approximate killing vectors on S^2 . *Phys. Rev. D* **76**, 041501 (2007)
40. C. Beetle, Approximate killing fields as an eigenvalue problem. (2008) [arXiv:0808.1745](https://arxiv.org/abs/0808.1745)
41. F.G. Friedlander, *The Wave Equation on a Curved Space-time* (Cambridge University Press, Cambridge, 1975)
42. T.C. Quinn, Axiomatic approach to radiation reaction of scalar point particles in curved space-time. *Phys. Rev. D* **62**, 064029 (2000)
43. I. Bailey, W. Israel, Relativistic dynamics of extended bodies and polarized media: an eccentric approach. *Ann. Phys. (NY)* **130**, 188 (1980)
44. W.G. Dixon, Dynamics of extended bodies in general relativity. II. Moments of the charge-current vector. *R. Soc. Lond. Proc. Ser. A* **319**, 509 (1970)
45. A.K. Harding, D. Lai, Physics of strongly magnetized neutron stars. *Rep. Prog. Phys.* **69**, 2631 (2006)
46. J.M. Hobbs, A vierbein formalism of radiation damping. *Ann. Phys. (NY)* **47**, 141 (1968)

47. L.D. Landau, E.M. Lifshitz, *The Classical Theory of Fields* (Pergamon Press, New York, 1975)
48. P.A.M. Dirac, Classical theory of radiating electrons. R. Soc. Lond. Proc. Ser. A **167**, 148 (1938)
49. B. Krishnan, C.O. Lousto, Y. Zlochower, Quasilocal linear momentum in black-hole binaries. Phys. Rev. D **76**, 081501 (2007)
50. J.L. Jaramillo, R.P. Macedo, P. Moesta, L. Rezzolla, Black-hole horizons as probes of black-hole dynamics. II. Geometrical insights. Phys. Rev. D **85**, 084031 (2012)
51. D. Keppel, D.A. Nichols, Y. Chen, K.S. Thorne, Momentum flow in black-hole binaries. I. Post-Newtonian analysis of the inspiral and spin-induced bobbing. Phys. Rev. D **80**, 124015 (2009)
52. G. Lovelace, Y. Chen, M. Cohen, J.D. Kaplan, D. Keppel, K.D. Matthews, D.A. Nichols, M.A. Scheel, U. Sperhake, Momentum flow in black-hole binaries. II. Numerical simulations of equal-mass, head-on mergers with antiparallel spins. Phys. Rev. D **82**, 064031 (2010)
53. S.E. Gralla, R.M. Wald, A rigorous derivation of gravitational self-force. Class. Quantum Gravity **25**, 205009 (2008)
54. A. Pound, Self-consistent gravitational self-force. Phys. Rev. D **81**, 024023 (2010)
55. R. Schattner, M. Streubel, Properties of extended bodies in spacetimes admitting isometries. Annales de l'institut Henri Poincaré A **34**, 117 (1981)
56. M. Streubel, R. Schattner, The connection between local and asymptotic structures for isolated gravitating systems with isometries. Annales de l'institut Henri Poincaré A **34**, 145 (1981)
57. A. Pound, Second-order gravitational self-force. Phys. Rev. Lett. **109**, 051101 (2012)
58. S.E. Gralla, Second-order gravitational self-force. Phys. Rev. D **85**, 124011 (2012)
59. J. Llosa, J. Carot, Flat deformation theorem and symmetries in spacetime. Class. Quantum Gravity **26**, 055013 (2009)
60. P.-N. Chen, M.-T. Wang, S.-T. Yau, Quasilocal angular momentum and center of mass in general relativity. (2013) [arXiv:1312.0990](https://arxiv.org/abs/1312.0990)
61. P.-N. Chen, M.-T. Wang, and S.-T. Yau, Conserved quantities in general relativity: from the quasi-local level to spatial infinity. (2013) [arXiv:1312.0985](https://arxiv.org/abs/1312.0985)
62. P.L. McGrath, Rigid Quasilocal Frames. (2014) [arXiv:1402.1443](https://arxiv.org/abs/1402.1443)

Motion of Small Objects in Curved Spacetimes: An Introduction to Gravitational Self-Force

Adam Pound

Abstract In recent years, asymptotic approximation schemes have been developed to describe the motion of a small compact object through a vacuum background to any order in perturbation theory. The schemes are based on rigorous methods of matched asymptotic expansions, which account for the object's finite size, require no "regularization" of divergent quantities, and are valid for strong fields and relativistic speeds. Up to couplings of the object's multipole moments to the external background curvature, these schemes have established that at least through second order in perturbation theory, the object's motion satisfies a generalized equivalence principle: it moves on a geodesic of a certain smooth metric satisfying the vacuum Einstein equation. I describe the foundations of this result, particularly focusing on the fundamental notion of how a small object's motion is represented in perturbation theory. The three common representations of perturbed motion are (i) the "Gralla-Wald" description in terms of small deviations from a reference geodesic, (ii) the "self-consistent" description in terms of a worldline that obeys a self-accelerated equation of motion, and (iii) the "osculating geodesics" description, which utilizes both (i) and (ii). Because of the coordinate freedom in general relativity, any coordinate description of motion in perturbation theory is intimately related to the theory's gauge freedom. I describe asymptotic solutions of the Einstein equations adapted to each of the three representations of motion, and I discuss the gauge freedom associated with each. I conclude with a discussion of how gauge freedom must be refined in the context of long-term dynamics.

A. Pound (✉)

Mathematical Sciences, University of Southampton, Southampton SO17 1BJ, UK
e-mail: a.pound@soton.ac.uk

1 Preamble and Survey

Consider a small object moving through a curved spacetime. What path does it follow? At the level of undergraduate physics, the answer is satisfyingly simple: if the object is sufficiently small and light, it can be idealized as a test particle, which does not affect the geometry around it and which moves on a geodesic of that geometry. But what if we do away with that idealization? The real object *does* perturb the geometry around it; how, then, does the object move in that geometry, which it itself affects?

In Newtonian gravity, we may ask the analogous question—how does a massive body move when it contributes to the gravitational field around it?—and we may happily provide an answer without yet leaving undergraduate physics: if the body is sufficiently spherical, it can be treated as a point particle located at its center of mass, and the motion of that center of mass is governed by the *external* gravitational fields produced by all *other* masses in the system; the object does not feel its *own* field, at least in so far as its center-of-mass motion is concerned.

However, in general relativity, the situation becomes radically more complicated. Because of the nonlinearity of the Einstein equations, an extended object cannot, in general, be modelled as a point particle without invoking post-hoc regularization procedures [1, 2]. Furthermore, in a curved background, an object, even an asymptotically small one, *does* feel its own field, for reasons discussed below (and elsewhere in these proceedings). Hence, the field is said to exert a *gravitational self-force* on the object.

One might wonder if this effect is actually relevant in any realistic scenarios. The answer, unequivocally, is “Yes”. Suppose we are interested in a bound binary of widely separated compact objects of comparable masses m_1 and m_2 moving slowly in each other’s weak mutual gravity. Each of the objects is small compared to the other scales in the system (for example, the typical orbital separation R , or the radius of curvature of m_1 ’s field at m_2 ’s position). In a Newtonian approximation, m_1 is subject only to m_2 ’s Newtonian field, which at the position of m_1 exerts a force (per unit mass) $F_N \sim m_2/R^2$. But if one requires anything more accurate than the Newtonian approximation, the moment one steps to the post-Newtonian level, self-forces can no longer be ignored: m_1 ’s field, which we can think of as scaling like $\Phi_N \sim m_1/R$, modifies the Newtonian fields, giving rise to a post-Newtonian force per unit mass that scales like $F_{PN} \sim \Phi_N F_N \sim m_1 m_2 / R^3$ [3], similar in magnitude to any other post-Newtonian effect.¹

In these systems just described, however, each object, while small compared to the radius of curvature of the ambient external field it finds itself in, is not small compared

¹In a certain sense, an object’s mass affects its own motion even in a Newtonian binary. Each object follows a Keplerian orbit about the system’s center of mass, not about the center of the other object. Since the center of mass is shifted by the object’s own mass, the object affects its own motion; more plainly, m_1 influences its own motion by influencing that of m_2 . This is a more indirect effect than the type described above, but in practice, distinguishing it from any other post-test-body effect is nontrivial. See Ref. [4] for a discussion.

to the other object. What if we are interested in a case where there are truly only two scales? Take a binary system of compact objects of mass m and M satisfying $m \ll M$, and specifically focus on the regime in which the orbital separation R is of order M . In this case, it seems the gravity of m must certainly have a very small effect on its own motion, and it must very nearly follow a geodesic of the metric of M . And yet, even in this scenario, m 's gravitational self-force cannot be neglected. Although the effect is very small over a few orbits, the system continually radiates energy in the form of gravitational waves (or equivalently, the self-force does negative work), causing the orbit to shrink, and eventually causing m to collide with M (or plunge into M , if M is a black hole). In other words, the self-force has long-term, secular effects on the motion which make it impossible to ignore.

Both of these two types of systems—binaries of widely separated bodies whose mutual gravity is weak, and binaries of objects with very dissimilar masses, called extreme-mass-ratio inspirals (EMRIs)—are of increasing relevance to modern astrophysics. The prospect of directly detecting gravitational waves emitted from compact binaries, and extracting information about the binaries' strong-field dynamics from those waves, has spurred an international effort to study them. In the case of widely separated bodies of comparable mass, the main method of analysis has been post-Newtonian theory,² a historied subject modern overviews of which can be found in the review articles [5, 6] and the recent textbook [7]. In the case of EMRIs, the main method of analysis has been self-force theory; for summaries of efforts to model EMRIs, I refer the reader to the reviews [8, 9], the more up-to-date but brief survey [10], and the contributions of Babak et al., Wardell, and Vega to these proceedings.

In this paper, I seek to provide a single, unified description of gravitational self-force theory. Roughly speaking, this formalism consists of a perturbative expansion in powers of the small object's mass m . Although I will refer to EMRIs to motivate many of the methods and problems I discuss, my focus will instead be on foundational issues related to the problem of motion of a small object. My aim is to complement extant reviews [8, 9] by concentrating on three themes given limited attention in those reviews: (i) self-force theory at arbitrary perturbative order, (ii) differing ways to represent perturbed motion, and the asymptotic expansions of the metric corresponding to each, and (iii) the relationship between perturbed motion and gauge freedom. My presentation mostly follows the methods and viewpoint of Refs. [11–17] though it takes additional inspiration from the work of Gralla and Wald [18–20] and the classic papers of Mino et al. [21] and Detweiler and Whiting [22, 23]. To avoid excessive length, rather than striving for complete self-containment, I will often refer the reader to Refs. [9, 11, 15, 16] for mathematical tools and technical details.

Most of what I discuss could be applied to objects carrying scalar or electric charges, but for simplicity I restrict my attention to the purely gravitational case. I refer the reader to Refs. [9, 24–28] for discussions of self-forces due to scalar and

²Of course, once the two bodies are sufficiently close to each other, they interact in a highly nonlinear, highly relativistic way. In that regime, one must use numerical relativity to solve the fully nonlinear Einstein equations for the system.

electromagnetic fields on fixed background geometries, and to Refs. [29, 30] for recent work on the coupled system in which the metric reacts to both the mass and the scalar or electromagnetic field.

In the remainder of this introduction, I make an extensive survey of the main concepts and results of self-force theory, beginning with the standard picture of a point mass in linearized perturbation theory and proceeding to describe the more robust framework now available for studying the motion of extended (but small) objects at any order in perturbation theory.

Notation. Throughout this paper, Greek indices run from 0 to 4 and are raised and lowered with a background metric $g_{\mu\nu}$. Latin indices run from 1 to 3 and are freely raised and lowered with the Euclidean metric δ_{ij} . Sans-serif symbols such as $g_{\mu\nu}$ refer to tensors on the perturbed spacetime rather than on the background. A semicolon and ∇ refer to a covariant derivative compatible with $g_{\mu\nu}$, ${}^g\nabla_\mu$ to the covariant derivative compatible with $g_{\mu\nu}$, and $\tilde{\nabla}_\mu$ to the covariant derivative compatible with an “effective metric” $\tilde{g}_{\mu\nu}$. $\epsilon \equiv 1$ is used to count powers of m , and labels such as the “ n ” in $h_{\mu\nu}^n$ refer to perturbative order ϵ^n ; I freely write these labels as either super- or subscripts. I work in geometric units with $G = c = 1$.

1.1 A Point Particle Picture: The MiSaTaQuWa Equation and Its Interpretations

1.1.1 Self-Interaction with the Tail of the Perturbation

As mentioned above, a point particle stress-energy tensor is not a well-defined source in the nonlinear Einstein equations. However, it *is* a fine source in the *linearized* theory. For simplicity, assume our object of mass m is isolated, such that in some large region, we can take it to be the sole source of stress-energy in the system. Now consider a metric $g_{\mu\nu} = g_{\mu\nu} + \epsilon h_{\mu\nu}^1 + \mathcal{O}(\epsilon^2)$, where the background metric $g_{\mu\nu}$ is a vacuum solution to the nonlinear Einstein equations, and $h_{\mu\nu}^1$ is the leading-order perturbation due to our small object. Linearizing the Einstein equations in $h_{\mu\nu}^1$, we obtain

$$\delta G_{\mu\nu}[h^1] = 8\pi T_{\mu\nu}^1, \quad (1)$$

where $\delta G_{\mu\nu}[h] \equiv \frac{dG_{\mu\nu}[g+\lambda h]}{d\lambda} \big|_{\lambda=0}$ is the linearized Einstein tensor, and $T_1^{\mu\nu}$ is the leading-order approximation to the object’s stress-energy tensor. Now suppose that the object’s stress-energy can be approximated by

$$T_1^{\mu\nu}(x; z) = \int_\gamma m u^\mu u^\nu \delta(x, z(\tau)) d\tau, \quad (2)$$

which is the stress-energy of a point mass moving on a worldline γ with coordinates z^μ in the background spacetime. Here $u^\mu \equiv \frac{dz^\mu}{d\tau}$ is the particle's four-velocity, τ is its proper time (as measured in $g_{\mu\nu}$), and $\delta(x, z) \equiv \frac{\delta^4(x^\alpha - z^\alpha)}{\sqrt{-g}}$ is a covariant delta distribution, with g being the determinant of $g_{\mu\nu}$.

Unlike the nonlinear Einstein equations with a point particle source, Eq. (1) has a perfectly well-defined solution. If we introduce the trace-reversed perturbation $\bar{h}^1_{\mu\nu} \equiv h^1_{\mu\nu} - \frac{1}{2}g_{\mu\nu}g^{\alpha\beta}h^1_{\alpha\beta}$ and impose the Lorenz gauge condition $\nabla^\nu \bar{h}^1_{\mu\nu} = \mathcal{O}(\epsilon)$, then the linearized Einstein equation takes the form of a wave equation,

$$E_{\mu\nu}[\bar{h}^1] = -16\pi T^1_{\mu\nu}, \quad (3)$$

where

$$E_{\mu\nu}[\bar{h}^1] \equiv \square \bar{h}^1_{\mu\nu} + 2R_{\mu}{}^{\alpha}{}_{\nu}{}^{\beta} \bar{h}^1_{\alpha\beta}, \quad (4)$$

$\square \equiv g^{\mu\nu}\nabla_\mu\nabla_\nu$, and $R_{\mu\alpha\nu\beta}$ is the Riemann tensor of the background. Assuming the existence of a global retarded Green's function $G_{\mu\nu\mu'\nu'}(x, x')$ ³ for this wave equation, we can write the retarded solution as

$$\bar{h}^1_{\mu\nu}(x; z) = 4 \int G_{\mu\nu\mu'\nu'} T^{\mu'\nu'}_1 dV = 4 \int m G_{\mu\nu\mu'\nu'} u^{\mu'} u^{\nu'} d\tau, \quad (5)$$

where a primed index refers to the tangent space at the source point x' .

Now, if the background were flat, waves would propagate precisely on the light cone, and the retarded Green's function would be supported only on points connected by a null curve: $G^{\mu\nu}{}_{\mu'\nu'} = \delta^{\mu}_{\mu'}\delta^{\nu}_{\nu'} \frac{\delta(t' - [t - |x^a - x^{a'}|])}{|x^a - x^{a'}|}$, where (t, x^a) is a Cartesian coordinate system, $t - |x^a - x^{a'}|$ is the retarded time, and $|x^a - x^{a'}| \equiv \sqrt{\delta_{ab}(x^a - x^{a'})(x^b - x^{b'})}$ is the spatial distance between the points x and x' . However, in a curved spacetime, Huygen's principle no longer holds. Waves scatter off the spacetime curvature, causing them to propagate from a source point x' both on the future null cone of x' and *within* that cone. Correspondingly, the Green's function at a point x has support both on the past null cone of x and within it. This implies that if we look at the field $\bar{h}^1_{\mu\nu}$ at a point x near the worldline, we can split it into two pieces: a *direct* piece, corresponding to the portion of the field that propagated to x from a point $z^\mu(\tau_{\text{ret}})$ along a null curve; and a so-called *tail* piece, $h^{\text{tail}}_{\mu\nu}$, corresponding to the portion of the field that propagated from all *earlier* points $z^\mu(\tau < \tau_{\text{ret}})$ on the worldline. The direct piece diverges like a Coulomb field, behaving as $1/r$ (where r is a geodesic distance from the particle). The tail piece, on the other hand, is finite.

A detailed analysis (such as the one presented in the bulk of this paper) reveals that at leading order, the mass m is constant, and the force on the particle vanishes; in other

³My conventions for the Green's function are those of Ref. [9]; Ref. [9] also contains a pedagogical introduction to bitensors, objects which live in the tangent spaces of two different points x and x' .

words, it behaves as a test particle in $g_{\mu\nu}$. The same analysis applied at subleading order reveals that the direct piece of the field exerts no force on the particle, but the tail piece *does* exert a force, and the equation of motion is found to be

$$\frac{D^2 z^\mu}{d\tau^2} = -\frac{1}{2}\epsilon P^{\mu\nu} \left(2h_{\nu\alpha\beta}^{\text{tail}} - h_{\alpha\beta\nu}^{\text{tail}} \right) u^\alpha u^\beta + \mathcal{O}(\epsilon^2), \quad (6)$$

where $\frac{D}{d\tau} = u^\mu \nabla_\mu$, $P^{\mu\nu} = g^{\mu\nu} + u^\mu u^\nu$ projects orthogonally to the worldline, and the tail term is given by

$$h_{\mu\nu\rho}^{\text{tail}}(z(\tau)) = 4m \int_{-\infty}^{\tau-0^+} \nabla_\rho \bar{G}_{\mu\nu\mu'\nu'} u^{\mu'} u^{\nu'} d\tau'; \quad (7)$$

the integral covers all of the worldline earlier than the point $z^\mu(\tau)$ at which the force is evaluated. The bar atop $G^{\mu\nu}_{\mu'\nu'}$ again denotes a trace reversal.

Equation (6) is termed the MiSaTaQuWa equation, after Mino et al. [21], who first derived it, and Quinn and Wald [24], who re-derived it very shortly thereafter using a very different, independent method. The intuitive picture to glean from the MiSaTaQuWa result is that the direct piece of the field is analogous to a Coulomb field, moving with the particle and exerting no force on it, in the same way the self-field exerts no force on a body in Newtonian gravity. Very loosely speaking, from the perspective of the particle, the tail, consisting as it does of backscattered radiation, is indistinguishable from any other incoming radiation. In other loose words, it is effectively an external field, and like an external field, it exerts a force.

Much of this paper is devoted to showing how the MiSaTaQuWa result can be robustly justified, and higher-order corrections to it can be found, within a systematic expansion of the Einstein equations. As a byproduct of that analysis, in Sect. 4.1 I will show that the setup of the linearized system with a point particle source in this section is rigorously justified—even for a non-material object such as a black hole, and even though at nonlinear orders the field equations cannot be written in terms of such a source. However, before moving on to those matters, we may say significantly more on the basis of the point-particle result.

1.1.2 The Detweiler-Whiting Description: A Generalized Equivalence Principle

In the original MiSaTaQuWa papers [21, 24], the authors noted that Eq. (6) appears to have the form of the geodesic equation in a metric $g_{\mu\nu} + h_{\mu\nu}^{\text{tail}}$, when that geodesic equation is expanded to linear order in $h_{\mu\nu}^{\text{tail}}$.⁴ However, $h_{\mu\nu}^{\text{tail}}$ is not in any way a nice field. It does not satisfy any particularly meaningful field equation, nor is it even differentiable at the particle [9] [despite superficial appearances in Eq. (6)].

⁴I refer the reader to Appendix 1 for the expansion of the geodesic equation in powers of a metric perturbation.

Detweiler and Whiting provided a more compelling form of the MiSaTaQuWa result [22, 23]. Rather than splitting the retarded field into a direct piece and a tail, they split it as

$$h_{\mu\nu}^1 = h_{\mu\nu}^{S1} + h_{\mu\nu}^{R1}. \quad (8)$$

The *singular field* $h_{\mu\nu}^{S1}$ can be interpreted as the bound self-field of the particle. Like the direct piece of the field, it exhibits a $1/r$, Coulomb divergence at the particle; but unlike the direct piece, it satisfies the inhomogeneous linearized Einstein equation $E_{\mu\nu}[\bar{h}^{S1}] = -16\pi T_{\mu\nu}^1$, bolstering its interpretation as a self-field. Similarly, the *regular field* $h_{\mu\nu}^{R1}$ improves on the interpretation of the tail: it includes all the backscattered radiation in the tail, but it is a smooth solution to the homogeneous wave equation $E_{\mu\nu}[\bar{h}^{R1}] = 0$. Hence, more than we could of the tail, we can think of $h_{\mu\nu}^{R1}$ as an effectively external field, propagating independently of the particle. From it we can define what I will variously call an *effective metric* or *effectively external metric* $\tilde{g}_{\mu\nu} = g_{\mu\nu} + \epsilon h_{\mu\nu}^{R1}$.

Fittingly, given this interpretation of $h_{\mu\nu}^{R1}$, Detweiler and Whiting showed that the MiSaTaQuWa equation (6) can be equivalently written as

$$\frac{D^2 z^\mu}{d\tau^2} = -\frac{1}{2}\epsilon P^{\mu\nu} \left(2h_{\nu\alpha;\beta}^{R1} - h_{\alpha\beta;\nu}^{R1} \right) u^\alpha u^\beta + \mathcal{O}(\epsilon^2), \quad (9)$$

or (following Appendix 1) explicitly as the geodesic equation in the metric $\tilde{g}_{\mu\nu}$,

$$\frac{\tilde{D}^2 z^\mu}{d\tilde{\tau}^2} = \mathcal{O}(\epsilon^2), \quad (10)$$

where $\frac{\tilde{D}}{d\tilde{\tau}} \equiv \tilde{u}^\mu \tilde{\nabla}_\mu$ is a covariant derivative compatible with $\tilde{g}_{\mu\nu}$, $\tilde{u}^\mu = \frac{dz^\mu}{d\tilde{\tau}}$ is the four-velocity normalized in $\tilde{g}_{\mu\nu}$, and $\tilde{\tau}$ is the proper time along z^μ as measured in $\tilde{g}_{\mu\nu}$. Equation (9) is equivalent to Eq. (6) because on the worldline, $h_{\mu\nu}^{R1}$ differs from $h_{\mu\nu}^{\text{tail}}$ only by (i) background Riemann terms that cancel in Eq. (9) and (ii) terms proportional to the worldline's acceleration, which can be treated as effectively higher order because the acceleration is already $\sim \epsilon$.

Allow me to dwell longer on the interpretation of the regular field. Because $\tilde{g}_{\mu\nu}$ is a smooth vacuum solution, at the particle's position an observer cannot distinguish it from $g_{\mu\nu}$. Although a portion of $\tilde{g}_{\mu\nu}$ comes from the retarded field sourced by the particle, to the observer on the worldline, it appears just as would any metric sourced by a distant object. However, this interpretation of the effective metric as an effectively *external* metric is delicate. To effect the desired split into $h_{\mu\nu}^{S1}$ and $h_{\mu\nu}^{R1}$, both fields must be made acausal when evaluated off the worldline [9, 23]. More precisely, in addition to depending on the particle's causal past, $h_{\mu\nu}^{R1}(x)$ depends on the particle at *spatially* related points x' . So in that sense its interpretability as a physical external field is limited. Yet when evaluated *on* the worldline, $h_{\mu\nu}^{R1}$ and its

derivatives *are* causal, and that is the sense in which $\tilde{g}_{\mu\nu}$ appears as a physical metric on the worldline.

I impress upon the reader the significance of these properties of $h_{\mu\nu}^{R1}$; they are what makes Eq. (10) a meaningful result. Although it may not be an obvious fact at first glance, *any equation of motion can be written as the geodesic equation in some smooth piece of the metric*. This is most easily seen by writing the equation of motion in a frame that comoves with the particle. In locally Cartesian coordinates (t, x^i) adapted to that frame, such as Fermi-Walker coordinates [9], the particle's equation of motion reads $a_i = F_i$, where $a^\mu \equiv \frac{D^2 z^\mu}{d\tau^2}$ is the particle's covariant acceleration and F^μ is the force (per unit mass) acting on it. Now suppose we were to define some smooth field $h_{\mu\nu}^{r1}$ and a corresponding singular field $h_{\mu\nu}^{s1} \equiv h_{\mu\nu}^1 - h_{\mu\nu}^{r1}$. In the comoving coordinates, the linearized geodesic equation in the regular metric $g_{\mu\nu} + h_{\mu\nu}^{r1}$, in the form analogous to Eq. (9), reads $a_i = -h_{ti,t}^{r1} + \frac{1}{2}h_{ti,i}^{r1}$. No matter what force F^μ acts on the particle, the equation of motion $a_i = F_i$ could be written as the geodesic equation in $g_{\mu\nu} + h_{\mu\nu}^{r1}$ simply by choosing $h_{ti,t}^{r1}|_\gamma = 0$ and $h_{ti,i}^{r1}|_\gamma = 2F_i$, for example. Besides those two conditions, the regular field $h_{\mu\nu}^{r1}$ could be entirely freely specified, and regardless of the specification we made, we would have defined a split $h_{\mu\nu}^1 = h_{\mu\nu}^{s1} + h_{\mu\nu}^{r1}$ in which $h_{\mu\nu}^{s1}$ is singular and exerts no force, and $g_{\mu\nu} + h_{\mu\nu}^{r1}$ is a regular metric in which the motion is geodesic.

Given this fact, it is of no special significance that the MiSaTaQuWa equation is equivalent to geodesic motion in *some* effective metric. But it *is* significant that the MiSaTaQuWa equation is equivalent to geodesic motion in the *particular* effective metric $\tilde{g}_{\mu\nu} = g_{\mu\nu} + h_{\mu\nu}^{R1}$ identified by Detweiler and Whiting, because of the particular, ‘physical’ properties of that metric: $\tilde{g}_{\mu\nu}$ is a smooth vacuum solution that is causal on the particle's worldline. Because of those properties, we may think of the MiSaTaQuWa equation as a generalized equivalence principle: any object, if it is sufficiently compact and slowly spinning, regardless of its internal composition, falls freely in a gravitational field $\tilde{g}_{\mu\nu}$ that can be thought of (loosely if not precisely) as the physical ‘external’ gravitational field at its ‘position’. I stress that this is a derived result, not an assumption, as will be shown in Sect. 3. By that stage in the paper, the principle's reference to extended, “sufficiently compact and slowly spinning” objects will have become clear.

Another aspect that will have become clearer is the non-uniqueness of the effective metric and the limitations of interpreting it in a strongly physical way. Nonetheless, the split of the metric into a self-field and an effective metric will be a recurring theme. In many ways, the generalized equivalence principle just described is both the central tool and the core result of self-force theory. It is conceptually more compelling than the expression for the force in terms of a tail,⁵ it is less tied to any particular choice

⁵Another compelling physical interpretation is provided by Quinn and Wald [24]. They showed that the MiSaTaQuWa equation follows from the assumption that the net force is equal to an average over a certain “bare” force over a sphere around the particle. (This assumption was later proved to be true in a large class of gauges [18, 19, 31].) In the language of Detweiler and Whiting fields, the force lines of the singular field are symmetric around the particle and vanish upon averaging, while the force lines of the regular field are asymmetric and add up to a net force on the particle.

of gauge [17], and it is often easier to use as a starting point from which to derive formal results. Perhaps most importantly, it is easily carried to nonlinear orders: as I describe in later sections, at least through second order in ϵ , the generalized equivalence principle stated above holds true [14, 16].

1.2 Extended Bodies and the Trouble with Point Particles

Although the point-particle picture seemingly works well within linearized theory, it is not obvious *a priori* how it fits within a systematic asymptotic expansion that goes to higher perturbative orders. For as I have reiterated above, one cannot use a point particle in the full nonlinear theory. Let me now expound on that point.

Suppose we attempt to model the extended object as a point particle in the exact spacetime, with a stress-energy tensor

$$T^{\mu\nu} = \int m \frac{dz^\mu}{dt} \frac{dz^\nu}{dt} \frac{\delta^4(x^\alpha - z^\alpha)}{\sqrt{-g}} dt, \quad (11)$$

where t is proper time on z^μ as measured in $g_{\mu\nu}$. If we expand the metric as $g_{\mu\nu} = g_{\mu\nu} + \sum_{n>0} \epsilon^n h_{\mu\nu}^n$, the linearized Einstein equation is exactly as described in the previous section. But at second order, severe problems arise. The second-order term in the Einstein equation $G^{\mu\nu}[g] = 8\pi T^{\mu\nu}$ reads

$$\delta G^{\mu\nu}[h^2] = -\delta^2 G^{\mu\nu}[h^1, h^1] + 8\pi T_2^{\mu\nu}, \quad (12)$$

where $\delta^2 G^{\mu\nu}[h, h] \equiv \frac{1}{2} \frac{d^2 G^{\mu\nu}[g+\lambda h]}{d\lambda^2} \Big|_{\lambda=0}$ and $T_2^{\mu\nu}$ is the second-order term in $T^{\mu\nu}$. There are two problems with Eq. (12). Most obviously, $T_2^{\mu\nu}$ contains terms like

$$\int m u^\mu u^\nu \left(-\frac{1}{2} g^{\rho\delta} h_{\rho\delta}^1 \right) \frac{\delta^4(x^\alpha - z^\alpha)}{\sqrt{-g}} d\tau.$$

As described in the preceding section, $h_{\mu\nu}^1$ diverges as $1/r$ near the particle; hence, the stress-energy diverges in the distributionally ill-defined manner $\frac{1}{r} \delta(r)$. Even if we could somehow mollify the ill behavior of this piece of the source, the other source term in Eq. (12) would still present a problem. $\delta^2 G^{\mu\nu}[h^1, h^1]$ behaves schematically as $(\partial h^1)^2 + h^1 \partial^2 h^1$. Therefore, it diverges as $1/r^4$. Such a divergence is non-integrable, meaning it is well defined as a distribution only if it can be expressed as a linear operator acting on an integrable function. In the present case, there does not appear to be a unique way of so expressing it.

These arguments make clear that a point particle poses increasingly worsening difficulties at nonlinear orders in perturbation theory. And it is well known that in any well-behaved space of functions *there exists no solution* to the original, fully nonlinear equation $G^{\mu\nu}[g] = 8\pi T^{\mu\nu}$ with a point particle source [1, 2].

Despite these obstacles, one might suppose that the point-particle model could be adopted and the divergences resolved using post-hoc regularization methods. Evidence for this reasoning is given by the successful use of dimensional regularization in post-Newtonian theory [5]. In the fully relativistic context, the most promising route to such regularization appears to be effective field theory [32, 33].

However, at a fundamental level, there should be no need for such regularization in general relativity. Outside of curvature singularities inside black holes, everything in the problem should be perfectly finite. For that reason, in this paper I will be interested only in formalisms that deal with finite, well-defined quantities throughout.

So let us do away with the fiction of a point particle and think of an extended object. Perhaps the most obvious route, at least at first glance, to determining this object's motion is to go to the opposite extreme from the linearized point particle model, by looking instead at a generic extended object in fully nonlinear general relativity; if one is interested in the case of a small object, one can always examine an appropriate limit of one's generic results. This line of attack has been most famously pursued by Dixon [34] (inspired by early work by Mathisson [35]) and Harte [36]. Specializing to material bodies, Dixon showed that all information in the stress-energy $T^{\mu\nu}$ can be encoded in a set of multipole moments, and all information in the conservation law $\nabla_\mu T^{\mu\nu} = 0$ can be encoded in laws of motion for the body. These laws take the form of evolution equations for some suitable representative worldline in the object's interior and for the object's spin about that worldline. A "good" choice of representative worldline may be made by, for example, defining the object's mass dipole moment relative to any given worldline and then choosing the worldline for which the mass dipole moment vanishes, establishing the worldline as a center of mass [37]. However, in order to transform these general results into practical equations of motion, Dixon's method requires an assumption that the metric and its derivatives do not vary much in the body's interior. Given that assumption, the force and torque appearing on the right-hand side of the equations of motion can be written as a simple expansion composed of couplings of the metric's curvature to the object's higher multipole moments; the higher moments, beginning with the quadrupole, may be freely specified, and their specification is entirely equivalent to a specification of the object's stress-energy tensor. Equations of motion of this form can be viewed in Eqs. (13) and (14) below.

Unfortunately, for a reasonably compact, strongly gravitating body, the physical metric does *not* vary slowly in its interior, due to the body's own contribution to the metric. To make progress, one must treat the object as a test body, an extended object that is non-gravitating but is equipped with a multipole structure—or, as discussed in Sect. 13 of Ref. [34], one must find an efficacious means of separating the object's self-field from the "external" field, analogous to the trivial split in Newtonian theory and to the Detweiler-Whiting split in the linearized point particle model. A well-chosen "external" field will vary little in the body's interior, a well-chosen "self-field" will have minimal influence on the motion, and one can hope to arrive at equations of motion expressed in terms of couplings to the curvature of the external field alone.

In the fully nonlinear theory, finding such a split would seem to be highly non-trivial. Nevertheless, in a series of papers [26, 27, 38] culminating in Ref. [36]

(see also Harte’s contribution to these proceedings [28]), Harte has succeeded in finding a suitable split by directly generalizing the Detweiler-Whiting decomposition. He has shown that the “self-field” he defines modifies the equation of motion only by shifting the values of the object’s multipole moments, and the object behaves as a test body moving in the effectively external metric he defines. This extends the Detweiler-Whiting result from the linearized model to the fully nonlinear problem. However, there is one caveat to this generalization: beyond linear order, Harte’s effective metric loses one of the compelling properties of the Detweiler-Whiting field: it is not a solution to the vacuum Einstein equation. Despite this feature, Harte’s work is a tour de force in the problem of motion.

The approach I take in this paper is complementary to Harte’s. Rather than beginning with the fully nonlinear problem, I will proceed directly to perturbation theory. There are several advantages to this. The perturbative approach naturally applies to black holes, while Harte’s formalism, because it is based on integrals over the object’s interior, is restricted to material bodies. The perturbative approach also naturally leads to a split into self-field and effective metric in which the effective metric satisfies the vacuum Einstein equation at all orders and is causal on the worldline. Most importantly, the perturbative approach provides a practical means of solving the Einstein equations. In the fully nonlinear approach, one arrives at equations of motion given the metric, but not a practical way to find that metric.

In the next section, I will begin to discuss the perturbative formalism. First, I note that with the work of Dixon and Harte, a new theme has been introduced: an object’s bulk motion can be expressed in terms of a set of multipole moments, and the $\ell \geq 2$ moments are freely specifiable. Like the decomposition of the metric into a self-field and effectively external field, this second theme will appear prominently in the remainder of this paper.

1.3 When Perturbation Theory Fails Near a Submanifold: The Method of Matched Asymptotic Expansions

As soon as we seek a perturbative description of the problem, we run into a new challenge. Say we assume an expansion of the exact spacetime ($g_{\mu\nu}^\epsilon, \mathcal{M}_\epsilon$) about a background spacetime ($g_{\mu\nu}, \mathcal{M}_0$), as in $g_{\mu\nu}^\epsilon = g_{\mu\nu} + \epsilon h_{\mu\nu}^1 + \mathcal{O}(\epsilon^2)$, where all ϵ -dependent terms are created by the small object (or by nonlinear interactions of its field with itself). This expansion assumes the object has only a small effect on the metric. Clearly, if the object is compact, this cannot be true everywhere: sufficiently near the object, where $r \sim \epsilon$, the object’s own gravitational field will contain a Coulomb term $\sim m/r \sim \epsilon^0$ —just as large as the background $g_{\mu\nu}$, and because it varies on the spatial scale ϵ rather than ϵ^0 , having much stronger curvature than $g_{\mu\nu}$.

This fact motivates the use of *matched asymptotic expansions*. At distances $r \sim \epsilon^0$ from the object (for example, $r \sim M$ in an EMRI), we expand the exact spacetime around ($g_{\mu\nu}, \mathcal{M}_0$), as above; I will call this the *outer expansion*. At distances $r \sim \epsilon$

from the object (or $r \sim m$ in dimensionful units), we introduce a second expansion, $g_{\mu\nu} = g_{\mu\nu}^{\text{obj}} + \epsilon H_{\mu\nu}^1 + \mathcal{O}(\epsilon^2)$, where $(g_{\mu\nu}^{\text{obj}}, \mathcal{M}_{\text{obj}})$ is the spacetime of the object were it isolated, and the perturbations $H_{\mu\nu}^n$ are due to the fields of external objects (and to nonlinear interactions); I call this the *inner expansion*. In a *buffer region* around the object, defined by $\epsilon \ll r \ll \epsilon^0$, we assume a *matching condition* is satisfied: if the outer expansion is re-expanded in the limit $r \ll \epsilon^0$ and the inner expansion is re-expanded in the limit $r \gg \epsilon$, the two expansions must agree term by term in powers of r and ϵ , since they both began as expansions of the same metric. The relationship between the various regions and expansions is shown schematically in Fig. 1, and it will be described precisely in Sect. 2.

Historically, matched asymptotic expansions have been a highly successful way of treating singular perturbation problems in which the behavior of the solution rapidly changes in a localized region. For general discussions of singular perturbation theory in applied mathematics, I refer readers to the textbook [39], and for more rigorous treatments, to Refs. [40, 41]. For general discussions in the context of general relativity, I refer them to [12, 42].

In the context of spacetimes containing small objects, matched expansions have been the standard method of tackling the problem; Refs. [11, 14, 18, 20–22, 43–46] are but a small sample. When it comes to obtaining equations of motion,

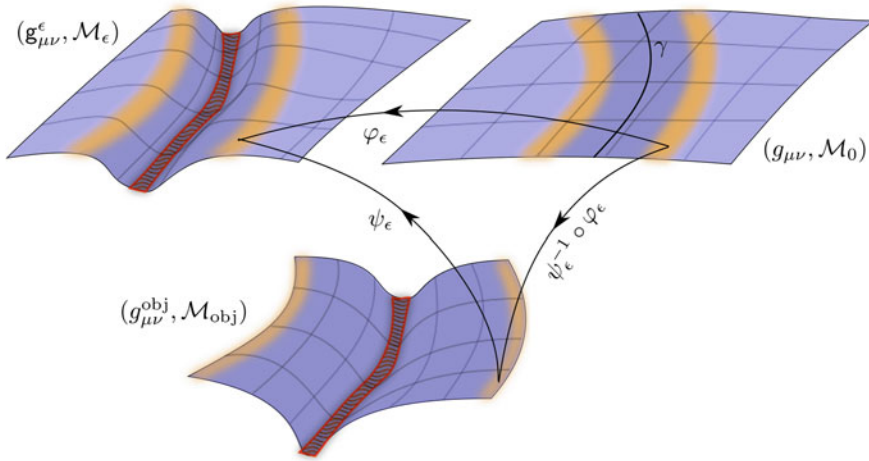


Fig. 1 The exact spacetime (top left), external background spacetime (top right), and inner background spacetime (bottom), with maps between them. In the exact spacetime, we have some small compact object, here shown as a material body (in dark red and black), but possibly a black hole or more exotic object. Around the object is a buffer region, shown in orange. Points outside the object can be identified (via the identification map φ_ϵ) with points in the external background manifold \mathcal{M}_0 . In a chart $(t, x^i) : \mathcal{M}_0 \rightarrow \mathbb{R}^4$ centered on a worldline $\gamma \in \mathcal{M}_0$, the points $p \in \mathcal{M}_0$ and $\varphi_\epsilon(p) \in \mathcal{M}_\epsilon$ are assigned the same coordinate values $(t(p), x^i(p))$. The map $\psi_\epsilon^{-1} \circ \varphi_\epsilon$ zooms in on the object by rescaling spatial coordinates; in the same chart (t, x^i) , the point $q = \psi_\epsilon^{-1}(\varphi_\epsilon(p))$ is assigned coordinate values $(\tilde{t}(q), \tilde{x}^i(q)) = (t(p), x^i(p)/\epsilon)$

the method hearkens back to an early insight of Einstein and others [3, 47–49]: an object’s equations of motion can be determined from the Einstein equations in a region *outside* the object. Specifically, it can be determined from the field equations in the buffer region defined above. Relative to the object’s scale $r \sim \epsilon$, the buffer region $\epsilon \ll r \ll \epsilon^0$ is at asymptotically large distances, allowing one to make an asymptotic characterization of how well “centered” the buffer region is around the object. One such characterization is based on a definition of multipole moments in the buffer region. Again, because the buffer region is at asymptotic infinity in the object’s metric $g_{\mu\nu}^{\text{obj}}$, we can define the object’s multipole moments by examining the form of the metric there, rather than having to refer to the object’s stress-energy. We can then use the metric’s mass dipole moment in the buffer region as a measure of centeredness: if we install a timelike curve γ in the background spacetime and define the mass dipole moment in coordinates centered on that worldline, then γ is a good representative worldline if the mass dipole moment vanishes. Centeredness conditions along these lines will be described in more detail in Sects. 2 and 7; for a schematic preview, see Figs. 1 and 2.

Prior to its application to self-force analyses [11, 14, 18, 20–22], this program was pursued furthest by Thorne and Hartle [46]. Where Dixon stood relative to the later non-perturbative work of Harte, Thorne and Hartle stand in the same position relative to perturbative self-force constructions. As did Dixon, they derived general laws of motion and precession for compact objects. They considered an object immersed

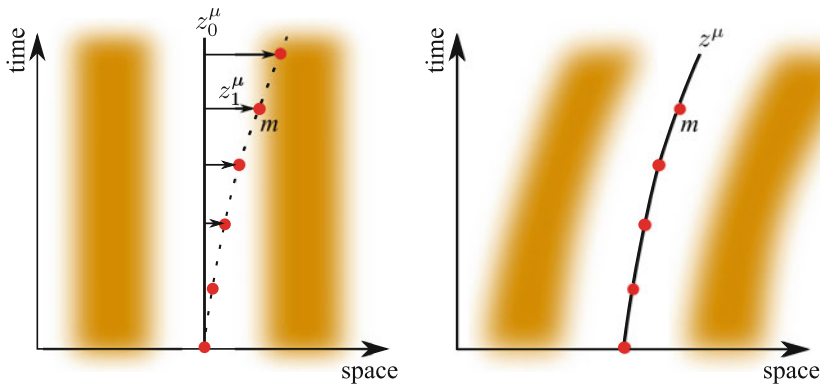


Fig. 2 Perturbative motion of a small object as defined in the Gralla-Wald (*left*) and self-consistent (*right*) approximations. In the Gralla-Wald case, the buffer region is centered on a zeroth-order worldline $\gamma_0 \subset \mathcal{M}_0$, which in a given coordinate system $x^\mu : \mathcal{M}_0 \rightarrow \mathbb{R}^4$ has coordinates $z_0^\mu(s)$. In a generic gauge, the self-force drives the object (shown as a sequence of *red circles*) away from γ_0 , and this deviation is represented by $z_1^\mu(s)$, a vector defined on γ_0 . In the self-consistent case, the buffer region is centered on an accelerated worldline $\gamma_\epsilon \subset \mathcal{M}_0$, which in the same coordinates x^μ has coordinates $z^\mu(s, \epsilon)$. The accelerated worldline faithfully tracks the object’s motion, such that the object is always at the “center” of the region enclosed by the buffer. On timescales much smaller than the dephasing time, we have that the two approximations are related by $z^\mu(s, \epsilon) = z_0^\mu(s) + \epsilon z_1^\mu(s) + \mathcal{O}(\epsilon^2)$

in some external spacetime, say $(g_{\mu\nu}, \mathcal{M})$, and found forces and torques made up of couplings between the external curvature and the object's multipole moments; specifically, in Cartesian coordinates (t, x^i) that are at rest relative to a geodesic z^μ of the external spacetime (and in which the mass dipole moment vanishes), they found

$$\frac{dp^i}{dt} = -\mathfrak{B}^i_j S^j + \mathcal{O}(\epsilon^3), \quad (13)$$

$$\frac{dS^i}{dt} = -\epsilon^i_{ab}(\mathfrak{E}^b_c Q^{ac} + \frac{4}{3}\mathfrak{B}^b_c Q^{ac}) + \mathcal{O}(\epsilon^4), \quad (14)$$

where p^μ and S^μ are the object's linear and angular momentum relative to z^μ , Q^{ab} and \mathcal{Q}^{ab} are its “mass and current” quadrupole moments (see the ends of Sects. 3.2 and 3.4), t is proper time (as measured in $g_{\mu\nu}$) on z^μ , and ϵ_{ijk} is the flat-space, Cartesian Levi-Civita tensor. The quantities \mathfrak{E}_{ab} and \mathfrak{B}_{ab} are the electric-type and magnetic-type quadrupole tidal moments of the external universe, which describe the tidal environment the object is placed in; they are related to the Riemann tensor of $g_{\mu\nu}$ according to $\mathfrak{E}_{ab} \equiv \mathfrak{R}_{\iota a \iota b}$ and $\mathfrak{B}_{ab} \equiv -\frac{1}{2}\epsilon^{pq}{}_{(a}\mathfrak{R}_{b)\iota pq}$.

Physically, Eqs. (13) and (14) say that *the object moves as a test body in the external metric*; the equations have the same structure as the test-body equations of motion mentioned above in the context of Dixon's work [34]. Up to the coupling of the object's moments to the tidal moments of the external universe, the motion is geodesic, and the spin parallel-propagated, in the external metric. But just as in Dixon's work, *these results become useful only once one knows how to split the full metric into a self-field and an effectively external metric*. What Thorne and Hartle call the “external metric” is not $g_{\mu\nu}$, but rather it is essentially defined to be whatever creates tidal fields across the object. As Thorne and Hartle themselves remarked, this “external” field includes a contribution from the object's own field. (Likewise, the “object's” multipole moments can be altered by the external field.)

In this sense, the self-force game is played by finding a useful split in which Thorne and Hartle's general laws are valid. Doing so requires developing a systematic theory of matched expansions for spacetimes containing small objects, as described in the body of this paper. Using those matched expansions, we will find that at linear order, we can circle back to the point particle picture: as first shown by D'Eath [43, 44], the linearized perturbation $h^1_{\mu\nu}$ in the outer expansion *is identical to the linearized field sourced by a point particle* (see also Refs. [11, 15, 18] for more refined derivations). And at that linearized level, we will find that the effectively external metric $g_{\mu\nu}$ of Thorne and Hartle can be taken to be the Detweiler-Whiting effective metric $\tilde{g}_{\mu\nu} = g_{\mu\nu} + \epsilon h^{\text{R1}}_{\mu\nu}$.

1.4 Gauge, Motion, and Long-Term Dynamics

Despite all the above preparation, we are still not ready to broach the problem of motion in perturbation theory. Two additional facts must first be understood: in perturbation theory, motion is intimately related to gauge freedom [17, 19, 50]; and in problems of astrophysical interest, the most important dynamical effects occur on the very long time scale $\sim 1/\epsilon$ [51].

To the first point. At leading order, the object's motion is geodesic in the background metric $g_{\mu\nu}$; all deviation from that motion is driven by an order- ϵ force. Suppose the self-accelerated worldline γ is a smooth function of ϵ . Then we can write its coordinates as an expansion

$$z^\mu(s, \epsilon) = z_0^\mu(s) + \epsilon z_1^\mu(s) + \mathcal{O}(\epsilon^2), \quad (15)$$

where s is a parameter on the worldline, and the zeroth-order term z_0^μ is a geodesic of $g_{\mu\nu}$. Now consider the effect of a gauge transformation. Under a transformation generated by a vector $\epsilon\xi^\mu$, a curve z^μ is shifted to a curve $z'^\mu = z^\mu - \epsilon\xi^\mu + \mathcal{O}(\epsilon^2)$. Nothing prevents us from choosing $\xi^\mu = z_1^\mu$, which leaves us with $z'^\mu = z_0^\mu + \mathcal{O}(\epsilon^2)$, entirely eliminating the first-order deviation from z_0^μ . This same idea can be carried to arbitrary order, meaning we can precisely set $z'^\mu = z_0^\mu$. In other words, the effect of the self-force appears to be pure gauge.

In one sense, this result is true. If we look at any finite region of spacetime and consider the limit $\epsilon \rightarrow 0$ in that region, the deviation from a background geodesic is, indeed, pure gauge. This does not mean it is irrelevant: in any given gauge, it must be accounted for to obtain the correct metric in that gauge. But it need not be accounted for in the *linearized* metric. We can always substitute the expansion (15) into $h_{\mu\nu}^1(x; z)$ to obtain

$$\epsilon h_{\mu\nu}^1(x; z) = \epsilon h_{\mu\nu}^1(x; z_0) + \epsilon^2 \delta h_{\mu\nu}^1(x; z_0, z_1) + \mathcal{O}(\epsilon^3), \quad (16)$$

and we can then transfer the term $\delta h_{\mu\nu}^1(x; z_0, z_1)$ into the second-order perturbation, $\epsilon^2 h_{\mu\nu}^2$. [An explicit expression for $\delta h_{\mu\nu}^1(x; z_0, z_1)$ is given in Eq. (221).]

However, this analysis assumes we work in a fixed, finite domain—and as mentioned in the first paragraph of this section, we do *not* typically work in such a domain in problems of interest. Consider an EMRI. Gravitational waves carry away orbital energy from the EMRI at a rate $\dot{E}/E \sim \epsilon$. It follows that the inspiral occurs on the time scale $t_{rr} \sim E/\dot{E} \sim 1/\epsilon$, which is called the *radiation-reaction time*. So in practice, we are not looking at the limit $\epsilon \rightarrow 0$ on a finite interval of time $[0, T]$, where T is independent of ϵ ; instead, we are looking at the limit $\epsilon \rightarrow 0$ on a time interval $[0, T/\epsilon]$ that blows up.

This consideration forces us to adjust our thinking about motion and gauge. Loosely speaking, the deviation from geodesic motion, ϵz_1^μ , is governed by an

equation of the form $\frac{d^2 z_1^\mu}{dt^2} \sim F_1^\mu$.⁶ On the radiation-reaction time scale, it therefore behaves as $\epsilon z_1^\mu \sim \epsilon F_1^\mu t_{rr}^2 \sim 1/\epsilon$. In other words, it blows up in the limit $\epsilon \rightarrow 0$. So on this domain, one cannot rightly write the worldline as a geodesic plus a self-forced correction, and one cannot use a small gauge transformation to shift the perturbed worldline onto a background geodesic; the gauge transformation would have to blow up in the limit $\epsilon \rightarrow 0$.

Because we are solving partial differential equations and not ordinary ones, these arguments about time scales translate into arguments about spatial scales. For example, if we seek a solution in a Schwarzschild background spacetime, fields (including inaccuracies in them) propagates outward toward null infinity along curves of constant $t - r^*$, or inward toward the future horizon along curves of constant $t + r^*$, where r^* is the tortoise coordinate. If one's accuracy is limited to a time span Δt , then it is also limited to a spatial region of similar size.

To organize our thinking, let us denote by $\mathcal{D}_{\zeta(\epsilon)}$ a spacetime region roughly of size $\zeta(\epsilon)$ (both temporal and spatial). I call an asymptotic solution to the Einstein equations a “good” solution in $\mathcal{D}_{\zeta(\epsilon)}$ if it is uniform in $\mathcal{D}_{\zeta(\epsilon)}$. That is, the asymptotic expansion $\mathfrak{g}_{\mu\nu} = g_{\mu\nu} + \sum_{n>0} \epsilon^n h_{\mu\nu}^n$ must satisfy $\lim_{\epsilon \rightarrow 0} \frac{\epsilon h_{\mu\nu}^1}{g_{\mu\nu}} = 0$ and $\lim_{\epsilon \rightarrow 0} \frac{\epsilon^n h_{\mu\nu}^n}{\epsilon^{n-1} h_{\mu\nu}^{n-1}} = 0$ *uniformly* (e.g., in a sup norm).

For the EMRI problem, we are interested in obtaining a good solution in a domain $\mathcal{D}_{1/\epsilon}$. Suppose we use an asymptotic expansion of the form (16) and incorporate $\delta h_{\mu\nu}^1(x; z_0, z_1)$ into $h_{\mu\nu}^2$. In a gauge such as the Lorenz gauge, z_1^μ grows as $\sim F_1^\mu t^2$, and so $\delta h_{\mu\nu}^1(x; z_0, z_1)$ likewise grows as t^2 . Hence, on $\mathcal{D}_{1/\epsilon}$, its contribution to $\epsilon^2 h_{\mu\nu}^2$ behaves at best as ϵ^0 , comparable to $g_{\mu\nu}$. Clearly, this is not a good approximation. Suppose we instead eliminated z_1^μ using a gauge transformation generated by $\xi^\mu = z_1^\mu$. This removes the offending growth in $h_{\mu\nu}^2$, but it commits a worse offense: it alters $\epsilon h_{\mu\nu}^1$ by an amount $2\epsilon \xi_{(\mu;\nu)}$, which behaves at best as ϵt , or as ϵ^0 on $\mathcal{D}_{1/\epsilon}$. Hence, if we are in a gauge where the self-force is nonvanishing, $h_{\mu\nu}^2$ behaves poorly; if we are in a gauge where the self-force is vanishing, even $h_{\mu\nu}^1$ behaves poorly.

Let us chase the consequences of this. To obtain a good approximation in $\mathcal{D}_{1/\epsilon}$, we need to work in a class of gauges compatible with uniformity in $\mathcal{D}_{1/\epsilon}$. This means, in particular, that if we obtain a good approximation in a particular gauge—call it a *good gauge*—we must confine ourselves to a class of gauges related to the good gauge by uniformly small gauge transformations. In turn, this means that the effects of the self-force are *not* pure gauge on $\mathcal{D}_{1/\epsilon}$. Due to dissipation, z^μ will deviate from any given geodesic z_0^μ by a very large amount in $\mathcal{D}_{1/\epsilon}$, but by using an allowed gauge transformation we may shift it only by a very small amount, of order ϵ , on that domain. In other words, *although the self-forced deviation from z_0^μ is pure gauge on a domain like \mathcal{D}_{ϵ^0} , it is no longer pure gauge in the domain $\mathcal{D}_{1/\epsilon}$.*

⁶More precisely, it is governed by Eq. (35).

1.5 Self-Consistent, Gralla-Wald, and Osculating-Geodesics Approximations

In the preceding sections, we encountered several core concepts pertaining to the motion of a small object: (i) the metric can be usefully split into a self-field and an effectively external metric in which the object behaves as a test body, (ii) the bulk motion of the object can be described in terms of forces and torques generated by freely specifiable multipole moments, (iii) by using matched expansions, all of this can be done in a vacuum region *outside* the object, where multipole moments can be defined from the metric and laws of motion can be derived from the vacuum Einstein equation, and (iv) the representation of the object's bulk motion, the asymptotic expansion of the metric, and notions of gauge must all be tailored to suit the long timescales on which self-force effects accumulate.

Let me now combine this information into a cohesive framework, mostly following Ref. [11] (but see also Refs. [14–17, 52]). The overarching method I describe consists of solving the Einstein equation with an “outer expansion” in some vacuum region $\mathcal{D}_{\zeta(\epsilon)}$ outside the object, using only minimal information from the “inner expansion” to determine the behavior of the solution very near the object.

Since we work in the vacuum region $\mathcal{D}_{\zeta(\epsilon)}$, we seek an asymptotic solution to the vacuum Einstein equation

$$R_{\mu\nu}[g] = 0. \quad (17)$$

Following the lessons of post-Newtonian theory, I write this equation in a “relaxed” form [5–7]. I define $h_{\mu\nu} \equiv g_{\mu\nu} - g_{\mu\nu}$, impose the Lorenz gauge condition⁷

$$L_\nu[h] \equiv \nabla^\mu (h_{\mu\nu} - \frac{1}{2} g_{\mu\nu} g^{\alpha\beta} h_{\alpha\beta}) = 0, \quad (18)$$

and write Eq. (17) with that condition imposed, making it read

$$E_{\mu\nu}[h] = S_{\mu\nu}[h], \quad (19)$$

where $E_{\mu\nu}$ is the wave operator introduced in Eq. (4) (but here acting on the metric perturbation rather than on its trace reverse),⁸ and the “source” $S_{\mu\nu} \equiv R_{\mu\nu}[g + h] - E_{\mu\nu}[h]$ is a nonlinear functional of $h_{\mu\nu}$. The background $g_{\mu\nu}$ is chosen to be a smooth solution to $R_{\mu\nu}[g] = 0$ (if matter exists outside the object, it is assumed to be sufficiently far away to lie outside $\mathcal{D}_{\zeta(\epsilon)}$). This makes Eq. (19) a weakly nonlinear hyperbolic equation for the perturbation $h_{\mu\nu}$; at this stage, that equation is still exact.

⁷Reference [15] describes how the entirety of this section can be performed in any gauge in which the linearized Einstein tensor is hyperbolic. Section 6 below offers a more general discussion of gauge.

⁸In the Lorenz gauge in a vacuum background, the linearized curvature tensors are related by $E_{\mu\nu}[h] = -2\delta R_{\mu\nu}[h] = -2\delta \bar{G}_{\mu\nu}[\bar{h}] = E_{\mu\nu}[\bar{h}]$.

I wish to solve Eq. (19) in $\mathcal{D}_{\zeta(\epsilon)}$ subject to two types of boundary conditions:

- (BC1) *Global boundary conditions.* Examples of these are retarded boundary conditions or specified Cauchy data.
- (BC2) *The matching condition.* In the buffer region, the solution must be compatible with an inner expansion.

Together these conditions ensure we are describing the correct physical situation. But they do not yet uniquely determine the solution. Equation (19) is called “relaxed” because, unlike Eq. (17), it can be solved no matter how the object moves; this relaxation arises because Eq. (19) is not constrained by the Bianchi identity, unlike Eq. (17). The object’s motion is determined only once the gauge condition is also imposed, thereby making the solution to the relaxed equation also a solution to the unrelaxed one. As discussed earlier, in the present problem, the motion of the object is defined by the mass dipole moment of the metric in the buffer region, and we will find that the evolution of that mass dipole moment is determined by the gauge condition.

Beyond these broad ideas, the specifics of the method, and the size of the region $\mathcal{D}_{\zeta(\epsilon)}$ in which it applies, depend crucially on how one represents the object’s perturbed motion, which determines how one formulates the asymptotic solution to the Einstein equation. Here I describe three representations and corresponding asymptotic solutions: what I call “self-consistent”, “Gralla-Wald”, and “osculating geodesics” approximations.

1.5.1 Self-Consistent Approximation

In the self-consistent approximation, to avoid the secularly growing errors described in Sect. 1.4, I seek to directly determine an accelerated worldline $z_\epsilon^\mu(s)$ that represents the object’s bulk motion; I do *not* wish to expand that worldline in powers of ϵ . To accommodate this, I write the perturbation $h_{\mu\nu}$ as $h_{\mu\nu}(x, \epsilon; z_\epsilon, \dot{z}_\epsilon)$, where $\dot{z}_\epsilon^\mu \equiv \frac{dz_\epsilon^\mu}{ds}$ and the quantities after the semicolon denote a functional dependence. I expand this functional as

$$h_{\mu\nu}(x, \epsilon; z_\epsilon, \dot{z}_\epsilon) = \sum_{n>0} \epsilon^n h_{\mu\nu}^n(x; z_\epsilon, \dot{z}_\epsilon). \quad (20)$$

Despite the fact that z_ϵ^μ and \dot{z}_ϵ^μ depend on ϵ , they are not expanded; in other words, I hold them fixed while taking the limit $\epsilon \rightarrow 0$. Later, I will suppress the functional dependence on \dot{z}_ϵ^μ and simply write $h_{\mu\nu}^n(x; z_\epsilon)$.

The self-consistent representation of motion is given its name because z_ϵ^μ must be determined simultaneously with $h_{\mu\nu}^n(x; z_\epsilon)$. It was the representation adopted in the original derivations of the MiSaTaQuWa equation [21, 24, 53], and it is the one I used in describing that equation in Sect. 1.1. It was first put on a sound and robust basis, as part of a systematic expansion of the Einstein equation, in Ref. [11]. In this section, I outline that expansion.

I first refine the region in which I seek a solution to the relaxed Einstein equation (19). Install the timelike curve γ_ϵ (with coordinates z_ϵ^μ) in the background space-time, and let $D_{\zeta(\epsilon)} \supset \gamma_\epsilon$ be a region of size $\zeta(\epsilon)$. I define $\mathcal{B}_{\gamma_\epsilon}$ to be a region of proper radius r_B centered on γ_ϵ , with $\epsilon \ll r_B \ll \epsilon^0$. The region I seek a solution in is then $\mathcal{D}_{\gamma_\epsilon, \zeta(\epsilon)} = D_{\zeta(\epsilon)} \setminus \mathcal{B}_{\gamma_\epsilon}$. The inner boundary of this region lies in the buffer region, and there the solution must satisfy the matching condition (BC2).

1.5.2 Field Equations

Since the coefficients $h_{\mu\nu}^n(x; z_\epsilon)$ in the expansion (20) depend on ϵ , it may seem they are not uniquely determined. However, here I define the functional $h_{\mu\nu}(x, \epsilon; z)$ to be the solution to the *relaxed* Einstein equation (19); the relaxed equation places no constraints on z^μ , and each function $z^\mu : \mathbb{R} \rightarrow \mathbb{R}^4$ yields a different solution. (In the present context this means there are no constraints on the motion of the region $\mathcal{B}_{\gamma_\epsilon}$.) The coefficients $h_{\mu\nu}^n(x; z)$ are then uniquely determined to be the solution to the n th-order term in an ordinary power-series expansion of the relaxed Einstein equation. That n th-order term has the form $E_{\mu\nu}[h^n] = S_{\mu\nu}^n[h^1, \dots, h^{n-1}]$. Up to $n = 3$, it reads

$$E_{\mu\nu}[h^1] = 0 \quad x \in \mathcal{D}_{\gamma, \zeta(\epsilon)}, \quad (21a)$$

$$E_{\mu\nu}[h^2] = 2\delta^2 R_{\mu\nu}[h^1, h^1] \quad x \in \mathcal{D}_{\gamma, \zeta(\epsilon)}, \quad (21b)$$

$$E_{\mu\nu}[h^3] = 2\delta^3 R_{\mu\nu}[h^1, h^1, h^1] + 4\delta^2 R_{\mu\nu}[h^1, h^2] \quad x \in \mathcal{D}_{\gamma, \zeta(\epsilon)}, \quad (21c)$$

where I have defined the “ n th-order Ricci tensor” to be the n th variation⁹

$$\delta^n R_{\mu\nu}[h, \dots, h] = \frac{1}{n!} \frac{d^n}{d\lambda^n} R_{\mu\nu}[g + \lambda h] \Big|_{\lambda=0}. \quad (22)$$

In the concrete calculations in this paper, I will require only $\delta^2 R_{\mu\nu}$, which is given explicitly by

$$\begin{aligned} \delta^2 R_{\alpha\beta}[h, h] = & -\frac{1}{2} \bar{h}^{\mu\nu}{}_{;\nu} (2h_{\mu(\alpha;\beta)} - h_{\alpha\beta;\mu}) + \frac{1}{2} h^{\mu}{}_{\beta}{}^{;\nu} (h_{\mu\alpha;\nu} - h_{\nu\alpha;\mu}) \\ & + \frac{1}{4} h^{\mu\nu}{}_{;\alpha} h_{\mu\nu;\beta} - \frac{1}{2} h^{\mu\nu} (2h_{\mu(\alpha;\beta)\nu} - h_{\alpha\beta;\mu\nu} - h_{\mu\nu;\alpha\beta}). \end{aligned} \quad (23)$$

Solving Eqs. (21) subject to the boundary conditions (BC1)–(BC2) yields a functional-valued asymptotic solution to the relaxed Einstein equation (19). Now we must find a particular function $z^\mu = z_\epsilon^\mu$ for which $h_{\mu\nu}(x, \epsilon; z)$ is also an asymptotic solution to the unrelaxed equation (17). To do this, we must ensure $h_{\mu\nu}(x, \epsilon; z)$ also satisfies the gauge condition (18) to the same order.¹⁰

⁹Cross terms like $\delta^2 R_{\mu\nu}[h^1, h^2]$ are as defined in Eq. (227).

¹⁰Equation (222) illustrates more explicitly, using a point-particle field, how the gauge condition implies an equation of motion.

I accomplish this in a systematic way by writing the accelerated equation of motion of z_ϵ^μ as

$$a_\epsilon^\mu \equiv \frac{D^2 z_\epsilon^\mu}{d\tau^2} = F^\mu(\tau, \epsilon), \quad (24)$$

and then assuming that like $h_{\mu\nu}$, the force (per unit mass) appearing on the right-hand side can be expanded as

$$F^\mu(\tau, \epsilon) = \sum_{n \geq 0} \epsilon^n F_n^\mu(\tau; z_\epsilon, \dot{z}_\epsilon). \quad (25)$$

I substitute this expansion, together with the one in Eq. (20), into the gauge condition (18) and solve order by order in ϵ while holding $(z_\epsilon^\mu, \dot{z}_\epsilon^\mu)$ fixed. By holding $(z_\epsilon^\mu, \dot{z}_\epsilon^\mu)$ fixed during this procedure, rather than expanding their ϵ dependence, I preserve the particular accelerated worldline that satisfies some appropriate mass-centeredness condition, such as the vanishing of a suitably defined mass dipole moment in the buffer region centered on γ_ϵ . Solving the sequence of gauge conditions to higher and higher order yields a better and better approximation to the equation of motion of that particular worldline, *without ever expanding the worldline itself*. The first few of these gauge conditions are

$$L_\mu[h^1, F_0] = 0, \quad (26a)$$

$$\delta L_\mu[h^1, F_1] = -L_\mu[h^2, F_0], \quad (26b)$$

$$\delta L_\mu[h^1, F_2] = -L_\mu[h^3, F_0] - \delta L_\mu[h^2, F_1] - \delta^2 L_\mu[h^1, F_1, F_1], \quad (26c)$$

where I have defined $L_\mu[h, F] = L_\mu[h]|_{a=F}$ and

$$\delta^n L_\mu[h, F, \dots, F] \equiv \frac{1}{n!} \frac{d^n}{d\lambda^n} L_\mu[h, F_0 + \lambda F]|_{\lambda=0}. \quad (27)$$

This sequence determines the forces F_n^μ ,¹¹ thereby determining the equation of motion (24).

1.5.3 Solution Method

We solve Eqs. (21) and (26) by working outward from the buffer region. Solving them in the buffer region using a local expansion, subject to (BC2), yields two things: the local form of the metric outside the object, and an equation of motion for the object.

¹¹It also constrains other quantities in $h_{\mu\nu}$, particularly determining the evolution of the object's mass and spin.

The local form of the metric is described in Sect. 3. In line with the themes of the earlier sections, it allows a natural split into an effectively external metric $\tilde{g}_{\mu\nu} = g_{\mu\nu} + h_{\mu\nu}^R$ and a self-field $h_{\mu\nu}^S \equiv h_{\mu\nu} - h_{\mu\nu}^R$, where $\tilde{g}_{\mu\nu}$ satisfies all the “nice” properties of the Detweiler-Whiting regular field.

Derivations of the equations of motion at first and second order are sketched in Sects. 3 and 7. If at leading order the object’s spin and quadrupole moment both vanish, then the equation of motion is [14, 16].

$$\frac{D^2 z_\epsilon^\mu}{d\tau^2} = -\frac{1}{2} P^{\mu\gamma} (g_\gamma^\nu - h_\gamma^{R\nu}) (2h_{\rho\nu;\sigma}^R - h_{\rho\sigma;\nu}^R) u^\rho u^\sigma + \mathcal{O}(\epsilon^3), \quad (28)$$

where $h_{\mu\nu}^R = \epsilon h_{\mu\nu}^{R1} + \epsilon^2 h_{\mu\nu}^{R2} + \mathcal{O}(\epsilon^3)$. Following the steps of Appendix 1, this equation of motion can also be written as $\frac{\tilde{D}^2 z_\epsilon^\mu}{d\tilde{\tau}^2} = \mathcal{O}(\epsilon^3)$, the geodesic equation in the effective (smooth, vacuum) metric $\tilde{g}_{\mu\nu}$. In other words, at least through second order in ϵ , the generalized equivalence principle described in Sect. 1.1.2 holds.

After obtaining the local results in the buffer region, one might think to solve Eqs. (21) and (26) globally in $\mathcal{D}_{\gamma_\epsilon, \varsigma(\epsilon)}$ by imposing agreement with the local results on the inner boundary $\partial\mathcal{B}_{\gamma_\epsilon}$ and then moving $\partial\mathcal{B}_{\gamma_\epsilon}$ using the equation of motion. However, in practice, a global solution is instead obtained by analytically extending the buffer-region results into $\mathcal{B}_{\gamma_\epsilon} \setminus \gamma_\epsilon$, replacing the physical metric there with the fictitious, analytically extended metric, while insisting that outside $\mathcal{B}_{\gamma_\epsilon}$, the metric is unaltered. This procedure (described in detail in Sect. 4) allows us to work with field equations on the whole of $\mathcal{D}_{\varsigma(\epsilon)} = \mathcal{D}_{\gamma_\epsilon, \varsigma(\epsilon)} \cup \mathcal{B}_{\gamma_\epsilon}$. At order ϵ , the procedure reveals that $h_{\mu\nu}^1(x; z_\epsilon)$ in $\mathcal{D}_{\gamma_\epsilon, \varsigma(\epsilon)}$ is precisely equal to the perturbation produced by a point mass moving on z_ϵ^μ , as promised in Sect. 1.1.1. More generally, at all orders, it leads to a practical *puncture scheme* [15, 52, 54–57], in which the *puncture* $h_{\mu\nu}^P$, a local approximation to $h_{\mu\nu}^S$, moves on γ_ϵ , and the field equations in $\mathcal{B}_{\gamma_\epsilon}$ are recast as equations for a *residual field* $h_{\mu\nu}^R$ that locally approximates $h_{\mu\nu}^R$.¹²

The setup of a puncture scheme is compactly summarized in Eqs. (98)–(100) below. Using this scheme, one can directly solve for the effective metric on the worldline and use it to evolve that worldline via the equation of motion, and at the same time one can obtain the physical metric outside $\mathcal{B}_{\gamma_\epsilon}$. Although we begin with a potentially complicated extended object, this scheme illuminates the fact that in self-force theory, we do not need to know anything about the particularities of that object: *at the end of the day, all necessary physical information about it is absorbed into the puncture and the motion of that puncture.*

¹²Note that although a puncture scheme utilizes approximations to $h_{\mu\nu}^S$ and $h_{\mu\nu}^R$, it is designed to *exactly* obtain $h_{\mu\nu}^R$ (and any finite number of its derivatives) on the worldline, meaning it does not introduce any approximation into the motion of γ_ϵ . Nor does it introduce approximations into the physical field $h_{\mu\nu} = h_{\mu\nu}^R + h_{\mu\nu}^S = h_{\mu\nu}^R + h_{\mu\nu}^P$.

1.5.4 Accuracy Estimates

How accurate will this self-consistent approximation be on a domain $\mathcal{D}_{\gamma, \varsigma(\epsilon)}$? Let us make the reasonable assumption that the largest secularly growing error in the approximation arises from truncating the expansion (25) at some order ϵ^n , leading to an error in z^μ of order $\delta z^\mu \sim \epsilon^{n+1} F_{n+1}^\mu t^2$.¹³ The largest error in $h_{\mu\nu}$ is then

$$\text{Error in } h_{\mu\nu} \sim \epsilon h_{\mu\nu}^1 \cdot \delta z^\alpha = \mathcal{O}(\epsilon^{n+2} t^2). \quad (29)$$

The order of accuracy depends on the size of the domain we work in. Suppose we work in $\mathcal{D}_{\gamma, 1/\epsilon}$, corresponding to the radiation-reaction time. On that domain, the error from neglecting F_{n+1}^μ is $\mathcal{O}(\epsilon^{n+2} \cdot 1/\epsilon^2) = \mathcal{O}(\epsilon^n)$. Therefore, if we include only F_1^μ in the equation of motion, solving (via a puncture scheme) the coupled system comprising Eqs. (21a) and (9), then the result contains errors $\mathcal{O}(\epsilon^3 \cdot 1/\epsilon^2) = \mathcal{O}(\epsilon)$ —which is as large as our first-order perturbation. In other words, this approximation fails on $\mathcal{D}_{1/\epsilon}$. If in addition we include F_2^μ , solving the coupled system comprising Eqs. (21a), (21b), and (28), then the error is $\mathcal{O}(\epsilon^4 \cdot 1/\epsilon^2) = \mathcal{O}(\epsilon^2)$; hence, with this approximation, we can have faith in our field $h_{\mu\nu}^1(x; z)$.

In the smaller domain $\mathcal{D}_{1/\sqrt{\epsilon}}$, corresponding to the so-called *dephasing time* $t_{\text{dph}} \sim 1/\sqrt{\epsilon}$, the approximations are more accurate. Including only F_1^μ , by solving Eqs. (21a) and (9), yields a first-order-accurate solution with errors $\mathcal{O}(\epsilon^3 \cdot 1/\epsilon) = \mathcal{O}(\epsilon^2)$. Including F_2^μ , by solving Eqs. (21a), (21b), and (28), yields a second-order-accurate solution with errors $\mathcal{O}(\epsilon^4 \cdot 1/\epsilon) = \mathcal{O}(\epsilon^3)$.

1.5.5 Gralla-Wald Approximation

I next consider the Gralla-Wald representation of perturbative motion, named after the authors of Refs. [18, 20]. In this approximation, as in Eqs. (15) and (16), one considers the effect of the self-force to be a small perturbation of the worldline, and one expands the worldline as

$$z^\mu(s, \epsilon) = \sum_{n \geq 0} \epsilon^n z_n^\mu(s), \quad (30)$$

where the terms $z_{n>0}^\mu$ measure the deviation of z^μ from the zeroth-order worldline z_0^μ . Substituting this expansion into Eq. (20), one obtains a new expansion of the metric perturbation:

$$h_{\mu\nu}(x, \epsilon; z, \dot{z}) = \sum_{n \geq 0} \epsilon^n \check{h}_{\mu\nu}^n(x; z_0, \dots, z_{n-1}). \quad (31)$$

¹³Here I return to what will become my common practice of dropping the subscript ϵ on z^μ for simplicity, though I refer to the self-consistently determined center-of-mass worldline, not the freely specifiable worldline for which the relaxed Einstein equation can be solved.

Section 5 describes this expansion in some detail. Explicitly, at first and second order, $h_{\mu\nu}^1(x; z_0) = h_{\mu\nu}^1(x; z_0)$ and $\check{h}_{\mu\nu}^2(x; z_0, z_1) = h_{\mu\nu}^2(x; z_0) + \delta h_{\mu\nu}^1(x; z_0, z_1)$, as described below Eq. (16). Since the individual terms $z_n^\mu(s)$ are independent of ϵ in Eq. (30), Eq. (31) is an ordinary expansion in which the coefficients $\check{h}_{\mu\nu}^n$ do not depend on ϵ , unlike in Eq. (20). Rather than starting from the self-consistent representation and then expanding the worldline, one could instead simply start with this ordinary expansion, as was done by Gralla and Wald. In this paper, to explicate the relationship between the two, I will instead almost always derive Gralla-Wald results from self-consistent results.

In the Gralla-Wald approximation, the role of the domain $\mathcal{D}_{\gamma, \varsigma(\epsilon)}$ is played by $\mathcal{D}_{\gamma_0, \varsigma(\epsilon)}$, which excludes a small region around γ_0 (the worldline with coordinates z_0^μ). In that region Eqs. (21) become

$$E_{\mu\nu}[\check{h}^1] = 0 \quad x \in \mathcal{D}_{\gamma_0, \varsigma(\epsilon)}, \quad (32a)$$

$$E_{\mu\nu}[\check{h}^2] = 2\delta^2 R_{\mu\nu}[\check{h}^1, \check{h}^1] \quad x \in \mathcal{D}_{\gamma_0, \varsigma(\epsilon)}, \quad (32b)$$

$$E_{\mu\nu}[\check{h}^3] = 2\delta^3 R_{\mu\nu}[\check{h}^1, \check{h}^1, \check{h}^1] + 4\delta^2 R_{\mu\nu}[\check{h}^1, \check{h}^2] \quad x \in \mathcal{D}_{\gamma_0, \varsigma(\epsilon)}. \quad (32c)$$

The gauge conditions (26) become simply

$$L_\mu[\check{h}^n] = 0. \quad (33)$$

The equation of motion (28) becomes a sequence of equations for z_n^μ :

$$\frac{D^2 z_0^\mu}{d\tau_0^2} = 0, \quad (34)$$

$$\frac{D^2 z_1^\mu}{d\tau_0^2} = \check{F}_1^\mu(\tau_0; z_0) - R^\mu{}_{\alpha\beta\gamma} u_0^\alpha z_1^\beta u_0^\gamma, \quad (35)$$

$$\begin{aligned} \frac{D^2 z_{2F}^\mu}{d\tau_0^2} &= \check{F}_2^\mu(\tau_0; z_0, z_1) - R^\mu{}_{\alpha\beta\gamma} \left(u_0^\alpha z_{2F}^\beta u_0^\gamma + 2u_1^\alpha z_1^\beta u_0^\gamma \right) \\ &\quad + 2R^\mu{}_{\alpha\beta\gamma;\delta} z_1^{(\alpha} u_0^{\beta)} z_1^{[\gamma} u_0^{\delta]}, \end{aligned} \quad (36)$$

where τ_0 is proper time on γ_0 as measured in $g_{\mu\nu}$, $u_0^\mu \equiv \frac{dz_0^\mu}{d\tau_0}$, $u_1^\mu \equiv \frac{Dz_1^\mu}{d\tau_0}$, and the forces \check{F}_1^μ and \check{F}_2^μ are constructed from $\check{h}_{\mu\nu}^R$ according to Eqs. (206)–(207). The Riemann terms in these equations of motion are geodesic-deviation terms; they correspond to the fact that even in the absence of a force, two neighbouring curves z^μ and z_0^μ will deviate from one another due to the background curvature. Appendix 1 describes how Eqs. (34)–(36) are derived from Eq. (28). As explained more thoroughly there, the quantities z_1^μ and z_{2F}^μ are vectors that live on γ_0 . z_{2F}^μ is defined by applying the expansion (30) in a normal coordinate system centered on γ_0 ; it is related to z_2^μ in any other coordinate system by the coordinate-dependent relation $z_{2F}^\mu = z_2^\mu + \frac{1}{2} \Gamma_{\nu\rho}^\mu(z_0) z_1^\nu z_1^\rho$.

Just as in the self-consistent case, we can work with field equations on $\mathcal{D}_{\varsigma(\epsilon)} = \mathcal{D}_{\gamma_0, \varsigma(\epsilon)} \cup \mathcal{B}_{\gamma_0}$ by replacing the physical metric in \mathcal{B}_{γ_0} with the analytical extension of the buffer-region metric. Re-expanding the results from the self-consistent case, we find that $\check{h}_{\mu\nu}^1(x; z_0)$ in $\mathcal{D}_{\gamma_0, \varsigma(\epsilon)}$ is identical to the perturbation sourced by a point particle moving on z_0^μ ; the expansion of $h_{\mu\nu}^1(x; z)$ around $\check{h}_{\mu\nu}^1(x; z_0)$ is derived in Appendix 2. We also arrive at a substantially simplified practical puncture scheme: rather than having to solve for z^μ and $h_{\mu\nu}$ together, as a coupled system, one can first specify a geodesic z_0^μ and then calculate in sequence (i) the perturbations $\check{h}_{\mu\nu}^1(x; z_0)$ and $\check{h}_{\mu\nu}^{R1}(x; z_0)$, (ii) the deviation z_1^μ driven by $\check{h}_{\mu\nu}^{R1}$, (iii) the perturbations $\check{h}_{\mu\nu}^2(x; z_0, z_1)$ and $\check{h}_{\mu\nu}^{R2}(x; z_0, z_1)$, (iv) the deviation z_2^μ , and so on. *At all orders, the puncture moves on z_0^μ ; the deviations $z_{n>0}^\mu$, through their appearance in $\check{h}_{\mu\nu}^{n>1}$, merely alter the singularity structure of the puncture.* This puncture scheme is compactly summarized in Eqs. (117)–(119) below.

On what domain is the Gralla-Wald approximation valid? There is no obvious estimate for the rate of growth of the terms $z_{n>1}^\mu$, but as in Sect. 1.4, we can easily estimate the growth of ϵz_1^μ to be of order ϵt^2 .¹⁴ If we assume that the dominant error in $h_{\mu\nu}$ arises from the z_1^μ term in $\check{h}_{\mu\nu}^2$, then we have

$$\text{Error in } \check{h}_{\mu\nu} \sim \epsilon^2 \check{h}_{\mu\nu}^1 z_1^\alpha = \mathcal{O}(\epsilon^2 t^2). \quad (37)$$

If this estimate is valid, we can make the approximation valid to any order on domains $\mathcal{D}_{\gamma_0, \varsigma(\epsilon)}$ with sufficiently small $\varsigma(\epsilon) \ll t_{dph} = 1/\sqrt{\epsilon}$. On domains comparable to the dephasing time, $\mathcal{D}_{\gamma_0, 1/\sqrt{\epsilon}}$, the deviation vector ϵz_1^μ becomes of order 1, the second-order metric perturbation becomes as large as the first, and the expansion of the worldline ceases to be sensible. If higher-order deviations $z_{n>1}^\mu$ grow large much more quickly than z_1^μ , as we might surmise from Eq. (36), then the domain of validity of the expansion may be substantially smaller than $\mathcal{D}_{\gamma_0, 1/\sqrt{\epsilon}}$ even for first-order accuracy; if at each higher order the deviations grow more rapidly than the last, it may be the case that the domain of validity cannot be extended beyond $\mathcal{D}_{\gamma_0, 1}$.

1.5.6 Osculating Geodesics

Finally, I consider an approximation intermediate between the self-consistent and Gralla-Wald expansions, one which makes use of both the expanded and unexpanded representations of the worldline. Starting from the self-consistent representation, the idea is at each instant τ on γ , to perform a Gralla-Wald expansion in a region $\mathcal{D}_{\gamma_0(\tau), \varsigma(\epsilon)}$, where $\gamma_0(\tau)$ is a geodesic of $g_{\mu\nu}$ that is instantaneously tangential to γ at time τ ; $\gamma_0(\tau)$ is called an *osculating geodesic* [59].¹⁵ By solving the field equations

¹⁴See Ref. [58] for an explicit solution to Eq. (35) in a particular scenario.

¹⁵The scheme I describe here should not be confused with the general method of osculating geodesics, which is simply a way of using instantaneously tangential geodesics to rewrite an equation

of the Gralla-Wald approximation, one may calculate the self-force at time τ , and then use that force to evolve z^μ to the next time step. By following this procedure at each time step, one eventually obtains γ over the entire timespan of interest. The terms in the self-consistent approximation $h_{\mu\nu}(x; z) = \sum_\epsilon \epsilon^n h_{\mu\nu}^n(x; z)$ can then be found simply by solving Eqs. (21a)–(21c) (and higher-order analogues) with γ already pre-determined.

More concretely, at each instant τ on the worldline, one perform a Gralla-Wald expansion $z^\mu(\tau', \epsilon) = \sum \epsilon^n z_{n(\tau)}^\mu(\tau')$, where τ is the specific instant of interest and τ' is variable, and one substitutes this expansion into the right-hand side of Eq. (25)—*but not into the left-hand side*—to obtain

$$\frac{D^2 z^\mu}{d\tau^2} = \epsilon \check{F}_1^\mu(\tau; z_{0(\tau)}) + \epsilon^2 \check{F}_2^\mu(\tau; z_{0(\tau)}, z_{1(\tau)}) + \mathcal{O}(\epsilon^3). \quad (38)$$

The forces on the right-hand side are constructed from fields $\check{h}_{\mu\nu}^{\text{R1}}(x; z_{0(\tau)})$ and $\check{h}_{\mu\nu}^{\text{R2}}(x; z_{0(\tau)}, z_{1(\tau)})$ (and higher-order fields for higher order forces) according to Eqs. (206) and (207). For example, in terms of the tail of the perturbation, $\check{F}_1^\mu(\tau; z_{0(\tau)})$ is given by the order- ϵ term on the right-hand side of Eq. (6) but with the tail integral (7) evaluated over $z_{0(\tau)}^\mu$ rather than over z^μ . These fields are found by solving the following sequence of equations at each value of τ : (34) for the osculating geodesic $z_{0(\tau)}^\mu$; (32a) for $\check{h}_{\mu\nu}^1(x; z_{0(\tau)})$ in $\mathcal{D}_{\gamma_{0(\tau)}, \varsigma(\epsilon)}$; (35) for $z_{1(\tau)}^\mu$; and (32b) for $\check{h}_{\mu\nu}^2(x; z_{0(\tau)}, z_{1(\tau)})$ in $\mathcal{D}_{\gamma_{0(\tau)}, \varsigma(\epsilon)}$. This suffices to compute $\check{F}_1^\mu(\tau; z_{0(\tau)})$ and $\check{F}_2^\mu(\tau; z_{0(\tau)}, z_{1(\tau)})$, but in principle the calculations could proceed to higher order. All of these equations are to be solved subject to the “osculation conditions” $z_{0(\tau)}^\mu = z^\mu(\tau)$, $u_{0(\tau)}^\mu(\tau) = u^\mu(\tau)$, $z_{n>0(\tau)}^\mu = 0$, and $u_{n>0(\tau)}^\mu(\tau) = 0$, which state that $\gamma_{0(\tau)}$ is tangential to γ at time τ . They must also be solved subject to boundary conditions that ensure the sum $\sum_{n>0} \epsilon^n \check{h}_{\mu\nu}^n(x; z_{0(\tau)})$ agrees with the full field $h_{\mu\nu}$ in $\mathcal{D}_{\gamma_{0(\tau)}, \varsigma(\epsilon)}$; at nonlinear orders, finding those boundary conditions may be highly nontrivial.

At linear order, the osculating-geodesic approximation has already been concretely implemented to find z^μ using the force $\check{F}_1^\mu(\tau; z_{0(\tau)})$ [60–62] (building on the framework in Ref. [59]) and to compute $h_{\mu\nu}^1(x; z)$ [61, 62]. However, to my knowledge, the brief sketch above is the first time it has been described at nonlinear orders (although possibly equivalent ideas have been presented by Mino [63]). Considerably more work must be done to establish that the scheme is viable beyond linear order. If it is, then one may naively estimate that it is valid to the same order on the same domain as the self-consistent expansion: including only $\check{F}_1^\mu(\tau; z_{0(\tau)})$ in

(Footnote 15 continued)

of motion $\frac{D^2 z^\mu}{d\tau^2} = F^\mu$ in terms of more convenient variables; that general method, inherited from celestial mechanics, is exact and does not inherently involve an expansion of z^μ , although it is particularly well suited to the osculating-geodesic approximation discussed here [59].

Eq. (38) yields an approximation valid up to $\mathcal{O}(\epsilon^2)$ errors in a domain $\mathcal{D}_{\gamma,1/\sqrt{\epsilon}}$, and including both $\check{F}_1^\mu(\tau; z_{0(\tau)})$ and $\check{F}_2^\mu(\tau; z_{0(\tau)}, z_{1(\tau)})$ yields an approximation valid up to $\mathcal{O}(\epsilon^2)$ errors in a domain $\mathcal{D}_{\gamma,1/\epsilon}$.

1.6 Outline of This Paper

As discussed above, the bulk of this paper focuses on the formalism presented in Ref. [11] and further developed in the series of papers [12, 14–18, 52].

I begin in Sect. 2 with a more complete description of matched asymptotic expansions, the concepts of which underly most of self-force theory. I focus on the importance of the buffer region and formulating appropriate definitions of the small object’s representative worldline.

Sections 3 and 4 present an algorithm for constructing an n th-order expansion in the self-consistent approximation. In Sect. 3, I describe how to obtain the general solution in the buffer region. This algorithm determines the equation of motion as well as a natural split of the general solution into a self-field and an effectively external field. In Sect. 4, I describe how to generate the global solution in $\mathcal{D}_{\gamma,\varsigma(\epsilon)}$, using as input the self-field obtained in the buffer region. Along the way, I show how at linear order, the point-particle picture is recovered, and how at nonlinear orders, a certain point-particle “skeleton” can be defined to characterize the object’s multipole structure.

In Sect. 5, I show how to recover a Gralla-Wald expansion or an osculating-geodesics expansion from the results of the self-consistent expansion.

In Sect. 6, I discuss the gauge freedom in each of the three types of expansions—self-consistent, Gralla-Wald, and osculating-geodesics—and how that freedom relates to the representation of perturbative motion in each.

In Sect. 7, I sketch how one can derive equations of motion by obtaining further information about the inner expansion and then utilizing the relationship between gauge and motion. This is an alternative to the algorithmic approach in the buffer region, and it is the method that has been used in practice to derive second-order equations of motion [14, 16, 20].

I conclude in Sect. 8 with a summary and a discussion of future directions.

The appendices contain more general results: expansions of the geodesic equation in a perturbed spacetime, expansions of point particle functionals of an accelerated worldline around a geodesic, and some identities pertaining to gauge transformations of curvature tensors.

2 Matched Asymptotic Expansions

2.1 Outer, Inner, and Buffer Expansions

Traditionally in applied mathematics, the method of matched asymptotic expansions has been used to find both inner and outer expansions to some desired degree of accuracy and then combine them to obtain a uniformly accurate solution in the entire domain. But for my purposes here, I will not be interested in obtaining an accurate solution in the region $r \sim \epsilon$; instead, I will be interested in the inner expansion only insofar as it constrains the outer expansion. Finding an accurate inner expansion would require specifying the type of compact object we are examining, while here I am interested in generic results that apply for any compact object. As it turns out, finding those generic results requires only minimal knowledge of the inner expansion—in fact, just its general form in the buffer region suffices.

To build toward that conclusion, let me describe the formalism more geometrically. I focus for the moment on the self-consistent case. In the outer expansion, we wish to approximate the exact spacetime $(g_{\mu\nu}, \mathcal{M}_\epsilon)$ in the domain $\mathcal{D}_{\gamma, \zeta(\epsilon)}$ outside a small region of size $r \ll \epsilon^0$ around the object. I expand the exact spacetime around a background $(g_{\mu\nu}, \mathcal{M}_0)$ by adopting some identification $\varphi : \mathcal{D}_{\gamma, \zeta(\epsilon)} \subset \mathcal{M}_0 \rightarrow \mathcal{M}_\epsilon$ between the spacetimes (in the region outside the inner region). In a given coordinate system $x^\mu : \mathcal{M}_0 \rightarrow \mathbb{R}^4$, the identification map assigns points $p \in \mathcal{M}_0$ and $\varphi(p) \in \mathcal{M}_\epsilon$ the same coordinate values $x^\mu(p)$. I next write $g_{\mu\nu}$ as a functional of a worldline $\gamma \subset \mathcal{M}_0$ as $g_{\mu\nu}(x, \epsilon; z)$ in those coordinates, where $z^\mu(s) = x^\mu(\gamma(s))$, and I then expand for small ϵ while holding both x^μ and z^μ fixed. I thence arrive at Eq. (20).¹⁶ Note that z^μ is defined in the background, not in the perturbed spacetime; the identification map is assumed to exist only in $\mathcal{D}_{\gamma, \zeta(\epsilon)}$, not in the inner region where there may lie a black hole rather than an identifiable worldline, for example. Later, I will replace the physical metric in the interior of the object with the effective metric $\tilde{g}_{\mu\nu}$, and via the identification map, the worldline will have identical coordinate values in the effective spacetime $(\tilde{g}_{\mu\nu}, \tilde{\mathcal{M}})$ as in the background.

Now, the inner expansion is constructed by choosing some coordinates (t, x^i) centered on γ , and then rescaling spatial distances according to $\bar{x}^i \equiv x^i/\epsilon$. The inner expansion is performed by expanding for $\epsilon \rightarrow 0$ while holding the scaled coordinates (t, \bar{x}^i) fixed, as in¹⁷

¹⁶In truth, it is unlikely that any of the expansions I consider, whether self-consistent, Gralla-Wald, or osculating-geodesics, is convergent. More likely, they are asymptotic approximations only. So when performing the self-consistent expansion, I actually assume that $|g_{\mu\nu}(x, \epsilon) - g_{\mu\nu}^N(x, \epsilon; z)| = o(\epsilon^N)$, where $g_{\mu\nu}^N(x, \epsilon; z) = g_{\mu\nu}(x) + \sum_{n=1}^N \epsilon^n h_{\mu\nu}^n(x; z)$. The notation $o(k(\epsilon))$ means “goes to zero faster than $k(\epsilon)$ ”.

¹⁷Here indices refer to the unscaled coordinates (t, x^i) . If components are written in the scaled coordinates, overall factors ϵ and ϵ^2 appear in front of ta and ab components, respectively. These overall factors have no practical impact.

$$g_{\mu\nu}(t, \bar{x}^a, \epsilon) = g_{\mu\nu}^{\text{obj}}(t, \bar{x}^a) + \sum_{n \geq 1} \epsilon^n H_{\mu\nu}^n(t, \bar{x}^a; z). \quad (39)$$

Tensors in this expansion live on a manifold \mathcal{M}_{obj} , where $(g_{\mu\nu}^{\text{obj}}, \mathcal{M}_{\text{obj}})$ is identified as the object's spacetime were it isolated. The perturbations $H_{\mu\nu}^n(t, \bar{x}^a; z)$ describe the effect of interaction with the external spacetime. What is the meaning of this expansion? The scaled coordinates serve to keep distances fixed relative to the object's mass in the limit $\epsilon \ll 1$, effectively zooming in on the object by sending all distances much larger than the mass off toward infinity. The use of a single scaling factor makes the approximation most appropriate for compact objects, whose linear dimension is comparable to their mass. Scaling only distances, not t , is equivalent to assuming the object possesses no fast internal dynamics; that is, there is no evolution on the short timescale of the object's mass and size.

Note that the treatment of the “region around the object” depends strongly on whether one considers a self-consistent or Gralla-Wald expansion. In the self-consistent case, the outer expansion takes the limit as the object shrinks toward zero size around the self-consistently determined, accelerated worldline $\gamma \subset \mathcal{M}_0$, and the inner expansion blows up a region around that accelerated worldline; in the Gralla-Wald case, the outer expansion takes the limit as the object shrinks to zero size around the zeroth-order, background geodesic γ_0 , and the inner expansion blows up a region around that background geodesic.

In either case, the relationship between the two expansions is illustrated in Fig. 1. I now use this relationship to feed information from the inner expansion out to the outer expansion. This exchange of information is done in the buffer region around the object. From the perspective of the inner expansion, the buffer region lies at asymptotic infinity in \mathcal{M}_{obj} . In that region, the inner expansion can be expressed in unscaled coordinates as

$$g_{\mu\nu}(t, x^a/\epsilon, \epsilon) = g_{\mu\nu}^{\text{obj}}(t, x^a/\epsilon) + \sum_{n \geq 1} \epsilon^n H_{\mu\nu}^n(t, x^a/\epsilon; z) \quad (40)$$

and then re-expanded for small ϵ (or equivalently, expanded for $r \gg \epsilon$; i.e., for distances that are large on the scale of the inner expansion). Conversely, from the perspective of the outer expansion, the buffer region lies in a tiny region around the worldline. Hence, in that region the outer expansion can be expanded for $r \ll \epsilon^0$ (i.e., for distances that are small on the scale of the outer expansion). Since the inner and outer expansions are assumed to approximate the same metric, it is assumed that the results of these re-expansions in the buffer region must match order by order in both r and ϵ .¹⁸

¹⁸This matching condition amounts to the assumption that nothing too “funny” happens in the buffer region. It can instead be replaced by more explicit assumptions on the behavior of the full metric $g_{\mu\nu}$, such as the conditions assumed in Ref. [18] or various others discussed in Ref. [41].

Now, say the n th-order outer perturbation is expanded as $h_{\mu\nu}^n(t, x^i) = \sum_p r^p h_{\mu\nu}^{np}(t, n^i)$ in the buffer region, where $n^i = x^i/r$.¹⁹ One must allow negative powers of r , since at least part of the field will fall off with distance from the body. But there is a bound on the most negative power at a given order in ϵ : Since the inner expansion is assumed to be well behaved, it must include no negative powers of ϵ . And since any term in $\epsilon^n h_{\mu\nu}^n$ must correspond to a term in the inner expansion, if $\epsilon^n h_{\mu\nu}^n$ is written as a function of the scaled distance $\bar{r} = r/\epsilon$, it must likewise have no negative powers of ϵ . From this it follows that

$$\epsilon^n h_{\mu\nu}^n(t, x^i) = \frac{\epsilon^n}{r^n} h_{\mu\nu}^{n,-n}(t, n^i) + \mathcal{O}(\epsilon^n r^{-n+1}). \quad (41)$$

Any higher power of $1/r$ would induce illegal powers of ϵ ; for example, $\frac{\epsilon^n}{r^{n+1}} = \frac{1}{\epsilon \bar{r}^{n+1}}$.

We can go one step further with this general analysis. Since ϵ^n/r^n is independent of ϵ in the scaled coordinates, and $g_{\mu\nu}^{\text{obj}}$ is the only term in the inner expansion (39) that does not depend on ϵ , it must be that $h_{\mu\nu}^{n,-n}$ is equal to a term in $g_{\mu\nu}^{\text{obj}}$. If we write $g_{\mu\nu}^{\text{obj}}(t, \bar{x}^i)$ in terms of the unscaled coordinates and expand for $r \gg \epsilon$, we find its form in the buffer region is²⁰

$$g_{\mu\nu}^{\text{obj}}(t, \bar{x}^i/\epsilon) = \sum_{n \geq 0} \frac{\epsilon^n}{r^n} g_{\mu\nu}^{\text{obj},n}(t, n^i). \quad (42)$$

From the matching condition, we then have

$$h_{\mu\nu}^{n,-n} = g_{\mu\nu}^{\text{obj},n}. \quad (43)$$

Therefore, at each order in ϵ , the most singular (as a function of r) piece of the metric perturbation $h_{\mu\nu}^n$ in the buffer region is determined by the $r \gg \epsilon$ asymptotic behavior of the object's unperturbed metric. In addition, note that because quantities in the inner expansion vary slowly in time relative to their variation in space, they are quasistationary: after changing to scaled coordinates, a derivative with respect to t effectively increases the power of ϵ relative to a derivative with respect to \bar{x}^i . Hence, on any short time, we can think of $g_{\mu\nu}^{\text{obj}}$ being stationary, and we can write its asymptotic form (42) in terms of a canonical set of multipole moments [64, 65]. So our final statement is that the inner expansion constrains the outer expansion to

¹⁹In r terms also generically arise. For simplicity, I incorporate those terms into $h_{\mu\nu}^{np}$ for the moment. Their presence does not spoil the well-orderedness of the expansion, since $r^p (\ln r)^q \ll r^{p'} (\ln r)^{q'}$ for $p > p'$. Similarly, $\ln \epsilon$ terms can occur in solving the relaxed Einstein equation [15], and I absorb them into the coefficients $h_{\mu\nu}^n(x; z)$.

²⁰The fact that the inner background must be asymptotically flat, containing no positive powers of r , follows from the assumption that the outer expansion contains no negative powers of ϵ , in the same manner as the cutoff on powers of $1/r$ in Eq. (41).

have the form (41), and the coefficients $h_{\mu\nu}^{n,-n}$ can be expressed in terms of multipole moments of the small object's unperturbed spacetime $(g_{\mu\nu}^{\text{obj}}, \mathcal{M}_{\text{obj}})$. This is all the information that will be required from the inner expansion (until we get to Sect. 7).

2.2 Defining the Worldline

Let us now use the above formalism to define what we mean by the object's worldline. First consider the self-consistent case. In the coordinates (t, x^i) centered on γ , calculate the mass dipole moment M^i of the spacetime $g_{\mu\nu}^{\text{obj}}$. A mass dipole moment indicates the position of the center of mass relative to the origin of the coordinates. If the coordinates are mass-centered, a Coulomb-like piece of the field behaves as m/r ; if the origin lies slightly away from the center of mass, by an amount ξ^i , then the Coulomb-like field behaves as $m/|x^i - \xi^i|$. Expanding this around $\xi^i = 0$, we find $m/r + m\xi_i n^i/r^2 + \mathcal{O}(|\xi|^2)$. The quantity $m\xi^i$ is the mass dipole moment M^i . Ergo, if this mass dipole moment vanishes in the coordinates centered on γ , then the object is appropriately centered “on” γ , and we identify γ as a good representative worldline.²¹ Because the definition only utilizes quantities in the buffer region, this definition makes sense even if the object is a black hole or contains topological oddities such as a wormhole: even if there exists no identification map between the background and the exact spacetime in the region inside the object, at least in the buffer region the coordinates (t, x^i) can be used to chart the manifolds \mathcal{M}_ϵ and \mathcal{M}_{obj} , and in those coordinates the metrics $g_{\mu\nu}$ and $g_{\mu\nu}^{\text{obj}}$ have reference to the worldline γ that is defined only in \mathcal{M}_0 . I refer the reader again to Fig. 1 to illuminate this.

Now consider the Gralla-Wald case. Here γ_0 is the worldline around which the inner expansion is performed. In a generic gauge (in particular, in the Lorenz gauge I work in), the small object's center of mass deviates from this worldline, as assumed in the expansion (30). Gauges in which the object does not deviate from γ_0 (on short timescales) are discussed in Sect. 7, but in a generic gauge, clearly we do not have $M^i = 0$ in coordinates centered on γ_0 . Instead, we calculate M^i in those coordinates and then define the first-order correction to the motion to be

$$z_1^i \equiv M^i/m. \quad (44)$$

Figure 2 illustrates the difference between this setup and the self-consistent one.

²¹This notion of mass-centeredness based on the mass dipole moment of $g_{\mu\nu}^{\text{obj}}$ applies only to order- ϵ deviations from z^μ . For higher-order deviations, mass-dipole-moment terms in the perturbations $H_{\mu\nu}^n$ must also be considered, or some other copacetic centeredness condition must be imposed, as discussed in Sects. 3 and 7.

3 Algorithm for an n th-Order Self-Consistent Approximation: General Solution in the Buffer Region

We are now positioned to actually obtain an outer expansion. In this section, I present an algorithm for finding the outer expansion in the buffer region. In Sect. 4, I describe an algorithm for obtaining a global solution using as input the results from the buffer region. In both cases, I specialize to the self-consistent case.

My method of finding the general solution in the buffer region is modeled on the post-Minkowskian methods of Blanchet and Damour [66]. Like them, I write the general solution in terms of a set of *algorithmic multipole moments*, which are defined simply from the algorithm of solving the relaxed Einstein equation, but a subset of which can be concretely identified with the physical multipole moments of $g_{\mu\nu}^{\text{obj}}$. All the moments are completely unconstrained so long as we solve only the relaxed Einstein equations (21). Once we impose the gauge condition, as in Eqs. (26), the moments become constrained, and in particular, evolution equations arise for the mass monopole, mass dipole, and spin dipole moments. The equation for the mass dipole moment will be used to identify the center-of-mass worldline γ for which $M^i = 0$.

The solution thus obtained will be a general solution in the sense that it is made to satisfy the matching condition (BC2) but not any particular global boundary conditions (BC1). (Refer back to the opening portion of Sect. 1.5.) Because the explicit calculations, as well as their results, are exceedingly lengthy, I merely sketch the algorithm and the form of the results. I refer the reader to Refs. [9, 11, 15, 52] for more detailed expositions.

3.1 Setup

For concreteness, I work in Fermi-Walker coordinates (t, x^a) centered on γ , in which t is proper time on γ , $r = \sqrt{\delta_{ij}x^i x^j}$ is the proper distance from γ along a spatial geodesic β that intersects γ perpendicularly, n^i is a unit radial vector that labels the direction along which β is sent out, and the spatial coordinate is $x^i = rn^i$. Reference [9] contains a pedagogical introduction.

The background metric in these coordinates is given by

$$g_{tt} = -(1 + a_i x^i)^2 - R_{0i0j} x^i x^j + \mathcal{O}(r^3), \quad (45a)$$

$$g_{ta} = -\frac{2}{3} R_{0iaj} x^i x^j + \mathcal{O}(r^3), \quad (45b)$$

$$g_{ab} = \delta_{ab} - \frac{1}{3} R_{aibj} x^i x^j + \mathcal{O}(r^3), \quad (45c)$$

where the Riemann terms are evaluated on the worldline and contracted with members of a tetrad (u^α, e_a^α) on γ that satisfies $\frac{\partial y^\mu}{\partial x^i} = e_i^\mu$ for any coordinates y^μ . For example,

$R_{0iaj}(t) \equiv R_{\alpha\mu\beta\nu}(z(t))u^\alpha e_i^\mu e_a^\beta e_j^\nu$. An overdot will indicate a covariant derivative along the worldline, such as $\dot{R}_{0iaj} \equiv R_{\alpha\mu\beta\nu;\rho}|_\gamma u^\alpha e_i^\mu e_a^\beta e_j^\nu u^\rho$. Relating back to the discussion below Eqs. (13) and (14), the Riemann tensor on γ can be written in terms of two tidal moments:

$$\mathcal{E}_{ab} \equiv R_{0a0b}, \quad \mathcal{B}_{ab} \equiv -\frac{1}{2}\epsilon^{pq}{}_{(a}R_{b)0pq}, \quad (46)$$

and $R_{abcd} = \mathcal{E}_{ac}\delta_{bd} + \mathcal{E}_{bd}\delta_{ac} + \mathcal{E}_{ad}\delta_{bc} + \mathcal{E}_{bc}\delta_{ad}$.

Reference [15] displays the metric (45) to higher order in r . At all orders in r , all terms are made from the acceleration, Riemann tensor, and derivatives of the Riemann tensor. Because the coordinates are tethered to an ϵ -dependent worldline, the background picks up an ϵ dependence, seen most obviously in the acceleration terms a^i . However, this is purely a coordinate effect. In any global coordinates covering $\mathcal{D}_{\gamma,\zeta(\epsilon)}$, $g_{\mu\nu}$ is ϵ -independent by definition. In a Gralla-Wald expansion, the ϵ -dependent coordinate transformation to Fermi-Walker coordinates would be expanded in powers of ϵ , splitting it into an ϵ -independent coordinate transformation (to Fermi coordinates centered on γ_0) plus a gauge transformation. Because I wish to at no point expand z^μ , I do not expand the transformation in this way.

In these coordinates, I expand $h_{\mu\nu}^n$ as in Eq. (41). I further assume that the coefficients in that expansion are smooth, and I make logarithms explicit; these logarithms appear generically in solutions to inhomogeneous hyperbolic equations.²² We then have an expansion of the form

$$h_{\mu\nu}^n(t, x^a; z) = \sum_{p \geq -n} \sum_{\ell=0}^{\ell_{\max}} \sum_{q=0}^{q_{\max}} r^p (\ln r)^q h_{\mu\nu L}^{npq\ell}(t; z) \hat{n}^L, \quad (47)$$

where $L = i_1 \cdots i_\ell$ is a multi-index, $h_{\mu\nu L}^{npq\ell}$ is a smooth function of t , and $\hat{n}^L \equiv n^{(i_1} \cdots n^{i_\ell)}$ is an STF combination of unit vectors. The decomposition in terms of \hat{n}^L is equivalent to an expansion in spherical harmonics, and like a spherical harmonic, \hat{n}^L is an eigenfunction of the flat-space Laplacian, satisfying $\partial^i \partial_i \hat{n}^L = -\frac{\ell(\ell+1)}{r^2} \hat{n}^L$. References [66, 68] contain excellent introductions to this type of decomposition, along with many useful identities. Favoring n^a over angles (θ, ϕ) , and \hat{n}^L over spherical harmonics, is useful because $g_{\mu\nu}$ is naturally written, as above, in terms of $x^a = rn^a$.

²²Intuitively, the logarithms are caused by the object perturbing the spacetime's light cones. One can expect the solution to the exact Einstein equation to propagate on (and within) null cones of the exact spacetime, and given that the mass of the body induces a logarithmic correction to the retarded time, logarithmic corrections then naturally appear in $h_{\mu\nu}^n$. This effect is well known from solutions to the Einstein equation in harmonic coordinates (see, e.g., Refs. [66, 67]). For generality, I allow logarithms at any value of n , but I assume that for each finite n , p , and ℓ , the highest power of $\ln r$ is a finite number $q_{\max}(n, p, \ell)$. For simplicity, to make sure that term-by-term differentiation is valid without worrying about issues of convergence, I also assume for a given, finite n and p , ℓ has a maximum $\ell_{\max}(n, p)$.

3.2 Seed Solutions

By definition, $h_{\mu\nu}^n$ is the solution to the n th-order relaxed Einstein equation, which has the form $E_{\mu\nu}[h^n] = S_{\mu\nu}^n[h^1, \dots, h^{n-1}]$. Before considering the general solution to this equation, let us first consider solutions to the corresponding homogeneous equation $E_{\mu\nu}[h^n] = 0$. We shall find that every solution of the form (47) is a member of a set $\{h_{\mu\nu}^{\text{seed}}(x; z, I_\ell^n) : 0 \leq \ell \leq n\}$ or of a set $\{h_{\mu\nu}^{\text{free}}(x; z, k_\ell^n) : \ell \geq 0\}$, or it is a superposition of such members. For a given background metric, the *seed solutions* $h_{\mu\nu}^{\text{seed}}(x; z, I_\ell^n)$ and the *free solutions* $h_{\mu\nu}^{\text{free}}(x; z, k_\ell^n)$ are completely determined by the worldline z^μ and functions of time $I_{\mu\nu L}^n(t)$ or $k_{\mu\nu L}^n(t)$ along that worldline. The quantities $I_{\mu\nu L}^n$ will be identified as *algorithmic multipole moments* that describe the object's multipole structure, while each of the quantities $k_{\mu\nu L}^n$ will identify an effectively external, freely propagating perturbation.

We arrive at these conclusions simply by substituting the expansion (47) into $E_{\mu\nu}[h^n] = 0$. First note that spatial derivatives reduce the order in r by one power, while temporal derivatives do not affect the order in r . This means we can write $E_{\mu\nu}[h^n] = \partial^i \partial_i h_{\mu\nu}^n + W_{\mu\nu}[h^n]$, where $W_{\mu\nu}[h^n] \sim h_{\mu\nu}^n/r$. Solving for $h_{\mu\nu}^{npq\ell}$ order by order in r is hence reduced to solving a sequence of Poisson equations $\partial^i \partial_i h_{\mu\nu}^n = -W_{\mu\nu}[h^n]$. Substituting the expansion (47) into this, we find that the coefficient of $r^{p-2}(\ln r)^q \hat{n}^L$ in the equation is

$$\begin{aligned} & [p(p+1) - \ell(\ell+1)]h_{\mu\nu L}^{npq\ell} + (q+1)(2p+1)h_{\mu\nu L}^{n,p,q+1,\ell} + (q+1)(q+2)h_{\mu\nu L}^{n,p,q+2,\ell} \\ &= \left\{ \sum_{p'=-n}^{p-1} \sum_{\ell'=0}^{\ell_{\max}} \sum_{q'=0}^{q_{\max}} W_{\mu\nu} \left[r^{p'} (\ln r)^{q'} \hat{n}^{L'} h_{\mu\nu L'}^{np'q'\ell'} \right] \right\}^{p-2,q,\ell}, \end{aligned} \quad (48)$$

where $\{\cdot\}^{pq\ell}$ means “pick off the coefficient of $r^{p-2}(\ln r)^q \hat{n}^L$ ”. The important thing to note is that the right-hand side depends only on coefficients with $p' < p$. So start with the term with the lowest power of r , $1/r^{n+2}$, such that the right-hand side of Eq. (48) vanishes. Further, start with $q = q_{\max}$, and suppose $q_{\max} > 0$. By assumption, $h_{\mu\nu L}^{n,-n,q_{\max}+1,\ell}$ and $h_{\mu\nu L}^{n,-n,q_{\max}+1,\ell}$ vanish, and so Eq. (48) becomes $[n(n-1) - \ell(\ell+1)]h_{\mu\nu L}^{n,-n,q_{\max},\ell} = 0$. This has a nontrivial solution only if $\ell = n-1$. Now look at the equation for the same ℓ and p but for $q = q_{\max} - 1$. It reads $[n(n-1) - \ell(\ell+1)]h_{\mu\nu L}^{n,-n,q_{\max}-1,\ell} + q_{\max}(1-2n)h_{\mu\nu L}^{n,-n,q_{\max},\ell} = 0$. But the first term vanishes because $\ell = n-1$. Hence, $h_{\mu\nu N-1}^{n,-n,q_{\max},n-1} = 0$ if $q_{\max} > 0$, and we conclude that $h_{\mu\nu N-1}^{n,-n,0,n-1} \hat{n}^{N-1}/r^n$ is the only nontrivial solution to the $1/r^{n+2}$ term in the homogeneous equation $E_{\mu\nu}[h^n] = 0$. I define the algorithmic moment

$$I_{\mu\nu L}^n \equiv h_{\mu\nu L}^{n,-n,0,n-1}. \quad (49)$$

Now proceed to sequentially higher orders in r , and at every order, set to zero all free functions that arise. The result is a solution to $E_{\mu\nu}[h^n] = 0$ of the form

$$h_{\mu\nu}^{\text{seed}}(x; z, I_{n-1}^n) = \frac{I_{\mu\nu N-1}^n(t) \hat{n}^{N-1}}{r^n} + \mathcal{O}(1/r^{n-1}) \quad (50)$$

in which every single term is linear in $I_{\mu\nu N-1}^n(t)$ (and t -derivatives of it), specifically consisting of $I_{\mu\nu N-1}^n(t)$ (and its derivatives) contracted with the other available Cartesian tensors n^i , a^i , δ^{ij} , ϵ^{ijk} , pieces of the background Riemann tensor, and pieces of derivatives of the background Riemann tensor.

Now set $I_{\mu\nu N-1}^n$ to zero and solve the $1/r^{n+1}$ and higher-order terms in Eq. (48), following exactly the same steps as above. Again the result is a homogeneous solution that is completely determined by a single function, in this case $I_{\mu\nu N-2}^n \equiv h_{\mu\nu N-2}^{n, -n+1, 0, n}$. Now keep doing the same by beginning at each following order up to (and including) $1/r^3$, always setting every free function to zero except the first one encountered. This procedure completely populates the set $\{h_{\mu\nu}^{\text{seed}}(x; z, I_\ell^n) : 0 \leq \ell \leq n\}$ with solutions of the form

$$h_{\mu\nu}^{\text{seed}}(x; z, I_\ell^n) = \frac{I_{\mu\nu L}^n(t) \hat{n}^L}{r^{\ell+1}} + \mathcal{O}(1/r^\ell), \quad (51)$$

where every term in the solution is proportional to $I_{\mu\nu L}^n(t) \equiv h_{\mu\nu L}^{n, -\ell-1, 0, \ell}(t)$ or its derivatives. The algorithmic multipole moments $I_{\mu\nu L}^n$ are symmetric in their first two indices and STF in their last ℓ indices.

Continuing the same procedure to higher orders in r , we completely populate the other set, $\{h_{\mu\nu}^{\text{free}}(x; z, I_\ell^n) : \ell \geq 0\}$, with solutions

$$h_{\mu\nu}^{\text{free}}(x; z, k_\ell^n) = r^\ell k_{\mu\nu L}^n(t) \hat{n}^L + \mathcal{O}(r^{\ell+1}), \quad (52)$$

where every term in the solution is proportional to $k_{\mu\nu L}^n(t) \equiv h_{\mu\nu L}^{n, \ell, 0, \ell}(t)$ or its derivatives. The change in behavior from $1/r^{\ell+1}$ to r^ℓ arises because the factor $[p(p+1) - \ell(\ell+1)]$ in Eq. (48) vanishes for $p = -\ell - 1$ if $p < 0$ and for $p = \ell$ if $p \geq 0$. As with $I_{\mu\nu L}^n$, the quantities $k_{\mu\nu L}^n$ are symmetric in their first two indices and STF in their last ℓ indices.

It is easy to see from the above steps that the set of seed solutions $h_{\mu\nu}^{\text{seed}}(x; z, I_\ell^n)$ and free solutions $h_{\mu\nu}^{\text{free}}(x; z, k_\ell^n)$ form a complete basis of solutions to $E_{\mu\nu}[h^n] = 0$ of the form (47). If extended down to $r = 0$, each seed solution diverges at $r = 0$, while each free solution is smooth there.

For later purposes, it will be convenient to split each algorithmic multipole moment into a mass and current moment,

$$I_{\mu\nu L}^n = M_{\mu\nu L}^n + S_{\mu\nu L}^n, \quad (53)$$

where the mass moment $M_{\mu\nu L}^n$ is the even-parity part of $I_{\mu\nu L}^n$, satisfying $M_{\mu j L}^n = M_{\mu(j i_1) i_2 \dots i_\ell}^n$, and the current moment $S_{\mu\nu L}^n$ is the odd-parity part, satisfying $S_{\mu j L}^n = S_{\mu[j i_1] i_2 \dots i_\ell}^n$. This splits each seed solution into two, $h_{\mu\nu}^{\text{seed}}(x; z, M_\ell^n)$ and $h_{\mu\nu}^{\text{seed}}(x; z, S_\ell^n)$.

3.3 General Solution

Now turn to the inhomogeneous equation $E_{\mu\nu}[h^n] = S_{\mu\nu}^n[h^1, \dots, h^{n-1}]$. Start at the $n = 1$ equation, (21a). The source vanishes, and the general solution is made up of a single seed solution,

$$h_{\mu\nu}^{\text{seed}}(x; z, I_0^1) = \frac{I_{\mu\nu}^1(t)}{r} + \mathcal{O}(r^0), \quad (54)$$

plus the sum of all free solutions $h_{\mu\nu}^{\text{free}}(x; z, k_\ell^1)$. That is,

$$h_{\mu\nu}^1 = h_{\mu\nu}^{\text{seed}}(x; z, I_0^1) + \sum_{\ell \geq 0} h_{\mu\nu}^{\text{free}}(x; z, k_\ell^1). \quad (55)$$

Next move to the $n = 2$ equation, (21b). The $1/r^{p+2}$ term in the equation looks essentially the same as Eq. (48), except that the right-hand side contains a term coming from $S_{\mu\nu}^2[h^1, h^1]$. One can straightforwardly solve for the functions $h_{\mu\nu L}^{2pq\ell}$ to find that each one of them is either the starting point for a new seed or free solution ($h_{\mu\nu i}^{2,-2,0,1}$, $h_{\mu\nu}^{2,-1,0,0}$, or $h_{\mu\nu L}^{2,\ell,0,\ell}$ for $\ell \geq 0$) or it is directly proportional to a $pq\ell$ mode of the source. Since the source is constructed from quadratic combinations of $h_{\mu\nu}^1$, it follows that the general solution is made up of the two seed solutions

$$h_{\mu\nu}^{\text{seed}}(x; z, I_1^2) = \frac{I_{\mu\nu i}^2(t)n^i}{r^2} + \mathcal{O}(1/r), \quad (56)$$

$$h_{\mu\nu}^{\text{seed}}(x; z, I_0^2) = \frac{I_{\mu\nu}^2(t)}{r} + \mathcal{O}(r^0), \quad (57)$$

plus the sum of all free solutions $h_{\mu\nu}^{\text{free}}(x; z, k_\ell^2)$, plus a particular inhomogeneous solution made up entirely of terms that are quadratic combinations of members of the set $\{I_{\mu\nu}^1, k_{\mu\nu L}^1 : \ell \geq 0\}$ (in other words, a particular solution in which all seed solutions and free solutions are set to zero). That is,

$$\begin{aligned} h_{\mu\nu}^2 = & h_{\mu\nu}^{\text{seed}}(x; z, I_1^2) + h_{\mu\nu}^{\text{seed}}(x; z, I_0^2) + \sum_{\ell \geq 0} h_{\mu\nu}^{\text{free}}(x; z, k_\ell^2) \\ & + h_{\mu\nu}^{2IH}(x; z, I_0^1, \{k_\ell^1\}_{\ell \geq 0}). \end{aligned} \quad (58)$$

The promised logarithms of r first appear in $h_{\mu\nu}^{2IH}(x; z, I_0^1, \{k_\ell^1\}_{\ell \geq 0})$ [11, 15].

Carrying this procedure to n th order, we find

$$\begin{aligned} h_{\mu\nu}^n = & \sum_{\ell=0}^{n-1} h_{\mu\nu}^{\text{seed}}(x; z, I_\ell^n) + \sum_{\ell \geq 0} h_{\mu\nu}^{\text{free}}(x; z, k_\ell^n) \\ & + h_{\mu\nu}^{nIH}(x; z, \{I_\ell^m\}_{m < n, \ell < n}, \{k_\ell^m\}_{m < n, \ell \geq 0}), \end{aligned} \quad (59)$$

where all functions $h_{\mu\nu L}^{npq\ell}$ appearing in $h_{\mu\nu}^{nIH}$ are made up of explicit products of members of the set $\{I_{\mu\nu L}^m : m < n, \ell < n - 1\} \cup \{k_{\mu\nu L}^m : m < n, \ell \geq 0\}$ (or their t derivatives) contracted with combinations of n^i , a^i , δ^{ij} , ϵ^{ijk} , pieces of the background Riemann tensor, and pieces of derivatives of the background Riemann tensor.

In any particular solution of the form (47) to the relaxed Einstein equation outside a small object, every term, to all orders in r and ϵ , is a linear or nonlinear combination of the functions $I_{\mu\nu L}^n(t) = h_{\mu\nu L}^{n,-\ell-1,0,\ell}(t)$ and $k_{\mu\nu L}^n(t) = h_{\mu\nu L}^{n,\ell,0,\ell}(t)$. Specifying all the functions $I_{\mu\nu L}^n(t)$ and $k_{\mu\nu L}^n(t)$ corresponds to making a specific choice of small object and of global boundary conditions.

3.4 Imposing Matching and Gauge Conditions

To satisfy the unrelaxed Einstein equation, the general solution described above must also satisfy the gauge conditions (26), which we can write generically as

$$L_\mu[h^n, F_0] = P_\mu[\{h^m, F_m\}_{m=1}^{n-1}], \quad (60)$$

for some P_μ that is linear in the h 's but not usually in the F 's. Recasting this as a constraint on the seed and free solutions in terms of lower-order fields, we have

$$\begin{aligned} \sum_{\ell=0}^{n-1} L_\mu[h^{\text{seed}}[I_\ell^n], F_0] + \sum_{\ell \geq 0} L_\mu[h^{\text{free}}[k_\ell^n], F_0] \\ = P_\mu[\{h^m, F_m\}_{m=1}^{n-1}] - L_\mu[h^{nIH}]. \end{aligned} \quad (61)$$

Like the relaxed Einstein equation, Eq. (61) can be solved order by order in r , thereby constraining the functions $I_{\mu\nu L}^n$ and $k_{\mu\nu L}^n$, which in the general solution to the relaxed Einstein equation were entirely arbitrary. Working through sequential orders in r first constrains each $I_{\mu\nu L}^n$ in sequence, from $\ell = n - 1$ to $\ell = 0$, and then each $k_{\mu\nu L}^n$ in sequence from $\ell = 0$ to $\ell = \infty$. The most important outcome is evolution equations for the moments $I_{\mu\nu L}^n(t)$.

At $n = 1$, the term with the lowest power of r in Eq. (26a), $1/r^2$, is $\partial^b(h_{\alpha b}^{\text{seed}}[I_0^1] - \frac{1}{2}\eta_{\alpha b}\eta^{\mu\nu}h_{\mu\nu}^{\text{seed}}[I_0^1]) = \mathcal{O}(1/r)$, which determines $I_{\mu\nu}^1 = 2m(t)\delta_{\mu\nu}$. The overall factor is written as $2m(t)$ for good reason: from Eq. (42), the inner background metric has an expansion $g_{\mu\nu}^{\text{obj}} = \frac{I_{\mu\nu}^1}{r} + \mathcal{O}(1/r^2)$, and substituting that expansion into the formula for the Arnowitt-Deser-Misner (ADM) mass, one finds that $m(t)$ is precisely the ADM mass of $g_{\mu\nu}^{\text{obj}}$. We call this the leading-order mass of the object. Proceeding to the next order in r , $1/r$, time derivatives and acceleration terms appear, and we find our sought evolution equations

$$\frac{dm}{dt} = 0, \quad F_0^\mu = 0, \quad (62)$$

which tell us that the object behaves approximately as a test body in $g_{\mu\nu}$. The remainder of the content of the $n = 1$ gauge condition, at all orders in r , is to enforce various uninteresting relationships between the functions $k_{\mu\nu}^n$.

At $n = 2$, the lowest order in r in the gauge condition (26b), $1/r^3$, similarly determines (after a very slight gauge refinement that remains within the Lorenz gauge [11]) that $I_{\mu\nu i}^2$ divides into mass and current moments of the form

$$M_{\mu\nu i}^2 = 2M_i(t)\delta_{\mu\nu}, \quad S_{\mu\nu i}^2 = 4u_{(\mu}\epsilon_{\nu)ji}S^j(t) \quad (63)$$

where $\epsilon_{tij} \equiv 0$. M_i and S^i are, respectively, the mass dipole moment and ADM angular momentum of $g_{\mu\nu}^{\text{obj}}$; we call these the object's leading-order mass dipole moment relative to γ and leading-order spin about γ . Defining $\delta m_{\mu\nu}(t) \equiv I_{\mu\nu}^2(t)$, we also find (from the order- $1/r^2$ and $1/r$ terms in the gauge condition) that

$$\begin{aligned} \delta m_{\alpha\beta} = & \frac{1}{3}m \left(2k_{\alpha\beta}^1 + g_{\alpha\beta}g^{\mu\nu}k_{\mu\nu}^1 \right) + m(g_{\alpha\beta} + 2u_\alpha u_\beta)u^\mu u^\nu k_{\mu\nu}^1 \\ & + 4u_{(\alpha}(mk_{\beta)\mu}^1 u^\mu + 2\dot{M}_\beta), \end{aligned} \quad (64)$$

where $\dot{M}^\beta \equiv \frac{DM^\beta}{d\tau}$. $\delta m_{\alpha\beta}$ can be thought of loosely as a correction to the object's monopole moment, but it is not invariant; a smooth gauge perturbation $2\xi_{(\alpha;\beta)}$ that is nonvanishing on γ will add directly to $k_{\alpha\beta}^1$. This is why the moments are called algorithmic: they arise in the algorithm of solving the field equations, but they are not invariant descriptions of the perturbed object. Furthermore, $\delta m_{\alpha\beta}$ is determined only up to a constant $c\delta_{\alpha\beta}$, but I choose to incorporate that term into $m\delta_{\alpha\beta}$.

Finally, the $1/r^2$ term in the $n = 2$ gauge condition determines the evolution equation $\frac{dS^i}{dt} = 0$, which tells us that the leading-order spin is parallelly propagated along γ , and the $1/r$ term determines

$$\frac{d^2 M_a}{dt^2} = -R_{a0b0}M^b - mF_a^1 - m\frac{dk_{ta}^1}{dt} + \frac{1}{2}mk_{tta}^1 + \frac{1}{2}R_{0aij}S^{ij}, \quad (65)$$

where I have defined $S^{ij} \equiv \epsilon^{ijk}S_k$. I call this the *master equation of motion*. It describes how the small object moves relative to any choice of nearby worldline γ . That motion is influenced by (i) geodesic deviation (evinced by the first term on the right), (ii) the acceleration of γ (manifesting as F_a^1), (iii) the ambient free fields in the neighbourhood, and (iv) the Mathisson-Papapetrou force created by coupling of the spin to the curvature of the external background metric. In the self-consistent expansion, we choose γ such that $M^i = 0$. Therefore,

$$F_a^1 = -\frac{dk_{ta}^1}{dt} + \frac{1}{2}k_{tta}^1 + \frac{1}{2m}R_{0aij}S^{ij}. \quad (66)$$

This is the MiSaTaQuWa force (albeit in an atypical form) plus the Mathisson-Papapetrou force. We see more clearly now that the practical consequence of the self-consistent approach, by utilizing a worldline relative to which M^i vanishes, is to prevent the term $M_i n^i / r^2$ from appearing in the second-order field (58). According to Eq. (65), this term would otherwise grow quadratically with time; this is the same undesirable growth discussed in Sect. 1.4.

As at $n = 1$, at $n = 2$ the gauge condition imposes relationships between the functions $k_{\mu\nu L}^2$, these relationships do not involve any of the algorithmic moments, and they leave each $k_{\mu\nu L}^n$ written in terms of arbitrary functions of time.

Extrapolating to arbitrary order n , we draw several conclusions: (i) The moment $I_{\mu\nu N-1}^n$ appearing in the leading order term $h_{\mu\nu}^{n,-n}/r^n$ is directly identified with a moment of $g_{\mu\nu}^{\text{obj}}$. Explicitly, as the mass appears at order ϵ and the spin at order ϵ^2 , so the quadrupole moment will appear at order ϵ^3 , the octupole at order ϵ^4 , etc.²³ We interpret these moments $I_{\mu\nu N-1}^n$ as the leading-order moments of the object. (ii) The others, $I_{\mu\nu \ell}^n$ with $\ell < n - 1$, we interpret as perturbations to the object's moments, and the gauge condition determines that each of these corrections involve some linear or nonlinear factors of moments of $g_{\mu\nu}^{\text{obj}}$. (iii) Even after the gauge and matching conditions are imposed, every coefficient $h_{\mu\nu L}^{npq\ell}(t)$ appearing in the free fields is made up entirely of arbitrary functions of time that are determined only once global boundary conditions (BC1) are also imposed.²⁴

When going to higher order, it is not obvious what condition should be imposed to make the worldline a good representation of the object's bulk motion. A natural candidate would be to set the corrections $M_{\mu\nu i}^{n>2}$ to the object's mass dipole moment to zero. However, one would have to investigate the third- and higher-order gauge conditions to see whether (i) doing so is possible and (ii) doing so prevents unwanted secular growth that can be associated with a growing displacement of the object away from the chosen representative worldline. Section 7 offers a different method of choosing a good worldline, at least at second order.

²³To relate back to the Thorne and Hartle results (13) and (14), canonical mass and current quadrupole moments Q_{ij} and \mathcal{Q}_{ij} can be defined from $M_{\mu\nu ij}^3$ and $S_{\mu\nu ij}^3$ according to

$$M_{\mu\nu ij}^3 = 3Q_{ij}\delta_{\mu\nu}, \quad S_{\mu\nu ij}^3 = 8u_{(\mu}\epsilon_{\nu)ki}\mathcal{Q}^k_{\ j}, \quad (67)$$

similarly to Eq. (63). In choosing the normalization factors of these moments, I follow Ref. [68].

²⁴A proof of statement (iii) will be presented elsewhere. Here it can be taken as a conjecture, although it is known to be true at all orders in ϵ and r that have been explicitly considered. Intuitively, it can be inferred from the fact that we can choose boundary conditions for which all $k_{\mu\nu L}^n$ vanish at a given n , and with that choice we must still be able to satisfy the gauge condition; hence, the constraints on the $I_{\mu\nu L}^n$'s cannot involve the $k_{\mu\nu L}^n$'s of the same n .

3.5 Split into Self-Field and Effective Field

I now define a convenient split of $h_{\mu\nu}^n$ into a self-field $h_{\mu\nu}^{Sn}$ and an effectively external field $h_{\mu\nu}^{Rn}$. Specifically, I define $h_{\mu\nu}^{Rn}$ to be the piece of Eq. (59) that contains no linear or nonlinear combinations of the algorithmic moments $I_{\mu\nu L}^n$:

$$h_{\mu\nu}^{Rn} = \sum_{\ell \geq 0} h_{\mu\nu}^{\text{free}}(x; z, k_\ell^n) + h_{\mu\nu}^{RnIH}(x; z, \{k_\ell^m\}_{m < n, \ell \geq 0}), \quad (68)$$

where $h_{\mu\nu}^{RnIH}$ is the part of $h_{\mu\nu}^{nIH}$ containing no factors of $I_{\mu\nu L}^n$. This implicitly defines the self-field $h_{\mu\nu}^{Sn} = h_{\mu\nu}^n - h_{\mu\nu}^{Rn}$ to be

$$h_{\mu\nu}^{Sn} = \sum_{\ell=0}^{n-1} h_{\mu\nu}^{\text{seed}}(x; z, I_\ell^n) + h_{\mu\nu}^{SnIH}(x; z, \{I_\ell^m\}_{m < n, \ell < n}, \{k_\ell^m\}_{m < n, \ell \geq 0}), \quad (69)$$

where every term in $h_{\mu\nu}^{SnIH}$ contains at least one factor of at least one algorithmic moment. I also define $h_{\mu\nu}^R = \sum_n \epsilon^n h_{\mu\nu}^{Rn}$ and $h_{\mu\nu}^S = \sum_n \epsilon^n h_{\mu\nu}^{Sn}$. Conclusion (iii) at the end of the last section implies that each of these two fields separately satisfies the Lorenz gauge condition.²⁵

More explicitly, at first order, $h_{\mu\nu}^1 = h_{\mu\nu}^{S1} + h_{\mu\nu}^{R1}$, with

$$h_{\mu\nu}^{S1} = h_{\mu\nu}^{\text{seed}}(x; z, m) = \frac{2m\delta_{\mu\nu}}{r} + \mathcal{O}(r^0), \quad (70)$$

$$h_{\mu\nu}^{R1} = \sum_{\ell \geq 0} h_{\mu\nu}^{\text{free}}(x; z, k_\ell^1) = k_{\mu\nu}^1(t) + rk_{\mu\nu i}^1(t)n^i + \mathcal{O}(r^2). \quad (71)$$

Recall that for any particular solution of the form (47), the functions in the free fields are $k_{\mu\nu L}^n = h_{\mu\nu L}^{n, \ell, 0, \ell}$.

At second order, $h_{\mu\nu}^2 = h_{\mu\nu}^{S2} + h_{\mu\nu}^{R2}$, with

$$h_{\mu\nu}^{S2} = h_{\mu\nu}^{\text{seed}}(x; z, S) + h_{\mu\nu}^{\text{seed}}(x; z, \delta m) + h_{\mu\nu}^{S2IH}(x; z, m, \{k_\ell^1\}_{\ell \geq 0}), \quad (72)$$

$$h_{\mu\nu}^{R2} = \sum_{\ell \geq 0} h_{\mu\nu}^{\text{free}}(x; z, k_\ell^2) + h_{\mu\nu}^{R2IH}(x; z, \{k_\ell^1\}_{\ell \geq 0}), \quad (73)$$

where

$$h_{\mu\nu}^{\text{seed}}(x; z, S) = \frac{4S^j n^i}{r^2} u_{(\mu} \epsilon_{\nu) ji} + \mathcal{O}(1/r), \quad (74)$$

²⁵If the statements were not true, one could always slightly alter the singular-regular split to make the two fields independently satisfy the gauge condition. Doing so would involve appropriately moving part of the free fields into $h_{\mu\nu}^S$ [15].

$$h_{\mu\nu}^{\text{seed}}(x; z, \delta m) = \frac{\delta m_{\mu\nu}}{r} + \mathcal{O}(r^0), \quad (75)$$

$$h_{\mu\nu}^{\text{R2}} = k_{\mu\nu}^2(t) + r k_{\mu\nu i}^2(t) n^i + \mathcal{O}(r^2), \quad (76)$$

$h_{\mu\nu}^{S2IH}(x; z, m, \{k_\ell^1\}_{\ell \geq 0})$ is made up exclusively of terms quadratic in m or products of m and $h_{\mu\nu}^{\text{R1}}$ (and derivatives of $h_{\mu\nu}^{\text{R1}}$), and $h_{\mu\nu}^{\text{R2IH}}(x; z, \{k_\ell^1\}_{\ell \geq 0})$ is made up of terms quadratic in $h_{\mu\nu}^{\text{R1}}$ (and derivatives of $h_{\mu\nu}^{\text{R1}}$).

I remind the reader that in Sect. 1.1.2 I identified three “nice” properties I wish an effectively external metric to satisfy:

1. it should be a vacuum solution
2. it should be causal on the worldline
3. the object should move as a test body in it.

There is no guarantee a priori that these conditions can simultaneously be satisfied at all orders in ϵ , but with the definitions given above, the first nice property is met: the effective metric $\tilde{g}_{\mu\nu} = g_{\mu\nu} + h_{\mu\nu}^{\text{R}}$ is a smooth solution to the vacuum Einstein equation $R_{\mu\nu}[\tilde{g}] = 0$ even at $r = 0$. This can be seen from the facts that (i) by construction, for $r > 0$ we still have a solution even if we set all moments $I_{\mu\nu L}^n$ to zero (i.e., if there is no object in \mathcal{B}_γ), and (ii) for the free fields the construction applies even at $r = 0$. Note that here I am taking a particular series (68) obtained outside the object and simply analytically extending it down to $r = 0$. In this way, I define an effective spacetime $(\tilde{g}_{\mu\nu}, \mathcal{M})$ in \mathcal{B}_γ , where the object lies in the physical spacetime.

More explicitly, the first- and second-order regular fields satisfy the vacuum equations

$$E_{\mu\nu}[h^{\text{R1}}] = 0, \quad L_\mu[h^{\text{R1}}, F_0] = 0, \quad (77)$$

$$E_{\mu\nu}[h^{\text{R2}}] = 2\delta^2 R_{\mu\nu}[h^{\text{R1}}, h^{\text{R1}}], \quad L_\mu[h^{\text{R2}}, F_0] = -\delta L_\mu[h^{\text{R1}}, F_1], \quad (78)$$

for all $r \geq 0$. The self-fields are left to satisfy

$$E_{\mu\nu}[h^{\text{S1}}] = 0, \quad L_\mu[h^{\text{S1}}, F_0] = 0, \quad (79)$$

$$E_{\mu\nu}[h^{\text{S2}}] = 2\delta^2 R_{\mu\nu}[h^{\text{S1}}, h^{\text{S1}}] + 4\delta^2 R_{\mu\nu}[h^{\text{S1}}, h^{\text{R1}}], \quad (80)$$

$$L_\mu[h^{\text{S2}}, F_0] = -\delta L_\mu[h^{\text{S1}}, F_1]. \quad (81)$$

The third “nice” condition is also met, at least through order ϵ : combining Eqs. (66) and (71), we get, in covariant form,

$$\frac{D^2 z^\mu}{d\tau^2} = -\frac{1}{2} P^{\mu\nu} (2h_{\rho\nu;\sigma}^{\text{R1}} - h_{\rho\sigma;\nu}^{\text{R1}}) u^\rho u^\sigma + \frac{1}{2m} R^\mu{}_{\nu\rho\sigma} u^\nu S^{\rho\sigma} + \mathcal{O}(\epsilon^2), \quad (82)$$

where I have defined the antisymmetric 4-tensor $S^{\mu\nu} = e_i^\mu e_j^\nu S^{ij}$.²⁶ Together with $\frac{dS^i}{dt} = 0$, Eq. (82) is the equation of motion of a test body in $\tilde{g}_{\mu\nu}$. It can be put in the form of the Thorne-Hartle equations (13) and (14) by using the results of Appendix 1 to absorb the $h_{\mu\nu}^{\text{R1}}$ terms into the covariant derivative and proper time in $\tilde{g}_{\mu\nu}$, using $p^\mu = m\tilde{u}^\mu + \mathcal{O}(\epsilon^3)$ and the fact that m is constant, and using Eq. (46) to write the Riemann tensor in terms of the tidal field \mathcal{B}_{ij} (noting $\mathfrak{B}_{ij} = \mathcal{B}_{ij} + \mathcal{O}(\epsilon)$). Doing so allows us to identify $\tilde{g}_{\mu\nu}$ with Thorne and Hartle’s “external” metric $\mathfrak{g}_{\mu\nu}$, at least in the weak sense that $\tilde{g}_{\mu\nu} = \mathfrak{g}_{\mu\nu} + \mathcal{O}(\epsilon^2, \epsilon r^2)$; since only first derivatives of $h_{\mu\nu}^{\text{R1}}$ appear in Eq. (82), we can make no claims on agreement at order r^2 or higher.

I show in the next section that my definition of the regular field also satisfies the remaining nice property: it is causal on the worldline. I also note that at least through order r^2 , my definition of $h_{\mu\nu}^{\text{R1}}$ agrees with the Detweiler-Whiting definition [52], despite the fact that the Detweiler-Whiting field is defined in a wholly different manner based on Green’s functions [9, 23]. However, despite all these reassuring facts, I stress that in general, *even if the effective metric I define is found to satisfy each of the three “nice” properties at a given order ϵ^n , it is not the unique field satisfying those properties*. One can simply shift any given free field $h_{\mu\nu}^{\text{free}}(x; z, k_\ell^{n'})$ (with $n' \leq n$ and ℓ sufficiently large for $k_{\mu\nu L}^{n'}$ to not appear in the n th equation of motion), and its nonlinear combinations, from the regular field into the self-field. The strongest of my “nice conditions” appears to be that the object behaves as a test *body* in the effective metric: since higher multipole moments couple to higher derivatives of the effective metric, this strongly constrains which part of the full metric should go into the effective one. At any finite perturbative order, however, one can always alter the effective metric’s higher derivatives without spoiling any of its nice properties. Nonetheless, I deem my “nice” choice most natural as a part of the process of solving the relaxed Einstein equations using the local expansion (47): before making reference to global boundary conditions, I simply put all the terms that involve the object’s multipole moments into the self-field, and I put all the terms made up entirely of unknown functions into the effective field.

3.6 Summary at First and Second Order

To extract the key pragmatic information of the preceding sections, I restate the conclusions at first and second order: The first-order field is given by Eqs. (70) and (71), where the self-field $h_{\mu\nu}^{\text{S1}}$ is locally determined by the (constant) mass m , and the effective field $h_{\mu\nu}^{\text{R1}}$ is to be determined by global boundary conditions. The

²⁶The monopole correction (64) can also be trivially rewritten in terms of $h_{\mu\nu}^{\text{R1}}$ as

$$\delta m_{\alpha\beta} = \frac{1}{3}m \left(2h_{\alpha\beta}^{\text{R1}} + g_{\alpha\beta}g^{\mu\nu}h_{\mu\nu}^{\text{R1}} \right) + m(g_{\alpha\beta} + 2u_\alpha u_\beta)u^\mu u^\nu h_{\mu\nu}^{\text{R1}} + 4u_{(\alpha}m h_{\beta)\mu}^{\text{R1}}u^\mu, \quad (83)$$

where I have set $M^i = 0$, and all fields are evaluated on γ .

second-order field is given by Eqs. (72) and (73), where the self-field $h_{\mu\nu}^{S2}$ is locally determined by (i) the mass m , (ii) the first-order effective field $h_{\mu\nu}^{R1}$, (iii) the (parallelly propagated) spin S^μ , and (iv) the monopole correction $\delta m_{\mu\nu}$ given in Eq. (83); the effective field $h_{\mu\nu}^{R2}$ is to be determined by global boundary conditions and by $h_{\mu\nu}^{R1}$. I encourage readers to examine the more explicit expressions for these fields given in, e.g., Ref. [52].

Finally, the object moves on a worldline governed by Eq. (82).

4 Algorithm for an n th-Order Self-Consistent Approximation: Point Particles, Punctures, and Global Solutions

With the general solution in the buffer region ready at hand, I now describe how to use it to generate a global solution. In short, this relies on a rigorous procedure of replacing the physical field in \mathcal{B}_γ with a fictitious field *without altering the field elsewhere*. What are the fictitious fields? Simply the analytical expansion (59) from the buffer region, extended to apply to all $r > 0$. This was done already for $h_{\mu\nu}^R$ in the previous section. Continuing the expression for $h_{\mu\nu}^S$ into \mathcal{B}_γ makes it into a field that diverges at $r = 0$: the true self-field in the interior of the body, whatever it may be, is replaced with this divergent field, and the self-field becomes the *singular field*. Since this extension into \mathcal{B}_γ does not affect the field in the buffer region, it also does not affect the field values outside the buffer, out in the external universe.

Section 4.1 describes how this analytical extension can be used to ascribe a certain pointlike stress-energy distribution to the object, thereby recovering the point particle picture at linear order (though this stress-energy I construct cannot be taken as a physical source in the Einstein equations beyond linear order). Section 4.2 then describes how the analytical extension can be used to obtain a global solution at any order; this will be the first point at which a global boundary condition (BC1) is finally imposed.

4.1 Skeletal Stress-Energy

Consider the solution (59) extended down to $r > 0$. For reasons described in Sect. 1.2, there is no known distributional source for this solution on a domain that includes $r = 0$. However, we can devise the following setup: each of the seed solutions can be thought of as being sourced by a pointlike stress-energy supported on γ . Everything else in the general solution then grows from these seeds, either being generated by nonlinearities or in the case of the free fields, being determined by global boundary conditions.

I refer to the stress-energy for the seed solutions as the skeletal stress energy, taking after a similar phrase in Ref. [35]; the idea is that in some sense, the object (or body) can be replaced by a skeleton. That skeleton is made up of multipole moments living on the object's worldline.

For each seed solution $h_{\mu\nu}^{\text{seed}}(x; z, I_\ell^n)$, I roughly follow the approach taken by Gralla and Wald at first order [18], defining the (trace-reversed) distributional stress-energy tensor

$$\bar{T}_{\mu\nu}^{n\ell} \equiv -\frac{1}{16\pi} E_{\mu\nu}[h^{\text{seed}}[I_\ell^n]]. \quad (84)$$

The right-hand side can be written as

$$E_{\mu\nu}[h^{\text{seed}}[I_\ell^n]] = \partial^i \partial_i \frac{I_{\mu\nu L}^n \hat{n}^L}{r^{\ell+1}} + N_{\mu\nu}[h^{\text{seed}}[I_\ell^n]], \quad (85)$$

where $N_{\mu\nu}[h^{\text{seed}}[I_\ell^n]] = \partial^i \partial_i \left(h_{\mu\nu}^{\text{seed}}[I_\ell^n] - I_{\mu\nu L}^n \hat{n}^L / r^{\ell+1} \right) + W_{\mu\nu}[h^{\text{seed}}[I_\ell^n]]$.

First examine the most singular term. Using the identities $\partial_L r^{-1} = (-1)^\ell (2\ell - 1)!! \frac{\hat{n}_L}{r^{\ell+1}}$ and $\partial^i \partial_i r^{-1} = -4\pi \delta^3(\vec{x})$, we have

$$\partial^i \partial_i \frac{I_{\mu\nu L}^n \hat{n}^L}{r^{\ell+1}} = \frac{4\pi(-1)^{\ell+1} I_{\mu\nu L}^n}{(2\ell - 1)!!} \partial_L \delta^3(\vec{x}). \quad (86)$$

Integrating the right-hand side against a test function $\psi^{\mu\nu}$, we find

$$\int \psi^{\mu\nu} I_{\mu\nu L}^n \partial_L \delta^3(\vec{x}) \sqrt{-g} d^3x dt = (-1)^\ell \int_\gamma \partial_L \left(\sqrt{-g} \psi_{\mu\nu} I_n^{\mu\nu L} \right) dt \quad (87)$$

$$= (-1)^\ell \int_\gamma (\psi_{\mu\nu} I_n^{\mu\nu\alpha_1 \dots \alpha_\ell})_{;\alpha_1 \dots \alpha_\ell} dt, \quad (88)$$

where in going from the second line to the third I have utilized the identity $\partial_i \sqrt{-g} = \Gamma_{\beta i}^\beta \sqrt{-g}$. Here I have defined $I_n^{\mu\nu\alpha_1 \dots \alpha_\ell}$ to be the tensor that agrees with $I_n^{\mu\nu L}$ if all α_i are spatial indices and zero otherwise, meaning that $I_n^{\mu\nu\alpha_1 \dots \alpha_\ell}$ is STF with respect to $g_{\mu\nu}$ and that $I_n^{\mu\nu\alpha_1 \dots \alpha_i \dots \alpha_\ell} u_{\alpha_i} = 0$. Equation (88) shows that

$$I_{(n)}^{\mu\nu L} \partial_L \delta^3(\vec{x}) = \int_\gamma I_{(n)}^{\mu\nu\alpha_1 \dots \alpha_\ell} \delta(x, z)_{;\alpha_1 \dots \alpha_\ell} d\tau, \quad (89)$$

Equation (85) now reads

$$E_{\mu\nu}[h^{\text{seed}}[I_\ell^n]] = \frac{4\pi(-1)^{\ell+1}}{(2\ell - 1)!!} \int_\gamma I_{(n)}^{\mu\nu\alpha_1 \dots \alpha_\ell} \delta(x, z)_{;\alpha_1 \dots \alpha_\ell} d\tau + N_{\mu\nu}. \quad (90)$$

Now note that, by construction, $N_{\mu\nu}[h^{\text{seed}}_\ell[I_\ell^n]]$ vanishes pointwise for $r > 0$. If it is nonvanishing as a distribution,²⁷ it must have support only on γ , in which case it must be proportional to $\delta^3(x)$ or a derivative thereof; but from the calculation just performed, that would lead to a different algorithmic moment $I_{\mu\nu L'}^n$ (with $\ell' \neq \ell$) appearing in the solution, which would contradict the definition of the seed field $h^{\text{seed}}_{\mu\nu}[I_\ell^n]$. So $N_{\mu\nu}[h^{\text{seed}}_\ell[I_\ell^n]]$ vanishes as a distribution.

Therefore, Eq. (84) becomes

$$\bar{T}_n^{\mu\nu}(x; z, I_\ell^n) = \frac{(-1)^\ell}{4(2\ell - 1)!!} \int_\gamma I_n^{\mu\nu\alpha_1 \dots \alpha_\ell} \delta(x, z)_{;\alpha_1 \dots \alpha_\ell} d\tau. \quad (91)$$

If we add up all the multipole moments, we arrive at a skeletal stress-energy tensor

$$\bar{T}^{\mu\nu} = \sum_{n, \ell} \bar{T}_n^{\mu\nu}(x; z, I_\ell^n) = \sum_\ell \int_\gamma I^{\mu\nu\alpha_1 \dots \alpha_\ell} \delta(x, z)_{;\alpha_1 \dots \alpha_\ell} d\tau, \quad (92)$$

where I have defined the corrected and normalized moments $I^{\mu\nu\alpha_1 \dots \alpha_\ell} \equiv \sum_n \frac{(-1)^\ell}{4(2\ell - 1)!!} I_n^{\mu\nu\alpha_1 \dots \alpha_\ell}$. Notably, this skeletal stress-energy agrees in form with that of the traditional multipolar expansion of a material body's stress-energy tensor [35, 69, 70].

At first order in ϵ , there is only one seed field, $h^{\text{seed}}_{\mu\nu}(x; z, m)$, and Eq. (91) gives

$$T_1^{\mu\nu}(x; z, m) = \int_\gamma m u^\mu u^\nu \delta(x, z) d\tau \quad (93)$$

—precisely the point particle stress-energy used in Sect. 1.1. Because $h_{\mu\nu}^1 = h_{\mu\nu}^{\text{R}1} + h^{\text{seed}}_{\mu\nu}(x; z, m)$, and $E_{\mu\nu}[h^{\text{R}1}] = 0$, we can conclude that $E_{\mu\nu}[h^1] = T_1^{\mu\nu}(x; z)$. In other words, *the first-order field is identical to one sourced by a point particle*. Of course, this is derived from the analytically extended field, but it also applies to the physical field at distances $r \gg \epsilon$ from the worldline.

At second order, there are seed fields, $h^{\text{seed}}_{\mu\nu}(x; z, \delta m)$, $h^{\text{seed}}_{\mu\nu}(x; z, S)$, and $h^{\text{seed}}_{\mu\nu}(x; z, M)$; although the last of these three we set to zero with our choice of z^μ , it is worth displaying the skeletal stress-energy that would source it if we chose a different z^μ . Equation (91) gives

$$T_2^{\mu\nu}(x; z, \delta m) = \frac{1}{4} \int_\gamma \bar{\delta m}^{\mu\nu} \delta(x, z) d\tau, \quad (94)$$

²⁷That it must be well defined as a distribution follows from it being the result of linear operations on $h^{\text{seed}}_{\mu\nu}[I_\ell^n]$, and $h^{\text{seed}}_{\mu\nu}[I_\ell^n]$ itself being a sum of terms constructed from linear operations on an integrable function. The latter fact follows from the first term in the sum being expressible as the linear operation ∂_L on an integrable function proportional to r^{-1} [as in the text above Eq. (86)], and all higher-order terms in the sum being constructed from linear operations on lower order terms in the sum (as described in Sect. 3.2).

$$T_2^{\mu\nu}(x; z, S) = - \int_{\gamma} u^{(\mu} S^{\nu)\alpha} \nabla_{\alpha} \delta(x, z) d\tau, \quad (95)$$

$$T_2^{\mu\nu}(x; z, M) = - \int_{\gamma} u^{\mu} u^{\nu} M^{\alpha} \nabla_{\alpha} \delta(x, z) d\tau, \quad (96)$$

where the overline indicates trace reversal. Appendix 2 shows that $T_2^{\mu\nu}(x; z_0, M)$ [plus a piece of $T_2^{\mu\nu}(x; z_0, \delta m)$] is precisely equal to the linear term in the expansion of $T_1^{\mu\nu}(x; z, m)$ given $z^{\mu} = z_0^{\mu} + \epsilon M^{\mu}/m + \mathcal{O}(\epsilon)$.

4.2 Puncture Schemes

I now describe how one can use the results from the buffer region to obtain a global solution. The method is called a *puncture scheme*. It has become standard in the linearized problem [54–57], and it is the only known practical way to obtain numerical results at second order and higher [14, 15, 20, 52, 71].

A puncture scheme begins with the construction of a *puncture* $h_{\mu\nu}^{\mathcal{P}}$, defined by truncating the local expansion of the singular field from the buffer region at some specified order. One then defines the residual field

$$h_{\mu\nu}^{\mathcal{R}} \equiv h_{\mu\nu} - h_{\mu\nu}^{\mathcal{P}} \quad (97)$$

and in a region covering the object, writes a field equation for $h_{\mu\nu}^{\mathcal{R}}$, rather than one for (the analytically continued) physical field $h_{\mu\nu}$. Since $h_{\mu\nu}^{\mathcal{P}} \approx h_{\mu\nu}^S$, so too $h_{\mu\nu}^{\mathcal{R}} \approx h_{\mu\nu}^R$. The better $h_{\mu\nu}^{\mathcal{P}}$ represents $h_{\mu\nu}^S$, the better $h_{\mu\nu}^{\mathcal{R}}$ represents $h_{\mu\nu}^R$. For example, if $\lim_{x \rightarrow \gamma} [h_{\mu\nu}^{\mathcal{P}}(x) - h_{\mu\nu}^S(x)] = 0$, then $\lim_{x \rightarrow \gamma} h_{\mu\nu}^{\mathcal{R}}(x) = \lim_{x \rightarrow \gamma} h_{\mu\nu}^R(x)$; that is, the residual field agrees with the regular field on the worldline. If $h_{\mu\nu}^{\mathcal{P}}$ agrees with $h_{\mu\nu}^S$ to one order higher, meaning $h_{\mu\nu}^{\mathcal{P}} - h_{\mu\nu}^S = o(r)$, then $\lim_{x \rightarrow \gamma} \nabla_{\rho} h_{\mu\nu}^{\mathcal{R}} = \lim_{x \rightarrow \gamma} \nabla_{\rho} h_{\mu\nu}^R$; since the self-force is constructed from first derivatives of $h_{\mu\nu}^R$, this condition guarantees that the force can be calculated from $h_{\mu\nu}^{\mathcal{R}}$, as in Eq. (100) below.

There are several schemes that can be developed from the starting point of the puncture. Here I describe a worldtube scheme in the tradition of Refs. [54, 56]. In this type of scheme one uses the field variables $h_{\mu\nu}^{\mathcal{R}n}$ inside a worldtube Γ surrounding γ , the field variables $h_{\mu\nu}^n$ outside that worldtube, and the change of variables $h_{\mu\nu}^n = h_{\mu\nu}^{\mathcal{R}n} + h_{\mu\nu}^{\mathcal{P}n}$ when moving between the two regions.²⁸ Concretely, a second-order puncture scheme is then summarized by the coupled system of equations²⁹

²⁸One does not solve the problem in each domain separately, since the separate problems would be ill-posed. Instead, when calculating $h_{\mu\nu}^n$ at a point just outside Γ that depends on points on past time slices inside Γ , one makes use of the values of $h_{\mu\nu}^{\mathcal{R}n}$ already calculated at those earlier points, and vice versa; see Sect. VB of Ref. [54].

²⁹The effective sources $S_{\mu\nu}^{\text{eff}n}$ are usually written to include the skeletal stress-energy terms, which are canceled by distributional content in $E_{\mu\nu}[h^{\mathcal{P}n}]$. Here I have instead followed Ref. [20] by

$$E_{\mu\nu}[h^{\mathcal{R}1}] = -E_{\mu\nu}[h^{\mathcal{P}1}] \equiv S_{\mu\nu}^{\text{eff}1} \quad \text{inside } \Gamma, \quad (98a)$$

$$E_{\mu\nu}[h^1] = 0 \quad \text{outside } \Gamma, \quad (98b)$$

$$E_{\mu\nu}[h^{\mathcal{R}2}] = 2\delta^2 R_{\mu\nu}[h^1, h^1] - E_{\mu\nu}[h^{\mathcal{P}2}] \equiv S_{\mu\nu}^{\text{eff}2} \quad \text{inside } \Gamma, \quad (99a)$$

$$E_{\mu\nu}[h^2] = 2\delta^2 R_{\mu\nu}[h^1, h^1] \quad \text{outside } \Gamma, \quad (99b)$$

$$\frac{D^2 z^\mu}{d\tau^2} = -\frac{1}{2} P^{\mu\nu} \left(g_\nu{}^\gamma - h_\nu^{\mathcal{R}\gamma} \right) \left(2h_{\gamma\alpha;\beta}^{\mathcal{R}} - h_{\alpha\beta;\gamma}^{\mathcal{R}} \right) u^\alpha u^\beta, \quad (100)$$

where the puncture diverges on the worldline z^μ determined by Eq. (100). Here I have looked ahead by using the second-order equation of motion (for an object whose spin and quadrupole moments vanish); the first-order equation (9) could be used instead, though as discussed in Sect. 1.5.4, the results would be accurate in a smaller region of spacetime.

In this scheme, Eqs. (98)–(100) must be solved together, as a coupled system for the variables z^μ , $h_{\mu\nu}^{\mathcal{R}1}/h_{\mu\nu}^1$ (inside/outside Γ), and $h_{\mu\nu}^{\mathcal{R}2}/h_{\mu\nu}^2$. The residual fields govern the position of the puncture, and the position of the puncture effectively sources the residual fields. This system of equations is to be solved subject to some global boundary conditions. For simplicity, we can consider using specified initial data on a Cauchy surface.³⁰

I make two technical asides: $h_{\mu\nu}^{\mathcal{P}2}$, according to Eq. 72, contains terms proportional to the first-order regular field $h_{\mu\nu}^{\mathcal{R}1}$. So at each timestep in a numerical evolution, one must first calculate the first-order residual field from the first-order puncture, then use that residual field to calculate the second-order effective source, and so forth. Also, the divergence of the individual sources is quite strong at the worldline, with the terms $2\delta^2 R_{\mu\nu}[h^1, h^1]$ and $E_{\mu\nu}[h^{\mathcal{P}2}]$ in Eq. (99) each going as $1/r^4$; by construction, these divergences analytically cancel each other, but the cancellation is numerically delicate.

In principle, there is no obstacle to using a puncture scheme at any order in ϵ . Outside Γ , one may solve the physical problem $E_{\mu\nu}[h^n] = S_{\mu\nu}^n[h^1, \dots, h^{n-1}]$, inside Γ one may solve the effective problem $E_{\mu\nu}[h^{\mathcal{R}n}] = S_{\mu\nu}^n[h^1, \dots, h^{n-1}] - E_{\mu\nu}[h^{\mathcal{P}n}] \equiv S_{\mu\nu}^{\text{eff}n}$, and when crossing Γ , one may change variables from the residual field to the full field via $h_{\mu\nu}^n = h_{\mu\nu}^{\mathcal{R}n} + h_{\mu\nu}^{\mathcal{P}n}$. Of course, this requires sufficiently high-order expressions for the puncture and for the equation of motion governing how the puncture moves. But we know how to obtain both expressions from a local analysis in the buffer region.

(Footnote 29 continued)

writing the source pointwise, off γ ; if the puncture agrees with the singular field sufficiently well, the source at points on γ can be defined as the limit from off γ .

³⁰Because the approximation is accurate only within a finite region of size $1/\epsilon$, one might better solve the equations in the future domain of dependence of a partial Cauchy surface.

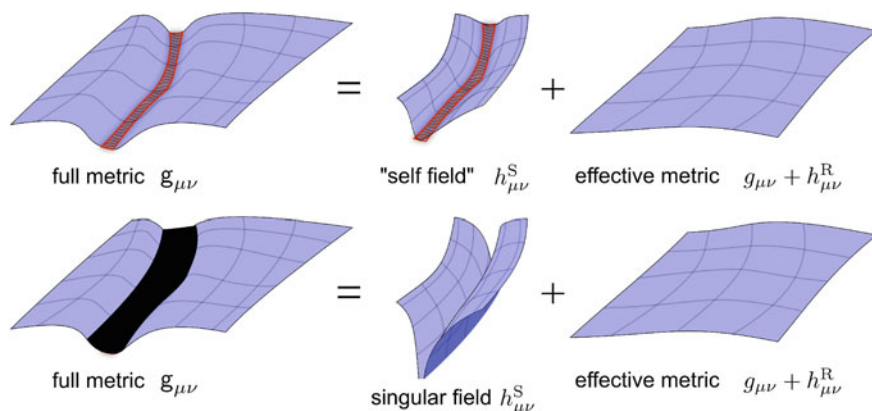


Fig. 3 Replacement of the physical metric with an effective metric plus a puncture. In the top row, the physical metric $g_{\mu\nu}$ is split into a self-field $h^S_{\mu\nu}$ plus an “effectively external” metric $\tilde{g}_{\mu\nu} = g_{\mu\nu} + h^R_{\mu\nu}$. In the bottom row, we “black out” the region in and very near the object, and we replace the physical metric with a singular field $h^S_{\mu\nu}$ (any local approximation to which is called a puncture) plus the “effectively external” metric. The replacement of the self-field with the singular field is made only very near the object: the self-field and singular field are identical to one another in the buffer region and beyond; the effective metric $\tilde{g}_{\mu\nu}$ is completely unaltered everywhere it is defined

The basic picture of a puncture scheme is illustrated in Fig. 3. Physically, the scheme replaces the actual problem in the region covering the body, with all its matter fields, singularities (in the case of a black hole), or other oddities (in the case of exotic matter), with an *effective* problem. But it yields the correct physical field outside the object. Hence, while we must abandon the point particle model at nonlinear orders, we can replace it with the more general concept of a puncture, a local singularity that encodes all the necessary information about the object in its multipole moments.

4.3 The Causality of the Regular Field

I now return to the question of how “nice” the regular field is, by which I specifically mean the three enumerated properties in Sect. 3.5. I have already shown that at all orders, the regular field I defined is a vacuum solution. I have also shown that at first order, the object moves as a test body in the effective geometry it induces, and (for spherical, nonspinning objects) this result will be extended to second order in Sect. 7. Now the final property follows immediately, at all orders in ϵ , from the design of the puncture scheme: the residual field and its derivatives manifestly depend only on the causal past, and by construction, the residual field and any number of its derivatives agree with those of the regular field on the worldline. Taking the limit of an infinite number of derivatives, we get the desired result.

4.4 A Note on “regularization”

In the gravitational self-force literature, one often speaks of “regularizing” the field or the self-force. This can mistakenly give the impression that one has introduced infinities into the problem, and that one must regularize them to recover the physical result. But in the formalism I have described here, one only ever deals with finite quantities. The force on the object, for example, is derived from the field equations outside the object, and it is written in terms of manifestly finite fields in that region. Those fields outside the object are then written in terms of quantities on the worldline by identifying $S^i(t)$, a field off the worldline, with $e^i_\mu S^\mu(z(t))$, for example; or similarly, by defining the regular field such that $h^{\text{R}1}_{\mu\nu}(z(t)) = k^1_{\mu\nu}(t)$ and $h^{\text{R}1}_{\mu\nu,i}(z(t)) = k^1_{\mu\nu i}(t)$.

From this perspective, the various “regularization” methods that have been used in the self-force problem to remove the ‘singular part’ of the field [8, 9] arise only as a practical necessity: we cannot easily determine the physical metric *inside* the object, nor are we interested in doing so, which prompts us to replace it with the fiction of a singular field solely as a means of calculating the physical metric *outside* the object. Computational techniques such as puncture schemes and mode-sum “regularization” [8, 9] are not methods of removing singularities; they are simply methods of calculating the particular finite quantities in question. In mode-sum regularization, for example, one rigorously writes a spherical-harmonic mode decomposition of $h^{\text{R}1}_{\mu\nu}(z)$ by decomposing $h^{\text{R}1}_{\mu\nu}(z) = \lim_{x \rightarrow z} (h^1_{\mu\nu} - h^{\text{S}1}_{\mu\nu})$, with $h^1_{\mu\nu}$ being the field of a point mass. Every quantity in the calculation is finite every step of the way.

5 Gralla-Wald and Osculating-Geodesics Approximations

Given results in the self-consistent approximation, one can always obtain analogous results in a Gralla-Wald or osculating-geodesics approximation by performing an expansion of the worldline, as described in Sects. 1.5.5 and 1.5.6. In this section I present that procedure and those results.

5.1 Gralla-Wald Approximation

There are two ways to obtain the Gralla-Wald approximation from prior results: by expanding the worldline in the self-consistent results; or more simply, by returning to the results in the buffer region and simply choosing the worldline at $r = 0$ to be γ_0 , the zeroth-order worldline.

For the moment, let us take the second route. All the local results are unchanged, except that $F_{n>0}^\mu$ is set to zero and the mass dipole moment M^i is *not* set to zero. This means that the metric perturbations $\check{h}_{\mu\nu}^n = \check{h}_{\mu\nu}^{Sn} + \check{h}_{\mu\nu}^{Rn}$ are modified from Eqs. (70)–(73) to be

$$\check{h}_{\mu\nu}^{S1} = h_{\mu\nu}^{\text{seed}}(x; z_0, m) = \frac{2m\delta_{\mu\nu}}{r} + \mathcal{O}(r^0), \quad (101)$$

$$\check{h}_{\mu\nu}^{R1} = \sum_{\ell \geq 0} h_{\mu\nu}^{\text{free}}(x; z_0, k_\ell^1), \quad (102)$$

and

$$\begin{aligned} \check{h}_{\mu\nu}^{S2} &= h_{\mu\nu}^{\text{seed}}(x; z_0, M) + h_{\mu\nu}^{\text{seed}}(x; z_0, S) + h_{\mu\nu}^{\text{seed}}(x; z_0, \check{\delta}m) \\ &\quad + h_{\mu\nu}^{S2IH}(x; z_0, m, \{k_\ell^1\}_{\ell \geq 0}), \end{aligned} \quad (103)$$

$$\check{h}_{\mu\nu}^{R2} = \sum_{\ell \geq 0} h_{\mu\nu}^{\text{free}}(x; z_0, k_\ell^2) + h_{\mu\nu}^{R2IH}(x; z_0, \{k_\ell^1\}_{\ell \geq 0}), \quad (104)$$

where

$$h_{\mu\nu}^{\text{seed}}(x; z_0, M) = \frac{2M_i n^i}{r^2} \delta_{\mu\nu} + \mathcal{O}(1/r), \quad (105)$$

and $\check{\delta}m_{\mu\nu}$ differs from Eq. (83) by the inclusion of the M_i term in Eq. (64), becoming

$$\begin{aligned} \check{\delta}m_{\alpha\beta} &= \frac{1}{3}m \left(2\check{h}_{\alpha\beta}^{R1} + g_{\alpha\beta}g^{\mu\nu}\check{h}_{\mu\nu}^{R1} \right) + m(g_{\alpha\beta} + 2u_\alpha u_\beta)u^\mu u^\nu \check{h}_{\mu\nu}^{R1} \\ &\quad + 4u_{(\alpha}(m\check{h}_{\beta)\mu}^{R1}u^\mu + 2\dot{M}_{\beta)}). \end{aligned} \quad (106)$$

Otherwise, all functionals remain completely unchanged, except that they are evaluated as functionals of z_0^μ rather than of z^μ . The regular field naturally remains a vacuum solution even on γ_0 , its first two orders satisfying $E_{\mu\nu}[\check{h}^{R1}] = 0$, $E_{\mu\nu}[\check{h}^{R2}] = 2\delta^2 R_{\mu\nu}[\check{h}^{R1}, \check{h}^{R1}]$, and $L_\mu[\check{h}^{Rn}] = 0$.

Finally, if we define $z_{1\perp}^\mu \equiv M^\mu/m$ to be the deviation perpendicular to γ_0 (defining $M^i = 0$), then from the master equation (65), we get the Gralla-Wald equation

$$\begin{aligned} \frac{D^2 z_{1\perp}^\mu}{d\tau_0^2} &= -R^\mu{}_{\alpha\nu\beta} u_0^\alpha z_{1\perp}^\nu u_0^\beta - \frac{1}{2} P_0^{\mu\nu} (2\check{h}_{\rho\nu;\sigma}^{R1} - \check{h}_{\rho\sigma;\nu}^{R1}) u_0^\rho u_0^\sigma \\ &\quad + \frac{1}{2m} R^\mu{}_{\nu\rho\sigma} u_0^\nu S^{\rho\sigma}. \end{aligned} \quad (107)$$

Just as in the self-consistent case, these local results can be used in the design of a puncture scheme to obtain global results. However, before describing that scheme, I return to the other method of obtaining the Gralla-Wald approximation: by substituting an expansion of the worldline into the self-consistent results.

5.1.1 Expansion of the Worldline

We would like to express the expansion covariantly, in terms of vectors that live on γ_0 . Suppose we begin with an expansion $z^\mu(s, \epsilon) = z_0^\mu(s) + \epsilon z_1^\mu(s) + \epsilon^2 z_2^\mu(s) + \dots$, where $z_n^\mu(s) = \frac{1}{n!} \frac{\partial^n z^\mu}{\partial \epsilon^n} \Big|_{\epsilon=0}$. The linear term, $z_1^\mu(s)$, is automatically a vector on γ_0 , since it is a first derivative along the curve of constant s and increasing ϵ . However, beyond linear order, the terms are no longer tensorial; each of them is simply a collection of four scalars dependent upon the particular chart x^μ in which $z^\mu(s, \epsilon) = x^\mu(\gamma(s, \epsilon))$.

So let us approach the problem more geometrically. To facilitate the expansion, I introduce a Lie derivative \mathcal{L} that acts on a functional's dependence on z^μ :

$$\mathcal{L}_\xi A_\Lambda(x; z) \equiv \frac{d}{d\lambda} A_\Lambda(x; z + \lambda \xi) \Big|_{\lambda=0}, \quad (108)$$

where Λ is a multi-index of any covariant and contravariant rank. This is closely related to a Lie derivative acting at x^μ . \mathcal{L} moves the field point relative to the worldline; \mathcal{L} moves the worldline relative to the field point. The two operations are not identical, since the tensorial character of the functional is different at the two points. For example, in Eq. (217) we see that $h_{\mu\nu}^1(x; z)$ is a rank-two tensor at x^μ but a scalar at z^μ .

An expansion of a functional of the worldline $z^\mu(s, \epsilon)$ in the limit $\epsilon \rightarrow 0$ is really an expansion along the flow of increasing ϵ . We can write this as

$$A_\Lambda(x; z_\epsilon) = A_\Lambda(x; z_0) + \epsilon \delta A_\Lambda(x; z_0) + \epsilon^2 \delta^2 A_\Lambda(x; z_0) + \dots, \quad (109)$$

where

$$\delta^n A_\Lambda(x; z_0) = \frac{1}{n!} \mathcal{L}_v^n A_\Lambda(x; z_0); \quad (110)$$

here $v^\mu \equiv \frac{\partial z^\mu}{\partial \lambda}$ is the generator of the flow.

Now, let $z_{2F}^\mu = \frac{1}{2} v^\mu \nabla_\mu v^\nu \Big|_{\epsilon=0}$. This is a vector on γ_0 . It is equal to z_2^μ if the expansion of the worldline is performed in Fermi normal coordinates. One can obtain a covariant evolution equation for it from a second-order self-consistent equation of motion, as described in Appendix 1. Beginning from Eq. (191), this procedure leads to Eq. (205), for example. More importantly for the present analysis, we can also write the expansion (110) in terms of this quantity. As an instance of that, the second-order term is

$$\frac{1}{2}\mathcal{L}_v^2 A_\Lambda(x; z_0) = z_0^{\mu'} \nabla_{\mu'} A_\Lambda(x; z_0) + \frac{1}{2} z_1^{\mu'} z_1^{\nu'} \nabla_{\mu'} \nabla_{\nu'} A_\Lambda(x; z_0), \quad (111)$$

where primed indices refer to the point z_0^μ . One can do the same at any order: from the equation of motion for z^μ , obtain evolution equations for vectors on z_0^μ , and write the expansion (109) in terms of those vectors.

Applying this expansion to the perturbations from the self-consistent approximation, we have

$$\epsilon^n h_{\mu\nu}^n(x; z) = \epsilon^n h_{\mu\nu}^n(x; z_0) + \epsilon^{n+1} \mathcal{L}_{z_1} h_{\mu\nu}^n(x; z_0) + \mathcal{O}(\epsilon^{n+2}). \quad (112)$$

Therefore, the Gralla-Wald expansion (31) reads

$$h_{\mu\nu} = \epsilon \check{h}_{\mu\nu}^1(x; z_0) + \epsilon^2 \check{h}_{\mu\nu}^2(x; z_0, z_1) + \mathcal{O}(\epsilon^3), \quad (113)$$

with $\check{h}_{\mu\nu}^1(x; z_0)$ being the same functional as $h_{\mu\nu}^1(x; z)$, but with z_0^μ having replaced z^μ in its argument, and with the second-order perturbation given by the new functional

$$\check{h}_{\mu\nu}^2(x; z_0, z_1) = h_{\mu\nu}^2(x; z_0) + \delta h_{\mu\nu}^1(x; z_0, z_1). \quad (114)$$

where $\delta h_{\mu\nu}^n(x; z_0, z_1) = \mathcal{L}_{z_1} h_{\mu\nu}^n(x; z_0)$.

The same expansions are applied in precise analogy for the singular and regular fields, yielding $\check{h}_{\mu\nu}^n = \check{h}_{\mu\nu}^{Sn} + \check{h}_{\mu\nu}^{Rn}$ with

$$\check{h}_{\mu\nu}^{S/R1} = h_{\mu\nu}^{S/R1}(x; z_0), \quad (115)$$

$$\check{h}_{\mu\nu}^{S/R2} = h_{\mu\nu}^{S/R2}(x; z_0) + \delta h_{\mu\nu}^{S/R1}(x; z_0, z_1). \quad (116)$$

Appendix 2 describes these expansions in more detail. But in a few words, the end result is that the procedure exactly recovers Eqs. (101)–(107). All of the meat of the result is in $\delta h_{\mu\nu}^1(x; z_0, z_1)$: the action of \mathcal{L} on $h_{\mu\nu}^1$ precisely generates the mass dipole moment seed field $h_{\mu\nu}^{\text{seed}}(x; z_0, M)$ and the contribution of the mass dipole moment to $\check{m}_{\mu\nu}$. Appendix 2 also shows that (i) the generation and modification of these two seed fields precisely corresponds to the linear term in the expansion of the skeletal stress-energy $T_1^{\mu\nu}(x; z)$ around $z^\mu = z_0^\mu$, and (ii) the term $\delta h_{\mu\nu}^1(x; z_0, z_1)$ [and analogously, $\delta h_{\mu\nu}^{S/R1}(x; z_0, z_1)$] can be written as a functional $\delta h_{\mu\nu}^1(x; z_0, z_{1\perp})$ that depends only on the perpendicular piece of z_1^μ . Result (ii) is in agreement with the fact that the seed fields depend only on $M^\mu = m z_{1\perp}^\mu$. Physically, this results from the field equations' indifference to the piece of the deviation that is tangential to the worldline, which can always be set to zero by reparametrizing the family $z^\mu(s, \epsilon)$ with a parameter $s' = s'(s, \epsilon)$ that ensures curves of fixed s' strike z_0^μ orthogonally at $\epsilon = 0$.

5.1.2 Global Metric

A global solution can be obtained from the local results just as in the self-consistent case. I first note that the local singularity structure of the singular field $\check{h}_{\mu\nu}^S = \epsilon \check{h}_{\mu\nu}^{S1} + \epsilon^2 \check{h}_{\mu\nu}^{S2}$ is identical to the self-consistent singular field, but for two important alterations:

- The divergent terms diverge on γ_0 , not on γ .
- The second-order singular field depends on the correction z_1^μ to the position.

Because the point at which the puncture diverges is independent of the perturbations $\check{h}_{\mu\nu}^n$ in this expansion, the puncture scheme becomes a sequence of equations, rather than a coupled system: first, the zeroth-order worldline is prescribed as a solution to the background geodesic equation,

$$\frac{D^2 z_0^\mu}{d\tau_0^2} = 0, \quad (117)$$

then the first order field is found from

$$E_{\mu\nu}[\check{h}^{\mathcal{R}1}] = -E_{\mu\nu}[\check{h}_{\alpha\beta}^{\mathcal{P}1}] \quad \text{inside } \Gamma_0, \quad (118a)$$

$$E_{\mu\nu}[\check{h}^1] = 0 \quad \text{outside } \Gamma_0, \quad (118b)$$

then that field is used to find the first-order correction to the position by solving the Gralla-Wald equation (107), and finally the second-order field is found from

$$E_{\mu\nu}[\check{h}^{\mathcal{R}2}] = 2\delta^2 R_{\mu\nu}[\check{h}^1, \check{h}^1] - E_{\mu\nu}[\check{h}^{\mathcal{P}2}] \quad \text{inside } \Gamma_0, \quad (119a)$$

$$E_{\mu\nu}[\check{h}^2] = 2\delta^2 R_{\mu\nu}[\check{h}^1, \check{h}^1] \quad \text{outside } \Gamma_0. \quad (119b)$$

Here Γ_0 is a tube around γ_0 ; unlike in the self-consistent case, neither γ_0 nor Γ_0 need be updated over the course of the numerical simulation. Like the self-consistent puncture scheme, these equations can be solved given initial data on a Cauchy surface.³¹

Again, there is no obstacle to carrying a puncture scheme like this to arbitrary order, given the local solution in the buffer region.

5.2 Osculating-Geodesics Approximation

I refer the reader back to Sect. 1.5.6 for a reminder of how the osculating-geodesics approximation works. In brief, it obtains a self-consistent approximation by first

³¹ Since the approximation is held to be valid in a region of size $\varsigma(\epsilon) \ll 1/\sqrt{\epsilon}$, a reasonable approach would be to solve the equations in the causal future of a partial Cauchy surface of that size.

using a sequence of Gralla-Wald approximations to find the self-consistent worldline z^μ , then solving the relaxed field equations with z^μ already determined. Concretely, through second order one seeks a solution to the self-consistent system (98)–(100) by applying the Gralla-Wald approximation (113) to the right-hand side of Eq. (100) at each instant τ , with the expansion $z^\mu(\tau', \epsilon) = z_{0(\tau)}^\mu(\tau') + \epsilon z_{1(\tau)}^\mu + \mathcal{O}(\epsilon)$ being around the geodesic $z_{0(\tau)}^\mu$ that is instantaneously tangential to z^μ at time τ . The terms $\check{h}_{\mu\nu}^{\mathcal{R}n}(z(\tau); z_0, \dots, z_{n-1})$ that then appear in Eq. (100) are found by solving Eqs. (117)–(119). By using the resulting sequence of forces $\epsilon F_1^\mu(\tau; z_{0(\tau)}) + \epsilon^2 F_2^\mu(\tau; z_{0(\tau)}, z_{1(\tau)})$, one can solve Eq. (100). Finally, one can solve Eqs. (98) and (99) using the z^μ one has already found.

What is the advantage of this over simply solving Eqs. (98)–(100) directly? At linear order, the advantage is that one can solve Eq. (118) very easily in the frequency domain, while the self-consistent equations do not seem to admit a frequency decomposition. One can then compute a table of values of $F_1^\mu(\tau; z_{0(\tau)})$ for different geodesics and easily solve $\frac{D^2 z^\mu}{d\tau^2} = \epsilon F_1^\mu(\tau; z_{0(\tau)})$ to obtain an approximation to z^μ [60]. But at second-order, it is not obvious whether the scheme is simpler than a direct solution of the self-consistent equations. The term $\delta h_{\mu\nu}^1(x; z_{0(\tau)}, z_{1(\tau)})$ that appears in the second-order field (and a piece of which appears in the puncture $\check{h}_{\mu\nu}^{2\mathcal{P}}$) grows with time away from the osculation point $x^\mu = z^\mu(\tau)$; can it be handled in an efficient way? Furthermore, one must ensure that appropriate boundary conditions are used in each Gralla-Wald expansion to reproduce desired global boundary conditions (such as no incoming radiation) on the self-consistent field; since the approximations only apply in a region of size $\ll 1/\sqrt{\epsilon}$, is there any simple way to find these boundary conditions? I leave these questions open.

6 Gauge Transformations in Perturbative Descriptions of Motion

Thus far, all the explicit results I have presented have been confined to a single choice of gauge. But as I described in Sect. 1.4, gauge and motion are intimately related in perturbation theory: any worldline z^μ one finds can always be shifted by an amount $\epsilon \xi^\mu$. Precisely how this impacts one's approximation scheme depends strongly on how one represents the worldline.

The effect of a gauge transformation on the worldline (or equivalently, on the self-force) was first explored by Barack and Ori [50]. Their results were extended to discontinuous gauge transformations by Gralla and Wald [18, 19]³² and to even more singular transformations in Ref. [31]. In this section I focus, for simplicity, on smooth transformations, and I aim mostly at (i) clarifying the gauge freedom in each of the

³²The extension of Gralla and Wald's result to the self-consistent case [12] unfortunately contained a significant error, leading to a result that held only in gauges continuously related to Lorenz, as in the Barack-Ori analysis.

different representations of motion and their corresponding approximation schemes, and (ii) defining appropriate rules for the gauge transformations of the singular and regular fields. Reference [18] contains a more comprehensive treatment.

6.1 Review of Gauge Freedom in Perturbation Theory

Before considering the question of gauge in self-force theory, I briefly remind the reader of the basics, following Refs. [72–74]. It will be convenient in this section to adopt index-free notation for tensors. In perturbation theory, we consider a family of metrics $g_{\mu\nu}(x, \epsilon)$, or simply g in the absence of a chart. This family lives on a family of manifolds \mathcal{M}_ϵ , and a given choice of gauge refers to an identification map $\phi_\epsilon^X : \mathcal{M}_0 \rightarrow \mathcal{M}_\epsilon$. The identification map induces a flow through the family down to the base manifold \mathcal{M}_0 where the background metric $g \equiv g_0$ lives. Call the generator of this flow $X \equiv \frac{d\phi_\epsilon^X}{d\epsilon}$. We wish to approximate a tensor A at a point $\phi_\epsilon^X(p) \in \mathcal{M}_\epsilon$ as an expansion around its value at $\epsilon = 0$. This expansion is given by

$$(\phi_\epsilon^{X*} A)(p) = (e^{\epsilon \mathcal{L}_X} A)(p) = \sum_{n \geq 0} \frac{\epsilon^n}{n!} (\mathcal{L}_X^n A)(p), \quad (120)$$

where ϕ_ϵ^{X*} denotes the pullback of ϕ_ϵ^X , \mathcal{L} is the Lie derivative, and $p \in \mathcal{M}_0$. We define the n th-order perturbation A_n^X in this gauge to be

$$A_n^X(p) \equiv \frac{1}{n!} (\mathcal{L}_X^n A)(p). \quad (121)$$

Now say we work in a different gauge. This corresponds to a different choice of identification map $\phi_\epsilon^Y : \mathcal{M}_0 \rightarrow \mathcal{M}_\epsilon$ and flow generator $Y \equiv \frac{d\phi_\epsilon^Y}{d\epsilon}$. The approximation of the tensor A in terms of tensors at the point $p \in \mathcal{M}_0$ is now given by

$$(\phi_\epsilon^{Y*} A)(p) = (e^{\epsilon \mathcal{L}_Y} A)(p), \quad (122)$$

and the n th-order perturbation is

$$A_n^Y(p) \equiv \frac{1}{n!} (\mathcal{L}_Y^n A)(p). \quad (123)$$

The gauge transformation of A is the difference between the two expansions when evaluated at a point in \mathcal{M}_0 : in more common notation, we say $A_n \rightarrow A'_n = A_n + \Delta A_n$, where the primed tensor refers to the Y gauge, the unprimed to the X gauge, and their difference is

$$\Delta A_n(p) = \frac{1}{n!} (\mathcal{L}_Y^n A)(p) - \frac{1}{n!} (\mathcal{L}_X^n A)(p). \quad (124)$$

The first- and second-order terms are easily expressed in the familiar form

$$\Delta A_1 = \mathcal{L}_{\xi_1} A_0, \quad (125a)$$

$$\Delta A_2 = \mathcal{L}_{\xi_2} A_0 + \frac{1}{2} \mathcal{L}_{\xi_1}^2 A_0 + \mathcal{L}_{\xi_1} A_1, \quad (125b)$$

where $\xi_1 \equiv Y - X$ and $\xi_2 \equiv \frac{1}{2}[X, Y]$ are the usual gauge vectors. Higher-order terms are straightforwardly written down, but since concrete self-force results are not available beyond second order, I stop here.

In a chart, one can show that a gauge transformation can equivalently be thought of as a near-identity coordinate transformation rather than a change in identification map. First lay a chart x^μ on each \mathcal{M}_ϵ using some identification, say $x^\mu(\phi_\epsilon^X(p)) = x^\mu(p)$ for each $p \in \mathcal{M}_0$. The two identification maps ϕ_ϵ^X and ϕ_ϵ^Y identify the point p in \mathcal{M}_0 with two different points $q = \phi_\epsilon^X(p)$ and $q' = \phi_\epsilon^Y(p)$ in \mathcal{M}_ϵ , which are related by the active diffeomorphism $q \mapsto \phi_\epsilon^Y((\phi_\epsilon^X)^{-1}(q))$ and which have slightly different coordinate values. Since the chart x^μ consists of four ordinary scalar fields, we can apply the general expansion (122) to write the coordinates at q' as

$$x^\mu(q') = x^\mu(q) + \epsilon \xi_1^\mu(x(q)) + \epsilon^2 \left[\xi_2^\mu(x(q)) + \frac{1}{2} \xi_1^\nu(x(q)) \partial_\nu \xi_2^\mu(x(q)) \right] + \mathcal{O}(\epsilon^3), \quad (126)$$

where I have used $\mathcal{L}_X x^\mu = 0$ to express Y derivatives as ξ derivatives, and I have used the fact that $x^\mu(p) = x^\mu(q)$ to express the components on the right-hand side as functions of $x^\mu(q)$. Now, rather than an active diffeomorphism on \mathcal{M}_ϵ , let us consider this as a passive change in the chart, $x^\mu(q) \mapsto x'^\mu(x(q))$. Define the coordinate transformation such that $x'^\mu(q') = x^\mu(q)$. Rewriting Eq. (126) as an equation for $x^\mu(q)$ as a function of $x^\mu(q')$, we get

$$x'^\mu(q') = x^\mu(q') - \epsilon \xi_1^\mu(x(q')) - \epsilon^2 \left[\xi_2^\mu(x(q')) - \frac{1}{2} \xi_1^\nu(x(q')) \partial_\nu \xi_1^\mu(x(q')) \right] + \mathcal{O}(\epsilon^3). \quad (127)$$

Gauge transformation laws for components of tensors can be derived directly from this coordinate transformation. For example, by rewriting Eq. (127) as an equation for $x^\mu(x'(p'))$ and substituting it into the ordinary transformation law for the components of the metric, one finds

$$g'_{\mu\nu}(x', \epsilon) = \frac{\partial x^\alpha}{\partial x'^\mu} \frac{\partial x^\beta}{\partial x'^\nu} g_{\alpha\beta}(x(x'), \epsilon) \quad (128a)$$

$$= g_{\mu\nu}(x', \epsilon) + \mathcal{L}_\xi g_{\mu\nu}(x', \epsilon) + \frac{1}{2} \mathcal{L}_\xi^2 g_{\mu\nu}(x', \epsilon) + \mathcal{O}(\epsilon^3), \quad (128b)$$

where $\xi^\mu = \epsilon \xi_1^\mu + \epsilon^2 \xi_2^\mu + \mathcal{O}(\epsilon^3)$; the analogous transformation law for a tensor of arbitrary rank is also easily found. To relate this to the language used above, note that we are now using a single identification map ϕ_ϵ , and given that identification, components of g have identical coordinate values as $(\phi_\epsilon^* g)$. Equation (128) applies even if $g_{\mu\nu}(x', \epsilon)$ is not expanded for small ϵ . If it is so expanded, then Eq. (128) returns Eq. (125).

Of course, we are ultimately interested in solving the Einstein equation, and so in addition to transformations of the metric, we must consider transformations of curvature tensors. Useful identities for the transformations of curvature tensors are derived in Appendix 3. One of their consequences is that when examining perturbations of a curvature tensor, one can derive transformation laws in two equally natural ways: directly from Eq. (125) or from the transformations of the metric perturbations. For example, in a vacuum background, Eq. (125) directly implies

$$\Delta \delta R_{\mu\nu}[h^1] = \mathcal{L}_{\xi_1} R_{\mu\nu}[g] = 0, \quad (129)$$

$$\Delta(\delta R_{\mu\nu}[h^2] + \delta^2 R_{\mu\nu}[h^1, h^1]) = \mathcal{L}_\xi \delta R_{\mu\nu}[h^1]; \quad (130)$$

or the same equations can be found by instead using Eq. (125) for the metric itself, writing

$$\begin{aligned} & \Delta(\delta R_{\mu\nu}[h^2] + \delta^2 R_{\mu\nu}[h^1, h^1]) \\ &= \delta R_{\mu\nu}[h'^2] + \delta^2 R_{\mu\nu}[h'^1, h'^1] - (\delta R_{\mu\nu}[h^2] + \delta^2 R_{\mu\nu}[h^1, h^1]) \\ &= \delta R_{\mu\nu}[\mathcal{L}_{\xi_2} g] + \frac{1}{2} \delta R_{\mu\nu}[\mathcal{L}_{\xi_1}^2 g] + \delta R_{\mu\nu}[\mathcal{L}_{\xi_1} h^1] \\ & \quad + 2\delta^2 R_{\mu\nu}[h^1, \mathcal{L}_{\xi_1} g] + \delta^2 R_{\mu\nu}[\mathcal{L}_{\xi_1} g, \mathcal{L}_{\xi_1} g] \end{aligned} \quad (131)$$

and then applying Eqs. (231)–(233).

6.2 Gauge in the Gralla-Wald Approximation

I reverse my usual ordering by first considering transformations in the Gralla-Wald approximation, which allows the most straightforward treatment. Since the Gralla-Wald expansion is an ordinary one, with coefficients independent of ϵ , all the ordinary rules apply.

6.2.1 Transformation of the Metric and the Worldline

First, let us examine the transformation of the deviation terms in the expansion of the worldline. According to Eq. (127), under a gauge transformation the coordinates $z^\mu(s, \epsilon) = x^\mu(\gamma_\epsilon(s))$ on the worldline become

$$z'^{\mu}(s, \epsilon) = z^{\mu}(s, \epsilon) - \epsilon \xi_1^{\mu}(z) - \epsilon^2 \left[\xi_2^{\mu}(z) - \frac{1}{2} \xi_1^{\nu}(z) \partial_{\nu} \xi_1^{\mu}(z) \right] + O(\epsilon^3), \quad (132)$$

where functions of z^{μ} are evaluated at $z^{\mu}(s)$. By expanding this in powers of ϵ , we immediately find

$$z_0'^{\mu}(s) = z_0^{\mu}(s), \quad (133a)$$

$$z_1'^{\mu}(s) = z_1^{\mu}(s) - \xi_1^{\mu}(z_0), \quad (133b)$$

$$z_2'^{\mu}(s) = z_2^{\mu}(s) - \xi_2^{\mu}(z_0) + \frac{1}{2} \xi_1^{\nu}(z_0) \partial_{\nu} \xi_1^{\mu}(z_0) - z_1^{\nu}(s) \partial_{\nu} \xi_1^{\mu}(z_0), \quad (133c)$$

where functions of z_0^{μ} are evaluated at $z_0^{\mu}(s)$. Note that the zeroth-order worldline is unchanged; the effect of the transformation is to alter the deviations relative to that worldline.

Now let us examine the transformation of the metric perturbations. Applying the transformation laws (125) to the metric, we find $\check{h}_{\mu\nu}^n \rightarrow \check{h}_{\mu\nu}^n + \Delta \check{h}_{\mu\nu}^n$ with

$$\Delta \check{h}_{\mu\nu}^1(x; z_0) = \mathcal{L}_{\xi_1} g_{\mu\nu}, \quad (134a)$$

$$\Delta \check{h}_{\mu\nu}^2(x; z_0) = \mathcal{L}_{\xi_2} g_{\mu\nu} + \frac{1}{2} \mathcal{L}_{\xi_1}^2 g_{\mu\nu} + \mathcal{L}_{\xi_1} \check{h}_{\mu\nu}^1(x; z_0). \quad (134b)$$

Corresponding to the treatment of the worldline, all $\check{h}_{\mu\nu}^n$, like all $\check{h}_{\mu\nu}^n$, diverge at $z_0^{\mu}(s)$. Instead of altering the curve on which the fields diverge, the gauge transformation alters the singularity on that curve, by altering the functions $z_{n>0}^{\mu}$ that appear in $\check{h}_{\mu\nu}^{n>1}$.

In fact, one need not even appeal to Eq. (132) to determine how the deviation vectors are transformed: the transformation laws for $z_{n>0}^{\mu}$, as given in Eq. (133), can be derived directly from those for $\check{h}_{\mu\nu}^{n>1}$. For example, z_1^{μ} appears in the metric as the mass dipole moment M^{μ}/m , and the transformation of M^{μ} can be determined from the transformation law for $\check{h}_{\mu\nu}^2$. By applying Eq. (134b) to the results (101)–(104) in Fermi normal coordinates³³ and comparing to Eq. (105), one quickly finds that $\mathcal{L}_{\xi_1} \check{h}_{\mu\nu}^1$ is the only part of $\Delta \check{h}_{\mu\nu}^2$ that contributes a mass dipole term. More specifically, $\mathcal{L}_{\xi_1} \frac{2m\delta_{\mu\nu}}{r}$ contributes the relevant term, given by $\frac{-2m\xi_1^i n_i}{r^2} \delta_{\mu\nu}$. This modifies M^i by an amount $\Delta M^i = -m\xi_1^i$, from which we read off the same result as in Eq. (133b).

6.2.2 Transformation of the Singular and Regular Fields

Though deriving the transformation laws for $\check{h}_{\mu\nu}^n$ was trivial, we must put some thought into how to do the same for the singular and regular fields $\check{h}_{\mu\nu}^{Sn}$ and $\check{h}_{\mu\nu}^{Rn}$. We

³³At this stage the transformation is applied only to the sums $\check{h}_{\mu\nu}^n = \check{h}_{\mu\nu}^{Rn} + \check{h}_{\mu\nu}^{Sn}$; one does not yet need transformation laws for the individual pieces $\check{h}_{\mu\nu}^{Rn}$ and $\check{h}_{\mu\nu}^{Sn}$.

are free to split $\check{h}_{\mu\nu}^n$ into a singular piece and a regular piece however we like, just as we were with $\check{h}_{\mu\nu}^n$. However, ideally, we can do so in such a way that we preserve the nice properties of the split. Allow me to specialize to a nonspinning, spherical object, such that there is no force from coupling of moments to external curvature. This means the properties I wish to preserve are that the transformed worldline z'^μ [in its expanded form (133)] should satisfy the geodesic equation in the transformed effective metric $\check{g}'_{\mu\nu} = g_{\mu\nu} + h_{\mu\nu}^R$, and that effective metric should satisfy the vacuum Einstein equation.

Appropriate transformation laws can be found by noting that for a smooth metric and smooth worldline, both the geodesic equation and the vacuum Einstein equation are manifestly invariant under a generic smooth coordinate transformation. It follows that if the worldline and the metric in those two equations are expanded in a power series, and the metric and the expanded geodesic transform according to the standard laws of gauge transformations, then the perturbative expansions of the worldline and metric continue to satisfy the perturbative geodesic equation and the perturbative Einstein equation. In our case, we already have the worldline transforming according to the standard transformation law. Accordingly, if we define the regular field to transform like an ordinary smooth perturbation, as $\check{h}_{\mu\nu}^{Rn} = \check{h}_{\mu\nu}^{Rn} + \Delta\check{h}_{\mu\nu}^{Rn}$, where

$$\Delta\check{h}_{\mu\nu}^{R1}(x; z_0) = \mathcal{L}_{\xi_1} g_{\mu\nu}, \quad (135a)$$

$$\Delta\check{h}_{\mu\nu}^{R2}(x; z_0) = \mathcal{L}_{\xi_2} g_{\mu\nu} + \frac{1}{2} \mathcal{L}_{\xi_1}^2 g_{\mu\nu} + \mathcal{L}_{\xi_1} \check{h}_{\mu\nu}^{R1}(x; z_0), \quad (135b)$$

then all the nice properties of the regular field are maintained under a gauge transformation. However, at the same time, the total field $\check{h}_{\mu\nu}^n = \check{h}_{\mu\nu}^{Sn} + \check{h}_{\mu\nu}^{Rn}$ must satisfy Eq. (134). This means the singular field must satisfy

$$\check{h}_{\mu\nu}^{Sn} = \check{h}_{\mu\nu}^{Sn} + (\Delta\check{h}_{\mu\nu}^n - \Delta\check{h}_{\mu\nu}^{Rn}) \quad (136)$$

—or more explicitly,

$$\Delta\check{h}_{\mu\nu}^{S1}(x; z_0) = 0, \quad (137a)$$

$$\Delta\check{h}_{\mu\nu}^{S2}(x; z_0) = \mathcal{L}_{\xi_1} \check{h}_{\mu\nu}^{S1}(x; z_0). \quad (137b)$$

6.2.3 Governing Equations in Alternative Gauges

By design, the transformation laws (133)–(137) ensure that *the governing equations of the Gralla–Wald representation are invariant under a gauge transformation*: in any gauge, the regular field satisfies the vacuum equations $\delta R_{\mu\nu}[\check{h}^{R1}] = 0$, $\delta R_{\mu\nu}[\check{h}^{R2}] =$

$-\delta^2 R_{\mu\nu}[\check{h}^{R1}, \check{h}^{R1}]; z_0^\mu$ is unaltered and the deviations from it satisfy (35) and (36)³⁴; and assuming the gauge choice admits a well-posed initial value problem, the full field off the worldline can be calculated using the puncture scheme encapsulated in Eqs. (117)–(119). These facts follow from the invariance of the geodesic equation and Eqs. (129)–(131). However, because of Eq. (137b), the singularity structure of the second-order field, and hence the puncture in the puncture scheme, is altered by a gauge transformation. We can assess the impact of this change by examining how it manifests in the second-order field equation. Using Eq. (233), we have

$$\delta R_{\mu\nu}[\mathcal{L}_{\xi_1} \check{h}^{S1}] = \mathcal{L}_{\xi_1} \delta R_{\mu\nu}[\check{h}^{S1}] - 2\delta^2 R_{\mu\nu}[h^{S1}, \mathcal{L}_{\xi_1} g] \quad (139a)$$

$$= 8\pi \mathcal{L}_{\xi_1} \bar{T}_{\mu\nu}^1 - 2\delta^2 R_{\mu\nu}[\check{h}^{S1}, \Delta \check{h}^{R1}]. \quad (139b)$$

The second term on the right is precisely the term required to make $h'^{S2}_{\mu\nu}$ a solution to the correct equation, $\delta R_{\mu\nu}[\check{h}'^{S2}] = -\delta^2 R_{\mu\nu}[\check{h}'^{S1}, \check{h}'^{S1}] - 2\delta^2 R_{\mu\nu}[\check{h}'^{S1}, \check{h}'^{R1}]$ at points off γ_0 . The first term on the right-hand side of Eq. (139b) indicates a change in the skeletal stress-energy: $\bar{T}_{\mu\nu}^2 \rightarrow \bar{T}_{\mu\nu}^2 + \mathcal{L}_{\xi_1} \bar{T}_{\mu\nu}^1$. This change in skeleton corresponds to a change in the seed solutions $h_{\mu\nu}^{\text{seed}}(x; z_0, \delta m)$ and $h_{\mu\nu}^{\text{seed}}(x; z_0, M)$. An explicit expression for $\mathcal{L}_{\xi_1} \bar{T}_{\mu\nu}^1$ can be derived from one for $\mathcal{L}_{\xi_1} T_1^{\mu\nu}$, given in Eq. (215). From that latter equation, we see that $\mathcal{L}_{\xi_1} T_1^{\mu\nu}$ both alters $\delta m_{\mu\nu}$ and more notably, shifts the mass dipole moment by an amount $\Delta M^\mu = -m \xi_{1\perp}^\mu$, in agreement with the discussion above.

Of course, to make use of the fact that the governing equations are the same in all smoothly related gauges, one must first find an effective metric satisfying them in a particular gauge. And given that multiple effective metrics can satisfy the same governing equations, one must realize that under a gauge transformation, one is referring to the transformation of one's particular choice of effective metric. Furthermore, there is the potentially more dangerous caveat that the entire analysis of this section assumes smooth transformations. Under a transformation that is singular on the worldline, the singularity structure of the field can be significantly altered, the transformation laws for the deviation vectors are no longer given by Eq. (133), and the relation between the “nice” effective metrics in the two gauges will not be given by Eq. (135).

³⁴Rather than saying the equation of motion (35) is invariant, self-force literature usually talks about a transformation of the self-force. At first order, the equation in the new gauge is $\frac{D^2 z_{1\perp}^\mu}{d\tau_0^2} + R_{\alpha\nu\beta}^\mu u_0^\alpha z_{1\perp}^\nu u_0^\beta = \check{F}_1^\mu$. The force is given by

$$\check{F}_1^\mu = -\frac{1}{2} P_0^{\mu\nu} (2\check{h}_{\nu\alpha;\beta}^{R1} - \check{h}_{\alpha\beta;\nu}^{R1}) u_0^\alpha u_0^\beta = \check{F}_1^\mu - \left(\frac{D^2 \xi_{1\perp}^\mu}{d\tau_0^2} + R_{\alpha\nu\beta}^\mu u_0^\alpha \xi_{1\perp}^\nu u_0^\beta \right), \quad (138)$$

where the second equality follows from $\check{h}_{\mu\nu}^{R1} = \check{h}_{\mu\nu}^{R1} + \mathcal{L}_{\xi_1} g_{\mu\nu}$. With $z_{1\perp}'^\mu = z_{1\perp}^\mu - \epsilon \xi_{1\perp}^\mu$ in the left-hand side of the equation of motion, the equation's invariance is transparent.

6.3 Gauge in the Self-Consistent Approximation

I now consider the freedom in the self-consistent expansion, which is slightly thornier than the Gralla-Wald case.

6.3.1 Transformation of the Metric and the Worldline

First, I note that the self-consistently determined worldline z^μ transforms according to Eq. (132). Unlike in the Gralla-Wald case, neither z^μ nor z'^μ are expanded around z_0^μ .

Now to the metric. Let us adopt the passive view. Suppose we performed the self-consistent expansion in two slightly different coordinate systems x^μ and x'^μ . In the unprimed coordinates, the expansion is performed by writing $g_{\mu\nu}$ as $g_{\mu\nu}(x, \epsilon; z)$ and expanding for small ϵ while holding x^μ and z^μ fixed. In the primed coordinates, we write $g'_{\mu\nu}$ as $g'_{\mu\nu}(x', \epsilon; z')$ and expand while holding x'^μ and z'^μ fixed. In terms of the perturbations $h_{\mu\nu} \equiv g_{\mu\nu} - g_{\mu\nu}$ and $h'_{\mu\nu} \equiv g'_{\mu\nu} - g_{\mu\nu}$, we have expansions

$$h_{\mu\nu}(x, \epsilon; z) = \sum \epsilon^n h_{\mu\nu}^n(x; z), \quad (140)$$

$$h'_{\mu\nu}(x', \epsilon; z') = \sum \epsilon^n h'_{\mu\nu}{}^n(x'; z'). \quad (141)$$

The metric in the two coordinate systems are related, as in Eq. (128), according to

$$g'_{\mu\nu}(x', \epsilon; z') = \frac{\partial x^\alpha}{\partial x'^\mu} \frac{\partial x^\beta}{\partial x'^\nu} g_{\alpha\beta}(x(x'), \epsilon; z(z')), \quad (142a)$$

$$\begin{aligned} &= g_{\mu\nu}(x', \epsilon; z(z')) + \mathcal{L}_\xi g_{\mu\nu}(x', \epsilon; z(z')) \\ &\quad + \frac{1}{2} \mathcal{L}_\xi^2 g_{\mu\nu}(x', \epsilon; z(z')) + \mathcal{O}(\epsilon^3). \end{aligned} \quad (142b)$$

Expanding $g_{\mu\nu}(x', \epsilon; z(z'))$ returns

$$\begin{aligned} h'_{\mu\nu}(x', \epsilon) &= \epsilon [h_{\mu\nu}^1(x'; z) + \mathcal{L}_{\xi_1} g_{\mu\nu}(x')] + \epsilon^2 [h_{\mu\nu}^2(x'; z) + \mathcal{L}_{\xi_2} g_{\mu\nu}(x')] \\ &\quad + \mathcal{L}_{\xi_1} h_{\mu\nu}^1(x'; z) + \frac{1}{2} \mathcal{L}_{\xi_1}^2 g_{\mu\nu}(x')] + \mathcal{O}(\epsilon^3). \end{aligned} \quad (143)$$

In Eq. (143) I have simply left $z^\mu(z')$ as z^μ . Just as in the Gralla-Wald case, the term $\mathcal{L}_{\xi_1} h_{\mu\nu}^1(x'; z)$ introduces a mass dipole moment relative to the reference worldline—in this case, relative to z^μ . But if we now expand $z^\mu(z')$ around $z^\mu = z'^\mu$, the perturbation reads

$$\begin{aligned} h'_{\mu\nu}(x', \epsilon) &= \epsilon [h_{\mu\nu}^1(x'; z') + \mathcal{L}_{\xi_1} g_{\mu\nu}(x')] + \epsilon^2 [h_{\mu\nu}^2(x'; z') + \mathcal{L}_{\xi_2} g_{\mu\nu}(x')] \\ &\quad + (\mathcal{L}_{\xi_1} + \mathcal{L}_{\xi_1}) h_{\mu\nu}^1(x'; z') + \frac{1}{2} \mathcal{L}_{\xi_1}^2 g_{\mu\nu}(x')] + \mathcal{O}(\epsilon^3). \end{aligned} \quad (144)$$

where $\mathcal{L}_{\xi_1} h_{\mu\nu}^1(x'; z') = \delta h_{\mu\nu}^1(x'; z', \xi)$ uses the Lie derivative introduced in Sect. 5. The two Lie derivatives $(\mathcal{L}_{\xi_1} + \mathcal{L}_{\xi_1})h_{\mu\nu}^1(x'; z')$ do not precisely cancel one another, but \mathcal{L}_{ξ_1} does precisely remove the mass dipole moment induced by \mathcal{L}_{ξ_1} ; simply put, \mathcal{L}_{ξ_1} moves everything relative to the worldline, and \mathcal{L}_{ξ_1} moves the worldline by the same amount, such that there is no net change relative to the worldline. In other words, as we expect, $h'_{\mu\nu}$ contains no mass dipole term when written as a functional of the transformed worldline z'^μ . The fact that the dipole moment cancels in this way can be seen more explicitly by acting with $(\mathcal{L}_{\xi_1} + \mathcal{L}_{\xi_1})$ on the leading term in $h_{\mu\nu}^1$, $\frac{2m\delta_{\mu\nu}}{r} \sim \frac{2m\delta_{\mu\nu}}{|x^i - z^i|}$; it can also be inferred from the result (216).

Equation (144) is an expansion at fixed x'^μ and z'^μ . Hence, we can read off the coefficients of ϵ^n and say that the individual terms in the two expansions (140) and (141) are related as

$$h'^1_{\mu\nu}(x'; z') = h^1_{\mu\nu}(x'; z') + \mathcal{L}_{\xi_1} g_{\mu\nu}(x'), \quad (145)$$

$$h'^2_{\mu\nu}(x'; z') = h^2_{\mu\nu}(x'; z') + (\mathcal{L}_{\xi_1} + \mathcal{L}_{\xi_1})h^1_{\mu\nu}(x'; z') + \mathcal{L}_{\xi_2} g_{\mu\nu}(x') + \frac{1}{2}\mathcal{L}_{\xi_1}^2 g_{\mu\nu}(x'). \quad (146)$$

We can see from this analysis that a gauge transformation acts quite differently here than in the Gralla-Wald case. In the Gralla-Wald approximation, the zeroth-order worldline, on which the singular field diverges, is invariant; in the self-consistent approximation, a gauge transformation actually shifts the curve on which the singular field diverges.

6.3.2 Transformation of the Singular and Regular Fields

As in the Gralla-Wald case, I define the split into singular and regular fields in the primed gauge in the simplest way that preserves the properties of the split. In other words, we must have the effective metric $\tilde{g}_{\mu\nu}$ transform as any ordinary smooth tensor field would: $\tilde{g}'_{\mu\nu}(x') = \frac{\partial x^\alpha}{\partial x'^\mu} \frac{\partial x^\beta}{\partial x'^\nu} \tilde{g}_{\alpha\beta}(x(x'))$, which implies $\tilde{g}'_{\mu\nu}(x', \epsilon; z') = \frac{\partial x^\alpha}{\partial x'^\mu} \frac{\partial x^\beta}{\partial x'^\nu} \tilde{g}_{\alpha\beta}(x(x'), \epsilon; z(z'))$, and from there,

$$h'^{\text{R1}}_{\mu\nu}(x'; z') = h^{\text{R1}}_{\mu\nu}(x'; z') + \mathcal{L}_{\xi_1} g_{\mu\nu}(x'), \quad (147)$$

$$h'^{\text{R2}}_{\mu\nu}(x'; z') = h^{\text{R2}}_{\mu\nu}(x'; z') + (\mathcal{L}_{\xi_1} + \mathcal{L}_{\xi_1})h^{\text{R1}}_{\mu\nu}(x'; z') + \mathcal{L}_{\xi_2} g_{\mu\nu}(x') + \frac{1}{2}\mathcal{L}_{\xi_1}^2 g_{\mu\nu}(x'). \quad (148)$$

At the same time we must satisfy Eqs. (145) and (146), which leaves the singular field to transform as

$$h'^{S1}_{\mu\nu}(x'; z') = h^{S1}_{\mu\nu}(x'; z'), \quad (149)$$

$$h'^{S2}_{\mu\nu}(x'; z') = h^{S2}_{\mu\nu}(x'; z') + (\mathcal{L}_{\xi_1} + \mathcal{L}_{\xi_1})h^{S1}_{\mu\nu}(x'; z'). \quad (150)$$

With these choices, the worldline z'^μ is a geodesic of $\tilde{g}'_{\mu\nu}$, and $\tilde{g}'_{\mu\nu}$ is a smooth solution to the vacuum Einstein equation.

6.3.3 Governing Equations in Alternative Gauges

Again as in the Gralla-Wald case, by design, the transformation laws (147)–(150) ensure that *the governing equations of the self-consistent approximation are invariant under a gauge transformation*: in any gauge X , the regular field satisfies $\delta R^X_{\mu\nu}[h^{R1}] = 0$, $\delta R^X_{\mu\nu}[h^{R2}] = -\delta^2 R^X_{\mu\nu}[h^{R1}, h^{R1}]$, where $\delta R^X_{\mu\nu}$ is the linearized Ricci tensor in the X gauge; the center-of-mass worldline on which the field diverges satisfies (28); and assuming well-posedness, the full field off the worldline can be computed using the puncture scheme (98)–(100), with the replacement $E_{\mu\nu} \rightarrow -2\delta R^X_{\mu\nu}$. The only change is to the form of the second-order puncture. The nature of this change can be inferred from the analogue of Eq. (139b), which reads

$$\delta R_{\mu\nu}[(\mathcal{L}_{\xi_1} + \mathcal{L}_{\xi_1})h^{S1}] = 8\pi(\mathcal{L}_{\xi_1} + \mathcal{L}_{\xi_1})\bar{T}^1_{\mu\nu} - 2\delta^2 R_{\mu\nu}[h^{S1}, \Delta h^{R1}]. \quad (151)$$

This is just as in the Gralla-Wald case but for the presence of the \mathcal{L} term. The two Lie derivatives induce a change in the skeletal stress-energy, and hence in the seed solutions contained in the puncture, but unlike in the Gralla-Wald case, this change does not alter the mass dipole moment; the presence of \mathcal{L}_{ξ_1} ensures the mass dipole moment remains zero, as discussed above. So $h^{\text{seed}}_{\mu\nu}(x; z, M)$ vanishes in all smoothly related gauges, and only $h^{\text{seed}}_{\mu\nu}(x; z, \delta m)$ is altered.

6.4 Gauge in the Osculating-Geodesics Approximation

Gauge freedom in the osculating-geodesics approximation is more complicated than in either of the previous two cases. Here, there is freedom at two levels: in the calculations in the Gralla-Wald expansion at each osculation instant, and in the calculation of the self-consistent perturbation $h_{\mu\nu}(x; z)$ that stitches together the Gralla-Wald expansions.

If we always use the same gauge at the two levels, then there is no real complication: a gauge transformation at the self-consistent level can be expanded out to find the induced gauge transformation at the Gralla-Wald level in a straightforward way. However, in principle, calculations at the two levels can be performed in different gauges. In that case, one must have good control over the relationships between the gauges, since the final self-consistent approximation $h_{\mu\nu}(x; z) = \sum_{n=1}^N \epsilon^n h^n_{\mu\nu}(x; z)$ satisfies the Einstein equation through order ϵ^N only if z^μ is in the same gauge as $h_{\mu\nu}$.

Suppose we wish to calculate $h_{\mu\nu}^n(x; z)$ in a gauge X (denoted by unprimed symbols), but at an osculation instant τ we wish to calculate the Gralla-Wald perturbations $\check{h}_{\mu\nu}^n(x; z_{0(\tau)})$ in a gauge Y (denoted by primed symbols). To find the curve z^μ in gauge X , we need to solve

$$\frac{D^2 z^\mu}{d\tau^2} = F^\mu(\tau; z) = \epsilon \check{F}_1^\mu(\tau; z_{0(\tau)}) + \epsilon^2 \check{F}_1^\mu(\tau; z_{0(\tau)}) \quad (152)$$

with the forces in gauge X . But as input we have only the Y -gauge perturbations $\check{h}_{\mu\nu}^n(x; z_{0(\tau)})$. For simplicity, consider only the first-order force in gauge X . It is related to Y -gauge quantities as [see Eq. (139)]

$$\check{F}_1^\mu(\tau) = \check{F}'^\mu_1(\tau) + \left(\frac{D^2 \xi_{1\perp}^\mu}{d\tau_0^2} + R^\mu{}_{\alpha\nu\beta} u_{0(\tau)}^\alpha \xi_{1\perp}^\nu u_{0(\tau)}^\beta \right), \quad (153)$$

where $F_1'^\mu(\tau) = -\frac{1}{2} P_0^{\mu\nu} [2\check{h}_{\nu\alpha;\beta}^{\text{R1}}(x; z_{0(\tau)}) - \check{h}_{\alpha\beta;\nu}^{\text{R1}}(x; z_{0(\tau)})] u_0^\alpha u_0^\beta$. To know the correct force for our self-consistent evolution, we need to know the gauge vector ξ_1^μ . However, this gauge vector is constrained by the osculation condition: we must have $z^\mu(\tau) = z_{0(\tau)}^\mu(\tau)$ and $u^\mu(\tau) = u_{0(\tau)}^\mu(\tau)$. Hence, we should impose $\xi_1^\mu(z(\tau)) = 0$, reducing Eq. (153) to

$$\check{F}_1^\mu = \check{F}'^\mu_1 + \frac{D^2 \xi_{1\perp}^\mu}{d\tau_0^2}. \quad (154)$$

Using this relation, one can calculate the force that appears in Eq. (152) using the force calculated from the Gralla-Wald expansion in gauge Y —but one must know $\frac{D^2 \xi_{1\perp}^\mu}{d\tau_0^2}$ at the osculation instant τ . The same analysis can be straightforwardly generalized to the second-order force $\check{F}_2^\mu(\tau; z_{0(\tau)})$.

7 Equations of Motion from a Rest Gauge

In the algorithm of Sect. 3, the n th-order equation of motion is obtained by solving the $(n+1)$ th-order Einstein equation in the buffer region. However, at least in certain cases, we can instead obtain an equation of motion using only the n th-order solution. This is accomplished by finding the relationship between one's desired gauge—call it the *practical gauge*—and what I call a *rest gauge*, which is, essentially, any of the gauges that have been used to study tidally perturbed objects in the context of matched expansions (see Ref. [75] and the many references therein for examples of these studies). Methods along these lines were the first ones used to derive the MiSaTaQuWa equation [21] and currently, they are the only ones that have been used to derive second-order equations of motion [14, 16, 20, 76], although different notations and descriptions have obscured the shared underlying features of these derivations.

Throughout this section, I specialize to the case of an approximately spherical, nonspinning object whose leading-order dipole and quadrupole moments vanish: $I_{\mu\nu i}^2 = I_{\mu\nu ij}^3 = 0$. I only sketch the calculations in this section refer the reader to Refs. [16, 20] for the details of the calculations in this section.

7.1 Metric in a Rest Gauge

By a rest gauge, I mean a gauge in which the object is manifestly at rest relative to a worldline z^μ and manifestly centered on that worldline. To motivate this idea, I return to the themes of the introduction. In Sect. 1.1.2, I argued that any equation of motion can be written as the geodesic equation in some smooth piece of the metric. In Sect. 1.3, I recalled the results of Thorne and Hartle, who showed something slightly stronger: that the equations of motion and precession for any compact object can be written as those for a test body immersed in some effectively external metric. In Eq. (82), the self-force program has recovered their result for the center-of-mass motion, and it has shown that the “external” metric in their formalism is in fact (at least through order ϵr) the effective metric $\tilde{g}_{\mu\nu} = g_{\mu\nu} + h_{\mu\nu}^R$.

At second order in ϵ and beyond, the algorithm of Sect. 3 has not yet revealed how $\tilde{g}_{\mu\nu}$ relates to Thorne and Hartle’s external metric. But if we can establish the relationship, we can establish the equation of motion. Notably, they derived their equations by working in an inertial frame of their external metric; if the object possesses no spin or quadrupole moments, then there is no force on the object in this frame, and it is what I call the rest gauge. Why I call it a gauge rather than a frame will become clear as we move forward.

The metric in this gauge is most easily constructed through the inner expansion (39) rather than the outer. To do so, I first note that just as the matching condition fixes a lowest allowed power of r in the outer expansion, so it determines a highest power of r in the inner expansion: expanding the n th-order inner perturbation $\epsilon^n H_{\mu\nu}^n(t, \bar{x}^i)$ in the buffer region, we find $\epsilon^n \sum_p (\epsilon/r)^p H_{\mu\nu}^{np}(t, n^i)$; the condition that no negative powers of ϵ occur in the outer expansion then determines

$$H_{\mu\nu}^n(t, \bar{x}^i) = \sum_{p \leq n} \bar{r}^p H_{\mu\nu}^{np}(t, n^i). \quad (155)$$

Here and in what follows, I assume some locally Cartesian coordinates centered on the center-of-mass worldline z^μ . Given an appropriate choice of rest gauge, the coordinates will later be identified with Fermi-Walker coordinates centered on z^μ .

For our approximately spherical, approximately nonspinning object, the inner background metric, when expanded in the buffer region according to Eq. (42), is equal to the Schwarzschild metric through order $1/\bar{r}^4$. It has the schematic form

$$g^{\text{obj}} \sim \eta + \frac{m}{\bar{r}} + \frac{m^2}{\bar{r}^2} + \frac{m^3}{\bar{r}^3} + \mathcal{O}(1/\bar{r}^4); \quad (156)$$

here I do not specify any particular coordinate system, though I insist that the coordinates are mass-centered, such that no mass dipole moment appears in the expansion of g^{obj} ; every term in Eq. (156), at the orders displayed, is fully determined by m . Using our previous results, we know m is constant. Hence, we can find the perturbations $H_{\mu\nu}^n$ in the buffer region using the well-developed formalism of perturbations of Schwarzschild. Furthermore, given the assumption that the perturbations are quasistationary (because, as explained in Sect. 2, the inner expansion scales space but not time), time derivatives appear as higher-order terms in the Einstein equations. That is, one first solves the time-independent linearized Einstein equation

$$\delta R_{\mu\nu}^0[g^{\text{obj}}, H^1] = 0 \quad (157)$$

for $H_{\mu\nu}^1$, with t fixed; here $\delta R_{\mu\nu}[g^{\text{obj}}, H^1] = 0$ means the Ricci tensor linearized off the background $g_{\mu\nu}^{\text{obj}}$, and the superscript “0” means “terms in $\delta R_{\mu\nu}$ containing no t derivatives”. Next, one solves

$$\delta R_{\mu\nu}^0[g^{\text{obj}}, H^2] = -\delta^2 R_{\mu\nu}^0[g^{\text{obj}}, H^1, H^1] - \delta R_{\mu\nu}^1[g^{\text{obj}}, H^1] \quad (158)$$

for $H_{\mu\nu}^2$ at fixed t and for the time derivative of $H_{\mu\nu}^1$, where the superscript “1” in $\delta R_{\mu\nu}^1$ means “terms in $\delta R_{\mu\nu}$ containing one t derivative”. At this point, the pattern should be obvious.

Just as when constructing the outer expansion in the buffer region, we here solve a sequence of spatial differential equations. Furthermore, it is well known that in an appropriate gauge, stationary vacuum perturbations of Schwarzschild behave as $1/\bar{r}^{\ell+1}$ or \bar{r}^ℓ at large \bar{r} , where ℓ is the spherical harmonic index, just as in the outer expansion. Let us label the $1/\bar{r}^{\ell+1}$ solutions as $\frac{1}{\bar{r}^{\ell+1}} H_{\mu\nu}^{n,\ell,-}(t, \bar{x}^i)$ and the \bar{r}^ℓ solutions as $\bar{r}^\ell H_{\mu\nu}^{n,\ell,+}(t, \bar{x}^i)$, where $H_{\mu\nu}^{n,\ell,\pm}$ tends to a finite function $H_{\mu\nu L}^{n,\ell,\pm}(t) \hat{n}^L$ as $\bar{r} \rightarrow \infty$. Combining this with Eq. (155), we find that at first order, where there is no source, the solution behaves as

$$H^1 \sim \bar{r} H^{1,1,+} + \bar{r}^0 H^{1,0,+} + \frac{1}{\bar{r}} H^{1,0,-} + \frac{1}{\bar{r}^2} H^{1,1,-} + \mathcal{O}(1/\bar{r}^3). \quad (159)$$

It is well known that the monopole and dipole solutions $r^0 H_{\mu\nu}^{n,0,+}$ and $r H_{\mu\nu}^{n,0,+}$ are pure gauge. Hence, I set them to zero. The gauge-invariant content in $\frac{\epsilon^2}{r} H_{\mu\nu}^{1,0,-}$ is a correction to m , and in $\frac{\epsilon^3}{r^2} H_{\mu\nu}^{1,1,-}$ it is a perturbation toward the Kerr metric—that is, a small spin. With a bit of work, one can show from Eq. (158) that these perturbations are independent of t , and we can freely set them to zero, absorbing the mass correction into m and specifying that the object remains unspinning at this order. Physically, this time-independence corresponds to the fact that physical changes in mass and angular momentum are caused by tidal heating and torquing, which are caused by nonlinear effects at much higher order in ϵ . So in the end, we have

$$H_{\mu\nu}^1 = 0. \quad (160)$$

Since $H_{\mu\nu}^1$ vanishes, Eq. (158) is again the linearized vacuum equation: $\delta R_{\mu\nu}^0 [g^{\text{obj}}, H^2] = 0$. The solution behaves as

$$H^2 \sim \bar{r}^2 H^{2,2,+} + \bar{r} H^{2,1,+} + \bar{r}^0 H^{2,0,+} + \frac{1}{\bar{r}} H^{2,0,-} + \mathcal{O}(1/\bar{r}^2). \quad (161)$$

Again, $H_{\mu\nu}^{2,1,+}$ and $H_{\mu\nu}^{2,0,+}$ can be gauged away. The invariant part of $H_{\mu\nu}^{2,0,-}$ is another correction to m , which again can be absorbed into a redefinition of m . Writing $H_{\mu\nu}^{2,2,+} = H_{\mu\nu ij}^{2,2,+} \hat{n}^{ij}$, we then have

$$H_{\mu\nu}^2 \sim \bar{r}^2 H_{\mu\nu ij}^{2,2,+}(t, \bar{r}) \hat{n}^{ij} + \mathcal{O}(1/\bar{r}^2). \quad (162)$$

$\lim_{\bar{r} \rightarrow \infty} H_{\mu\nu ij}^{2,2,+}(t, \bar{r})$ can be written in terms of two STF functions $\mathcal{E}_{ij}(t)$ and $\mathcal{B}_{ij}(t)$, and in the expansion of $H_{\mu\nu ij}^{2,2,+}(t, \bar{r})$ for large r , every term is directly proportional to one of those two functions (i.e., constructed from contractions of one of them with δ_{ij} or ϵ_{ijk}). These two quantities can be interpreted as quadrupole tidal moments in the neighbourhood of the object, and from the matching condition they will be identified with those of the external background metric, defined in Eq. (46).

The third-order Einstein equation now reads

$$\delta R_{\mu\nu}^0 [g^{\text{obj}}, H^3] = -\delta R_{\mu\nu}^1 [g^{\text{obj}}, H^2]. \quad (163)$$

Following the same steps as at the previous orders, we find

$$H_{\mu\nu}^3 \sim \bar{r}^3 H_{\mu\nu ijk}^{3,3,+}(t, \bar{r}) \hat{n}^{ijk} + \bar{r}^3 \dot{H}_{\mu\nu ij}^{2,2,+}(t, \bar{r}) \hat{n}^{ij} + \bar{r}^2 H_{\mu\nu ij}^{3,2,+}(t, \bar{r}) \hat{n}^{ij} + \mathcal{O}(1/\bar{r}). \quad (164)$$

$H_{\mu\nu ijk}^{3,3,+}(t, \bar{r})$ can be written in terms of two STF functions $\mathcal{E}_{ijk}(t)$ and $\mathcal{B}_{ijk}(t)$, such that every term in its large- \bar{r} expansion is directly proportional to one or the other. These two quantities can be interpreted as octupole tidal moments in the neighbourhood of the object, and they will be identified with those of the external background metric, which are constructed from covariant derivatives of the Riemann tensor of $g_{\mu\nu}$. Equation (164) additionally contains corrections to the quadrupole fields, both in the form of the time derivatives $\dot{\mathcal{E}}_{ij}$ and $\dot{\mathcal{B}}_{ij}$ appearing in $\dot{H}_{\mu\nu ij}^{2,2,+}$, and in the field $H_{\mu\nu ij}^{3,2,+}$, which like $H_{\mu\nu ij}^{2,2,+}$ can be written in terms of two STF functions, call them $\delta\mathcal{E}_{ij}$ and $\delta\mathcal{B}_{ij}$.

Now let us put the results together. After we rewrite it in terms of unscaled coordinates $r = \epsilon \bar{r}$ and re-expand in ϵ , the metric $g_{\mu\nu} = g_{\mu\nu}^{\text{obj}}(\bar{r}) + \epsilon^2 H_{\mu\nu}^2(\bar{r}) + \epsilon^3 H_{\mu\nu}^3(\bar{r}) + \mathcal{O}(\epsilon^4)$ reads $g_{\mu\nu} = g_{\mu\nu}(r) + \epsilon h_{\mu\nu}^1(r) + \epsilon^2 h_{\mu\nu}^2(r) + \epsilon^3 h_{\mu\nu}^3(r) + \mathcal{O}(\epsilon^4)$, with

$$\begin{aligned}
g &= \eta + r^2 \mathcal{E}_{ij} + r^3 (\mathcal{E}_{ijk} + \dot{\mathcal{E}}_{ij}) + \mathcal{O}(r^4) \\
h'^1 &\sim \frac{m}{r} + mr \mathcal{E}_{ij} + r^2 \delta \mathcal{E}_{ij} + mr^2 (\mathcal{E}_{ijk} + \dot{\mathcal{E}}_{ij}) + \mathcal{O}(r^3), \\
h'^2 &\sim \frac{m^2}{r^2} + m^2 \mathcal{E}_{ij} + mr \delta \mathcal{E}_{ij} + m^2 r (\mathcal{E}_{ijk} + \dot{\mathcal{E}}_{ij}) + \mathcal{O}(r^2), \\
h'^3 &\sim \frac{m^3}{r^3} + \frac{m^3}{r} \mathcal{E}_{ij} + m^2 \delta \mathcal{E}_{ij} + m^3 (\mathcal{E}_{ijk} + \dot{\mathcal{E}}_{ij}) + \mathcal{O}(r),
\end{aligned} \tag{165}$$

where primes refer to quantities in the rest gauge, and $\eta = \text{diag}(-1, 1, 1, 1)$. ‘+’ signs here mean “plus terms directly proportional to”. For compactness, I have omitted the magnetic-type moments \mathcal{B}_{ij} , $\dot{\mathcal{B}}_{ij}$, $\delta \mathcal{B}_{ij}$, and \mathcal{B}_{ijk} ; they appear in exact analogy with the electric type moments \mathcal{E}_{ij} , $\dot{\mathcal{E}}_{ij}$, $\delta \mathcal{E}_{ij}$, and \mathcal{E}_{ijk} . All terms in the tableau, at the displayed orders, are directly proportional to one of these moments and/or to a power of m . Every term in the first column is $\ell = 0$, every term in the second is $\ell = 2$, and every term in the third is either $\ell = 2$ (the $\dot{\mathcal{E}}_{ij}$ and $\dot{\mathcal{B}}_{ij}$ terms) or $\ell = 3$ (the \mathcal{E}_{ijk} and \mathcal{B}_{ijk} terms). In this gauge, the object is manifestly at rest on z^μ : there are no mass dipole moment terms, which have the even-parity dipolar behavior n^i/r^2 , nor any acceleration terms, which have the even-parity dipolar behavior rn^i .

By choosing the gauge of the inner expansion appropriately, we can put the external background metric $g_{\mu\nu}$, given by the top row of Eq. (165), in precisely the form (45) that it takes in Fermi-Walker coordinates—except that no acceleration terms appear. Since we know that the center-of-mass worldline is accelerated in $g_{\mu\nu}$, this tells us that Eq. (165) is actually incomplete. *The construction we have followed here is valid for any worldline z^μ , regardless of whether it is accelerating in $g_{\mu\nu}$ or not.* The fact that we see no explicit acceleration terms is equivalent to the empty statement that any worldline z^μ can be written as a geodesic in *some* smooth piece of the full metric. Ergo, at this stage we know nothing at all about z^μ , and to make $g_{\mu\nu}$ the external background spacetime, we must insert into it by hand the acceleration terms appearing in Eq. (45). At the same time, in our choice of gauge, no acceleration terms appear in the full metric $\mathfrak{g}_{\mu\nu}$. Therefore, we must insert F_n^μ terms into the perturbations $h_{\mu\nu}^n$ such that the sum $g_{\mu\nu}(r) + \epsilon h_{\mu\nu}^1(r) + \epsilon^2 h_{\mu\nu}^2(r) + \epsilon^3 h_{\mu\nu}^3(r) + \mathcal{O}(\epsilon^4)$ contains no acceleration terms when one applies the expansion (25).

The form of $\mathfrak{g}_{\mu\nu}$ in the rest gauge invites us to make a new split into an effectively external metric $\mathfrak{g}_{\mu\nu} = g_{\mu\nu} + h_{\mu\nu}^R$ that contains the m -independent tidal terms in Eq. (165), plus a self-field $h_{\mu\nu}^S = \mathfrak{g}_{\mu\nu} - g_{\mu\nu}$, every term of which is directly proportional to a power of m . With an appropriate choice of rest gauge, $\mathfrak{g}_{\mu\nu}$ looks exactly like Eq. (45) with none of the acceleration terms; that is, our gauge makes the Fermi coordinates refer to proper distances, times, Riemann curvature, and parallel transport defined with respect to $\mathfrak{g}_{\mu\nu}$. We have

$$\mathfrak{g}_{tt} = -1 - \mathfrak{R}_{0i0j} x^i x^j + \mathcal{O}(r^3), \tag{166a}$$

$$\mathfrak{g}_{ta} = -\frac{2}{3} \mathfrak{R}_{0iaj} x^i x^j + \mathcal{O}(r^3), \tag{166b}$$

$$\mathfrak{g}_{ab} = \delta_{ab} - \frac{1}{3} \mathfrak{R}_{aibj} x^i x^j + \mathcal{O}(r^3), \tag{166c}$$

where $\mathfrak{R}_{\mu\alpha\nu\beta} = R_{\mu\alpha\nu\beta} + \epsilon\delta R_{\mu\alpha\nu\beta}[\mathfrak{h}^{\text{R}1}] + \mathcal{O}(\epsilon^2)$ is the Riemann tensor of $\mathfrak{g}_{\mu\nu}$. As per the discussion of acceleration terms in the preceding paragraph, the new “regular field” reads

$$\mathfrak{h}_{it}^{\text{R}1} = 2F_1^i n_i - \delta R_{0i0j}[\mathfrak{h}^{\text{R}}]x^i x^j + \mathcal{O}(r^3), \quad (167a)$$

$$\mathfrak{h}_{ta}^{\text{R}1} = -\frac{2}{3}\delta R_{0iaj}[\mathfrak{h}^{\text{R}}]x^i x^j + \mathcal{O}(r^3), \quad (167b)$$

$$\mathfrak{h}_{ab}^{\text{R}1} = -\frac{1}{3}\delta R_{aibj}[\mathfrak{h}^{\text{R}}]x^i x^j + \mathcal{O}(r^3), \quad (167c)$$

$$\mathfrak{h}_{it}^{\text{R}2} = 2F_2^i n_i + \mathcal{O}(r^2), \quad \mathfrak{h}_{ta}^{\text{R}2} = \mathfrak{h}_{ab}^{\text{R}2} = \mathcal{O}(r^2), \quad (168)$$

and $\mathfrak{h}_{\mu\nu}^{\text{R}3} = \mathcal{O}(r)$. For visual clarity, I have truncated these equations at lower orders in r than Eq. (165).

In summary, in a rest gauge the metric perturbations take the form

$$h_{\mu\nu}^n = \mathfrak{h}_{\mu\nu}^{Sn} + \mathfrak{h}_{\mu\nu}^{Rn}, \quad (169)$$

where $\mathfrak{h}_{\mu\nu}^{Sn}$ is made up entirely of terms containing explicit factors of m^n , no mass monopole corrections, no spin moment, no quadrupole moment, no mass dipole moment, and no acceleration terms, and $\mathfrak{h}_{\mu\nu}^{Rn}$ is given by Eq. (167)–(168). Equation (169) is the *general solution in the buffer region outside an approximately spherical and nonspinning object*, just written in a particular gauge. In this gauge, z^μ is manifestly a geodesic of an effectively external metric, and $\mathfrak{g}_{\mu\nu}$ is being *defined* as that effectively external metric in which z^μ is a geodesic.³⁵ A priori, $\mathfrak{g}_{\mu\nu}$ *need not be related to* $\tilde{g}_{\mu\nu}$; the latter was defined in a very different manner and is not yet known to be the metric in which the motion is geodesic (except at zeroth and first order).

7.2 Self-Consistent Approximation: Worldline-Preserving Gauge Transformations

Metrics in local rest gauges are common in the literature, usually derived in the context of tidally perturbed compact objects. The goal of the self-force game is not simply to construct such a metric, but to find the equation of motion in whichever “practical gauge” one wants to use to compute a global solution.

³⁵Note that without some additional input beyond that definition, the split of $\mathfrak{g}_{\mu\nu}$ into $g_{\mu\nu}$, $\mathfrak{h}_{\mu\nu}^{\text{R}}$, and $\mathfrak{h}_{\mu\nu}^{\text{S}}$ is quite ambiguous. Suppose there were a zeroth-order force acting on the object. One could still write the equation of motion as a geodesic in some smooth piece of the metric, but to do so, one would have to shift part of $g_{\mu\nu}$ into $\mathfrak{h}_{\mu\nu}^{\text{S}}$; one would not simply be splitting the perturbations $h_{\mu\nu}^n$. With the present setup, the ambiguity is lifted by assuming the expansion (25) and utilizing the independently determined fact that $F_0^\mu = 0$.

Let us take the Lorenz gauge as the practical gauge. I wish to find a unique gauge transformation between the rest-gauge perturbations (169) and the Lorenz-gauge perturbations (70)–(73). That is, I seek gauge vectors ξ_1^μ and ξ_2^μ satisfying

$$\mathcal{L}_{\xi_1} g_{\mu\nu} = h_{\mu\nu}^{\prime 1} - h_{\mu\nu}^1, \quad (170)$$

$$\mathcal{L}_{\xi_2} g_{\mu\nu} = h_{\mu\nu}^{\prime 2} - h_{\mu\nu}^2 - \frac{1}{2} \mathcal{L}_{\xi_1}^2 g_{\mu\nu} - \mathcal{L}_{\xi_1} h_{\mu\nu}^1. \quad (171)$$

Note that here I do not utilize the third-order perturbation, though its form $h_{\mu\nu}^{\prime 3}$ was found in the rest-frame gauge. What is its relevance? Only that it contains no mass dipole moment term; in other words, it shows that with this choice of gauge, the correction to the mass dipole moment can unambiguously be set to zero to define a center-of-mass-worldline.

These equations are to be solved subject to one crucial condition: *they must preserve the location of the worldline*. The rest-gauge solution shows that the object is at rest on some worldline, the Lorenz-gauge solution is written in coordinates centered on some worldline, and in order to claim that the worldline of the Lorenz-gauge solution is the desired center-of-mass worldline, we must enforce that it be identical to the worldline of the rest-gauge solution. In the simplest scenario, Eqs. (170) and (171) can be solved with a smooth gauge transformation of the form

$$\xi_n^\mu = \sum_{p \geq 0} \sum_{\ell \leq p} r^p \xi_{np\ell}^{\mu L}(t) \hat{n}_L. \quad (172)$$

Given Eq. (132), the condition that the worldline not be altered is that

$$\xi_{n00}^\mu(t) = \xi_n^\mu|_\gamma = 0. \quad (173)$$

I call a transformation satisfying this condition a *worldline-preserving transformation*. This condition was first used in Ref. [21]. A more general condition is used in Refs. [14, 16].

By working through sequential orders of r in Eqs. (170) and (171), one uniquely determines $\xi_{np\ell}^{\mu L}(t)$ (up to residual gauge freedom in the rest gauge and Lorenz gauge). I do not present details of that process here, but the explicit solution to the first-order equation (170), with particular choices of rest gauge, can be found in various references; see, e.g., Ref. [12]. The explicit solution at second order is presented in Ref. [16]. What is the essential result in these solutions? At first order, they uniquely determine F_1^μ , which appears via Eq. (167), to be the MiSaTaQuWa force (66) (with $S^i = 0$), as we already know. At second-order, they uniquely determine the second-order force F_2^μ , which appears via Eq. (168), to be

$$F_i^2 = \frac{1}{2} \partial_i h_{tt}^{R2} - \partial_t h_{ti}^{R2} - \frac{11}{3} m \dot{F}_i^1 + F_i^1 h_{tt}^{R1} - \frac{1}{2} h_{ti}^{R1} \partial_t h_{tt}^{R1}. \quad (174)$$

Following Appendix 1, the results for F_1^μ and F_2^μ can be combined to write the equation of motion $\frac{D^2 z^\mu}{d\tau^2} = \epsilon F_1^\mu + \epsilon^2 F_2^\mu + \mathcal{O}(\epsilon^3)$ as the geodesic equation $\frac{\tilde{D}^2 z^\mu}{d\tilde{\tau}^2} = \mathcal{O}(\epsilon^3)$ in $\tilde{g}_{\mu\nu} = g_{\mu\nu} + h_{\mu\nu}^R$. This is the result promised way back in Sect. 1.5.1.

What is the meaning of this result? In the rest gauge, we knew that z^μ was a geodesic in $g_{\mu\nu}$. Now we know it is a geodesic in $\tilde{g}_{\mu\nu}$. Either of $g_{\mu\nu}$ or $\tilde{g}_{\mu\nu}$ can be thought of as a “nice” effectively external metric. Are they the same metric? Not necessarily. The two geodesic equations only restrict the metrics $g_{\mu\nu}$ and $\tilde{g}_{\mu\nu}$ on the worldline and their first derivatives on the worldline; they place no constraint on higher derivatives. But one of the results of the process of finding ξ_1^μ and ξ_2^μ is that the two metrics are related by

$$h_{\mu\nu}^{R1} = h_{\mu\nu}^{R1} + \mathcal{L}_{\xi_1} g_{\mu\nu} + \mathcal{O}(r^2) \quad (175)$$

$$h_{\mu\nu}^{R2} = h_{\mu\nu}^{R2} + \mathcal{L}_{\xi_2} g_{\mu\nu} + \frac{1}{2} \mathcal{L}_{\xi_1}^2 g_{\mu\nu} + \mathcal{L}_{\xi_1} h_{\mu\nu}^{R1} + \mathcal{O}(r^2). \quad (176)$$

In other words, they are equivalent up to possible $\mathcal{O}(r^2)$ differences. Are they the same at order r^2 and higher? The answer depends on precisely how the rest gauge, and the tidal moments $\delta\mathcal{E}_{ij}$, $\delta\mathcal{B}_{ij}$ (and at higher order in r , octupolar and higher order moments) appearing in $h_{\mu\nu}^{R1}$, is constructed; this construction is, unfortunately, not unique. Reference [16] demonstrates explicitly that the two effective fields can differ at order r^2 .

Is there a way to determine which effective field is the “best one”? As described in Sect. 3.5, the most promising route is by solving the field equations outside an object with spin and higher moments, since those moments will couple to *some* tidal moments, and we can determine *which* metric the tidal moments belong to, and thence the metric in which the object moves as a test body. But just with the results at hand, we can confidently say that $\tilde{g}_{\mu\nu}$ has all the nice properties one might desire of it for a spherical, nonspinning object: it is a vacuum solution, causal on the worldline, and the object moves on a geodesic of its geometry.

7.3 Gralla-Wald Approximation

Starting from the self-consistent results, one can readily derive the second-order Gralla-Wald equation of motion (36) following the expansion procedure of Appendix 1.

Alternatively, one can derive a second-order equation of motion directly, as was done by Gralla [20]. In the Gralla-Wald case, the rest gauge is constructed in coordinates centered not on z^μ but on z_0^μ . The results are the same as in Sect. 7.1, but all acceleration terms are set to zero in $g_{\mu\nu}$ (and likewise for the F_n^μ terms in $h_{\mu\nu}^n$ that cancel them). When transforming to a “practical gauge”, one uses

$$\check{h}_{\mu\nu}^1 = \check{h}_{\mu\nu}^{\prime 1} + \mathcal{L}_{\xi_1} g_{\mu\nu}, \quad (177)$$

$$\check{h}_{\mu\nu}^2 = \check{h}_{\mu\nu}^{\prime 2} + \mathcal{L}_{\xi_2} g_{\mu\nu} + \frac{1}{2} \mathcal{L}_{\xi_1}^2 g_{\mu\nu} + \mathcal{L}_{\xi_1} \check{h}_{\mu\nu}^1, \quad (178)$$

and *one does not impose the worldline-preserving condition*. The gauge transformation is allowed to move the object relative to z_0^μ . Since $z_1^{\prime\mu} = z_2^{\prime\mu} = 0$ in the rest gauge, we have from Eq. (133) that in the practical gauge

$$z_1^\mu(s) = -\xi_1^\mu(z_0), \quad (179)$$

$$z_2^\mu(s) = -\xi_2^\mu(z_0) + \frac{1}{2} \xi_1^\nu(z_0) \partial_\nu \xi_1^\mu(z_0), \quad (180)$$

and the covariant second deviation is $z_{2F}^\mu(s) = -\xi_2^\mu(z_0) + \frac{1}{2} \xi_1^\nu(z_0) \nabla_\nu \xi_1^\mu(z_0)$.

Following Gralla, one can use this procedure to obtain results in any gauge smoothly related to a particular rest gauge. Defining regular fields

$$\check{h}_{\mu\nu}^{\text{R1}} = \check{h}_{\mu\nu}^{\text{R1}} + \mathcal{L}_{\xi_1} g_{\mu\nu}, \quad (181)$$

$$\check{h}_{\mu\nu}^{\text{R2}} = \check{h}_{\mu\nu}^{\text{R2}} + \mathcal{L}_{\xi_2} g_{\mu\nu} + \frac{1}{2} \mathcal{L}_{\xi_1}^2 g_{\mu\nu} + \mathcal{L}_{\xi_1} \check{h}_{\mu\nu}^{\text{R1}}, \quad (182)$$

one finds evolution equations for z_n^μ in terms of $\check{h}_{\mu\nu}^{\text{Rn}}$ by taking appropriate derivatives of these relations; any desired gauge condition is imposed on $\check{h}_{\mu\nu}^{\text{Rn}}$, $\check{h}_{\mu\nu}^{\text{Rn}}$ is computed via a puncture scheme, and z_n^μ is computed from $\check{h}_{\mu\nu}^{\text{Rn}}$. Because of the particular method of construction, in which the rest gauge is defined with respect to z_0^μ rather than z^μ , the evolution equations for z_n^μ do not correspond to an expansion of the geodesic equation in the metric $\mathfrak{g}_{\mu\nu} = g_{\mu\nu} + \mathfrak{h}_{\mu\nu}^{\text{R}}$ that Gralla defines; this lack of geodesic motion in $g_{\mu\nu} + \mathfrak{h}_{\mu\nu}^{\text{R}}$ should amount to a slightly different definition of $\mathfrak{h}_{\mu\nu}^{\text{R}}$ than the one used in the self-consistent expansion, although no one has yet carried out a detailed comparison of Gralla's second-order results to those of the self-consistent method.

8 Conclusion

8.1 Summary

In this review, we began with the idea of a point particle interacting with its own backscattered field; we ended with the idea of using laws of gauge transformation to obtain laws of motion for extended objects. And yet, reassuringly, from the latter description we have recovered the former.

Along the circuitous way, I have emphasized several core ideas. First, the laws of motion of an extended object, to all orders in perturbation theory, are determinable from the metric *outside* the object; all information about the object's shape and

internal composition is encoded in a discrete set of multipole moments, themselves defined from the form of the metric in the buffer region outside the object. To obtain an equation of motion of order ϵ^n in perturbation theory, moments of multipole order $\ell = n$ are required. Second, the laws of motion found in this way show that at least through second order in perturbation theory, a small, sufficiently spherical, sufficiently slowly spinning compact object moves on a geodesic of an effectively external metric that (i) satisfies the vacuum Einstein equations and (ii) behaves causally on the object's representative worldline. Furthermore, the analysis of the metric outside the object provides a clean way of separating the metric into two constituents: a suitable effectively external metric satisfying the above properties, and a self-field that, loosely speaking, locally characterizes the object.

This treatment weds several traditions that run through the history of the problem of motion in general relativity, from the characterization of motion of a material body in terms of suitably defined multipole moments in the tradition of Mathisson [35] and Dixon [34], to the method of algorithmically characterizing the metric in terms of multipole moments in the multipolar post-Minkowskian theory of Blanchet and Damour [5, 66], to the derivation of laws of motion of asymptotically small objects from the Einstein equation outside the objects in the tradition of Einstein [49], D'Eath [43], and Thorne and Hartle [46]. The perturbative treatment here also complements the non-perturbative treatment of Harte [36]. Just as Harte brought Dixon's project to fruition by finding a utile separation of the metric into a self-field and an effectively external metric, so the same can be said about the method here bringing to fruition the project of Thorne and Hartle.

An important aspect of any perturbative treatment of motion is the relationship between that motion and gauge freedom. It is well known that on short timescales, the self-force is pure gauge; it can be freely set to zero by a suitable choice of gauge. Equivalently, one can say that on short timescales, the perturbed worldline of the object can be transformed to a geodesic of the background spacetime.

What physical role, then, does the self-force play? On short timescales, one can say the following: the deviation from geodesic motion appears explicitly in the second-order field. Hence, in order to get gauge-invariant information about the second-order field from the solution to the Einstein equation in any given gauge, one must include the effect of the self-force. (Note that the argument doesn't run in reverse. Since the first-order deviation is determined entirely by the first-order gauge choice, one does not need the entire second order perturbation to obtain invariant information involving the first-order deviation [77].) However, on these short timescales, the perturbative correction to the motion need not be accounted for to obtain physical information from the first-order metric.

As I have argued, this situation changes when one considers long scales. If one seeks a solution valid on a large domain, such as over the course of a binary inspiral, then one *must* account for the correction to the motion in order to obtain a well-defined perturbation theory. If one were to attempt to put the perturbative shift in the motion into the second-order field, then on this timescale the second-order field would grow larger than the first-order field. Hence, one must incorporate the effect on the motion into the first-order perturbation. In this sense, the perturbed worldline

itself is quasi-invariant under a gauge transformation on long timescales; it may only be shifted by a small amount of order ϵ , while the shift due to the self-force is a much larger effect, of order $\sim 1/\epsilon$ (or $\sim \epsilon^0$, depending on whether one is looking at orbital phase or orbital radius in an inspiral, for example).

For this same reason, if one is interested in long timescales, one need not include the second-order perturbation in order to obtain gauge-invariant information about an inspiral. For any given short patch of that inspiral, the effects of the self-force will be pure gauge; but the *accumulation* of those effects over long timescales is invariant within the class of gauges that are well behaved on these timescales.

8.2 Future Directions

Although the foundations seem in place and the second-order results seem sufficient for the practical purposes we can presently imagine, several open avenues remain to be explored.

First, at present we have obtained second-order equations only for objects whose spin and quadrupole moments vanish at leading order. It would be worthwhile, and astrophysically relevant, to obtain second-order equations of motion for more generic compact objects. As is well known [34], the object's leading order quadrupole moment would generate a force by coupling to the external curvature. Additionally, there may be an effect due the correction δS^i to the object's spin.

The mention of this subleading spin raises another question to consider: what is the physical content of the perturbed multipole moments? I have discussed above how the monopole correction $\delta m_{\mu\nu}$ is pure gauge (at least on short timescales). Will higher corrections, or corrections to higher moments, contain more physical information than this? We can expect that they will: tidal heating and torquing, for example, should create physical corrections to the mass and spin [78, 79], and at least for a material body, the external tidal fields should correct the higher moments by physically deforming the object [80–82]. Ultimately, to model the motion of a particular class of objects, such as realistic neutron stars, one will need to explicitly match an inner expansion to the outer expansion I have discussed; the matching procedure will uniquely identify the multipole moments of the objects as they appear in the metric in the buffer region. To this end, one might consider metrics of tidally perturbed neutron stars, such as those described in Refs. [80, 81].

One might also try to describe less compact astrophysical objects, or more exotic objects, by broadening the scope of the perturbative expansion. Rather than assuming the object is compact, such that its linear dimension d is of the same order as its mass m , one might consider a two-parameter family corresponding to m and d . This would alter the orders at which various multipole moments appear in the buffer region, since they scale as md^ℓ . One could even try to describe approximately string-like objects by examining a limit in which two of the object's linear dimensions go to zero while one linear dimension remains finite.

To gain further insight into the physical content of the multipole moments, one could also relate them to the moments appearing in other formalisms, such as the non-perturbative formalism of Harte [36]. Another point of comparison with Harte would be the definition of the effectively external (i.e., the “regular”) field. As I have discussed, the choice of effectively external field is far from unique, and in fact an infinite number of choices could be made that would still guarantee the center-of-mass motion is geodesic in the effective metric. Here, I have taken as my guideline that the effective metric should be a vacuum solution that is causal on the worldline and in which the motion is geodesic; these conditions still do not uniquely identify an effective field, but they narrow the range of options, and I have shown how a choice satisfying these conditions arises naturally in the process of solving the Einstein equation in the buffer region outside the object. However, Harte makes a different choice, which does not satisfy the vacuum Einstein equation. How are the two related? The answer is not obvious. One way of establishing a stronger relationship would be to find perturbative equations of motion for objects with higher multipole moments: because moments of higher ℓ couple to higher derivatives of the metric, they feel much more of the field than does a monopole. With Harte’s definition of effective field, the equation of motion is precisely that of a test body in the effective metric. Would the same be true in the effective metric I have defined here?

In addition to comparison with Harte, the results I have described should be related to Gralla’s more closely related, perturbative results [20]. At second order, Gralla makes a choice of regular field that *is* a vacuum solution (at least to the order in r to which he defines it), but in which the center-of-mass motion is *not* geodesic.

Although I have emphasized the idea of splitting the physical metric into a self-field and an “effectively external” metric, and although I have linked that split to a generalized equivalence principle, the array of choices of regular field should make clear that there is a danger of over-interpreting the physical meaning of any particular choice, no matter how nice its properties. This risk is also present because in general, a regular field satisfying nice properties on the object’s worldline is acausal when evaluated away from the worldline. As a practical matter, the freedom to define different effective metrics may make future comparisons of self-force results to post-Newtonian results more hairy; given the vast freedom—even while maintaining the property that the motion is geodesic in the effective metric, for example—it is remarkable and fortuitous that agreement has so far been found for so many different effects that appear to rely on particular choices of this field [83–85].

Acknowledgments I thank Leor Barack, Eric Poisson, and Abraham Harte for thought-provoking discussions that helped shape my thinking on self-force theory. This work received funding from the European Research Council under the European Union’s Seventh Framework Programme (FP7/2007-2013)/ERC Grant No. 304978.

Appendix 1: Expansions of the Geodesic Equation

Expansion in Powers of a Metric Perturbation

In this appendix, I examine the expansion of the geodesic equation in any sufficiently smooth metric $g_{\mu\nu}$; the treatment is generic, not specialized to a spacetime containing a small object. I expand only in powers of a sufficiently smooth metric perturbation; I do not expand the worldline itself. Hence, the analysis is meant to apply to the self-consistent representation of motion, not to the Gralla-Wald representation.

The geodesic equation reads

$$\frac{d\dot{z}^\mu}{ds} + {}^g\Gamma_{\nu\rho}^\mu \dot{z}^\nu \dot{z}^\rho = \kappa \dot{z}^\mu, \quad (183)$$

where s is a potentially non-affine parameter on the curve $z^\mu(s)$, $\dot{z}^\mu \equiv \frac{dz^\mu}{ds}$ is its tangent vector field, ${}^g\Gamma_{\nu\rho}^\mu$ is the Christoffel symbol corresponding to $g_{\mu\nu}$, and $\kappa = \frac{d}{ds} \ln \sqrt{-g_{\mu\nu} \dot{z}^\mu \dot{z}^\nu}$.

If we now write the metric as the sum of two pieces, $g_{\mu\nu} = g_{\mu\nu} + h_{\mu\nu}$, and if we take $s = \tau$, the proper time on z^μ in $g_{\mu\nu}$, and if we rewrite the geodesic equation in terms of covariant derivatives compatible with $g_{\mu\nu}$, we find

$$a^\mu = -\Delta\Gamma_{\nu\rho}^\mu u^\nu u^\rho + \kappa u^\mu, \quad (184)$$

where $a^\mu \equiv \frac{D^2 z^\mu}{d\tau^2}$, $u^\mu \equiv \frac{dz^\mu}{d\tau}$, and

$$\Delta\Gamma_{\beta\gamma}^\alpha \equiv {}^g\Gamma_{\beta\gamma}^\alpha - \Gamma_{\beta\gamma}^\alpha = \frac{1}{2} g^{\alpha\delta} (2h_{\delta(\beta;\gamma)} - h_{\beta\gamma;\delta}) \quad (185)$$

is the difference between the Christoffel symbol associated with the full metric $g_{\mu\nu}$ and that associated with the background metric $g_{\mu\nu}$. With τ as a parameter, κ becomes

$$\kappa = \frac{\frac{d}{d\tau} \sqrt{1 - h_{\mu\nu} u^\mu u^\nu}}{\sqrt{1 - h_{\mu\nu} u^\mu u^\nu}}. \quad (186)$$

So far no approximation has been made; Eq. (184) is exact. If we now expand $\Delta\Gamma_{\nu\rho}^\mu$ and κ in powers of $h_{\mu\nu}$, we find

$$\begin{aligned} a^\alpha = & -\frac{1}{2} (g^{\alpha\delta} - h^{\alpha\delta}) (2h_{\delta(\beta;\gamma)} - h_{\beta\gamma;\delta}) u^\beta u^\gamma - \frac{1}{2} h_{\beta\gamma;\delta} u^\alpha u^\beta u^\gamma u^\delta \\ & - \frac{1}{2} h_{\mu\nu} h_{\beta\gamma;\delta} u^\alpha u^\beta u^\gamma u^\delta u^\mu u^\nu - h_{\beta\gamma} u^\alpha a^\beta u^\gamma + \mathcal{O}(h^3). \end{aligned} \quad (187)$$

This equation is complicated by the fact that the acceleration appears on both sides in a nontrivial way. To disentangle the acceleration from the perturbation, I assume that a^μ , too, has an expansion in powers of $h_{\mu\nu}$,

$$a^\mu = a_{\text{lin}}^\mu + a_{\text{quad}}^\mu + \mathcal{O}(h^3), \quad (188)$$

where a_{lin}^μ is linear in $h_{\mu\nu}$ and a_{quad}^μ is quadratic in it. Substituting this expansion into Eq. (187), one finds

$$a_{\text{lin}}^\alpha = -\frac{1}{2}P^{\alpha\delta}(2h_{\delta(\beta;\gamma)} - h_{\beta\gamma;\delta})u^\beta u^\gamma, \quad (189)$$

$$a_{\text{quad}}^\alpha = -\frac{1}{2}P^{\alpha\mu}h_{\mu}^\delta(2h_{\delta(\beta;\gamma)} - h_{\beta\gamma;\delta})u^\beta u^\gamma, \quad (190)$$

where $P^{\alpha\mu} \equiv g^{\alpha\mu} + u^\alpha u^\mu$. Summing these, we have

$$\frac{D^2 z^\mu}{d\tau^2} = -\frac{1}{2}P^{\alpha\mu}(g_{\mu}^\delta - h_{\mu}^\delta)(2h_{\delta(\beta;\gamma)} - h_{\beta\gamma;\delta})u^\beta u^\gamma + \mathcal{O}(h^3). \quad (191)$$

As applied to the case of the effective metric $\tilde{g}_{\mu\nu} = g_{\mu\nu} + h_{\mu\nu}^{\text{R}}$ (i.e., replacing $h_{\mu\nu}$ with $h_{\mu\nu}^{\text{R}}$), Eq. (191) agrees with the second-order self-forced equation of motion derived in the body of the paper.

Expansion in Powers of a Metric Perturbation and a Worldline Deviation

In the last section, I expanded the geodesic equation while holding the solution $z_\epsilon^\mu(s)$ to that equation fixed. I now expand $z_\epsilon^\mu(s)$ as well. This procedure yields a sequence of equations for the terms in the expansion of $z_\epsilon^\mu(s)$, suitable for a Gralla-Wald approximation. My approach to the expansion closely follows the treatment of geodesic deviation in Sect. 1.10 in Ref. [86]

I first describe the geometry of the situation. Consider a family of worldlines $z^\mu(\tau, \epsilon)$, with each member $z_\epsilon^\mu(\tau) = z^\mu(\tau, \epsilon)$ governed by the equation of motion (184). Each member satisfies

$$\frac{D^2 z_\epsilon^\mu}{d\tau^2} = F^\mu(\tau, \epsilon), \quad (192)$$

where τ is proper time on z_ϵ^μ , and F^μ is given by the right-hand side of Eq. (184). The family generates a two dimensional surface \mathcal{S} with a tangent bundle spanned by

$u^\mu \equiv \frac{\partial x^\mu}{\partial \tau}$ and $v^\mu \equiv \frac{\partial x^\mu}{\partial \epsilon}$. An important relation between these vector fields can be found from $\frac{\partial^2 x^\mu}{\partial \tau \partial \epsilon} = \frac{\partial^2 x^\mu}{\partial \epsilon \partial \tau}$, which implies $\mathcal{L}_u v^\mu = 0 = \mathcal{L}_v u^\mu$, and from there,

$$v^\mu{}_{;\nu} u^\nu = u^\mu{}_{;\nu} v^\nu. \quad (193)$$

Now, we seek to describe the deviation of an accelerated worldline $z^\mu_\epsilon(\tau)$ from the zeroth order, geodesic worldline $z^\mu_0(\tau) \equiv z^\mu(\tau, 0)$. The first step is to expand the worldline in the power series

$$z^\mu(\tau, \epsilon) = z^\mu_0(\tau) + \epsilon z^\mu_1(\tau) + \epsilon^2 z^\mu_2(\tau) + O(\epsilon^3), \quad (194)$$

where

$$z^\mu_n(\tau) = \frac{1}{n!} \epsilon^n \frac{\partial^n z^\mu}{\partial \epsilon^n}(\tau, 0). \quad (195)$$

We may also write the expansion as $z^\mu(\tau, \epsilon) = \sum \frac{1}{n!} \epsilon^n \mathcal{L}_v^n z^\mu|_{z_0(\tau)}$. Note that here z^μ is a scalar field equal to the μ th coordinate field on the surface \mathcal{S} . The leading-order term is the family member $z^\mu_0(\tau) \equiv z^\mu(\tau, 0)$. The second term is $z^\mu_1(\tau) = \mathcal{L}_v z^\mu|_{z_0} = v^\mu(z_0(\tau))$, a vector on z^μ_0 . But at second order and beyond, a subtlety arises: unlike the first derivative along a curve, which is a tangent vector, second and higher derivatives are not immediately vectorial quantities. The function $z^\mu(\tau, \epsilon)$ describes a curve in a particular set of coordinates, and the corrections z^μ_n depend on the coordinate system in which one defines $z^\mu(\tau, \epsilon)$. Since my notion of an object's center is established with reference to a comoving normal coordinate system, I wish my covariant measure of the second-order deviation to agree, component by component, with $\frac{1}{2} \frac{\partial^2 z^\mu}{\partial \epsilon^2}(\tau, 0)$ when evaluated in a normal coordinate system centered on z^μ_0 ; Sect. 5 describes the utility of this choice when re-expanding a self-consistent approximation into Gralla-Wald or osculating-geodesics form. With that in mind, I define the vector

$$w^\alpha \equiv \frac{1}{2} \frac{Dv^\alpha}{d\epsilon} = \frac{1}{2} v^\beta \nabla_\beta v^\alpha \quad (196)$$

and I seek an evolution equation for its restriction to z^μ_0 ,

$$z^\alpha_{2F}(\tau) \equiv w^\alpha|_{z_0(\tau)}. \quad (197)$$

z^α_{2F} is the second-order term in the expansion (194) when that expansion is performed in Fermi normal coordinates centered on z^μ_0 .

In addition to the choice of coordinates, the expansion (194) depends on the particular choice of parametrization (τ, ϵ) of the surface \mathcal{S} . A change of parametrization alters the direction of expansion away from z^μ_0 . Here, the parametrization is chosen such that τ is proper time along each curve $z^\mu_\epsilon(\tau)$, and a flow line generated by v^μ links points on different curves $z^\mu_\epsilon(\tau)$ at the same value of τ . When restricted to z^μ_0 , the parameter τ is τ_0 , the proper time on z^μ_0 .

With all preliminaries established, I now proceed to find the evolution equations for z_0^μ , z_1^μ , and z_2^μ . The leading term clearly satisfies

$$\frac{D^2 z_0^\mu}{d\tau_0^2} = F^\mu(\tau, 0) = 0. \quad (198)$$

For the others, I first find evolution equations for v^μ and w^μ and then evaluate the results on z_0^μ . At first order, using Eqs. (192) and (193), we have

$$\frac{D^2 v^\alpha}{d\tau^2} = \left(v^\alpha{}_{;\beta} u^\beta \right)_{;\gamma} u^\gamma \quad (199)$$

$$= \left(u^\alpha{}_{;\beta} v^\beta \right)_{;\gamma} u^\gamma \quad (200)$$

$$= F^\alpha{}_{;\gamma} v^\gamma - R^\alpha{}_{\mu\beta\nu} u^\mu v^\beta u^\nu, \quad (201)$$

where the second line follows from Eq. (193) and the third line follows from the Ricci identity and Eq. (192). Evaluating on z_0^μ , I write this as

$$\frac{D^2 z_1^\alpha}{d\tau_0^2} = \check{F}_1^\alpha(\tau_0) - R^\alpha{}_{\mu\beta\nu} u_0^\mu z_1^\beta u_0^\nu, \quad (202)$$

where $\check{F}_1^\alpha \equiv \frac{DF^\alpha}{d\epsilon}|_{\gamma_0}$. This is a generalization from the usual geodesic deviation equation to the deviation between neighbouring accelerating worldlines; it is valid even if $F^\mu(\tau, 0) \neq 0$.

At second order, repeated use of Eq. (193) and Ricci's identity leads to

$$\frac{D^2 w^\alpha}{d\tau^2} = \frac{1}{2} \left[\left(v^\alpha{}_{;\beta} v^\beta \right)_{;\mu} u^\mu \right]_{;\nu} u^\nu \quad (203)$$

$$= \frac{1}{2} \left[\left(u^\alpha{}_{;\beta} u^\beta \right)_{;\gamma} v^\gamma \right]_{;\delta} v^\delta + \frac{1}{2} R^\alpha{}_{\mu\beta\nu;\gamma} \left(v^\mu u^\beta v^\nu u^\gamma - u^\mu v^\beta u^\nu v^\gamma \right) \\ - R^\alpha{}_{\mu\beta\nu} \left(u^\mu w^\beta u^\nu + 2u^\mu{}_{;\gamma} v^\gamma v^\beta u^\nu + \frac{1}{2} v^\mu v^\beta u^\nu{}_{;\gamma} u^\gamma \right). \quad (204)$$

Evaluating on z_0^μ and using Eq. (192), we can write this as

$$\frac{D^2 z_{2F}^\alpha}{d\tau_0^2} = \check{F}_2^\alpha(\tau_0) - R^\alpha{}_{\mu\beta\nu} \left(u_0^\mu z_{2F}^\beta u_0^\nu + 2u_1^\mu z_1^\beta u_0^\nu \right) + 2R^\alpha{}_{\mu\beta\nu;\gamma} z_1^{(\mu} u_0^{\beta)} z_1^{[\nu} u_0^{\gamma]} \quad (205)$$

where $\check{F}_2^\alpha \equiv \frac{1}{2} \frac{D^2 F^\alpha}{d\epsilon^2}|_{\gamma_0}$ and $u_1^\mu \equiv \frac{Dz_1^\mu}{d\tau}$. Equation (205) describes the second deviation between neighbouring accelerating worldlines. In the case of neighbouring geodesics, it agrees with ‘‘Bazanski’s equation’’ in the form given in Eq. (5.9) of Ref. [87].

The quantities \check{F}_n^μ appearing in Eqs. (202) and (205) can be straightforwardly evaluated by performing the expansion $h_{\mu\nu}(x, \epsilon) = \epsilon \check{h}_{\mu\nu}^1(x) + \epsilon^2 \check{h}_{\mu\nu}^2(x) + \mathcal{O}(\epsilon^3)$ in Eq. (191) and then taking covariant derivatives with respect to v^μ . The results are

$$\check{F}_1^\mu = \frac{1}{2} P_0^{\mu\nu} \left(\check{h}_{\sigma\lambda;\rho}^1 - 2\check{h}_{\rho\sigma;\lambda}^1 \right) u_0^\sigma u_0^\lambda \quad (206)$$

and

$$\begin{aligned} \check{F}_2^\mu = & -\frac{1}{2} P_0^{\mu\nu} \left(2\check{h}_{\nu\sigma;\lambda}^2 - \check{h}_{\sigma\lambda;\nu}^2 \right) u_0^\sigma u_0^\lambda - \frac{1}{2} P_0^{\mu\nu} \left(2\check{h}_{\nu\sigma;\lambda\delta}^1 - \check{h}_{\sigma\lambda;\nu\delta}^1 \right) u_0^\sigma u_0^\lambda z_1^\delta \\ & - \left(2\check{h}_{\nu\sigma;\lambda}^1 - \check{h}_{\sigma\lambda;\nu}^1 \right) \left(u_1^{(\mu} u_0^{\nu)} u_0^\sigma u_0^\lambda + P_0^{\mu\nu} u_1^{(\sigma} u_0^{\lambda)} \right) \\ & + P_0^{\mu\nu} \check{h}_{\nu}^{1\rho} \left(2\check{h}_{\rho\sigma;\lambda}^1 - \check{h}_{\sigma\lambda;\rho}^1 \right) u_0^\sigma u_0^\lambda. \end{aligned} \quad (207)$$

As applied to the case of the effective metric $\check{g}_{\mu\nu} = g_{\mu\nu} + h_{\mu\nu}^R$ (i.e., replacing $\check{h}_{\mu\nu}^n$ with $\check{h}_{\mu\nu}^{Rn}$), Eqs. (202) and (205), together with Eqs. (206) and (207), are the second-order expansion of the motion that apply in a Gralla-Wald approximation.

Appendix 2: Expansion of Point-Particle Fields in Powers of a Worldline Deviation

In this appendix, I derive the linear terms in expansions of the point particle stress-energy $T_1^{\mu\nu}(x; z)$ and the Lorenz-gauge retarded field $h_{\mu\nu}^1(x; z)$ when the worldline is expanded as $z^\mu(s, \epsilon) = z_0^\mu(s) + \epsilon z_1^\mu(s) + \mathcal{O}(\epsilon^2)$, where s is an arbitrary parameter. I also establish the identification of these linear terms with the mass dipole moment terms found from the local analysis in Sect. 3.

Stress-Energy

I write the stress-energy in the parametrization-invariant form [9]

$$T_1^{\alpha\beta}(x; z) = m \int_\gamma g_{\alpha'}^\alpha(x, z) g_{\beta'}^\beta(x, z) \dot{z}^{\alpha'} \dot{z}^{\beta'} \delta(x, z) \frac{ds}{\sqrt{-g_{\mu'\nu'}(z) \dot{z}^{\mu'} \dot{z}^{\nu'}}}, \quad (208)$$

where $g_{\alpha'}^\alpha(x; z)$ is a parallel propagator from the source point $x' = z(s, \epsilon)$ to the field point x , and $\dot{z}^\mu \equiv \frac{dz^\mu}{ds}$.

Substituting the expansion (30) into this stress-energy tensor, we obtain

$$\begin{aligned}
 T_1^{\alpha\beta}(x; z) = m \int_{\gamma_0} & \left[g_{\alpha'}^\alpha(x, z_0) g_{\beta'}^\beta(x, z_0) \dot{z}_0^{\alpha'} \dot{z}_0^{\beta'} + \epsilon z_1^{\mu'} \nabla_{\mu'} (g_{\alpha'}^\alpha g_{\beta'}^\beta \dot{z}_0^{\alpha'} \dot{z}_0^{\beta'}) \Big|_{\epsilon=0} \right] \\
 & \times \left[\delta(x, z_0) + \epsilon z_1^{\nu'} \nabla_{\nu'} \delta(x, z) \Big|_{\epsilon=0} \right] \left[1 - \epsilon \frac{\dot{z}_{0\delta'} z_1^{\gamma'} \nabla_{\gamma'} \dot{z}_0^{\delta'}}{\dot{z}_0^{\kappa'} \dot{z}_{0\kappa'}} \right] \frac{ds}{\sqrt{-\dot{z}_0^{\rho'} \dot{z}_{0\rho'}}} \\
 & + O(\epsilon^2).
 \end{aligned} \tag{209}$$

In each instance, the evaluation at $\epsilon = 0$ occurs *after* taking the derivative.

I simplify this expression using the distributional identities $\nabla_{\mu'} \delta(x, z) = -g_{\mu'}^\mu \nabla_\mu \delta(x, z)$ and $g_{\alpha'; \beta'}^\alpha \delta(x, z) = 0$ [9]. I also use the identity

$$z_1^{\mu'} (\nabla_{\mu'} \dot{z}_0^{\alpha'}) \Big|_{\epsilon=0} = \frac{Dz_1^{\alpha'}}{ds} \equiv \dot{z}_1^{\alpha'}, \tag{210}$$

which follows in the same manner as Eq. (193).

The result of those simplifications is

$$\epsilon T_1^{\alpha\beta}(x; z) = \epsilon T_1^{\alpha\beta}(x; z_0) + \epsilon^2 \delta T_1^{\alpha\beta}(x; z_0, z_1) + O(\epsilon^3), \tag{211}$$

with

$$T_1^{\alpha\beta}(x; z_0) = m \int_{\gamma_0} g_{\alpha'}^\alpha g_{\beta'}^\beta u_0^{\alpha'} u_0^{\beta'} \delta(x, z_0) d\tau'_0, \tag{212}$$

$$\begin{aligned}
 \delta T_1^{\alpha\beta}(x; z_0, z_1) = m \int_{\gamma_0} & g_{\alpha'}^\alpha g_{\beta'}^\beta \left[\left(2u_0^{(\alpha'} u_1^{\beta')} - u_0^{\alpha'} u_0^{\beta'} u_{0\gamma'} u_1^{\gamma'} \right) \delta(x, z_0) \right. \\
 & \left. - u_0^{\alpha'} u_0^{\beta'} z_1^{\gamma'} g_{\gamma'}^\gamma \nabla_\gamma \delta(x, z_0) \right] d\tau'_0,
 \end{aligned} \tag{213}$$

where $u_1^\mu(\tau_0) \equiv \frac{Dz_1^\mu}{d\tau_0}$, and the parallel propagators are evaluated at $(x, z_0(\tau'_0))$. I have simplified these expressions by reparametrizing z_0^μ in terms of τ_0 , the proper time on γ_0 , but note that this does *not* correspond to choosing the original parameter $s = \tau_0$. Equations (211)–(213) are valid for any choice of parameter s , and $z_1^\mu(\tau_0)$ actually *depends* on the original choice of s : a change of parametrization $s \rightarrow s'(s, \epsilon)$ will change the direction of z_1^μ , in particular changing whether or not z_1^μ is orthogonal to u_0^μ .

To eliminate this dependence on the initial choice of parametrization, I rewrite $\delta T_1^{\alpha\beta}$ in terms of the orthogonal part of z_1^μ , $z_{1\perp}^\mu \equiv (\delta_\nu^\mu + u_0^\mu u_{0\nu}) z_1^\nu$. The result is

$$\delta T_1^{\alpha\beta} = m \int_{\gamma_0} g_{\alpha'}^\alpha g_{\beta'}^\beta \left[2u_0^{(\alpha'} u_{1\perp}^{\beta')} \delta(x, z_0) - u_0^{\alpha'} u_0^{\beta'} z_{1\perp}^{\gamma'} g_{\gamma'}^\gamma \nabla_\gamma \delta(x, z_0) \right] d\tau'_0, \tag{214}$$

where $u_{1\perp}^\mu \equiv \frac{Dz_{1\perp}^\mu}{d\tau_0}$. Note that the part of z_1^μ parallel to u_0^μ does not appear in this expression. Again, this result does not depend on the initial choice of parametrization. One need not choose a parametrization by hand that enforces $z_1^\mu u_{0\mu} = 0$; no matter the choice, only the perpendicular part plays a role in the field equations.

The quantity $\delta T_1^{\mu\nu}(x; z_0)$ is equal to $\mathcal{L}_v T^{\mu\nu}(x; z_0)$, where $v^\mu = \frac{\partial z_1^\mu(s, \epsilon)}{\partial \epsilon}$ is introduced in Appendix 1, and \mathcal{L}_v is the Lie derivative introduced in Sect. 5. In fact, for any vector ξ^μ , $\mathcal{L}_\xi T^{\mu\nu}(x; z)$ is given by Eq. (214) with the replacement $z_1^\mu \rightarrow \xi^\mu$ and $u_0^\mu \rightarrow u^\mu$. This quantity is useful when considering gauge transformations in the self-consistent approximation. Also useful is the ordinary Lie derivative of $T_1^{\mu\nu}$; taking similar steps as above, one finds

$$\begin{aligned} \mathcal{L}_\xi T_1^{\alpha\beta}(x; z) = & -m \int_\gamma g_{\alpha'}^\alpha g_{\beta'}^\beta \left\{ \left[2u^{(\alpha'} \frac{D\xi_{\perp}^{\beta')}}{d\tau'} + u^{\alpha'} u^{\beta'} \left(\frac{d\xi_{\parallel}}{d\tau} + \xi^{\rho'}{}_{;\rho'} \right) \right] \delta(x, z) \right. \\ & \left. - u^{\alpha'} u^{\beta'} \xi_{\perp}^{\gamma'} \nabla_\gamma \delta(x, z) \right\} d\tau', \end{aligned} \quad (215)$$

where $\xi_{\perp}^{\beta'} \equiv P^{\beta'}{}_{\alpha'} \xi^{\alpha'}$ and $\xi_{\parallel} \equiv u_{\mu'} \xi^{\mu'}$. The sum of the two Lie derivatives yields the simple result

$$(\mathcal{L}_\xi + \mathcal{L}_\epsilon) T_1^{\mu\nu}(x; z) = -m \int g_{\mu'}^\mu g_{\nu'}^\nu u^{\mu'} u^{\nu'} \left(\frac{d\xi_{\parallel}}{d\tau} + \xi^{\rho'}{}_{;\rho'} \right) \delta(x, z) d\tau'. \quad (216)$$

A $\xi^\mu \nabla_\mu \delta(x, z)$ term signals that the mass m is displaced from z^μ by an amount ξ^μ ; the lack of any $\nabla_\mu \delta(x, z)$ term in Eq. (216) signals that the displacements due to the two derivatives cancel one another, leaving the mass m moving on z^μ .

Metric Perturbation

In the Lorenz gauge, the first-order self-consistent field, given some global boundary conditions, is given by

$$h_{\mu\nu}^1(x; z) = 4m \int \bar{G}_{\mu\nu\mu'\nu'} u^{\mu'} u^{\nu'} d\tau', \quad (217)$$

where $G_{\mu\nu\mu'\nu'}$ is the Green's function that comports with the global boundary conditions. I wish to expand this about $z^\mu = z_0^\mu$ to obtain something of the form

$$\epsilon h_{\mu\nu}^1(x; z) = \epsilon h_{\mu\nu}^1(x; z_0) + \epsilon^2 \delta h_{\mu\nu}^1(x; z_0, z_1) + \mathcal{O}(\epsilon^3). \quad (218)$$

There are two methods available for achieving this: directly, following steps analogous to those in the previous section; or by making use of the result of the previous section.

Here I adopt the second method. Noting that $\delta h_{\mu\nu}^1(x; z_0, z_1) = \mathcal{L}_\nu h_{\mu\nu}^1(x; z_0)$, that $\delta T_1^{\alpha\beta} = \mathcal{L}_\nu T_1^{\mu\nu}(x; z_0)$, and that \mathcal{L}_ν commutes with derivatives acting at x , we have

$$E_{\mu\nu}[\mathcal{L}_\nu \bar{h}^1](x; z_0) = \mathcal{L}_\nu E_{\mu\nu}[\bar{h}^1](x; z_0) = -16\pi \mathcal{L}_\nu T_{\mu\nu}^1(x; z_0). \quad (219)$$

Hence,

$$\delta h_{\mu\nu}^1(x; z_0, z_1) = \mathcal{L}_\nu h_{\mu\nu}^1(x; z_0) = 4 \int \bar{G}_{\mu\nu\mu'\nu'} \delta T^{\mu'\nu'}(x'; z_0, z_1) dV'. \quad (220)$$

From Eq. (214), this evaluates to

$$\delta h_{\mu\nu}^1(x; z_0, z_1) = 4m \int_{\gamma_0} \left(2\bar{G}_{\mu\nu\mu'\nu'} u_0^{(\mu'} u_{1\perp}^{\nu')} + \bar{G}_{\mu\nu\mu'\nu';\gamma} u_0^{\mu'} u_0^{\nu'} z_{1\perp}^{\gamma'} \right) d\tau_0'. \quad (221)$$

Gauge Condition

It is worth examining how $h_{\alpha\beta}^1(x; z)$ and $\delta h_{\alpha\beta}^1(x; z_0, z_1)$ contribute to the Lorenz gauge condition. Those contributions are easily found by invoking the identity $\nabla^\nu G_{\mu\nu\mu'\nu'} = -G_{\mu(\mu';\nu')}$ [9], where $G_{\mu\mu'}$ is a Green's function for the vector wave equation $\square V_\mu = S_\mu$, and both Green's functions must satisfy the same boundary conditions. Performing a trace-reversal on Eq. (217), taking the divergence of the result, using the Green's-function identity, and integrating by parts yields

$$\nabla^\beta \bar{h}_{\alpha\beta}^1(x; z) = 4 \int G_{\alpha\alpha'} \frac{D}{d\tau'} (m u^{\alpha'}) d\tau'. \quad (222)$$

(Earlier results in this section assumed constant m , but here I momentarily leave it arbitrary for generality.) The contribution to the gauge condition is determined entirely by $\frac{dm}{d\tau}$ and the acceleration of z^μ . In a Gralla-Wald expansion, one has $\nabla^\beta \check{h}_{\alpha\beta}^1(x; z_0) = 0$, from which one can read off $\frac{dm}{d\tau} = 0$ and $a_0^\mu = 0$. In a self-consistent expansion, one instead has $\nabla^\beta [\epsilon \bar{h}_{\alpha\beta}^1(x; z) + \epsilon^2 \bar{h}_{\alpha\beta}^2(x; z)] = \mathcal{O}(\epsilon^3)$ [or more precisely, Eq. (26)], which determines Eq. (9).

Doing the same with Eq. (221) yields

$$\nabla^\beta \delta \bar{h}_{\alpha\beta}^1(x; z_0, z_1) = 4m \int G_{\alpha\alpha'} \left(\frac{D^2 z_{1\perp}^{\alpha'}}{d\tau_0'^2} + R^{\alpha'}_{\beta'\gamma'\delta'} u_0^{\beta'} z_{1\perp}^{\gamma'} u_0^{\delta'} \right) d\tau_0'. \quad (223)$$

The contribution to the gauge condition is determined entirely by the acceleration of the deviation from z_0^μ (together with the geodesic-deviation term). In a Gralla-Wald expansion, $\delta h_{\alpha\beta}^1(x; z_0, z_1)$ is included in $\check{h}_{\alpha\beta}^2(x; z_0)$, and $\nabla^\beta \check{h}_{\alpha\beta}^2(x; z_0) = 0$ determines Eq. (35).

Local Expansion and Identification of Mass Dipole Moment

In Sect. 4.1, I showed that the mass dipole moment of the object creates a term (96) [and contributes to the term (94)] in the object's skeletal stress-energy. By comparing that result to Eq. (214), we can make the identification $M^i = m z_1^i$, exactly as concluded elsewhere in the paper. Since the two stress-energy tensors are the same, it follows that $\delta h_{\mu\nu}^1(x; z_0, z_1)$ includes the entire contribution to $\check{h}_{\mu\nu}^2$ coming from the mass dipole moment.

Here, I complete the circle by performing a local expansion of Eq. (221) near z_0^μ and showing $\delta h_{\mu\nu}^1(x; z_0, z_1)$ reproduces the order- $1/r^2$ and $1/r$ terms for the mass dipole seed solution in Fermi normal coordinates. The method of local expansion is elaborated in Ref. [9]. In particular, I follow steps analogous to those in Sect. 23.2 of that reference. To avoid belabouring the details, here I provide only the barest sketch; I leave it to the interested reader to fill in the gaps using the tools of Ref. [9].

The starting point is the Hadamard decomposition of the retarded Green's function, $G_{\mu\nu\mu'\nu'} = U_{\mu\nu\mu'\nu'}\delta_+(\sigma) + V_{\mu\nu\mu'\nu'}\theta_+(-\sigma)$. Here $\delta_+(\sigma)$ is a Dirac delta function supported on the past light cone of x , and $\theta_+(-\sigma)$ is a Heaviside step function supported in the interior of that light cone. $\sigma(x, x')$ is one-half the squared geodesic distance from x' to x , such that it vanishes when a null geodesic connects the two points.

From this starting point, the final result is obtained by a two-step process: (i) evaluating the integrals over τ'_0 by changing the integration variable to σ , and (ii) writing the retarded distance from x' to x in terms of the Fermi radial coordinate r . The results for the two terms in Eq. (221) are

$$8m \int \bar{G}_{\mu\nu\mu'\nu'} u_0^{(\mu'} \frac{Dz_{1\perp}^{\nu')}{d\tau'_0} d\tau'_0 = \frac{8m}{r} u_{0(\mu} e_{\nu)}^i \dot{z}_{1i} + \mathcal{O}(r^0), \quad (224)$$

where $\dot{z}_1^i = \frac{dz_1^i}{dt}$, and

$$4m \int \bar{G}_{\mu\nu\mu'\nu';\gamma'} u_0^{\mu'} u_0^{\nu'} z_{1\perp}^{\gamma'} d\tau'_0 = \frac{2m}{r^2} z_1^a n_a \delta_{\mu\nu} + \mathcal{O}(r^0). \quad (225)$$

The components in Fermi coordinates are

$$\delta h_{tt}^1 = \frac{2m\dot{z}_1^i n_i}{r^2} + \mathcal{O}(r^0), \quad (226a)$$

$$\delta h_{ta}^1 = \frac{4m\dot{z}_1^i a_i}{r} + \mathcal{O}(r^0), \quad (226b)$$

$$\delta h_{ab}^1 = \frac{2m\dot{z}_1^i n_i}{r^2} \delta_{ab} + \mathcal{O}(r^0). \quad (226c)$$

Here we see that with the identification $M^i = m\dot{z}_1^i$, the tt and ab components are precisely those in Eq. (105), and the ta component is precisely the term proportional to \dot{M}^i in Eq. (106). In other words, the integral (224) corresponds to the mass dipole moment's contribution to the monopole seed $h_{\mu\nu}^{\text{seed}}(x; z_0, \delta m)$, while the integral (225) corresponds to the mass-dipole seed $h_{\mu\nu}^{\text{seed}}(x; z_0, M)$.

Appendix 3: Identities for Gauge Transformations of Curvature Tensors

Let $A[g]$ be a tensor of any rank constructed from a metric g . (To streamline the presentation, I adopt index-free notation throughout most of this appendix.) Now define

$$\delta^n A[f_1, \dots, f_n] \equiv \frac{1}{n!} \frac{d^n}{d\lambda_1 \dots d\lambda_n} A[g + \lambda_1 f_1 + \dots + \lambda_n f_n] \Big|_{\lambda_1 = \dots = \lambda_n = 0}. \quad (227)$$

This tensor is linear in each of its arguments f_1, \dots, f_n ; it is also symmetric in them. In the case that all the arguments are the same, we have $\delta^n A[h, \dots, h] = \frac{1}{n!} \frac{d^n}{d\lambda^n} A[g + \lambda h] \Big|_{\lambda=0}$, the piece of $A[g + h]$ containing precisely n factors of h and its derivatives.

The following identities are easily proved by writing Lie derivatives as ordinary derivatives:

$$\mathcal{L}_\xi A[g] = \delta A[\mathcal{L}_\xi g], \quad (228)$$

$$\frac{1}{2} \mathcal{L}_\xi^2 A[g] = \frac{1}{2} \delta A[\mathcal{L}_\xi^2 g] + \delta^2 A[\mathcal{L}_\xi g, \mathcal{L}_\xi g], \quad (229)$$

$$\mathcal{L}_\xi \delta A[h] = \delta A[\mathcal{L}_\xi h] + 2\delta^2 A[\mathcal{L}_\xi g, h]. \quad (230)$$

Note that $\delta^2 A[\mathcal{L}_\xi g, h] = \delta^2 A[h, \mathcal{L}_\xi g] = \frac{1}{2} (\delta^2 A[h, \mathcal{L}_\xi g] + \delta^2 A[\mathcal{L}_\xi g, h])$. As an example, if A is the Ricci tensor, then

$$\mathcal{L}_\xi R_{\mu\nu}[g] = \delta R_{\mu\nu}[\mathcal{L}_\xi g], \quad (231)$$

$$\frac{1}{2} \mathcal{L}_\xi^2 R_{\mu\nu}[g] = \frac{1}{2} \delta R_{\mu\nu}[\mathcal{L}_\xi^2 g] + \delta^2 R_{\mu\nu}[\mathcal{L}_\xi g, \mathcal{L}_\xi g], \quad (232)$$

$$\mathcal{L}_\xi \delta R_{\mu\nu}[h] = \delta R_{\mu\nu}[\mathcal{L}_\xi h] + 2\delta^2 R_{\mu\nu}[h, \mathcal{L}_\xi g], \quad (233)$$

where I have restored indices to avoid confusion with the Ricci scalar.

To establish Eq. (228), one can write the metric as a function of a parameter λ along the flow generated by ξ and then perform a Taylor expansion:

$$\mathcal{L}_\xi A[g] = \frac{d}{d\lambda} A \left[g(0) + \lambda \frac{dg}{d\lambda} \Big|_{\lambda=0} \right] \Big|_{\lambda=0} = \delta A \left[\frac{dg}{d\lambda} \Big|_{\lambda=0} \right] = \delta A[\mathcal{L}_\xi g]. \quad (234)$$

Similarly, to establish Eq. (229), one can write

$$\frac{1}{2} \mathcal{L}_\xi^2 A[g] = \frac{1}{2} \frac{d^2}{d\lambda^2} A \left[g(0) + \lambda \frac{dg}{d\lambda} \Big|_{\lambda=0} + \frac{1}{2} \lambda^2 \frac{d^2 g}{d\lambda^2} \Big|_{\lambda=0} \right] \Big|_{\lambda=0} \quad (235a)$$

$$= \frac{1}{2} \delta A[\mathcal{L}_\xi^2 g] + \delta^2 A[\mathcal{L}_\xi g, \mathcal{L}_\xi g], \quad (235b)$$

and to establish Eq. (230), one can write g as a function of parameters (λ, ϵ) , where $h \equiv \frac{dg}{d\epsilon} \Big|_{\epsilon=0}$, and then write

$$\mathcal{L}_\xi \delta A[h] = \frac{d^2}{d\lambda d\epsilon} A \left[g(\lambda, 0) + \epsilon \frac{dg}{d\epsilon}(\lambda, 0) \right] \Big|_{\lambda=\epsilon=0} \quad (236a)$$

$$= \frac{d^2}{d\lambda d\epsilon} A \left[g(0, 0) + \lambda \frac{dg}{d\lambda}(0, 0) + \epsilon \frac{dg}{d\epsilon}(0, 0) + \lambda \epsilon \frac{d^2 g}{d\lambda d\epsilon}(0, 0) \right] \Big|_{\lambda=\epsilon=0} \\ = \delta A[\mathcal{L}_\xi h] + 2\delta^2 A[h, \mathcal{L}_\xi g]. \quad (236b)$$

References

1. R. Geroch, J. Traschen, Strings and other distributional sources in general relativity. *Phys. Rev. D* **36**, 1017–1031 (1987)
2. R. Steinbauer, J.A. Vickers, On the Geroch-Traschen class of metrics. *Class. Quantum Gravity* **26**, 065001 (2009)
3. A. Einstein, L. Infeld, B. Hoffmann, The gravitational equations and the problem of motion. *Ann. Math.* **39**, 65–100 (1938)
4. S. Detweiler, Perspective on gravitational self-force analyses. *Class. Quantum Gravity* **22**, S681–S716 (2005)
5. L. Blanchet, Gravitational radiation from post-Newtonian sources and inspiralling compact binaries. *Living Rev. Relativ.* **17**, 2 (2014)
6. T. Futamase, Y. Itoh, The post-Newtonian approximation for relativistic compact binaries. *Living Rev. Relativ.* **10**, 2 (2007)
7. E. Poisson, C.M. Will, *Gravity: Newtonian, Post-Newtonian, and Relativistic* (Cambridge University Press, Cambridge, 2014)
8. L. Barack, Gravitational self force in extreme mass-ratio inspirals. *Class. Quantum Gravity* **26**, 213001 (2009)
9. E. Poisson, A. Pound, I. Vega, The motion of point particles in curved spacetime. *Living Rev. Relativ.* **14**, 7 (2011)
10. P. Amaro-Seoane, J.R. Gair, A. Pound, S.A. Hughes, C.F. Sopuerta, Research Update on Extreme-Mass-Ratio Inspirals (2014)
11. A. Pound, Self-consistent gravitational self-force. *Phys. Rev. D* **81**(2), 024023 (2010)
12. A. Pound, Singular perturbation techniques in the gravitational self-force problem. *Phys. Rev. D* **81**, 124009 (2010)

13. A. Pound, Motion of small bodies in general relativity: foundations and implementations of the self-force. Ph.D. thesis, University of Guelph (2010)
14. A. Pound, Second-order gravitational self-force. *Phys. Rev. Lett.* **109**, 051101 (2012)
15. A. Pound, Nonlinear gravitational self-force: field outside a small body. *Phys. Rev. D* **86**, 084019 (2012)
16. A. Pound, Nonlinear gravitational self-force: second-order equation of motion. In preparation
17. A. Pound, Gauge and motion in perturbation theory. In preparation
18. S.E. Gralla, R.M. Wald, A rigorous derivation of gravitational self-force. *Class. Quantum Gravity* **25**, 205009 (2008)
19. S.E. Gralla, Gauge and averaging in gravitational self-force. *Phys. Rev. D* **84**, 084050 (2011)
20. S.E. Gralla, Second order gravitational self force. *Phys. Rev. D* **85**, 124011 (2012)
21. Y. Mino, M. Sasaki, T. Tanaka, Gravitational radiation reaction to a particle motion. *Phys. Rev. D* **55**, 3457–3476 (1997)
22. S.L. Detweiler, Radiation reaction and the self-force for a point mass in general relativity. *Phys. Rev. Lett.* **86**, 1931–1934 (2001)
23. S.L. Detweiler, B.F. Whiting, Self-force via a Green's function decomposition. *Phys. Rev. D* **67**, 024025 (2003)
24. T.C. Quinn, R.M. Wald, An axiomatic approach to electromagnetic and gravitational radiation reaction of particles in curved space-time. *Phys. Rev. D* **56**, 3381–3394 (1997)
25. S.E. Gralla, A.I. Harte, R.M. Wald, A rigorous derivation of electromagnetic self-force. *Phys. Rev. D* **80**, 024031 (2009)
26. A.I. Harte, Self-forces from generalized killing fields. *Class. Quantum Gravity* **25**, 235020 (2008)
27. A.I. Harte, Electromagnetic self-forces and generalized killing fields. *Class. Quantum Gravity* **26**, 155015 (2009)
28. A.I. Harte, Motion in classical field theories and the foundations of the self-force problem (2014)
29. T.M. Linz, J.L. Friedman, A.G. Wiseman, Combined gravitational and electromagnetic self-force on charged particles in electrovac spacetimes (2014)
30. P. Zimmerman, E. Poisson, Gravitational self-force in nonvacuum spacetimes (2014)
31. A. Pound, C. Merlin, L. Barack, Gravitational self-force from radiation-gauge metric perturbations. *Phys. Rev. D* **89**, 024009 (2014)
32. C.R. Galley, B.L. Hu, Self-force on extreme mass ratio inspirals via curved spacetime effective field theory. *Phys. Rev. D* **79**, 064002 (2009)
33. C.R. Galley, A Nonlinear scalar model of extreme mass ratio inspirals in effective field theory II. Scalar perturbations and a master source. *Class. Quantum Gravity* **29**, 015011 (2012)
34. W.G. Dixon, Dynamics of extended bodies in general relativity. iii. equations of motion. *Phil. Trans. R. Soc. Lond. A* **277**, 59 (1974)
35. M. Mathisson, Neue mechanik materieller systeme. *Acta Phys. Pol.* **6**, 163 (1937)
36. A.I. Harte, Mechanics of extended masses in general relativity. *Class. Quantum Gravity* **29**, 055012 (2012)
37. J. Ehlers, E. Rudolph, Dynamics of extended bodies in general relativity: center-of-mass description and quasirigidity. *Gen. Relativ. Gravit.* **8**, 197–217 (1977)
38. A.I. Harte, Effective stress-energy tensors, self-force, and broken symmetry. *Class. Quantum Gravity* **27**, 135002 (2010)
39. J. Kevorkian, J.D. Cole, *Multiple Scale and Singular Perturbation Methods* (Springer, New York, 1996)
40. N. Fenichel, Geometric singular perturbation theory for ordinary differential equations. *J. Differ. Equ.* **31**(1), 53–98 (1979)
41. W. Eckhaus, *Asymptotic Analysis of Singular Perturbations* (Elsevier North-Holland, New York, 1979)
42. R.E. Kates, Underlying structure of singular perturbations on manifolds. *Ann. Phys. (N.Y.)* **132**, 1–17 (1981)

43. P. D'Eath, Dynamics of a small black hole in a background universe. *Phys. Rev. D* **11**, 1387 (1975)
44. P.D. D'Eath, *Black Holes: Gravitational Interactions* (Oxford University Press, New York, 1996)
45. R.E. Kates, Motion of a small body through an external field in general relativity calculated by matched asymptotic expansions. *Phys. Rev. D* **22**, 1853 (1980)
46. K.S. Thorne, J.B. Hartle, Laws of motion and precession for black holes and other bodies. *Phys. Rev. D* **31**, 1815 (1985)
47. H. Weyl, *Raum, Zeit, Materie*, 4th edn., Chapter 36 (Springer, Berlin, 1921)
48. A. Einstein, J. Grommer, Allgemeine relativitätstheorie und bewegungsgesetz. *Sitzungsber. Preuss. Akad. Wiss. Phys. Math. Kl.* **2** (1927)
49. A. Einstein, L. Infeld, On the motion of particles in general relativity theory. *Can. J. Math.* **1**, 209 (1949)
50. L. Barack, A. Ori, Gravitational self-force and gauge transformations. *Phys. Rev. D* **64**, 124003 (2001)
51. T. Hinderer, E.E. Flanagan, Two timescale analysis of extreme mass ratio inspirals in Kerr. I. Orbital motion. *Phys. Rev. D* **78**, 064028 (2008)
52. A. Pound, J. Miller, A practical, covariant puncture for second-order self-force calculations. *Phys. Rev. D* **89**, 104020 (2014)
53. T. Tanaka, Private communication
54. L. Barack, D.A. Golbourn, Scalar-field perturbations from a particle orbiting a black hole using numerical evolution in 2+1 dimensions. *Phys. Rev. D* **76**, 044020 (2007)
55. I. Vega, S.L. Detweiler, Regularization of fields for self-force problems in curved spacetime: foundations and a time-domain application. *Phys. Rev. D* **77**, 084008 (2008)
56. S.R. Dolan, L. Barack, Self force via m-mode regularization and 2+1D evolution: foundations and a scalar-field implementation on Schwarzschild. *Phys. Rev. D* **83**, 024019 (2011)
57. I. Vega, B. Wardell, P. Diener, Effective source approach to self-force calculations. *Class. Quantum Gravity* **28**, 134010 (2011)
58. A. Pound, A conservative effect of the second-order gravitational self-force on quasicircular orbits in Schwarzschild spacetime. *Phys. Rev. D* **90**, 084039 (2014)
59. A. Pound, E. Poisson, Osculating orbits in Schwarzschild spacetime, with an application to extreme mass-ratio inspirals. *Phys. Rev. D* **77**, 044013 (2008)
60. N. Warburton, S. Akcay, L. Barack, J.R. Gair, N. Sago, Evolution of inspiral orbits around a Schwarzschild black hole. *Phys. Rev. D* **85**, 061501 (2012)
61. K.A. Lackeos, L.M. Burko, Self-forced gravitational waveforms for extreme and Intermediate mass ratio inspirals. *Phys. Rev. D* **86**, 084055 (2012)
62. L.M. Burko, G. Khanna, Self-force gravitational waveforms for extreme and intermediate mass ratio inspirals. II: importance of the second-order dissipative effect. *Phys. Rev. D* **88**(2), 024002 (2013)
63. Y. Mino, Self-force in the radiation reaction formula. *Prog. Theor. Phys.* **113**, 733–761 (2005)
64. R. Geroch, Multipole moments. ii. curved space. *J. Math. Phys.* **11**, 2580–2588 (1970)
65. R.O. Hansen, Multipole moments of stationary spacetimes. *J. Math. Phys.* **15**, 46–52 (1974)
66. L. Blanchet, T. Damour, Radiative gravitational fields in general relativity I. General structure of the field outside the source. *Philos. Trans. R. Soc. Lond. A* **320**, 379–430 (1986)
67. L. Blanchet, *Proc. R. Soc. Lond. Ser. A* **409**, 383–399 (1987)
68. T. Damour, B.R. Iyer, Multipole analysis for electromagnetism and linearized gravity with irreducible cartesian tensors. *Phys. Rev. D* **43**, 3259–3272 (1991)
69. W. Tulczyjew, Motion of multipole particles in general relativity theory. *Acta Phys. Pol.* **18**, 393 (1959)
70. J. Steinhoff, D. Puetzfeld, Multipolar equations of motion for extended test bodies in general relativity. *Phys. Rev. D* **81**, 044019 (2010)
71. S. Detweiler, Gravitational radiation reaction and second order perturbation theory. *Phys. Rev. D* **85**, 044048 (2012)
72. R. Geroch, Limits of spacetimes. *Commun. Math. Phys.* **13**(3), 180–193 (1969)

73. J.M. Stewart, M. Walker, Perturbations of space-times in general relativity. *Proc. R. Soc. Lond. A* **341**, 49–74 (1974)
74. M. Bruni, S. Matarrese, S. Mollerach, S. Sonego, Perturbations of space-time: gauge transformations and gauge invariance at second order and beyond. *Class. Quantum Gravity* **14**, 2585–2606 (1997)
75. E. Poisson, Tidal deformation of a slowly rotating black hole (2014)
76. E. Rosenthal, Second-order gravitational self-force. *Phys. Rev. D* **74**, 084018 (2006)
77. L. Barack, N. Sago, Beyond the geodesic approximation: conservative effects of the gravitational self-force in eccentric orbits around a Schwarzschild black hole. *Phys. Rev. D* **83**, 084023 (2011)
78. E. Poisson, Absorption of mass and angular momentum by a black hole: time-domain formalisms for gravitational perturbations, and the small-hole/slow-motion approximation. *Phys. Rev. D* **70**, 084044 (2004)
79. K. Chatziioannou, E. Poisson, N. Yunes, Tidal heating and torquing of a Kerr black hole to next-to-leading order in the tidal coupling. *Phys. Rev. D* **87**(4), 044022 (2013)
80. T. Damour, A. Nagar, Relativistic tidal properties of neutron stars. *Phys. Rev. D* **80**, 084035 (2009)
81. T. Binnington, E. Poisson, Relativistic theory of tidal love numbers. *Phys. Rev. D* **80**, 084018 (2009)
82. P. Landry, E. Poisson, Relativistic theory of surficial love numbers (2014)
83. S.L. Detweiler, A consequence of the gravitational self-force for circular orbits of the Schwarzschild geometry. *Phys. Rev. D* **77**, 124026 (2008)
84. S.R. Dolan, N. Warburton, A.I. Harte, A. Le Tiec, B. Wardell et al., Gravitational self-torque and spin precession in compact binaries. *Phys. Rev. D* **89**, 064011 (2014)
85. S.R. Dolan, P. Nolan, A.C. Ottewill, N. Warburton, B. Wardell, Tidal invariants for compact binaries on quasi-circular orbits (2014)
86. E. Poisson, *A Relativist's Toolkit* (Cambridge University Press, Cambridge, 2004)
87. J. Vines, Geodesic deviation at higher orders via covariant bitensors (2014)

Self-force: Computational Strategies

Barry Wardell

Abstract Building on substantial foundational progress in understanding the effect of a small body's self-field on its own motion, the past 15 years has seen the emergence of several strategies for explicitly computing self-field corrections to the equations of motion of a small, point-like charge. These approaches broadly fall into three categories: (i) mode-sum regularization, (ii) effective source approaches and (iii) worldline convolution methods. This paper reviews the various approaches and gives details of how each one is implemented in practice, highlighting some of the key features in each case.

1 Introduction

Compact-object binaries are amongst the most compelling sources of gravitational waves. In particular, the ubiquity of supermassive black holes residing in galactic centres [1] has made the extreme mass ratio regime a prime target for the eLISA mission [2–6]. Meanwhile, the comparable and intermediate mass ratio regimes are an intriguing target for study by the imminent Advanced LIGO detector [7]. In order to maximise the scientific gain realised from gravitational-wave observations, highly accurate models of gravitational-wave sources are essential. For the case of extreme mass ratio inspirals (EMRIs)—binary systems in which a compact, solar mass object inspirals into an approximately million solar mass black hole—the demands of gravitational wave astronomy are particularly stringent; the promise of groundbreaking scientific advances—including precision tests of general relativity in the strong-field regime [8–10] and a better census of black hole populations—hinges on our ability to track the phase of their gravitational waveforms throughout the long inspiral, with an accuracy of better than 1 part in 10,000 [2]. This, in turn requires highly accurate, long time models of the orbital motion.

B. Wardell (✉)

Department of Astronomy, Cornell University, Ithaca, NY 14853, USA

e-mail: barry.wardell@gmail.com

URL: <http://www.barrywardell.net>

For the past two decades, these demands have stimulated an intense period of EMRI research among the gravitational physics community. Despite of the impressive progress made by numerical relativists towards tackling the two-body problem in general relativity (for reviews see Refs. [11–13]), the disparity of length scales characterising the EMRI regime is a significant roadblock for existing numerical relativity techniques. Indeed, to this day EMRIs remain intractable by current numerical relativity methods, and successful approaches have instead tackled the problem perturbatively or through post-Newtonian approximations (see Ref. [14] for a review). This article will focus on the first of these; by treating the smaller object as a perturbation to the larger mass, the so-called “self-force approach” reviewed here has been a resoundingly successful tool for EMRI research.

Within the self-force approach, the smaller mass, $\mu \ll M$, is assumed to be sufficiently small that it may be used as a perturbative expansion parameter in the background of the larger mass, M . Expanding the Einstein equation in μ , we see the smaller object as an effective point particle generating a perturbation about the background of the larger mass. At zeroth order in μ , the smaller object merely follows a geodesic of the background. At first order in μ , it deviates from this geodesic due to its interaction with its self-field. Viewing this deviation as a force acting on the smaller object, the calculation of this self-force is critical to the accurate modelling of the evolution of the system. For the purposes of producing an accurate waveform for space-based detectors, and for producing accurate intermediate mass ratio inspiral (IMRI) models, it will be necessary to include further effects up to second perturbative order [15, 16]. Indeed, recent compelling work [17, 18] suggests that IMRIs—and even comparable mass binaries—may be modelled using self-force techniques.

A naïve calculation of the first order perturbation due to a point particle leads to a retarded field which diverges at the location of the particle. The self-force, being the derivative of the field, also diverges at the location of the particle and one obtains equations of motion which are not well-defined and must be regularized. A series of formal derivations of the regularized first order equations of motion (now commonly referred to as the MiSaTaQuWa equations, named after Mino et al. [19] and Quinn and Wald [20] who first derived them) for a point particle in curved spacetime have been developed [19–30], culminating in a rigorous work by Gralla and Wald [31] and Pound [32] in the gravitational case and by Gralla et al. [33] in the electromagnetic case. This was subsequently extended to second perturbative order by Rosenthal [34–37], Pound [38–40], Gralla [41] and Detweiler [42]. These derivations eliminate the ambiguities associated with the divergent self-field of a point particle and provide a well-defined, finite equation of motion. Building upon this foundational progress, several practical computational strategies have emerged from these formal derivations:

- *Dissipative self-force approaches*: While the full first-order self-force is divergent, it turns out that the dissipative component is finite and requires no regularization. This fact has prompted the development of methods for computing the dissipative component alone, sidestepping the issue of regularization altogether. These dissipative approaches fall into two categories:

1. *Flux methods*: By measuring the orbit-averaged flux of gravitational waves onto the horizon of the larger black hole and out to infinity, the fact that the field is evaluated far away from the worldline means that no divergent quantities are ever encountered. This approach yields the time-averaged¹ dissipative component of the self-force [43–50].
2. *Local/instantaneous dissipative self-force*: The time averaging element of flux methods can be eliminated by instead computing the local, instantaneous dissipative component of the self-force from the half-advanced-minus-half-retarded field [43, 51–53].

Both methods, however, fundamentally rely on neglecting potentially important conservative effects which can significantly alter the orbital phase of the system.

- The *mode-sum* approach: Introduced in Refs. [54, 55], and having since been successfully used in many applications, the approach relies on the decomposition of the retarded field into spherical harmonic modes (which are finite, but not differentiable at the particle), numerically solving for each mode independently and subtracting analytically-derived “regularization parameters”, then summing over modes.
- The *effective source* approach: Proposed in [56, 57], the approach implements the regularization before solving the wave equation. This has the advantage that all quantities are finite throughout the calculation and one can directly solve a wave equation for the regularized field.
- The *worldline convolution* approach: First suggested in [58, 59], one computes the regularized retarded field as a convolution of the retarded Green function along the past worldline of the particle. Although the approach is the most closely related to the early formal derivations, it is only recently that it has been successfully applied to calculations in black hole spacetimes.

For a comprehensive review of the self-force problem, see Refs. [60–63]. In this paper, I will review the various approaches and give details of how each one is implemented in practice, highlighting the advantages and disadvantages in each case.

This paper follows the conventions of Misner et al. [64]; a “mostly positive” metric signature, $(-, +, +, +)$, is used for the spacetime metric, the connection coefficients are defined by $\Gamma_{\mu\nu}^{\lambda} = \frac{1}{2}g^{\lambda\sigma}(g_{\sigma\mu,\nu} + g_{\sigma\nu,\mu} - g_{\mu\nu,\sigma})$, the Riemann tensor is $R^{\alpha}_{\lambda\mu\nu} = \Gamma^{\alpha}_{\lambda\nu,\mu} - \Gamma^{\alpha}_{\lambda\mu,\nu} + \Gamma^{\sigma}_{\sigma\mu}\Gamma^{\sigma}_{\lambda\nu} - \Gamma^{\sigma}_{\sigma\nu}\Gamma^{\sigma}_{\lambda\mu}$, the Ricci tensor and scalar are $R_{\alpha\beta} = R^{\mu}_{\alpha\mu\beta}$ and $R = R^{\alpha}_{\alpha}$, and the Einstein equations are $G_{\alpha\beta} = R_{\alpha\beta} - \frac{1}{2}g_{\alpha\beta}R = 8\pi T_{\alpha\beta}$. Standard geometrized units are used, with $c = G = 1$. Greek indices are used for four-dimensional spacetime components, symmetrisation of indices is denoted using parenthesis [e.g. $(\alpha\beta)$], anti-symmetrisation is denoted using square brackets (e.g. $[\alpha\beta]$) and indices are excluded from symmetrisation by surrounding them by vertical bars [e.g. $(\alpha|\beta|\gamma)$]. Latin letters starting from i are used for indices summed only over spatial dimensions and capital letters are used to denote the spinorial/tensorial indices appropriate to the field being considered. Either x or x^{μ} are used when

¹For the case of inclined orbits in Kerr spacetime, this is more appropriately formulated as a torus-average.

referring to a spacetime field point and $z(\tau)$ or $z^\mu(\tau)$ are used when referring to a point on a worldline parametrised by proper time τ . Finally, a retarded (or source) point is denoted using a prime, i.e. z' .

2 Equations of Motion

The formal equations of motion of a compact object moving in a curved spacetime are now well established up to second perturbative order. Writing the perturbed spacetime in terms of a background plus perturbation, $g_{\alpha\beta} = g_{\alpha\beta}^{(0)} + h_{\alpha\beta}$, the equations of motion essentially amount to those of an accelerated worldline in the background spacetime, with the acceleration given by a well-defined regular field which is sourced by the worldline. To order μ , this coupled system of equations for the worldline and its self-field are commonly referred to as the MiSaTaQuWa equations and are given (in Lorenz gauge, assuming a Ricci-flat background spacetime) by

$$\square \bar{h}_{\alpha\beta}^{\text{ret}} + 2C_{\alpha}{}^{\gamma}{}_{\beta}{}^{\delta} \bar{h}_{\gamma\delta}^{\text{ret}} = -16\pi\mu \int g_{\alpha'(\alpha} u^{\alpha'} g_{\beta)\beta'} u^{\beta'} \delta_4(x, z(\tau')) d\tau' \quad (1a)$$

$$\mu a^\alpha = \mu k^{\alpha\beta\gamma\delta} \bar{h}_{\beta\gamma;\delta}^{\text{R}} \quad (1b)$$

with

$$k^{\alpha\beta\gamma\delta} = \frac{1}{2} g_{(0)}^{\alpha\delta} u^\beta u^\gamma - g_{(0)}^{\alpha\beta} u^\gamma u^\delta - \frac{1}{2} u^\alpha u^\beta u^\gamma u^\delta + \frac{1}{4} u^\alpha g_{(0)}^{\beta\gamma} u^\delta + \frac{1}{4} g_{(0)}^{\alpha\delta} g_{(0)}^{\beta\gamma}.$$

Here, μ is mass of the object, $g_{\alpha'\alpha}$ is the bivector of parallel transport, $C_{\alpha\beta\gamma\delta}$ is the Weyl tensor of the background spacetime, and we use the trace-reversed metric perturbation $\bar{h}_{\alpha\beta} = h_{\alpha\beta} - \frac{1}{2} g_{\alpha\beta}^{(0)} h$, $h = h^\gamma{}_\gamma$.

One can also consider compact objects possessing other types of charge. For example, a particularly simple case is that of a scalar charge q with mass m and scalar field Φ , in which case the equations of motion are given by^{2,3}

$$(\square - \xi R) \Phi^{\text{ret}} = -4\pi q \int \delta_4(x, z(\tau')) d\tau' \quad (2a)$$

$$ma^\alpha = q (g_{(0)}^{\alpha\beta} + u^\alpha u^\beta) \Phi_{,\beta}^{\text{R}} \quad (2b)$$

$$\frac{dm}{d\tau} = -q u^\alpha \Phi_{,\alpha}^{\text{R}}. \quad (2c)$$

²In the scalar case, it is important to distinguish between the self-force $F^\alpha = \nabla^\alpha \Phi$ and the self-acceleration, which is given by projecting to self-force orthogonal to the worldline, $a^\alpha = (g_{(0)}^{\alpha\beta} + u^\alpha u^\beta) F_\beta$. In the electromagnetic and gravitational cases the self-force has no component along the worldline and the two may be used interchangeably.

³We assume that the mass m is small and ignore its effect on the equations of motion.

Here, R is the Ricci scalar of the background spacetime and ξ is the coupling to scalar curvature. Similarly, for an electric charge, e , one obtains equations of motion which are given in Lorenz gauge by

$$\square A_{\alpha}^{\text{ret}} - R_{\alpha}^{\beta} A_{\beta}^{\text{ret}} = -4\pi e \int g_{\alpha\alpha'} u^{\alpha'} \delta_4(x, z(\tau')) d\tau' \quad (3a)$$

$$ma^{\alpha} = e(g_{(0)}^{\alpha\beta} + u^{\alpha} u^{\beta}) A_{[\gamma, \beta]}^{\text{R}} u^{\gamma}, \quad (3b)$$

where $R_{\alpha\beta}$ is the Ricci tensor of the background spacetime and A^{μ} is the vector potential.

The key component in all instances is the identification of the appropriate regularized field on the worldline. Detweiler and Whiting identified a particularly elegant choice for the regularized field, written in terms of the difference between the retarded field and a locally-defined singular field,

$$\Phi^{\text{R}} = \Phi^{\text{ret}} - \Phi^{\text{S}}, \quad A_{\alpha}^{\text{R}} = A_{\alpha}^{\text{ret}} - A_{\alpha}^{\text{S}}, \quad h_{\alpha\beta}^{\text{R}} = h_{\alpha\beta}^{\text{ret}} - h_{\alpha\beta}^{\text{S}}. \quad (4)$$

In addition to giving the physically-correct self-force, the Detweiler-Whiting regular field has the appealing feature of being a solution of the homogeneous field equations in the vicinity of the worldline. Most computational strategies essentially amount to differing ways of representing this singular field⁴ and obtaining the regularized field on the worldline.

3 Numerical Regularization Strategies

In a numerical implementation, it is essential to avoid the evaluation of divergent quantities. In the case of self-force calculations, both the retarded and singular fields diverge on the worldline so one must avoid evaluating them there. Several strategies for doing so have emerged over the years (see Table 1 for a summary).

One option is to only ever evaluate finite, dissipative quantities (e.g. the retarded field far from the worldline or the half-advanced-minus-half-retarded field on the worldline). This is the basis of the dissipative methods mentioned in the introduction. Since these methods effectively avoid the problem of regularization, they will not be discussed further here; we will return to them in Sect. 4. It is worth noting, however, that the methods typically used by dissipative calculations are essentially the same as those used by mode-sum regularization for computing the retarded field, but without the additional regularization step.

This leaves three regularization strategies which allow the regularized field to be computed on the worldline without encountering numerical divergences: worldline convolution, mode-sum regularization, and the effective source approach.

⁴Some methods [65, 66] rely on alternative prescriptions for the singular field than that proposed by Detweiler and Whiting.

Table 1 Summary of regularization methods employed by self-force calculations in black hole spacetimes

Case	Worldline	Mode-sum	Effective source
<i>Scalar</i>			
Schwarzschild	Circular (apprx) [59]; generic (quasilocal) [67, 68]; generic [69–71]; static [72]; accelerated [73]	Radial [74]; circular [75–78]; eccentric [79–83]; static [72]	Circular [56, 57, 65, 84–86]; eccentric [87]; evolving [88]
Kerr	Generic [68]; accelerated [73]	Circular [89]; equatorial [90, 91]; inclined circular [92]; accelerated [93]; static [94, 95]	Circular [96]; eccentric [97]
<i>EM</i>			
Schwarzschild	Static [72]	Static [72]; eccentric [82, 98]; static (Schwarzschild-de Sitter) [99]; radial (Reissner-Nordström) [100]	–
Kerr	–	Equatorial [90]; accelerated [93]	–
<i>Gravity</i>			
Schwarzschild	Generic (quasilocal) [101]	Radial [102]; circular [103–111]; eccentric [82, 112–120]; osculating [121]	Circular [122]
Kerr	Circular (quasilocal) [59]; branch cut [123]	Equatorial [90]; accelerated [93]; circular [119, 124]	Circular [125]; generic [126]

3.1 Worldline Convolution

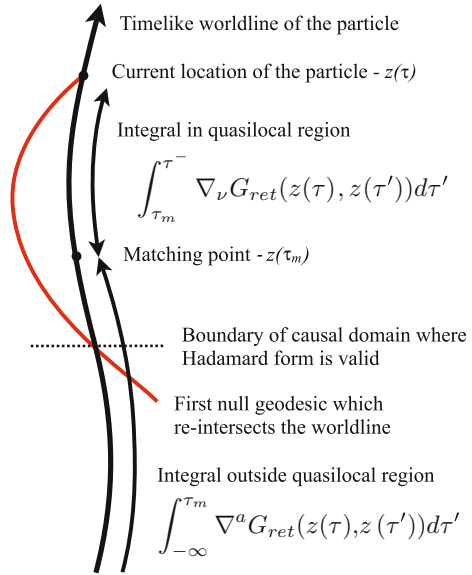
The worldline convolution method relies on a split of the regularized self-force into an “instantaneous” piece and a history-dependent term. The instantaneous piece is easily calculated from local quantities evaluated at the particle’s position,

$$\Phi_{,\alpha}^{\text{inst}} = q \left[\frac{1}{2} \left(\xi - \frac{1}{6} \right) R u_{\alpha} + \left(g_{\alpha\beta}^{(0)} + u_{\alpha} u_{\beta} \right) \left(\frac{1}{3} \dot{a}^{\beta} + \frac{1}{6} R^{\beta}{}_{\gamma} u^{\gamma} \right) \right], \quad (5a)$$

$$A_{[\beta;\alpha]}^{\text{inst}} u^{\beta} = e \left(g_{\alpha\beta}^{(0)} + u_{\alpha} u_{\beta} \right) \left(\frac{1}{3} \dot{a}^{\beta} + \frac{1}{6} R^{\beta}{}_{\gamma} u^{\gamma} \right), \quad (5b)$$

$$\bar{h}_{\alpha\beta;\gamma}^{\text{inst}} u^{\beta} u^{\gamma} = \bar{h}_{\alpha\beta;\gamma}^{\text{inst}} u^{\alpha} u^{\beta} = 0. \quad (5c)$$

Fig. 1 Schematic representation of the worldline convolution method. The equations shown are for the case of the self-force on a scalar charge, but are representative of similar equations in the electromagnetic and gravitational cases. Reproduced from Ref. [69]



The history-dependent term is much more difficult to calculate, as it is given in terms of a convolution of the derivative of the retarded Green function along the worldline's entire past-history (see Fig. 1),

$$\Phi_{,\alpha}^{\text{hist}} = q \int_{-\infty}^{\tau^-} \nabla_{\alpha} G^{\text{ret}}[x, z(\tau')] d\tau', \quad (6a)$$

$$A_{\alpha;\beta}^{\text{hist}} = e \int_{-\infty}^{\tau^-} \nabla_{\beta} G_{\alpha\alpha'}^{\text{ret}}[x, z(\tau')] u^{\alpha'} d\tau', \quad (6b)$$

$$\bar{h}_{\alpha\beta;\gamma}^{\text{hist}} = 4\mu \int_{-\infty}^{\tau^-} \nabla_{\gamma} G_{\alpha\beta\alpha'\beta'}^{\text{ret}}[x, z(\tau')] u^{\alpha'} u^{\beta'} d\tau'. \quad (6c)$$

The covariant derivatives here are taken with respect to the first argument of the retarded Green function. Likewise, the regularized self-field can be obtained from a worldline convolution of the retarded Green function itself; similar formulae can also be derived for higher derivatives. The retarded Green function appearing in these equations is a solution of the wave equation with a delta-function source,

$$(\square - \xi R) G^{\text{ret}} = -4\pi \delta^4(x, x'), \quad (7a)$$

$$\square G_{\alpha\alpha'}^{\text{ret}} - R_{\alpha}{}^{\beta} G_{\beta\alpha'}^{\text{ret}} = -4\pi g_{\alpha\alpha'} \delta^4(x, x'), \quad (7b)$$

$$\square G_{\alpha\beta\alpha'\beta'}^{\text{ret}} + 2R_{\alpha}{}^{\gamma}{}_{\beta}{}^{\delta} G_{\gamma\delta\alpha'\beta'}^{\text{ret}} = -4\pi g_{\alpha\alpha'} g_{\beta\beta'} \delta^4(x, x'), \quad (7c)$$

with boundary conditions such that the solutions correspond to purely outgoing radiation at infinity and no radiation emerging from the horizon.

The regularization (i.e. subtraction of the Detweiler-Whiting singular field) is formally achieved by the limiting procedure in the upper limit of integration, i.e. by cutting off the integration at τ^- , slightly before the coincidence point $z = x$. In practice, this is done by taking the integration all the way up to coincidence, but excluding the *direct* contribution to the Green function at coincidence (i.e. the term proportional to $\delta(\sigma)$ in the Hadamard form for the Green function). Although the retarded Green function also diverges at certain other points along the past worldline (in particular at null-geodesic intersections where the particle sees null rays emitted from its past), it turns out that these are all integrable singularities (of the form $1/\sigma$ and $\delta(\sigma)$) and the integral may be accurately evaluated to give a finite and accurate value for the regularized self-force.

Despite having been proposed in the early days of EMRI self-force calculations [58], the worldline convolution method was largely ignored for a long time by numerical implementations (the notable exception being investigative studies [59, 127] which did not complete a full calculation of the self-force). A likely reason is that the method relies on knowledge of the retarded Green function for all points on the particle's past worldline. While methods have existed for decades for computing portions of the retarded Green function, it turns out to be very difficult to obtain it accurately everywhere that it is needed for the worldline convolution.

Thankfully, recent progress has led to two practical computational strategies, both of which have been successfully applied to compute the self-force in black hole spacetimes. The first of these is based on a frequency-domain decomposition of the Green function, and builds on the rich history of black hole perturbation theory developed over the past several decades. The second, a time-domain approach, has been a very recent development and shows a great deal of promise for the future.

Independently of whether a frequency-domain or a time-domain scheme is used, a common problem with both is that they fail at early times when source and field points are close together; in the frequency-domain case the convergence is poor at early times, while in the time-domain case features from the numerical approximation pollute the data at early times. A relatively straightforward solution which has been successfully applied in both scenarios is to only rely on their results at late times and to supplement them at early times with a quasilocal Taylor series expansion. Provided a sufficiently early time can be chosen where both the distant past and quasilocal calculations converge, this yields a global approximation for the Green function which is sufficient for producing an accurate result for the self-force. To date this has been shown to be possible in the case of a scalar charge in Nariai [128], Schwarzschild [69, 70] and Kerr [129] spacetimes.

Given an approximation for the Green function valid throughout the past worldline, it is then trivial to numerically integrate Eq. (6) to obtain the self-force (see Fig. 1). As mentioned previously, the divergences in the retarded Green function at null-geodesic intersections on the past worldline are all integrable singularities and do not pose a significant obstacle to accurate numerical evaluation of the integrals.

3.1.1 Quasilocal Expansion

In order to obtain an approximation to the retarded Green function which is valid at early times, it is convenient to start with the Hadamard form for the Green function (in Lorenz gauge)

$$G_{AB'}^{\text{ret}}(x, x') = \Theta_- \left[U_{AB'} \delta(\sigma) - V_{AB'} \Theta(-\sigma) \right], \quad (8)$$

where Θ_- is analogous to the Heaviside step-function, being 1 when x' is in the causal past of x , and 0 otherwise, $\delta(\sigma)$ is the covariant form of the Dirac delta function, $U_{AB'}$ and $V_{AB'}$ are symmetric bi-spinors/tensors and are regular for $x' \rightarrow x$. The bi-scalar $\sigma(x, x')$ is the Synge world function, which is equal to one half of the squared geodesic distance between x and x' . In particular, $\sigma(x, x) = 0$ and $\sigma(x, z) < 0$ when x and z are timelike separated. Because of the limiting procedure in the history integral, Eq. (6), only the term involving $V_{AB'}$ is non-zero, and at all required points along the worldline $\Theta_- = 1 = \Theta(-\sigma)$. The problem of determining the retarded Green function at early times therefore reduces to finding an approximation for $V_{AB'}(x, x')$ which is valid for x and x' close together.

Several methods have been developed for computing approximations to $V_{AB'}$. Fundamentally, they rely on either the use of a series expansion, or on the use of numerically evolved transport equations (ordinary differential equations defined along a worldline). The series expansion approach has been the most fruitful to date with results including: leading-order coordinate expansions in Schwarzschild and Kerr spacetimes for scalar [68, 73] and gravitational cases [101], high-order coordinate expansions in spherically symmetric spacetimes (including Schwarzschild) [67], formal covariant expansions in generic spacetimes [130–133], and moderately high-order coordinate expansions in Schwarzschild [82] and Kerr [90] spacetimes. The only numerical calculation I am aware of was done in [133] for generic spacetimes (with an example application in Schwarzschild spacetime).

The series expansion method produces an expression for $V(x, x')$ as a power series in the coordinate distance between x and x' . For example, for the scalar case in Schwarzschild spacetime it takes the form

$$V(x, x') = \sum_{i,j,k=0}^{\infty} v_{ijk}(r) (t - t')^{2i} (1 - \cos \gamma)^j (r - r')^k, \quad (9)$$

where γ is the angular separation of the points and the v_{ijk} are analytic functions of r and M . It is straightforward to take partial derivatives of these expressions at either spacetime point to obtain the derivative of the Green function. Although this series on its own may be sufficient for use in the quasilocal component of a worldline convolution, it turns out that some simple tricks allow for a vast improvement in accuracy. It turns out that, because $V(x, x')$ diverges at the edge of the normal neighbourhood, the series approximation benefits significantly from Padé resummation

which incorporates information about the form of the divergence [67]. One minor caveat is that since Padé re-summation is only well defined for series expansions in a single variable, it is necessary to first expand r' and γ in a Taylor series in $t - t'$, using the equations of motion to determine the higher derivatives appearing in the series coefficients. Then, with $V(x, x')$ written as a power series in $t - t'$ alone, a standard diagonal Padé approximant provides an accurate representation of the Green function in the quasi-local region.

3.1.2 Frequency Domain Methods

Frequency domain methods for computing the retarded Green function rely crucially on the separability of the wave equation. In the scalar, Schwarzschild case that represents the current state-of-the-art⁵ [69] (also see [128] for a related calculation in Nariai spacetime), this can be achieved by writing the Green function as a sum of spherical harmonic and Fourier modes

$$G^{\text{ret}}(x, x') = \frac{1}{r r'} \sum_{\ell=0}^{\infty} P_{\ell}(\cos \gamma) \frac{1}{2\pi} \int_{-\infty+i\epsilon}^{\infty+i\epsilon} \hat{g}_{\ell}(r, r'; \omega) e^{-i\omega(t-t')} d\omega. \quad (10)$$

Here, $\epsilon > 0$ is a formal parameter to ensure the correct boundary conditions are satisfied for a retarded Green function. Substituting this into the wave equation, Eq. (7a), one obtains an independent set of ordinary differential equations for $\hat{g}_{\ell}(r, r'; \omega)$, one equation for each ℓ and ω ,

$$\left[\frac{d^2}{dr_*^2} + \omega^2 - V_{\ell}(r) \right] \hat{g}_{\ell}(r, r'; \omega) = -\delta(r_* - r'_*), \quad (11)$$

with

$$V_{\ell}(r) \equiv \left(1 - \frac{2M}{r} \right) \left[\frac{\ell(\ell+1)}{r^2} + \frac{2M}{r^3} \right]. \quad (12)$$

Here, $r_* \equiv r + 2M \ln \left(\frac{r}{2M} - 1 \right)$ is the radial tortoise coordinate.

⁵More generally, Teukolsky [134, 135] showed that the field equations may be separated in Kerr spacetime in the gravitational case by making use of the spin-weighted spheroidal harmonics in place of the spherical harmonics. A series of works—pioneered by Regge and Wheeler [136] and improved upon by others [137–143]—achieved a similar separation in the Schwarzschild gravitational case by making use of tensor spherical harmonics. However, separability alone is not sufficient and there remain some technical issues which have yet to be solved before solutions of the Teukolsky or Regge-Wheeler equations could be used in a worldline convolution approach. Most important is the issue of gauge; the MiSaTaQuWa equations, Eqs. (5) and (6), were derived in the Lorenz gauge, whereas solutions of the Teukolsky and Regge-Wheeler equations are in a gauge different from Lorenz gauge. Fortunately, recent work [119] has resolved many of the conceptual issues associated with gauge choice.

Given two linearly-independent solutions, $p(r; \omega)$ and $q(r; \omega)$, of the homogeneous version of (11), $\hat{g}_\ell(r, r'; \omega)$ is given by

$$\hat{g}_\ell(r, r'; \omega) = \frac{p_\ell(r_<, \omega)q_\ell(r_>, \omega)}{W(p, q)}, \quad (13)$$

where $r_> \equiv \max(r, r')$, $r_< \equiv \min(r, r')$ and $W(p, q)$ is the Wronskian. One is then faced with the integral over frequencies in the inverse Fourier transform appearing in (10). This may be achieved through straightforward integration along the real- ω axis (see Fig. 2); the only caveat is that the formally-infinite integral over frequencies should be cut off at some finite maximum frequency using a smooth window function, for example

$$g_\ell(r, r'; t - t') = \frac{1}{2\pi} \int_{-\infty+i\epsilon}^{\infty+i\epsilon} \hat{g}_\ell(r, r'; \omega) e^{-i\omega(t-t')} (1 - \text{erf}[2(\omega - \omega_{\max}))]/2 d\omega. \quad (14)$$

Alternatively, as was done in [69], the integration contour can be deformed into the complex frequency plane following a proposal by Leaver [144, 145]. In Schwarzschild spacetime, $\hat{g}_\ell(r, r'; \omega)$ has simple poles in the lower semi-plane at

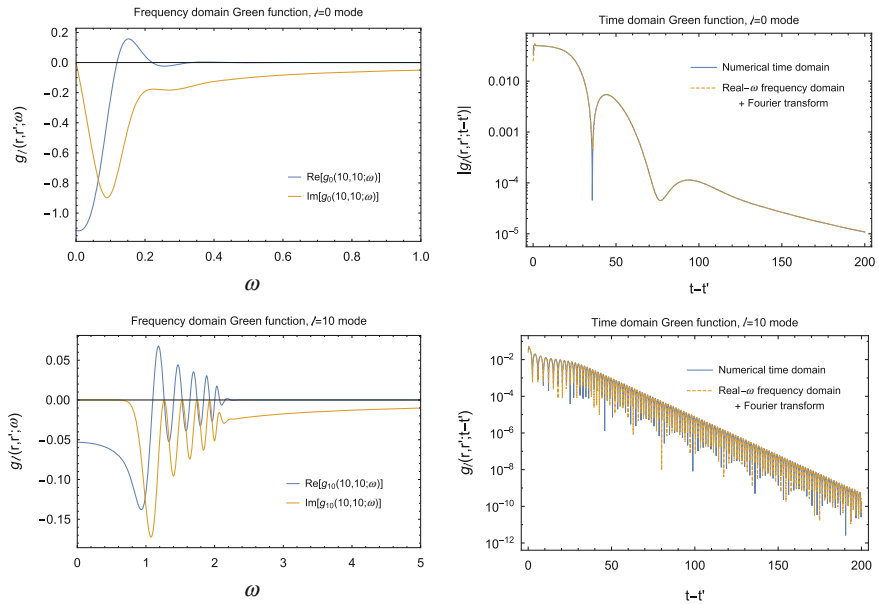


Fig. 2 Spherical harmonic modes of the Schwarzschild scalar Green function. *Left* the frequency domain Green function, $\hat{g}_\ell(r, r'; \omega)$, as a function of real frequency for $r = r' = 10M$, $\ell = 0$ (top) and $\ell = 10$ (bottom). *Right* the corresponding time domain Green function, $g_\ell(r, r'; t - t')$ computed by Fourier transforming the frequency domain Green function using Eq. (14) with $\omega_{\max} = 8.5$ (blue, solid line), and by using the time domain methods described in Sect. 3.1.3 (orange, dashed line)

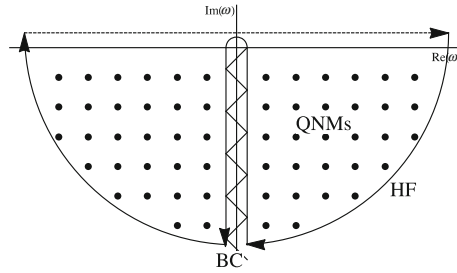


Fig. 3 Contour deformation in the complex-frequency plane. The residue theorem of complex analysis allows one to re-express the integral over (just above) the real line of the Fourier modes, $\hat{g}_\ell(r, r'; \omega)$, as an integral over a high-frequency arc plus an integral around a branch cut and a sum over the residues at the poles. Reproduced from Ref. [69]

the quasinormal mode frequencies, along with a branch cut starting at $\omega = 0$ and continuing along the negative imaginary axis (see Fig. 3). The deformed frequency integral is therefore given by an integral over a high-frequency arc, an integral around a branch cut, and an integral over the residues at the poles.⁶

The high-frequency arcs can be disregarded as they are likely to only contribute at very early times, where the quasilocal approximation can be used. There are well-established methods for accurately computing the location of the poles (quasinormal mode frequencies) and the residues at the poles. The biggest difficulty in the frequency-domain approach is in evaluating the branch cut integral, about which very little was known until recently (other than asymptotic approximations for e.g. large radius or late times). Substantial recent progress has established methods for calculating this branch cut contribution [146]; these methods were used in [69] to compute the self-force in Schwarzschild spacetime.

The final step in the frequency domain approach is to sum over spherical harmonic modes to produce the full Green function. Here, the distributional parts of the full Green function can cause poor convergence in the mode-sum. Fortunately, there is a straightforward solution to this problem: by smoothly cutting off the mode sum at large ℓ ,

$$G^{\text{ret}}(x, x') = \frac{1}{r r'} \sum_{\ell=0}^{\ell_{\text{max}}} P_\ell(\cos \gamma) g_\ell(r, r'; t - t') e^{-\ell^2/2\ell_{\text{cut}}^2} \quad (15)$$

one obtains a mollified retarded Green which is appropriate for use in a self-force calculation, and whose sum over ℓ converges. Empirically, it has been found that choosing $\ell_{\text{cut}} \approx \ell_{\text{max}}/5$ gives good results.

⁶In the Kerr spacetime there are indications that there may be additional branch cuts to consider [123].

3.1.3 Time Domain Approaches

The frequency domain approach to computing the retarded Green function has several shortcomings. It relies on relatively difficult technical calculations and has poor convergence properties at early times and in scenarios where the worldline is not well-represented by a discrete spectrum of frequencies. Recent work has shown that the Green function may also be accurately computed (at least for the purposes of self-force calculations) in the time domain using straightforward numerical evolutions. A time domain calculation sidesteps issues related to a wide frequency spectrum and appears to exhibit much better convergence properties at early times.

There are two closely-related proposals for computing the Green function in the time domain. In [71], Eq. (7a) was numerically solved as an initial value problem, with the delta-function source approximated by a narrow Gaussian. A reformulation of this approach as a homogeneous problem with Gaussian initial data was subsequently given in [70]. It was found that these “numerical Gaussian” approaches are able to approximate the retarded Green function remarkably well in a large region of the space required by worldline convolutions. The size of the Gaussian limits the scale of the smallest features which can be resolved, but it turns out that this is not significantly detrimental to a self-force calculation.

The only regimes where the numerical Gaussian approach is not well suited to computing the retarded Green function are at very early and very late times. At early times the direct $\delta(\sigma(x, x))$ term (which must be excluded from the worldline convolution of the retarded Green function) is smeared out and is difficult to isolate from the rest of the Green function. There is no conceptual difficulty at late times, but the reality of a numerical evolution is that it can only be run for a finite time. Fortunately, both of these issues are easily overcome; the former by using the quasilocal expansion at early times, and the latter by using a late-time expansion of the branch cut integral (see Fig. 4).

In the time domain approach, each numerical time domain evolution gives the Green function $G(x_0, x')$ for a single base point x_0 , and for all source points, x . As a result, a single numerical calculation can only be used to compute the self-force at a single spacetime point, but it can be computed for any past-worldline ending up at that point. This is in contrast to other self-force methods, where a single orbit is considered at a time, but a single calculation gives the self-force at all points on the orbit. The problem of efficiently spanning the parameter space of base points x_0 is an ideal application of reduced order methods [129, 147].

3.2 Mode-Sum Regularization

The mode-sum regularization scheme, first proposed by Barack and Ori [54], has proven highly successful as a computational self-force strategy, having been applied to the computation of the self force for a variety of configurations in Schwarzschild [74–81, 83, 102, 107–110, 113, 114, 148, 149] and Kerr [89, 91,

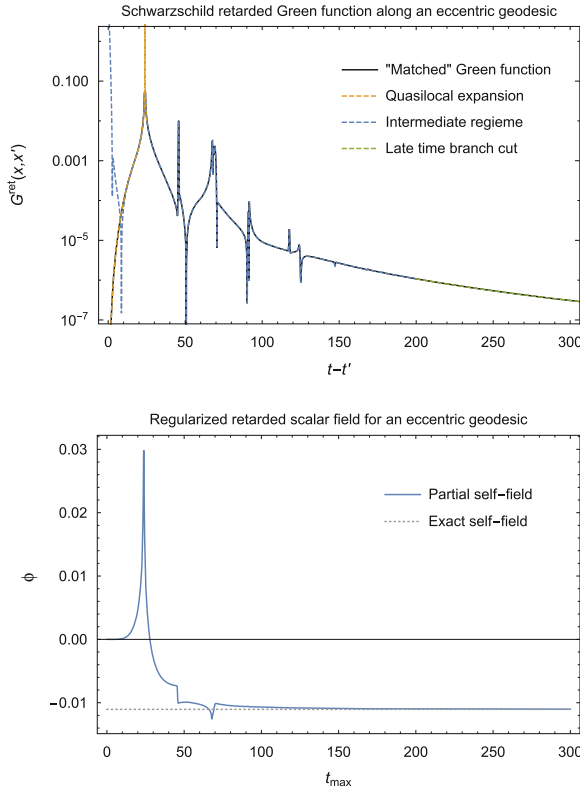


Fig. 4 *Top* Matched Green function along an eccentric orbit (eccentricity $e = 0.5$ and semilatus rectum $p = 7.2$) in Schwarzschild spacetime. The full Green function (black) is constructed by combining a quasilocal approximation at early times (orange, dashed line) with a time domain calculation at intermediate times (blue, dashed line) and a late-time branch cut approximation at late times (green, dashed line). *Bottom* Integrating the retarded Green function (excluding the direct part) up to some time point on the past worldline gives the contribution to the regularized self-field from all points on the past worldline up to that time. With an eccentric orbit of period $\approx 317M$, we see that a good approximation to the self-field is obtained by including the contributions from less than one full orbit. Note that the formal divergences of the Green function are integrable and do not cause significant numerical difficulty in computing the self-force

92, 124, 150] spacetimes. The success of the method hinges on the fact that the first order retarded field diverges in a way which can be effectively smoothed out by a spectral decomposition in the angular directions. More specifically, the divergence appears as an odd power of $1/s$, where $s^2 = (g^{\alpha\beta} + u^\alpha u^\beta)\sigma_{;\alpha}\sigma_{;\beta}$ is an appropriate measure of distance from the worldline. The result is that the $1/s$ divergence of the field near the worldline turns into an infinite sum of modes, each of which are individually finite (but possibly discontinuous) on the worldline. The divergence of the field then manifests itself through the failure of the (infinite) sum over modes to converge. Conveniently, this odd-in- $1/s$ property of the retarded field also holds for its derivatives, both the first derivatives required for the self-force and higher

derivatives which are useful for computing higher-multipole gauge invariants [104, 105]. As a result, an arbitrary number of derivatives of the first order retarded field is represented by an infinite sum of modes, each of which are individually finite (but possibly discontinuous) on the worldline. The trade-off is that as the number of derivatives increases the divergence of the sum over modes becomes increasingly strong.

Since the individual modes are finite, numerical calculations of the retarded field and its derivatives can be done in the reduced (t, r) space without encountering any numerical divergences. The remaining piece of the problem is a method for rendering the divergent sum over modes finite. An analytic decomposition of the angular dependence of the Detweiler-Whiting singular field yields “regularization parameters” which may be subtracted mode-by-mode from the numerical retarded field values. Provided all parts of the Detweiler-Whiting singular field which don’t vanish on the worldline are included in the calculation, the regularized sum over modes is convergent on the worldline and one never encounters any numerical divergences.

It is important to note that the use of the Detweiler-Whiting singular field is not merely a convenience; it also provides well-motivated physical grounds to justify the mode-sum regularization approach. Other ad-hoc approaches based on identifying the asymptotically divergent contributions to the mode-sum often produce the correct regularization parameters, but their use is difficult to justify rigorously and can easily lead to incorrect results. Crucially, there is no way of knowing whether such an ad-hoc regularization procedure is producing a physically correct result, or if important contributions are being overlooked. They should therefore not be relied on without extreme care.

Unfortunately, despite its success in first order calculations, mode-sum regularization alone is not an effective tool for computing the second order self-force. The reason for this is straightforward: the second order retarded field contains divergent terms which appears in the form of even powers of $1/s$. Intuitively, this arises from the fact that the second order field contains terms which depend quadratically on the first order field. Unlike the odd-in- $1/s$ case, the angular decomposition of $1/s^2$ leads to individual modes which diverge logarithmically as the worldline is approached. Fortunately, all is not lost for the mode-sum method as a computational tool at second order. Provided the leading order logarithmic divergence is subtracted by some other means (for example, using the effective source approach), regularization parameters may be used to accelerate the rate of convergence of the mode sum. Such a hybrid scheme complements the generality of the effective source approach with the computational efficiency of mode-sum regularization.

3.2.1 Regularization Parameters

The computation of regularization parameters has been addressed by a series of calculations stemming from the original Barack-Ori derivation. Barack and Ori’s original work gave the first two self-force regularization parameters for scalar, electromagnetic and Lorenz-gauge gravitational cases in both Schwarzschild and Kerr

spacetimes. These are sufficient for computing the regularized self-force, but they yield mode-sums which have relatively poor quadratic convergence with the number of modes included. Since the Detweiler-Whiting regularized field is a smooth, homogeneous function in the vicinity of the worldline, its mode-sum representation converges exponentially. This spectral convergence is spoiled by the fact that only the portion of the Detweiler-Whiting singular field which does not vanish on the worldline is subtracted by the leading order regularization parameters. The mode decomposition effectively contains information about the extension of the field off the worldline to the entire two-sphere, so the regularized field contains residual pieces of the Detweiler-Whiting singular field off the worldline, but on a two-sphere of the same radius. By deriving higher-order regularization parameters one can subtract these residual pieces order-by-order, leaving a mode-sum which is more and more rapidly convergent (see Fig. 5). The derivation of these higher-order parameters is closely related to the computation of the quasilocal expansion of the Green function and has been addressed in a series of papers: the first higher order parameter was given in [76] for the case of a scalar charge on a circular orbit in Schwarzschild spacetime, and for eccentric geodesic orbits in [80]. This was subsequently extended by several further orders for equatorial geodesic motion in the scalar, electromagnetic and gravitational cases in both Schwarzschild [82] and Kerr [90] spacetimes. Recent work has also produced parameters for accelerated worldlines [72, 93].

Within these derivations of high-order regularization parameters, a subtle ambiguity appears through the elevation of the four-velocity from a quantity defined on a worldline to a quantity defined everywhere on the two-sphere. A natural, covariant choice is to define this off-worldline extension through parallel transport, $u^{\alpha'} = g_{\alpha}^{\alpha'} u^{\alpha}$. However, in practical calculations it is often convenient to make a coordinate choice. For example, a common choice is to define the extension in terms of “constant coordinate components”, i.e. to define $u^{\alpha'}$ such that its components in some coordinate system have a constant value everywhere on the two-sphere. This is

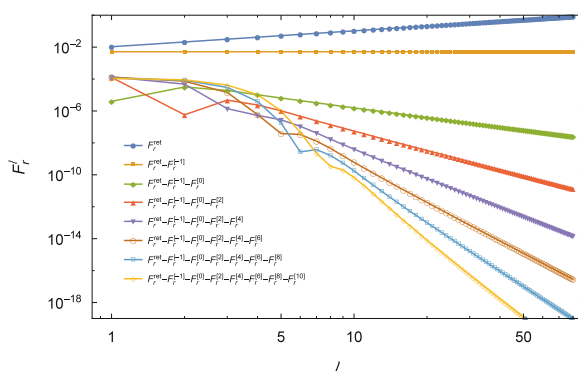


Fig. 5 Spherical harmonic modes of the self-force for a point scalar charge on a circular orbit of radius $r_0 = 6M$ in Schwarzschild spacetime. By subtracting analytically determined high-order “regularization parameters”, the sum over modes is rendered more and more rapidly convergent. Each regularization parameter, $F_l^{[n]}$, behaves asymptotically for large- ℓ as $1/\ell^n$

a perfectly valid choice, as is any other choice where $u^{\alpha'}$ agrees with the actual four-velocity when evaluated on the worldline. The only caveat is that the regularization parameters beyond the leading two orders change depending on the particular choice of extension. As a result, in order to use higher-order regularization parameters it is essential that a compatible choice of off-worldline extension is used in the retarded field calculation.

3.2.2 Choice of Basis and Gauge

There are two other factors which must be considered in the mode-sum scheme: the choice of angular basis functions for the spectral decomposition and the choice of gauge in the electromagnetic and gravitational cases.

The choice of basis functions is typically motivated by their ability to produce separability of the retarded field equations; an appropriate choice of basis functions yields an independent set of equations in (t, r) space for each individual mode. For the case of a scalar charge in Schwarzschild spacetime, the appropriate basis functions are the standard spherical harmonics. In the Kerr case the spheroidal harmonics are required for separability. For electromagnetic and gravitational cases, there are several choices. For Schwarzschild spacetime one can choose between a tensor harmonic basis and a basis of spin-weighted spherical harmonics. In the Kerr case only the spin-weighted spheroidal harmonics are known to yield separability [134, 135].

This choice of angular basis also affects the regularization parameters. The parameters for scalar spherical harmonic modes, tensor harmonic modes, spin-weighted spherical harmonic modes and spheroidal harmonic modes are all potentially different. However, it is always possible project the tensor, spin-weighted, or spheroidal harmonic modes onto the scalar spherical harmonic basis. In fact, since the regularization parameters are most easily obtained for the scalar spherical harmonic basis, calculations of the retarded field are typically done using the computationally most convenient basis and the result is then projected onto the scalar spherical harmonics before the regularization and sum-over-modes steps are done [113].

A more difficult issue in the electromagnetic and gravitational cases is the choice of gauge. The Detweiler-Whiting singular field is defined in Lorenz gauge (since it is derived from a Lorenz gauge Green function), but numerical calculations of the retarded field are more easily done in either radiation or Regge-Wheeler gauge. The existence of tensor spherical harmonics makes a Lorenz-gauge calculation possible, if somewhat cumbersome in the Schwarzschild case [111, 118, 120]. One obtains a coupled set of 10 equations for the metric perturbation, but there is no coupling between different different tensor-harmonic modes. Unfortunately, this does not hold for the Kerr case as there are no known tensor spheroidal harmonics. Rather than trying to derive tensor spheroidal harmonics, a better approach is to work with the relatively straightforward Teukolsky equation in radiation gauge [124]. The difficulty then is in identifying the appropriate regularization parameters, particularly since the gauge transformation from Lorenz gauge is itself often singular. This remained an

open problem until recently, when an understanding of how to apply the mode-sum regularization scheme in radiation gauge was finally established [119] and applied in a self-force calculation [108].

3.2.3 Mode-Sum Regularization in the Frequency Domain

The mode-sum scheme provides a method for computing the regularized self-force using numerical data for the modes of the retarded field in the reduced (t, r) space. There are, however, several possibilities for computing this numerical data. One option relies on a further decomposition of the time dependence into Fourier-frequency modes, in an analogous way to the frequency-domain Green function described in Sect. 3.1.2 above. Using a spin-weighted spheroidal harmonic basis, this leads to a radial equation for the Teukolsky function,

$$\Delta^{-s} \frac{d}{dr} \left(\Delta^{s+1} \frac{dR}{dr} \right) + V(r)R = \mathcal{T}(r) \quad (16)$$

with the potential given by

$$V(r) = \frac{K^2 - 2is(r - M)K}{\Delta} + 4ir\omega s - \lambda. \quad (17)$$

Here, $\Delta \equiv r^2 - 2Mr + a^2$, $K \equiv (r^2 + a^2)\omega - am$, λ is an eigenvalue of the spheroidal equation,

$$\left[\frac{1}{\sin \theta} \frac{d}{d\theta} \left(\sin \theta \frac{d}{d\theta} \right) - a^2 \omega^2 \sin^2 \theta - \frac{(m + s \cos \theta)^2}{\sin^2 \theta} - 2a\omega s \cos \theta + s + 2ma\omega + \lambda \right]_s S_{\ell m} = 0 \quad (18)$$

and a and M are the Kerr spin and mass parameters. For $a = 0$, $\lambda = (\ell - s)(\ell + s + 1)$ and this reduces to the Schwarzschild wave equation decomposed into spin-weighted spherical harmonics (in radiation gauge for the gravitational case), while for $s = 0$ it reduces to the scalar wave equation. A decomposition of the point-particle source term yields a source involving $\delta(r - r_p)$ (and in some cases its derivative), where r_p is the radial location of the particle. In practice, the frequency domain mode-sum approach proceeds in the same way as for the Green function: two independent solutions of the homogeneous radial equation are obtained and are matched at the particle's location.⁷ Then, the distributional sources do not introduce any numerical difficulty as they simply appear as jumps when matching the homogeneous inner and outer solutions.

⁷For eccentric orbits where the particle can not be considered to be at a single radial location in the frequency domain this matching must be modified slightly using, for example, the method of extended homogeneous solutions [112, 116].

The solutions of the Teukolsky equation for a given (ℓ, m, ω) can be obtained either through straightforward numerical integration of the radial ordinary differential equation (typically with some modifications to improve numerical accuracy [151, 152]) or as an approximation in the form of an infinite convergent series of hypergeometric functions. The latter method is based on an idea originally developed by Leaver [153] and now commonly referred to as the “MST” method, after Mano et al. [154] who reformulated it into its current form. It provides an efficient and highly accurate method for computing solutions of the radial equation. For example, recent results have used it to compute solutions accurate to several hundred decimal places, allowing the solutions to be used to determine previously unknown high-order post-Newtonian parameters [155–159]. For a comprehensive review of the MST approach, see the living review by Sasaki and Tagoshi [160] and references therein.

The frequency-domain approach is particularly appropriate in scenarios where the worldline is well represented by a discrete spectrum involving a small number of frequencies. In such cases, mode-sum regularization is by far the optimal choice and is unparalleled in its accuracy and computational efficiency [161]. The prototypical example is a circular orbit, in which only a single frequency is present. In the case of eccentric equatorial orbits (and inclined circular orbits in the Kerr case), there are two fundamental frequencies, and also an infinite number of higher harmonics produced from combinations of the fundamental frequencies. For mildly eccentric orbits this does not cause a great deal of difficulty. However, for more eccentric orbits (with eccentricities $e \gtrsim 0.5$) an increasingly large number of frequencies must be included and the competitive advantage of the frequency domain approach is lost [161]. Even worse, generic geodesic orbits in Kerr spacetime have three fundamental frequencies and the computational difficulty is so high that a calculation has yet to be attempted. Similarly, unbound orbits and other cases such as radial infall are not well suited to frequency domain methods. Apart from these deficiencies, the frequency domain mode-sum approach has been highly successful for producing results.

3.2.4 Mode-Sum Regularization in the Time Domain

The mode-sum scheme may also be applied in the time domain by skipping the Fourier decomposition step and instead solving a set of 1 + 1D partial differential equations in (t, r) space. The main difficulty then is in appropriately handling the distributional source term which has the form $\delta(r - r_p(t))$. One solution, used in [49, 79, 98, 113, 149, 162], is to use a discretised representation of a delta function and to construct the computational grid such that the worldline only ever passes *between* grid points.

An alternative approach is to reformulate the problem in an analogous way to the frequency-domain method. By splitting the computational domain into two domains—one either side of the particle—the delta-function source can be reformulated in terms of a jump in the fields and their derivatives at the interface of the two domains. This method is well suited to highly-accurate spectral numerical methods as all of the numerically evolved fields are smooth functions. It was implemented

using discontinuous-Galerkin methods in [106, 115] and using Chebyshev pseudo-spectral methods in [78, 81]. Eccentric orbits present a small additional complexity in this case as the particle must always lie on the domain interface. This is easily achieved by introducing a time-dependent mapping between the computational and physical coordinates of the system [81, 106].

3.2.5 Limitations of the Mode-Sum Regularization Scheme

Despite its resounding success to date, the mode-sum regularization scheme has some unfortunate disadvantages which make it ill-suited as a general-purpose method for self-force calculations:

1. Its application in the Kerr case is only straightforward in the frequency domain, since the field equations are not separable in the time domain⁸
2. It relies on the use of Lorenz gauge for regularization in the gravitational case. This is not a major issue in the Schwarzschild case since the tensor spherical harmonics may be used to decouple the Lorenz gauge field equations in the angular directions (leaving 10 coupled 1 + 1D equations for each ℓ, m mode). However, there are no known tensor spheroidal harmonics which would be required for the Kerr case, and even if there were they would likely not be applicable in the time domain (again, it is conceivable that a coupled system of equations involving tensor spherical harmonics could be used, but the coupling would result in considerable complexity).
3. It is not applicable beyond first perturbative order, since the modes of the second order perturbation diverge logarithmically near the worldline.

The first two issues are not necessarily showstoppers. There have been several attempts at 1 + 1D time-domain implementations using coupled spherical-harmonic modes in the Kerr case [163, 164], and recent progress on reformulating mode-sum regularization for radiation gauge has clarified the regularization issue [119]. The third point, however, appears insurmountable. For these reasons, among others, the effective source method, described in the next section, was developed.

3.3 Effective Source Approach

Proposed in 2007 as a solution to the shortcomings of mode-sum regularization, the effective source approach⁹ provides an alternative method for handling the divergence of the retarded field. Rather than first computing the retarded field and then

⁸It may still be possible to use mode-sum regularization for the Kerr case in the time domain by decomposing the field equations into *spherical* harmonics and evolving the resulting infinitely coupled set of 1 + 1D partial differential equations in a similar manner to the Schwarzschild case.

⁹Note that the effective source proposed by Lousto and Nakano [65] is similar in spirit, but differs in that it is not derived from the Detweiler-Whiting singular field.

subtracting the singular piece as a post-processing step, one can instead work directly with an equation for the regular field. This idea—independently proposed by Barack and Golbourn [56] and by Vega and Detweiler [57]—has the distinct advantage of involving only regular quantities from the outset, making it applicable in a wider variety of scenarios than the mode-sum scheme. In particular, since it does not rely on a mode decomposition of the retarded field, it can be used by any numerical prescription for solving the retarded field equations, whether in the frequency domain (where the method is really just a generalisation of mode-sum regularization) or in the time domain as a 1 + 1D, 2 + 1D or even 3 + 1D problem.

The basic idea is to use the split of the retarded field into regular and singular pieces, Eq. (4), to rewrite the field equations, Eqs. (1a), (2a) and (3a) as equations for the Detweiler-Whiting regular field,

$$\begin{aligned} (\square - \xi R)\Phi^R &= (\square - \xi R)(\Phi^{\text{ret}} - \Phi^S) \\ &= -4\pi\rho - (\square - \xi R)\Phi^S, \end{aligned} \quad (19a)$$

$$\begin{aligned} (\square\delta_\alpha^\beta - R_\alpha^\beta)A_\beta^R &= (\square\delta_\alpha^\beta - R_\alpha^\beta)(A_\beta^{\text{ret}} - A_\beta^S) \\ &= -4\pi e \int g_{\alpha\alpha'} u^{\alpha'} \delta_4(x, z(\tau')) d\tau' - (\square\delta_\alpha^\beta - R_\alpha^\beta)(A_\beta^S), \end{aligned} \quad (19b)$$

$$\begin{aligned} (\square\delta_\alpha^\gamma \delta_\beta^\delta + 2C_\alpha^\gamma \delta_\beta^\delta) \bar{h}_{\gamma\delta}^R &= (\square\delta_\alpha^\gamma \delta_\beta^\delta + 2C_\alpha^\gamma \delta_\beta^\delta) (\bar{h}_{\gamma\delta}^{\text{ret}} - \bar{h}_{\gamma\delta}^S) \\ &= -16\pi\mu \int g_{\alpha'(\alpha} u^{\alpha'} g_{\beta)\beta'} u^{\beta'} \delta_4(x, z(\tau')) d\tau' - (\square\delta_\alpha^\gamma \delta_\beta^\delta + 2C_\alpha^\gamma \delta_\beta^\delta) (\bar{h}_{\gamma\delta}^S). \end{aligned} \quad (19c)$$

If the singular field used in the subtraction is exactly the Detweiler-Whiting singular field, then the two terms on the right hand side of this equation cancel and the regularized field would be a homogeneous solution of the wave equation. Unfortunately, one typically does not have access to an exact expression for the singular field. Indeed, the Detweiler-Whiting singular field is only defined through a Hadamard parametrix which is not even defined globally. Instead, the best one can typically do is a local expansion which is valid only in the vicinity of the worldline. Borrowing the language of Barack and Golbourn, we refer to an approximation to the singular field as a “puncture” field, $\Phi^S \approx \Phi^P$, $A_\alpha^S \approx A_\alpha^P$, $\bar{h}_{\alpha\beta}^S \approx \bar{h}_{\alpha\beta}^P$. Then, the corresponding approximate regular field—referred to as the “residual field”—is no longer a solution of the homogeneous equation, but instead is a solution of the sourced equation with an *effective source* (see Fig. 6) which is defined to be the right-hand side of Eq. (19) with the puncture field substituted for the singular field

$$S^{\text{eff}} = -4\pi q \int \delta_4(x, z(\tau')) d\tau' - (\square - \xi R)\Phi^P, \quad (20a)$$

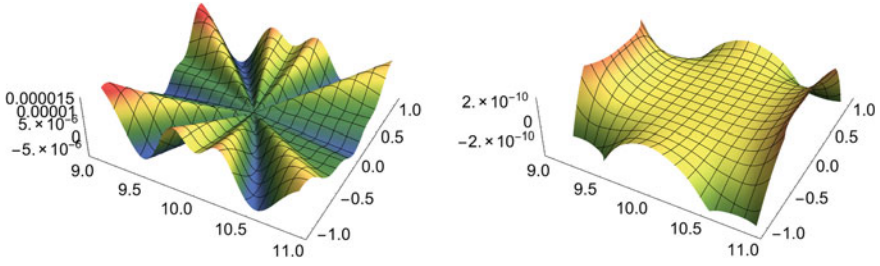


Fig. 6 The effective source for a scalar particle on a circular orbit in Schwarzschild spacetime. The source is generically non-smooth in the vicinity of the worldline (*left*), but the smoothness can be improved by incorporating higher-order parts of the Detweiler-Whiting singular field into the source

$$S_{\alpha}^{\text{eff}} = -4\pi e \int g_{\alpha\alpha'} u^{\alpha'} \delta_4(x, z(\tau')) d\tau' - (\square \delta_{\alpha}^{\beta} - R_{\alpha}^{\beta})(A_{\beta}^{\text{P}}), \quad (20b)$$

$$S_{\alpha\beta}^{\text{eff}} = -16\pi\mu \int g_{\alpha'(\alpha} u^{\alpha'} g_{\beta)\beta'} u^{\beta'} \delta_4(x, z(\tau')) d\tau' - (\square \delta_{\alpha}^{\gamma} \delta_{\beta}^{\delta} + 2C_{\alpha}^{\gamma} \delta_{\beta}^{\delta})(\bar{h}_{\gamma\delta}^{\text{P}}). \quad (20c)$$

Note that the presence of a distributional component of the source on the worldline is merely a formal prescription; in practice the puncture field is chosen so that it exactly cancels this distributional component on the worldline. This effective source is then finite everywhere, but has limited differentiability on the worldline. This makes it well-suited to numerical implementations since no divergent quantities are ever encountered. The only numerical difficulty arises from the non-smoothness of the source in the vicinity of the worldline (see Fig. 6), which leads to numerical noise in the computed self force. The noise can be reduced by making the source smoother using higher-order parts of the Detweiler-Whiting singular field. As shown in Fig. 7, at the same numerical resolution a higher order source (C^2 in this case) eliminates the vast majority of the numerical noise that is present when using a lower order source (C^0 in the case in the figure). The cost of this improved accuracy is a source which is considerably more complicated, and costly to compute in a numerical code.

An additional level of complexity arises from the fact that the puncture field is defined only in the vicinity of the worldline. To avoid ambiguities in its definition far from the worldline, one must ensure that the puncture field goes to zero there. This is most easily achieved by multiplying it by a window function, \mathcal{W} , with properties such that it only modifies the puncture field in a way that its local expansion about the worldline is preserved to some chosen order. In a first-order calculation of the self-force, it suffices to choose \mathcal{W} such that $\mathcal{W}(x_p) = 1$, $\mathcal{W}'(x_p) = 0$, $\mathcal{W}''(x_p) = 0$ and $\mathcal{W} = 0$ far away from the worldline. The residual field (see Fig. 8) then obeys

$$(\square - \xi R)\Phi^{\text{res}} = S^{\text{eff}} \quad (21a)$$

$$(\square \delta_{\alpha}^{\beta} - R_{\alpha}^{\beta})A_{\beta}^{\text{res}} = S_{\alpha}^{\text{eff}} \quad (21b)$$

$$(\square \delta_{\alpha}^{\gamma} \delta_{\beta}^{\delta} + 2C_{\alpha}^{\gamma} \delta_{\beta}^{\delta})\bar{h}_{\gamma\delta}^{\text{res}} = S_{\alpha\beta}^{\text{eff}} \quad (21c)$$

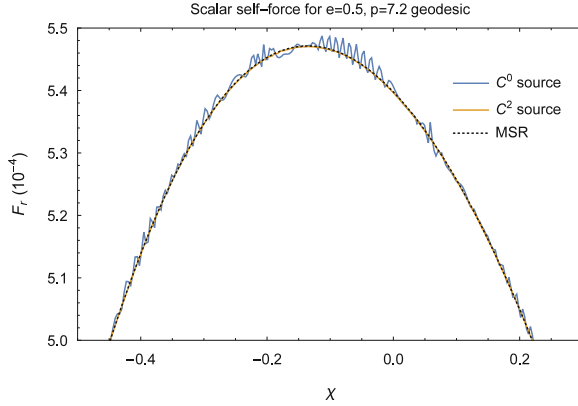
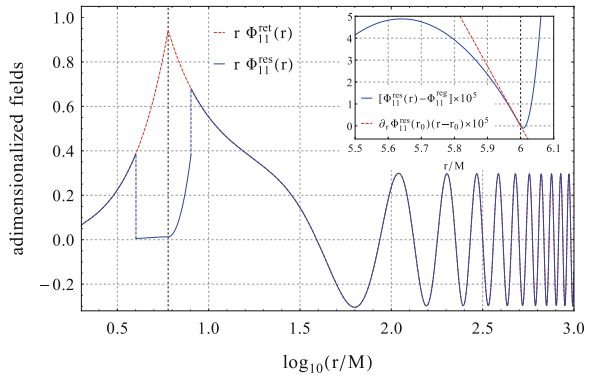


Fig. 7 Radial self-force for a scalar particle on an eccentric orbit in Schwarzschild spacetime, computed with a $3 + 1\text{D}$ implementation of the effective source scheme. Here, the independent variable χ is a “relativistic anomaly parameter” defined through $r = pM/(1 + e \cos \chi)$, with p the semilatus rectum and e the eccentricity. The high-frequency errors using a continuous but non-differentiable source (blue) are dramatically decreased by using a twice differentiable source (orange) obtained from a higher-order approximation to the Detweiler-Whiting singular field. For reference, a highly accurate value computed using frequency-domain mode-sum regularization is also included (dashed, black). Figure based on version presented in Ref. [165]

Fig. 8 The $\ell = 1, m = 1$ spherical-harmonic mode of the residual field, Φ^{res} , for a scalar point particle on a circular orbit in Schwarzschild spacetime. This was produced in [86] using a frequency-domain effective source approach



and has the properties

$$\begin{aligned} \Phi^{\text{res}}(x_p) &= \Phi^{\text{R}}(x_p), \quad \nabla_\alpha \Phi^{\text{res}}(x_p) = \nabla_\alpha \Phi^{\text{R}}(x_p), \\ \Phi^{\text{res}}(x) &= \Phi^{\text{ret}}(x) \quad \text{for } x \notin \text{supp}(\mathcal{W}), \end{aligned} \quad (22a)$$

$$\begin{aligned} A_\alpha^{\text{res}}(x_p) &= A_\alpha^{\text{R}}(x_p), \quad \nabla_\alpha A_\alpha^{\text{res}}(x_p) = \nabla_\alpha A_\alpha^{\text{R}}(x_p), \\ A_\alpha^{\text{res}}(x) &= A_\alpha^{\text{ret}}(x) \quad \text{for } x \notin \text{supp}(\mathcal{W}), \end{aligned} \quad (22b)$$

$$\begin{aligned}
h_{\alpha\beta}^{\text{res}}(x_p) &= h_{\alpha\beta}^{\text{R}}(x_p), \quad \nabla_\alpha h_{\alpha\beta}^{\text{res}}(x_p) = \nabla_\alpha h_{\alpha\beta}^{\text{R}}(x_p), \\
h_{\alpha\beta}^{\text{res}}(x) &= h_{\alpha\beta}^{\text{ret}}(x) \quad \text{for } x \notin \text{supp}(\mathcal{W}).
\end{aligned}
\tag{22c}$$

As the residual field coincides with the retarded field far from the particle we can use the usual retarded field boundary conditions when solving Eqs. (21a)–(21c). The details of a numerical implementation of the effective source approach are then much the same as for the Green function and mode-sum regularization schemes. One can use either a frequency domain or a time domain method for solving the field equations, the key differences now being that there is no restriction to 1 + 1D, and that the effective source must be included as a source term. A more thorough review of the effective source approach—including a detailed description of methods for obtaining explicit expressions for the effective source—can be found in Refs. [126, 166].

The effective source approach has been successfully applied in the frequency domain [86], and in the time domain in 1 + 1D [57], 2 + 1D [84, 96, 122] and 3 + 1D [85, 87, 88] contexts. It has also been formulated—but not yet implemented—in the gravitational case to second order in the mass ratio [40, 41]; for the second order problem it is currently the only viable computational strategy. Since the effects of the second-order metric perturbation will be very small—being suppressed by two orders of the mass ratio relative to test body effects—it is likely that a highly accurate numerical scheme will be required, suggesting a frequency domain treatment of the problem where one encounters *ordinary differential equations* (ODEs) which are relatively easy to solve numerically to high accuracy.

4 Evolution Schemes

The calculation of the self-force is only the first stage in the production of an inspiral model. Another critical component is a scheme for evolving the orbit using this self-force information. Various approaches have been proposed, each of which brings with it its own advantages and disadvantages. Approaches which make approximations in the self-force used to drive the inspiral can give substantial decreases in the computational cost of an inspiral simulation, but come at the cost of ignoring potentially relevant physical effects.

4.1 Dissipation Driven Inspirals

A straightforward model for the inspiral can be obtained from energy balance considerations. Using a flux calculation—in which fluxes of energy and angular momentum are obtained by evaluating the point-particle retarded field near the horizon and out at infinity—the entire issue of regularization is avoided and one obtains

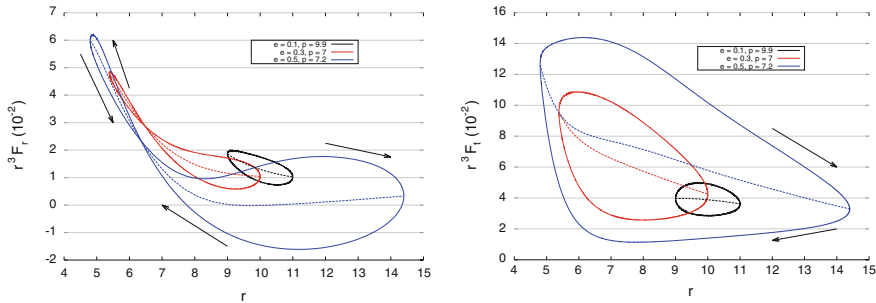


Fig. 9 Radial (*left*) and time (*right*) components of the self-force through one radial cycle, for three different geodesic orbits in Schwarzschild spacetime. *Solid lines* indicate the full self-force and *dashed lines* indicate the conservative-only (*left*) or dissipative-only (*right*) pieces. *Arrows* denote the direction of the geodesic motion. Reproduced from Ref. [87]

an approximation to the contributions to the inspiral coming from dissipative self-force effects. However, this is inadequate for capturing all relevant effects from the first-order self-force. Being a dissipative approximation, it completely misses all conservative corrections to the motion. Furthermore, there is no well-defined way of associating fluxes far from the worldline with an instantaneous local self-force on the worldline; a flux model can only be used to drive an inspiral in a time-averaged sense, ignoring some potentially important dissipative contributions. Nevertheless, the relative straightforwardness and computational efficiency of their implementation have made flux models a compelling approach to assessing qualitative features of self-force driven inspirals. These “kludge” models have been used to produce kludge waveforms for EMRI systems which capture at least some of the qualitative physical effects [44, 45, 48, 49, 162].

To improve on the flux-based dissipative model, one can instead make use of a half-retarded minus half-advanced scheme [43, 51–53] to compute a local, instantaneous dissipative self-force (see Fig. 9). This approach captures all dissipative effects responsible for driving the inspiral, but still neglects small but potentially important conservative corrections to the orbital phase of the system [121].

4.2 Osculating Self-Forced Geodesics

In order to account for both conservative and dissipative effects from the first order self-force, it is essential to build an inspiral model around a full calculation of the local self-force. This, however, still leaves some flexibility in the choice of method for computing this local self-force. One option, based on the osculating geodesics framework [167] is particularly compelling as it allows for dramatic improvements in computational efficiency by separating the coupled problem of simultaneously solving for the orbit and for the regularized retarded field into two independent,

largely uncoupled computational problems. The basic idea is to perturbatively expand the worldline about a geodesic of the background spacetime, $z(\tau) = z_0(\tau) + \dots$. Then, the self-force at first order is a functional not of the evolving orbit $z(\tau)$, but of the geodesic orbit, $z_0(\tau)$, which is instantaneously tangent to the worldline. This expansion is valid in the adiabatic regime, where the orbit is evolving slowly and the difference between the geodesic and evolving orbits is small; the error introduced by the approximation appears at the same order in the equations of motion as a second-order perturbative correction to the field equations.

The improvements in computational efficiency brought about by the osculating geodesics approximation are dramatic. The problem of self-consistently computing the regularized self-force coupled to an arbitrarily evolving orbit is reduced to the much simpler problem of determining the self-force for geodesic worldlines. Since orbits of black hole spacetimes are parametrised by at most three conserved quantities (energy and angular momentum in the Schwarzschild case, supplemented by the Carter constant in the Kerr case), it is computationally tractable to span the entire parameter space of moderately-eccentric geodesic orbits. Even better, the highly-accurate frequency domain mode-sum method can be used because bound geodesic orbits are efficiently represented by a small frequency spectrum. In Ref. [121] this approach was explored over an entire radiation-reaction timescale for moderately-eccentric inspirals in the Schwarzschild spacetime.¹⁰ This was achieved by tabulating the values for the self-force in a relevant portion of the energy-angular momentum phase space of geodesic orbits, and using an interpolated model of the tabulated results to drive an orbital inspiral.

4.3 Self-Consistent Evolution

Unfortunately, the adiabatic approximation responsible for the dramatic improvements in computational efficiency brought by the osculating geodesics framework also introduces errors in the equation of motion at second perturbative order, making the method inadequate for the purposes of precision EMRI astrophysics. One possible solution, implemented in [88] for the scalar field case, is to avoid expanding out the worldline and instead evolve the self-consistent coupled system of equations, Eqs. (1a) and (1b); (2a), (2b) and (2c); or (3a) and (3b). This is a computationally much more difficult problem as the field equations must be solved in the time domain and one cannot rely on an efficient off-line tabulation of self-force values. This self-consistent evolution can in principal be implemented using a time-domain mode-sum scheme, but in practice implementations have instead used the effective source approach since that will be necessary at second perturbative order (see Sect. 3.2 for an explanation of this issue).

¹⁰See also Ref. [168] for an approximate version which assumes a sequence of quasi-circular orbits.

While a self-consistent evolution incorporates all effects contributing to the first order self-force, and only neglects second order contributions from the second order field equations, this comes at the cost of computational efficiency. Whereas an osculating geodesics framework can evolve a large number ($\sim 10,000$) of orbits with ease once the initial off-line tabulation phase is complete [121], the self-consistent scheme requires a long calculation of the solutions of the first-order field equations for each new orbit. In reality, this limits the practicality of the scheme to tens of orbits using current methods. The self-consistent evolution scheme is therefore most valuable as a benchmark against which other, less accurate but more efficient methods can be validated. In fact, comparisons between the self-consistent and osculating geodesics scheme for the scalar case indicate that the osculating geodesics scheme performs remarkably well [169].

4.4 Two-Timescale Expansions

The osculating geodesics scheme is fast, but inaccurate, while the self-consistent evolution scheme is accurate, but slow. This begs the question of whether there is a middle ground which incorporates most of the accuracy of a self-consistent evolution while maintaining the computational efficiency of the osculating geodesics scheme. One promising possibility is that the use of a two-timescale expansion could give just such a scheme. In the two-timescale scheme, rather than using an expansion about a background geodesic (which is valid over short timescales characterised by the orbital motion), one introduces an additional radiation reaction timescale into the problem and incorporates the relevant effects over this radiation reaction timescale.

The relevant two-timescale expansion of the worldline equations of motion was completed in Ref. [52], and follow-up work has improved our understanding of important resonance effects for inspiral orbits [53, 170–179]. In order to consistently incorporate a two-timescale expansion into an orbital evolution scheme, it will also be necessary to have a two-time expansion of the field equations. Promising progress towards such an expansion was recently reported in [180], indicating that it is likely that a self-consistent orbital evolution using a two-timescale expansion is indeed feasible.

5 Discussion

The techniques described in this review represent the current state of the art of self-force calculations. The three primary approaches: worldline convolutions, mode-sum regularization and the effective source approach can be considered complimentary, with each having regimes where they are most appropriate:

- The mode-sum scheme gives unparalleled accuracy (particularly in the frequency domain) for orbits which have a small frequency spectrum.
- The worldline convolution method provides valuable physical insight and can be easily applied to arbitrary orbital configurations, including those inaccessible by other means.
- The effective source approach can be used in arbitrary spacetimes without relying on any symmetries, and also stands out as the most applicable to a second order calculation.

There still remain important developments to be made in each case. For example, the mode sum and effective source schemes are still under development for the Kerr gravitational case, and worldline convolution approaches have yet to be fully applied to the gravitational case for any spacetime.

Finally, it should be pointed out that this review is not an exhaustive exposition of all self-force computation strategies. Many other calculations have not been described, including alternative regularization strategies [66, 181, 182], near-horizon waveform calculations [183–186], methods based on effective field theory [187–190], analytic calculations in particularly simple cases [95, 191, 192], black holes in higher dimensions [193], and calculations in non-black hole spacetimes such as wormholes [194, 195] and cosmological models [196, 197]. More details can be found in the reviews [60, 61], and references therein.

Acknowledgments I am grateful to Scott Field and David Nichols for helpful discussions during the preparation of this article, to Peter Diener for providing the data used in Fig. 7, and to Niels Warburton, Scott Field and Eanna Flanagan for helpful comments on an early draft of this paper. This material is based upon work supported by the National Science Foundation under Grant Number 1417132. B.W. was supported by Science Foundation Ireland under Grant No. 10/RFP/PHY2847, by the John Templeton Foundation New Frontiers Program under Grant No. 37426 (University of Chicago) - FP050136-B (Cornell University), and by the Irish Research Council, which is funded under the National Development Plan for Ireland.

References

1. J. Magorrian, S. Tremaine, D. Richstone, R. Bender, G. Bower et al., The Demography of massive dark objects in galaxy centers. *Astron. J.* **115**, 2285 (1998)
2. J.R. Gair, L. Barack, T. Creighton, C. Cutler, S.L. Larson et al., Event rate estimates for LISA extreme mass ratio capture sources. *Class. Quantum Gravity* **21**, S1595–S1606 (2004)
3. P. Amaro-Seoane, J.R. Gair, M. Marc Freitag, C. Miller, I. Mandel et al., Astrophysics, detection and science applications of intermediate- and extreme mass-ratio inspirals. *Class. Quantum Gravity* **24**, R113–R169 (2007)
4. J.R. Gair, Probing black holes at low redshift using LISA EMRI observations. *Class. Quantum Gravity* **26**, 094034 (2009)
5. P. Amaro-Seoane, S. Aoudia, S. Babak, P. Binétruy, E. Berti, A. Bohé, C. Caprini, M. Colpi, N.J. Cornish, K. Danzmann, J.-F. Dufaux, J. Gair, I. Hinder, O. Jennrich, P. Jetzer, A. Klein, R.N. Lang, A. Lobo, T. Littenberg, S.T. McWilliams, G. Nelemans, A. Petiteau, E.K. Porter, B.F. Schutz, A. Sesana, R. Stebbins, T. Sumner, M. Vallisneri, S. Vitale, M. Volonteri, H.

- Ward, B. Wardell, eLISA: Astrophysics and cosmology in the millihertz regime. *GW Notes* **6**, 4–110 (2013)
6. <http://www.elisascience.org>
 7. <http://www.ligo.org/>
 8. L. Barack, C. Cutler, LISA capture sources: approximate waveforms, signal-to-noise ratios, and parameter estimation accuracy. *Phys. Rev.* **D69**, 082005 (2004)
 9. S. Babak, J.R. Gair, A. Petiteau, A. Sesana, Fundamental physics and cosmology with LISA. *Class. Quantum Gravity* **28**, 114001 (2011)
 10. J.R. Gair, A. Sesana, E. Berti, M. Volonteri, Constraining properties of the black hole population using LISA. *Class. Quantum Gravity* **28**, 094018 (2011)
 11. I. Hinder, The current status of binary black hole simulations in numerical relativity. *Class. Quantum Gravity* **27**, 114004 (2010)
 12. H.P. Pfeiffer, Numerical simulations of compact object binaries. *Class. Quantum Gravity* **29**, 124004 (2012)
 13. U. Sperhake, The numerical relativity breakthrough for binary black holes. *Class. Quantum Gravity* (in press)
 14. A. Le Tiec, The overlap of numerical relativity, perturbation theory and post-Newtonian theory in the binary black hole problem. *Int. J. Mod. Phys.* **D23**(10), 1430022 (2014)
 15. S. Isoyama, R. Fujita, N. Sago, H. Tagoshi, T. Tanaka, Impact of the second-order self-forces on the dephasing of the gravitational waves from quasicircular extreme mass-ratio inspirals. *Phys. Rev.* **D87**(2), 024010 (2013)
 16. L.M. Burko, G. Khanna, Self-force gravitational waveforms for extreme and intermediate mass ratio inspirals. II: importance of the second-order dissipative effect. *Phys. Rev.* **D88**(2), 024002 (2013)
 17. A. Le Tiec, A.H. Mroue, L. Barack, A. Buonanno, H.P. Pfeiffer et al., Periastron advance in black hole binaries. *Phys. Rev. Lett.* **107**, 141101 (2011)
 18. A. Le Tiec, A. Buonanno, A.H. Mroue, H.P. Pfeiffer, D.A. Hemberger et al., Periastron advance in spinning black hole binaries: gravitational self-force from numerical relativity. *Phys. Rev.* **D88**(12), 124027 (2013)
 19. Y. Mino, M. Sasaki, T. Tanaka, Gravitational radiation reaction to a particle motion. *Phys. Rev.* **D55**, 3457–3476 (1997)
 20. T.C. Quinn, R.M. Wald, An axiomatic approach to electromagnetic and gravitational radiation reaction of particles in curved space-time. *Phys. Rev.* **D56**, 3381–3394 (1997)
 21. P.A.M. Dirac, Classical theory of radiating electrons. *Proc. R. Soc. Lond.* **A167**, 148–169 (1938)
 22. B.S. DeWitt, R.W. Brehme, Radiation damping in a gravitational field. *Ann. Phys.* **9**, 220–259 (1960)
 23. J.M. Hobbs, A vierbien formalism of radiation damping. *Ann. Phys.* **47**, 141 (1968)
 24. T.C. Quinn, Axiomatic approach to radiation reaction of scalar point particles in curved space-time. *Phys. Rev.* **D62**, 064029 (2000)
 25. S.L. Detweiler, B.F. Whiting, Selfforce via a Green's function decomposition. *Phys. Rev.* **D67**, 024025 (2003)
 26. A.I. Harte, Self-forces from generalized Killing fields. *Class. Quantum Gravity* **25**, 235020 (2008)
 27. A.I. Harte, Electromagnetic self-forces and generalized Killing fields. *Class. Quantum Gravity* **26**, 155015 (2009)
 28. A.I. Harte, Effective stress-energy tensors, self-force, and broken symmetry. *Class. Quantum Gravity* **27**, 135002 (2010)
 29. C.R. Galley, A nonlinear scalar model of extreme mass ratio inspirals in effective field theory I. Self force through third order. *Class. Quantum Gravity* **29**, 015010 (2012)
 30. C.R. Galley, A Nonlinear scalar model of extreme mass ratio inspirals in effective field theory II. Scalar perturbations and a master source. *Class. Quantum Gravity* **29**, 015011 (2012)
 31. S.E. Gralla, R.M. Wald, A rigorous derivation of gravitational self-force. *Class. Quantum Gravity* **25**, 205009 (2008)

32. A. Pound, Self-consistent gravitational self-force. *Phys. Rev.* **D81**, 024023 (2010)
33. S.E. Gralla, A.I. Harte, R.M. Wald, A rigorous derivation of electromagnetic self-force. *Phys. Rev.* **D80**, 024031 (2009)
34. E. Rosenthal, Regularization of second-order scalar perturbation produced by a point-particle with a nonlinear coupling. *Class. Quantum Gravity* **22**, S859 (2005)
35. E. Rosenthal, Regularization of the second-order gravitational perturbations produced by a compact object. *Phys. Rev.* **D72**, 121503 (2005)
36. E. Rosenthal, Construction of the second-order gravitational perturbations produced by a compact object. *Phys. Rev.* **D73**, 044034 (2006)
37. E. Rosenthal, Second-order gravitational self-force. *Phys. Rev.* **D74**, 084018 (2006)
38. A. Pound, Second-order gravitational self-force. *Phys. Rev. Lett.* **109**, 051101 (2012)
39. A. Pound, Nonlinear gravitational self-force. I. Field outside a small body. *Phys. Rev.* **D86**, 084019 (2012)
40. A. Pound, J. Miller, A practical, covariant puncture for second-order self-force calculations. *Phys. Rev.* **D89**, 104020 (2014)
41. S.E. Gralla, Second order gravitational self force. *Phys. Rev.* **D85**, 124011 (2012)
42. S. Detweiler, Gravitational radiation reaction and second order perturbation theory. *Phys. Rev.* **D85**, 044048 (2012)
43. Y. Mino, Perturbative approach to an orbital evolution around a supermassive black hole. *Phys. Rev.* **D67**, 084027 (2003)
44. K. Glampedakis, D. Kennefick, Zoom and whirl: eccentric equatorial orbits around spinning black holes and their evolution under gravitational radiation reaction. *Phys. Rev.* **D66**, 044002 (2002)
45. S.A. Hughes, S. Drasco, E.E. Flanagan, J. Franklin, Gravitational radiation reaction and inspiral waveforms in the adiabatic limit. *Phys. Rev. Lett.* **94**, 221101 (2005)
46. N. Sago, T. Tanaka, W. Hikida, K. Ganz, H. Nakano, The Adiabatic evolution of orbital parameters in the Kerr spacetime. *Prog. Theor. Phys.* **115**, 873–907 (2006)
47. S. Drasco, E.E. Flanagan, S.A. Hughes, Computing inspirals in Kerr in the adiabatic regime. I. The scalar case. *Class. Quantum Gravity* **22**, S801–S846 (2005)
48. S. Drasco, S.A. Hughes, Gravitational wave snapshots of generic extreme mass ratio inspirals. *Phys. Rev.* **D73**(10), 024027 (2006)
49. P.A. Sundararajan, G. Khanna, S.A. Hughes, Towards adiabatic waveforms for inspiral into Kerr black holes. I. A new model of the source for the time domain perturbation equation. *Phys. Rev.* **D76**, 104005 (2007)
50. R. Fujita, W. Hikida, H. Tagoshi, An efficient numerical method for computing gravitational waves induced by a particle moving on eccentric inclined orbits around a Kerr black hole. *Prog. Theor. Phys.* **121**, 843–874 (2009)
51. S.E. Gralla, J.L. Friedman, A.G. Wiseman, Numerical radiation reaction for a scalar charge in Kerr circular orbit (2005). [arXiv:gr-qc/0502123](https://arxiv.org/abs/gr-qc/0502123)
52. T. Hinderer, E.E. Flanagan, Two timescale analysis of extreme mass ratio inspirals in Kerr I. Orbital motion. *Phys. Rev.* **D78**, 064028 (2008)
53. E.E. Flanagan, S.A. Hughes, U. Ruangsri, Resonantly enhanced and diminished strong-field gravitational-wave fluxes. *Phys. Rev.* **D89**(8), 084028 (2014)
54. L. Barack, A. Ori, Mode sum regularization approach for the selfforce in black hole space-time. *Phys. Rev.* **D61**, 061502 (2000)
55. L. Barack, Y. Mino, H. Nakano, A. Ori, M. Sasaki, Calculating the gravitational selfforce in Schwarzschild space-time. *Phys. Rev. Lett.* **88**, 091101 (2002)
56. L. Barack, D.A. Golbourn, Scalar-field perturbations from a particle orbiting a black hole using numerical evolution in 2+1 dimensions. *Phys. Rev.* **D76**, 044020 (2007)
57. I. Vega, S.L. Detweiler, Regularization of fields for self-force problems in curved spacetime: foundations and a time-domain application. *Phys. Rev.* **D77**, 084008 (2008)
58. E. Poisson, A.G. Wiseman, Suggestion at the 1st Capra Ranch meeting on radiation reaction (1998)

59. W.G. Anderson, A.G. Wiseman, A matched expansion approach to practical self-force calculations. *Class. Quantum Gravity* **22**, S783–S800 (2005)
60. E. Poisson, A. Pound, I. Vega, The motion of point particles in curved spacetime. *Living Rev. Relativ.* **14**, 7 (2011)
61. S.L. Detweiler, Perspective on gravitational self-force analyses. *Class. Quantum Gravity* **22**, S681–S716 (2005)
62. L. Barack, Gravitational self force in extreme mass-ratio inspirals. *Class. Quantum Gravity* **26**, 213001 (2009)
63. L. Blanchet, A. Spallicci, B. Whiting, Mass and motion in general relativity, in *Proceedings of School on Mass*, Orleans, France, 23–25 June 2008. *Fundam. Theor. Phys.* **162**, 1–624 (2011)
64. C.W. Misner, K.S. Thorne, J.A. Wheeler, *Gravitation* (Freeman, San Francisco, 1973)
65. C.O. Lousto, H. Nakano, A new method to integrate (2+1)-wave equations with Dirac’s delta functions as sources. *Class. Quantum Gravity* **25**, 145018 (2008)
66. B. Kol, Self force from equivalent periodic sources (2013). [arXiv:1307.4064](https://arxiv.org/abs/1307.4064)
67. M. Casals, S. Dolan, A.C. Ottewill, B. Wardell, Pade approximants of the Green function in spherically symmetric spacetimes. *Phys. Rev.* **D79**, 124044 (2009)
68. A.C. Ottewill, B. Wardell, Quasilocal contribution to the scalar self-force: Geodesic motion. *Phys. Rev.* **D77**, 104002 (2008)
69. M. Casals, S. Dolan, A.C. Ottewill, B. Wardell, Self-force and Green function in Schwarzschild spacetime via quasinormal modes and branch cut. *Phys. Rev.* **D88**, 044022 (2013)
70. B. Wardell, C.R. Galley, A. Zenginoglu, M. Casals, S.R. Dolan et al., Self-force via Green functions and worldline integration. *Phys. Rev.* **D89**, 084021 (2014)
71. A. Zenginoglu, C.R. Galley, Caustic echoes from a Schwarzschild black hole. *Phys. Rev.* **D86**, 064030 (2012)
72. M. Casals, E. Poisson, I. Vega, Regularization of static self-forces. *Phys. Rev.* **D86**, 064033 (2012)
73. A.C. Ottewill, B. Wardell, Quasi-local contribution to the scalar self-force: non-geodesic motion. *Phys. Rev.* **D79**, 024031 (2009)
74. L. Barack, L.M. Burko, Radiation reaction force on a particle plunging into a black hole. *Phys. Rev.* **D62**, 084040 (2000)
75. L.M. Burko, Selfforce on particle in orbit around a black hole. *Phys. Rev. Lett.* **84**, 4529 (2000)
76. S.L. Detweiler, E. Messaritaki, B.F. Whiting, Selfforce of a scalar field for circular orbits about a Schwarzschild black hole. *Phys. Rev.* **D67**, 104016 (2003)
77. L.-M. Diaz-Rivera, E. Messaritaki, B.F. Whiting, S.L. Detweiler, Scalar field self-force effects on orbits about a Schwarzschild black hole. *Phys. Rev.* **D70**, 124018 (2004)
78. P. Canizares, C.F. Sopuerta, An efficient pseudospectral method for the computation of the self-force on a charged particle: circular geodesics around a Schwarzschild black hole. *Phys. Rev.* **D79**, 084020 (2009)
79. R. Haas, Scalar self-force on eccentric geodesics in Schwarzschild spacetime: a time-domain computation. *Phys. Rev.* **D75**, 124011 (2007)
80. R. Haas, E. Poisson, Mode-sum regularization of the scalar self-force: formulation in terms of a tetrad decomposition of the singular field. *Phys. Rev.* **D74**, 044009 (2006)
81. P. Canizares, C.F. Sopuerta, J.L. Jaramillo, Pseudospectral collocation methods for the computation of the self-force on a charged particle: generic orbits around a Schwarzschild black hole. *Phys. Rev.* **D82**, 044023 (2010)
82. A. Heffernan, A. Ottewill, B. Wardell, High-order expansions of the Detweiler-Whiting singular field in Schwarzschild spacetime. *Phys. Rev.* **D86**, 104023 (2012)
83. J. Thornburg, Highly accurate and efficient self-force computations using time-domain methods: Error estimates, validation, and optimization (2010). [arXiv:1006.3788](https://arxiv.org/abs/1006.3788)
84. S.R. Dolan, L. Barack, Self force via m-mode regularization and 2+1D evolution: foundations and a scalar-field implementation on Schwarzschild. *Phys. Rev.* **D83**, 024019 (2011)

85. I. Vega, P. Diener, W. Tichy, S.L. Detweiler, Self-force with (3+1) codes: a Primer for numerical relativists. *Phys. Rev.* **D80**, 084021 (2009)
86. N. Warburton, B. Wardell, Applying the effective-source approach to frequency-domain self-force calculations. *Phys. Rev.* **D89**, 044046 (2014)
87. I. Vega, B. Wardell, P. Diener, S. Cupp, R. Haas, Scalar self-force for eccentric orbits around a Schwarzschild black hole. *Phys. Rev.* **D88**, 084021 (2013)
88. P. Diener, I. Vega, B. Wardell, S. Detweiler, Self-consistent orbital evolution of a particle around a Schwarzschild black hole. *Phys. Rev. Lett.* **108**, 191102 (2012)
89. N. Warburton, L. Barack, Self force on a scalar charge in Kerr spacetime: circular equatorial orbits. *Phys. Rev.* **D81**, 084039 (2010)
90. A. Heffernan, A. Ottewill, B. Wardell, High-order expansions of the Detweiler-Whiting singular field in Kerr spacetime. *Phys. Rev.* **D89**, 024030 (2014)
91. N. Warburton, L. Barack, Self force on a scalar charge in Kerr spacetime: eccentric equatorial orbits. *Phys. Rev.* **D83**, 124038 (2011)
92. N. Warburton, Self force on a scalar charge in Kerr spacetime: inclined circular orbits. *Phys. Rev.* **D91**, 024045 (2015)
93. T.M. Linz, J.L. Friedman, A.G. Wiseman, Self force on an accelerated particle. *Phys. Rev.* **D90**, 024064 (2014)
94. L.M. Burko, Y.T. Liu, Selfforce on a scalar charge in the space-time of a stationary, axisymmetric black hole. *Phys. Rev.* **D64**, 024006 (2001)
95. A.C. Ottewill, P. Taylor, Static Kerr Green's function in closed form and an analytic derivation of the self-force for a static scalar charge in Kerr space-time. *Phys. Rev.* **D86**, 024036 (2012)
96. S.R. Dolan, L. Barack, B. Wardell, Self force via m -mode regularization and 2+1D evolution: II. Scalar-field implementation on Kerr spacetime. *Phys. Rev.* **D84**, 084001 (2011)
97. J. Thornburg, Scalar self-force for highly eccentric orbits in Kerr spacetime, in *17th Capra Meeting on Radiation Reaction in General Relativity*, <http://www.tapir.caltech.edu/~capra17/talks/by-id/a425ec3f30f7f652d27107b1ec5538c8/thornburg-caltech-capra-2014-06-23.pdf>
98. R. Haas, Time domain calculation of the electromagnetic self-force on eccentric geodesics in Schwarzschild spacetime (2011). [arXiv:1112.3707](https://arxiv.org/abs/1112.3707)
99. J. Kuchar, E. Poisson, I. Vega, Electromagnetic self-force on a static charge in Schwarzschild-de Sitter spacetimes. *Class. Quantum Gravity* **30**, 235033 (2013)
100. P. Zimmerman, I. Vega, E. Poisson, R. Haas, Self-force as a cosmic censor. *Phys. Rev.* **D87**(4), 041501 (2013)
101. W.G. Anderson, E.E. Flanagan, A.C. Ottewill, Quasi-local contribution to the gravitational self-force. *Phys. Rev.* **D71**, 024036 (2005)
102. L. Barack, C.O. Lousto, Computing the gravitational selfforce on a compact object plunging into a Schwarzschild black hole. *Phys. Rev.* **D66**, 061502 (2002)
103. L. Barack, C.O. Lousto, Perturbations of Schwarzschild black holes in the Lorenz gauge: formulation and numerical implementation. *Phys. Rev.* **D72**, 104026 (2005)
104. S.R. Dolan, N. Warburton, A.I. Harte, A. Le Tiec, B. Wardell et al., Gravitational self-torque and spin precession in compact binaries. *Phys. Rev.* **D89**(6), 064011 (2014)
105. S.R. Dolan, P. Nolan, A.C. Ottewill, N. Warburton, B. Wardell, Tidal invariants for compact binaries on quasi-circular orbits. *Phys. Rev.* **D91**, 023009 (2015)
106. S.E. Field, J.S. Hesthaven, S.R. Lau, Persistent junk solutions in time-domain modeling of extreme mass ratio binaries. *Phys. Rev.* **D81**, 124030 (2010)
107. T.S. Keidl, A.G. Shah, J.L. Friedman, D.-H. Kim, L.R. Price, Gravitational self-force in a radiation gauge. *Phys. Rev.* **D82**, 124012 (2010)
108. C. Merlin, A.G. Shah, Self-force from reconstructed metric perturbations: numerical implementation in Schwarzschild spacetime. *Phys. Rev.* **D91**(2), 024005 (2015)
109. N. Sago, L. Barack, S.L. Detweiler, Two approaches for the gravitational self force in black hole spacetime: comparison of numerical results. *Phys. Rev.* **D78**, 124024 (2008)
110. A.G. Shah, T.S. Keidl, J.L. Friedman, D.-H. Kim, L.R. Price, Conservative, gravitational self-force for a particle in circular orbit around a Schwarzschild black hole in a radiation gauge. *Phys. Rev.* **D83**, 064018 (2011)

111. S. Akcay, A fast frequency-domain algorithm for gravitational self-force: I. Circular orbits in Schwarzschild spacetime. *Phys. Rev.* **D83**, 124026 (2011)
112. L. Barack, A. Ori, N. Sago, Frequency-domain calculation of the self force: the high-frequency problem and its resolution. *Phys. Rev.* **D78**, 084021 (2008)
113. L. Barack, N. Sago, Gravitational self-force on a particle in eccentric orbit around a Schwarzschild black hole. *Phys. Rev.* **D81**, 084021 (2010)
114. N. Sago, Gravitational self-force effects on a point mass moving around a Schwarzschild black hole. *Class. Quantum Gravity* **26**, 094025 (2009)
115. S.E. Field, J.S. Hesthaven, S.R. Lau, Discontinuous Galerkin method for computing gravitational waveforms from extreme mass ratio binaries. *Class. Quantum Gravity* **26**, 165010 (2009)
116. S. Hopper, C.R. Evans, Gravitational perturbations and metric reconstruction: method of extended homogeneous solutions applied to eccentric orbits on a Schwarzschild black hole. *Phys. Rev.* **D82**, 084010 (2010)
117. S. Hopper, C.R. Evans, Metric perturbations from eccentric orbits on a Schwarzschild black hole: I. Odd-parity Regge-Wheeler to Lorenz gauge transformation and two new methods to circumvent the Gibbs phenomenon. *Phys. Rev.* **D87**(6), 064008 (2013)
118. S. Akcay, N. Warburton, L. Barack, Frequency-domain algorithm for the Lorenz-gauge gravitational self-force. *Phys. Rev.* **D88**(10), 104009 (2013)
119. A. Pound, C. Merlin, L. Barack, Gravitational self-force from radiation-gauge metric perturbations. *Phys. Rev.* **D89**, 024009 (2014)
120. T. Osburn, E. Forseth, C.R. Evans, S. Hopper, Lorenz gauge gravitational self-force calculations of eccentric binaries using a frequency domain procedure. *Phys. Rev.* **D90**(10), 104031 (2014)
121. N. Warburton, S. Akcay, L. Barack, J.R. Gair, N. Sago, Evolution of inspiral orbits around a Schwarzschild black hole. *Phys. Rev.* **D85**, 061501 (2012)
122. S.R. Dolan, L. Barack, Self-force via m -mode regularization and 2+1D evolution: III. Gravitational field on Schwarzschild spacetime. *Phys. Rev.* **D87**, 084066 (2013)
123. C. Kavanagh, Scalar Green function in Kerr spacetime: branch cut contribution, in *17th Capra Meeting on Radiation Reaction in General Relativity*, http://www.tapir.caltech.edu/~capra17/talks/by-id/6c0aa3c2d1f42cfb4b61b26db5d729b4/Capra17_CKavanagh.pdf
124. A.G. Shah, J.L. Friedman, T.S. Keidl, EMRI corrections to the angular velocity and redshift factor of a mass in circular orbit about a Kerr black hole. *Phys. Rev.* **D86**, 084059 (2012)
125. S. Dolan, Approaches to self-force calculations on Kerr spacetime, in *16th Capra Meeting on Radiation Reaction in General Relativity*, <http://maths.ucd.ie/capra16/talks/Dolan.pdf>
126. B. Wardell, I. Vega, J. Thornburg, P. Diener, A generic effective source for scalar self-force calculations. *Phys. Rev.* **D85**, 104044 (2012)
127. R.A. Capon, Radiation reaction near black holes. Ph.D. thesis, University of Wales (1998)
128. M. Casals, S.R. Dolan, A.C. Ottewill, B. Wardell, Self-force calculations with matched expansions and quasinormal mode sums. *Phys. Rev. D* **79**, 124043 (2009)
129. B. Wardell M. Casals, Self-force via worldline integration of the Green function, in *17th Capra Meeting on Radiation Reaction in General Relativity*, <http://www.tapir.caltech.edu/~capra17/talks/by-id/cd6fd7365091903b9748c2ff48b477a3/GreenFunctions.pdf>
130. I.G. Avramidi, Covariant methods for the calculation of the effective action in quantum field theory and investigation of higher derivative quantum gravity. Ph.D. thesis, Moscow State University (1986)
131. I.G. Avramidi, Heat kernel and quantum gravity. *Lect. Notes Phys.* **M64**, 1–149 (2000)
132. Y. Decanini, A. Folacci, Off-diagonal coefficients of the Dewitt-Schwinger and Hadamard representations of the Feynman propagator. *Phys. Rev.* **D73**, 044027 (2006)
133. A.C. Ottewill, B. Wardell, A transport equation approach to calculations of Hadamard Green functions and non-coincident DeWitt coefficients. *Phys. Rev.* **D84**, 104039 (2011)
134. S.A. Teukolsky, Rotating black holes—separable wave equations for gravitational and electromagnetic perturbations. *Phys. Rev. Lett.* **29**, 1114–1118 (1972)

135. S.A. Teukolsky, Perturbations of a rotating black hole. I. Fundamental equations for gravitational electromagnetic and neutrino field perturbations. *Astrophys. J.* **185**, 635–647 (1973)
136. T. Regge, J.A. Wheeler, Stability of a Schwarzschild singularity. *Phys. Rev.* **108**, 1063–1069 (1957)
137. F.J. Zerilli, Gravitational field of a particle falling in a Schwarzschild geometry analyzed in tensor harmonics. *Phys. Rev.* **D2**, 2141–2160 (1970)
138. C.V. Vishveshwara, Stability of the Schwarzschild metric. *Phys. Rev.* **D1**, 2870–2879 (1970)
139. V. Moncrief, Gravitational perturbations of spherically symmetric systems I. The exterior problem. *Ann. Phys.* **88**, 323–342 (1974)
140. C.T. Cunningham, R.H. Price, V. Moncrief, Radiation from collapsing relativistic stars. I—linearized odd-parity radiation. *Astrophys. J.* **224**, 643 (1978)
141. C.T. Cunningham, R.H. Price, V. Moncrief, Radiation from collapsing relativistic stars. II—linearized even parity radiation. *Astrophys. J.* **230**, 870–892 (1979)
142. K. Martel, E. Poisson, Gravitational perturbations of the Schwarzschild spacetime: a practical covariant and gauge-invariant formalism. *Phys. Rev.* **D71**, 104003 (2005)
143. M.V. Berndtson, Harmonic gauge perturbations of the Schwarzschild metric. Ph.D. thesis, University of Colorado (1996)
144. E.W. Leaver, Spectral decomposition of the perturbation response of the Schwarzschild geometry. *Phys. Rev.* **D34**, 384–408 (1986)
145. E.W. Leaver, Erratum: spectral decomposition of the perturbation response of the schwarzschild geometry. *Phys. Rev.* **D38**, 725–725 (1988)
146. M. Casals, A. Ottewill, The branch cut and quasi-normal modes at large imaginary frequency in Schwarzschild space-time. *Phys. Rev.* **D86**, 024021 (2012)
147. S.E. Field, C.R. Galley, J.S. Hesthaven, J. Kaye, M. Tiglio, Fast prediction and evaluation of gravitational waveforms using surrogate models. *Phys. Rev.* **X4**, 031006 (2014)
148. J.L. Jaramillo, C.F. Sopuerta, P. Canizares, Are Time-Domain Self-Force Calculations Contaminated by Jost Solutions? *Phys. Rev.* **D83**, 061503 (2011)
149. L. Barack, N. Sago, Gravitational self force on a particle in circular orbit around a Schwarzschild black hole. *Phys. Rev.* **D75**, 064021 (2007)
150. S. Isoyama, L. Barack, S.R. Dolan, A. Le Tiec, H. Nakano et al., Gravitational self-force correction to the innermost stable circular equatorial orbit of a Kerr black hole. *Phys. Rev. Lett.* **113**(16), 161101 (2014)
151. M. Sasaki, T. Nakamura, A class of new perturbation equations for the Kerr geometry. *Phys. Lett.* **A89**, 68–70 (1982)
152. M. Sasaki, T. Nakamura, Gravitational radiation from a Kerr black hole. 1. Formulation and a method for numerical analysis. *Prog. Theor. Phys.* **67**, 1788 (1982)
153. E.W. Leaver, Solutions to a generalized spheroidal wave equation: Teukolsky’s equations in general relativity, and the two-center problem in molecular quantum mechanics. *J. Math. Phys.* **27**, 1238–1265 (1986)
154. S. Mano, H. Suzuki, E. Takasugi, Analytic solutions of the Teukolsky equation and their low frequency expansions. *Prog. Theor. Phys.* **95**, 1079–1096 (1996)
155. A.G. Shah, J.L. Friedman, B.F. Whiting, Finding high-order analytic post-Newtonian parameters from a high-precision numerical self-force calculation. *Phys. Rev.* **D89**, 064042 (2014)
156. A.G. Shah, Gravitational-wave flux for a particle orbiting a Kerr black hole to 20th post-Newtonian order: a numerical approach. *Phys. Rev.* **D90**(4), 044025 (2014)
157. D. Bini, T. Damour, Analytic determination of the eight-and-a-half post-Newtonian self-force contributions to the two-body gravitational interaction potential. *Phys. Rev.* **D89**(10), 104047 (2014)
158. D. Bini, T. Damour, Two-body gravitational spin-orbit interaction at linear order in the mass ratio. *Phys. Rev.* **D90**, 024039 (2014)
159. D. Bini, T. Damour, Gravitational self-force corrections to two-body tidal interactions and the effective one-body formalism. *Phys. Rev.* **D90**(12), 124037 (2014)
160. M. Sasaki, H. Tagoshi, Analytic black hole perturbation approach to gravitational radiation. *Living Rev. Relativ.* **6**, 6 (2003)

161. J.L. Barton, D.J. Lazar, D.J. Kennefick, G. Khanna, L.M. Burko, Computational efficiency of frequency and time-domain calculations of extreme mass-ratio binaries: equatorial orbits. *Phys. Rev. D* **78**, 064042 (2008)
162. P.A. Sundararajan, G. Khanna, S.A. Hughes, S. Drasco, Towards adiabatic waveforms for inspiral into Kerr black holes: II. Dynamical sources and generic orbits. *Phys. Rev. D* **78**, 024022 (2008)
163. S.R. Dolan, Superradiant instabilities of rotating black holes in the time domain. *Phys. Rev. D* **87**(12), 124026 (2013)
164. L.C. Stein, Probes of strong-field gravity. Ph.D. thesis, Massachusetts Institute of Technology (2012)
165. P. Diener, I. Vega, B. Wardell, A smoother effective source for scalar self-force simulations. APS April meeting (2014). <http://meetings.aps.org/link/BAPS.2014.APR.X15.5>
166. I. Vega, B. Wardell, P. Diener, Effective source approach to self-force calculations. *Class. Quantum Gravity* **28**, 134010 (2011)
167. A. Pound, E. Poisson, Osculating orbits in Schwarzschild spacetime, with an application to extreme mass-ratio inspirals. *Phys. Rev. D* **77**, 044013 (2008)
168. K.A. Lackeos, L.M. Burko, Self-forced gravitational waveforms for extreme and intermediate mass ratio inspirals. *Phys. Rev. D* **86**, 084055 (2012)
169. N. Warburton, Numerical approaches to computing the self-force and related quantities, in *17th Capra Meeting on Radiation Reaction in General Relativity*. http://www.tapir.caltech.edu/~capra17/talks/by-id/e8888ab334817da52763737c8ab5f984/Capra_17_Warburton1_flatten_stages.pdf
170. E.E. Flanagan, T. Hinderer, Transient resonances in the inspirals of point particles into black holes. *Phys. Rev. Lett.* **109**, 071102 (2012)
171. C.M. Hirata, Resonant recoil in extreme mass ratio binary black hole mergers. *Phys. Rev. D* **83**, 104024 (2011)
172. R. Grossman, J. Levin, G. Perez-Giz, The harmonic structure of generic Kerr orbits. *Phys. Rev. D* **85**, 023012 (2012)
173. R. Grossman, J. Levin, G. Perez-Giz, Faster computation of adiabatic extreme mass-ratio inspirals using resonances. *Phys. Rev. D* **88**(2), 023002 (2013)
174. J. Gair, N. Yunes, C.M. Bender, Resonances in extreme mass-ratio inspirals: asymptotic and hyperasymptotic analysis. *J. Math. Phys.* **53**, 032503 (2012)
175. S. Isoyama, R. Fujita, N. Sago, T. Tanaka, Evolution of the Carter constant for resonant inspirals into a Kerr black hole: I. The scalar case. *PTEP* **2013**(6), 063E01 (2013)
176. J. Brink, M. Geyer, T. Hinderer, Orbital resonances around Black holes *Phys. Rev. Lett.* **114**, (8) 081102 (2015). [arXiv:1304.0330](https://arxiv.org/abs/1304.0330)
177. U. Ruangsri, S.A. Hughes, Census of transient orbital resonances encountered during binary inspiral. *Phys. Rev. D* **89**(8), 084036 (2014)
178. M. van de Meent, Conditions for sustained orbital resonances in extreme mass ratio inspirals. *Phys. Rev. D* **89**(8), 084033 (2014)
179. M. van de Meent, Resonantly enhanced kicks from equatorial small mass-ratio inspirals. *Phys. Rev. D* **90**(4), 044027 (2014)
180. J. Moxon, Higher-order expansions of self-forces for use in two-timescale analyses, in *17th Capra Meeting on Radiation Reaction in General Relativity*, http://www.tapir.caltech.edu/~capra17/talks/by-id/235094cbacbd7089b07b3cc37c96eea5/Capra17_Moxon.pdf
181. E. Rosenthal, Massive field approach to the scalar selfforce in curved space-time. *Phys. Rev. D* **69**, 064035 (2004)
182. E. Rosenthal, Scalar self-force on a static particle in Schwarzschild using the massive field approach. *Phys. Rev. D* **70**, 124016 (2004)
183. G. d'Ambrosi, J.W. van Holten, Ballistic orbits in Schwarzschild space-time and gravitational waves from EMR binary mergers. *Class. Quantum Gravity* **32**(1), 015012 (2015)
184. S. Hadar, B. Kol, Post-ISCO ringdown amplitudes in extreme mass ratio inspiral. *Phys. Rev. D* **84**, 044019 (2011)

185. S. Hadar, B. Kol, E. Berti, V. Cardoso, Comparing numerical and analytical calculations of post-ISCO ringdown amplitudes. *Phys. Rev.* **D84**, 047501 (2011)
186. S. Hadar, A.P. Porfyriadis, A. Strominger, Gravity waves from extreme-mass-ratio plunges into Kerr black holes. *Phys. Rev.* **D90**(6), 064045 (2014)
187. O. Birnholtz, S. Hadar, B. Kol, Theory of post-Newtonian radiation and reaction. *Phys. Rev.* **D88**(10), 104037 (2013)
188. O. Birnholtz, S. Hadar, Action for reaction in general dimension. *Phys. Rev.* **D89**(4), 045003 (2014)
189. O. Birnholtz, S. Hadar, B. Kol, Radiation reaction at the level of the action. *Int. J. Mod. Phys.* **A29**(24), 1450132 (2014)
190. O. Birnholtz, Comments on initial conditions for the Abraham-Lorentz(-Dirac) equation *Int. J. Mod. Phys.* **A30**, (2), 1550011 (2015). [arXiv:1410.5871](https://arxiv.org/abs/1410.5871)
191. A.G. Wiseman, The Selfforce on a static scalar test charge outside a Schwarzschild black hole. *Phys. Rev.* **D61**, 084014 (2000)
192. D.H.J. Cho, A.A. Tsokaros, A.G. Wiseman, The self-force on a non-minimally coupled static scalar charge outside a Schwarzschild black hole. *Class. Quantum Gravity* **24**, 1035–1048 (2007)
193. M.J.S. Beach, E. Poisson, B.G. Nickel, Self-force on a charge outside a five-dimensional black hole. *Phys. Rev.* **D89**(12), 124014 (2014)
194. P. Taylor, Self-force on an arbitrarily coupled static scalar particle in a wormhole space-time. *Phys. Rev.* **D87**, 024046 (2013)
195. P. Taylor, Propagation of test particles and scalar fields on a class of wormhole space-times. *Phys. Rev.* **D90**(2), 024057 (2014)
196. L.M. Burko, A.I. Harte, E. Poisson, Mass loss by a scalar charge in an expanding universe. *Phys. Rev.* **D65**, 124006 (2002)
197. R. Haas, E. Poisson, Mass change and motion of a scalar charge in cosmological spacetimes. *Class. Quantum Gravity* **22**, S739–S752 (2005)

On the Self-force in Electrodynamics and Implications for Gravity

Volker Perlick

Abstract We consider the motion of charged point particles on Minkowski spacetime. The questions of whether the self-force is finite and whether mass renormalisation is necessary are discussed within three theories: In the standard Maxwell vacuum theory, in the non-linear Born-Infeld theory and in the higher-order Bopp-Podolsky theory. In a final section we comment on possible implications for the theory of the self-force in gravity.

1 Introduction

The problem of the electromagnetic self-force has a long history. It began in the late 19th century when Lorentz, Abraham and others tried to formulate a classical theory of the electron. The idea was to model the electron as an extended, at least approximately spherical, charged body and to determine the equations of motion for the electron. Based on earlier results by Lorentz, Abraham succeeded in writing the equation of motion in terms of a power series with respect to the radius of the electron. If the radius tended to zero, i.e., for a point charge, an infinity occurred. The reason for this infinity is in the fact that, in the point-particle limit, the electric field strength diverges so strongly at the position of the charge that the field energy in an arbitrarily small sphere becomes infinitely large. To get rid of this infinity, it was necessary to “renormalise the mass” of the particle by assuming that it carries a negative infinite “bare mass”. After this mass renormalisation, one got a differential equation of third order for the motion of the particle which is known as the Abraham-Lorentz equation. It is a non-relativistic equation in the sense that, on the basis of special relativity, it can hold only if the particle’s speed is small in comparison to the speed of light.

A fully relativistic treatment of the problem had to wait until Dirac’s work [1] of 1938. The resulting equation of motion is known as the Lorentz-Dirac equation or as the Abraham-Lorentz-Dirac equation. Clearly, everyone would call it the Dirac equation except for the fact that this name was already occupied by another, even

V. Perlick (✉)

ZARM, University of Bremen, Am Fallturm, 28359 Bremen, Germany
e-mail: perlick@zarm.uni-bremen.de

more famous equation. Neither Lorentz nor Abraham has ever seen the (Abraham-) Lorentz-Dirac equation, because both had passed away in the 1920s. In particular in the case of Abraham it is rather clear that he would not have liked this equation because he was an ardent opponent of relativity. Therefore, it seems appropriate to omit his name and call it the Lorentz-Dirac equation. For the derivation of the Lorentz-Dirac equation, again mass renormalisation was necessary and one arrived at a third-order equation of motion. The latter fact means that, in contrast to other equations of motion, not only the position and the velocity but also the acceleration of the particle has to be prescribed at an initial instant for fixing a unique solution. Moreover, the Lorentz-Dirac equation is notorious for showing unphysical behaviour such as run-away solutions and pre-acceleration. For a detailed discussion of the Lorentz-Dirac equation, including historical issues, we refer to Rohrlich [2] and to Spohn [3].

The trouble with the Lorentz-Dirac equation clearly has its origin in the fact that the electric field strength of a point charge becomes infinite at the position of the charge, and that this singularity is so strong that the field energy in an arbitrarily small ball around the charge is infinite. A possible way out is to modify the underlying vacuum Maxwell theory in such a way that this field energy becomes finite. Two such modified vacuum Maxwell theories have been suggested in the course of history, the non-linear Born-Infeld theory [4] and the linear but higher-order Bopp-Podolsky theory [5, 6]. It is the main purpose of this article to discuss to what extent these theories have succeeded in providing a theory of classical charged point particles with a finite self-force and a finite field energy.

Some people are of the opinion that there is no need for a consistent theory of classical charged point particles. They say that either one should deal with extended classical charge distributions or with quantum particles. However, this is not convincing. E.g. in accelerator physics it is common to describe beams in terms of classical point particles; neither a description in terms of extended charge distributions nor in terms of quantum matter seems to be appropriate or even feasible. Therefore, a consistent and conceptually well-founded theory of classical charged point particles is actually needed.

The problem of the electromagnetic self-force of a charged particle has a counterpart in the gravitational self-force of a massive particle. In comparison with the electromagnetic self-force, the gravitational self-force is plagued with additional conceptual issues. The latter are related to the facts that Einstein's field equation does not admit solutions for sources concentrated on a worldline, see Geroch and Traschen [7], and that an extended massive particle becomes a black hole if it is compressed beyond its Schwarzschild radius. However, by considering the self-interacting massive particle as a perturbation of a fixed background spacetime one arrives at a formalism which is similar to the electromagnetic case, see the comprehensive review by Poisson et al. [8]. At this level of approximation it is reasonable to ask if modifications of the vacuum Maxwell theory can be mimicked by modifying Einstein's theory in such a way that the (approximated) gravitational self-force becomes finite. We will come back to this question at the end of this article, after a detailed discussion of the electromagnetic case.

2 Maxwell's Equations and the Constitutive Law for Vacuum

Maxwell's equations are universal and they do not involve a metric or a connection. They read

$$dF = 0, \quad dH = j, \quad (1)$$

where F is an untwisted two-form, H is a twisted two-form and j is a twisted three-form. (A differential form is twisted if its sign depends on the choice of an orientation. The difference between twisted and untwisted differential forms becomes irrelevant if the underlying manifold is oriented.) F gives the electromagnetic field strength, H gives the electromagnetic excitation and j gives the electromagnetic current. Our notation follows Hehl and Obukhov [9].

The Eqs. (1) are referred to as the *premetric* form of Maxwell's equations. These equations immediately imply that on simply connected domains F can be represented in terms of a potential,

$$F = dA, \quad (2)$$

and that charge conservation is guaranteed,

$$dj = 0. \quad (3)$$

If j is given, Maxwell's equations must be supplemented with a constitutive law relating F and H to specify the dynamics of the electromagnetic field. There is a particular constitutive law for vacuum, and there is a particular constitutive law for each type of medium. In any case, the constitutive law will involve some background geometry. In the following we consider vacuum electrodynamics on Minkowski spacetime. Then the constitutive law should involve the Minkowski metric tensor and no other background fields.

On Minkowski spacetime, we may choose an orthonormal coframe, i.e., four linearly independent covector fields $\theta^0, \theta^1, \theta^2, \theta^3$ such that the Minkowski metric is represented as

$$g = \eta_{ab} \theta^a \otimes \theta^b \quad (4)$$

where $(\eta_{ab}) = \text{diag}(-1, 1, 1, 1)$. Here and in the following we use the summation convention for latin indices that take values 0, 1, 2, 3 and for greek indices that take values 1, 2, 3. Latin indices will be lowered and raised with η_{ab} and its inverse η^{ab} , respectively, while greek indices will be lowered and raised with the Kronecker symbol $\delta_{\mu\nu}$ and its inverse $\delta^{\mu\nu}$, respectively.

With respect to the chosen orthonormal coframe, the electromagnetic field strength can be decomposed into electric and magnetic parts,

$$F = E_\mu \theta^\mu \wedge \theta^0 + \frac{1}{2} B^\rho \varepsilon_{\rho\mu\nu} \theta^\mu \wedge \theta^\nu. \quad (5)$$

Here the wedge denotes the antisymmetrised tensor product and $\varepsilon_{\rho\mu\nu}$ is the Levi-Civita symbol, defined by the properties that it is totally antisymmetric and satisfies $\varepsilon_{123} = 1$. The electromagnetic excitation can be decomposed in a similar fashion,

$$H = -\mathcal{H}_\mu \theta^\mu \wedge \theta^0 + \frac{1}{2} D^\rho \varepsilon_{\rho\mu\nu} \theta^\mu \wedge \theta^\nu. \quad (6)$$

If we apply the Hodge star operator of the Minkowski metric to F and H , we find

$$*F = -B_\mu \theta^\mu \wedge \theta^0 + \frac{1}{2} E^\rho \varepsilon_{\rho\mu\nu} \theta^\mu \wedge \theta^\nu, \quad (7)$$

$$*H = -D_\mu \theta^\mu \wedge \theta^0 - \frac{1}{2} \mathcal{H}^\rho \varepsilon_{\rho\mu\nu} \theta^\mu \wedge \theta^\nu. \quad (8)$$

The field energy density measured by an observer whose 4-velocity V satisfies $\theta^\mu(V) = 0$ for $\mu = 1, 2, 3$ is given by

$$\varepsilon = \frac{1}{2} (E_\mu D^\mu + \mathcal{H}_\mu B^\mu). \quad (9)$$

With the help of the Hodge star operator we can form out of F the untwisted scalar invariant

$$*(F \wedge *F) = B_\mu B^\mu - E_\mu E^\mu \quad (10)$$

and the twisted scalar invariant

$$*(F \wedge F) = -2E_\mu B^\mu. \quad (11)$$

All these equations are valid with respect to any orthonormal coframe. In particular, we may choose a holonomic coframe, i.e., we may choose inertial coordinates on Minkowski spacetimes,

$$g = \eta_{ab} dx^a \otimes dx^b \quad (12)$$

and then write $\theta^a = dx^a$. In the following we will see that it is sometimes convenient to work with an anholonomic orthonormal coframe on Minkowski spacetime.

We will now discuss the vacuum constitutive law in three different theories.

2.1 Standard Maxwell Vacuum Theory

In the standard Maxwell theory, the constitutive law of vacuum reads

$$H = {}^*F. \quad (13)$$

By comparison of (6) and (7) we see that this implies

$$D^\rho = E^\rho, \quad \mathcal{H}^\mu = B^\mu. \quad (14)$$

Here and in the following, we use units making the permittivity of vacuum, ε_0 , the permeability of vacuum, μ_0 , and thus the vacuum speed of light, $c = (\varepsilon_0\mu_0)^{-1/2}$, equal to one.

2.2 Born-Infeld Theory

In 1934, Born and Infeld [4] suggested a non-linear modification of the vacuum constitutive law,

$$H = \frac{{}^*F - \frac{{}^*(F \wedge F)}{2b^2}F}{\sqrt{1 + \frac{{}^*(F \wedge {}^*F)}{b^2} - \frac{({}^*(F \wedge F))^2}{4b^4}}} \quad (15)$$

where b is a new hypothetical constant of nature with the dimension of a (magnetic or electric) field strength. The idea behind this modified constitutive law is to find a theory where the field energy of a point charge remains bounded. We will discuss in the following sections to what extent this goal was achieved.

Maxwell's equations with the Born-Infeld constitutive law (15) can be derived from a Lagrangian that depends only on the invariants (10) and (11). This demonstrates that the theory is not only gauge invariant but also Lorentz invariant. However, we will not need the Lagrangian formulation in the following.

As the constitutive law (15) does not involve any derivatives, in the Born-Infeld theory the vacuum Maxwell equations are still of first order with respect to the field strength (i.e., of second order with respect to the potential), just as in the standard Maxwell theory. However, they are now non-linear.

Obviously, the Born-Infeld constitutive law (15) approaches the standard vacuum constitutive law (13) in the limit $b \rightarrow \infty$. This implies that the Born-Infeld theory is indistinguishable from the standard Maxwell vacuum theory if b is sufficiently big. In this sense, any experiment that confirms the standard Maxwell vacuum theory is in agreement with Born-Infeld theory as well, and it gives a lower bound for b . For the purpose of this article, the specific value of b is irrelevant as long as it is finite.

Decomposing the constitutive law (15) into electric and magnetic parts results in

$$D^\rho = \frac{E^\rho + \frac{E_\tau B^\tau}{b^2} B^\rho}{\sqrt{1 + \frac{1}{b^2} (B_\sigma B^\sigma - E_\sigma E^\sigma) - \frac{(E_\nu B^\nu)^2}{b^4}}}, \quad (16)$$

$$\mathcal{H}^\mu = \frac{B^\mu - \frac{E_\tau B^\tau}{b^2} E^\mu}{\sqrt{1 + \frac{1}{b^2} (B_\sigma B^\sigma - E_\sigma E^\sigma) - \frac{(E_\nu B^\nu)^2}{b^4}}}. \quad (17)$$

2.3 Bopp-Podolsky Theory

Another modification of the vacuum constitutive law, again motivated by the wish of having the field energy of a point charge finite, was brought forward in 1940 by Bopp [5]. The same theory was independently re-invented two years later by Podolsky [6]. The Bopp-Podolsky theory is equivalent to another theory that was suggested in 1941 by Landé and Thomas [10].

The Bopp-Podolsky vacuum constitutive law reads

$$H = {}^*F - \ell^2 \square {}^*F \quad (18)$$

where

$$\square = {}^*d {}^*d + d {}^*d^* \quad (19)$$

is the wave operator on Minkowski spacetime and ℓ is a new hypothetical constant of nature with the dimension of a length. In contrast to the Born-Infeld constitutive law, the Bopp-Podolsky constitutive law is linear. However, it involves second derivatives of the field strength, so Maxwell's equations give a system of fourth-order differential equations for the potential A . In the Landé-Thomas version of the theory one splits the potential into two parts each of which satisfies a second-order differential equation, see Sect. 4.3 below. Just as the Born-Infeld theory, the Bopp-Podolsky can be derived from a gauge-invariant and Lorentz-invariant Lagrangian (see Bopp [5] or Podolsky [6]) but we will not use the Lagrangian formulation in the following.

For $\ell \rightarrow 0$, the Bopp-Podolsky constitutive law (18) approaches the standard vacuum law (13). So any experiment that is in agreement with the standard Maxwell theory is in agreement with the Bopp-Podolsky theory as long as ℓ is sufficiently small. However, dealing with the limit $\ell \rightarrow 0$ requires some care because it is a *singular* limit of Maxwell's equations in the sense that it kills the highest-derivative term.

3 Field of a Static Point Charge

It is our goal to discuss the field of a point charge in arbitrary motion on Minkowski spacetime (subluminal, of course) according to the standard Maxwell vacuum theory, the Born-Infeld theory and the Bopp-Podolsky theory. As a preparation for that, it is useful to consider first the simple case of a point charge that is at rest in the spatial origin of an appropriately chosen inertial coordinate system. (Obviously, in any other inertial system the charge is then in uniform and rectilinear motion.) In this inertial system, the field produced by the charge must be spherically symmetric and static because there are no background structures that could introduce a deviation from these symmetries. Writing $\vec{r} = (x^1, x^2, x^3)$ for the coordinates and $\vec{E} = (E^1, E^2, E^3)$ etc. for the fields in the chosen inertial system, Maxwell's equations (1) reduce to

$$\nabla \times \vec{E} = \vec{0}, \quad \nabla \cdot \vec{B} = 0, \quad \nabla \times \vec{\mathcal{H}} = \vec{0}, \quad \nabla \cdot \vec{D} = q\delta^{(3)}(\vec{r}), \quad (20)$$

where q is the charge and $\delta^{(3)}$ is the three-dimensional Dirac delta distribution. While the curl equations are satisfied by any spherically symmetric \vec{E} and $\vec{\mathcal{H}}$ fields, the divergence equations determine the spherically symmetric \vec{D} and \vec{B} fields uniquely,

$$\vec{D} = \frac{q}{4\pi r^2} \vec{e}_r, \quad \vec{B} = \vec{0}, \quad (21)$$

where \vec{e}_r is the radial unit vector. So whatever the constitutive law may be, the electric excitation \vec{D} always has its standard Coulomb form, i.e., it diverges like r^{-2} if the position of the charge is approached, and the magnetic field strength \vec{B} vanishes everywhere. The corresponding (spherically symmetric) electric field strength \vec{E} and magnetic excitation $\vec{\mathcal{H}}$ are not restricted by Maxwell's equations; they have to be determined from the constitutive law.

3.1 Standard Maxwell Vacuum Theory

In the standard Maxwell vacuum theory the constitutive law simply requires $\vec{E} = \vec{D}$ and $\vec{B} = \vec{\mathcal{H}}$. Hence, (21) says that \vec{E} is the standard Coulomb field and that $\vec{\mathcal{H}}$ vanishes,

$$\vec{E} = \frac{q}{4\pi r^2} \vec{e}_r, \quad \vec{\mathcal{H}} = \vec{0}. \quad (22)$$

Clearly, $|\vec{E}|$ becomes infinite at the origin, i.e., at the position of the charge. The direction of \vec{E} is always radial, so in the limit $r \rightarrow 0$ the direction may be any unit vector depending on how the origin is approached. As these direction vectors average to zero, the Lorentz force ($\sim \vec{E}$) exerted by the static particle onto itself vanishes. Here

we follow the widely accepted hypothesis that the self-force results from averaging over directions, cf. e.g. Poisson et al. [8]. This hypothesis is very natural if one thinks of the point particle as being the limiting case of an extended (spherical) body.

The field energy in a ball K_R of radius R around the origin is

$$W(R) = \int_{K_R} \frac{1}{2} \vec{D} \cdot \vec{E} r^2 \sin \vartheta dr d\vartheta d\varphi = \frac{q^2}{8\pi} \int_0^R \frac{dr}{r^2}. \quad (23)$$

Clearly, this expression is infinite, for arbitrarily small R . Both \vec{E} and \vec{D} throw in a factor of r^{-2} ; one of them is killed by a factor of r^2 from the volume element but the other one makes the integral diverge. We see that we can cure this infinity by introducing a modified constitutive law that leaves \vec{E} bounded if the position of the charge is approached. We will now verify that both the Born-Infeld theory and the Bopp-Podolsky theory have this desired property.

3.2 Born-Infeld Theory

As $\vec{B} = \vec{0}$ by (21), in the Born-Infeld theory the constitutive law requires

$$\vec{D} = \frac{\vec{E}}{\sqrt{1 - \frac{1}{b^2} |\vec{E}|^2}}, \quad \vec{H} = \vec{0}. \quad (24)$$

With \vec{D} given by (21), we have to solve the equation

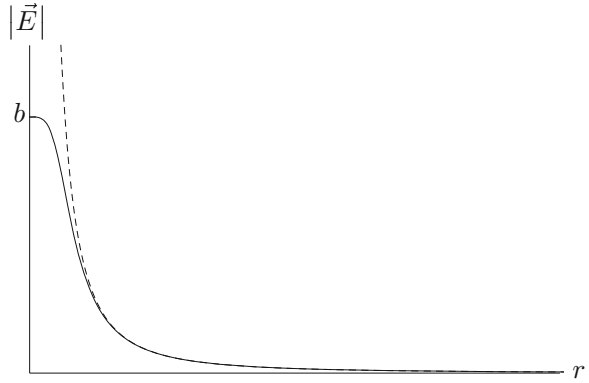
$$\frac{\vec{E}}{\sqrt{1 - \frac{1}{b^2} |\vec{E}|^2}} = \frac{q}{4\pi r^2} \vec{e}_r \quad (25)$$

for \vec{E} to determine the electric field strength. The result is (Born and Infeld [4])

$$\vec{E} = \frac{q}{4\pi \sqrt{r_0^4 + r^4}} \vec{e}_r, \quad r_0^2 = \frac{q}{4\pi b}. \quad (26)$$

Hence $|\vec{E}| \rightarrow b$ for $r \rightarrow 0$, see Fig. 1. Note that the limit of \vec{E} for $r \rightarrow 0$ does not exist because the *direction* of the limit vector depends on how the position of the point charge is approached. One may say that the electric field strength stays bounded but has a *directional singularity* at the origin. By averaging over directions, the self-force ($\sim \vec{E}$) of the static particle vanishes.

Fig. 1 Modulus of the electric field strength for a static charge in the Born-Infeld theory (*solid*) and in the standard Maxwell vacuum theory (*dashed*)



The field energy in a ball K_R of radius R around the origin is

$$W(R) = \int_{K_R} \frac{1}{2} \vec{D} \cdot \vec{E} r^2 \sin \vartheta dr d\vartheta d\varphi = \frac{q^2}{8\pi} \int_0^R \frac{dr}{\sqrt{r_0^4 + r^4}}. \quad (27)$$

This is an elliptic integral which is finite as long as $r_0 > 0$, i.e., as long as b is finite. Even the field energy in the whole space is finite,

$$\lim_{R \rightarrow \infty} W(R) = \frac{q^2 \Gamma(5/4)^2}{2r_0 \pi^{3/2}}, \quad (28)$$

where Γ is the Euler gamma function.

3.3 Bopp-Podolsky Theory

In this case the constitutive law requires

$$\vec{D} = \vec{E} - \ell^2 \Delta \vec{E}, \quad \vec{\mathcal{H}} = \vec{0}. \quad (29)$$

With \vec{D} given by (21), we have to solve the second-order differential equation

$$\vec{E} - \ell^2 \Delta \vec{E} = \frac{q}{4\pi r^2} \vec{e}_r \quad (30)$$

to determine \vec{E} . For a spherically symmetric field, $\vec{E}(\vec{r}) = E(r)\vec{e}_r(\vec{r})$, this reduces to

$$E - \frac{\ell^2}{r^2} \left(\frac{d}{dr} \left(r^2 \frac{dE}{dr} \right) - 2E \right) = \frac{q}{4\pi r^2}. \quad (31)$$

The general solution is

$$\vec{E} = \frac{q}{4\pi r^2} \left\{ 1 + C_1 \ell(r - \ell)e^{r/\ell} - C_2 \ell(r + \ell)e^{-r/\ell} \right\} \vec{e}_r \quad (32)$$

with two integration constants C_1 and C_2 . The first integration constant is fixed if we require \vec{E} to fall off towards infinity; this yields $C_1 = 0$. The second integration constant is fixed if we require \vec{E} to stay bounded if the position of the charge is approached; this yields $C_2 = \ell^{-2}$. This gives us the Bopp-Podolsky analogue of the Coulomb \vec{E} field (Bopp [5]; Podolsky [6])

$$\vec{E} = \frac{q}{4\pi r^2} \left\{ 1 - \left(\frac{r}{\ell} + 1 \right) e^{-r/\ell} \right\} \vec{e}_r \quad (33)$$

which satisfies $|\vec{E}| \rightarrow q/(8\pi\ell^2)$ for $r \rightarrow 0$, see Fig. 2. Just as in the Born-Infeld case, the electric field strength stays bounded but has a directional singularity at the origin.

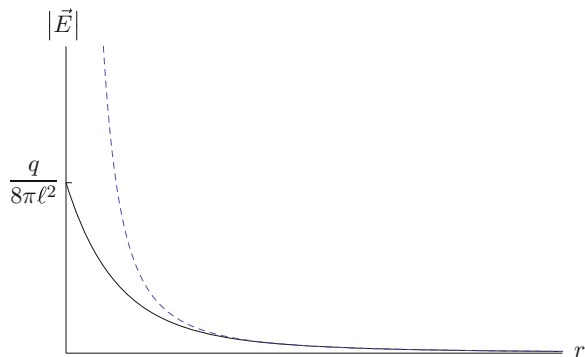
The field energy in a ball K_R of radius R around the origin is

$$\begin{aligned} W(R) &= \int_{K_R} \frac{1}{2} \vec{D} \cdot \vec{E} r^2 \sin\vartheta dr d\vartheta d\varphi \\ &= \frac{q^2}{8\pi} \int_0^R \left(\frac{1}{r^2} - \frac{e^{-r/\ell}}{r^2} - \frac{e^{-r/\ell}}{r\ell} \right) dr = \frac{q^2}{8\pi} \left(\frac{1}{\ell} + \frac{e^{-R/\ell} - 1}{R} \right) \end{aligned} \quad (34)$$

which is finite as long as $\ell > 0$. As in the Born-Infeld theory, even the field energy in the whole space is finite,

$$\lim_{R \rightarrow \infty} W(R) = \frac{q^2}{8\pi\ell}. \quad (35)$$

Fig. 2 Modulus of the electric field strength for a static charge in the Bopp-Podolsky theory (*solid*) and in the standard Maxwell vacuum theory (*dashed*)



4 Field of an Accelerated Point Charge

We have seen that both the Born-Infeld theory and the Bopp-Podolsky theory modify the Coulomb \vec{E} field of a point charge *at rest* in such a way that $|\vec{E}|$ is bounded and that the field energy in a ball around the charge is finite. Of course, what one is really interested in is the field produced by an *accelerated* charge. We will now try to find out what can be said about this case.

We choose an inertial coordinate system on Minkowski spacetime, $g = \eta_{ab}dx^a \otimes dx^b$. We fix a timelike C^∞ curve $z^a(\tau)$ parametrised by proper time,

$$\eta_{ab}\dot{z}^a\dot{z}^b = -1. \quad (36)$$

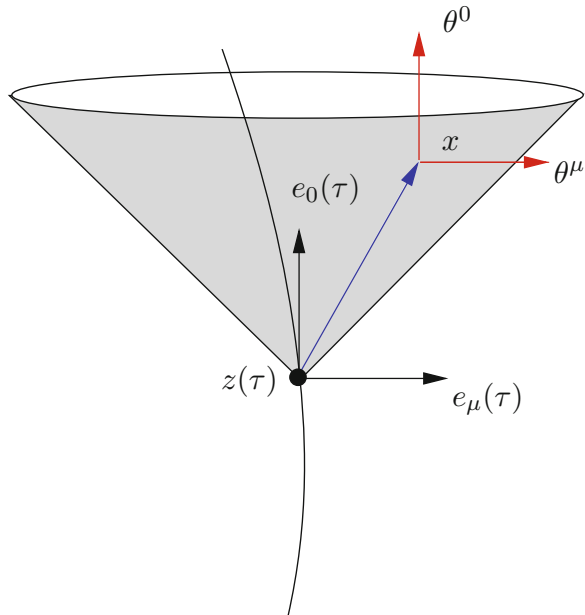
We assume that this timelike curve is inextendible. As an accelerated worldline may reach (past or future) infinity in a finite proper time, this does not necessarily mean that the parameter τ ranges over all of \mathbb{R} . We denote the interval on which τ is defined by $]\tau_{\min}, \tau_{\max}[$ where $-\infty \leq \tau_{\min} < \tau_{\max} \leq \infty$.

We want to determine the electromagnetic field of a point charge that moves on the worldline $z^a(\tau)$. For convenience, we introduce an orthonormal tetrad $(e_0(\tau), e_1(\tau), e_2(\tau), e_3(\tau))$ along the worldline of the charged particle such that

$$e_0^a(\tau) = \dot{z}^a(\tau), \quad a(\tau)e_3^b(\tau) = \ddot{z}^b(\tau), \quad (37)$$

see Fig. 3. Along the worldline, this fixes the timelike vector $e_0(\tau)$ everywhere and the spacelike vector $e_3(\tau)$, up to sign, at all events where the acceleration $\ddot{z}(\tau)$ is

Fig. 3 Retarded light-cone coordinates and orthonormal coframe



non-zero. $e_1(\tau)$ and $e_2(\tau)$ are then fixed up to a rotation in the plane perpendicular to $e_3(\tau)$. At points where the acceleration is zero, $e_3(\tau)$ is ambiguous; there are pathological cases where it is not possible to extend it into such points such that the resulting vector field e_3 is continuously differentiable. We exclude such cases in the following and assume that the tetrad is smoothly dependent on τ and satisfies (37) along the entire worldline.

With respect to this tetrad, we can introduce retarded light-cone coordinates $(\tau, r, \vartheta, \varphi)$ which are related to the inertial coordinates (x^0, x^1, x^2, x^3) by

$$x^a = z^a(\tau) + r \left(\dot{z}^a(\tau) + n^a(\tau, \vartheta, \varphi) \right) \quad (38)$$

where

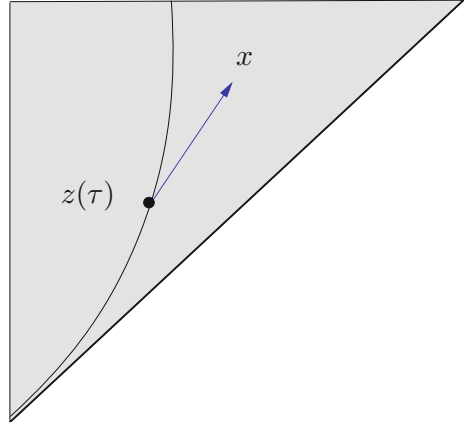
$$n^a(\tau, \vartheta, \varphi) = \cos\varphi \sin\vartheta e_1^a(\tau) + \sin\varphi \sin\vartheta e_2^a(\tau) + \cos\vartheta e_3^a(\tau). \quad (39)$$

Retarded light-cone coordinates are routinely used nowadays when treating self-force problems, cf. e.g. Poisson et al. [8]. These coordinates have a long history. In connection with electrodynamics on Minkowski spacetime, they were introduced by Newman and Unti [11] in 1963. In particular, Newman and Unti demonstrated that in these coordinates the Liénard-Wiechert potential takes a surprisingly simple form. In general relativity the history of light-cone coordinates is even older. They made their first appearance in a 1938 paper by Temple [12] who called the time-reversed version (i.e., the advanced light-cone coordinates) “optical coordinates”. Advanced light-cone coordinates are used in gravitational lensing and in cosmology where the worldline is interpreted as an observer who receives light (rather than as a source that emits radiation).

In retarded light-cone coordinates, the “temporal” coordinate τ labels the future light-cones with vertex on the chosen worldline; r is a radius coordinate along each light-cone and (ϑ, φ) are standard spherical coordinates that parametrise the spheres $(\tau, r) = \text{constant}$. Of course, there are the usual coordinate singularities of the spherical coordinates at the poles $\sin\vartheta = 0$ and φ is defined only modulo 2π . If these coordinate singularities are understood, the system of retarded light-cone coordinates is well-defined on an open subset, U , which equals the causal future of the worldline with the worldline itself being omitted. Figure 4 shows a worldline that approaches the speed of light in the past. In this case the causal future of the worldline is bounded by a lightlike hyperplane to which the worldline is asymptotic. For a worldline that does not approach the speed of light in the past, the causal future is all of Minkowski spacetime. (Recall that we consider only worldlines that are inextendible.)

With the retarded light-cone coordinates $(\tau, r, \vartheta, \varphi)$ we can associate an orthonormal coframe $(\theta^0, \theta^1, \theta^2, \theta^3)$ defined by

Fig. 4 Domain of definition, U , of the retarded light-cone coordinates



$$\theta^0 = d\tau + dr + ra(\tau)\cos\vartheta d\tau \quad (40)$$

$$\theta^1 = dr + ra(\tau)\cos\vartheta d\tau$$

$$\theta^2 = rd\vartheta - ra(\tau)\sin\vartheta d\tau$$

$$\theta^3 = r\sin\vartheta d\varphi,$$

see Fig. 3.

The electromagnetic field of the point charge is to be determined by solving the Maxwell equations (1) with

$$*j(x) = q \left(\int_{\tau_{\min}}^{\tau_{\max}} \delta^{(4)}(x - z(\tau)) \dot{z}^a(\tau) d\tau \right) \eta_{ab} dx^b \quad (41)$$

where $\delta^{(4)}$ is the 4-dimensional Dirac delta distribution. The solution has to satisfy the vacuum constitutive law on the open domain U and it should be retarded. By the latter requirement we mean that the field strength at an event $x \in U$ should be completely determined by what the point charge did in the causal past of the event x .

4.1 Standard Maxwell Vacuum Theory

In the case of the standard Maxwell vacuum theory, finding the field of a point charge on Minkowski spacetime is a standard text-book matter. The solution is $F = dA$, $H = *F$, where

$$A = -\frac{q\theta^0}{4\pi r} = -\frac{q}{4\pi} \left(\frac{d\tau + dr}{r} + a(\tau)\cos\vartheta d\tau \right) \quad (42)$$

is the (retarded) Liénard-Wiechert potential. At an event $x \in U$, the potential is determined by the 4-velocity and the 4-acceleration of the point charge at the retarded time which is given by the coordinate τ . There are no “tail terms”, i.e., there is no dependence on the earlier history of the point charge.

For deriving the Liénard-Wiechert potential in a systematic way, one introduces the potential, $F = dA$, and imposes the Lorenz gauge condition, $*dA = 0$. Then the first Maxwell equation, $dF = 0$, is automatically satisfied and the second Maxwell equation, $dH = j$, becomes an inhomogeneous wave equation for A ,

$$\square A = (*d*d + d*d*)A = *d*F = *dH = *j. \quad (43)$$

With the well-known (retarded) Green function of the wave operator \square , the (retarded) solution can be written as an integral over $*j$. Inserting the current from (41) gives the desired result.

From the Liénard-Wiechert potential we find that the field strength $F = dA$ and the excitation $H = *dA$ are given by

$$\begin{aligned} F &= \frac{q}{4\pi} \left(\frac{\theta^1 \wedge \theta^0}{r^2} + \frac{a(\tau)}{r} \sin\vartheta \theta^2 \wedge (\theta^0 - \theta^1) \right) \\ &= \frac{q}{4\pi} \left(\frac{dr \wedge d\tau}{r^2} + a(\tau) \sin\vartheta d\vartheta \wedge d\tau \right) \end{aligned} \quad (44)$$

and

$$\begin{aligned} H &= \frac{q}{4\pi} \left(\frac{\theta^2 \wedge \theta^3}{r^2} - \frac{a(\tau)}{r} \sin\vartheta \theta^3 \wedge (\theta^0 - \theta^1) \right) \\ &= \frac{q}{4\pi} \sin\vartheta d\vartheta \wedge d\varphi, \end{aligned} \quad (45)$$

respectively. Decomposing into electric and magnetic parts yields

$$E_\mu \theta^\mu = D_\mu \theta^\mu = \frac{q}{4\pi} \left\{ \frac{\theta^1}{r^2} + a(\tau) \sin\vartheta \frac{\theta^2}{r} \right\}, \quad (46)$$

$$B_\mu \theta^\mu = \mathcal{H}_\mu \theta^\mu = \frac{q}{4\pi} a(\tau) \sin\vartheta \frac{\theta^3}{r}. \quad (47)$$

In addition to the “Coulomb part”, which goes with $1/r^2$, we have in the case of a non-vanishing acceleration a “radiation part” which goes with $1/r$. The self-force, i.e. the Lorentz force exerted onto the point charge by its own field, is given as the limit of $q E_\mu \theta^\mu$ if the position of the point charge is approached. The Coulomb part averages to zero, as in the case of a static charge. The radiation part, however, does not average to zero; it gives an infinite self-force whenever the acceleration $a(\tau)$ is non-zero. As in the static case, the field energy in an arbitrarily small sphere around the point charge is infinite. It is this infinite amount of energy carried by

the point charge with itself that makes mass renormalisation necessary if one wants to formulate an equation of motion for the point charge taking the self-force into account.

4.2 Born-Infeld Theory

If one wants to find the field of an accelerated point charge in the Born-Infeld theory, one would try to mimic the derivation of the Liénard-Wiechert potential as far as possible. As in the standard Maxwell theory, one can satisfy the first Maxwell equation by introducing the potential and one can impose the Lorenz gauge condition (or any other gauge condition if this appears to be more appropriate). However, with H given in terms of $F = dA$ by the Born-Infeld constitutive law, the second Maxwell equation now becomes a *non-linear* inhomogeneous wave equation for A . There are no standard methods for solving such an equation; in particular, Green function methods are not applicable. Therefore, we cannot write down a Born-Infeld analogue of the Liénard-Wiechert potential. In the Born-Infeld theory, no explicit solution of the electromagnetic field of a point charge with non-vanishing acceleration seems to be known.

One might say that it is not actually necessary to write down a solution explicitly. It would be sufficient if one could verify some properties of the solution. Firstly, it would be highly desirable to prove that, for a point charge moving on an arbitrary worldline or on a worldline subject to some conditions, the retarded electromagnetic field is unique and regular on U . Secondly, it would be highly desirable to know if for this solution the self-force and the energy in a ball around the charge are finite. However, very little is known about these issues in the Born-Infeld theory beyond the case of an unaccelerated point charge.

As to regularity, it seems worthwhile to point out that even for a *time-independent* and smooth j the question of regularity is highly non-trivial. It was shown only recently by Kiessling [13] that in this case the electromagnetic field is, indeed, free of singularities or discontinuities. Although this result seems to be intuitively quite obvious, the proof is difficult and very technical. It is based on series expansions with respect to $1/b^2$, where b is the Born-Infeld constant, and the hard part is in the proof of convergence. For the field of an accelerated point charge, it is very well conceivable that infinities or discontinuities (“shocks”) are formed. It is true that Boillat [14] has shown the non-existence of some kind of shocks in the Born-Infeld theory, but these results do not apply to the case at hand where the equations become singular along a worldline.

Even if it is possible to show that the electromagnetic field of a point charge is regular on U , either for all worldlines or for a special class of worldlines, it is far from obvious that the field has the same behaviour as in the static case if the position of the point charge is approached. A discussion of related issues can be found in a paper by Chruściński [15]; this, however, is based on the *assumption* that the electric field strength remains bounded and that the electric excitation diverges like r^{-2} if the position of the point charge is approached. In contrast to the retarded light-cone

coordinates used here, Chruściński used Fermi coordinates in a similar fashion as they had been used already earlier by Kijowski [16] in the context of the standard Maxwell vacuum theory.

Something can be said, at least, for the case of a point charge that is initially at rest and then starts accelerating. In this case, conservation of energy guarantees that the total field energy must be finite for all times. However, even in this case it is not clear if shocks are excluded.

For approaching the problem in a systematic way, one may write the electromagnetic field strength as a power series with respect to $1/b^2$,

$$F = \sum_{N=0}^{\infty} \frac{F_N}{b^{2N}} = F_0 + \frac{F_1}{b^2} + \dots, \quad F_N = dA_N. \quad (48)$$

Inserting this expression into the Born-Infeld constitutive law (15) and collecting terms of equal powers of $1/b^2$ gives

$$H = \sum_{N=0}^{\infty} \frac{H_N}{b^{2N}} = \sum_{N=0}^{\infty} \frac{1}{b^{2N}} (*F_N + \mathcal{W}_N(F_0, \dots, F_{N-1})) \quad (49)$$

where $\mathcal{W}_N(F_0, \dots, F_{N-1})$ stands for an expression depending on F_0, \dots, F_{N-1} that can be explicitly calculated for every N . We have to determine the $F_N = dA_N$ such that $dH = j$ with the current given by (41). This can be done by requiring

$$dH_0 = j, \quad dH_N = 0 \text{ for } N = 1, 2, \dots \quad (50)$$

and solving these equations iteratively. We may impose the Lorenz gauge condition on each A_N . Then the zeroth order retarded solution is known to be the standard Liénard-Wiechert field, $F_0 = dA_0$ with A_0 given by the right-hand side of (42). The higher-order $F_N = dA_N$ are determined by

$$d(*dA_N + \mathcal{W}_N(dA_0, \dots, dA_{N-1})) = 0. \quad (51)$$

In the Lorenz gauge, this is the standard inhomogeneous wave equation for A_N , with the inhomogeneity given in terms of the lower-order solutions A_0, \dots, A_{N-1} ,

$$\square A_N = *\tilde{j}_N, \quad \tilde{j}_N = -d\mathcal{W}_N(dA_0, \dots, dA_{N-1}). \quad (52)$$

The retarded solution of this equation is known from classical electrodynamics: It is the retarded potential of the “current” three-form \tilde{j}_N . In this way, we can iteratively determine the A_N and write the solution $F = dA$ as a formal power series.

The big question, unanswered so far, is whether or not this series converges. We do know that it does converge in the case of vanishing acceleration; then we get the field of a static point charge discussed in Sect. 3.2. For non-zero acceleration, however, no convergence results are known.

4.3 Bopp-Podolsky Theory

In the case of the Bopp-Podolsky theory the situation is much better than in the case of the Born-Infeld theory. The Bopp-Podolsky theory is linear, so it allows for applications of the Green function method.

With $F = dA$ and choosing the Lorenz gauge, $d^*A = 0$, the remaining field equation reads

$$\square A - \ell^2 \square^2 A = {}^*j. \quad (53)$$

This fourth-order equation for A can be reduced to a pair of second-order equations

$$\square \hat{A} = {}^*j, \quad \square \tilde{A} - \ell^{-2} \tilde{A} = j, \quad (54)$$

if we write

$$A = \hat{A} - \tilde{A} \quad (55)$$

$$\hat{A} := A - \ell^2 \square A, \quad \tilde{A} := -\ell^2 \square A. \quad (56)$$

If rewritten in this way, a quantised version of the theory would predict the existence of a massless photon, described by \hat{A} , and a massive photon with Compton wavelength ℓ , described by \tilde{A} . Both Bopp [5] and Podolsky [6] had realised that their higher-order theory can be rewritten in this way as a two-field theory. This two-field theory is precisely what Landé and Thomas [10] independently suggested one year after Bopp and one year before Podolsky.

One can thus construct the (retarded) solution to the fourth-order equation (53) from the (retarded) Green functions of the wave equations (54). The latter are well known, see e.g. the original paper by Landé and Thomas [10]. This gives the retarded solution to (53) for the current (41) of a point charge as

$$A(x) = \left(\int_{-\infty}^{\tau} \frac{J_1(s(x, \tau')/\ell)}{\ell s(x, \tau')} \dot{z}^a(\tau') d\tau' \right) \eta_{ab} dx^b \quad (57)$$

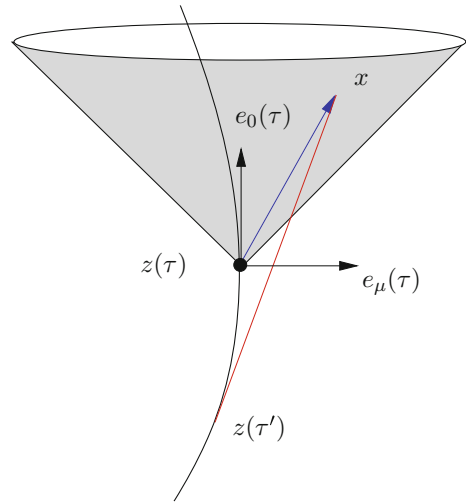
where

$$s(x, \tau')^2 = -(x^a - z^a(\tau'))(x_a - z_a(\tau')) \quad (58)$$

and J_1 is the Bessel function of the first kind. The geometric meaning of $s(x, \tau')$ is illustrated in Fig. 5.

The potential (57) is the Bopp-Podolsky analogue of the Liénard-Wiechert potential. In contrast to the standard Liénard-Wiechert potential, it depends on the entire earlier history of the point charge up to the retarded time τ . Such “tail terms” are nothing peculiar; they also occur in the standard vacuum Maxwell theory on a curved

Fig. 5 $s(x, \tau')$ is the Lorentz length of the timelike line segment that connects x with $z(\tau')$



background, see e.g. Poisson et al. [8]. The integral in (57) and in the corresponding expression for the field strength can be expanded in a formal power series with respect to ℓ . For the self-force, after averaging over directions this results in a series with terms of order ℓ^{-1} , ℓ^0 , ℓ , $\ell^2 \dots$, see Zayats [17] (also cf. McManus [18], Frenkel [19] and Frenkel and Santos [20]). However, these series are non-convergent and, therefore, of limited use.

So in contrast to the Born-Infeld theory, in the Bopp-Podolsky theory the electromagnetic potential (and, thereupon, the electromagnetic field strength) produced by an arbitrarily accelerated point charge can be explicitly written down, albeit in terms of an integral over the particle's earlier history. A detailed discussion of the class of worldlines for which this integral absolutely converges will be given elsewhere [21]. This demonstrates that, for a large class of worldlines, the electric field stays bounded and there is no need for mass renormalisation. As an important example, the self-force of a *uniformly* accelerated point charge was calculated by Zayats [17].

Because of the tail terms, the equation of motion is no longer a differential equation but rather an integro-differential equation for the worldline. It is unknown if the equation of motion admits run-away solutions. For some partial results, indicating that run-away solutions cannot exist if ℓ is bigger than a certain critical value, see Frenkel and Santos [20].

5 Implications for Gravity

The preceding discussion can be summarised in the following way. In the standard Maxwell vacuum theory, the self-force is infinite and mass renormalisation is necessary. Postulating a negative infinite bare mass is conceptually not satisfactory and the

resulting equation of motion, the Lorentz-Dirac equation, is highly pathological. In the Born-Infeld theory, the properties of the field of a static charge look promising, but for an accelerated charge very little can be calculated and the properties of the field are largely unknown. For the Bopp-Podolsky theory, the field of an accelerated point charge can be calculated, in terms of an integral over the history of the particle which is manageable to a certain extent, and it can be shown for a large class of accelerated worldlines that the field is, actually, finite. No negative infinite bare mass needs to be postulated, and the equation of motion can be assumed to be the usual Lorentz-force equation with the (finite) self-field included after averaging over directions. The explicit expression of the electromagnetic field, given by the analogue of the Liénard-Wiechert potential, is more complicated than in the standard vacuum Maxwell theory on Minkowski spacetime, because of the tail terms. However, such tail terms are familiar from the standard vacuum Maxwell theory on a curved spacetime and should not be viewed as a reason for discarding the theory. Although there are still several open issues—most notably the absence or non-absence of run-away solutions has to be clarified—it seems fair to say that in the Bopp-Podolsky theory the infinities associated with point charges are cured to a large extent. We may therefore view it as the best candidate for a conceptually satisfactory theory of classical charged point particles. (This does not necessarily mean that the Bopp-Podolsky theory is “the correct theory of electromagnetism” at a fundamental, quantum field theoretical, level).

Do these observations teach a lesson with respect to the gravitational self-force? In the approximation where the self-gravitating particle is viewed as a perturbation of a fixed background spacetime, the theory is very similar to the electromagnetic case in the standard Maxwell vacuum theory. Modifying the theory along the lines of the Born-Infeld theory seems to be of no use: Firstly, it is largely unclear if the Born-Infeld theory really cures the infinities in the field of an accelerated point charge. Secondly, the original Einstein theory was already a non-linear theory whose non-linearities had been killed by setting up the approximation formalism for the self-gravitating point mass. Therefore, it seems rather meaningless to re-introduce non-linear terms. The situation is quite different for the Bopp-Podolsky theory. Here linearity is kept but higher-order terms are added. It seems not unreasonable to assume that Einstein’s theory can be modified by adding higher-order terms in such a way that they survive the approximation, giving rise to a regularising term of the same kind as it occurs in the Bopp-Podolsky theory. Higher-order theories of gravity have been investigated intensively. They are mainly motivated by the observation that quantum corrections to Einstein’s theory are expected to give a Lagrangian that is of quadratic or higher order in the curvature, resulting in field equations that involve fourth derivatives of the metric. (The simplest class of such theories is the class of $f(R)$ theories which are reviewed, e.g., in the Living Review by de Felice and Tsujikawa [22]). Looking for a version that gives rise to a Bopp-Podolsky-like term seems to be a promising programme that might give a new theoretical framework for getting a finite gravitational self-force.

Acknowledgments This work was financially supported by the Deutsche Forschungsgemeinschaft, Grant LA905/10-1, and by the German-Israeli-Foundation, Grant 1078/2009. Moreover, I gratefully acknowledge support from the Deutsche Forschungsgemeinschaft within the Research Training Group 1620 “Models of Gravity”. As to the part on Bopp-Podolsky theory, I wish to thank Robin Tucker and Jonathan Gratus for many helpful discussions and for the ongoing collaboration on this subject. Finally, I am grateful to the organisers of the Heraeus-Seminar “Equations of motion in relativistic gravity” for inviting this contribution.

References

1. P.A.M. Dirac, Classical theory of radiating electrons. Proc. R. Soc. Lond., A **167**, 148, (1938)
2. F. Rohrlich, *Classical Charged Particles* (World Scientific, New York, 2007)
3. H. Spohn, *Dynamics of Charged Particles and Their Radiation Field* (Cambridge University Press, Cambridge, 2007)
4. M.Born, L.Infeld, Foundations of the new field theory. Proc. R. Soc. Lond., A **144**, 425 (1934)
5. F. Bopp, Eine lineare Theorie des Elektrons. Ann. Phys. **430**, 345 (1940)
6. B. Podolsky, A generalized electrodynamics. Part I: non-quantum. Phys. Rev. **62**, 68 (1942)
7. R. Geroch, J. Traschen, Strings and other distributional sources in general relativity. Phys. Rev. D **36**, 1017 (1987)
8. E. Poisson, A. Pound, I. Vega, The motion of point particles in curved spacetime. Living Rev. Relativ. **14**, 7 (2011)
9. F.W. Hehl, Y. Obukhov, *Foundations of Classical Electrodynamics* (Birkhäuser, Basel, 2003)
10. A. Landé, L.H. Thomas, Finite self-energies in radiation theory. Part II. Phys. Rev. **60**, 514 (1941)
11. E.T. Newman, T.W.J. Unti, A class of null flat-space coordinate systems. J. Math. Phys. **4**, 1467 (1963)
12. G. Temple, New systems of normal co-ordinates for relativistic optics. Proc. R. Soc. Lond., A **168**, 122 (1938)
13. M. Kiessling, Convergent perturbative power series solution of the stationary Born-Infeld field equations with regular sources. J. Math. Phys. **52**, 022902 (2011)
14. G. Boillat, Nonlinear electrodynamics: Lagrangians and equations of motion. J. Math. Phys. **11**, 941 (1970)
15. D. Chruściński, Point charge in the Born-Infeld electrodynamics. Phys. Lett. A **240**, 8 (1998)
16. J. Kijowski, Electrodynamics of moving particles. Gen. Relativ Gravity **26**, 167 (1994)
17. A.E. Zayats, Self-interaction in the Bopp-Podolsky electrodynamics: can the observable mass of a charged particle depend on its acceleration? Ann. Phys., N.Y., **342**, 11 (2014)
18. H. McManus, Classical electrodynamics without singularities. Proc. R. Soc. Lond., A **195**, 323 (1948)
19. J. Frenkel, 4/3 problem in classical electrodynamics. Phys. Rev. E **54**, 5859 (1996)
20. J. Frenkel, R. Santos, The self-force of a charged particle in classical electrodynamics. Int. J. Mod. Phys. B **13**, 315 (1999)
21. J. Gratus, V. Perlick, R. Tucker, [arXiv:1502.01945](https://arxiv.org/abs/1502.01945)
22. A. de Felice, S. Tsujikawa, $f(R)$ theories. Living Rev. Relativ. **13**, 3 (2010)

Self-gravitating Elastic Bodies

Lars Andersson

Abstract Extended objects in GR are often modelled using distributional solutions of the Einstein equations with point-like sources, or as the limit of infinitesimally small “test” objects. In this note, I will consider models of finite self-gravitating extended objects, which make it possible to give a rigorous treatment of the initial value problem for (finite) extended objects.

1 Introduction

Extended objects in GR are often modelled using distributional solutions of the Einstein equations with point-like sources, or as the limit of infinitesimally small “test” objects. In this context, gravitational self-force manifests itself through corrections to geodesic motion, in analogy to radiation reaction. This is relevant for example in the analysis of extreme mass ratio inspirals, see [1]. See also the papers by Harte [2] and Pound [3] for background on the self-force problem.

A widely studied model for objects with internal structure in general relativity are so-called spinning particles. There are several formal approaches to deriving the corrections to geodesic motion for such object, see [4] for a survey. These works rely to a large extent on the study of distributional stress-energy tensors representing the particle-like objects. On the other hand, limiting procedures have been applied to study objects with internal structure by Wald and collaborators, cf. [5]. In this note, I will consider models of finite self-gravitating extended objects, which make it possible to give a rigorous treatment of the initial value problem for (finite) extended objects. Such models could serve as a basis for the above mentioned limiting considerations.

A serious difficulty in treating self-gravitating material bodies in general relativity, is that matter distributions with finite extent are typically irregular at the surface of the body. This phenomenon can be seen already by considering a stationary Newtonian polytrope, with equation of state

L. Andersson (✉)

Albert Einstein Institute, Am Mühlenberg 1, 14476 Potsdam, Germany
e-mail: laan@aei.mpg.de

$$p = K\rho^\gamma$$

Then the density ρ behaves as

$$\rho(x) \sim d^{\frac{1}{\gamma-1}}(x, \partial\Omega)$$

where $d(x, \partial\Omega)$ is the distance to the boundary of the body. Recall that the sound speed c_s for such a polytrope is given by

$$c_s = \sqrt{\frac{dp}{d\rho}} = \sqrt{K\gamma\rho^{\frac{\gamma-1}{2}}}$$

and hence c_s tends to zero at $\partial\Omega$. It follows that the hyperbolicity of the Euler equations degenerates at the free boundary, characterized by the vanishing of pressure, of a typical polytrope in vacuum. In particular the particles at the boundary move as if in free fall.

Perfect fluid bodies in vacuum with equation of state such that the density at the free boundary is non-vanishing are sometimes referred to as liquid bodies. An example of an equation of state of this type is

$$p = D(\rho - \rho_0)$$

where D, ρ_0 are suitable constants. For a steady fluid body with this equation of state, the density will be ρ_0 at the boundary of the body. In this particular case, we also see that the sound speed does not go to zero at the boundary, and there is no degeneration of hyperbolicity. However, for liquid bodies this is not generally the case. See [6, Sect. 3.5] for discussion.

For elastic bodies, like liquid bodies, we may expect the density of the material to be non-zero at the boundary, and hence there will be a jump in the density at the surface of the body. Further, for elastic bodies, we may expect that the field equations remain non-degenerate and hyperbolic up to boundary. For elastic bodies, the free boundary condition, which can be formulated as saying that the normal pressure at the boundary vanishes, is known as the zero traction boundary condition.

Following the qualitative discussion above, we shall now mention some results on the Cauchy problem in continuum mechanics. First we consider infinitely extended bodies. For the case of fluids, Christodoulou [7] gives a conditions for shock formation for small data, while for elastic materials John [8] gives a condition (genuine nonlinearity) under which small data lead to formation of singularities. Sideris [9] gives a version of the null condition for elasticity and proves global existence for small data.

For bounded matter distributions, the situation is more complex. As mentioned above, for liquid or fluid bodies in vacuum, the hyperbolicity of the evolution equation degenerates at boundary. This problem can be overcome by using e.g. weighted energy estimates. See [10–12] for recent work on this problem. The Cauchy problem

for elastic bodies with free boundary can in Lagrange coordinates be written as a quasi-linear hyperbolic problem with boundary condition of Neumann type and treated using the methods of e.g. [13]. See [14, 15] for applications of these techniques in elasticity.

If we on the other hand consider self-gravitating material bodies, much less is known. In fact, apart from some limited results which we shall mention below, the problem of constructing solutions of the initial value problem for self-gravitating liquid or fluid bodies in vacuum (both in Newtonian gravity and GR) is largely open.

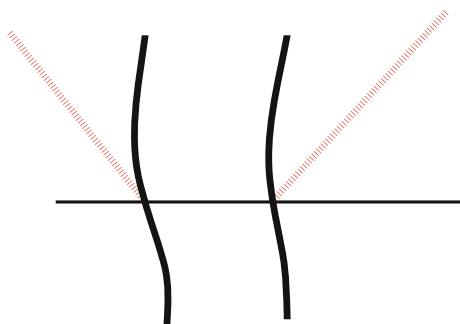
The Einstein equations imply hyperbolic equations for the components of curvature. Hence the irregularity at the boundary of a self-gravitating body could in general be expected to radiate into the surrounding spacetime, preventing this from being regular, cf. Fig. 1. As this clearly does not occur for realistic self-gravitating bodies, there must be a geometric “conspiracy” at the boundary of a self-gravitating body undergoing a regular evolution in Einstein gravity. This then has to be reflected in compatibility conditions on the Cauchy data for such a body, see [16].

It has in recent work been possible to prove local well-posedness for the the initial value problem for self-gravitating elastic bodies in Newtonian gravity, cf. [15], and general relativity, cf. [17, 18], see also Sect. 4 below. In both cases, one finds that corner conditions on the initial data originating from the free boundary condition, which from a PDE point of view is of Neumann type, as well as compatibility conditions on the Cauchy data.

If we turn to dynamical liquid or fluid bodies in general relativity, the results are quite limited. Choquet-Bruhat and Friedrich [19] considered the initial value problem for a dust body in Einstein gravity, assuming a density which is regular at the boundary. The work of Kind and Ehlers [20] on self-gravitating fluid bodies in general relativity restricts to spherical symmetry but allows a discontinuity at the boundary for the matter density. Rendall [21] was able to prove local well-posedness for Einstein-fluid bodies with certain restricted class of equations of state, and with smooth density at the boundary.

Steady states of self-gravitating bodies provide in particular solutions of the initial value problem, and thus, apart from their intrinsic interest, a study of steady states gives useful information for the study of the dynamics of self-gravitating bodies.

Fig. 1 It is a priori possible that the irregularity at the boundary of a body causes the surrounding spacetime to be irregular



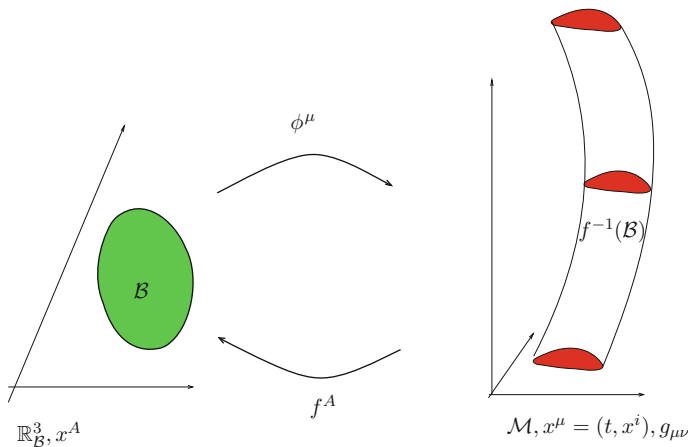
Steady states of fluid configurations in Newtonian gravity may be complicated, examples are Dedekind and Jacobi ellipsoids, cf. [22, 23]. Lichtenstein [24] constructed static and rotating fluid Newtonian fluid bodies. His results have been extended to elastic matter by Beig and Schmidt [25]. For general Newtonian liquid or fluid bodies there are only limited results available. Lindblad and Nordgren proved a priori estimates for incompressible Newtonian fluid bodies [26]. Further, problems of dynamics and stability of self-gravitating fluid and liquid bodies in Newtonian gravity have been studied by Solonnikov, see e.g. [27, 28] and references therein.

Static self-gravitating fluid bodies are spherically symmetric, in Newtonian gravity as well as in general relativity, cf. [29]. Lindblom [30] gave an argument showing that viscous stationary fluids in GR are axi-symmetric. Heilig [31] constructed rotating fluid bodies in GR. It is an open problem whether helically symmetric rotating states exist in GR, cf. [32–34] for related work.

Although relativistic elasticity has been studied since shortly after the introduction of relativity, cf. [35] (special relativity), [36–39], until recently no existence or well-posedness results except in the spherically symmetric case, cf. [40]. Work by the author with Beig and Schmidt shows that there are examples of static self-gravitating elastic bodies in general relativity which have no symmetries, cf. [41]. Similarly, there are rigidly rotating self-gravitating elastic bodies in general relativity with minimal symmetry, i.e. which are stationary and axially symmetric [42].

2 Classical Elasticity

An elastic body is described in terms of configurations with respect to a *reference body* \mathcal{B} , a domain in the extended body $\mathbb{R}^3_{\mathcal{B}}$.



The *configuration maps* f from the physical spacetime to the reference body, and the *deformation maps* ϕ from the reference body to spacetime are assumed to satisfy

$$f \circ \phi|_{\mathcal{B}} = \text{id}.$$

The role of the configuration map f in the Eulerian variational formulation of elasticity in the context of general relativity has been stressed by Kijowski and Magli [38]. See the books by Marsden and Hughes [43] and Truesdell and Noll [44] for background on elasticity.

The physical body $f^{-1}(\mathcal{B})$ moves in spacetime \mathcal{M} with coordinates $x^\mu = (t, x^i)$ and metric $g_{\mu\nu}$. Coordinates as well as coordinate indices on \mathcal{B} are denoted with capital letters, X^A . It is convenient to endow the body \mathcal{B} with a *body metric* b_{AB} . For many situations, this can be taken to be the Euclidean metric $b_{AB} = \delta_{AB}$.

We start by considering the non-relativistic case. In the non-relativistic case it is natural to take $\mathcal{M} = \mathbb{R}_t \times \mathbb{R}_S^3$, where \mathbb{R}_S^3 is the space-manifold, metric g_{ij} , which in the non-relativistic case can be taken to be Euclidean. The action for a hyperelastic body in Newtonian gravity takes the form

$$S = \int \Lambda dt d^3x \quad (2.1)$$

where

$$\Lambda = \Lambda^{kin} - [\Lambda^{grav} + \Lambda^{pot} + \Lambda^{elast}] \quad (2.2)$$

where

$$\begin{aligned} \Lambda^{kin} &= \frac{1}{2} \rho v^2 \chi_{f^{-1}(\mathcal{B})}, \\ \Lambda^{grav} &= \frac{|\nabla U|^2}{8\pi G}, \\ \Lambda^{pot} &= \rho U \chi_{f^{-1}(\mathcal{B})}, \\ \Lambda^{elast} &= n \epsilon \chi_{f^{-1}(\mathcal{B})}. \end{aligned}$$

See [6, Sect. 3]. Here $n = \det \partial f$ is the number density, and $\epsilon = \epsilon(f, \partial f)$ is the stored energy function, representing the internal energy of the material. We have, for clarity included the indicator function $\chi_{f^{-1}(\mathcal{B})} = \chi_{\mathcal{B}} \circ f$ of the physical body, where $\chi(X) = 1$ for $X \in \mathcal{B}$, and $\chi(X) = 0$ otherwise. The physical mass density is $\rho = nm$ where m is the specific mass of the material particles. Further, U is the Newtonian potential and

$$|\nabla U|^2 = \partial_i U \partial_j U g^{ij}.$$

The kinetic term in the action is defined in terms of the square velocity

$$v^2 = v^i v^j g_{ij},$$

with the 3-velocity, given by $v^i = -\phi^i{}_{,A} f^A{}_{,t}$, representing the motion in space of the material particles. It should be stressed that the terms Λ^{pot} , Λ^{kin} , Λ^{elast} are supported on $f^{-1}(\mathcal{B})$ while the term Λ^{grav} should be viewed having support on the whole \mathbb{R}_S .

Remark 2.1

1. Defining the Newtonian potential by the Poisson integral

$$U(x) = -G \int_{f^{-1}(\mathcal{B})} \frac{\rho(x')}{|x - x'|} d^3 x', \quad (2.3)$$

the term $\Lambda^{grav} + \Lambda^{pot}$ can be replaced by

$$\frac{1}{2} \rho U \chi_{f^{-1}(\mathcal{B})}$$

2 The Lagrangian given in (2.2) is of the familiar form

$$L = T - V$$

with T , V the kinetic and potential terms, respectively. The corresponding Hamiltonian (or energy) is then

$$H = T + V$$

The elastic stress tensor is

$$\tau_j^i = n \frac{\partial \epsilon}{\partial f^A{}_{,i}} f^A{}_{,j}$$

This is the canonical energy-momentum tensor for the elastic part of the action. Assuming suitable asymptotic behavior for the fields, the Euler-Lagrange equation for the action (2.1) is

$$\rho v^\mu \partial_\mu v_i \chi_{f^{-1}(\mathcal{B})} + \partial_j (\tau_i^j \chi_{f^{-1}(\mathcal{B})}) + \rho \partial_i U \chi_{f^{-1}(\mathcal{B})} = 0 \quad (2.4)$$

Now, an important fact is that the divergence

$$\partial_j (\tau_i^j \chi_{f^{-1}(\mathcal{B})})$$

is a function in L^p only if the normal stress vanishes at the boundary of the body, i.e.

$$\tau_i^j n_j|_{\partial f^{-1}(\mathcal{B})} = 0,$$

cf. [41, Lemma 2.2]. This is due to the fact that the gradient of the indicator function is of the form

$$\partial_i \chi^{f^{-1}(\mathcal{B})} = -\nu_i \delta_{\partial f^{-1}(\mathcal{B})}$$

where $\delta_{\partial f^{-1}(\mathcal{B})}$ is the surface delta function. Thus,

$$\rho v^\mu \partial_\mu v_i + \partial_j \tau_i^j + \rho \partial_i U = 0, \quad \text{in } f^{-1}(\mathcal{B}), \quad (2.5a)$$

$$\tau_i^j n_j|_{\partial f^{-1}(\mathcal{B})} = 0 \quad \text{on } \partial f^{-1}(\mathcal{B}) \quad (2.5b)$$

coupled to the Poisson equation

$$\Delta U = 4\pi G \rho \chi_{f^{-1}(\mathcal{B})} \quad (2.5c)$$

which has solution given by (2.3). Here

$$v^\mu \partial_\mu = \partial_t + v^i \partial_i$$

so that

$$v^\mu \partial_\mu v^i$$

gives the acceleration of the physical particles. Equation (2.5a) corresponds to Newton's force law $F = ma$, where now the force includes both force generated by elastic stress as well as the gravitational force, together with the free boundary, or zero traction, boundary condition (2.5b). The boundary condition represents the fact that the motion of the boundary is not subject to any external forces.

We recall some facts from potential theory. We can write the Newtonian (volume) potential given by (2.3) as

$$U = \Delta^{-1}(4\pi G \rho \chi_{f^{-1}(\mathcal{B})})$$

Differentiating gives

$$\partial_{x^i} U = \Delta^{-1}[\partial_{x^i} 4\pi G \rho] - \mathcal{S}[\text{tr}_{\partial f^{-1}(\mathcal{B})} 4\pi G \rho \nu^i], \quad (2.6)$$

where \mathcal{S} is the layer potential and ν^i is the normal to $\partial f^{-1}(\mathcal{B})$. Similarly, $\partial_{x^i} \mathcal{S}$ can be expressed in terms of the double layer potential \mathcal{D} . Standard estimates for \mathcal{S} , \mathcal{D} and an inductive argument can be used to estimate U . Due to the jump in the matter density $\rho \chi_{f^{-1}(\mathcal{B})}$ we have that $\partial^2 U$ is discontinuous at $\partial f^{-1}(\mathcal{B})$. However, U has full regularity up to $\partial f^{-1}(\mathcal{B})$. See [6, Appendix A] for details.

In the material frame (Lagrange coordinates) the physical body is represented by the deformation map $\phi(\mathcal{B})$. The material form of the action is got by simply pulling back the Lagrange density from the Eulerian picture (in spacetime) to get

$$S_{\text{material}} = \int \phi^*(\Lambda dt d^3x).$$

The Euler-Lagrange equation can then be calculated purely in the material picture. An important simplification is gained due to the fact that the domain of the body in the material picture is the reference body \mathcal{B} , which is time-independent. One finds that under suitable assumptions on the stored energy function, the Cauchy problem for the elastic body in material frame is an initial-boundary value problem on \mathcal{B} with Neumann type boundary conditions.

Since we have $\tau_i^j = \tau_i^j(f, \partial f)$, the expression $\partial_j \tau_i^j$ is a quasi-linear second order operator on f . Disregarding the gravitational self-interaction for the moment, hyperbolicity of the system (2.5) is determined by the properties of the *elasticity tensor*

$$L_A^i B^j = \frac{\partial^2 \epsilon}{\partial f^A_{,i} \partial f^B_{,j}}$$

e.g. rank-one positivity

$$L_A^i B^j \xi^A \eta_i \xi^B \eta_j \geq C |\xi|^2 |\eta|^2$$

or pointwise stability

$$L_A^i B^j \xi^A_{,i} \xi^B_{,j} \geq C \xi^A_{,i} \xi^B_{,j} b_{AB} g^{ij}$$

where C is some positive constant. If one of these conditions hold, the system (2.5) forms a quasi-linear elliptic-hyperbolic system with Neumann-type boundary conditions.

A formulation of elasticity compatible with general relativity requires the elastic action to be generally covariant. This implies that the stored energy function is *frame indifferent*. Define the strain tensor γ^{AB} by

$$\gamma^{AB} = f^A_{,i} f^B_{,j} g^{ij}$$

and let λ_i , $i = 1, 2, 3$ be the fundamental invariants of $\gamma^A_B = \gamma^{AC}(b)_{CB}$. The material is frame indifferent if $\epsilon = \epsilon(f, \gamma^{AB})$ and isotropic if $\epsilon = \epsilon(\lambda_i)$.

Remark 2.2

1. In the variational problem of classical elasticity (with energy determined purely by the elastic term), polyconvexity [45], i.e. the condition

$$\epsilon(F) = \hat{\epsilon}(F, \text{Cof} F, \det F)$$

where $F = (\phi^i_{,A})$, with $\hat{\epsilon}$ convex, leads to cancellations which in certain circumstances allow one to show convergence of minimizing sequences.

2. Small perturbations around a stress free state are governed by the quasi-linear wave equation

$$\partial_t^2 \phi - c_2^2 \Delta \phi - (c_1^2 - c_2^2) \text{grad div } \phi = F(\nabla \phi, \nabla^2 \phi),$$

cf. [46].

3. The field equation of classical elasticity is analogous to membrane equation which has action

$$S = \int \sqrt{|\phi^* g|}$$

For the vacuum Einstein equation in wave coordinates, L^2 bounded curvature (which corresponds to H^2 regular data) implies local well-posedness [47]. For elasticity and the membrane equation, the analogous result would be well-posedness for H^3 regular initial data.

A static body is in equilibrium, in particular, the elastic load must balance the load from e.g. the gravitational force. Further, in Newtonian gravity, Newtons principle *actio est reactio* implies further that each component of a body must be in equilibrium. The following equilibration condition is a consequence of the assumption that the total load on a body from elastic stress and gravitational force does not generate a motion. Gauss' law and the zero traction boundary condition gives for any Euclidean Killing field ξ^i with $\xi_{i,j} = \xi_{[i,j]}$

$$\int_{f^{-1}(\mathcal{B})} \xi^j \partial_i \tau_j^i = \int_{\partial f^{-1}(\mathcal{B})} \xi^j \tau_j^i n_i = 0,$$

The body is static if the stress load balances the gravitational load

$$\partial_i \tau_j^i = b_i := \rho \partial_j U$$

In particular such a load must be *equilibrated*

$$\int_{f^{-1}(\mathcal{B})} \xi^i b_i = 0,$$

for any Killing field ξ^i . For a general load this is a non-trivial condition, but a gravitational load is automatically equilibrated.

As mentioned above, it is convenient in applying PDE techniques to elastic bodies, to consider the system in the material frame. This is true both in the construction of steady states of Newtonian elasticity, see [25] and references therein, but also for the Cauchy problem. Assuming suitable constitutive relations, the initial value problem for a Newtonian self-gravitating body in material frame is an elliptic-hyperbolic system with Neumann type boundary conditions. Well-posedness has been proved for this system in [15], assuming suitable constitutive relations. This result gives the

first construction of self-gravitating dynamical extended bodies with *no symmetries*. One finds that the initial data must satisfy *compatibility conditions* induced by the Neumann boundary conditions.

3 Elastic Bodies in General Relativity

The action for an general relativistic elastic body is

$$S = - \int \frac{R\sqrt{-g}}{16\pi G} d^4x + \int \Lambda \sqrt{-g} d^4x. \quad (3.1)$$

where $\Lambda = \Lambda(f, \partial f, g) = n\epsilon\chi_{f^{-1}(\mathcal{B})}$ is the energy density of the material in its own rest frame. Here we have included the indicator function $\chi_{f^{-1}(\mathcal{B})}$ for space-time trajectory of the body explicitly in the action. The relativistic number density is given by $n = \det(\gamma^{AB})^{1/2}$ with $\gamma^{AB} = f^A{}_{,\mu} f^B{}_{,\nu} g^{\mu\nu}$, and ϵ is the stored energy function. As mentioned above, general covariance demands *frame invariance*, i.e. $\epsilon = \epsilon(f, \gamma^{AB}, g)$.

The Euler-Lagrange equations for this action are the Einstein equations

$$G_{\mu\nu} = 8\pi G T_{\mu\nu} \chi_{f^{-1}(\mathcal{B})}, \quad (3.2a)$$

where

$$G_{\mu\nu} = R_{\mu\nu} - \frac{1}{2} R g_{\mu\nu}, \quad T_{\mu\nu} = 2 \frac{\partial \Lambda}{\partial g^{\mu\nu}} - \Lambda g_{\mu\nu}$$

The elasticity equations, including the free boundary condition

$$T_{\mu\nu} \nu^\nu \big|_{\partial f^{-1}(\mathcal{B})} = 0,$$

where ν^ν is the normal to the (typically time-like) boundary of the spacetime domain of the body are consequences of the conservation equation

$$\nabla^\mu (T_{\mu\nu} \chi_{f^{-1}(\mathcal{B})}) = 0 \quad (3.2b)$$

which in turn follows from the Einstein equation (3.2a), but which can also be derived as the Euler-Lagrange equation for the action with respect to variations of the configuration map. The field equations for a general relativistic elastic body may thus be viewed as the Einstein equation (3.2a) or, equivalently, as the coupled system (3.2).

3.1 Static Body in GR

We next consider the case of static self-gravitating bodies in general relativity. Thus, we assume $(\mathcal{M}, g_{\mu\nu})$ is static, i.e. there is a global timelike, hypersurface orthogonal, Killing field ξ^μ . Then we have that $\mathcal{M} = \mathbb{R} \times M$ and we may introduce coordinates $x^\mu = (t, x^i)$ such that the Killing field is $\xi^\mu \partial_\mu = \partial_t$, with norm $e^{2U} = -\xi^\mu \xi_\mu$. For a static spacetime we can write

$$g_{\alpha\beta} dx^\alpha dx^\beta = -e^{2U} dt^2 + e^{-2U} h_{ij} dx^i dx^j$$

where U, h_{ij} depend only on x^i . Kaluza-Klein reduction applied to (3.1) gives the action

$$S = - \int_M \frac{1}{16\pi G} \sqrt{h} (R_h - 2|\nabla U|_h^2) + \int_M e^U n^\epsilon \sqrt{h} \quad (3.3)$$

The Euler-Lagrange equations are

$$\begin{aligned} \nabla_j (e^U \sigma_i^j) &= e^U (n^\epsilon - \sigma_l^l) \nabla_i U \quad \text{in } f^{-1}(\mathcal{B}), \quad \sigma_i^j n_j|_{f^{-1}(\partial\mathcal{B})} = 0 \\ \Delta_h U &= 4\pi G e^U (n^\epsilon - \sigma_l^l) \chi_{f^{-1}(\mathcal{B})} \quad \text{in } \mathbb{R}_S^3 \\ G_{ij} &= 8\pi G (\Theta_{ij} - e^U \sigma_{ij} \chi_{f^{-1}(\mathcal{B})}) \quad \text{in } \mathbb{R}_S^3 \end{aligned}$$

where

$$\Theta_{ij} = \frac{1}{4\pi G} \left[\nabla_i U \nabla_j U - \frac{1}{2} h_{ij} |\nabla U|^2 \right].$$

This system is equivalent to the 3 + 1 dimensional Einstein equations for the static elastic body.

Let a relaxed reference body \mathcal{B} be given. For small G , we construct a static self-gravitating body, i.e. a solution to the static Einstein-elastic equations, which is a deformation of \mathcal{B} , cf. [41]. The construction is carried out in the material frame. Working in harmonic coordinate gauge, the reduced Einstein-elastic system can be cast in the form

$$\mathcal{F}(G, Z) = 0,$$

where G is Newtons constant and Z denotes the fields in the material frame version of the system, i.e. the deformation map ϕ as well as the material version of the Newtonian potential U and the 3-metric h_{ij} . Assuming suitable constitutive relations, the reduced system of Einstein-elastic equations is an elliptic boundary value problem with Neumann type boundary condition. Given a relaxed background configuration Z_0 , which can be viewed as a solution of the Einstein-elastic system with Newtons constant $G = 0$, we would like to apply the implicit function theorem to construct solutions to (3.2) for small G .

However, an obstacle to doing so is the fact that the linearized operator $D_Z \mathcal{F}(0, Z_0)$ necessarily fails to be an isomorphism. In fact, due to invariance properties of the the equilibration condition, the infinitesimal Euclidean motions, i.e. the Killing vector fields on Euclidean 3-space, are in the kernel. Further, due to the linearized operator $D_Z \mathcal{F}(0, Z_0)$ has a non-trivial co-kernel, which also corresponds to the infinitesimal Euclidean motions. This is due to the fact that the the linearized elasticity operator at the reference configuration is automatically equilibrated. Thus, we have a kernel and cokernel corresponding to the Killing fields of the Euclidean reference metric on M and on \mathbb{R}_B^3 . Applying a projection to $D_Z \mathcal{F}(0, Z_0)$ in order to get an isomorphism we are in a position to apply the implicit function theorem to construct a solution for small G to the projected system

$$\mathbb{P}_B \mathcal{F}(G, Z) = 0.$$

The proof is completed by showing that the solution to the projected system is *automatically equilibrated*, i.e. it is a solution to the full system, including the harmonic coordinate condition.

By choosing the reference body to be non-symmetric, we thus get the first construction of self-gravitating static elastic bodies in general relativity *with no symmetries*. Outside the body, the spacetime is a solution of the vacuum Einstein equations, which will be asymptotically flat, but with no Killing vector fields except for the static Killing field.

In Newtonian gravity there are many examples of static self-gravitating many-body systems, consisting of rigid bodies of the type shown schematically in Fig. 2. The method described above in the case of static self-gravitating bodies extends to N -body configurations [48]. In this case, one takes a Newtonian static configuration N -body configuration consisting of rigid, self-gravitating bodies as the starting point. Under some conditions on the Newtonian potential one can apply a deformation

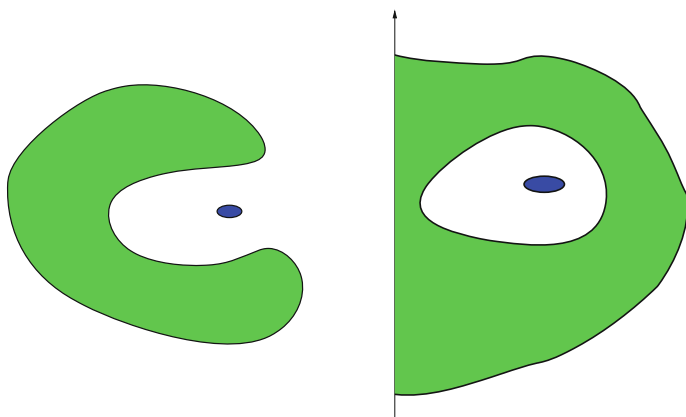
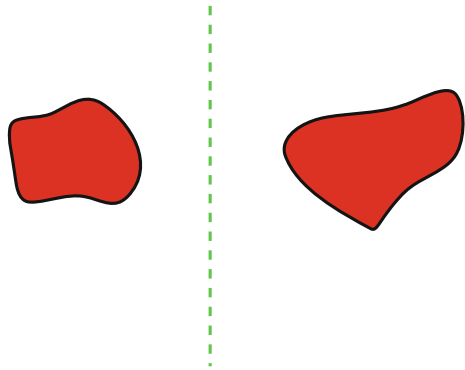


Fig. 2 Examples of two-body configurations in equilibrium

Fig. 3 Bodies separated by a plane cannot be in equilibrium in Newtonian gravity. This holds in GR if the plane is replaced by a totally geodesic hypersurface. It would be interesting to find a more general characterization of what static configurations are possible



technique related to that used in the construction of static self-gravitating bodies to construct N -body configurations. A particular case consist of placing a small body at a stationary point of the gravitational potential of a large body.

The proof makes use of the additional degree of freedom corresponding to the difference in the centers of mass and alignments of the bodies to achieve equilibration. In Newtonian gravity, one proves easily that a two bodies separated by a plane cannot be in static equilibrium, cf. Fig. 3. This relates to Newton's principle *actio est reactio*, also mentioned above, which implies that each body must be equilibrated with respect to its own self-gravity.

In general relativity, we lack the concept of force (see however [49] for related ideas in the static case) and the problem of characterizing "allowed" n -body configurations is open. Partial results on this problem have been proved by Beig and Schoen [50], and Beig et al. [51]. In particular, bodies separated by a totally geodesic surface cannot be in static equilibrium.

In order to describe rotating, self-gravitating bodies, we must consider stationary spacetimes, i.e. spacetimes with a Killing field which in the relevant situation will be timelike, but not hypersurface orthogonal. In this case, Kaluza-Klein reduction gives action

$$S = - \int_M \frac{\sqrt{h}}{16\pi G} \left(R_h - 2|DU|_h^2 + e^{4U} |\omega|_h^2 \right) + \int_M n e^U \sqrt{h},$$

In this case, one may use techniques related to those discussed above to construct self-gravitating rotating bodies in general relativity as deformations of axi-symmetric relaxed, non-rotating, reference states, see [42]. By choosing the reference body appropriately we get rigidly rotating self-gravitating elastic bodies with a minimal amount of symmetry, i.e. with no additional Killing vector fields than the stationary and axial Killing vector fields. The asymptotically flat vacuum region surrounding the rotating body can in that case be shown to have exactly these two Killing symmetries. It is plausible that all stationary, asymptotically flat spacetimes which are vacuum near infinity, are axisymmetric.

4 Dynamics of Elastic Bodies in General Relativity

We write the Einstein-elastic system, cf. (3.2), in the form

$$\begin{aligned} R_{\mu\nu} &= 8\pi G(T_{\mu\nu} - \frac{1}{2}Tg_{\mu\nu})\chi_{f^{-1}(\mathcal{B})} \\ \nabla^\mu T_{\mu\nu} &= 0 \quad \text{in } f^{-1}(\mathcal{B}) \\ T_\mu{}^\nu \nu_\mu|_{\partial f^{-1}(\mathcal{B})} &= 0 \end{aligned}$$

In order to construct solutions to the Einstein equation it is convenient to work in wave coordinates gauge,

$$g^{\mu\nu}\Gamma_{\mu\nu}^\alpha = 0 \quad (4.1)$$

A standard calculation, cf. [52, Sect. 10.2] shows that with (4.1) imposed, the Einstein equation takes the form becomes a quasi-linear wave equation of the form

$$-\frac{1}{2}\square_g g_{\mu\nu} + S_{\mu\nu}(g, \partial g) = 8\pi G(T_{\mu\nu} - \frac{1}{2}Tg_{\mu\nu})$$

where $\square_g = \nabla^\alpha \nabla_\alpha$ is the scalar d'Alembertian and $S_{\mu\nu}$ is an expression which is quadratic in derivatives of $g_{\mu\nu}$. Assuming suitable constitutive relations for the elastic material, the Einstein-elastic system now becomes a quasi-linear hyperbolic system, and one can proceed to construct solutions along standard lines.

A serious obstacle however is the fact that the matter density has a jump at the surface of the body. This means that using standard techniques it appears difficult to prove local well-posedness for this system, even using sophisticated harmonic analysis techniques, as appears in the proof of the L^2 curvature conjecture. In a joint paper with Oliynyk [17] we have given a proof of local existence for solutions of quasi-linear systems with the appropriate discontinuity in the source term. There we have also given an outline of the application of the results of that paper to the Einstein-elastic system [17, Sect. 5]. Details will appear in a joint paper with Oliynyk and Schmidt [18].

An important aspect of the problem can be seen by considering the following model problem. In $\mathbb{R}^{n,1}$ with coordinates $(x^\alpha) = (t, x^i)$, let $\square = -\partial_t^2 + \Delta$ and consider the Cauchy problem

$$\square u = F(t, x, u, \partial u)\chi_\Omega, \quad (4.2a)$$

$$u(0) = u^0, \quad \partial_t u(0) = u^1. \quad (4.2b)$$

Let $u_\ell = \partial_t^\ell u$, $F_\ell = \partial_t^\ell F$ and let s be a given, sufficiently large integer, and let the spaces \mathcal{H}^s be defined by

$$\mathcal{H}^s = \begin{cases} H^s(\mathbb{R}^n), & s = 0, 1, \\ H^s(\mathbb{R}^n) \cap H^s(\Omega) \cap H^s(\mathbb{R}^n \setminus \Omega), & s \geq 2. \end{cases}$$

Suppose we are given data satisfying the *compatibility conditions*

$$u_\ell(0) \in \mathcal{H}^{s+1-\ell}, \quad (4.3)$$

and assume that $F_\ell(\cdot, t) \in H^{s-\ell}(\Omega)$, for $0 \leq \ell \leq s$. Time differentiating the equation yields

$$\square u_j = F_j \chi_\Omega, \quad j = 0, \dots, s. \quad (4.4)$$

A standard energy estimate shows that u_s, u_{s+1} are bounded in H^1 and L^2 , respectively. One gets improved regularity for lower time derivatives by an induction argument. From (4.4) for $j = s - 1$, we have

$$\begin{aligned} \Delta u_{s-1} &= F_{s-1} \chi_\Omega + \partial_t^2 u_{s-1} \\ &= F_{s-1} \chi_\Omega + u_{s+1}. \end{aligned}$$

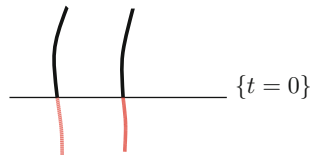
The potential theory results mentioned in Sect. 2 imply that $u_{s-1} \in \mathcal{H}^2$. Suppose now we have for $\ell \geq 1$ an estimate for $u_{s-\ell}$ in $\mathcal{H}^{\ell+1}$ in terms of the initial data and the bound on $F_{s-\ell}$ in $H^\ell(\Omega)$. Then we have from Eq. (4.4) for $j = s - 1 - \ell$,

$$\Delta u_{s-1-\ell} = F_{s-1-\ell} \chi_\Omega + u_{s+1-\ell} \in \mathcal{H}^\ell.$$

and the potential theory results we can now be used together with the assumptions on the initial data and F , to give an estimate for $u_{s-1-\ell}$ in $\mathcal{H}^{\ell+2}$. Induction with $\ell = 1$ as base yields an estimate for u in \mathcal{H}^{s+1} .

An argument similar to the above forms an important part in the proofs of local well-posedness in the papers [17, 18] mentioned above. The compatibility conditions (4.3) on initial data can be interpreted as implying that the body (or in the model problem, the source) existed and was regular in the past of the initial Cauchy surface, i.e. one must have the situation illustrated in Fig. 4.

Fig. 4 The solution to the Cauchy problem is regular provided the Cauchy data is compatible with the source having existed in the past



References

1. L. Barack, TOPICAL REVIEW: Gravitational self-force in extreme mass-ratio inspirals. *Class. Quantum Gravity* **26**(21), 213001 (2009)
2. A.I. Harte, Motion in classical field theories and the foundations of the self-force problem (2014). (In this volume)
3. A. Pound, Motion of small bodies in curved spacetimes: an introduction to gravitational self-force (In this volume)
4. W.G. Dixon, The new mechanics of Myron Mathisson and its subsequent development (In this volume)
5. R.M. Wald, Introduction to gravitational self-force (2009)
6. L. Andersson, R. Beig, B.G. Schmidt, Elastic deformations of compact stars (2014)
7. D. Christodoulou, *The Formation of Shocks in 3-dimensional Fluids*. EMS Monographs in Mathematics. (European Mathematical Society, Zürich, 2007)
8. F. John, Formation of singularities in elastic waves. *Trends and Applications of Pure Mathematics to Mechanics (Palaiseau, 1983)* Lecture Notes in Physics, vol. 195, (Springer, Berlin, 1984), pp. 194–210
9. T.C. Sideris, The null condition and global existence of nonlinear elastic waves. *Invent. Math.* **123**(2), 323–342 (1996)
10. H. Lindblad, Well-posedness for the motion of an incompressible liquid with free surface boundary. *Ann. Math. (2)* **162**(1), 109–194 (2005)
11. D. Coutand, S. Shkoller, Well-posedness in smooth function spaces for the moving-boundary 3-D compressible Euler equations in physical vacuum (2010)
12. Y. Trakhinin, Local existence for the free boundary problem for the non-relativistic and relativistic compressible Euler equations with a vacuum boundary condition (2008)
13. H. Koch, Mixed problems for fully nonlinear hyperbolic equations. *Math. Z.* **214**(1), 9–42 (1993)
14. R. Beig, M. Wernig-Pichler, On the motion of a compact elastic body. *Commun. Math. Phys.* **271**(2), 455–465 (2007)
15. L. Andersson, T.A. Oliynyk, B.G. Schmidt, Dynamical elastic bodies in Newtonian gravity. *Class. Quantum Gravity* **28**(23), 235006 (2011)
16. H. van Elst, G.F.R. Ellis, B.G. Schmidt, Propagation of jump discontinuities in relativistic cosmology. *Phys. Rev. D* **62**(10), 104023 (2000)
17. Lars Andersson, Todd A. Oliynyk, A transmission problem for quasi-linear wave equations. *J. Differ. Equ.* **256**(6), 2023–2078 (2014)
18. L. Andersson, T. Oliynyk, B. Schmidt, Dynamics of self-gravitating elastic bodies in general relativity (in preparation)
19. Yvonne Choquet-Bruhat, Helmut Friedrich, Motion of isolated bodies. *Class. Quantum Gravity* **23**, 5941–5950 (2006)
20. S. Kind, I. Ehlers, Initial-boundary value problem for the spherically symmetric Einstein equations for a perfect fluid. *Class. Quantum Gravity* **10**, 2123–2136 (1993)
21. A.D. Rendall, The initial value problem for a class of general relativistic fluid bodies. *J. Math. Phys.* **33**, 1047–1053 (1992)
22. S. Chandrasekhar, *Ellipsoidal Figures of Equilibrium* (Dover, New York, 1987)
23. R. Meinel, M. Ansorg, A. Kleinwächter, G. Neugebauer, D. Petroff, *Relativistic Figures of Equilibrium* (Cambridge University Press, Cambridge, 2008)
24. Leon Lichtenstein, *Gleichgewichtsfiguren rotierende flüssigkeiten* (Springer, Berlin, 1933)
25. Robert Beig, Bernd G. Schmidt, Celestial mechanics of elastic bodies. *Math. Z.* **258**(2), 381–394 (2008)
26. Hand Lindblad, Karl Hakan Nordgren, A priori estimates for the motion of a self-gravitating incompressible liquid with free surface boundary (2008)
27. V.A. Solonnikov, The problem on evolution of a self-gravitating isolated fluid mass that is not subject to the surface tension forces. *J. Math. Sci. (N. Y.)* **122**(3), 3310–3330 (2004). Problems in mathematical analysis

28. V.A. Solonnikov, On estimates for potentials related to the problem of stability of a rotating self-gravitating liquid. *J. Math. Sci. (N. Y.)* **154**(1), 90–124 (2008). Problems in mathematical analysis. No. 37
29. A.K.M. Masood-ul-Alam, Proof that static stellar models are spherical. *Gen. Relativ. Gravit.* **39**(1), 55–85 (2007)
30. Lee Lindblom, Stationary stars are axisymmetric. *Astrophys. J.* **208**(3, part 1), 873–880 (1976)
31. Uwe Heilig, On the existence of rotating stars in general relativity. *Commun. Math. Phys.* **166**(3), 457–493 (1995)
32. R. Beig, J.M. Heinzle, B.G. Schmidt, Helically symmetric N-Particle solutions in scalar gravity. *Phys. Rev. Lett.* **98**(12), 121102–+ (2007)
33. R. Beig, B.G. Schmidt, Helical solutions in scalar gravity. *Gen. Relativity Gravit.* **41**, 2031–2043 (2009)
34. K. Uryū, F. Limousin, J.L. Friedman, E.ourgoulhon, M. Shibata, Nonconformally flat initial data for binary compact objects. *Phys. Rev. D* **80**(12), 124004–+ (2009)
35. Gustav Herglotz, Über die mechanik des deformierbaren Körpers vom Standpunkte der Relativitätstheorie. *Annalen der Physik* **36**, 493–533 (1911)
36. C.B. Rayner, Elasticity in general relativity. *Proc. R. Soc. Ser. A* **272**, 44–53 (1963)
37. B. Carter, H. Quintana, Foundations of general relativistic high-pressure elasticity theory. *Proc. R. Soc. Lond. Ser. A* **331**, 57–83 (1972)
38. Jerzy Kijowski, Giulio Magli, Unconstrained variational principle and canonical structure for relativistic elasticity. *Rep. Math. Phys.* **39**(1), 99–112 (1997)
39. A. Shadi Tahvildar-Zadeh, Relativistic and nonrelativistic elastodynamics with small shear strains. *Ann. Inst. H. Poincaré Phys. Théor.* **69**(3):275–307 (1998)
40. Jiseong Park, Spherically symmetric static solutions of the Einstein equations with elastic matter source. *Gen. Relativity Gravit.* **32**(2), 235–252 (2000)
41. Lars Andersson, Robert Beig, Bernd G. Schmidt, Static self-gravitating elastic bodies in Einstein gravity. *Commun. Pure Appl. Math.* **61**(7), 988–1023 (2008)
42. Lars Andersson, Robert Beig, Bernd G. Schmidt, Rotating elastic bodies in Einstein gravity. *Commun. Pure Appl. Math.* **63**(5), 559–589 (2010)
43. J.E. Marsden, T.J.R. Hughes, *Mathematical Foundations of Elasticity* (Dover Publications Inc., New York, 1994). Corrected reprint of the 1983 original
44. C. Truesdell, W. Noll, *The Non-linear Field Theories of Mechanics*, 3rd edn. (Springer, Berlin, 2004). Edited and with a preface by Stuart S. Antman
45. J.M. Ball, Convexity conditions and existence theorems in nonlinear elasticity. *Arch. Ration. Mech. Anal.* **63**(4), 337–403 (1976/77)
46. R. Agemi, Global existence of nonlinear elastic waves. *Inventiones Mathematicae* **142**, 225–250 (2000)
47. S. Klainerman, I. Rodnianski, J. Szeftel, The bounded L2 curvature conjecture (2012)
48. L. Andersson, B.G. Schmidt, Static self-gravitating many-body systems in Einstein gravity. *Class. Quantum Gravity* **26**(16), 165007–+ (2009)
49. C. Cederbaum, Geometrostatics: the geometry of static space-times (2012)
50. R. Beig, R.M. Schoen, On static n-body configurations in relativity. *Class. Quantum Gravity* **26**(7), 075014–+ (2009)
51. R. Beig, G.W. Gibbons, R.M. Schoen, Gravitating opposites attract. *Class. Quantum Gravity* **26**(22), 225013–+ (2009)
52. Robert M. Wald, *General Relativity* (University of Chicago Press, Chicago, 1984)

On Geodesic Dynamics in Deformed Black-Hole Fields

O. Semerák and P. Suková

Abstract “Almost all” seems to be known about isolated stationary black holes in asymptotically flat space-times and about the behaviour of *test* matter and fields in their backgrounds. The black holes likely present in galactic nuclei and in some X-ray binaries are commonly being represented by the Kerr metric, but actually they are not isolated (they are detected only thanks to a strong interaction with the surroundings), they are not stationary (black-hole sources are rather strongly variable) and they also probably do not live in an asymptotically flat universe. Such “perturbations” may query the classical black-hole theorems (how robust are the latter against them?) and certainly affect particles and fields around, which can have observational consequences. In the present contribution we examine how the geodesic structure of the static and axially symmetric black-hole space-time responds to the presence of an additional matter in the form of a thin disc or ring. We use several different methods to show that geodesic motion may become chaotic, to reveal the strength and type of this irregularity and its dependence on parameters. The relevance of such an analysis for galactic nuclei is briefly commented on.

1 Introduction

Geodesic structure is a very comprehensive and demonstrative attribute of space (-time). As traversing regions of all possible sizes, geodesics can unveil a local behaviour of a given system as well as tiny tendencies only discernible over an extensive span of time. A default example of the latter are weak irregularities attending a lack of

O. Semerák (✉)

Institute of Theoretical Physics, Faculty of Mathematics and Physics,
Charles University in Prague, Prague, Czech Republic
e-mail: oldrich.semerak@mff.cuni.cz
URL: utf.mff.cuni.cz/en/index.html

P. Suková

Center for Theoretical Physics, Polish Academy of Sciences, Warsaw, Poland
e-mail: psukova@cft.edu.pl
URL: <http://www.cft.edu.pl/en/index.php>

a complete set of integrals of the motion. Actually, the long-term geodesic dynamics is a suitable tool how to detect, illustrate, evaluate, classify and compare different deviations of a chosen system from a certain simple, “regular” ideal. In mathematics and physics, such an ideal is represented by linear systems (the finite-dimensional in particular). However, within the last 150 years it has become clear that even in these highly abstract fields the linear systems represent just marginal tips within a vast non-linear tangle which is typically prone to “irregularities” and which can display “chaotic” behaviour even in rather simple settings.

The modern *theory of chaos* was apparently inspired by Henri Poincaré’s treatment of a three-body system, and our interest will also focus on systems driven by *gravitational* interaction in this contribution. Specifically, we consider a simplest possible gravitational centre, the Schwarzschild black hole, and study how the time-like geodesics in its field respond on perturbation due to the presence of a very simple additional source, namely a static and axially symmetric thin annular disc or ring. Such a topic has an extra *attraction* in general relativity, due to the latter’s non-linearity. Besides that, as reminded in [1], it is doubly apropos to seek for chaos around black holes, because in ancient Greek CHAOS meant a gaping bottomless void, where everything falls endlessly... A more sophisticated reason was articulated nicely by [2]: “...even the most pristine black-hole space-time harbours the seeds of chaos in the form of isolated unstable orbits. A small perturbation causes these unstable orbits to break out and infect large regions of phase space. Note that the experience with Newtonian systems is very misleading. For example, the Kepler problem has more integrals of motion than are needed for integrability. Keplerian systems are thus impervious to small perturbations. In contrast, black hole space-times are at the edge of chaos, just waiting for the proverbial butterfly to flap its wings.”

However, the space-time of a black hole enclosed by a disc or ring has not been chosen only for theoretical reasons: the black holes probably present in galactic nuclei and in some X-ray binaries are supposed to be interacting with their surroundings through disc accretion, and, besides that, galactic nuclei are also typically encircled, at larger distance, by tori of colder molecular gas and dust (called circum-nuclear rings). These structures (at least the inner accretion disc) are assumed to be rather lightweight with respect to the central black hole, and theoretical models actually treat them as test (not contributing to the gravitational field at all). Such an approximation is certainly adequate concerning the potential (metric) and its gradient (field), but may not hold for higher derivatives (curvature). However, the curvature terms are important for stability of the motion, so one can expect that a gravitating matter would assume a *different* configuration than a test one. This could be important in the physics of accretion discs, as the latter e.g. depends crucially on position of the disc inner radius (approximated by the innermost stable circular orbit); this in turn plays a key role in estimating the black-hole spin from observations. The issue was pointed out already by [3] on Newtonian grounds and later confirmed in analysis of the sequences of exact space-times describing the fields of a black hole with concentric thin discs (e.g. [4, 5] and references therein). It turned out, in particular, that the properties of circular motion in the disc plane are indeed altered due to the orbiting-matter own gravity, for example, the frequencies of epicyclic oscillations indicate that the disc

may remain stable closer to the horizon, whereas it rather inclines to instability at larger (intermediate) radii (e.g. [6]).

It should be stressed right away that a test body orbiting in a black-hole field has various other reasons why to behave in a chaotic way. Even if leaving aside the most probable perturbation, namely due to a *mechanical* interaction with the ambient medium, and focusing only on *gravitational* effects, the dynamics depends on how the body is described (whether it is point-like, i.e. without structure, or endowed with more multipoles than just mass), on whether/how it is influenced by incident gravitational and electromagnetic waves, and on whether/how the gravitational and electromagnetic emissions of the body and corresponding reactions on itself are taken into account. Besides that, in reality the body also feels back reaction due to its own gravity (it is not strictly test). Finally, one has to take care of what kind and amount of chaos is added by the numerical code alone: numerical truncations are easily under control for regular orbits along which a sufficient number of quantities (a “complete set of integrals”) remains constant, but for chaotic trajectories such a full check is not at hand. It is really confirmed by experience that even with just slightly modified code it is almost impossible to reproduce *accurately* a given long-term chaotic evolution. This urges caution in interpreting the results of chaotic-dynamics modelling and suggests not to trust it uncritically down to quantitative details.

In such an area, it is of particular importance to use several independent methods (and, if possible, also different basic codes for integration of the equations of motion) and compare their outcomes. The rapid progress that the field of chaotic dynamics have been experiencing since the middle of the 20th century has indeed yielded a number of techniques which, starting from the beginning of 1990s, have been also applied to general relativistic systems. One can roughly divide them into two groups: those which require the knowledge of the system’s dynamics (evolution equations) and those which can manage with just series of values (time series of experimental data, for example). Of the first group, we employed the Poincaré surfaces of section, the Lyapunov exponents and two other similar indicators (abbreviated as FLI and MEGNO) and also followed the evolution of the so called latitudinal action (given by the component of four-momentum which is not bound by any constant of motion). Concerning the second group of methods, we drew the power spectrum of a certain dynamical variable (“vertical” position of the particle in our case) and subjected the motion to two variants of recurrence analysis, one focused on directions in which the orbits recurrently traverse “pixels” of a prescribed phase-space grid and the other based on recurrences to the chosen cells themselves.

Below we first describe our system in more detail. Then, in Sect. 3, we briefly outline methods we have used to analyse the regime of geodesic dynamics in the chosen black-hole–disc/ring field, and review basic observations they provide. Comments concerning astrophysical relevance of the results and possible further extensions of the work are given in Concluding remarks. We will not go into details, especially not concerning the theory of chaos itself and the diagnostic methods used, focusing mainly on results and their interpretation. For a thorough account, please, see the papers [1, 7, 8] and references therein. Let us add that we use geometrized units in which $c = 1$ and $G = 1$ and the metric ($g_{\mu\nu}$) signature $(- + + +)$.

2 Static and Axially Symmetric Metrics for a Black Hole Surrounded by Discs or Rings

Due to the non-linearity of Einstein equations, the fields of multiple sources are very difficult to find in general. In some situations, however, the equations simplify to a form which permits to solve at least a certain part of the problem in a Newtonian manner (namely, certain metric components superpose linearly). One very important example of such a setting is a static and axially symmetric case. Choosing the parameters of these symmetries as the time and azimuthal coordinates, t and ϕ , the *vacuum* metric can always be written then in the Weyl form

$$ds^2 = -e^{2\nu} dt^2 + \rho^2 e^{-2\nu} d\phi^2 + e^{2\lambda-2\nu} (d\rho^2 + dz^2) \quad (1)$$

involving just two unknown functions ν and λ depending only on coordinates ρ and z (cylindrical-type radius and “vertical” axis) which cover the meridional surfaces. The ν function represents Newtonian gravitational potential and is given by Laplace equation, hence it superposes linearly. The other function λ represents non-Newtonian part of the problem. It is given by line integration of the derivatives of ν , reducing to zero along the vacuum parts of the axis; it does not superpose linearly and except some special cases it has to be found numerically.

In general relativity, the motion has 3 degrees of freedom in general, because four-velocity u^μ is always constrained by normalization $g_{\mu\nu} u^\mu u^\nu = -1$. In the above space-times, we have two independent constants of *geodesic* motion thanks to the stationarity and axial symmetry, namely energy and angular momentum with respect to infinity per unit particle mass, $\mathcal{E} = -g_{tt} u^t$ and $\ell = g_{\phi\phi} u^\phi$. In contrast to the space-times of *isolated* stationary black holes, there is no irreducible Killing tensor and consequently no other independent conserved quantity (the so-called Carter constant quadratic in four-velocity), which implies that the geodesic motion may become chaotic.

We have been interested in time-like geodesic dynamics in the field of a Schwarzschild black hole surrounded, in a concentric way, by an annular thin disc or ring. Specifically, we considered one of the discs (mainly the first one) of the counter-rotating Morgan-Morgan family, inverted (Kelvin-transformed) with respect to their rim (see e.g. [4, 9]),¹ and also the Bach-Weyl solution for a circular ring (e.g. [10, 11]). The Newtonian surface densities of the inverted Morgan-Morgan (iMM) discs are

$$w_{\text{iMM}}^{(m)} = \frac{2^{2m} (m!)^2}{(2m)! \pi^2} \frac{\mathcal{M}b}{\rho^3} \left(1 - \frac{b^2}{\rho^2}\right)^{m-1/2} \quad (2)$$

¹We also checked that the results are similar for discs of the family with power-law density profile [5] which are however more demanding computationally.

and their fields are described by the potentials

$$\nu_{\text{iMM}}^{(m)} = -\frac{2^{2m+1}(m!)^2}{\pi} \frac{\mathcal{M}}{b} \frac{\sum_{n=0}^m C_{2n}^{(m)} i Q_{2n}\left(\frac{|y|}{\sqrt{x^2+1-y^2}}\right) P_{2n}\left(\frac{x}{\sqrt{x^2+1-y^2}}\right)}{\sqrt{x^2+1-y^2}}, \quad (3)$$

where the coefficients read

$$C_{2n}^{(m)} = \frac{(-1)^n (4n+1)(2n)!(m+n)!}{(n!)^2 (m-n)!(2m+2n+1)!} \quad (n \leq m),$$

$P_{2n}(y)$ are Legendre polynomials and $Q_{2n}(ix)$ are Legendre functions of the second kind, \mathcal{M} and b are the disc mass and Weyl inner radius and (x, y) are oblate spheroidal coordinates related to the Weyl coordinates by

$$\rho^2 = b^2(x^2 + 1)(1 - y^2), \quad z = bxy.$$

On the symmetry axis ($\rho = 0$) where $x = \frac{|z|}{b}$, $y = \text{sign } z$, $\frac{|y|}{\sqrt{x^2+1-y^2}} = \frac{1}{x}$ and $\frac{x}{\sqrt{x^2+1-y^2}} = 1$, the disc potentials simplify to

$$\nu_{\text{iMM}}^{(m)}(\rho = 0) = -\frac{2^{2m+1}(m!)^2}{\pi} \frac{\mathcal{M}}{|z|} \sum_{n=0}^m C_{2n}^{(m)} i Q_{2n}\left(\frac{ib}{|z|}\right).$$

Our second external source, the Bach-Weyl ring (of mass \mathcal{M} and Weyl radius b), generates potential

$$\nu_{\text{BW}} = -\frac{2\mathcal{M}K(k)}{\pi l_2}, \quad l_{1,2} = \sqrt{(\rho \mp b)^2 + z^2}, \quad (4)$$

where $K(k) = \int_0^{\pi/2} \frac{d\alpha}{\sqrt{1-k^2 \sin^2 \alpha}}$ is the complete elliptic integral of the 1st kind, with modulus and complementary modulus given by

$$k^2 = 1 - \frac{(l_1)^2}{(l_2)^2} = \frac{4b\rho}{(l_2)^2}, \quad k'^2 = 1 - k^2 = \frac{(l_1)^2}{(l_2)^2}.$$

Especially on the axis $\rho = 0$, one has $k = 0$, $K = \pi/2$, so $\nu_{\text{BW}} = -\frac{\mathcal{M}}{z^2+b^2}$.

Our main goal has been to analyse the behaviour of the geodesic flow in dependence on parameters of the system, namely on the relative mass and radius of the disc/ring and on energy and angular momentum of the particles. It should be admitted that both sources are singular (the discs are 2D in space and the ring is even 1D) and curvature scalars really diverge at the ring as well as at the inner edge of the first iMM disc which we consider mostly (the higher- m is the disc, the less singular it

is at the edge). Hence, it is desirable to exclude from study the orbits which would approach the ring or the inner edge of the disc too closely, because there the space-time hardly corresponds to the astrophysical fields we want to approximate. Anyway, we assume that the test particles do not interact with the external source *mechanically* (in particular, they traverse the disc without collision).

3 Geodesic Chaos in the Black-Hole–Disc/Ring Fields

Turning first to Poincaré surfaces, we were recording transitions of suitably chosen large sets of bound orbits through the equatorial plane (the plane of symmetry defined by the disc or ring) and drew the passages in terms of a radial component of four-velocity against radial coordinate. The results showed typical properties of a weakly non-integrable dynamical system, well described by the KAM theory. They were also confirmed by power spectra which we computed from vertical-coordinate time series, and by evolution of the “latitudinal action” given by integral of the latitudinal component of momentum over an orbital period. (The character of dynamics can be well estimated from the time series itself, as well as from a spatial plot of the orbit.) Without repeating details from [1], let us list our main observations:

- Geodesic flow tends to irregularity with increasing relative mass of the external source. The strongest chaos typically occurs when the disc mass is comparable to that of the black hole (for the ring it happens about 1/10 of the black-hole mass). For still heavier external source, the system rather returns to a more regular behaviour.
- Similarly with the dependence on particle energy: chaos first develops with \mathcal{E} increasing, but for very high values it rather reduces back.
- The above are just overall tendencies, however the change of the system with parameters is by no means smooth. Indeed, one of the most typical and interesting aspects of chaotic dynamics is its *chaotic* dependence on parameters, with abrupt changes of the phase portrait occurring/disappearing within very narrow parameter ranges.
- The dependence on angular momentum ℓ is opposite: larger ℓ means larger part of energy allotted to azimuthal motion; and this component of motion is “held” exactly by the conserved value of ℓ , so its larger value favours regularity.
- The ring being stronger source than the disc, it also induces stronger perturbation of the geodesic dynamics. In particular, the ring presence within the region accessible to the particles generates so many higher-periodic regular islands (surrounded by chaotic layers) that the resulting Poincaré diagrams can (also) be used as sophisticated wallpapers. However, if close encounters of the particles with the ring are prevented, the geodesic flow gets only moderately chaotic.
- On (equatorial) Poincaré sections, the geodesic dynamics rather tends to break up from the boundaries of the accessible phase-space region (these boundaries correspond to a zero vertical/latitudinal component of velocity, thus to a motion within the equatorial plane), while a certain regular region often survives in the interior.

- Chaos is a “global” phenomenon and its notion is being used in connection with sufficient time spans, yet it is possible (and practically even inevitable) to speak of a degree of (ir)regularity of a certain restricted *section* of an orbit. Different sections of the same orbit may display very different degrees of chaoticity and the dynamics may switch between these modes quite suddenly. Orbits with such a variable behaviour are typical for weakly perturbed systems and at the same time they are most interesting for comparing different methods.
- Consistently with experience from the literature, such “weakly chaotic” (parts of the) orbits which at times range over the chaotic “sea” but also linger for a considerable intervals very close to regular regions of phase space (they “stick” to them, hence *sticky* orbits) rather produce “1/frequency” spectrum (i.e. approximated by a straight line in the log-log plot), whereas the “strongly chaotic” (parts of the) orbits typically produce “cat-back” spectral profile with (say, 100-times) less power at the low-frequency end, with less distinct peaks and more of tiny irregularities.

In [7] we subjected the above dynamical system to two recurrence methods. The first of them, abbreviated WADV (from “weighted average of directional vectors”), was proposed by [12] as a way to distinguish between deterministic and random systems. Employing it within general relativity for the first time (as far as we know), we found it is even fairly sensitive to different degrees of (deterministic) chaos, especially in the regime of very weak perturbations (which we are mainly interested in). Briefly speaking, one takes a time series of some dynamical variable (we take vertical coordinate $z(\tau)$ as a function of the particle proper time τ) and reconstructs the (3D) phase space from $z(\tau)$, $z(\tau - \Delta\tau)$, $z(\tau - 2\Delta\tau)$, where $\Delta\tau$ is some time delay; this space is then “rasterized” into a grid of boxes of some chosen size. The main point is to add (unit) directions in which orbits recurrently cross the prescribed boxes, average the length of the accumulated vector over the cells with respect to the number of passages and analyse its dependence on $\Delta\tau$ (and on the box size). Finally, the result is evaluated against its counter-part obtained for unit-step random walk, namely, one computes

$$\bar{\Lambda} = \text{average} \left[\frac{\left(\frac{V_j}{n_j} \right)^2 - \left(\bar{R}_{n_j}^d \right)^2}{1 - \left(\bar{R}_{n_j}^d \right)^2} \right]_{\text{over cells (over } j)}, \quad (5)$$

where V_j is the norm of the vector accumulated after n_j passages through the j th box and

$$\bar{R}_n^d = \frac{\Gamma(\frac{d+1}{2})}{\Gamma(\frac{d}{2})} \sqrt{\frac{2}{nd}}, \quad \text{in particular} \quad \bar{R}_n^3 = \frac{4}{\sqrt{6\pi n}}$$

denotes the average shift per step for random walk in d dimensions, obtained for n steps (with particular value given for $d = 3$ which is relevant in our case). Now, the $\bar{\Lambda}$ realizes a normalized autocorrelation parameter: in theoretical limit (infinite

evolution and infinitely fine grain), $\bar{\Lambda} = 1$ for a deterministic signal, whereas $\bar{\Lambda} = 0$ for random data; in practice, $\bar{\Lambda}(\Delta\tau)$ more or less decreases from 1, the faster the more chaotic (or even random) is the evolution.

The second recurrence method we applied rests on recurrences themselves of the orbits to chosen neighbourhoods of their past points. Denoting by $\mathbf{X}_{(i)} = \mathbf{X}(\tau_{(i)})$ the N successive points of a phase-space trajectory,² the recurrences are simply recorded in the so called recurrence matrix

$$R_{i,j}(\epsilon) = \Theta(\epsilon - \|\mathbf{X}_{(i)} - \mathbf{X}_{(j)}\|), \quad i, j = 1, \dots, N, \quad (6)$$

where ϵ is the radius of a chosen neighbourhood (the selected threshold of “close return”), $\|\cdot\|$ denotes the chosen norm (the picture of long-term dynamics only slightly depends on which one is used) and Θ is the Heaviside step function. The matrix thus contains only units and zeros and can be easily visualized by filling black dots (units) or blank spaces (zeros) at the respective coordinates (i, j) ; such figures are called *recurrence plots* and were introduced by [13]. For regular systems, the recurrences (black points) arrange in distinct structures, in particular in long parallel diagonal lines (their distance scales with period), and weak chaos brings checkerboard structures, whereas for random systems the recurrences are scattered without order; chaotic (deterministic) systems yield the most interesting plots, consisting of rectangular blocks of almost-diagonal patterns as well as irregular ones, often looking like placed one over another. The pattern of recurrences yields rich and credible data which can be further processed in numerous ways (see [14] for a thorough survey). Within general relativity, the method has been employed e.g. by [15, 16].

Finally, one of the most characteristic symptoms of chaos is a sensitive dependence on initial conditions, following from the fast deviation of trajectories in the phase space. This divergence can be quantified by various indicators, of which Lyapunov characteristic exponents (λ_i) are the most well known, but other useful suggestions have also been given. The divergence quantifiers can be computed in two ways, either by following two nearby trajectories and the evolution of their phase-space separation, or by solving an appropriate variational equation (geodesic-deviation equation in our case) along one trajectory. We have adhered to the first, two-particle approach, using the procedure proposed—within general relativity—by [17, 18]. They argued, in particular, that it is sufficient to compute the orbital divergence in configuration space only, without including the momenta. This claim seems plausible and we have followed it, but a careful verification is still to be performed. Anyway, of the Lyapunov exponents, each characterizing the rate of separation change in a certain (i -th) independent direction, the most important is the maximal one (which prevails automatically in a longer evolution),

²The series of just one variable (e.g. position) suffices actually, since the phase space can be reconstructed from a sequence of its time-delayed copies as in the WADV method summarized above.

$$\lambda_{\max} = \lim_{\tau \rightarrow \infty} \frac{1}{\tau} \ln \frac{|\Delta \vec{x}(\tau)|}{|\Delta \vec{x}(0)|}, \quad \text{where } |\Delta \vec{x}(\tau)| = \sqrt{|g_{\mu\nu} \Delta x^\mu \Delta x^\nu|(\tau)}. \quad (7)$$

We use small x for the position in configuration space, $\mathbf{X} \equiv (x^\mu, p^\alpha)$, so $\Delta \vec{x}$ is the separation vector whose norm represents the momentary proper distance between the two neighbouring orbits. If $\lambda_{\max} > 0$, then at least one direction exists in which the nearby orbits deviate exponentially.³

Due to typically very slow convergence of the above limit, a number of related quantifiers has been proposed whose computation converges faster and which thus reveal the nature of orbits in a significantly shorter integration time. We have tried two of them, often used in celestial and galactic mechanics, the *fast Lyapunov indicator* (FLI) and the *mean exponential growth of nearby orbits* (MEGNO). The FLI, suggested by [19], is given by

$$\text{FLI}(\tau) = \log_{10} \frac{|\Delta \vec{x}(\tau)|}{|\vec{x}(0)|} \quad (8)$$

(restricting only to the configuration-space separation again). $\text{FLI}(\tau)$ grows considerably faster for chaotic than for regular trajectories and this trend is evident much earlier than $\lambda_{\max}(\tau)$ approaches its limit value. In general relativity (motion in black-hole fields), the FLI has been employed by [20, 21]. The second indicator, MEGNO, was proposed by [22] as

$$Y(T) = \frac{2}{T} \int_0^T \frac{1}{|\Delta \vec{x}(\tau)|} \frac{d|\Delta \vec{x}(\tau)|}{d\tau} \tau d\tau. \quad (9)$$

The content of this quantity is simply its *value* (rather than rate of growth or even “irregularity of behaviour”), which makes it suitable for automatic surveys over large areas of phase space. Importantly, the MEGNO distinguishes between regular and chaotic evolutions securely, because for regular orbits it tends to 2 (with an additional bounded oscillating term), whereas for chaotic orbits it grows linearly, with a slope corresponding to the value of the maximal Lyapunov exponent ($Y \approx \lambda_{\max} T$ for large enough proper time). A few years ago, [23] found an analytic relation between FLI and MEGNO,

$$Y(T) = 2 [\text{FLI}(T) - \overline{\text{FLI}}(T)] \ln(10), \quad (10)$$

where $\overline{\text{FLI}}(T)$ is the FLI time averaged over the period $\langle 0, T \rangle$,

³The exponents should reveal the nature of the flow *in the vicinity* of the reference world-line, hence, while time is running, the separation vector has to be renormalized whenever it reaches a certain “too large” value; the velocity deviation vector, given by difference between four-velocities of the neighbouring world-lines, has to be renormalized by the same factor.

$$\overline{\text{FLI}}(T) = \frac{1}{T} \int_0^T \text{FLI}(\tau) d\tau.$$

Note that one can in turn average the MEGNO over some period in a similar manner (cf. the last part of Fig. 8).

We presented the results obtained using Lyapunov exponents, FLI and MEGNO in paper [8], together with more details and remarks e.g. on often queried (non-) invariance of the world-line deviation indicators. A thorough comparison of these quantities with other similar indicators has recently been given by [24] using the variational approach.

3.1 Relations Between Chaotic Indicators—An Example

Besides relations like that between the FLI and MEGNO indicators (which are of similar nature), yet more interesting are relations between quantities whose origins are more independent. One illustration is an estimate of the maximal Lyapunov exponent which can be obtained from the MEGNO slope as indicated above, but also (for instance) from the 2nd-order Rényi's entropy (also called correlation entropy), one of the indicators derived from the recurrence analysis. Namely, [14] showed that this quantity yields a lower estimate of the sum of positive Lyapunov exponents, and they also suggested that it can be approximated by

$$K_2(\epsilon, l) \approx -\frac{1}{l\Delta\tau} \ln p_c(\epsilon, l), \quad (11)$$

where $\Delta\tau$ is the sampling time step and $p_c(\epsilon, l)$ is the probability of finding a diagonal line whose length is at least l in the recurrence matrix (ϵ is the radius of a chosen “close neighbourhood”). This means that K_2 is estimated from a slope of the cumulative histogram of diagonal lines (of diagonals at least l points long), plotted in logarithmic scale against the length l . We computed both estimates (from MEGNO slope and from Rényi's entropy) and confirmed that they are in line with the values of λ_{\max} obtained by direct computation.

Let us make a remark concerning the “value/price ratio” of the above indicators. Whereas MEGNO was introduced as a handy “condensate” of Lyapunov exponents which can be quite easily implemented in automated scans, the Rényi's entropy is more sophisticated, but also less accessible for routine computer evaluation, mainly because it has to be determined from a proper part of the histogram. Namely, only a certain middle section of the histogram, reasonably following a straight line, is relevant, since the short-length end typically diverges due to increasing number of “sojourn” points (successive points between which the orbit does not leave the given ϵ -neighbourhood⁴), while the long-length end typically falls off quickly due to a

⁴These points does *not* represent true recurrences and are usually discarded from the statistics.

finite length of the trajectory. One should stress that the histogram is theoretically to be computed in the limit $l \rightarrow \infty$, so the short-length end has actually no sense, while the long-length end is of course determined by the fact that practically the trajectories cannot be infinitely long. We are depicting this to point out the benefits of some simpler recurrence quantifiers, especially of the one called DIV, given by inverse of the length of the longest diagonal. We compared the K_2 entropy with the DIV, in particular, we coloured several Poincaré diagrams according to the values of K_2 and DIV obtained for the orbits followed in a given run, and observed that both the quantifiers provide virtually the same information (cf. Fig. 7).

4 Numerical Illustrations

Let us give several examples of how the varying degrees of chaoticity are revealed by the methods we have mentioned above. The passages through a suitably chosen plane, plotted in a suitably chosen variables (called Poincaré maps), provide a direct, reliable and indicative picture of a studied motion. We naturally start with them, showing how the nature of geodesic flow around a black hole changes when a more and more massive thin disc (Fig. 1) or ring (Fig. 2) are placed around in a concentric manner. In both cases, the passages are recorded of some bunch of bound time-like geodesics through the equatorial plane of the system, and plotted in terms of the Schwarzschild-type radius r and of the corresponding component of four-velocity u^r . Figure 3 compares a regular geodesic with a chaotic one, using four representations: their spatial tracks, equatorial Poincaré sections, time dependence of the “vertical” (z) position and the corresponding power spectra. Figure 4 compares two different parts of the *same* geodesic, one “sticking” to a regular island and the other filling a chaotic sea. Four plots are shown—equatorial Poincaré sections, time series of the u^r four-velocity component, the power spectra of $z(t)$ and, in the second part of the figure, recurrence plots; the difference between the two orbital phases is clearly seen in all of them. Four different parts of the same orbit are also shown in Fig. 5 and their increasing chaoticity revealed on the $u^r(t)$ evolution and on the power spectra of $z(t)$.

The above representations are illustrative for a human eye, but less suitable for a quantitative judgement about the “degree of chaoticity” of the system, mainly if such a judgement should be entrusted to a computer. The recurrence methods we tested offer several “quantifiers” that are more suitable in this respect and which assign to every single orbit a single number or a single dependence on some parameter. In the first method, the character of the orbit is recognized from the average of directions in which the orbit recurrently crosses the prescribed phase-space cells (the Kaplan-Glass WADV method described in previous section). In Fig. 6, this averaged autocorrelation parameter is compared for a geodesic lying deep in a primary regular island and for a one inhabiting a large chaotic region; also added are the respective Poincaré diagrams and $z(t)$ evolutions. Figure 7 presents several quantifiers computed from the recurrence matrix and requires some commentary. The quantifiers shown

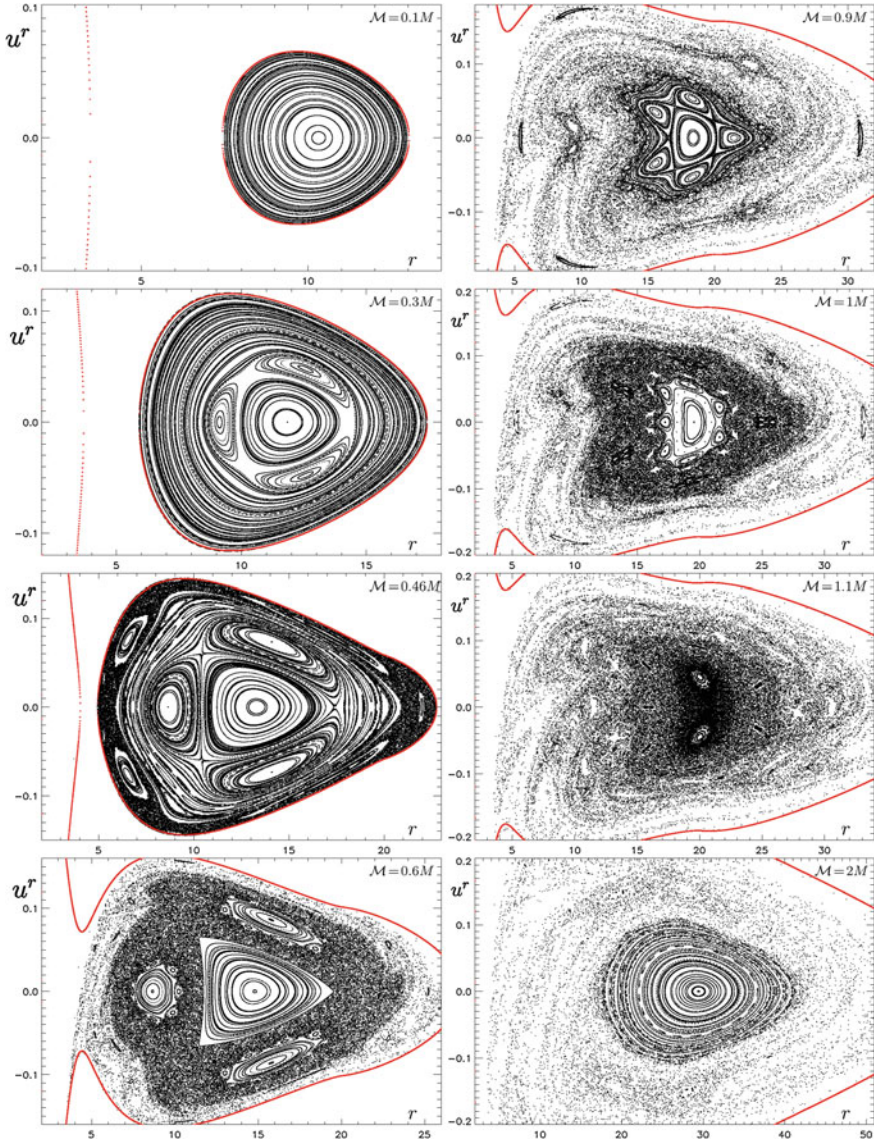


Fig. 1 Passages of geodesics with $\ell = 3.75M$ and $\mathcal{E} = 0.955$ through the equatorial plane of a Schwarzschild black hole (with mass M) surrounded by the inverted 1st Morgan-Morgan disc (with inner Schwarzschild radius $r_{\text{disc}} = 20M$), drawn for different relative disc masses \mathcal{M}/M (indicated in the plots). Red line bounds the accessible region. Adopted from [1]

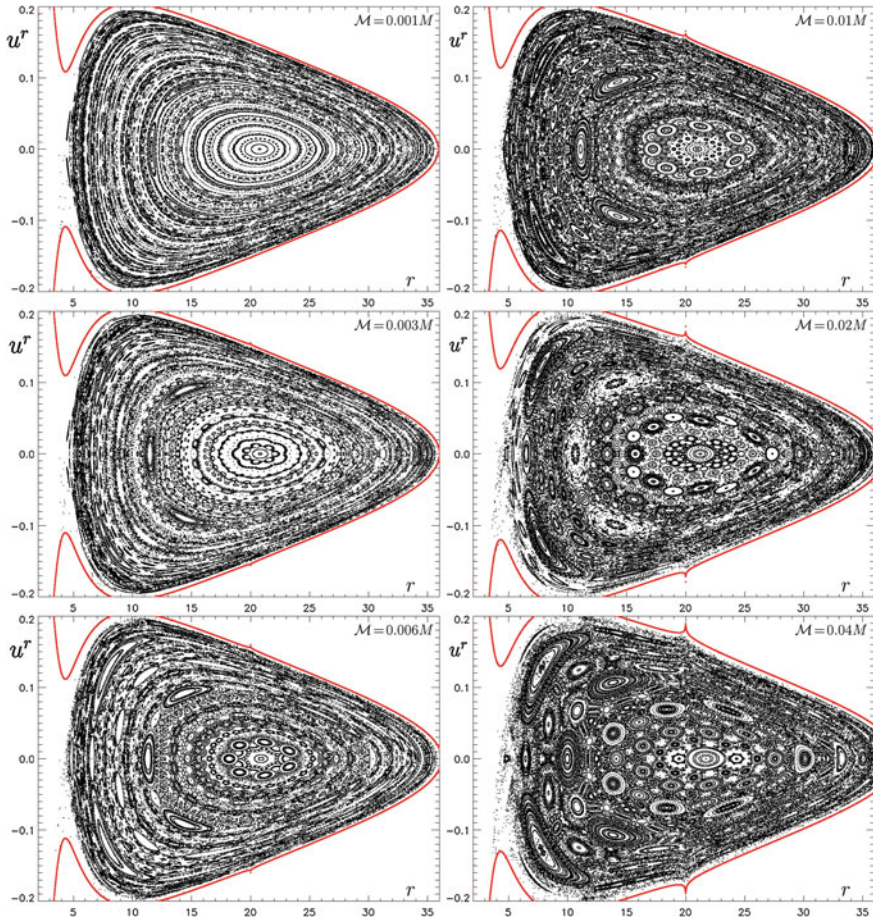


Fig. 2 Passages of geodesics with $\ell = 3.75M$ and $\mathcal{E} = 0.977$ through the equatorial plane of a Schwarzschild black hole (with mass M) surrounded by a Bach-Weyl ring (with Schwarzschild radius $r_{\text{ring}} = 20M$), drawn for different relative ring masses \mathcal{M}/M (indicated in the plots). Red line bounds the accessible region. With growing mass of the ring, the phase space apparently becomes very complex, containing many islands formed by higher-periodic regular orbits, interwoven with chaotic layers. For very high relative masses, the primary regular island restores and dominates the plot again. However, if the particles could not get close to the ring (if the latter did not lie within their accessible region), their motion would be considerably less irregular. The figure is adopted from [1]

are called RR, DET, DIV and VENTROPY (see [14]). The *recurrence rate* RR is given by ratio of the recurrence points (black ones) within all points of the recurrence matrix,

$$\text{RR}(\epsilon) = \frac{1}{N^2} \sum_{i,j=1}^N R_{i,j}(\epsilon).$$

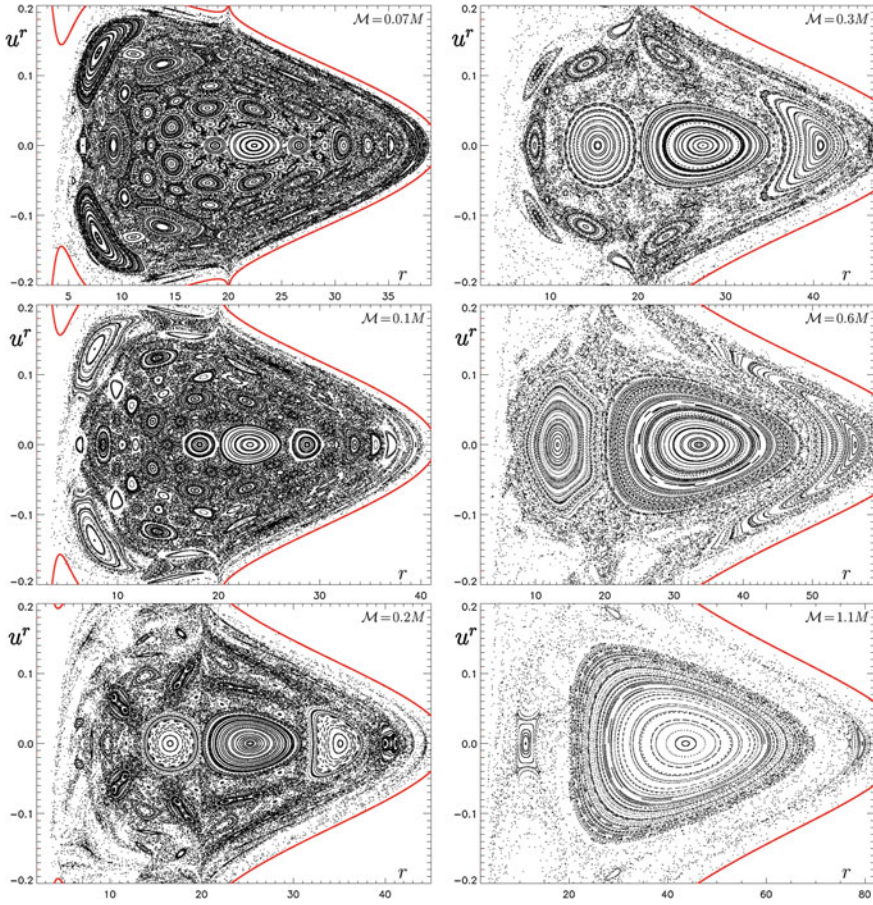


Fig. 2 (continued)

The DIV (“divergence”) quantifier is just reciprocal of the length of the recurrence-matrix longest diagonal. The DET (“determinism”) is a ratio of the points which form a diagonal line longer than a certain l_{\min} within all recurrence points,

$$\text{DET}(\epsilon) = \frac{\sum_{l=l_{\min}}^N l P(\epsilon, l)}{\sum_{l=1}^N l P(\epsilon, l)},$$

where $P(\epsilon, l)$ denotes histogram of lengths of the diagonal lines (length spectrum of the diagonals). Finally, the VENTROPY represents the Shannon entropy of the probability $p(v)$ that a vertical line has length v ,

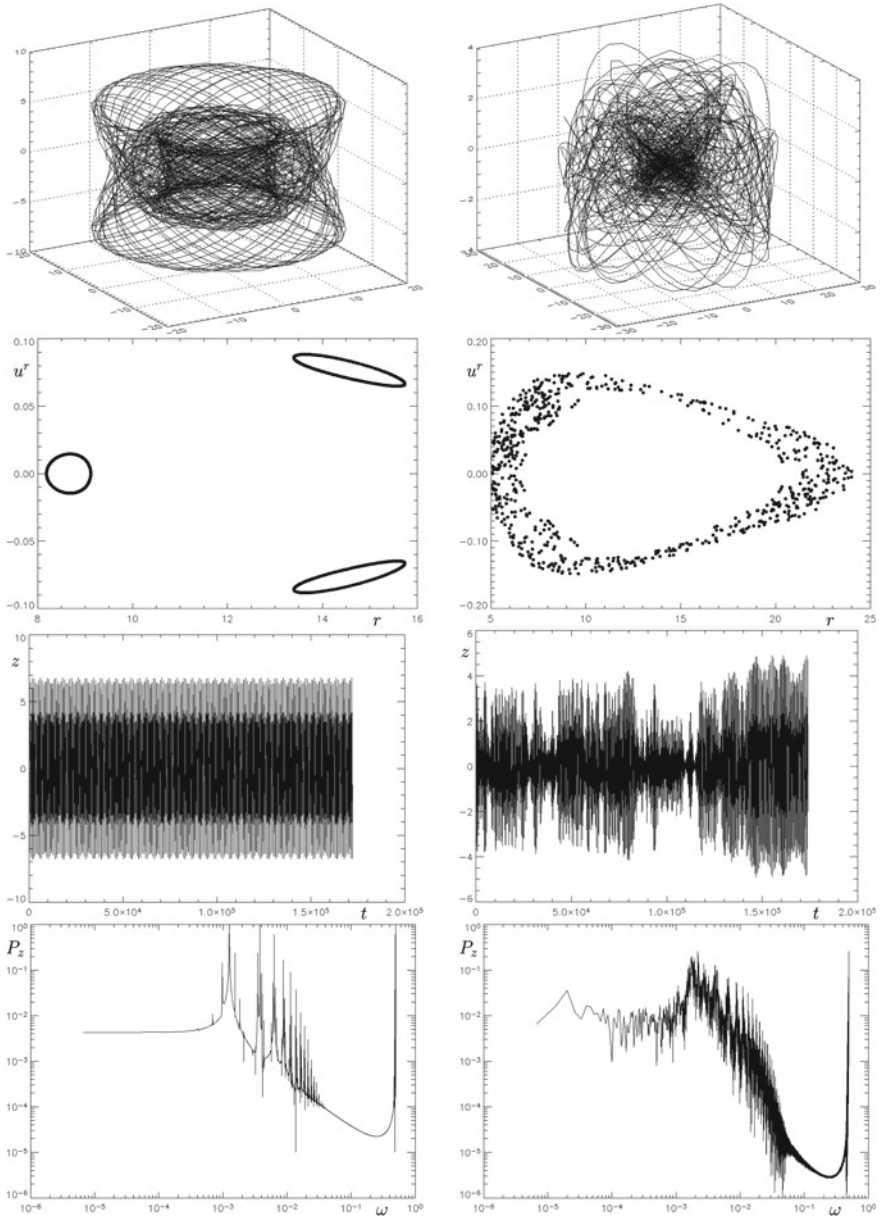


Fig. 3 Example of a regular (*left*) and chaotic (*right*) geodesic, both with $\mathcal{E}=0.955$ and $\ell=3.75M$, in the field of a Schwarzschild black hole surrounded by the inverted 1st Morgan-Morgan disc with $\mathcal{M}=0.5M$, $r_{\text{disc}}=20M$. From *top to bottom*, the rows show their spatial tracks, Poincaré sections $z=0$ (r, u^r), time series of the z position and corresponding power spectra. Coordinates are in $[M]$, frequencies in $[1/M]$. Adopted from [1]

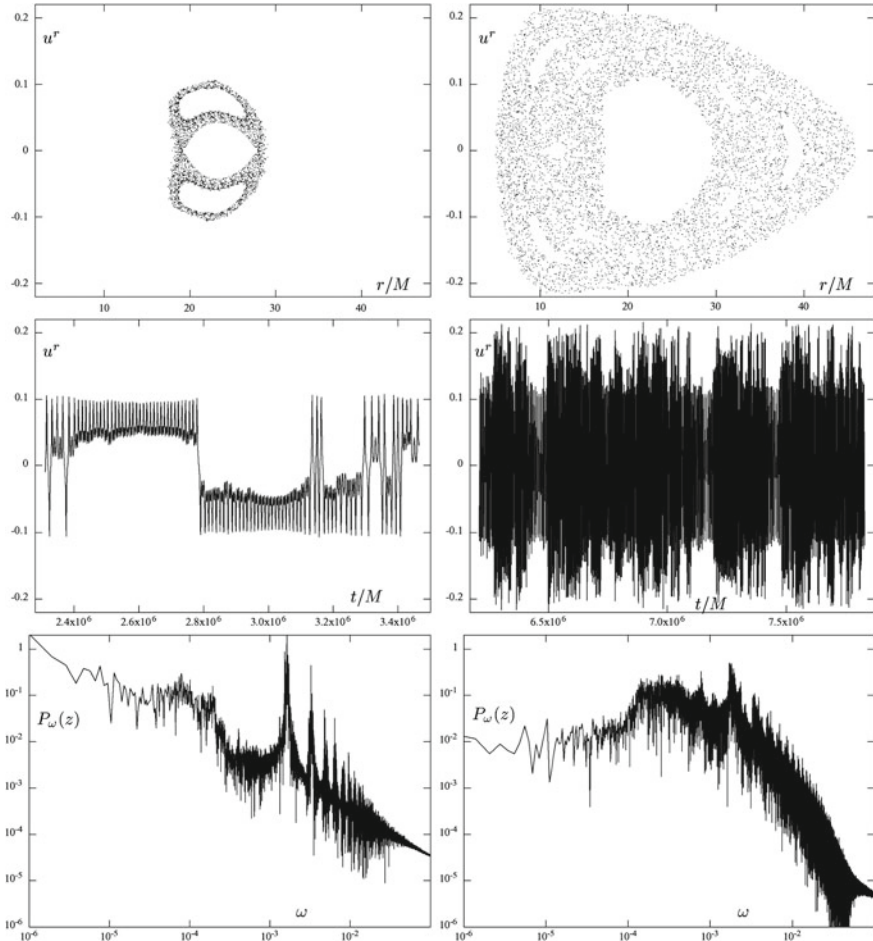


Fig. 4 Example of a “sticky” (*left column*) and strongly chaotic (*right column*) phases of one and the same geodesic (having $\mathcal{E} = 0.956$ and $\ell = 4M$) in the field of a black hole plus an inverted 1st Morgan-Morgan disc (with $\mathcal{M} = 1.3M$, $r_{\text{disc}} = 20M$): Poincaré sections $z = 0$ (r, u^r), time series of u^r and power spectra of the z position. Adopted from [7]. Recurrence plots for the same two orbital sections. Considering the recurrence-matrix symmetry, we give just halves of the plots in one square: the weakly chaotic section is above the main diagonal, while the strongly chaotic one is below the main diagonal. The axis values indicate proper time in units of M . Adopted from [7]

$$\text{V ENTROPY} = - \sum_{v=v_{\min}}^N p(\epsilon, v) \ln p(\epsilon, v), \quad p(\epsilon, v) = \frac{P(\epsilon, v)}{\sum_{v=v_{\min}}^N P(\epsilon, v)}.$$

In Fig. 7 we went along the $u^r = 0$ axis of the Poincaré diagrams and plotted the value of the above quantifiers for geodesics starting tangentially from the respective radii; it represents 470 geodesics in total, starting from radii between $5M$ and $24M$.

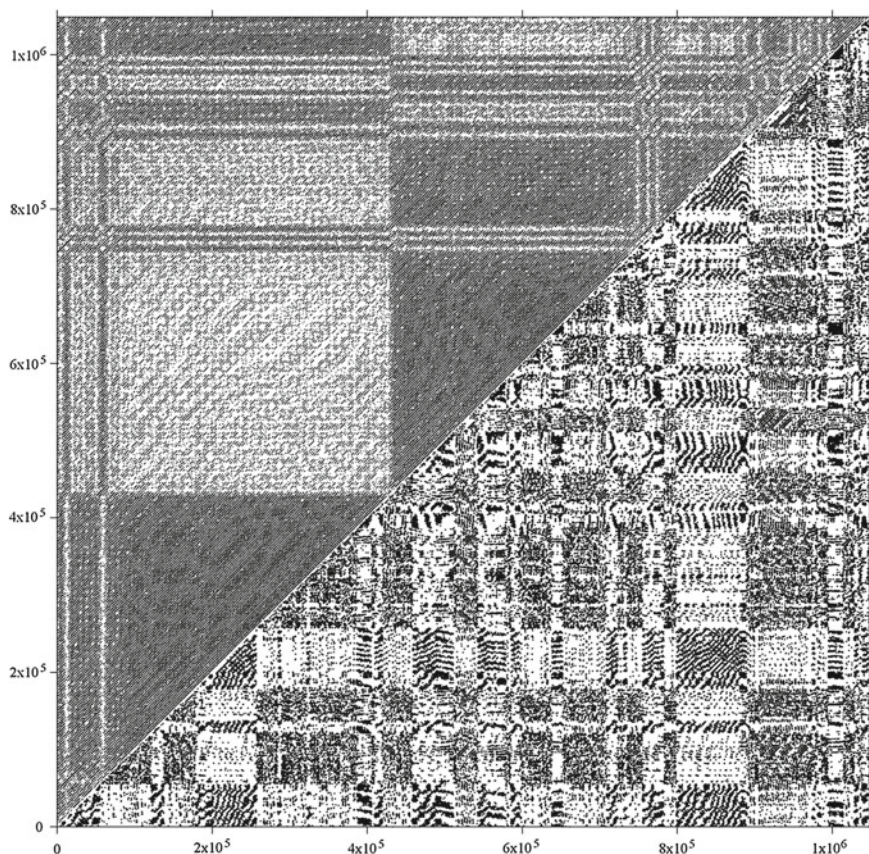


Fig. 4 (continued)

As already noted at the end of previous section, the colouring of the Poincaré maps by the values of the “rough” quantity DIV and its “sophisticated” relative K_2 shows that both bring practically the same information. It is also obvious that the quantifiers (including DIV) are quite sensitive and can uncover even tiny features of phase space.

In the last two figures, the quantifiers of geodesic deviation are illustrated and their message compared with that provided by previous methods. Three orbits of different degrees of chaoticity are analyzed in Fig. 8, first on Poincaré sections and by computing the maximal Lyapunov exponents, then on power spectra of $z(t)$ and on behaviour of the Kaplan-Glass directional autocorrelation in dependence on time shift applied to $z(t)$, and finally by computing the FLI and MEGNO indicators. All the methods clearly distinguish between the orbits and yield consistent results. Figure 9 presents Poincaré maps of three different phase-space situations, coloured

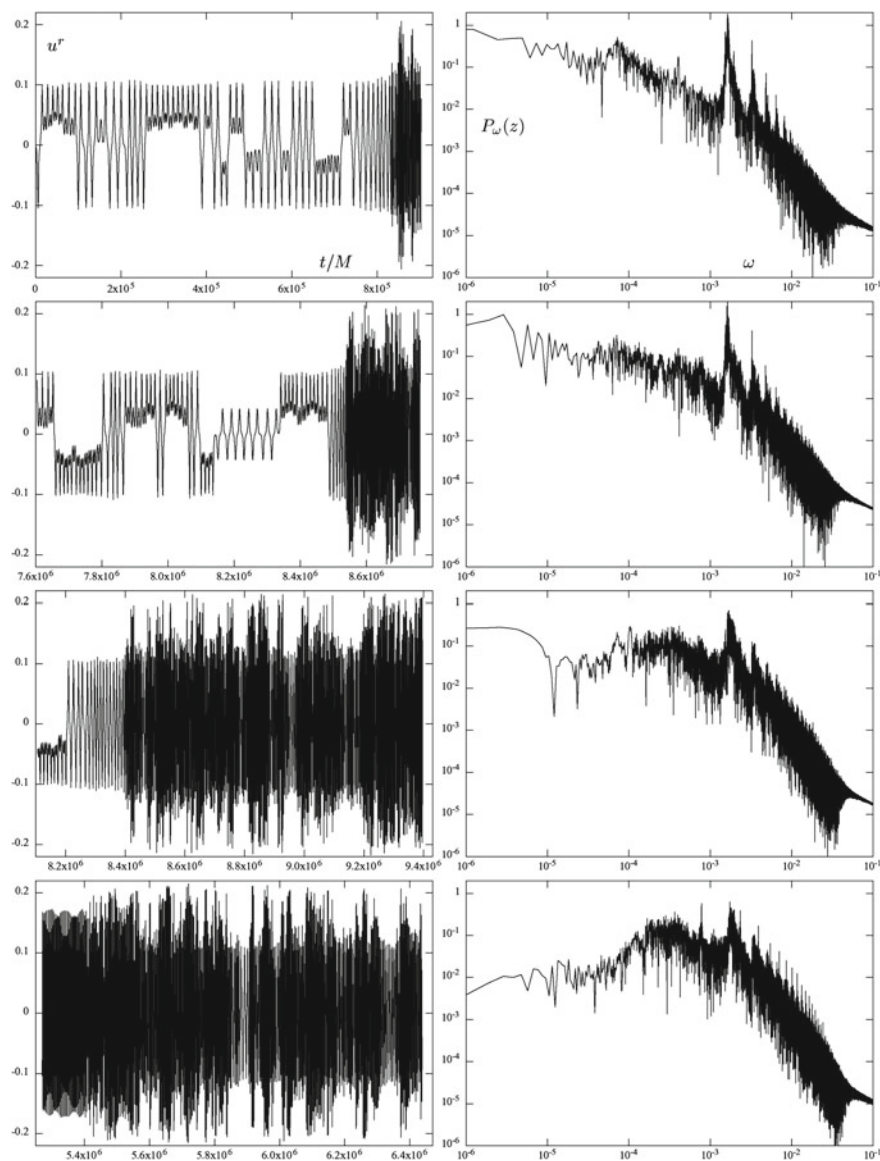


Fig. 5 The $u'(t)$ behaviour (left column) and power spectra of $z(t)$ evolution (right column) of four different sections of the same orbit as in Fig. 4. Chaoticity clearly grows from top to bottom. Adopted from [7]

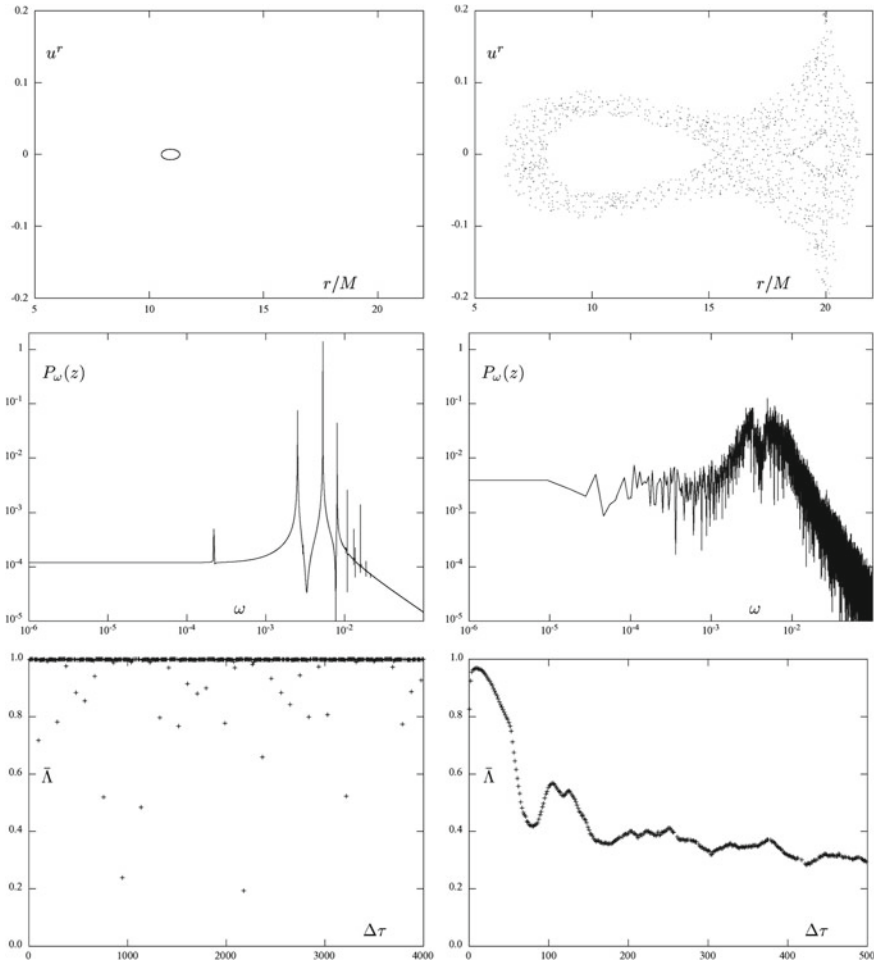


Fig. 6 Difference between a geodesic lying deep in a primary regular island (*left column*) and the one living in a chaotic sea (*right column*), as seen on Poincaré diagram (*top*), $z(t)$ evolution (*middle*) and the Kaplan-Glass averaged autocorrelation parameter $\bar{\Lambda}(\Delta\tau)$ (*bottom*). Both geodesics have $\mathcal{E} = 0.93$ and $\ell = 3.75M$ and the background is determined by a black hole surrounded by a Bach-Weyl ring with $\mathcal{M} = 0.5M$ and $r_{\text{ring}} = 20M$. Adopted from [7]

by $\text{FLI}(\tau_{\text{max}})$ and $\text{MEGNO}(\tau_{\text{max}})$. The quantities apparently provide almost the same message, but MEGNO is somewhat more helpful, because, due to its definite value of 2 for regular orbits, it is more precise in distinguishing them from the chaotic ones (whose MEGNO value is bigger); to benefit from this graphically, one can, for example, increase all the values of MEGNO indicating chaotic evolution by some constant (we did it with all values above 4, in order to be on the safe side).

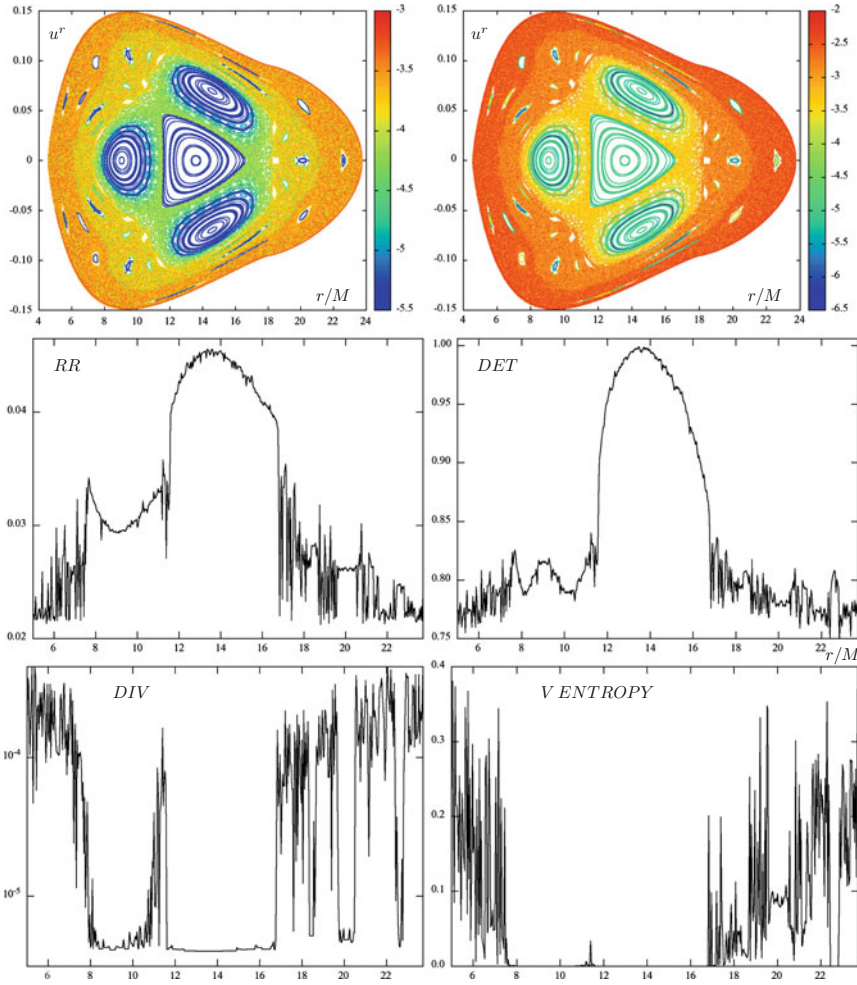


Fig. 7 Examples of quantifiers extracted from the recurrence matrix, as computed for 470 geodesics launched with $\mathcal{E}=0.9532$, $\ell=3.75M$ tangentially (with $u^r=0$) from radii between $5M$ and $24M$ from equatorial plane of a black hole (M) surrounded by the inverted 1st MM disc ($\mathcal{M}=0.5M$, $r_{\text{disc}}=18M$). The orbits were followed for about $250,000M$ of proper time with “sampling” $\Delta\tau=45M$. In Poincaré diagram (top), they are coloured according to their DIV (left) and K_2 (right) values (log scale). The quantifiers shown (see text for description) are clearly sensitive to tiny phase-space features (behaviour along the top-diagram r -axis). Adopted from [7]

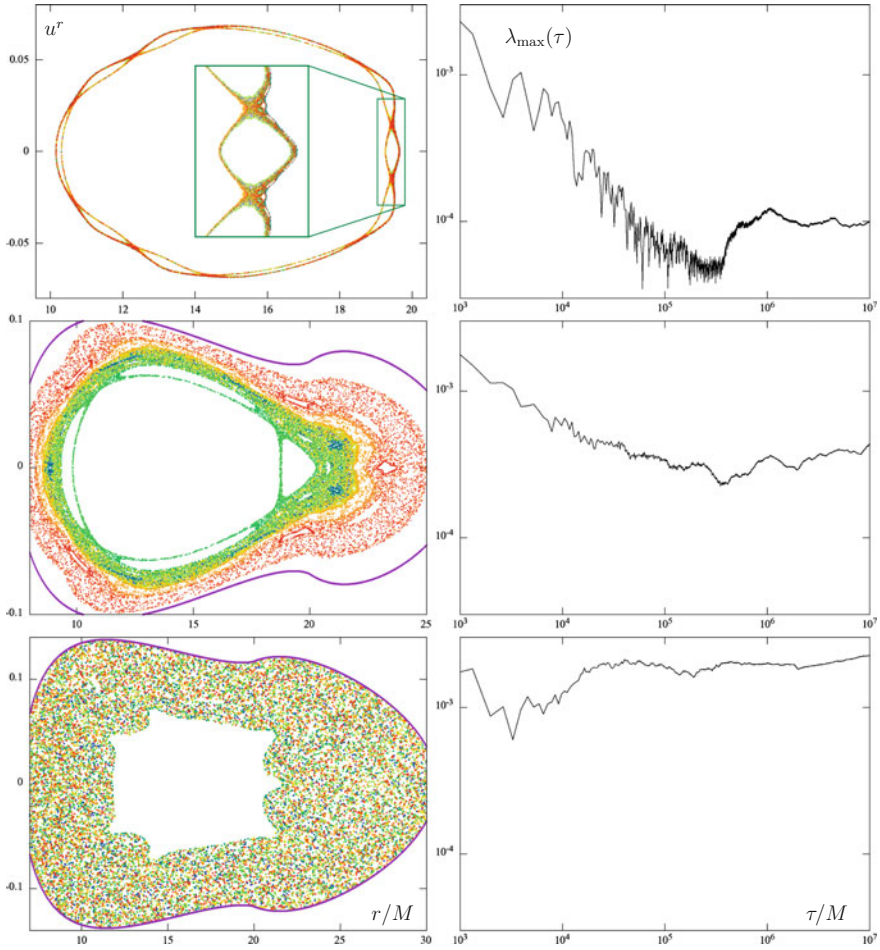


Fig. 8 Poincaré sections (left) and maximal Lyapunov exponents (right) for three orbits (D, E, F) of different degrees of irregularity, with parameters $\mathcal{M}=0.94M$, $r_{\text{disc}}=20M$, $\mathcal{E}=0.947$, $\ell=4M$ in the upper row (D); $\mathcal{M}=1.3M$, $r_{\text{disc}}=20M$, $\mathcal{E}=0.9365$, $\ell=4M$ in the middle row (E); and $\mathcal{M}=1.3M$, $r_{\text{disc}}=20M$, $\mathcal{E}=0.941$, $\ell=4M$ in the bottom row (F). The orbits fill phase-space layers of different volumes, in agreement with the obtained values $\lambda_{\text{max}}(\tau_{\text{max}}) \doteq 9.88 \cdot 10^{-5} M^{-1}$ (top), $4.28 \cdot 10^{-4} M^{-1}$ (middle) and $2.25 \cdot 10^{-3} M^{-1}$ (bottom). The Poincaré-surface passages are coloured by proper time (it increases in the order blue \rightarrow green \rightarrow yellow \rightarrow red). Power spectra of $z(t)$ (left column) and the Kaplan-Glass average of the recursion directions $\bar{\Lambda}$ (right column), plotted for the same three orbits D, E, F (for their parts up to $\tau_{\text{max}} = 10^6 M$). The $\bar{\Lambda}(\Delta\tau)$ dependence is drawn for three separate time-shift ($\Delta\tau$) intervals, $(2500-3300)M$, $(25,000-25,800)M$ and $(100,000-100,800)M$. Note that vertical-axes ranges are different on the right, 0.5–1.0 for the top orbit whereas 0.1–0.6 for the remaining two. FLI(τ) on the left and $Y(\tau)$ (MEGNO) on the right, computed for the same three orbits (D, E, F). The average MEGNO $2\bar{Y}(\tau)$ is drawn in blue and its linear fit is in red. The maximal-Lyapunov-exponent values inferred from the average-MEGNO slope are $9.172 \cdot 10^{-5} M^{-1}$ for orbit D (bottom), $4.192 \cdot 10^{-4} M^{-1}$ for orbit E (middle) and $2.278 \cdot 10^{-3} M^{-1}$ for orbit F (top). All three plots are adopted from [8]

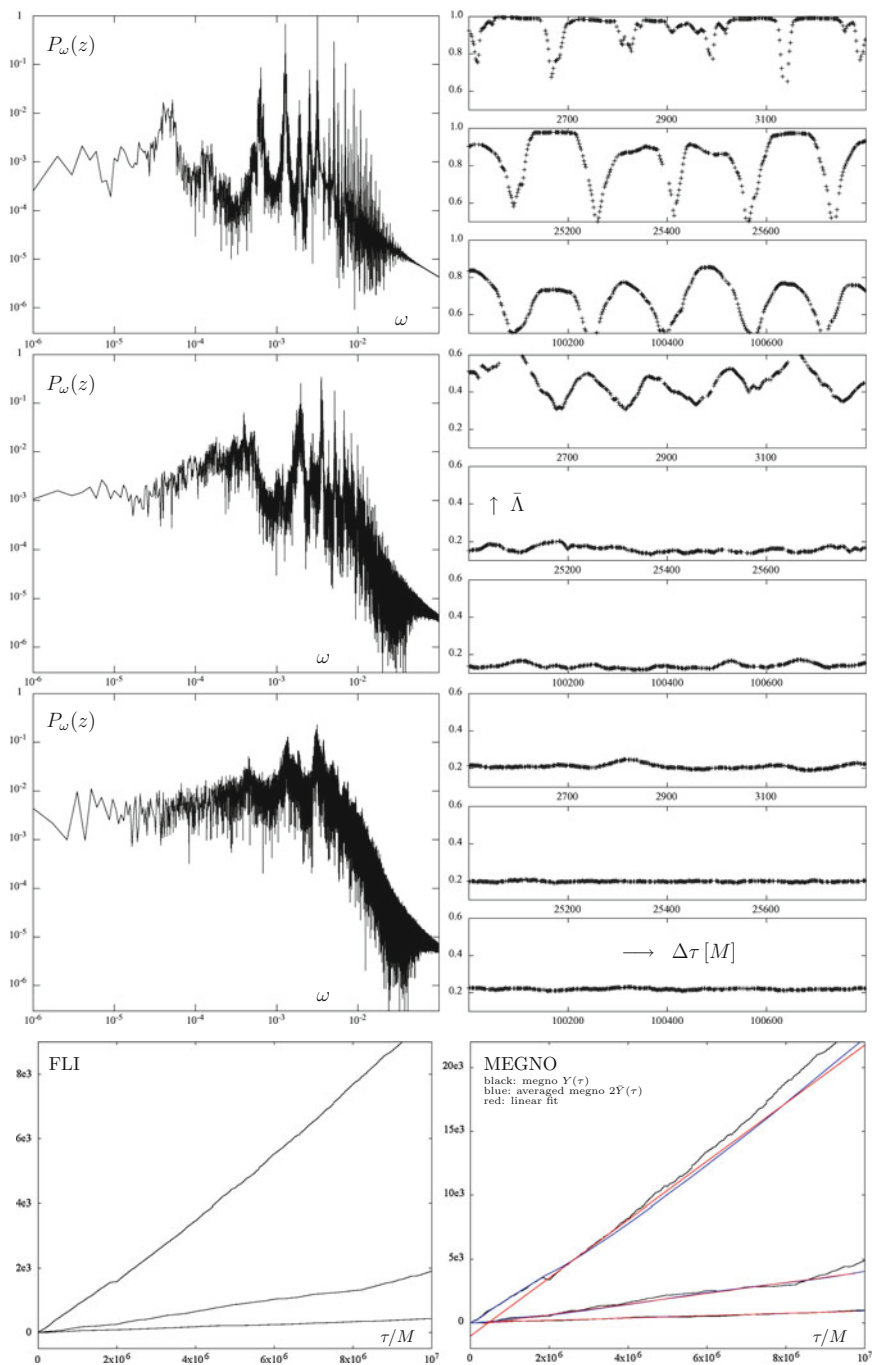


Fig. 8 (continued)

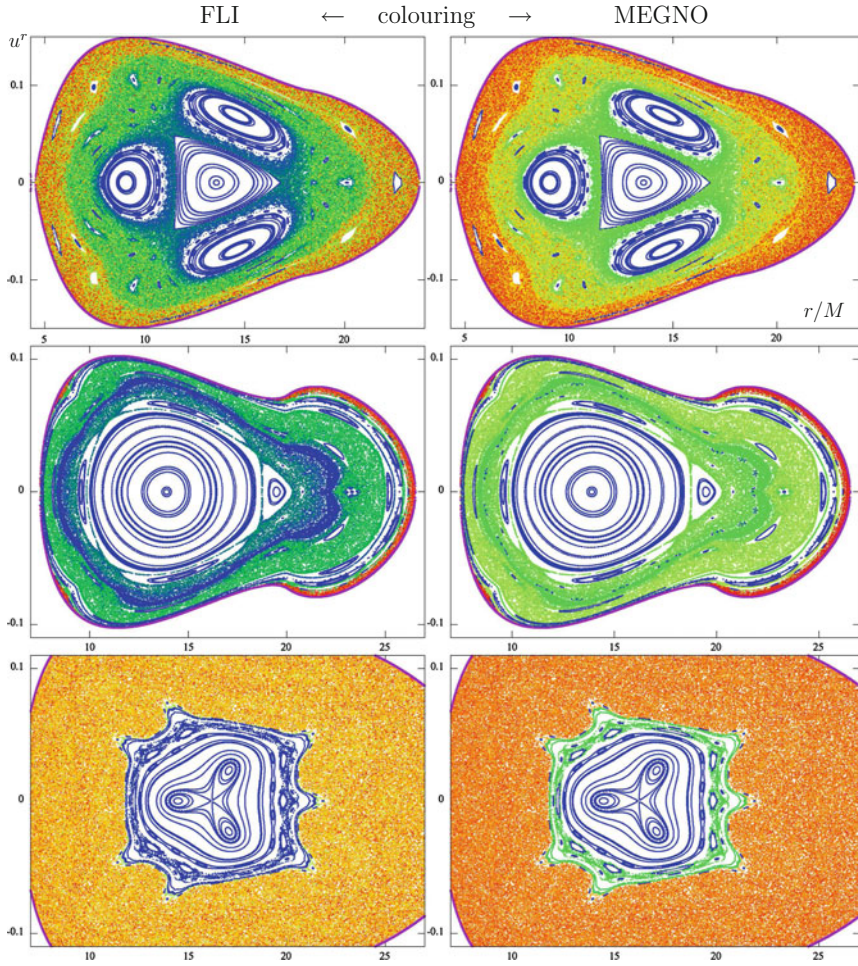


Fig. 9 Equatorial Poincaré maps of three phase portraits, coloured according to $\text{FLI}(\tau_{\max})$ (left column) and $\tilde{Y}(\tau_{\max})$ (right column) values, where $\tau_{\max} = 250,000M$. Parameters: $\mathcal{M} = M/2$, $r_{\text{disc}} = 18M$, $\mathcal{E} = 0.9532$, $\ell = 3.75M$ in the 1st row; $\mathcal{M} = 1.3M$, $r_{\text{disc}} = 20M$, $\mathcal{E} = 0.9365$, $\ell = 4M$ in the 2nd row; and $\mathcal{M} = 1.3M$, $r_{\text{disc}} = 20M$, $\mathcal{E} = 0.941$, $\ell = 4M$ in the 3rd row. Whenever $\tilde{Y}(\tau_{\max}) > 4$, we add another 200 to it in order to enhance distinction between regular and weakly chaotic regions. The colours going from blue to red in the visible-spectrum order correspond to FLI increasing from 0 to 350 (left) and to MEGNO increasing from 0 to 500. Adopted from [8]

5 Concluding Remarks

In the Introduction, we indicated black-hole dominated cores of galactic nuclei as a natural astrophysical motivation. Indeed, the individual stars there can be approximated as point test particles and if the environment is sufficiently sparse, their motion is close to a geodesic one. In our Galaxy, for instance, there is a black hole of mass $M \doteq 4.3 \cdot 10^6 M_\odot$, probably surrounded by a rather tiny accretion structure and by *two* much larger circum-nuclear rings, one with radius 2 parsecs and mass $M/10$ and the other around the 80 parsec radius with mass $10M$. (These are average values learned from literature, see [8] for references.) There is also a considerable nuclear star cluster which could be incorporated by adding a suitable spherical term in our potential ν . Of the above structures, only the smaller circum-nuclear ring has been observed to be able to partially destabilize the motion of stars, and only if their orbits can get sufficiently close to it.

The dynamics of astrophysical systems clearly has observable consequences conveyed by electromagnetic as well as gravitational radiation. The character of dynamics is crucial for the long-term evolution of these systems, although examples like the motion of stars in galactic nuclei are happening over too long intervals to provide well detectable signatures of chaos in “real time”. The characteristic periods are of course the shorter the closer to the horizon the motion takes place and [25] argued that it could be possible to recognize whether the central object is Kerr-like or different from the radiation of an inspiralling captured geodesic orbiter. Without doubt, the astrophysical black holes *should* differ from the Kerr ideal for other reasons (than considered here) as well: they must be interacting (if only to be “observable”), so not only they are not isolated, but also not stationary; and probably they do not live in an asymptotically flat universe. In any case, the study of motion in deformed black-hole fields can lead to fundamental questions concerning the nature of objects supposed to play a key role in the most engaging cosmic systems.

Let us conclude by several suggestions of further possible work. One could certainly subject the system to still another methods and codes in order to check the results, but also to evaluate the methods/codes themselves and their practical features within general relativity; such analyses like [24] (on the usage of several indicators of orbital deviation in GR) will be helpful. For example, the Melnikov-integral method has already been employed several times in general relativity, as well as the study of the dimension of “basin boundaries” (boundaries between initial-condition sets which evolve to distinct end states), which are of particular appeal due to their coordinate-independent message. It would be interesting to perform a similar analysis for the “corresponding” (pseudo-)Newtonian or post-Newtonian systems, at least to infer how good approximations they provide. Also, for better insight, one should study in detail the unstable periodic orbits and their asymptotic orbits whose behaviour under perturbation is crucial for the system properties.

The other direction is to make the model of the astrophysical system more realistic. Speaking about the galactic nucleus, one could include the central star cluster (at least in terms of a spherical potential), replace the thin ring by a toroid of finite

cross-section, or/and possibly try to account for mechanical interaction of the orbiters with the putative gaseous medium. From the point of view of general relativity, it would however be most interesting to include *rotation* (which generates dragging effects, no longer compatible with *static* solution). Actually, rotation is almost omnipresent in astrophysics and mainly expected in the case of very compact bodies like black holes, and certainly in the case of orbiting matter like that of accretion discs. Unfortunately, it has proved very difficult to extend the scope from static to *stationary* axisymmetric exact setting. It is well known that under such symmetries Einstein equations reduce to the Ernst equation which is completely integrable, but explicit solutions of the corresponding boundary-value problem are rather involved [26–28] and not friendly as backgrounds for further extensive numerical studies. Although several related algorithms called *generating techniques* have been recognized which can in principle provide *any* solution with given (two commuting) symmetries (e.g. [29]), none of those actually considered in more detail turned out to have satisfactory properties (besides basic ones already familiar before, like the Kerr metric). In particular, simple attempts to “generate” a *physically reasonable* metric for a black hole surrounded by an additional matter or field have not been very successful (e.g. [30–34] and references therein).

To conclude with the main topic of this seminar, let us also notice that in reality the body whose motion is studied differs from the point-test-particle ideal (and thus the motion from a geodesic one): it is likely endowed with spin or even higher moments; the radiation reaction due to its gravitational emission could be taken into account as well as back reaction due to its non-zero effect on space-time geometry; and, needless to say, if the orbiter was charged, it would also be affected by electromagnetic field, if there was any around. It would be sensible to employ the methods used in the theory of chaos in order to estimate and compare the significance of various such “perturbations” which affect the motion in real astrophysical situations.

Acknowledgments We thank for support the Czech grants GACR 14-10625S (O.S.) and SVV-267301 (P.S.). O.S. is grateful to Dirk Puetzfeld for invitation to the Bad Honnef conference and to the Wilhelm und Else Heraeus Stiftung for support there.

References

1. O. Semerák, P. Suková, Free motion around black holes with discs or rings: between integrability and chaos—I. Mon. Not. R. Astron. Soc. **404**, 545 (2010)
2. N.J. Cornish, N.E. Frankel, The black hole and the pea. Phys. Rev. D **56**, 1903 (1997)
3. M.A. Abramowicz, A. Curir, A. Schwarzenberg-Czerny, R.E. Wilson, Self-gravity and the global structure of accretion discs. Mon. Not. R. Astron. Soc. **208**, 279 (1984)
4. O. Semerák, Gravitating discs around a Schwarzschild black hole—III. Class. Quantum Gravity **20**, 1613 (2003)
5. O. Semerák, Exact power-law discs around static black holes. Class. Quantum Gravity **21**, 2203 (2004)
6. M. Žáček, O. Semerák, Gravitating discs around a Schwarzschild black hole II. Czech. J. Phys. **52**, 19 (2002)

7. O. Semerák, P. Suková, Free motion around black holes with discs or rings: between integrability and chaos—II. *Mon. Not. R. Astron. Soc.* **425**, 2455 (2012)
8. P. Suková, O. Semerák, Free motion around black holes with discs or rings: between integrability and chaos—III. *Mon. Not. R. Astron. Soc.* **436**, 978 (2013)
9. J.P.S. Lemos, P.S. Letelier, Exact general relativistic thin disks around black holes. *Phys. Rev. D* **49**, 5135 (1994)
10. O. Semerák, T. Zellerin, M. Žáček, The structure of superposed Weyl fields. *Mon. Not. R. Astron. Soc.* **308**, 691 (1999)
11. L.A. D'Afonseca, P.S. Letelier, S.R. Oliveira, Geodesics around Weyl-Bach's ring solution. *Class. Quantum Gravity* **22**, 3803 (2005)
12. D.T. Kaplan, L. Glass, Direct test for determinism in a time series. *Phys. Rev. Lett.* **68**, 427 (1992)
13. J.-P. Eckmann, S. Oliffson Kamphorst, D. Ruelle, Recurrence plots of dynamical systems. *Europhys. Lett.* **4**, 973 (1987)
14. N. Marwan, M.C. Romano, M. Thiel, J. Kurths, Recurrence plots for the analysis of complex systems. *Phys. Rep.* **438**, 237 (2007)
15. O. Kopáček, V. Karas, J. Kovář, Z. Stuchlík, Transition from regular to chaotic circulation in magnetized coronae near compact objects. *Astrophys. J.* **722**, 1240 (2010)
16. J. Kovář, O. Kopáček, V. Karas, Y. Kojima, Regular and chaotic orbits near a massive magnetic dipole. *Class. Quantum Gravity* **30**, 025010 (2013)
17. X. Wu, T.-Y. Huang, Computation of Lyapunov exponents in general relativity. *Phys. Lett. A* **313**, 77 (2003)
18. X. Wu, T.-Y. Huang, H. Zhang, Lyapunov indices with two nearby trajectories in a curved spacetime. *Phys. Rev. D* **74**, 083001 (2006)
19. C. Froeschlé, E. Lega, R. Gonczi, Fast Lyapunov indicators. Application to asteroidal motion. *Celest. Mech. Dyn. Astron.* **67**, 41 (1997)
20. W. Han, Chaos and dynamics of spinning particles in Kerr spacetime. *Gen. Relativ. Gravit.* **40**, 1831 (2008)
21. W. Han, Revised research about chaotic dynamics in Manko, et al., spacetime. *Phys. Rev. D* **77**, 123007 (2008)
22. P.M. Cincotta, C. Simó, Simple tools to study global dynamics in non-axisymmetric galactic potentials—I. *Astron. Astrophys. Suppl. Ser.* **147**, 205 (2000)
23. M.F. Mestre, P.M. Cincotta, C.M. Giordano, Analytical relation between two chaos indicators: FLI and MEGNO. *Mon. Not. R. Astron. Soc.* **414**, L100 (2011)
24. G. Lukes-Gerakopoulos, Adjusting chaotic indicators to curved spacetimes. *Phys. Rev. D* **89**, 043002 (2014)
25. G. Lukes-Gerakopoulos, T.A. Apostolatos, G. Contopoulos, Observable signature of a back-ground deviating from the Kerr metric. *Phys. Rev. D* **81**, 124005 (2010)
26. G. Neugebauer, R. Meinel, Progress in relativistic gravitational theory using the inverse scattering method. *J. Math. Phys.* **44**, 3407 (2003)
27. C. Klein, O. Richter, *Ernst Equation and Riemann Surfaces: Analytical and Numerical Methods*. Lecture Notes in Physics, vol. 685 (Springer, Berlin 2005)
28. J. Lenells, Boundary value problems for the stationary axisymmetric Einstein equations: a disk rotating around a black hole. *Commun. Math. Phys.* **304**, 585 (2011)
29. V. Belinski, E. Verdaguer, *Gravitational Solitons* (Cambridge University Press, Cambridge, 2001)
30. A. Tomimatsu, Distorted rotating black holes. *Phys. Lett.* **103A**, 374 (1984)
31. K.D. Krori, R. Bhattacharjee, A Kerr object embedded in a gravitational field. II. *J. Math. Phys.* **31**, 147 (1990)
32. T. Zellerin, O. Semerák, Two-soliton stationary axisymmetric sprouts from Weyl seeds. *Class. Quantum Gravity* **17**, 5103 (2000)
33. O. Semerák, Thin disc around a rotating black hole, but with support in-between. *Class. Quantum Gravity* **19**, 3829 (2002)
34. G.M. de Castro, P.S. Letelier, Black holes surrounded by thin rings and the stability of circular orbits. *Class. Quantum Gravity* **28**, 225020 (2011)

Higher Order Post-Newtonian Dynamics of Compact Binary Systems in Hamiltonian Form

Gerhard Schäfer

Abstract The Hamiltonian formalism developed by Arnowitt, Deser, and Misner (ADM) is used to derive and discuss the higher order post-Newtonian dynamics and motion of compact binary systems in general relativity including proper rotation of the components. Various explicit analytic Hamiltonians will be presented for the conservative and dissipative dynamics, the latter resulting from gravitational radiation damping. Explicit analytic expressions for the orbital motion will be given.

1 Introduction

The convincing explanation of the anomalous perihelion advance of Mercury, the first success of general relativity, has been right a post-Newtonian (PN) achievement. So PN approximation techniques are part of the application of the Einstein theory from the very beginning. Since 1915, the year of the birth of general relativity, a lot of work has been invested into the exploration of the theory in terms of PN approximation schemes. Typical for all these PN schemes is the Newtonian theory as starting point and the expansion of the structure of general relativity, in the weak-field and slow-motion regime, in inverse powers of the speed of light c in the form of terms containing powers of v^2/c^2 and Gm/rc^2 , where v and m respectively denote a typical velocity and a typical mass of the bodies in question and r a typical relative distance; G is the Newtonian gravitational constant, e.g. [1–3]. The n PN order of approximation means the n th power $(v^2/c^2)^n$. For bound systems, the virial terms guarantees $v^2/c^2 \sim Gm/rc^2$. Starting with the level where radiation reaction enters for the first time, half-integer n enter. The first radiation-reaction level is of 2.5PN order. If the internal dynamics of a body is decoupled from its external one, the internal dynamics must not have weak gravitational fields to participate in the external weak-field and slow-motion dynamics; so neutron stars and black holes can be objects of PN systems. Famous is the derivation of the 1PN dynamics of n -body

G. Schäfer (✉)

Theoretisch-Physikalisches Institut, Friedrich-Schiller-Universität Jena,
Max-Wien-Platz 1, 07743 Jena, Germany
e-mail: gos@tpi.uni-jena.de

systems with strong self interaction published by Einstein, Infeld, and Hoffmann (EIH) in 1938, [4]. Here the technique of closed surface integrals around the bodies has been applied, themselves located in the weak field regime. Thinking in terms of Gauss's theorem it is understandable why with the help of Dirac delta functions the same result could have been achieved later on; however, with much less amount of computational work. The interested reader may compare the two different techniques in the recent computations of the 3PN binary dynamics, where Itoh and Futamase made use out of an EIH-type approach [5, 6] whereas Damour et al. [7] and Blanchet et al. [8] applied the Dirac delta function ansatz. Also a recent rederivation of the 3PN binary dynamics by Foffa and Sturani [9] within the effective field theory formalism used the Dirac delta function or its Fourier transform.

The Hamiltonian formalism of general relativity has been inaugurated in two seminal papers by Dirac in the years 1958–1959, [10, 11], and developed in great detail by Arnowitt, Deser, and Misner (ADM) in the years 1959–1960, see review [12, 13]. Also Schwinger devised a Hamiltonian formalism based on the ADM formalism but with applying tetrads in a first-order formulation of general relativity, in 1963, [14]. Already in the same year, Kibble implemented the Dirac field into the Schwinger formalism, [15], which, in the realm of the Dirac approach, [16], was fully worked through by Nelson and Teitelboim in 1978 only, [17]. DeWitt, in 1967, [18], and Regge and Teitelboim, in 1974, [19], delivered refined treatments of the Hamiltonian formulations of general relativity with respect to the involved surface integrals, particularly the famous Hamiltonian one of ADM.

The ADM formalism of general relativity is the most often applied one out of these formalisms. Its application to the PN approximation already started with Kimura in 1961 who rederived the 1PN dynamics of EIH, [20]. In the 1970s a lot of work has been performed in Kimura's research group for the obtention of the 2PN dynamics, particularly in the ADM formalism [21]. The full set of expressions of the 2PN dynamics in Hamiltonian form was finally obtained by Damour and the author in 1985, [22]. Later on in 2001, by Damour, Jaranowski, and the author, for the first time, the 3PN binary dynamics has been computed and finally, most recently, the 4PN compact binary dynamics, where in both cases judicious dimensional regularization procedures were applied, [7, 23]. The paper by Damour, Jaranowski, and the author about the Hamiltonian of two spinning compact bodies with next-to-leading order gravitational spin-orbit coupling, published in 2008, can be regarded as the beginning of the PN treatment of gravitationally interacting spinning bodies in genuine Hamiltonian form, [24]. Already in 2009, a seminal paper appeared where the implementation of classical spinning bodies into general relativity was performed to linear order in spin, [25]; a detailed presentation is given in [26]. The state of the affairs in the derivation of higher order gravitational Hamiltonians with spinning compact objects can be found in [27]. Our list of References mainly contains papers of Hamiltonian provenance. In the lists of References presented therein, related papers applying non-Hamiltonian approaches can be found.

2 Newtonian Dynamics in Hamiltonian Form

A full set of mathematical relations for a Newtonian ideal fluid is given by the equations, e.g. [28], the Einstein summation notation applied, (i)

$$\partial_t \varrho_* + \partial_i (\varrho_* v^i) = 0, \quad (1)$$

the mass conservation equation, where ϱ_* denotes the mass density and v^i the velocity field of the fluid, (ii)

$$\varrho_* \partial_t v^i + \partial_j (\varrho_* v^i v^j) = -\partial_i p + \varrho_* \partial_i U, \quad (2)$$

the equations of motion, where p is the pressure of the fluid and U the Newtonian gravitational potential, (iii)

$$\frac{ds}{dt} \equiv \partial_t s + v^i \partial_i s = 0, \quad (3)$$

the entropy conservation equation for the mass elements along their motion in space, where s denotes the specific entropy, (iv)

$$\epsilon = \epsilon(\varrho_*, s), \quad (4)$$

the equation of state, where ϵ is the specific internal energy, (v)

$$d\epsilon = \frac{p}{\varrho_*^2} d\varrho_* + T ds, \quad (5)$$

the Gibbs fundamental form, with T being the temperature, (vi)

$$U(\mathbf{x}, t) = G \int d^3 x' \frac{\varrho_*(\mathbf{x}', t)}{|\mathbf{x} - \mathbf{x}'|}, \quad (6)$$

the gravitational potential expression in terms of its source, or

$$\Delta U = -4\pi G \varrho_*, \quad (7)$$

the Newtonian gravitational field equation. Δ denotes the Laplace operator and $|\dots|$ the standard euclidean distance. Partial derivatives with respect time and space, employing cartesian coordinates $\mathbf{x} = (x^i)$, ($i = 1, 2, 3$), are denoted ∂_t and ∂_i , respectively.

In a Hamiltonian formulation, e.g. [28], all the dynamical equations are derived with the aid of a Hamiltonian functional $H = H[\varrho_*, \pi_i, s]$ which depends on such a set of variables that the equations of motion follow by variations. The new variable herein is the momentum density π_i . It relates to the velocity field through $v^i = \frac{\delta H}{\delta \pi_i}$. The dynamical equations presented above, are now,

(i) mass conservation,

$$\frac{\partial \varrho_*}{\partial t} = -\partial_i \left(\frac{\delta H}{\delta \pi_i} \varrho_* \right), \quad (8)$$

(ii) equations of motion,

$$\frac{\partial \pi_i}{\partial t} = -\partial_j \left(\frac{\delta H}{\delta \pi_j} \pi_i \right) - \partial_i \left(\frac{\delta H}{\delta \pi_j} \right) \pi_j - \partial_i \left(\frac{\delta H}{\delta \varrho_*} \right) \varrho_* + \frac{\delta H}{\delta s} \partial_i s, \quad (9)$$

(iii) entropy conservation,

$$\frac{\partial s}{\partial t} = -\frac{\delta H}{\delta \pi_i} \partial_i s. \quad (10)$$

In terms of generalized brackets, the so-called Lie-Poisson brackets, e.g. [28], equations of motion generally read

$$\partial_t A(\mathbf{x}, t) = \{A(\mathbf{x}, t), H\}. \quad (11)$$

In our case, the fundamental variables fulfil the following Lie-Poisson-bracket relations

$$\{\pi_i(\mathbf{x}, t), \varrho_*(\mathbf{x}', t)\} = \frac{\partial}{\partial x'^i} [\varrho_*(\mathbf{x}', t) \delta(\mathbf{x} - \mathbf{x}')], \quad (12)$$

$$\{\pi_i(\mathbf{x}, t), s(\mathbf{x}', t)\} = \frac{\partial s(\mathbf{x}', t)}{\partial x'^i} \delta(\mathbf{x} - \mathbf{x}'), \quad (13)$$

$$\{\pi_i(\mathbf{x}, t), \pi_j(\mathbf{x}', t)\} = \pi_i(\mathbf{x}', t) \frac{\partial}{\partial x'^j} \delta(\mathbf{x} - \mathbf{x}') - \pi_j(\mathbf{x}, t) \frac{\partial}{\partial x^i} \delta(\mathbf{x} - \mathbf{x}'), \quad (14)$$

where $\int d^3x \delta(\mathbf{x}) = 1$.

The introduction of Lagrangian variables $q^A(\mathbf{x}, t)$ and $P_A(\mathbf{x}, t)$, with $A = 1, 2, 3$, turn the Lie-Poisson brackets into standard Poisson brackets, reading

$$\{q^A(\mathbf{x}, t), P_B(\mathbf{x}', t)\} = \delta_B^A \delta(\mathbf{x} - \mathbf{x}'), \quad \text{zero otherwise}, \quad (15)$$

where the following relations between the Eulerian and Lagrangian variables hold,

$$\varrho_* = \varrho_L[q^A(\mathbf{x}, t)] \det \left[\frac{\partial q^A(\mathbf{x}, t)}{\partial x^i} \right], \quad (16)$$

$$s(\mathbf{x}, t) = s_L[q^A(\mathbf{x}, t)], \quad (17)$$

$$\pi_i(\mathbf{x}, t) = -\frac{\partial q^A(\mathbf{x}, t)}{\partial x^i} P_A(\mathbf{x}, t). \quad (18)$$

As each fluid matter element keeps its Lagrangian “name”, say A or B, the Lagrangian position field fulfills a conservation equation,

$$\partial_t q^A + v^i \partial_i q^A = 0. \quad (19)$$

Finally, the Hamiltonian functional of our ideal fluid is

$$H = \frac{1}{2} \int d^3x \frac{\pi_i \pi_i}{\varrho_*} - \frac{G}{2} \int d^3x d^3x' \frac{\varrho_*(\mathbf{x}, t) \varrho_*(\mathbf{x}', t)}{|\mathbf{x} - \mathbf{x}'|} + \int d^3x \varrho_* \epsilon. \quad (20)$$

The total linear momentum of the fluid is given by

$$P_i = \int d^3x \pi_i, \quad (21)$$

its total orbital angular momentum reads,

$$J_i = \int d^3x \epsilon_{ijk} x^j \pi_k, \quad (22)$$

and the center-of-mass vector takes the form,

$$G_i = \int d^3x x^i \varrho_*. \quad (23)$$

The transition to point particles is achieved through the settings

$$\varrho_* = \sum_a m_a \delta(\mathbf{x} - \mathbf{x}_a), \quad \pi_i = \sum_a p_{ai} \delta(\mathbf{x} - \mathbf{x}_a), \quad (24)$$

which result in standard Poisson brackets,

$$\{x_a^i, p_{aj}\} = \delta_{ij}, \quad \text{zero otherwise}, \quad (25)$$

and in the standard Hamiltonian of gravitationally interacting point masses,

$$H = \sum_a \frac{p_{ai} p_{ai}}{2m_a} - \frac{1}{2} \sum_{a \neq b} \frac{G m_a m_b}{|\mathbf{x}_a - \mathbf{x}_b|}, \quad (26)$$

with mass parameters m_a and linear momenta p_a , ($a = 1, 2, 3, \dots, N$), the number of point masses being denoted by N . Dusty matter would have been obtained by imposing $p = \epsilon = s = 0$.

Evidently, the total dynamical quantities of above read,

$$P_i = \sum_a p_{ai}, \quad (27)$$

$$J_i = \sum_a \epsilon_{ijk} x_a^j p_{ak}, \quad (28)$$

and

$$K_i = G_i - t P_i, \quad G_i = \sum_a m_a x_a^i, \quad (29)$$

where the constant boost vector K_i has been introduced.

Independently from its structure, any isolated system has to fulfil the well known Galileo algebra

$$\{P_i, H\} = \{J_i, H\} = 0, \quad (30)$$

$$\{J_i, P_j\} = \epsilon_{ijk} P_k, \quad \{J_i, J_j\} = \epsilon_{ijk} J_k, \quad (31)$$

$$\{J_i, G_j\} = \epsilon_{ijk} G_k, \quad (32)$$

$$\{G_i, H\} = P_i, \quad (33)$$

$$\{G_i, P_j\} = M \delta_{ij}, \quad (34)$$

$$\{G_i, G_j\} = 0, \quad (35)$$

where M is the total mass, $M = \sum_a m_a$. Notice in view of the following section that the components of the center-of-mass vector commute in Poisson brackets and that the total mass breaks the otherwise uniform appearance of the dynamical quantities.

3 Relativistic Systems in External Gravitational Fields in Hamiltonian Form

The energy-momentum tensor of an ideal fluid takes the form, e.g. [3, 28],

$$T_\nu^\mu = (\varrho c^2 + \varrho \epsilon + p) u_\nu u^\mu + p \delta_\nu^\mu, \quad u_\nu u^\nu = -1, \quad u_\nu = g_{\nu\mu} u^\mu, \quad (36)$$

where ϱ is the proper rest mass density of the fluid and u^ν its 4-dimensional timelike velocity field with its 3-dimensional components reading $u^i = u^0 v^i / c$. The space-time metric is $g_{\nu\mu}$, ($\mu, \nu = 0, 1, 2, 3$), and δ_ν^μ denotes the standard Kronecker delta. ϵ and p have the same meaning as in the previous section which is also the case for s and T ,

$$\epsilon = \epsilon(\varrho, s), \quad (37)$$

$$d\epsilon = \frac{p}{\varrho^2} d\varrho + T ds. \quad (38)$$

The independent variables are defined by, $(\bar{g} = \det(g_{\mu\nu}))$,

$$\varrho_* = \sqrt{-\bar{g}} u^0 \varrho, \quad s, \quad \pi_i = \frac{1}{c} \sqrt{-\bar{g}} T_i^0. \quad (39)$$

They do have the same Lie-Poisson-bracket structure as in the Newtonian dynamics case,

$$\{\pi_i(\mathbf{x}, t), \varrho_*(\mathbf{x}', t)\} = \frac{\partial}{\partial x'^i} [\varrho_*(\mathbf{x}', t) \delta(\mathbf{x} - \mathbf{x}')], \quad (40)$$

$$\{\pi_i(\mathbf{x}, t), s(\mathbf{x}', t)\} = \frac{\partial s(\mathbf{x}', t)}{\partial x'^i} \delta(\mathbf{x} - \mathbf{x}'), \quad (41)$$

$$\{\pi_i(\mathbf{x}, t), \pi_j(\mathbf{x}', t)\} = \pi_i(\mathbf{x}', t) \frac{\partial}{\partial x'^j} \delta(\mathbf{x} - \mathbf{x}') - \pi_j(\mathbf{x}, t) \frac{\partial}{\partial x^i} \delta(\mathbf{x} - \mathbf{x}'). \quad (42)$$

Also the equations of motion do have the same form as in the Newtonian case,

$$\frac{\partial \varrho_*}{\partial t} = -\partial_i \left(\frac{\delta H}{\delta \pi_i} \varrho_* \right) \iff \partial_\mu (\sqrt{-\bar{g}} \varrho u^\mu) = 0, \quad (43)$$

$$\frac{\partial s}{\partial t} = -\frac{\delta H}{\delta \pi_i} \partial_i s \iff u^\mu \partial_\mu s = 0, \quad (44)$$

$$\begin{aligned} \frac{\partial \pi_i}{\partial t} &= -\partial_j \left(\frac{\delta H}{\delta \pi_j} \pi_i \right) - \partial_i \left(\frac{\delta H}{\delta \pi_j} \right) \pi_j - \partial_i \left(\frac{\delta H}{\delta \varrho_*} \right) \varrho_* + \frac{\delta H}{\delta s} \partial_i s \\ &\iff \nabla_\mu \left(\sqrt{-\bar{g}} T_i^\mu \right) = 0, \end{aligned} \quad (45)$$

with ∇_μ the 4-dimensional covariant derivative, where again

$$v^i = \frac{\delta H}{\delta \pi_i}, \quad v^i = c \frac{u^i}{u^0} \quad (46)$$

hold. The total linear and orbital momenta read

$$P_i = \int d^3x \pi_i, \quad J_i = \int d^3x \epsilon_{ijk} x^j \pi_k. \quad (47)$$

Dusty matter is again obtained through

$$\epsilon = p = s = 0, \quad (48)$$

and the transition to point particles is made by

$$\varrho_* = \sum_a m_a \delta(\mathbf{x} - \mathbf{x}_a), \quad \pi_i = \sum_a p_{ai} \delta(\mathbf{x} - \mathbf{x}_a), \quad v_a^i = \frac{dx_a^i}{dt} \quad (49)$$

with standard Poisson brackets,

$$\{x_a^i, p_{aj}\} = \delta_{ij}, \quad \text{zero otherwise,} \quad (50)$$

and standard equations of motion,

$$\frac{dp_{ai}}{dt} = -\frac{\partial H}{\partial x_a^i}, \quad \frac{dx_a^i}{dt} = \frac{\partial H}{\partial p_{ai}}. \quad (51)$$

The Poincaré algebra, reading, e.g. [29],

$$\{P_i, H\} = \{J_i, H\} = 0, \quad (52)$$

$$\{J_i, P_j\} = \varepsilon_{ijk} P_k, \quad \{J_i, J_j\} = \varepsilon_{ijk} J_k, \quad (53)$$

$$\{J_i, G_j\} = \varepsilon_{ijk} G_k, \quad (54)$$

$$\{G_i, H\} = P_i, \quad (55)$$

$$\{G_i, P_j\} = \frac{1}{c^2} H \delta_{ij}, \quad (56)$$

$$\{G_i, G_j\} = -\frac{1}{c^2} \varepsilon_{ijk} J_k, \quad (57)$$

generalizes the Galileo algebra to relativity. The boost vector K_i fulfills the relations $K_i = -t P_i + G_i$, $dK_i/dt = \partial K_i/\partial t + \{K_i, H\} = -P_i + \{G_i, H\} = 0$.

Canonical expressions for a non-interacting particle are, setting $c = 1$, the

total angular momentum: $\mathbf{J} = \hat{\mathbf{X}} \times \mathbf{P} + \hat{\mathbf{S}}$,

Hamiltonian: $H = \sqrt{m^2 + \mathbf{P}^2}$,

Lorentz boost: $\mathbf{K} = -t\mathbf{P} + H\hat{\mathbf{X}} - \frac{1}{H+m}\hat{\mathbf{S}} \times \mathbf{P}$,

center-of-energy position vector: $\bar{\mathbf{X}} = \hat{\mathbf{X}} - \frac{1}{(H+m)H} \hat{\mathbf{S}} \times \mathbf{P}$.

The constant boost vector can be written: $\mathbf{K} = -t\mathbf{P} + H\bar{\mathbf{X}}$, $\mathbf{G} = H\bar{\mathbf{X}}$.

For isolated conservative many particle systems with interaction one gets, using again standard notations $\mathbf{p}_a = (p_{ai})$, etc., for the

total linear momentum: $\mathbf{P} = \sum_a \mathbf{p}_a$,

total angular momentum: $\mathbf{J} = \sum_a (\mathbf{r}_a \times \mathbf{p}_a + \mathbf{s}_a)$,

total rest mass squared: $\mathcal{M}^2 \equiv H^2 - \mathbf{P}^2$, $H = \sqrt{\mathcal{M}^2 + \mathbf{P}^2}$,

center-of-energy vector: $\mathbf{G} = H\hat{\mathbf{X}} - \frac{1}{H+\mathcal{M}}(\mathbf{J} - \hat{\mathbf{X}} \times \mathbf{P}) \times \mathbf{P}$.

The standard Poisson brackets read,

$$\{\hat{X}^i, \hat{X}^j\} = \{P^i, P^j\} = 0, \quad \{\hat{X}^i, P^j\} = \delta^{ij},$$

$$\{\mathcal{M}, \hat{X}^j\} = \{\mathcal{M}, P^j\} = \{\mathcal{M}, H\} = 0.$$

There are various center-of-body definitions in use, the

(i), center of spin: $\hat{\mathbf{X}}$; $\{\hat{X}^i, \hat{X}^j\} = 0$ (Newton-Wigner coordinates),

(ii), center of energy: $\bar{\mathbf{X}} = \hat{\mathbf{X}} - \frac{1}{(H+m)H} \hat{\mathbf{S}} \times \mathbf{P}$,

(iii), center of inertia: $\mathbf{X} = \hat{\mathbf{X}} + \frac{1}{(H+m)m} \hat{\mathbf{S}} \times \mathbf{P}$.

Connected herewith are spin supplementary conditions (SSC), for

(i), center of inertia: $S^{\mu\nu} P_\nu = 0$,

(ii), center of energy: $\bar{S}^{\mu\nu} n_\nu = 0$, $n_\mu = (-1, 0, 0, 0)$,

(iii), center of spin: $m\hat{S}^{\mu\nu} n_\nu + \hat{S}^{\mu\nu} P_\nu = 0$,

where, say, $S^{\mu\nu} = -S^{\nu\mu}$ and $S^{ij} = \epsilon^{ijk} S^k$. The various center definitions are intimately connected with the fact that the components of the center-of-energy vector have non-vanishing Poisson brackets; also see [2].

4 General Relativity in Hamiltonian Form

Following the work by ADM [12, 13], general relativity can be put into a non-degenerate canonical form if e.g. the following four coordinate conditions are applied,

$$g_{ij} = \left(1 + \frac{1}{8}\phi\right)^4 \delta_{ij} + h_{ij}^{\text{TT}}, \quad (58)$$

which mean three coordinate conditions, where h_{ij}^{TT} is transverse and traceless, i.e. $\partial_j h_{ij}^{\text{TT}} = h_{ii}^{\text{TT}} = 0$, and, $(g = \det(g_{ij}))$,

$$\pi^{ii} = 0, \quad \pi^{ij} = -g^{1/2}(K^{ij} - \gamma^{ij}K), \quad \pi_i^i \equiv g_{ij}\pi^{ij} = \pi^{ij}h_{ij}^{\text{TT}}, \quad (59)$$

which means one coordinate condition. K_{ij} is the extrinsic curvature tensor of hypersurfaces $t = \text{const}$ ($K = g_{ij}K^{ij}$) and $\gamma^{ik}g_{kj} = \delta_j^i$. A unique decomposition is possible, reading $\pi^{ij} = \tilde{\pi}^{ij} + \pi_{\text{TT}}^{ij}$ with

$$\tilde{\pi}^{ij} = \partial_i \pi^j + \partial_j \pi^i - \frac{2}{3} \delta_{ij} \partial_k \pi^k. \quad (60)$$

Again, π_{TT}^{ij} is transverse and traceless. The canonical conjugate field to h_{ij}^{TT} is denoted $\pi_{\text{TT}}^{ij} c^3 / 16\pi G$. These both fields are the independent canonical variables of the gravitational field. The field functions ϕ and $\tilde{\pi}^{ij}$ are determined by the four constraint equations,

$$g^{1/2}R = \frac{1}{g^{1/2}} \left(\pi_i^i \pi_j^j - \frac{1}{2} \pi_i^i \pi_j^j \right) + \frac{16\pi G}{c^3} \sum_a \left(m_a^2 c^2 + \gamma^{ij} p_{ai} p_{aj} \right)^{1/2} \delta_a, \quad (61)$$

the Hamiltonian constraint, which is equivalent to the Einstein field equation $G^{00} = \frac{8\pi G}{c^4} T^{00}$, and

$$-2\partial_j \pi_i^j + \pi^{kl} \partial_i g_{kl} = \frac{16\pi G}{c^3} \sum_a p_{ai} \delta_a, \quad (62)$$

the momentum constraint, which corresponds to the Einstein field equations $G_i^0 = \frac{8\pi G}{c^4} T_i^0$.

The famous ADM Hamiltonian is defined by

$$H \left[x_a^i, p_{ai}, h_{ij}^{\text{TT}}, \pi_{\text{TT}}^{ij} \right] = -\frac{c^4}{16\pi G} \int d^3x \Delta \phi \left[x_a^i, p_{ai}, h_{ij}^{\text{TT}}, \pi_{\text{TT}}^{ij} \right] \quad (63)$$

which also can be brought into a surface integral form using the Gauss theorem.

The description of the conservative dynamics part is most efficiently performed with a Routh functional, e.g. [30],

$$R \left[x_a^i, p_{ai}, h_{ij}^{\text{TT}}, \partial_t h_{ij}^{\text{TT}} \right] = H - \frac{c^3}{16\pi G} \int d^3x \pi_{\text{TT}}^{ij} \partial_t h_{ij}^{\text{TT}} \quad (64)$$

resulting in the following evolution equations,

$$\frac{\delta \int R(t') dt'}{\delta h_{ij}^{\text{TT}}(x^k, t)} = 0, \quad \dot{p}_{ai} = -\frac{\partial R}{\partial x_a^i}, \quad \dot{x}_a^i = \frac{\partial R}{\partial p_{ai}}. \quad (65)$$

The on-field-shell Routhian describes the conservative dynamics,

$$R_{\text{on}}(t) = R \left[x_a^i, p_{ai}, h_{ij}^{\text{TT}}[x_a^k, p_{ak}], \partial_t h_{ij}^{\text{TT}}[x_a^k, p_{ak}] \right], \quad (66)$$

$$\dot{p}_{ai}(t) = -\frac{\delta \int R_{\text{on}}(t') dt'}{\delta x_a^i(t)}, \quad \dot{x}_a^i(t) = \frac{\delta \int R_{\text{on}}(t') dt'}{\delta p_{ai}(t)}, \quad (67)$$

$$\frac{\delta \int R_{\text{on}}(t') dt'}{\delta z(t)} = \frac{\partial R_{\text{on}}}{\partial z(t)} - \frac{d}{dt} \frac{\partial R_{\text{on}}}{\partial \dot{z}(t)} + \dots, \quad z = (x_a^i, p_{ai}). \quad (68)$$

Within the present context, the fundamental PN expansion reads

$$R \left[x_a^i, p_{ai}, h_{ij}^{\text{TT}}, \partial_t h_{ij}^{\text{TT}} \right] = Mc^2 + \sum_{n=0}^{\infty} \left(\frac{1}{c^2} \right)^n R_n \left[x_a^i, p_{ai}, \hat{h}_{ij}^{\text{TT}}, \partial_t \hat{h}_{ij}^{\text{TT}} \right], \quad (69)$$

where $h_{ij}^{\text{TT}} = \frac{G}{c^4} \hat{h}_{ij}^{\text{TT}}$. Hereof the PN expansion of the field evolution equation follows in the form (symbolic writing),

$$\left(\Delta - \frac{\partial_t^2}{c^2} \right) h^{\text{TT}} = \frac{G}{c^4} \sum_{m=0}^{\infty} \left(\frac{1}{c^2} \right)^m D_m^{\text{TT}}[x, x_a(t), p_a(t), \hat{h}^{\text{TT}}(t), \partial_t \hat{h}^{\text{TT}}(t)]. \quad (70)$$

The order c^{-2n} is called the n th PN order. Also the multipole expansion of the gravitational field is of PN type, e.g. in far zone (FZ), [31],

$$h_{ij}^{\text{TT}}(\mathbf{x}, t) = \frac{G}{c^4} \frac{P_{ijkl}(\mathbf{n})}{r} \sum_{l=2}^{\infty} \left\{ \left(\frac{1}{c^2} \right)^{\frac{l-2}{2}} \frac{4}{l!} M_{kmi_3 \dots i_l}^{(l)} \left(t - \frac{r_*}{c} \right) N_{i_3 \dots i_l} \right. \\ \left. + \left(\frac{1}{c^2} \right)^{\frac{l-1}{2}} \frac{8l}{(l+1)!} \epsilon_{pq(k} S_{m)pi_3 \dots i_l}^{(l)} \left(t - \frac{r_*}{c} \right) n_q N_{i_3 \dots i_l} \right\}, \quad (71)$$

where the mass quadrupole tensor is given by, showing the standard Newtonian mass quadrupole tensor \widehat{M}_{ij} and the leading order backscattering or tail contribution, [32], M denoting the total mass and b a scaling constant,

$$M_{ij}(t - \frac{r_*}{c}) = \widehat{M}_{ij} \left(t - \frac{r_*}{c} \right)$$

$$\begin{aligned}
& + \frac{2GM}{c^3} \int_0^\infty dv \ln\left(\frac{v}{2b}\right) \widehat{M}_{ij}^{(2)}\left(t - \frac{r_*}{c} - v\right) + O(1/c^4), \\
r_* = r + \frac{2GM}{c^2} \ln\left(\frac{r}{cb}\right) + O(1/c^3).
\end{aligned} \tag{72}$$

Through second PN order in the wave emission, i.e. two PN orders beyond the leading order or, symbolically, order $c^{-5}(1 + c^{-2} + c^{-4})$, the time-averaged gravitational wave luminosity $\langle \mathcal{L}(t) \rangle$ and energy loss $\langle \frac{dE}{dt} \rangle$ are given by,

$$\mathcal{L}(t) = \frac{c^3}{32\pi G} \oint_{\text{FZ}} (\partial_t h_{ij}^{\text{TT}})^2 r^2 d\Omega \tag{73}$$

$$\begin{aligned}
\mathcal{L} &= \frac{G}{5c^5} \sum_{n=0}^{\infty} \left(\frac{1}{c^2}\right)^n \hat{\mathcal{L}}_n \\
&= \frac{G}{5c^5} \left\{ M_{ij}^{(3)} M_{ij}^{(3)} + \frac{1}{c^2} \left[\frac{5}{189} M_{ijk}^{(4)} M_{ijk}^{(4)} + \frac{16}{9} S_{ij}^{(3)} S_{ij}^{(3)} \right] \right. \\
&\quad \left. + \frac{1}{c^4} \left[\frac{5}{9072} M_{ijkm}^{(5)} M_{ijkm}^{(5)} + \frac{5}{84} S_{ijk}^{(4)} S_{ijk}^{(4)} \right] \right\},
\end{aligned} \tag{74}$$

and

$$- \left\langle \frac{dE(t - r_*/c)}{dt} \right\rangle = \langle \mathcal{L}(t) \rangle. \tag{75}$$

The leading term is known as the famous “Einstein quadrupole formula”.

5 Spin and Gravity

The implementation into gravity of proper angular momentum (spin) of a classical or quantum particle is most efficiently performed with the aid of a tetrad field e_a^μ , e.g. [14–16],

$$e_a^\mu e_{b\mu} = \eta_{ab}, \quad e_{a\mu} e_{b\nu} \eta^{ab} = g_{\mu\nu} = g_{\nu\mu}, \tag{76}$$

where $\eta_{ab} = \eta^{ab}$ denotes the Minkowski metric, $a, b = (0), (1), (2), (3)$, and $g_{\mu\nu}$ the metric of physical spacetime. A local Lorentz transformation L^b_a operates in the form

$$e'^\mu_a = L^b_a e^\mu_b, \quad L^a_c \eta_{ab} L^b_d = \eta_{cd}. \tag{77}$$

A linear connection ω_μ^{ab} is needed for the spacetime derivatives to transform homogeneously under local Lorentz transformations, e.g. [33],

$$D_\mu \phi \equiv \partial_\mu \phi + \frac{1}{2} \omega_\mu^{ab} G_{[ab]} \phi \quad (78)$$

with

$$\omega_\mu'^{ab} = L^a_c L^b_d \omega_\mu^{cd} + L^a_d \partial_\mu L^{bd}, \quad \partial_\mu \equiv \frac{\partial}{\partial x^\mu}. \quad (79)$$

Infinitesimal local Lorentz transformations with group parameters $\delta \xi^{ab}$ induce the change

$$\delta \phi = \delta \xi^{ab} G_{[ab]} \phi \quad (80)$$

on the mathematical object ϕ .

The curvature tensor of the tetrad field, $R_{\mu\nu}^{ab}$, is defined by

$$D_\mu D_\nu \phi - D_\nu D_\mu \phi = R_{\mu\nu}^{ab} G_{[ab]} \phi, \quad (81)$$

and results in

$$R_{\mu\nu}^{ab} = \partial_\mu \omega_\nu^{ab} - \partial_\nu \omega_\mu^{ab} + \omega_\nu^{ac} \omega_\mu^{bd} \eta_{cd} - \omega_\mu^{ac} \omega_\nu^{bd} \eta_{cd}. \quad (82)$$

The Lagrangian density of the gravitational field is given by

$$\mathcal{L}_G = \frac{1}{16\pi} \det(e_\gamma^c) e_a^\mu e_b^\nu R_{\mu\nu}^{ab}(\omega) + \partial_\mu \mathcal{C}^\mu. \quad (83)$$

The vacuum Einstein field equations take the forms,

$$0 = \frac{\delta \mathcal{L}_G}{\delta e_a^\mu} e_{a\nu} \equiv 2 \det(e_\gamma^c) (R_{\mu\nu} - \frac{1}{2} g_{\mu\nu} R) \quad (84)$$

and

$$0 = \frac{\delta \mathcal{L}_G}{\delta \omega_\mu^{ab}} \Rightarrow \omega_\mu^{ab} = \omega_\mu^{ab}(e, \partial_\nu e). \quad (85)$$

The latter equation eliminates torsion from the tetrad field. If this condition is also kept if matter sources for the gravitational field are included, no torsion will enter the gravitational field.

The Lagrangian for spinning objects coupled to gravity reads, e.g. [26] and References therein,

$$\mathcal{L}_M = \int d\tau \left[\left(p_\mu - \frac{1}{2} S_{ab} \omega_\mu^{ab} \right) \frac{dz^\mu}{d\tau} + \frac{1}{2} S_{ab} \frac{\delta\theta^{ab}}{d\tau} \right] \delta_{(4)}, \quad (86)$$

where S_{ab} is the spin tensor in tetrad components and $\delta\theta^{ab}/d\tau$ the angular velocity tensor. This Lagrangian is degenerate and thus needs an additional Lagrangian which imposes supplementary conditions,

$$\mathcal{L}_C = \int d\tau \left[\lambda_1^a p^b S_{ab} + \lambda_{2[i]} \Lambda^{[i]a} p_a - \frac{\lambda_3}{2} (p^2 + m^2) \right] \delta_{(4)}, \quad (87)$$

where λ_1^a , $\lambda_{2[i]}$, λ_3 are Lagrange multipliers, $p_a = \eta_{ab} p^b$ the four-dimensional linear momentum of the particle with $p^2 = p_a p^a$, and Λ^{Ca} the rotational matrix between the spacetime tetrad e_a^μ and a body fixed one; the latter tetrad has capital latin indices as names, $C = [0], [i]$, whereas the former one has small latin ones, $a = (0), (i)$,

$$\delta\theta^{ab} = \Lambda_C^a d\Lambda^{Cb} = -\delta\theta^{ba}. \quad (88)$$

Obviously, $\delta\theta^{ab}$ is not an exact one-form.

The equations of motion which originate from our Lagrangians read,

$$\frac{DS_{ab}}{D\tau} = 0, \quad (89)$$

$$\frac{Dp_\mu}{D\tau} = -\frac{1}{2} R_{\mu\rho ab} u^\rho S^{ab}, \quad (90)$$

or, in well known spacetime component representation,

$$\frac{DS^{\mu\nu}}{D\tau} = 0, \quad S^{\mu\nu} = e_a^\mu e_b^\nu S^{ab}, \quad (91)$$

$$\frac{Dp_\mu}{D\tau} = -\frac{1}{2} R_{\mu\rho\alpha\beta} u^\rho S^{\alpha\beta}, \quad R_{\mu\rho\alpha\beta} = e_\alpha^a e_\beta^b R_{\mu\rho ab}, \quad (92)$$

where

$$u^\mu \equiv \frac{dz^\mu}{d\tau} = \lambda_3 p^\mu. \quad (93)$$

The energy-momentum tensor $T^{\mu\nu}$ of the spinning body has the form

$$\sqrt{-g} T^{\mu\nu} = \int d\tau \left[\lambda_3 p^\mu p^\nu \delta_{(4)} + \nabla_\alpha \left(u^{(\mu} S^{\nu)\alpha} \delta_{(4)} \right) \right], \quad (94)$$

where $\delta_{(4)}$ is the four-dimensional delta function and τ the proper time of the body. This tensor is the well known pole-dipole energy-momentum tensor by Tulczyjew [34].

As we are interested in a canonical formulation of the gravitational spin dynamics, the line element of the spacetime metric has to be put into the ADM representation,

$$ds^2 = -(Ncdt)^2 + g_{ij}(dx^i + N^i cdt)(dx^j + N^j cdt), \quad (95)$$

where N and N^i denote the lapse and shift functions, respectively, coined so by J. A. Wheeler in 1964, [35].

The non-reduced Hamiltonian has the general form, $(,{}_i = \partial_i)$,

$$H = \int d^3x (N\mathcal{H} - N^i \mathcal{H}_i) + \frac{c^4}{16\pi G} \oint_{i^0} d^2s_i (g_{ij,j} - g_{jj,i}), \quad (96)$$

where \mathcal{H} and \mathcal{H}_i are the super-Hamiltonian and super-momentum, respectively. The surface integral is taken at spatial infinity, denoted i^0 . At i^0 , the lapse and shift functions are assumed to behave as

$$N|_{i^0} = 1 + \mathcal{O}(1/r), \quad N^i|_{i^0} = \mathcal{O}(1/r). \quad (97)$$

The famous constraint equations

$$\mathcal{H} = 0 \quad \text{and} \quad \mathcal{H}_i = 0 \quad (98)$$

result from the fact that the functions N and N^i are Lagrange multipliers.

If the constraint equations are fulfilled and adapted coordinate conditions are applied, then

$$H = \frac{c^4}{16\pi G} \oint_{i^0} d^2s_i (g_{ij,j} - g_{jj,i}) \equiv H_{\text{ADM}} \quad (99)$$

describes the Hamilton functional of the total system, called the ADM Hamiltonian.

To simplify notation, from now on and for the rest of this section we put $c = G = 1$. The solutions for the matter supplementary conditions read, for

(i), λ_1 :

$$nS_i \equiv n^\mu S_{\mu i} = \frac{p_k \gamma^{kj} S_{ji}}{np} = g_{ij} n S^j, \quad (100)$$

(ii), λ_2 :

$$\Lambda^{[j](0)} = \Lambda^{[j](i)} \frac{p_{(i)}}{p^{(0)}}, \quad \Lambda^{[0]a} = -\frac{p^a}{m}, \quad (101)$$

(iii), λ_3 :

$$np \equiv n^\mu p_\mu = -\sqrt{m^2 + \gamma^{ij} p_i p_j}, \quad \gamma^{ik} g_{kj} = \delta_j^i, \quad (102)$$

where the timelike unit vector orthogonal to the $t = \text{const}$ slices reads,

$$n^\mu = (1, -N^i)/N, \quad n_\mu = (-N, 0, 0, 0). \quad (103)$$

The time gauge for the tetrad field, coined so by Schwinger [14], is defined by, also see [16],

$$e_{(0)}^\mu = n^\mu, \quad e_{(0)}^0 = \frac{1}{N}, \quad e_{(0)}^i = -\frac{N^i}{N}, \quad (104)$$

thus,

$$g_{ij} = e_i^{(m)} e_{(m)j}. \quad (105)$$

The matter part of the constraint Lagrangian density takes the form

$$\mathcal{L}_{MC} = -N\mathcal{H}^{\text{matter}} + N^i \mathcal{H}_i^{\text{matter}} \quad (106)$$

with

$$\mathcal{H}^{\text{matter}} = -np\delta - K^{ij} \frac{p_i n S_j}{np} \delta - (nS^k \delta)_{;k} \quad (107)$$

and

$$\mathcal{H}_i^{\text{matter}} = (p_i + K_{ij} n S^j) \delta + \left(\frac{1}{2} \gamma^{mk} S_{ik} \delta + \delta_i^{(k} \gamma^{l)m} \frac{p_k n S_l}{np} \delta \right)_{;m}. \quad (108)$$

Here, a semicolon denotes three-dimensional covariant derivative.

The transformation to canonical matter variables, $\hat{z}^i, \hat{S}_{ij}, \hat{\lambda}^{[i](k)}, P_i$, reads

$$z^i = \hat{z}^i - \frac{nS^i}{m - np}, \quad nS_i = -\frac{p_k \gamma^{kj} \hat{S}_{ji}}{m}, \quad (109)$$

$$S_{ij} = \hat{S}_{ij} - \frac{p_i n S_j}{m - np} + \frac{p_j n S_i}{m - np}, \quad (110)$$

$$\lambda^{[i](j)} = \hat{\lambda}^{[i](k)} \left(\delta_{kj} + \frac{p_{(k} p^{(j)}}{m(m - np)} \right), \quad (111)$$

$$P_i = p_i + K_{ij}nS^j + \hat{A}^{kl}e_{(j)k}e_{l,i}^{(j)} - \left(\frac{1}{2}S_{kj} + \frac{p_{(k}nS_{j)}}{np} \right) \Gamma_i^{kj}, \quad (112)$$

where Γ_i^{kj} are 3-dimensional Christoffel symbols and

$$g_{ik}g_{jl}\hat{A}^{kl} = \frac{1}{2}\hat{S}_{ij} + \frac{mp_{(i}nS_{j)}}{np(m-np)}. \quad (113)$$

The spin tensors and vectors have constant three-dimensional length,

$$S^{ab}S_{ab} = \hat{S}_{(i)(j)}\hat{S}_{(i)(j)} = 2\hat{S}_{(i)}\hat{S}_{(i)} = 2s^2 = \text{const}, \quad (114)$$

and the canonical three-dimensional rotation matrix $\hat{\lambda}_{[k]}^{(i)}$ is orthogonal,

$$\hat{\lambda}_{[k]}^{(i)}\hat{\lambda}^{[k](j)} = \delta_{ij}; \quad (115)$$

also, it holds,

$$\delta\hat{\theta}^{(i)(j)} \equiv \hat{\lambda}_{[k]}^{(i)}d\hat{\lambda}^{[k](j)} = -\delta\hat{\theta}^{(j)(i)}. \quad (116)$$

The purely kinetic Lagrangian density of the body takes the form,

$$\hat{\mathcal{L}}_{KM} = P_i\dot{z}^i\delta + \frac{1}{2}\hat{S}_{(i)(j)}\dot{\theta}^{(i)(j)}\delta \quad (117)$$

and a gravitational Lagrangian related with the body reads,

$$\hat{\mathcal{L}}_{GM} = \hat{A}^{ij}e_{(k)i}e_{j,0}^{(k)}\delta. \quad (118)$$

Adding the Lagrangian density of gravity, \mathcal{L}_G , yields,

$$\hat{\mathcal{L}}_{GM} + \mathcal{L}_G = \frac{1}{8\pi}[\pi^{ij} + 8\pi\hat{A}^{ij}\delta]e_{(k)i}e_{j,0}^{(k)} + \mathcal{L}_{GC} - \frac{1}{16\pi}\mathcal{E}_{i,i}, \quad (119)$$

where $\mathcal{E}_i = g_{ij,j} - g_{jj,i}$ and the total energy is given by

$$E = \frac{1}{16\pi} \oint d^2s_i \mathcal{E}_i = \frac{1}{16\pi} \int d^3x \mathcal{E}_{i,i}. \quad (120)$$

The gravitational constraint Lagrangian density is

$$\mathcal{L}_{GC} = -N\mathcal{H}^{\text{field}} + N^i\mathcal{H}_i^{\text{field}}, \quad (121)$$

where

$$\mathcal{H}^{\text{field}} = -\frac{1}{16\pi\sqrt{g}} \left[gR + \frac{1}{2}(g_{ij}\pi^{ij})^2 - g_{ij}g_{kl}\pi^{ik}\pi^{jl} \right], \quad (122)$$

with R the 3-dimensional curvature scalar, and

$$\mathcal{H}_i^{\text{field}} = \frac{1}{8\pi} g_{ij}\pi^{jk}{}_{;k}. \quad (123)$$

The pure field momentum reads,

$$\pi^{ij} = \sqrt{g}(\gamma^{ij}\gamma^{kl} - \gamma^{ik}\gamma^{jl})K_{kl}. \quad (124)$$

The spatially symmetric time gauge, introduced by Kibble in 1963, [15], is defined by

$$e_{(i)j} = e_{ij} = e_{ji}, \quad e_{ij}e_{jk} = g_{ik} \quad \text{or}, \quad e_{ij} = \sqrt{(g_{kl})}. \quad (125)$$

It allows the elimination of the tetrad field from the formalism (otherwise the Einstein theory of gravity could not be fully regained),

$$e_{(k)i}e_{j,\mu}^{(k)} = B_{ij}^{kl}g_{kl,\mu} + \frac{1}{2}g_{ij,\mu}, \quad (126)$$

where $B_{ij}^{kl} = B_{ij}^{lk} = -B_{ji}^{kl}$.

The new canonical field momentum is then given by, cf. [15],

$$\pi_{\text{can}}^{ij} = \pi^{ij} + 8\pi\hat{A}^{(ij)}\delta + 16\pi B_{kl}^{ij}\hat{A}^{[kl]}\delta. \quad (127)$$

Additionally, for the obtention of unique dynamical evolution also appropriate spacetime coordinate conditions must be imposed, in the ADM case,

$$3g_{ij,j} - g_{jj,i} = 0, \quad \pi_{\text{can}}^{ii} = 0 \quad (128)$$

or,

$$g_{ij} = \Psi^4\delta_{ij} + h_{ij}^{\text{TT}}, \quad \pi_{\text{can}}^{ij} = \tilde{\pi}^{ij} + \pi_{\text{TTcan}}^{ij}. \quad (129)$$

Again, transverse traceless conditions apply,

$$h_{ii}^{\text{TT}} = \pi_{\text{TTcan}}^{ii} = h_{ij,j}^{\text{TT}} = \pi_{\text{TTcan},j}^{ij} = 0, \quad (130)$$

as well as longitudinal traceless ones,

$$\tilde{\pi}^{ij} = V^i_{,j} + V^j_{,i} - \frac{2}{3}\delta_{ij}V^k_{,k}. \quad (131)$$

The constraint equations read,

$$\mathcal{H}^{\text{field}} + \mathcal{H}^{\text{matter}} = 0, \quad \mathcal{H}_i^{\text{field}} + \mathcal{H}_i^{\text{matter}} = 0. \quad (132)$$

Finally, the total canonical action results in the form,

$$W = \frac{1}{16\pi} \int d^4x \pi_{\text{can}}^{ij\text{TT}} h_{ij,0}^{\text{TT}} + \int dt \left[P_i \dot{z}^i + \frac{1}{2} \hat{S}_{(i)(j)} \dot{\theta}^{(i)(j)} - E \right], \quad (133)$$

and the Hamiltonian reads

$$E \equiv H_{\text{ADM}} = -\frac{1}{2\pi} \int d^3x \Delta \Psi [\hat{z}^i, P_i, \hat{S}_{(i)(j)}, h_{ij}^{\text{TT}}, \pi_{\text{TTcan}}^{ij}]. \quad (134)$$

The Poisson brackets take the particularly simple form,

$$\{\hat{z}^i, P_j\} = \delta_{ij}, \quad \{\hat{S}_{(i)}, \hat{S}_{(j)}\} = \epsilon_{ijk} \hat{S}_{(k)}, \quad (135)$$

$$\{h_{ij}^{\text{TT}}(\mathbf{x}, t), \pi_{\text{TTcan}}^{kl}(\mathbf{x}', t)\} = 16\pi \delta_{ij}^{\text{TTkl}} \delta(\mathbf{x} - \mathbf{x}'), \quad (136)$$

and zero otherwise, where $\delta_{ij}^{\text{TTkl}} \delta(\mathbf{x})$ is a transverse traceless Dirac delta function, e.g. [12, 13].

6 Higher Order Post-Newtonian Hamiltonians

In the following, reduced variables in the the center-of-mass system will be used, defining $\hat{H} = (H - Mc^2)/\mu$, $\mu = m_1 m_2 / M$, $M = m_1 + m_2$, $\nu = \mu / M$, $0 \leq \nu \leq 1/4$ with test-body case $\nu = 0$ and equal-mass case $\nu = 1/4$. In the center-of-mass system $\mathbf{p}_1 + \mathbf{p}_2 = 0$ and $\mathbf{p} \equiv \mathbf{p}_1 / \mu$. Furthermore, $p_r = (\mathbf{n} \cdot \mathbf{p})$, $\mathbf{q} \equiv (\mathbf{x}_1 - \mathbf{x}_2) / GM$, $\mathbf{n} = \mathbf{q} / |\mathbf{q}|$.

The 3PN conservative binary black hole dynamics has Hamiltonian, [7, 36],

$$\hat{H} = \hat{H}_{\text{N}} + \frac{1}{c^2} \hat{H}_{[1\text{PN}]} + \frac{1}{c^4} \hat{H}_{[2\text{PN}]} + \frac{1}{c^6} \hat{H}_{[3\text{PN}]}, \quad (137)$$

where

$$\hat{H}_N = \frac{p^2}{2} - \frac{1}{q}, \quad (138)$$

$$\hat{H}_{[1\text{PN}]} = \frac{1}{8}(3\nu - 1)p^4 - \frac{1}{2}[(3 + \nu)p^2 + \nu p_r^2]\frac{1}{q} + \frac{1}{2q^2}, \quad (139)$$

$$\begin{aligned} \hat{H}_{[2\text{PN}]} &= \frac{1}{16}(1 - 5\nu + 5\nu^2)p^6 \\ &+ \frac{1}{8}[(5 - 20\nu - 3\nu^2)p^4 - 2\nu^2 p_r^2 p^2 - 3\nu^2 p_r^4]\frac{1}{q} \\ &+ \frac{1}{2}[(5 + 8\nu)p^2 + 3\nu p_r^2]\frac{1}{q^2} - \frac{1}{4}(1 + 3\nu)\frac{1}{q^3}, \end{aligned} \quad (140)$$

$$\begin{aligned} \hat{H}_{[3\text{PN}]} &= \frac{1}{128}(-5 + 35\nu - 70\nu^2 + 35\nu^3)p^8 \\ &+ \frac{1}{16}[(-7 + 42\nu - 53\nu^2 - 5\nu^3)p^6 + (2 - 3\nu)\nu^2 p_r^2 p^4 \\ &+ 3(1 - \nu)\nu^2 p_r^4 p^2 - 5\nu^3 p_r^6]\frac{1}{q} \\ &+ \left[\frac{1}{16}(-27 + 136\nu + 109\nu^2)p^4 + \frac{1}{16}(17 + 30\nu)\nu p_r^2 p^2 \right. \\ &+ \left. \frac{1}{12}(5 + 43\nu)\nu p_r^4 \right]\frac{1}{q^2} \\ &+ \left[\left(-\frac{25}{8} + \left(\frac{1}{64}\pi^2 - \frac{335}{48} \right)\nu - \frac{23}{8}\nu^2 \right) p^2 \right. \\ &+ \left. \left(-\frac{85}{16} - \frac{3}{64}\pi^2 - \frac{7}{4}\nu \right) \nu p_r^2 \right]\frac{1}{q^3} \\ &+ \left[\frac{1}{8} + \left(\frac{109}{12} - \frac{21}{32}\pi^2 \right)\nu \right]\frac{1}{q^4}. \end{aligned} \quad (141)$$

The dissipative dynamics is non-autonomous with Hamiltonians explicitly depending on time, $H_{2.5\text{PN}}(t) + H_{3.5\text{PN}}(t) + \dots$. The leading order 2.5PN binary black hole orbital Hamiltonian reads, e.g. [37],

$$H_{2.5\text{PN}}(t) = \frac{2G}{5c^5} Q_{ij}(t) \left(\frac{p_{1i} p_{1j}}{m_1} + \frac{p_{2i} p_{2j}}{m_2} - \frac{Gm_1 m_2}{r_{12}} n_{12}^i n_{12}^j \right), \quad (142)$$

where the variables in

$$Q_{ij}(t) = \sum_{a=1,2} m_a \left(x_a^i x_a^j - \frac{1}{3} \mathbf{x}_a^2 \delta_{ij} \right) \quad (143)$$

are allowed to be identified with the variables outside $Q_{ij}(t)$ only after the Hamilton equations of motion have been derived.

The spin-gravity interactions of compact objects have the forms, [38–40], to leading order spin-orbit coupling, ($\mathbf{S} \equiv \hat{\mathbf{S}}$, $\mathbf{p} \equiv$ canonical momentum),

$$H_{\text{SO}}^{\text{LO}} = \frac{G}{c^2} \sum_a \sum_{b \neq a} \frac{1}{r_{ab}^2} (\mathbf{S}_a \times \mathbf{n}_{ab}) \cdot \left[\frac{3m_b}{2m_a} \mathbf{p}_a - 2\mathbf{p}_b \right], \quad (144)$$

to leading order spin(1)-spin(2) coupling,

$$H_{\text{S}_1\text{S}_2}^{\text{LO}} = \frac{G}{c^2} \sum_a \sum_{b \neq a} \frac{1}{2r_{ab}^3} [3(\mathbf{S}_a \cdot \mathbf{n}_{ab})(\mathbf{S}_b \cdot \mathbf{n}_{ab}) - (\mathbf{S}_a \cdot \mathbf{S}_b)], \quad (145)$$

and to leading order spin(1)-squared coupling,

$$H_{\text{S}_1^2}^{\text{LO}} = \frac{G}{c^2} \frac{m_2 C_{Q_1}}{2m_1 r_{12}^3} [3(\mathbf{S}_1 \cdot \mathbf{n}_{12})(\mathbf{S}_1 \cdot \mathbf{n}_{12}) - (\mathbf{S}_1 \cdot \mathbf{S}_1)], \quad (146)$$

where $C_{Q_1} = 1$ for black holes and $C_{Q_1} > 1$ otherwise, e.g. [41, 42].

For the next to leading order couplings, the corresponding expressions are, for spin-orbit coupling, [24, 43],

$$\begin{aligned} H_{\text{SO}}^{\text{NLO}} = & \frac{G}{c^4 r^2} \left[-((\mathbf{p}_1 \times \mathbf{S}_1) \cdot \mathbf{n}_{12}) \left[\frac{5m_2 \mathbf{p}_1^2}{8m_1^3} + \frac{3(\mathbf{p}_1 \cdot \mathbf{p}_2)}{4m_1^2} \right. \right. \\ & - \frac{3\mathbf{p}_2^2}{4m_1 m_2} + \frac{3(\mathbf{p}_1 \cdot \mathbf{n}_{12})(\mathbf{p}_2 \cdot \mathbf{n}_{12})}{4m_1^2} + \frac{3(\mathbf{p}_2 \cdot \mathbf{n}_{12})^2}{2m_1 m_2} \left. \right] \\ & + ((\mathbf{p}_2 \times \mathbf{S}_1) \cdot \mathbf{n}_{12}) \left[\frac{(\mathbf{p}_1 \cdot \mathbf{p}_2)}{m_1 m_2} + \frac{3(\mathbf{p}_1 \cdot \mathbf{n}_{12})(\mathbf{p}_2 \cdot \mathbf{n}_{12})}{m_1 m_2} \right] \\ & + ((\mathbf{p}_1 \times \mathbf{S}_1) \cdot \mathbf{p}_2) \left[\frac{2(\mathbf{p}_2 \cdot \mathbf{n}_{12})}{m_1 m_2} - \frac{3(\mathbf{p}_1 \cdot \mathbf{n}_{12})}{4m_1^2} \right] \left. \right] \\ & + \frac{G^2}{c^4 r^3} \left[-((\mathbf{p}_1 \times \mathbf{S}_1) \cdot \mathbf{n}_{12}) \left[\frac{11m_2}{2} + \frac{5m_2^2}{m_1} \right] \right. \\ & + ((\mathbf{p}_2 \times \mathbf{S}_1) \cdot \mathbf{n}_{12}) \left[6m_1 + \frac{15m_2}{2} \right] \left. \right] + (1 \leftrightarrow 2), \quad (147) \end{aligned}$$

for spin(1)-spin(2) coupling, [44],

$$\begin{aligned}
H_{S_1 S_2}^{\text{NLO}} = & (G/2m_1 m_2 c^4 r^3) [3((\mathbf{p}_1 \times \mathbf{S}_1) \cdot \mathbf{n}_{12})((\mathbf{p}_2 \times \mathbf{S}_2) \cdot \mathbf{n}_{12})/2 \\
& + 6((\mathbf{p}_2 \times \mathbf{S}_1) \cdot \mathbf{n}_{12})((\mathbf{p}_1 \times \mathbf{S}_2) \cdot \mathbf{n}_{12}) \\
& - 15(\mathbf{S}_1 \cdot \mathbf{n}_{12})(\mathbf{S}_2 \cdot \mathbf{n}_{12})(\mathbf{p}_1 \cdot \mathbf{n}_{12})(\mathbf{p}_2 \cdot \mathbf{n}_{12}) \\
& - 3(\mathbf{S}_1 \cdot \mathbf{n}_{12})(\mathbf{S}_2 \cdot \mathbf{n}_{12})(\mathbf{p}_1 \cdot \mathbf{p}_2) + 3(\mathbf{S}_1 \cdot \mathbf{p}_2)(\mathbf{S}_2 \cdot \mathbf{n}_{12})(\mathbf{p}_1 \cdot \mathbf{n}_{12}) \\
& + 3(\mathbf{S}_2 \cdot \mathbf{p}_1)(\mathbf{S}_1 \cdot \mathbf{n}_{12})(\mathbf{p}_2 \cdot \mathbf{n}_{12}) + 3(\mathbf{S}_1 \cdot \mathbf{p}_1)(\mathbf{S}_2 \cdot \mathbf{n}_{12})(\mathbf{p}_2 \cdot \mathbf{n}_{12}) \\
& + 3(\mathbf{S}_2 \cdot \mathbf{p}_2)(\mathbf{S}_1 \cdot \mathbf{n}_{12})(\mathbf{p}_1 \cdot \mathbf{n}_{12}) - 3(\mathbf{S}_1 \cdot \mathbf{S}_2)(\mathbf{p}_1 \cdot \mathbf{n}_{12})(\mathbf{p}_2 \cdot \mathbf{n}_{12}) \\
& + (\mathbf{S}_1 \cdot \mathbf{p}_1)(\mathbf{S}_2 \cdot \mathbf{p}_2) - (\mathbf{S}_1 \cdot \mathbf{p}_2)(\mathbf{S}_2 \cdot \mathbf{p}_1)/2 + (\mathbf{S}_1 \cdot \mathbf{S}_2)(\mathbf{p}_1 \cdot \mathbf{p}_2)/2] \\
& + (3/2m_1^2 r^3) [-((\mathbf{p}_1 \times \mathbf{S}_1) \cdot \mathbf{n}_{12})((\mathbf{p}_1 \times \mathbf{S}_2) \cdot \mathbf{n}_{12}) \\
& + (\mathbf{S}_1 \cdot \mathbf{S}_2)(\mathbf{p}_1 \cdot \mathbf{n}_{12})^2 - (\mathbf{S}_1 \cdot \mathbf{n}_{12})(\mathbf{S}_2 \cdot \mathbf{p}_1)(\mathbf{p}_1 \cdot \mathbf{n}_{12})] \\
& + (3/2m_2^2 r^3) [-((\mathbf{p}_2 \times \mathbf{S}_2) \cdot \mathbf{n}_{12})((\mathbf{p}_2 \times \mathbf{S}_1) \cdot \mathbf{n}_{12}) \\
& + (\mathbf{S}_1 \cdot \mathbf{S}_2)(\mathbf{p}_2 \cdot \mathbf{n}_{12})^2 - (\mathbf{S}_2 \cdot \mathbf{n}_{12})(\mathbf{S}_1 \cdot \mathbf{p}_2)(\mathbf{p}_2 \cdot \mathbf{n}_{12})] \\
& + (6G^2(m_1 + m_2)/c^4 r^4) [(\mathbf{S}_1 \cdot \mathbf{S}_2) - 2(\mathbf{S}_1 \cdot \mathbf{n}_{12})(\mathbf{S}_2 \cdot \mathbf{n}_{12})], \quad (148)
\end{aligned}$$

and for spin-squared coupling, [45, 46],

$$\begin{aligned}
H_{S_1^2}^{\text{NLO}} = & \frac{G}{c^4 r^3} \left[\frac{m_2}{m_1^3} \left(\left(-\frac{21}{8} + \frac{9}{4} C_{Q_1} \right) \mathbf{p}_1^2 (\mathbf{S}_1 \cdot \mathbf{n})^2 \right. \right. \\
& + \left(\frac{15}{4} - \frac{9}{2} C_{Q_1} \right) (\mathbf{p}_1 \cdot \mathbf{n}) (\mathbf{S}_1 \cdot \mathbf{n}) (\mathbf{p}_1 \cdot \mathbf{S}_1) \\
& + \left(-\frac{5}{4} + \frac{3}{2} C_{Q_1} \right) (\mathbf{p}_1 \cdot \mathbf{S}_1)^2 + \left(-\frac{9}{8} + \frac{3}{2} C_{Q_1} \right) (\mathbf{p}_1 \cdot \mathbf{n})^2 \mathbf{S}_1^2 \\
& + \left(\frac{5}{4} - \frac{5}{4} C_{Q_1} \right) \mathbf{p}_1^2 \mathbf{S}_1^2 \Big) + \frac{1}{m_1^2} \left(-\frac{15}{4} C_{Q_1} (\mathbf{p}_1 \cdot \mathbf{n}) (\mathbf{p}_2 \cdot \mathbf{n}) (\mathbf{S}_1 \cdot \mathbf{n})^2 \right. \\
& + \left(3 - \frac{21}{4} C_{Q_1} \right) (\mathbf{p}_1 \cdot \mathbf{p}_2) (\mathbf{S}_1 \cdot \mathbf{n})^2 \\
& + \left(-\frac{3}{2} + \frac{9}{2} C_{Q_1} \right) (\mathbf{p}_2 \cdot \mathbf{n}) (\mathbf{p}_1 \cdot \mathbf{S}_1) (\mathbf{S}_1 \cdot \mathbf{n}) \\
& + \left(-3 + \frac{3}{2} C_{Q_1} \right) (\mathbf{p}_1 \cdot \mathbf{n}) (\mathbf{p}_2 \cdot \mathbf{S}_1) (\mathbf{S}_1 \cdot \mathbf{n}) \\
& + \left(\frac{3}{2} - \frac{3}{2} C_{Q_1} \right) (\mathbf{p}_1 \cdot \mathbf{S}_1) (\mathbf{p}_2 \cdot \mathbf{S}_1) + \left(\frac{3}{2} - \frac{3}{4} C_{Q_1} \right) (\mathbf{p}_1 \cdot \mathbf{n}) (\mathbf{p}_2 \cdot \mathbf{n}) \mathbf{S}_1^2 \\
& + \left(-\frac{3}{2} + \frac{9}{4} C_{Q_1} \right) (\mathbf{p}_1 \cdot \mathbf{p}_2) \mathbf{S}_1^2 \Big) + \frac{C_{Q_1}}{m_1 m_2} \left(-\frac{3}{4} \mathbf{p}_2^2 \mathbf{S}_1^2 + \frac{9}{4} \mathbf{p}_2^2 (\mathbf{S}_1 \cdot \mathbf{n})^2 \right) \Big] \\
& + \frac{G^2 m_2}{c^4 r^4} \left[\left(2 + \frac{1}{2} C_{Q_1} + \frac{m_2}{m_1} (1 + 2C_{Q_1}) \right) \mathbf{S}_1^2 \right. \\
& \left. - \left(3 + \frac{3}{2} C_{Q_1} + \frac{m_2}{m_1} (1 + 6C_{Q_1}) \right) (\mathbf{S}_1 \cdot \mathbf{n})^2 \right]. \quad (149)
\end{aligned}$$

This expression goes beyond the general linear-in-spin structure and needed additional considerations as undertaken in the quoted References.

Properly augmenting the discussed Hamiltonians, the present knowledge reads,

$$\begin{aligned}
 H(t) = & H_N + H_{1\text{PN}} + H_{2\text{PN}} + H_{3\text{PN}} + H_{4\text{PN}} \\
 & + H_{\text{SO}}^{\text{LO}} + H_{\text{S}_1\text{S}_2}^{\text{LO}} + H_{\text{S}_1^2}^{\text{LO}} + H_{\text{S}_2^2}^{\text{LO}} \\
 & + H_{\text{SO}}^{\text{NLO}} + H_{\text{S}_1\text{S}_2}^{\text{NLO}} + H_{\text{S}_1^2}^{\text{NLO}} + H_{\text{S}_2^2}^{\text{NLO}} \\
 & + H_{\text{SO}}^{\text{NNLO}} + H_{\text{S}_1\text{S}_2}^{\text{NNLO}} \\
 & + H_{2.5\text{PN}}(t) + H_{3.5\text{PN}}(t) \\
 & + H_{\text{SO}}^{\text{DLO}}(t) + H_{\text{S}_1\text{S}_2}^{\text{DLO}}(t).
 \end{aligned} \tag{150}$$

All the higher order dissipative Hamiltonians, including the leading order spin-orbit and spin(1)-spin(2) coupling ones, have been computed in the Refs. [47–50].

7 Applications

Important applications of the dynamics of binary systems are the computation of their orbital and spin motions. Here particularly, the orbital period, the periastron advance, the innermost stable circular orbit (ISCO), and the spin precessions are of great interest. For not entering into complicated expressions within higher order PN settings, only spinless particles will be considered. For the case of spinning bodies, the reader may consult the Refs. [51–54].

7.1 Orbital Motion

The derivation of orbital observables is most elegant with starting from the action functional of the particles. The radial action, denoted by $i_r(E, j)$ with E reduced energy and j reduced angular momentum, is defined by

$$i_r(E, j) = \frac{1}{2\pi} \oint dr \, p_r, \tag{151}$$

where the integration has to be performed from minimal radial separation to minimal radial separation ($p_r = 0$), notice $p^2 = p_r^2 + j^2/r^2$. In reduced variables, the full revolution of phase, Φ , is given by

$$\frac{\Phi}{2\pi} = 1 + k = -\frac{\partial}{\partial j} i_r(E, j) \tag{152}$$

and the orbital period, P , results in the form

$$\frac{P}{2\pi GM} = \frac{\partial}{\partial E} i_r(E, j), \quad (153)$$

see, e.g., [55].

Through 3PN order, the periastron advance k turns out to be,

$$\begin{aligned} k = & \frac{1}{c^2} \frac{3}{j^2} \left[1 + \frac{1}{c^2} \left[\frac{5}{4} (7 - 2\nu) \frac{1}{j^2} + \frac{1}{2} (5 - 2\nu) E \right] \right. \\ & \left. + \frac{1}{c^4} \left[a_1(\nu) \frac{1}{j^4} + a_2(\nu) \frac{E}{j^2} + a_3(\nu) E^2 \right] \right], \end{aligned} \quad (154)$$

and the orbital period results in,

$$\begin{aligned} \frac{P}{2\pi GM} = & \frac{1}{(-2E)^{3/2}} \left[1 - \frac{1}{c^2} \frac{1}{4} (15 - \nu) E \right. \\ & + \frac{1}{c^4} \left[\frac{3}{2} (5 - 2\nu) \frac{(-2E)^{3/2}}{j} - \frac{3}{32} (35 + 30\nu + 3\nu^2) E^2 \right] \\ & \left. + \frac{1}{c^6} \left[a_2(\nu) \frac{(-2E)^{3/2}}{j^3} - 3a_3(\nu) \frac{(-2E)^{5/2}}{j} + a_4(\nu) E^3 \right] \right] \end{aligned} \quad (155)$$

with

$$a_1(\nu) = \frac{5}{2} \left(\frac{77}{2} + \left(\frac{41}{64} \pi^2 - \frac{125}{3} \right) \nu + \frac{7}{4} \nu^2 \right), \quad (156)$$

$$a_2(\nu) = \frac{105}{2} + \left(\frac{41}{64} \pi^2 - \frac{218}{3} \right) \nu + \frac{45}{6} \nu^2, \quad (157)$$

$$a_3(\nu) = \frac{1}{4} (5 - 5\nu + 4\nu^2), \quad (158)$$

$$a_4(\nu) = \frac{5}{128} (21 - 105\nu + 15\nu^2 + 5\nu^3). \quad (159)$$

The orbital motion takes the form,

$$\begin{aligned} r &= a_r (1 - e_r \cos u), \\ \frac{2\pi}{P} (t - t_0) &= u - e_t \sin u + F_{v-u} (v - u) + F_v \sin v + \dots, \\ \frac{2\pi}{\Phi} (\phi - \phi_0) &= v + G_v \sin v + G_{2v} \sin(2v) + G_{3v} \sin(3v) + \dots, \end{aligned} \quad (160)$$

where the true anomaly v is parametrized in terms of the eccentric anomaly u in the form

$$v = 2\arctan \left[\sqrt{\frac{1+e_\phi}{1-e_\phi}} \tan \frac{u}{2} \right].$$

More details can be found in [36, 55–58].

7.2 Innermost Stable Circular Orbit

In the Einstein theory binary systems show the phenomenon of innermost stable circular orbits (ISCO) beyond which no stable motion is possible. For a test body orbiting a Schwarzschild black hole of mass M the ISCO is located at $6GM/c^2$, in Schwarzschild coordinates, or in terms of orbital angular frequency, ω , which not depends on the chosen coordinate system, with $x = (GM\omega)^{2/3}/c^2$, yielding $x = 1/6$. For binary systems an exact result is not known. Clearly, the ISCO is only connected with the conservative part of the dynamics, the dissipative part makes the orbits shrinking, [59].

In reduced variables the (reduced) Hamiltonian may read $H = H(\mathbf{p}, \mathbf{r})$. Circular motion holds if $p_r = (\mathbf{p} \cdot \mathbf{r})/r = 0$ is valid. Then the Hamiltonian takes the form $H = H(j, r)$, where j is the reduced angular momentum, $p^2 = p_r^2 + j^2/r^2$. Circular motion takes place if $\frac{\partial}{\partial r} H(j, r) = 0$ holds. Then the Hamiltonian is a function of j only, $H = H(j)$. The orbital angular frequency ω results in the form $\omega = \frac{dH(j)}{dj}$ which can be inverted to obtain $H = H(\omega)$. The ISCO results from the condition $\frac{dH(\omega)}{d\omega} = 0$. This is a fully coordinate-invariant approach. Another possibility to obtain the ISCO is to impose $\frac{\partial^2}{\partial r^2} H(j, r) = 0$. In the following we will best keep to the coordinate-invariant definition.

In case of a Schwarzschild black hole, the reduced Hamiltonian reads, $\hat{H} = c^2 \mathcal{E}(x)$,

$$\begin{aligned} \mathcal{E}(x) &= \frac{1-2x}{(1-3x)^{1/2}} - 1 \\ &= -\frac{1}{2}x + \frac{3}{8}x^2 + \frac{27}{16}x^3 + \frac{675}{128}x^4 + \frac{3969}{256}x^5 + \dots \end{aligned} \quad (161)$$

In terms of our previously defined orbital variables, the orbital angular frequency for circular orbits reads,

$$\omega = \omega_{\text{radial}} + \omega_{\text{periastron}} = \frac{2\pi(1+k)}{P}. \quad (162)$$

Use of the most advanced knowledge, i.e. 4PN approximation,

$$c^2 \mathcal{E}(x) \equiv \hat{H}_N + \frac{1}{c^2} \hat{H}_{[1\text{PN}]} + \frac{1}{c^4} \hat{H}_{[2\text{PN}]} + \frac{1}{c^6} \hat{H}_{[3\text{PN}]} + \frac{1}{c^8} \hat{H}_{[4\text{PN}]}, \quad (163)$$

results in

$$\begin{aligned} \mathcal{E}(x) = & -\frac{1}{2}x + \left(\frac{3}{8} + \frac{1}{24}\nu\right)x^2 + \left(\frac{27}{16} - \frac{19}{16}\nu + \frac{1}{48}\nu^2\right)x^3 \\ & + \left(\frac{675}{128} + \left(-\frac{34445}{1152} + \frac{205\pi^2}{192}\right)\nu + \frac{155}{192}\nu^2 + \frac{35}{10368}\nu^3\right)x^4 \\ & + \left(\frac{3969}{256} + \left(\frac{123671}{11520} - \frac{9037\pi^2}{3072} - \frac{224}{15}(2\gamma_E + \ln(16x))\right)\nu\right. \\ & \left. + \left(\frac{498449}{6912} - \frac{3157\pi^2}{1152}\right)\nu^2 - \frac{301}{3456}\nu^3 - \frac{77}{62208}\nu^4\right)x^5, \end{aligned} \quad (164)$$

where $\gamma_E = 0.577\dots$ denotes the Euler constant. Both the γ_E -term and the log-term originate from the interaction of the binary with its near-zone tail field. The formula Eq. (164) as such is the state of the affairs in 2013, [60, 61], i.e. the full 4PN information as given in [23] was not needed. The ISCO is obtained by applying the condition $\frac{d\mathcal{E}(x)}{dx} = 0$ (minimum for \mathcal{E} as function of orbital frequency). For $\nu = 0$, the ISCO reads $x = 0.179\dots$ which is about 7.7% larger than the exact value of $1/6$; for $\nu = 1/4$, the equal mass case, one finds $x = 0.236\dots$ (more information is given in [60]).

References

1. S. Weinberg, *Gravitation and Cosmology* (Wiley, New York, 1972)
2. C.W. Misner, K.S. Thorne, J.A. Wheeler, *Gravitation* (W. H. Freeman, San Francisco, 1973)
3. N. Straumann, *General Relativity* (Springer, Dordrecht, 2013)
4. A. Einstein, L. Infeld, B. Hoffmann, The gravitational equations and the problem of motion. *Ann. Math.* **39**, 65 (1938)
5. Y. Itoh, T. Futamase, New derivation of the third post-Newtonian equation of motion for relativistic compact binaries without ambiguity. *Phys. Rev. D* **68**, 121501(R) (2003)
6. Y. Itoh, Equation of motion for relativistic compact binaries with the strong field point particle limit: third post-Newtonian order. *Phys. Rev. D* **69**, 064018 (2004)
7. T. Damour, P. Jaranowski, G. Schäfer, Dimensional regularization of the gravitational interaction of point masses. *Phys. Lett. B* **513**, 147 (2001)
8. L. Blanchet, T. Damour, G. Esposito-Farèse, Dimensional regularization of the third post-Newtonian dynamics of point particles in harmonic coordinates. *Phys. Rev. D* **69**, 124007 (2004)
9. S. Foffa, R. Sturani, Effective field theory calculation of conservative binary dynamics at third post-Newtonian order. *Phys. Rev. D* **84**, 044031 (2011)
10. P.A.M. Dirac, The theory of gravitation in Hamiltonian form. *Proc. R. Soc. (Lond.)* **A246**, 333 (1958)

11. P.A.M. Dirac, Fixation of coordinates in the Hamiltonian theory of gravitation. *Phys. Rev.* **114**, 924 (1959)
12. R. Arnowitt, S. Deser, C.M. Misner, The dynamics of general relativity, in *Gravitation: An Introduction to Current Research*, ed. by L. Witten (Wiley, New York, 1962), p. 227
13. R. Arnowitt, S. Deser, C.M. Misner, The dynamics of general relativity. *Gen. Relativ. Gravit.* **40**, 1997 (2008)
14. J. Schwinger, Quantized gravitational field. *Phys. Rev.* **130**, 1253 (1963)
15. T.W.B. Kibble, Canonical variables for the interacting gravitational and Dirac fields. *J. Math. Phys.* **4**, 1433 (1963)
16. P.A.M. Dirac, Interacting gravitational and spinor fields, in *Recent Developments in General Relativity* (PWN-Polish Scientific Publishers, Pergamon Press, Oxford, 1962), p. 191
17. J.E. Nelson, C. Teitelboim, Hamiltonian formulation of the theory of interacting gravitational and electron fields. *Ann. Phys. (N.Y.)* **116**, 86 (1978)
18. B.S. DeWitt, Quantum theory of gravity. I. The canonical theory. *Phys. Rev.* **160**, 1113 (1967)
19. T. Regge, C. Teitelboim, Role of surface integrals in the Hamiltonian formulation of general relativity. *Ann. Phys. (N.Y.)* **88**, 286 (1974)
20. T. Kimura, Fixation of physical space-time coordinates and equation of motion of two-body problem. *Prog. Theor. Phys.* **26**, 157 (1961)
21. T. Ohta, H. Okamura, T. Kimura, K. Hiida, Coordinate conditions and higher order gravitational potential in canonical formalism. *Prog. Theor. Phys.* **51**, 1598 (1974)
22. T. Damour, G. Schäfer, Lagrangians for n point masses at the second post-Newtonian approximation of general relativity. *Gen. Relativ. Gravit.* **17**, 879 (1985)
23. T. Damour, P. Jaranowski, G. Schäfer, Nonlocal-in-time action for the fourth post-Newtonian conservative dynamics of two-body systems. *Phys. Rev. D* **89**, 064058 (2014)
24. T. Damour, P. Jaranowski, G. Schäfer, Hamiltonian of two spinning compact bodies with next-to-leading order gravitational spin-orbit coupling. *Phys. Rev. D* **77**, 064032 (2008)
25. J. Steinhoff, G. Schäfer, Canonical formulation of self-gravitating spinning-object systems. *Europhys. Lett.* **87**, 50004 (2009)
26. J. Steinhoff, Canonical formulation of spin in general relativity. *Ann. Phys. (Berlin)* **523**, 296 (2011)
27. J. Hartung, J. Steinhoff, G. Schäfer, Next-to-next-to-leading order post-Newtonian linear-in-spin binary Hamiltonians. *Ann. Phys. (Berlin)* **525**, 359 (2013)
28. D.D. Holm, Hamiltonian formalism for general-relativistic adiabatic fluids. *Phys. D* **17**, 1 (1985)
29. S. Weinberg, *The Quantum Theory of Fields. Volume I: Foundations* (Cambridge University Press, Cambridge, 1995)
30. P. Jaranowski, G. Schäfer, Third post-Newtonian higher order ADM Hamilton dynamics for two-body point mass systems. *Phys. Rev. D* **57**, 7274 (1998)
31. L. Blanchet, Gravitational radiation from post-Newtonian sources and inspiralling compact binaries. *Living Rev. Relativ.* **17**, 2 (2014)
32. G. Schäfer, Reduced Hamiltonian formalism for general-relativistic adiabatic fluids and applications. *Astron. Nachrichten* **311**, 213 (1990)
33. B.S. DeWitt, Dynamical theory of groups and fields, in *Relativity, Groups and Topology*, eds. by C. DeWitt, B. DeWitt (Gordon and Breach, New York, 1964) p. 585
34. W.M. Tulczyjew, Motion of multipole particles in general relativity. *Acta Phys. Pol.* **18**, 393 (1959)
35. J.A. Wheeler, Geometrodynamics and the issue of the final state, in *Relativity, Groups and Topology*, eds. by C. DeWitt, B. DeWitt (Gordon and Breach, New York, 1964), p. 315
36. T. Damour, P. Jaranowski, G. Schäfer, Dynamical invariants for general relativistic two-body systems at the third post-Newtonian approximation. *Phys. Rev. D* **62**, 044024 (2000)
37. G. Schäfer, The general relativistic two-body problem. Theory and experiment, in *Symposia Gaussiana, Conference A: Mathematical and Theoretical Physics*, eds. by M. Behara, R. Fritsch, R.G. Lintz (Walter de Gruyter, Berlin, 1995), p. 667

38. B.M. Barker, R.F. O'Connell, Gravitational two-body problem with arbitrary masses, spins, and quadrupole moments. *Phys. Rev. D* **12**, 329 (1975)
39. P.D. D'Eath, Interaction of two black holes in the slow-motion limit. *Phys. Rev. D* **12**, 2183 (1975)
40. K.S. Thorne, J.B. Hartle, Laws of motion and precession for black holes and other bodies. *Phys. Rev. D* **31**, 1815 (1985)
41. B.M. Barker, R.F. O'Connell, The gravitational interaction: Spin, rotation, and quantum effects—a review. *Gen. Relativ. Gravit.* **11**, 149 (1979)
42. E. Poisson, Gravitational waves from inspiraling compact binaries: the quadrupole-moment term. *Phys. Rev. D* **57**, 5287 (1998)
43. J. Steinhoff, G. Schäfer, S. Hergt, ADM canonical formalism for gravitating spinning objects. *Phys. Rev. D* **77**, 104018 (2008)
44. J. Steinhoff, S. Hergt, G. Schäfer, Next-to-leading order gravitational spin(1)-spin(2) dynamics in Hamiltonian form. *Phys. Rev. D* **77**, 081501 (2008)
45. J. Steinhoff, S. Hergt, G. Schäfer, Spin-squared Hamiltonian of next-to-leading order gravitational interaction. *Phys. Rev. D* **78**, 101503(R) (2008)
46. S. Hergt, J. Steinhoff, G. Schäfer, The reduced Hamiltonian for next-to-leading-order spin-squared dynamics of general compact binaries. *Class. Quantum Gravity* **27**, 135007 (2010)
47. P. Jaranowski, G. Schäfer, Radiative 3.5 post-Newtonian ADM Hamiltonian for many-body point-mass systems. *Phys. Rev. D* **55**, 4712 (1997)
48. C. Königsdörffer, G. Faye, G. Schäfer, Binary black-hole dynamics at the third-and-a-half post-Newtonian order in the ADM formalism. *Phys. Rev. D* **68**, 044004 (2003)
49. J. Steinhoff, H. Wang, Canonical formulation of gravitating spinning objects at 3.5 post-Newtonian order. *Phys. Rev. D* **81**, 024022 (2010)
50. H. Wang, J. Steinhoff, J. Zeng, G. Schäfer, Leading-order spin-orbit and spin(1)-spin(2) radiation-reaction Hamiltonians. *Phys. Rev. D* **84**, 124005 (2011)
51. G. Schäfer, Gravitomagnetic effects. *Gen. Relativ. Gravit.* **36**, 2223 (2004)
52. M. Tessmer, J. Hartung, G. Schäfer, Aligned spins: orbital elements, decaying orbits, and last stable circular orbit to high post-Newtonian orders. *Class. Quantum Gravity* **30**, 015007 (2013)
53. M. Tessmer, J. Steinhoff, G. Schäfer, Canonical angles in a compact binary star system with spinning components: approximative solution through next-to-leading-order spin-orbit interaction for circular orbits. *Phys. Rev. D* **87**, 064035 (2013)
54. S. Hergt, A. Shah, G. Schäfer, Observables of a test-mass along an inclined orbit in a post-Newtonian approximated Kerr spacetime to leading-order-quadratic-in-spin. *Phys. Rev. Lett.* **111**, 021101 (2013)
55. T. Damour, G. Schäfer, Higher-order relativistic periastron advances and binary pulsars. II *Nuovo Cimento B* **101**, 127 (1988)
56. G. Schäfer, N. Wex, Second post-Newtonian motion of compact binaries. *Phys. Lett. A* **174**, 196 (1993)
57. G. Schäfer, N. Wex, Second post-Newtonian motion of compact binaries. *Phys. Lett. A* **177**, 461(E) (1993)
58. R.M. Memmesheimer, A. Gopakumar, G. Schäfer, Third post-Newtonian accurate generalized quasi-Keplerian parametrization for compact binaries in eccentric orbits. *Phys. Rev. D* **70**, 104011 (2004)
59. T. Damour, P. Jaranowski, G. Schäfer, On the determination of the last stable orbit for circular general relativistic binaries at the third post-Newtonian approximation. *Phys. Rev. D* **62**, 084011 (2000)
60. P. Jaranowski, G. Schäfer, Dimensional regularization of local singularities in the 4th post-Newtonian two-point-mass Hamiltonian. *Phys. Rev. D* **87**, 081503(R) (2013)
61. D. Bini, T. Damour, Analytical determination of the two-body gravitational interaction potential at the 4th post-Newtonian approximation. *Phys. Rev. D* **87**, 121501(R) (2013)

Spin and Quadrupole Contributions to the Motion of Astrophysical Binaries

Jan Steinhoff

Abstract Compact objects in general relativity approximately move along geodesics of spacetime. It is shown that the corrections to geodesic motion due to spin (dipole), quadrupole, and higher multipoles can be modeled by an extension of the point mass action. The quadrupole contributions are discussed in detail for astrophysical objects like neutron stars or black holes. Implications for binaries are analyzed for a small mass ratio situation. There quadrupole effects can encode information about the internal structure of the compact object, e.g., in principle they allow a distinction between black holes and neutron stars, and also different equations of state for the latter. Furthermore, a connection between the relativistic oscillation modes of the object and a dynamical quadrupole evolution is established.

1 Introduction

The problem of motion is among of the most fundamental ones in general relativity. As a part of the present proceedings on “Equations of Motion in Relativistic Gravity” this does probably not require any explanations. The problem is addressed using multipolar approximation schemes, the most prominent are due to Mathisson [1, 2] and Dixon [3], and another one is due to Papapetrou [4]. These particular methods have in common that equations of motion for extended bodies are derived from the conservation of energy-momentum. In the present contribution, the focus lies on theoretical models for compact stars and black holes based on point-particle actions. There equations of motions follow from a variational principle instead of conservation of energy-momentum. These point-particle actions were probably first discussed in general relativity by Westpfahl [5] for the case of a pole-dipole particle and later generalized by Bailey and Israel [6] to generic multipoles.

J. Steinhoff (✉)

Centro Multidisciplinar de Astrofísica (CENTRA), Instituto Superior Técnico (IST),
Avenida Rovisco Pais 1, 1049-001 Lisbon, Portugal

e-mail: jan.steinhoff@ist.utl.pt

URL: <http://jan-steinhoff.de/physics/>

However, without further justification, it is not obvious how a point-particle action relates to an actual extended body. Most important is the effacing principle [7], which indicates that a nonrotating star can be represented by a point mass up to a high order within the post-Newtonian approximation. (More details on the use of point-masses for self-gravitating bodies within this approximation can be found in other contributions to these proceedings, see, e.g., the contribution by G. Schäfer) This suggests that extensions of the point-mass action can serve as models for extended bodies, even in the self-gravitating case. A similar conclusion arises from the framework of effective field theory applied to gravitating compact bodies [8]. Indeed, the effective action belonging to a compact body naturally takes on the form of a point-particle action, which puts previous works on similar actions [5, 6] into a different light. This provides enough motivation for us to further elaborate the action approach of [6] in Sect. 2, where it is combined with useful aspects of more recent literature [9–13]. An application to the post-Newtonian approximation of self-gravitating extended bodies is omitted, because various formalisms exist for it and the aim is to highlight aspects that are independent of (and hopefully useful for) all of them.

It is worth mentioning that the effective field theory framework offers a machinery which can be used, at least in principle, to *compute* the effective point-particle action from a complete microphysical description of the extended body. In practice, however, this procedure is not viable for realistic astrophysical objects and one must be satisfied with a more phenomenological construction of the effective action. This is in fact analogous to other situations in physics. For instance, it is usually admitted that thermodynamic potentials can be derived from a microscopic description. Yet an explicit calculation is often too complicated, or the microscopic description is even unclear. But a phenomenological construction of thermodynamic potentials or equations of state is usually possible. This analogy is further elaborated in Sect. 5. There an adiabatic quadrupole deformation due to spin [14] is discussed. An application to a binary system in the extreme mass ratio case is given. Quadrupole deformation due to an external gravitational fields is discussed in Sects. 4, 5 and 6, both in an adiabatic [15–17] and a dynamical situation [18, 19].

A main critique against point-particles arises from the fact that Dirac delta distributions are ill-defined sources for the nonlinear Einstein equations. But the situation changes once one softens the Dirac delta using regularization techniques. It is then possible to solve the field equations iteratively within some approximation, like the post Newtonian one. If one regards the chosen regularization prescription as a part of the phenomenological model, then point-particles must be accepted as viable sources in general relativity (at least for applications within approximation schemes). This point is further stressed in Sect. 6.4. It is important that a weak field approximation for the point-particle mimics the field of the actual self-gravitating extended body away from the source. (This is precisely the criterion for the phenomenological construction of the effective point-particle source.) Hence, though one applies the effective source to weak field approximations, e.g., to compute predictions for a binary, strong-field effects from the interior of the bodies are taken into account.

The signature of spacetime is taken to be $+2$. Units are such that the speed of light c is equal to one. The gravitational constant is denoted by G . We are going to utilize three different frames, denoted by different indices. Greek indices refer to the coordinate frame, lower case Latin indices from the beginning of the alphabet belong to a local Lorentz frame, and upper case Latin indices from the beginning of the alphabet denote the so called body-fixed Lorentz frame. Round and square brackets are used for index symmetrization and antisymmetrization, respectively, e.g., $A^{(\mu\nu)} \equiv \frac{1}{2}(A^{\mu\nu} + A^{\nu\mu})$. The convention for the Riemann tensor is

$$R^\mu{}_{\nu\alpha\beta} = \Gamma^\mu{}_{\nu\beta,\alpha} - \Gamma^\mu{}_{\nu\alpha,\beta} + \Gamma^\rho{}_{\nu\beta}\Gamma^\mu{}_{\rho\alpha} - \Gamma^\rho{}_{\nu\alpha}\Gamma^\mu{}_{\rho\beta}. \quad (1)$$

2 Point-Particle Actions

Action principles for spinning point particles have a long tradition, see, e.g., [5, 6, 9–13, 20–24]. In this section, the advantages from several of these references are brought together. Our approach is most similar to [6]. Compared to the presentation in [11], a simpler (manifestly covariant) variation technique is applied and the transition to tetrad gravity is discussed at a later stage. This makes the derivation more transparent.

2.1 Manifestly Covariant Variation

Before we start to formulate the action principle, let us introduce a useful notation due to DeWitt [25], see also [12, Appendix A]. One can define a linear operator $G^\nu{}_\mu$ such that the covariant derivative ∇_α and the Lie derivative \mathcal{L}_ξ read

$$\nabla_\alpha := \partial_\alpha + \Gamma^\mu{}_{\nu\alpha} G^\nu{}_\mu, \quad \mathcal{L}_\xi := \xi^\mu \partial_\mu - (\partial_\nu \xi^\mu) G^\nu{}_\mu. \quad (2)$$

For instance, $G^\nu{}_\mu$ operates on a tensor $T_\alpha{}^\beta$ as $G^\nu{}_\mu T_\alpha{}^\beta := -\delta_\alpha^\nu T_\mu{}^\beta + \delta_\mu^\beta T_\alpha{}^\nu$. That is, $G^\nu{}_\mu$ is a linear operator that acts on the spacetime indices of a tensor. Notice that $G^\nu{}_\mu$ does not act on indices of the body-fixed frame. Further, $G^\nu{}_\mu$ obeys a product rule like a differential operator. Similarly, we can construct a covariant differential D and a covariant variation Δ of quantities defined along a worldline z^α by

$$D := d + \Gamma^\mu{}_{\nu\alpha}(dz^\alpha) G^\nu{}_\mu, \quad \Delta := \delta + \Gamma^\mu{}_{\nu\alpha}(\delta z^\alpha) G^\nu{}_\mu. \quad (3)$$

For scalars the contributions from the connection vanish. Notice that a variation of the worldline δz^α is not manifestly covariant if the component values of tensors defined on the worldline are held fixed. The variation Δ instead parallel transports to the varied worldline. When it is applied to a tensor *field* taken at the worldline,

e.g., $T_\alpha^\beta(z)$, then the variation δ splits into a part due to the shift of the worldline δz^ρ and a part coming from the variation of the field itself. Let us denote the latter part by $\delta_z T_\alpha^\beta := (\delta T_\alpha^\beta)(z)$, so we have

$$\delta \equiv \delta_z + (\delta z^\rho) \partial_\rho, \quad \Delta \equiv \delta_z + (\delta z^\alpha) \nabla_\alpha, \quad (\text{for fields}). \quad (4)$$

For instance, the metric compatibility of ∇_α then leads to

$$\Delta g_{\mu\nu} = \delta_z g_{\mu\nu}. \quad (5)$$

2.2 Action Principle

We envisage an action principle localized on a worldline $z^\rho(\lambda)$. Here λ is an arbitrary parameter, not necessarily identical to the proper time τ . (Let us require that the action is invariant under reparametrizations of the worldline.) We further assume that the action is varied with respect to a “body-fixed” frame defined by Lorentz-orthonormal basis vectors $\Lambda_A^\mu(\lambda)$ labeled by A ,

$$\Lambda_A^\mu \Lambda_B^\nu g_{\mu\nu} \equiv \eta_{AB}, \quad \Lambda_A^\mu \Lambda_B^\nu \eta^{AB} \equiv g^{\mu\nu}. \quad (6)$$

Now, stars are in general differentially rotating and it is difficult to interpret a body-fixed frame. Such a frame is thus rather an abstract element of our theoretical model, inspired by the Newtonian theory of rigid bodies (see, e.g., [11, Sect. 3.1.1]).

The constraint (6) implies that Λ_A^μ and $g_{\mu\nu}$ are in general not independent and one should take special care when both are varied at the same time. In order to address this problem, we split the variation $\Delta \Lambda_A^\nu$ as

$$\Lambda^{A\mu} \Delta \Lambda_A^\nu = \Lambda^{A[\mu} \Delta \Lambda_A^{\nu]} + \frac{1}{2} \Delta (\Lambda^{A\mu} \Lambda_A^\nu) = \Delta \Theta^{\mu\nu} - \frac{1}{2} g^{\mu\alpha} g^{\nu\beta} \delta_z g_{\alpha\beta}. \quad (7)$$

where we used $\delta g^{\mu\nu} = -g^{\mu\alpha} g^{\nu\beta} \delta g_{\alpha\beta}$ and (5). In the last step, we also introduced the abbreviation

$$\Delta \Theta^{\mu\nu} := \Lambda^{A[\mu} \Delta \Lambda_A^{\nu]}, \quad (8)$$

which is similar to the antisymmetric variation symbol used in [22], see also [13, Eq. (2.7)]. The independence of $\Delta \Theta^{\mu\nu}$ from the metric variation $\delta_z g_{\alpha\beta}$ will be made more manifest in Sect. 2.4. For now let us just appeal to the fact that the 6 degrees of freedom of the antisymmetric symbol $\Delta \Theta^{\mu\nu}$ exactly matches the degrees of freedom of a Lorentz frame (3 boosts and 3 rotations). Thus $\Delta \Theta^{\mu\nu}$ corresponds to the independent variation of the body-fixed Lorentz frame.

Let us consider an action that is as generic as possible,

$$W = W_F + W_M, \quad W_F[g_{\mu\nu}, \dots] = \frac{1}{16\pi G} \int d^4x \sqrt{-g} R + \dots, \quad (9)$$

$$W_M[g_{\mu\nu}, z^\rho, \Lambda_A^\mu, \dots] = \int d\lambda L_M(g_{\mu\nu}, u^\mu, \Lambda_A^\mu, \Omega^{\mu\nu}, \phi_I), \quad (10)$$

Here ϕ_I collectively denotes other dependencies of the Lagrangian L_M and the dots denote other fields, like the electromagnetic one. (In this section I is a multi-index that may comprise any sort of spacetime, Lorentz, or label indices.) Notice that fields like $g_{\mu\nu}$ are taken at the worldline position z^ρ in W_M . The 4-velocity u^μ and the angular velocity $\Omega^{\mu\nu}$ are defined by

$$u^\mu := \frac{dz^\mu}{d\lambda}, \quad \Omega^{\mu\nu} := \Lambda^{A\mu} \frac{D\Lambda_A^\nu}{d\lambda}, \quad (11)$$

Notice that $\Omega^{\mu\nu}$ is antisymmetric due to (6) and $Dg_{\mu\nu}/d\lambda = 0$.

2.3 Variation

For the sake of deriving equations of motion, we may assume $\delta\lambda = 0$. Then the variation can be commuted with ordinary or partial λ -derivatives. Furthermore, the Lagrangian L_M is a scalar and we can make use of $\delta L_M \equiv \Delta L_M$ to write its variation in a manifestly covariant manner,

$$\delta L_M = p_\mu \Delta u^\mu + \frac{1}{2} S_{\mu\nu} \Delta \Omega^{\mu\nu} + \frac{\partial L_M}{\partial \Lambda_A^\mu} \Delta \Lambda_A^\mu + \frac{\partial L_M}{\partial g_{\mu\nu}} \Delta g_{\mu\nu} + \frac{\partial L_M}{\partial \phi_I} \Delta \phi_I, \quad (12)$$

where we have defined the linear momentum p_μ and spin $S_{\mu\nu} = -S_{\nu\mu}$ as generalized momenta belonging to the velocities u^μ and $\Omega^{\mu\nu}$,

$$p_\mu := \frac{\partial L_M}{\partial u^\mu}, \quad S_{\mu\nu} := 2 \frac{\partial L_M}{\partial \Omega^{\mu\nu}}. \quad (13)$$

It should be noted that (12) can be checked using a usual variation δ together with the identity (21), but here it is a simple consequence of the chain rule for Δ . Obviously this method nicely organizes the Christoffel symbols.

The 5 individual terms in (12) are transformed as follows:

- The 1st term of (12) is evaluated with the help of

$$\Delta u^\mu \equiv \delta u^\mu + \Gamma^\mu_{\alpha\beta} u^\alpha \delta z^\beta = \frac{D\delta z^\mu}{d\lambda}. \quad (14)$$

- The 2nd term of (12) requires the most work. In order to evaluate $\Delta\Omega^{\mu\nu}$, we need to commute Δ with the covariant differential D contained in $\Omega^{\mu\nu}$, Eq. (11). The definitions in (3) lead to

$$[\Delta, D] = [(\delta_z \Gamma^\mu_{\nu\alpha}) - (\delta z^\beta) R^\mu_{\nu\alpha\beta}](dz^\alpha) G^\nu_\mu. \quad (15)$$

Notice the analogy to the commutator of covariant derivatives, which also gives rise to curvature. It is useful to derive intermediate commutators first, for instance

$$[G^\nu_\mu, G^\beta_\alpha] = \delta^\beta_\mu G^\nu_\alpha - \delta^\nu_\alpha G^\beta_\mu. \quad (16)$$

Next, we express $\delta_z \Gamma^\mu_{\nu\alpha}$ in (15) with the help of

$$\delta \Gamma^\nu_{\beta\alpha} = \frac{1}{2} g^{\nu\rho} [\nabla_\beta \delta g_{\alpha\rho} + \nabla_\alpha \delta g_{\beta\rho} - \nabla_\rho \delta g_{\alpha\beta}]. \quad (17)$$

Now it is straightforward to evaluate $\Delta\Omega^{\mu\nu}$. In the result, we replace $\Delta\Lambda_A^\mu$ using (7), make use of

$$\frac{D\delta_z g_{\rho\sigma}}{d\lambda} = u^\alpha (\nabla_\alpha \delta g_{\rho\sigma})(z), \quad (18)$$

and finally arrive at

$$\begin{aligned} \Delta\Omega^{\mu\nu} &= \frac{D(\Delta\Theta^{\mu\nu})}{d\lambda} + 2\Omega_\alpha^{[\mu} \Delta\Theta^{\nu]\alpha} + R^{\mu\nu}_{\alpha\beta} u^\alpha \delta z^\beta \\ &\quad + \Omega^{\alpha[\mu} g^{\nu]\beta} \delta_z g_{\alpha\beta} + g^{\beta[\mu} g^{\nu]\rho} u^\alpha (\nabla_\beta \delta g_{\rho\alpha})(z). \end{aligned} \quad (19)$$

- Before proceeding to the 3rd term of (12), let us recall the transformation property of a tensor under an infinitesimal coordinate transformation $x^{\mu'} = x^\mu - \xi^\mu$,

$$\phi_{I'} - \phi_I = -(\partial_\nu \xi^\mu) G^\nu_\mu \phi_I, \quad \text{e.g.,} \quad u^{\mu'} - u^\mu = -u^\nu \partial_\nu \xi^\mu. \quad (20)$$

The Lagrangian is a scalar and thus invariant, but it depends on tensors which transform. As $\partial_\nu \xi^\mu$ is quite arbitrary, the invariance of the Lagrangian L_M leads to the identity

$$p_{\mu} u^\nu + S_{\mu\alpha} \Omega^{\nu\alpha} + \frac{\partial L_M}{\partial \Lambda_A^\mu} \Lambda_A^\nu - 2 \frac{\partial L_M}{\partial g_{\nu\alpha}} g_{\mu\alpha} + \frac{\partial L_M}{\partial \phi_I} G^\nu_\mu \phi_I \equiv 0. \quad (21)$$

We eliminate the partial derivative of L_M with respect to Λ_A^μ using this relation and we replace $\Delta\Lambda_A^\mu$ using (7) to arrive at

$$\begin{aligned} \frac{\partial L_M}{\partial \Lambda^{A\mu}} \Delta \Lambda^{A\mu} = & \frac{1}{2} \left[p^\mu u^\nu - S_{\alpha}{}^\mu \Omega^{\nu\alpha} + (G^{\mu\nu} \phi_I) \frac{\partial L_M}{\partial \phi_I} - 2 \frac{\partial L_M}{\partial g_{\mu\nu}} \right] \delta_z g_{\mu\nu} \\ & + \left[p_\mu u_\nu - S_{\alpha\mu} \Omega_\nu{}^\alpha - (G_{\mu\nu} \phi_I) \frac{\partial L_M}{\partial \phi_I} \right] \Delta \Theta^{\mu\nu}. \end{aligned} \quad (22)$$

- In the 4th term of (12) we use (5).
- The 5th term of (12) is not touched for now, as this requires a specialization of ϕ_I . This is discussed in the Sect. 3.1.

All these transformations are now applied to (12). Furthermore, we insert a unity in the form of

$$1 \equiv \int d^4x \delta_{(4)}, \quad \delta_{(4)} := \delta(x^\mu - z^\mu), \quad (23)$$

into the terms containing field variations of type δ_z . This allows one to rewrite these variations at the spacetime point x^μ and perform partial integrations. Notice that $\delta_{(4)}$ has compact support for finite λ -intervals, so these partial integrations do not require assumptions on field variations at the spatial boundary. Finally, (12) turns into

$$\begin{aligned} \delta L_M = & \int d^4x \left[p^\mu u^\nu \delta_{(4)} + (G^{\mu\nu} \phi_I) \frac{\partial L_M}{\partial \phi_I} \delta_{(4)} - \nabla_\alpha (S^{\alpha\mu} u^\nu \delta_{(4)}) \right] \frac{\delta g_{\mu\nu}(x)}{2} \\ & + \frac{\partial L_M}{\partial \phi_I} \Delta \phi_I + \left[p_\mu u_\nu - (G_{\mu\nu} \phi_I) \frac{\partial L_M}{\partial \phi_I} - \frac{1}{2} \frac{D S_{\mu\nu}}{d\lambda} \right] \Delta \Theta^{\mu\nu} \\ & + \left[\frac{1}{2} S_{\alpha\beta} R^{\alpha\beta}{}_{\rho\mu} u^\rho - \frac{D p_\mu}{d\lambda} \right] \delta z^\mu + \frac{d}{d\lambda} \left[p_\mu \delta z^\mu + \frac{1}{2} S_{\mu\nu} \Delta \Theta^{\mu\nu} \right]. \end{aligned} \quad (24)$$

Notice that the covariant and ordinary derivatives with respect to λ are identical for the last term.

2.4 Metric Versus Tetrad Gravity

The separation of metric and body-fixed-frame variations by means of (7) is an elegant trick to derive equations of motion. However, if further calculations at the level of the action are performed, one often needs an explicit split between gravitational and body-fixed-frame degrees of freedom. This can be achieved by introducing a tetrad gravitational field $e_a{}^\mu(x)$, that is, a field of Lorentz-orthonormal basis vectors labeled by a and defined at every spacetime point x^ρ ,

$$e_a{}^\mu e_b{}^\nu g_{\mu\nu} \equiv \eta_{ab}, \quad e_a{}^\mu e_b{}^\nu \eta^{ab} \equiv g^{\mu\nu}. \quad (25)$$

Tetrad gravity replaces the metric by virtue of the latter relation and regards e_a^μ as the fundamental gravitational field in the variation principle. This allows us to split Λ_A^μ as

$$\Lambda_A^\mu = \Lambda_A^a e_a^\mu(z), \quad (26)$$

where Λ_A^a is now just a usual (flat-spacetime) Lorentz matrix

$$\Lambda_A^a \Lambda_B^b \eta_{ab} \equiv \eta_{AB}, \quad \Lambda_A^a \Lambda_B^b \eta^{AB} \equiv \eta^{ab}. \quad (27)$$

Thus Λ_A^a is independent of the gravitational field e_a^μ and the announced manifest split is indeed given by (26).

Based on this split, we can understand the meaning of $\Delta\Theta^{\mu\nu}$ in more detail. As Λ_A^a is a usual Lorentz matrix, we can follow Ref. [22] and describe its independent variations by an antisymmetric symbol $\delta\theta^{ab} := \Lambda^{Aa} \delta\Lambda_A^b$. Then $\Delta\Theta^{\mu\nu}$ reads explicitly

$$\Delta\Theta^{\mu\nu} = e_a^\mu e_b^\nu \delta\theta^{ab} + \left(\Gamma^{[\nu\mu]}_\alpha + e^{a[\mu} \partial_\alpha e_a^{\nu]} \right) \delta z^\alpha + e^{a[\mu} \delta z_\alpha e_a^{\nu]}. \quad (28)$$

One can be even more explicit and write $\delta\theta^{ab}$ as a linear combination of six independent variations of angle variables parameterizing Λ^{Aa} , see [22, Sect. 3.A]. Anyway, $\Delta\Theta^{\mu\nu}$ is in fact a linear combination of the independent frame variations $\delta\theta^{ab}$ with other variations. Now, it is legitimate to regard $\Delta\Theta^{\mu\nu}$, δz^α , and δe_a^μ as independent variations instead of $\delta\theta^{ab}$, δz^α , and δe_a^μ . This just corresponds to a linear recombining of the equations of motion following from the variation. Equation (28) shows that this recombination manifestly removes noncovariant terms related to the δz^α -variation and an antisymmetric part of the energy-momentum tensor due to $e^{a[\mu} \delta z_\alpha e_a^{\nu]}$ (the symmetric part arises from $e^{a(\mu} \delta e_a^{\nu)} = \frac{1}{2} \delta g^{\mu\nu}$ as usual). All of this is important for the next section, where equations of motion are deduced from (24).

In the next step it is possible to return to metric gravity by a partial gauge fixing of the tetrad. For instance, a possible gauge condition is to require that the matrix $(e_{a\mu})$ is symmetric (in spite of the different nature of its indices). Then e_a^μ is given by the matrix square-root of the metric. This gauge choice leads to the same conclusions as in [9, Sect. IV.B], where a more direct construction was followed. In the end, the partially gauge-fixed tetrad is a function of the metric, so we have obtained a metric gravity theory. It might look like the introduction of a tetrad field accompanied by an enlarged gauge group of gravity is just extra baggage. However, more gauge freedom is important for applications, as gauges can and should be adopted to the problem at hand. For instance, for an ADM-like canonical formulation of spinning particles, it is a wise choice to adopt the Schwinger time-gauge for the tetrad [10]. Further, some subtle aspects of the consistency of the theory can be analyzed more easily within tetrad gravity (e.g., the algebra of gravitational constraints, because after reduction to metric gravity the gravitational field momentum receives complicated corrections [10]). Spinning particles should always be coupled to tetrad gravity in the first place.

3 Equations of Motion

In order to draw conclusions from (24), one must further specialize the so far arbitrary ϕ_I . The assumptions we are going to introduce in the following are not the least restrictive, but already allow important insights on the structure of the equations of motion.

3.1 Further Assumptions

Let us assume from now on that the ϕ_I can be split into two groups. We denote by ϕ_I^{field} the part that contains spacetime fields (functions of x), so its variation $\Delta\phi_I^{\text{field}}$ can be evaluated using (4). The second group ϕ_I^{wl} contains variables defined on the worldline only (functions of λ) and its first order derivatives $\dot{\phi}_I^{\text{wl}}$, where $\dot{} := D/d\lambda$. Most importantly, we assume that the $\delta\phi_I^{\text{wl}}$ correspond to independent variational degrees of freedom, like Lagrange multipliers or the dynamical multipoles introduced in Sect. 6. Without loss of generality, one can then assume that the ϕ_I^{wl} carry indices of the body-fixed frame instead of spacetime indices, so that $G^\nu{}_\mu \phi_I^{\text{wl}} = 0$.

Notice that our assumptions do not allow time (i.e., λ) derivatives of u^μ and $\Omega^{\mu\nu}$ as part of the ϕ_I^{wl} . If such accelerations would appear in subleading contributions of the Lagrangian (within some approximation scheme), then one can often remove them by a redefinition of variables [26]. Further, acceleration-dependent Lagrangians are often problematic due to Ostrogradsky instability. For these reasons, we also assumed that at most first-order time derivatives of the ϕ_I^{wl} appear in L_M . However, our assumptions here are not entirely exhaustive. For instance, a concrete situation for which our assumptions should be relaxed in the future is discussed at the end of Sect. 5.1.

3.2 Equations of Motion for Linear Momentum and Spin

With these assumptions, we have

$$\begin{aligned} \frac{\partial L_M}{\partial \phi_I} \Delta\phi_I &= \frac{\partial L_M}{\partial \phi_I^{\text{field}}} \left[\delta_z \phi_I^{\text{field}} + (\delta z^\alpha) \nabla_\alpha \phi_I^{\text{field}} \right] \\ &+ \left[\frac{\partial L_M}{\partial \phi_I^{\text{wl}}} - \frac{d\psi_{\text{wl}}^I}{d\lambda} \right] \delta\phi_I^{\text{wl}} + \frac{d}{d\lambda} \left[\psi_{\text{wl}}^I \delta\phi_I^{\text{wl}} \right], \end{aligned} \quad (29)$$

where we used that the worldline variables do not carry spacetime indices and we introduced their canonical generalized momenta,

$$\psi_{\text{wl}}^I := \frac{\partial L_M}{\partial \dot{\phi}_I^{\text{wl}}}. \quad (30)$$

The second line leads to the usual Euler-Lagrange equations for the worldline degrees of freedom ϕ_I^{wl} , which are discussed in Sect. 6.4. Let us focus on the other terms for now. Using the arbitrariness and independence of δz^μ and $\Delta\Theta^{\mu\nu}$, we can read off the equations of motion for the linear momentum and the spin from (24) and (29),

$$\frac{Dp_\mu}{d\lambda} = \frac{1}{2}S_{\alpha\beta}R^{\alpha\beta}{}_{\rho\mu}u^\rho + (\nabla_\mu\phi_I^{\text{field}})\frac{\partial L_M}{\partial\phi_I^{\text{field}}}, \quad (31)$$

$$\frac{DS_{\mu\nu}}{d\lambda} = 2p_{[\mu}u_{\nu]} - 2(G_{[\mu\nu]}\phi_I^{\text{field}})\frac{\partial L_M}{\partial\phi_I^{\text{field}}}. \quad (32)$$

The total λ -derivative in the last line of (24) was ignored here. (Here we assume that the variation vanishes at the end points of the worldline). The energy-momentum tensor density $\sqrt{-g}T^{ab}$ is simply given by the coefficient in front of $\delta g_{\mu\nu}/2$ in (24). However, an explicit determination requires yet another specialization of ϕ_I^{field} , because the fields can dependent on the metric. In the absence of ϕ_I^{field} , one immediately recovers the result of Tulczyjew [27].

3.3 Quadrupole

Let us now explore the case that $\phi_I^{\text{field}} = \{R_{\mu\nu\alpha\beta}\}$. It is useful to introduce an abbreviation for the corresponding partial derivative of the Lagrangian,

$$J^{\mu\nu\alpha\beta} := -6\frac{\partial L_M}{\partial R_{\mu\nu\alpha\beta}}. \quad (33)$$

The conventional factor of -6 is motivated by comparing (31), now reading

$$\frac{Dp_\mu}{d\lambda} = \frac{1}{2}S_{\alpha\beta}R^{\alpha\beta}{}_{\rho\mu}u^\rho - \frac{1}{6}\nabla_\mu R_{\nu\rho\beta\alpha}J^{\nu\rho\beta\alpha}, \quad (34)$$

with the corresponding result of Dixon at the quadrupolar approximation level. An identification of $J^{\mu\nu\alpha\beta}$ with Dixon's reduced quadrupole moment is tempting, as this makes (34) formally identical to Dixon's result. It is important that $J^{\mu\nu\alpha\beta}$ inherits the symmetries of the Riemann tensor. From these symmetries and the properties of the operator $G^\mu{}_\nu$, we obtain

$$J^{\sigma\rho\alpha\beta}G^\mu{}_\nu R_{\sigma\rho\alpha\beta} = -4J^{\sigma\rho\alpha\beta}\delta^\mu_\sigma R_{\nu\rho\alpha\beta} = -4J^{\mu\rho\alpha\beta}R_{\nu\rho\alpha\beta}. \quad (35)$$

This simplifies (32) to

$$\frac{DS_{\mu\nu}}{d\lambda} = 2p_{[\mu}u_{\nu]} + \frac{4}{3}R_{\alpha\beta\rho[\mu}J_{\nu]}{}^{\rho\beta\alpha}, \quad (36)$$

and formally agrees with Dixon's spin equation of motion, too. Finally, the energy-momentum tensor agrees with the explicit result in [28] (in the present conventions, see (5.3) in [11]). This derives from

$$\delta R^\mu{}_{\nu\alpha\beta} = \nabla_\alpha \delta \Gamma^\mu{}_{\nu\beta} - \nabla_\beta \delta \Gamma^\mu{}_{\nu\alpha}, \quad (37)$$

which must be further expanded using (17) and then leads to

$$\frac{\partial L_M}{\partial R_{\mu\nu\alpha\beta}} \delta_z R_{\mu\nu\alpha\beta} = \int d^4x \left[-\frac{1}{3} J^{\mu\rho\alpha\beta} R^\nu{}_{\rho\alpha\beta} \delta_{(4)} - \frac{2}{3} \nabla_\beta \nabla_\alpha (J^{\mu\alpha\beta\nu} \delta_{(4)}) \right] \frac{\delta g_{\mu\nu}}{2}. \quad (38)$$

This is the contribution coming from the first term in (29). Another contribution arises from the second term in the first row of (24), which is evaluated using (35). Collecting all terms in front of $\delta g_{\mu\nu}$ in (24), we can read off the energy momentum tensor density as

$$\begin{aligned} \sqrt{-g} T^{\mu\nu} = \int d\lambda \bigg[& u^{(\mu} p^{\nu)} \delta_{(4)} - \nabla_\alpha (S^{\alpha(\mu} u^{\nu)} \delta_{(4)}) \\ & + \frac{1}{3} R_{\beta\alpha\rho}{}^{(\mu} J^{\nu)\rho\alpha\beta} \delta_{(4)} - \frac{2}{3} \nabla_\beta \nabla_\alpha (J^{\mu(\alpha\beta)\nu} \delta_{(4)}) \bigg]. \end{aligned} \quad (39)$$

3.4 Other Multipoles

Dixon's moments are essentially defined as integrals over the energy-momentum tensor of the extended body. Though these definitions can be applied to self-gravitating bodies, the derivation of the equations of motions based on these definitions only succeeds for test-bodies [3]. It was shown in [29] (see also the corresponding contribution by A. Harte in these proceedings) using methods for self-force calculations that for self-gravitating objects the equations of motions are still of the same form, but the multipole moments must be renormalized. The multipoles arising from the effective action should therefore be related to these renormalized moments. For self-gravitating bodies, one can not in general calculate the moments in the equations of motion using Dixon's integral formulas any more. In the language of effective field theory, the multipoles are calculated through a "matching" procedure instead, which will be explained in Sect. 5.

Other gravitational multipoles can be incorporated by including symmetrized covariant derivatives of the curvature in ϕ_I^{field} . Similarly, electromagnetic multipoles arise from an analogous construction based on the Faraday tensor $F_{\mu\nu}$. A quite exhaustive case is therefore

$$\phi_I^{\text{field}} = \{R_{\mu\nu\alpha\beta}, \nabla_\rho R_{\mu\nu\alpha\beta}, \nabla_{(\sigma} \nabla_{\rho)} R_{\mu\nu\alpha\beta}, \dots, F_{\mu\nu}, \nabla_{(\rho} F_{\mu)\nu}, \nabla_{(\sigma} \nabla_{\rho)} F_{\mu)\nu}, \dots\}. \quad (40)$$

Notice that the commutation of covariant derivatives results in curvature terms and that, e.g., $3\nabla_\alpha F_{\mu\nu} = 2\nabla_{(\alpha} F_{\mu)\nu} - 2\nabla_{(\alpha} F_{\nu)\mu}$, which can be checked using $\nabla_{[\alpha} F_{\mu\nu]} = 0$. Again the partial derivatives of L_M with respect to the ϕ_I^{field} can be called multipole moments. However, these multipoles and also p_μ are probably not unique, because L_M is not unique. For instance, contractions of covariant derivatives with u^μ can be written as λ -derivatives and one can partially integrate them. Notice that Dixon's multipole moments have the same symmetries as ours, but satisfy additional orthogonality relations to a timelike vector defined on the worldline.

It is also possible to include a term proportional to $A_\mu u^\mu$ in the Lagrangian, as this combination transforms into a total λ -derivative under a gauge transformation of the electromagnetic potential A_μ . It just leads to the well-known Lorentz force. However, in the present approach a part of the Lorentz force is hidden in the definition of p_μ , making the equations of motion not manifestly gauge-invariant.

4 Symmetries, Transformations, and Conditions

In this section we discuss symmetries, conservation laws, various transformations of the action, and conditions it must fulfill.

4.1 Symmetries and Conserved Quantities

Action principles have the advantage that one can easily derive conserved quantities from the Noether theorem [30]. Here we are going to consider only symmetry transformations where the fields are not transformed. Further, we assume $\delta\lambda = 0$, so the variational formula (24) together with (29) is still valid.

On the one hand, we require that the Lagrangian transforms under such a symmetry into a total derivative

$$\delta L_M = \frac{dK}{d\lambda}, \quad (41)$$

without making use of the equations of motion. On the other hand, if we assume that the equations of motion hold, then only the total time derivatives from (24) with (29) inserted contribute to δL_M . These total derivatives are located in the last lines of (24) and (29). (The first lines of (24) and (29) vanish because fields are not transformed here.) We therefore have the conservation law

$$\frac{d}{d\lambda} \left[p_\mu \delta z^\mu + \frac{1}{2} S_{\mu\nu} \Delta \Theta^{\mu\nu} + \psi_{\text{wl}}^I \delta \phi_I^{\text{wl}} - K \right] = 0. \quad (42)$$

A simple example is given by the global symmetry under a change of the body-fixed frame. In order to make things even more simple, we assume that L_M does not

depend on Λ_A^μ and on the $\dot{\phi}_I^{\text{wl}}$, so that $\psi_{\text{wl}}^I = 0$. But L_M still implicitly depends on Λ_A^μ through $\Omega^{\mu\nu}$. A constant infinitesimal Lorentz transformation of the body-fixed frame then reads

$$\delta z^a = 0, \quad \delta \Lambda^{AB} = \omega^{AB} \Lambda_B^\mu, \quad (43)$$

where ω^{AB} is a constant infinitesimal antisymmetric matrix. Obviously $\Omega^{\mu\nu}$ is invariant under this transformation, so (41) is fulfilled with $K = 0$. Further, we have $\Delta \Theta^{ab} = \Lambda_A^a \Lambda_B^b \omega^{AB}$ and (42) reads

$$\frac{1}{2} \omega^{AB} \frac{d}{d\lambda} \left[S_{\mu\nu} \Lambda_A^\mu \Lambda_B^\nu \right] = 0. \quad (44)$$

As ω^{AB} is arbitrary, we see that the components of the spin in the body-fixed frame $S_{AB} \equiv S_{\mu\nu} \Lambda_A^\mu \Lambda_B^\nu$ are constant. A corollary of this fact is that the spin length S is constant, where $2S^2 = S_{AB} S^{AB} = S_{\mu\nu} S^{\mu\nu}$.

The next important example is a symmetry of the spacetime described by a Killing vector field ξ^μ , $\mathcal{L}_\xi g_{\mu\nu} = 0$. (Notice that also $\mathcal{L}_\xi R_{abcd} = 0$ etc.) Other fields entering L_M are assumed to be invariant under this symmetry, too, e.g., $\mathcal{L}_\xi F_{\mu\nu} = 0$. We consider an infinitesimal shift of the worldline coordinate

$$\delta z^\mu = \epsilon \xi^\mu, \quad \Delta \Lambda_A^\nu = -\epsilon \mathcal{L}_\xi \Lambda_A^\nu = \epsilon \Lambda_A^\mu \nabla_\mu \xi^\nu, \quad \delta \phi_I^{\text{wl}} = 0, \quad (45)$$

where ϵ is an infinitesimal constant and we assume parallel transport of Λ_A^μ along ξ^ν , i.e., $\xi^\nu \nabla_\nu \Lambda_A^\mu = 0$. Notice that the fields are not transformed, but their symmetry along ξ^μ is important. Recall that $-\epsilon \mathcal{L}_\xi$ generates an infinitesimal coordinate transformation. Therefore, L_M is invariant under this transformation if all the variables it depends on, including the fields, would be transformed by $-\epsilon \mathcal{L}_\xi$. But the shift (45) only applies to z^μ , Λ_A^μ , and ϕ_I^{wl} , so the result of (45) on L_M is exactly opposite to the case when all variables *except* z^μ , Λ_A^μ , and ϕ_I^{wl} are transformed. These variables are all the fields, so the δL_M produced by (45) can be obtained by transforming all the fields using $+\epsilon \mathcal{L}_\xi$. But the fields were assumed to be invariant under this transformation. Hence we have argued that (45) is a symmetry of the action, $\delta L_M = 0$, and $K = 0$. Combining (42) and (45), we find the conserved quantity

$$E_\xi := p_\mu \xi^\mu + \frac{1}{2} S^{\mu\nu} \nabla_\mu \xi_\nu = \text{const}, \quad (46)$$

where $\Delta \Theta^{\mu\nu} = \epsilon \nabla^{[\mu} \xi^{\nu]}$ was used. It is interesting that this covers to all multipole orders. This was also shown in [31, p. 210] based on the equations of motion.

A special kind of conserved quantities that is not covered by the Noether theorem here are mass-like quantities. We will see later on that masses enter the action as parameters and are therefore constant by assumption.

4.2 Legendre Transformations

Before proceeding, it is worth to point out that of course not every conceivable Lagrangian L_M is acceptable. Some choices are mathematically inconsistent or physically unacceptable for other reasons. Some Lagrangians L_M are technically more difficult to handle and it makes sense to assume simplifying conditions for L_M for a first study. One such assumption we make here is that the relation between spin and angular velocity is a bijection. Notice that this relation is fixed by L_M through our definition of $S_{\mu\nu}$ in (13). A violation of our assumption can have the interesting implication that the spin supplementary condition follows from (13), see [22], but we will not consider this scenario here. The supplementary conditions are discussed in the next section.

With this assumption on the relation between spin and angular velocity, we can solve for $\Omega^{\mu\nu}$ in terms of $S^{\mu\nu}$ (and probably other variables). This allows a Legendre transformation in $\Omega^{\mu\nu}$, i.e.,

$$W_M[e_a^\mu, z^\rho, \Lambda_A^\mu, S_{\mu\nu}, \dots] = \int d\lambda \left[\frac{1}{2} S_{\mu\nu} \Omega^{\mu\nu} + R_M(g_{\mu\nu}, u^\mu, \Lambda_A^\mu, S_{\mu\nu}, \phi_I) \right]. \quad (47)$$

It is important that the spin is varied independently now. Notice that this notion of Legendre transformation is unusual in mechanics, as $\Omega^{\mu\nu}$ is not a time derivative, but a combination of time derivatives. Still Legendre transformations are applicable in much more generic situations, which is heavily used, i.e., in thermodynamics. The function R_M establishes the connection to Routhian approaches [32–34]. The Routhian is a mixture of a Hamiltonian and a Lagrangian. Here it is essentially the sum of R_M and the connection part in $\frac{1}{2} S_{\mu\nu} \Omega^{\mu\nu}$. Notice that therefore the Routhian is not manifestly covariant and covariance only becomes apparent at the level of the equations of motion. In contrast, in our construction R_M is manifestly covariant.

A consequence of reparametrization invariance is that L_M must be a homogeneous function of degree one in all (first-order) λ -derivatives. For our assumptions in Sect. 3.1 this applies only to u^μ , $\Omega^{\mu\nu}$, and $\dot{\phi}_I^{\text{wl}}$, so Euler's theorem on homogeneous functions reads

$$L_M = \frac{\partial L_M}{\partial u^\mu} u^\mu + \frac{\partial L_M}{\partial \Omega^{\mu\nu}} \Omega^{\mu\nu} + \frac{\partial L_M}{\partial \dot{\phi}_I^{\text{wl}}} \dot{\phi}_I^{\text{wl}} = p_\mu u^\mu + \frac{1}{2} S_{\mu\nu} \Omega^{\mu\nu} + \psi_{\text{wl}}^I \dot{\phi}_I^{\text{wl}}. \quad (48)$$

This is a consequence of reparametrization-gauge invariance, so in this sense it is analogous to (21), which follows from coordinate-gauge invariance. Let us proceed with a Legendre transformation in u^μ . This is more subtle, as the relation between u^μ and p_μ can not be a bijection. To see this, first notice that (48) can be interpreted as a constraint on the component $p_\mu u^\mu$ of p_μ . This can be formulated as the famous mass-shell constraint

$$p_\mu p^\mu + \mathcal{M}^2 = 0, \quad (49)$$

where \mathcal{M} is called dynamical mass and usually depends on the dynamical variables. Thus the momentum only has three independent components. On the other hand, u^μ has four independent components: three physical and one gauge degree of freedom due to reparametrization invariance in λ . (If we would choose λ to be the proper time, then just 3 components are independent. But the constraint $u^\mu u_\mu = -1$ makes the variational principle more subtle.) That is, the constraint (49) produces a mismatch in degrees of freedom between u^μ and p_μ , so they can not be connected by a bijection. However, the Legendre transformation can in fact be generalized to the case where constraints appear. One can perform the Legendre transformation “as usual” if all constraints are added to the action using Lagrange multipliers [35, 36]. Here we need one Lagrange multiplier α for (49), which together with the three independent components of p_μ provides a total of four independent variables. This exactly matches the four independent degrees of freedom of u^μ . The Lagrange multiplier α isolates the reparametrization-gauge degree of freedom, while p_μ represents the physical degrees of freedom. Again we require L_M to be such that no pathologies for this “constraint” Legendre transformation arise.

Finally, the result of the transformation is

$$\begin{aligned} W_M \left[e_a^\mu, z^\rho, p_\mu, \alpha, S_{\mu\nu}, \Lambda_A^\mu, \phi_I^{\text{wl}}, \psi_I^I, \dots \right] \\ = \int d\lambda \left[p_\mu u^\mu + \frac{1}{2} S_{\mu\nu} \Omega^{\mu\nu} + \psi_I^I \dot{\phi}_I^{\text{wl}} - \frac{\alpha}{2} (p_\mu p^\mu + \mathcal{M}^2) \right], \end{aligned} \quad (50)$$

where

$$\mathcal{M} = \mathcal{M} \left(g_{\mu\nu}, p_\mu, \Lambda_A^\mu, S_{\mu\nu}, \phi_I^{\text{wl}}, \psi_I^I, \phi_I^{\text{field}} \right). \quad (51)$$

We assume that we can also Legendre transform in the $\dot{\phi}_I^{\text{wl}}$ without giving rise to further constraints or pathologies. From the variations of p_μ , $S_{\mu\nu}$, and ψ_I^I , we obtain

$$u^\mu = \alpha p^\mu + \frac{\alpha}{2} \frac{\partial \mathcal{M}^2}{\partial p_\mu}, \quad \Omega^{\mu\nu} = \alpha \frac{\partial \mathcal{M}^2}{\partial S_{\mu\nu}}, \quad \dot{\phi}_I^{\text{wl}} = \frac{\alpha}{2} \frac{\partial \mathcal{M}^2}{\partial \psi_I^I}. \quad (52)$$

These are just the inverses to variable transformations used in the Legendre transformations. Because we did not touch the variables $g_{\mu\nu}$, ϕ_I^{wl} , Λ_A^μ and ϕ_I^{field} , it is clear that

$$\frac{\partial L_M}{\partial g_{\mu\nu}} \equiv -\frac{\alpha}{2} \frac{\partial \mathcal{M}^2}{\partial g_{\mu\nu}}, \quad \frac{\partial L_M}{\partial \Lambda_A^\mu} \equiv -\frac{\alpha}{2} \frac{\partial \mathcal{M}^2}{\partial \Lambda_A^\mu}, \quad (53)$$

$$\frac{\partial L_M}{\partial \phi_I^{\text{wl}}} \equiv -\frac{\alpha}{2} \frac{\partial \mathcal{M}^2}{\partial \phi_I^{\text{wl}}}, \quad \frac{\partial L_M}{\partial \phi_I^{\text{field}}} \equiv -\frac{\alpha}{2} \frac{\partial \mathcal{M}^2}{\partial \phi_I^{\text{field}}}. \quad (54)$$

The Lagrange multiplier α is determined by choosing a normalization for u^μ , which corresponds to a gauge choice for λ . For a given dynamical mass function \mathcal{M} , one can then evaluate the equations of motion (31) and (32).

Coming back to the plan outlined in the introduction, we have the option to construct either L_M , R_M , or \mathcal{M} in a phenomenological manner. Let us explore the last option here, e.g., because it promotes both p_μ and $S_{\mu\nu}$ to dynamical variables, which are probably easier to identify in realistic situations compared to u^μ and $\Omega^{\mu\nu}$. Further, it is suggestive that the mass \mathcal{M} of the object as a function of the dynamical variables completely determines the macroscopic dynamics of the body. This situation is analogous to a thermodynamic potential (like the internal energy) describing the large-scale behavior of a thermodynamic system. This is the first indication that thinking in terms of thermodynamic analogies is very useful here.

4.3 Supplementary Conditions

The model for spinning bodies developed up to now comprises too many degrees of freedom. We expect three rotational degrees of freedom instead of six provided by the Lorentz frame Λ_A^μ . Similarly, the spin should only have three independent components, too. It is suggestive to impose that the time direction of the body-fixed frame is aligned to a (to be defined) rest frame described by a unit time-like vector r^μ , and that the spin only has spatial components in this rest frame,

$$\Lambda_0^\mu = r^\mu, \quad S_{\mu\nu}r^\nu = 0. \quad (55)$$

One can also envision different time-like vectors in each of these conditions. However, using the same vector seems to fit well to the interpretation of r^μ as a rest frame. The condition on the spin is usually called spin supplementary condition. Two specific options are $r^\mu = u^\mu / \sqrt{-u_\nu u^\nu}$ or $r^\mu = p^\mu / \sqrt{-p_\nu p^\nu}$. The latter condition is usually considered as the best choice, as it uniquely fixes the representative worldline of the extended object [37–39] (if Dixon’s definitions for the multipoles are used). A more detailed discussion of supplementary conditions is given in the contributions by D. Giulini, L.F. Costa and J. Natário. But notice that in flat space the choice of this condition can be related to the choice of the representative worldline for the extended body. In curved spacetime this relation could not be established yet. From a careful perspective one should therefore reckon that different spin supplementary conditions may lead to inequivalent models. As long as the relation to the choice of center is not clarified for curved spacetimes, one must regard this condition as a constitutive relation of the model. For this reason, one should also avoid conditions which are not manifestly covariant.

The most straightforward way to implement (55) into a given action is to add these conditions using Lagrange multipliers. In general, this will modify the dynamics by constraint forces. As in classical mechanics, one requires that (55) is preserved in time, which should fix the Lagrange multipliers. This can lead to inconsistencies,

in which case one should revise the action or the choice for r^μ . It can also lead to further constraints, which we regard as unphysical here as they further reduces the number of independent variables (we want exactly three rotational degrees of freedom). Similarly, if some of the Lagrange multipliers remain undetermined, then the degrees of freedom are increased, which we also regard as unphysical. The last possibility is that the Lagrange multipliers are uniquely fixed by requiring that (55) is preserved. In the end, we can insert this solution for the Lagrange multipliers into the action. In this way we obtain an action without Lagrange multipliers which preserves (55).

4.4 Conditions on the Dynamical Mass

Having this said, we can try to directly construct an action which preserves (55). This approach is in fact very natural here. For instance, one can make an ansatz for \mathcal{M}^2 and use this requirement to fix some of the coefficients. The first condition in (55) can be written as $\eta_{0A} = \Lambda_{A\mu} r^\mu$ and is preserved in time if

$$0 = \frac{Dr^\mu}{d\lambda} + \Omega^{\mu\nu} r_\nu, \quad \text{where } \Omega^{\mu\nu} = \alpha \frac{\partial \mathcal{M}^2}{\partial S_{\mu\nu}}. \quad (56)$$

Using (21) and (53), we can write the spin equation of motion (32) in the form

$$\frac{DS_{\mu\nu}}{d\lambda} = 2S_{\alpha[\mu} \Omega_{\nu]}^\alpha + \alpha \frac{\partial \mathcal{M}^2}{\partial \Lambda_A^\alpha} \delta_\alpha^{[\mu} \Lambda_A^{\nu]}. \quad (57)$$

With the help of this equation, we see that the spin supplementary condition is preserved in time if it holds (56) and additionally

$$0 = \frac{\partial \mathcal{M}^2}{\partial \Lambda_A^\alpha} \delta_\alpha^{[\mu} \Lambda_A^{\nu]} r_\nu. \quad (58)$$

This condition is often trivially fulfilled, namely when \mathcal{M}^2 does not explicitly depend on Λ_A^μ . We are going to construct a simple example now, in order to show that functions \mathcal{M} exist which are consistent with all of our requirements.

4.5 A Simple Construction of the Dynamical Mass

Instead of constructing an action which fulfills (56) and (58) for a specific choice of r^μ , one can look at a specific action and construct a r^μ such that the requirements (56) and (58) are fulfilled. Let us consider a simple example where \mathcal{M}^2 is a nonconstant

analytic function f depending only on $S^2 := S^{\mu\nu}S_{\mu\nu}/2$, i.e., $\mathcal{M}^2 = f(S^2)$. It is clear that (58) is fulfilled, because there is no explicit dependence on the body-fixed frame. We still need to satisfy (56), which reads explicitly

$$0 = \frac{Dr^\mu}{d\lambda} + \alpha f' S^{\mu\nu} r_\nu = \frac{Dr^\mu}{d\lambda}. \quad (59)$$

That is, the vector r^μ must be parallel transported along the worldline. This does indeed characterize a suitable spin supplementary condition, which was first discussed in [40, Sect. 3.4]. Although, with this condition, r^μ lacks an immediate interpretation as a rest frame, the numerical results in [40] show that it leads to similar predictions as the choice $r^\mu = p^\mu / \sqrt{-p_\nu p^\nu}$. Further discussions on this supplementary condition are given in other contributions to these proceedings.

For the case of a black hole, the laws of black hole dynamics [41, Box 33.4] suggests that

$$\mathcal{M}_{\text{BH}}^2 = f(S^2) = m_0^2 + \frac{S^2}{(2Gm_0)^2}. \quad (60)$$

where m_0 is the constant irreducible mass related to the horizon area. We can now have a look at the angular velocity with respect to asymptotic time, so we have $\alpha = \mathcal{M}^{-1}$ (for a body at rest). Evaluating (52), we find agreement with what is usually identified as the angular velocity of the horizon. This is a nice check for the consistency of the interpretation of our variables. Notice that the laws of black hole dynamics owe their name to their similarity to the laws of thermodynamics. Further, an action principle similar to the one presented here can be used to derive the so called first law of black hole *binary* dynamics [13]. Again we encounter the thermodynamic character of the approach.

For objects other than black holes, we can derive \mathcal{M} from the moment of inertia. One usually defines the moment of inertia $I(S^2)$ as the proportionality factor between spin and angular velocity, which can be read off from (52). Again we have $\alpha = \mathcal{M}^{-1} = f^{-1/2}$, so (52) leads to the differential equation $I^{-1} = f^{-1/2} f'$. Its solution reads

$$\mathcal{M}^2 = f(S^2) = \left[m_0 + \int_0^{S^2} \frac{dx}{2I(x)} \right]^2, \quad (61)$$

where the irreducible mass m_0 enters as an integration constant. For neutron stars, the function $I(S^2)$ can be obtained numerically, e.g., using the RNS code [42, 43]. Alternatively, one can numerically compute the gravitating mass \mathcal{M} directly as a function of S for a fixed number of baryons in the star. It would be interesting to see if both methods lead to compatible results. It should be noted that both black holes and neutron stars possess a quadrupole (and other multipoles) when they are spinning, which was neglected here. It will be included in the next section.

Interestingly, it is implied by [44] that for the pole-dipole case one can construct a \mathcal{M}^2 such that (56) and (58) are fulfilled for $r^\mu = p^\mu / \sqrt{-p_\nu p^\nu}$ without the need for approximations or truncations of \mathcal{M}^2 . Then, however, \mathcal{M}^2 is not solely dependent on S . The details on this are left for a future work.

5 Spin-Induced Quadrupole

In this section, we are going to develop a simple phenomenological model for \mathcal{M}^2 describing the spin-induced quadrupole of a star. This is the quadrupole of a star arising from a deformation away from spherical symmetry due to rotation. We start with a reasonable ansatz for \mathcal{M}^2 . The main idea for this ansatz is to include all possible covariant (general coordinate invariant) terms up to a certain power in spin and curvature. The unknown coefficients in this ansatz are then fixed by comparing to the Kerr metric and to numerical solutions for the gravitational field of a rotating neutron star. One should emphasize that a truncation of \mathcal{M}^2 requires negligibly small interaction energies, not small multipoles.

5.1 Construction of the Action

We are going to include in our ansatz the quadratic order in spin and second order derivatives of the metric. This means that we include terms linear in the curvature and covariant derivatives of the curvature are not allowed. This implies that we exclude λ -derivatives of the curvature for now, but this restriction will be loosened below. Symbolically we have $\phi_I^{\text{field}} = \{R_{\mu\nu\alpha\beta}\}$, which according to Sect. 3.4 implies that we neglect interaction terms involving octupole and higher multipoles. Finally, let us assume the absence of further worldline degrees of freedom in this section, or $\phi_I^{\text{wl}} = \emptyset$, so we have no need for a dependence of \mathcal{M}^2 on Λ_A^μ . [Then (58) is already fulfilled.]

The main task is to collect all possible interaction terms. One must take care of including only independent terms, which can be tricky due to the symmetries of the Riemann tensor. A procedure for this was applied to the construction of effective Lagrangians or Routhians in [8, 34, 45]. Instead, we are going to construct \mathcal{M}^2 directly, but the arguments are essentially the same. We will follow a different approach to implement the spin supplementary condition, too, by making an ansatz for r^μ around the case

$$r^\mu = \frac{p^\mu}{\sqrt{-p_\nu p^\nu}} + \mathcal{O}(R_{\mu\nu\alpha\beta}). \quad (62)$$

As a first simplification, one can replace $R_{\mu\nu\alpha\beta}$ by its tracefree version, the Weyl tensor $C_{\mu\nu\alpha\beta}$. The traces are given by $R_{\mu\nu} := g^{\alpha\beta} R_{\mu\alpha\nu\beta}$ and $R := g^{\mu\nu} R_{\mu\nu}$, which

are related to the energy momentum tensor $T^{\mu\nu}$ through Einstein's gravitational field equations

$$R^{\mu\nu} = 8\pi G \left(T^{\mu\nu} - \frac{1}{2} T^\alpha{}_\alpha g_{\mu\nu} \right). \quad (63)$$

The energy momentum tensor can contain contributions from fields penetrating the compact object, like electromagnetic or dark matter fields. We assume that these can be neglected, i.e., the bodies are mainly interacting via the gravitational field. But in the case of self-gravitating bodies, the energy momentum tensor also includes a singular contribution from the point-particle (39) itself. Let us assume that these singular self-interactions can be dropped. Then we can effectively make use of the vacuum field equations $R^{\mu\nu} = 0$ at the particle location, so we have $R_{\mu\nu\alpha\beta} = C_{\mu\nu\alpha\beta}$. However, in general one is not allowed to use field equations at the level of the action. But in the current context this is essentially a valid procedure, as it is equivalent to a field redefinition in the action, see [8, 26], or [46, Appendix A]. Without loss of generality, we can therefore restrict to $\phi_I^{\text{field}} = \{C_{\mu\nu\alpha\beta}\}$ in the quadrupole case.

The most important and most obvious requirement on the allowed interaction terms in \mathcal{M}^2 is general coordinate invariance. Further restrictions on the terms and transformations identifying equivalent terms (equivalent within our truncation) are:

1. In four spacetime dimensions, the Weyl tensor can be split into an electric $E_{\mu\nu}$ and a magnetic part $B_{\mu\nu}$ with respect to a time-like unit vector. Choosing this vector to be r^μ , it holds

$$E_{\mu\nu} = C_{\mu\alpha\nu\beta} r^\alpha r^\beta, \quad B_{\mu\nu} = \frac{1}{2} \eta_{\mu\alpha\rho\sigma} C_{\nu\beta}{}^{\rho\sigma} r^\alpha r^\beta, \quad (64)$$

where $\eta_{\mu\nu\alpha\beta}$ is the volume form. These tensors have the properties

$$E_{\mu\nu} = E_{\nu\mu}, \quad E_{\mu\nu} g^{\mu\nu} = 0, \quad E_{\mu\nu} r^\nu = 0, \quad (65)$$

$$B_{\mu\nu} = B_{\nu\mu}, \quad B_{\mu\nu} g^{\mu\nu} = 0, \quad B_{\mu\nu} r^\nu = 0. \quad (66)$$

These properties make $E_{\mu\nu}$ and $B_{\mu\nu}$ much easier to handle compared to $C_{\mu\nu\alpha\beta}$.

2. We include only terms invariant under parity transformations. In this respect it is important to notice that $B_{\mu\nu}$ is of odd parity. We conclude that any terms with an odd number of magnetic Weyl tensors must also include an odd number of volume forms $\eta_{\mu\nu\alpha\beta}$. Due to the antisymmetry of $\eta_{\mu\nu\alpha\beta}$, it will always be contracted with both indices of the spin at the current level of truncation. Then we can rewrite all terms involving $\eta_{\mu\nu\alpha\beta}$ in terms of the dual of the spin tensor

$$*S_{\alpha\beta} := \frac{1}{2} S^{\mu\nu} \eta_{\mu\nu\alpha\beta}. \quad (67)$$

Notice that we have the identity [22, Eq. (A.7)]

$$S_{\mu\alpha} * S^{\alpha\nu} = -\frac{1}{4} \delta_{\mu}^{\nu} S_{\alpha\beta} * S^{\alpha\beta}. \quad (68)$$

As a consequence, it holds $B_{\mu\nu} S^{\mu}{}_{\alpha} * S^{\alpha\nu} = 0$. It is customary to define a spin vector $S^{\mu} := r_{\nu} * S^{\nu\mu}$.

3. It should be noticed that one is in general not allowed to neglect terms involving the combination $S_{\mu\nu} r^{\nu}$, though these numerically vanish due to the spin supplementary condition (55): A variation of these terms can lead to nonvanishing contributions to the equations of motion. Instead, terms in the action which are at least quadratic in $S_{\mu\nu} r^{\nu}$ can be neglected, as their contributions to the equations of motion are at least linear in the spin supplementary condition and thus always vanish.
4. The quadrupole interaction terms can be simplified using the leading order truncation of the mass-shell constraint $p_{\mu} p^{\mu} + \mathcal{M}^2 = 0$. (For the ansatz in (70) given below, this implies that we can set $p_{\mu} p^{\mu} \approx -\mu^2$ in the higher order terms of \mathcal{M}^2 .) This transformation does in fact just correspond to a redefinition of the Lagrange multiplier α , and the idea is therefore similar to the field redefinitions mentioned above [26].
5. Time derivatives of p_{μ} and $S_{\mu\nu}$ can also be removed by redefinitions of variables, which follows from the ideas in [26] and is again analogous to the mentioned field redefinitions. Besides that, the absence of higher order time derivatives was already assumed in Sect. 3.1.

The last point also shows that our ansatz will automatically cover time derivatives of $E_{\mu\nu}$ and $B_{\mu\nu}$ of arbitrary order. As we work at linear level in the curvature, the time derivatives can always be removed from the curvature through partial integration. After this transformation, all time derivatives finally apply to p_{μ} and $S_{\mu\nu}$ only, which can be removed by virtue of the argument 5 above. This suggests that these terms belong to the quadrupole level, too, although time derivatives of the fields are in fact covariant derivatives $D/d\lambda = u^{\mu} \nabla_{\mu}$. This is of course related to the ambiguity of the multipoles pointed out in Sect. 3.4. At linear level in the curvature, one can assume that the covariant derivatives are projected orthogonal to r^{μ} , because $r^{\mu} \nabla_{\mu} \approx u^{\mu} \nabla_{\mu} = D/d\lambda$ up to higher order terms, which can be partially integrated.

The first point mentioned above suggests to include just $E_{\mu\nu}$ and $B_{\mu\nu}$ in ϕ_I^{field} . However, this is currently not possible, because we assumed in Sect. 3.1 that the ϕ_I^{field} contain just fields, but r^{μ} in (64) is only defined on the worldline. For instance, one would have to clarify the meaning of $\nabla_{\alpha} r^{\mu}$ arising from $\nabla_{\alpha} E_{\mu\nu}$ in (31). For simplicity, let us stick to $\phi_I^{\text{field}} = \{C_{\mu\nu\alpha\beta}\}$ here, but have in mind that \mathcal{M}^2 depends on $C_{\mu\nu\alpha\beta}$ only through the combinations $E_{\mu\nu}$ and $B_{\mu\nu}$. The equations of motion are initially expressed in terms the quadrupole moment related to $C_{\mu\nu\alpha\beta}$,

$$\tilde{J}^{\mu\nu\alpha\beta} := -6 \frac{\partial L_M}{\partial C_{\mu\nu\alpha\beta}}. \quad (69)$$

see (33), but these are at once related to the moments belonging to $E_{\mu\nu}$ and $B_{\mu\nu}$ through the chain rule. The interpretation of the latter moments as quadrupoles is much more obvious than for (69), as $E_{\mu\nu}$ and $B_{\mu\nu}$ are symmetric tracefree spatial tensors in the rest frame defined by r^μ . These moments can be called electric and magnetic quadrupoles, respectively. They match the quadrupole degrees of freedom of the gravitational field outside the body [47], in contrast to (33), which in general is not tracefree. This approach to define electric and magnetic quadrupoles was briefly discussed in [11]. An explicit split into electric and magnetic quadrupoles at the level of the equations of motion was performed in [48].

5.2 Ansatz

The most general ansatz for \mathcal{M}^2 now reads

$$\mathcal{M}^2 = \mu^2 + C_{BS^2p} B_{\mu\nu} S^\mu S^{\nu\alpha} \hat{p}_\alpha + C_{ES^2} E_{\mu\nu} S^{\mu\alpha} S^\nu{}_\alpha + \mathcal{O}(E^2, B^2, S^3), \quad (70)$$

where we introduced the abbreviation $\hat{p}_\mu = p_\mu/\mu$. We assume that μ , C_{BS^2p} , and C_{ES^2} are constants. Remember that within the curvature terms we can set $r^\mu \approx \hat{p}^\mu$, which is due to (62) and point 4 of the last section. Notice that μ must be a function of the constant spin length, $\mu^2 = f(S^2)$, cf. (61). Otherwise the Legendre transformation would be problematic. Consistent with our truncation, we may write

$$\mu^2 = m_0^2 + \frac{m_0}{I_0} S^2 + \mathcal{O}(S^4), \quad (71)$$

where $I_0 \equiv I(0)$ is the moment of inertia in a slow rotation limit $S \rightarrow 0$. Furthermore, the constants C_{BS^2p} and C_{ES^2} will in general depend on μ and S . This is further discussed below.

Next, we want to check if (56) is fulfilled. Notice that (56) is required to hold at linear order in spin only. For this purpose, let us make an ansatz for r^μ to linear order in S ,

$$r^\mu = C_{rp} \hat{p}^\mu + G C_{rBS} B^{\mu\nu} S_\nu + \mathcal{O}(E^2, B^2, S^2). \quad (72)$$

The normalization $r^\mu r_\mu = -1$ leads to $C_{rp} = 1$. Inspecting (56), we see that most of the contributions from the C_{rBS} -term are shifted to higher orders, namely quadratic level in spin: This is due to $\Omega = \mathcal{O}(S)$ and $\dot{S}_\nu = \mathcal{O}(S^2)$. The only C_{rBS} -term linear in spin contains $\dot{B}^{\mu\nu}$. Though this is a derivative of the curvature, it is not of higher order, because we realized that our ansatz effectively also covers λ -derivatives of the curvature. We conclude that $C_{rBS} = 0$, or $r^\mu \approx \hat{p}^\mu$. For calculating \dot{r}^μ in (56), it is useful to rewrite (31) as

$$\frac{Dp_\mu}{d\lambda} = \alpha(E_{\alpha[\mu} S_{\nu]}{}^\alpha - B_{\alpha[\mu} r_{\nu]} S^\alpha) \left[2p^\nu + \frac{\partial \mathcal{M}^2}{\partial p_\nu} \right] - \frac{\alpha}{2} (\nabla_\mu \phi_I^{\text{field}}) \frac{\partial \mathcal{M}^2}{\partial \phi_I^{\text{field}}}. \quad (73)$$

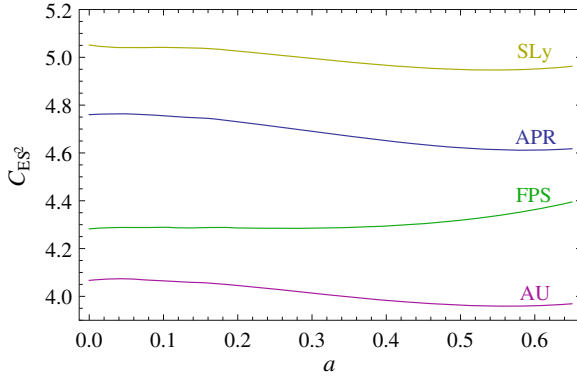


Fig. 1 The coefficient C_{ES^2} as a function of the dimensionless spin $a = S/G\mu^2$, where μ is identified with the gravitating mass and is given by $\mu = 1.4M_\odot$ here. The data points were generated using the RNS code [42, 43], where a multipole extraction according to [49] was used. The labels SLy, APR, FPS, and AU refer to equations of state considered in [50]

Finally, the condition (56) is fulfilled to linear order in spin if $C_{BS^2p} = 2$ in our ansatz (70). The condition (58) is of course also fulfilled. In summary, we must have

$$C_{rp} = 1, \quad C_{rBS} = 0, \quad C_{BS^2p} = 2, \quad (74)$$

while C_{ES^2} is not determined by basic principles, but depends on the specific object. Instead of fixing r^μ algebraically like in (72), it would be interesting to view (56) as an evolution equation for r^μ in the future, analogous to (59) in the pole-dipole case.

In Fig. 1 the numerical value of C_{ES^2} is shown as a function of the spin length for fixed mass μ but different neutron star models. It is apparent from the plot that C_{ES^2} is approximately independent of the spin length. However, one should be careful and check this assumption for the specific case of interest. This determination of C_{ES^2} is actually a simple example of a matching procedure. The quadrupole moment J of the effective point particle is parametrized through the ansatz (70) as $J \sim C_{ES^2} S^2$. This is compared (or matched) to the quadrupole moment of a numeric neutron star spacetime computed with the RNS code [42, 43]. Here the quadrupole moment is identified through the exterior spacetime. This means that the effective point particle mimics the exterior spacetime of a numerically constructed neutron star model, which depends crucially on strong field effects in the interior. This makes C_{ES^2} an interesting indicator for both the neutron star equation of state and strong-field modifications of gravity. For black holes, a comparison with the Kerr metric leads to $C_{ES^2} = 1$.

Finally, we come back to the thermodynamic analogy to our approach. The quadrupole relation $J \sim C_{ES^2} S^2$ can be viewed as a simple (idealized) “equation of state” relating the macroscopic variables J and S . As in the case of the ideal gas, this model can be improved to meet the required accuracy. This can be done systematically here by extending the ansatz (70) to higher orders.

5.3 Application

As an application for the spin-induced quadrupole constructed in the last section, we consider the case of a test particle moving in a Kerr spacetime. This test particle can be characterized as a pole-dipole-quadrupole particle. We aim at an estimate for the relevance of the spin-squared contributions, so we may consider a specific orbital configuration that simplifies the discussion. This is obviously a circular orbit in the equatorial plane of the Kerr geometry. Let us further assume that the spin of the test body is aligned with the rotation axis of the background spacetime.

In the absence of a quadrupole, these orbits can be constructed in a simple manner, which was first used in [51]. This method is in fact still applicable for the considered quadrupole model [52]. It requires that conserved quantities, spin supplementary condition, and constraints on the orbital configuration are enough to uniquely fix the 10 dynamic variables contained in p_μ and $S^{\mu\nu}$. This is just an algebraic calculation, in contrast to solving the differential equations of motion. A numeric study for Schwarzschild spacetime is given in [53].

The spin supplementary condition ($S^{\mu\nu} p_\nu = 0$) contains three independent equations. The constraint on the orbit provides three further independent conditions: one due to equatorial orbits ($p^\theta = 0$) and two due to spin alignment ($S^{\mu\theta} = 0$). So we need to identify $10 - 3 - 3 = 4$ conserved quantities in order to solve for p_μ and $S^{\mu\nu}$ algebraically. Three conserved quantities were already identified in Sect. 4.1.

These are the spin-length $S := \sqrt{\frac{1}{2} S_{ab} S^{ab}}$ and the quantities derived from the two Killing vectors of Kerr spacetime (∂_t and ∂_ϕ) through (46). We call the latter two the energy $E := E_{\partial_t}$ and total angular momentum $J_\phi := E_{-\partial_\phi}$ of the particle. The last remaining conserved quantity is just the mass-like parameter μ , which in the action approach is constant by assumption. However, one should remember that (70) is truncated and thus only approximately valid. One can equivalently say that μ is only conserved approximately, corresponding to the truncation of (70). This point of view was taken in [52].

Now we are in a position to solve for p_a and S^{ab} . Most important is the equation for p^r . After some algebra [52], one finds that $(p^r)^2$ is given by a polynomial of second order in E . We denote the roots of this polynomial by U_+ and U_- , i.e.,

$$(p^r)^2 \propto (E - U_+)(E - U_-). \quad (75)$$

For p^r to be a real number, we need to have both $E \leq U_+$ and $E \leq U_-$, or both $E \geq U_+$ and $E \geq U_-$. It turns out that the important relation is just $E \geq U_+$ for the most relevant part of the parameter space. This justifies to call U_+ effective potential: The test body can only move in the region where $E \geq U_+$ and its turning points are given by $E = U_+$, because then $p^r = 0$ (which implies $u^r = 0$, see [52]). Therefore the minimum of U_+ as a function of r defines circular orbits. This completes our construction.

The various contributions to the dimensionless binding energy $e := E/\mu - 1$ are plotted in Fig. 2 for the case of a very rapidly rotating (small) black hole in a

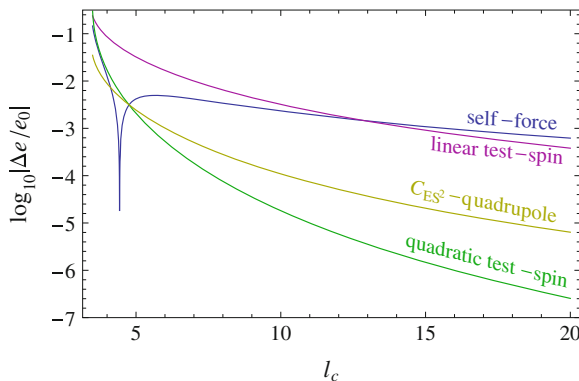


Fig. 2 Various corrections to the binding energy e for a maximally spinning (small) black hole in a Schwarzschild background. Here $l_c := J_\phi - S$ is the *orbital* angular momentum. The mass ratio is formally taken to be $q = 1$ in the plot, though the result are only valid for $q \ll 1$. The curves can be scaled to the case of interest ($q \lesssim 10^{-2}$): self-force and linear spin effects scale as $\propto q$, the others as $\propto q^2$

Schwarzschild background. A comparison with recent results for the conservative part of the self-force [54] is also included. In a Kerr background, the last stable circular orbit can be very close to the horizon, so that the discussed effects can be some orders of magnitude stronger. The reader is referred to [52] for a more complete discussion.

6 Dynamical Quadrupole and Tidal Forces

For the model developed in the last section, the quadrupole adiabatically follows the spin evolution. Thus, the quadrupole is not an independent dynamical variable. In this section, we are going to investigate dynamical quadrupoles, but restrict to the nonspinning case for simplicity.

6.1 Basic Idea

We have already discovered that the dynamical mass \mathcal{M} plays a role similar to a thermodynamic potential. From this perspective, one can compare the variables it depends on, like p_μ and $S_{\mu\nu}$, to thermodynamic state variables. Noticing that p_μ and $S_{\mu\nu}$ are the monopole and dipole moment, a natural extension is to introduce dynamical “state” variables for other multipoles, too. A possible motivation arises from the realization that stars have oscillation modes and that these modes can be excited by tidal forces from an external time-dependent gravitational field. This phenomenon is

well understood in Newtonian gravity [55], see also [56–58] and references therein. If one wants to capture it by our approach, one obviously must introduce dynamical worldline variables corresponding to these oscillation modes. Suitable point-particle actions were already discussed in [45, 59], though with applications to absorption or binary systems in mind.

The key to find a model for dynamical multipoles is to understand the reaction of the multipoles to external fields. We focus here on the response of the quadrupole to external tidal fields. In fact, we will encode the quadrupole dynamics in terms of a response function. This function can equivalently be called the propagator of the quadrupole [45], which better highlights the fact that it is a necessary ingredient for deriving predictions using perturbative calculations, e.g., in the post-Newtonian approximation. A third possible naming is correlation function between quadrupole and external field. This better accentuates the parallels to statistical mechanics or thermodynamics. The idea is that if one would be able to model the correlations of the most important multipoles among each other and with external fields, then one can in principle predict the motion of extended objects (with complicated internal structure) to any desired precision.

It is important to notice that the multipole moments of a compact object can be defined through their exterior field. The response functions of the multipoles to externally applied tidal fields can therefore be obtained by analyzing the gravitational field outside of the body. The final goal is to extract these functions from numerical simulations of a *single* compact object. However, for a first simpler investigation one can restrict to linear perturbations of nonrotating compact objects. The unperturbed metric in the exterior is then just the Schwarzschild one. Because this metric is static and spherically symmetric, its linear perturbations can then be decomposed into Fourier basis in the time direction and spherical harmonic basis $Y^{lm}(\theta, \phi)$ in angular directions. Then their radial dependence is described by the famous Zerilli [60] or Regge-Wheeler [61] equations for electric- or magnetic-parity-type perturbations, respectively. The Zerilli equation can be transformed into the simpler Regge-Wheeler form [62], so we can focus just on the latter one. It reads

$$\frac{d^2 X}{dr_*^2} + \left[\left(1 - \frac{R_S}{r} \right) \frac{l(l+1) - \frac{3R_S}{r}}{r^2} + \omega^2 \right] X = 0, \quad (76)$$

where ω is the frequency of the perturbation, l is the angular momentum quantum number, r is radial coordinate in the Regge-Wheeler gauge, R_S is the Schwarzschild radius (representing the mass of the body), $r_* = r + R_S \log(r/R_S - 1)$ is the tortoise radial coordinate, and X denotes the Regge-Wheeler master function. Given some boundary values for X at the surface of the body (which result from a solution to the more complicated interior perturbation equations), it is straightforward to integrate this equation numerically. The question is how one can decompose X into external (applied) tidal field and multipolar field generated by the body in response to the external field. This is a complicated problem in the general relativistic case. Let us therefore start with the Newtonian theory in order to get a better understanding of the problem [19].

6.2 Newtonian Case

The Newtonian case can be obtained as a weak field and slow motion approximation of general relativity. That is, we have to set $R_S = 0$ (weak field) and $\omega = 0$ (slow motion) in (76). The perturbation of the Newtonian potential Φ_{pert} can be reconstructed as

$$\Phi_{\text{pert}} = -\frac{1}{2\pi} \int d\omega \sum_{lm} e^{i\omega t} Y^{lm} \frac{1}{2} \left[\frac{d}{dr} + \frac{l(l+1)}{2r} \right] X_{lm\omega}, \quad (77)$$

where the $X_{lm\omega}$ are solutions to the Newtonian limit of (76) for all values of the parameters l , m , and ω .

The generic solution to the Newtonian limit of (76) reads

$$X = C_1 r^{l+1} + C_2 r^{-l}, \quad (78)$$

where C_1 and C_2 are integration constants. The r^{l+1} part diverges asymptotically, which means that its source is located at infinity. Therefore, C_1 is the strength of the external field. Similarly, the r^{-l} part is singular at the origin and emanates from the compact body, so C_2 describes the l -polar field of the body. The frequency-domain response \tilde{F}_l of the multipoles to external fields is then proportional to the ratio of C_2 and C_1 . In the conventions used in [18, 19], it holds

$$\tilde{F}_l(\omega) = \frac{l(l-1)}{G(l+1)(l+2)(2l-1)!!} \frac{C_2}{C_1} \quad (79)$$

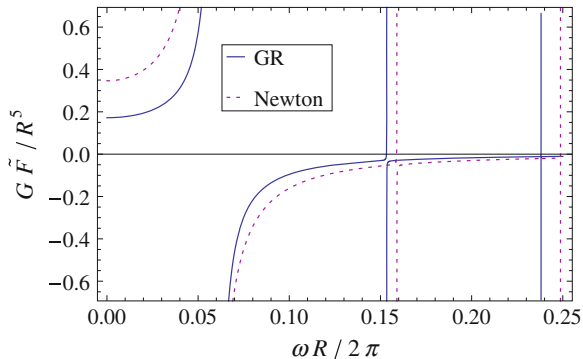
This response must in general be computed numerically. The first step is to numerically solve the interior problem of a perturbed body, including the interior gravitational field perturbation. Then the gravitational field is matched to (78) at the surface, which leads to numeric values for the integration constants and thus for the response (79). This response can in general acquire a complicated frequency dependence through the internal dynamics. Usually one defines normal oscillation modes by requiring that the body keeps up a multipolar field without external excitation, i.e., for $C_1 = 0$. Therefore the response (79) has a pole at normal mode frequencies.

In the case of linear perturbations of a nonrotating barotropic star, the response turns out to be quite simple. For the quadrupolar case $l = 2$, the outcome is shown in Fig. 3. In fact, the form of the response can even be computed analytically and reads [19]

$$\tilde{F}_l = \sum_n \frac{I_{nl}^2}{\omega_{nl}^2 - \omega^2}. \quad (80)$$

This is just the sum of response functions of harmonic oscillators with resonance frequencies (poles) at ω_{nl} . Here n labels the type and overtone number of the oscillation

Fig. 3 Response function of the quadrupole, $l = 2$, for a one solar mass star. The equation of state is a polytrope with index 1 and such that the radius R is 17.7 km in the Newtonian case or 15.7 km in the relativistic case



modes. The constants I_{nl} are the so called overlap integrals, which here simply take the role of coupling constants between the oscillators and the external driving forces. As a consequence, the internal dynamics can be captured by an effective action through just a set of harmonic oscillators, which are coupled to the tidal force of the gravitational field [19] (with coupling constants I_{nl}). By fitting the numeric result for \tilde{F}_l to (80), one can extract the constants ω_{nl} and I_{nl} .

It is worth to point out that the presented Newtonian setup is simple enough to perform explicitly the effective field theory procedure of integrating out small scales, see [19]. This turns a compact fluid configuration into a point particle on macroscopic scales.

6.3 Relativistic Case at Zero Frequency

Let us now return to the relativistic case, but restrict to even parity and the adiabatic case $\omega = 0$. The connection between the relativistic tidal constants defined in [15–17, 63] and the response function is given by a Taylor-expansion,

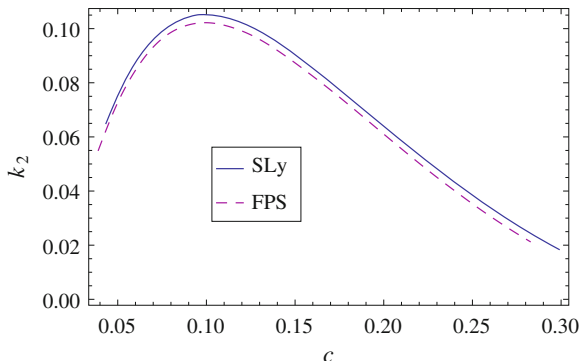
$$\frac{\tilde{F}_l(\omega)}{l!} = \mu_l + i\lambda_l\omega + \mu'_l\omega^2 + \mathcal{O}(\omega^3), \quad (81)$$

see [19]. Here the constants μ_l are named after the astronomer A.E.H. Love, who introduced them for tidal effects in the Earth-Moon system. A dimensionless version of the Love numbers μ_l is often defined as

$$k_l = \frac{(2l-1)!!}{2R^{2l+1}} G\mu_l, \quad (82)$$

where R is the radius of the star. The λ_l -term in (81) is related to absorption [45] and μ'_2 was introduced in [63].

Fig. 4 Dimensionless quadrupolar Love number k_2 as a function of the compactness $c = R_S/2R$ for two different equations of state (SLy, FPS)



It remains to define how the response should be computed in the adiabatic relativistic case. First, we again solve (76), this time for $\omega = 0$, and find an analytic result in terms of the Gauss hypergeometric function ${}_2F_1$,

$$X = C_1 r^{l+1} {}_2F_1(-l-2, 2-l, -2l; R_S/r) + C_2 r^{-l} {}_2F_1(l-1, l+3, 2(l+1); R_S/r), \quad (83)$$

see, e.g., [64]. Again we can obtain numeric values for the integration constants by solving the perturbation equations inside the body and then match the gravitational field to (83) at the surface. In the limit of $1/r \rightarrow 0$ the hypergeometric functions are equal to 1, so (83) turns into (78). This implies that the interpretation of the integration constants as magnitudes of external field and response is still valid. The even-parity response in the adiabatic case $\omega = 0$ then follows from (79) as before. A plot of the outcome in terms of the dimensionless Love number k_2 is given in Fig. 4. An extension of the application from Sect. 5.3 to adiabatic tidal deformations can be found in [52].

For integer values of l , the hypergeometric functions in (83) turn into polynomials (which possibly contain logarithms). Then one might worry that the exponents on r from the two independent solutions in (83) can overlap and spoil a unique identification of external field and response. However, this is avoided by examining X for generic values of l , in the sense of an analytic continuation. This is in spirit similar to working in generic dimension, as done in [64].

6.4 Relativistic Case for Generic Frequency

We now turn our attention to the case of generic frequency in the even parity sector [18]. One can still solve (76) analytically [65], this time in terms of a series involving hypergeometric functions. We write the generic solution schematically as

$$X = A_1 X_{\text{MST}}^l + A_2 X_{\text{MST}}^{-l-1}, \quad (84)$$

where we denote the solution from [65] by a subscript MST.

Note here that $X_{\text{MST}}^l \sim r^l$ and $X_{\text{MST}}^{-l-1} \sim r^{-l}$, which means that (79) essentially still works. Of course, one has to take into account the normalization of the X_{MST} in order to rewrite the C_i in (79) in terms of the A_i . This introduces complicated ω -dependent corrections into (79). These are computed through a matching of the asymptotic field of the extended body to the field of the point-particle model. The details of this procedure can be found in [18]. The basic steps are as follows:

- The field of the effective theory is obtained from an inhomogeneous version of (76) with a point particle source. It is understood that the post-Minkowskian approximation is applied, as this removes the singular point of (76) at the Schwarzschild radius. The explicit form of the source term derives from (39).
- The solution to the inhomogeneous equation is constructed from the homogeneous solution (84) using the method of variation of parameters. This method involves integrals over products of singular source and the X_{MST} . The integration constants just represent a generic solution to the homogeneous solution that can always be added.
- Here the integration constants must be restricted further. Due to the singular behavior of the differential equation at $r = 0$, the homogeneous solution might actually not be homogeneous at $r = 0$. But the externally applied field is homogeneous everywhere, including $r = 0$. The restriction of the integration constants is therefore equivalent to the identification of the external part of the field and the part generated by the particle.
- Notice that an l -pole source involves l partial derivatives of a delta distribution. This suggests to identify the self-field by $X_{\text{MST}}^{-l-1} \sim r^{-l}$ and the external field by $X_{\text{MST}}^l \sim r^l$ for dimensional reasons. Here the idea of analytic continuation in l is again crucial.
- The integrals arising in the variation of parameters are actually singular. This is not surprising, as the self-field of point-particles always leads to this kind of problem. A regularization method must be introduced.

These steps lead to a refined (frequency dependent) version of (79) expressing the response function in terms of A_1 and A_2 . The final step is again to obtain numeric values for A_1 and A_2 for an actual (extended) neutron star.

The result for the general relativistic response function is shown in Fig. 3. It can still be fitted by (80) very well. This implies that the internal dynamics can be approximated by a set of harmonic oscillators. Restricting to the quadrupolar level $l = 2$ for simplicity, this translates to a dynamical mass of the form

$$\mathcal{M}^2 \approx \mu^2 + \mu \sum_n \left(\psi_n^{AB} \psi_{nAB} + \omega_n^2 \phi_{nAB} \phi_n^{AB} + 2I_n E^{AB} \phi_{nAB} \right), \quad (85)$$

where the internal dynamical variables ϕ_{nAB} and ψ_n^{AB} only have spatial components in the body-fixed frame ($\phi_{n0B} = 0 = \psi_n^{0B}$) and are symmetric tracefree in the

indices A and B . The dynamical equations for the quadrupolar worldline variables can be extracted from (52), (29), and (54),

$$\dot{\phi}_n{}^{AB} = \frac{\alpha}{2} \frac{\partial \mathcal{M}^2}{\partial \psi_{nAB}}, \quad \dot{\psi}_{nAB} = -\frac{\alpha}{2} \frac{\partial \mathcal{M}^2}{\partial \phi_n{}^{AB}}. \quad (86)$$

In the linear perturbation regime, the contributions of the internal dynamical variables are small compared to μ^2 . The index n still labels the type of the oscillation mode. The mass quadrupole is the coefficient in front of E^{AB} , i.e., $Q_{AB} := \sum_n I_n \phi_{nAB}$. Now the frame enters through $E^{AB} = \lambda^A{}_\mu \lambda^B{}_\nu E^{\mu\nu}$, so we need to check if (58) is fulfilled. Using $\Lambda_0{}^\mu = r^\mu$ and $E_{\mu\nu} r^\nu = 0$ it is easy to see that this is the case. In fact, (58) is always fulfilled if the time direction of the body-fixed frame $\Lambda_0{}^\mu$ drops out of the action.

Some final remarks on the problem of regularization of point particles are in order. It was shown already in [59] that the quadrupole diverges at order ω^2 in dimensional regularization. It is therefore not surprising that poles appear in the generalization of (79) at order ω^2 , which must be subtracted within some renormalization scheme. At the same time, the poles give rise to an explicit appearance of a renormalization scale parameter, which in a sense parametrizes the ambiguity in the choice of the renormalization scheme. An important point is that this scale parameter is in fact fixed by the requirement that the response function has an asymptotic behavior for $\omega \rightarrow \infty$ compatible with (80). Different regularization and renormalization schemes will in general lead to slightly different numeric values for this scale parameter. However, within a given scheme its value can be uniquely matched and is therefore not ambiguous. In this sense, the regularization and renormalization scheme is a part of the phenomenological model.

7 Conclusions

We considered point-particle models for extended bodies in gravity, in particular for black holes and neutron stars. The multipoles of the point particles are adjusted such that their field predicted from a weak field approximation matches an exact/numerical solution for the extended object in question. This incorporates strong field effects from the interior of the extended object in the model. This is of particular importance when binary systems are considered using weak field approximations, e.g., for gravitational wave source modeling or pulsar timing.

Therefore, point-particle actions are far more powerful than what was probably envisioned when they were first investigated [5, 6]. The resulting equations of motion are similar to Dixon's results. Here we developed astrophysical realistic models for the multipoles in these equations. The latest development is the inclusion of oscillation modes in relativistic tidal interaction of neutron stars.

An interesting topic not discussed here are universal relations for various neutron star properties. Here “universal” refers to an approximate independence among various proposed realistic equations of state. In [66, 67] universal relations between the dimensionless moment of inertia $I/G^2\mu^3$, the quadrupolar Love number $\mu_2/G^4\mu^5$, and the quadrupole constant C_{ES^2} were found and coined I-Love-Q relations. Further investigations, also including higher multipoles, followed shortly afterwards [68–73]. This indicates that coefficients in (70) arising at higher orders are actually not independent, but are (approximately) fixed by universality. (For black holes, in fact all coefficients are fixed, which is guaranteed by the no hair theorem.) This makes the expansion (70) a meaningful tool to study the impact of the equation of state on observations, as predictions of the effective model are then parametrized by only a small set of constants.

The most interesting development for the future is probably the description of oscillation modes for rotating bodies, which can be tried in a slow rotation approximation. It is also interesting to investigate if universal properties hold for the ingredients of the response function, e.g., for the overlap integrals.

Acknowledgments I am indebted to all of my collaborators contributing directly or indirectly to the material presented here: Sayan Chakrabarti, Trencé Delsate, Norman Gürlebeck, Johannes Hartung, Steven Hergt, Dirk Puetzfeld, Gerhard Schäfer, and Manuel Tessmer. This work was supported by DFG (Germany) through projects STE 2017/1-1 and STE 2017/2-1, and by FCT (Portugal) through projects SFRH/BI/52132/2013 and PCOFUND-GA-2009-246542 (co-funded by Marie Curie Actions).

References

1. M. Mathisson, *Neue Mechanik materieller Systeme*. Acta Phys. Pol. **6**, 163–200 (1937)
2. M. Mathisson, *Republication of: new mechanics of material systems*. Gen. Relativ. Gravit. **42**, 1011–1048 (2010)
3. W.G. Dixon, *Extended bodies in general relativity: their description and motion*, in *Proceedings of the International School of Physics Enrico Fermi LXVII*, ed. by J. Ehlers (North Holland, Amsterdam, 1979), pp. 156–219
4. A. Papapetrou, *Spinning test-particles in general relativity*. I. Proc. R. Soc. A **209**, 248–258 (1951)
5. K. Westpfahl, *Relativistische Bewegungsprobleme*. VI. Rotator-Spinteilchen und allgemeine Relativitätstheorie. Ann. Phys. (Berlin) **477**, 361–371 (1969)
6. I. Bailey, W. Israel, *Lagrangian dynamics of spinning particles and polarized media in general relativity*. Commun. Math. Phys. **42**, 65–82 (1975)
7. T. Damour, *Gravitational radiation and the motion of compact bodies*, in *Gravitational Radiation*, ed. by N. Deruelle, T. Piran (North Holland, Amsterdam, 1983), pp. 59–144
8. W.D. Goldberger, I.Z. Rothstein, *An effective field theory of gravity for extended objects*. Phys. Rev. D **73**, 104029 (2006)
9. R.A. Porto, *Post-Newtonian corrections to the motion of spinning bodies in nonrelativistic general relativity*. Phys. Rev. D **73**, 104031 (2006)
10. J. Steinhoff, G. Schäfer, *Canonical formulation of self-gravitating spinning-object systems*. Europhys. Lett. **87**, 50004 (2009)
11. J. Steinhoff, *Canonical formulation of spin in general relativity*. Ann. Phys. (Berlin) **523**, 296–353 (2011)

12. B.S. DeWitt, *Bryce DeWitt's Lectures on Gravitation*, vol. 826, 1st edn. Lecture Notes in Physics (Springer, Berlin, 2011)
13. L. Blanchet, A. Buonanno, A. Le Tiec, First law of mechanics for black hole binaries with spins. *Phys. Rev. D* **87**, 024030 (2013)
14. W.G. Laarakkers, E. Poisson, Quadrupole moments of rotating neutron stars. *Astrophys. J.* **512**, 282–287 (1999)
15. T. Damour, A. Nagar, Relativistic tidal properties of neutron stars. *Phys. Rev. D* **80**, 084035 (2009)
16. T. Binnington, E. Poisson, Relativistic theory of tidal love numbers. *Phys. Rev. D* **80**, 084018 (2009)
17. T. Hinderer, Tidal love numbers of neutron stars. *Astrophys. J.* **677**, 1216–1220 (2008)
18. S. Chakrabarti, T. Delsate, J. Steinhoff, New perspectives on neutron star and black hole spectroscopy and dynamic tides (2013)
19. S. Chakrabarti, T. Delsate, J. Steinhoff, Effective action and linear response of compact objects in Newtonian gravity. *Phys. Rev. D* **88**, 084038 (2013)
20. H. Goenner, K. Westpfahl, Relativistische Bewegungsprobleme. II. Der starre Rotator. *Ann. Phys. (Berlin)* **475**, 230–240 (1967)
21. H. Römer, K. Westpfahl, Relativistische Bewegungsprobleme. IV. Rotator-Spinteilchen in schwachen Gravitationsfeldern. *Ann. Phys. (Berlin)* **477**, 264–276 (1969)
22. A.J. Hanson, T. Regge, The relativistic spherical top. *Ann. Phys. (N.Y.)* **87**, 498–566 (1974)
23. M. Leclerc, Mathisson-Papapetrou equations in metric and gauge theories of gravity in a Lagrangian formulation. *Class. Quantum Gravity* **22**, 3203–3222 (2005)
24. J. Natario, Tangent Euler top in general relativity. *Commun. Math. Phys.* **281**, 387–400 (2008)
25. B.S. DeWitt, Dynamical theory of groups and fields, in *Relativity, Groups, and Topology, Les Houches 1963* (Gordon and Breach, New York, 1964)
26. T. Damour, G. Schäfer, Redefinition of position variables and the reduction of higher order Lagrangians. *J. Math. Phys.* **32**, 127–134 (1991)
27. W.M. Tulczyjew, Motion of multipole particles in general relativity theory. *Acta Phys. Pol.* **18**, 393–409 (1959)
28. J. Steinhoff, D. Puetzfeld, Multipolar equations of motion for extended test bodies in general relativity. *Phys. Rev. D* **81**, 044019 (2010)
29. A.I. Harte, Mechanics of extended masses in general relativity. *Class. Quantum Gravity* **29**, 055012 (2012)
30. E. Noether, Invariante Variationsprobleme. *Nachr. Akad. Wiss. Gött.* 235–257 (1918)
31. J. Ehlers, E. Rudolph, Dynamics of extended bodies in general relativity—center-of-mass description and quasirigidity. *Gen. Relativ. Gravit.* **8**, 197–217 (1977)
32. K. Yee, M. Bander, Equations of motion for spinning particles in external electromagnetic and gravitational fields. *Phys. Rev. D* **48**, 2797–2799 (1993)
33. R.A. Porto, I.Z. Rothstein, Spin(1)spin(2) effects in the motion of inspiralling compact binaries at third order in the post-Newtonian expansion. *Phys. Rev. D* **78**, 044012 (2008)
34. R.A. Porto, I.Z. Rothstein, Next to leading order spin(1)spin(1) effects in the motion of inspiralling compact binaries. *Phys. Rev. D* **78**, 044013 (2008)
35. L. Rosenfeld, Zur Quantelung der Wellenfelder. *Ann. Phys. (Berlin)* **397**, 113–152 (1930)
36. P.A.M. Dirac, Generalized Hamiltonian dynamics. *Can. J. Math.* **2**, 129–148 (1950)
37. W. Beiglböck, The center-of-mass in Einsteins theory of gravitation. *Commun. Math. Phys.* **5**, 106–130 (1967)
38. R. Schattner, The center of mass in general relativity. *Gen. Relativ. Gravit.* **10**, 377–393 (1979)
39. R. Schattner, The uniqueness of the center of mass in general relativity. *Gen. Relativ. Gravit.* **10**, 395–399 (1979)
40. K. Kyrian, O. Semerák, Spinning test particles in a Kerr field – II. *Mon. Not. R. Astron. Soc.* **382**, 1922–1932 (2007)
41. C.W. Misner, K.S. Thorne, J.A. Wheeler, *Gravitation* (W. H. Freeman and Company, New York, 1973)
42. N. Stergioulas, S. Morsink, RNS code

43. N. Stergioulas, J.L. Friedman, Comparing models of rapidly rotating relativistic stars constructed by two numerical methods. *Astrophys. J.* **444**, 306–311 (1995)
44. H.P. Künzle, Canonical dynamics of spinning particles in gravitational and electromagnetic fields. *J. Math. Phys.* **13**, 739–744 (1972)
45. W.D. Goldberger, I.Z. Rothstein, Dissipative effects in the worldline approach to black hole dynamics. *Phys. Rev. D* **73**, 104030 (2006)
46. T. Damour, G. Esposito-Farèse, Gravitational-wave versus binary-pulsar tests of strong-field gravity. *Phys. Rev. D* **58**, 042001 (1998)
47. K.S. Thorne, Multipole expansions of gravitational radiation. *Rev. Mod. Phys.* **52**, 299–339 (1980)
48. D. Bini, A. Geralico, Deviation of quadrupolar bodies from geodesic motion in a Kerr spacetime. *Phys. Rev. D* **89**, 044013 (2014)
49. G. Pappas, T.A. Apostolatos, Revising the multipole moments of numerical spacetimes, and its consequences. *Phys. Rev. Lett.* **108**, 231104 (2012)
50. S. Chakrabarti, T. Delsate, N. Gürlebeck, J. Steinhoff, The I-Q relation for rapidly rotating neutron stars (2013)
51. S.N. Rasband, Black holes and spinning test bodies. *Phys. Rev. Lett.* **30**, 111–114 (1973)
52. J. Steinhoff, D. Puetzfeld, Influence of internal structure on the motion of test bodies in extreme mass ratio situations. *Phys. Rev. D* **86**, 044033 (2012)
53. D. Bini, A. Geralico, Dynamics of quadrupolar bodies in a Schwarzschild spacetime. *Phys. Rev. D* **87**, 024028 (2013)
54. A. Le Tiec, E. Barausse, A. Buonanno, Gravitational self-force correction to the binding energy of compact binary systems. *Phys. Rev. Lett.* **108**, 131103 (2012)
55. W.H. Press, S.A. Teukolsky, On formation of close binaries by two-body tidal capture. *Astrophys. J.* **213**, 183–192 (1977)
56. M.E. Alexander, Tidal resonances in binary star systems. *Mon. Not. R. Astron. Soc.* **227**, 843–861 (1987)
57. Y. Rathore, A.E. Broderick, R. Blandford, A variational formalism for tidal excitation: Non-rotating, homentropic stars. *Mon. Not. R. Astron. Soc.* **339**, 25–32 (2003)
58. É.E. Flanagan, É. Racine, Gravitomagnetic resonant excitation of Rossby modes in coalescing neutron star binaries. *Phys. Rev. D* **75**, 044001 (2007)
59. W.D. Goldberger, A. Ross, Gravitational radiative corrections from effective field theory. *Phys. Rev. D* **81**, 124015 (2010)
60. F.J. Zerilli, Effective potential for even parity Regge-Wheeler gravitational perturbation equations. *Phys. Rev. Lett.* **24**, 737–738 (1970)
61. T. Regge, J.A. Wheeler, Stability of a Schwarzschild singularity. *Phys. Rev.* **108**, 1063–1069 (1957)
62. S. Chandrasekhar, On the equations governing the perturbations of the Schwarzschild black hole. *Proc. R. Soc. A* **343**, 289–298 (1975)
63. D. Bini, T. Damour, G. Faye, Effective action approach to higher-order relativistic tidal interactions in binary systems and their effective one body description. *Phys. Rev. D* **85**, 124034 (2012)
64. B. Kol, M. Smolkin, Black hole stereotyping: induced gravito-static polarization. *JHEP* **1202**, 010 (2012)
65. S. Mano, E. Takasugi, Analytic solutions of the Teukolsky equation and their properties. *Prog. Theor. Phys.* **97**, 213–232 (1997)
66. K. Yagi, N. Yunes, I-Love-Q: Unexpected universal relations for neutron stars and quark stars. *Science* **341**, 365–368 (2013)
67. K. Yagi, N. Yunes, I-Love-Q relations in neutron stars and their applications to astrophysics, gravitational waves and fundamental physics. *Phys. Rev. D* **88**, 023009 (2013)
68. A. Maselli, V. Cardoso, V. Ferrari, L. Gualtieri, P. Pani, Equation-of-state-independent relations in neutron stars. *Phys. Rev. D* **88**, 023007 (2013)
69. M. Bauböck, E. Berti, D. Psaltis, F. Özel, Relations between neutron-star parameters in the Hartle-Thorne approximation. *Astrophys. J.* **777**, 68 (2013)

70. B. Haskell, R. Ciolfi, F. Pannarale, L. Rezzolla, On the universality of I-Love-Q relations in magnetized neutron stars. *Mon. Not. R. Astron. Soc. Lett.* **438**, L71–L75 (2014)
71. D.D. Doneva, S.S. Yazadjiev, N. Stergioulas, K.D. Kokkotas, Breakdown of I-Love-Q universality in rapidly rotating relativistic stars. *Astrophys. J. Lett.* **781**, L6 (2014)
72. G. Pappas, T.A. Apostolatos, Universal behavior of rotating neutron stars in GR: even simpler than their Newtonian counterparts (2013)
73. K. Yagi, Multipole love relations (2013)

Testing the Motion of Strongly Self-Gravitating Bodies with Radio Pulsars

Norbert Wex

Abstract Before the 1970s, precision tests for gravity theories were constrained to the weak-field environment of the Solar System. In terms of relativistic equations of motion, the Solar System gave access to the first order corrections to Newtonian dynamics. Testing anything beyond the first post-Newtonian contributions was for a long time out of reach. The discovery of the first binary pulsar by Russell Hulse and Joseph Taylor in the summer of 1974 initiated a completely new field for testing the relativistic dynamics of gravitationally interacting bodies. For the first time the back reaction of gravitational wave emission on the binary motion could be studied. Furthermore, the Hulse-Taylor pulsar provided the first test bed for the orbital dynamics of strongly self-gravitating bodies. To date, there are a number of binary pulsars known which can be utilized to test different aspects of relativistic dynamics. So far GR has passed these tests with flying colors, while many alternative theories, like scalar-tensor gravity, are tightly constraint by now. This article gives an introduction to gravity tests with pulsars, and summarizes some of the most important results. Furthermore, it gives a brief outlook into the future of this exciting field of experimental gravity.

1 Introduction

In about two years from now we will be celebrating the centenary of Einstein's general theory of relativity. On November 25th 1915 Einstein presented his field equations of gravitation (without cosmological term) to the Prussian Academy of Science [1]. With this publication, general relativity (GR) was finally completed as a logically consistent physical theory ("*Damit ist endlich die allgemeine Relativitätstheorie als logisches Gebäude abgeschlossen.*"). Already one week before, based on the vacuum form of his field equations, Einstein was able to show that his theory of gravitation naturally explains the anomalous perihelion advance of the planet

N. Wex (✉)

Max-Planck-Institut für Radioastronomie, Auf dem Hügel 69, 53121 Bonn, Germany

e-mail: wex@mpifr-bonn.mpg.de

URL: <http://www.mpifr-bonn.mpg.de/staff/nwex/>

Mercury [2]. While in hindsight this can be seen as the first experimental test for GR, back in 1915 astronomers were still searching for a Newtonian explanation [3]. In his 1916 comprehensive summary of GR [4], Einstein proposed three experimental tests:

- Gravitational redshift.
- Light deflection.
- Perihelion precession of planetary orbits.

Gravitational redshift, a consequence of the equivalence principle, is common to all metric theories of gravity, and therefore in some respect its measurement has less discriminating power than the other two tests [5]. The first verification of gravitational light bending during the total eclipse on May 29th 1919 was far from being a high precision test, but clearly decided in favor of GR, against the Newtonian prediction, which is only half the GR value [6]. In the meantime this test has been greatly improved, in the optical with the astrometric satellite HIPPARCOS [7], and in the radio with very long baseline interferometry [8, 9]. The deflection predicted by GR has been verified with a precision of 1.5×10^{-4} . An even better test for the curvature of spacetime in the vicinity of the Sun is based on the Shapiro delay, the so-called “fourth test of GR” [10]. A measurement of the frequency shift of radio signals exchanged with the Cassini spacecraft lead to a 10^{-5} confirmation of GR [11]. Apart from the four “classical” tests, GR has passed many other tests in the Solar system with flying colors: Lunar Laser Ranging tests for the strong equivalence principle and the de-Sitter precession of the Moon’s orbit [12], the Gravity Probe B experiment for the relativistic spin precession of a gyroscope (geodetic and frame dragging) [13], and the Lense-Thirring effect in satellite orbits [14], just to name a few.

GR, being a theory where fields travel with finite speed, predicts the existence of gravitational waves that propagate with the speed of light [15] and extract energy from (non-axisymmetric) material systems with accelerated masses [16]. This is also true for a self-gravitating system, where the acceleration of the masses is driven by gravity itself, a question which was settled in a fully satisfactory manner only several decades after Einstein’s pioneering papers (see [17] for an excellent review). This fundamental property of GR could not be tested in the slow-motion environment of the Solar system, and the verification of the existence of gravitational waves had to wait until the discovery of the first binary pulsar in 1974 [18]. Also, all the experiments in the Solar system can only test the weak-field aspects of gravity. The spacetime of the Solar system is close to Minkowski space everywhere: To first order (in standard coordinates) the spatial components of the spacetime metric can be written as $g_{ij} = (1 - 2\Phi/c^2)\delta_{ij}$, where Φ denotes the Newtonian gravitational potential. At the surface of the Sun one finds $\Phi/c^2 \sim -2 \times 10^{-6}$, while at the surface of a neutron star $\Phi/c^2 \sim -0.2$. Consequently, gravity experiments with binary pulsars, not only yielded the first tests of the radiative properties of gravity, they also took our gravity tests into a new regime of gravity.

To categorize gravity tests with pulsars and to put them into context with other gravity tests it is useful to introduce the following four gravity regimes:

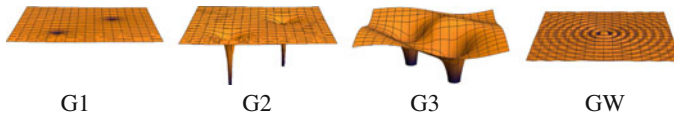


Fig. 1 Illustration of the different gravity regimes used in this article

G1 *Quasi-stationary weak-field regime*: The motion of the masses is slow compared to the speed of light ($v \ll c$) and spacetime is only very weakly curved, i.e. close to Minkowski spacetime everywhere. This is, for instance, the case in the Solar system.

G2 *Quasi-stationary strong-field regime*: The motion of the masses is slow compared to the speed of light ($v \ll c$), but one or more bodies of the system are strongly self-gravitating, i.e. spacetime in their vicinity deviates significantly from Minkowski space. Prime examples here are binary pulsars, consisting of two well-separated neutron stars.

G3 *Highly-dynamical strong-field regime*: Masses move at a significant fraction of the speed of light ($v \sim c$) and spacetime is strongly curved and highly dynamical in the vicinity of the masses. This is the regime of merging neutron stars and black holes.

GW *Radiation regime*: Synonym for the collection of the radiative properties of gravity, most notably the generation of gravitational waves by material sources, the propagation speed of gravitational waves, and their polarization properties.

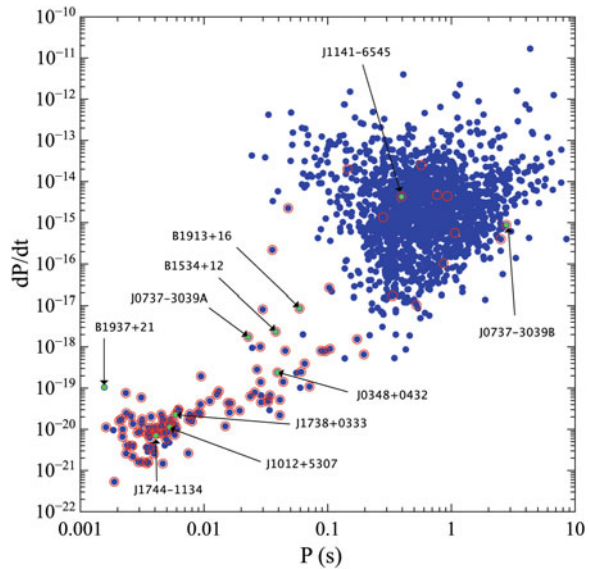
Figure 1 illustrates the different regimes. Gravity regime G1 is well tested in the Solar system. Binary pulsar experiments are presently our only precision experiments for gravity regime G2, and the best tests for the radiative properties of gravity (regime GW).¹ In the near future, gravitational wave detectors will allow a direct detection of gravitational waves (regime GW) and probe the strong and highly dynamical spacetime of merging compact objects (regime G3). As we will discuss at the end of this article, pulsar timing arrays soon should give us direct access to the nano-Hz gravitational wave band and probe the properties of these ultra-low-frequency gravitational waves (regime GW).

1.1 Radio Pulsars and Pulsar Timing

Radio pulsars, i.e. rotating neutron stars with coherent radio emission along their magnetic poles, were discovered in 1967 by Jocelyn Bell and Antony Hewish [20]. Seven years later, Russell Hulse and Joseph Taylor discovered the first binary pulsar, a pulsar in orbit with a companion star [18]. This discovery marked the beginning of

¹ Gravitational wave damping has also been observed in a double white-dwarf system, which has an orbital period of just 13 min [19]. This experiment combines gravity regimes G1 (note, $v/c \sim 3 \times 10^{-3}$) and GW of Fig. 1.

Fig. 2 The $P-\dot{P}$ diagram for radio pulsars. Binary pulsars are indicated by a *red circle*. Pulsars that play a particular role in this article are marked with a *green dot* and have their name as a label. The data are taken from the *ATNF Pulsar Catalogue* [21]



gravity tests with radio pulsars. Presently, more than 2000 radio pulsars are known, out of which about 10 % reside in binary systems [21]. The population of radio pulsars can be nicely presented in a diagram that gives the two main characteristics of a pulsar: the rotational period P and its temporal change \dot{P} due to the loss of rotational energy (see Fig. 2). Fast rotating pulsars with small \dot{P} (millisecond pulsars) appear to be particularly stable in their rotation. On long time-scales, some of them rival the best atomic clocks in terms of stability [22, 23]. This property makes them ideal tools for precision astrometry, and hence (most) gravity tests with pulsars are simply clock comparison experiments to probe the spacetime of the binary pulsar, where the “pulsar clock” is read off by counting the pulses in the pulsar signal (see Fig. 3). As a result, a wide range of relativistic effects related to orbital binary dynamics, time dilation and delays in the signal propagation can be tested. The technique used is the so-called *pulsar timing*, which basically consists of measuring the exact arrival time of pulses at the radio telescope on Earth, and fitting an appropriate *timing model* to these arrival times, to obtain a phase-connected solution. In the phase-connected approach lies the true strength of pulsar timing: the timing model has to account for every (observed) pulse over a time scale of several years, in some cases even several decades. This makes pulsar timing extremely sensitive to even tiny deviations in the model parameters, and therefore vastly superior to a simple measurement of Doppler-shifts in the pulse period. Table 1 illustrates the current precision capabilities of pulsar timing for various experiments, like mass determination, astrometry and gravity tests. We will not go into the details of pulsar observations and pulsar timing here, since there are numerous excellent reviews on these topics, for instance [24, 25], just to mention two. In this article we focus on the relativistic effects that play a role in pulsar-timing observations, and how pulsar timing can be used to test gravitational phenomena in generic as well as theory-based frameworks.

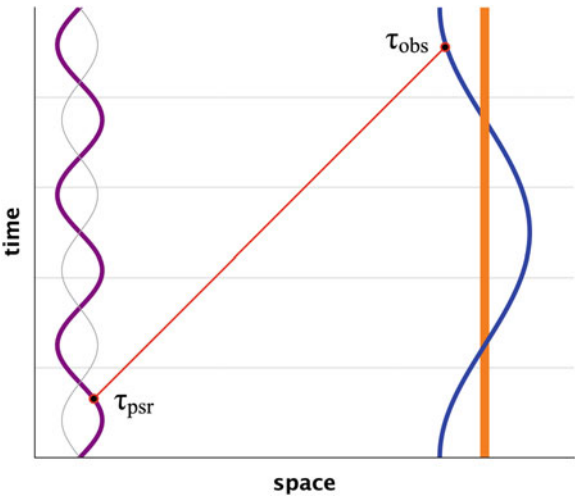


Fig. 3 Spacetime diagram illustration of pulsar timing. Pulsar timing connects the proper time of emission τ_{psr} , defined by the pulsar’s intrinsic rotation, and the proper time of the observer on Earth τ_{obs} , measured by the atomic clock at the location of the radio telescope. The timing model, which expresses τ_{obs} as a function of τ_{psr} , accounts for various “relativistic effects” associated with the metric properties of the spacetime, i.e. the world line of the pulsar and the null-geodesic of the radio signal. In addition, it contains a number of terms related to the Earth motion and relativistic corrections in the Solar system, like time dilation and signal propagation delays (see [26] for details)

Table 1 Examples of precision measurements using pulsar timing

Rotational period	5.757451924362137(2) ms	[27]
Orbital period	0.102251562479(8) d	[*]
Small eccentricity	$(3.5 \pm 1.1) \times 10^{-7}$	[28]
Distance	157(1) pc	[27]
Proper motion	140.915(1) mas yr ^{−1}	[27]
Masses of neutron stars	$m_p = 1.4398(2) M_\odot$	[29]
	$m_c = 1.3886(2) M_\odot$	[29]
Mass of millisecond pulsar	1.667(7) M_\odot	[30]
Mass of white-dwarf companion	0.207(2) M_\odot	[31]
Mass of Jupiter and moons	$9.547921(2) \times 10^{-4} M_\odot$	[32]
Relativistic periastron advance	4.226598(5) deg yr ^{−1}	[29]
Gravitational wave damping	0.504(3) pico-Hz yr ^{−1}	[*]
GR validity (observed/GR)	1.0000(5)	[*]

A number in bracket indicates the (one-sigma) uncertainty in the last digit of each value. The symbol M_\odot stands for the Solar mass. (cf. Table 1 in [33])
[*] Kramer et al., in prep.

1.2 Binary Pulsar Motion in Gravity Theories

While in Newtonian gravity there is an exact solution to the equations of motion of two point masses that interact gravitationally, no such exact analytic solution is known in GR. In GR, the two-body problem has to be solved numerically or on the basis of approximation methods. A particularly well established and successful approximation scheme, to tackle the problem of motion of a system of well-separated bodies, is the *post-Newtonian approximation*, which is based on the weak-field slow-motion assumption. However, to describe the motion and gravitational wave emission of binary pulsars, there are two main limitations of the post-Newtonian approximation that have to be overcome (cf. [34]):

- (A) Near and inside the pulsar (and its companion, if it is also a neutron star) the gravitational field is strong and the weak-field assumption no longer holds.
- (B) When it comes to generation of gravitational waves (of wavelength λ_{GW}) and their back-reaction on the orbit (of size r and period P_b), the post-Newtonian approximation is only valid in the near zone ($r \ll \lambda_{\text{GW}} = c P_b/2$), and breaks down in the radiation zone ($r > \lambda_{\text{GW}}$) where gravitational waves propagate and boundary conditions are defined, like the ‘no incoming radiation’ condition.

The discovery of the Hulse-Taylor pulsar was a particularly strong stimulus for the development of consistent approaches to compute the equations of motion for a binary system with strongly self-gravitating bodies (gravity regime G2). As a result, by now there are fully self-consistent derivations for the gravitational wave emission and the damping of the orbit due to gravitational wave back-reaction for such systems. In fact, in GR, there are several independent approaches that lead to the same result, giving equations of motion for a binary system with non-rotating components that include terms up to 3.5 post-Newtonian order (v^7/c^7) [35, 36]. For the relative acceleration in the center-of-mass frame one finds the general form

$$\ddot{\mathbf{r}} = -\frac{GM}{r^2} \left[(1 + A_2 + A_4 + A_5 + A_6 + A_7) \frac{\mathbf{r}}{r} + (B_2 + B_4 + B_5 + B_6 + B_7) \dot{\mathbf{r}} \right], \quad (1)$$

where the coefficients A_k and B_k are of order c^{-k} , and are functions of $r \equiv |\mathbf{r}|$, \dot{r} , $v \equiv |\dot{\mathbf{r}}|$, and the masses (see [35] for explicit expressions). The quantity M denotes the total mass of the system. At this level of approximation, these equations of motion are also applicable to binaries containing strongly self-gravitating bodies, like neutron stars and black holes. This is a consequence of a remarkable property of Einstein’s theory of gravity, the *effacement of the internal structure* [34, 37]: In GR, strong-field contributions are absorbed into the definition of the body’s mass.

In GR’s post-Newtonian approximation scheme, gravitational wave damping enters for the first time at the 2.5 post-Newtonian level (order v^5/c^5), as a term in the equations of motion that is not invariant against time-reversal. The corresponding loss of orbital energy is given by the *quadrupole formula*, derived for the

first time by Einstein within the linear approximation, for a material system where the gravitational interaction between the masses can be neglected [16]. As it turns out, the quadrupole formula is also applicable for gravity regime G2 of Fig. 1, and therefore valid for binary pulsars as well (cf. [34]).

In alternative gravity theories, the gravitational wave back-reaction, generally, already enters at the 1.5 post-Newtonian level (order v^3/c^3). This is the result of the emission of dipolar gravitational waves, and adds terms A_3 and B_3 to Eq. (1) [5, 38]. Furthermore, one does no longer have an effacement of the internal structure of a compact body, meaning that the orbital dynamics, in addition to the mass, depends on the “sensitivity” of the body, a quantity that depends on its structure/compactness. Such modifications already enter at the “Newtonian” level, where the usual Newtonian gravitational constant G is replaced by a (body-dependent) effective gravitational constant \mathcal{G} . For alternative gravity theories, it therefore generally makes an important difference whether the pulsar companion is a compact neutron star or a much less compact white dwarf. In sum, alternative theories of gravity generally predict deviations from GR in both the quasi-stationary and the radiative properties of binary pulsars [39, 40].

At the first post-Newtonian level, for fully conservative gravity theories without preferred location effects, one can construct a generic *modified Einstein-Infeld-Hoffmann Lagrangian* for a system of two gravitationally interacting masses m_p (pulsar) and m_c (companion) at relative (coordinate) separation $r \equiv |\mathbf{x}_p - \mathbf{x}_c|$ and velocities $\mathbf{v}_p = \dot{\mathbf{x}}_p$ and $\mathbf{v}_c = \dot{\mathbf{x}}_c$:

$$\begin{aligned}
 L_O = & -m_p c^2 \left(1 - \frac{\mathbf{v}_p^2}{2c^2} - \frac{\mathbf{v}_p^4}{8c^4} \right) - m_c c^2 \left(1 - \frac{\mathbf{v}_c^2}{2c^2} - \frac{\mathbf{v}_c^4}{8c^4} \right) \\
 & + \frac{\mathcal{G} m_p m_c}{r} \left[1 - \frac{\mathbf{v}_p \cdot \mathbf{v}_c}{2c^2} - \frac{(\mathbf{r} \cdot \mathbf{v}_p)(\mathbf{r} \cdot \mathbf{v}_c)}{2c^2 r^2} + \varepsilon \frac{(\mathbf{v}_p - \mathbf{v}_c)^2}{2c^2} \right] \\
 & - \xi \frac{\mathcal{G}^2 M m_p m_c}{2c^2 r^2}, \tag{2}
 \end{aligned}$$

where $M \equiv m_p + m_c$. The body-dependent quantities \mathcal{G} , ε and ξ account for deviations from GR associated with the self-energy of the individual masses [5, 39]. In GR one simply finds $\mathcal{G} = G$, $\varepsilon = 3$, and $\xi = 1$. There are various analytical solutions to the dynamics of (2). The most widely used in pulsar astronomy is the quasi-Keplerian parametrization by Damour and Deruelle [41]. It forms the basis of pulsar-timing models for relativistic binary pulsars, as we will discuss in more details in Sect. 1.4.

Beyond the first post-Newtonian level there is no fully generic framework for the gravitational dynamics of a binary system. However, one can find equations of motion valid for a general class of gravity theories, like in [42] where a framework based on multi-scalar-tensor theories is introduced to discuss tests of relativistic gravity to the second post-Newtonian level, or in [43] where the explicit equations of motion for non-spinning compact objects to 2.5 post-Newtonian order for a general class of scalar-tensor theories of gravity are given.

1.3 Gravitational Spin Effects in Binary Pulsars

In relativistic gravity theories, in general, the proper rotation of the bodies of a binary system directly affects their orbital and spin dynamics. Equations of motion for spinning bodies in GR have been developed by numerous authors, and in the meantime go way beyond the leading order contributions (for reviews and references see, e.g., [34, 44–46]). For present day pulsar-timing experiments it is sufficient to have a look at the post-Newtonian leading order contributions. There, one finds three contributions: the spin-orbit (SO) interaction between the pulsar’s spin \mathbf{S}_p and the orbital angular momentum \mathbf{L} , the SO interaction between the companion’s spin \mathbf{S}_c and the orbital angular momentum, and finally the spin-spin interaction between the spin of the pulsar and the spin of the companion [44].

Spin-spin interaction will remain negligible in binary pulsar experiments for the foreseeable future. They are many orders of magnitude below the second post-Newtonian and spin-orbit effects [47], and many orders of magnitude below the measurement precision of present timing experiments. For this reason, we will not further discuss spin-spin effects here.

For a boost invariant gravity theory, the (acceleration-dependent) Lagrangian for the spin-orbit interaction has the following general form (summation over spatial indices i, j)

$$L_{\text{SO}}(\mathbf{x}_A, \mathbf{v}_A, \mathbf{a}_A) = \frac{1}{c^2} \sum_A S_A^{ij} \left[\frac{1}{2} v_A^i a_A^j + \sum_{B \neq A} \frac{\Gamma_A^B m_B}{r_{AB}^3} (v_A^i - v_B^i)(x_A^j - x_B^j) \right], \quad (3)$$

where $S_A^{ij} \equiv \varepsilon^{ijk} S_A^k$ is the antisymmetric spin tensor of body A [34, 39, 48]. The coupling function Γ_A^B can also account for strong-field effects in the spin-orbit coupling. In GR $\Gamma_A^B = 2G$. For bodies with negligible gravitational self-energy, one finds in the framework of the *parametrized post-Newtonian (PPN) formalism*² $\Gamma_A^B = (\gamma_{\text{PPN}} + 1)G$, a quantity that is actually most tightly constrained by the light-bending and Shapiro-delay experiments in the Solar system, which test γ_{PPN} [8, 9, 11, 49].

In binary pulsars, spin-orbit coupling has two effects. On the one hand, it adds spin-dependent terms to the equations of motion (1), which cause a Lense-Thirring precession of the orbit (for GR see [44, 50]). So far this contribution could not be tested in binary pulsar experiments. Prospects of its measurement will be discussed in the future outlook in Sect. 5. On the other hand it leads to secular changes in the orientation of the spins of the two bodies (geodetic precession), most importantly the observed pulsar in a pulsar binary [44, 51, 52]. As we discuss in more details in Sect. 3, a change in the rotational axis of the pulsar causes changes in the observed

²The PPN formalism uses 10 parameters to parametrize in a generic way deviations from GR at the post-Newtonian level, within the class of metric gravity theories (see [5] for details).

emission properties of the pulsar, as the line-of-sight gradually cuts through different regions of the magnetosphere.

As can be derived from (3), to first order in GR the geodetic precession of the pulsar, averaged over one orbit, is given by ($\hat{\mathbf{L}} \equiv \mathbf{L}/|\mathbf{L}|$)

$$\Omega_p^{\text{SO}} = \frac{n_b}{1-e^2} \left[2 + \frac{3m_c}{2m_p} \right] \frac{m_p m_c}{M^2} \frac{V_b^2}{c^2} \hat{\mathbf{L}}, \quad (4)$$

where $n_b \equiv 2\pi/P_b$ and $V_b \equiv (GMn_b)^{1/3}$.

It is expected that in alternative theories relativistic spin precession generally depends on self-gravitational effects, meaning, the actual precession may depend on the compactness of a self-gravitating body. For the class of theories that lead to the Lagrangian (3), Eq. (4) modifies to

$$\Omega_p^{\text{SO}} = \frac{n_b}{1-e^2} \left[\frac{\Gamma_p^c}{\mathcal{G}} + \left(\frac{\Gamma_p^c}{\mathcal{G}} - \frac{1}{2} \right) \frac{m_c}{m_p} \right] \frac{m_p m_c}{M^2} \frac{\mathcal{V}_b^2}{c^2} \hat{\mathbf{L}}, \quad (5)$$

where $\mathcal{V}_b \equiv (\mathcal{G}Mn_b)^{1/3}$ is the strong-field generalization of V_b .

Effects from spin-induced quadrupole moments are negligible as well. For double neutron-star systems they are many orders of magnitude below the second post-Newtonian and spin-orbit effects, due to the small extension of the bodies [47]. If the companion is a more extended star, like a white dwarf or a main-sequence star, the rotationally-induced quadrupole moment might become important. For all the binary pulsars discussed here, the quadrupole moments of pulsar and companion are (currently) negligible.

Finally, certain gravitational phenomena, not present in GR, can even lead to a spin precession of isolated pulsars, for instance, a violation of the local Lorentz invariance in the gravitational sector, as we will discuss in more details in Sect. 4.

1.4 Phenomenological Approach to Relativistic Effects in Binary Pulsar Observations

For binary pulsar experiments that test the quasi-stationary strong-field regime (G2) and the gravitational wave damping (GW), a phenomenological parametrization, the so-called ‘parametrized post-Keplerian’ (PPK) formalism, has been introduced by Damour [53] and extended by Damour and Taylor [39]. The PPK formalism parametrizes all the observable effects that can be extracted independently from binary pulsar timing and pulse-structure data. Consequently, the PPK formalism allows to obtain theory-independent information from binary pulsar observations by fitting for a set of *Keplerian* and *post-Keplerian parameters*.

The description of the orbital motion is based on the quasi-Keplerian parametrization of Damour and Deruelle, which is a solution to the first post-Newtonian equations of motion [41, 54]. The corresponding *Roemer delay* in the arrival time of the pulsar signals is

$$\Delta_R = x \sin \omega [\cos U - e(1 + \delta_r)] + x \cos \omega \left[1 - e^2(1 + \delta_\theta)^2 \right]^{1/2} \sin U, \quad (6)$$

where the eccentric anomaly U is linked to the proper time of the pulsar T via the Kepler equation

$$U - e \sin U = 2\pi \left[\left(\frac{T - T_0}{P_b} \right) - \frac{\dot{P}_b}{2} \left(\frac{T - T_0}{P_b} \right)^2 \right]. \quad (7)$$

The five Keplerian parameters P_b , e , x , ω , and T_0 denote the orbital period, the orbital eccentricity, the projected semi-major axis of the pulsar orbit, the longitude of periastron, and the time of periastron passage, respectively. The post-Keplerian parameter δ_r is not separately measurable, i.e. it can be absorbed into other timing parameters, and the post-Keplerian parameter δ_θ has not been measured up to now in any of the binary pulsar systems. The relativistic precession of periastron changes the longitude of periastron ω according to

$$\omega = \omega_0 + \dot{\omega} \frac{P_b}{\pi} \arctan \left[\left(\frac{1+e}{1-e} \right)^{1/2} \tan \frac{U}{2} \right], \quad (8)$$

meaning, that averaged over a full orbit, the location of periastron shifts by an angle $\dot{\omega} P_b$. The parameter $\dot{\omega}$ is the corresponding post-Keplerian parameter. A change in the orbital period, due to the emission of gravitational waves, is parametrized by the post-Keplerian parameter \dot{P}_b .

Besides the Roemer delay Δ_R , there are two purely relativistic effects that play an important role in pulsar timing experiments. In an eccentric orbit, one has a changing time dilation of the “pulsar clock” due to a variation in the orbital velocity of the pulsar and a change of the gravitational redshift caused by the gravitational field of the companion. This so-called *Einstein delay* is a periodic effect, whose amplitude is given by the post-Keplerian parameter γ , and to first order can be written as

$$\Delta_E = \gamma \sin U. \quad (9)$$

For sufficiently edge-on and/or eccentric orbits the propagation delay suffered by the pulsar signals in the gravitational field of the companion becomes important. This so-called *Shapiro delay*, to first order, reads

$$\Delta_S = -2r \ln \left[1 - e \cos U - s \sin \omega (\cos U - e) - s \cos \omega (1 - e^2)^{1/2} \sin U \right], \quad (10)$$

where the two post-Keplerian parameters r and s are called *range* and *shape* of the Shapiro delay. The latter is linked to the inclination of the orbit with respect to the line of sight, i , by $s = \sin i$. It is important to note, that for $i \rightarrow 90^\circ$ Eq. (10) breaks down and higher order corrections are needed. But so far, Eq. (10) is fully sufficient for the timing observations of known pulsars [55].

Concerning the post-Keplerian parameters related to quasi-stationary effects, for the wide class of boost-invariant gravity theories one finds that they can be expressed as functions of the Keplerian parameters, the masses, and parameters generically accounting for gravitational self-field effects (cf. Eq. (2)) [5, 39]:

$$\dot{\omega} = \frac{n_b}{1-e^2} \left[\varepsilon - \frac{\xi}{2} + \frac{1}{2} \right] \frac{\mathcal{V}_b^2}{c^2}, \quad (11)$$

$$\gamma = \frac{e}{n_b} \left[\frac{G_{0c}}{\mathcal{G}} + \mathcal{K}_p^c + \frac{m_c}{M} \right] \frac{m_c}{M} \frac{\mathcal{V}_b^2}{c^2}, \quad (12)$$

$$r = \frac{1 + \varepsilon_{0c}}{4} \frac{G_{0c} m_c}{c^3}, \quad (13)$$

$$s = x n_b \frac{M}{m_c} \frac{c}{\mathcal{V}_b}, \quad (14)$$

plus Ω^{SO} from Eq. (5). Here we have listed only those parameters that play a role in this article. For a complete list and a more detailed discussion, the reader is referred to [39]. The quantities G_{0c} and ε_{0c} are related to the interaction of the companion with a test particle or a photon. The parameter \mathcal{K}_p^c accounts for a possible change in the moment of inertia of the pulsar due to a change in the local gravitational constant. In GR one finds $\mathcal{G} = G_{0c} = G$, $\varepsilon = \varepsilon_{0c} = 3$, $\xi = 1$ and $\mathcal{K}_p^c = 0$. Consequently

$$\dot{\omega}^{\text{GR}} = \frac{3n_b}{1-e^2} \frac{V_b^2}{c^2}, \quad (15)$$

$$\gamma^{\text{GR}} = \frac{e}{n_b} \left[1 + \frac{m_c}{M} \right] \frac{m_c}{M} \frac{V_b^2}{c^2}, \quad (16)$$

$$r^{\text{GR}} = \frac{G m_c}{c^3}, \quad (17)$$

$$s^{\text{GR}} = x n_b \frac{M}{m_c} \frac{c}{V_b}. \quad (18)$$

These parameters are independent of the internal structure of the neutron star(s), due to the effacement of the internal structure, a property of GR [34, 37]. For most alternative gravity theories this is not the case. For instance, in the mono-scalar-tensor theories $T_1(\alpha_0, \beta_0)$ of [56, 57], one finds³

³The mono-scalar-tensor theories $T_1(\alpha_0, \beta_0)$ of [56, 57] have a conformal coupling function $A(\varphi) = \alpha_0(\varphi - \varphi_0) + \beta_0(\varphi - \varphi_0)^2/2$. The Jordan-Fierz-Brans-Dicke gravity is the sub-class with $\beta_0 = 0$, and $\alpha_0^2 = (2\omega_{\text{BD}} + 3)^{-1}$.

$$\dot{\omega}^{T_1} = \frac{n_b}{1-e^2} \left[\frac{3 - \alpha_p \alpha_c}{1 + \alpha_p \alpha_c} - \frac{m_p \alpha_p^2 \beta_c + m_c \alpha_c^2 \beta_p}{2M(1 + \alpha_p \alpha_c)^2} \right] \frac{\mathcal{V}_b^2}{c^2}, \quad (19)$$

$$\gamma^{T_1} = \frac{e}{n_b} \left[\frac{1 + k_p \alpha_c}{1 + \alpha_p \alpha_c} + \frac{m_c}{M} \right] \frac{m_c}{M} \frac{\mathcal{V}_b^2}{c^2}, \quad (20)$$

$$r^{T_1} = \frac{G_* m_c}{c^3}, \quad (21)$$

$$s^{T_1} = x n_b \frac{M}{m_c} \frac{c}{\mathcal{V}_b}, \quad (22)$$

where $\mathcal{V}_b = [G_*(1 + \alpha_p \alpha_c) M n_b]^{1/3}$. The body-dependent quantities α_p and α_c denote the effective scalar coupling of pulsar and companion respectively, and $\beta_A \equiv \partial \alpha_A / \partial \varphi_0$ where φ_0 denotes the asymptotic value of the scalar field at spatial infinity. The quantity k_p is related to the moment of inertia I_p of the pulsar via $k_p \equiv -\partial \ln I_p / \partial \varphi_0$. For a given equation of state, the parameters α_A , β_A , and k_A depend on the fundamental constants of the theory, e.g. α_0 and β_0 in $T_1(\alpha_0, \beta_0)$, and the mass of the body. As we will demonstrate later, these “gravitational form factors” can assume large values in the strong gravitational fields of neutron stars. Depending on the value of β_0 , this is even the case for a vanishingly small α_0 , where there are practically no measurable deviations from GR in the Solar system. In fact, even for $\alpha_0 = 0$, a neutron star, above a certain β_0 -dependent critical mass, can have an effective scalar coupling α_A of order unity. This non-perturbative strong-field behavior, the so-called “spontaneous scalarization” of a neutron star, was discovered 20 years ago by Damour and Esposito-Farèse [56].

Finally, there is the post-Keplerian parameter \dot{P}_b , related to the damping of the orbit due to the emission of gravitational waves. We have seen above that in alternative gravity theories the back reaction from the gravitational wave emission might enter the equations of motion already at the 1.5 post-Newtonian level, giving rise to a $\dot{P}_b \propto \mathcal{V}_b^3 / c^3$. To leading order one finds in mono-scalar-tensor gravity the dipolar contribution from the scalar field [57–59]:

$$\dot{P}_b = -2\pi \frac{m_p m_c}{M^2} \frac{1 + e^2/2}{(1 - e^2)^{5/2}} \frac{\mathcal{V}_b^3}{c^3} \frac{(\alpha_p - \alpha_c)^2}{1 + \alpha_p \alpha_c} + \mathcal{O}(\mathcal{V}_b^5 / c^5). \quad (23)$$

As one can see, the change in the orbital period due to dipolar radiation depends strongly on the difference in the effective scalar coupling α_A . Binary pulsar systems with a high degree of asymmetry in the compactness of their components are therefore ideal to test for dipolar radiation. An order unity difference in the effective scalar coupling would lead to a change in the binary orbit, which is several orders of magnitude ($\sim c^2 / \mathcal{V}_b^2$) stronger than the quadrupolar damping predicted by GR. For GR one finds from the well-known *quadrupole formula* [60]:

$$\dot{P}_b^{\text{GR}} = -\frac{192\pi}{5} \frac{m_p m_c}{M^2} \frac{1 + 73e^2/24 + 37e^4/96}{(1 - e^2)^{7/2}} \frac{\mathcal{V}_b^5}{c^5}. \quad (24)$$

Apart from a change in the orbital period, gravitational wave damping will also affect other post-Keplerian parameters. While gravitational waves carry away orbital energy and angular momentum, Keplerian parameters like the eccentricity and the semi-major axis of the pulsar orbit change as well. The corresponding post-Keplerian parameters are \dot{e} and \dot{x} respectively. However, these changes affect the arrival times of the pulsar signals much less than the \dot{P}_b , and therefore do (so far) not play a role in the radiative tests with binary pulsars.

As already mentioned in Sect. 1.2, there is no generic connection between the higher-order gravitational wave damping effects and the parameters \mathcal{G} , ε , and ξ of the modified Einstein-Infeld-Hoffmann formalism. Such higher order, mixed radiative and strong-field effects depend in a complicated way on the structure of the gravity theory [39].

The post-Keplerian parameters are at the foundation of many of the gravity tests conducted with binary pulsars. As shown above, the exact functional dependence differs for given theories of gravity. A priori, the masses of the pulsar and the companion are undetermined, but they represent the only unknowns in this set of equations. Hence, once two post-Keplerian parameters are measured, the corresponding equations can be solved for the two masses, and the values for other post-Keplerian parameters can be predicted for an assumed theory of gravity. Any further post-Keplerian measurement must therefore be consistent with that prediction, otherwise the assumed theory has to be rejected. In other words, if $N \geq 3$ post-Keplerian parameters can be measured, a total of $N - 2$ independent tests can be performed. The method is very powerful, as any additionally measured post-Keplerian parameter is potentially able to fail the prediction and hence to falsify the tested theory of gravity. The standard graphical representation of such tests, as will become clear below, is the mass-mass diagram. Every measured post-Keplerian parameter defines a curve of certain width (given by the measurement uncertainty of the post-Keplerian parameter) in a m_p - m_c diagram. A theory has passed a binary pulsar test, if there is a region in the mass-mass diagram that agrees with all post-Keplerian parameter curves.

2 Gravitational Wave Damping

2.1 The Hulse-Taylor Pulsar

The first binary pulsar to ever be observed happened to be a rare double neutron star system. It was discovered by Russell Hulse and Joseph Taylor in summer 1974 [18]. The pulsar, PSR B1913+16, has a rotational period of 59 ms and is in a highly eccentric ($e = 0.62$) 7.75-h orbit around an unseen companion. Shortly after the discovery of PSR B1913+16, it has been realized that this system may allow the observation of gravitational wave damping within a time span of a few years [61, 62].

Table 2 Observed orbital timing parameters of PSR B1913+16, based on the Damour-Deruelle timing model (taken from [29])

T_0	Time of periastron passage (MJD)	52144.90097841(4)
x	Projected semi-major axis of the pulsar orbit (s)	2.341782(3)
e	Orbital eccentricity	0.6171334(5)
P_b	Orbital period at T_0 (d)	0.322997448911(4)
ω_0	Longitude of periastron at T_0 (deg)	292.54472(6)
$\dot{\omega}$	Secular advance of periastron (deg/yr)	4.226598(5)
γ	Amplitude of Einstein delay (ms)	4.2992(8)
\dot{P}_b	Secular change of orbital period	$-2.423(1) \times 10^{-12}$

Figures in parentheses represent estimated uncertainties in the last quoted digit

The first relativistic effect seen in the timing observations of the Hulse-Taylor pulsar was the secular advance of periastron $\dot{\omega}$. Thanks to its large value of 4.2 deg/yr, this effect was well measured already one year after the discovery [63]. Due to the, a priori, unknown masses of the system, this measurement could not be converted into a quantitative gravity test. However, assuming GR is correct, Eq. (15) gives the total mass M of the system. From the modern value given in Table 2 one finds $M = m_p + m_c = 2.828378 \pm 0.000007 M_\odot$ [29].⁴

It took a few more years to measure the Einstein delay (9) with good precision. In a single orbit this effect is exactly degenerate with the Roemer delay, and only due to the relativistic precession of the orbit these two delays become separable [61, 65]. By the end of 1978, the timing of PSR B1913+16 yielded a measurement of the post-Keplerian parameter γ , which is the amplitude of the Einstein delay [66]. Together with the total mass from $\dot{\omega}^{\text{GR}}$, Eq. (16) can now be used to calculate the individual masses. With the modern value for γ from Table 2, and the total mass given above, one finds the individual masses $m_p = 1.4398 \pm 0.0002 M_\odot$ and $m_c = 1.3886 \pm 0.0002 M_\odot$ for pulsar and companion respectively [29].

With the knowledge of the two masses, m_p and m_c , the binary system is fully determined, and further GR effects can be calculated and compared with the observed values, providing an intrinsic consistency check of the theory. In fact, Taylor et al. [66] reported the measurement of a decrease in the orbital period \dot{P}_b , consistent with the quadrupole formula (24). This was the first proof for the existence of gravitational waves as predicted by GR. In the meantime the \dot{P}_b is measured with a precision of 0.04 % (see Table 2). However, this is not the precision with which the validity of the quadrupole formula is verified in the PSR B1913+16 system. The observed \dot{P}_b needs to be corrected for extrinsic effects, most notably the differential Galactic acceleration and the Shklovskii effect, to obtain the intrinsic value caused by gravitational wave

⁴Strictly speaking, this is the total mass of the system scaled with an unknown Doppler factor D , i.e. $M^{\text{observed}} = D^{-1} M^{\text{intrinsic}}$ [39]. For typical velocities, $D - 1$ is expected to be of order 10^{-4} , see for instance [64]. In gravity tests based on post-Keplerian parameters, the factor D drops out and is therefore irrelevant [54].

damping [67, 68]. The extrinsic contribution due to the Galactic gravitational field (acceleration \mathbf{g}) and the proper motion (transverse angular velocity in the sky μ) are given by

$$\delta \dot{P}_b^{\text{ext}} = \frac{P_b}{c} \left[\hat{\mathbf{K}}_0 \cdot (\mathbf{g}_{\text{PSR}} - \mathbf{g}_{\odot}) + \mu^2 d \right], \quad (25)$$

where $\hat{\mathbf{K}}_0$ is the unit vector pointing towards the pulsar, which is at a distance d from the Solar system. For PSR B1913+16, P_b and $\hat{\mathbf{K}}_0$ are measured with very high precision, and also μ is known with good precision ($\sim 8\%$). However, there is a large uncertainty in the distance d , which is also needed to calculate the Galactic acceleration of the PSR B1913+16 system, \mathbf{g}_{PSR} , in Eq. (25). Due to its large distance, there is no direct parallax measurement for d , and estimates of d are based on model-dependent methods, like the measured column density of free electrons between PSR B1913+16 and the Earth. Such methods are known to have large systematic uncertainties, and for this reason the distance to PSR B1913+16 is not well known: $d = 9.9 \pm 3.1$ kpc [29, 69]. In addition, there are further uncertainties, e.g. in the Galactic gravitational potential and the distance of the Earth to the Galactic center. Accounting for all these uncertainties leads to an agreement between $\dot{P}_b - \delta \dot{P}_b^{\text{ext}}$ and \dot{P}_b^{GR} at the level of about 0.3 % [29]. The corresponding mass-mass diagram is given in Fig. 4. As the precision of the radiative test with PSR B1913+16 is limited by the model-dependent uncertainties in Eq. (25), it is not expected that this test can be significantly improved in the near future.

Fig. 4 Mass-mass diagram for PSR B1913+16 based on GR and the three observed post-Keplerian parameters $\dot{\omega}$ (black), γ (red) and \dot{P}_b (blue). The dashed \dot{P}_b curve is based on the observed \dot{P}_b , without corrections for Galactic and Shklovskii effects. The solid \dot{P}_b curve is based on the corrected (intrinsic) \dot{P}_b , where the *thin lines* indicate the one-sigma boundaries. Values are taken from Table 2

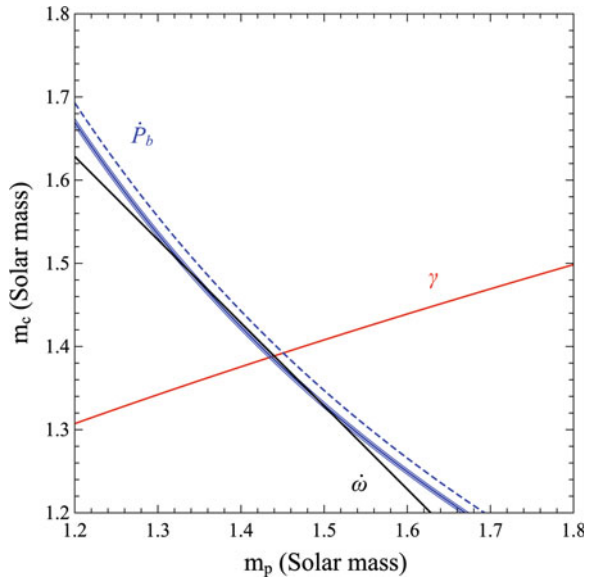
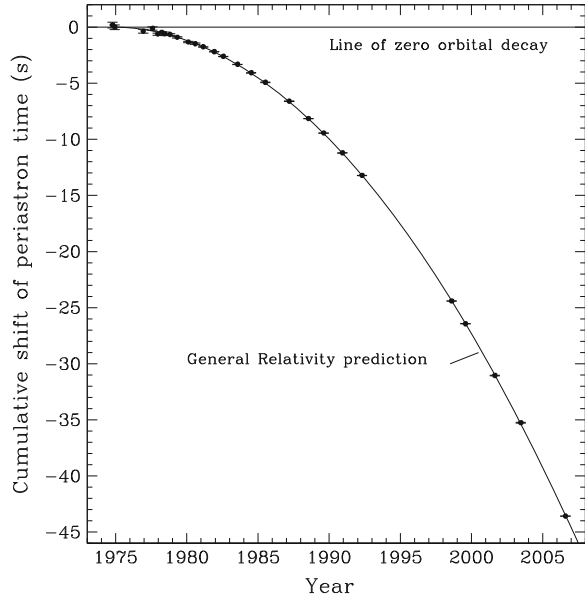


Fig. 5 Shift in the time of periastron passage of PSR B1913+16 due to gravitational wave damping. The parabola represents the GR prediction and the data points the timing measurements, with (vertical) error bars mostly too small to be resolved. The observed shift in periastron time is a direct measurement of the change in the world-line of the pulsar due to the back-reaction of the emitted gravitational waves (cf. Figure 3). The corresponding spatial shift amounts to about 20,000 km. Figure is taken from [29]



Finally, besides the mass-mass diagram, there is a different way to illustrate the test of gravitational wave damping in PSR B1913+16. According to Eq. (7), the change in the orbital period, i.e. the post-Keplerian parameter \dot{P}_b , is measured from a shift in the time of periastron passage, where U is a multiple of 2π . One finds for the shift in periastron time, as compared to an orbit with zero decay

$$\Delta T = \frac{1}{2} P_b \dot{P}_b n^2 + \mathcal{O}(P_b \dot{P}_b^2 n^3), \quad (26)$$

where $n = 0, 1, 2, \dots$ denotes the number of the periastron passage, and is given by $n \simeq (T - T_0)/P_b$. Equation (26) represents a parabola in time, which can be calculated with high precision using the masses that come from $\dot{\omega}^{\text{GR}}$ and γ^{GR} (see above). On the other hand, the observed cumulative shift in periastron can be extracted from the timing observations with high precision. A comparison of observed and predicted cumulative shift in the time of the periastron passage is given in Fig. 5.

2.2 The Double Pulsar—The Best Test for Einstein’s Quadrupole Formula, and More

In 2003 a binary system was discovered where, at first, one member was identified as a pulsar with a 23 ms period [70], before about half a year later, the companion was also recognized as a radio pulsar with a period of 2.8 s [71]. Both pulsars, known as

PSRs J0737–3039A and J0737–3039B, respectively, (or *A* and *B* hereafter), orbit each other in less than 2.5 h in a mildly eccentric ($e = 0.088$) orbit. As a result, the system is not only the first and only double neutron star system where both neutron stars are visible as active radio pulsars, but it is also the most relativistic binary pulsar laboratory for gravity known to date [72]. Just to give an example for the strength of relativistic effects, the advance of periastron, $\dot{\omega}$, is 17 degrees per year, meaning that the eccentric orbit does a full rotation in just 21 years. In this subsection, we briefly discuss the properties of this unique system, commonly referred to as the *Double Pulsar*, and highlight some of the gravity tests that are based on the radio observations of this system. For detailed reviews of the Double Pulsar see [72, 73].

In the Double Pulsar system a total of six post-Keplerian parameters have been measured by now. Five arise from four different relativistic effects visible in pulsar timing [74], while a sixth one can be determined from the effects of geodetic precession, which will be discussed in detail below. The relativistic precession of the orbit, $\dot{\omega}$, was measured within a few days after timing of the system commenced, and by 2006 it was already known with a precision of 0.004 % (see Table 3). At the same time the measurement of the amplitude of Einstein delay, γ , reached 0.7 % (see Table 3). Due to the periastron precession of 17 degrees per year, the Einstein delay was soon well separable from the Roemer delay. Two further post-Keplerian parameters came from the detection of the Shapiro delay: the *shape* and *range* parameters s and r . They were measured with a precision of 0.04 and 5 %, respectively (see Table 3). From the measured value $s = \sin i = 0.99974^{+0.00016}_{-0.00039}$ ($i = 88.7^{+0.5}_{-0.8}^\circ$) one can already see how exceptionally edge-on this system is. Finally, the decrease of the orbital period due to gravitational wave damping was measured with a precision of 1.4 % just three years after the discovery of the system (see Table 3).

A unique feature of the Double Pulsar is its nature as a “dual-line source”, i.e. we measure the orbits of both neutron stars at the same time. Obviously, the sizes of the two orbits are not independent from each other as they orbit a common center

Table 3 A selection of observed orbital timing parameters of the Double Pulsar, based on the Damour-Deruelle timing model (taken from [74])

$x_A \equiv a_A \sin i/c$	Projected semi-major axis of <i>A</i> (s)	1.415032(1)
$x_B \equiv a_B \sin i/c$	projected semi-major axis of <i>B</i> (s)	1.5161(16)
e	Orbital eccentricity	0.0877775(9)
P_b	Orbital period (d)	0.10225156248(5)
$\dot{\omega}$	Secular advance of periastron (deg/yr)	16.89947(68)
γ	amplitude of Einstein delay for <i>A</i> (ms)	0.3856(26)
\dot{P}_b	Secular change of orbital period	$-1.252(17) \times 10^{-12}$
s	<i>Shape</i> of Shapiro delay for <i>A</i>	0.99974(−39, +16)
r	<i>Range</i> of Shapiro delay for <i>A</i> (μ s)	6.21(33)

All post-Keplerian parameters below are obtained from the timing of pulsar *A*. The timing precision for pulsar *B* is considerably lower, and allows only for a, in comparison, low precision measurement ($\sim 0.3\%$) of $\dot{\omega}$ [74]. Figures in parentheses represent estimated uncertainties in the last quoted digit

of mass. In GR, up to first post-Newtonian order the relative size of the orbits is identical to the inverse ratio of masses. Hence, by measuring the orbits of the two pulsars (relative to the centre of mass), we obtain a precise measurement of the mass ratio. This ratio is directly observable, as the orbital inclination angle is obviously identical for both pulsars, i.e.

$$R \equiv \frac{m_A}{m_B} = \frac{a_B}{a_A} = \frac{a_B \sin i/c}{a_A \sin i/c} \equiv \frac{x_B}{x_A}. \quad (27)$$

This expression is not just limited to GR. In fact, it is valid up to first post-Newtonian order and free of any explicit strong-field effects in any Lorentz-invariant theory of gravity (see [40] for a detailed discussion). Using the parameter values of Table 3, one finds that in the Double Pulsar the masses are nearly equal with $R = 1.0714 \pm 0.0011$.

As it turns out, all the post-Keplerian parameters measured from timing are consistent with GR. In addition, the region of allowed masses agrees well with the measured mass ratio R (see Fig. 6). One has to keep in mind, that the test presented here is based on data published in 2006 [74]. In the meantime continued timing lead to a significant decrease in the uncertainties of the post-Keplerian parameters of the Double pulsar. This is especially the case for \dot{P}_b , for which the uncertainty typically decreases with $T_{\text{obs}}^{-2.5}$ [75], T_{obs} being the total time span of timing observations. The new results will be published in an upcoming publication (Kramer et al., in prep.).

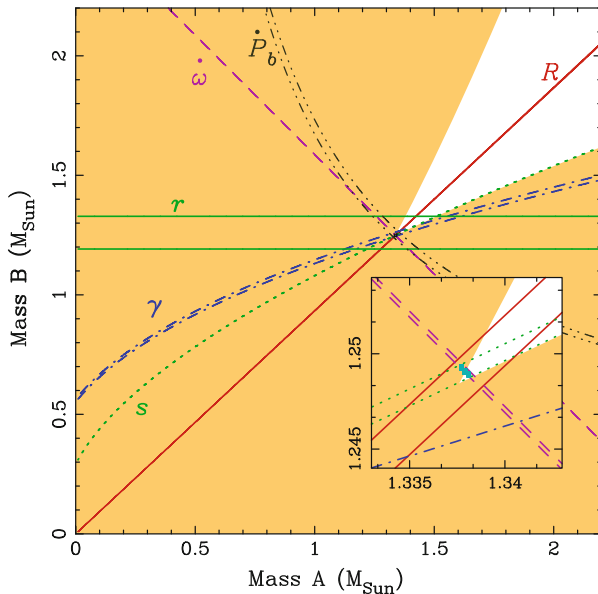


Fig. 6 GR mass-mass diagram based on timing observations of the Double Pulsar. The *orange areas* are excluded simply by the fact that $\sin i \leq 1$. The figure is taken from [72] (Ω_{SO} lines removed) and based on the timing solution published in [74]

As reported in [33], presently the Double Pulsar provides the best test for the GR quadrupole formalism for gravitational wave generation, with an uncertainty well below the 0.1 % level. As discussed above, the Hulse-Taylor pulsar is presently limited by uncertainties in its distance. This raises the valid question, at which level such uncertainties will start to limit the radiative test with the Double Pulsar as well. Compared to the Hulse-Taylor pulsar, the Double Pulsar is much closer to Earth. Because of this, a direct distance estimate of $1.15^{+0.22}_{-0.16}$ kpc based on a parallax measurement with long-baseline interferometry was obtained [76]. Thus, with the current accuracy in the measurement of distance and transverse velocity, GR tests based on \dot{P}_b can be taken to the 0.01 % level.

With the large number of post-Keplerian parameters and the known mass ratio, the Double Pulsar is the most over-constrained binary pulsar system. For this reason, one can do more than just testing specific gravity theories. The Double Pulsar allows for certain generic tests on the orbital dynamics, time dilation, and photon propagation of a spacetime with two strongly self-gravitating bodies [72]. First, the fact that the Double Pulsar gives access to the mass ratio, R , in any Lorentz-invariant theory of gravity, allows us to determine $m_A/M = R/(1 + R) = 0.51724 \pm 0.00026$ and $m_B/M = 1/(1 + R) = 0.48276 \pm 0.00026$. With this information at hand, the measurement of the shape of the Shapiro delay s can be used to determine \mathcal{V}_b via Eq. (14): $\mathcal{V}_b/c = (2.0854 \pm 0.0014) \times 10^{-3}$. At this point, the measurement of the post-Keplerian parameters $\dot{\omega}$, γ , and r (Eqs. (11)–(13)) can be used to impose restrictions on the “strong-field” parameters of Lagrangian (2) [72]:

$$\frac{2\varepsilon - \xi}{5} = 0.9995 \pm 0.0016, \quad (28)$$

$$\frac{G_{0B}}{\mathcal{G}} + \mathcal{K}_A^B = 1.005 \pm 0.010, \quad (29)$$

$$\frac{\varepsilon_{0B} + 1}{4} \frac{G_{0B}}{\mathcal{G}} = 1.009 \pm 0.054. \quad (30)$$

This is in full agreement with GR, which predicts one for all three of these expressions. Consequently, nature cannot deviate much from GR in the quasi-stationary strong-field regime of gravity (G2 in Fig. 1).

2.3 PSR J1738+0333—The Best Test for Scalar-Tensor Gravity

The best “pulsar clocks” are found amongst the fully recycled millisecond pulsars, which have rotational periods less than about 10 ms (see e.g. [77]). A result of the stable mass transfer between companion and pulsar in the past—responsible for the recycling of the pulsar—is a very efficient circularization of the binary orbit, that leads to a pulsar-white dwarf system with very small residual eccentricity [78]. For

such systems, the post-Keplerian parameters $\dot{\omega}$ and γ are generally not observable. There are a few cases where the orbit is seen sufficiently edge-on, so that a measurement of the Shapiro delay gives access to the two post-Keplerian parameters r and s with good precision (see e.g. [79], which was the first detection of a Shapiro delay in a binary pulsar). With these two parameters the system is then fully determined, and in principle can be used for a gravity test in combination with a third measured (or constrained) post-Keplerian parameter (e.g. \dot{P}_b). Besides the Shapiro delay parameters, some of the circular binary pulsar systems offer a completely different access to their masses, which is not solely based on the timing observations in the radio frequencies. If the companion star is bright enough for optical spectroscopy, then we have a dual-line system, where the Doppler shifts in the spectral lines can be used, together with the timing observations of the pulsar, to determine the mass ratio R . Furthermore, if the companion is a white dwarf, the spectroscopic information in combination with models of the white dwarf and its atmosphere can be used to determine the mass of the white dwarf m_c , ultimately giving the mass of the pulsar via $m_p = R m_c$. As we will see in this and the following subsection, two of the best binary pulsar systems for gravity tests have their masses determined through such a combination of radio and optical astronomy.

PSR J1738+0333 was discovered in 2001 [80]. It has a spin period P of 5.85 ms and is a member of a low-eccentricity ($e < 4 \times 10^{-7}$) binary system with an orbital period P_b of just 8.5 h. The companion is an optically bright low-mass white dwarf. Extensive timing observation over a period of 10 years allowed a determination of astrometric, spin and orbital parameters with high precision [28], most notably

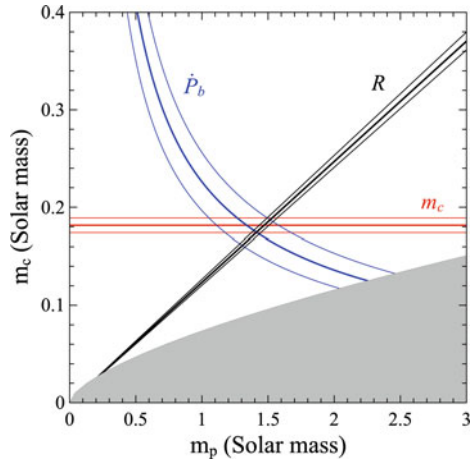
- A change in the orbital period of $(-17.0 \pm 3.1) \times 10^{-15}$.
- A timing parallax, which gives a model independent distance estimate of $d = 1.47 \pm 0.10$ kpc.

The latter is important to correct for the Shklovskii effect and the differential Galactic acceleration to obtain the intrinsic \dot{P}_b (cf. Eq. (25)). Additional spectroscopic observations of the white dwarf gave the mass ratio $R = 8.1 \pm 0.2$ and the companion mass $m_c = 0.181_{-0.005}^{+0.007} M_\odot$, and consequently the pulsar mass $m_p = 1.47_{-0.06}^{+0.07} M_\odot$ [81]. It is important to note, that the mass determination for PSR B1738+0333 is free of any explicit strong-field contributions, since this is the case for the mass ratio [40], and certainly for the mass of the white dwarf, which is a weakly self-gravitating body, i.e. a gravity regime that has been well tested in the Solar system (G1 in Fig. 1).

After using Eq. (25) to correct for the Shklovskii contribution, $\delta \dot{P}_b = P_b \mu^2 d / c = (8.3_{-0.5}^{+0.6}) \times 10^{-15}$, and the contribution from the Galactic differential acceleration, $\delta \dot{P}_b = (0.58_{-0.14}^{+0.16}) \times 10^{-15}$, one finds an intrinsic orbital period change due to gravitational wave damping of $\dot{P}_b^{\text{intr}} = (-25.9 \pm 3.2) \times 10^{-15}$. This value agrees well with the prediction of GR, as can be seen in Fig. 7.

The radiative test with PSR J1738+0333 represents a $\sim 15\%$ verification of GR's quadrupole formula. A comparison with the $< 0.1\%$ test from the Double Pulsar (see Sect. 2.2) raises the valid question of whether the PSR J1738+0333 experiment is teaching us something new about the nature of gravity and the validity of GR. To

Fig. 7 GR mass-mass diagram based on the timing observations of PSR J1738+0333 and the optical observations of its white-dwarf companion respectively. The *thin lines* indicate the one-sigma errors of the measured parameters. The *grey area* is excluded by the condition $\sin i \leq 1$



address this question, let's have a look at Eq. (23). Dipolar radiation can be a strong source of gravitational wave damping, if there is a sufficient difference between the effective coupling parameters α_p and α_c of pulsar and companion respectively. For the Double Pulsar, where we have two neutron stars with $m_p \approx m_c$, one generally expects that $\alpha_p \approx \alpha_c$, and therefore the effect of dipolar radiation would be strongly suppressed. On the other hand, in the PSR J1738+0333 system there is a large difference in the compactness of the two bodies. For the weakly self-gravitating white-dwarf companion $\alpha_c \simeq \alpha_0$, i.e. it assumes the weak-field value,⁵ while the strongly self-gravitating pulsar can have an α_p that significantly deviates from α_0 . In fact, as discussed in Sect. 1.4, α_p can even be of order unity in the presence of effects like strong-field scalarization. In the absence of non-perturbative strong-field effects one can do a first order estimation $(\alpha_p - \alpha_c) \propto (\epsilon_p - \epsilon_c) + \mathcal{O}(\epsilon^2)$. For the Double Pulsar one finds $(\epsilon_p - \epsilon_c)^2 \approx 6 \times 10^{-5}$, which is significantly smaller than for the PSR J1738+0333 system, which has $(\epsilon_p - \epsilon_c)^2 \approx 0.012$.⁶ As a consequence, the orbital decay of asymmetric systems like PSR J1738+0333 could still be dominated by dipolar radiation, even if the Double Pulsar agrees with GR. For this reason, PSR J1738+0333 is particularly useful to test gravity theories that violate the strong equivalence principle and therefore predict the emission of dipolar radiation. A well known class of gravity theories, where this is the case, are scalar-tensor theories. As it turns out, PSR J1738+0333 is currently the best test system for these alternatives to GR (see Fig. 8). In terms of Eq. (23), one finds

$$|\alpha_p - \alpha_c| < 2 \times 10^{-3} \quad (95\% \text{ confidence}), \quad (31)$$

⁵From the Cassini experiment [11] one obtains $|\alpha_0| < 3 \times 10^{-3}$ (95 % confidence).

⁶These numbers are based on the equation of state MPA1 in [82]. Within GR, MPA1 has a maximum neutron-star mass of $2.46 M_\odot$, which can also account for the high-mass candidates of [83–85].

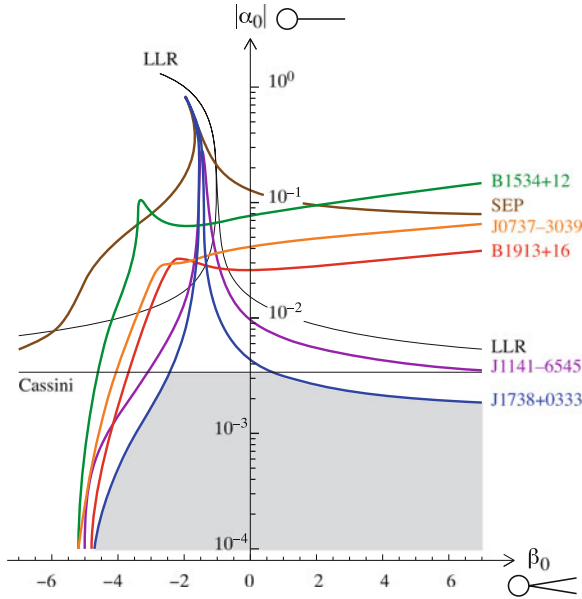


Fig. 8 Constraints on the class of $T_1(\alpha_0, \beta_0)$ scalar-tensor theories of [56, 57], from different binary pulsar and Solar system (Cassini and Lunar Laser Ranging) experiments. The *grey area* indicates the still allowed T_1 theories, and includes GR ($\alpha_0 = \beta_0 = 0$). It is obvious that PSR J1738+0333 is the most constraining experiment for most of the β_0 range, and is even competitive with Cassini in testing the Jordan-Fierz-Brans-Dicke theory ($\beta_0 = 0$). As can be clearly seen, the double neutron-star systems PSR B1534+12 [86], PSR B1913+16 (Hulse-Taylor pulsar) and PSR J0737–3039A/B (Double Pulsar) are considerably less constraining, as explained in the text. Figure is taken from [28]

where for the weakly self-gravitating white dwarf companion $\alpha_c \simeq \alpha_0$. This limit can be interpreted as a generic limit on dipolar radiation, where $\alpha_p - \alpha_c$ is the difference of some hypothetical (scalar- or vector-like) “gravitational charges” [38].

2.4 PSR J0348+0432—A Massive Pulsar in a Relativistic Orbit

PSR J0348+0432 was discovered in 2007 in a drift scan survey using the Green Bank radio telescope (GBT) [87, 88]. PSR J0348+0432 is a mildly recycled radio-pulsar with a spin period of 39 ms. Soon it was found to be in a 2.46-h orbit with a low-mass white-dwarf companion. In fact, the orbital period is only 15 s longer than that of the Double Pulsar, which by itself makes this already an interesting system for gravity. Initial timing observations of the binary yielded an accurate astrometric position, which allowed for an optical identification of its companion [89]. As it turned out, the companion is a relatively bright white dwarf with a spectrum that shows deep Balmer lines. Like in the case of PSR J1738+0333, one could use

high-resolution optical spectroscopy to determine the mass ratio $R = 11.70 \pm 0.13$ and the companion mass $m_c = 0.172 \pm 0.003 M_\odot$. For the mass of the pulsar one then finds $m_p = R m_c = 2.01 \pm 0.04 M_\odot$, which is presently the highest, well determined neutron star mass, and only the second neutron star with a well determined mass close to $2 M_\odot$.⁷

Since the discovery of PSR J0348+0432 there have been regular timing observations with three of the major radio telescopes in the world, the 100-m Green Bank Telescope, the 305-m radio telescope at the Arecibo Observatory, and the 100-m Effelsberg radio telescope. Based on the timing data, in 2013 Antoniadis et al. [89] reported the detection of a decrease in the orbital period of $\dot{P}_b = (-2.73 \pm 0.45) \pm 10^{-13}$ that is in full agreement with GR. In numbers:

$$\dot{P}_b / \dot{P}_b^{\text{GR}} = 1.05 \pm 0.18. \quad (32)$$

As it turns out, using the distance inferred from the photometry of the white dwarf ($d \sim 2.1$ kpc) corrections due to the Shklovskii effect and differential acceleration in the Galactic potential (see Eq. (25)) are negligible compared to the measurement uncertainty in \dot{P}_b .

Like PSR 1738+0333, PSR J0348+0432 is a system with a large asymmetry in the compactness of the components, and therefore well suited for a dipolar radiation test. Using Eq. (23), the limit (32) can be converted into a limit on additional gravitational scalar or vector charges:

$$|\alpha_p - \alpha_0| < 5 \times 10^{-3} \quad (95 \% \text{ confidence}). \quad (33)$$

This limit is certainly weaker than the limit (32), but it has a new quality as it tests a gravity regime in neutron stars that has not been tested before. Gravity tests before [89] were confined to “canonical” neutron star masses of $\sim 1.4 M_\odot$. PSR J0348+0432 for the first time allows a test of the relativistic motion of a massive neutron star, which in terms of gravitational self-energy lies clearly outside the tested region (see Fig. 9).

Although an increase in fractional binding energy of about 50 % does not seem much, in the highly non-linear gravity regime of neutron stars it could make a significant difference. To demonstrate this, [89] used the scalar-tensor gravity $T_1(\alpha_0, \beta_0)$ of [56, 57], which is known to behave strongly non-linear in the gravitational fields of neutron stars, in particular for $\beta_0 < -4.0$. As shown in Fig. 10, PSR J0348+0432 excludes a family of scalar-tensor theories that predict significant deviations from GR in massive neutron stars and were not excluded by previous experiments, most notably the test done with PSR J1738+0333.

With PSR J0348+0432, gravity tests now cover a range of neutron star masses from $1.25 M_\odot$ (PSR J0737–3039B) to $2 M_\odot$. No significant deviation from GR in the orbital motion of these neutron stars was found. These findings have interesting

⁷The first well determined two Solar mass neutron star is PSR J1614–2230 [90], which is in a wide orbit and therefore does not provide any gravity test.

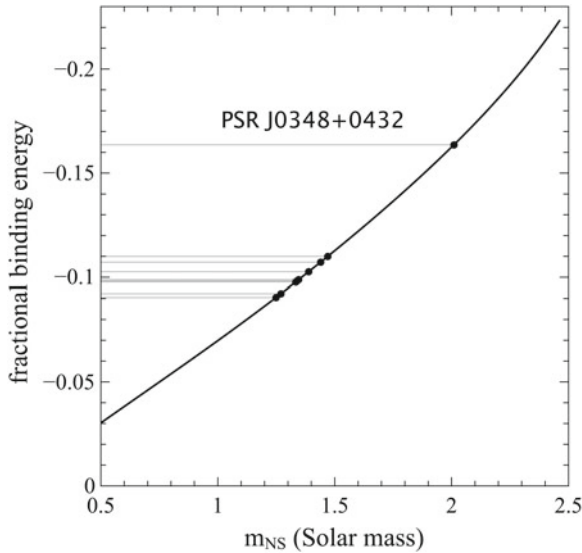


Fig. 9 Fractional gravitational binding energy of a neutron star as a function of its (inertial) mass, based on equation of state MPA1 [82]. The plot clearly shows the prominent position of PSR J0348+0432. The other dots indicate the neutron star masses of the individual test systems in Fig. 8

implications for the upcoming ground-based gravitational wave experiments, as a significant amount of dipolar radiation would drive the phase evolution of the merging binary many cycles away from the GR template and, consequently, degrade the ability to accurately determine the parameters of the merging system or even prevent the detection of the signal. A detailed discussion can be found in [89].

3 Geodetic Precession

A few months after the discovery of the Hulse-Taylor pulsar, Damour and Ruffini [51] proposed a test for geodetic precession in that system. If the pulsar spin is sufficiently tilted with respect to the orbital angular momentum, the spin direction should gradually change over time (see Sect. 1.3). A change in the orientation of the spin-axis of the pulsar with respect to the line-of-sight should lead to changes in the observed pulse profile. These pulse-profile changes manifest themselves in various forms [92], such as changes in the amplitude ratio or separation of pulse components [93, 94], the shape of the characteristic swing of the linear polarization [95], or the absolute value of the position angle of the polarization in the sky [72]. In principle, such changes could allow for a measurement of the precession rate and by this yield a test of GR. In practice, it turned out to be rather difficult to convert changes in the pulse profile into a quantitative test for the precession rate. Indeed, the Hulse-Taylor

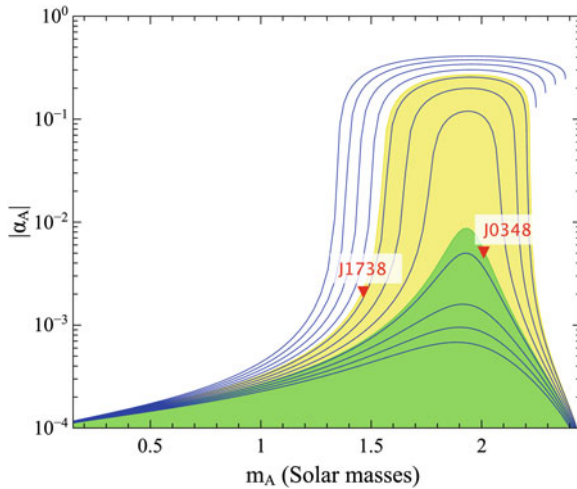


Fig. 10 Effective scalar coupling as a function of the neutron-star mass, in the $T_1(\alpha_0, \beta_0)$ mono-scalar-tensor gravity theory of [56, 57]. For the linear coupling of matter to the scalar field we have chosen $\alpha_0 = 10^{-4}$, a value well below the sensitivity of any near-future Solar system experiment, like GAIA [91]. The *blue curves* correspond to stable neutron-star configurations for different values of the quadratic coupling β_0 : -5 to -4 (*top to bottom*) in steps of 0.1 . The *yellow area* indicates the parameter space still allowed by the limit (31) [label ‘J1738’], whereas only the *green area* is in agreement with the limit (33) [label ‘J0348’]. The plot shows clearly how the massive pulsar PSR J0348+0432 probes deep into a new gravity regime. Neutron-star calculations are based on equation of state MPA1 [82] (see [89] for a different equation-of-state)

pulsar, in spite of prominent profile changes due to geodetic precession [93, 94], does not (yet) allow for a quantitative test of geodetic precession. This is mostly due to uncertainties in the orientation of the magnetic axis and the intrinsic beam shape [96].

Profile and polarization changes due to geodetic precession have been observed in other binary pulsars as well [97, 98], but again did not lead to a quantitative gravity test. A complete list of binary pulsars that up to date show signs of geodetic precession can be found in [33]. Out of the six pulsars listed in [33], so far only two allowed for quantitative constraints on their rate of geodetic precession: PSR B1534+12 [95] and pulsar *B* of the Double Pulsar [99]. In the following we will discuss the latter in more details, as it currently provides the best test for the geodetic precession of a binary pulsar.

In Sect. 2.2, we have seen the Double Pulsar as one of the most exciting “laboratories” for relativistic gravity, with a wealth of relativistic effects measured, allowing the determination of 5 post-Keplerian parameters from timing observations: $\dot{\omega}$, γ , \dot{P}_b , r , s . Calculating the inclination angle of the orbit i from $s = \sin i$, one finds that the line-of-sight is inclined with respect to the plane of the binary orbit by just about 1.3° [74]. As a consequence, during the superior conjunction the signals of pulsar *A* pass pulsar *B* at a distance of only 20,000 km. This is small compared to

the extension of pulsar B 's magnetosphere, which is roughly given by the radius of the light-cylinder⁸ $r_{lc} \equiv cP/2\pi \sim 130,000$ km. And indeed, at every superior conjunction pulsar A gets eclipsed for about 30 s due to absorption by the plasma in the magnetosphere of pulsar B [71]. A detailed analysis revealed that during every eclipse the light curve of pulsar A shows flux modulations that are spaced by half or integer numbers of pulsar B 's rotational period [100]. This pattern can be understood by absorbing plasma that co-rotates with pulsar B and is confined within the closed field lines of the magnetic dipole of pulsar B . As such, the orientation of pulsar B 's spin is encoded in the observed light curve of pulsar A [99]. Over the course of several years, Breton et al. [99] observed characteristic shifts in the eclipse pattern, that can be directly related to a precession of the spin of pulsar B . From this analysis, Breton et al. were able to derive a precession rate of

$$\Omega^{\text{SO}} = 4.77^{+0.66}_{-0.65} \text{ deg/yr.} \quad (34)$$

The measured rate of precession is consistent with that predicted by GR ($\Omega_{\text{GR}}^{\text{SO}} = 5.07$ deg/yr) within its one-sigma uncertainty. This is the sixth(!) post-Keplerian parameter measured in the Double-Pulsar system. Furthermore, for the coupling function Γ_B^A , which parametrizes strong-field deviation in alternative gravity theories (see Eq. (5)), one finds

$$\Gamma_B^A/G = 1.90 \pm 0.22, \quad (35)$$

which agrees with the GR value $\Gamma_B^A/G = 2$. Although the geodetic precession of a gyroscope was confirmed to better than 0.3 % by the Gravity Probe B experiment [13], the clearly less precise test with Double Pulsar B (13 %) for the first time gives a good measurement of this effect for a strongly self-gravitating “gyroscope”, and by this represents a qualitatively different test.

The geodetic precession of pulsar B not only changes the pattern of the flux modulations observed during the eclipse of pulsar A , it also changes the orientation of pulsar B 's emission beam with respect to our line-of-sight. As a result of this, geodetic precession has by now turned pulsar B in such a way, that since 2009 it is no longer seen by radio telescopes on Earth [101]. From their model, Perera et al. [101] predicted that the reappearance of pulsar A is expected to happen around 2035 with the same part of the beam, but could be as early as 2014 if one assumes a symmetric beam shape.

Finally, for pulsar A GR predicts a precession rate of 4.78 deg/yr, which is comparable to that of pulsar B . However, since the light-cylinder radius of pulsar A (~ 1000 km) is considerably smaller than that of pulsar B , there are no eclipses that could give insight into the orientation of its spin. Moreover, long-term pulse profile observations indicate that the misalignment between the spin of pulsar A and the orbital angular momentum is less than 3.2° (95 % confidence) [102]. For such a close alignment, geodetic precession is not expected to cause any significant changes in

⁸The light-cylinder is defined as the surface where the co-rotating frame reaches the speed of light.

the spin direction (cf. Eqs. (4) and (5)). This, on the other hand, is good news for tests based on timing observations. One does not expect a complication in the analysis of the pulse arrival times due to additional modeling of a changing pulse profile.

4 Local Lorentz Invariance of Gravity

Some alternative gravity theories allow the Universal matter distribution to single out the existence of a preferred frame, which breaks the symmetry of local Lorentz invariance (LLI) for the gravitational interaction. In the post-Newtonian parametrization of semi-conservative gravity theories, LLI violation is characterized by two parameters, α_1 and α_2 [5]. Non-vanishing α_1 and α_2 modify the dynamics of self-gravitating systems that move with respect to the preferred frame (preferred-frame effects). In GR one finds $\alpha_1 = \alpha_2 = 0$.

As the most natural preferred frame, generally one chooses the frame associated with the isotropic cosmic microwave background (CMB), meaning that the preferred frame is assumed to be fixed by the global matter distribution of the Universe. From the five-year Wilkinson Microwave Anisotropy Probe (WMAP) satellite experiment, a CMB dipole measurement with high precision was obtained [103]. The CMB dipole corresponds to a motion of the Solar system with respect to the CMB with a velocity of 369.0 ± 0.9 km/s in direction of Galactic longitude and latitude $(l, b) = (263.99^\circ \pm 0.14^\circ, 48.26^\circ \pm 0.03^\circ)$. The numbers quoted in the next two sub-sections, will be with respect to the CMB frame. A generalization to other frames is straightforward, and was done in some of the references cited below.

The most important (weak-field) constraints on preferred-frame effects do come from Lunar Laser Ranging (LLR) [104],

$$\alpha_1 = (-0.7 \pm 1.8) \times 10^{-4} \quad (95 \% \text{ CL}), \quad (36)$$

and the alignment of the Sun's spin with the total angular momentum of the planets in the Solar system [105],

$$|\alpha_2| < 2.4 \times 10^{-7}. \quad (37)$$

4.1 Constraints on $\hat{\alpha}_1$ from Binary Pulsars

In binary pulsars, the isotropic violation of Lorentz invariance in the gravitational sector should lead to characteristic preferred frame effects in the binary dynamics, if the barycenter of the binary is moving relative to the preferred frame with a velocity \mathbf{w} . For small-eccentricity binaries, the effects induced by $\hat{\alpha}_1$ and $\hat{\alpha}_2$ (the hat indicates possible modifications by strong-field effects) decouple, and can therefore be tested independently [106, 107].

In case of a non-vanishing $\hat{\alpha}_1$, the observed eccentricity vector \mathbf{e} of a small-eccentricity binary pulsar is a vectorial superposition of a ‘rotating eccentricity’ $\mathbf{e}_R(t)$ and a fixed ‘forced eccentricity’ \mathbf{e}_F : $\mathbf{e}(t) = \mathbf{e}_F + \mathbf{e}_R(t)$ [106]. The rotating eccentricity has a constant length e_R , and rotates with the relativistic precession of periastron, $\dot{\omega}$, in the orbital plane. This is identical to the dynamics caused by a violation of the strong equivalence principle [106, 108], with the forced eccentricity pointing into the direction of $\hat{\mathbf{L}} \times \mathbf{w}$. As a consequence, the binary orbit changes from a less to a more eccentric configuration and back on a time scale of

$$T_{\dot{\omega}} \equiv \frac{2\pi}{\dot{\omega}} \simeq (1140 \text{ yr}) \left(\frac{P_b}{1 \text{ day}} \right)^{5/3} \left(\frac{M}{2M_{\odot}} \right)^{-2/3}, \quad (38)$$

where we have assumed that the true $\dot{\omega}$ does not deviate significantly from the one predicted by GR (Eq. (15)), an assumption that is well justified by other binary-pulsar experiments, like the generic tests in the Double Pulsar (cf. Sect. 2.2).

The forced eccentricity \mathbf{e}_F is determined by the strength of the preferred frame effect. Its magnitude is approximately given by

$$e_F \simeq 0.093 \hat{\alpha}_1 \frac{m_p - m_c}{M} \left(\frac{M}{2M_{\odot}} \right)^{-1/3} \left(\frac{P_b}{1 \text{ day}} \right)^{1/3} \left(\frac{w \sin \psi}{300 \text{ km/s}} \right), \quad (39)$$

where ψ is the angle between \mathbf{w} and $\hat{\mathbf{L}}$ (see [106] for a detailed expression). The observation of small eccentricities in binary pulsars, like $e \sim 10^{-7}$ for PSR J1738+0333 does not directly constrain $\hat{\alpha}_1$. The orientation of the a priori unknown intrinsic \mathbf{e}_R could be such, that it compensates for a large \mathbf{e}_F . If the system is sufficiently old, one can assume a uniform probability distribution in $[0^\circ, 360^\circ]$ for $\theta(t)$. Like in the Damour-Schäfer test for SEP, one can now set a probabilistic upper limit on e_F , and by this on $\hat{\alpha}_1$, by excluding θ values close to alignment of \mathbf{e}_R and \mathbf{e}_F . Based on this method, [106] found a limit of $|\hat{\alpha}_1| < 5 \times 10^{-4}$ with 90% confidence.

But even if θ happens to be close to 0° , due to the relativistic precession it will not remain there, and a large e_F cannot remain hidden for ever. In fact, if $\dot{\omega}$ is sufficiently large (greater than $\sim 1^\circ$ per year) a significant change in the orbital eccentricity should become observable over time scales of a few years, even if at the start of the observation there was a complete cancellation between \mathbf{e}_R and \mathbf{e}_F . This can be used to constrain $\hat{\alpha}_1$ [107]. The best such test comes from PSR J1738+0333 (see Sect. 2.3). This binary pulsar is ideal for this test for several reasons:

- The orbit has an extremely small, well constrained eccentricity of $\sim 10^{-7}$ [28].
- The (calculated) relativistic precession of periastron is about 1.6 deg/yr , and the binary has been observed by now for about 10 years [28]. Hence, $\theta(t)$ has covered an angle of 16° in that time.
- The 3D velocity with respect to the Solar system is known with good precision from timing and optical observations, meaning that one can compute \mathbf{w} [28, 81].

- The orientation of the system is such, that the unknown angle of the ascending node Ω has little influence on the $\hat{\alpha}_1$ limit, hence there is no need for probabilistic considerations to exclude certain values of Ω [107].

Consequently, PSR J1738+0333 leads to the best constraints of α_1 -like violations of the local Lorentz invariance of gravity, giving [107]

$$\hat{\alpha}_1 = -0.4^{+3.7}_{-3.1} \times 10^{-5} \quad (95\% \text{ confidence}). \quad (40)$$

This limit is not only five times better than the current most stringent limit on α_1 obtained in the Solar system (cf. Eq.(36)), it is also sensitive to potential deviations related to the strong self-gravity of the pulsar. For non-perturbative deviations one can, for illustration purposes, do an expansion with respect to the fractional binding energy ϵ of the neutron star,

$$\hat{\alpha}_1 = \alpha_1 + \mathcal{C}_1 \epsilon + \mathcal{O}(\epsilon^2). \quad (41)$$

Since $\epsilon \sim -0.1$ for PSR J1738+0333, we get tight constraints for \mathcal{C}_1 , a parameter that is virtually unconstrained by the LLR experiment, since $\epsilon \sim -5 \times 10^{-10}$ for the Earth.

4.2 Constraints on $\hat{\alpha}_2$ from Binary and Solitary Pulsars

In the presence of a non-vanishing $\hat{\alpha}_2$, a small-eccentricity binary system experiences a precession of the orbital angular momentum around the fixed direction \mathbf{w} with an angular frequency

$$\Omega_{\hat{\alpha}_2}^{\text{prec}} = -\hat{\alpha}_2 \frac{\pi}{P_b} \left(\frac{w}{c} \right)^2 \cos \psi, \quad (42)$$

where ψ is the angle between the orbital angular momentum and \mathbf{w} [107]. In binary pulsars, such a precession should become visible as a secular change in the projected semi-major axis of the pulsar orbit, \dot{x} , which is an observable timing parameter. The two binary pulsars PSRs J1012+5307 and J1738+0333 turn out to be particularly useful for such a test, since both of them have optically bright white dwarf companions, which allowed the determination of the masses in the system, and the 3D systemic velocity with respect to the preferred frame [81, 109, 110].

Unfortunately, in general, the orientation of a binary pulsar orbit with respect to \mathbf{w} and the line-of-sight cannot be fully determined from timing observations. As a consequence, one cannot directly test $\hat{\alpha}_2$ from observed constraints for \dot{x} . In fact, since the longitude of the ascending node Ω is not measured, neither for PSR J1012+5307 nor for PSR J1738+0333, the orientation of these systems could in principle be such, that an $\hat{\alpha}_2$ -induced precession would not lead to a significant \dot{x} . Assuming a random distribution of Ω in the interval $[0^\circ, 360^\circ)$, one can use probabilistic considerations

to exclude such unfavorable orientations. A detailed discussion of this test can be found in [107], where the following 95 % confidence limits are derived

$$\begin{aligned} |\hat{\alpha}_2| &< 3.6 \times 10^{-4} && \text{from PSR J1012+5307,} \\ |\hat{\alpha}_2| &< 2.9 \times 10^{-4} && \text{from PSR J1738+0333,} \\ |\hat{\alpha}_2| &< 1.8 \times 10^{-4} && \text{from PSRs J1012+5307 and J1738+0333 combined.} \end{aligned} \quad (43)$$

It is important to note, that for the last limit, based on the statistical combination of the two systems, one has to assume that $\hat{\alpha}_2$ has only a weak functional dependence on the neutron-star mass in the range of $1.3 - 2.0 M_\odot$.

The limit for $\hat{\alpha}_2$ obtained from binary pulsars are still several orders of magnitude weaker than the α_2 limit which Nordtvedt derived in 1987 from the alignment of the Sun's spin with the orbital planes of the planets [105]. In the same paper, Nordtvedt pointed out that solitary fast-rotating pulsars could be used in a similar way to obtain tight constraints for α_2 . This can be directly seen from Eq. (42), which holds for a rotating self-gravitating star if P_b is replaced by the rotational period P of the star. While the five-billion-year base-line for the Solar experiment is typically a factor of $\sim 10^9$ longer than the observational time-span T_{obs} of pulsars, for millisecond pulsars P is $\sim 10^9$ shorter than the rotational period of the Sun. In fact, the first millisecond pulsar PSR B1937+21, discovered in 1982 [111], by now has a figure of merit T_{obs}/P that is ~ 10 times larger than that of the Sun.

The precession of a solitary pulsar due to a non-vanishing $\hat{\alpha}_2$ would lead to characteristic changes in the observed pulse profile over time-scales of years, just like in the case of binary pulsars that experience geodetic precession (cf. Sect. 3). Consequently, a non-detection of such changes can be converted into constraints for $\hat{\alpha}_2$. Recently, Shao et al. [112] used the two solitary millisecond pulsars PSRs B1937+21 and J1744–1134 for such an experiment. For both pulsars they utilized a consistent set of data, taken over a time span of approximately 15 years with the same observing system at the 100-m Effelsberg radio telescope. The continuity in the observing system was key for an optimal comparison of the high signal-to-noise ratio profiles over time. As it turns out, both pulsars, PSRs B1937+21 and J1744–1134, do not show any detectable profile evolution in the last 15 years. As an example of such a non-detection see Fig. 11, which shows two pulse profiles of PSR B1937+21 obtained at different epochs.

Similarly to the $\hat{\alpha}_2$ test with the binary pulsars, there are unknown angles in the orientation of the pulsar spin, for which certain values have to be excluded based on probabilistic considerations. From extensive Monte-Carlo simulations Shao et al. found with 95 % confidence

$$\begin{aligned} |\hat{\alpha}_2| &< 2.5 \times 10^{-8} && \text{from PSR B1937+21,} \\ |\hat{\alpha}_2| &< 1.5 \times 10^{-8} && \text{from PSR J1744–1134,} \\ |\hat{\alpha}_2| &< 1.6 \times 10^{-9} && \text{from PSRs B1937+21 and J1744–1134 combined.} \end{aligned} \quad (44)$$

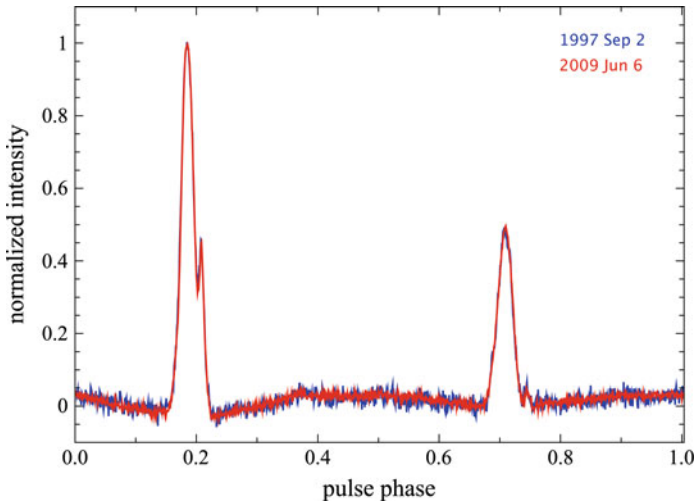


Fig. 11 Comparison of two pulse profiles of PSR B1937+21 obtained at two different epochs. The *blue* one was obtained on September 2, 1997, while the *red* one was obtained on June 6, 2009. The main peak is aligned and scaled to have the same intensity. There exists no visible difference within the noise level. Profiles were taken from [112]

These limits are significantly tighter than the α_2 limit from the Sun's spin orientation. Like in the case of the $\hat{\alpha}_1$ test (previous subsection), this test also covers potential deviations related to the strong self-gravity of the pulsar, and in the combination of the two pulsars, makes the assumption that $\hat{\alpha}_2$ depends only weakly on the neutron-star mass.

An important difference to the aforementioned tests with binary pulsars is, that for solitary pulsars one cannot determine the radial velocity. It enters the determination of \mathbf{w} as a free parameter. However, as shown in [112], the unknown radial velocities for PSRs B1937+21 and J1744–1134 only have a marginal effect on the limits. For the limits above it was assumed that both pulsars are gravitationally bound in the Galactic potential. But even if one relaxes this assumption and allows for unphysically large radial velocities, exceeding 1000 km/s, the limits get weaker by at most $\sim 40\%$.

5 Summary and Outlook

With their discovery of the first binary pulsar four decades ago, Joseph Taylor and Russell Hulse opened a new field of experimental gravity, which has been an active field of research ever since. Besides the Hulse-Taylor pulsar, which led to the first confirmation of the existence of gravitational waves, astronomy has seen the discovery of many new binary pulsars suitable for precision gravity tests. Arguably, the most exiting discovery was the Double Pulsar in 2003, which by now provides the best test for GR's quadrupole formalism of gravitational wave generation ($<0.1\%$ uncertainty),

and the best test for the relativistic spin precession of a strongly self-gravitating body. In addition to this, it is the binary pulsar with the most post-Keplerian parameters measured, allowing for a number of generic constraints on strong-field deviations from GR. For certain aspects of gravity, binary pulsars with white dwarf companions have proven to be even better “test laboratories” than the Double Pulsar. These are gravitational phenomena, predicted by alternatives to GR, that depend on the difference in the compactness/binding energy of the two components, like gravitational dipolar radiation. By now, pulsar-white dwarf systems, like PSR J1738+0333, set quite stringent limits (coupling strength less than about 10^{-3}) on the existence of any additional “gravitational charges” associated with light or massless fields. The recent discovery of a massive pulsar in a relativistic binary system (PSR J0348+0432), for the first time allowed to test the orbital motion of a neutron star that is significantly more compact than pulsars of previous gravity tests. For certain aspects of gravity, solitary pulsars turned out to be ideal probes. The current best limit on the PPN parameters α_2 , related to the existence of a preferred frame for gravity, does come from pulse-profile observations of two solitary millisecond pulsars. In all these tests, pulsars go beyond Solar system tests, since they are also sensitive to deviations that occur only in the strong-field environment of neutron stars.

So far, GR has passed all these tests with flying colors. Will this continue for ever? Is GR our final answer to the macroscopic description of gravity? Pulsar astronomy will certainly continue to investigate this question. Many of the tests mentioned here will simply improve by continued timing observations of the known pulsars. In fact, the measurement precision for some of the post-Keplerian parameters increases fast with time. For instance, in regular observations (with the same hardware) the uncertainty in the change of the orbital period \dot{P}_b decreases with $T_{\text{obs}}^{-2.5}$, T_{obs} denoting the observing time span. Improvements in the hardware, like new broad-band receivers (e.g. [113]), will further boost the timing precision. For pulsars like PSR J1738+0333 and PSR J0348+0432 soon the modeling of the white dwarf will be the limiting factor, while for the Double Pulsar the corrections of the external contributions to \dot{P}_b will be the challenging bit, in particular if one wants to reach the $\sim 10^{-5}$ level at which higher order contributions to \dot{P}_b [114, 115] and the Lense-Thirring contribution to the orbital dynamics [44, 50] become relevant (see [72] for a detailed discussion). The upcoming next generation of radio telescopes, like the Five-hundred-meter Aperture Spherical radio Telescope (FAST) [116] and the The Square Kilometre Array (SKA) [117], certainly promise a big step towards this goal. With SKA, for many pulsars one can hope for a factor of 100 improvement in timing precision [118]. The SKA also promises to provide excellent direct distance measurements to pulsars, either directly by utilizing the long baselines of the SKA to form high angular resolution images, or by fitting for the timing parallax in the arrival times of the pulsar signals [119]. In combination with new models for the gravitational potential of our Galaxy, in particular after new missions like GAIA [120], one will be able to accurately determine the extrinsic “contaminations” of \dot{P}_b via Eq. (25), and by this know the intrinsic \dot{P}_b . This is key for any high precision gravitational wave test with binary pulsars, but also crucial to measure the Lense-Thirring drag in the Double Pulsar [72].

Reducing the parameter uncertainties for known pulsars is one way to push gravity tests forward, finding new, more relativistic systems is the other. Presently there are a number of pulsar surveys underway that promise the discovery of many new pulsars. New techniques, like acceleration searches [121] and high performance computing, e.g. Einstein@Home [122], promise the detection of pulsars in tight orbits, which generally cannot be found with traditional methods. There is considerable hope among pulsar astronomers, that this will finally also lead to the discovery of a pulsar-black hole system, occasionally called the “holy grail” of pulsar astronomy. Such a system is expected to provide a superb new probe of relativistic gravity and black hole properties, like the dragging of spacetime by the rotation of the black hole [123–125]. According to GR, for an astrophysical black hole (Kerr solution) there is an upper limit for its spin, given by $S_{\max} = GM^2/c$. It would pose an interesting challenge to GR, if the timing of a pulsar-black hole system indicates a spin $S > S_{\max}$. But even for gravity theories that predict the same properties for black holes as in GR, a pulsar-black hole system would constitute an excellent test system, due to the high grade of asymmetry in the strong-field properties of these two components (see [125] for simulations based on $T_1(\alpha_0, \beta_0)$ scalar-tensor theories). A pulsar in a close orbit ($P_b < 1$ yr) around the super-massive black hole ($m_{\text{BH}} \approx 4 \times 10^6 M_\odot$) in the center of our Galaxy would be the ultimate test system, in that context. According to the mock data analysis in [126], for such a system a precise measurement of the quadrupole moment of the black hole, and therefore a test of the no-hair theorem, should be possible, provided that the environment of the pulsar orbit is sufficiently clean. Finding and timing a pulsar in the center of our Galaxy is certainly challenging. A promising result in that direction is the very recent detection of radio signals from a magnetar near the Galactic center black hole [127], even if this pulsar is still too far away from the super-massive black hole (~ 0.1 pc) to probe its spacetime.

Until now, all gravitational wave tests are based on probing the near-zone of a binary spacetime by measuring how the back reaction of the gravitational radiation changes the world lines of the source masses. As outlined above, with the Double Pulsar this test has reached a precision of better than 0.1 %. Presently there are considerable efforts to achieve a direct detection of gravitational waves, i.e. measure the far-field properties of such radiative spacetimes by using appropriate test masses. Ground based laser interferometric gravitational wave observatories, like LIGO and VIRGO, have mirrors with separations of a few kilometers. Their sensitivity is in the range from 10 Hz to few 10^3 Hz. Planned space-based detectors, like eLISA, will have three drag-free satellites as test masses with a typical separation of $\sim 10^6$ km, and should be sensitive to gravitational waves from about 10^{-4} to 0.1 Hz. For the ultra-low frequency band (few nano-Hz) pulsar timing arrays are currently the most promising detectors [128]. In these experiments the Earth/Solar system and a collection of very stable pulsars act as the test masses. A gravitational wave becomes apparent in a pulsar timing array by the changes it causes in the arrival times of the pulsar signals. Due to the fitting of the rotational frequency ν and its time derivative $\dot{\nu}$ for every pulsar, such

a detector is only sensitive to wavelengths up to $\sim c T_{\text{obs}}$.⁹ This leads to the special situation that the length of the “detector arms” is much larger than the wavelength. As a consequence, the observed timing signal contains two contributions, the so-called *pulsar term*, related to the impact of the gravitational wave on the pulsar when the radio signal is emitted, and the *Earth term* corresponding to the impact of the gravitational wave on the Earth during the arrival of the radio signal at the telescope [131, 132]. The most promising source in the nano-Hz frequency band is a stochastic gravitational wave background, as a result of many mergers of super-massive black hole binaries in the past history of the Universe [133, 134]. With the large number of “detector arms”, pulsar timing arrays have enough information to explore the properties of the nano-Hz gravitational wave background in details, once its signal is clearly detected in the data. Are there more than the two Einsteinian polarization modes (alternative metric theories can have up to six)? Is the propagation speed of nano-Hz gravitational waves frequency depended? Does the graviton carry mass? These are some of the main questions that can be addressed with pulsar timing arrays [135, 136]. The isolation of a single source in the pulsar timing array data would give us a unique opportunity to study the merger evolution of a super-massive black hole binary, since the signal in the Earth term and the signal in the pulsar term show two different states of the system, which are typically several thousand years apart [137]. For these kind of gravity experiments, however, we might have to wait till the full SKA has collected a few years of data, which probably brings us close to the year 2030.

Acknowledgments I would like to thank the workshop organizers for their hospitality, and John Antoniadis for carefully reading the manuscript.

References

1. A. Einstein, Sitzungsberichte der Königlich Preußischen Akademie der Wissenschaften (Berlin), pp. 844–847 (1915)
2. A. Einstein, Sitzungsberichte der Königlich Preußischen Akademie der Wissenschaften (Berlin), pp. 831–839 (1915)
3. H. Seeliger, Astronomische Nachrichten **201**, 273 (1915)
4. A. Einstein, Annalen der Physik **354**, 769–822 (1916)
5. C.M. Will, *Theory and Experiment in Gravitational Physics*, 2nd edn. (Cambridge University Press, Cambridge, 1993)
6. F.W. Dyson, A.S. Eddington, C. Davidson, R. Soc. Lond. Philos. Trans. Ser. A **220**, 291–333 (1920)
7. M. Froeschle, F. Mignard, F. Arenou, in *Hipparcos—Venice ’97*, vol. 402, ed. by R.M. Bonnet, E. Høg, P.L. Bernacca, et al. (ESA Special Publication, The Netherlands, 1997), pp. 49–52
8. S.S. Shapiro, J.L. Davis, D.E. Lebach, J.S. Gregory, Phys. Rev. Lett. **92**, 121101 (2004)
9. E. Fomalont, S. Kopeikin, G. Lanyi, J. Benson, Astrophys. J. **699**, 1395–1402 (2009)
10. I.I. Shapiro, Phys. Rev. Lett. **13**, 789–791 (1964)

⁹It has been suggested to use the orbital period of binary pulsars to test for gravitational waves of considerably longer wavelength [129, 130].

11. B. Bertotti, L. Iess, P. Tortora, *Nature* **425**, 374–376 (2003)
12. K. Nordtvedt, *Class. Quantum Gravity* **16**, A101–A112 (1999)
13. C.W.F. Everitt, D.B. Debra, B.W. Parkinson et al., *Phys. Rev. Lett.* **106**, 221101 (2011)
14. I. Ciufolini, E.C. Pavlis, *Nature* **431**, 958–960 (2004)
15. A. Einstein, *Sitzungsberichte der Königlich Preußischen Akademie der Wissenschaften (Berlin)*, pp. 688–696 (1916)
16. A. Einstein, *Sitzungsberichte der Königlich Preußischen Akademie der Wissenschaften (Berlin)*, pp. 154–167 (1918)
17. D. Kennefick, *Traveling at the Speed of Thought: Einstein and the Quest for Gravitational Waves*, (Princeton University Press, Princeton, 2007)
18. R.A. Hulse, J.H. Taylor, *Astrophys. J.* **195**, L51–L53 (1975)
19. J.J. Hermes, M. Kilic, W.R. Brown et al., *Astrophys. J.* **757**, L21 (2012)
20. A. Hewish, S.J. Bell, J.D.H. Pilkington et al., *Nature* **217**, 709–713 (1968)
21. R.N. Manchester, G.B. Hobbs, A. Teoh, M. Hobbs, *Astrophys. J.* **129**, 1993–2006 (2005). <http://www.atnf.csiro.au/research/pulsar/psrcat/>
22. D.R. Lorimer, *Living Rev. Relativ.* **8** (2005). <http://www.livingreviews.org/lrr-2005-7>
23. G. Hobbs, W. Coles, R.N. Manchester et al., *Mon. Not. R. Astron. Soc.* **427**, 2780–2787 (2012)
24. I.H. Stairs, *Living Rev. Relativ.* **6** (2003). <http://www.livingreviews.org/lrr-2003-5>
25. D.R. Lorimer, M. Kramer, *Handbook of Pulsar Astronomy*, (Cambridge University Press, Cambridge, 2004)
26. R.T. Edwards, G.B. Hobbs, R.N. Manchester, *Mon. Not. R. Astron. Soc.* **372**, 1549–1574 (2006)
27. J.P.W. Verbiest, M. Bailes, W. van Straten et al., *Astrophys. J.* **679**, 675–680 (2008)
28. P.C.C. Freire, N. Wex, G. Esposito-Farèse et al., *Mon. Not. R. Astron. Soc.* **423**, 3328–3343 (2012)
29. J.M. Weisberg, D.J. Nice, J.H. Taylor, *Astrophys. J.* **722**, 1030–1034 (2010)
30. P.C.C. Freire, C.G. Bassa, N. Wex et al., *Mon. Not. R. Astron. Soc.* **412**, 2763–2780 (2011)
31. A.W. Hotan, M. Bailes, S.M. Ord, *Mon. Not. R. Astron. Soc.* **369**, 1502–1520 (2006)
32. D.J. Champion, G.B. Hobbs, R.N. Manchester et al., *Astrophys. J.* **720**, L201–L205 (2010)
33. M. Kramer, *Proc. Int. Astron. Union* **8**, 19–26 (2012)
34. T. Damour, in *Three Hundred Years of Gravitation*, ed. by S.W. Hawking, W. Israel (Cambridge University Press, Cambridge, 1987), pp. 128–198
35. L. Blanchet, *Living Rev. Relativ.* **9**, 4 (2006)
36. T. Futamase, Y. Itoh, *Living Rev. Relativ.* **10** (2007). <http://www.livingreviews.org/lrr-2007-2>
37. T. Damour, in *Gravitational Radiation*, ed. by N. Deruelle, T. Piran (North-Holland, Amsterdam, 1983), pp. 59–144
38. J.-M. Gérard, Y. Wiaux, *Phys. Rev. D* **66**, 024040 (2002)
39. T. Damour, J.H. Taylor, *Phys. Rev. D* **45**, 1840–1868 (1992)
40. T. Damour, in *Astrophysics and Space Science Library*, vol. 359, ed. by M. Colpi, P. Casella, V. Gorini, U. Moschella, A. Possenti (Springer, New York, 2009), pp. 1–41
41. T. Damour, N. Deruelle, *Ann. Inst. Henri Poincaré Phys. Théor.* **43**, 107–132 (1985)
42. T. Damour, G. Esposito-Farèse, *Phys. Rev. D* **53**, 5541–5578 (1996)
43. S. Mirshekari, C.M. Will, *Phys. Rev. D* **87**, 084070 (2013)
44. B.M. Barker, R.F. O’Connell, *Phys. Rev. D* **12**, 329–335 (1975)
45. V.A. Brumberg, *Essential Relativistic Celestial Mechanics*, (Adam Hilger, Bristol, 1991)
46. J. Hartung, J. Steinhoff, G. Schäfer, *Annalen der Physik* **525**, 359–394 (2013)
47. N. Wex, *Class. Quantum Gravity* **12**, 983–1005 (1995)
48. T. Damour, *C. R. Acad. Sci. Paris Sér. II* **294**, 1355–1357 (1982)
49. D.E. Lebach, B.E. Corey, I.I. Shapiro et al., *Phys. Rev. Lett.* **75**, 1439–1442 (1995)
50. T. Damour, G. Schäfer, *Nuovo Cimento B* **101**, 127 (1988)
51. T. Damour, R. Ruffini, *Académie des Sciences Paris Comptes Rendus Serie Sciences Mathématiques* **279**, 971–973 (1974)

52. G. Börner, J. Ehlers, E. Rudolph, *Astron. Astrophys.* **44**, 417–420 (1975)
53. T. Damour, in *Proceedings of the 2nd Canadian Conference on General Relativity and Relativistic Astrophysics*, ed. by A. Coley, C. Dyer, T. Tupper, (University of Toronto, 1988), pp. 315–334
54. T. Damour, N. Deruelle, *Ann. Inst. Henri Poincaré Phys. Théor.* **44**, 263–292 (1986)
55. M. Ali, Master thesis, University of Bonn, Germany (2011)
56. T. Damour, G. Esposito-Farèse, *Phys. Rev. Lett.* **70**, 2220–2223 (1993)
57. T. Damour, G. Esposito-Farèse, *Phys. Rev. D* **54**, 1474–1491 (1996)
58. D.M. Eardley, *Astrophys. J.* **196**, L59–L62 (1975)
59. C.M. Will, *Astrophys. J.* **214**, 826–839 (1977)
60. P.C. Peters, *Phys. Rev.* **136**, B1224–B1232 (1964)
61. V.A. Brumberg, I.B. Zeldovich, I.D. Novikov, N.I. Shakura, *Sov. Astron. Lett.* **1**, 2–4 (1975)
62. R.V. Wagoner, *Astrophys. J.* **196**, L63–L65 (1975)
63. J.H. Taylor, R.A. Hulse, L.A. Fowler et al., *Astrophys. J.* **206**, L53–L58 (1976)
64. N. Wex, V. Kalogera, M. Kramer, *Astrophys. J.* **528**, 401–409 (2000)
65. R. Blandford, S.A. Teukolsky, *Astrophys. J.* **198**, L27–L29 (1975)
66. J.H. Taylor, L.A. Fowler, P.M. McCulloch, *Nature* **277**, 437–440 (1979)
67. I.S. Shklovskii, *Sov. Astron.* **13**, 562–565 (1970)
68. T. Damour, J.H. Taylor, *Astrophys. J.* **366**, 501–511 (1991)
69. J.M. Weisberg, S. Stanimirović, K. Xilouris et al., *Astrophys. J.* **674**, 286–294 (2008)
70. M. Burgay, N. D’Amico, A. Possenti et al., *Nature* **426**, 531–533 (2003)
71. A.G. Lyne, M. Burgay, M. Kramer et al., *Science* **303**, 1153–1157 (2004)
72. M. Kramer, N. Wex, *Class. Quantum Gravity* **26**, 073001 (2009)
73. M. Kramer, I.H. Stairs, *Annu. Rev. Astron. Astrophys.* **46**, 541–572 (2008)
74. M. Kramer, I.H. Stairs, R.N. Manchester et al., *Science* **314**, 97–102 (2006)
75. R. Blandford, S.A. Teukolsky, *Astrophys. J.* **205**, 580–591 (1976)
76. A.T. Deller, M. Bailes, S.J. Tingay, *Science* **323**, 1327–1329 (2009)
77. J.P.W. Verbiest, M. Bailes, W.A. Coles et al., *Mon. Not. R. Astron. Soc.* **400**, 951–968 (2009)
78. E.S. Phinney, *R. Soc. Lond. Philos. Trans. Ser. A* **341**, 39–75 (1992)
79. M.F. Ryba, J.H. Taylor, *Astrophys. J.* **371**, 739–748 (1991)
80. B.A. Jacoby, Ph.D. thesis, California Institute of Technology, California, USA (2005)
81. J. Antoniadis, M.H. van Kerkwijk, D. Koester et al., *Mon. Not. R. Astron. Soc.* **423**, 3316–3327 (2012)
82. H. Muther, M. Prakash, T.L. Ainsworth, *Phys. Lett. B* **199**, 469–474 (1987)
83. P.C.C. Freire, S.M. Ransom, S. Bégin et al., *Astrophys. J.* **675**, 670–682 (2008)
84. M.H. van Kerkwijk, R.P. Breton, S.R. Kulkarni, *Astrophys. J.* **728**, 95 (2011)
85. R.W. Romani, A.V. Filippenko, J.M. Silverman et al., *Astrophys. J.* **760**, L36 (2012)
86. I.H. Stairs, S.E. Thorsett, J.H. Taylor, A. Wolszczan, *Astrophys. J.* **581**, 501–508 (2002)
87. J. Boyles, R.S. Lynch, S.M. Ransom et al., *Astrophys. J.* **763**, 80 (2013)
88. R.S. Lynch, J. Boyles, S.M. Ransom et al., *Astrophys. J.* **763**, 81 (2013)
89. J. Antoniadis, P.C.C. Freire, N. Wex et al., *Science* **340**, 448 (2013)
90. P.B. Demorest, T. Pennucci, S.M. Ransom et al., *Nature* **467**, 1081–1083 (2010)
91. D. Hobbs, B. Holl, L. Lindegren et al., *Proc. Int. Astron. Union* **5**, 315–319 (2009)
92. N.D.H. Dass, V. Radhakrishnan, *Astrophys. J.* **16**, L135–L139 (1975)
93. J.M. Weisberg, R.W. Romani, J.H. Taylor, *Astrophys. J.* **347**, 1030–1033 (1989)
94. M. Kramer, *Astrophys. J.* **509**, 856–860 (1998)
95. I.H. Stairs, S.E. Thorsett, Z. Arzoumanian, *Phys. Rev. Lett.* **93**, 141101 (2004)
96. J.M. Weisberg, J.H. Taylor, *Astrophys. J.* **576**, 942–949 (2002)
97. R.N. Manchester, M. Kramer, I.H. Stairs et al., *Astrophys. J.* **710**, 1694–1709 (2010)
98. G. Desvignes, M. Kramer, I. Cognard et al., *Proc. Int. Astron. Union* **8**, 199–202 (2012)
99. R.P. Breton, V.M. Kaspi, M. Kramer et al., *Science* **321**, 104–107 (2008)
100. M.A. McLaughlin, A.G. Lyne, D.R. Lorimer et al., *Astrophys. J.* **616**, L131–L134 (2004)
101. B.B.P. Perera, M.A. McLaughlin, M. Kramer et al., *Astrophys. J.* **721**, 1193–1205 (2010)
102. R.D. Ferdman, I.H. Stairs, M. Kramer et al., *Astrophys. J.* **767**, 85 (2013)

103. G. Hinshaw, J.L. Weiland, R.S. Hill et al., *Astrophys. J. Suppl.* **180**, 225–245 (2009)
104. J. Müller, J.G. Williams, S.G. Turyshev, *Astrophysics and space science library*, in *Lasers, Clocks and Drag-Free Control: Exploration of Relativistic Gravity in Space*, vol. 349, ed. by H. Dittus, C. Lammerzahn, S.G. Turyshev (Springer, Berlin, 2008), pp. 457–472
105. K. Nordtvedt, *Astrophys. J.* **320**, 871–874 (1987)
106. T. Damour, G. Esposito-Farèse, *Phys. Rev. D* **46**, 4128–4132 (1992)
107. L. Shao, N. Wex, *Class. Quantum Gravity* **29**, 215018 (2012)
108. T. Damour, G. Schäfer, *Phys. Rev. Lett.* **66**, 2549–2552 (1991)
109. P.J. Callanan, P.M. Garnavich, D. Koester, *Mon. Not. R. Astron. Soc.* **298**, 207–211 (1998)
110. K. Lazaridis, N. Wex, A. Jessner et al., *Mon. Not. R. Astron. Soc.* **400**, 805–814 (2009)
111. D.C. Backer, S.R. Kulkarni, C. Heiles et al., *Nature* **300**, 615–618 (1982)
112. L. Shao, R.N. Caballero, M. Kramer et al., *Class. Quantum Gravity* **30**, 165019 (2013)
113. S. Weinreb, J. Bardin, H. Mani, G. Jones, *Rev. Sci. Instrum.* **80**, 044702 (2009)
114. L. Blanchet, G. Schäfer, *Mon. Not. R. Astron. Soc.* **239**, 845–867 (1989)
115. L. Blanchet, G. Schäfer, *Mon. Not. R. Astron. Soc.* **242**, 704 (1990)
116. R. Nan, D. Li, C. Jin et al., *Int. J. Mod. Phys. D* **20**, 989–1024 (2011)
117. A.R. Taylor, *Proc. Int. Astron. Union* **8**, 337–341 (2012)
118. R. Smits, M. Kramer, B. Stappers et al., *Astron. Astrophys.* **493**, 1161–1170 (2009)
119. R. Smits, S.J. Tingay, N. Wex et al., *Astron. Astrophys.* **528**, A108 (2011)
120. M.A.C. Perryman, K.S. de Boer, G. Gilmore et al., *Astron. Astrophys.* **369**, 339–363 (2001)
121. S.M. Ransom, J.M. Cordes, S.S. Eikenberry, *Astrophys. J.* **589**, 911–920 (2003)
122. B. Allen, B. Knispel, J.M. Cordes et al., *Astrophys. J.* **773**, 91 (2013)
123. N. Wex, S.M. Kopeikin, *Astrophys. J.* **514**, 388–401 (1999)
124. K. Liu, Ph.D. thesis, University of Manchester, UK (2012)
125. N. Wex, K. Liu, R.P. Eatough et al., *Proc. Int. Astron. Union* **8**, 171–176 (2012)
126. K. Liu, N. Wex, M. Kramer et al., *Astrophys. J.* **747**, 1 (2012)
127. R.P. Eatough, H. Falcke, R. Karuppusamy, et al., *Nature* (2013), in press [arXiv:1308.3147](https://arxiv.org/abs/1308.3147)
128. G. Hobbs, A. Archibald, Z. Arzoumanian et al., *Class. Quantum Gravity* **27**, 084013 (2010)
129. B. Bertotti, B.J. Carr, M.J. Rees, *Mon. Not. R. Astron. Soc.* **203**, 945–954 (1983)
130. S.M. Kopeikin, *Phys. Rev. D* **56**, 4455–4469 (1997)
131. F.B. Estabrook, H.D. Wahlquist, *Gen. Relativ. Gravit.* **6**, 439–447 (1975)
132. S. Detweiler, *Astrophys. J.* **234**, 1100–1104 (1979)
133. A. Sesana, A. Vecchio, C.N. Colacino, *Mon. Not. R. Astron. Soc.* **390**, 192–209 (2008)
134. A. Sesana, A. Vecchio, M. Volonteri, *Mon. Not. R. Astron. Soc.* **394**, 2255–2265 (2009)
135. K.J. Lee, F.A. Jenet, R.H. Price, *Astrophys. J.* **685**, 1304–1319 (2008)
136. K.J. Lee, F.A. Jenet, R.H. Price et al., *Astrophys. J.* **722**, 1589–1597 (2010)
137. F.A. Jenet, A. Lommen, S.L. Larson, L. Wen, *Astrophys. J.* **606**, 799–803 (2004)

Equations of Motion in an Expanding Universe

Sergei M. Kopeikin and Alexander N. Petrov

Abstract We make use of an effective field-theoretical approach to derive post-Newtonian equations of motion of hydrodynamical inhomogeneities in cosmology. The matter Lagrangian for the perturbed cosmological model includes dark matter, dark energy, and ordinary baryonic matter. The Lagrangian is expanded in an asymptotic Taylor series around a Friedmann-Lemaître-Robertson-Walker background. The small parameter of the decomposition is the magnitude of the metric tensor perturbation. Each term of the expansion series is gauge-invariant and all of them together form a basis for the successive post-Newtonian approximations around the background metric. The approximation scheme is covariant and the asymptotic nature of the Lagrangian decomposition does not require the post-Newtonian perturbations to be small though computationally it works the most effectively when the perturbed metric is close enough to the background metric. Temporal evolution of the background metric is governed by dark matter and dark energy and we associate the large-scale inhomogeneities of matter as those generated by the primordial cosmological perturbations in these two components with $\delta\rho/\rho \leq 1$. The small scale inhomogeneities are generated by the baryonic matter which is considered as a bare perturbation of the background gravitational field, dark matter and energy. Mathematically, the large scale structure inhomogeneities are given by the homogeneous solution of the post-Newtonian equations while the small scale inhomogeneities are described by a particular solution of these equations with the stress-energy tensor of the baryonic matter that admits $\delta\rho/\rho \gg 1$. We explicitly work out the field equations of the first post-Newtonian approximation in cosmology and derive the

S.M. Kopeikin (✉)

Department of Physics & Astronomy, University of Missouri,
322 Physics Bldg., Columbia, MO 65211, USA
e-mail: kopeikins@missouri.edu

S.M. Kopeikin

Siberian State Academy of Geodesy,
10 Plakhotny Stz., Novosibirsk 630108, Russia

A.N. Petrov

Sternberg Astronomical Institute, Lomonosov Moscow State University,
Universitetskii Prospect 13, Moscow 119992, Russia
e-mail: alex.petrov55@gmail.com

post-Newtonian equations of motion of the large and small scale inhomogeneities which generalize the covariant law of conservation of stress-energy-momentum tensor of matter in asymptotically-flat spacetime.

1 Introduction

1.1 Brief Overview of Perturbation Techniques

The multiwavelength satellite observations of cosmic microwave background (CMB) radiation have opened a new chapter in cosmology [1]. The standard cosmological model has been worked out to fit the model parameters to CMB [2–5]. The agreement between the standard theory and CMB observations was achieved at the decisive confidence level of 95 % [6]. The Planck satellite observations provide further evidences in robustness of the standard model [7, 8] (see <http://www.sciops.esa.int/index.php?project=PLANCK> for a comprehensive list of Planck collaboration papers) though it might be still difficult to discern between various scenarios of the early universe [9].

Study of the formation and evolution of the large scale structure in the universe is a key for understanding the present state of the universe and for prediction its uttermost fate [10]. It is extensively researched but, as of today, remains yet unsolved problem in physical cosmology. It is dark matter which plays a key role in structure formation. The dark matter consists of weakly interacting massive particles and interacts with baryons only by the force of gravity. The baryonic matter forms galaxies which, at early stage of structure formation, simply follow the evolution of dark matter. Therefore, the large scale distribution of galaxies is to trace the distribution of dark matter. At the linear stage the density contrast $\delta\rho = \rho - \bar{\rho}$ is much smaller than the background (mean) density $\bar{\rho}$ of the universe: $\delta\rho/\bar{\rho} \ll 1$. At later stages of cosmological evolution the structure formation enters non-linear regime when $\delta\rho/\bar{\rho} \simeq 1$ and caustics are formed. Further growth of the perturbations leads to formation of small scale structures like nuclei of galaxies, dwarf galaxies, globular clusters, stars and more compact relativistic objects which have $\delta\rho/\bar{\rho} \gg 1$. Gravitational field and matter of these super-dense baryonic objects counteract with the gravitational potential of dark matter and dark energy but details of this process are still unknown because it involves fluid's magnetohydrodynamics, turbulence and the physics of strong gravity field that implies a general relativistic approach taking into account the non-linear interaction of gravitational field with itself and the surrounding matter. Presumably, some insight to the solution of this problem can be gained by exploring exact Lemaître-Tolman cosmological solution of Einstein's equations admitting spatially inhomogeneity along radial coordinate [11–13]. This purely geometric approach is mathematically sound but physically unrealistic as it describes a pressureless, spherically-symmetric accretion of dust to a single point on the cosmological manifold while the real universe has a continuous set of the accretion points

determined by the initial spectrum of the primordial density fluctuations [3–5] and the baryonic fluid pressure cannot be ignored at non-linear regime.

It is supposed that non-linear gravitational effects in the formation of small-scale structure in the universe can be treated with the help of the general relativistic post-Newtonian approximations. They had been developed in asymptotically-flat space-time by a number of researchers [14–18] and were very successful in describing non-linear gravitational effects of fluids, for example, in derivation of equations of motion of binary stars [19–22], in calculation of equilibrium models of rapidly rotating neutron stars [23–25], etc. Post-Newtonian approximations in the baryonic component of the cosmological matter are more entrapped because the background manifold is not flat and we have to take into account not only the perturbations of the background metric tensor, $\bar{g}_{\alpha\beta}$, but those of the background stress-energy tensor of dark matter and dark energy as well. Furthermore, the formalism of the post-Newtonian approximations in cosmology is to separate the contribution of bare, small-scale perturbations of the baryonic matter from the large-scale perturbations of the background matter and the metric tensor of spacetime manifold.

A number of theoretical attempts was undertaken to work out the first post-Newtonian approximation and equations of motion of perfect fluid on cosmological manifold [26–29]. These works provide a good insight to the possible solution of the problem but are insufficiently consistent in separation of perturbations from their background values. They do not suggest a systematic approach for extending the calculations of the linear perturbation theory to the second, and higher, post-Newtonian approximations either. We also point out a rather surprising result by Oliynyk [30, 31] who analysed the general structure of the post-Newtonian expansions on cosmological manifold and arrived to the conclusion that the post-Newtonian series are analytic with respect to the small parameter $\varepsilon = v/c$, where v is a peculiar velocity of fluid with respect to the Hubble flow and c is the constant fundamental speed [32]. The Oliynyk's conclusion disagrees with that established for the post-Newtonian expansions in asymptotically-flat spacetime [33–35].

Recently, a new interest for developing a self-consistent theory of post-Newtonian approximations in precision cosmology was triggered by a lively discussion [36–40] on whether the small-scale structure of the universe affects its Hubble expansion rate and, thus, can explain the cosmic acceleration of the universe discovered in 1998–99 [41, 42] without invoking a dark energy. This is a, so-called, backreaction problem which intimately relates to the procedure of averaging the small-scale matter perturbations on a curved cosmological manifold [43, 44]. A certain progress in this direction was achieved but many mathematical aspects of the backreaction problem are still poorly understood [45]. The task is to build a rigorous mathematical formalism being able to describe on equal footing both the large-scale perturbations of the background matter of cosmological manifold with the density contrast $\delta\rho/\bar{\rho} \ll 1$ and the small-scale perturbations at present epoch caused by small-scale structures (galaxy, globular cluster, star) having the density contrast $\delta\rho/\bar{\rho} \gg 1$. Einstein's equations tell us that the density perturbation, $\delta\rho/\bar{\rho}$, is proportional to the second derivatives of the metric tensor perturbation which can be very large if $\delta\rho/\bar{\rho} \gg 1$. At the same time, the metric tensor perturbation, $\varkappa_{\alpha\beta} = g_{\alpha\beta} - \bar{g}_{\alpha\beta}$, and its first derivatives, $\varkappa_{\alpha\beta,\gamma}$,

can still remain small enough in order to apply a perturbation technique for solving the Einstein equations. This is similar to the situation in the solar system where the matter density contrast is huge but, nonetheless, the gravitational weak-field approximation for solving Einstein's equations is fully applicable [46]. It supports the idea that the perturbation technique in cosmology (under above assumptions) is valid for calculating physical effects of inhomogeneities on both the large and small scales [39, 47, 48]. The question is what mathematical technique is the most adequate to deal with physical applications.

Historically, the very first perturbation scheme in cosmology was worked out by Lifshitz [49, 50]. It is technically convenient for calculating time evolution of matter's large scale structure inhomogeneities and gravitational field perturbations [4, 51] but is unsuitable for discussing the process of formation and time evolution of the small scale structures in universe. This is because the Lifshitz approach uses the synchronous gauge where the time-time component of the metric tensor is fixed, $g_{00} = -1$, at any order of approximation. The small scale structure in cosmology corresponds to a localized astronomical system having a large density contrast, $\delta\rho/\bar{\rho}$, and governed by the Newtonian law of gravity which demands the presence of the Newtonian potential, U , making $g_{00} = -1 + 2U/c^2$. It breaks down the synchronous gauge condition at the regime of $\delta\rho/\bar{\rho} \gg 1$.

Bardeen's perturbation approach [52] (see also [53]) is more flexible as it admits a rather large freedom in choosing a particular gauge condition for solving cosmological problems [3, 5]. In the framework of this approach, the longitudinal (conformal-Newtonian) gauge is the most appropriate for discussing the small scale structure formation and its physical effects [54]. Some mathematical disadvantage of Bardeen's approach is in imposing a scalar-vector-tensor decomposition on the metric tensor. It requires application of the Helmholtz theorem [55] that demands to foliate spacetime by a family of spacelike hypersurfaces and to integrate the metric tensor over these hypersurfaces. It makes Bardeen's approach non-local as contrasted to Lifshitz's perturbation scheme. Moreover, in order to preserve the gauge-invariance of the Bardeen perturbation scheme one has to decompose the gauge functions in the same fashion as the metric tensor. As the universe evolves the gauge-invariance of the overall Bardeen's scheme can be preserved, if and only if, one maintains the mapping of spatial points on the foliations along the vector field of time coordinate world lines. Evidently, this approximation scheme differs significantly from the post-Newtonian approximations in asymptotically flat spacetime [14, 46, 56] which are more similar to Lifshitz's approach but use a different gauge condition (harmonic gauge).

A gauge-invariant alternative to Bardeen's approach was suggested by Ellis and Bruni [57] (see also [58, 59]), who developed a perturbation scheme based on a reduction of full Einstein's equations down to a system of field equations that are linear around a particular background. The Ellis-Bruni approach uses gauge-invariant variables which are spatial projections on the local comoving-observer frame threading the entire space-time of a real universe. Thus, the Bardeen's foliation has been replaced in Ellis-Bruni approach with the frame threading and, thus, observer dependent. This is not convenient, and is not used, for developing the post-Newtonian approximations in asymptotically-flat spacetime.

At the epoch of precise cosmology we need more transparent theoretical scheme of the post-Newtonian approximations for handling the iterative calculation of cosmological perturbations and derivation of their equations of motion. This iterative scheme must satisfy a number of well-established criteria like to be covariant, gauge-invariant, operate with locally defined quantities, be systematic and self-consistent in improving the order of approximations, clearly separate the large-scale from small-scale matter perturbations, be independent of the mathematical ambiguities introduced by the averaging procedures, etc. Some steps in developing such a scheme were done by Green and Wald [39, 40]. However, their work was focused mainly on the discussion of the averaging procedure in cosmology, on the proof that the small-scale, post-Newtonian inhomogeneities do not produce a noticeable backreaction and on finding mathematical evidences that the Newtonian approximation is sufficient in numerical N-body simulations of large scale structure formation [60].

No doubt, theoretical questions about how to perform the averaging in cosmology and whether it produces any backreaction at all, are important for understanding the mathematics of averaging of differential operators in non-linear equations and for clarification of the true nature of dark matter and dark energy. However, the post-Newtonian approximation scheme in cosmology has broader implications that are going beyond the discussion of averaging and backreaction problems and relates to the problem of interpretation of precise measurement of cosmological parameters by the advanced gravitational wave detector's technique [61, 62] and formation of small-scale structures in the universe at the non-linear regime. The formalism of the post-Newtonian approximations can be also helpful in better understanding of the influence of cosmological expansion on celestial mechanics of isolated astronomical systems like binary pulsars which are currently the best laboratories for testing non-linear regime of general relativity [63, 64]. These tests will be made significantly more precise with advent of gravitational-wave astronomy and Square Kilometer Array (SKA) radio telescope [65].

Recently, we have started a systematic investigation of the dynamics of small-scale inhomogeneities moving on the FLRW background manifold. We have set up a Lagrangian formalism to derive the post-Newtonian field equations for linearised cosmological perturbations [48] and analysed the Newtonian limit of these equations [66]. The present paper goes beyond the linear regime and explores some non-linear effects. In particular, we derive the post-Newtonian hydrodynamic equations of motion of the background matter (dark matter and dark energy) along with the equations of motion of the baryonic matter forming a small-scale structure with high-density contrast like a star, or galaxy or a cluster of galaxies.

We discuss the concept of the covariant and Lie derivatives on manifold in Sect. 2. Geometric theory of Euler-type variational perturbations of arbitrary background manifold is set up in Sect. 3. This theory is applied to the FLRW universe, governed by dark matter and dark energy, in Sect. 4. Section 5 derives the stress-energy tensors for perturbations of the gravitational field, dark matter and dark energy. Finally, we derive equations of motion of the small-scale (bare) perturbations in Sect. 6. Appendix outlines some particular mathematical aspects of our derivation.

Before going into details of our presentation we explain the notations adopted in the present paper.

1.2 Notations

We use G to denote the universal gravitational constant and c for the ultimate speed in Minkowski spacetime. Every time, when there is no confusion about the system of units, we use a geometrized system of units where $G = c = 1$. We put a bar over any function that belongs to the background manifold of the FLRW cosmological model. Any function without such a bar belongs to the perturbed manifold. The other notations used in the present paper are as follows:

- T and $X^i = \{X, Y, Z\}$ are the coordinate time and isotropic spatial coordinates on the background manifold;
- $X^\alpha = \{X^0, X^i\} = \{c\eta, X^i\}$ are the conformal coordinates with η being a conformal time;
- $x^\alpha = \{x^0, x^i\} = \{ct, x^i\}$ is an arbitrary coordinate chart on the background manifold;
- Greek indices $\alpha, \beta, \gamma, \dots$ run through values 0, 1, 2, 3, and label spacetime coordinates;
- Roman indices i, j, k, \dots take values 1, 2, 3, and label spatial coordinates;
- Einstein summation rule is applied for repeated (dummy) indices, for example, $P^\alpha Q_\alpha \equiv P^0 Q_0 + P^1 Q_1 + P^2 Q_2 + P^3 Q_3$, and $P^i Q_i \equiv P^1 Q_1 + P^2 Q_2 + P^3 Q_3$;
- $g_{\alpha\beta}$ is a full metric on the cosmological spacetime manifold;
- $\bar{g}_{\alpha\beta}$ is the FLRW metric on the background spacetime manifold;
- $\mathfrak{g}^{\mu\nu} = \sqrt{-g}g^{\mu\nu}$ —the metric tensor density of a unit weight +1;
- $\bar{\mathfrak{g}}^{\mu\nu} = \sqrt{-\bar{g}}\bar{g}^{\mu\nu}$ —the background metric tensor density of a unit weight +1;
- $\mathfrak{f}_{\alpha\beta}$ is the metric on the conformal spacetime manifold;
- $\eta_{\alpha\beta} = \text{diag}\{-1, +1, +1, +1\}$ is the Minkowski metric;
- the scale factor of the FLRW metric is denoted as $R = R(T)$, or as $a = a(\eta) = R[T(\eta)]$;
- the Hubble parameter, $H = R^{-1}dR/dT$;
- the conformal Hubble parameter, $\mathcal{H} = a'/a$;
- \mathcal{F} denotes a geometric object on the manifold. It can be either a scalar, or a vector, or a tensor field, or a corresponding tensor density;
- a bar, $\bar{\mathcal{F}}$ above a geometric object \mathcal{F} , denotes the unperturbed value of \mathcal{F} on the background manifold;
- the tensor indices of geometric objects on the background manifold are raised and lowered with the background metric $\bar{g}_{\alpha\beta}$, for example $\mathcal{F}_{\alpha\beta} = \bar{g}_{\alpha\mu}\bar{g}_{\beta\nu}\mathcal{F}^{\mu\nu}$;
- the tensor indices of geometric objects on the conformal spacetime are raised and lowered with the conformal metric $\mathfrak{f}_{\alpha\beta}$;
- symmetry of a geometric object with respect to two indices is denoted with round parenthesis, $\mathcal{F}_{(\alpha\beta)} \equiv (1/2)(\mathcal{F}_{\alpha\beta} + \mathcal{F}_{\beta\alpha})$;

- antisymmetry of a geometric object with respect to two indices is denoted with square parenthesis, $\mathcal{F}_{[\alpha\beta]} \equiv (1/2) (\mathcal{F}_{\alpha\beta} - \mathcal{F}_{\beta\alpha})$;
- a prime $\mathcal{F}' = d\mathcal{F}/d\eta$ denotes a total derivative with respect to the conformal time η ;
- a dot $\dot{\mathcal{F}} = d\mathcal{F}/dT$ denotes a total derivative with respect to the coordinate time T ;
- $\partial_\alpha = \partial/\partial x^\alpha$ is a partial derivative with respect to the coordinate x^α ;
- a comma with a following index $\mathcal{F}_{,\alpha} \equiv \partial_\alpha \mathcal{F}$ is an other designation of a partial derivative with respect to a coordinate x^α which is more convenient in some cases. In some cases which may not cause confusion, the comma as a symbol of the partial derivative is omitted. For example, we denote the partial derivatives of the perturbations of matter variables as $\phi_\alpha \equiv \phi_{,\alpha}$, $\psi_\alpha \equiv \psi_{,\alpha}$, etc.;
- a vertical bar, $\mathcal{F}_|$ denotes a covariant derivative of a geometric object \mathcal{F} with connection referred to the background metric $\bar{g}_{\alpha\beta}$. Covariant derivatives of scalar fields coincide with their partial derivatives;
- a semicolon, $\mathcal{F};_\alpha$ denotes a covariant derivative of a geometric object \mathcal{F} with the connection referred to the conformal metric $\bar{g}_{\alpha\beta}$;
- a covariant derivative with the connection referred to the full metric, $g_{\alpha\beta}$ is denoted with the help of ∇_α ;
- Φ^A —a multiplet of $A = \{1, 2, \dots, a\}$ matter fields. In other words, Φ^A denotes a set of fields $\Phi^A \equiv \{\Phi^1, \Phi^2, \dots, \Phi^a\}$ where each of the fields Φ^1, Φ^2, \dots is a tensor density of its own weight m_1, m_2, \dots respectively. These fields generate the full metric $g_{\mu\nu}$ of FLRW universe via the Einstein equations;
- $\bar{\Phi}^A$ —the background value of the fields Φ^A . These fields generate the background metric $\bar{g}_{\mu\nu}$ of FLRW universe via the unperturbed Einstein equations;
- Θ^B —a multiplet of $B = \{1, 2, \dots, b\}$ matter fields, $\Theta^B = \{\Theta^1, \Theta^2, \dots, \Theta^b\}$ which can be also tensor densities. They generate the stress energy tensor of the bare perturbation of the metric tensor $g_{\mu\nu}$ and that of the fields Φ^A ;
- $\bar{\Theta}^B$ —the background value of the fields Θ^B ;
- $\phi^A \equiv \Phi^A - \bar{\Phi}^A$ —the perturbation of the field Φ^A . Fields Φ^A and $\bar{\Phi}^A$ refer to the same point on the manifold;
- $\tau^B \equiv \Theta^B - \bar{\Theta}^B$ —the perturbation of the field Θ^B caused by the counteraction of the metric tensor perturbations $l_{\mu\nu}$ and those of the dynamic fields ϕ^A on the stress-energy tensor of the bare perturbations;
- $\varkappa_{\mu\nu} \equiv g_{\mu\nu} - \bar{g}_{\mu\nu}$ —the metric tensor perturbation. Fields $g_{\mu\nu}$ and $\bar{g}_{\mu\nu}$ refer to the same point on the manifold;
- $\mathfrak{h}^{\mu\nu} \equiv g^{\mu\nu} - \bar{g}^{\mu\nu}$ —the perturbation of the metric density caused by Θ^B ;
- $l^{\mu\nu} \equiv \mathfrak{h}^{\mu\nu}/\sqrt{-\bar{g}}$. In a linear approximation, $l^{\mu\nu} = -\varkappa^{\mu\nu} + \frac{1}{2}\bar{g}^{\mu\nu}\varkappa^\alpha{}_\alpha$, where $\varkappa^\alpha{}_\alpha = \bar{g}^{\alpha\beta}\varkappa_{\alpha\beta}$;
- the Christoffel symbols, $\Gamma^\alpha{}_{\beta\gamma} = \frac{1}{2}g^{\alpha\nu}(g_{\nu\beta,\gamma} + g_{\nu\gamma,\beta} - g_{\beta\gamma,\nu})$;
- the Riemann tensor, $R^\alpha{}_{\beta\mu\nu} = \Gamma^\alpha{}_{\beta\nu,\mu} - \Gamma^\alpha{}_{\beta\mu,\nu} + \Gamma^\alpha{}_{\mu\gamma}\Gamma^\gamma{}_{\beta\nu} - \Gamma^\alpha{}_{\nu\gamma}\Gamma^\gamma{}_{\beta\mu}$;
- the Ricci tensor, $R_{\alpha\beta} = R^\mu{}_{\alpha\mu\beta}$;
- the Ricci scalar, $R = g^{\alpha\beta}R_{\alpha\beta}$.

We shall often employ the term *on-shell*. By *on-shell* we mean *satisfying the equations of motion*. For instance, Noether's theorem links conserved quantities to symmetries of the system on-shell. It is invalid off-shell. We shall introduce and explain other notations as they appear in the main text of the paper.

2 Derivatives on the Geometric Manifold

2.1 Variational Derivative

Theory of perturbations of physical fields on manifolds rely upon the principle of the least action of a functional S called action. Variational derivative arises in the problem of finding solutions of the gravitational field equation that extremize the action

$$S = \int \mathcal{F} d^4x, \quad (1)$$

where $\mathcal{F} \equiv f\sqrt{-g}$, is a scalar density of weight +1. Let $\mathcal{F} = \mathcal{F}(Q, Q_\alpha, Q_{\alpha\beta})$ depend on the field variable Q , its first— $Q_\alpha \equiv Q_{,\alpha}$ and second— $Q_{\alpha\beta} \equiv Q_{,\alpha\beta}$ partial derivatives that play here a similar role as velocity and acceleration in the Lagrangian mechanics of point-like particles. The field variable Q can be a tensor field of an arbitrary type with the covariant and/or contravariant indices. For the time being, we suppress the tensor indices of Q as it may not lead to a confusion. Function \mathcal{F} depends on the determinant g of the metric tensor and can also depend on its derivatives. We shall discuss this case in the sections that follow.

A certain care should be taken in choosing the dynamic variables of the Lagrangian formalism in case when the variable Q is a tensor field. For example, if we choose a covariant vector field A_μ as an independent variable, the corresponding “velocity” and “acceleration” variables must be chosen as $A_{\mu,\alpha}$ and $A_{\mu,\alpha\beta}$ respectively. On the other hand, if the independent variable is chosen as a contravariant vector A^μ , the corresponding “velocity” and “acceleration” variables must be chosen as $A^{\mu,\alpha}$ and $A^{\mu,\alpha\beta}$. The same remark is applied to any other tensor field. The reason behind is that A_μ and A^μ are interrelated via the metric tensor, $A^\mu = g^{\mu\nu} A_\nu$. Therefore, derivative of A^μ differs from that of A_μ by an additional term involving the derivative of the metric tensor which, if being improperly introduced, can bring about spurious terms to the field equations derived from the principle of the least action.

Variational derivative, $\delta\mathcal{F}/\delta Q$, taken with respect to the variable Q relates a change, δS , in the functional S to a change, $\delta\mathcal{F}$, in the function \mathcal{F} that the functional depends on,

$$\delta S = \int \delta\mathcal{F} d^4x, \quad (2)$$

where

$$\delta \mathcal{F} = \frac{\partial \mathcal{F}}{\partial Q} \delta Q + \frac{\partial \mathcal{F}}{\partial Q_\alpha} \delta Q_\alpha + \frac{\partial \mathcal{F}}{\partial Q_{\alpha\beta}} \delta Q_{\alpha\beta}. \quad (3)$$

This is a functional increment of \mathcal{F} . The variational derivative is obtained after we single out a total divergence in the right side of (3) by making use of the commutation relations, $\delta Q_\alpha = (\delta Q)_{,\alpha}$ and $\delta Q_{\alpha\beta} = (\delta Q)_{,\alpha\beta}$. The total divergence is reduced to a surface term in the integral (2) which vanishes on the boundary of the volume of integration. Thus, the variation of S with respect to Q is given by

$$\delta S = \int \frac{\delta \mathcal{F}}{\delta Q} \delta Q d^4x, \quad (4)$$

where

$$\frac{\delta \mathcal{F}}{\delta Q} \equiv \frac{\partial \mathcal{F}}{\partial Q} - \frac{\partial}{\partial x^\alpha} \frac{\partial \mathcal{F}}{\partial Q_\alpha} + \frac{\partial^2}{\partial x^\alpha \partial x^\beta} \frac{\partial \mathcal{F}}{\partial Q_{\alpha\beta}}. \quad (5)$$

Similar procedure can be applied to S by varying it with respect to Q_α and $Q_{\alpha\beta}$. In such a case we get the variational derivatives of \mathcal{F} with respect to Q_α

$$\frac{\delta \mathcal{F}}{\delta Q_\alpha} \equiv \frac{\partial \mathcal{F}}{\partial Q_\alpha} - \frac{\partial}{\partial x^\beta} \frac{\partial \mathcal{F}}{\partial Q_{\alpha\beta}}, \quad (6)$$

and that of \mathcal{F} with respect to $Q_{\alpha\beta}$,

$$\frac{\delta \mathcal{F}}{\delta Q_{\alpha\beta}} \equiv \frac{\partial \mathcal{F}}{\partial Q_{\alpha\beta}} \quad (7)$$

Let us assume that there is another geometric object, $\mathcal{T}(Q, Q_\alpha, Q_{\alpha\beta})$, which differs from the original one $\mathcal{F}(Q, Q_\alpha, Q_{\alpha\beta})$ by a total divergence

$$\mathcal{T}(Q, Q_\alpha, Q_{\alpha\beta}) = \mathcal{F}(Q, Q_\alpha, Q_{\alpha\beta}) + \partial_\beta H^\beta(Q, Q_\alpha). \quad (8)$$

It is well-known [67, 68] that taking the variational derivative (5) from \mathcal{T} and \mathcal{F} yields the same result

$$\frac{\delta \mathcal{T}}{\delta Q} \equiv \frac{\delta \mathcal{F}}{\delta Q}, \quad (9)$$

because the variational derivative from the divergence is zero identically. In fact, it is straightforward to prove a more general result, namely, that the variational derivative (5), after it applies to a partial derivative of an arbitrary smooth function, vanishes identically

$$\frac{\delta}{\delta Q} \left(\frac{\partial \mathcal{F}}{\partial x^\alpha} \right) \equiv 0. \quad (10)$$

However, this property does not hold for a covariant derivative in the most general case [68].

The variational derivatives are covariant geometric object that is they do not depend on the choice of a particular coordinates on manifold [46, 68]. In case, when the dynamic variable Q is not a metric tensor, this statement can be proved by taking the first, $Q_\alpha \equiv Q_{;\alpha}$, and second, $Q_{\alpha\beta} \equiv Q_{;\alpha\beta}$, covariant derivatives of Q as independent dynamic variables instead of its partial derivatives, Q_α and $Q_{\alpha\beta}$. In this case the procedure of derivation of variational derivatives (5), (6) remains the same and the result is

$$\frac{\delta \mathcal{F}}{\delta Q} = \frac{\partial \mathcal{F}}{\partial Q} - \left[\frac{\partial \mathcal{F}}{\partial Q_\alpha} \right]_{;\alpha} + \left[\frac{\partial \mathcal{F}}{\partial Q_{\alpha\beta}} \right]_{;\beta\alpha}. \quad (11)$$

The order, in which the covariant derivatives are taken, is imposed by the procedure of the extracting the total divergence from the variation of the action in (2). The order of the derivatives is important because the covariant derivatives do not commute.

Variational derivative of \mathcal{F} with respect to the metric tensor $g_{\mu\nu}$ is defined by the same Eqs. (5)–(7) where we identify $Q \equiv g_{\mu\nu}$, $Q_\alpha \equiv g_{\mu\nu,\alpha}$, and $Q_{\mu\nu} \equiv g_{\mu\nu,\alpha\beta}$. It yields

$$\frac{\delta \mathcal{F}}{\delta g_{\mu\nu}} \equiv \frac{\partial \mathcal{F}}{\partial g_{\mu\nu}} - \frac{\partial}{\partial x^\alpha} \frac{\partial \mathcal{F}}{\partial g_{\mu\nu,\alpha}} + \frac{\partial^2}{\partial x^\alpha \partial x^\beta} \frac{\partial \mathcal{F}}{\partial g_{\mu\nu,\alpha\beta}} \quad (12)$$

$$\frac{\delta \mathcal{F}}{\delta g_{\mu\nu,\alpha}} \equiv \frac{\partial \mathcal{F}}{\partial g_{\mu\nu,\alpha}} - \frac{\partial}{\partial x^\beta} \frac{\partial \mathcal{F}}{\partial g_{\mu\nu,\alpha\beta}}, \quad (13)$$

$$\frac{\delta \mathcal{F}}{\delta g_{\mu\nu,\alpha\beta}} \equiv \frac{\partial \mathcal{F}}{\partial g_{\mu\nu,\alpha\beta}} \quad (14)$$

Covariant generalization of (12)–(14) is not quite straightforward because the covariant derivative of the metric tensor $g_{\mu\nu;\alpha} = 0$, and we cannot use it as a dynamic variable. In this case, we consider the set of the metric tensor, $g_{\mu\nu}$, the Christoffel symbols $\Gamma^\alpha_{\mu\nu}$, and the Riemann tensor $R^\alpha_{\beta\mu\nu}$ as a set of independent dynamic variables. The action is given by (1) where $\mathcal{F} \equiv \sqrt{-g} f(g_{\mu\nu}, \Gamma^\alpha_{\mu\nu}, R^\alpha_{\beta\mu\nu})$ is a scalar density of weight +1. Variation of \mathcal{F} is

$$\delta \mathcal{F} = \frac{\partial \mathcal{F}}{\partial g_{\mu\nu}} \delta g_{\mu\nu} + \frac{\partial \mathcal{F}}{\partial \Gamma^\alpha_{\mu\nu}} \delta \Gamma^\alpha_{\mu\nu} + \frac{\partial \mathcal{F}}{\partial R^\alpha_{\beta\mu\nu}} \delta R^\alpha_{\beta\mu\nu}, \quad (15)$$

where variations of the Christoffel symbols and the Riemann tensor are tensors that can be expressed in terms of the variation $\delta g_{\mu\nu}$ of the metric tensor [51]

$$\delta \Gamma^\alpha_{\mu\nu} = \frac{1}{2} g^{\alpha\sigma} [(\delta g_{\sigma\mu})_{;\nu} + (\delta g_{\sigma\nu})_{;\mu} - (\delta g_{\mu\nu})_{;\sigma}], \quad (16)$$

$$\delta R^\alpha_{\beta\mu\nu} = (\delta \Gamma^\alpha_{\beta\nu})_{;\mu} - (\delta \Gamma^\alpha_{\beta\mu})_{;\nu}. \quad (17)$$

Now, we replace (16), (18) in (15) and single out a total divergence.¹ It yields

$$\delta\mathcal{F} = \frac{\delta\mathcal{F}}{\delta g_{\mu\nu}} \delta g_{\mu\nu} + \mathcal{B}^\alpha{}_{,\alpha}, \quad (18)$$

where the total divergence vanishes on the boundary of integration of the action, and the covariant variational derivative is

$$\begin{aligned} \frac{\delta\mathcal{F}}{\delta g_{\mu\nu}} &= \frac{\partial\mathcal{F}}{\partial g_{\mu\nu}} \\ &- \frac{1}{2} \left(g^{\sigma\mu} \frac{\partial\mathcal{F}}{\partial\Gamma^\sigma{}_{\nu\alpha}} + g^{\sigma\nu} \frac{\partial\mathcal{F}}{\partial\Gamma^\sigma{}_{\mu\alpha}} - g^{\sigma\alpha} \frac{\partial\mathcal{F}}{\partial\Gamma^\sigma{}_{\mu\nu}} \right)_{;\alpha} \\ &+ \left(g^{\sigma\mu} \frac{\partial\mathcal{F}}{\partial R^\sigma{}_{\alpha\beta\nu}} + g^{\sigma\nu} \frac{\partial\mathcal{F}}{\partial R^\sigma{}_{\mu\beta\alpha}} - g^{\sigma\alpha} \frac{\partial\mathcal{F}}{\partial R^\sigma{}_{\mu\beta\nu}} \right)_{;\beta\alpha} \end{aligned} \quad (19)$$

Variational derivative with respect to the contravariant metric tensor is

$$\frac{\delta\mathcal{F}}{\delta g^{\mu\nu}} = \frac{\partial g_{\alpha\beta}}{\partial g^{\mu\nu}} \frac{\delta\mathcal{F}}{\delta g_{\alpha\beta}} = -g_{\alpha\mu} g_{\beta\nu} \frac{\delta\mathcal{F}}{\delta g_{\alpha\beta}}. \quad (20)$$

The variational derivatives are not linear operators. For example, they do not obey Leibniz's rule [69, Sect. 2.3]. More specifically, for any geometric object, $\mathcal{H} = \mathcal{F}\mathcal{T}$, that is a corresponding product of two other geometric objects, $\mathcal{F} = \mathcal{F}(Q, Q_\alpha, Q_{\alpha\beta})$ and $\mathcal{T} = \mathcal{T}(Q, Q_\alpha, Q_{\alpha\beta})$, the variational derivative

$$\frac{\delta(\mathcal{F}\mathcal{T})}{\delta Q} \neq \frac{\delta\mathcal{F}}{\delta Q} \mathcal{T} + \mathcal{F} \frac{\delta\mathcal{T}}{\delta Q}, \quad (21)$$

in the most general case. The chain rule with regard to the variational derivative is preserved in a limited sense. More specifically, let us consider a geometric object $\mathcal{F} = \mathcal{F}(Q, Q_\alpha, Q_{\alpha\beta})$ where Q is a function of a variable P , that is $Q = Q(P)$. Then, the variational derivative

$$\frac{\delta\mathcal{F}}{\delta P} = \frac{\delta\mathcal{F}}{\delta Q} \frac{\partial Q}{\partial P}, \quad (22)$$

that can be confirmed by inspection [70]. On the other hand, if we have a singled-valued function $\mathcal{H} = \mathcal{H}(Q)$, and $Q = Q(P, P_\alpha, P_{\alpha\beta})$, the chain rule

$$\frac{\delta\mathcal{H}}{\delta P} = \frac{\partial\mathcal{F}}{\partial Q} \frac{\delta Q}{\delta P}, \quad (23)$$

¹The fact that \mathcal{F} is a scalar density is essential for the transformation of covariant derivatives to the total divergence. The total divergences can be converted to surface integrals which vanish on the boundary of integration and, hence, can be dropped off the calculations.

is also valid. The chain rule (23) will be often used in calculations of the present paper.

2.2 Lie Derivative

Lie derivative on the manifold can be viewed as being induced by a diffeomorphism

$$x'^\alpha = x^\alpha + \xi^\alpha(x), \quad (24)$$

such that a vector field ξ^α has no self-intersections, thus, defining a congruence of curves which provides a natural mapping of the manifold into itself. Lie derivative of a geometric object \mathcal{F} is denoted as $\mathcal{L}_\xi \mathcal{F}$. It is defined by a standard rule

$$\mathcal{L}_\xi \mathcal{F} = \mathcal{F}'(x) - \mathcal{F}(x), \quad (25)$$

where \mathcal{F}' is calculated by doing its coordinate transformation induced by the change of the coordinates (24) with subsequent pulling back the transformed object from the point x'^α to x^α along the congruence ξ^α [46]. In particular, for any tensor density $\mathcal{F} = \mathcal{F}_{\nu_1 \dots \nu_q}^{\mu_1 \dots \mu_p}$ of type (p, q) and weight m one has

$$\begin{aligned} \mathcal{L}_\xi \mathcal{F}_{\nu_1 \dots \nu_q}^{\mu_1 \dots \mu_p} = & \xi^\alpha \mathcal{F}_{\nu_1 \dots \nu_q, \alpha}^{\mu_1 \dots \mu_p} + m \xi^\alpha_{, \alpha} \mathcal{F}_{\nu_1 \dots \nu_q}^{\mu_1 \dots \mu_p} \\ & + \mathcal{F}_{\alpha \dots \nu_q}^{\mu_1 \dots \mu_p} \xi^\alpha_{, \nu_1} + \dots + \mathcal{F}_{\nu_1 \dots \alpha}^{\mu_1 \dots \mu_p} \xi^\alpha_{, \nu_q} \\ & - \mathcal{F}_{\nu_1 \dots \nu_q}^{\alpha \dots \mu_p} \xi^{\mu_1}_{, \alpha} - \dots - \mathcal{F}_{\nu_1 \dots \nu_q}^{\mu_1 \dots \alpha} \xi^{\mu_p}_{, \alpha}. \end{aligned} \quad (26)$$

We notice that *all* partial derivatives in the right side of Eq. (26) can be simultaneously replaced with the covariant derivatives because the terms containing the Christoffel symbols cancel each other.

The Lie derivative commutes with a partial (but not a covariant) derivative

$$\partial_\alpha (\mathcal{L}_\xi \mathcal{F}) = \mathcal{L}_\xi (\partial_\alpha \mathcal{F}). \quad (27)$$

This property allows us to prove that a Lie derivative from a geometric object $\mathcal{F}(Q, Q_\alpha, Q_{\alpha\beta})$ can be calculated in terms of its variational derivative. Indeed,

$$\mathcal{L}_\xi \mathcal{F} = \frac{\partial \mathcal{F}}{\partial Q} \mathcal{L}_\xi Q + \frac{\partial \mathcal{F}}{\partial Q_\alpha} \mathcal{L}_\xi Q_\alpha + \frac{\partial \mathcal{F}}{\partial Q_{\alpha\beta}} \mathcal{L}_\xi Q_{\alpha\beta}. \quad (28)$$

Now, after using the commutation property (27) and changing the order of partial derivatives in $\mathcal{L}_\xi Q_\alpha$ and $\mathcal{L}_\xi Q_{\alpha\beta}$, one can express (28) as an algebraic sum of the variational derivative and a total divergence

$$\mathcal{L}_\xi \mathcal{F} = \frac{\delta \mathcal{F}}{\delta Q} \mathcal{L}_\xi Q + \frac{\partial}{\partial x^\alpha} \left(\frac{\delta \mathcal{F}}{\delta Q_\alpha} \mathcal{L}_\xi Q + \frac{\delta \mathcal{F}}{\delta Q_{\alpha\beta}} \mathcal{L}_\xi Q_\beta \right). \quad (29)$$

This property of the Lie derivative indicates its close relation to the variational derivative on the manifold and will be used in the calculations that follow. It is also worth pointing out that (29) is used for derivation of Noether's theorem of conservation of the canonical stress-energy tensor of the field Q in case when $\mathcal{F} = \mathcal{L}$ is the Lagrangian density of the field for which the variational derivative vanishes on-shell, $\delta \mathcal{F} / \delta Q = \delta \mathcal{L} / \delta Q = 0$, and $\mathcal{L}_\xi \mathcal{L} = \partial_\alpha (\xi^\alpha \mathcal{L})$.

2.3 Partial Derivatives with Respect to the Metric Tensor

Calculation of variational derivatives requires calculation of partial derivatives with respect to the metric tensor and other geometric objects like the Christoffel symbols, the Riemann tensor, etc. An example is the partial derivatives from the determinant of the metric tensor

$$\frac{\partial \sqrt{-g}}{\partial g^{\mu\nu}} = -\frac{1}{2} \sqrt{-g} g_{\mu\nu}, \quad \frac{\partial \sqrt{-g}}{\partial g_{\mu\nu}} = \frac{1}{2} \sqrt{-g} g^{\mu\nu}, \quad (30)$$

where g is the determinant of the metric tensor.

Taking partial derivatives from \mathcal{F} with respect to $g_{\mu\nu}$, $\Gamma_{\mu\nu}^\alpha$ and $R_{\beta\mu\nu}^\alpha$ is facilitated with the help of the following formulas

$$\frac{\partial g_{\alpha\beta}}{\partial g_{\mu\nu}} = \delta_\alpha^{(\mu} \delta_\beta^{\nu)}, \quad (31)$$

$$\frac{\partial \Gamma_{\mu\nu}^\sigma}{\partial \Gamma_{\rho\mu\nu}^\sigma} = \delta_\rho^\sigma \delta_\alpha^{(\mu} \delta_\beta^{\nu)}, \quad (32)$$

$$\frac{\partial R_{\kappa\mu\nu}^\sigma}{\partial R_{\rho\mu\nu}^\sigma} = \delta_\rho^\sigma \delta_\gamma^\kappa \delta_\alpha^{[\mu} \delta_\beta^{\nu]}, \quad (33)$$

where we have accounted for the symmetry of the Christoffel symbols and the anti-symmetry of the Riemann tensor.

Variational derivative with respect to the contravariant metric tensor is achieved with the help of the derivative

$$\frac{\delta}{\delta g^{\mu\nu}} = \frac{\partial g_{\alpha\beta}}{\partial g^{\mu\nu}} \frac{\delta}{\delta g_{\alpha\beta}} = -g_{\alpha\mu} g_{\nu\beta} \frac{\delta}{\delta g_{\alpha\beta}}. \quad (34)$$

We will also need to calculate the variational derivative with respect to the density of the metric tensor, $g^{\mu\nu}$. It relates to the variational derivative of the metric tensor as follows,

$$\frac{\delta}{\delta g^{\mu\nu}} = \frac{\partial g^{\rho\sigma}}{\partial g^{\mu\nu}} \frac{\delta}{\delta g^{\rho\sigma}} = A_{\mu\nu}^{\rho\sigma} \frac{1}{\sqrt{-g}} \frac{\delta}{\delta g^{\rho\sigma}}, \quad (35)$$

where

$$A_{\mu\nu}^{\rho\sigma} = \frac{1}{2} \left(\delta_{\mu}^{\rho} \delta_{\nu}^{\sigma} + \delta_{\nu}^{\rho} \delta_{\mu}^{\sigma} - g_{\mu\nu} g^{\rho\sigma} \right). \quad (36)$$

Partial derivatives of any geometric object with respect to either the metric tensor or its first, or second derivatives can be easily calculated after making use of

$$\frac{\partial g^{\alpha\beta}}{\partial g^{\mu\nu}} = \delta_{\mu}^{(\alpha} \delta_{\nu}^{\beta)}, \quad (37)$$

$$\frac{\partial g^{\alpha\beta}_{,\gamma}}{\partial g^{\mu\nu}_{,\sigma}} = \delta_{\mu}^{(\alpha} \delta_{\nu}^{\beta)} \delta_{\gamma}^{\sigma}, \quad (38)$$

$$\frac{\partial g^{\alpha\beta}_{,\gamma\kappa}}{\partial g^{\mu\nu}_{,\rho\sigma}} = \delta_{\mu}^{(\alpha} \delta_{\nu}^{\beta)} \delta_{\gamma}^{(\rho} \delta_{\kappa}^{\sigma)}. \quad (39)$$

3 Geometric Perturbation Theory of Arbitrary Background Manifold

Let us consider a field theory on a background pseudo-Riemannian manifold $\bar{\mathcal{M}}$ having the metric tensor $\bar{g}_{\alpha\beta}$ that is a solution of Einstein's equations with the stress-energy tensor $\bar{T}_{\alpha\beta}$ of the physical fields $\bar{\Phi}^A$, where the index A numerates the fields and takes values $A = 1, 2, \dots, a$. Let us perturb the manifold by “injecting” into it some matter with a bare stress-energy tensor $\mathfrak{T}_{\alpha\beta}$ that is generated by a set of physical fields Θ^B where the index B numerates the bare fields and takes values $B = 1, 2, \dots, b$. We denote the unperturbed value of the bare fields, $\bar{\Theta}^B$. The tensor $\mathfrak{T}_{\alpha\beta}$ is the source of the bare perturbations of the background values of the metric tensor $\bar{g}_{\mu\nu}$ and the fields $\bar{\Phi}^A$ on the background manifold $\bar{\mathcal{M}}$. We assume that the fields Φ^A and Θ^B are both minimally coupled to the curvature of spacetime in the sense of the strong equivalence principle [46, Sect. 3.8.2], [71, Sect. 6.13]. We also assume for the sake of simplicity that the fields Φ^A and Θ^B do not directly interact one with another. The basic geometric theory of the present paper is Einstein's general relativity. Other geometric theories beyond general relativity can be considered after making corresponding modifications in the Lagrangian formalism presented in this paper but we shall not proceed in this direction here (see, e.g. [72]).

The perturbation caused by tensor $\mathfrak{T}_{\alpha\beta}$ changes the metric $\bar{g}_{\alpha\beta}$ to $g_{\alpha\beta} = \bar{g}_{\alpha\beta} + \varkappa_{\alpha\beta}$, and the fields $\bar{\Phi}^A$ to $\Phi^A = \bar{\Phi}^A + \phi^A$, where $\varkappa_{\alpha\beta}$ and ϕ^A are the perturbations of the metric and the physical fields respectively. Due to the non-linearity of Einstein's equations the perturbations interact one with another through gravitational coupling in Einstein's equations. It makes the geometric structure of the perturbed manifold \mathcal{M} rather entangled. This section describes how to find out the perturbed structure

of the manifold \mathcal{M} , the field equations, and the equations of motion of matter on the basis of the Lagrangian variational principle [70, 73].

3.1 Variational Principle

Lagrangian formulation of the dynamic theory of physical perturbations starts off the Hilbert-Einstein action defined on an unperturbed (background) manifold $\bar{\mathcal{M}}$

$$\bar{S} = \int d^4x \bar{\mathcal{L}}(\bar{g}_{\mu\nu}, \bar{\Phi}^A), \quad (40)$$

where $\bar{\mathcal{L}} = \sqrt{-\bar{g}}\bar{L}$ is a scalar density of weight +1, $\bar{L} = \bar{L}(\bar{g}_{\mu\nu}, \bar{\Phi}^A)$ is the Lagrangian depending on the metric tensor, the multiplet of matter (tensor density) fields $\bar{\Phi}^A = \{\bar{\Phi}^1, \bar{\Phi}^2, \dots, \bar{\Phi}^a\}$, and their partial derivatives. We did not show explicitly (but are keeping in mind) the dependence of the Lagrangian on the derivatives to avoid superfluous notations. The tensor fields $\bar{\Phi}^A$ determine the dynamic and geometric structure of the background manifold $\bar{\mathcal{M}}$ via Einstein's equations. For short, we shall call the Lagrangian density $\bar{\mathcal{L}}$ simply the Lagrangian.

The Lagrangian \mathcal{L} is split in two parts

$$\bar{\mathcal{L}}(\bar{g}_{\mu\nu}, \bar{\Phi}^A) = \bar{\mathcal{L}}^G(\bar{g}_{\mu\nu}) + \bar{\mathcal{L}}^M(\bar{g}_{\mu\nu}, \bar{\Phi}^A), \quad (41)$$

where the gravitational (Hilbert) Lagrangian

$$\bar{\mathcal{L}}^G(\bar{g}_{\alpha\beta}) \equiv -\frac{1}{16\pi}\sqrt{-\bar{g}}\bar{R}, \quad (42)$$

depends on the background metric tensor $\bar{g}_{\mu\nu}$, its first and second derivatives. The matter Lagrangian, $\bar{\mathcal{L}}^M$ depends solely on the metric tensor and (for instance, in case of Yang-Mills fields) its first derivatives. Of course, it also depends on the matter fields $\bar{\Phi}^A$ and their derivatives.

Dynamic equations of the gravitational field and matter are derived from the principle of the least action by varying the action (40) and equating its variation to zero. This procedure is equivalent to taking the variational derivatives (5) from the Lagrangian (41) that yields

$$\frac{\delta \bar{\mathcal{L}}^M}{\delta \bar{\Phi}^A} = 0, \quad (43)$$

$$\frac{\delta \bar{\mathcal{L}}^G}{\delta \bar{g}^{\mu\nu}} + \frac{\delta \bar{\mathcal{L}}^M}{\delta \bar{g}^{\mu\nu}} = 0. \quad (44)$$

Equation (43) describes dynamic evolution of the matter fields $\bar{\Phi}^A$. Equation (44) can be recognized as the Einstein equations for the background gravitational field (the metric) after noticing that the variational derivatives

$$\frac{\delta \bar{\mathcal{L}}^G}{\delta \bar{g}^{\mu\nu}} = -\frac{1}{16\pi} \bar{R}_{\mu\nu}, \quad (45)$$

$$\frac{\delta \bar{\mathcal{L}}^M}{\delta \bar{g}^{\mu\nu}} = \frac{1}{2} \left(\bar{T}_{\mu\nu}^M - \frac{1}{2} \bar{g}_{\mu\nu} \bar{T}^M \right), \quad (46)$$

where $\bar{R}_{\mu\nu}$ is the background value of the Ricci tensor calculated with the help of the background metric $\bar{g}_{\mu\nu}$, and $\bar{T}_{\mu\nu}^M$ is the stress-energy tensor of the fields $\bar{\Phi}^A$. Equation (46) is just a definition of the metrical stress-energy tensor of matter [46, Sect. 3.9.5]. Equation (45) is usually derived by varying the gravitational action (see, for instance, [46, p. 310], [51, p. 364]) and extracting the total derivative that vanishes on the boundary of the volume of integration. We emphasize that the variational derivative (45) given by Eqs. (19) and (20) achieves the same goal in much more simple and attractive way. Indeed, the Lagrangian (42) is equivalent to

$$\bar{\mathcal{L}}^G = -\frac{1}{16\pi} \bar{g}^{\kappa\lambda} \delta_\rho^\sigma \bar{R}^\rho{}_{\kappa\sigma\lambda} \quad (47)$$

This expression depends only on the metric tensor and the Riemann tensor as a linear algebraic function. Hence, partial derivatives with respect to the Christoffel symbols are automatically nil. Moreover, the covariant derivatives from the metric tensor vanish identically. Hence, the variational derivative (20) is reduced to a simple partial derivative

$$\frac{\delta \bar{\mathcal{L}}^G}{\delta \bar{g}^{\mu\nu}} = -\frac{1}{16\pi} \frac{\partial \bar{g}^{\kappa\lambda}}{\partial \bar{g}^{\mu\nu}} \bar{R}_{\kappa\lambda}, \quad (48)$$

that immediately results in (45). Of course, we could calculate the variational derivative in (45) by applying a more conventional definition (12). It yields the same result but the calculations are lengthy and less obvious. We explain details of this calculation in Appendix section “Variational Derivative from the Hilbert Lagrangian”.

For many astrophysical applications the background value of the metric tensor $\bar{g}_{\mu\nu}$ is the Minkowski metric $\eta_{\mu\nu}$ which is a trivial solution of the field equations (44). However, this assumption is not applicable in cosmology where (44) are the dynamic Friedmann equations describing the expanding universe by means of the FLRW metric

$$d\bar{s}^2 = -dT^2 + R^2(T) \left(1 + \frac{1}{4}kr^2 \right)^{-2} \delta_{ij} dX^i dX^j, \quad (49)$$

where $X^\alpha = (T, X^i)$ are the global coordinates associated with the Hubble flow, $r = \sqrt{\delta_{ij} X^i X^j}$, T is the cosmic time, k is the curvature of space taking one of

the three values $k = -1, 0, +1$, and $R(T)$ is the scale factor which exact time-dependence is governed by the solution of Einstein's equations with the background stress-energy tensor determined by the matter fields $\bar{\Phi}^A$ [4, 5, 51].

Physical perturbations of the background manifold $\bar{\mathcal{M}}$ are caused by the bare matter field $\bar{\Theta}^B$ with the Lagrangian $\bar{\mathcal{L}}^P = \sqrt{-\bar{g}}\bar{L}^P$ where $\bar{L}^P \equiv \bar{L}^P(\bar{g}_{\mu\nu}, \bar{\Theta}^B)$ is a scalar function. The present paper assumes that $\bar{\Theta}^B$ is minimally coupled with gravity but does not interact directly with the fields $\bar{\Phi}^A$. We postulate that the absolute value of $\bar{\mathcal{L}}^P$ is much smaller than the Lagrangian $\bar{\mathcal{L}}$ of the background manifold, that is $\bar{\mathcal{L}}^P \ll \bar{\mathcal{L}}$. The fields $\bar{\Theta}^B$ can be conceived, for example, as a matter composing of an isolated astronomical system like our solar system or a galaxy, or a cluster of galaxies. However, it also admissible to consider $\bar{\Theta}^B$ as a seed perturbations of the fields $\bar{\Phi}^A$, for example, in case of discussion of the formation of the large-scale structure of the universe from the primordial cosmological perturbations. The assumptions imposed on the Lagrangian of the fields $\bar{\Theta}^B$ presume that in order to describe the dynamic evolution of the perturbed manifold \mathcal{M} we should add algebraically the Lagrangian $\bar{\mathcal{L}}^P$ of the bare perturbations to the unperturbed Lagrangian $\bar{\mathcal{L}}$ of the background manifold, write down the perturbed Einstein equations for the metric tensor perturbations $l_{\mu\nu}$ along with the equations for the perturbations ϕ^A of the fields $\bar{\Phi}^A$, solve them, and proceed to the second, third, etc. iterations if necessary. The iterative theory of the Lagrangian perturbations of the manifold is described in the following sections.

3.2 The Lagrangian Perturbations of Dynamic Fields

Lagrangian formulation of the dynamic theory of physical perturbations of a manifold starts off the Hilbert-Einstein action

$$S = \int d^4x \mathcal{L}(g_{\mu\nu}, \Phi^A, \Theta^B), \quad (50)$$

where $\mathcal{L} = \sqrt{-g}L$ is the scalar density of weight +1, and $L = L(g_{\mu\nu}, \Phi^A, \Theta^B)$ is the Lagrangian depending on the metric tensor, the matter fields $\Phi^A = \{\Phi^1, \Phi^2, \dots, \Phi^a\}$, and the fields $\Theta^B = \{\Theta^1, \Theta^2, \dots, \Theta^b\}$ representing the bare perturbation of the manifold.

The Lagrangian \mathcal{L} consists of three parts

$$\mathcal{L}(g_{\mu\nu}, \Phi^A, \Theta^B) = \mathcal{L}^G(g_{\mu\nu}) + \mathcal{L}^M(g_{\mu\nu}, \Phi^A) + \mathcal{L}^P(g_{\mu\nu}, \Theta^B), \quad (51)$$

where the gravitational (Hilbert) Lagrangian

$$\mathcal{L}^G(g_{\alpha\beta}) \equiv -\frac{1}{16\pi}\sqrt{-g}R, \quad (52)$$

depends on the metric tensor $g_{\mu\nu}$, its first and second derivatives. The Lagrangians of matter, \mathcal{L}^M and \mathcal{L}^P , depend solely on the metric tensor and its first derivatives. They also depend directly on the matter fields Φ^A and Θ^B and their partial derivatives but we did not show it explicitly to avoid tedious notations. The matter fields Φ^A and Θ^B are minimally coupled to gravity but we assume that they are not directly coupled to each other. Hence, the Lagrangian of the interaction between these fields does not appear explicitly in (51). This assumption can be relaxed in some alternative theories of gravity [74]. Such cases can be handled with the formalism of the present paper but the computational algebra becomes more intricate and will be considered somewhere else.

It is worth noticing that \mathcal{L}^M and \mathcal{L}^P depend on the metric tensor $g_{\mu\nu}$ both explicitly and implicitly through the mathematical definition of the matter fields Φ^A and Θ^B . For example, consider the Lagrangian of the perfect fluid $\mathcal{L}^M = \rho(1 + \Pi)\sqrt{-g}$, where Π is the specific internal energy of the fluid and ρ is the energy density. The metric tensor appears explicitly as $\sqrt{-g}$ and implicitly in ρ that is defined as the ratio of the rest energy of the fluid's element to its comoving volume which depends on the determinant of the metric tensor [46].

We define perturbations of the gravitational and matter fields residing on the background manifold by the following equations,

$$g^{\mu\nu}(x) = \bar{g}^{\mu\nu}(x) + h^{\mu\nu}(x), \quad (53)$$

$$\Phi^A(x) = \bar{\Phi}^A(x) + \phi^A(x), \quad (54)$$

$$\Theta^B(x) = \bar{\Theta}^B(x) + \theta^B(x), \quad (55)$$

where all functions are taken at one and the same point $x \equiv x^\alpha$ of the unperturbed manifold. The perturbed values of the fields are assumed to be small compared with their background counterparts: $|h^{\mu\nu}| < |\bar{g}^{\mu\nu}|$, $|\phi^A| < |\bar{\Phi}^A|$ and $|\theta^B| < |\bar{\Theta}^B|$. There are no specific limitations on the rate of change of the perturbations that is on their first partial derivatives. The second partial derivatives of the fields are comparable (due to the field equations) with the magnitude of the stress-energy tensor, $\mathcal{T}^{\mu\nu}$, of the bare perturbations that is $|h^{\mu\nu}_{,\alpha\beta}| \sim |\phi^A_{,\alpha\beta}| \sim |\mathcal{T}^{\mu\nu}|$.

We consider the perturbations $h^{\mu\nu}$, ϕ^A along with the perturbing field θ^B as a set of independent dynamic variables which propagate on the background manifold $\bar{\mathcal{M}}$ with the metric $\bar{g}_{\mu\nu}$. In order to derive differential equations governing the evolution of the perturbations we substitute the field decompositions (53), (54) to the Lagrangian \mathcal{L} defined by Eq. (51) which yields

$$\mathcal{L} = \mathcal{L}^G(\bar{g}^{\mu\nu} + h^{\mu\nu}) + \mathcal{L}^M(\bar{\Phi}^A + \phi^A, \bar{g}^{\mu\nu} + h^{\mu\nu}) + \mathcal{L}^P(\bar{\Theta}^B + \theta^B, \bar{g}^{\mu\nu} + h^{\mu\nu}). \quad (56)$$

Because the perturbations $h^{\mu\nu}$, ϕ^A , θ^B are linearly superimposed with the background values of the metric tensor $\bar{g}_{\mu\nu}$ and the fields $\bar{\Phi}$, $\bar{\Theta}^B$ respectively, the perturbed (total) Lagrangian (56) admits the following property of the variational derivatives,

$$\frac{\delta \mathcal{L}}{\delta \mathfrak{h}^{\mu\nu}} = \frac{\delta \mathcal{L}}{\delta \bar{\mathfrak{g}}^{\mu\nu}}, \quad \frac{\delta \mathcal{L}}{\delta \phi^A} = \frac{\delta \mathcal{L}}{\delta \bar{\Phi}^A}, \quad \frac{\delta \mathcal{L}}{\delta \theta^B} = \frac{\delta \mathcal{L}}{\delta \bar{\Theta}^B}. \quad (57)$$

These relations allow us to replace the variational derivatives with respect to the dynamic perturbation of the field for that taken with respect to the background value of the field. It turns out to be useful in calculations that follow.

3.3 The Lagrangian Series Decomposition

Let us now expand the total Lagrangian (56) in a Taylor series by making use of the variational derivatives of \mathcal{L} with respect to $\mathfrak{h}^{\mu\nu}$ and ϕ^A . The Taylor expansion of \mathcal{L} with respect to θ is not important at this stage of the calculation procedure because physical measurements yield access to the total value of the bare perturbation Θ .

We assume at the beginning that the perturbations and their derivatives are small enough to ensure the convergence of the expansion. For the Lagrangian is a function of several variables, the Taylor series has terms with mixed derivatives starting from the second order. There is a nice way of handling the mixed derivatives in the Taylor expansion of the Lagrangian by noticing the following property of the commutator of two variational derivatives [70]

$$\mathfrak{h}^{\alpha\beta} \frac{\delta}{\delta \bar{\mathfrak{g}}^{\alpha\beta}} \left(\phi^A \frac{\delta \bar{\mathcal{L}}}{\delta \bar{\Phi}^A} \right) - \phi^A \frac{\delta}{\delta \bar{\Phi}^A} \left(\mathfrak{h}^{\alpha\beta} \frac{\delta \bar{\mathcal{L}}}{\delta \bar{\mathfrak{g}}^{\alpha\beta}} \right) = \partial_\alpha \mathcal{H}^\alpha, \quad (58)$$

where \mathcal{H}^α denotes a vector density of weight +1 made of the partial derivatives from the background Lagrangian $\bar{\mathcal{L}}$, and the repeated field label A denotes Einstein's summation over all fields Φ^A . This commutation rule is also valid for any two fields from the field multiplet Φ^A . Equation (58) allows us to change the order of the variational derivatives to reshuffle the terms with the mixed derivatives in the Taylor expansion of the perturbed Lagrangian \mathcal{L} . All terms representing the total divergence are omitted from the Taylor expansion since the variational derivative from them vanishes and they do not contribute to the field equations according to (8), (9). After all terms with the mixed derivatives are put in order by applying the commutator rule (58) and the total divergences are discarded, the Taylor expansion of the Lagrangian takes the following simple form

$$\mathcal{L} = \mathcal{L}^p + \sum_{n=0}^{\infty} \mathcal{L}_n. \quad (59)$$

Here, \mathcal{L}^p is the Lagrangian of the bare perturbation, $\mathcal{L}_0 \equiv \bar{\mathcal{L}}$ is the Lagrangian (42) describing dynamic properties of the background manifold, and for any $n \geq 1$,

$$\mathcal{L}_n = \frac{1}{n} \left(\mathfrak{h}^{\mu\nu} \frac{\delta \mathcal{L}_{n-1}}{\delta \bar{\mathfrak{g}}^{\mu\nu}} + \phi^A \frac{\delta \mathcal{L}_{n-1}}{\delta \bar{\Phi}^A} \right), \quad (60)$$

represents a collection of terms of the power n with respect to the perturbations $\mathfrak{h}^{\mu\nu}$ and ϕ^A . In particular, the linear and quadratic terms of the expansion in (59) read

$$\mathcal{L}_1 = \mathfrak{h}^{\mu\nu} \frac{\delta \bar{\mathcal{L}}}{\delta \bar{\mathfrak{g}}^{\mu\nu}} + \phi^A \frac{\delta \bar{\mathcal{L}}}{\delta \bar{\Phi}^A}, \quad (61)$$

$$\mathcal{L}_2 = \frac{1}{2} \left(\mathfrak{h}^{\mu\nu} \frac{\delta \mathcal{L}_1}{\delta \bar{\mathfrak{g}}^{\mu\nu}} + \phi^A \frac{\delta \mathcal{L}_1}{\delta \bar{\Phi}^A} \right), \quad (62)$$

and so on. Equation (60) can be proved by induction starting from the value of \mathcal{L}_1 in (61) which is apparently true, and operating with the commutation rule (58) in higher orders in order to confirm that the result is reduced to the original Taylor series. The commutation property (58) of the variational derivatives allows us to write down the Taylor expansion (59) as follows

$$\mathcal{L} = \exp \left(\mathfrak{h}^{\mu\nu} \frac{\delta}{\delta \bar{\mathfrak{g}}^{\mu\nu}} + \phi^A \frac{\delta}{\delta \bar{\Phi}^A} \right) \bar{\mathcal{L}} + \mathcal{L}^P, \quad (63)$$

that establishes a relation between the perturbed and unperturbed Lagrangians in the most succinct, exponential form.

By applying Eq. (57) to the Taylor series (59), and making use of $\delta \mathcal{L}^P / \delta \mathfrak{h}^{\mu\nu} = \delta \mathcal{L}^P / \delta \bar{\mathfrak{g}}^{\mu\nu}$, we get an important relation between the variational derivatives of the consecutive terms in the series

$$\frac{\delta \mathcal{L}_n}{\delta \mathfrak{h}^{\mu\nu}} = \frac{\delta \mathcal{L}_{n-1}}{\delta \bar{\mathfrak{g}}^{\mu\nu}}, \quad \frac{\delta \mathcal{L}_n}{\delta \phi^A} = \frac{\delta \mathcal{L}_{n-1}}{\delta \bar{\Phi}^A}. \quad (64)$$

These relations can be confirmed directly by making use of (60) that establishes a relation between the adjacent orders of the Lagrangian expansion (59).

The Lagrangian of the bare perturbation can be also expanded in the Taylor series with respect to $\mathfrak{h}^{\mu\nu}$,

$$\begin{aligned} \mathcal{L}^P &= \mathcal{L}^\Theta + \mathfrak{h}^{\mu\nu} \frac{\delta \mathcal{L}^\Theta}{\delta \bar{\mathfrak{g}}^{\mu\nu}} + \frac{1}{2!} \mathfrak{h}^{\alpha\beta} \frac{\delta}{\delta \bar{\mathfrak{g}}^{\alpha\beta}} \left(\mathfrak{h}^{\mu\nu} \frac{\delta \mathcal{L}^\Theta}{\delta \bar{\mathfrak{g}}^{\mu\nu}} \right) + \dots \\ &= \exp \left(\mathfrak{h}^{\mu\nu} \frac{\delta}{\delta \bar{\mathfrak{g}}^{\mu\nu}} \right) \mathcal{L}^\Theta, \end{aligned} \quad (65)$$

where we have defined $\mathcal{L}^\Theta \equiv \mathcal{L}^P(\Theta^B, \bar{\mathfrak{g}}^{\mu\nu})$. However, in practical calculations it is more convenient to hold \mathcal{L}^P unexpanded, keeping in mind that at each iteration the metric tensor $g_{\mu\nu}$ and the field Θ entering \mathcal{L}^P are known up to the order of the approximation under consideration.

3.4 Dynamic and Effective Lagrangians

The principle of the least action tells us that the Lagrangian (56) must be stationary with respect to variations of the metric tensor $g_{\mu\nu}$ and the field variables Φ^A ,

$$\frac{\delta \mathcal{L}}{\delta g^{\mu\nu}} = 0, \quad \frac{\delta \mathcal{L}}{\delta \Phi^A} = 0. \quad (66)$$

We also assume that the background Lagrangian (51) is stationary with respect to the variations of the background variables $\bar{g}^{\mu\nu}$ and $\bar{\Phi}^A$, and the field equations (43), (44) are valid. It means that the variational derivatives with respect to $\mathfrak{h}^{\mu\nu}$ and ϕ^A from the background Lagrangian $\mathcal{L}_0 \equiv \bar{\mathcal{L}}$ vanish identically. Therefore, applying Eq. (64) to $n = 1$ yields

$$\frac{\delta \mathcal{L}_1}{\delta \mathfrak{h}^{\mu\nu}} = \frac{\delta \bar{\mathcal{L}}}{\delta \bar{g}^{\mu\nu}} = 0, \quad (67)$$

$$\frac{\delta \mathcal{L}_1}{\delta \phi^A} = \frac{\delta \bar{\mathcal{L}}}{\delta \bar{\Phi}^A} = 0, \quad (68)$$

due to the background field equations (43), (44).

Equations (67), (68) point out that dynamics of physical perturbations are governed solely by the quadratic, cubic and higher-order polynomial terms in the Lagrangian decomposition (59). We define the *dynamic* Lagrangian of the dynamic perturbations as follows [70, 73]

$$\mathcal{L}^{\text{dyn}} \equiv \mathcal{L}_2 + \mathcal{L}_3 + \cdots, \quad (69)$$

so that the total Lagrangian (59) can be written down in the following form

$$\mathcal{L} = \bar{\mathcal{L}} + \mathcal{L}_1 + \mathcal{L}^{\text{dyn}} + \mathcal{L}^{\text{p}}. \quad (70)$$

The background Lagrangian, $\bar{\mathcal{L}}$, does not depend on the dynamic variables, $\mathfrak{h}^{\mu\nu}$, ϕ^A and θ^B . Hence, the variational derivative from $\bar{\mathcal{L}}$ taken with respect to any of these variables is identically zero. On the other hand, the variational derivatives from \mathcal{L}_1 taken with respect to $\mathfrak{h}^{\mu\nu}$ and/or ϕ^A vanish on-shell due to the background field equations, as shown in (67), (68). Hence, the Lagrangian perturbation theory of dynamic fields residing on the background manifold can be built on-shell with the *effective* Lagrangian

$$\mathcal{L}^{\text{eff}} \equiv \mathcal{L}^{\text{dyn}} + \mathcal{L}^{\text{p}}. \quad (71)$$

The effective Lagrangian is convenient for deriving the field equations of the physical perturbations and equations of motion of matter which are discussed in the rest of the present paper.

3.5 Field Equations for Gravitational Perturbations

The Einstein field equations for the metric perturbations are obtained after taking the variational derivative (5) from the effective Lagrangian \mathcal{L}^{eff} with respect to $\mathfrak{h}^{\mu\nu}$, and equating it to zero,

$$\frac{\delta \mathcal{L}^{\text{eff}}}{\delta \mathfrak{h}^{\mu\nu}} = 0. \quad (72)$$

Because of (67), it is equivalent to equation $\delta (\mathcal{L} - \bar{\mathcal{L}}) / \delta \mathfrak{h}^{\mu\nu} = 0$ or, after applying (57), to $\delta (\mathcal{L} - \bar{\mathcal{L}}) / \delta \bar{\mathfrak{g}}^{\mu\nu} = 0$. Replacing \mathcal{L} in this equation with expansion (70) and accounting for the background Einstein equations, $\delta \bar{\mathcal{L}} / \delta \bar{\mathfrak{g}}^{\mu\nu} = 0$, we recast (72) into the following form

$$-\frac{\delta \mathcal{L}_1}{\delta \bar{\mathfrak{g}}^{\mu\nu}} = \frac{\delta \mathcal{L}^{\text{eff}}}{\delta \bar{\mathfrak{g}}^{\mu\nu}}, \quad (73)$$

where we have used (35) in order to replace the variational derivative with respect to $\bar{\mathfrak{g}}^{\mu\nu}$ for that with respect to $\bar{g}^{\mu\nu}$. The Euler-Lagrangian equation (73) is convenient to work with. It is worth emphasizing that is fully equivalent to the first variational equation (66).

By taking the variational derivatives one can reduce Eq. (73) to a more tractable tensor form

$$F_{\mu\nu}^{\text{G}} + F_{\mu\nu}^{\text{M}} = 8\pi \Lambda_{\mu\nu}, \quad (74)$$

where

$$\Lambda_{\mu\nu} = \frac{2}{\sqrt{-\bar{g}}} \frac{\delta \mathcal{L}^{\text{eff}}}{\delta \bar{\mathfrak{g}}^{\mu\nu}}, \quad (75)$$

is the effective stress-energy tensor and the left side of (74) is a Laplace-Beltrami operator for tensor fields on curved manifolds [48] that consists of two parts

$$F_{\mu\nu}^{\text{G}} \equiv -\frac{16\pi}{\sqrt{-\bar{g}}} \frac{\delta}{\delta \bar{\mathfrak{g}}^{\mu\nu}} \left(\mathfrak{h}^{\rho\sigma} \frac{\delta \bar{\mathcal{L}}^{\text{G}}}{\delta \bar{\mathfrak{g}}^{\rho\sigma}} \right), \quad (76)$$

$$F_{\mu\nu}^{\text{M}} \equiv -\frac{16\pi}{\sqrt{-\bar{g}}} \frac{\delta}{\delta \bar{\mathfrak{g}}^{\mu\nu}} \left(\mathfrak{h}^{\rho\sigma} \frac{\delta \bar{\mathcal{L}}^{\text{M}}}{\delta \bar{\mathfrak{g}}^{\rho\sigma}} + \phi^A \frac{\delta \bar{\mathcal{L}}^{\text{M}}}{\delta \bar{\Phi}^A} \right). \quad (77)$$

Operator $F_{\mu\nu}^{\text{G}}$ describes perturbation of the Ricci tensor and can be easily calculated on any background manifold. Indeed, taking into account (45), we immediately get

$$F_{\mu\nu}^{\text{G}} = \frac{1}{\sqrt{-\bar{g}}} \frac{\delta}{\delta \bar{\mathfrak{g}}^{\mu\nu}} (\mathfrak{h}^{\rho\sigma} \bar{R}_{\rho\sigma}). \quad (78)$$

Now, according to the rule of rising and lowering indices of the variational derivatives, we can recast (78) to

$$F_{\mu\nu}^G = -\frac{1}{\sqrt{-\bar{g}}} \bar{g}_{\mu\chi} g_{\nu\epsilon} \frac{\delta}{\delta \bar{g}_{\chi\epsilon}} \left(\mathfrak{h}^{\rho\gamma} \delta_{\lambda}^{\kappa} \bar{R}^{\lambda}_{\rho\kappa\gamma} \right). \quad (79)$$

Variational derivative in (79) is calculated with the help of the covariant definition (19) where the covariant derivatives are taken on the background manifold and are denoted with a vertical bar. We recall that $\mathfrak{h}^{\rho\gamma}$ is an independent dynamic variable while the term under the sign of the variational derivative in (79) depends merely on the background Riemann tensor. Therefore, the derivative in (79) is taken only with respect to the Riemann tensor in accordance with (19). It yields

$$\begin{aligned} & \frac{\delta}{\delta \bar{g}_{\chi\epsilon}} \left(\mathfrak{h}^{\rho\gamma} \delta_{\lambda}^{\kappa} \bar{R}^{\lambda}_{\rho\kappa\gamma} \right) \\ &= \left[\mathfrak{h}^{\rho\gamma} \delta_{\lambda}^{\kappa} \left(\bar{g}^{\sigma\chi} \delta_{\sigma}^{\lambda} \delta_{\rho}^{\alpha} \delta_{\kappa}^{[\beta} \delta_{\gamma}^{\epsilon]} + \bar{g}^{\sigma\epsilon} \delta_{\sigma}^{\lambda} \delta_{\rho}^{\chi} \delta_{\kappa}^{[\beta} \delta_{\gamma}^{\alpha]} - \bar{g}^{\sigma\alpha} \delta_{\sigma}^{\lambda} \delta_{\rho}^{\chi} \delta_{\kappa}^{[\beta} \delta_{\gamma}^{\epsilon]} \right) \right]_{|\beta\alpha} \\ &= \left(\mathfrak{h}^{\alpha[\epsilon} \bar{g}^{\beta]\chi} + \mathfrak{h}^{\chi[\alpha} \bar{g}^{\beta]\epsilon} - \mathfrak{h}^{\chi[\epsilon} \bar{g}^{\beta]\alpha} \right)_{|\beta\alpha} \\ &= \frac{1}{2} \left(\mathfrak{h}^{\alpha\chi} \bar{g}^{\beta\epsilon} + \mathfrak{h}^{\alpha\epsilon} \bar{g}^{\beta\chi} - \mathfrak{h}^{\chi\epsilon} \bar{g}^{\alpha\beta} - \mathfrak{h}^{\alpha\beta} \bar{g}^{\chi\epsilon} \right)_{|\beta\alpha}, \end{aligned} \quad (80)$$

where we have taken into account that the expression enclosed in the brackets, is symmetric with respect to indices α and β . We substitute (80) to (79) and recollect definition of $\mathfrak{h}^{\mu\nu} = \sqrt{-\bar{g}} l^{\mu\nu}$ along with the constancy of the background metric tensor $\bar{g}_{\mu\nu}$ with respect to the covariant derivative. It results in

$$F_{\mu\nu}^G = \frac{1}{2} \left(l_{\mu\nu} |^{\alpha}_{|\alpha} + \bar{g}_{\mu\nu} l^{\alpha\beta} |_{\alpha\beta} - l^{\alpha}_{\mu} |_{\nu\alpha} - l^{\alpha}_{\nu} |_{\mu\alpha} \right), \quad (81)$$

where each vertical bar denotes a covariant derivative with respect to the background metric $\bar{g}_{\mu\nu}$, and $l_{\alpha\beta} \equiv \mathfrak{h}_{\alpha\beta} / \sqrt{-\bar{g}}$.

Operator $F_{\mu\nu}^M$ describes perturbation of the stress-energy tensor of the matter governing the evolution of the background manifold. Hence, it vanishes on any Ricci-flat spacetime manifold in general relativity. Cosmological FLRW spacetime is not Ricci flat. Therefore, $F_{\mu\nu}^M$ makes a non-trivial contribution to the field equations for gravitational perturbations. Variational derivative in definition (77) of $F_{\mu\nu}^M$ is taken from the Lagrangian, \mathcal{L}^M , characterizing the background matter fields $\bar{\Phi}^A$, and depends crucially on its particular form which must be specified in each individual case. We can bring (77) to a more explicit form by accounting for the definition of the metrical stress-energy tensor of the background matter [46]

$$\bar{T}_{\mu\nu}^M \equiv \frac{2}{\sqrt{-\bar{g}}} \frac{\delta \bar{\mathcal{L}}^M}{\delta \bar{g}^{\mu\nu}}, \quad (82)$$

and introducing a new function

$$\bar{I}_A^{\mathbf{M}} \equiv \frac{2}{\sqrt{-\bar{g}}} \frac{\delta \bar{\mathcal{L}}^{\mathbf{M}}}{\delta \bar{\Phi}^A}. \quad (83)$$

We notice that $\bar{I}_A^{\mathbf{M}}$ vanishes on-shell because of the field equation (43). However, this equation should not be applied immediately in the definition of $F_{\mu\nu}^{\mathbf{M}}$ as we have to take the variational derivative with respect to the metric tensor which is off-shell operation. With these remarks Eq. (77) takes on the following form

$$F_{\mu\nu}^{\mathbf{M}} = -\frac{8\pi}{\sqrt{-\bar{g}}} \frac{\delta}{\delta \bar{g}^{\mu\nu}} \left(\mathfrak{h}^{\rho\sigma} \bar{T}_{\rho\sigma}^{\mathbf{M}} - \frac{1}{2} \mathfrak{h} \bar{T}^{\mathbf{M}} + \sqrt{-\bar{g}} \phi^A \bar{I}_A^{\mathbf{M}} \right). \quad (84)$$

We shall calculate (84) later on for an ideal fluid and a scalar field in the case of the FLRW universe governed by dark matter and dark energy.

The right side of Eq. (74) contains the effective stress-energy tensor consisting of two contributions

$$\Lambda_{\mu\nu} = \mathfrak{T}_{\mu\nu} + \mathcal{T}_{\mu\nu}, \quad (85)$$

where

$$\mathfrak{T}_{\mu\nu} \equiv \frac{2}{\sqrt{-\bar{g}}} \frac{\delta \mathcal{L}^{\mathbf{P}}}{\delta \bar{g}^{\mu\nu}}, \quad (86)$$

is the stress-energy tensor of the bare perturbation, and

$$\mathcal{T}_{\mu\nu} \equiv \frac{2}{\sqrt{-\bar{g}}} \frac{\delta \mathcal{L}^{\text{dyn}}}{\delta \bar{g}^{\mu\nu}}, \quad (87)$$

is the stress-energy tensor associated with the dynamic field perturbations $\mathfrak{h}^{\mu\nu}$ and ϕ^A .

We notice that tensor $\mathfrak{T}_{\mu\nu}$ is defined as a variational derivative with respect to the background metric, $\bar{g}_{\mu\nu}$. Hence, it differs from

$$T_{\alpha\beta} = \frac{2}{\sqrt{-g}} \frac{\delta \mathcal{L}^{\mathbf{P}}}{\delta g^{\alpha\beta}}, \quad (88)$$

which is defined in terms of the variational derivative with respect to the full metric $g_{\mu\nu} = \bar{g}_{\mu\nu} + \mathfrak{x}_{\mu\nu} + \dots$. Relation of the two tensors can be found by making use of equations

$$\frac{\partial \mathfrak{g}^{\mu\nu}}{\partial \bar{g}^{\alpha\beta}} = \sqrt{-\bar{g}} \left[\delta_{\alpha}^{(\mu} \delta_{\beta}^{\nu)} - \frac{1}{2} \bar{g}^{\mu\nu} \bar{g}_{\alpha\beta} \right], \quad (89)$$

$$\frac{\partial g^{\rho\sigma}}{\partial \bar{g}^{\mu\nu}} = \frac{1}{\sqrt{-g}} \left[\delta_{\mu}^{(\rho} \delta_{\nu}^{\sigma)} - \frac{1}{2} g^{\rho\sigma} g_{\mu\nu} \right], \quad (90)$$

and

$$\frac{\delta}{\delta \bar{g}^{\alpha\beta}} = \frac{\partial \mathbf{g}^{\mu\nu}}{\partial \bar{g}^{\alpha\beta}} \frac{\partial g^{\rho\sigma}}{\partial \mathbf{g}^{\mu\nu}} \frac{\delta}{\delta g^{\rho\sigma}}. \quad (91)$$

It yields an exact relation

$$\mathfrak{T}_{\mu\nu} = T_{\mu\nu} - \frac{1}{2} g_{\mu\nu} T - \frac{1}{2} \bar{g}_{\mu\nu} \bar{g}^{\alpha\beta} \left(T_{\alpha\beta} - \frac{1}{2} g_{\alpha\beta} T \right), \quad (92)$$

where the trace of the stress energy tensor is defined as $T \equiv g^{\alpha\beta} T_{\alpha\beta}$. Relation (92) can be inverted leading to

$$T_{\mu\nu} = \mathfrak{T}_{\mu\nu} - \frac{1}{2} \bar{g}_{\mu\nu} \mathfrak{T} - \frac{1}{2} g_{\mu\nu} g^{\alpha\beta} \left(\mathfrak{T}_{\alpha\beta} - \frac{1}{2} \bar{g}_{\alpha\beta} \mathfrak{T} \right), \quad (93)$$

where $\mathfrak{T} = \bar{g}^{\alpha\beta} \mathfrak{T}_{\alpha\beta}$.

Tensor $\mathcal{T}_{\mu\nu}$ can be split in two algebraically-independent parts

$$\mathcal{T}_{\mu\nu} = \mathfrak{t}_{\mu\nu} + \tau_{\mu\nu}, \quad (94)$$

where $\mathfrak{t}_{\mu\nu}$ is the stress-energy tensor of pure gravitational perturbations $\mathfrak{h}^{\mu\nu}$ while $\tau_{\mu\nu}$ is the stress-energy tensor characterizing gravitational coupling of the matter field ϕ^A with the gravitational perturbations $\mathfrak{h}^{\mu\nu}$.

For example, in the second-order approximation, when $\mathcal{L}^{\text{dyn}} = \mathcal{L}_2$, the corresponding stress-energy tensors are given by equations

$$\mathfrak{t}_{\mu\nu} = -\frac{1}{16\pi\sqrt{-\bar{g}}} \frac{\delta}{\delta \bar{g}^{\mu\nu}} \left(\mathfrak{h}^{\rho\sigma} F_{\rho\sigma}^{\text{G}} - \frac{1}{2} \mathfrak{h} F^{\text{G}} \right), \quad (95)$$

$$\tau_{\mu\nu} = -\frac{1}{16\pi\sqrt{-\bar{g}}} \frac{\delta}{\delta \bar{g}^{\mu\nu}} \left(\mathfrak{h}^{\rho\sigma} F_{\rho\sigma}^{\text{M}} - \frac{1}{2} \mathfrak{h} F^{\text{M}} + \sqrt{-\bar{g}} \phi^A F_A^{\text{M}} \right), \quad (96)$$

where F_A^{M} is defined in (101).

As soon as the differential operators and the source terms in Eq. (74) are specified, it can be solved by successive iterations. It requires decomposition of the perturbations $\mathfrak{h}^{\mu\nu} = \phi^a$ in the post-Friedmanian series

$$\mathfrak{h}^{\mu\nu} = \mathfrak{h}_1^{\mu\nu} + \mathfrak{h}_2^{\mu\nu} + \mathfrak{h}_3^{\mu\nu} + \dots, \quad (97)$$

$$\phi^A = \phi_1^A + \phi_2^A + \phi_3^A + \dots, \quad (98)$$

where the terms with indices $n = 1, 2, 3, \dots$ represent the successive approximations of the corresponding order of magnitude. We conjecture that the series (97), (98) are analytic and convergent for a sufficiently small magnitude of the perturbations. However, this requires a special mathematical study.

The iteration procedure starts off the substitution of the unperturbed values of $\mathfrak{h}^{\mu\nu} = \phi^a = 0$ to the right side of (74) and finding the linear perturbation $\mathfrak{h}_1^{\mu\nu}$. The solution is substituted back to the right side of (74), which is solved again to find $\mathfrak{h}_2^{\mu\nu}$, and so on. However, we need additional set of differential equations for the perturbations of the matter fields ϕ^A .

3.6 Field Equations for Matter Perturbations

Equations for the matter field perturbation ϕ^A are derived from the Lagrangian (71) by taking the variational derivative with respect to ϕ^A . Since the Lagrangian \mathcal{L}^P does not depend on ϕ^A it drops out from calculations. Moreover, we assume that the background field equations (43) are satisfied. Thus, the stationarity of the Lagrangian (70) with respect to the perturbations ϕ^A yields

$$\frac{\delta \mathcal{L}^{\text{dyn}}}{\delta \phi^A} = 0. \quad (99)$$

After making use of the second relation in (57), Eq. (99) recasts to

$$F_A^M = 8\pi \Sigma_A^M, \quad (100)$$

where the linear differential operator

$$F_A^M \equiv -\frac{16\pi}{\sqrt{-g}} \frac{\delta}{\delta \bar{\Phi}^A} \left(\mathfrak{h}^{\mu\nu} \frac{\delta \bar{\mathcal{L}}^M}{\delta \bar{\mathfrak{g}}^{\mu\nu}} + \phi^A \frac{\delta \bar{\mathcal{L}}^M}{\delta \bar{\Phi}^A} \right), \quad (101)$$

and the source density

$$\Sigma_A^M \equiv \frac{2}{\sqrt{-g}} \frac{\delta \mathcal{L}^{\text{dyn}}}{\delta \bar{\Phi}^A}. \quad (102)$$

All linear with respect to $\mathfrak{h}^{\alpha\beta}$ and ϕ^A terms are included in the left side of Eq. (100) while the non-linear terms have been put in Σ_A^M . More explicit form of the operator F_A^M can be obtained with the help of (82), (83) that results in

$$F_A^M = -\frac{8\pi}{\sqrt{-g}} \frac{\delta}{\delta \bar{\Phi}^A} \left(\mathfrak{h}^{\rho\sigma} \bar{T}_{\rho\sigma}^M - \frac{1}{2} \mathfrak{h} \bar{T}^M + \sqrt{-g} \phi^A \bar{I}_A^M \right). \quad (103)$$

Further specification of F_A^M requires a particular model of the background matter Lagrangian $\bar{\mathcal{L}}^M$ which will be discussed in the following section.

Equations of motion of the field Θ^B are obtained after taking the variational derivative from the Lagrangian (71) with respect to the variable Θ^B . Because the

only part of the Lagrangian which depends on this field, is \mathcal{L}^P , the equations are reduced to

$$\frac{\delta \mathcal{L}^P}{\delta \Theta^B} = 0. \quad (104)$$

Particular form of this equation depends on a specific choice of the Lagrangian of the bare perturbation. In the lowest order approximation Eqs. (100) and (104) describe evolution of the dynamic variables ϕ^A and Θ^B on the unperturbed cosmological background. The next-order approximations take into account the back reaction of the background on these fields.

3.7 Gauge Invariance of the Field Equations

Gauge invariance of the dynamic perturbations is an important geometric property that allows us to distinguish physical degrees of freedom of gravitational and matter fields from the spurious modes generated by transformations of the local coordinates on manifold. Any self-consistent perturbation theory must clearly separate the coordinate-dependent effects from physical perturbations which do not depend on the choice of coordinates. The gauge transformation is understood in the sense of the exponential mapping of the background spacetime to itself that is induced by a non-singular vector flow with a tangent vector $\xi^\alpha \equiv \xi^\beta(x^\alpha)$ that is a generator of a (finite) coordinate transformation

$$x'^\alpha = \exp\left(\xi^\beta \partial_\beta\right) x^\alpha = x^\alpha + \xi^\alpha + \frac{1}{2!} \xi^\beta \partial_\beta \xi^\alpha + \dots \quad (105)$$

The mapping of any geometric object $Q \equiv Q(x^\alpha)$ to another one $Q' \equiv Q'(x^\alpha)$ being induced by transformation (105) defines the gauge transformation of Q that is given by the exponential Lie transform

$$Q'(x^\alpha) = (\exp \mathcal{L}_\xi) Q(x^\alpha) = Q(x^\alpha) + \mathcal{L}_\xi Q(x^\alpha) + \frac{1}{2!} \mathcal{L}_\xi^2 Q(x^\alpha) + \dots, \quad (106)$$

where the Lie derivative \mathcal{L}_ξ has been defined in Sect. 2.2, $\mathcal{L}_\xi^2 \equiv \mathcal{L}_\xi \mathcal{L}_\xi$, $\mathcal{L}_\xi^3 \equiv \mathcal{L}_\xi \mathcal{L}_\xi \mathcal{L}_\xi$, and so on.

The gauge transformation of the metric tensor, $g_{\mu\nu}$, and the matter fields, $\Phi^A \Theta^B$, implies that their background values do not change under the gauge transformation, only the dynamic perturbations, $h^{\mu\nu}$, ϕ^A , θ^B change. Hence, the gauge transformation (106) applied to these variables read

$$h'^{\mu\nu} = h^{\mu\nu} + (\exp \mathcal{L}_\xi - 1) (\bar{g}^{\mu\nu} + h^{\mu\nu}), \quad (107)$$

$$\phi'^A = \phi^A + (\exp \mathcal{L}_\xi - 1) (\bar{\Phi}^A + \phi^A), \quad (108)$$

$$\theta'^B = \theta^B + (\exp \mathcal{L}_\xi - 1) (\bar{\Theta}^B + \theta^B), \quad (109)$$

Let us consider the gauge transformation of the Lagrangian (51) induced by the gauge transformations of its arguments in more detail. The transformed Lagrangian \mathcal{L}' has the same functional form as \mathcal{L} that depends now on the new values of the dynamic variables, $\mathcal{L}' \equiv \mathcal{L}(\bar{g}^{\mu\nu} + h^{\mu\nu}, \bar{\Phi}^A + \phi^A, \bar{\Theta}^B + \theta'^B)$. Replacing the primed variables by making use of Eqs. (107)–(109), yields

$$\mathcal{L}' = \mathcal{L} \left[\exp \mathcal{L}_\xi (\bar{g}^{\mu\nu} + h^{\mu\nu}), \exp \mathcal{L}_\xi (\bar{\Phi}^A + \phi^A), \exp \mathcal{L}_\xi (\bar{\Theta}^B + \theta^B) \right]. \quad (110)$$

This equation can be further transformed by making use of the following commutation relation [70]

$$\begin{aligned} \mathcal{L} \left[\exp \mathcal{L}_\xi (\bar{g}^{\mu\nu} + h^{\mu\nu}), \exp \mathcal{L}_\xi (\bar{\Phi}^A + \phi^A), \exp \mathcal{L}_\xi (\bar{\Theta}^B + \theta^B) \right] \\ = \exp \mathcal{L}_\xi \mathcal{L} \left(\bar{g}^{\mu\nu} + h^{\mu\nu}, \bar{\Phi}^A + \phi^A, \bar{\Theta}^B + \theta^B \right), \end{aligned} \quad (111)$$

that is valid modulo total divergence which is inessential in the variational calculus. Expanding the right side of (111) in a Taylor series, like in (106), and taking into account that $\mathcal{L}_\xi \mathcal{L} = \partial_\alpha (\xi^\alpha \mathcal{L})$, yields the gauge transformation of the Lagrangian,

$$\begin{aligned} \mathcal{L}' = \mathcal{L} + \partial_\alpha (\xi^\alpha \mathcal{L}) \\ + \frac{1}{2!} \partial_\beta (\xi^\beta \partial_\alpha (\xi^\alpha \mathcal{L})) + \frac{1}{3!} \partial_\gamma (\xi^\gamma \partial_\beta (\xi^\beta \partial_\alpha (\xi^\alpha \mathcal{L}))) + \dots, \end{aligned} \quad (112)$$

where the second, third, and all other terms in the right side of this infinite series represent a divergence. The divergence vanishes when one takes the variational derivative from it and, hence, it can be omitted from the action functional S given in (50). The conclusion is that both the action S and the Lagrangian (56) are gauge invariant with respect to the gauge transformation of their arguments. This assertion is valid both on-shell and off-shell.

On the other hand, the effective Lagrangian (71) is gauge-invariant only on-shell that is only when the background equations of motion (43), (44) are satisfied. Indeed, the effective Lagrangian can be represented as a difference $\mathcal{L}^{\text{eff}} = \mathcal{L} - \mathcal{L}_1 - \bar{\mathcal{L}}$. After making the gauge transformations (107)–(109) of the dynamic variables, we get a new effective Lagrangian $\mathcal{L}'^{\text{eff}} = \mathcal{L}' - \mathcal{L}'_1 - \bar{\mathcal{L}}$. The difference $\delta \mathcal{L}^{\text{eff}} = \mathcal{L}'^{\text{eff}} - \mathcal{L}^{\text{eff}}$ is

$$\delta \mathcal{L}^{\text{eff}} = \delta \mathcal{L} + (\exp \mathcal{L}_\xi - 1) \left[(\bar{g}^{\mu\nu} + h^{\mu\nu}) \frac{\delta \bar{\mathcal{L}}}{\delta \bar{g}^{\mu\nu}} + (\bar{\Phi}^A + \phi^A) \frac{\delta \bar{\mathcal{L}}}{\delta \bar{\Phi}^A} \right], \quad (113)$$

where the terms being enclosed in the square brackets, vanish on-shell due to the background equations of motion (43), (44). Therefore, $\delta \mathcal{L}^{\text{eff}} = \delta \mathcal{L} \equiv \mathcal{L}' - \mathcal{L}$ is a total divergence as follows from (112). Hence, \mathcal{L}^{eff} is gauge-invariant on-shell.

The gauge invariance of the Lagrangian suggests that the Einstein equations (74) for metric perturbations are gauge invariant as well. It is straightforward to prove it by direct but otherwise tedious calculation which technical details are given in [70]. Gauge transformations (107)–(109) applied to the Einstein equations (74) transform them as follows

$$F'^G_{\mu\nu} + F'^M_{\mu\nu} - 8\pi\Lambda'_{\mu\nu} = F^G_{\mu\nu} + F^M_{\mu\nu} - 8\pi\Lambda_{\mu\nu} + \exp \mathcal{L}_\xi \mathcal{F}, \quad (114)$$

where function \mathcal{F} vanishes on-shell similar to (113). Therefore, if one assumes that the field equations are valid at least in one gauge, the last term in the right side of (114) vanishes, thus, proving that the field equations are valid in any other gauge.

4 The Lagrangian Formalism in Cosmology

We shall use the cosmological model that is in a close agreement with modern observational data. In this model the background manifold represents the spatially homogeneous and isotropic FLRW universe which temporal evolution is governed by a doublet of matter fields, $\Phi^A = \{\Phi^1, \Phi^2\}$. We identify $\Phi^1 \equiv \Phi$ with the Clebsch potential of an ideal fluid with pressure, and $\Phi^2 \equiv \Psi$ —with a scalar field having the potential $W = W(\Psi)$ depending only on the scalar field Ψ . The ideal fluid models a self-interacting dark matter [75] while the scalar field describes dark energy in the form of quintessence [76]. The dark matter without self-interaction is included in our theoretical scheme as a pressureless ideal fluid.

The overall Lagrangian of the model under consideration is given by Eq. (51) with the Lagrangian of the matter consisting of two non-directly interacting pieces

$$\mathcal{L}^M = \mathcal{L}^m + \mathcal{L}^q, \quad (115)$$

where \mathcal{L}^m is the Lagrangian of dark matter, and \mathcal{L}^q is the Lagrangian of dark energy.

4.1 Lagrangian of Dark Matter

Dark matter is modelled as an ideal fluid that is characterized by four thermodynamic parameters: the rest-mass density ρ_m , the specific internal energy per unit mass Π_m , pressure p_m , and entropy s_m where the sub-index ‘m’ stands for the dark ‘matter’. We shall assume that the entropy of the ideal fluid remains constant (isentropic motion) and dissipative processes are neglected. The total energy density of the fluid

$$\epsilon_m = \rho_m(1 + \Pi_m). \quad (116)$$

One more thermodynamic parameter is the specific enthalpy of the fluid defined as

$$\mu_m = \frac{\epsilon_m + p_m}{\rho_m} = 1 + \Pi_m + \frac{p_m}{\rho_m}. \quad (117)$$

We shall consider barotropic fluid which thermodynamic equation of state is given by equation $p_m = p_m(\rho_m, \Pi_m)$, where the specific internal energy Π_m is related to pressure by the first law of thermodynamics

$$d\Pi_m + p_m d\left(\frac{1}{\rho_m}\right) = 0. \quad (118)$$

It is used to derive the following thermodynamic relationships

$$dp_m = \rho_m d\mu_m, \quad (119)$$

$$d\epsilon_m = \mu_m d\rho_m, \quad (120)$$

which are derived directly from (116)–(118). Equation (119) immediately tells us that the partial derivatives

$$\frac{\partial p_m}{\partial \mu_m} = \rho_m, \quad (121a)$$

$$\frac{\partial \epsilon_m}{\partial \rho_m} = \mu_m. \quad (121b)$$

Equation (121) elucidate that all thermodynamic quantities are functions of only one thermodynamic potential. We accept that this potential is the specific enthalpy μ_m . Equation of state, relating pressure and the energy density, becomes $p_m = p_m(\epsilon_m)$, and it is also an implicit function of the same thermodynamic variable μ_m because $\epsilon_m = \epsilon_m(\mu_m)$.

Partial derivatives of the thermodynamic quantities with respect to μ_m can be calculated by making use of (119), (120), and the equation of state $p_m = p_m(\epsilon_m)$ giving rise to definition of the (adiabatic) speed of sound c_s propagating in the fluid

$$\frac{\partial p_m}{\partial \epsilon_m} = \frac{c_s^2}{c^2}, \quad (122)$$

where the partial derivative is taken under a condition that the entropy, s_m , does not change. Notice that the speed of sound in dark matter is *not* constant in the most general case of a non-linear equation of state. In this case, the speed of sound depends on the thermodynamic potential μ_m through the equation of state, that is $c_s = c_s(\mu_s)$. It is also worth emphasizing that Eq. (122) is valid for any wavelength of sound wave in the ideal fluid, not only for short wavelengths.

Other partial derivatives of the thermodynamic quantities can be calculated with the help of the equation of state and derivatives (121), (122) which can be inverted, if necessary, because all thermodynamic relations in the ideal fluid are single-valued. We have, for example,

$$\frac{\partial \epsilon_m}{\partial \mu_m} = \frac{c^2}{c_s^2} \rho_m, \quad \frac{\partial \rho_m}{\partial \mu_m} = \frac{c^2}{c_s^2} \frac{\rho_m}{\mu_m}, \quad (123)$$

where all partial derivatives are performed under the same condition of the constant entropy.

Theoretical description of the ideal fluid as a dynamic system on space-time manifold is given the most conveniently in terms of the Clebsch potential, Φ which is also known as the velocity or the Taub potential [77]. The Clebsch potential is a continuous scalar field which can be taken as an independent dynamic variable characterizing the motion of the fluid. This description is complimentary (dual) to the Lagrangian formalism of the ideal fluid based on the coordinates and four-velocity of the fluid particles.

In the case of a single-component fluid the Clebsch potential is introduced by the following relationship

$$\mu_m w_\alpha = -\Phi_\alpha, \quad (124)$$

where $w^\alpha = dx^\alpha/d\tau$ is the four-velocity of the fluid, $w_\alpha = g_{\alpha\beta} w^\beta$, τ is the proper time of the fluid element taken along its world line, and we denote $\Phi_\alpha \equiv \Phi_{,\alpha}$ from now on. Equation (124) solves the relativistic Euler equation of motion of the ideal fluid [78]. The four-velocity is normalized, $g_{\alpha\beta} w^\alpha w^\beta = -1$, so that the specific enthalpy can be expressed in the following form

$$\mu_m = \sqrt{-g^{\alpha\beta} \Phi_\alpha \Phi_\beta}. \quad (125)$$

One may also notice that

$$\mu_m = w^\alpha \Phi_\alpha. \quad (126)$$

The Clebsch potential Φ has no direct physical meaning as it can be changed to another value $\Phi \rightarrow \Phi' = \Phi + \tilde{\Phi}$ such that the gauge function, $\tilde{\Phi}$, is constant along the worldlines of the fluid in the sense that $w^\alpha \tilde{\Phi}_\alpha = 0$.

The Lagrangian of the ideal fluid is usually taken in the form of the total energy density, $\mathcal{L}^m = \sqrt{-g} \epsilon_m$ [79]. However, this form is less convenient for applying the Lagrangian formalism on manifolds as it does not contain the kinetic energy ($\sim g^{\alpha\beta} \Phi_\alpha \Phi_\beta$) of dynamic field variables directly. For this reason, the Lagrangian of the ideal fluid in the form of pressure, $L^m = -\sqrt{-g} p_m$, is used in the present paper. It differs from the Lagrangian in the form of energy by a total divergence (see [46, pp. 334–335] for more detail) which is unimportant as it vanishes when the variational derivative from the Lagrangian is taken. The Lagrangian in the form of pressure includes the kinetic energy term

$$\mathcal{L}^m = \sqrt{-g} (\epsilon_m - \rho_m \mu_m) = \sqrt{-g} \left(\epsilon_m - \rho_m \sqrt{-g^{\alpha\beta} \Phi_\alpha \Phi_\beta} \right). \quad (127)$$

Metrical stress-energy tensor of the ideal fluid is obtained by taking a variational derivative of the Lagrangian (127) with respect to the metric tensor,

$$T_{\alpha\beta}^m = \frac{2}{\sqrt{-g}} \frac{\delta \mathcal{L}^m}{\delta g^{\alpha\beta}}. \quad (128)$$

In our field-theoretical approach to the description of the ideal fluid the metric tensor enters all thermodynamic quantities only through the specific enthalpy in the form of (125). Therefore, taking the variational derivative in (128) with respect to the metric tensor can be done with the help of the chain rule (23) and the results are given in Appendix section “Variational Derivatives of Dark Matter Variables”. Finally, the stress-energy tensor (128) is

$$T_{\alpha\beta}^m = (\epsilon_m + p_m) w_\alpha w_\beta + p_m g_{\alpha\beta}, \quad (129)$$

that is a standard form of the stress-energy tensor of the ideal fluid [79].

4.2 Lagrangian of Dark Energy

The Lagrangian of dark energy is taken in the form of a quintessence of a scalar field Ψ

$$\mathcal{L}^q = \sqrt{-g} \left(\frac{1}{2} g^{\alpha\beta} \Psi_\alpha \Psi_\beta + W \right), \quad (130)$$

where $W \equiv W(\Psi)$ is a potential of the scalar field and we denote $\Psi_\alpha \equiv \Psi_{,\alpha}$ from now on. We assume that there is no direct coupling between the Lagrangian of dark energy and that of dark matter. They interact only indirectly through the gravitational field. Many various forms of the potential W are used in cosmology [80] but at the present paper we do not need to specify it further.

The metrical stress-energy tensor of the scalar field is obtained by taking a variational derivative

$$T_{\alpha\beta}^q = \frac{2}{\sqrt{-g}} \frac{\delta \mathcal{L}^q}{\delta g^{\alpha\beta}}, \quad (131)$$

that yields

$$T_{\alpha\beta}^q = \Psi_\alpha \Psi_\beta - g_{\alpha\beta} \left[\frac{1}{2} g^{\mu\nu} \Psi_\mu \Psi_\nu + W(\Psi) \right]. \quad (132)$$

One can *formally* reduce tensor (132) to the form similar to that of the ideal fluid by making use of the following procedure. First, we define the analogue of the specific enthalpy of the scalar field “fluid”

$$\mu_q = \sqrt{-g^{\alpha\beta} \Psi_\alpha \Psi_\beta}, \quad (133)$$

and the effective four-velocity, v^α , of the “fluid”

$$\mu_q v_\alpha = -\Psi_\alpha. \quad (134)$$

The four-velocity v^α is normalized to $g_{\alpha\beta} v^\alpha v^\beta = -1$. Therefore, the scalar field enthalpy μ_q can be expressed in terms of the partial derivative from the scalar field

$$\mu_q = v^\alpha \Psi_\alpha. \quad (135)$$

We introduce the analogue of the rest mass density ρ_q of the scalar field “fluid” by defining,

$$\rho_q = \mu_q = v^\alpha \Psi_\alpha = \sqrt{-g^{\alpha\beta} \Psi_\alpha \Psi_\beta}. \quad (136)$$

As a consequence of the above definitions, the energy density, ϵ_q and pressure p_q of the scalar field “fluid” can be introduced as follows

$$\epsilon_q \equiv -\frac{1}{2} g^{\alpha\beta} \Psi_\alpha \Psi_\beta + W(\Psi) = \frac{1}{2} \rho_q \mu_q + W(\Psi), \quad (137)$$

$$p_q \equiv -\frac{1}{2} g^{\alpha\beta} \Psi_\alpha \Psi_\beta - W(\Psi) = \frac{1}{2} \rho_q \mu_q - W(\Psi). \quad (138)$$

We notice that relation

$$\mu_q = \frac{\epsilon_q + p_q}{\rho_q}, \quad (139)$$

between the specific enthalpy μ_q , density ρ_q , pressure p_q and the energy density, ϵ_q , of the scalar field “fluid” formally holds on the same form (117) as in the case of the barotropic ideal fluid.

After substituting the above-given definitions of various “thermodynamic” quantities into Eq. (132), it formally reduces to the stress-energy tensor of an ideal “fluid”

$$T_{\alpha\beta}^q = (\epsilon_q + p_q) v_\alpha v_\beta + p_q g_{\alpha\beta}. \quad (140)$$

It is worth emphasizing that the analogy between the stress-energy tensor (140) of the scalar field “fluid” with that of the barotropic ideal fluid (129) is rather formal since the scalar field, in the most general case, does not satisfy *all* required thermodynamic equations because of the presence of the potential $W = W(\Psi)$ in the energy density ϵ_q , and pressure p_q of the scalar field. The dark energy is physically different from dark matter!

4.3 Lagrangian of the Bare Perturbation

The Lagrangian \mathcal{L}^p of bare perturbation that appears in (51), can be chosen arbitrary. We assume that the matter of the bare perturbation is described by a variable Θ which may be a scalar or tensor field. The Lagrangian of the bare perturbation is given by $\mathcal{L}^p = \sqrt{-g} L^p(\Theta, g_{\alpha\beta})$. Stress-energy tensor of the bare perturbation, $T_{\alpha\beta}$, is defined in (88). Tensor $T_{\alpha\beta}$ is a source of the bare gravitational perturbation of the background manifold which generates the large-scale structure of the universe. Its structure should be specified depending on a particular physical situation. In this paper we focus on derivation of hydrodynamic equations of motion of an ideal fluid on background manifold with taking into account the manifold back reaction. Therefore, we assume

$$T_{\alpha\beta} = (\epsilon + p) U_\alpha U_\beta + p g_{\alpha\beta}, \quad (141)$$

where ϵ , p are the energy density and pressure of the fluid comprising the bare perturbation, and U^α is its four-velocity normalized to $U_\alpha U^\alpha = -1$. It is worth emphasizing that the four-velocity of the bare perturbation is not a part of the background fluid flow and is decoupled from it in the first approximation. Notice that the stress-energy tensor $\mathfrak{T}_{\mu\nu}$ defined in (85), is not equal to $T_{\mu\nu}$. We have derived relation between the two tensors in (92) and (93).

4.4 Background Manifold

All geometric objects on background cosmological manifold $\bar{\mathcal{M}}$ will be denoted with a bar over the object. The FLRW metric on the background manifold is given in (49). It is convenient to introduce global isotropic coordinates $X^\alpha = (X^0, X^i)$ by changing the cosmic time T to the conformal time $\eta \equiv X^0$ via differential equation $dT = a(\eta)d\eta$. The FLRW metric tensor in the isotropic coordinates reads

$$\bar{g}_{\mu\nu} = a^2(\eta) \bar{\mathfrak{f}}_{\mu\nu}, \quad (142)$$

where a cosmological scale factor, $a(\eta) \equiv R[T(\eta)]$. The conformal metric $\bar{\mathfrak{f}}_{\mu\nu} = (-1, \bar{\mathfrak{f}}_{ij})$, where the spatial part of the metric

$$\bar{\mathfrak{f}}_{ij} = \left(1 + \frac{1}{4}r^2\right)^{-2} \delta_{ij}, \quad (143)$$

depends on the curvature of the spatial hypersurfaces, $k = \{-1, 0, +1\}$. In case, $k = 0$, the conformal metric $\bar{\mathfrak{f}}_{\mu\nu}$ is reduced to the Minkowski metric, $\eta_{\mu\nu}$. Four-velocity of the Hubble flow in the isotropic coordinates is $\bar{U}^\alpha = dX^\alpha/dT = (a^{-1}, 0, 0, 0, 0)$.

Due to the maximal symmetry of FLRW spacetime, all background geometric objects depend only on time η in the isotropic coordinates. We can, and will use

arbitrary coordinates $x^\alpha = (x^0, x^i)$ which are connected to the isotropic coordinates X^α by a smooth diffeomorphism $x^\alpha = x^\alpha(X^\beta)$. Partial derivative of a background geometric object, $\bar{Q} = \bar{Q}(\eta)$, in the arbitrary coordinates is given by

$$\bar{Q}_{,\alpha} = -\frac{\bar{Q}'}{a}\bar{u}_\alpha = -\dot{\bar{Q}}\bar{u}_\alpha, \quad (144)$$

where \bar{u}^α is four-velocity of the Hubble flow in arbitrary coordinates. Equation (144) applied to the scale factor, yields $a_{,\alpha} = -\dot{a}\bar{u}_\alpha = -\mathcal{H}\bar{u}_\alpha$, and the partial derivative from the conformal Hubble parameter $\mathcal{H}_{,\alpha} = -\dot{\mathcal{H}}\bar{u}_\alpha$.

Einstein's field equations on the background manifold are given by (44)–(46) which yield two Friedmann equations for the temporal evolution of the scale factor a ,

$$H^2 = \frac{8\pi}{3}\bar{\epsilon} - \frac{k}{a^2}, \quad (145)$$

$$2\dot{H} + 3H^2 = -8\pi\bar{p} - \frac{k}{a^2} \quad (146)$$

where $\bar{\epsilon}$ and \bar{p} are the effective energy density and pressure of the background matter.

A consequence of the Friedmann equations (145), (146) is an equation

$$\dot{H} = -4\pi(\bar{\epsilon} + \bar{p}) + \frac{k}{a^2}, \quad (147)$$

relating the time derivative of the Hubble parameter with the sum of the overall energy density and pressure of dark matter and dark energy

$$\bar{\epsilon} + \bar{p} = \bar{\rho}_m\bar{\mu}_m + \bar{\rho}_q\bar{\mu}_q. \quad (148)$$

The equation of continuity for the rest mass density $\bar{\rho}_m$ of the background dark matter is (43) for $\bar{\Phi}^A \rightarrow \bar{\Phi}$. It reads

$$(\bar{\rho}_m\bar{u}^\alpha)_{|\alpha} = 0, \quad (149)$$

that is equivalent to

$$\bar{\rho}_m|_\alpha - 3H\bar{\rho}_m\bar{u}_\alpha = 0. \quad (150)$$

The background equation of the conservation of energy of dark matter is

$$\bar{\epsilon}_m|_\alpha - 3H(\bar{\epsilon}_m + \bar{p}_m)\bar{u}_\alpha = 0, \quad (151)$$

where we have employed the definition of energy (116), and Eqs. (118), (150).

Background equation for the scalar field $\bar{\Psi}$ is (43) for $\bar{\Phi}^A \rightarrow \bar{\Psi}$. It reads

$$\bar{g}^{\alpha\beta}\bar{\Psi}_{|\alpha\beta} - \frac{\partial\bar{W}}{\partial\bar{\Psi}} = 0. \quad (152)$$

After making use of the definition of the background enthalpy of the scalar field $\bar{\mu}_q \equiv \bar{u}^\alpha \bar{\Psi}_{|\alpha}$, an equality $\bar{\mu}_q = \bar{\rho}_q$, and definition (137) of the specific energy $\bar{\epsilon}_q$ of the scalar field, the Eq. (152) can be recast to

$$\bar{\epsilon}_{q|\alpha} - 3H(\bar{\epsilon}_q + \bar{\rho}_q)\bar{u}_\alpha = 0, \quad (153)$$

that is similar to the hydrodynamic equation (150) of the conservation of energy of dark matter. Because of this similarity, the second Friedmann equation (146) is not independent and can be derived directly from the first Friedmann equation (145) by taking a time derivative and applying the energy conservation Eqs. (151) and (153).

The equation of continuity for the density $\bar{\rho}_q$ of dark energy is obtained by differentiating definition (136) of $\bar{\rho}_q$, and making use of (152). It yields

$$(\bar{\rho}_q \bar{u}^\alpha)_{|\alpha} = -\frac{\partial\bar{W}}{\partial\bar{\Psi}}, \quad (154)$$

or, equivalently,

$$\bar{\rho}_{q|\alpha} - 3H\bar{\rho}_q\bar{u}_\alpha = \frac{\partial\bar{W}}{\partial\bar{\Psi}}\bar{u}_\alpha, \quad (155)$$

which shows that the density $\bar{\rho}_q$ is not conserved. There is no violation of physical laws here since (155) is simply another way of writing (152) and dark energy is not thermodynamically equivalent to dark matter.

4.5 Perturbations of Dynamic Variables

In the present paper, FLRW background manifold is defined by the metric $\bar{g}_{\alpha\beta}$ which dynamics is governed by the two fields—the Clebsch potential $\bar{\Phi}$ of dark matter and the scalar field $\bar{\Psi}$ of dark energy. We assume that the background metric and the fields are perturbed by the presence of a bare matter field θ . Perturbations are considered to be sufficiently small so that the perturbed metric and the matter fields can be split in their background values and the corresponding perturbations,

$$g_{\alpha\beta} = \bar{g}_{\alpha\beta} + \varkappa_{\alpha\beta}, \quad \Phi = \bar{\Phi} + \phi, \quad \Psi = \bar{\Psi} + \psi. \quad (156)$$

These equations are exact. Perturbation of the contravariant component of the metric is not independent and is determined from the isomorphism $g_{\alpha\gamma}g^{\gamma\beta} = \bar{g}_{\alpha\gamma}\bar{g}^{\gamma\beta} = \delta_\alpha^\beta$, and is given by

$$g^{\alpha\beta} = \bar{g}^{\alpha\beta} - \varkappa^{\alpha\beta} + \varkappa^\alpha_\gamma \varkappa^{\gamma\beta} + \dots, \quad (157)$$

where the ellipses denote terms of the higher order.

We consider perturbation of the metric— $\varkappa_{\alpha\beta}$, that of the potential of dark matter— ϕ , and that of the potential of dark energy— ψ as weak with respect to their corresponding background values $\bar{g}_{\alpha\beta}$, $\bar{\Phi}$, and $\bar{\Psi}$, which dynamics is governed by equations that have been explained in Sect. 4.4. Because the field variable θ is the source of the *bare* perturbation, we postulate that its background value is equal to zero. The perturbations $\varkappa_{\alpha\beta}$, ϕ , and ψ have the same order of magnitude as θ . More convenient dynamic variable of gravitational field is a contravariant (Gothic) metric

$$\mathfrak{g}^{\alpha\beta} = \sqrt{-g} g^{\alpha\beta}. \quad (158)$$

The covariant Gothic metric $\mathfrak{g}_{\beta\gamma}$ is defined by $\mathfrak{g}^{\alpha\beta} \mathfrak{g}_{\beta\gamma} = \delta_{\gamma}^{\alpha}$ that yields $\mathfrak{g}_{\alpha\beta} = g_{\alpha\beta} / \sqrt{-g}$. The Gothic metric $\mathfrak{g}^{\alpha\beta}$ is expanded around its background value, $\bar{\mathfrak{g}}^{\alpha\beta} = \sqrt{-\bar{g}} \bar{g}^{\alpha\beta}$, as shown in (53). Calculations also prompt to single out $\sqrt{-\bar{g}}$ from $\mathfrak{h}^{\alpha\beta}$, and operate with a variable

$$l^{\alpha\beta} \equiv \frac{\mathfrak{h}^{\alpha\beta}}{\sqrt{-\bar{g}}}. \quad (159)$$

Tensor indices of the metric tensor perturbations, $l^{\alpha\beta}$, $\mathfrak{h}^{\alpha\beta}$, etc., are raised and lowered with the help of the background metric, for example, $l_{\alpha\beta} \equiv \bar{g}_{\alpha\mu} \bar{g}_{\beta\nu} l^{\mu\nu}$. The field variable $l^{\alpha\beta}$ relates to the perturbation $\varkappa_{\alpha\beta}$ of the metric tensor as follows

$$l^{\alpha\beta} = -\varkappa^{\alpha\beta} + \frac{1}{2} \bar{g}^{\alpha\beta} \varkappa + \varkappa^{\mu(\alpha} \varkappa^{\beta)}_{\mu} - \frac{1}{2} \varkappa^{\alpha\beta} \varkappa - \frac{1}{4} \bar{g}^{\alpha\beta} \left(\varkappa^{\mu\nu} \varkappa_{\mu\nu} - \frac{1}{2} \varkappa^2 \right) + \dots, \quad (160)$$

where $\varkappa \equiv \varkappa^{\sigma}_{\sigma} = \bar{g}^{\rho\sigma} \varkappa_{\rho\sigma}$, and ellipses denote terms of higher orders in $\varkappa_{\alpha\beta}$.

Perturbations of four-velocities, w^{α} and v^{α} , entering definitions of the stress-energy tensors (129), (140), are fully determined by the perturbation of the metric and those of the potentials of dark matter and dark energy. Indeed, according to definitions (124) and (136) the four-velocities are defined by the following equations

$$w_{\alpha} = -\frac{\Phi_{\alpha}}{\mu_{\text{m}}}, \quad v_{\alpha} = -\frac{\Psi_{\alpha}}{\mu_{\text{q}}}. \quad (161)$$

where $\mu_{\text{m}} = \sqrt{-g^{\alpha\beta} \Phi_{\alpha} \Phi_{\beta}}$ and $\mu_{\text{q}} = \sqrt{-g^{\alpha\beta} \Psi_{\alpha} \Psi_{\beta}}$ in accordance with (125) and (133) respectively. We define perturbation of the covariant components of the four-velocities as follows

$$w_{\alpha} = \bar{w}_{\alpha} + \delta w_{\alpha}, \quad v_{\alpha} = \bar{v}_{\alpha} + \delta v_{\alpha}, \quad (162)$$

where the unperturbed values of the four-velocities coincide and are equal to the four-velocity of the Hubble flow due to the requirement of the homogeneity and isotropy of the background FLRW spacetime that is $\bar{w}^{\alpha} = \bar{v}^{\alpha} = \bar{u}^{\alpha}$. Hence, we have

$$\bar{u}_\alpha = -\frac{\bar{\Phi}_\alpha}{\bar{\mu}_m}, \quad \bar{u}_\alpha = -\frac{\bar{\Psi}_\alpha}{\bar{\mu}_q}. \quad (163)$$

Making use of (161) and (163) in the left side of definitions (161), and expanding its right side by making use of expansions (156) and (157), yield

$$\delta w_\alpha = -\frac{1}{\bar{\mu}_m} \bar{P}^\beta{}_\alpha \phi_{|\beta} - \frac{1}{2} \mathfrak{q} \bar{u}_\alpha, \quad \delta v_\alpha = -\frac{1}{\bar{\mu}_q} \bar{P}^\beta{}_\alpha \psi_{|\beta} - \frac{1}{2} \mathfrak{q} \bar{u}_\alpha, \quad (164)$$

where $\bar{P}_{\alpha\beta} = \bar{g}_{\alpha\beta} + \bar{u}_\alpha \bar{u}_\beta$ is projector onto the hypersurface orthogonal to the Hubble flow, and

$$\mathfrak{q} \equiv -\bar{u}^\alpha \bar{u}^\beta \varkappa_{\alpha\beta} = \bar{u}^\alpha \bar{u}^\beta l_{\alpha\beta} + \frac{l}{2}, \quad (165)$$

is projection of the metric tensor perturbation on the Hubble flow.

4.6 Field Equations

4.6.1 Gravitational Field

Field equations for metric tensor perturbation are given by the Euler-Lagrange equations (74) where the operator

$$F_{\mu\nu}^M = F_{\mu\nu}^m + F_{\mu\nu}^q, \quad (166)$$

consists of two pieces corresponding to dark matter (index ‘m’) and dark energy (index ‘q’). These pieces are defined in accordance with (77) or, more exactly,

$$F_{\mu\nu}^m \equiv -\frac{16\pi}{\sqrt{-\bar{g}}} \frac{\delta}{\delta \bar{g}^{\mu\nu}} \left(\mathfrak{h}^{\rho\sigma} \frac{\delta \bar{\mathcal{L}}^m}{\delta \bar{g}^{\rho\sigma}} + \phi \frac{\delta \bar{\mathcal{L}}^m}{\delta \bar{\Phi}} \right), \quad (167)$$

$$F_{\mu\nu}^q \equiv -\frac{16\pi}{\sqrt{-\bar{g}}} \frac{\delta}{\delta \bar{g}^{\mu\nu}} \left(\mathfrak{h}^{\rho\sigma} \frac{\delta \bar{\mathcal{L}}^q}{\delta \bar{g}^{\rho\sigma}} + \psi \frac{\delta \bar{\mathcal{L}}^q}{\delta \bar{\Psi}} \right). \quad (168)$$

Taking variational derivatives from various functions entering the Lagrangians \mathcal{L}^m and \mathcal{L}^q is rather straightforward and follows from their definitions, the chain rule (23), and a set of variational derivatives of thermodynamic quantities given in Appendix section “Variational Derivatives of Dynamic Variables with Respect to the Metric Tensor”. Making use of the Lagrangians (127) and (130) taken on the background manifold and calculating variational derivatives in (167), (168), we obtain

$$F_{\mu\nu}^m = -4\pi(\bar{\rho}_m - \bar{\epsilon}_m)l_{\mu\nu} + 8\pi\bar{\rho}_m(\bar{u}_\mu\phi_\nu + \bar{u}_\nu\phi_\mu - \bar{g}_{\mu\nu}\bar{u}^\alpha\phi_\alpha) \quad (169)$$

$$+ 8\pi\bar{\rho}_m\left(1 - \frac{c^2}{c_s^2}\right)\left(\bar{u}^\alpha\phi_\alpha - \frac{1}{2}\bar{\mu}_m\mathfrak{q}\right)\bar{u}_\mu\bar{u}_\nu,$$

$$F_{\mu\nu}^q = -4\pi(p_q - \epsilon_q)l_{\mu\nu} + 8\pi\bar{\rho}_q(\bar{u}_\mu\psi_\nu + \bar{u}_\nu\psi_\mu - \bar{g}_{\mu\nu}\bar{u}^\alpha\psi_\alpha) \quad (170)$$

$$+ 8\pi\bar{g}_{\mu\nu}\frac{\partial\bar{W}}{\partial\bar{\Psi}}\psi,$$

where $\bar{\rho}_q = \mu_q \equiv \dot{\bar{\Psi}}/a$ in accordance with definition (136) projected on the background manifold. The dark energy potential function, $\bar{W} = \bar{W}(\bar{\Psi})$, is arbitrary.

Substituting (169), (170) along with (81) to the left side of (74) yields field equations for gravitational perturbations $l^{\alpha\beta}$ in a covariant form [48, Eq. 161]

$$l_{\mu\nu}{}^{|\alpha}{}_{|\alpha} + \bar{g}_{\mu\nu}A^\alpha{}_{|\alpha} - 2A_{(\mu}l_{\nu)\alpha} - 2\bar{R}^\alpha{}_{(\mu}l_{\nu)\alpha} - 2\bar{R}_{\mu\alpha\beta\nu}l^{\alpha\beta} + 2F_{\mu\nu}^M = 16\pi\Lambda_{\mu\nu}, \quad (171)$$

where $A^\alpha \equiv l^{\alpha\beta}{}_{|\beta}$ is the gauge vector function. They can be drastically simplified by choosing the gauge condition imposed on the variable $A^\alpha \equiv l^{\alpha\beta}{}_{|\beta}$ in the following form

$$A^\alpha = -2Hl^{\alpha\beta}\bar{u}_\beta + 16\pi(\bar{\rho}_m\phi + \bar{\rho}_q\psi)\bar{u}^\alpha. \quad (172)$$

This gauge condition cancels a significant number of terms in the field equations (171) and allows us to decouple equations for different components of $l^{\alpha\beta}$. Picking up the isotropic coordinates of the Hubble observers we bring the gravity field equations to the following form [48]

$$\square q + 2Hq_{,0} + 4kq - 4\pi\left(1 - \frac{c^2}{c_s^2}\right)\bar{\rho}_m\bar{\mu}_mq = 8\pi(\Lambda_{00} + \Lambda_{kk}) \quad (173a)$$

$$- 8\pi a\bar{\rho}_m\left(1 - \frac{c^2}{c_s^2}\right)\phi_0$$

$$- 16\pi a^2\frac{\partial\bar{W}}{\partial\bar{\Psi}}\psi$$

$$+ 32\pi aH(\bar{\rho}_m\phi + \bar{\rho}_q\psi),$$

$$\square l_{0i} + 2Hl_{0i,0} + 2kl_{0i} = 16\pi\Lambda_{0i}, \quad (173b)$$

$$\square l_{<ij>} + 2Hl_{<ij>,0} + 2(\dot{H} - k)l_{<ij>} = 16\pi\Lambda_{<ij>}, \quad (173c)$$

$$\square l + 2Hl_{,0} + 2(\dot{H} + 2k)l = 16\pi\Lambda_{kk}. \quad (173d)$$

where we denoted the wave operators $\square q \equiv \mathfrak{F}^{\mu\nu}g_{;\mu\nu}$ and $\square l_{\mu\nu} \equiv \bar{\mathfrak{F}}^{\alpha\beta}l_{\mu\nu;\alpha\beta}$. Other notations are $\phi_0 \equiv \phi_{,0}$, $q \equiv (l_{00} + l_{kk})/2$, $l \equiv l_{kk} = l_{11} + l_{22} + l_{33}$, $l_{<ij>} = l_{ij} - (1/3)\delta_{ij}l_{kk}$, and the same index notations are applied to the effective stress-energy tensor $\Lambda_{<ij>}$.

4.6.2 Dark Matter

Evolution of dark matter perturbation is described by the perturbation of the Clebsch potential ϕ . Equation for ϕ is derived from a general equation (100) is, in case of dark matter, reads

$$F_{\Phi}^m = 8\pi \Sigma^m. \quad (174)$$

All terms in this equation can now be explicitly written down because the Lagrangian of dark matter is fully determined by (127). The linear differential operator F_{Φ}^m is derived from (103) which yields

$$F_{\Phi}^m \equiv -\frac{8\pi}{\sqrt{-\bar{g}}} \frac{\delta}{\delta \bar{\Phi}} \left(\bar{\eta}^{\rho\sigma} \bar{T}_{\rho\sigma}^m - \frac{1}{2} \bar{\eta} \bar{T}^m + \sqrt{-\bar{g}} \phi \bar{T}^m \right), \quad (175)$$

where

$$\bar{T}^m = 2 \left(\bar{\rho}_m \bar{u}^\alpha \right)_{|\alpha}. \quad (176)$$

The source density

$$\Sigma^m \equiv \frac{2}{\sqrt{-\bar{g}}} \frac{\delta \mathcal{L}^{\text{dyn}}}{\delta \bar{\Phi}}, \quad (177)$$

and we shall calculate it explicitly in next section.

Calculation of variational derivative in (175) requires taking variational derivative from the density $\bar{\rho}_m$ of the ideal fluid with respect to the background value of the Clebsch potential $\bar{\Phi}$. The density implicitly depends on the potential through the specific enthalpy, $\bar{\rho}_m = \bar{\rho}(\bar{\mu}_m)$ which depends only on the derivatives Φ_α of the potential. Hence,

$$\frac{\delta \rho_m}{\delta \bar{\Phi}} = -\frac{\partial}{\partial x^\alpha} \frac{\partial \rho_m}{\partial \bar{\Phi}_\alpha} = -\frac{\partial}{\partial x^\alpha} \left(\frac{\partial \rho_m}{\partial \bar{\mu}_m} \frac{\partial \mu_m}{\partial \bar{\Phi}_\alpha} \right), \quad (178)$$

where the partial derivative of the density with respect to the specific enthalpy is calculated with the help of (123) by making use of equation of state of the ideal fluid, and the partial derivative

$$\frac{\partial \mu_m}{\partial \bar{\Phi}_\alpha} = \bar{u}^\alpha. \quad (179)$$

It reveals that

$$F_{\Phi}^m = 8\pi Y^\alpha_{|\alpha}, \quad (180)$$

where the vector field

$$Y^\alpha \equiv \frac{\bar{\rho}_m}{\bar{\mu}_m} \phi^\alpha - \bar{\rho}_m l^{\alpha\beta} \bar{u}_\beta + \left(1 - \frac{c^2}{c_s^2} \right) \left(\frac{\bar{\rho}_m}{\bar{\mu}_m} \bar{u}^\beta \phi_\beta - \frac{1}{2} \bar{\rho}_m \mathfrak{q} \right) \bar{u}^\alpha. \quad (181)$$

Taking covariant derivative in (180) brings about the field equations for ϕ

$$\begin{aligned} & \phi^\alpha{}_\alpha - \mu_m A^\alpha \bar{u}_\alpha - 4\bar{\mu}_m H (4q - l) \\ & + \left(1 - \frac{c^2}{c_s^2}\right) \left(\bar{u}^\alpha \bar{u}^\beta \phi_{\alpha\beta} - \frac{1}{2} \bar{\mu}_m \bar{u}^\alpha q_\alpha \right) \\ & - 3H \bar{\mu}_m \frac{\partial \ln c_s^2}{\partial \bar{\mu}_m} \left(\bar{u}^\alpha \phi_\alpha - \frac{1}{2} \bar{\mu}_m q \right) = \Sigma^m, \end{aligned} \quad (182)$$

where the very last term accounts for the fact that the speed of sound is not constant in inhomogeneous medium [78]. Indeed, the speed of sound, c_s , relates to other thermodynamic quantities by equation of state making the speed of sound a function of the specific enthalpy. Hence, $c_s = c_s(\bar{\mu}_m)$. Covariant derivative from the speed of sound is $c_{s|\alpha} = (\partial c_s / \partial \bar{\mu}_m) \bar{\mu}_{m|\alpha}$, where the covariant derivative $\bar{\mu}_{m|\alpha} = (\partial \bar{\mu}_m / \partial \bar{\rho}_m) \bar{\rho}_{m|\alpha}$ and, according to equation of continuity, $\bar{\rho}_{m|\alpha} = 3H \bar{\rho}_m \bar{u}_\alpha$. It yields

$$\left(1 - \frac{c^2}{c_s^2}\right)_{|\alpha} = 3H \bar{\mu}_m \frac{\partial \ln c_s^2}{\partial \bar{\mu}_m} \bar{u}_\alpha, \quad (183)$$

that explains the origin of the last term in (182).

After imposing the gauge condition (172), Eq. (182) is reduced to

$$\begin{aligned} & \phi^\alpha{}_\alpha + 16\pi \bar{\mu}_m (\bar{\rho}_m \phi + \bar{\rho}_q \psi) - 2\bar{\mu}_m H q \\ & + \left(1 - \frac{c^2}{c_s^2}\right) \left(\bar{u}^\alpha \bar{u}^\beta \phi_{\alpha\beta} - \frac{1}{2} \bar{\mu}_m \bar{u}^\alpha q_\alpha \right) \\ & - 3H \bar{\mu}_m \frac{\partial \ln c_s^2}{\partial \bar{\mu}_m} \left(\bar{u}^\beta \phi_\beta - \frac{1}{2} \bar{\mu}_m q \right) = \Sigma^m. \end{aligned} \quad (184)$$

4.6.3 Dark Energy

Calculation of the field equation for dark energy perturbation ψ follows similar path like in previous subsection. The field equations follows from (100), and they are

$$F_\Psi^q = 8\pi \Sigma^q, \quad (185)$$

where F_Ψ^q and Σ^q are determined by the Lagrangian of dark energy (130). Making use of this Lagrangian in (103) we obtain

$$F_\Psi^q \equiv -\frac{8\pi}{\sqrt{-\bar{g}}} \frac{\delta}{\delta \bar{\Psi}} \left(\bar{h}^{\rho\sigma} \bar{T}_{\rho\sigma}^q - \frac{1}{2} \bar{h} \bar{T}^q + \sqrt{-\bar{g}} \bar{\psi} \bar{I}^q \right), \quad (186)$$

where

$$\bar{I}^q = 2 \left[(\bar{\rho}_q \bar{u}^\alpha)_{|\alpha} + \frac{\partial \bar{W}}{\partial \bar{\Psi}} \right]. \quad (187)$$

The source density

$$\Sigma^q \equiv \frac{2}{\sqrt{-\bar{g}}} \frac{\delta \mathcal{L}^{\text{dyn}}}{\delta \bar{\Psi}}, \quad (188)$$

and we shall calculate it explicitly in next section.

According to Eq. (130), the Lagrangian density of the scalar field \mathcal{L}^q depends on both the field Ψ and its first derivative, Ψ_α . For this reason, the differential operator F^q is not reduced to the covariant derivative from a vector field as the partial derivative of the Lagrangian with respect to Ψ does not vanish. We have

$$F_\Psi^q \equiv 8\pi \left(Z^\alpha_{|\alpha} - \frac{l}{2} \frac{\partial \bar{W}}{\partial \bar{\Psi}} - \psi \frac{\partial^2 \bar{W}}{\partial \bar{\Psi}^2} \right) \quad (189)$$

where $l \equiv \bar{g}^{\alpha\beta} l_{\alpha\beta}$, and vector field

$$Z^\alpha \equiv \psi^{|\alpha} - \bar{\rho}_q l^{\alpha\beta} \bar{u}_\beta, \quad (190)$$

where we have used equation $\bar{\Psi}_{|\alpha} = -\bar{u}^\beta \bar{\Psi}_{|\beta} \bar{u}_\alpha = -\bar{\rho}_q \bar{u}_\alpha$. Taking covariant derivative in (189) yields the field equations for ψ

$$\psi^\alpha_{|\alpha} + 16\pi \bar{\mu}_m (\bar{\rho}_m \phi + \bar{\rho}_q \psi) - \left(2\bar{\mu}_q H + \frac{\partial \bar{W}}{\partial \bar{\Psi}} \right) \bar{q} - \frac{\partial^2 \bar{W}}{\partial \bar{\Psi}^2} \psi = \Sigma^q, \quad (191)$$

where Eq. (172) has been used along with the equality $\bar{\rho}_q = \bar{\mu}_q$.

5 Stress-Energy Tensor of Dynamic Perturbations

The effective stress-energy tensor $\Lambda_{\mu\nu}$ is defined as a variational derivative (75) taken from the effective Lagrangian (71). According to (85), it consists of two parts—the stress-energy tensor of matter of the bare perturbation $\mathcal{T}_{\mu\nu}$, and the stress-energy tensor of dynamic perturbations $\mathcal{T}_{\mu\nu}$. We shall keep tensor $\mathcal{T}_{\mu\nu}$ unspecified as long as theory permits and focus on calculation of $\mathcal{T}_{\mu\nu}$ which also consists of two parts, $\mathfrak{t}_{\mu\nu}$ and $\tau_{\mu\nu}$, according to (287). Tensor $\mathfrak{t}_{\mu\nu}$ is the stress-energy tensor of gravitational field perturbations (95). Tensor $\tau_{\mu\nu}$ is the stress-energy tensor due to the coupling of matter perturbations on the background manifold and the gravitational field perturbations. General formula for calculating $\tau_{\mu\nu}$ is given in (96). In case of FLRW universe governed by dark matter and dark energy, tensor $\tau_{\mu\nu}$ is linearly split in two counterparts

$$\tau_{\alpha\beta} = \tau_{\alpha\beta}^m + \tau_{\alpha\beta}^q, \quad (192)$$

where $\tau_{\alpha\beta}^m$ and $\tau_{\alpha\beta}^q$ describe contributions of dark matter and dark energy respectively.

5.1 Stress-Energy Tensor of Gravitational Field Perturbations

Stress-energy tensor of gravitational perturbations, $t_{\mu\nu}$, has a universal presentation on any manifold. We begin its calculation from definition (95) and notice that variational derivative is insensitive to terms which are total divergences. Hence, it is reasonable to single out a total divergence in the argument of variational derivative, $\mathcal{F}^G \equiv h^{\rho\sigma} F_{\rho\sigma}^G - (1/2)h F^G$ entering definition (95) of the gravitational stress-energy tensor. We substitute (81) for $F_{\rho\sigma}^G$ to calculate \mathcal{F}^G , and, then, employ the Leibniz rule to single out the total divergence from the products of two functions. We arrive to

$$\mathcal{F}^G = h^{\rho\sigma|\lambda} l_{\lambda\rho|\sigma} - \frac{1}{2} h^{\rho\sigma|\lambda} l_{\rho\sigma|\lambda} + \frac{1}{4} h^{|\lambda} l_{|\lambda} + \text{div}, \quad (193)$$

where $h^{\rho\sigma} = \sqrt{-\bar{g}} l^{\rho\sigma}$, $h = \bar{g}_{\rho\sigma} h^{\rho\sigma}$, $l = \bar{g}^{\mu\nu} l_{\mu\nu}$, and div is a total divergence that can be discarded from the calculation of the variational derivative.

Next step is to apply the covariant definition (19) of variational derivative to (193) in definition (95) of $t_{\alpha\beta}$. After accounting for transformation (34), definition (95) can be written as follows

$$16\pi t_{\alpha\beta} = \frac{1}{\sqrt{-\bar{g}}} \bar{g}_{\alpha\mu} \bar{g}_{\beta\nu} \frac{\delta \mathcal{F}^G}{\delta \bar{g}_{\mu\nu}}, \quad (194)$$

that conforms with the lower position of indices in variational derivative (19). It is worthwhile to remind the reader that we consider perturbation $h^{\rho\sigma}$ as independent variable which has been used in derivation of (95). It means that the partial derivative

$$\frac{\partial h^{\alpha\beta}}{\partial \bar{g}_{\mu\nu}} = 0. \quad (195)$$

The covariant components of the gravitational perturbation, $h_{\alpha\beta} = \bar{g}_{\alpha\kappa} \bar{g}_{\beta\lambda} h^{\kappa\lambda}$, contain the background metric tensor and cannot be considered as independent from the background metric tensor. We have

$$\frac{\partial h_{\alpha\beta}}{\partial \bar{g}_{\mu\nu}} = \frac{\partial \bar{g}_{\alpha\kappa}}{\partial \bar{g}_{\mu\nu}} \bar{g}_{\beta\lambda} h^{\kappa\lambda} + \frac{\partial \bar{g}_{\beta\lambda}}{\partial \bar{g}_{\mu\nu}} \bar{g}_{\alpha\kappa} h^{\kappa\lambda} = \delta_{\alpha}^{(\mu} h^{\nu)}_{\beta} + \delta_{\beta}^{(\mu} h^{\nu)}_{\alpha}. \quad (196)$$

Let us consider now the dependence of the covariant derivative $\mathfrak{h}^{\alpha\beta}{}_{|\lambda}$ on the metric tensor. We notice that the perturbation $\mathfrak{h}^{\alpha\beta}$ is a tensor density of weight -1 . Therefore, its covariant derivative has one more term as compared with that of a tensor of a second rank. More specifically,

$$\mathfrak{h}^{\alpha\beta}{}_{|\kappa} = \mathfrak{h}^{\alpha\beta}{}_{,\kappa} + \Gamma^\alpha_{\sigma\kappa} \mathfrak{h}^{\sigma\beta} + \Gamma^\beta_{\sigma\kappa} \mathfrak{h}^{\sigma\alpha} - \Gamma^\sigma_{\sigma\kappa} \mathfrak{h}^{\alpha\beta}. \quad (197)$$

It reveals that the derivative depends merely directly on the Christoffel symbols and is independent of the metric tensor $\bar{g}_{\alpha\beta}$. Hence, the partial derivative

$$\frac{\partial \mathfrak{h}^{\alpha\beta}{}_{|\lambda}}{\partial \bar{g}_{\mu\nu}} = 0. \quad (198)$$

It confirms that the metric tensor and the Christoffel symbols are true independent variables along with the tensor density $\mathfrak{h}^{\alpha\beta}$ and its covariant derivative $\mathfrak{h}^{\alpha\beta}{}_{|\lambda}$.

Equation (193) given in terms of the independent variables, reads

$$\mathcal{F}^G = \frac{\bar{g}^{\kappa\lambda} \bar{g}_{\beta\rho}}{\sqrt{-\bar{g}}} \left(\bar{g}_{\alpha\lambda} \mathfrak{h}^{\rho\sigma}{}_{|\kappa} \mathfrak{h}^{\alpha\beta}{}_{|\sigma} - \frac{1}{2} \bar{g}_{\alpha\sigma} \mathfrak{h}^{\rho\sigma}{}_{|\kappa} \mathfrak{h}^{\alpha\beta}{}_{|\lambda} + \frac{1}{4} \bar{g}_{\alpha\sigma} \mathfrak{h}^{\alpha\sigma}{}_{|\kappa} \mathfrak{h}^{\beta\rho}{}_{|\lambda} \right), \quad (199)$$

where we have discarded the total divergence.

Variational derivative (19) from (193) engages the partial derivatives with respect to the background metric tensor and those with respect to the Christoffel symbols. Partial derivative with respect to the metric tensor yields

$$\begin{aligned} \frac{1}{\sqrt{-\bar{g}}} \frac{\partial \mathcal{F}^G}{\partial \bar{g}_{\mu\nu}} = & -\frac{1}{2} \bar{g}^{\mu\nu} \left(l^{\rho\sigma|\lambda} l_{\lambda\rho|\sigma} - \frac{1}{2} l^{\rho\sigma|\lambda} l_{\rho\sigma|\lambda} + \frac{1}{4} l^{|\lambda} l_{|\lambda} \right) \\ & - l^{\mu\sigma|\rho} l^\nu{}_{\sigma|\rho} + l^{\mu\sigma|\rho} l^\nu{}_{\rho|\sigma} \\ & + \frac{1}{2} l^{\rho\sigma|\mu} l_{\rho\sigma}{}^{|\nu} + \frac{1}{2} l^{\mu\nu|\sigma} l_{|\sigma} - \frac{1}{4} l^{|\mu} l^{|\nu}. \end{aligned} \quad (200)$$

Partial derivative with respect to the Christoffel symbols taken from $\mathfrak{h}^{\rho\sigma|\kappa}$ is calculated with the help of (197). It gives

$$\frac{\partial \mathfrak{h}^{\rho\sigma}{}_{|\kappa}}{\partial \Gamma^\alpha_{\lambda\gamma}} = \delta^\rho_\alpha \delta^\lambda_\kappa \mathfrak{h}^{\gamma\sigma} + \delta^\sigma_\alpha \delta^\lambda_\kappa \mathfrak{h}^{\rho\gamma} - \delta^\lambda_\alpha \delta^\gamma_\kappa \mathfrak{h}^{\rho\sigma}. \quad (201)$$

After making use of this formula, the partial derivative of \mathcal{F}^G with respect to the Christoffel symbols results in

$$\begin{aligned} \frac{1}{\sqrt{-\bar{g}}} \frac{\partial \mathcal{F}^G}{\partial \Gamma^\alpha_{\mu\gamma}} = & 2l^{\rho\gamma} l^\mu{}_{(\rho|\alpha)} + 2l^{\rho\mu} l^\gamma{}_{(\rho|\alpha)} - 2l_{\rho\alpha}{}^{|\mu} l^{\gamma\rho)} \\ & - 2\delta^\mu_\alpha l^{(\gamma)}{}_{\rho|\sigma} l^{\rho\sigma} + l_\alpha{}^{(\gamma} l^{|\mu)} + l^{\rho\sigma} l^{|\mu}{}_{\rho\sigma} \delta^\gamma_\alpha - \frac{1}{2} \delta^\mu_\alpha l^{(\gamma)} l^{\gamma)}. \end{aligned} \quad (202)$$

It allows us to calculate the linear combination of the partial derivatives entering definition of variational derivative (19),

$$\begin{aligned}
 & -\frac{1}{2} \frac{1}{\sqrt{-\bar{g}}} \left(\bar{g}^{\sigma\nu} \frac{\partial \mathcal{F}^G}{\partial \Gamma^\sigma_{\mu\gamma}} + \bar{g}^{\sigma\mu} \frac{\partial \mathcal{F}^G}{\partial \Gamma^\sigma_{\nu\gamma}} - \bar{g}^{\sigma\gamma} \frac{\partial \mathcal{F}^G}{\partial \Gamma^\sigma_{\mu\nu}} \right) \\
 & = 2l_\rho^{(\mu} l^{\nu)\rho|\gamma} - 2l^{\gamma\rho} l^{(\mu} l^{\nu)}_{\rho} - l_\rho{}^\gamma l^{\mu\nu|\rho} - \frac{1}{2} l^{\mu\nu} l^{|\gamma} \\
 & + \bar{g}^{\mu\nu} \left(l^{\rho\sigma} l^\gamma_{\rho|\sigma} - \frac{1}{2} l^{\rho\sigma} l_{\rho\sigma}{}^{|\gamma} + \frac{1}{4} l l^{|\gamma} \right).
 \end{aligned} \tag{203}$$

After replacing (200) and (203) into variational derivative (194) defined by the rule (19), the stress-energy tensor of gravitational field takes on the following form

$$\begin{aligned}
 16\pi t_{\mu\nu} = & -\frac{1}{2} \bar{g}_{\mu\nu} \left(l^{\rho\sigma|\gamma} l_{\gamma\rho|\sigma} - \frac{1}{2} l^{\rho\sigma|\gamma} l_{\rho\sigma|\gamma} + \frac{1}{4} l l^{|\gamma} l_{|\gamma} \right) \\
 & - l_{\mu\sigma|\rho} l_\nu{}^{\sigma|\rho} + l_{\mu\sigma|\rho} l_\nu{}^{\rho|\sigma} + \frac{1}{2} l_{\rho\sigma|\mu} l^{\rho\sigma}{}_{|\nu} + \frac{1}{2} l_{\mu\nu|\sigma} l^{|\sigma} - \frac{1}{4} l_{|\mu} l_{|\nu} \\
 & + \bar{g}_{\mu\nu} \left(l^{\rho\sigma} l^\gamma_{\rho|\sigma} - \frac{1}{2} l^{\rho\sigma} l_{\rho\sigma}{}^{|\gamma} + \frac{1}{4} l l^{|\gamma} \right)_{|\gamma} \\
 & + \left(2l_{\rho(\mu} l_{\nu)}{}^{\rho|\gamma} - l_{\nu\rho} l^{\gamma\rho}{}_{|\mu} - l_{\mu\rho} l^{\gamma\rho}{}_{|\nu} - l^{\gamma\rho} l_{\mu\nu|\rho} - \frac{1}{2} l_{\mu\nu} l^{|\gamma} \right)_{|\gamma}.
 \end{aligned} \tag{204}$$

It apparently depends on the second derivatives of the gravitational perturbation, $l_{\mu\nu}$. Significant number of the second derivatives can be eliminated on-shell by making use of the covariant field equation (171). We take the covariant derivative (204) and express the commutator of the second-order derivatives from the metric tensor perturbation in terms of the Riemann tensor

$$l^\alpha_{\rho|\sigma\beta} = l^\alpha_{\rho|\beta\sigma} - l^\gamma_{\rho} \bar{R}^\alpha_{\gamma\sigma\beta} + l^\alpha_{\gamma} \bar{R}^\gamma_{\rho\sigma\beta}. \tag{205}$$

A useful consequence of this equation is

$$l^\alpha_{\rho|\sigma\alpha} = A_{\rho|\sigma} + l^\alpha_{\rho} \bar{R}_{\sigma\alpha} + l^\alpha_{\gamma} \bar{R}^\gamma_{\rho\sigma\alpha}, \tag{206}$$

where $A^\alpha \equiv l^{\alpha\beta}{}_{|\beta}$. Straightforward but tedious rearrangement of the second-order derivatives from the metric tensor perturbations with the help of (205), (206) allows us to put (204) into the following form

$$\begin{aligned}
16\pi t_{\mu\nu} = & 2l_{\mu\rho|\sigma}l_{\nu}^{(\rho|\sigma)} - l^{\rho\sigma}{}_{|\mu}l_{\nu\rho|\sigma} - l^{\rho\sigma}{}_{|\nu}l_{\mu\rho|\sigma} \\
& + \frac{1}{2}l_{\rho\sigma|\mu}l^{\rho\sigma}{}_{|\nu} - \frac{1}{4}l_{|\mu}l_{|\nu} - l^{\rho\sigma}l_{\mu\nu|\rho\sigma} \\
& + \frac{1}{2}\bar{g}_{\mu\nu} \left(l^{\rho\sigma|\gamma}l_{\gamma\rho|\sigma} - \frac{1}{2}l^{\rho\sigma|\gamma}l_{\rho\sigma|\gamma} + \frac{1}{4}l^{|\gamma}l_{|\gamma} \right) \\
& + 2l^{\rho}{}_{(\mu}A_{\nu)\rho} - l_{\mu\nu}A^{\rho}{}_{|\rho} - l_{\mu\nu|\rho}A^{\rho} \\
& + 8\pi \left[4l^{\rho}{}_{(\mu}\Theta_{\nu)\rho} - l_{\mu\nu}\Theta - \bar{g}_{\mu\nu} \left(l^{\rho\sigma}\Theta_{\rho\sigma} - \frac{l}{2}\Theta \right) \right] \\
& + 2l^{\rho}{}_{\mu}l^{\sigma}{}_{\nu}\bar{R}_{\rho\sigma} + 2l^{\alpha\beta}l^{\rho}{}_{(\mu}\bar{R}_{\nu)\alpha\beta\rho}
\end{aligned} \tag{207}$$

where

$$\Theta_{\alpha\beta} = \mathfrak{T}_{\alpha\beta} - \frac{1}{8\pi} \left(F_{\alpha\beta}^{\mathfrak{m}} + F_{\alpha\beta}^{\mathfrak{q}} \right), \tag{208}$$

and the spur, $\Theta \equiv \bar{g}^{\alpha\beta}\Theta_{\alpha\beta}$. Notice that the on-shell form (207) of the stress-energy tensor $t_{\mu\nu}$ for gravitational field depends on the choice of the gauge function A^{α} as well as on the value of the Riemann tensor of the background manifold.

5.2 Stress-Energy Tensor of Dark Matter Perturbations

The part of the stress-energy tensor describing the dark matter perturbation is given in (192) by $\tau_{\mu\nu}^{\mathfrak{m}}$ that, according to (96), is calculated as a variational derivative

$$16\pi\tau_{\alpha\beta}^{\mathfrak{m}} = \frac{1}{\sqrt{-\bar{g}}} \bar{g}_{\alpha\mu}\bar{g}_{\beta\nu} \frac{\delta\mathcal{F}^{\mathfrak{m}}}{\delta\bar{g}_{\mu\nu}}, \tag{209}$$

where

$$\mathcal{F}^{\mathfrak{m}} \equiv \mathfrak{h}^{\rho\sigma}F_{\rho\sigma}^{\mathfrak{m}} - \frac{1}{2}\mathfrak{h}F^{\mathfrak{m}} + \sqrt{-\bar{g}}\phi F_{\Phi}^{\mathfrak{m}} \tag{210}$$

Individual terms entering the right side of (210) are taken from (169) and (180). We single out the total divergence and brings (210) to the following form

$$\mathcal{F}^{\mathfrak{m}} \equiv \mathfrak{h}^{\rho\sigma}F_{\rho\sigma}^{\mathfrak{m}} - \frac{1}{2}\mathfrak{h}F^{\mathfrak{m}} - 8\pi\sqrt{-\bar{g}}\phi_{\alpha}Y^{\alpha}, \tag{211}$$

where the total divergence has been dropped off, $\phi_{\alpha} \equiv \phi_{|\alpha}$, and Y^{α} is given in (181). After reducing similar terms Eq. (211) takes on the following form

$$\begin{aligned}
\mathcal{F}^m = & -8\pi\sqrt{-\bar{g}} \left(\frac{\bar{\rho}_m}{\bar{\mu}_m} \phi^\alpha \phi_\alpha - 3\bar{\rho}_m l^{\alpha\beta} \bar{u}_\alpha \phi_\beta \right) \\
& - 4\pi\sqrt{-\bar{g}} (\bar{p}_m - \bar{\epsilon}_m) \left(l^{\alpha\beta} l_{\alpha\beta} - \frac{1}{2} l^2 \right) \\
& - 8\pi\sqrt{-\bar{g}} \frac{\bar{\rho}_m}{\bar{\mu}_m} \left(1 - \frac{c^2}{c_s^2} \right) \left[(\bar{u}^\alpha \phi_\alpha)^2 - \frac{3}{2} \bar{\mu}_m \mathfrak{q} \bar{u}^\alpha \phi_\alpha + \frac{1}{2} \mu_m^2 \mathfrak{q}^2 \right].
\end{aligned} \tag{212}$$

where again we have used notation $\phi_\alpha \equiv \phi|_\alpha$.

Taking variational derivative in (209) is rather straightforward but tedious procedure. Because the Lagrangian \mathcal{F}^m depends neither on the Christoffel symbols nor on the curvature tensor, the variational derivative (209) is reduced to a partial derivative with respect to the metric tensor $\delta\mathcal{F}^m/\delta g_{\mu\nu} = \partial\mathcal{F}^m/\partial g_{\mu\nu}$. Calculation of the partial derivative is done with the help of the chain rule and equations in Appendix section “Variational Derivatives”. It yields the stress-energy tensor of dark matter

$$\begin{aligned}
\tau_{\mu\nu}^m = & \frac{\bar{\rho}_m}{2\bar{\mu}_m} \phi_\mu \phi_\nu \\
& - \frac{\bar{\rho}_m}{2\bar{\mu}_m} \left(1 - \frac{c^2}{c_s^2} \right) \left[\left(\frac{3}{2} \bar{\mu}_m \mathfrak{q} - 2\bar{u}^\alpha \phi_\alpha \right) \bar{u}_{(\mu} \phi_{\nu)} - \frac{3}{4} \bar{\mu}_m \bar{u}^\alpha \phi_\alpha l_{\mu\nu} \right] \\
& + \frac{\bar{\rho}_m}{4\bar{\mu}_m} \left(1 - \frac{c^2}{c_s^2} \right) \left(\phi^\alpha \phi_\alpha - 3\bar{\mu}_m l^{\alpha\beta} \bar{u}_\alpha \phi_\beta + \frac{3}{2} \bar{\mu}_m l \bar{u}^\alpha \phi_\alpha \right) \bar{u}_\mu \bar{u}_\nu \\
& + \frac{\bar{\rho}_m}{4\bar{\mu}_m} \left[\left(1 - \frac{c^2}{c_s^2} \right) \left(3 - \frac{c^2}{c_s^2} \right) - \bar{\rho}_m \bar{\mu}_m \frac{c^2}{c_s^2} \frac{\partial \ln c_s^2}{\partial \bar{p}_m} \right] \\
& \times \left[(\bar{u}^\alpha \phi_\alpha)^2 - \frac{3}{2} \bar{\mu}_m \mathfrak{q} \bar{u}^\alpha \phi_\alpha + \frac{1}{2} \mu_m^2 \mathfrak{q}^2 \right] \bar{u}_\mu \bar{u}_\nu \\
& - \frac{\bar{\rho}_m}{4\bar{\mu}_m} \left[\phi^\alpha \phi_\alpha + \left(1 - \frac{c^2}{c_s^2} \right) (\bar{u}^\alpha \phi_\alpha)^2 \right] \bar{g}_{\mu\nu} \\
& - \frac{1}{8} \bar{\rho}_m \bar{\mu}_m \left(1 - \frac{c^2}{c_s^2} \right) \left[2\mathfrak{q} l_{\mu\nu} - \mathfrak{q}^2 \bar{g}_{\mu\nu} + \left(l^{\alpha\beta} l_{\alpha\beta} - \frac{1}{2} l^2 + 2\mathfrak{q} l \right) \bar{u}_\mu \bar{u}_\nu \right] \\
& - \frac{1}{2} (\bar{p}_m - \bar{\epsilon}_m) \left[l_{\alpha\mu} l_\nu{}^\alpha - \frac{1}{2} l l_{\mu\nu} - \frac{1}{4} \left(l^{\alpha\beta} l_{\alpha\beta} - \frac{1}{2} l^2 \right) \bar{g}_{\mu\nu} \right],
\end{aligned} \tag{213}$$

where we have used (117) to make a replacement $\bar{\epsilon}_m + \bar{p}_m = \bar{\rho}_m \bar{\mu}_m$.

5.3 Stress-Energy Tensor of Dark Energy Perturbations

The part of the stress-energy tensor describing the dark energy perturbation is given in (192) by $\tau_{\mu\nu}^q$ that, according to (96), is calculated as a variational derivative

$$16\pi\tau_{\alpha\beta}^q = \frac{1}{\sqrt{-\bar{g}}} \bar{g}_{\alpha\mu} \bar{g}_{\beta\nu} \frac{\delta \mathcal{F}^q}{\delta \bar{g}_{\mu\nu}}, \quad (214)$$

where

$$\mathcal{F}^q \equiv \mathfrak{h}^{\rho\sigma} F_{\rho\sigma}^q - \frac{1}{2} \mathfrak{h} F^q + \sqrt{-\bar{g}} \psi F_{\Psi}^q \quad (215)$$

Individual terms entering the right side of (215) are taken from (170) and (189). We single out the total divergence and bring (215) to the following form

$$\mathcal{F}^q \equiv \mathfrak{h}^{\rho\sigma} F_{\rho\sigma}^q - \frac{1}{2} \mathfrak{h} F^q - 8\pi\sqrt{-\bar{g}} \psi_{\alpha} Z^{\alpha} - 4\pi\sqrt{-\bar{g}} \psi \left(l \frac{\partial \bar{W}}{\partial \bar{\Psi}} + 2\psi \frac{\partial^2 \bar{W}}{\partial \bar{\Psi}^2} \right), \quad (216)$$

where the total divergence has been dropped off. More explicitly,

$$\begin{aligned} \mathcal{F}^q = & -8\pi\sqrt{-\bar{g}} \left[\psi^{\alpha} \psi_{\alpha} + \frac{3}{2} l \psi \frac{\partial \bar{W}}{\partial \bar{\Psi}} + \psi^2 \frac{\partial^2 \bar{W}}{\partial \bar{\Psi}^2} - 3\bar{\mu}_q l^{\alpha\beta} \bar{u}_{\alpha} \psi_{\beta} \right] \\ & + 8\pi\sqrt{-\bar{g}} \bar{W}(\bar{\Psi}) \left(l^{\alpha\beta} l_{\alpha\beta} - \frac{1}{2} l^2 \right), \end{aligned} \quad (217)$$

where $\psi_{\alpha} \equiv \psi_{,\alpha}$. Taking variational derivative with respect to $\bar{g}_{\mu\nu}$, we obtain the stress-energy tensor of dark energy perturbation

$$\begin{aligned} \tau_{\mu\nu}^q = & \frac{1}{2} \psi_{\mu} \psi_{\nu} - \frac{1}{4} \left(\psi^{\alpha} \psi_{\alpha} + \psi^2 \frac{\partial^2 \bar{W}}{\partial \bar{\Psi}^2} \right) \bar{g}_{\mu\nu} - \frac{3}{4} l_{\mu\nu} \psi \frac{\partial \bar{W}}{\partial \bar{\Psi}} \\ & + \bar{W}(\bar{\Psi}) \left[l_{\alpha\mu} l_{\nu}^{\alpha} - \frac{1}{2} l l_{\mu\nu} - \frac{1}{4} \left(l^{\alpha\beta} l_{\alpha\beta} - \frac{1}{2} l^2 \right) \bar{g}_{\mu\nu} \right]. \end{aligned} \quad (218)$$

6 Post-Newtonian Equations of Motion in Cosmology

6.1 General Formulation

Let us consider a general manifold with the effective Lagrangian $\mathcal{L}^{\text{eff}} = \mathcal{L}^{\text{eff}}(\bar{g}^{\mu\nu}, \bar{\Phi}^A, \mathfrak{h}^{\mu\nu}, \phi^A, \theta^B)$ depending on five independent variables and their derivatives which we intentionally omitted from the argument of the Lagrangian to avoid a cumbersome notation. We have proved in Sect. 3.7 that the effective Lagrangian \mathcal{L}^{eff} is gauge-invariant modulo a total divergence. The gauge invariance of \mathcal{L}^{eff} suggests that its Lie derivative must be also nil modulo a total divergence of a vector field: $\mathcal{L}_{\xi} \mathcal{L}^{\text{eff}} = \partial_{\alpha} A^{\alpha}$. Because the total divergences do not affect field equations we drop all of them out of the subsequent equations.

We compute the Lie derivative of the effective Lagrangian by making use of (29) that reduce calculation of the Lie derivative to that of variational derivatives modulo

a total divergence. After dropping off the divergence, we have

$$\begin{aligned}\mathcal{L}_\xi \mathcal{L}^{\text{eff}} &= \frac{\delta \mathcal{L}^{\text{eff}}}{\delta \bar{g}^{\alpha\beta}} \mathcal{L}_\xi \bar{g}^{\alpha\beta} + \frac{\delta \mathcal{L}^{\text{eff}}}{\delta \bar{\Phi}^A} \mathcal{L}_\xi \bar{\Phi}^A + \frac{\delta \mathcal{L}^{\text{eff}}}{\delta \mathfrak{h}^{\mu\nu}} \mathcal{L}_\xi \mathfrak{h}^{\mu\nu} \\ &+ \frac{\delta \mathcal{L}^{\text{eff}}}{\delta \phi^A} \mathcal{L}_\xi \phi^A + \frac{\delta \mathcal{L}^{\text{eff}}}{\delta \theta^B} \mathcal{L}_\xi \theta^B.\end{aligned}\quad (219)$$

Field equations (72), (99), (104) describing evolution of perturbations $\mathfrak{h}^{\mu\nu}$, ϕ^A , θ^B on the background manifold exterminate the last three terms in the right side of (219). The first term in the right side of (219) can be written down as follows

$$\frac{\delta \mathcal{L}^{\text{eff}}}{\delta \bar{g}^{\alpha\beta}} \mathcal{L}_\xi \bar{g}^{\alpha\beta} = -\sqrt{-\bar{g}} \Lambda_{\alpha\beta} \xi^{\alpha|\beta}, \quad (220)$$

where we have used definitions (75), (85)–(87), and equation $\mathcal{L}_\xi \bar{g}^{\alpha\beta} = -\xi^{\alpha|\beta} - \xi^{\beta|\alpha}$.

The Lie derivative of the field $\bar{\Phi}^A$ depends on its geometric properties. In a particular case of tensor density $\bar{\Phi}^A \equiv (\bar{\Phi}^A)^{\mu_1 \dots \mu_p}_{\nu_1 \dots \nu_q}$, the Lie derivative is given by (26) that can be written symbolically as follows

$$\mathcal{L}_\xi \bar{\Phi}^A = \xi^\alpha \bar{\Phi}^A_{|\alpha} + \bar{K}^A_{\alpha\beta} \xi^{\alpha|\beta}, \quad (221)$$

where $\bar{\Phi}^A_{|\alpha} \equiv (\bar{\Phi}^A)^{\mu_1 \dots \mu_p}_{\nu_1 \dots \nu_q |\alpha}$, $\bar{K}^A_{\alpha\beta} = \bar{K}^{A\sigma}_{\alpha} \bar{g}_{\sigma\beta}$, and

$$\begin{aligned}\bar{K}^{A\sigma}_{\alpha} &\equiv m \delta^\sigma_{\alpha} \left(\bar{\Phi}^A \right)^{\mu_1 \dots \mu_p}_{\nu_1 \dots \nu_q} \\ &- \delta^{\mu_1}_{\alpha} \left(\bar{\Phi}^A \right)^{\sigma \mu_2 \dots \mu_p}_{\nu_1 \dots \nu_q} - \dots - \delta^{\mu_p}_{\alpha} \left(\bar{\Phi}^A \right)^{\mu_1 \dots \mu_{p-1} \sigma}_{\nu_1 \dots \nu_q} \\ &+ \delta^\sigma_{\nu_1} \left(\bar{\Phi}^A \right)^{\mu_1 \dots \mu_p}_{\alpha \nu_2 \dots \nu_q} + \dots + \delta^\sigma_{\nu_q} \left(\bar{\Phi}^A \right)^{\mu_1 \dots \mu_p}_{\nu_1 \dots \nu_{q-1} \alpha}.\end{aligned}\quad (222)$$

Making use of definition (102) and (222) we can present the second term in the right side of (219) in the following form

$$\frac{\delta \mathcal{L}^{\text{eff}}}{\delta \bar{\Phi}^A} \mathcal{L}_\xi \bar{\Phi}^A = \frac{1}{2} \sqrt{-\bar{g}} \Sigma^M_A \left(\xi^\alpha \bar{\Phi}^A_{|\alpha} + \bar{K}^A_{\alpha\beta} \xi^{\alpha|\beta} \right) \quad (223)$$

Substituting (220), (223) to the right side of (219) results in

$$\mathcal{L}_\xi \mathcal{L}^{\text{eff}} = \frac{1}{2} \sqrt{-\bar{g}} \Sigma^M_A \bar{\Phi}^A_{|\alpha} \xi^\alpha + \sqrt{-\bar{g}} \left(-\Lambda_{\alpha\beta} + \frac{1}{2} \Sigma^M_A \bar{K}^A_{\alpha\beta} \right) \xi^{\alpha|\beta}. \quad (224)$$

Applying the Leibniz rule to change the order of differentiation in the terms depending on $\xi^{\alpha|\beta}$, we can recast (219) to the following form

$$\mathcal{L}_\xi \mathcal{L}^{\text{eff}} = \sqrt{-\bar{g}} \left[\frac{1}{2} \Sigma_A^M \bar{\Phi}_{|\alpha}^A + \Lambda_{\alpha\beta}{}^{|\beta} - \frac{1}{2} \left(\Sigma_A^M \bar{K}_{\alpha\beta}^A \right)^{|\beta} \right] \xi^\alpha + \sqrt{-\bar{g}} W_\beta{}^{|\alpha}, \quad (225)$$

where the vector field

$$W_\beta \equiv \left(-\Lambda_{\alpha\beta} + \frac{1}{2} \Sigma_A^M \bar{K}_{\alpha\beta}^A \right) \xi^\alpha \quad (226)$$

The last term in (225) is reduced to the total divergence of a vector density

$$\sqrt{-\bar{g}} W_\beta{}^{|\beta} = \left(\sqrt{-\bar{g}} W^\beta \right)_{,\beta}, \quad (227)$$

where $W^b = \bar{g}^{\alpha\beta} W_\alpha$. Therefore, the variational derivative of the effective Lagrangian can be equal to zero modulo the divergence of the vector field if, and only if, the combination of terms enclosed to the square brackets in (225) is nil. It yields the equations of motion of the matter of bare perturbation

$$\Lambda_{\alpha\beta}{}^{|\beta} = -\frac{1}{2} \Sigma_A^M \bar{\Phi}_{|\alpha}^A + \frac{1}{2} \left(\Sigma_A^M \bar{K}_{\alpha\beta}^A \right)^{|\beta}. \quad (228)$$

It should be compared with the law of conservation of matter in flat background spacetime where it has a similar form $\Lambda_{\alpha\beta}{}^{|\beta} = 0$ of the total divergence [79]. The presence of the background matter fields $\bar{\Phi}^A$ makes the right side of (228) different from zero. This result was established in [73].

Equation (228) can be also interpreted as the integrability condition of the gravitational field equation (74). Taking a covariant derivative from both sides of the field equation (74) and applying the equations of motion (228) yields

$$\left(F_{\alpha\beta}^G + F_{\alpha\beta}^M \right)^{|\beta} = -4\pi \left[\Sigma_A^M \bar{\Phi}_{|\alpha}^A - \left(\Sigma_A^M \bar{K}_{\alpha\beta}^A \right)^{|\beta} \right]. \quad (229)$$

In the linear approximation, when all quadratic and higher-order terms with respect to the perturbations are discarded ($\Sigma_A^M \rightarrow 0$), the covariant divergence $(F_{\alpha\beta}^G + F_{\alpha\beta}^M)^{|\beta} = 0$. It agrees with the assumption that the stress-energy tensor of the bare perturbation is conserved in the linearized perturbative order, $\mathfrak{T}_{\alpha\beta}{}^{|\beta} = 0$. Now we are set to start calculating equations of motion of matter of the bare perturbation in FLRW universe.

6.2 Equations of Motion in the Universe Governed by Dark Matter and Dark Energy

The dark matter and dark energy components of matter that governs the temporal evolution of the universe are modelled by scalar fields Φ and Ψ . Hence, the tensor, $\bar{K}_{\alpha\beta}^A \equiv 0$, and, consequently, the second term in the right side of (228) is identically

nil. Therefore, equations of motion of matter (228) can be written more explicitly in the following form

$$\mathfrak{T}_{\mu\nu}{}^{|\nu} + \mathfrak{t}_{\mu\nu}{}^{|\nu} + \tau_{\mu\nu}^{\text{m}}{}^{|\nu} + \tau_{\mu\nu}^{\text{q}}{}^{|\nu} = \frac{1}{2} (\bar{\mu}_{\text{m}} \Sigma^{\text{m}} + \bar{\mu}_{\text{q}} \Sigma^{\text{q}}) \bar{u}_{\mu}, \quad (230)$$

where we have used definitions (163) of the gradients of the scalar fields $\bar{\Phi}$ and $\bar{\Psi}$ in terms of the background four-velocity \bar{u}^{α} . Next step is to calculate the explicit form of Σ^{m} and Σ^{q} as well as the covariant divergences of stress-energy tensors entering (230). We split the process of calculation in three parts—for gravitational field, for dark matter, and dark energy.

6.2.1 Gravitational Field

Covariant divergence from the stress-energy tensor of gravitational field, $\mathfrak{t}_{\mu\nu}$, is derived from (207). We again need to employ the commutation relations (205), (206) along with a rule for the third order derivative

$$l^{\lambda}{}_{\mu|\rho\sigma\nu} = l^{\lambda}{}_{\mu|\rho\nu\sigma} - l^{\gamma}{}_{\mu|\rho} \bar{R}^{\lambda}{}_{\gamma\sigma\nu} + l^{\lambda}{}_{\gamma|\rho} \bar{R}^{\gamma}{}_{\mu\sigma\nu} + l^{\lambda}{}_{\mu|\gamma} \bar{R}^{\gamma}{}_{\rho\sigma\nu}, \quad (231)$$

which allows us (after one more commutation of the covariant derivative in $l^{\lambda}{}_{\mu|\rho\nu\sigma}$) to derive

$$\begin{aligned} l^{\nu}{}_{\mu|\rho\sigma\nu} &= A_{\mu|\rho\sigma} + l^{\alpha}{}_{\mu|\sigma} \bar{R}_{\alpha\rho} + l^{\alpha}{}_{\mu|\rho} \bar{R}_{\alpha\sigma} + l^{\alpha}{}_{\beta|\sigma} \bar{R}^{\beta}{}_{\mu\rho\alpha} \\ &\quad + l^{\alpha}{}_{\beta|\rho} \bar{R}^{\beta}{}_{\mu\sigma\alpha} + l^{\alpha}{}_{\mu|\beta} \bar{R}^{\beta}{}_{\rho\sigma\alpha} + l^{\alpha}{}_{\mu} \bar{R}_{\alpha\rho|\sigma} + l^{\alpha}{}_{\beta} \bar{R}^{\beta}{}_{\mu\rho\alpha|\sigma}. \end{aligned} \quad (232)$$

Significant number of terms cancel out, and after long calculation we obtain a rather simple result

$$\mathfrak{t}_{\mu\nu}{}^{|\nu} = \left(l^{\rho}{}_{\nu} \Theta_{\rho\mu} - \frac{1}{2} l_{\mu\nu} \Theta \right)^{|\nu} - \frac{1}{2} \left(l^{\rho\sigma} \Theta_{\rho\sigma|\mu} - \frac{1}{2} l \Theta_{|\mu} \right), \quad (233)$$

where $\Theta_{\alpha\beta}$ was defined in (208). After taking the covariant divergence, it is convenient to algebraically split (233) in three parts

$$\begin{aligned} \mathfrak{t}_{\mu\nu}{}^{|\nu} &= \left(l^{\rho}{}_{\nu} \mathfrak{T}_{\rho\mu} - \frac{1}{2} l_{\mu\nu} \mathfrak{T} \right)^{|\nu} - \frac{1}{2} \left(l^{\rho\sigma} \mathfrak{T}_{\rho\sigma|\mu} - \frac{1}{2} l \mathfrak{T}_{|\mu} \right) \\ &\quad - \frac{1}{8\pi} \left(l^{\rho}{}_{\nu} F^{\text{m}}_{\rho\mu} - \frac{1}{2} l_{\mu\nu} F^{\text{m}} \right)^{|\nu} + \frac{1}{16\pi} \left(l^{\rho\sigma} F^{\text{m}}_{\rho\sigma|\mu} - \frac{1}{2} l F^{\text{m}}_{|\mu} \right) \\ &\quad - \frac{1}{8\pi} \left(l^{\rho}{}_{\nu} F^{\text{q}}_{\rho\mu} - \frac{1}{2} l_{\mu\nu} F^{\text{q}} \right)^{|\nu} + \frac{1}{16\pi} \left(l^{\rho\sigma} F^{\text{q}}_{\rho\sigma|\mu} - \frac{1}{2} l F^{\text{q}}_{|\mu} \right), \end{aligned} \quad (234)$$

where the first line describes the coupling of gravity with the stress-energy tensor $\mathfrak{T}_{\mu\nu}$ of the bare perturbation, and the second and the third lines outline the contribution of dark matter (index ‘m’) and dark energy (index ‘q’).

6.2.2 Dark Matter

The source density of dark matter, Σ^m , depends only on the derivatives of the scalar field $\bar{\Phi}$, and can be written in the form of a covariant divergence

$$\Sigma^m = J_\nu^m |^\nu, \quad (235)$$

with the matter current

$$J_\nu^m = \frac{1}{16\pi\sqrt{-g}} \frac{\partial \mathcal{F}^m}{\partial \bar{\Phi}^\nu}. \quad (236)$$

The current is split in two components

$$J_\alpha^m = \bar{\rho}_m \bar{u}_\alpha j + \bar{\rho}_m \bar{P}_\alpha{}^\beta j_\beta, \quad (237)$$

where

$$\begin{aligned} j = & \frac{1}{2\bar{\mu}_m^2} \left(1 - \frac{c^2}{c_s^2}\right) \left[\phi^\alpha \phi_\alpha + \left(1 - \frac{c^2}{c_s^2}\right) (\bar{u}^\alpha \phi_\alpha)^2 \right] \\ & + \frac{3}{2\bar{\mu}_m} \frac{c^2}{c_s^2} \left[l^{\alpha\beta} \bar{u}_\alpha \phi_\beta + \frac{1}{2} \left(1 - \frac{c^2}{c_s^2}\right) (\bar{u}^\alpha \phi_\alpha) q \right] \\ & - \frac{1}{4} \left(1 - \frac{c^2}{c_s^2}\right) \left[\left(1 + \frac{c^2}{c_s^2}\right) q^2 + l^{\alpha\beta} l_{\alpha\beta} - \frac{l^2}{2} \right] \\ & - \frac{1}{2\bar{\mu}_m} \frac{c^2}{c_s^2} \frac{\partial \ln c_s^2}{\partial \bar{\mu}_m} \left[(\bar{u}^\alpha \phi_\alpha)^2 - \frac{3}{2} \bar{\mu}_m q (\bar{u}^\alpha \phi_\alpha) + \frac{1}{2} \bar{\mu}_m^2 q^2 \right], \end{aligned} \quad (238)$$

$$\begin{aligned} j_\beta = & \frac{1}{\bar{\mu}_m^2} \left(1 - \frac{c^2}{c_s^2}\right) (\bar{u}^\alpha \phi_\alpha) \phi_\beta \\ & - \frac{3}{2\bar{\mu}_m} l_\beta{}^\alpha \phi_\alpha - \frac{3}{2\bar{\mu}_m} \left(1 - \frac{c^2}{c_s^2}\right) \left[(\bar{u}^\alpha \phi_\alpha) l_\beta{}^\gamma \bar{u}_\gamma + \frac{1}{2} q \phi_\beta \right] \\ & + \left(1 - \frac{c^2}{c_s^2}\right) q l_\beta{}^\alpha \bar{u}_\alpha. \end{aligned} \quad (239)$$

Taking covariant divergence from J_α^m entangles a lot of algebraic operations which number can be significantly reduced by making use of the following procedure. We notice that the first term in the right side of (230) can be transformed to

$$\bar{\mu}_m \Sigma^m \bar{u}_\mu = (\bar{\mu}_m J_\nu^m \bar{u}_\mu)^{|\nu} + 3 \frac{c_s^2}{c^2} H \bar{\rho}_m \bar{\mu}_m j \bar{u}_\mu - H \bar{\rho}_m \bar{\mu}_m j_\nu \bar{P}_\mu{}^\nu. \quad (240)$$

Furthermore,

$$16\pi \sqrt{-\bar{g}} \tau_{\mu\nu}^m = \bar{g}_{\mu\rho} \bar{g}_{\nu\sigma} \left(\frac{\partial \mathcal{F}^m}{\partial \bar{g}_{\rho\sigma}} + \frac{\partial \mathcal{F}^m}{\partial \bar{\mu}_m} \frac{\delta \bar{\mu}_m}{\delta \bar{g}_{\rho\sigma}} \right), \quad (241)$$

$$16\pi \sqrt{-\bar{g}} J_\nu^m = \frac{\partial \mathcal{F}^m}{\partial \bar{\Phi}^\nu} + \frac{\partial \mathcal{F}^m}{\partial \bar{\mu}_m} \frac{\delta \bar{\mu}_m}{\delta \bar{\Phi}^\nu}, \quad (242)$$

Accounting for the variational derivatives (299), (322) we obtain

$$\tau_{\mu\nu}^m - \frac{1}{2} \bar{\mu}_m J_\nu^m \bar{u}_\mu = \frac{1}{16\pi \sqrt{-\bar{g}}} \left(\bar{g}_{\mu\rho} \bar{g}_{\nu\sigma} \frac{\partial \mathcal{F}^m}{\partial \bar{g}_{\rho\sigma}} - \frac{1}{2} \frac{\partial \mathcal{F}^m}{\partial \bar{\Phi}^\nu} \bar{u}_\mu \right). \quad (243)$$

This equation elucidates that we do not need to directly calculate the partial derivatives with respect to the specific enthalpy $\bar{\mu}_m$ when calculating the equations of motion (230). It saves us from doing a lot of algebra.

We combine (243) with the divergence from the second line of (234) and denote

$$X_{\mu\nu} \equiv \tau_{\mu\nu}^m - \frac{1}{2} \bar{\mu}_m J_\nu^m \bar{u}_\mu - \frac{1}{8\pi} \left(l^\rho{}_\nu F_{\rho\mu}^m - \frac{1}{2} l_{\mu\nu} F^m \right). \quad (244)$$

Notice that $X_{\mu\nu}$ is not symmetric with respect to its indices. Calculation reveals

$$\begin{aligned} X_{\mu\nu} = & \frac{\bar{\rho}_m}{2\bar{\mu}_m} \left(\phi_\mu \phi_\nu - \frac{1}{2} \phi^\alpha \phi_\alpha \bar{g}_{\mu\nu} \right) \\ & + \frac{\bar{\rho}_m}{2\bar{\mu}_m} \left(1 - \frac{c^2}{c_s^2} \right) \left[(\bar{u}^\alpha \phi_\alpha) \phi_\mu \bar{u}_\nu - \frac{1}{2} (\bar{u}^\alpha \phi_\alpha)^2 \bar{g}_{\mu\nu} \right] \\ & - \bar{\rho}_m \left(\phi_\mu l_\nu{}^\rho \bar{u}_\rho + \frac{1}{4} \bar{u}_\mu l_\nu{}^\rho \phi_\rho \right) \\ & - \bar{\rho}_m \left(1 - \frac{c^2}{c_s^2} \right) \left[\frac{3}{8} \mathfrak{q} \phi_\mu \bar{u}_\nu + (\bar{u}^\alpha \phi_\alpha) \left(\frac{1}{8} l_{\mu\nu} + \frac{1}{4} \bar{u}_\mu l_\nu{}^\rho \bar{u}_\rho \right) \right] \\ & + \frac{1}{8} \left[\bar{\rho}_m \bar{\mu}_m \left(1 - \frac{c^2}{c_s^2} \right) \mathfrak{q}^2 + (\bar{p}_m - \bar{\epsilon}_m) \left(l^{\rho\sigma} l_{\rho\gamma} - \frac{1}{2} l^2 \right) \right] \bar{g}_{\mu\nu}. \end{aligned} \quad (245)$$

Let us denote the density of the force caused by dark matter on the motion of the matter of the bare perturbation, by f_μ^m . After grouping all terms together the force density is defined by the following expression

$$f_\mu^m \equiv -X_{\mu\nu}{}^{|\nu} - \frac{1}{16\pi} \left(l^{\rho\sigma} F_{\rho\sigma|\mu}^m - \frac{1}{2} l F_{|\mu}^m \right) \quad (246)$$

$$+ \frac{3}{2} \frac{c_s^2}{c^2} H \bar{\rho}_m \bar{\mu}_m j \bar{u}_\mu - \frac{1}{2} H \bar{\rho}_m \bar{\mu}_m j_\nu \bar{P}_\mu{}^\nu,$$

which can be split in two orthogonal components

$$f_\mu^m = a^m \bar{u}_\mu + a_\mu^m \bar{P}^\nu{}_\mu, \quad (247)$$

where $a^m \equiv -\bar{u}^\nu f_\nu^m$ and $a_\mu^m \equiv \bar{P}_\mu{}^\nu f_\nu^m$. We have

$$a^m = \frac{1}{4} \bar{\rho}_m \left[l^{\alpha\beta} \phi_{\alpha\beta} + A^\alpha \phi_\alpha - 2 (\bar{u}^\alpha \phi_\alpha) (\bar{u}^\beta A_\beta) \right] \quad (248)$$

$$+ \frac{1}{8} \bar{\rho}_m \left(1 - \frac{c^2}{c_s^2} \right)$$

$$\times \left[\bar{u}^\alpha \bar{u}^\beta l_{\beta}{}^\gamma \phi_{\alpha\gamma} + \mathfrak{q} \bar{u}^\alpha \bar{u}^\beta \phi_{\alpha\beta} - (\bar{u}^\alpha \phi_\alpha) (\bar{u}^\beta \mathfrak{q}_\beta) + (\bar{u}^\alpha \phi_\alpha) (\bar{u}^\beta A_\beta) \right]$$

$$+ 2 \bar{\rho}_m H (\bar{u}^\alpha \phi_\alpha) \left(2\mathfrak{q} - \frac{1}{2} l \right)$$

$$+ \frac{1}{8} \bar{\rho}_m H \left(1 - \frac{c^2}{c_s^2} \right) \left[l^{\alpha\beta} \bar{u}_\alpha \phi_\beta + (\bar{u}^\alpha \phi_\alpha) (3\mathfrak{q} - l) \right]$$

$$+ \frac{3}{8} \bar{\rho}_m \bar{\mu}_m H \frac{\partial \ln c_s^2}{\partial \bar{\mu}_m} \left(\mathfrak{q} - \frac{l}{2} \right) (\bar{u}^\alpha \phi_\alpha),$$

$$a_\mu^m = \frac{1}{2} \bar{\rho}_m (\bar{u}^\alpha A_\alpha) \phi_\mu \quad (249)$$

$$+ \frac{1}{8} \bar{\rho}_m \left(1 - \frac{c^2}{c_s^2} \right) \left[l_\mu{}^\alpha \bar{u}^\beta \phi_{\alpha\beta} - \mathfrak{q} \bar{u}^\alpha \phi_{\mu\alpha} + (\bar{u}^\alpha \mathfrak{q}_\alpha) \phi_\mu + (\bar{u}^\alpha \phi_\alpha) A_\mu \right]$$

$$- 2 \bar{\rho}_m H \left(2\mathfrak{q} - \frac{1}{2} l \right) \phi_\mu$$

$$+ \frac{1}{2} \bar{\rho}_m H \left(1 - \frac{c^2}{c_s^2} \right) \left[(\bar{u}^\alpha \phi_\alpha) l_{\mu\beta} \bar{u}^\beta - \frac{1}{4} \mathfrak{q} \phi_\mu + \frac{1}{4} l_\mu{}^\alpha \phi_\alpha \right]$$

$$+ \frac{3}{8} \bar{\rho}_m \bar{\mu}_m H \frac{\partial \ln c_s^2}{\partial \bar{\mu}_m} [(\bar{u}^\alpha \phi_\alpha) l_\mu{}^\alpha \bar{u}_\alpha - \mathfrak{q} \phi_\mu].$$

6.2.3 Dark Energy

The dark energy source, $\Sigma^{\mathfrak{q}}$, depends not only on the derivatives of the scalar field $\bar{\Psi}$ but on the field itself through the field potential $W = W(\Phi)$. Therefore, according to definition (102)

$$\Sigma^q = \frac{1}{16\pi\sqrt{-\bar{g}}} \left[-\frac{\partial \mathcal{F}^q}{\partial \bar{\Psi}} + \left(\frac{\partial \mathcal{F}^q}{\partial \bar{\Psi}_\nu} \right)_{|\nu} \right]. \quad (250)$$

After taking the variational derivatives we obtain

$$\begin{aligned} \Sigma^q = & \frac{1}{2} \psi^2 \frac{\partial^3 \bar{W}}{\partial \bar{\Psi}^3} + \frac{3}{4} l \psi \frac{\partial^2 \bar{W}}{\partial \bar{\Psi}^2} - \frac{1}{2} \frac{\partial \bar{W}}{\partial \bar{\Psi}} \left(l^{\alpha\beta} l_{\alpha\beta} - \frac{1}{2} l^2 \right) \\ & + \frac{3}{2} \left(l^{\alpha\beta} {}_{|\gamma} \psi_a \bar{u}_\beta \bar{u}^{\gamma} + l^{\alpha\beta} \psi_{\alpha\gamma} \bar{u}_\beta \bar{u}^{\gamma} + 3H l^{\alpha\beta} \bar{u}_\alpha \psi_\beta \right). \end{aligned} \quad (251)$$

The force caused by dark energy on the motion of the matter of the bare perturbation is

$$\begin{aligned} f_\mu^q \equiv & -\tau_{\mu\nu}^q{}^{|\nu} + \frac{1}{8\pi} \left(l^\rho{}_\nu F_{\rho\mu}^q - \frac{1}{2} l_{\mu\nu} F^q \right)^{|\nu} \\ & - \frac{1}{16\pi} \left(l^{\rho\sigma} F_{\rho\sigma|\mu}^q - \frac{1}{2} l F^q{}_{|\mu} \right) + \frac{1}{2} \bar{\mu}_q \Sigma^q \bar{u}_\mu, \end{aligned} \quad (252)$$

After long but straightforward calculation we get

$$\begin{aligned} f_\mu^q = & \bar{\rho}_q \bar{u}_\mu \\ & \times \left(l^{\alpha\beta} \psi_{\alpha\beta} + \frac{3}{4} l^{\alpha\beta} {}_{|\gamma} \psi_\alpha \bar{u}_\beta \bar{u}^{\gamma} + \frac{3}{4} l^{\alpha\beta} \psi_{\alpha\gamma} \bar{u}_\beta \bar{u}^{\gamma} + \frac{9}{4} H l^{\alpha\beta} \bar{u}_\alpha \psi_\beta \right) \\ & + (A^\alpha \psi_\alpha) \bar{u}_\mu + \frac{1}{2} (A^\alpha \bar{u}_\alpha) \psi_\mu + \bar{\rho}_q H \left(2q - \frac{1}{2} l \right) \psi_\mu \\ & - \frac{1}{4} \frac{\partial \bar{W}}{\partial \bar{\Psi}} (\psi A_\mu + l_\mu{}^\nu \psi_\nu - 2q \psi_\mu) + \frac{1}{4} \bar{\rho}_q \psi \frac{\partial^2 \bar{W}}{\partial \bar{\Psi}^2} \left(l_{\mu\nu} \bar{u}^\nu - \frac{1}{2} l \bar{u}_\mu \right). \end{aligned} \quad (253)$$

6.3 Final Form of the Equations of Motion

After making use of the results of the presiding section, equations of motion (230) take on the following form

$$\begin{aligned} \mathfrak{T}_\mu{}^\nu{}_{|\nu} + l^{\rho\nu} \left(\mathfrak{T}_{\rho\mu|\nu} - \frac{1}{2} \mathfrak{T}_{\rho\nu|\mu} \right) - \frac{1}{2} \left(l_\mu{}^\nu - \frac{l}{2} \delta_\mu{}^\nu \right) \mathfrak{T}_{|\nu} \\ + A^\rho \mathfrak{T}_{\rho\mu} - \frac{1}{2} A_\mu \mathfrak{T} = f_\mu^m + f_\mu^q. \end{aligned} \quad (254)$$

The left side of this equation can be brought to a more conventional form if we use relation (93) between the stress-energy tensor of the bare perturbation $T_{\mu\nu}$ and $\mathfrak{T}_{\mu\nu}$.

Let us take a covariant divergence of $T_{\mu\nu}$ with respect to the full metric $g_{\mu\nu}$ that is $\nabla_\nu T_\mu{}^\nu \equiv g^{\nu\rho} \nabla_\nu T_{\rho\mu}$ where ∇_ν denotes a covariant derivative with the connection

referred to the full metric so that $\nabla_\alpha g_{\beta\gamma} \equiv 0$. The covariant derivatives from the stress-energy tensor $\mathfrak{T}_{\mu\nu}$ are calculated with the help of

$$\nabla_\alpha \mathfrak{T}_{\mu\nu} = \mathfrak{T}_{\mu\nu|\alpha} - \mathfrak{G}_{\alpha\mu}^\beta \mathfrak{T}_{\nu\beta} - \mathfrak{G}_{\alpha\nu}^\beta \mathfrak{T}_{\mu\beta}, \quad (255)$$

where $\mathfrak{G}_{\alpha\mu}^\beta \equiv \Gamma_{\alpha\mu}^\beta - \bar{\Gamma}_{\alpha\mu}^\beta$ is a tensor describing the difference between the perturbed and unperturbed values of the Christoffel symbols which we shall call the Christoffel tensor. In terms of the metric tensor perturbations

$$\mathfrak{G}_{\alpha\mu}^\beta = \frac{1}{2} g^{\beta\gamma} (\mathfrak{K}_{\gamma\alpha|\mu} + \mathfrak{K}_{\gamma\mu|\alpha} - \mathfrak{K}_{\alpha\mu|\gamma}). \quad (256)$$

Equation (256) is exact. In the linear approximation with respect to the $l_{\mu\nu}$ it can be expressed in terms of the background metric and perturbations $l_{\mu\nu}$ as follows

$$\mathfrak{G}_{\alpha\mu}^\beta = -\frac{1}{2} \bar{g}^{\beta\gamma} (l_{\gamma\alpha|\mu} + l_{\gamma\mu|\alpha} - l_{\alpha\mu|\gamma}) + \frac{1}{4} (\delta_\alpha^\beta l_{|\mu} + \delta_\mu^\beta l_{|\alpha} - \bar{g}_{\alpha\mu} l^{|\beta}), \quad (257)$$

where all quadratic terms with respect to $l_{\mu\nu}$ have been neglected. Two contracted values of the Christoffel tensor are

$$\mathfrak{G}_\alpha \equiv \mathfrak{G}_{\alpha\beta}^\beta = \frac{1}{2} l_{|\alpha}, \quad \bar{g}^{\alpha\beta} \mathfrak{G}_{\alpha\beta}^\gamma = -l^{\gamma\beta}_{|\beta} = -A^\gamma, \quad (258)$$

Making use of these notations and definitions and doing direct calculation allows us to show that

$$\begin{aligned} \nabla_\nu T_\mu{}^\nu &= \mathfrak{T}_\mu{}^\nu{}_{|\nu} + l^{\rho\nu} \left(\mathfrak{T}_{\rho\mu|\nu} - \frac{1}{2} \mathfrak{T}_{\rho\nu|\mu} \right) \\ &\quad - \frac{1}{2} \left(l_\mu{}^\nu - \frac{l}{2} \delta_\mu{}^\nu \right) \mathfrak{T}_{|\nu} + A^\rho \mathfrak{T}_{\rho\mu} - \frac{1}{2} A_\mu \mathfrak{T}. \end{aligned} \quad (259)$$

Hydrodynamic equation of motion (254) becomes

$$\nabla_\nu T_\mu{}^\nu = f_\mu^{\text{m}} + f_\mu^{\text{q}}. \quad (260)$$

Were the background spacetime flat, the right side of (260) would vanish. However, in cosmology the background spacetime is given by FLRW metric, thus, making the divergence of the stress-energy-momentum tensor of the bare perturbation different from zero. The reader should not be confused here. Equation (260) is the law of conservation of the total stress-energy-momentum tensor given in the form, in which the covariant divergence of the stress-energy-momentum tensor of the bare perturbation is singled out and put to the left side. The right side represents the covariant divergence of the stress-energy-momentum tensor of the background matter in the disguised form of the sum of two vectors, f_μ^{m} and f_μ^{q} .

Acknowledgments Sergei Kopeikin thanks the Center of Applied Space Technology and Microgravity (ZARM) of the University of Bremen for providing partial financial support for travel and Physikzentrum at Bad Honnef (Germany) for hospitality and accommodation. The work of Sergei Kopeikin has been supported by the grant 14-27-00068 of the Russian Scientific foundation.

Appendix 1: Hilbert and Einstein Lagrangians

We define the Christoffel symbols of the second kind as usual [46]

$$\Gamma^\alpha{}_{\beta\gamma} \equiv \frac{1}{2} g^{\alpha\delta} (g_{\delta\beta,\gamma} + g_{\delta\gamma,\beta} - g_{\beta\gamma,\delta}). \quad (261)$$

The Christoffel symbols of the first type

$$\Gamma_{\alpha\beta\gamma} = g_{\alpha\sigma} \Gamma^\sigma{}_{\beta\gamma} = \frac{1}{2} (g_{\alpha\beta,\gamma} + g_{\alpha\gamma,\beta} - g_{\beta\gamma,\alpha}), \quad (262)$$

We notice the symmetry with respect to the last two indices $\Gamma_{\alpha\beta\gamma} = \Gamma_{\alpha(\beta\gamma)}$. There is no any symmetry with respect to the first two indices. In general,

$$\Gamma_{\alpha\beta\gamma} = \Gamma_{(\alpha\beta)\gamma} + \Gamma_{[\alpha\beta]\gamma}, \quad (263)$$

where

$$\Gamma_{(\alpha\beta)\gamma} = \frac{1}{2} g_{\alpha\beta,\gamma}, \quad \Gamma_{[\alpha\beta]\gamma} = \frac{1}{2} (g_{\gamma\alpha,\beta} - g_{\gamma\beta,\alpha}), \quad (264)$$

There are two, particularly useful symbols that are obtained by contracting indices of the Christoffel symbols of the first kind. They are denoted as

$$\mathcal{Y}_\alpha \equiv \Gamma^\beta{}_{\alpha\beta}, \quad \mathcal{Y}^\alpha = g^{\alpha\beta} \mathcal{Y}_\beta, \quad (265)$$

and

$$\Gamma^\alpha \equiv g^{\beta\gamma} \Gamma^\alpha{}_{\beta\gamma}, \quad \Gamma_\alpha = g_{\alpha\beta} \Gamma^\beta, \quad (266)$$

Direct inspection shows that

$$\mathcal{Y}_\alpha = -\frac{1}{2} g^{\beta\gamma} g_{\beta\gamma,\alpha} = (\ln \sqrt{-g})_{,\alpha}. \quad (267)$$

The two symbols are interrelated

$$\Gamma_\alpha = -\mathcal{Y}_\alpha + g^{\beta\gamma} g_{\alpha\beta,\gamma}, \quad (268)$$

$$\Gamma^\alpha = -\mathcal{Y}^\alpha - g^{\alpha\beta}{}_{,\beta}, \quad (269)$$

We define the Riemann tensor as follows [46]

$$R^\alpha{}_{\mu\beta\nu} = \Gamma^\alpha{}_{\mu\nu,\beta} - \Gamma^\alpha{}_{\mu\beta,\nu} + \Gamma^\alpha{}_{\beta\gamma}\Gamma^\gamma{}_{\mu\nu} - \Gamma^\alpha{}_{\nu\gamma}\Gamma^\gamma{}_{\mu\beta}. \quad (270)$$

Second covariant derivatives of tensors do not commute due to the curvature of spacetime. For example, denoting the covariant derivatives with a vertical bar we have for a covector field \mathcal{F}_α and a covariant tensor of second rank, $\mathcal{F}_{\alpha\beta}$ the following commutation relations

$$\mathcal{F}_{\alpha|\beta\gamma} = \mathcal{F}_{\alpha|\gamma\beta} + R^\mu{}_{\alpha\beta\gamma}\mathcal{F}_\mu, \quad (271)$$

$$\mathcal{F}_{\alpha\beta|\gamma\delta} = \mathcal{F}_{\alpha\beta|\delta\gamma} + R^\mu{}_{\alpha\gamma\delta}\mathcal{F}_{\mu\beta} + R^\mu{}_{\beta\gamma\delta}\mathcal{F}_{\alpha\mu}. \quad (272)$$

Riemann tensor can be also expressed in terms of the second partial derivatives of the metric tensor and the Christoffel symbols

$$R_{\alpha\mu\beta\nu} = \frac{1}{2} (g_{\mu\beta,\alpha\nu} + g_{\nu\alpha,\beta\mu} - g_{\alpha\beta,\mu\nu} - g_{\mu\nu,\alpha\beta}) + \Gamma_{\rho\mu\beta}\Gamma^\rho{}_{\alpha\nu} - \Gamma_{\rho\mu\nu}\Gamma^\rho{}_{\alpha\beta}. \quad (273)$$

Contraction of two indices in the Riemann tensor yields the Ricci tensor

$$R_{\mu\nu} = \Gamma^\alpha{}_{\mu\nu,\alpha} - \mathcal{Y}_{\mu,\nu} + \mathcal{Y}_\gamma\Gamma^\gamma{}_{\mu\nu} - \Gamma^\alpha{}_{\nu\gamma}\Gamma^\gamma{}_{\mu\alpha}, \quad (274)$$

or, in terms of the second derivatives from the metric tensor and the Christoffel symbols,

$$R_{\mu\nu} = \frac{1}{2} g^{\kappa\epsilon} (g_{\mu\kappa,\epsilon\nu} + g_{\nu\kappa,\epsilon\mu} - g_{\kappa\epsilon,\mu\nu} - g_{\mu\nu,\kappa\epsilon}) + g^{\kappa\epsilon}\Gamma_{\rho\mu\epsilon}\Gamma^\rho{}_{\kappa\nu} - \Gamma_{\rho\mu\nu}\Gamma^\rho{}_{\kappa\epsilon}. \quad (275)$$

One more contraction of indices in the Ricci tensor brings about the Ricci scalar which we shall write down in the form suggested by Fock [14, Appendix B]

$$R = L + \mathcal{Y}_\alpha\Gamma^\alpha - \mathcal{Y}_\alpha\mathcal{Y}^\alpha + \Gamma^\alpha{}_{,\alpha} - \mathcal{Y}^\alpha{}_{,\alpha}, \quad (276)$$

where

$$L = g^{\mu\nu} (\Gamma^\alpha{}_{\nu\gamma}\Gamma^\gamma{}_{\mu\alpha} - \mathcal{Y}_\alpha\Gamma^\alpha{}_{\mu\nu}), \quad (277)$$

is (up to a constant factor) the gravitational Lagrangian introduced by Einstein [79] as an alternative to the gravitational Lagrangian, R , of Hilbert. The Hilbert Lagrangian is the Ricci scalar which depends on the second derivatives of the metric tensor while the Einstein Lagrangian does not.

The two Lagrangians are interrelated

$$R = L + (-g)^{-1/2} \mathcal{A}^\alpha{}_{,\alpha}, \quad (278)$$

where

$$\mathcal{A}^\alpha = \sqrt{-g} (\Gamma^\alpha - \mathcal{Y}^\alpha), \quad (279)$$

is a vector density of weight +1. After performing differentiation in (278), and accounting for (265) we can easily prove that (278) reproduces (276).

One more form of relation between R and L will be useful for calculating the variational derivative in Appendix section “Variational Derivative from the Hilbert Lagrangian”. To this end we introduce a new notation

$$\Gamma \equiv \Gamma^\alpha_{,\alpha} + \mathcal{Y}_\alpha \Gamma^\alpha, \quad (280)$$

and notice that

$$g^{\alpha\beta} \mathcal{Y}_{\alpha,\beta} = \mathcal{Y}^\alpha_{,\alpha} + \mathcal{Y}_\alpha \Gamma^\alpha + \mathcal{Y}_\alpha \mathcal{Y}^\alpha, \quad (281)$$

Equations (280), (281) allows us to cast (276) to the following form

$$R = L + \Gamma + \mathcal{Y}_\alpha \Gamma^\alpha - g^{\alpha\beta} \mathcal{Y}_{\alpha,\beta}, \quad (282)$$

that was found by Fock [14, Appendix B].

Appendix 2: Variational Derivatives

Variational Derivative from the Hilbert Lagrangian

The goal of this section is to prove relation (45) being valid on the background manifold $\bar{\mathcal{M}}$. We shall omit the bar over the background geometric objects as it does not bring about confusion. We notice that the Hilbert Lagrangian density, $\mathcal{L}^G = -(16\pi)^{-1} \sqrt{-g} R$, differs from $\mathcal{L}^E = -(16\pi)^{-1} \sqrt{-g} L$ by a total derivative that is a consequence of (278). Due to relation (9) the Lagrangian derivatives from \mathcal{L}^G and \mathcal{L}^E coincides

$$\frac{\delta \mathcal{L}^G}{\delta g^{\mu\nu}} = \frac{\delta \mathcal{L}^E}{\delta g^{\mu\nu}}, \quad (283)$$

thus, pointing out that we can safely operate with the Einstein Lagrangian density \mathcal{L}^E . Because of (35), we have

$$\frac{\delta \mathcal{L}^E}{\delta g^{\mu\nu}} = \frac{1}{\sqrt{-g}} A^{\rho\sigma}_{\mu\nu} \frac{\delta \mathcal{L}^E}{\delta g^{\rho\sigma}}, \quad (284)$$

which suggests that calculation of the variational derivative with respect to the metric tensor is sufficient.

Calculation of the variational derivative $\delta \mathcal{L}^E / \delta g^{\rho\sigma}$ demands the partial derivatives of the contravariant metric and Christoffel symbols with respect to $g^{\mu\nu}$. The partial

derivatives of the metric are calculated with the help of (37), (30). The Christoffel symbols are given in terms of the partial derivatives from covariant metric tensor, $g_{\alpha\beta,\gamma}$ which are not conjugated with the dynamic variable $g^{\alpha\beta}$. Thus, calculation of the partial derivative with respect to $g^{\mu\nu}$ from the Christoffel symbols demands its transformation to the form where the conjugated variables $g^{\alpha\beta}_{,\gamma}$ are used instead. This form of the Christoffel symbols is

$$\Gamma^\alpha{}_{\beta\gamma} = \frac{1}{2} (g^{\rho\kappa}{}_{,\sigma} g^{\alpha\sigma} g_{\rho\beta} g_{\kappa\gamma} - g^{\alpha\sigma}{}_{,\beta} g_{\gamma\sigma} - g^{\alpha\sigma}{}_{,\gamma} g_{\beta\sigma}). \quad (285)$$

Taking the partial derivative of (285) with respect to the contravariant metric yields

$$\frac{\partial \Gamma^\alpha{}_{\beta\gamma}}{\partial g^{\mu\nu}} = -g^{\alpha\sigma} \{ \Gamma_{[\sigma\beta](\mu} g_{\nu)\gamma} + \Gamma_{[\sigma\gamma](\mu} g_{\nu)\beta} + \Gamma_{(\beta\gamma)(\mu} g_{\nu)\sigma} \}, \quad (286)$$

and

$$\frac{\partial \mathcal{Y}_\alpha}{\partial g^{\mu\nu}} = -\Gamma_{(\mu\nu)\alpha}, \quad (287)$$

where we have used (263). Contracting (286), (287) with the Christoffel symbols and the metric tensor results in

$$g^{\sigma\gamma} \frac{\partial \Gamma^\alpha{}_{\beta\gamma}}{\partial g^{\mu\nu}} \Gamma^\beta{}_{\sigma\alpha} = -2\Gamma^\alpha{}_{\beta\mu} \Gamma^\beta{}_{\nu\alpha}, \quad (288)$$

$$g^{\sigma\gamma} \frac{\partial \mathcal{Y}_\beta}{\partial g^{\mu\nu}} \Gamma^\beta{}_{\sigma\gamma} = -\Gamma_{(\mu\nu)\alpha} \Gamma^\alpha, \quad (289)$$

$$g^{\sigma\gamma} \frac{\partial \Gamma^\beta{}_{\sigma\gamma}}{\partial g^{\mu\nu}} \mathcal{Y}_\beta = \Gamma_{(\mu\nu)\alpha} \mathcal{Y}^\alpha - \Gamma_{\alpha\mu\nu} \mathcal{Y}^\alpha - \mathcal{Y}_\mu \mathcal{Y}_\nu. \quad (290)$$

Partial derivatives of the Christoffel symbols with respect to the metric derivatives are calculated from (285) with the help of (38). We get

$$\frac{\partial \Gamma^\alpha{}_{\beta\gamma}}{\partial g^{\mu\nu}{}_{,\rho}} = \frac{1}{2} \left[g^{\rho\alpha} g_{\beta(\mu} g_{\nu)\gamma} - \delta^\rho_\gamma \delta^\alpha_{(\mu} g_{\nu)\beta} - \delta^\rho_\beta \delta^\alpha_{(\mu} g_{\nu)\gamma} \right], \quad (291)$$

$$\frac{\partial \mathcal{Y}_\beta}{\partial g^{\mu\nu}{}_{,\rho}} = -\frac{1}{2} g_{\mu\nu} \delta^\rho_\beta. \quad (292)$$

Contracting (291), (292) with the Christoffel symbols and the metric tensor results in

$$g^{\sigma\gamma} \frac{\partial \Gamma^{\alpha}{}_{\beta\gamma}}{\partial g^{\mu\nu}{}_{,\rho}} \Gamma^{\beta}{}_{\sigma\alpha} = -\frac{1}{2} \Gamma^{\rho}{}_{\mu\nu}, \quad (293)$$

$$g^{\sigma\gamma} \frac{\partial \mathcal{Y}_{\beta}}{\partial g^{\mu\nu}{}_{,\rho}} \Gamma^{\beta}{}_{\sigma\gamma} = -\frac{1}{2} g_{\mu\nu} \Gamma^{\rho}, \quad (294)$$

$$g^{\sigma\gamma} \frac{\partial \Gamma^{\beta}{}_{\sigma\gamma}}{\partial g^{\mu\nu}{}_{,\rho}} \mathcal{Y}_{\beta} = \frac{1}{2} g_{\mu\nu} \mathcal{Y}^{\rho} - \delta^{\rho}{}_{(\mu} \mathcal{Y}_{\nu)}. \quad (295)$$

Explicit expression for the variational derivative of the Einstein Lagrangian is

$$\begin{aligned} -16\pi \frac{\delta \mathcal{L}^E}{\delta g^{\mu\nu}} = & \left(\frac{\partial \sqrt{-g}}{\partial g^{\mu\nu}} g^{\sigma\gamma} + \sqrt{-g} \frac{\partial g^{\sigma\gamma}}{\partial g^{\mu\nu}} \right) \left(\Gamma^{\alpha}{}_{\beta\gamma} \Gamma^{\beta}{}_{\sigma\alpha} - \mathcal{Y}_{\beta} \Gamma^{\beta}{}_{\sigma\gamma} \right) \\ & + \sqrt{-g} g^{\sigma\gamma} \left(2 \frac{\partial \Gamma^{\alpha}{}_{\beta\gamma}}{\partial g^{\mu\nu}} \Gamma^{\beta}{}_{\sigma\alpha} - \frac{\partial \mathcal{Y}_{\beta}}{\partial g^{\mu\nu}} \Gamma^{\beta}{}_{\sigma\gamma} - \frac{\partial \Gamma^{\beta}{}_{\sigma\gamma}}{\partial g^{\mu\nu}} \mathcal{Y}_{\beta} \right) \\ & - \frac{\partial}{\partial x^{\rho}} \left[\sqrt{-g} g^{\sigma\gamma} \left(2 \frac{\partial \Gamma^{\alpha}{}_{\beta\gamma}}{\partial g^{\mu\nu}{}_{,\rho}} \Gamma^{\beta}{}_{\sigma\alpha} - \frac{\partial \mathcal{Y}_{\beta}}{\partial g^{\mu\nu}{}_{,\rho}} \Gamma^{\beta}{}_{\sigma\gamma} - \frac{\partial \Gamma^{\beta}{}_{\sigma\gamma}}{\partial g^{\mu\nu}{}_{,\rho}} \mathcal{Y}_{\beta} \right) \right] \end{aligned} \quad (296)$$

Replacing the partial derivatives in (296) with the corresponding right sides of Eqs.(37), (30), (293)–(295) and taking the partial derivative with respect to spatial coordinates, yields

$$-16\pi \frac{\delta \mathcal{L}^E}{\delta g^{\mu\nu}} = \sqrt{-g} \left(R_{\mu\nu} - \frac{1}{2} g_{\mu\nu} R \right), \quad (297)$$

where we have used expressions (274), (276) for the Ricci tensor and Ricci scalar respectively. Substituting Eq.(297) to (284) yields

$$\frac{\delta \mathcal{L}^E}{\delta g^{\mu\nu}} = -\frac{1}{16\pi} R_{\mu\nu}. \quad (298)$$

Variational Derivatives of Dynamic Variables with Respect to the Metric Tensor

Variational Derivatives of Dark Matter Variables

The primary thermodynamic variable of dark matter is μ_m defined in (125). Variational derivative from μ_m is calculated directly from its definition and yields

$$\frac{\delta \bar{\mu}_m}{\delta \bar{g}_{\mu\nu}} = \frac{1}{2} \bar{\mu}_m \bar{u}^{\mu} \bar{u}^{\nu}. \quad (299)$$

Variational derivative of pressure \bar{p}_m is obtained from thermodynamic relation (121a) by making use of the chain differentiation rule along with (299), that is

$$\frac{\delta \bar{p}_m}{\delta \bar{g}_{\mu\nu}} = \frac{1}{2} \bar{\rho}_m \bar{\mu}_m \bar{u}^\mu \bar{u}^\nu. \quad (300)$$

Variational derivative of the rest mass and energy density are obtained by making use of (299) along with equation of state that allows us to express partial derivatives of ρ_m and ϵ_m in terms of the variational derivative for μ_m . More specifically,

$$\frac{\delta \bar{\rho}_m}{\delta \bar{g}_{\mu\nu}} = \frac{1}{2} \frac{c^2}{c_s^2} \bar{\rho}_m \bar{u}^\mu \bar{u}^\nu, \quad (301)$$

$$\frac{\delta \bar{\epsilon}_m}{\delta \bar{g}_{\mu\nu}} = \frac{1}{2} \frac{c^2}{c_s^2} \bar{\rho}_m \bar{\mu}_m \bar{u}^\mu \bar{u}^\nu \quad (302)$$

where the speed of sound appears explicitly. Variational derivatives from products and/or ratios of the thermodynamic quantities are calculated by applying the chain rule of differentiation and the above equations,

$$\frac{\delta (\bar{\rho}_m \bar{\mu}_m)}{\delta \bar{g}_{\mu\nu}} = \frac{1}{2} \left(1 + \frac{c^2}{c_s^2} \right) \bar{\rho}_m \bar{\mu}_m \bar{u}^\mu \bar{u}^\nu, \quad (303)$$

$$\frac{\delta}{\delta \bar{g}_{\mu\nu}} \left(\frac{\bar{\rho}_m}{\bar{\mu}_m} \right) = -\frac{1}{2} \left(1 - \frac{c^2}{c_s^2} \right) \frac{\bar{\rho}_m}{\bar{\mu}_m} \bar{u}^\mu \bar{u}^\nu, \quad (304)$$

$$\frac{\delta (\bar{p}_m - \bar{\epsilon}_m)}{\delta \bar{g}_{\mu\nu}} = \frac{1}{2} \left(1 - \frac{c^2}{c_s^2} \right) \bar{\rho}_m \bar{\mu}_m \bar{u}^\mu \bar{u}^\nu. \quad (305)$$

Variational Derivatives of Dark Energy Variables

The primary thermodynamic variable of dark energy is $\bar{\mu}_q$ defined in (125). Variational derivative from $\bar{\mu}_q$ is calculated directly from its definition,

$$\frac{\delta \bar{\mu}_q}{\delta \bar{g}_{\mu\nu}} = \frac{1}{2} \bar{\mu}_q \bar{u}^\mu \bar{u}^\nu. \quad (306)$$

Variational derivative of the mass density $\bar{\rho}_q$ of the dark energy “fluid” follows directly from $\bar{\rho}_q = \bar{\mu}_q$, and reads

$$\frac{\delta \bar{\rho}_q}{\delta \bar{g}_{\mu\nu}} = \frac{1}{2} \bar{\rho}_q \bar{u}^\mu \bar{u}^\nu. \quad (307)$$

Variational derivative of pressure \bar{p}_q is obtained from definition (138) along with (306), which yields

$$\frac{\delta \bar{p}_q}{\delta \bar{g}_{\mu\nu}} = \frac{1}{2} \bar{\rho}_q \bar{\mu}_q \bar{u}^\mu \bar{u}^\nu. \quad (308)$$

Variational derivative of energy density $\bar{\epsilon}_q$ is obtained by making use of (306) along with (137). More specifically,

$$\frac{\delta \bar{\epsilon}_q}{\delta \bar{g}_{\mu\nu}} = \frac{1}{2} \bar{\rho}_q \bar{\mu}_q \bar{u}^\mu \bar{u}^\nu. \quad (309)$$

Variational derivatives from products and ratios of other quantities are calculated by making use of the chain rule of differentiation and the above equations

$$\frac{\delta (\bar{\rho}_q \bar{\mu}_q)}{\delta \bar{g}_{\mu\nu}} = \bar{\rho}_q \bar{\mu}_q \bar{u}^\mu \bar{u}^\nu, \quad (310)$$

$$\frac{\delta}{\delta \bar{g}_{\mu\nu}} \left(\frac{\bar{\rho}_q}{\bar{\mu}_q} \right) = 0, \quad (311)$$

$$\frac{\delta (\bar{\rho}_q - \bar{\epsilon}_q)}{\delta \bar{g}_{\mu\nu}} = 0. \quad (312)$$

Variational Derivatives of Four-Velocity of the Hubble Flow

Variational derivatives from four-velocity of the fluid are derived from the definition (163) of the four-velocity given in terms of the potential Φ or Ψ which are independent dynamic variables that do not depend on the metric tensor. Taking variational derivative from (163) and making use either (299) or (306) we obtain

$$\frac{\delta \bar{u}_\alpha}{\delta \bar{g}_{\mu\nu}} = -\frac{1}{2} \bar{u}_\alpha \bar{u}^\mu \bar{u}^\nu, \quad (313)$$

$$\frac{\delta \bar{u}^\alpha}{\delta \bar{g}_{\mu\nu}} = -\frac{1}{2} \bar{u}^\alpha \bar{u}^\mu \bar{u}^\nu - \bar{g}^{\alpha(\mu} \bar{u}^{\nu)}, \quad (314)$$

$$\frac{\delta (\bar{u}^\alpha \phi_\alpha)}{\delta \bar{g}_{\mu\nu}} = -\phi^{(\mu} \bar{u}^{\nu)} - \frac{1}{2} \bar{u}^\mu \bar{u}^\nu (\bar{u}^\alpha \phi_\alpha), \quad (315)$$

where Eq. (315) accounts for the fact that ϕ_α is an independent variable that does not depend on the metric tensor.

Variational Derivatives of the Metric Tensor Perturbations

Variational derivatives from the metric tensor perturbations $l^{\alpha\beta}$ are determined by taking into account that $l^{\alpha\beta} = \mathfrak{h}^{\alpha\beta} / \sqrt{\bar{g}}$ and $\mathfrak{h}^{\alpha\beta}$ is an independent dynamic variable which does not depend on the metric tensor. Therefore, its variational derivative is nil, and we have

$$\frac{\delta l^{\alpha\beta}}{\delta \bar{g}_{\mu\nu}} = \frac{\delta}{\delta \bar{g}_{\mu\nu}} \left(\frac{\mathfrak{h}^{\alpha\beta}}{\sqrt{\bar{g}}} \right) = \mathfrak{h}^{\alpha\beta} \frac{\delta}{\delta \bar{g}_{\mu\nu}} \left(\frac{1}{\sqrt{\bar{g}}} \right) = -\frac{1}{2} l^{\alpha\beta} \bar{g}^{\mu\nu}. \quad (316)$$

Other variational derivatives are derived by making use of tensor operations of rising and lowering indices with the help of $\bar{g}_{\alpha\beta}$ and applying from (316). It gives

$$\frac{\delta l_{\alpha\beta}}{\delta \bar{g}_{\mu\nu}} = -\frac{1}{2} l_{\alpha\beta} \bar{g}^{\mu\nu} + 2l_{\alpha}^{(\mu} \delta_{\beta}^{\nu)}, \quad (317)$$

$$\frac{\delta l}{\delta \bar{g}_{\mu\nu}} = l^{\mu\nu} - \frac{1}{2} l \bar{g}^{\mu\nu}, \quad (318)$$

$$\frac{\delta \mathfrak{q}}{\delta \bar{g}_{\mu\nu}} = -\mathfrak{q} \left(\bar{u}^{\mu} \bar{u}^{\nu} + \frac{1}{2} \bar{g}^{\mu\nu} \right) + \frac{1}{2} (l^{\mu\nu} + l \bar{u}^{\mu} \bar{u}^{\nu}), \quad (319)$$

$$\frac{\delta}{\delta \bar{g}_{\mu\nu}} \left(l^{\alpha\beta} l_{\alpha\beta} - \frac{l^2}{2} \right) = 2l^{\alpha(\mu} l^{\nu)}_{\alpha} - l l^{\mu\nu} - \bar{g}^{\mu\nu} \left(l^{\alpha\beta} l_{\alpha\beta} - \frac{l^2}{2} \right). \quad (320)$$

Variational Derivatives with Respect to Matter Variables

Variational Derivatives of Dark Matter Variables

The dark matter variables do not depend on the Clebsch potential $\bar{\Phi}$ directly but merely on its first derivative $\bar{\Phi}_{\alpha}$. Therefore, any variational derivative of dark matter variable, say, $\mathcal{Q} = \mathcal{Q}(\bar{\Phi}_{\alpha})$, is reduced to a total divergence

$$\frac{\delta \mathcal{Q}}{\delta \bar{\Phi}} = -\frac{\partial}{\partial x^{\alpha}} \frac{\partial \mathcal{Q}}{\partial \bar{\Phi}_{\alpha}}. \quad (321)$$

We present a short summary of the partial derivatives with respect to $\bar{\Phi}_{\alpha}$.

$$\frac{\partial \bar{\mu}_{\text{m}}}{\partial \bar{\Phi}_{\alpha}} = \bar{u}^{\alpha}, \quad (322)$$

$$\frac{\partial \bar{\rho}_{\text{m}}}{\partial \bar{\Phi}_{\alpha}} = \bar{\rho}_{\text{m}} \bar{u}^{\alpha}, \quad (323)$$

$$\frac{\partial \bar{\rho}_{\text{m}}}{\partial \bar{\Phi}_{\alpha}} = \frac{c^2}{c_s^2} \frac{\bar{\rho}_{\text{m}}}{\bar{\mu}_{\text{m}}} \bar{u}^{\alpha}, \quad (324)$$

$$\frac{\partial \bar{\epsilon}_{\text{m}}}{\partial \bar{\Phi}_{\alpha}} = \frac{c^2}{c_s^2} \bar{\rho}_{\text{m}} \bar{u}^{\alpha}, \quad (325)$$

$$\frac{\partial (\bar{\rho}_{\text{m}} \bar{\mu}_{\text{m}})}{\partial \bar{\Phi}_{\alpha}} = \left(1 + \frac{c^2}{c_s^2} \right) \bar{\rho}_{\text{m}} \bar{u}^{\alpha}, \quad (326)$$

$$\frac{\partial}{\partial \bar{\Phi}_\alpha} \left(\frac{\bar{\rho}_m}{\bar{\mu}_m} \right) = - \left(1 - \frac{c^2}{c_s^2} \right) \frac{\bar{\rho}_m}{\bar{\mu}_m^2} \bar{u}^\alpha, \quad (327)$$

$$\frac{\partial (\bar{\rho}_m - \bar{\epsilon}_m)}{\partial \bar{\Phi}_\alpha} = + \left(1 - \frac{c^2}{c_s^2} \right) \bar{\rho}_m \bar{u}^\alpha. \quad (328)$$

Partial derivatives of four velocity

$$\frac{\partial \bar{u}_\alpha}{\partial \bar{\Phi}_\beta} = - \frac{\bar{P}_\alpha^\beta}{\bar{\mu}_m}, \quad \frac{\partial \bar{u}^\alpha}{\partial \bar{\Phi}_\beta} = - \frac{\bar{P}^{\alpha\beta}}{\bar{\mu}_m}. \quad (329)$$

It allows us to deduce, for example,

$$\frac{\partial (\bar{u}^\alpha \phi_\alpha)}{\partial \bar{\Phi}_\beta} = - \frac{1}{\bar{\mu}_m} \bar{P}^{\alpha\beta} \phi_\beta, \quad (330)$$

$$\frac{\partial \bar{q}}{\partial \bar{\Phi}_\alpha} = - \frac{2}{\bar{\mu}_m} \bar{P}^\alpha_{\mu} l^{\mu\nu} \bar{u}_\nu. \quad (331)$$

Variational Derivatives of Dark Energy Variables

The dark energy variables depend on both the scalar potential $\bar{\Psi}$ and its first derivative $\bar{\Psi}_\alpha$ in the most generic situation. This is because there is a potential of the scalar field $W(\bar{\Phi})$ that is absent in case of the dark matter. Therefore, variational derivative of the dark energy variable, say, $\mathcal{A} = \mathcal{A}(\bar{\Psi}, \bar{\Psi}_\alpha)$, is

$$\frac{\delta \mathcal{A}}{\delta \bar{\Psi}} = \frac{\partial \mathcal{A}}{\partial \bar{\Psi}} - \frac{\partial}{\partial x^\alpha} \frac{\partial \mathcal{A}}{\partial \bar{\Psi}_\alpha}. \quad (332)$$

Partial derivatives $\partial \mathcal{A} / \partial \bar{\Psi} = (\partial \mathcal{A} / \partial W)(\partial W / \partial \bar{\Psi})$, and their particular form depends on the shape of the potential W . As for the partial derivatives with respect to the derivatives of the field, they can be calculated explicitly for each variable, and we present a short summary of these partial derivatives below. More specifically,

$$\frac{\partial \bar{\mu}_q}{\partial \bar{\Psi}_\alpha} = \bar{u}^\alpha, \quad (333)$$

$$\frac{\partial \bar{p}_q}{\partial \bar{\Psi}_\alpha} = \bar{\rho}_q \bar{u}^\alpha, \quad (334)$$

$$\frac{\partial \bar{\rho}_q}{\partial \bar{\Psi}_\alpha} = \bar{u}^\alpha, \quad (335)$$

$$\frac{\partial \bar{\epsilon}_q}{\partial \bar{\Psi}_\alpha} = \bar{\rho}_q \bar{u}^\alpha, \quad (336)$$

$$\frac{\partial (\bar{\rho}_q \bar{\mu}_q)}{\partial \bar{\Psi}_\alpha} = 2 \bar{\rho}_q \bar{u}^\alpha, \quad (337)$$

$$\frac{\partial}{\partial \bar{\Psi}_\alpha} \left(\frac{\bar{\rho}_q}{\bar{\mu}_q} \right) = 0, \quad (338)$$

$$\frac{\partial (\bar{p}_q - \bar{\epsilon}_q)}{\partial \bar{\Psi}_\alpha} = 0. \quad (339)$$

Partial derivatives of four velocity

$$\frac{\partial \bar{u}_\alpha}{\partial \bar{\Psi}_\beta} = -\frac{\bar{P}_\alpha^\beta}{\bar{\mu}_q}, \quad \frac{\partial \bar{u}^\alpha}{\partial \bar{\Psi}_\beta} = -\frac{\bar{P}^{\alpha\beta}}{\bar{\mu}_q}. \quad (340)$$

It allows us to deduce, for example,

$$\frac{\partial (\bar{u}^\alpha \psi_\alpha)}{\partial \bar{\Psi}_\beta} = -\frac{1}{\bar{\mu}_q} \bar{P}^{\alpha\beta} \psi_\beta, \quad (341)$$

$$\frac{\partial q}{\partial \bar{\Psi}_\alpha} = -\frac{2}{\bar{\mu}_q} \bar{P}^\alpha_\mu l^{\mu\nu} \bar{u}_\nu. \quad (342)$$

References

1. O.V. Verkhodanov, A.G. Doroshkevich, *Advances in Machine Learning and Data Mining for Astronomy*, chapter Cosmic Microwave Background Mapping (CRC Press, Taylor & Francis Group, Boca Raton, 2012), pp. 133–159
2. J. Peacock, *Encyclopedia of Astronomy and Astrophysics*, chapter Cosmology: Standard Model (2002)
3. V. Mukhanov, *Physical Foundations of Cosmology* (Cambridge University Press, Cambridge, 2005), p. 442
4. S. Weinberg, *Cosmology* (Oxford University Press, Oxford, 2008)
5. D.S. Gorbunov, V.A. Rubakov, *Introduction to the Theory of the Early Universe* (World Scientific Publishing Company, Singapore, Hackensack, 2011)
6. M. Tegmark, M.A. Strauss, M.R. Blanton, K. Abazajian, S. Dodelson, H. Sandvik, X. Wang, D.H. Weinberg, I. Zehavi, N.A. Bahcall, F. Hoyle, D. Schlegel, R. Scoccimarro, M.S. Vogeley, A. Berlind, T. Budavari, A. Connolly, D.J. Eisenstein, D. Finkbeiner, J.A. Frieman, J.E. Gunn, L. Hui, B. Jain, D. Johnston, S. Kent, H. Lin, R. Nakajima, R.C. Nichol, J.P. Ostriker, A. Pope, R. Scranton, U. Seljak, R.K. Sheth, A. Stebbins, A.S. Szalay, I. Szapudi, Y. Xu, J. Annis, J. Brinkmann, S. Burles, F.J. Castander, I. Csabai, J. Loveday, M. Doi, M. Fukugita, B. Gillespie, G. Hennessy, D.W. Hogg, Ž. Ivezić, G.R. Knapp, D.Q. Lamb, B.C. Lee, R.H. Lupton, T.A. McKay, P. Kunszt, J.A. Munn, L. O’Connell, J. Peoples, J.R. Pier, M. Richmond, C. Rockosi, D.P. Schneider, C. Stoughton, D.L. Tucker, D.E. vanden Berk, B. Yanny, D.G. York, Cosmological parameters from SDSS and WMAP. *Phys. Rev. D* **69**(10), 103501 (2004)
7. Planck Collaboration, P.A.R. Ade, N. Aghanim, C. Armitage-Caplan, M. Arnaud, M. Ashdown, F. Atrio-Barandela, J. Aumont, C. Baccigalupi, A.J. Planck Banday et al., Planck 2013 results. XVI. Cosmological parameters, ArXiv e-prints, March 2013
8. Planck Collaboration, P.A.R. Ade, N. Aghanim, C. Armitage-Caplan, M. Arnaud, M. Ashdown, F. Atrio-Barandela, J. Aumont, C. Baccigalupi, A.J. Planck Banday et al., Planck 2013 results. XXIV. Constraints on primordial non-gaussianity, ArXiv e-prints, March 2013
9. J.-L. Lehnert, P.J. Steinhardt, Planck 2013 results support the cyclic universe. *Phys. Rev. D* **87**(12), 123533 (2013)

10. A.R. Liddle, D.H. Lyth, *Cosmological Inflation and Large-Scale Structure* (Cambridge University Press, Cambridge, 2000)
11. A. Krasinski, C. Hellaby, Structure formation in the Lemaître-Tolman model. *Phys. Rev. D* **65**(2), 023501 (2002)
12. A. Krasinski, C. Hellaby, Formation of a galaxy with a central black hole in the Lemaître-Tolman model. *Phys. Rev. D* **69**(4), 043502 (2004)
13. P. Jacewicz, A. Krasinski, Formation of Gyrs old black holes in the centers of galaxies within the Lemaître-Tolman model. *Gen. Relativ. Gravit.* **44**, 81–105 (2012)
14. V.A. Fock, *The Theory of Space, Time and Gravitation* (Pergamon Press, Oxford, 1964)
15. A. Papapetrou, Equations of motion in general relativity. *Proc. Phys. Soc. A* **64**, 57–75 (1951)
16. S. Chandrasekhar, Y. Nutku, The second post-Newtonian equations of hydrodynamics in general relativity. *Astrophys. J.* **158**, 55 (1969)
17. S. Chandrasekhar, F.P. Esposito, The $2\frac{1}{2}$ -post-Newtonian equations of hydrodynamics and radiation reaction in general relativity. *Astrophys. J.* **160**, 153 (1970)
18. J.L. Anderson, T.C. Decanio, Equations of hydrodynamics in general relativity in the slow motion approximation. *Gen. Relativ. Gravit.* **6**, 197–237 (1975)
19. N. Spyrou, Relativistic celestial mechanics of binary stars. *Gen. Relativ. Gravit.* **13**, 473–485 (1981)
20. S.M. Kopeikin, General relativistic equations of binary motion for extended bodies with conservative corrections and radiation damping. *Sov. Astron.* **29**, 516–524 (1985)
21. R.A. Breuer, E. Rudolph, The force law for the dynamic two-body problem in the second post-Newtonian approximation of general relativity. *Gen. Relativ. Gravit.* **14**, 181–211 (1982)
22. R.A. Breuer, E. Rudolph, Radiation reaction and energy loss in the post-Newtonian approximation of general relativity. *Gen. Relativ. Gravit.* **13**, 777–793 (1981)
23. S.T. Shapiro, A.P. Lightman, Rapidly rotating, post-Newtonian neutron stars. *Astrophys. J.* **207**, 263–278 (1976)
24. I. Ciufolini, R. Ruffini, Equilibrium configurations of neutron stars and the parametrized post-Newtonian metric theories of gravitation. *Astrophys. J.* **275**, 867–877 (1983)
25. S.L. Shapiro, S. Zane, Bar mode instability in relativistic rotating stars: A post-Newtonian treatment. *Astrophys. J. Suppl.* **117**, 531 (1998)
26. M. Takada, T. Futamase, A post-Newtonian Lagrangian perturbation approach to large-scale structure formation. *Mon. Not. R. Astron. Soc.* **306**, 64–88 (1999)
27. W. Petry, Cosmological post-Newtonian approximation in flat space-time theory of gravitation. *Astrophys. Space Sci.* **272**(4), 353–368 (2000)
28. P. Szekeres, T. Rainsford, Post-newtonian cosmology. *Gen. Relativ. Gravit.* **32**, 479–490 (2000)
29. J.-C. Hwang, H. Noh, D. Puetzfeld, Cosmological non-linear hydrodynamics with post-Newtonian corrections. *J. Cosmol. Astropart. Phys.* **3**, 10 (2008)
30. T.A. Oliynyk, Cosmological post-Newtonian expansions to arbitrary order. *Commun. Math. Phys.* **295**, 431–463 (2010)
31. T.A. Oliynyk, The fast Newtonian limit for perfect fluids. *Adv. Theor. Math. Phys.* **16**(2), 359–391 (2012)
32. S.M. Kopeikin, The speed of gravity in general relativity and theoretical interpretation of the Jovian deflection experiment. *Class. Quantum Gravity* **21**, 3251–3286 (2004)
33. J.L. Anderson, R.E. Kates, L.S. Kegeles, R.G. Madonna, Divergent integrals of post-Newtonian gravity: nonanalytic terms in the near-zone expansion of a gravitationally radiating system found by matching. *Phys. Rev. D* **25**, 2038–2048 (1982)
34. L. Blanchet, Post-Newtonian gravitational radiation, in *Einstein's Field Equations and Their Physical Implications*. Lecture Notes in Physics, vol. 540, ed. by B.G. Schmidt (Springer, Berlin, 2000), p. 225
35. G. Schäfer, *Post-Newtonian methods: analytic results on the binary problem*. In: L. Blanchet, A. Spallicci and B. Whiting (Eds.), *Mass and Motion in General Relativity*. *Fundam. Theor. Phys.* **162**, 167–210 (2011)
36. T. Buchert, Dark energy from structure: a status report. *Gen. Relativ. Gravit.* **40**, 467–527 (2008)

37. E.W. Kolb, V. Marra, S. Matarrese, Description of our cosmological spacetime as a perturbed conformal Newtonian metric and implications for the backreaction proposal for the accelerating universe. *Phys. Rev. D* **78**(10), 103002 (2008)
38. E.W. Kolb, V. Marra, S. Matarrese, Cosmological background solutions and cosmological backreactions. *Gen. Relat. Gravit.* **42**, 1399–1412 (2010)
39. Stephen R. Green, Robert M. Wald, New framework for analyzing the effects of small scale inhomogeneities in cosmology. *Phys. Rev. D* **83**, 084020 (2011)
40. S.R. Green, R.M. Wald, Newtonian and relativistic cosmologies. *Phys. Rev. D* **85**(6), 063512 (2012)
41. A.G. Riess, A.V. Filippenko, P. Challis, A. Clocchiatti, A. Diercks, P.M. Garnavich, R.L. Gilliland, C.J. Hogan, S. Jha, R.P. Kirshner, B. Leibundgut, M.M. Phillips, D. Reiss, B.P. Schmidt, R.A. Schommer, R.C. Smith, J. Spyromilio, C. Stubbs, N.B. Suntzeff, J. Tonry, Observational evidence from supernovae for an accelerating universe and a cosmological constant. *Astron. J.* **116**, 1009–1038 (1998)
42. S. Perlmutter, G. Aldering, G. Goldhaber, R.A. Knop, P. Nugent, P.G. Castro, S. Deustua, S. Fabbro, A. Goobar, D.E. Groom, I.M. Hook, A.G. Kim, M.Y. Kim, J.C. Lee, N.J. Nunes, R. Pain, C.R. Pennypacker, R. Quimby, C. Lidman, R.S. Ellis, M. Irwin, R.G. McMahon, P. Ruiz-Lapuente, N. Walton, B. Schaefer, B.J. Boyle, A.V. Filippenko, T. Matheson, A.S. Fruchter, N. Panagia, H.J.M. Newberg, W.J. Couch and Supernova Cosmology Project, Measurements of omega and lambda from 42 high-redshift supernovae. *Astrophys. J.* **517**, 565–586 (1999)
43. R. Zalaletdinov, The averaging problem in cosmology and macroscopic gravity. *Int. J. Mod. Phys. A* **23**, 1173–1181 (2008)
44. T. Futamase, Averaging of a locally inhomogeneous realistic universe. *Phys. Rev. D* **53**, 681–689 (1996)
45. C. Clarkson, G. Ellis, J. Larena, O. Umeh, Does the growth of structure affect our dynamical models of the universe? The averaging, backreaction and fitting problems in cosmology. *Rep. Prog. Phys.* **74**, 112901 (2011)
46. S. Kopeikin, M. Efroimsky, G. Kaplan, *Relativistic Celestial Mechanics of the Solar System* (Wiley, Weinheim, 2011)
47. G.F.R. Ellis, Inhomogeneity effects in cosmology. *Class. Quantum Gravity* **28**(16), 164001 (2011)
48. S.M. Kopeikin, A.N. Petrov, Post-Newtonian celestial dynamics in cosmology: field equations. *Phys. Rev. D* **87**(4), 044029 (2013)
49. E.M. Lifshitz, I.M. Khalatnikov, Special issue: problems of relativistic cosmology. *Sov. Phys. Uspekhi* **6**, 495–522 (1964)
50. E. Lifshitz, On the gravitational stability of the expanding universe. *JETP* **10**, 116–129 (1946). <http://www.citebase.org/abstract?id=oai>
51. S. Weinberg, *Gravitation and Cosmology: Principles and Applications of the General Theory of Relativity* (Wiley, New York, 1972)
52. J.M. Bardeen, Gauge-invariant cosmological perturbations. *Phys. Rev. D* **22**, 1882–1905 (1980)
53. H. Kodama, M. Sasaki, Cosmological perturbation theory. *Prog. Theor. Phys. Suppl.* **78**, 1 (1984)
54. A. Ishibashi, R.M. Wald, Can the acceleration of our universe be explained by the effects of inhomogeneities? *Class. Quantum Gravity* **23**, 235–250 (2006)
55. R. Baierlein, Representing a vector field: Helmholtz's theorem derived from a Fourier identity. *Am. J. Phys.* **63**, 180–182 (1995)
56. V.A. Brumberg, *Essential Relativistic Celestial Mechanics* (Adam Hilger, Bristol, 1991), p. 271
57. G.F.R. Ellis, M. Bruni, Covariant and gauge-invariant approach to cosmological density fluctuations. *Phys. Rev. D* **40**, 1804–1818 (1989)
58. G.F.R. Ellis, J. Hwang, M. Bruni, Covariant and gauge-independent perfect-fluid Robertson-Walker perturbations. *Phys. Rev. D* **40**, 1819–1826 (1989)
59. C.G. Tsagas, A. Challinor, R. Maartens, Relativistic cosmology and large-scale structure. *Phys. Rep.* **465**, 61–147 (2008)

60. S. Shandarin, S. Habib, K. Heitmann, Cosmic web, multistream flows, and tessellations. *Phys. Rev. D* **85**(8), 083005 (2012)
61. W. Del Pozzo, Inference of cosmological parameters from gravitational waves: Applications to second generation interferometers. *Phys. Rev. D* **86**(4), 043011 (2012)
62. S.R. Taylor, J.R. Gair, I. Mandel, Cosmology using advanced gravitational-wave detectors alone. *Phys. Rev. D* **85**(2), 023535 (2012)
63. M. Kramer, N. Wex, The double pulsar system: a unique laboratory for gravity. *Class. Quantum Gravity* **26**(7), 073001 (2009)
64. J.M. Weisberg, D.J. Nice, J.H. Taylor, Timing measurements of the relativistic binary pulsar PSR B1913+16. *Astrophys. J.* **722**, 1030–1034 (2010)
65. M. Kramer, Pulsars, SKA and time-domain studies in the future, in *IAU Symposium*, ed. by E. Griffin, R. Hanisch, R. Seaman, vol. 285, pp. 147–152, April 2012
66. S.M. Kopeikin, Celestial ephemerides in an expanding universe. *Phys. Rev. D* **86**(6), 064004 (2012)
67. S. Hojman, Problem of the identical vanishing of Euler-Lagrange derivatives in field theory. *Phys. Rev. D* **27**, 451–453 (1983)
68. N.V. Mitskevich, *Physical Fields in General Relativity* (Nauka, Moscow, 1969), p. 326
69. W. Greiner, J. Reinhardt, *Field Quantization* (Springer, Berlin, 1996). Translated from the German. With a foreword by D.A. Bromley
70. A.D. Popova, A.N. Petrov, Exact dynamic theories on a given background in gravitation. *Int. J. Mod. Phys. A* **3**, 2651–2679 (1988)
71. B. Schutz, *Geometrical Methods of Mathematical Physics* (Cambridge University Press, Cambridge, 1980)
72. A.N. Petrov, Noether and Belinfante corrected types of currents for perturbations in the Einstein-Gauss-Bonnet gravity. *Class. Quantum Gravity* **28**(21), 215021 (2011)
73. L.P. Grishchuk, A.N. Petrov, A.D. Popova, Exact theory of the (Einstein) gravitational field in an arbitrary background space-time. *Commun. Math. Phys.* **94**, 379–396 (1984)
74. C.M. Will, *Theory and Experiment in Gravitational Physics* (Cambridge University Press, Cambridge, 1993), p. 396
75. E. Bertschinger, Testing dark matter models with the phase space structure of dark matter halos, in *Probes of Dark Matter on Galaxy Scales*, p. 10001 (2013)
76. I. Zlatev, L. Wang, P.J. Steinhardt, Quintessence, cosmic coincidence, and the cosmological constant. *Phys. Rev. Lett.* **82**, 896–899 (1999)
77. B.F. Schutz, Perfect fluids in general relativity: velocity potentials and a variational principle. *Phys. Rev. D* **2**, 2762–2773 (1970)
78. L.D. Landau, E.M. Lifshitz, *Fluid Mechanics* (Pergamon Press, Oxford, 1959)
79. L.D. Landau, E.M. Lifshitz, *The Classical Theory of Fields* (Pergamon Press, Oxford, 1975)
80. L. Amendola, S. Tsujikawa, *Dark Energy: Theory and Observations* (Cambridge University Press, Cambridge, 2010)

The Galactic Center Black Hole Laboratory

A. Eckart, S. Britzen, M. Valencia-S., C. Straubmeier,
J.A. Zensus, V. Karas, D. Kunneriath, A. Alberdi, N. Sabha,
R. Schödel and D. Puetzfeld

Abstract The super-massive 4 million solar mass black hole Sagittarius A* (SgrA*) shows flare emission from the millimeter to the X-ray domain. A detailed analysis of the infrared light curves allows us to address the accretion phenomenon in a statistical way. The analysis shows that the near-infrared flare amplitudes are dominated by a single state power law, with the low states in SgrA* limited by confusion through the unresolved stellar background. There are several dusty objects in the immediate vicinity of SgrA*. The source G2/DSO is one of them. Its nature is unclear. It may be comparable to similar stellar dusty sources in the region or may consist predominantly of gas and dust. In this case a particularly enhanced accretion activity onto SgrA* may be expected in the near future. Here the interpretation of recent data and ongoing observations are discussed.

Sagittarius (SgrA*) at the center of our Galaxy is a highly variable radio, near-infrared (NIR), and X-ray source which is associated with a $4 \times 10^6 M_{\odot}$ super-massive central black hole (SMBH). SgrA* is the closest SMBH and can be taken as a paradigm for quiescent or very Low Luminosity Active Galactic Nuclei (LLAGN). It has been shown that the strong polarized (up to several 10 %) infrared flux density excursions (often referred to as flares) from SgrA* show patterns of strong gravity as expected from in-spiraling material very close to the black hole's horizon [1–3]. As a consequence of the strong gravitational field of the black hole these patterns

A. Eckart (✉) · M. Valencia-S. · C. Straubmeier · J.A. Zensus · N. Sabha
I. Physikalisches Institut, Universität zu Köln, Zùlpicher Str. 77, 50937 Cologne, Germany
e-mail: eckart@ph1.uni-koeln.de

A. Eckart · S. Britzen · J.A. Zensus
Max-Planck-Institut für Radioastronomie, Auf dem Hügel 69, 53121 Bonn, Germany

V. Karas · D. Kunneriath
Astronomical Institute, Academy of Sciences, 14131 Prague, Czech Republic

A. Alberdi · R. Schödel
Instituto de Astrofísica de Andalucía (CSIC), Glorieta de la Astronomía s/n,
18008 Granada, Spain

D. Puetzfeld
ZARM, University of Bremen, Am Fallturm, 28359 Bremen, Germany

express themselves in characteristic variations of the light curve due to the effect of relativistic boosting, light bending and the rotation of the polarization angle [1–5]. Therefore, it is mainly the polarization and the strong flux variability that give us certainty that we study the immediate vicinity of a SMBH [1–3, 6].

A fast moving infrared excess source G2, which is widely interpreted as a core-less gas and dust cloud [7], approaches SgrA* on a presumably elliptical orbit covering the region of the high velocity S-stars close to SgrA*. The passage of this Dusty S-cluster Object (DSO) is expected to result in accretion phenomena which will give an improved insight into the nature of the immediate surroundings of the SMBH SgrA*. The year 2013 certainly was only the first in an intense observing campaign during which the immediate vicinity of SgrA* is being monitored while the dusty object is close. Recent orbit determinations expect the peri-apse passage to occur in April/May 2014 [8]. Based on recent conference contributions (see Acknowledgments) on the Galactic Center this article concentrates on three major topics: (1) SgrA* and its environment, (2) its relation to extragalactic nuclei, and (3) new instrumentation and perspectives.

1 The Galactic Center

The DSO source approaching the super-massive black hole SgrA* at the center of the Milky Way has spawned great activities in observing that region covering the entire electromagnetic spectrum from radio, via infrared to X-ray wavelengths using telescopes across the world. The upcoming events underline the importance of the Galactic Center as a laboratory to investigate and understand phenomena in the immediate environment of super massive black holes [9, 10]. Gas and stars within the Galactic Center stellar cluster provide the fuel for the central super-massive black hole and hence the reason for most of the flux density variability observed from it.

1.1 The Variability of *Sagittarius A**

Progress has been made in the understanding of the emission process associated with the immediate surroundings of the super-massive black hole counterpart SgrA* as well as the three-dimensional dynamics and the population of the central stellar cluster. There is also ample evidence of interactions between the cluster and SgrA*.

Series of monitoring observations in the near-infrared (NIR), X-ray, and sub-millimeter (sub-mm) regimes accumulated over the years allowed us to perform for the first time detailed statistical studies of the variability of SgrA* [11–13]. The analyses show that the histogram of the near-infrared flux density is a pure power-law and the emission process is most likely dominated by synchrotron radiation. In [11], we present a comprehensive data description for NIR measurements of SgrA*. We characterized the statistical properties of the variability of SgrA* in the

near-infrared, which we found to be consistent with a single-state process forming a flux density power-law distribution. We discovered a linear rms-flux relation for the flux density range up to 12 mJy on a time scale of 24 min. This and the structure function of the flux density variations imply a phenomenological, formally nonlinear statistical behavior that can be modeled. In this way, we can simulate the observed variability and extrapolate its behavior to higher flux levels and longer time scales. SgrA* is also strongly variable in the X-ray domain [12–17] and references there in, as well as [18, 19] for a recent strong flares observed with Chandra and NuSTAR. The detailed statistical investigation in [11] also suggests that the past strong X-ray variations that give rise to the observed X-ray echos can in fact be explained by the NIR variability histogram under the assumption of a Synchrotron Self Compton (SSC) process. SgrA* is extremely faint in the X-ray bands, though strong activity has been revealed through the detection of flares. Therefore, SgrA* is the ideal target to investigate the mass accretion and the ejection physics in the case of an extremely low accretion rate onto a super-massive black hole. This is actually the phase in which super-massive black holes are thought to spend most of their lifetime. The activity phase onset of a magnetar (see section below) at a separation of only about 3 arcsec from the Galactic Center presented a problem for the SgrA* monitoring program in 2013 [20–22].

Simultaneous observations and modeling of the millimeter (mm), NIR, and X-ray flare emission of SgrA* are presented in [12, 13]. These data allowed us to investigate physical processes giving rise to the variable emission of SgrA* from the radio to the X-ray domain. In the radio cm-regime SgrA* is hardly linearly polarized but shows a fractional circular polarization of around 0.4 % [23, 24]. The circular polarization decreases towards the mm-domain [25], where as the authors of [26] report a variable linear polarization from SgrA* of a few percent in the mm-wavelength domain. The observations reveal flaring activity in all wavelength bands. The polarization degree and angle in the sub-mm are likely linked to the magnetic field structure or the general orientation of the source. In general—the NIR emission is leading the sub-mm with a delay of about one to two hours (see below) and the excursions in the NIR and X-ray emission are rather simultaneous. As a result we found that the observations can be modeled as the signal from an adiabatically expanding source component [27–29] of relativistic electrons emitting via the synchrotron/SSC process. A large fraction of the lower energy mm/cm- flux density excursions is not necessarily correlated with the NIR/X-ray variability (see, e.g., [30, 31] and details and further references in [12, 13]). One may compute the SSC spectrum produced by up-scattering of a power-law distribution of sub-mm-wavelength photons into the NIR and X-ray domain by using the formalism given by [32, 33]. Such a single SSC component model may be too simplistic, although it is considered as a possibility in most of the recent modeling approaches. It does not take into account possible deviations from the overall spectral index of $\alpha = 1.3$ at any specific wavelength domain like the NIR or X-ray regime.

The number density distribution of the relativistic electrons responsible for the synchrotron spectrum can be described by

$$N(E) = N_0 E^{-2\alpha+1}, \quad (1)$$

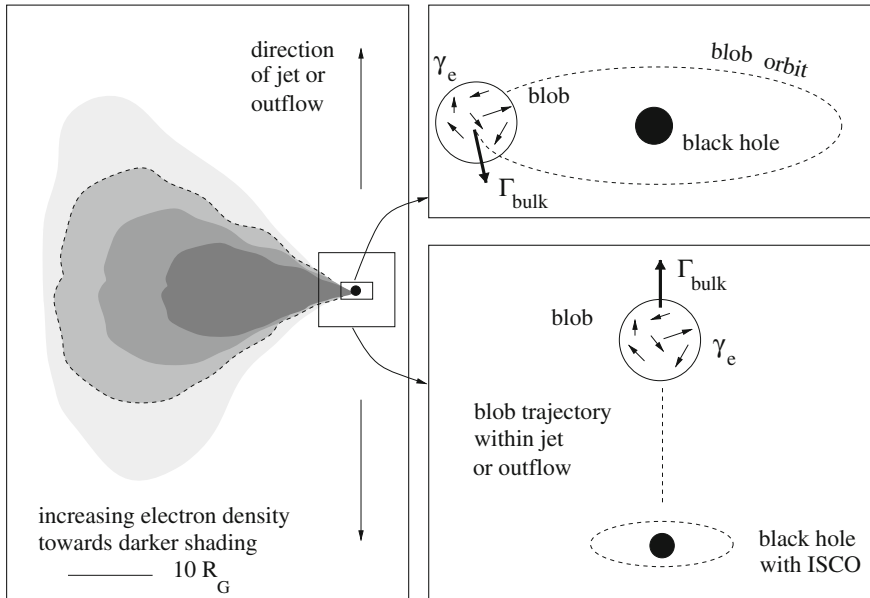


Fig. 1 Modeling approaches and the involved relativistic motions. We schematically compare the approaches through disk (*top right*) and jet (*bottom right*) modeling to relativistic magneto hydrodynamic modeling (*left*)

with γ_e between γ_1 and γ_2 which limit the lower and upper bound of the relativistic electron spectrum

$$\gamma_1 mc^2 < E = \gamma_e mc^2 < \gamma_2 mc^2. \quad (2)$$

Lorentz factors γ_e for the emitting electrons of the order of a few thousand are required to produce a sufficient SSC flux in the observed X-ray domain. In addition the relativistic bulk motion of the orbiting or outward traveling component is described by the bulk Lorentz factor Γ (see Fig. 1). On the left of this figure we show a sketch of a typical relativistic electron density distribution resulting from MHD calculations [30, 34, 35]. We show a cut through only one side of the three dimensional structure. The central plane and outflow region resulting from these calculations can be modeled in different, dedicated approaches (top and bottom right).

In the central plane modeling the flux variations are assumed to be the result of the motion of an orbiting blob or a hot spot (see for example [4]). In the outflow model the flux variations are assumed to be due to the ejection of a blob and its motion along the jet (with bulk motions close to the speed of light) or a much slower overall outflow component. In this case—for VLBI observations—the larger outflow extent at increasingly lower radio frequencies would be hidden by the decreasingly lower angular resolutions due to interstellar scattering. In Fig. 2 the accretion disk (here assumed to be edge-on) is shown as a vertical thick line to the right, the dashed part indicates the disk sections in the back- and foreground. Extending to the left

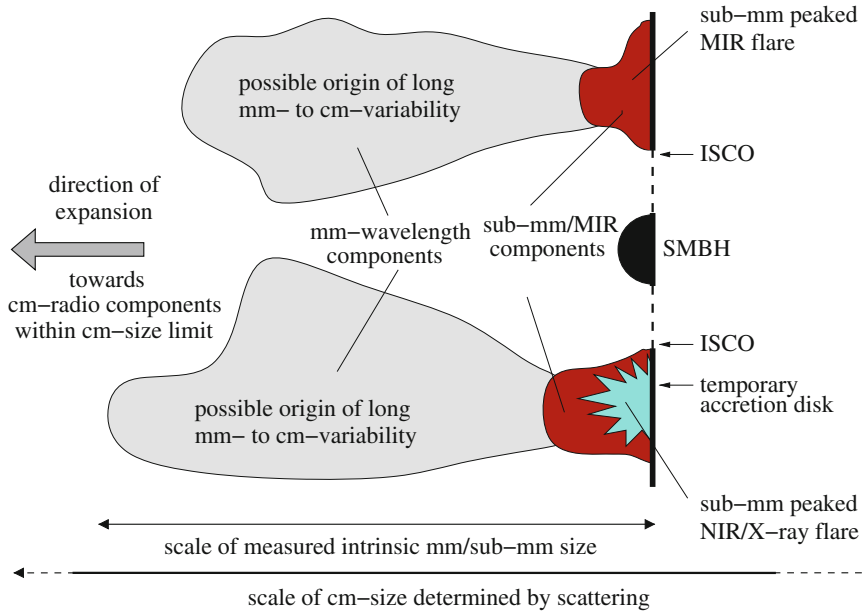


Fig. 2 Sketch of a possible source structure for the accretion disk around the SMBH associated with SgrA* following Fig. 12 in [36]

we show one side above the disk. Here higher energy flare emission (lower part) is assumed to be responsible for the observed NIR/X-ray flare emission. Lower energy flare emission (upper part) may substantially contribute to long wavelength infrared emission. In addition to the expansion towards and beyond the mm-source size, radial and azimuthal expansion within the disk may occur. Hence, long mm/cm-wavelength variability may originate from different source components of SgrA* and may be difficult to be disentangled based on radio data alone.

In Fig. 1 the relativistic boosting vectors for the electrons γ_e and the bulk motion Γ_{bulk} are not drawn to a proper relative scale. One can assume $\gamma_e \geq \Gamma_{bulk}$. In the case of relativistically orbiting gas as well as relativistic outflows one may use modest values for Γ . Both dynamical phenomena are likely to be relevant in the case of SgrA*. The size of the central plane synchrotron component is assumed to be of the order of or at most a few times the Schwarzschild radius. From the overall variable radio/sub-mm spectrum we can assume a turnover frequency ν_m of a few 100 GHz (see details in [12]). The motion of the synchrotron emitting cloud can be described via

$$\delta = \Gamma_{bulk}^{-1} (1 - \beta \cos \phi)^{-1}, \quad (3)$$

$$\Gamma_{bulk} = (1 - \beta^2)^{-1/2}. \quad (4)$$

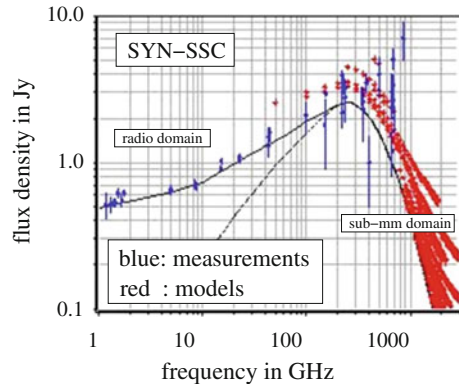
Here $\beta = v/c$ and v is the speed of the bulk motion of the synchrotron cloud, δ is the Doppler factor and ϕ the angle to the line of sight. For a relativistic bulk motion with Γ_{bulk} around 1.7 ± 0.3 (i.e. angles ϕ of about $30^\circ \pm 15^\circ$) the corresponding magnetic field strengths are often assumed to be of the order of a few ten Gauss, which is also within the range of magnetic fields expected for RIAF models [37, 38].

Modeling of the light curves shows that (at least for the brighter events) typically the sub-mm flux density excursions follow the NIR emission with a delay of about one to two hours with an expansion velocity of about $0.01\text{--}0.001\text{ c}$ [27–29]. We find source component sizes of around one Schwarzschild radius, flux densities of a few Janskys, and steep spectral indices. Typical model parameters suggest that either the adiabatically expanding source components have a bulk motion larger than its expansion velocity or the expanding material contributes to a corona or disk, confined to the immediate surroundings of SgrA*. For the bulk of the synchrotron and SSC models, we find synchrotron turnover frequencies in the range of 300–400 GHz. For the pure synchrotron models, this results in densities of relativistic particles in the mid-plane of the assumed accretion flow of the order of $10^{6.5}\text{ cm}^{-3}$, and for the SSC models the median densities are about one order of magnitude higher. However, to obtain a realistic description of the frequency-dependent variability amplitude of SgrA*, models with higher turnover frequencies and even higher densities are required. This modeling approach also successfully reproduces the degree of flux density variability across the radio to far-infrared spectrum of SgrA*. In Fig. 3 we show observed flux densities of SgrA* taken from the literature (blue) compared to a combined model that consists of the fit given in [39, 40] (black line), and [34] (black dashed line). We plotted in red the spectra of synchrotron self-absorption frequencies for the range of models. Here we show results for the preferred synchrotron plus SSC (SYN-SSC) model that most closely represents the observed variability of SgrA*.

In [41] theoretical polarimetric light curves expected in the case of optically thin NIR emission from over-dense regions close to the marginal stable orbit are presented (see also [1–5]). Using a numerical code the authors track the time evolution of detectable polarization properties produced by synchrotron emission of compact sources in the vicinity of the black hole. They show that the different setups lead to very special patterns in the time-profiles of polarized flux and the orientation of the polarization vector. As such, they may be used for determining the geometry of the accretion flow around SgrA* (see also [2, 3, 42]).

During the 2013 Bad Honnef and the Granada conference (see Acknowledgments) efforts to monitor SgrA* during the DSO fly-by and first observational results from 2013 were reported in [8, 43–49]. The NRAO Karl G. Jansky Very Large Array (VLA) is undertaking an ongoing community service observing program to follow the expected encounter of the DSO cloud with the black hole SgrA* in 2013/2014 [50]. The NRAO VLA has been observing the Sgr A region since October 2012 on roughly a bi-monthly interval, cycling through eight observing bands. For monitoring the flux densities and in particular the radio spectral indices the short wavelength observations ($\lambda < 6\text{ cm}$) are most useful. For 2012/2013 no particular flux density variation was detected that could be attributed to the interaction between SgrA* and the DSO. This may be linked with the fact that the newly determined periaapse passage is now

Fig. 3 The variable radio spectrum of SgrA*: measurements and model results (see text and [12, 13] for details)



expected to happen in April/May of 2014 [8], i.e. later than originally anticipated. However, in the radio-shock frame in which variations of up to several Janskys were expected even during the pre-periapse time. Hence, the lack of strong radio flares indicates that the medium is less dense than expected and/or that the bow-shock size i.e. the cross-section of the dust source is much smaller than assumed [51–56].

1.2 VLBI Imaging of SgrA*

There is also profound progress in imaging and modeling of the central putative accretion disk of SgrA* as well as the jet that may be associated with the source [35, 41, 57]. In fact imaging of SgrA* may turn out to be a Rosetta Stone in the attempts of distinguishing between different relativity theories of black holes (see [58], e.g., 2013, on astronomical tests of general relativity and the pseudo-complex theory).

VLBI (Very Long Baseline Interferometry) observations at very short millimeter radio wavelengths can overcome the effects of interstellar scattering and allow us to study the source intrinsic structure of SgrA*. Large mm/sub-mm facilities like the VLBA (Very Long Baseline Array), VERA (VLBI Exploration of Radio Astrometry), ALMA (Atacama Large Millimeter Array), PdBI (Plateau de Bure Interferometer) and the sensitive mm-telescopes in the EVN (European VLBI Network)—such as the IRAM 30 m and the 100 m Effelsberg telescopes—are participating in this effort, which will eventually culminate in the project EHT (Event Horizon Telescope), a VLBI array especially designed to image the structures close to the event horizons of the largest SMBHs in the sky—namely SgrA* and M87, with 1 Schwarzschild radius extending to an angular size of about 10 and $3.7 \mu\text{as}$, respectively. Multi-epoch imaging observations will allow to constrain the locations and sizes of the flaring region of SgrA* within the putative temporal accretion disk of the accretion stream/flow towards or an accretion wind from SgrA*. These measurements will also constrain the acceleration processes (e.g. magnetic reconnection events or

non-axisymmetric standing shocks) that give rise to the population of relativistic electrons and the variable emission we see from SgrA*. Ultimately, alternative black hole models will be probed and attempts to test the black hole no-hair theorem will be possible with the new VLB mm/sub-mm facilities [43, 44, 59–65].

These VLBI experiments will eventually enable spatially resolved studies on sub-horizon scales, leading to an unprecedented exploration of a putative predicted black-hole shadow [66] as an evidence for light trapping by the black hole as well as its interaction with the surrounding material. It will be possible to monitor the possible expansion of source components during flare activity. Furthermore, when a rotating black hole is immersed in a magnetic field of external origin, the gravito-magnetic interaction is capable of triggering the magnetic reconnection, accelerating the particles to very high energy [67–69]. This frame-dragging phenomenon is particularly interesting in the context of exploring the strong-gravity effects in astrophysical black holes because the effect does not have a Newtonian counterpart and it operates on the border of the ergospheric region [70], i.e. very close to the black hole horizon, and it can be probed with the future EHT. Also, one can investigate if the black hole proximity generates conditions favorable to incite the magnetic reconnection that eventually leads to plasma heating and particle acceleration. This effect could contribute to the flaring activity.

1.3 The Importance of Dusty Sources Close to the Center

A major discussion point is if and how the DSO source will be disrupted during its peri-bothron¹ passage. It may be only its dusty envelope that will be disrupted since the K_s-band identifications of the source suggest that it can also be associated with a star [45]. In addition to the VLT NACO and the Keck NIRC detections of the DSO NIR continuum emission [46], here we show the detection of the DSO continuum at about $K \sim 19$ using SINFONI data (Fig. 4). The detection of the continuum emission in data sets taken with three different instrumental setups over many years strengthens the case for a substantial continuum emission from that dusty source. As posted in the astronomer's telegram No. 6110 on 2 May 2014 [72], the DSO was detected $3.8 \mu\text{m}$ during its peri-bothron passage around the central black hole SgrA*. Hence, it appears to be intact and up to this point not yet heavily affected by tidal effects. This clearly supports our finding [46] that it may very well be a dusty star rather than a pure gas and dust cloud.

In contrast to a pure dust and gas nature of the DSO its possible stellar (i.e. a dust enshrouded star) nature is discussed and partially favoured in [8, 45–47, 49, 73–75]. Eckart et al. [45] investigate the possible mass transfer across Lagrange point

¹Peri- or apo-bothron is the term used for peri- or apoapsis—i.e. closest or furthest separation—for an elliptical orbit with a black hole present at one of the foci. As already mentioned by Frank and Rees in [71] the word ‘bothros’ was apparently first suggested in the context of black holes by W.R. Stoeger. It originates from the greek word $\delta\beta\theta\rho\varsigma$ with the equivalent meaning of ‘the sink’ or ‘the deep dark pit’.

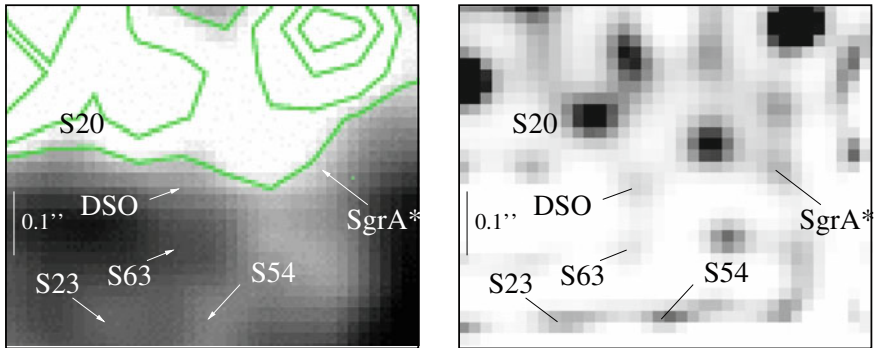


Fig. 4 The DSO detected in its K-band continuum emission in 2010 SINFONI data. *Left* The original image (positive greyscale); *Right* A LUCY deconvolved image (negative greyscale) shown at an angular resolution close to the diffraction limit of the VLT UT4

L1 in a simple Roche model. If the star has a mass of about $1 M_{\odot}$, the separation of L1 from it will be about 0.1 AU. For a Herbig Ae/Be stars with $2\text{--}8 M_{\odot}$ that distance will be between 0.2 and 0.5 AU. For a typical S-cluster stellar mass of $\sim 20\text{--}30 M_{\odot}$ the separation will be closer to one AU. The interferometrically determined inner ring sizes that one typically finds for young Herbig Ae/Be and T Tauri stars can indeed be as small as 0.1–1 AU [76]. Any stellar disk or shell may already have been stripped substantially if the DSO has performed more than a single orbit. If the source has a size of about 1 AU (as determined from its MIR-luminosity; [7]) then a significant amount of the dusty circumstellar material may pass beyond L1 during peri-bothron passage. This material will then start to move into the Roche lobe associated with SgrA*.

However, it is not at all clear what will happen to the transferred material after the peri-bothron passage around May 2014 or beyond. The fact that this dusty object may be a dust enshrouded star rather than a dust cloud will have an influence on the expected flux density variations resulting from the close approach. They may be much weaker than expected. Simulations [77–79] that have discussed the feeding rate of SgrA* as a function of radius indicate that a portion of the material may fall towards SgrA*. If SgrA* is associated with a significant wind on scale of the peri-bothron separation, then a large part of the material may be blown away again by an out-bound accretion wind. Shcherbakov and Baganoff [80] have discussed the feeding rate of SgrA* as a function of radius. Based on their modeling one may suggest that the bow-shock sources X3 and X7 [81] are still in the regime in which most of the in-flowing mass is blown away again. Another case for comparison is the star S2. During its peri-bothron passage the star has been well within the zone in which matter of its (weak) stellar wind could have been accreted by SgrA*. The DSO peri-bothron will be at a larger radius than that of S2 [8]. This may imply that no enhanced accretion effect will result from it during the peri-bothron passage. Until May 2014 no increase in variability and no significant flux density increase well above normal levels has been reported in the radio to X-ray domains.

The fate of the DSO and the cometary sources X3 and X7 underline the importance of investigating the wind properties in the vicinity of SgrA* in more detail. IRS 8 is a unique possibility to study the bow shock properties and polarization features in the dusty environment at the Galactic Center. Based on a detailed study of near-infrared emission Rauch et al. [82] present interstellar dust properties for the northern arm in the vicinity of the IRS 8 bow shock. This study allowed us for the first time to determine the relative positioning of IRS 8 with respect to the northern arm and the super-massive black hole SgrA*. The result indicates that the central star of IRS 8 is in fact located closer towards the observer than the northern arm. In [45] we investigated the near-infrared proper motions and spectra of infrared excess sources at the Galactic Center. The work concentrated on a small but dense cluster of comoving sources (IRS13N) located 3'' west of SgrA*. Our analysis shows that these stars are spectroscopically and dynamically young and can indeed be identified with continuum emission at 2 μ m and shortward, indicating that these mid-infrared sources are not only dust sources but young stars. The possibility of ongoing star formation at the Galactic Center is supported through simulations [48]. In fact the DSO may be a representative of dusty sources similar to those discussed in [29, Fig.14] and compare also to the discussion of sources X3 and X7 in [81]. Meyer et al. [73] present NIR spectroscopic data of several of these sources. They also show that the DSO does not seem to be unique, since several red emission-line objects can be found in the central arcsecond. In summary, the authors of [73] conclude that it seems more likely that G2 is ultimately a stellar source that is clearly associated with gas and dust (see also [45–47]).

1.4 Stellar Dynamics and Tests of Relativity

SgrA*, the super-massive black hole at the center of the Milky Way, is surrounded by a small cluster of high velocity stars, known as the S-stars [83]. Sabha et al. [84] aimed at constraining the amount and nature of the stellar and dark mass that is associated with the cluster in the immediate vicinity of SgrA*. The authors use near-infrared imaging to determine the Ks-band luminosity function of the S-star cluster members, the distribution of the diffuse background emission and the stellar number density counts around the central black hole. This allows us to determine the stellar light and mass contribution expected from the faint members of the cluster. In [84] post-Newtonian N-body simulations are used to investigate the effect of stellar perturbations on the motion of S2, as a means of detecting the number and masses of the perturbers. The authors find that the stellar mass derived from the Ks-band luminosity extrapolation is much smaller than the amount of mass that might be present considering the uncertainties in the orbital motion of the star S2. Also the amount of light from the fainter S-cluster members is below the amount of the residual light at the position of the S-star cluster after one removes the bright cluster members. If the distribution of stars and stellar remnants is peaked near SgrA* strongly enough, observed changes in the orbital elements of S2 can be used to constrain both the

masses and the number of objects inside its orbit. Based on simulations of the cluster of high velocity stars we find that in the NIR K-band—close to the confusion level for 8 m class telescopes—blended stars will occur preferentially near the position of SgrA* which is the direction towards which we find the highest stellar density. These blended stars consist of several faint, (with the current facilities) individually undetectable stars that get aligned along the line-of-sight, producing the visual effect of a new point source. The proper motion of stars and the corresponding velocity dispersion leads to the fact that such a blended star configuration dissolves typically after 3 years.

Stars that get very close to the super massive black hole are ideal probes to analyze the gravitational field and to search for effects of relativity due to the presence of the high mass concentration and its effect on space time. This can be done by tracing the orbit of stars through proper motions and radial velocities. As discussed in [85] relativistic effects should express themselves spectroscopically. The redshift z of a black hole orbiting star can be written as:

$$z = \Delta\lambda/\lambda = B_0 + B_1\beta + B_2\beta^2 + O(\beta^3) \quad (5)$$

with B_0 being an offset, $B_1\beta$ describing the Doppler velocity and $B_2\beta^2$ expressing the relativistic effects. Here the value B_2 contains equal contributions from the gravitational redshift and the special relativistic transverse Doppler effect. The combined effect gives a redshift that is about an order of magnitude larger than the currently achieved spectral resolution of $\delta\lambda/\lambda \sim 10^{-4}$. For S2 one expects about a 150–200 km/s signal measurable over a few months on top of an orbit-depending radial velocity of more than 4000 km/s. Expectations are high that this will be observable during the next peri-boethron for S2 around 2017.9 ± 0.35 [86, 87] or S2-102 around 2021.0 ± 0.3 [49]. Realistically, however, one needs several stars on different orbits to detect the relativistic effect with certainty ([85]; see also [88] for peri-boethron shift). Alternatively, one has to find stars that are (or get) closer than S2 and S2-102 ([49]; see below) to SgrA*.

Detailed imaging and the analysis of proper motions may be another way to trace relativistic effects. An important deviation from Keplerian motion occurs as a result of relativistic corrections to the equations of motion, which to the lowest order predict a certain advance of the argument of peri-boethron each orbital period. Choosing $a = 5.0$ mpc and $e = 0.88$ for the semi-major axis and eccentricity of S2, respectively, and assuming a black hole mass of $M_\bullet = 4.0 \times 10^6 M_\odot$ this advance will be

$$(\Delta\omega)_{\text{GR}} = \frac{6\pi GM_\bullet}{c^2 a(1-e^2)} \approx 10.8'. \quad (6)$$

The relativistic precession is prograde, and leaves the orientation of the orbital plane unchanged.

The location of the peri-boethron advances for each orbital period due to the spherically-symmetric component of the distributed mass that is resolved by the elliptical orbit of the star. The amplitude of this Newtonian “mass precession” is

$$(\Delta\omega)_M = -2\pi G_M(e, \gamma) \sqrt{1 - e^2} \left[\frac{M_\star}{M_\bullet} \right]. \quad (7)$$

Here, $M_\star = M_\star(r < a)$ is the distributed mass within a radius $r = a$, and G_M is a dimensionless factor of order unity that depends on e and on the power-law index of the density, $\rho \propto r^{-\gamma}$ [89]. In the special case $\gamma = 2$,

$$G_M = \left(1 + \sqrt{1 - e^2}\right)^{-1} \approx 0.68 \text{ for S2}, \quad (8)$$

so that

$$(\Delta\omega)_M \approx -1.0' \left[\frac{M_\star}{10^3 M_\odot} \right]. \quad (9)$$

Mass precession is retrograde, i.e., opposite in sense to the relativistic precession.

The contribution of relativity to the peri-bothron advance is determined uniquely by the known values of a and e . A measured $\Delta\omega$ can then be used to constrain the mass enclosed within S2's orbit, by subtracting $(\Delta\omega)_{GR}$ and comparing the result with Eq. (9). So far, this technique has yielded only upper limits on M_\star of $\sim 10^{-2} M_\bullet$ [90]. First robust upper limits of that order have been derived in [91, 92]. The role of relativistic effects versus the gravitational effects of the nuclear star cluster and a ring of stars are summarized in [93].

In addition to the relativistic effects on the orbit of a test star, and the precession due to the smooth matter distribution, the granularity of the cluster stars and stellar remnants needs to be considered. The granularity of the distributed mass makes itself felt via the phenomenon of resonant relaxation (RR; [94, 95]). On current observational time scales the stellar orbits near SgrA* remain nearly fixed in their orientations. The perturbing effect of each field star on the motion of a test star (e.g. S2) can be approximated as a torque that is fixed in time and proportional to the mass m of the field star. Sabha et al. [84] show that the effects of RR are competing with the relativistic and Newtonian periastron effects on the orbits of the known high velocity S-cluster stars. Following [84], we show in Fig. 6 the predicted change in S2's orbital elements over the course of one orbital period (~ 15.6 year). The shift due to relativity, $\Delta\omega_{GR} \approx 11'$, has been subtracted from the total; what remains is due to Newtonian perturbations from the field stars. Each histogram was constructed from integrations of 100 random realizations of the same initial model, with field-star mass $m = 10M_\odot$, and four different values of the total number: $N = 200$ (solid/black); $N = 100$ (dotted/red); $N = 50$ (dashed/blue); and $N = 25$ (dot-dashed/green). The average value of the peri-bothron shift increases with increasing Nm , as predicted by Eq. (10). There is also a separate contribution that scales approximately as $\sim 1/\sqrt{N}$ and that results in a variance about the mean value.

Sabha et al. [84] show that the net effect of the torques from N field stars is to change the angular momentum, \mathbf{L} , of S2's orbit according to

$$\frac{|\Delta\mathbf{L}|}{L_c} \approx K \sqrt{N} \frac{m}{M_\bullet} \frac{\Delta t}{P} \quad (10)$$

where L_c is the angular momentum of a circular orbit having the same semi-major axis as that of the test star. Here Eq. 10 describes “coherent resonant relaxation”. Sabha et al. [84] state that the normalizing factor K should be of order unity [96].

Changes in \mathbf{L} imply changes in both the eccentricity of the test star orbit, as well as changes in its orbital plane. Changes in the orbital plane can be described in a coordinate-independent way via the angle $\Delta\theta$, where

$$\cos(\Delta\theta) = \frac{\mathbf{L}_1 \cdot \mathbf{L}_2}{L_1 L_2} \quad (11)$$

and $\{\mathbf{L}_1, \mathbf{L}_2\}$ are the values of \mathbf{L} at two times separated by Δt [84]. For small values of $\Delta\theta$ this can be written as

$$\Delta\theta \approx \sqrt{2 - 2 \frac{\mathbf{L}_1 \cdot \mathbf{L}_2}{L_1 L_2}} \approx 1 - \frac{\mathbf{L}_1 \cdot \mathbf{L}_2}{L_1 L_2}. \quad (12)$$

If we set Δt equal to the orbital period of the test star, the changes in its orbital elements due to resonant relaxation are expected to be

$$|\Delta e|_{\text{RR}} \approx K_e \sqrt{N} \frac{m}{M_\bullet}, \quad (13)$$

$$(\Delta\theta)_{\text{RR}} \approx 2\pi K_t \sqrt{N} \frac{m}{M_\bullet}, \quad (14)$$

where N is the number of stars having a -values similar to, or less than, that of the test star [84]. The constants K_e and K_t may depend on the properties of the orbits of the field star distribution in the Galactic Center stellar cluster. More details are given in [84]. The Kozai mechanism is another kind of resonant process that is thought to operate in the Galactic Center environment [97–99].

Figure 5 (following [100]) plots the location of the S stars in the (a, e) -plane (semimajor axis—ellipticity). The data for the two currently closest known stars S2 and S2-102 are indicated by pattern filled circles. For the two currently closest sources one finds:

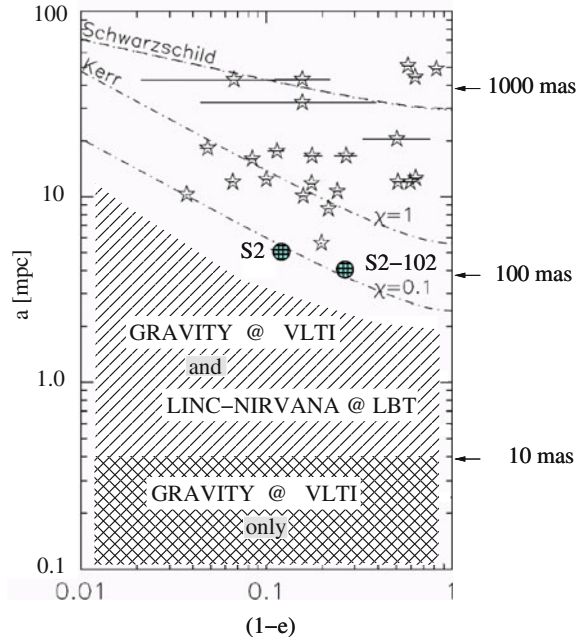
$$\text{S0} - 102 : T_{\text{orbit}} = 11.5 \pm 0.3 \text{ yr} \quad e = 0.680 \pm 0.020 \quad a = 0.100'' \pm 0.010''$$

$$\text{S2} : T_{\text{orbit}} = 15.6 \pm 0.4 \text{ yr} \quad e = 0.883 \pm 0.003 \quad a = 0.125'' \pm 0.002''$$

([49, 86, 87]; $1''$ at the distance of the Galactic Center corresponds to a linear scale of about $39 \text{ mpc} = 0.127 \text{ ly} = 8044 \text{ AU}$).

Also plotted in Fig. 5 are curves indicating where the effects of RR begin to be mediated by relativistic precession of the “test” star. The upper curve is the “Schwarzschild barrier” [101]; stars below this curve precess due to GR so rapidly that their precession, rather than the mean precession rate of the field stars, determines the coherence time over which the RR torques can act. This is reflected in the horizontal tick marks which give the expected amplitude of eccentricity changes as an orbit

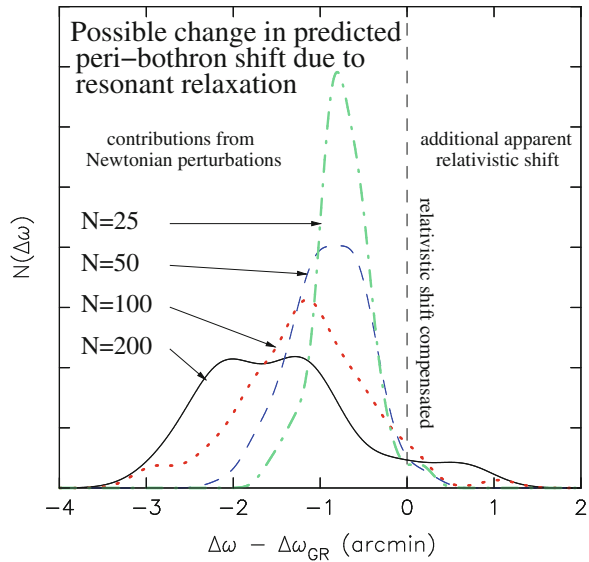
Fig. 5 An example for the location of the Galactic Center S-stars on the (a, e) -plane. See details in the text and [100], in particular the *left panel* of their Fig. 1



precesses in the essentially fixed torquing field due to the field stars. The location of the Schwarzschild barrier in the (a, e) -plane depends somewhat on the assumed spatial distribution of the stars in the nuclear cluster, but for most reasonable distributions, S2 lies below the barrier [100]. Closer to SgrA*, frame-dragging torques due to the spin of SgrA* begin to make themselves felt. The two lower curves on Fig. 6 mark where these torques begin to compete with RR torques. In this regime, orbits precess so rapidly that their eccentricities are essentially unaffected by the \sqrt{N} torques, but their orbital planes can still change (“vector RR”). Below the curves marked “Kerr” in Fig. 5 are curves indicating where the effects of RR begin to be changes in orbital planes due to frame dragging dominate the changes due to vector RR [102]. Stars in this regime can be used to test theories of gravity, e.g., “no-hair” theorems.

Figure 5 also shows the (a, e) -regions that will be experimentally accessible with the new upcoming interferometric instrumentation in the NIR like GRAVITY at the VLTI and LINC-NIRVANA at the LBT (see below). Only for stars at much smaller orbital separations from SgrA* than S2 or S2-102, as they may be found with infrared interferometers like GRAVITY at the VLTI or LINC-NIRVANA at the LBT (see below), are Newtonian perturbations (mass precession, RR) negligible compared with the effects of GR. However, even then one will need more than one star with different orbital elements in order to clearly demonstrate that the eventually observed orbital changes are truly due to relativistic effects (see, e.g., [85, 88, 102, 103]).

Fig. 6 Histograms of the predicted change in S2's argument of peri-bothron, ω , over the course of one orbital period (~ 15.6 year; see also [84]). See text for a detailed description of the figure



1.5 Effects Due to Stellar Collisions

The stellar density close to center is in excess of $10^5 M_\odot$ per cubic-parsec. This implies that in this region the evolution of stars is influenced by stellar collisions (e.g. [104, 105]). Observations of the stars at the Galactic Center show that there is a lack of red giants within about 0.5 pc of the super-massive black hole. The very high stellar number densities this close to the SMBH imply that the giants—or their progenitors—may have been destroyed by stellar collisions. The derivation of collisional rates between different types of stars at the Galactic Center and their likely effects are currently a field of intense investigation in order to quantify how large a contribution stellar collisions could make to the puzzle of the missing red giants [106]. As an example see recent contributions on star formation (see also references below), and on the structure of the central stellar cluster and stellar interactions in the Galactic Center area by [84, 107–112].

1.6 Pulsars at the Galactic Center

Another very promising way of investigating the super-massive black hole properties in great detail is to find pulsars orbiting SgrA*. If close enough, they would allow us to measure the spin and quadrupole moment of the central black hole with superb precision enabling us to test different theories of gravity [113]. The number of pulsars in the central cluster will depend on the star formation history in the overall

region. The discovery of radio pulsations from a magnetar PSR J1745-2900 with the Effelsberg telescope has highlighted the great value and the efforts that are currently being undertaken to find pulsars in the Galactic Center region [20, 114–117].

1.7 Star Formation and the Galactic Center

Star formation activity in the Galactic Center is an ongoing research topic (e.g. [54, 55, 118, 119]). Given the deep gravitational potential towards the very center, stars cannot form in the same way they do throughout the Milky Way. However, infrared observations have shown evidence that massive stars were formed in the hostile environment of SgrA* a few million years ago. VLA, ALMA and CARMA measurements suggest that star formation is still taking place in this region and has been going on during the past few 10^5 years. A broad variety of possible star formation scenarios can be discussed. Massive stars may have formed within a disk of molecular gas resulting from a passage of a giant molecular cloud interacting with SgrA* and then dispersed after having formed these stars [120]. Dense clumps originating from the CND loosing angular momentum and falling towards the very center may also be a source of constant or episodic star formation in the Galactic Center [48]. A fraction of the material associated with these phenomena may have accreted onto SgrA* probably in an episodic or transient manner [121]. This process may in part be responsible for the origin of the γ -ray emitting Fermi bubbles [122].

1.8 The Galactic Center on Larger Scales

Radio polarization observations by the Parkes radio telescope in Australia have recently led to the discovery of giant radio lobes emanating from the Galactic nucleus [123, 124]. These lobes are largely coincident with the Fermi Bubbles discovered in the γ -ray domain [122]. However, the radio outflows extend to even larger angular scales, covering about $55\text{--}60^\circ$ north and south of the Galactic plane. It is likely that the radio lobes—and the Fermi Bubbles—are the result of the concentrated star formation occurring in the Central Molecular Zone of the Milky Way rather than signatures of putative activity of the super-massive black hole. These Fermi bubbles may be related to the giant magnetized outflows from the Galactic Center [125–127]. These phenomena link the Galactic Center nuclei of nearby active galaxies and larger scale events (e.g. amounts of gas escaping from the potential well of the galaxy). Massive inflow of gas towards the centers, as well as star formation or jet driven outflows from the nuclear regions, are frequently observed and are directly or indirectly linked with the accretion processes onto super-massive black holes.

2 Extragalactic Nuclei

The observational results obtained on the Galactic Center during the past few years need to be put into perspective. The nucleus of our Galaxy has an extremely low luminosity. However, it also demonstrates that violent activity may take place at times. Hence, a comparison between the center of the Milky Way and the nuclei of galaxies hosting Low Luminosity Active Galactic Nuclei (LLAGN) appears to be imperative.

Footprints of AGN feeding and feedback in LLAGN can be observed in many cases [128–130]. The study of the content, distribution and kinematics of interstellar gas is a key to understanding the fueling of AGN and star formation activity in galaxy disks. Current mm-interferometers provide a sharp view of the distribution and kinematics of molecular gas in the circumnuclear disks of galaxies through extensive mapping of molecular line (mainly CO and to some extent high density tracers like HCN, HCO^+ , CS, etc.). The use of molecular tracers specific to the dense gas phase can probe the influence of feedback on the chemistry and energy balance in the interstellar medium of galaxies. Radiative and mechanical feedback are often used as a mechanism of self-regulation in galaxy evolution as well as thermal and non-thermal AGN activity. In the disks of galaxies the evolution is predominantly expressed in star formation and the evolution of stellar populations and the ISM properties. In galactic nuclei the thermal part is represented mainly by the properties of the nuclear ISM and by the NLR and BLR regions while the non-thermal part is dominated by synchrotron/SSC emission due to SMBH accretion and the presence of jets.

High angular resolution ($<1''$) observations with sub(mm)-interferometers (IRAM PdBI, ALMA) in the context of the Nuclei of GALaxies (NUGA) survey (see, e.g., [128, 129, 131–133] and upcoming more ALMA NUGA papers) allow us to study the mechanisms responsible for fueling AGN and star formation activity in the central $R < 1$ kpc disks of a sample of 25 active galaxies at the 10–100 pc scale. This study has revealed streaming motions towards and away from the nuclear region that do not necessarily have to be co-phased with current AGN activity. In several cases these observations also reveal the presence of molecular circumnuclear disks and massive molecular outflows.

These phenomena are directly coupled to black-hole fueling, feedback and duty cycles that are essential for understanding the activity in galactic nuclei [134–137], see also [138, 139]. The distribution of gas and stars in nearby galaxies traced by 3-D studies of molecular, neutral and ionized gas provides a unique view of the role of the multi-phase medium in triggering and fueling nuclear activity in galactic nuclei on scales ever closer to the central black hole. Radio- and mm-interferometers and in particular 3-dimensional imaging devices in the infrared and optical domain (like integral field units) allow us to obtain spectroscopic and photometric information at every position of the field-of-view. Such observations have been used to elaborate

comparative studies of gaseous and stellar dynamics in active and quiescent galaxies. Studying the inner kiloparsec of AGN is particularly important, since the activity and dynamical time scales become comparable in this region. These investigations also show that the variability observed in nearby radio-quiet AGN may provide parallels to our own Galactic Center. They also provide evidence that AGN duty cycles may be shorter than previously thought.

3 Black Hole Laboratory: New Instrumentation and Perspective

An improved link between theory and observations will be provided by new and upcoming instrumentation such as the future capability of measuring polarization in the X-ray domain [140, 141], and direct VLBI imaging of the event horizon region for e.g. M87 as a representative of the largest supermassive black holes, and SgrA* as a representative for low-mass SMBHs [59, 60, 142]. The SKA (Square Kilometer Array) will be key instrument to establish the census of pulsars at the Galactic Center, to determine the star formation history, and to provide the required precision to determine the spin and quadrupole of the central BH, testing the theories of gravity (see, e.g., [143]).

The beam combining instrument GRAVITY² at the VLTI (P.I. Frank Eisenhauer, MPE, Garching) will be able to measure the NIR image centroid paths during flux density excursions of SgrA* [12, 144–146]. These paths will depend on the geometrical structure and time evolution of the emitting region i.e. spot shape, e.g. presence of a torus or spiral-arm patterns, an emerging jet component. Figure 7 shows the fringe tracking spectrometer of GRAVITY being under construction at the University of Cologne. Operating on six interferometric baselines, i.e. using all four UTs, the 2nd generation VLTI instrument GRAVITY will deliver narrow angle astrometry with 10 μ as accuracy at the infrared K-band.

While most of the mentioned geometries are currently able to fit the observed variable emission from SgrA*, future NIR interferometry with GRAVITY at the VLTI will break some of the degeneracies between different emission models. GRAVITY will be able to detect the positional shift of the photo-center of a flare at the Galactic Center within the ~ 20 min orbital time scale of a source component close to the last stable orbit, using the flares as dynamical probes of the gravitational field around SgrA*. In particular GRAVITY observations of polarized NIR light could reveal a clear centroid track of bright spot(s) orbiting in the mid-plane of the accretion disk (see, e.g., [1–3]). A non-detection of centroid shifts may point at a multi-component

²<http://www.mpe.mpg.de/2441478/Team>.

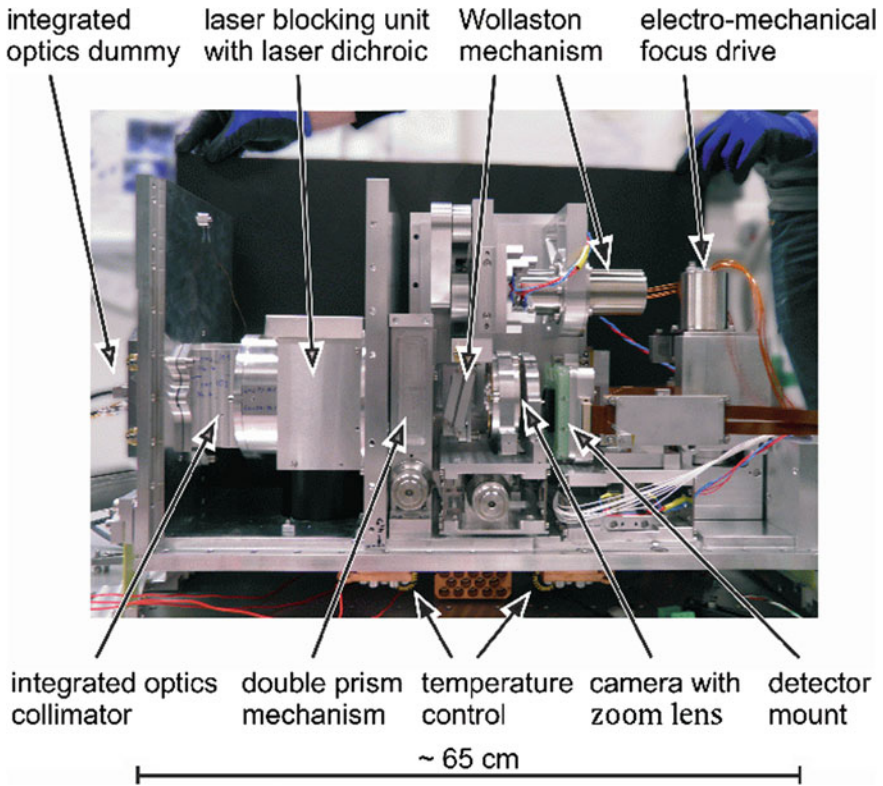


Fig. 7 The fringe tracking spectrometer of GRAVITY being under construction at the University of Cologne [144]

model or spiral arms scenarios. However, a clear wander between alternating centroid positions during the flares will strongly support the idea of bright long-lived spots occasionally orbiting the central black hole.

Acknowledgments In this article we summarize contributions on the Galactic Center, held at the conference ‘Equations of Motion in Relativistic Gravity’ at the Physikzentrum Bad Honnef, Bad Honnef, Germany, [(February 17–23, 2013) <http://www.puetzfeld.org/eom2013.html>] and the COST action MP0905—“Black Holes in a Violent Universe”—Galactic Center GC2013 conference (<http://www.astro.uni-koeln.de/gc2013> and <http://galacticcenter.iaa.es/>) titled ‘The Galactic Center Black Hole Laboratory’ held at the Instituto de Astrofísica de Andalucía (IAA-CSIC) in Granada, Spain (November 19–22, 2013). The main goal of the COST conference and the contribution in Bad Honnef was to focus on the new observational and theoretical results that are linked to the Galactic Center and to point out possible consequences for our understanding of galactic nuclei in general. The COST conference brought together scientists working on all mass-scales of Black Holes (Quantum to super-massive), observers and theoreticians as well as particle physicists.

We are grateful to D. Merritt for constructive comments on the draft thank especially the Local Organizing Committees of the Bad Honnef and the Granada conferences. For Bad Honnef we thank the organizers D. Puetzfeld, C. Laemmerzahl, B. F. Schutz as well as the staff of the Physikzentrum

Bad Honnef, Bad Honnef, Germany. The Granada conference was hosted by and held at the Instituto de Astrofísica de Andalucía (IAA-CSIC), Spain. We thank especially the Local Organizing Committee at the IAA-CSIC that was lead by Dr. Antxon Alberdi. The Granada conference was also closely linked to and substantially supported by the COST Action MP1104—“Polarization as a tool to study the Solar System and beyond”, the FP7 action “Probing Strong Gravity by Black Holes Across the Range of Masses” [FP7-SPACE-2012-1 (FP7-312789)], and the collaborative research center SFB956 “Conditions and Impact of Star Formation—Astrophysics, Instrumentation and Laboratory Research”. We also thank RadioNet for support. We are also grateful to all SOC members of the Granada conference: Vladimir Karas, Michal Dovciak, Devaky Kunneriath, Delphine Porquet, Andreas Eckart, Silke Britzen, Anton Zensus, Michael Kramer, Wolfgang Duschl, Antxon Alberdi, Rainer Schödel, Murat Hüdaver, Carole Mundell, Farhad Yusef-Zadeh, Andrea Ghez, Mark Morris. This work was supported in part by the Deutsche Forschungsgemeinschaft (DFG) via the Cologne Bonn Graduate School (BCGS), the Max Planck Society through the International Max Planck Research School (IMPRS) for Astronomy and Astrophysics, as well as special funds through the University of Cologne.

References

1. M. Zamaninasab et al., *A&A* **510**, 3 (2010)
2. M. Zamaninasab et al., *MNRAS* **413**, 322 (2011)
3. M. Zamaninasab et al., *ASPC* **439**, 323 (2011)
4. A. Eckart et al., *A&A* **455**, 1 (2006)
5. A.E. Broderick, A. Loeb, *MNRAS* **363**, 353 (2005)
6. T. Yoshikawa, S. Nishiyama, *ApJ* **778**, 92 (2013)
7. S. Gillessen et al., *Nature* **481**, 51 (2012)
8. K. Phifer et al., *ApJ* **773**, L13 (2013)
9. F. Eisenhauer, *IAUS* **261**, 269 (2010)
10. A. Ghez, *Astro2010: the astronomy and astrophysics decadal survey. Science White Papers* **89** (2009)
11. G. Witzel et al., *ApJS* **203**, 18 (2012)
12. A. Eckart et al., *A&A* **537**, 52 (2012)
13. A. Eckart et al., *SPIE* **8445**, 1 (2012)
14. F.K. Baganoff et al., *ApJ* **591**, 891 (2012)
15. F.K. Baganoff et al., *Nature* **413**, 45 (2001)
16. D. Porquet et al., *A&A* **407**, L17 (2003)
17. D. Porquet et al., *A&A* **488**, 549 (2008)
18. M.A. Nowak et al., *ApJ* **759**, 95 (2012)
19. M.A. Nowak et al., *ApJ* **786**, 46 (2014)
20. K. Mori et al., *ApJ* **770**, L23 (2013)
21. R.M. Shannon, S. Johnston, *MNRAS* **435**, L29 (2013)
22. N. Rea et al., *ApJ* **775**, L34 (2013)
23. G.C. Bower, H. Falcke, D.C. Backer, *ApJ* **523**, L29 (1999)
24. G.C. Bower et al., *ApJ* **521**, 582 (1999)
25. G.C. Bower, *Ap&SS* **288**, 69 (2003)
26. J.P. Macquart, *ApJ* **646**, L111 (2006)
27. A. Eckart et al., *A&A* **492**, 337 (2008)
28. F. Yusef-Zadeh, *ApJ* **650**, 189 (2006)
29. A. Eckart et al., *A&A* **450**, 535 (2006)
30. J. Dexter, PCh. Fragile, *MNRAS* **432**, 2252 (2013)
31. J. Dexter, B. Kelly, G.C. Bower, D.P. Marrone, *MNRAS* **442**, 2797 (2014)
32. A.P. Marscher, *ApJ* **264**, 296 (1983)

33. R.J. Gould, A&A **76**, 306 (1979)
34. J. Dexter et al., ApJ **717**, 1092 (2010)
35. M. Moscibrodzka, H. Falcke, A&A **559**, L3 (2013)
36. A. Eckart et al., A&A **479**, 625 (2008)
37. F. Yuan, Z.-Q. Shen, L. Huang, ApJ **642**, L45 (2006)
38. R. Narayan et al., ApJ **492**, 554 (1998)
39. H. Falcke, S. Markoff, A&A **362**, 113 (2000)
40. D.P. Marrone et al., ApJ **682**, 373 (2008)
41. M. Valencia-S et al., JPhCS **372**, 2073 (2012)
42. V. Karas, M. Dovciak, M. Zamaninasab, A. Eckart, ASPC **439**, 344 (2011)
43. K. Akiyama, R. Takahashi, M. Honma, T. Oyama, H. Kobayashi, PASJ **65**, 91 (2013)
44. K. Akiyama et al., (2013). [arXiv:1311.5852](#) [astro-ph.GA]
45. A. Eckart et al., A&A **551**, 18 (2013)
46. A. Eckart et al., (2013). [arXiv:1311.2743](#) [astro-ph.GA]
47. A. Eckart et al., (2013). [arXiv:1311.2753](#) [astro-ph.GA]
48. B. Jalali, I. Pelulessy, A. Eckart, (2013). [arXiv:1311.4881](#) [astro-ph.GA]
49. L. Meyer et al., (2013). [arXiv:1312.1715](#) [astro-ph.GA]
50. C. J. Chandler, L.O. Sjouwerman. The Astronomer's Telegram, No. 5727 and related ones (2014)
51. R. Narayan, F. Özel, L. Sironi, ApJ **757**, L20 (2012)
52. P. Crumley, P. Kumar, MNRAS **436**, 1955 (2013)
53. A. Sadowski et al., MNRAS **432**, 478 (2013)
54. F. Yusef-Zadeh, M. Wardle, ApJ **770**, L21 (2013)
55. F. Yusef-Zadeh et al., ApJ **767**, L32 (2013)
56. R.V. Shcherbakov, ApJ **783**, 31 (2014)
57. H. Falcke, S.B. Markoff, Class. Quantum Gravity **30**, 244003 (2013)
58. Th. Boller, A. Müller, *Exciting Interdisciplinary Physics*. FIAS Interdisciplinary Science Series (Springer International Publishing, Switzerland, 2013), p. 293. ISBN 978-3-319-00046-6
59. A.E. Broderick, T. Johannsen, A. Loeb, D. Psaltis, ApJ **784**, 7 (2014)
60. V.L. Fish et al., AAS, 22344304 (2014)
61. Z.-Q. Shen, F. Gao, L. Huang, ApJ **745**, L20 (2012)
62. A.E. Broderick et al., ApJ **738**, 38 (2011)
63. A.E. Broderick et al., ApJ **735**, 110 (2011)
64. V.L. Fish et al., ApJ **727**, L36 (2011)
65. R.-S. Lu et al., A&A **525**, 76 (2011)
66. L. Huang et al., MNRAS **379**, 833 (2007)
67. V. Karas, O. Kopacek, D. Kunneriath, Class. Quantum Gravity **29**, 035010 (2012)
68. V. Karas, O. Kopacek, D. Kunneriath, Int. J. Astron. Astrophys. **3**, 18 (2013)
69. V.S. Morozova, L. Rezzolla, B.J. Ahmedov, Phys. Rev. D **89**, 104030 (2014)
70. S. Koide, K. Arai, ApJ **682**, 1124 (2008)
71. J. Frank, M.J. Rees, MNRAS **176**, 633 (1976)
72. A.M. Ghez et al., The Astronomer's Telegram. No. 6110 (2014)
73. L. Meyer et al. AAS Meeting No. 223, No. 108.07 (2014)
74. N. Scoville, A. Burkert, ApJ **768**, 108 (2013)
75. A. Ballone et al., ApJ **776**, 13 (2013)
76. J.D. Monnier, R. Millan-Gabet, ApJ **579**, 694 (2002)
77. A. Burkert et al., ApJ **750**, 58 (2012)
78. M. Schartmann et al., ApJ **755**, 155 (2012)
79. M. Zajacek, V. Karas, A. Eckart, A&A **565**, A17 (2014)
80. R.V. Shcherbakov, F.K. Baganoff, ApJ **716**, 504 (2010)
81. K. Muzic et al., A&A **521**, 13 (2010)
82. Rauch et al., A&A **551A**, 35R (2013)
83. A. Eckart, R. Genzel, MNRAS **284**, 576 (1997)

84. N. Sabha et al., *A&A* **545**, 70 (2012)
85. S. Zucker et al., *ApJ* **639**, L21 (2006)
86. S. Gillessen et al., *ApJ* **707**, L114 (2009)
87. F. Eisenhauer et al., *ApJ* **597**, L121 (2003)
88. G.F. Rubilar, A. Eckart, *A&A* **374**, 95 (2001)
89. D. Merritt, *Dynamics and Evolution of Galactic Nuclei* (Princeton University Press, Princeton, 2012)
90. S. Gillessen et al., *ApJ* **692**, 1075 (2009)
91. N. Mouawad et al., *ANS* **324**, 315 (2003)
92. N. Mouawad et al., *AN* **326**, 83 (2005)
93. L. Subr, V. Karas, J.-M. Hure, *MNRAS* **354**, 1177 (2004)
94. K.P. Rauch, S. Tremaine, *New A* **1**, 149 (1996)
95. C. Hopman, T. Alexander, *ApJ* **645**, 1152 (2006)
96. E. Eilon, G. Kupi, T. Alexander, *ApJ* **698**, 641 (2009)
97. L. Subr, V. Karas, *A&A* **433**, 405 (2005)
98. P. Chang, *MNRAS* **393**, 224f (2009)
99. X. Chen, P. Amaro-Seoane, (2014) [arXiv:1401.6456](https://arxiv.org/abs/1401.6456) [astro-ph.GA]
100. F. Antonini, D. Merritt, *ApJ* **763**, L10 (2013)
101. D. Merritt et al., *Phys. Rev. D* **84**, 044024 (2011)
102. D. Merritt et al., *Phys. Rev. D* **81**, 062002 (2010)
103. C.M. Will, *ApJ* **674**, L25 (2008)
104. M.B. Davies et al., *ASPC* **439**, 212 (2011)
105. R.P. Church et al., *PASA* **26**, 92 (2009)
106. J. Dale et al., *MNRAS* **393**, 1016 (2009)
107. H.B. Perets, A. Mastrobuono-Battisti, (2014) [arXiv:1401.1824](https://arxiv.org/abs/1401.1824) [astro-ph.GA]
108. A. Mastrobuono-Battisti, H.B. Perets, *ApJ* **779**, 85 (2013)
109. J. Haas, L. Subr, *J. Phys. Conf. Ser.* **372**, 2059 (2012)
110. L. Subr, J. Haas, *J. Phys. Conf. Ser.* **372**, 2018 (2012)
111. J. Haas, L. Subr, D. Vokrouhlicky, *MNRAS* **416**, 1023 (2011)
112. A. Feldmeier, N. Lützgendorf, N. Neumayer, *A&A* **554**, 63 (2013)
113. D. Psaltis, *ApJ* **759**, 130 (2012)
114. L.G. Spitler et al., *ApJ* **780**, L3 (2014)
115. K.J. Lee et al., *The Astronomer's Telegram*. No. 5064 (2013)
116. R.P. Eatough, H. Falcke, R. Karuppusamy, *Nature* **501**, 391 (2013)
117. R.P. Eatough et al., *The Astronomer's Telegram*. No. 5027 (2013)
118. F. Yusef-Zadeh et al., *ApJ* **702**, 178 (2009)
119. F. Yusef-Zadeh et al., *ApJ* **725**, 1429 (2010)
120. S. Nayakshin, J. Cuadra, V. Springel, *MNRAS* **379**, 21 (2007)
121. B. Czerny et al., *A&A* **555**, A97 (2013)
122. M. Su, T.R. Slatyer, D.P. Finkbeiner, *ApJ* **724**, 1044 (2010)
123. K. Zubovas, S. Nayakshin, *MNRAS* **424**, 666 (2012)
124. J. Bland-Hawthorn et al., *ApJ* **778**, 58 (2013)
125. R.M. Crocker, *MNRAS* **423**, 3512 (2012)
126. R.M. Crocker, F. Aharonian, *Phys. Rev. Lett.* **106**, 1102 (2011)
127. R.M. Crocker et al., *MNRAS* **411**, L11 (2011)
128. S. Garcia-Burillo, F. Combes, *J. Phys. Conf. Ser.* **372**, 2050 (2012)
129. S. Garcia-Burillo et al., *A&A* **539**, 8 (2012)
130. I. Marquez, J. Masegosa, *RMxAC* **32**, 150 (2008)
131. S. Garcia-Burillo et al., *A&A* **407**, 485 (2003)
132. M. Krips et al., *A&A* **464**, 553 (2007)
133. L. Moser et al., (2013) [arXiv:1309.6921](https://arxiv.org/abs/1309.6921) [astro-ph.CO]
134. C.G. Mundell et al., *ApJ* **583**, 192 (2003)
135. C.G. Mundell et al., *ApJ* **614**, 648 (2004)
136. C.G. Mundell et al., *New Astron. Rev.* **51**, 34 (2007)

137. C.G. Mundell et al., *ApJ* **703**, 802 (2009)
138. F. Combes et al., *A&A* **565**, A97 (2014)
139. T. Heckman, P. Best, *Annu. Rev. Astron. Astrophys.* **52**, 589 (2014)
140. P. Soffitta et al., *SPIE* **8443**, 1 (2012)
141. P. Soffitta et al., *ExA* **36**, 523 (2013)
142. J. Dexter et al., *J. Phys. Conf. Ser.* **372**, 012023 (2012)
143. F. Aharonian et al., *Pathway to the square kilometer array*, The German White Paper (2013)
144. C. Straubmeier et al., *SPIE* **8445**, 2 (2012)
145. F. Eisenhauer et al., *Msngr* **143**, 16 (2011)
146. A. Eckart et al., *SPIE* **7734**, 27 (2010)

Extreme Mass Ratio Inspirals: Perspectives for Their Detection

Stanislav Babak, Jonathan R. Gair and Robert H. Cole

Abstract In this article we consider prospects for detecting extreme mass ratio inspirals (EMRIs) using gravitational wave (GW) observations by a future space borne interferometric observatory eLISA. We start with a description of EMRI formation channels. Different formation scenarios lead to variations in the expected event rate and predict different distributions of the orbital parameters when the GW signal enters the eLISA sensitivity band. Then we will briefly overview the available theoretical models describing the GW signal from EMRIs and describe proposed methods for their detection.

1 Introduction

Extreme mass ratio inspirals (EMRIs) arise following the capture of a small compact object (CO)—a white dwarf, neutron star or stellar mass black hole—by a massive black hole (MBH) in the centre of a galaxy. The astrophysical processes that lead to the formation of EMRIs are described in detail in Sect. 2. The inspiralling CO loses energy and angular momentum through emission of gravitational radiation, and the initially wide and very eccentric orbit gradually shrinks and becomes more circular. EMRIs are among the most interesting gravitational wave (GW) sources that could be observed by the proposed eLISA detector. eLISA (evolving Laser Space Interferometer Antenna) is a space-based gravitational wave detector which is scheduled for launch in 2034. It will be sensitive to GWs in the frequency range 0.1–100 mHz. Sources in this band include the mergers of massive black hole binaries, which will be observable up to a redshift $z = 20$, and numerous white dwarf

S. Babak (✉)

Albert Einstein Institute, Am Muehlenberg 1, 14476 Golm, Germany

e-mail: stba@aei.mpg.de

J.R. Gair · R.H. Cole

Institute of Astronomy, University of Cambridge, Cambridge CB3 0HA, UK

e-mail: jrg23@cam.ac.uk

R.H. Cole

e-mail: rhc26@ast.cam.ac.uk

binaries in the Milky Way, in addition to EMRIs. We will discuss the event rate and the expected precision of parameter estimation for EMRI sources in Sect. 2.

During an EMRI, the CO typically spends 10^5 – 10^6 orbital cycles in the eLISA band before plunging into the central MBH. We need to model the phase of GW signal from EMRIs with an accuracy of a fraction of a cycle in order to detect the signal and correctly extract the parameters of the binary system. This is a challenging problem, which has not yet been solved in full. Due to the extreme mass ratio, $m/M \sim 10^{-4} - 10^{-6}$, we can treat the problem perturbatively, considering the field of the CO and the emitted GWs as a small perturbation of the background spacetime of the central MBH. At the leading orders in mass ratio the internal structure of a CO is not important and so the CO is conventionally treated as a delta-function. As often happens in such an approximation, the self-field is divergent at the position of the CO, and requires proper treatment (regularization) [1]. The resulting perturbation has the form of a tail expression, and depends on an integral over the entire past history of the CO's trajectory. In the limit that the mass ratio goes to zero, the motion is described by a geodesic. However, the mass of a CO is small but not zero and due to interaction of the self field of the particle with a background, the trajectory slowly deviates from a geodesic path [2]. This can be described effectively as the action of a force (self-force) on the inspiraling object. In practice, the geodesic trajectory is used to compute the tail integral entering the self-force, and the resultant force is used to update the geodesic trajectory accordingly. In Sect. 3, we will summarize various ways to compute the GW signal from EMRIs and describe how the evolution of the orbital motion can be described using an osculating elements approach. The CO may also be spinning and this spin is coupled to the background curvature and alters the trajectory of the CO, forcing it to deviate from the corresponding geodesic of a non-spinning body. The trajectory of a spinning particle (in the limit of vanishing mass ratio) is described by the Mathisson-Papapetrou equation. Attaching a spin to a point particle is not uniquely defined, leaving a freedom to choose the dipole moment of a body (see [3] for a description of spinning objects in the weak field approximation). This freedom manifests itself through the need to specify a spin supplementary condition (SSC) in order to obtain a unique solution to the equations of motion. In order to understand these complications, we consider in Sect. 3.3 the motion of a spinning particle in de Sitter space time. This space time possesses a non-trivial curvature but is still fully symmetric. For more details on the computation of the self-force and on the Mathisson-Papapetrou equations we refer to other articles in this issue.

Last, but not least we want to consider the question of detectability of GW signals from EMRIs. The GWs generated by an EMRI system are characterized by 14 parameters: two masses m , M , the dimensionless spin of the MBH, a , and its orientation, θ_K , ϕ_K ; six parameters describing the CO's position and velocity at some fiducial time or equivalently the instantaneous shape and phase of the orbit at that time (eccentricity e , inclination of the orbital plane to the spin of MBH ι , semi-latus rectum p and the initial phases ϕ_r , ϕ_θ , φ corresponding to the three coordinate degrees of freedom); the sky location of the source, θ , ϕ , and its luminosity distance, D_L . Many of these parameters are highly correlated. The GW signal comprises a

superposition of orbital harmonics, with the number of harmonics and their relative strength strongly dependent on the eccentricity and binary orientation. The strength of the signal observed in the detector varies with time as eLISA moves around the sun (amplitude modulation) and the relative motion of the detector and the source induces a time-dependent Doppler modulation of the phase. The main challenge in detecting EMRIs is the multi-modality of the likelihood. The likelihood can be seen as a hyper-surface embedded in the 14-dimensional parameter space. It has multiple strong maxima and the main challenge is to find the highest (global) maximum. In Sect. 4 we describe algorithms to do this which were successfully demonstrated on the Mock LISA data challenges [4].

Throughout this paper we use geometrical units $G = c = 1$.

2 Astrophysics of Extreme Mass Ratio Inspirals

In this section we will consider possible channels leading to EMRI formation, the expected number of EMRI events that will be observed for eLISA and the likely accuracy with which eLISA will constrain their parameters. Then we will briefly summarize some of the potential impact of EMRI detections for astrophysics and fundamental physics.

2.1 Formation of EMRIs

The “extreme mass ratio” refers to the fact that the mass of the CO is of order of $1\text{--}10M_\odot$, while the mass of the central (capturing) object is in the range $10^5\text{--}10^7M_\odot$. Current astrophysical observations indicate that massive compact objects of this kind are present in the nuclei of all sufficiently massive galaxies for which the central part can be resolved. The best example is the nucleus of the Milky Way, in which a few dozen bright O-B stars (so called S-stars) have been observed in Keplerian orbits around a central object with an estimated mass of $\sim 4 \times 10^6M_\odot$. In addition, the compactness of this object suggests that it must be a massive black hole.

These massive objects in the centres of galaxies are typically surrounded by clusters of stars. In the “standard” picture of EMRI formation, the stars are spherically distributed around the MBH (which should be approximately true for sufficiently large distances) and dense enough for efficient 2-body relaxation, i.e., mutual gravitational deflection and contact collisions. The timescale for this process, the relaxation time t_{rlx} , is defined as the time required to change the angular momentum of a star by an amount J_c , where J_c is the angular momentum of a star on a circular orbit with the same semi-major axis. A smaller t_{rlx} implies that stars can be more easily deflected on to very eccentric orbits with a small periapsis passage. If a CO object on an initially wide orbit is perturbed onto such a trajectory, it will lose energy to GW bursts emitted near periapsis (r_p) and its orbit will gradually shrink. While the semi-major axis is very large, the CO can still efficiently interact with other stars at the apoapsis and could be either deflected onto a plunging orbit with $r_p < 8M$

or onto a wide orbit which does not emit appreciable GW radiation. To become an observable EMRI, the CO must remain on the highly eccentric orbit until its period becomes smaller than $\sim 10^3\text{--}10^4$ s, at which point it is continually radiating GWs in the eLISA sensitivity band. While we will be primarily interested in such EMRIs here, the bursts of GWs produced during periapsis passages in the early stages of the process could also be potentially detected by eLISA if the event is in the nucleus of nearby galaxies [5].

When the stars interact gravitationally, they tend to divide the kinetic energy equally and, while equipartition is not reached in practice, this process causes more massive objects to sink deeper in the potential well of the MBH. This process is called mass segregation. As a result we expect stellar mass black holes to form a steep power-law density cusp around the MBH $n(r) \sim r^{-\alpha}$ with $\alpha \simeq 1.7 - 2.0$, which dominates for $r < 0.1\text{pc}$. The lighter stellar species form shallower density profiles with $\alpha \simeq 1.3 - 1.5$ [6]. The relaxation time is inverse proportional to the density of the CO and it should therefore be smaller for the stellar mass black holes.

In order for an object to become an EMRI, it should efficiently dissipate energy through GW emission, and have a sufficiently low probability to be deflected onto a different orbit. This condition implies that the time scale for orbital decay by GW emission, t_{GW} , should be smaller than $(1 - e)t_{rlx}$, where e is orbital eccentricity. Once the orbital period reaches $P < 10^4\text{s}$, the CO completely decouples from the cusp, which happens for orbits with semi-major axis $a_{EMRI} \sim 0.05\text{pc}$.

For typical orbits around an MBH, the number of stars enclosed by the orbit is rather small and so the gravitational potential created by the “field” stars is not a smooth symmetric function. This gives rise to a torque acting on a CO on an orbit with semi-major axis a_{CO} of $\tau \sim \sqrt{Nm_*/a_{CO}}$, where N is a number of field stars with mass m_* inside the CO orbit. If the precession of the CO orbit is slow compared to the timescale over which the distribution of field stars changes significantly, the CO experiences a nearly constant torque over some time. This mechanism, known as resonant relaxation, changes the angular momentum of the CO, but not its energy. The characteristic time scale associated with resonant relaxation, t_{RR} , is significantly smaller than t_{rlx} and so this process can significantly boost the EMRI event rate. Resonant relaxation plays an important role for orbits with $a_{CO} \leq a_{EMRI}$ [7–10]. However, for COs on eccentric orbits with small perhaps radii, the relativistic (GR) precession can be very high, which effectively destroys the resonant relaxation effect. The point at which this occurs is known as the “Schwarzschild barrier” [11]. The existence of this barrier means that resonant relaxation is not as effective at boosting EMRI rates as one might first think, although if the MBH has significant spin then the impact of the “Schwarzschild barrier” is somewhat diminished due to the lower value of the plunge periapsis for prograde orbits [12]. In this case, COs that would normally be considered as plunging and hence undetectable around a Schwarzschild MBH actually perform many cycles in the eLISA band and may contribute significantly to the event rate [13].

In this picture, the critical thing for having a high EMRI rate is to have compact objects in the “loss-cone” (orbits with impact parameter sufficiently small that they can be captured or tidally disrupted by the MBH). Several channels have been

suggested that can replenish the loss-cone and thereby significantly boost the EMRI rate, including triaxiality of the potential (non-spherical galactic nuclei) [14] or the presence of massive perturbers (such as intermediate mass BHs, and/or molecular clouds) in the vicinity of the orbits [15].

The complex dynamics of this standard capture scenario for EMRI formation means that the astrophysical event rates are very uncertain. To estimate event rates we will use a current best guess of 400Gyr^{-1} for Milky Way-like black holes, dominated by EMRIs in which the CO is a black hole. This rate is taken from [16].

As well as this standard mechanism for EMRI formation, there are two other plausible channels.

Tidal binary disruption. It is possible that within the radius of influence of a MBH there is a binary fraction of at least a few percent [17]. If a binary approaches the MBH it can be tidally disrupted and, if this happens, one star is ejected at very high velocity while the other star becomes tightly bound to the MBH. The captured CO is expected to end up on an orbit with a semi-major axis of a few hundred AU and a pericentre distance of a few to tens of AU, implying that it will circularise by the time it enters the eLISA frequency band [17, 18]. This is a distinct feature of this formation channel, since in the standard scenario we expect the EMRIs to have a significant residual eccentricity even at plunge [19], $e_{pl} \sim 0.1 - 0.3$. We observe in the Milky Way so called “hyper-velocity” stars [20], which are moving away from the galactic centre with large velocities. The best current explanation for the presence of short-lived S-stars in the vicinity of the Milky Way MBH is that they came there following the tidal disruption of binaries, while the observed hyper-velocity stars are the thrown away companions [21].

Formation of stellar remnants in a disk. Observation of active galactic nuclei suggests the presence of a circum-nuclear gaseous disk accreting onto the MBH. If the disk is thick and sufficiently massive, the outer part could fragment and form stars. If migration through the disk is sufficiently slow, stars formed in this way could evolve to form compact object remnants (neutron star or black hole) which subsequently spiral into the MBH as an EMRI in the equatorial plane (the accretion disk, at least its inner parts, is expected to be aligned with the MBH’s equatorial plane [22]). The interaction with the gas is also likely to keep the orbit of a CO close to circular, so the distinct feature of this channel of EMRI formation is a circular orbit in the black hole equatorial plane.

By measuring the orbital parameters we will be able to say which of these three channels provides the most likely explanation for how the EMRI was formed. For more details on the dynamics of galactic nuclei we refer the reader to the comprehensive review [23].

2.2 Expected Event Rate Estimation

In this section we follow [24] and briefly outline how the expected event rate of EMRIs observed by eLISA can be estimated. To make this estimation we require

an intrinsic event rate $\mathcal{R}(M, a, \mu)$, where M is the mass of the MBH, a its spin in units of M and $\mu = m/M$ is the mass ratio. The intrinsic event rate tells us how often EMRIs are formed (i.e., how often they enter the eLISA sensitivity band) per galaxy hosting a MBH with parameters M, a . The mass ratio parameter tells us the nature of a CO, i.e., whether it is a stellar mass BH, neutron star or white dwarf. As discussed in the previous subsection, due to mass segregation we expect stellar mass BHs to be the most likely candidate for EMRIs, so we choose a canonical value for the CO mass of $m = 10M_\odot$. We will normalize the mass of the MBH by the mass expected for a Milky Way type galaxy $M_{MW} \approx 3 \times 10^6 M_\odot$. So far we do not have information about the distribution of the spin of MBHs of this mass. X-ray observations of some active galactic nuclei provide information about the spin of accreting MBHs in the centre, but those black holes are of higher mass $> 10^7 M_\odot$ and embedded in the gaseous circum-nuclear disk. In addition all present estimations of the spin are heavily model dependent and could vary significantly depending on the underlying assumptions [25]. Therefore, here we assume a uniform distribution of the spin within its physical range $a \in (-1, 1)$. The estimation of the intrinsic event rate is a very challenging task, as described above and in more detail in [23], which depends quite heavily on the underlying assumptions about the efficiency of mass segregation, the relative importance of different EMRI formation channels and the interplay between resonant relaxation and the “Schwarzschild barrier”. Here we adopt the estimate derived in [16] which for stellar mass BHs is

$$\mathcal{R} = 400 \text{Gyr}^{-1} \left(\frac{M}{3 \times 10^6 M_\odot} \right)^\beta \quad (1)$$

where $\beta \approx 0.19$.

If the duration of EMRI signals was significantly shorter than the observation time, then the observed event rate would be determined by computing the distance at which the signal-to-noise ratio (SNR) equals some detection threshold ρ_{thr} and then multiplying the rate per unit volume by the volume contained by that distance, assuming a uniform distribution of EMRIs in the local Universe. However, EMRIs are long-lived, and the SNR can be accumulated for as much of the inspiral as coincides with the eLISA observation. Fixing all the parameters of the EMRI, we can compute the SNR as a function of the time left to plunge, t_{pl} . As we increase t_{pl} from zero, the SNR first increases, then reaches a maximum before starting to decrease. There is a decrease of SNR for large t_{pl} because the finite observation time means that we are ultimately only observing systems that are rather wide, with not very efficient GW emission, and with emission primarily at low frequencies where acceleration noise rises rather steeply. This means that if an EMRI is at all detectable, the SNR as a function of t_{pl} intersects the line $\text{SNR} = \rho_{thr}$ at two times, t_{early} , t_{late} , and we can define the EMRI observable lifetime as $\tau(\lambda_i) = t_{late}(\lambda_i) - t_{early}(\lambda_i)$, where λ_i corresponds to all the other parameters of the EMRI (besides t_{pl}) which we have fixed. If EMRIs plunge at a rate \mathcal{R} per year in a particular galaxy, then $\tau\mathcal{R}$ gives the expected number of events from that galaxy (after appropriate averaging over parameters λ_i).

Among all parameters describing the EMRI system the most important are M , a , and we denote the remaining parameters as $\hat{\lambda}_i$. We define $\mathcal{N}(M, a, z)dMda$ as the number of MBHs per comoving volume with mass $M \in [M, M + dM]$, spin $a \in [a, a + da]$, and at redshift z . We make two further assumptions (i) that the mass and spin distributions are independent; and (ii) that the distribution of MBH mass and spin are independent of redshift. The first assumption reflects our level of ignorance, and the second assumption is reasonable given how far we can observe EMRIs (with eLISA we will be able to see EMRIs up to $z_{\max} \approx 0.7$). In this range we can ignore the evolution of masses and spins with z . Under these assumptions $\mathcal{N}(M, a, z)dMda = (dn/d \ln M)(M)d \ln M p(a)da$, where $p(a)$ is the probability distribution function for the spin $\int p(a)da = 1$. As described above, we assume this is uniform in our calculations, but we keep it here in the equation for completeness.

The expected event rate is then

$$N_{eLISA} = \left\langle \int_{z=0}^{\infty} dz \int_{M_{low}}^{M_{high}} d \ln M \int_{a=-1}^1 da \mathcal{R}(M, a) \tau(M, a, z, \hat{\lambda}_i) \frac{dn}{d \ln M}(M) p(a) \frac{dV_c}{dz} \right\rangle_{\hat{\lambda}_i} \quad (2)$$

Here $(dV_c/dz)dz$ is the comoving volume in the redshift range $[z, z + dz]$. The triangular brackets denote the averaging over other EMRI parameters $\hat{\lambda}_i$. We note that in practice the intrinsic event rate could also depend on some parameters from the set $\hat{\lambda}_i$ (depending on the channel of EMRI formation). The mass function $(dn/d \ln M)$ can be deduced from measured galaxy luminosity functions using the observed $L - \sigma$, $M - \sigma$ correlations. In the range of interest to eLISA, these functions are approximately flat [26], so we adopt

$$\frac{dn}{d \ln M} = n_0 \left(\frac{M}{3 \times 10^6 M_{\odot}} \right)^{\alpha} \quad (3)$$

with canonical values $n_0 = 0.002 \text{ Mpc}^{-3}$, $\alpha = 0$. If we assume these canonical values, with $\beta = 0.19$, a mission duration of 2 years and a detection threshold of $\rho_{thr} = 20$, we estimate that eLISA would observe 25–50 events in two years [27, 28]. This spread in the predicted number of events comes from uncertainties in the waveform model and system parameters, but a much larger uncertainty, which is not taken into account here, arises from the uncertainty in the true value of \mathcal{R} .

2.3 Science Return from Observing GW Signals from EMRIs

Detection of EMRIs and measurement of their parameters provides unique astrophysical data which cannot be obtained by any other means. We expect to be able to learn information about stellar populations in the centre of the Milky Way in the

future by observing pulsars in the nuclear stellar cluster region using the SKA [29]. Inferring similar properties of other galaxies through observations of EMRIs will also us to compare the nucleus of the Milky Way with nuclei of other galaxies. The number of observed EMRI events and the mass distribution of the COs will tell us about the physics of mass segregation, the masses and spins of stellar mass compact objects and about the steepness of the stellar cusps in the centres of galaxies. In addition, EMRI observations will provide precise measurements of MBH masses and spins in a new mass range. EMRIs will probe galaxies containing black holes with masses 10^5 – $10^7 M_\odot$, and such galaxies tend to be of lower mass and not particularly luminous in the electromagnetic spectrum. Extracting information about the nuclei of those galaxies is therefore very challenging, if not impossible, using electromagnetic observations and eLISA therefore has tremendous potential to inform us about these systems. Observations show that the masses of black holes in galactic nuclei correlate with the mass, luminosity and the stellar velocity dispersion of their host galaxy [30]. These correlations imply that black holes evolve along with their hosts throughout cosmic time, but it is not yet known if this coevolution extends down to the lowest galaxy and black hole masses, since those systems may have differences in the accretion properties [31], dynamical effects [32], or cosmic bias [33]. eLISA observations of EMRIs will significantly improve our knowledge of the MBH mass function (e.g., inferring the parameter α in eqn. [3]), as well as allowing us to measure the intrinsic event rate (for example constraining the parameter β in eqn. [1]), determine the relative importance of different channels of EMRI formation and measure the spatial distribution (relative to the MBH) of different types of CO. This is made possible by the ultra-precise determination of EMRI parameters with GW observations. In Fig. 1 we show how accurately we expect to measure the most important parameters: MBH mass (M) and spin (a), CO mass (m), orbital eccentricity just before the plunge (end of inspiral) (e_{pl}). The last parameter, ΔQ , is a possible deviation in the MBH quadrupole moment away from the Kerr value, which will be discussed at the end of this subsection.

In addition an observation of an EMRI will allow us to determine the luminosity distance to the source (D_L) with an accuracy of $\leq 1\%$ and to localize the source on the sky to about 0.2 square degrees. Such a fantastic accuracy is achieved because the source is long lived—the CO spends 10^4 – 10^6 cycles in the close vicinity of a MBH. Using matched filtering we will be able to determine the phase of an EMRI to an accuracy of half a cycle, a fractional phase accuracy of 10^{-6} – 10^{-4} . All information about the binary system is encoded in the GW phase and so we can expect to make measurements of the intrinsic parameters to this same fractional accuracy. Measurements of the extrinsic parameters, such as sky localisation, are not as precise since these measurements come not from the phase but from the modulation of the GW signal (in amplitude and in phase) caused by eLISA’s orbital motion.

These precise phase measurements mean we can also use EMRIs to test the “no-hair” theorem: if the central massive compact object is indeed described by the Kerr metric, as general relativity predicts. The spacetime outside a stationary, axisymmetric object is fully determined by its mass, M_I , and current, S_I , multipole moments. Since these moments fully characterise the spacetime, the orbits of the

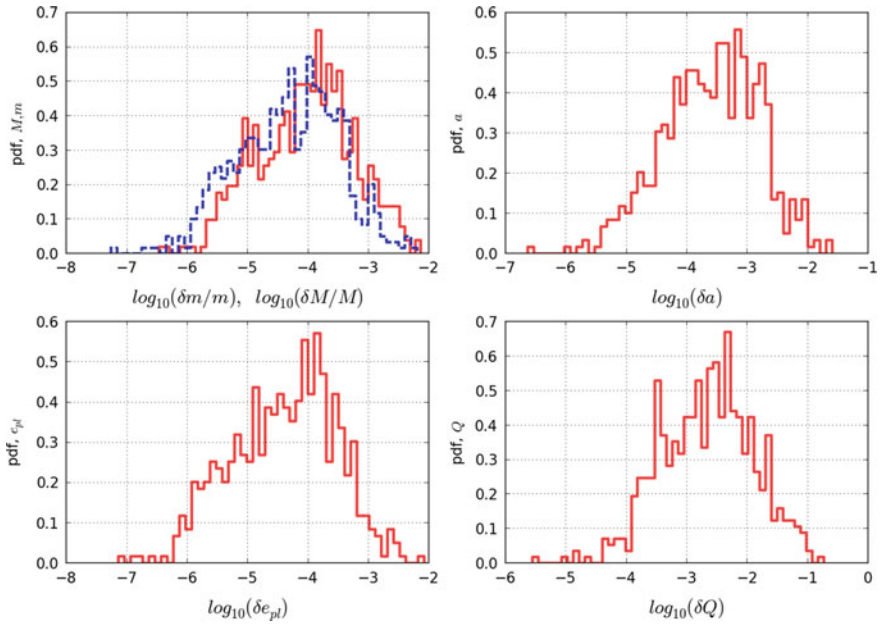


Fig. 1 Expected precision of parameter estimation from observed EMRI events, computed using the Fisher information matrix: MBH mass (M , dashed line), CO mass (m , solid line), MBH spin (a), orbital eccentricity before plunge (e_{pl}) and deviation of the MBH quadrupole moment from the Kerr value (Q)

smaller object and the gravitational waves it emits are determined by these multipole moments. The emitted GWs therefore encode a map of the spacetime structure and by observing these gravitational waves with eLISA we can precisely characterise the multipole structure of the central object. Extracting the moments from the EMRI waves is analogous to geodesy. If the central object is a Kerr black hole, then all multipole moments are determined by its mass and spin (“no-hair” theorem):

$$M_l + i S_l = (ia)^l M^{l+1}$$

If we can measure the first three moments we can therefore check whether the central object is consistent with being a Kerr black hole. Figure 1 shows that we should be able to measure a deviation in the mass quadrupole moment from the Kerr value, $Q = |M_2 - M_2^{Kerr}|$, to a precision of $\delta Q \approx (10^{-2} - 10^{-3})M^3$. EMRIs could therefore also serve as laboratories for testing fundamental physics. For more discussion on this topic we refer to [28, 34].

3 Modelling the GW Signal from EMRIs

For detection of EMRIs we will utilize matched filtering, this technique assumes that we can model the GW signal and then cross-correlate it with the data. The EMRI signal depends on 14 parameters (actually on 17 if we take into account the spin of CO), which we do not know a priori and need to infer from the measured data. To do this, we must generate many signals from a given model (templates) across the full, 14-D, parameter space to find the parameters that best fit the data (this set of parameters, which maximize the likelihood, are called “maximum likelihood estimators” of those parameters). We will describe the search procedure in detail in the next section.

The presence of noise in the data stream causes the best-fit parameters to differ from the true parameters of the GW signal. The size of this difference can be estimated using the Fisher information matrix, as shown in Fig. 1. If the data is analysed using an inaccurate model there will also be systematic errors in the parameter estimates, which could be larger than the statistical errors from detector noise. It is therefore important to accurately model the GW signal coming from EMRIs, to ensure reliable estimation of parameters and improve the detectability, since a mismatch between the signal and template will cause a drop in the SNR and decrease in the observed volume by $(\text{SNR}/\text{SNR}_{\text{optimal}})^3$.

In this section we will describe currently available models for EMRI signal and discuss their effectualness (if they are able to recover the optimal SNR) and faithfulness (if the systematic errors in parameter estimation is below the statistical errors due to presence of the noise). Note that effectualness does not imply faithfulness: a model could recover a significant fraction of the SNR with a large systematic bias in the parameters. In other words, the shift in the parameters from the true values could (partially) compensate for inaccuracies in the model.

3.1 Waveform Inventory

Unlike the inspiral of a comparable mass binary, the merger (here we call it plunge) of a CO with MBH and subsequent ring-down are suppressed by a factor of the mass-ratio and are therefore not observable by eLISA. We therefore only need to model the inspiral part of the signal up to a plunge. However, for the whole of the inspiral observable by eLISA, the CO is orbiting in the strong-field region close to the MBH and moving at ultra-relativistic speeds. This makes modelling an EMRI signal somewhat different from modelling GWs from a binary of two nearly-equal mass MBHs. Here we briefly outline some of the currently available models for GW signals from EMRIs. More detailed description can be found in other papers in this volume.

Post-newtonian expansion. The post-newtonian approach describes the GW signal as an expansion in velocity v . As mentioned above the CO in EMRI systems are fast

moving and spend 10^4 – 10^6 cycles in a regime where v is large. The EOB approach [35, 36] is the most suitable for modelling EMRIs by construction (the conservative dynamics reduces to the test-mass in the limit $m/M \rightarrow 0$), however the dissipative part (fluxes) are needed to a very high post-newtonian order, which is not currently known. In addition, the analytic expressions for the fluxes are known only for nearly circular and nearly equatorial orbits, while we expect EMRI orbits to be both eccentric and inclined [37].

Analytic “kludge” waveforms. This model was introduced primarily to study detection rates and parameter estimation for EMRIs [38]. The main advantage of these waveforms is that they are fast to generate, so they are suitable for large Monte-Carlo simulations, and they were extensively used to develop detection algorithms (see Sect. 4). This model is an extension of the work by Peters and Mathew [39], it represents emission from a CO in Keplerian orbit augmented by imposing (post-newtonian) relativistic precession of the orbital plane and the direction to perihelion. The dissipative evolution is taken from post-newtonian calculations. This model is not particularly accurate but it captures the main physical processes occurring in EMRIs.

Numerical “kludge” waveform, or semi-relativistic model. The idea of the numerical kludge waveforms is to combine an exact particle trajectory (up to inaccuracies in the phase space trajectory and conservative radiation reaction terms) with an approximate expression for the GW emission. By including the particle dynamics accurately, we hope to capture the main features of the waveform, even if we are using an approximation for the waveform construction. The idea was introduced in [40, 41] and was further evolved with some modifications in [42, 43].

The procedure to compute a numerical kludge waveform has two stages. Firstly, a phase-space inspiral trajectory is constructed, i.e., the sequence of geodesics that an inspiral passes through, by integrating prescriptions for the evolution of the six constants of the motion (energy, angular momentum, Carter constant and three initial phases). Initial work has used post-newtonian expressions (augmented by some consistency corrections and by fitting to solutions of the Teukolsky equations) to evolve these constants. This inspiralling trajectory is computed numerically thus the name “numerical kludge”. Once the trajectory has been constructed a waveform is generated by identifying the Boyer Lindquist coordinates along the trajectory with spherical-polar coordinates in a flat space time and applying weak-field GW emission formulae, in particular the quadrupole-octupole approximation:

$$\bar{h}^{jk} = \frac{2}{D_L} \left(\ddot{I}^{jk} - 2n_i \ddot{S}^{ijk} + n_i \ddot{M}^{ijk} \right) |_{t'=t-D_L}, \quad (4)$$

where I^{ik} , M^{ijk} are the mass quadrupole and octupole moments and S^{ijk} is the current quadrupole moment of the binary system, n^i is a unit vector pointing from MBH to the position of a CO, and overdots denote time derivatives. These waveforms are somewhat slower to generate as compared with the analytic kludge due to the numerical integration of the orbital trajectory, but it is far more faithful up to the last month or less (semilatus rectum $p \approx 6M$) before the plunge.

Adiabatic inspirals based on Teukolsky formalism. The very first framework for black hole perturbation theory in a Kerr background was the Teukolsky formalism [44], which encapsulates all gravitational radiative degrees of freedom in a single “master” wave equation (the “Teukolsky equation”) for the Weyl scalars, Ψ_0 and Ψ_4 . A key feature of this equation is that it admits separation of variables in the frequency domain, which effectively reduces it to a pair of ordinary differential equations. The Teukolsky equation has been solved in the frequency domain [45] and in the time domain [46], but both approaches assume the orbit that acts as the source of the perturbation is a geodesic. The rate of change in energy, angular momentum, Carter constant (averaged over several orbits) are evaluated from the gravitational wave field and then used to update the parameters of the geodesic in an adiabatic manner. This procedure misses the evolution of the other constants of motion (initial positions) as well as making the adiabatic assumption. As a result, the waveforms are not accurate on a very long time scale, but they are the most faithful model on time scales $\sim M^2/m$.

Self-force waveforms. An accurate description of the self-force and its derivation is given in other papers in this volume, so we only briefly mention it here. As mentioned above, the extreme mass ratio in an EMRI system allows the waveform to be determined using perturbation theory. The inspiralling object can be regarded as a small perturbation on the background spacetime of the central black hole, except very close to the small object. In the vicinity of the small object, the spacetime can be regarded as a Schwarzschild BH moving under the influence of an external tidal field due to the MBH. Matching these two regimes allows one to obtain an expression for the self-force acting on the CO. The self force can be seen to arise as a result of the interaction of the self field of the CO with the non-flat background geometry, which causes the lines of force to be bent and act back on the CO. The self-force can be conventionally split into two parts: non-time symmetric (dissipative) and time-symmetric (conservative). The former part causes the inspiral and dominates while the latter part can be eliminated by a redefinition of the orbital frequencies at each instance, which means it is effectively second-order in mass ratio. The adiabatic Teukolsky based waveforms take into account only the dissipative part of the self force, neglecting the conservative part, which defines the domain of its validity. The self force is computed assuming the CO is moving on a geodesic, then it is used to adjust the geodesic (inspiral) before the self-force is recomputed again. The computation of the self force is somewhat complicated as it treats the CO as a delta function in the background spacetime, which requires mathematical apparatus for regularization of some divergent integrals. It is possible to subtract the singular part from the field equations (by finding a singular solution valid in the vicinity of the CO) and the resulting equations are manifestly regular and contain on the right hand side a smooth effective source [47], which allows the field equations to be coupled to the equations of motion and integrated. This procedure can be written for a scalar field (representing a CO carrying a scalar charge and ignoring the gravitational part of the self-force) as [48]

$$(\Phi^r)_{;\alpha}{}^{;\alpha} = S(x; z(\tau), u(\tau)) \quad (5)$$

$$\frac{Du^\alpha}{d\tau} = \frac{q}{m(\tau)}(g^{\alpha\beta} + u^\alpha u^\beta) \nabla_\beta \Phi^r \quad (6)$$

$$\frac{dm}{d\tau} = -qu^\beta \nabla_\beta \Phi^r, \quad (7)$$

where Φ is the scalar field, q is the scalar charge, m the mass of the CO, S is an effective source term and u^α is the CO four-velocity. Greek indices are being used to indicate space-time components, and a semicolon denotes a covariant derivative with respect to the background spacetime, $g_{\alpha\beta}$. A similar procedure can be applied to the gravitational field. So far only the self-force waveform for a Schwarzschild background has been computed, but recent progress has been rapid and so we expect the extension to Kerr to be completed within a few years.

Numerical relativity waveforms. The ultimate goal would be to compute EMRI waveforms using numerical integration of the full GR field equations. State-of-the-art techniques have enabled the computation of waveforms for the last 20–50 cycles of the inspiral, merger and ring-down of comparable mass ratio binaries. The simulation of an EMRI requires the computation of a few orders of magnitude more cycles, plus the resolution of two very different spatial scales. This is far beyond the capability of current computational resources and techniques. In addition, the time step for explicit numerical integration is set by the smallest characteristic scale in the problem, which is the mass of the CO in this case. Numerical waveforms will be very useful for the calibration of current calculations based on perturbation techniques, but new numerical methods will have to be developed to handle EMRIs.

3.2 Evolving Perturbed Geodesic Motion

In this subsection we will focus on how we can compute the evolution of the orbit. The orbital evolution is the key ingredient for creating numerical kludge waveforms and waveforms based on the self force. In fact this is the same problem, the main difference is in how the waveform is computed from the orbital trajectory. To compute the orbital evolution we must solve the forced geodesic equation:

$$u^\beta u_\beta{}^{;\alpha} = a^\alpha, \quad (8)$$

where a^α is the 4-acceleration. The acceleration is essentially the self-force, but the method we will describe here for solving this equation is also applicable to the case where a^α represents some other kind of external perturbation. This perturbation could be caused by a second (intermediate) MBH (if the CO in the EMRI is inspiralling into an MBH that is in a wide MBH binary), a molecular cloud or disc, another star or compact objector basically anything that can cause a slow modification of the geodesic orbit. Here we assume that the acceleration has been derived in some other way and are only interested in the effect it has on the inspiral trajectory.

The rest of this subsection summarizes results described in more detail in [49]. We use an osculating elements approach to evolve Eq. (8). If the perturbing force is small,¹ we can represent the perturbed trajectory at each instant by the unique geodesic passing through the same position with the same velocity and see the orbital evolution as a slow variation of the constants of these instantaneously-tangent geodesics. A general geodesic in Kerr spacetime is described by eight constants of motion: $J = \{m, E, L_z, Q, \psi_0, \chi_0, \phi_0, t_0\}$, however two of them (CO mass and initial time m, t_0) are not truly dynamical, so we will work with the remaining 6: orbital energy (E), orbital angular momentum projected onto the spin of the MBH (J_z), Carter constant (Q) and three initial phases (ψ_0, χ_0, ϕ_0) describing the initial position of the CO on the orbit in r, θ and ϕ respectively. The osculating element for of the equation of motion $\ddot{\mathbf{r}} = \mathbf{f}_{geo} + \delta\mathbf{f}$, is

$$z^\alpha(\tau) = z_g^\alpha(J^A(\tau), \tau), \quad \rightarrow \quad \frac{\partial z_g^\alpha}{\partial J^A} \frac{\partial J^A}{\partial \tau} = 0 \quad (9)$$

$$\frac{\partial z^\alpha}{\partial \tau} = \frac{\partial z_g^\alpha}{\partial \tau}(J^A(\tau), \tau), \quad \rightarrow \quad \frac{\partial z_g^\alpha}{\partial J^A} \frac{\partial J^A}{\partial \tau} = \delta f^\alpha. \quad (10)$$

The first set of equations describes a “geodesic” motion with slowly changing orbital “constants”, and the second set gives us the evolution of the orbital “constants” as a function of the perturbing force.

The advantage of using the osculating elements approach is that we can use an adiabatic approximation (or, more generally, a two-time-scale expansion [50]) to evolve EMRIs, for which the radiation reaction time scale is much longer than the orbital time scale, allowing us to more easily study secular effects.

The osculating elements approach was first used in [51] to study Eq. 8 in Schwarzschild background, and was extended to Kerr in [49]. The authors in [49] wrote the osculating element equations on two different forms, using the Kinnersley tetrad or “Hughes” variables (i.e., in terms of the orbital constants and the total phase variables [45]). In both cases, the appearance of an apparent divergence in the osculating equations of motion at turning points is avoided. The techniques were applied to a toy problem in which an EMRI was evolving under the influence of a perturbing force due to drag from surrounding material. This “gas-drag” force was taken to be proportional to the velocity of the inspiralling compact object. The two different approaches were shown to give identical results, and the comparison of the exact and adiabatic solutions to the problem identified the domain of validity of the adiabatic approach. Although the gas-drag problem was considered only to illustrate the methods, it yielded interesting results. In particular, it was found that the influence of the drag force was to drive the inspiral of the object, but also to increase the eccentricity

¹In fact this formalism does not assume the force is small—there is a unique geodesic passing through any given point with a particular velocity and so any trajectory can be described as an osculating geodesic. However, the approach is most useful when the force is small since then the trajectory remains almost geodesic and parameterising it in terms of instantaneous geodesic motion is useful.

of the orbit and decrease the orbital inclination. A gravitational wave driven inspiral would tend to show a decreasing eccentricity and so these two types of perturbing force would be distinguishable in an EMRI observation.

Osculating elements were also used to generate inspirals in a Schwarzschild background under the influence of the gravitational self-force in [52]. The formalism developed for Kerr inspirals in [49] has not been used for any other studies so far, but this will be done once suitable models for perturbing forces are available. Another type of orbital perturbation, which can also be interpreted in terms of a perturbing force acting on a geodesic, is the influence of the spin of the CO on the trajectory. This will be discussed in detail in the next subsection.

3.3 *Spinning Particle in de Sitter Space-Time*

In this subsection we will consider a spinning CO. There are several contributions to this proceedings which describe the motion of a spinning body in a given background in great detail. Here we will give only a brief summary, then show how we can formulate the motion in terms of the osculating elements approach described in the last subsection. To understand the motion of a spinning CO in the MBH spacetime, we will first consider a simpler problem. We will describe analytically the motion of a spinning test body in de Sitter spacetime.

The motion of a test mass in an arbitrary spacetime is governed by the Mathisson-Papapetrou equations

$$D_\tau p^\alpha = -\frac{1}{2} R_{\mu\nu\beta}{}^\alpha u^\beta S^{\mu\nu} \quad (11)$$

$$D_\tau S^{\alpha\beta} = 2p^{[\alpha} u^{\beta]}. \quad (12)$$

The first complication is that the 4-momentum p^μ and 4-velocity u^μ are not parallel

$$p^\alpha = m u^\alpha + u_\beta D_\tau S^{\alpha\beta}. \quad (13)$$

Here D_τ denotes a covariant derivative with respect to the proper time, square brackets denote the anti-symmetric part, $R_{\mu\nu\beta}{}^\alpha$ is the Riemann tensor of the background space time and $S^{\mu\nu} = -S^{\nu\mu}$ is the spin tensor. The difference between p^α and u^α means that there is an ambiguity in what we call the mass—we can define this as $m = p^\alpha u_\alpha$ or $M^2 = p^\alpha p_\alpha$. The second complication is that there is not a sufficient number of equations to determine all of the unknowns. In order to close the system we need to introduce an additional “spin supplementary condition” (SSC). There is an arbitrariness in choosing the SSC, which is usually attributed to how we choose the representative world line of a test mass (this is equivalent to choosing a dipole moment of a spinning CO). The main reason that the SSC is needed is that there is an ambiguity in the definition of the spin tensor for a point mass. The point mass

is an approximation of an extended body (for which the spin tensor is well defined) when the size is much less than the radius of curvature of the background spacetime. The most common SSCs are

$$(i) \quad p_\alpha S^{\alpha\beta} = 0, \quad (ii) \quad u_\alpha S^{\alpha\beta} = 0, \quad (iii) \quad w_\alpha S^{\alpha\beta} = 0 \quad (14)$$

SSC (i) is usually referred to as the Tulczyjew condition [53], (ii) is the Frenkel-Pirani condition [54, 55] and (iii) was first introduced in [56] and is referred to as the w -condition.

As mentioned above we want to write the Mathisson-Papetrou equations as a set of first order equations using the osculating elements approach. To achieve this, we must first write the equations of motion in the form of a forced geodesic equation for a non-spinning particle:

$$\dot{u}^\alpha = \frac{d^2 x^\alpha}{ds^2} + \Gamma_{\rho\sigma}^\alpha \frac{dx^\rho}{ds} \frac{dx^\sigma}{ds} = f^\alpha, \quad (15)$$

which we want to rewrite later in the form (10). We denote the SSCs (i), (ii) and (iii) as “T” and “F” and “w”, and consider first the “T” condition, $S^{ab}p_b = 0$. In that case, we have $M = \text{const}$, but $\dot{m}(u^\alpha, \dot{u}^\alpha) = \dot{S}^{\alpha\beta}\dot{u}_\alpha u_\beta$. We can introduce a new time variable, λ , with $d\lambda = m d\tau$ and use \tilde{u}^α to denote the coordinate velocity in the new coordinates $\tilde{u}^\alpha := dx^\alpha/d\lambda = u^\alpha/m$. The equations then become

$$\begin{aligned} \frac{dp^\alpha}{d\lambda} + \Gamma_{\rho\sigma}^\alpha p^\rho \tilde{u}^\sigma &= -\frac{1}{2} S^{\rho\sigma} \tilde{u}^\mu R_{\rho\sigma\mu}{}^\alpha, \\ \frac{dS^{\alpha\beta}}{d\lambda} + \Gamma_{\rho\sigma}^\alpha S^{\beta\sigma} \tilde{u}^\rho + \Gamma_{\rho\sigma}^\beta S^{\alpha\sigma} \tilde{u}^\rho &= 2p^{[\alpha} \tilde{u}^{\beta]}, \\ \tilde{u}^\alpha = \frac{dx^\alpha}{d\lambda} &= \frac{1}{M^2} \left(p^\alpha + \frac{2S^{\alpha\beta} S^{\rho\sigma} R_{\beta\epsilon\rho\sigma} p^\epsilon}{4M^2 + S^{\mu\beta} S^{\rho\sigma} R_{\mu\beta\rho\sigma}} \right), \end{aligned} \quad (16)$$

which now have no explicit dependence on m and so we can proceed to write them in osculating element form. In particular, we can differentiate the third equation with respect to λ and then use the first equation to get an equation for $\frac{d\tilde{u}^\alpha}{d\lambda} + \Gamma_{\rho\sigma}^\alpha \tilde{u}^\beta \tilde{u}^\gamma$ that depends only on position and velocity, and not on derivatives of \tilde{u}^α . The explicit expression for the covariant total derivative of \tilde{u}^a is given by:

$$\begin{aligned} \frac{D\tilde{u}^\alpha}{d\lambda} &= m^2 \left(\tilde{u}^\mu + \tilde{u}_\beta \frac{DS^{\mu\beta}}{d\lambda} \right) \frac{d}{d\lambda} H^\alpha{}_\mu + \Gamma_{\rho\sigma}^\alpha \tilde{u}^\rho \tilde{u}^\sigma \\ &\quad - \Gamma_{\rho\sigma}^\mu \tilde{u}^\rho m^2 \left(\tilde{u}^\sigma + \tilde{u}_\nu \frac{DS^{\sigma\nu}}{d\lambda} \right) \left(H^\alpha{}_\mu - \frac{1}{M^2} \delta_\mu^\alpha \right) \\ &\quad - \frac{1}{2} S^{\rho\sigma} \tilde{u}^\beta R_{\rho\sigma\beta}{}^\mu \left(H^\alpha{}_\mu - \frac{1}{M^2} \delta_\mu^\alpha \right), \end{aligned} \quad (17)$$

where we made use of the following abbreviation:

$$H^\alpha{}_\mu := \frac{2S^{\alpha\beta}S^{\rho\sigma}R_{\rho\sigma\beta\mu}}{4M^4 + M^2S^{\epsilon\lambda}S^{\kappa\nu}R_{\kappa\nu\epsilon\lambda}}.$$

The third equation in (16) gives an implicit dependence of p^α on the spin tensor and velocity ($p^\alpha = p^\alpha(u^\beta, S^{\beta\gamma})$) which we can use to integrate the (second) equation for the spin tensor.

We note, however, that the standard osculating element formulation of the equations implicitly imposes the condition that $\tilde{u}^\alpha\tilde{u}_\alpha = 1$ and hence $\tilde{u}^\alpha f_\alpha = 0$. This is no longer true after this change of variables. However, there is a way to put the equations into this standard osculating element form when there is an arbitrary force on the right hand side. To tackle this problem we can again make a change of integration variable to a new variable, q say. We then have

$$\begin{aligned}\frac{dx^\alpha}{d\lambda} &= \frac{dq}{d\lambda} \frac{dx^\alpha}{dq} \\ \frac{d^2x^\alpha}{d\lambda^2} &= \left(\frac{dq}{d\lambda}\right)^2 \frac{d^2x^\alpha}{dq^2} + \frac{d^2q}{d\lambda^2} \frac{dx^\alpha}{dq}\end{aligned}\quad (18)$$

and the equations become

$$\frac{d^2x^\alpha}{d\lambda^2} + \Gamma_{\rho\sigma}{}^\alpha \frac{dx^\rho}{d\lambda} \frac{dx^\sigma}{d\lambda} = f'^\alpha = \frac{1}{(dq/d\lambda)^2} \left(f^\alpha - \frac{d^2q}{d\lambda^2} \frac{dx^\alpha}{dq} \right). \quad (19)$$

We can impose the orthogonality condition by solving

$$\frac{d^2q}{d\lambda^2} = \frac{f_\alpha dx^\alpha/dq}{g_{\alpha\beta}(dx^\alpha/dq)(dx^\beta/dq)} \quad (20)$$

and the force becomes

$$f'^\alpha = \frac{1}{(dq/d\lambda)^2} \left(f^\alpha - \frac{f_\gamma dx^\gamma/dq}{g_{\mu\nu}(dx^\mu/dq)(dx^\nu/dq)} \frac{dx^\alpha}{dq} \right). \quad (21)$$

So, to compute the new force we need to know the value of $dq/d\lambda$. We can set this to one initially and then simultaneously integrate the equation

$$\frac{d}{dq} \left(\frac{dq}{d\lambda} \right) = \frac{1}{dq/d\lambda} \frac{f_\alpha dx^\alpha/dq}{g_{\mu\nu}(dx^\mu/dq)(dx^\nu/dq)}. \quad (22)$$

This is a somewhat complicated procedure, but the right hand sides of the new equations now do not depend on derivatives of velocity and so the problems identified above no longer apply.

The (iii) SSC (w -condition) is the most suitable for the osculating elements approach. In this case, we use an arbitrary normalized time-like vector $w^\alpha w_\alpha = 1$ and impose the following conditions

$$w_\alpha S^{\alpha\beta} = 0, \quad D_\tau w^\alpha = 0. \quad (23)$$

The vector field w^α is parallel propagated along the world line of the test mass and these conditions imply $p^\alpha = mu^\alpha$ and m is conserved. This SSC is the most suited for the osculating elements approach.

Alternatively one can linearize the equations with respect to the spin $S_{\mu\nu}$. In this case the relation between the velocity and the 4-momentum takes the simple form

$$p^\alpha \stackrel{\text{L}}{=} mu^\alpha, \quad (24)$$

and the supplementary conditions “T” and “F” coincide. The equations of motion are now given by:

$$\dot{u}^\alpha \stackrel{\text{L}}{=} -\frac{1}{2m} S^{\rho\sigma} u^\beta R_{\rho\sigma\beta}{}^\alpha, \quad (25)$$

$$\dot{S}^{\alpha\beta} \stackrel{\text{L}}{=} 0. \quad (26)$$

As is apparent from (26), this form of the equations of motion is suitable for the osculating orbits method, yielding a perturbing force of the form

$$f^\alpha \stackrel{\text{L}}{=} f^\alpha(u^\alpha, S^{\alpha\beta}). \quad (27)$$

We will now stop considering a general background space time and focus on a particular choice: de Sitter. This is a spacetime with a constant curvature which is at the same time fully symmetric. This allows us to solve the equations of motion analytically and to gain better understanding of the trajectories and the role of the SSC.

The motion of spinning test particles in de Sitter spacetime has previously been investigated by [57] where it was found that under the Tulczyjew SSC, the trajectory is a geodesic with the parallel transport of an appropriately defined spin vector. In addition, under the Frenkel-Pirani SSC, it was found that the trajectory is perturbed about a geodesic by an oscillatory motion but the final solution for the trajectory was left as a numerical integration. We focus on this oscillatory motion in more detail and relate it to motion under the w -condition.

The first Mathisson-Papapetrou equation (11) simplifies in de Sitter spacetime to

$$D_\tau p^\alpha = \frac{1}{l^2} S^{\alpha\beta} u_\beta, \quad (28)$$

where l is a real constant, related to the Ricci scalar via $R = 12/l^2$. At first glance, it might appear that the Frenkel-Pirani SSC will lead to the simplest trajectories, as $D_\tau p^\alpha$ is identically zero in this case. However, due to the difference between 4-momentum and 4-velocity in (13), this generically leads to non-geodesic motion.

We can write the equation of motion under both the Frenkel-Pirani and the w -condition in the same functional form, given by

$$\begin{aligned} D_\tau u^\alpha &= \pm \frac{\omega \eta^{\alpha\beta\mu\nu} F_\beta u_\mu S_\nu}{\sqrt{(F_\sigma S^\sigma)^2 + (F_\sigma F^\sigma) S^2}}, \quad D_\tau F^\alpha = 0, \quad D_\tau S^\alpha = 0, \\ u_\alpha u^\alpha &= 1, \quad F_\alpha S^\alpha = u_\alpha S^\alpha, \quad F_\alpha F^\alpha = u_\alpha F^\alpha, \quad S_\alpha S^\alpha = -S^2, \end{aligned} \quad (29)$$

where S^α is a spin 4-vector constructed from the spin tensor such that the SSC is satisfied, S and ω are real constants, and $\eta^{\alpha\beta\mu\nu}$ is the permutation symbol. Differentiating the equation for $D_\tau u^\alpha$, results in

$$D_\tau^2 u^\alpha = -\omega^2 (u^\alpha - F^\alpha), \quad (30)$$

demonstrating that F^α can be viewed as a forcing term for the oscillations.

The frequency of oscillation ω and the forcing term F^α are different for the two SSCs: for the Frenkel-Pirani case, we find

$$F^\alpha \stackrel{\text{F}}{=} \frac{m}{M^2} p^\alpha, \quad (31)$$

$$\omega \stackrel{\text{F}}{=} \frac{2M}{S}; \quad (32)$$

while under the w -condition,

$$F^\alpha \stackrel{w}{=} (u_\sigma w^\sigma) w^\alpha - \frac{u_\sigma S^\sigma}{S^2} S^\alpha, \quad (33)$$

$$\omega \stackrel{w}{=} \frac{S}{2Ml^2}. \quad (34)$$

As we have an explicit equation for $D_\tau u^\alpha$, we could now numerically integrate, using the method of osculating elements, to find the trajectory. Instead, it is possible to find a general analytic solution to (29) for the motion of spinning test particles in de Sitter spacetime. As a starting point, we note that the solution in Minkowski spacetime has been determined previously (see [56, 58, 59], for example). Under both the Tulczyjew and w -conditions, the particle follows a geodesic whilst under the Frenkel-Pirani condition, the particle undergoes purely circular motion, boosted along a central geodesic.

Since the de Sitter and Minkowski geometries are both maximally symmetric, it might be expected that a similar solution representing circular motion will be found in de Sitter spacetime. We are interested in the 16 components of the position x^α , velocity u^α , forcing term F^α , and spin S^α 4-vectors, using spherically symmetric

static coordinates. Using the 10 isometries of the de Sitter spacetime and the four constraints in (29), it is possible to show that a completely general solution to the equations of motion is given by

$$x^\mu(\tau) = \left\{ t = u^t \tau, r, \theta = \frac{\pi}{2}, \phi = u^\phi \tau \right\}, \quad (35)$$

$$u^\mu(\tau) = \left\{ u^t = \sqrt{\frac{1 - r^2/l^2 + \omega^2 r^2}{1 - 2r^2/l^2}}, u^r = 0, u^\theta = 0, \right. \\ \left. u^\phi = \sqrt{\frac{r^2/l^2 + \omega^2 (l^2 - r^2)}{l^2 - 2r^2}} \right\}, \quad (36)$$

$$F^\mu(\tau) = \left\{ F^t = -\frac{u^\phi}{u^t} l^2 F^\phi, F^r = 0, F^\theta = 0, F^\phi = -\frac{u^\phi (u^t)^2}{\omega^2 l^2} \right\}, \quad (37)$$

$$S^\mu(\tau) = \left\{ S^t = -\frac{u^\phi}{u^t} l^2 S^\phi, S^r = 0, S^\theta = \pm \frac{1}{r} \sqrt{S^2 + \frac{\omega^2 l^4 (S^\phi)^2}{(u^t)^2}}, S^\phi \right\}, \quad (38)$$

where r and S^ϕ are free constants. This solution explicitly corresponds to circular motion about the origin at a frequency that tends to ω in the limit that $l \rightarrow \infty$, consistent with the Minkowski result.

In spacetimes with fewer symmetries than de Sitter, we do not anticipate that such an exact analytic solution for the trajectory can be found, although progress can still be made. Different classes of pole-dipole orbits have been identified in the equatorial plane of Kerr [60] and it has been shown numerically that the motion of spinning test particles in Schwarzschild is of a helical nature [61]. The existence of the exact de Sitter solution can be used to further our understanding of spinning test particle trajectories in these more physical spacetimes.

In addition, the similarity of the solutions in de Sitter under the w -condition and the Frenkel-Pirani SSC will hopefully lead to a better understanding of these SSCs. Particularly, we note here that the product of covariant frequencies, $\omega_p \omega_w = 1/l^2$ is dependent only on the curvature of de Sitter and not on the multipole moments of the test particle. If a similar fundamental link between the two SSCs exists in other spacetimes, it might allow us to infer properties of the Frenkel-Pirani trajectory by numerically integrating the simpler equation of motion under the w -condition.

4 Detecting GW Signals from EMRIs

In the previous two sections we have described the formation of EMRI systems and how the gravitational waves they generate can be modelled. Both those problems are very hard and not yet solved in full, and those astrophysical and theoretical

uncertainties in EMRI rates and in models of the GW signal are coupled to the data analysis challenges. Before we describe specific data analysis algorithms for extracting EMRI GW signals from the detector data we will give a general description of the signal and the problems we face in data analysis.

As mentioned earlier, an EMRI generates 10^5 – 10^6 gravitational waveform cycles in the eLISA band. We therefore need to model it very accurately if we want to avoid systematic biases in the inferred parameter estimates. The expected signal-to-noise ratio (SNR) from those systems is not very high (probably less than 50), but during the Mock LISA Data Challenges (MLDCs) successful extraction of EMRI signals with SNRs as low as 19 was demonstrated, using the same approximate EMRI model (the analytic kludge described earlier) for both injection and recovery. As described in Sect. 1, the EMRI signal depends on 14 parameters, if the spin of the CO is ignored, which is justifiable for mass ratios less than $\sim 10^{-4}$. It is convenient to describe the EMRI's dynamics in the frame fixed relative to the spin axis of the MBH. The spin direction is usually taken to be the z -axis, but we have full freedom in choosing the orientation of the x , y -axes, and this choice is degenerate with the initial azimuthal position of the CO. Since the signal is long lived (stays in band for the entire duration of observation) there is a significant modulation of the amplitude and the phase of the waveform caused by the orbital motion of the detector. This allows us to measure the source sky position with a precision of a few degrees for signals with SNR ~ 20 [4].

EMRIs are primarily GW sources for a future space-based detector like eLISA [28], and the data analysis discussion presented in this section is based on analysing data from such an instrument. Here we will always assume that the instrumental noise is Gaussian (but not white) and that EMRIs are the only GW sources in the data. These are not realistic assumptions for eLISA like data, but make the problem more tractable and the resulting algorithms are still likely to be effective when the assumptions are relaxed. For the purpose of developing data analysis algorithms and EMRI detection strategies we use somewhat simplified models of GW signal (in particular the analytic “kludge” model described in the Sect. 3.1), which capture the main physical features present in the expected signal (periapsis and orbital precession, slow inspiral, Doppler modulation, multiple harmonics) and are also fast to generate numerically and so can be used for computationally expensive parameter estimation. The need to quickly evaluate hundreds of thousands of waveforms to perform data analysis is the main factor which prevents us from using more realistic models. If the data analysis algorithms do not use any model specific features, they can be easily ported to use the best GW signal model available at the time the data is analysed.

There are two data analysis challenges associated with the search for EMRI signals. The first one is to find a signal in the noise, in other words to test the null hypothesis that the observed data is consistent with noise only. This could be a problem for signals with SNR below 20, however we do expect to see a few dozen signals from EMRIs with SNR above 20, which should be detected with high statistical significance. Therefore we will concentrate on such reliably detectable signals. The situation will become more complex when other GW signals are present in the data (especially the foreground from Galactic white dwarf binaries) and/or with realistic instrumental noise. We do expect some environmental and instrumental artefacts to

be present in the data and the LISA Pathfinder [62] measurements (scheduled for launch in July 2015) will allow us to simulate a more realistic eLISA data stream in the near future.

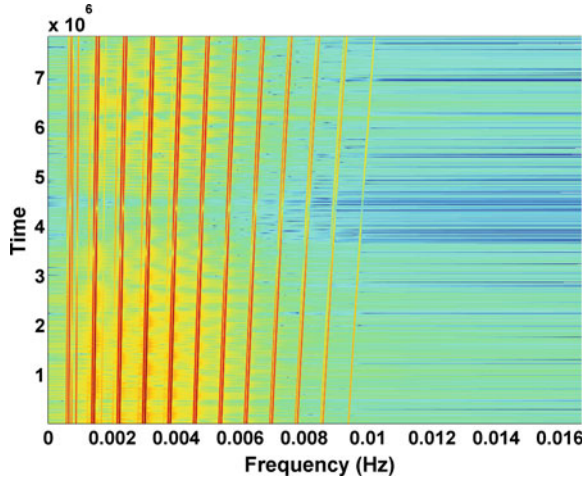
The second problem is what we will focus on in the rest of the current section. The large dimensionality of the parameter space of possible signals makes a grid-type search completely infeasible, so instead we will rely on (pseudo)-stochastic search methods, primarily based on Markov chain Monte-Carlo (MCMC) techniques. Various implementations of MCMC for searches for EMRI signals are described in [4, 63, 64], but the basic idea is to construct a chain which moves predominantly in the direction of increasing likelihood. The complication is that the EMRI likelihood hyper-surface has numerous local maxima some of which could be as much as 70–80% of the global maximum and these local maxima are widely separated in the parameter space. The problem is similar to finding the tallest tree in a forest. A standard MCMC based search will reach a local maximum and get stuck there for a significant number of steps. Theoretically MCMC has a non-zero probability of exploring the whole parameter space and finding the global maximum, but in practice it can get stuck on a strong local maximum for a very long time. Since we consider here only clearly detectable signals, when we refer to a detection we will mean successfully finding the global maximum of the likelihood (which is near the true parameters of a simulated signal and by “near” we mean comparable to the expected statistical deviations due to the presence of detector noise).

In order to detect a GW signal from an EMRI we need an algorithm which can explore efficiently a large part of the parameter space and at the same time concentrate more on regions of high likelihood. Parallel tempering MCMC is one such algorithm and it was used in the MLDCs by N. Cornish [65]. Here we describe two other methods which share the same core principle, based on understanding and exploiting the reason for the presence of local maxima. To understand this reason, we need to look carefully at the GW signal. The GW signal from an EMRI is a superposition of harmonics of three fundamental frequencies, which slowly evolve as the CO inspirals.

$$h(t) = \sum_{l,m,n} h_{lmn}(t) = \Re \left(\sum_{l,m,n} A_{lmn}(t) e^{i(l\Phi_r + m\Phi_\theta + n\Phi_\phi)} \right) \quad (39)$$

These fundamental frequencies (instantaneously or for a geodesic motion) are associated with three degrees of freedom: the radial frequency is associated with eccentric motion from periapsis to apoapsis and back; the polar frequency (θ -motion) is associated with spin-orbital coupling and the resulting precession of the orbital plane around the spin axis of the MBH; and finally the frequency of azimuthal motion [45, 66]. The frequencies evolve under radiation reaction (self-force) on a time scale associated with the mass ratio, which is for EMRIs significantly longer than the orbital time scale. As the CO spirals toward the MBH the overall amplitude of the signal is slightly increasing but the amplitude of individual harmonic depends on the instantaneous orbital parameters like eccentricity

Fig. 2 The time-frequency plot of a typical GW signal from an EMRI, there are 30 clearly identifiable harmonics slowly evolving in time. The amplitude is *colour* coded. The time is in seconds



and inclination. Due to orbital circularisation under radiation reaction [39] the amplitude of some harmonics (high l) will decrease while that of some other (low l) harmonics will increase, but in all cases the amplitude of each harmonic is a smooth and slowly varying function of time. We can construct a periodogram of the EMRI signal, and it looks like a comb in the time-frequency plane, see Fig. 2 as an example.

The global maximum corresponds to the case when two combs representing a signal and a search template coincide exactly in amplitude everywhere in the time-frequency plane. The reason for the local maxima is a partial overlap between the signal harmonics and the harmonics of a template. These might not be the same harmonics (the same set of l, m, n) and the strength of a given local maximum will depend on how long (in frequency and in time) the harmonics of the signal and template coincide.

In the search for a GW signal we use matched filtering which is an optimal detection technique in the presence of Gaussian noise and can be seen as an inner product of the data $x(t) = n(t) + s(t)$ with a template $h(t)$. Here $n(t)$ is the instrumental noise and the signal $s(t) = s(t; \vec{\lambda})$ depends on the parameters of the source ($\vec{\lambda}$), which we are trying to estimate. The inner product is defined as

$$(x, h) = 2\Re \int_0^\infty \frac{\tilde{x}^*(f)\tilde{h}(f)}{S_n(f)} df, \quad (40)$$

where tilde denotes a Fourier transformed quantity and $S_n(f)$ is the one-sided power spectral density of the noise in the detector. If the signal is confined within a narrow frequency band around f_0 , so that we can treat $S_n(f_0)$ as almost constant, the inner product can also be written in the time domain in a simple form:

$$(x, h) \approx \frac{1}{S_n(f_0)} \int_0^T x(t)h(t)dt, \quad (41)$$

where T is the observation time (or duration of a template). The assumption that $S_n(f)$ is approximately constant over the signal evolution is valid for signals of duration up to 2–5 months (dependent on the parameters). Since the amplitude of an EMRI signal is a slowly growing function of time, one can see from Eq. (41) that the SNR ($SNR^2 = (s, s)$) roughly grows as the square root of the observation time. We can use a maximum likelihood estimator to determine the GW parameters. The likelihood ratio is given by

$$\Lambda(\vec{\lambda}) = \frac{P(x|h(\vec{\lambda}))}{P(x|0)} = e^{(x, h(\vec{\lambda})) - \frac{1}{2}(h(\vec{\lambda}), h(\vec{\lambda}))}, \quad (42)$$

where $P(x|h(\vec{\lambda}))$ is the probability that the data x would be observed when a signal corresponding to the specified set of parameters is present in the data and $P(x|0)$ is the probability that the data would be observed when no signal was present. Usually the likelihood (or log-likelihood) can be maximised over some parameters of the signal analytically, whereas maximisation over other parameters requires a numerical search. The analytically maximised likelihood is quite often referred as the F -statistic [63, 64, 67].

Based on the Eqs. (40) and (41) we can introduce a cumulative likelihood (or cumulative F -statistic) in the time and/or in the frequency domain by varying the upper limit of integration. If the template matches the signal exactly we expect to have steady growth of the cumulative F -statistic as a function of time or frequency (in other words it should be a monotonic and not decreasing function). In the case of a local maxima we will observe “bursts” of increase in the F -statistic around instances of time (or frequency) where one or more harmonics of the template and signal match. This is illustrated in Fig. 3, the left panel shows schematically a harmonic of a template successively intersecting and overlapping with two different harmonics of the signal, one of which (in black) is stronger than the other.

In the right panel of the same Figure, we show the corresponding accumulation of the F -statistic, and the instances of two intersections are clearly seen here as a rapid increase in the F -statistic. This illustrates nicely the reason for the presence of strong local maxima in the parameter space which we hit while constructing the Markov chain: harmonics of a signal can reproduce (overlap) one or a few strong harmonics of a signal for a span of time sufficient to accumulate a significant value of the detection statistic. This makes a “curse” into a “blessing”: we can use the information of the locations of the local maxima to guide the search to find the global maximum of the likelihood. This is a key part of the search for EMRIs and the main basis for the two specific methods described in the following subsections. We find many local maxima by running multiple MCMC chains with different seeds, and then analyse the accumulation of the F -statistic to identify the parts (harmonics) of the signal that were found at each of those local maxima. Then we use this information to run a

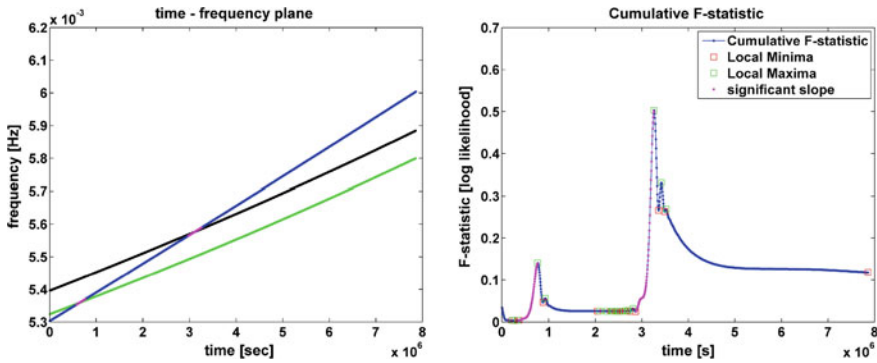


Fig. 3 Cartoon showing two harmonics of a signal in *green* and *black* (*black* being stronger) and a harmonic of the template intersecting the signal at two instances (*left* plot). In the *right* plot we give the corresponding accumulation of the F -statistic in time. The two significant positive slopes (in *pink*) corresponds to two instances of overlaps between a signal and a template

constrained MCMC (as described in Sect. 4.1) or place them on the time-frequency plane and fit them with the harmonic tracks of a template by varying the source parameters (as described in Sect. 4.2).

4.1 Constrained Markov Chain Monte Carlo Search

In this subsection we will summarize the method which was successfully used to analyse the Mock LISA data challenge [4] and described in greater detail in [63]. In this method we split the data into 6-month long subsets and start by analysing each of them separately, before joining them together once we have started to lock onto the signal.

In the first step we perform a stochastic search: we randomly draw parameters from the prior range and evaluate their likelihoods. This is continued until multiple statistically significant points have been identified in the parameter space. Those points are then refined by running small MCMC chains seeded at those points. The local maxima are then analysed to find common harmonics (in time and frequency). These are identified as sections of harmonics of the true signal, although usually we do not know the associated harmonic indices.

In the second step we run a constrained MCMC. The sections of harmonics found in the first stage serve as constraints. We do realise that those constraints might not be exact, so we first run the MCMC with the frequency constraints and adjust the other parameters then we release the constraint and allow the code to adjust the constrained frequencies before fixing these again and repeating. This works very well in practice, even if the frequency of some of the (especially weak) harmonics was not determined very accurately initially. We also run several chains simultaneously to check for convergence to a global maximum.

In the third step we join the 6-month-long subsets of data together and let the chains adjust to match together the best found solutions in each subset. This method was used to analyse simulated data with a single relatively strong (SNR between 50 and 130) EMRI signal [63]. The identification of a signal was remarkably good with an ultra-precise recovery of the system parameters. The technique was also used to analyse the third Mock LISA data challenge data set, for which there was a single data set with five weak (SNR about 20) EMRI signals. The technique successfully identified two signals, while for the other three signals we identified that they were present but did not determine reliable estimates of their parameters before the challenge deadline.

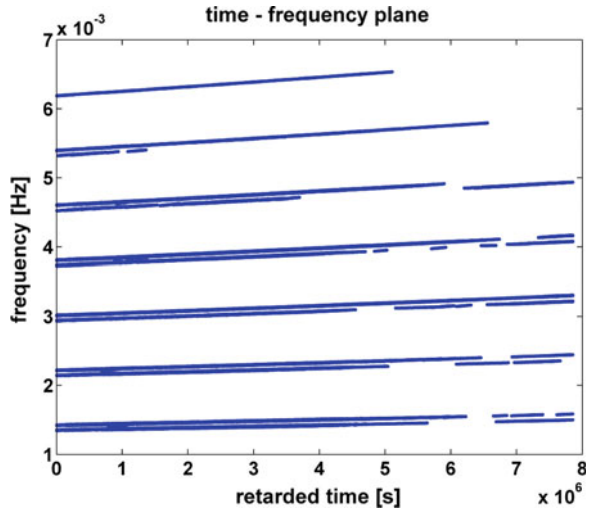
4.2 Detection of EMRIs Using a Phenomenological Template Family

In this subsection we summarise the method described in [64]. The main idea of this approach was to detect GW signals from EMRIs in a model independent way using a minimal set of assumptions about the signal: (1) the orbital motion can be described by six slowly (on the radiation reaction time scale) changing quantities; and (2) the signal is represented by a set of harmonics of those (three) orbital frequencies with slowly changing amplitude. Those are rather mild constraints and should describe also “dirty” EMRIs where the orbital motion is perturbed either by the astrophysical environment or by a deviation in the spacetime geometry of the central BH [34, 68].

We can use the assumption of slow frequency and amplitude evolution to decompose the phase and amplitude of each harmonic as a Taylor series and perform the search over the coefficients of the Taylor expansion. We call this a phenomenological EMRI template—the relationship between the Taylor series coefficients and the physical parameters depends on the specific model for the GW signal from an EMRI system. By searching over phenomenological parameters (Taylor coefficients) we do not restrict ourselves to any specific model within the framework of our assumptions above. The truncation of the Taylor series and the number of harmonics included depends mainly on the SNR of the signal: for weak signals we have to use a higher order expansion in order to match the signal for a longer time. Detection of EMRI signals in this model independent way allows us to relax stringent requirements on the accuracy of the theoretical model and to test alternatives to the assumption of a CO inspiral occurring in a pure vacuum Kerr spacetime.

Here we describe the simulations performed in [64]. Three month long data sets were simulated containing an EMRI signal ($SNR = 50$) using the numerical kludge as a model. Multiple MCMC searches using the phenomenological templates were carried out with different starting seeds. The results were collected and analysed for the presence of local maxima. For each identified maximum a patch of the signal harmonic which was found was extracted and placed on the time-frequency plane. The resulting map looks as presented in Fig. 4. In this example the injected source

Fig. 4 Recovered patches of the signal corresponding to a strong accumulation of the F -statistic



was a strong signal and the method recovered 13 harmonics. In more realistic cases we would expect to recover 3–5 harmonics only. We note that the strong harmonics (at low frequency) are better recovered (through the full duration of the observation). Notice also that the last month of the data is recovered less well than the first two, which is due to the orbital motion of the detector—the antenna beam pattern during the last month is pointing away from the source.

In the second stage it is necessary to assume a certain EMRI model, so that the found harmonics can be identified and the physical parameters of the system recovered. In particular it is here that we can assume several alternatives: a CO spiralling toward a Kerr MBH, a CO spiralling into a massive boson star, a “dirty” Kerr black hole (a bumpy BH or a complex astrophysical environment). Once the model is assumed, we can find the set of parameters which give the best fit to the found set of harmonics (in amplitude and in their evolution). One can use a simple chi-square test of goodness of fit to estimate how well the assumed model describes the observed harmonic tracks and hence make a statement about the model. Results for the recovery of orbital parameters if the same model is used for recovery and signal generation were presented in [64].

5 Conclusion

In this article we have described one of the most interesting GW sources for the future space based gravitational wave observatory eLISA. We have briefly described the various channels for EMRI formation and expected event rates. Then we went through an inventory of available models for the GW signal generated by EMRIs. We also briefly discussed the osculating element approach for integration of the forced (under

radiation reaction) motion of a CO in Kerr spacetime, and its application to the case of a spinning CO. One non-trivial question is the influence of the spin supplementary condition on the computed motion of a spinning CO and we have addressed this by looking at a simplified case: the motion of a spinning test mass in de Sitter spacetime. This should provide guidance on how to proceed in the case of a Schwarzschild or Kerr spacetime. Finally we have described the challenges which we will face in extracting GW signals generated by EMRIs from eLISA data. The main problem is to search for a global maximum of likelihood in the multidimensional parameter space, when multiple strong local maxima are also present. We have described how one can extract useful information about the signal from the locations of those local maxima in order to direct the search to the correct solution. In addition we have outlined the possibility that these methods can be used to verify that the central massive compact object is indeed described by the Kerr metric, as predicted by general relativity.

References

1. E. Poisson, A. Pound, I. Vega, The motion of point particles in curved spacetime. *Living Rev. Relativ.* **14**(7), (2011)
2. S.E. Gralla, R.M. Wald, A rigorous derivation of gravitational self-force. *Class. Quantum Gravity* **25**(20), 205009 (2008)
3. C.W. Misner, K.S. Thorne, J.A. Wheeler. *Gravitation*, 2 edn. (W.H. Freeman and Company, London, (1973)
4. S. Babak et al., The mock LISA data challenges: from challenge 3 to challenge 4. *Class. Quantum Gravity* **27**, 084009 (2010)
5. C.P.L. Berry, J.R. Gair, Extreme-mass-ratio bursts from extragalactic sources. *Mon. Not. R. Astron. Soc.* **433**(4), 3572–3583 (2013)
6. T. Alexander, C. Hopman, Strong mass segregation around a massive black hole. *Astrophys. J.* **697**, 1861–1869 (2009)
7. C. Hopman, T. Alexander, Resonant relaxation near the massive black hole in the galactic center. *J. Phys. Conf. Ser.* **54**, 321–327 (2006)
8. C. Hopman, T. Alexander, Resonant relaxation near a massive black hole: the stellar distribution and gravitational wave sources. *Astrophys. J.* **645**, 1152–1163 (2006)
9. E. Eilon, G. Kufi, T. Alexander, The efficiency of resonant relaxation around a massive black hole. *Astrophys. J.* **698**, 641–647 (2009)
10. T. Alexander, Stellar relaxation processes near the galactic massive black hole. February 2011
11. D. Merritt, T. Alexander, S. Mikkola, C.M. Will, Stellar dynamics of extreme-mass-ratio inspirals. *Phys. Rev.* **D84**, 044024 (2011)
12. P. Brem, P. Amaro-Seoane, C.F. Sopuerta, Blocking low-eccentricity EMRIs: A statistical direct-summation N-body study of the Schwarzschild barrier. *Mon. Not. R. Astron. Soc.* **437**(2), 1259–1267 (2014)
13. P. Amaro-Seoane, C.F. Sopuerta, M.D. Freitag, The role of the supermassive black hole spin in the estimation of the EMRI event rate. *Mon. Not. R. Astron. Soc.* **429**(4), 3155–3165 (2013)
14. D. Merritt, E. Vasiliev, Orbits around black holes in triaxial nuclei. *Astrophys. J.* **726**, 61 (2011)
15. H.B. Perets, C. Hopman, T. Alexander, Massive perturber-driven interactions of stars with a massive black hole. *Astrophys. J.* **656**, 709–720 (2007)
16. C. Hopman, Extreme mass ratio inspiral rates: dependence on the massive black hole mass. *Class. Quantum Gravity* **26**, 094028 (2009)
17. M. Coleman Miller, M. Freitag, D.P. Hamilton, V.M. Lauburg, Binary encounters with supermassive black holes. *Astrophys. J.* **631**, L117–L120 (2005)

18. C. Hopman, Binary dynamics near a massive black hole. *Astrophys. J.* **700**, 1933–1951 (2009)
19. P. Amaro-Seoane, J.R. Gair, M. Marc Freitag, C. Miller, I. Mandel et al., Astrophysics, detection and science applications of intermediate- and extreme mass-ratio inspirals. *Class. Quantum Gravity* **24**, R113–R169 (2007)
20. W.R. Brown, M.J. Geller, S.J. Kenyon, MMT hypervelocity star survey. *Astrophys. J.* **690**, 1639–1647 (2009)
21. K.M. Svensson, R.P. Church, M.B. Davies, The nature of hypervelocity stars as inferred from their galactic trajectories. *Mon. Not. Roy. Astron. Soc.* (2007)
22. Y. Levin, Starbursts near supermassive black holes: young stars in the Galactic Center, and gravitational waves in LISA band. *Mon. Not. R. Astron. Soc.* **374**, 515–524 (2007)
23. P. Amaro-Seoane, Stellar dynamics and extreme-mass ratio inspirals. ArXiv e-prints, May 2012
24. Jonathan R. Gair, Probing black holes at low redshift using LISA EMRI observations. *Class. Quantum Gravity* **26**, 094034 (2009)
25. L. Brenneman, Measuring supermassive black hole spins in active galactic nuclei (2013)
26. F. Shankar, D.H. Weinberg, J. Miralda-Escude, Self-consistent models of the AGN and black hole populations: duty cycles, accretion rates, and the mean radiative efficiency. *Astrophys. J.* **690**, 20–41 (2009)
27. P. Amaro-Seoane, S. Aoudia, S. Babak, P. Binetruy, E. Berti et al., Low-frequency gravitational-wave science with eLISA/NGO. *Class. Quantum Gravity* **29**, 124016 (2012)
28. P. Amaro-Seoane, S. Aoudia, S. Babak, P. Binetruy, E. Berti et al., eLISA/NGO: astrophysics and cosmology in the gravitational-wave millihertz regime. *GW Notes* **6**, 4–110 (2013)
29. K. Liu, N. Wex, M. Kramer, J.M. Cordes, T.J.W. Lazio, Prospects for probing the spacetime of Sgr A* with pulsars. *Astrophys. J.* **747**, 1 (2012)
30. K. Gültekin, D.O. Richstone, K. Gebhardt, T.R. Lauer, S. Tremaine et al., The M-sigma and M-L relations in galactic bulges and determinations of their intrinsic scatter. *Astrophys. J.* **698**, 198–221 (2009)
31. S. Mathur, D. Grupe, The locus of highly accreting AGNs on the M(BH)-sigma plane: selections, limitations, and implications. *Astrophys. J.* **633**, 688–692 (2005)
32. M. Volonteri, M. Sikora, J-P. Lasota, Black-Hole Spin and Galactic Morphology, (2007)
33. M. Volonteri, P. Natarajan, Journey to the $M_{\text{BH}} - \sigma$ relation: the fate of low mass black holes in the universe. *Mon. Not. Roy. Astron. Soc.* **400**, 1911 (2009)
34. S. Babak, J.R. Gair, A. Petiteau, A. Sesana, Fundamental physics and cosmology with LISA. *Class. Quantum Gravity* **28**, 114001 (2011)
35. A. Buonanno, T. Damour, Effective one-body approach to general relativistic two-body dynamics. *Phys. Rev.* **D59**, 084006 (1999)
36. T. Damour, A. Nagar, The effective one body description of the two-body problem. *Fundam. Theor. Phys.* **162**, 211–252 (2011)
37. Y. Mino, M. Sasaki, M. Shibata, H. Tagoshi, T. Tanaka, Black hole perturbation: Chapter 1. *Prog. Theor. Phys. Suppl.* **128**, 1–121 (1997)
38. L. Barack, C. Cutler, LISA capture sources: approximate waveforms, signal-to-noise ratios, and parameter estimation accuracy. *Phys. Rev.* **D69**, 082005 (2004)
39. P.C. Peters, J. Mathews, Gravitational radiation from point masses in a Keplerian orbit. *Phys. Rev.* **131**, 435–439 (1963)
40. R. Ruffini, M. Sasaki, On a semirelativistic treatment of the gravitational radiation from a mass thrust into a black hole. *Prog. Theor. Phys.* **66**, 1627–1638 (1981)
41. T. Tanaka, M. Shibata, M. Sasaki, H. Tagoshi, T. Nakamura, Gravitational wave induced by a particle orbiting around a Schwarzschild black hole. *Prog. Theor. Phys.* **90**, 65–84 (1993)
42. S. Babak, H. Fang, J.R. Gair, K. Glampedakis, S.A. Hughes, ‘Kludge’ gravitational waveforms for a test-body orbiting a Kerr black hole. *Phys. Rev.* **D75**, 024005 (2007)
43. C.F. Sopuerta, N. Yunes, New Kludge scheme for the construction of approximate waveforms for extreme-mass-ratio inspirals. *Phys. Rev.* **D84**, 124060 (2011)
44. S.A. Teukolsky, Perturbations of a rotating black hole. 1. Fundamental equations for gravitational electromagnetic and neutrino field perturbations. *Astrophys. J.* **185**, 635–647 (1973)

45. S. Drasco, S.A. Hughes, Gravitational wave snapshots of generic extreme mass ratio inspirals. *Phys. Rev.* **D73**, 024027 (2006)
46. K. Martel, Gravitational wave forms from a point particle orbiting a Schwarzschild black hole. *Phys. Rev.* **D69**, 044025 (2004)
47. I. Vega, B. Wardell, P. Diener, Effective source approach to self-force calculations. *Class. Quantum Gravity* **28**, 134010 (2011)
48. P. Diener, I. Vega, B. Wardell, S. Detweiler, Self-consistent orbital evolution of a particle around a Schwarzschild black hole. *Phys. Rev. Lett.* **108**, 191102 (2012)
49. J.R. Gair, E.E. Flanagan, S. Drasco, T. Hinderer, S. Babak, Forced motion near black holes. *Phys. Rev.* **D83**, 044037 (2011)
50. T. Hinderer, E.E. Flanagan, Two timescale analysis of extreme mass ratio inspirals in Kerr. I. Orbital Motion. *Phys. Rev.* **D78**, 064028 (2008)
51. A. Pound, E. Poisson, Osculating orbits in Schwarzschild spacetime, with an application to extreme mass-ratio inspirals. *Phys. Rev.* **D77**, 044013 (2008)
52. N. Warburton, S. Akcay, L. Barack, J.R. Gair, N. Sago, Evolution of inspiral orbits around a Schwarzschild black hole. *Phys. Rev.* **D85**(6), 061501 (2012)
53. W. Tulczyjew, Motion of multipole particles in general relativity theory. *Acta Phys. Pol.* **18**, 393 (1959)
54. J. Frenkel, Die Elektrodynamik des rotierenden Elektrons. *Z. Phys.* **37**, 243–262 (1926)
55. F.A.E. Pirani, On the physical significance of the Riemann tensor. *Acta Phys. Pol.* **15**, 389–405 (1956)
56. K. Kyrian, O. Semerak, Spinning test particles in a Kerr field. *Mon. Not. R. Astron. Soc.* **382**, 1922 (2007)
57. Y.N. Obukhov, D. Puetzfeld, Dynamics of test bodies with spin in de Sitter spacetime. *Phys. Rev.* **D83**, 044024 (2011)
58. L. Filipe, O. Costa, C.A.R. Herdeiro, J. Natario, M. Zilhao, Mathisson’s helical motions for a spinning particle: Are they unphysical? *Phys. Rev.* **D85**, 024001 (2012)
59. N. Kudryashova, Y.N. Obukhov, On the dynamics of classical particle with spin. *Phys. Lett. A* **374**, 3801–3805 (2010)
60. E. Hackmann, C. Lämmerzahl, Y.N. Obukhov, D. Puetzfeld, I. Schaffer, Motion of spinning test bodies in Kerr spacetime. *Phys. Rev.* **D90**, 064035 (2014)
61. R. Plyatsko, O. Stefanyshyn, M. Fenyk, Mathisson-Papapetrou-Dixon equations in the Schwarzschild and Kerr backgrounds. *Class. Quantum Gravity* **28**, 195025 (2011)
62. F. Antonucci, M. Armano, H. Audley, G. Auger, M. Benedetti et al., The LISA Pathfinder mission. *Class. Quantum Gravity* **29**, 124014 (2012)
63. S. Babak, J.R. Gair, E.K. Porter, An algorithm for detection of extreme mass ratio inspirals in LISA data. *Class. Quantum Gravity* **26**, 135004 (2009)
64. Y. Wang, Y. Shang, S. Babak, EMRI data analysis with a phenomenological waveform. *Phys. Rev.* **D86**, 104050 (2012)
65. N.J. Cornish, Detection strategies for extreme mass ratio inspirals. *Class. Quantum Gravity* **28**, 094016 (2011)
66. W. Schmidt, Celestial mechanics in Kerr space-time. *Class. Quantum Gravity* **19**, 2743 (2002)
67. P. Jaranowski, A. Krolak, B.F. Schutz, Data analysis of gravitational—wave signals from spinning neutron stars. I. The signal and its detection. *Phys. Rev.* **D58**, 063001 (1998)
68. E. Barausse, V. Cardoso, P. Pani, Can environmental effects spoil precision gravitational-wave astrophysics? *Phys. Rev.* **D89**, 104059 (2014)

Level Sets of the Lapse Function in Static GR

Carla Cederbaum

Abstract We present a novel physical interpretation of the level sets of the (canonical) lapse function in static isolated general relativistic spacetimes. Our interpretation uses a notion of *constrained test particles*. It leads to a definition of gravitational force on test particles and to a previously unknown uniqueness result for the lapse function. In Sect. 5, we discuss *photon spheres* in static isolated relativistic spacetimes and relate them to the level sets of the lapse function.

1 Static Isolated Relativistic Spacetimes

Static isolated relativistic spacetimes have been studied from a number of perspectives including regularity, asymptotics, construction of explicit solutions etc. They serve as models of static isolated star and black hole configurations. The standard example is the Schwarzschild family of spacetimes

$$ds^2 = -N^2 c^2 dt^2 + \frac{1}{N^2} dr^2 + r^2 d\Omega^2, \quad (1)$$

$$N = \left(1 - \frac{2M}{r}\right)^{\frac{1}{2}}, \quad (2)$$

modeling the vacuum exterior region of a black hole or spherically symmetric matter distribution. Here, $M = mGc^{-2}$ is the mass parameter and $d\Omega^2$ denotes the standard metric of the round sphere.

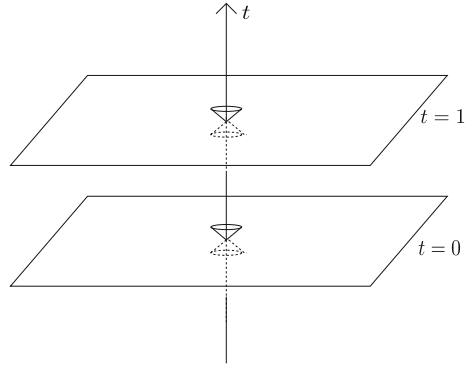
N is called the (*canonical*) *lapse function*. For $M = m = 0$, we find the Minkowski spacetime as a special case in the Schwarzschild family.

More generally, a static relativistic spacetime is given by a smooth Lorentzian metric ds^2 which has a smooth timelike Killing vector field $X = \partial_t$ which is hypersurface-orthogonal with respect to the induced Levi-Civita connection ∇ :

C. Cederbaum (✉)

Mathematisches Institut, Universität Tübingen, Auf der Morgenstelle 10,
72076 Tübingen, Germany
e-mail: cederbaum@math.uni-tuebingen.de

Fig. 1 The time-slices of a canonically decomposed static spacetime



$$X_{[\alpha} \nabla_{\beta} X_{\gamma]} = 0. \quad (3)$$

It follows that the (*canonical*) lapse function $N := \sqrt{-ds^2(X, X)}$ is positive and time-independent. The metric locally splits into a warped product

$$ds^2 = -N^2 c^2 dt^2 + g, \quad (4)$$

where g is a time-independent Riemannian metric on a time-slice $\{t = \text{const}\}$. All time-slices are isometric and extrinsically flat, cf. Fig. 1.

A static spacetime with metric ds^2 of the form (4) is said to model an *isolated system* if

$$g_{ij} \rightarrow \delta_{ij} \quad (5)$$

$$N \rightarrow 1 \quad (6)$$

as $r \rightarrow \infty$ and if the topology of the time-slices is that of Euclidean 3-space outside a ball. Thinking of the time-slices as only modeling the exterior region outside the (assumedly finitely extended) matter distribution and outside all black holes, let us additionally assume that ds^2 satisfies the vacuum Einstein equations. Making use of the time-translation symmetry, the vacuum Einstein equations reduce to the *static vacuum equations*

$$N \text{Ric} = \nabla^2 N \quad (7)$$

$$\Delta N = 0 \quad (8)$$

on any and every time-slice. Here, Ric denotes the Ricci curvature tensor, ∇^2 the covariant Hessian, and Δ the covariant Laplacian corresponding to the 3-dimensional Riemannian metric g on the time-slices.

While the Riemannian metric g captures the geometry of the time-slices, the lapse function N incorporates the information of how we have to arrange or stack the (isometric) time-slices in order to reproduce the static spacetime, cf. Eq. (4) and Fig. 1.

2 Physical Interpretation of the Lapse Function

What is the physical significance of the lapse function N ? Does it play a role similar to that of the Newtonian potential in static Newtonian gravity? Surprisingly, it (almost) does, and in a number of ways:

- **Newtonian limit:** The *pseudo-Newtonian potential* $U := c^2 \ln N$ converges to the Newtonian potential in the Newtonian limit (along any suitable family of static isolated spacetimes possessing a Newtonian limit in the sense of Ehlers' frame theory), cf. [1, 2].
- **Asymptotic behavior:** The pseudo-Newtonian potential $U = c^2 \ln N$ asymptotically behaves like

$$U = -\frac{mG}{r} + \mathcal{O}\left(\frac{1}{r^2}\right) \quad (9)$$

as $r \rightarrow \infty$, where m is the ADM-mass of the system, cf. [3]. Moreover, the next order term in the asymptotic expansion of U corresponds to a center of mass term of the same form as in the Newtonian setting

$$U = -\frac{mG}{r} - \frac{mG\vec{z} \cdot \vec{x}}{r^3} + \mathcal{O}\left(\frac{1}{r^3}\right), \quad (10)$$

cf. [2]. Both asymptotic decay statements are made precise using weighted Sobolev spaces.

- **Equipotential surfaces:** Relativistic test particles constrained to a given 2-surface Σ^2 generically accelerate along Σ^2 unless Σ^2 is a level set of the lapse function N and thus also of the pseudo-Newtonian potential $U = c^2 \ln N$. It is thus justified to call those level sets *equipotential*. We will describe this phenomenon in more detail in Sect. 3.
- **Uniqueness of lapse:** N and thus also $U = c^2 \ln N$ are uniquely determined outside the matter distribution by the spatial metric g – and everywhere in a given time-slice by the metric g and the matter variables induced on any time-slice by the energy momentum tensor. We will sketch how this follows from the equipotential nature of the level sets in Sect. 4. More details as well as two alternative proofs can be found in [2, 4].
- **Degrees of freedom:** Introducing asymptotically flat wave-harmonic coordinates (x^i) on a time-slice, N (or, alternatively, $U = c^2 \ln N$) together with the coordinates uniquely determine the components g_{ij} of the spatial metric g of a given static

isolated spacetime. So, in this sense, static isolated spacetimes have four degrees of freedom, namely those corresponding to the choice of (N, x^1, x^2, x^3) . This coincides with static isolated Newtonian gravity, where the degrees of freedom are given by the Newtonian potential and three Galilei coordinates.

3 Equipotential Surfaces and Gravitational Force

In static Newtonian gravity, the (negative) gradient of the Newtonian potential defines the force \vec{F} on a unit mass test body. This has a well-known consequence for the *equipotential* or level set surfaces: if a test body is constrained into one of the level set surfaces, the gravitational force \vec{F} is perpendicular to the path of the test body and does thus not have a tangential component. Hence the test body does not tangentially accelerate along any level set surface, see Fig. 2. If, on the other hand, a test body is constrained to an arbitrary surface Σ^2 , it will in general accelerate due to the tangential component of the force along Σ^2 .

Surprisingly, the “same” is true for the level sets of the lapse function N in a static isolated spacetime. To see that, we need to replace the constrained Newtonian test bodies in the above picture by “constrained (relativistic) test particles”. In order to define these, recall that a timelike curve $\mu(\tau)$ is called a (*freely falling relativistic*) *test particle* if it is a critical point of the time functional $T[\mu]$ given by

$$T[\mu] := \int_{\tau_0}^{\tau_1} |\dot{\mu}(\tau)| d\tau. \quad (11)$$

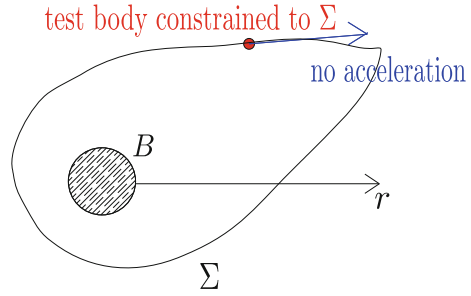
In the context of static isolated spacetimes, the warped product structure of the metric captured by (4) allows us to think of a timelike curve $\mu(\tau)$ as having temporal and spatial components such that

$$\mu(\tau) = (t(\tau), x(\tau)). \quad (12)$$

Accordingly, let us say that a timelike curve $\mu(\tau)$ is *constrained to a surface* $\Sigma^2 \subset \{t = \text{const}\}$ if $x(\tau) \in \Sigma^2$ for all τ . In other words, we ask the curve $\mu(\tau)$ to stay within the warped 3-dimensional timelike cylinder $(-\infty, \infty) \times \Sigma^2$ “over” Σ^2 in the spacetime. We then define a *constrained (relativistic) test particle* to be a timelike curve $\mu(\tau)$ which is a critical point of the time functional $T[\mu]$ as in (11) but subject to the constraint that it (and all its competitors in the variation of $T[\mu]$) is constrained to a given surface $\Sigma^2 \subset \{t = \text{const}\}$.

Equipped with this notion of constrained test particles, let us say that a closed surface Σ^2 sitting in a time-slice $\{t = \text{const}\}$ of a static isolated spacetime is an *equipotential surface* if **every** test particle constrained to Σ^2 is a geodesic in Σ^2 with respect to the induced 2-metric, i.e. does not accelerate within Σ^2 , see again Fig. 2. This is a geometrized analog of the Newtonian notion of equipotential surfaces.

Fig. 2 A (Newtonian) test body constrained to a surface Σ^2



A straightforward analysis of the Euler-Lagrange equations of the functional $T[\mu]$ subject to the constraint that $x(\tau) \in \Sigma^2$ for all τ shows that Σ^2 is an equipotential surface in a given static isolated spacetime if and only if Σ^2 is a level set of the lapse function N . Thus, in their effect on constrained test particles, the level sets of the lapse function N in static isolated spacetimes play precisely the same role as those of the Newtonian potential in static isolated Newtonian gravity.

3.1 Gravitational Force

In Newtonian gravity, the equipotential property of the level sets of the potential stems from the fact that the (negative) gradient of the potential determines the gravitational force per unit mass. It is thus tempting to define gravitational force per unit mass as the (negative) gradient of the lapse function N in our context. Our Newtonian limit analysis¹ however suggests that we should replace the lapse function N by the pseudo-Newtonian potential $U = c^2 \ln N$. Observe that U has the same level sets as N .

Moreover, it is more adequate² to take the gradient of U not with respect to the induced spatial metric g but instead with respect to the conformally equivalent Riemannian metric $\gamma := N^2 g$. We suggest to call γ the *pseudo-Newtonian metric* of the given static isolated spacetime.

Finally, it is important to realize that a notion of gravitational force constructed by the above equipotential principle will only apply to test particles.³ It will not

¹cf. Sect. 2 for a sketch of and [2] for more details on the Newtonian limit analysis of static isolated spacetimes.

²This follows from the Newtonian limit analysis combined with a more detailed study of the geometry of *pseudo-Newtonian gravity*, cf. [2].

³Our definition of gravitational force can be extended to general timelike curves that are not necessarily geodesics. These can be interpreted as test particles that are subject to not only gravitational but also to non-gravitational forces (e.g. electro-magnetic ones).

readily⁴ apply to extended bodies. This distinction is irrelevant in static Newtonian gravity due to the superposition principle for the linear Poisson equation satisfied by the Newtonian potential.

So let $\mu(\tau) = (t(\tau), x(\tau))$ be a test particle in a static isolated spacetime with metric ds^2 as in (4). Assume that μ has mass m or that

$$ds^2 \left(\frac{d\mu}{d\tau}, \frac{d\mu}{d\tau} \right) = -m^2 \quad (13)$$

for all τ . We then define the *gravitational force on the test particle* $\mu(\tau)$ as

$$\vec{F} := -m \, {}^\gamma \vec{\nabla} U, \quad (14)$$

where ${}^\gamma \vec{\nabla}$ denotes the (3-dimensional) γ -covariant gradient. Furthermore, we define its (3-dimensional) *acceleration*⁵ by

$$\vec{a} := {}^g \vec{\nabla}_{\frac{dx}{d\tau}} \frac{dx}{d\tau}. \quad (15)$$

Here, ${}^g \vec{\nabla}$ denotes the (3-dimensional) g -covariant gradient. A straightforward computation shows that with these definitions of gravitational force and acceleration, the second *pseudo*-Newtonian law of motion

$$\vec{F} = m\vec{a} \quad (16)$$

holds for all freely falling test particles of mass m , see [2].

4 Uniqueness Results

In a static isolated spacetime, the Einstein constraint equations on every time-slice reduces to

$$R = 0. \quad (17)$$

We observe that the lapse function N does not appear in this constraint equation. Using Choquet-Bruhat's local uniqueness theorem (see e.g. [5]) for the Einstein

⁴The author has some first ideas how to generalize the notion of gravitational force presented here to extended bodies. A second Newtonian law of motion for extended bodies, however, seems more difficult at the moment.

⁵The acceleration of the test particle is induced from the Lorentzian metric ds^2 and thus naturally refers to the spatial metric g and not to the conformally transformed metric γ because the definition of test particles relies on the “dynamics” of the spacetime. On the other hand, the definition of gravitational force uses the analogy of pseudo-Newtonian and Newtonian effects and thus should be formulated in pseudo-Newtonian terms.

equations, this implies that the spacetime corresponding to a given spatial metric g and lapse function N is in fact *independent*⁶ of the lapse function N . It follows that N is indeed **unique**: Suppose there was a second lapse function \tilde{N} such that $\tilde{N} \rightarrow 1$ as $r \rightarrow \infty$. Then by the above, the levels of N and \tilde{N} would be detected by constrained test particles. Those only depend on the Lorentzian metric ds^2 which we have seen to be independent of the lapse function whatsoever. Thus the level sets of N and \tilde{N} coincide so that $\tilde{N} = f \circ N$ for some real valued function f . The static vacuum equations (7) and (8) applied to N and \tilde{N} then imply

$$\begin{aligned} 0 &= \Delta \tilde{N} = \Delta(f \circ N) \\ &= f'' \circ N \|\nabla N\|_g^2 + f' \circ N \Delta N \\ &= f'' \circ N \|\nabla N\|_g^2 \end{aligned}$$

so that $f'' = 0$ and thus $\tilde{N} = \alpha N + \beta$ for some real numbers α, β . Moreover,

$$\begin{aligned} \nabla^2 \tilde{N} &= \tilde{N} \text{Ric} \\ &= (\alpha N + \beta) \text{Ric} \\ &= \alpha \nabla^2 N + \beta \text{Ric} \\ &= \nabla^2 \tilde{N} + \beta \text{Ric}. \end{aligned}$$

If g is not everywhere flat, this implies $\beta = 0$. Finally $N, \tilde{N} \rightarrow 1$ as $r \rightarrow \infty$ leads to $\alpha = 1$ so that $N = \tilde{N}$.

We interpret this result as saying that “there is only one way of synchronizing time at different locations in a geometrostatic spacetime such that one sees staticity” just as, for a Riemannian geodesic, “there is only one way of walking along a geodesic such that one does not accelerate (up to affine re-parametrizations)”. The affine freedom of the parameter along the geodesic does not make an appearance in the static isolated spacetime picture because we fixed the lapse function to asymptotically converge to 1 at spacelike infinity and therewith fixed the time unit.

5 Photon Spheres

It is well-known that the Schwarzschild spacetime (1) and (2) with positive mass parameter $M = mGc^{-2}$ possesses a so-called *photon sphere* at $r = 3M$. This is to say that photons (aka null geodesics) initially tangent to the timelike cylinder $(-\infty, \infty) \times \{r = 3M\}$ remain tangent to it or that “photons get caught in the sphere $\{r = 3M\}$ ”. Moreover, each photon’s energy and frequency is constant in time (as

⁶However, we do assume that the lapse function exists in the first place.

observed by the static observers $N^{-1}\partial_t$). This is a very interesting phenomenon. It has proved relevant for understanding questions related to dynamical stability and to gravitational lensing.⁷

As we have seen above, the positive mass Schwarzschild spacetimes are prime examples of static isolated spacetimes. It is thus natural to ask whether more general static isolated spacetimes can also possess photon spheres or whether the phenomenon is restricted to the spherically symmetric Schwarzschild case. To the best knowledge of the author, this question was first raised in [6].

To study this question, let us define⁸ a *photon surface* in a static isolated spacetime with metric ds^2 of the form (4) as a surface $\Sigma^2 \subset \{t = \text{const}\}$ such that **every** photon (i.e. null geodesic) initially tangent to the cylinder $(-\infty, \infty) \times \Sigma^2$ remains tangent to it. A photon surface possessing the property that the tangential photons have constant energy and frequency along the photon surface (in the eyes of the static observers) will be called a *photon sphere*. It turns out that this property is equivalent to constancy of the lapse function N along the photon surface, see Lemma 2.7 in [8].

An analysis⁹ of the null geodesic equation combined with the Gauß-Codazzi-Mainardi equations and the static vacuum equations (7) and (8) shows that a photon sphere Σ^2 in a static isolated spacetime must necessarily have constant mean curvature (or *expansion*). Furthermore, a photon sphere Σ^2 has constant (intrinsic) Gauß curvature and the normal derivative of the lapse function $\nu(N)$ must also be constant along Σ^2 .

In [8], the author shows that a static vacuum isolated spacetime with metric as in (4) possessing a—connected—photon sphere Σ^2 must be isometric to a Schwarzschild spacetime outside the photon sphere under a mild technical condition. This gives a partial answer to the question raised above; for a priori disconnected photon spheres, the issue will be addressed in [9], together with other results on photon surfaces.

This theorem can be interpreted as a photon sphere uniqueness theorem; its proof in fact mimics Israel's proof of static black hole uniqueness [10]. It allows to identify a given static vacuum isolated spacetime as in fact being a Schwarzschild spacetime whenever it is known to possess a photon sphere.

More precisely, if $\Sigma^2 \subset \{t = \text{const}\}$ is a photon sphere then we can¹⁰ use the lapse function N as a coordinate in the spatial slice $\{t = \text{const}\}$. As Israel showed in [10], the static vacuum equations (7) and (8) can be rephrased as inequalities on each level set of the coordinate N . Integrating those inequalities from the photon sphere all the way to spatial infinity, we obtain inequalities relating the mean and Gauß curvatures of the photon sphere to the ADM-mass m of the spacetime. Recall that we have already derived above that both of these curvatures are constant.

⁷See [4] for more information.

⁸See [6–8] for the origins of this definition.

⁹cf. [8] for an exposition of this analysis.

¹⁰Making the same mild technical assumption as Israel [10] that the lapse function foliates the region exterior to the photon sphere.

When combining the static vacuum equation (8) with the asymptotic decay of the spatial metric g discussed in (9) we can relate¹¹ the ADM-mass m of the spacetime to the normal derivative $\nu(N)$ of the lapse function via

$$\frac{c^2}{4\pi G} \int_{\Sigma^2} \nu(N) d\sigma = m. \quad (18)$$

This physical insight proves that the integrated inequalities are in fact equalities. This, however, implies that Israel's inequalities must be identities on each level set of N . From this, it is straightforward to compute that the spacetime is in fact Schwarzschild with N playing the role of a rescaled radial variable. For more details, we refer the reader to [8].

References

1. J. Ehlers, The Newtonian limit of general relativity, in *Classical Mechanics and Relativity: Relationship and Consistency* (Bibliopolis, Berkeley, 1989), pp. 95–106
2. C. Cederbaum, The Newtonian limit of geometrostatics. Ph.D. thesis, Free University Berlin (2011)
3. D. Kennefick, N.Ó Murchadha, Weakly decaying asymptotically flat static and stationary solutions to the Einstein equations. *Class. Quantum Grav.* **12**(1), 149 (1995)
4. C. Cederbaum. Uniqueness of the lapse function in static space-times. In preparation
5. Y. Choquet-Bruhat, J. Jork Jr, in *The Cauchy Problem*, ed. by A. Held. General Relativity and Gravitation, vol. 1. (Plenum Press, New York, 1980), pp. 99–172
6. C.-M. Claudel, K. Shwetketu, Virbhadra, G.F.R. Ellis, The geometry of photon surfaces. *J. Math. Phys.* **42**(2), 818–839 (2001)
7. V. Perlick, On totally umbilic submanifolds of semi-Riemannian manifolds. *Nonlinear Anal.* **63**(5–7), e511–e518 (2005)
8. C. Cederbaum. Uniqueness of photon spheres in static vacuum asymptotically flat spacetimes, in *Complex Analysis and Dynamical Systems VI.*, Contemporary mathematics - American Mathematical Society, (Providence, 2014) [to appear]
9. C. Cederbaum, G. Galloway, in preparation (2014)
10. W. Israel, Event horizons in static vacuum space-times. *Phys. Rev.* **164**(5), 1776–1779 (1967)

¹¹This relationship can actually be pursued much further; it even constitutes a central tool for showing that the Newtonian limit of the ADM-mass of a static isolated spacetime “is” the Newtonian mass of “its” Newtonian limit. For more details, see [2].

Aberrational Effects for Shadows of Black Holes

Arne Grenzebach

Abstract In this paper, we discuss how the shadow of a Kerr black hole depends on the motion of the observer. In particular, we derive an analytical formula for the boundary curve of the shadow for an observer moving with given four-velocity at given Boyer–Lindquist coordinates. We visualize the shadow for various values of parameters.

1 Introduction: What Is the “Shadow”?

For an observer at Boyer–Lindquist coordinates (r_O, ϑ_O) the *shadow* of a black hole is defined as that region of the observer’s celestial sphere which is left dark if all light sources are distributed on a sphere with radius $r_L > r_O$. To calculate the shadow, we consider light rays, i.e. lightlike geodesics, which are sent into the past from the observer’s position. Then, the boundary curve of the shadow corresponds to the limiting case between geodesics going towards the horizon (\rightarrow darkness) and geodesics going to the sphere at r_L with light sources (\rightarrow brightness). The limiting case are geodesics that asymptotically spiral towards (unstable) lightlike geodesics which fill a specific spatial region, the *photon region* \mathcal{K} , and are propagating on a sphere. Consequently, the shadow of the black hole is a mapping of this photon region \mathcal{K} and not of the horizon.

Starting with the theoretical work of Bardeen who for the first time calculated the shadow of a Kerr black hole correctly [1] we now reach the time where it seems to be possible to observe the shadow of the black hole near Sgr A* at the center of our Galaxy. The expected image is shown by calculations of how the shadow of a black hole would look like if matter, in the form of an accretion disc, a corona, or a jet, is included in the model. These calculations are based on ray tracing and GRMHD, see e.g. [2–7]. It is hoped that the shadow of Sgr A* will indeed be observed in the near future within the *Event Horizon Telescope* project, see [8], or the *Black Hole Cam* project.

A. Grenzebach (✉)

ZARM, University of Bremen, Am Fallturm, 28359 Bremen, Germany
e-mail: arne.grenzebach@zarm.uni-bremen.de

In the following, we discuss how differently moving observers at a given position see the shadow of a Kerr black hole. A detailed discussion of a more general space-time describing a Kerr–Newman–NUT black hole with cosmological constant can be found in [9]. There, we demonstrate how the shadow is influenced by a charge, the cosmological constant or the NUT parameter. Since there one can also find a discussion of metric properties and visualizations of the photon regions of the black holes, we restrict ourselves in this proceedings volume to the Kerr case. Our construction of the shadow is a geometrical one, based on the geodesic equation and ignoring the influence of matter.

2 The Kerr Metric

The Kerr space-time is a stationary, axially symmetric type D solution of the Einstein vacuum equations that describes a rotating black hole with mass m and spin a . In Boyer–Lindquist coordinates $(r, \vartheta, \varphi, t)$ the Kerr metric can be written as [10, p. 314]

$$g_{\mu\nu} dx^\mu dx^\nu = \Sigma \left(\frac{1}{\Delta} dr^2 + d\vartheta^2 \right) + \frac{1}{\Sigma} \left((\Sigma + a\chi)^2 \sin^2 \vartheta - \Delta \chi^2 \right) d\varphi^2 \\ + \frac{2}{\Sigma} (\Delta \chi - a(\Sigma + a\chi) \sin^2 \vartheta) dt d\varphi - \frac{1}{\Sigma} (\Delta - a^2 \sin^2 \vartheta) dt^2 \quad (1)$$

where we use the abbreviations

$$\Sigma = r^2 + (a \cos \vartheta)^2, \quad \chi = a \sin^2 \vartheta, \quad \Delta = r^2 - 2mr + a^2, \quad (2)$$

and rescaled units; hence, the speed of light and the gravitational constant are normalized ($c = 1$, $G = 1$). The coordinates t and r range over $]-\infty, \infty[$, while ϑ and φ are standard angular coordinates on the two-sphere. Whereas the parameter m for the mass of the black hole could take all values in \mathbb{R}^+ the absolute value of the spin parameter a is bounded by m since the event horizon of the Kerr black hole is at $r + \sqrt{m^2 - a^2}$.

3 Calculating the Shadows of Black Holes

As the geodesic equation in the Kerr space-time has four constants of motion—the Lagrangian \mathcal{L} , the energy and the z -component of angular momentum

$$E = -\frac{\partial \mathcal{L}}{\partial t} = -g_{\varphi t} \dot{\varphi} - g_{tt} \dot{t}, \quad L_z = \frac{\partial \mathcal{L}}{\partial \dot{\varphi}} = g_{\varphi\varphi} \dot{\varphi} + g_{\varphi t} \dot{t}, \quad (3)$$

plus the Carter constant K [11]—the lightlike geodesics ($\mathcal{L} = 0$) are given by four separated equations of motion

$$\Sigma \dot{t} = \frac{\chi(L_z - E\chi)}{\sin^2 \vartheta} + \frac{(\Sigma + a\chi)((\Sigma + a\chi)E - aL_z)}{\Delta}, \quad (4a)$$

$$\Sigma \dot{\phi} = \frac{L_z - E\chi}{\sin^2 \vartheta} + \frac{a((\Sigma + a\chi)E - aL_z)}{\Delta}, \quad (4b)$$

$$\Sigma^2 \dot{\vartheta}^2 = K - \frac{(\chi E - L_z)^2}{\sin^2 \vartheta} =: \Theta(\vartheta), \quad (4c)$$

$$\Sigma^2 \dot{r}^2 = ((\Sigma + a\chi)E - aL_z)^2 - \Delta K =: R(r). \quad (4d)$$

The existence of the *photon region* \mathcal{K} , i.e. the region filled with lightlike geodesics staying on a sphere $r = \text{constant}$, is crucial for calculating the shadow because it will give us a parametrization of the shadow's boundary curve. By (4d), the sphere conditions $\dot{r} = 0$ and $\ddot{r} = 0$ imply that $R(r) = 0$ and $R'(r) = 0$. Hence,

$$K_E = \frac{((\Sigma + a\chi) - aL_E)^2}{\Delta}, \quad K_E = \frac{2r((\Sigma + a\chi) - aL_E)}{r - m}, \quad (5)$$

where $L_E = \frac{L_z}{E}$ and $K_E = \frac{K}{E^2}$. Solving for these constants gives the expressions

$$K_E = \frac{4r^2 \Delta}{(r - m)^2}, \quad aL_E = (\Sigma + a\chi) - \frac{2r \Delta}{r - m} \quad (6)$$

for spherical light rays. Since $0 \leq \Sigma^2 \dot{\vartheta}^2$ we find by (4c) an inequality characterizing the photon region

$$\mathcal{K}: (2r \Delta - \Sigma(r - m))^2 \leq 4a^2 r^2 \Delta \sin^2 \vartheta. \quad (7)$$

Through each point (r, ϑ) of \mathcal{K} there is a light ray propagating on a sphere. Plots and a detailed discussion of the photon region for different space-times can be found in [9, Figs. 3–5].

4 Viewing the Shadows of Black Holes

For determining the shadow of a black hole we consider an observer at Boyer-Lindquist coordinates (r_O, ϑ_O) and assume, for the sake of simplicity, that the light sources are distributed on a sphere with radius $r_L > r_O$.

Lightlike geodesics reaching the observer can be divided into two types of orbits. There are geodesics which passed the sphere with light sources and there are those coming from the horizon. Thus, our observer would see brightness in the direction

of light rays of the first type and darkness for the other ones. The boundary curve of the shadow is therefore given by lightlike geodesics that spiraled from one of the unstable spherical light orbits of the photon region \mathcal{K} .

The shape of the shadow depends on the observer's state of motion. At Boyer–Lindquist coordinates (r_O, ϑ_O) , we choose an orthonormal tetrad adapted to the symmetry of the space-time [10, p.307]

$$\begin{aligned} e_0 &= \frac{(\Sigma + a\chi)\partial_t + a\partial_\varphi}{\sqrt{\Sigma\Delta}} \Big|_{(r_O, \vartheta_O)}, & e_1 &= \sqrt{\frac{1}{\Sigma}} \partial_\vartheta \Big|_{(r_O, \vartheta_O)}, \\ e_2 &= -\frac{\partial_\varphi + \chi\partial_t}{\sqrt{\Sigma} \sin \vartheta} \Big|_{(r_O, \vartheta_O)}, & e_3 &= -\sqrt{\frac{\Delta}{\Sigma}} \partial_r \Big|_{(r_O, \vartheta_O)}. \end{aligned} \quad (8)$$

It is chosen such that $e_0 \pm e_3$ are tangential to the *principal null congruences* of our metric. Here, e_0 is interpreted as the four-velocity of an observer at (r_O, ϑ_O) because it is a timelike vector; e_3 points into the direction towards the center of the black hole. An observer with this tetrad is called a *standard observer* in the following.

If another observer at (r_O, ϑ_O) moves with velocity $\mathbf{v} = (v_1, v_2, v_3)$, $v = |\mathbf{v}| < 1 = c$, with respect to our standard observer, we have to modify the tetrad. The four-velocity of the moving observer is

$$\tilde{e}_0 = \frac{v_1 e_1 + v_2 e_2 + v_3 e_3 + e_0}{\sqrt{1 - v^2}}. \quad (9a)$$

From $\tilde{e}_0, e_1, e_2, e_3$ we find an orthonormal tetrad $\tilde{e}_0, \tilde{e}_1, \tilde{e}_2, \tilde{e}_3$ with the Gram–Schmidt procedure by adding e_3, e_1, e_2 —in this order—successively to \tilde{e}_0

$$\begin{aligned} \tilde{e}_1 &= \frac{(1 - v_2^2)e_1 + v_1(v_2 e_2 + e_0)}{\sqrt{1 - v_2^2} \sqrt{1 - v_1^2 - v_2^2}}, \\ \tilde{e}_2 &= \frac{e_2 + v_2 e_0}{\sqrt{1 - v_2^2}}, \\ \tilde{e}_3 &= \frac{(1 - v_1^2 - v_2^2)e_3 + v_3(v_1 e_1 + v_2 e_2 + e_0)}{\sqrt{1 - v_1^2 - v_2^2} \sqrt{1 - v^2}}. \end{aligned} \quad (9b)$$

Note that $\tilde{e}_i = e_i$ if $v_i = 0$, i.e., for $\mathbf{v} = 0$ this procedure recovers the tetrad e_0, e_1, e_2, e_3 . As before, the spacelike vector \tilde{e}_3 corresponds to the direction towards the black hole. The interpretation of \tilde{e}_1 and \tilde{e}_2 becomes clear if we introduce celestial coordinates, see (11) and Fig. 1. Then, \tilde{e}_1 and \tilde{e}_2 point into the north–south respectively the west–east direction.

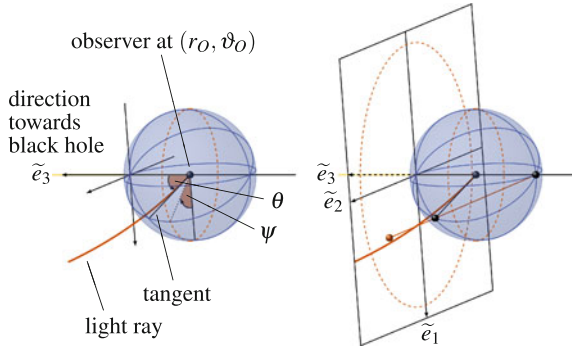


Fig. 1 The direction of each light ray reaching the observer is given by the celestial coordinates θ and ψ [Eq. (11)] of their tangents, see figure on the *left*. These points (θ, ψ) on the celestial sphere (*black ball*) can be identified with points in the plane (*red ball*) by stereographic projection, see figure on the *right*. The *dashed (red) circles* mark the celestial equator $\theta = \pi/2$ respectively its projection

We can now describe the tangent vector of a light ray $\lambda(s)$ by Boyer–Lindquist coordinates

$$\dot{\lambda} = \dot{r}\partial_r + \dot{\vartheta}\partial_{\vartheta} + \dot{\varphi}\partial_{\varphi} + \dot{t}\partial_t \quad (10)$$

and by celestial coordinates θ and ψ for our moving observer

$$\dot{\lambda} = \sigma(-\tilde{e}_0 + \sin\theta \cos\psi \tilde{e}_1 + \sin\theta \sin\psi \tilde{e}_2 + \cos\theta \tilde{e}_3) \quad (11)$$

where $\theta = 0$ corresponds to the direction towards the black hole. For the tetrad (9) we observe the following dependencies regarding (8):

$$\begin{aligned} \tilde{e}_0 &= k_{0r}\partial_r + k_{0\vartheta}\partial_{\vartheta} + k_{0\varphi}\partial_{\varphi} + k_{0t}\partial_t, \\ \tilde{e}_1 &= k_{1\vartheta}\partial_{\vartheta} + k_{1\varphi}\partial_{\varphi} + k_{1t}\partial_t, \\ \tilde{e}_2 &= k_{2\varphi}\partial_{\varphi} + k_{2t}\partial_t, \\ \tilde{e}_3 &= k_{3r}\partial_r + k_{3\vartheta}\partial_{\vartheta} + k_{3\varphi}\partial_{\varphi} + k_{3t}\partial_t. \end{aligned} \quad (12)$$

Hence

$$\begin{aligned} \dot{\lambda} &= \sigma((-k_{0r} + k_{3r} \cos\theta)\partial_r + (-k_{0\vartheta} + k_{1\vartheta} \sin\theta \cos\psi + k_{3\vartheta} \cos\theta)\partial_{\vartheta} \\ &\quad + (-k_{0\varphi} + k_{1\varphi} \sin\theta \cos\psi + k_{2\varphi} \sin\theta \sin\psi + k_{3\varphi} \cos\theta)\partial_{\varphi} \\ &\quad + (-k_{0t} + k_{1t} \sin\theta \cos\psi + k_{2t} \sin\theta \sin\psi + k_{3t} \cos\theta)\partial_t). \end{aligned} \quad (13)$$

Comparing coefficients of ∂_r , ∂_ϑ , and ∂_φ in (10) and (13) yields

$$\dot{r} = \sigma(-k_{0r} + k_{3r} \cos \theta), \quad (14)$$

$$\dot{\vartheta} = \sigma(-k_{0\vartheta} + k_{1\vartheta} \sin \theta \cos \psi + k_{3\vartheta} \cos \theta), \quad (15)$$

$$\dot{\varphi} = \sigma(-k_{0\varphi} + k_{1\varphi} \sin \theta \cos \psi + k_{2\varphi} \sin \theta \sin \psi + k_{3\varphi} \cos \theta). \quad (16)$$

These equations can be solved easily for $\cos \theta$ and $\sin \psi$ (using $k_{1\vartheta} \sin \theta \cos \psi = \frac{1}{\sigma} \dot{\vartheta} + k_{0\vartheta} - k_{3\vartheta} \cos \theta$),

$$\cos \theta = \frac{\frac{1}{\sigma} \dot{r} + k_{0r}}{k_{3r}}, \quad (17a)$$

$$\sin \psi = \frac{k_{3r} \left(\frac{1}{\sigma} \dot{\varphi} + k_{0\varphi} - \frac{k_{1\varphi}}{k_{1\vartheta}} \left(\frac{1}{\sigma} \dot{\vartheta} + k_{0\vartheta} \right) \right) - \left(k_{3\varphi} - \frac{k_{3\vartheta}}{k_{1\vartheta}} k_{1\varphi} \right) \left(\frac{1}{\sigma} \dot{r} + k_{0r} \right)}{k_{2\varphi} \sqrt{k_{3r}^2 - \left(\frac{1}{\sigma} \dot{r} + k_{0r} \right)^2}} \quad (17b)$$

where $\dot{\varphi}$, $\dot{\vartheta}$ and \dot{r} have to be substituted from the equations of motion (4b), (4c) and (4d); since \dot{r} and $\dot{\vartheta}$ are given as quadratic expressions, the signs have to be chosen consistently.

The remaining scalar factor σ can be calculated analogously to α in [9, Eq. (20)]. At first, express \tilde{e}_0 (9a) in terms of the tetrad $\{\partial_r, \partial_\vartheta, \partial_\varphi, \partial_t\}$

$$\tilde{e}_0 = \frac{1}{\sqrt{\Sigma} \sqrt{1-v^2}} \left(\frac{(\Sigma + a\chi) \partial_t + a \partial_\varphi}{\sqrt{\Delta}} + v_1 \partial_\vartheta - v_2 \frac{\partial_\varphi + \chi \partial_t}{\sin \vartheta} - v_3 \sqrt{\Delta} \partial_r \right). \quad (18)$$

As $\sigma = g(\dot{\lambda}, \tilde{e}_0)$, see (11) we get σ from (1), (10), and (18),

$$\sigma = \frac{1}{\sqrt{\Sigma} \sqrt{1-v^2}} \left(\frac{aL_z - (\Sigma + a\chi)E}{\sqrt{\Delta}} + v_1 \Sigma \dot{\vartheta} - v_2 \frac{L_z - \chi E}{\sin \vartheta} - v_3 \frac{\Sigma}{\sqrt{\Delta}} \dot{r} \right) \Big|_{(r_O, \vartheta_O)} \quad (19)$$

where $\dot{\varphi}$, $\dot{\vartheta}$ and \dot{r} have to be substituted from (4b), (4c) and (4d) as above.

With this expression, (17) indeed describes the boundary curve of the black hole's shadow for a moving observer. The boundary represents lightlike geodesics which, if you think of sending them from the observer's position into the past, reach the photon region asymptotically. Each such geodesic must have constants of motion

$$K_E = \frac{4r^2 \Delta}{(r-m)^2} \Big|_{r=r_p}, \quad aL_E = (\Sigma + a\chi) - \frac{2r\Delta}{r-m} \Big|_{r=r_p}, \quad (20)$$

given by (6) where r_p is the radius coordinate of the limiting spherical lightlike geodesic. For $a > 0$, this radius coordinate r_p is—as in [9]—extremal where the boundary of the exterior photon region intersects the cone $\vartheta = \vartheta_O$. Hence, the extremal values are the values of r where (7) holds with equality. Substituting K_E and L_E in (17) and (19) by the expressions (20) provides the shadow’s boundary curve $(\theta(r_p), \psi(r_p))$ where r_p runs between the extremal values.

If $a = 0$, then it is not possible to parametrize the boundary curve by r_p because the right hand side of (7) is zero, so it determines a unique r_p . By (20) this results in an unique value for K_E which, when inserted into (17), gives the shadow’s boundary curve in the form $(\psi(L_E), \theta(L_E))$. Here, L_E ranges between the extremal values determined by (4c) for $\Sigma^2 \dot{\vartheta}^2 = 0$.

5 Plots of Black Hole’s Shadows

As described before, we used our analytical parameter representation (17) with (19) and (20) to calculate the boundary curve of the shadow as seen by an observer moving with four-velocity \tilde{e}_0 . The results in Fig. 3 are visualized via stereographic projection from the celestial sphere onto a plane, as illustrated in Fig. 1. Standard Cartesian coordinates in this plane are given by

$$\begin{aligned} x(r_p) &= -2 \tan\left(\frac{\theta(r_p)}{2}\right) \sin(\psi(r_p)), \\ y(r_p) &= -2 \tan\left(\frac{\theta(r_p)}{2}\right) \cos(\psi(r_p)). \end{aligned} \quad (21)$$

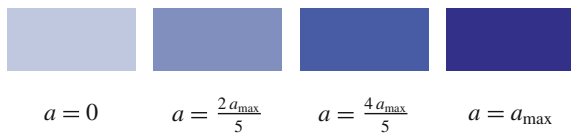
All plots of shadows shown in Fig. 3 belong to Kerr black holes where each subfigure combines the pictures for four spin values, see legend in Fig. 2.

In principle, the shadows for moving observers ($v \neq 0$) are calculable from the shadow seen by the standard observer ($v = 0$) with the help of Penrose’s aberration formula [12]

$$\tan \frac{\tilde{\alpha}}{2} = \sqrt{\frac{c-v}{c+v}} \tan \frac{\alpha}{2}. \quad (22)$$

But for applying this formula, one may need to make coordinate transformations since the angles α and $\tilde{\alpha}$ have to be measured against the direction of the motion. Hence, no transformations are needed if the observer moves in radial direction.

Fig. 2 Legend for the different spins a used for calculating the black hole’s shadows shown in Fig. 3



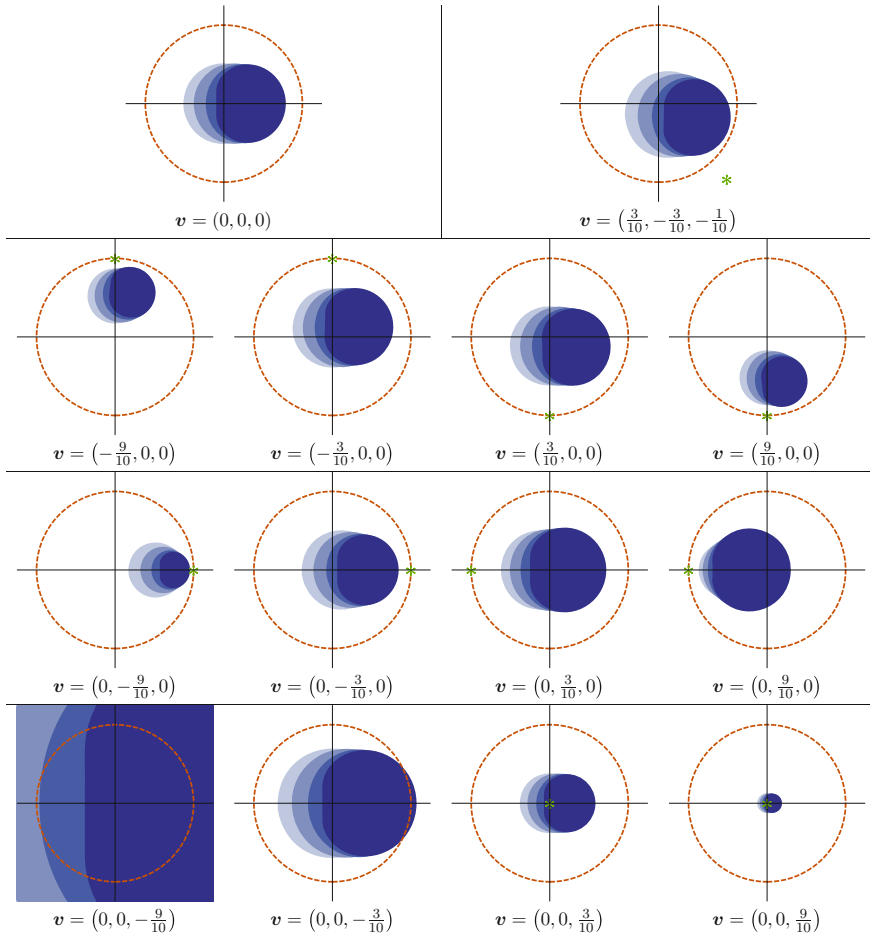


Fig. 3 Aberrational effects on the shadows of Kerr black holes. The subfigures show the stereographic projection of the shadow for observers moving with various velocities $\mathbf{v} = (v_1, v_2, v_3)$ which are noted beneath the plots ($r_O = 5m$, $\vartheta_O = \frac{\pi}{2}$). If $\mathbf{v} \neq 0$, the projected direction of the observer’s motion is marked by a (green) star. Each plot combines the silhouettes for four different spins ($a = \kappa \cdot a_{\text{max}}$ where $a_{\text{max}} = m$), see Fig. 2 for the corresponding legend

Then, the shadow is magnified if the observer moves away from the black hole, and demagnified if the observer moves towards the black hole. In this case, our formula (17a) reduces to the following common variant of Penrose’s aberration formula (22)

$$\cos \tilde{\theta} = \frac{v + \cos \theta}{1 + v \cos \theta}. \tag{23}$$

Penrose emphasized in his article [12] that the aberration formula maps circles on the celestial sphere onto circles. Thus, the shadow of a non-rotating black hole ($a = 0$) is always circular, independent of the observer's motion. Consequently, our pictures of the shadow are then always circular, because the stereographic projection (21) maps circles onto circles, too.

Figure 3 shows several pictures of shadows for differently moving observers in Kerr space-times. The results for the standard observer ($\mathbf{v} = 0$, $\tilde{e}_\mu = e_\mu$) are shown in the left plot in the first row of Fig. 3. The right plot is exemplary and belongs to an observer moving with velocity $\mathbf{v} = (\frac{3}{10}, -\frac{3}{10}, -\frac{1}{10})$. In each of the lower rows we vary only one component v_i of \mathbf{v} ; in the following we write \mathbf{v}_i as abbreviation for those observer velocities \mathbf{v} with $v_i \neq 0$ and $v_j = 0$, $j \neq i$. Due to our definition of the tetrad e_μ in (8) and of the observer's four-velocity \tilde{e}_0 in (9a) the observer moves in ϑ direction if $\mathbf{v} = \mathbf{v}_1$, and in r i.e. radial direction if $\mathbf{v} = \mathbf{v}_3$. For $\mathbf{v} = \mathbf{v}_2$ the motion is in φ direction.

Since the last row of Fig. 3 shows the plots of shadows seen by a radially moving observer ($\mathbf{v} = \mathbf{v}_3$), the shadows are magnified if the observer moves away from the black hole (v_3 negative), and demagnified, if the observer moves towards the black hole (v_3 positive), as mentioned before.

For velocities $\mathbf{v} = \mathbf{v}_1$ or $\mathbf{v} = \mathbf{v}_2$ the shadow is shifted in the direction of the observer's motion with bigger effects for higher velocities. Also the size of the shadow is affected. But all these aberrational changes are explainable if one relates the direction of the observer's motion to the spin of the black hole and to the equatorial plane as symmetry plane.

Furthermore, the shadow is symmetric with respect to a horizontal axis as long as the observer does not move in ϑ direction because $\sin \psi$, see (17b), depends on ϑ which is given by a quadratic expression, see (4c). Hence, the different signs of ϑ yield different solutions of (17) for the points (θ, ψ) and $(\theta, \pi - \psi)$. Without a ϑ component in the velocity, the symmetry of the shadow is not affected even if the observer is not in the equatorial plane, i.e. $\vartheta_0 \neq \frac{\pi}{2}$.

All in all, the shadows shown in Fig. 3 are calculated for relatively fast moving observers ($v = 0.3c$ up to $v = 0.9c$). Thus, the aberrational influence for the future observations of the shadow of Sgr A* within the Event Horizon Telescope or the Black Hole Cam project is expected to be very small since our solar system orbits the galactic center with roughly $250 \frac{\text{km}}{\text{s}} \approx \frac{1}{1000}c$, see [13]. Nevertheless, the study of aberrational effects are of interest from a fundamental point of view.

Acknowledgments I would like to thank Volker Perlick, Claus Lämmerzahl, Nico Giulini, Norman Gürlebeck, Eva Hackmann, Valeria Diemer (née Kagramanova), Jutta Kunz and Luciano Rezzolla for helpful discussions. Furthermore, I want to thank Dirk Pützfeld, Claus Lämmerzahl, and Bernard F. Schutz for organizing the 524th WE-Heraeus-Seminar and for the opportunity to contribute to this proceedings volume. The WE-Heraeus foundation deserves my gratitude for offering poster awards. I gratefully acknowledge support from the DFG within the Research Training Group 1620 “Models of Gravity” and from the “Centre for Quantum Engineering and Space-Time Research (QUEST)”.

References

1. J.M. Bardeen, Timelike and null geodesics in the Kerr metric, in *Black Holes (Les Astres Occlus)*, ed. by C. DeWitt, B.S. DeWitt (Gordon and Breach, New York, 1973), pp. 215–239
2. H. Falcke, F. Melia, E. Agol, Viewing the shadow of the black hole at the galactic center. *Astrophys. J.* **528**, L13–L16 (2000)
3. J. Dexter, E. Agol, P.C. Fragile, J.C. McKinney, Radiative models of sagittarius A* and M87 from relativistic MHD simulations. *J. Phys.* **372**, 012023 (2012)
4. J. Dexter, P.C. Fragile, Tilted black hole accretion disc models of sagittarius A*: time-variable millimetre to near-infrared emission. *Mon. Not. R. Astron. Soc.* **432**, 2252–2272 (2013)
5. Z. Younsi, K. Wu, S.V. Fuerst, General relativistic radiative transfer: formulation and emission from structured tori around black holes. *Astron. Astrophys.* **545**, A13 (2012)
6. M. Mościbrodzka, H. Falcke, H. Shiokawa, C.H.F. Gammie, Observational appearance of inefficient accretion flows and jets in 3D GRMHD simulations: application to Sgr A*. *Astron. Astrophys.* **570**, A7 (2014)
7. V.L. Fish, M.D. Johnson, R.-S. Lu, S.S. Doeleman, K.L. Bouman, D. Zoran, W.T. Freeman, D. Psaltis, R. Narayan, V. Pankratius, A.E. Broderick, C.R. Gwinn, L.E. Vertatschitsch, Imaging an event horizon: mitigation of scattering toward Sagittarius A*. *Astrophys. J.* **795**, 134 (2014)
8. S. Doeleman, Imaging an event horizon: submm-VLBI of a super massive black hole, *Astro 2010: astronomy and astrophysics. Decadal survey* (Science White Papers, 2009)
9. A. Grenzebach, V. Perlick, C. Lämmerzahl, Photon regions and shadows of Kerr-Newman-NUT black holes with a cosmological constant. *Phys. Rev. D* **89**, 124004 (2014)
10. J.B. Griffiths, J. Podolský, *Exact Space-Times in Einstein's General Relativity* (Cambridge University Press, Cambridge, 2009)
11. B. Carter, Hamilton-Jacobi and Schrodinger separable solutions of Einstein's equations. *Commun. Math. Phys.* **10**, 280–310 (1968)
12. R. Penrose, The apparent shape of a relativistically moving sphere. *Math. Proc. Camb. Philos. Soc.* **55**, 137–139 (1959)
13. M.J. Reid, K.M. Menten, X.W. Zheng et al., Trigonometric parallaxes of massive star-forming regions. VI. Galactic structure, fundamental parameters, and noncircular motions. *Astrophys. J.* **700**, 137–148 (2009)

Time-Domain Inspiral Templates for Spinning Compact Binaries in Quasi-Circular Orbits

Anuradha Gupta and Achamveedu Gopakumar

Abstract We present a prescription to compute the time-domain gravitational wave (GW) polarization states associated with spinning compact binaries inspiraling along quasi-circular orbits. We invoke the orbital angular momentum \mathbf{L} rather than its Newtonian counterpart \mathbf{L}_N to describe the orbits and the two spin vectors are freely specified in the source frame associated with the initial direction of the total angular momentum. We discuss the various implications of our approach.

1 Introduction

Gravitational waves (GWs) from coalescing compact binaries containing at least one spinning component are expected to be routinely detected by the second-generation laser interferometric detectors like advanced LIGO (aLIGO), Virgo and KAGRA [1]. The detection of GWs from such binaries and subsequent source characterization crucially depend on accurately modeling temporally evolving GW polarization states, $h_+(t)$ and $h_\times(t)$, from such binaries during their inspiral phase [2]. At present, $h_+(t)$ and $h_\times(t)$ associated with non-spinning compact binaries inspiraling along quasi-circular orbits have GW phase evolution accurate to 3.5PN order and amplitude corrections that are 3PN accurate [3]. Recall that the 3.5PN and 3PN orders correspond to corrections that are accurate to relative orders $(v/c)^7$ and $(v/c)^6$ beyond the ‘Newtonian’ estimates, where v and c are the orbital and light speeds, respectively. In the case of inspiraling compact binaries containing Kerr black hole (BHs), it is desirable to employ temporally evolving $h_+(t)$ and $h_\times(t)$ that incorporate the spin effects very accurately and the dominant spin effect arises due to the general relativistic spin-orbit coupling that appear at the relative 1.5PN order for maximally spinning Kerr BHs [4, 5]. Following Ref. [5], we define the spin of a compact object

A. Gupta (✉) · A. Gopakumar

Department of Astronomy and Astrophysics, Tata Institute of Fundamental Research,
Mumbai 400005, India

e-mail: arg@tifr.res.in; anuradha@iucaa.ernet.in

A. Gopakumar

e-mail: gopu@tifr.res.in

as $\mathbf{S} = G m_{\text{co}}^2 \chi \mathbf{s}/c$, where m_{co} , χ and \mathbf{s} are its mass, Kerr parameter and a unit vector along \mathbf{S} , respectively and for a maximally spinning Kerr BH $\chi = 1$. We note that it is customary to employ the Newtonian orbital angular momentum $\mathbf{L}_N = \mu \mathbf{r} \times \mathbf{v}$, where μ , \mathbf{r} and \mathbf{v} are the reduced mass, orbital separation and velocity, respectively, to specify these quasi-circular orbits [5, 6].

In what follows we provide a prescription to generate the time-domain amplitude corrected $h_+(t)$ and $h_\times(t)$ for spinning compact binaries inspiraling along quasi-circular orbits, described by their orbital angular momenta. Note that the amplitude corrected $h_+(t)$ and $h_\times(t)$ refer to GW polarization states that are PN-accurate both in its amplitude and phase. We describe our approach to compute the fully 1.5PN accurate amplitude corrected expression for $h_\times(t)$ while invoking \mathbf{L} , the PN-accurate orbital angular momentum, to characterize the binary orbits. We symbolically obtain the additional 1.5PN order amplitude corrections to $h_\times(t)$ in comparison with Eqs. (A3) in Ref. [6] that employ \mathbf{L}_N to describe the binary orbits. We also discuss certain implications of our approach while considering spin effects due to the leading order general relativistic spin-orbit coupling. Our attempt to perform GW phasing with the help of \mathbf{L} is motivated by a number of observations (we term accurate modeling of temporally evolving GW polarization states as ‘GW phasing’). First being Ref. [7] that provided a prescription to implement GW phasing for spinning compact binaries in inspiralling eccentric orbits in an accurate and efficient way. We are further influenced by the fact that it is customary to use precessional equation appropriate for \mathbf{L} to evolve \mathbf{L}_N while incorporating the effects due to the dominant order spin-orbit coupling [5, 6, 8]. Finally, we note that a seminal paper that explored the inspiral dynamics of spinning compact binaries and the influences of precessional dynamics on $h_{+,\times}(t)$ employed \mathbf{L} to describe their binary orbits [9]. Additionally, we specify the two spins in an inertial frame associated with the initial direction of the total angular momentum \mathbf{j}_0 while it is customary to invoke a non-inertial \mathbf{L}_N -based orbital triad to specify the two spins in the literature.

2 GW Phasing for Spinning Binaries Characterized by \mathbf{L}

We invoke, as noted earlier, the PN-accurate orbital angular momentum \mathbf{L} to describe binary orbits and we specify at the initial epoch both the orbital and spin angular momentum vectors in an inertial frame associated with the initial direction of total angular momentum (see Fig. 1). We begin by presenting an expression for the cross polarization state having Newtonian (quadrupolar) order amplitude and the relevant expression reads [10]

$$h_\times|_Q(t) = 2 \frac{G \mu}{c^2} \frac{v^2}{R'} \left\{ (1 - \cos \iota) S_\theta \sin \iota \sin(\alpha - 2\Phi) \right. \\ \left. - (1 + \cos \iota) S_\theta \sin \iota \sin(\alpha + 2\Phi) \right\}$$

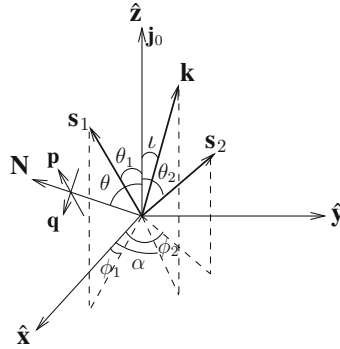


Fig. 1 The inertial frame and the Cartesian coordinate system where the \hat{z} axis points along \hat{j}_0 , the direction of total angular momentum at the initial epoch. We display the angles that characterize the orbital and spin angular momentum vectors, denoted by \mathbf{k} , \mathbf{s}_1 and \mathbf{s}_2 , while the line of sight vector \mathbf{N} is in the $x - z$ plane. The *dashed lines* depict the projections of various vectors on the $x - y$ plane

$$\begin{aligned} & -\frac{1}{2}(1 + 2 \cos \iota + \cos^2 \iota) C_\theta \sin(2\alpha + 2\Phi) \\ & -\frac{1}{2}(1 - 2 \cos \iota + \cos^2 \iota) C_\theta \sin(2\alpha - 2\Phi) \Big\}, \end{aligned} \quad (1)$$

where R' , S_θ and C_θ stand for the radial distance to the binary, $\sin \theta$ and $\cos \theta$, respectively. The dynamical angular variable Φ measures the orbital phase from the direction of ascending node in a plane perpendicular to \mathbf{k} while its derivative is required to define $v^2/c^2 = (G m \dot{\Phi}/c^3)^{2/3}$. To obtain temporally evolving $h_{\times|Q}(t)$ associated with spinning compact binaries inspiraling along quasi-circular orbits, we pursue the following steps. First, we specify how the Eulerian angles α and ι that specify the orientation of \mathbf{L} vary under the conservative orbital dynamics. This requires us to employ three differential equations that describe the precessional dynamics of the orbital and spin angular momenta and these differential equations contain an orbital like frequency ω [5]. The conservative evolution for Φ and $\dot{\Phi}$ are governed by the following differential equation

$$\dot{\Phi} = \omega - \cos \iota \dot{\alpha}, \quad (2)$$

where the orbital like frequency ω is defined by the relation $\omega = v/r$ that connects ω to the orbital separation and velocity. This PN-accurate equation arises from the vectorial expression for the orbital velocity in a co-moving triad [5]. It is convenient to introduce a dimensionless parameter $x \equiv (G m \omega_{\text{orb}}/c^3)^{2/3}$ such that the above equation reads $\dot{\Phi} = (x^{3/2}/(G m/c^3)) - \cos \iota \dot{\alpha}$. Thereafter, we impose the effects of gravitational radiation reaction on these differential equations by specifying how x , appearing in these differential equations, vary during the binary inspiral.

It turns out that we require to solve simultaneously the precessional equations for \mathbf{k} , \mathbf{s}_1 and \mathbf{s}_2 , the unit vectors along \mathbf{L} , \mathbf{S}_1 and \mathbf{S}_2 , to specify how α and ι vary under the conservative dynamics as the precessional dynamics of \mathbf{L} , \mathbf{S}_1 and \mathbf{S}_2 are intertwined. In Fig. 1, we display various angles that specify the orientations of these three unit vectors in the above inertial frame. The Cartesian components of these vectors are

$$\mathbf{k} = (\sin \iota \cos \alpha, \sin \iota \sin \alpha, \cos \iota), \quad (3a)$$

$$\mathbf{s}_1 = (\sin \theta_1 \cos \phi_1, \sin \theta_1 \sin \phi_1, \cos \theta_1), \quad (3b)$$

$$\mathbf{s}_2 = (\sin \theta_2 \cos \phi_2, \sin \theta_2 \sin \phi_2, \cos \theta_2). \quad (3c)$$

The precessional equations for the above three unit vectors, extractable from Refs. [4, 5], read

$$\dot{\mathbf{k}} = \frac{c^3}{Gm} x^3 \left\{ \delta_1 q \chi_1 (\mathbf{s}_1 \times \mathbf{k}) + \frac{\delta_2}{q} \chi_2 (\mathbf{s}_2 \times \mathbf{k}) \right\}, \quad (4a)$$

$$\dot{\mathbf{s}}_1 = \frac{c^3}{Gm} x^{5/2} \delta_1 (\mathbf{k} \times \mathbf{s}_1), \quad (4b)$$

$$\dot{\mathbf{s}}_2 = \frac{c^3}{Gm} x^{5/2} \delta_2 (\mathbf{k} \times \mathbf{s}_2), \quad (4c)$$

where $q = m_1/m_2$ and the symmetric mass ratio $\eta = \mu/m$ is required to define the quantities δ_1 and δ_2 ($\delta_{1,2} = \eta/2 + 3(1 \mp \sqrt{1-4\eta})/4$). We are now in a position to incorporate the effect of gravitational radiation damping and this is achieved by specifying the secular variations in x in the above differential equations. The PN-accurate differential equation for x arises from the usual energy balance arguments and may be obtained from Eq. (3.21) in Ref. [6].

We obtain numerically the time-domain GW polarization states for our binaries by simultaneously solving the differential equations for the Cartesian components of \mathbf{k} , \mathbf{s}_1 and \mathbf{s}_2 along with the PN-accurate equations for $\dot{\Phi}$ and dx/dt . This implies that we numerically solve a set of 11 differential equations and the resulting variations in α , ι , Φ and $\dot{\Phi}$ are implemented in Eq. (1) to obtain the temporally varying $h_{\times|Q}(t)$. A close inspection reveals that we require to specify four angles that provide the orientations of the two spins from \mathbf{j}_0 at the initial epoch to obtain $h_{\times|Q}(t)$. It should be noted that the two angles that specify the initial orientation of \mathbf{k} from \mathbf{j}_0 are not independent variables. This is because one may point the total angular momentum along the z -axis at the initial epoch without the loss of any generality. This allowed us to equate the x and y components of $\mathbf{J} = \mathbf{L} + \mathbf{S}_1 + \mathbf{S}_2$ to zero at that epoch and therefore to obtain the initial estimates for ι and α . In our numerical integrations, the bounding values for x are given by $x_0 = 2.9 \times 10^{-4} (m' \omega_0)^{2/3}$ and $x_f = 1/6$, where m' is the total mass of the binary in solar units and let $\omega_0 = 10 \pi$ Hz as customary for aLIGO along with $\Phi(x_0) = 0$. Finally, we note that the values of α and ι at every step of our numerical runs are obtained from the Cartesian components of \mathbf{k} by

the relations: $\alpha = \cos^{-1}(k_x / \sqrt{k_x^2 + k_y^2})$ and $\iota = \cos^{-1}(k_z)$. Therefore, we require eight independent parameters to specify the inspiral dynamics of compact binaries with spinning components and these eight parameters are the four basic (constant) parameters namely $(m_1, m_2, \chi_1, \chi_2)$ along with the above four angular dynamical variables that specify the two spin vectors in the inertial frame, namely (θ_1, ϕ_1) and (θ_2, ϕ_2) as displayed in Fig. 1.

In what follows we compare our approach with what is detailed in Ref. [6] that provided a way to obtain the time-domain ready-to-use GW polarization states for inspiraling compact binaries while incorporating all 1.5PN order spin effects both in amplitude and GW phase evolutions. Their approach differs from ours in two aspects. First, Ref. [6] employed $\mathbf{l} = \mathbf{L}_N / |\mathbf{L}_N|$ to characterize the orbital plane and following the earlier papers employed a precessional equation for \mathbf{l} that is identical to our Eq. (4a) for $\dot{\mathbf{k}}$ while replacing \mathbf{k} by \mathbf{l} . It is not very difficult to show that this is equivalent of using an orbital averaged expression for $\dot{\mathbf{l}}$ [5]. However, invoking an orbital averaged precessional equation for \mathbf{l} leads to an undesirable feature that the coefficient of \mathbf{l} in the expression for $\dot{\mathbf{n}}$ in the $(\mathbf{n}, \boldsymbol{\lambda} = \mathbf{l} \times \mathbf{n}, \mathbf{l})$ frame will not, in general, vanish. It is fairly straightforward to compute the time derivative of \mathbf{n} and express it in the $(\mathbf{n}, \boldsymbol{\lambda}, \mathbf{l})$ frame as

$$\frac{d\mathbf{n}}{dt} = \left(\frac{d\Phi'}{dt} + \cos \iota' \frac{d\alpha'}{dt} \right) \boldsymbol{\lambda} + \left(\frac{d\iota'}{dt} \sin \Phi' - \sin \iota' \cos \Phi' \frac{d\alpha'}{dt} \right) \mathbf{l}, \quad (5)$$

where ι', α' and Φ' are the usual 3 Eulerian angles required to define $\mathbf{n}, \boldsymbol{\lambda}$ and \mathbf{l} in the \mathbf{j}_0 -based inertial frame. The fact that $\mathbf{l} \equiv \mathbf{n} \times \dot{\mathbf{n}} / |\mathbf{n} \times \dot{\mathbf{n}}|$ clearly demands that the coefficient of \mathbf{l} in the above equation should be zero as also noted in Ref. [6]. However, if one employs Eq. (4a) to describe the precessional dynamics of \mathbf{l} then it is possible to show with some straightforward algebra that

$$\sin \Phi' \frac{d\iota'}{dt} - \cos \Phi' \sin \iota' \frac{d\alpha'}{dt} = -\frac{c^3}{Gm} x^3 \left\{ \delta_1 q \chi_1 (\mathbf{s}_1 \cdot \boldsymbol{\lambda}) + \frac{\delta_2}{q} \chi_2 (\mathbf{s}_2 \cdot \boldsymbol{\lambda}) \right\}, \quad (6)$$

as noted in Ref. [7]. It is not very difficult to conclude that the right hand side of above expression, in general, is not zero.

It turns out that $\dot{\mathbf{n}}$ having components along \mathbf{l} leads to certain anomalous terms that contribute to the Φ' evolution at the 3PN order and this is within the consideration of higher order spin effects available in the literature. Note that the higher order spin effects are known to 3.5PN order while dealing with the spin-orbit interactions [11]. We demonstrate our observation by noting that the definitions $\mathbf{v} = r \dot{\mathbf{n}}$ and $v = r \omega$ imply that $\omega^2 = \dot{\mathbf{n}} \cdot \dot{\mathbf{n}}$. With the help of our Eq. (5) the expression for ω reads

$$\omega = \left(\frac{d\Phi'}{dt} + \cos \iota' \frac{d\alpha'}{dt} \right) + \frac{1}{2\dot{\Phi}'} \left(\frac{d\iota'}{dt} \sin \Phi' - \sin \iota' \cos \Phi' \frac{d\alpha'}{dt} \right)^2, \quad (7)$$

where $\dot{\Phi}'$ stands for $d\Phi'/dt$ and the higher order terms that are cubic in the time derivatives of ι' and α' are neglected. Invoking the fact that $\dot{\Phi}'$ at the Newtonian order is given by $x^{3/2}/(Gm/c^3)$ and noting that the expression for $d\iota'/dt$ and $d\alpha'/dt$ arise from the 1.5PN order differential equation for $\dot{\mathbf{k}}$, we get

$$\dot{\Phi}' = \frac{c^3}{Gm} x^{3/2} \left(1 + x^{3/2} A' + x^3 B' \right), \quad (8)$$

such that A' and B' are given by

$$A' = -\frac{\cos \iota'}{\sin \iota'} \left\{ [\delta_1 q \chi_1 (\mathbf{s}_1 \cdot \boldsymbol{\lambda}) + \frac{\delta_2}{q} \chi_2 (\mathbf{s}_2 \cdot \boldsymbol{\lambda})] \cos \Phi' \right. \\ \left. + [\delta_1 q \chi_1 (\mathbf{s}_1 \cdot \mathbf{n}) + \frac{\delta_2}{q} \chi_2 (\mathbf{s}_2 \cdot \mathbf{n})] \sin \Phi' \right\}, \quad (9a)$$

$$B' = -\frac{1}{2} \left\{ \delta_1 q \chi_1 (\mathbf{s}_1 \cdot \boldsymbol{\lambda}) + \frac{\delta_2}{q} \chi_2 (\mathbf{s}_2 \cdot \boldsymbol{\lambda}) \right\}^2. \quad (9b)$$

It should be evident that the B' terms appear at the 3PN order while A' terms enter $\dot{\Phi}$ expression at the 1.5PN order. It is not very difficult to infer that these B' terms arise due to the non-vanishing \mathbf{l} component in the expression for $\dot{\mathbf{n}}$ and therefore are unphysical in nature. Therefore, these anomalous terms contribute to the Φ' evolution at the third post-Newtonian order and this is within the consideration of higher order spin effects currently available in the literature. It should be noted that these unphysical terms play no role in investigations in Ref. [6] that probed the leading order spin effects appearing at the 1.5PN order in the phase evolution.

Another consequence of invoking \mathbf{k} to specify the binary orbit is the appearance of certain new 1.5PN order contributions to the amplitudes of h_+ and h_\times in addition to what is provided by Eqs. (A1)–(A3) in Ref. [6]. We recall that Eqs. (A1)–(A3) in Ref. [6] provide the fully 1.5PN accurate expressions for h_+ and h_\times while invoking L_N to describe the binary orbits. The additional amplitude corrections to the GW polarization states arise mainly due to the fact that the component of \mathbf{v} along \mathbf{k} is of 1.5PN order. To demonstrate this point, we express \mathbf{r} and $\mathbf{v} = d\mathbf{r}/dt$ in the inertial frame $(\hat{\mathbf{x}}, \hat{\mathbf{y}}, \hat{\mathbf{z}})$ associated with \mathbf{j}_0 with the help of the three usual Eulerian angles Φ , α and ι as displayed in Fig. 1. The relevant expression for \mathbf{r} may be written as $\mathbf{r} = r\mathbf{n}$ where $\mathbf{n} = (-\sin \alpha \cos \Phi - \cos \iota \cos \alpha \sin \Phi)\hat{\mathbf{x}} + (\cos \alpha \cos \Phi - \cos \iota \sin \alpha \sin \Phi)\hat{\mathbf{y}} + \sin \iota \sin \Phi \hat{\mathbf{z}}$. To show that \mathbf{v} can have non-vanishing 1.5PN order terms along \mathbf{k} , we compute $d\mathbf{r}/dt$ in the co-moving frame defined by the triad $(\mathbf{n}, \boldsymbol{\xi} = \mathbf{k} \times \mathbf{n}, \mathbf{k})$ and this is easily achieved with the help of three rotations involving the three Eulerian angles appearing in the expression for \mathbf{r} [12]. The resulting expression for \mathbf{v} reads

$$\mathbf{v} = r \left(\frac{d\Phi}{dt} + \frac{d\alpha}{dt} \cos \iota \right) \boldsymbol{\xi} + r \left(\frac{d\iota}{dt} \sin \Phi - \sin \iota \cos \Phi \frac{d\alpha}{dt} \right) \mathbf{k}. \quad (10)$$

It is not very difficult to verify that $\mathbf{v} \cdot \mathbf{k} \neq 0$ while invoking Eq. (4a) for $\dot{\mathbf{k}}$ to evaluate the \mathbf{k} component of \mathbf{v} . Moreover, the coefficient of \mathbf{k} in the above expression for \mathbf{v} is at the 1.5PN order. The \mathbf{k} component of \mathbf{v} enters the expressions for h_+ and h_\times through the dot products $(\mathbf{p} \cdot \mathbf{v})$ $(\mathbf{q} \cdot \mathbf{v})$ and $(\mathbf{p} \cdot \mathbf{v})^2 - (\mathbf{q} \cdot \mathbf{v})^2$ that are required to compute the PN-accurate expressions for h_+ and h_\times (the vectors \mathbf{p} and \mathbf{q} are two unit vectors that lay in a plane perpendicular to \mathbf{N}). The resulting 1.5PN order amplitude corrections to h_\times symbolically read

$$h_\times \Big|_{1.5\text{PN}} = \frac{G \mu}{c^4 R'} \frac{G m}{c^3 \sqrt{x}} \left\{ \frac{d\iota}{dt} \kappa_1(\iota, \alpha, \Phi, \theta) + \frac{d\alpha}{dt} \kappa_2(\iota, \alpha, \Phi, \theta) \right\}, \quad (11)$$

where the explicit expressions for κ_1 and κ_2 are available in Ref. [10]. Therefore, the fully 1.5PN order amplitude corrected expression for h_\times associated with the spinning compact binaries in quasi-circular orbits, described by \mathbf{L} , is provided by Eq. (A3) along with the above Eq. (11). This statement also requires that the angular variables ι and α that appear in Eq. (A3) of Ref. [6] represent \mathbf{k} rather than \mathbf{l} . Let us emphasize again that Eqs. (A2) and (A3) in Ref. [6] indeed provide the fully 1.5PN accurate amplitude corrected h_+ and h_\times for spinning compact binaries in circular orbits described by \mathbf{L}_N .

Another aspect where we differ from Refs. [6, 8] is the way we specify the two spin and \mathbf{k} vectors to perform GW phasing. In the literature, it is common to freely specify spin vectors in an orthonormal triad defined by using \mathbf{l} [5, 6, 8]. In contrast, we freely specify the two spin vectors at the initial epoch in the inertial source frame associated with \mathbf{j}_0 . This choice allowed us to specify the x and y components of \mathbf{k} uniquely in terms of s_1 , s_2 and other intrinsic binary parameters at the initial epoch by demanding that the x and y components of $\mathbf{J} = \mathbf{L} + \mathbf{S}_1 + \mathbf{S}_2$ should be zero at that epoch. Therefore, we extract very easily the initial values of α and ι from the following expressions for the initial x and y components of \mathbf{k}

$$k_{x,i} = \sin \iota \cos \alpha = -\frac{G m^2}{c L_i} \{X_1^2 \chi_1 \sin \theta'_1 \cos \phi'_1 + X_2^2 \chi_2 \sin \theta'_2 \cos \phi'_2\},$$

$$k_{y,i} = \sin \iota \sin \alpha = -\frac{G m^2}{c L_i} \{X_1^2 \chi_1 \sin \theta'_1 \sin \phi'_1 + X_2^2 \chi_2 \sin \theta'_2 \sin \phi'_2\},$$

where $\theta'_1, \phi'_1, \theta'_2, \phi'_2$ are the values of $\theta_1, \phi_1, \theta_2, \phi_2$ at the initial epoch and L_i denotes the PN-accurate expression for $|\mathbf{L}|$ at initial orbital frequency.

For isolated unequal mass spinning compact binaries with $q > 3$ it should be advantageous to specify their spins in the inertial frame associated with \mathbf{j}_0 . This is because $\theta_1(x_0)$ that provides the dominant spin orientation from \mathbf{j}_0 at x_0 is expected to lie in a smaller range for such binaries spiraling into x_0 due to the emission of GWs. A recent study reveals that the dominant BH spin orientation from \mathbf{j}_0 at x_0 is more likely to be $\leq 90^\circ$ for angular momentum dominated unequal mass binaries ($|\mathbf{L}|(x_0) > S_1$) while $\theta_1(x_0) \leq 45^\circ$ for unequal mass binaries having $S_1 > |\mathbf{L}|$ at x_0 [13]. These inferences require that these binaries inherit spin-orbit misalignments

$\leq 160^\circ$ from various astrophysical processes responsible for the formation of such unequal mass spinning binaries. The physical explanation for these conclusions is the observed alignment of \mathbf{S}_1 towards \mathbf{j}_0 due to the action of gravitational radiation reaction, detailed in Ref. [9]. However, it will be difficult to provide similar bounds for the dominant spin orientation if the spins are freely specified in a non-inertial orbital triad associated with \mathbf{L} at x_0 . In this case $\mathbf{k} \cdot \mathbf{s}_1$ provides the dominant spin orientation at x_0 and it is not difficult to show that $\mathbf{k} \cdot \mathbf{s}_1$ remains fairly constant as these unequal mass binaries with $q > 3$ spiral into x_0 from initial orbital separations $\leq 1000 Gm/c^2$ due to the emission of GWs.

References

1. R.X. Adhikari, Gravitational Radiation Detection with Laser Interferometry. ArXiv e-prints, May (2013)
2. B.S. Sathyaprakash, B.F. Schutz, Physics, astrophysics and cosmology with gravitational waves. *Living Rev. Relativ.* **12**(2) (2009)
3. L. Blanchet, Gravitational radiation from post-Newtonian sources and inspiralling compact binaries. *Living Rev. Relativ.* **9**(4) (2006)
4. B.M. Barker, R.F. O’Connell, Gravitational two-body problem with arbitrary masses, spins, and quadrupole moments. *Phys. Rev. D* **12**, 329–335 (1975)
5. L.E. Kidder, Coalescing binary systems of compact objects to (post)^{5/2}-Newtonian order. v. spin effects. *Phys. Rev. D* **52**, 821–847 (1995)
6. K.G. Arun, A. Buonanno, G. Faye, E. Ochsner, Higher-order spin effects in the amplitude and phase of gravitational waveforms emitted by inspiraling compact binaries: ready-to-use gravitational waveforms. *Phys. Rev. D* **79**, 104023 (2009)
7. A. Gopakumar, G. Schäfer, Gravitational wave phasing for spinning compact binaries in inspiraling eccentric orbits. *Phys. Rev. D* **84**, 124007 (2011)
8. A. Buonanno, Y. Chen, M. Vallisneri, detecting gravitational waves from precessing binaries of spinning compact objects: adiabatic limit. *Phys. Rev. D* **67**, 104025 (2003)
9. T.A. Apostolatos, C. Cutler, G.J. Sussman, K.S. Thorne, Spin-induced orbital precession and its modulation of the gravitational waveforms from merging binaries. *Phys. Rev. D* **49**, 6274–6297 (1994)
10. A. Gupta, A. Gopakumar, Time-domain inspiral templates for spinning compact binaries in quasi-circular orbits described by their orbital angular momenta (2013). [arXiv:1308.1315](https://arxiv.org/abs/1308.1315)
11. S. Marsat, A. Bohe, G. Faye, L. Blanchet, Next-to-next-to-leading order spinorbit effects in the equations of motion of compact binary systems. *Class. Quantum Gravity* **30**(5), 055007 (2013)
12. T. Damour, G. Schafer, Higher-order relativistic periastron advances and binary pulsars. *Nuovo Cimento B Ser.* **101**, 127–176 (1988)
13. A. Gupta, A. Gopakumar. To be submitted (2013)